

AD-A136 749

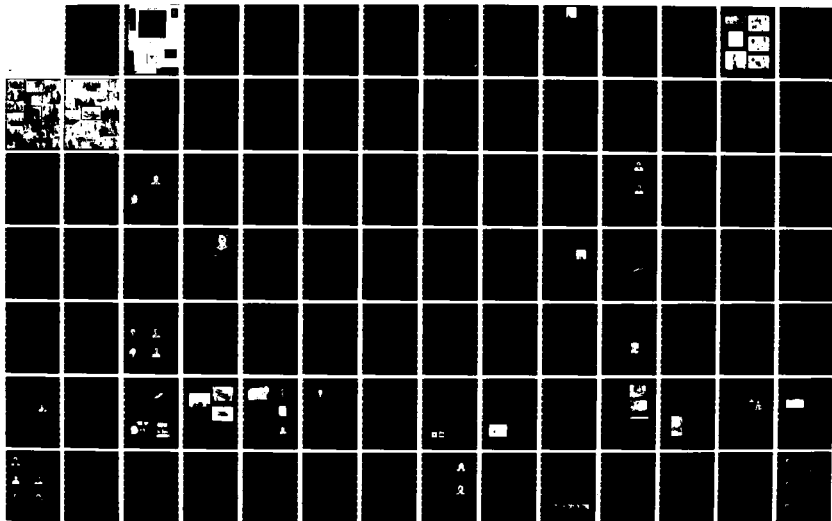
PROCEEDINGS OF THE INTERNATIONAL WIRE AND CABLE  
SYMPOSIUM (32ND) HELD AT (U) ARMY  
COMMUNICATIONS-ELECTRONICS COMMAND FORT MONMOUTH NJ  
17 NOV 83

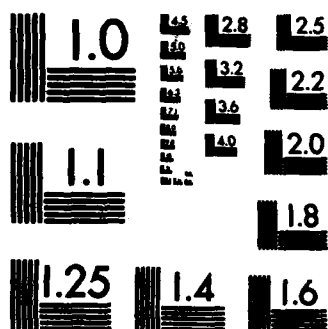
1/5

UNCLASSIFIED

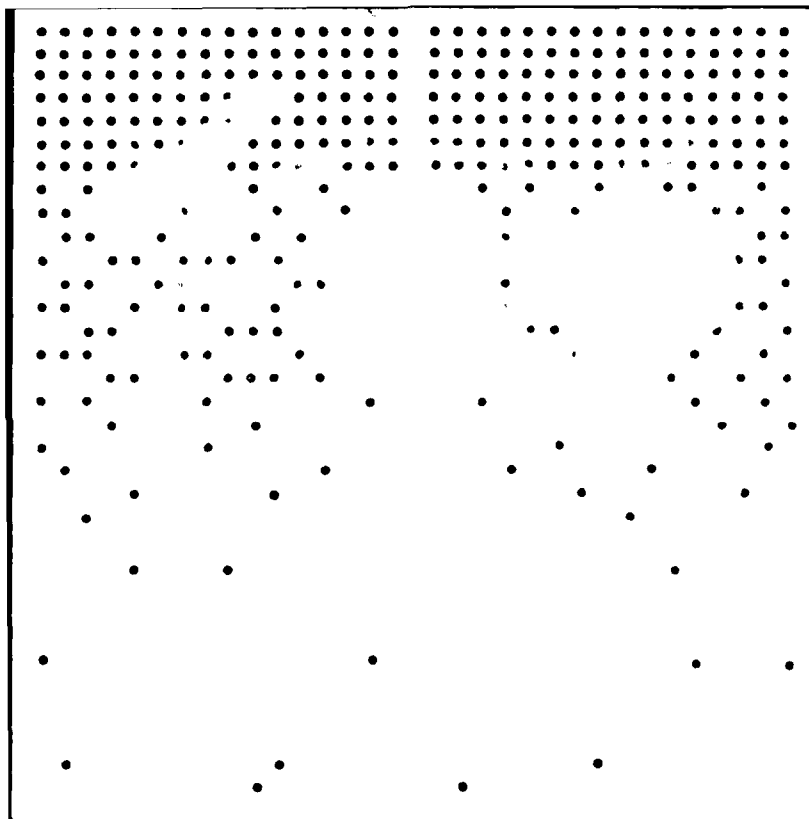
F/G 5/2

NL





MICROCOPY RESOLUTION TEST CHART  
NATIONAL BUREAU OF STANDARDS-1963-A



Total 58 documents

## COMPONENT PART NOTICE

THIS PAPER IS A COMPONENT PART OF THE FOLLOWING COMPILATION REPORT:

(TITLE): Proceedings of the International Wire and Cable Symposium (32nd) Held  
at Cherry Hill, New Jersey on November 15, 16 and 17, 1983.

(SOURCE): Army Communications-Electronics Command, Fort Monmouth, N.J.

TO ORDER THE COMPLETE COMPILATION REPORT USE AD-A136 749.

THE COMPONENT PART IS PROVIDED HERE TO ALLOW USERS ACCESS TO INDIVIDUALLY AUTHORED SECTIONS OF PROCEEDINGS, ANNALS, SYMPOSIA, ETC. HOWEVER, THE COMPONENT SHOULD BE CONSIDERED WITHIN THE CONTEXT OF THE OVERALL COMPILATION REPORT AND NOT AS A STAND-ALONE TECHNICAL REPORT.

THE FOLLOWING COMPONENT PART NUMBERS COMPRISE THE COMPILATION REPORT:

AD#: P002 526 TITLE: Use of Plain Copper Conductors in Lieu of Tinned-Copper for Internal Cables.

P002 527	Development of Copper-Coated Aluminum-Shielded Wire.
P002 528	Aluminum Foil Shield Effectiveness for Electronic Cables.
P002 529	Unbalanced Digital Crosstalk in Balanced, Twisted Pair, Inside Wiring Cable.
P002 530	Design and Characteristics of Radiating Pair Cable.
P002 531	New Wuality Assessment Procedure for Exchange Area Cable Transmission Parameters.
P002 532	Bell System Lightguide Cable Interconnection Equipment, Central Office to Customer Premises.
P002 533	Termination of Cylindrical Grooved Optical Cables.
P002 534	Field Trial of Composite Fiber-Optic Overhead Ground Wire.
P002 535	Factory Splicing of Optical Waveguide Fiber.
P002 536	Fabrication and Evaluation of a High Density Multi Fiber Plastic Connector.
P002 537	Lead Making for Improved Continuous-Flow Manufacturing Systems.
P002 538	Longitudinal Waterblocking Performance of Conductive and Non Conductive Waterswellable Nonwovens.
P002 539	Evaluation of Adhesive Materials for Bonded Sheath Cable Designs.
P002 540	New Data on Long Term Stabilization of Polyethylene for Telecommunication Wire Insulation.
P002 541	Behaviour of Four Non-Migratory Antioxidants in Solid Polyethylene Insulation.
P002 542	Equipment and Design Changes in Extrusion of Foamed Fluoropolymer Resins.
P002 543	Foamable PVFD (Polyvinylidene Fluoride) Fluoroplastic for Wire and Cable Applications.
P002 544	Development of Composite Fiber-Optic Electric-Power Umbilical Cable and Optical Feedthrough for Deep Ocean Mining.

## COMPONENT PART NOTICE (CON'T)

<b>ADM:</b> P002 545 —	<b>TITLE:</b> Analysis of Excess Attenuation in Optical Fibers Subjected to Low Temperatures.
P002 546 —	Buckling of Optical Fibers within Elastomers Used in an Embedded-Core Cable Structure.
P002 547 —	Design Aspects of Loose Buffer Tube Fiber Optics Cable.
P002 548 —	Non-Metallic Optical Cable with Optical Fiber Catenary for Long Span Aerial Application.
P002 549 —	Non-Metallic Long Span Aerial Cable with Optical Fibers for the Use at 1.3 Micrometers.
P002 550 —	New Silicone Rubber Cable Insulation Promises Circuit Integrity, in Flaming Environment.
P002 551 —	A Polytetrafluoroethylene Insulated Cable for High Temperature Oxygen Aerospace Applications.
P002 552 —	Development of Flame Retardant, Low Aggressivity Cables.
P002 553 —	Low-Smoke, Halogenfree Ship-Offshore/Onshore Cables with Improved Flame Retardance and Fire Resistance.
P002 554 —	Versatile Fire Barrier Systems for Telephone Cable.
P002 555 —	Cylindrical V-Grooved Non Metallic Optical Fibre Cable.
<i>Start</i> P002 556 —	Design and Test Results of Optical Fiber Units for Optical Submarine Cable.
P002 557 —	Metal-Free Cylindrical V-Grooved Optical Cable.
P002 558 —	Design, Fabrication and Testing of a Ruggedized Fiberoptic Cable.
P002 559 —	A Rodent and Lightning Protective Sheath for Fiber Optic Cables.
P002 560 —	A Radically New Approach to the Installation of Optical Fibre Using the Viscous Flow of Air.
P002 561 —	Material Requirements for Multimedia Communications Cable.
P002 562 —	Design of a Twisted Pair Cable for a Token Passing Local Area Network.
P002 563 —	Measurement of the Characteristic Impedance of Balanced Twisted Pairs Using Scattering Parameters.
P002 564 —	Design/Process Optimization of Paired Computer Interconnecting Cable for Local Area Networks.
P002 565 —	Evaluation of Foam-Skin Cables for Aerial Applications.
P002 566 —	A Practical Single-Mode System, 50 km at 140 Mbit/s.
P002 567 —	Performance Characteristics of VAD Single Mode Fibers in Mass Production Basis.
P002 568 —	Recent Developments in Mini-Unit Cable.
P002 569 —	Manufacture, Laying and Splicing of Monomode Optical Fiber Cables with Low Losses.
P002 570 —	A Field Splicing System for Single-Mode Optical Fiber.
P002 571 —	Optical and Mechanical Properties of Single-Mode Cables at 1300 nm.
P002 572 —	A New Engineering Approach for Cable in Fire Situations Using Halogenated Polymers.

AD: P002 573 — TITLE: Characteristics of Heat and Flame Resistant Optical Fiber Cables.  
P002 574 — Cable Fire Studies Using the Ohio State University Release Rate Apparatus.  
P002 575 — Circuit Transmission Integrity of Plenum Cables in a Developing Fire Scenario.  
P002 576 — Large Scale Fire Test of Cable Installed in Tunnels.  
P002 577 — Overall Fire Safety of Cable and Wiring Materials. Part 1.  
P002 578 — Fracture Mechanics Evaluation of the Static Fatigue Life of Optical Fibers in Bending.  
P002 579 — Computerised Optical Fibre Characterisation.  
P002 580 — Remote-Ended Time Domain Bandwidth Measurements on Installed Regenerator Sections of Multimode Optical Fibre Cable in the British Telecom Network.  
P002 581 — Development of Short-Distance Optical Transmission Cord.  
P002 582 — Thermal Properties of Loose Tube Secondary Coated Optical Fibres Experimentally Discussed by a Relative Light Pulse Delay Technique.  
P002 583 — Breakout Cables for Short Haul Fiber Optic Systems.

Accession For	
THIS GRA&I	<input checked="" type="checkbox"/>
IC TAB	<input type="checkbox"/>
Announced	<input type="checkbox"/>
Notification	
By	
Distribution/	
Availability Codes	
Avail and/or	
Special	
A-1	

**DTIC**  
**ELECTRIC**  
**JAN 13 1984**  
**A**

This document has been approved  
for public release and sale; its  
distribution is unlimited.

## **DISCLAIMER NOTICE**

**THIS DOCUMENT IS BEST QUALITY  
PRACTICABLE. THE COPY FURNISHED  
TO DTIC CONTAINED A SIGNIFICANT  
NUMBER OF PAGES WHICH DO NOT  
REPRODUCE LEGIBLY.**

# PROCEEDINGS OF 32nd INTERNATIONAL WIRE AND CABLE SYMPOSIUM

Sponsored by  
US Army Communications-Electronics Command  
(CECOM) Fort Monmouth, NJ

CHERRY HILL, NEW JERSEY  
NOVEMBER 15, 16 and 17, 1983

~~Copy available to DTIC does not  
guarantee fully legible reproduction~~

APPROVED FOR PUBLIC RELEASE: DISTRIBUTION UNLIMITED

Accession For	
NTIS GRA&I	<input checked="" type="checkbox"/>
DTIC TAB	<input type="checkbox"/>
Unannounced	<input type="checkbox"/>
Justification	
By	
Distribution/	
Availability Codes	
Dist	Avail and/or Special
A/1	code 27 CW



DTIC  
ELECTE  
DEC 21 1983  
D

# **32nd INTERNATIONAL WIRE AND CABLE SYMPOSIUM**

## **SYMPOSIUM COMMITTEE**

Elmer F. Godwin, Director, GEF Associates (201)741-8864  
Winnie Conti, Assistant, US Army CECOM (201)544-2770  
John Brazee, Northern Telecom Inc.  
William Chervenak, Corning Glass Works  
Robert Depp, Defense Electronics Supply Center  
Paul Dobson, Valtec Corporation  
Andrew Dunin, DuPont Canada Inc.  
Joseph McCann, US Army CECOM  
Kazuo Nomura, Sumitomo Electric, USA  
Eugene Riley, Anaconda-Ericsson, Inc.  
John Santos, Phelps Dodge Communications Company  
John Thompson, Nokia, Inc.  
James Typer, Essex Group  
George Webster, Bell Laboratories  
Austin Wetherell, Underwriters Laboratories

## **ADVISORY**

Michael A. DeLucia, David W. Taylor Naval Ship R&D Center  
Marta Farago, Northern Telecom Canada Ltd.  
Irving Kolodny, General Cable Company  
Joe Neigh, AMP, Inc.  
Frank Short, Belden Corporation

## **TECHNICAL SESSIONS**

### **Tuesday, 15 November 1983**

9:30 a.m.	Session I	Panel Discussion—Current Trends In Local Area Networks
2:00 p.m.	Session II	Design and Testing
2:00 p.m.	Session III	Fiber Optic Applications and Terminations

### **Wednesday, 16 November 1983**

9:00 a.m.	Session IV	Material I
9:00 a.m.	Session V	Fiber Optic Cable Design I
2:00 p.m.	Session VI	Materials II
2:00 p.m.	Session VII	Fiber Optics Cable Design II

### **Thursday, 17 November 1983**

9:00 a.m.	Session VIII	Applications and Local Area Networks
9:00 a.m.	Session IX	Single Mode Fiber and Applications
2:00 p.m.	Session X	Fire, Smoke and Toxicity
2:00 p.m.	Session XI	Fiber Optics Characterization and Testing

## **PAPERS**

Responsibility for contents rests upon the authors and not the symposium committee or its members. After the symposium, all the publication rights of each paper are reserved by their authors, and requests for republication of a paper should be addressed to the appropriate author. Abstracting is permitted, and it would be appreciated if the symposium is credited when abstracts or papers are republished. Requests for individual copies of papers should be addressed to the authors.



Message From The Director

On behalf of the US Army Communications-Electronics Command (CECOM) and the Symposium Committee, welcome to the 32nd Annual International Wire and Cable Symposium (IWCS). Last year's symposium was, again, a real success, with an attendance of over 1500, including representatives from 505 US Companies, 17 US Government Agencies, and 26 foreign countries. Of the 59 papers presented during the symposium, 34 were by foreign attendees.

The committee expects this year's excellent technical program to continue and attract worldwide interest and participation. Sixty (60) papers are scheduled for presentation, beginning with a tutorial session entitled, "Current Trends In Local Area Networks," followed by ten (10) session covering a variety of technical topics related to wire/cable and interconnections. The area of fiber optics continues to provide the greatest response to the "Call For Papers," and also includes the largest number of papers scheduled for presentation.


For the first time a press area will be available for representatives of participating companies and reporters or writers of periodicals/magazines. The committee hopes that the area will promote and enhance the collection and dissemination of information relating to symposium activities and developments in the wire/cable industry.

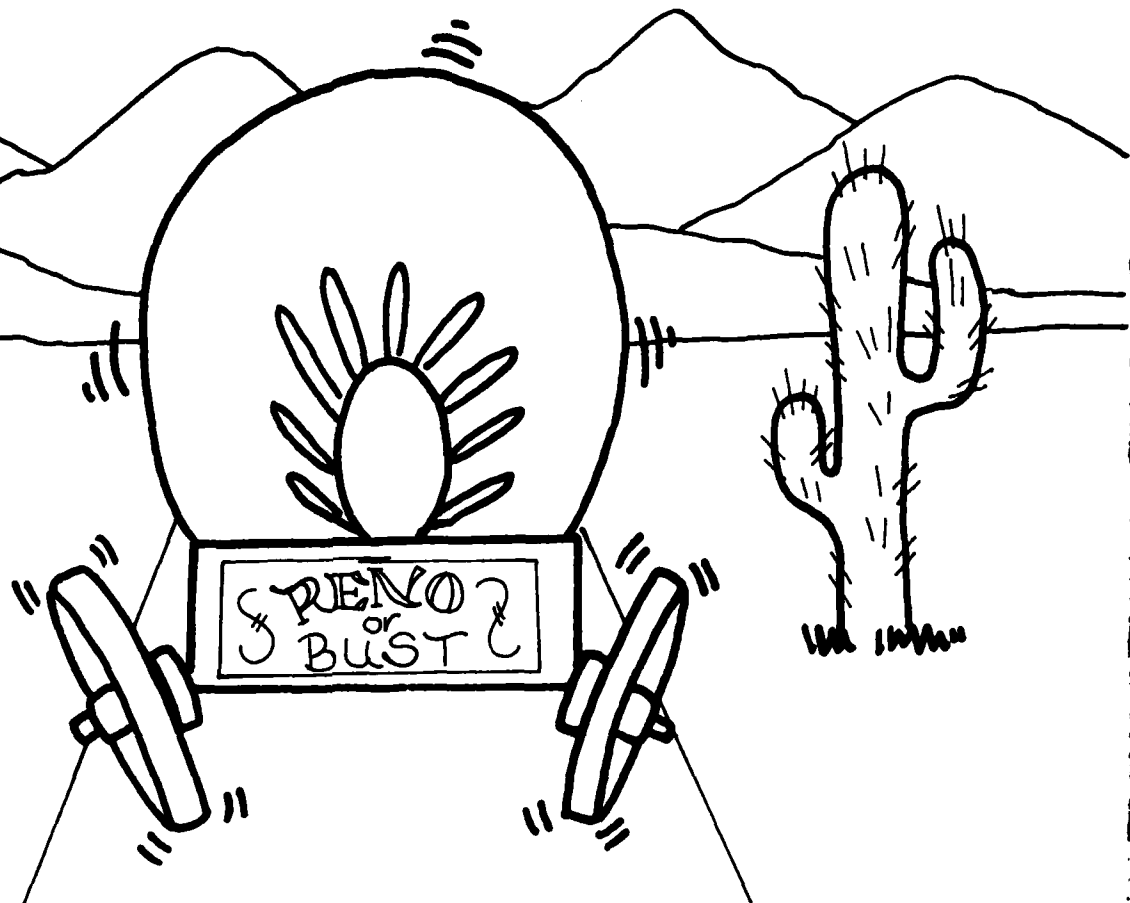
As announced during last year's symposium, the 33rd symposium (1984) will be held at the MGM Grand Hotel, Reno, Nevada (see committee's letter - next page). In 1985, the symposium will return to the Cherry Hill Hyatt Hotel, Cherry Hill, New Jersey. A location for the 1986 symposium has not been selected, however, symposium attendees will be informed of the location well in advance of the 1986 meeting.

Committee member John Brazee of Northern Telecom is retiring from the committee. John contributed significantly to the success of the symposium and on behalf of the committee, I thank John for his valuable contributions and wish him success in his future endeavors.

Ms. Winnie Conti was recently promoted and transferred to a new position, as a result, this will be her last year with the symposium. On behalf of the committee, a very special thanks to Winnie for her sincere dedication, cooperation, and support of the symposium. I personally thank Winnie for her valuable assistance and contributions and wish her success in her new position.

The committee requests the continued support of all members of the wire and cable industry. The objective of the committee is for the symposium to remain a reflection of the needs and interests of its attendees and supporters, therefore, comments and suggestions for improving the symposium are welcomed.

  
ELMER F. GODWIN  
Director



After 32 years of nurturing and growth in the east, the IWCS will head west and hold its 1984 Symposium at the MGM Grand Hotel in Reno, Nevada on 13, 14, and 15 November. While the move represents a major change in location it will not break the tradition of technical excellence forged with the wire and cable industry. It comes in response to the changing character of the industry: once concentrated in the New England area and now a truly coast-to-coast industry. The 1984 location will be an experiment to determine the feasibility and practicality of a west coast location with the possible eventual goal of alternating (east/west) locations. It is hoped that the new location will attract greater participation from portions of the industry who in the past have found it difficult and/or costly.

The committee is excited about the selection of the MGM Grand Hotel as its west coast headquarters. The large, modern facility will accommodate all symposium participants and activities. All technical sessions, speakers, hospitality suites and registrants will be under a single roof thus allowing for maximum interchange between participants. Adjacent to the hotel is the Reno International Airport allowing convenient travel connections for anywhere in the world. The possibility of low-cost group airfare is under investigation. You may even wish to make family vacations plans around the Symposium and take advantage of nearby Lake Tahoe, and ski resorts like Heavenly Valley and Squaw Valley.

It is the committee's sincere desire to make this transition smoothly. If you have any questions about the facility, a representative of the MGM Grand will be present at this years (1983) symposium (or you may call Mr. Bill Ellander (Tele 702-789-2000) at the hotel).

Spread the word 'round the industry!  
We're moving to Reno in '84.

The IWCS Committee

**PROCEEDINGS  
INTERNATIONAL WIRE & CABLE SYMPOSIUM  
BOUND—AVAILABLE AT FORT MONMOUTH**

27th International Wire & Cable Symposium Proceedings—1978—8.00  
28th International Wire & Cable Symposium Proceedings—1979—8.00  
29th International Wire & Cable Symposium Proceedings—Not Available  
30th International Wire & Cable Symposium Proceedings—1981—8.00  
31st International Wire & Cable Symposium Proceedings—1982—10.00  
\*32nd International Wire & Cable Symposium Proceedings—1983—15.00  
\*Extra copies: 1-3 \$15.00; next 4-10 \$10.00; next 11 & above \$8.00 each

Make check or bank draft Payable in US dollars to the INTERNATIONAL WIRE & CABLE SYMPOSIUM and forward request to:

International Wire & Cable Symposium  
US Army Communications - Electronics Command  
ATTN: DRSEL-COM-RM-3  
Fort Monmouth, NJ 07703  
USA

**PHOTOCOPIES—AVAILABLE AT DEPARTMENT OF COMMERCE**

Photocopies are available for complete sets of papers for 1964 and 1966 thru 1982. Information on prices and shipping charges should be requested from the:

US Department of Commerce  
National Technical Information Service  
Springfield, Virginia 22151  
USA

Include Title, Year and "AD" Number

13th Annual Wire & Cable Symposium (1964)	—AD 787164
15th Annual Wire & Cable Symposium (1966)	—AD A006601
16th International Wire & Cable Symposium (1967)	—AD 787165
17th International Wire & Cable Symposium (1968)	—AD 787166
18th International Wire & Cable Symposium (1969)	—AD 787167
19th International Wire & Cable Symposium Proceedings 1970	—AD 714985
20th International Wire & Cable Symposium Proceedings 1971	—AD 733399
21st International Wire & Cable Symposium Proceedings 1972	—AD 752908
22nd International Wire & Cable Symposium Proceedings 1973	—AD 772914
23rd International Wire & Cable Symposium Proceedings 1974	—AD A003251
24th International Wire & Cable Symposium Proceedings 1975	—AD A017787
25th International Wire & Cable Symposium Proceedings 1976	—AD A032801
26th International Wire & Cable Symposium Proceedings 1977	—AD A047609
27th International Wire & Cable Symposium Proceedings 1978	—AD A062322
28th International Wire & Cable Symposium Proceedings 1979	—AD A081428
29th International Wire & Cable Symposium Proceedings 1980	—AD A096308
30th International Wire & Cable Symposium Proceedings 1981	—AD A110859
31st International Wire & Cable Symposium Proceedings 1982	—AD A125662
Kwic Index of Technical Papers, International Wire & Cable Symposium (1952-1975)	—AD A027558

**Highlights of the 31st  
International Wire and Cable Symposium  
November 16, 17, & 18, 1982  
Hyatt Cherry Hill, Cherry Hill, NJ**



**Panel Members—Tutorial Session:**  
(left to right) N. Dean, Dir. and Chief Engineer of Telecommunications, B.I.C.C.; Mr. D. McMahon, V. Pres., Marketing, Essex Corp.; Mr. R. Sweitert, V. Pres., Planning, Siecor; Mr. A. Yebejs, Technical Manager, Bell Laboratories; and Dr. M. Biskeborn, Consultant, Research and Development, Phelps Dodge.



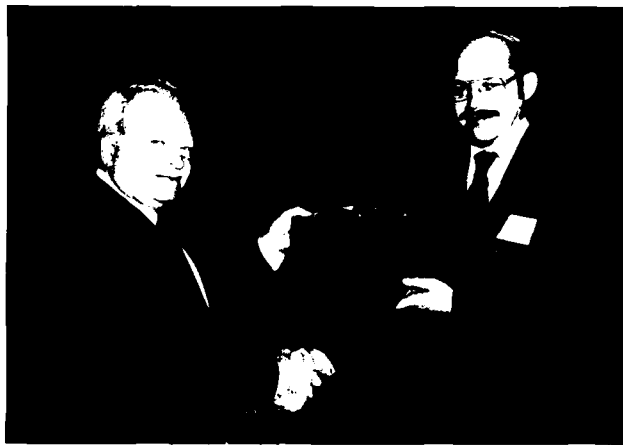
**Brigadier General A. Albright, Commander, Defense Electronic Supply Center, Introduction of Guest Speaker.**



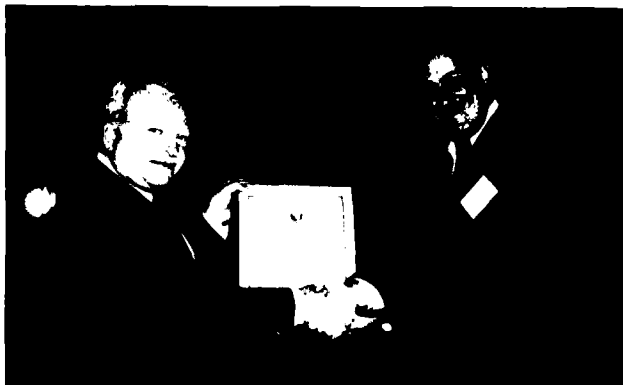
**Banquet Guest Speaker—Mr. Billy Oliver, Vice President of Planning and Design for AT&T Long Lines.**



**Mr. Leo Chattler, (Center) DCM Industries, Inc., presenting the award for Outstanding Technical Paper to (left to right) Messrs. J. Arroyo and N. Cagelia, Bell Laboratories and Mr. J. Darsey, Western Electric.**



**Mr. Leo Chattler, DCM Industries, Inc., presenting the award for Best Presentation to Mr. G. S. Anderson, Belden Corp.**



**Mr. E. Famolari, Director of CENCOMS, Fort Monmouth, Presenting Retirement Certificate to Committee Member Leo Chattler (left), missing from photo, Mr. Willaim Korcz, Shell Development Company.**

# AWARDS

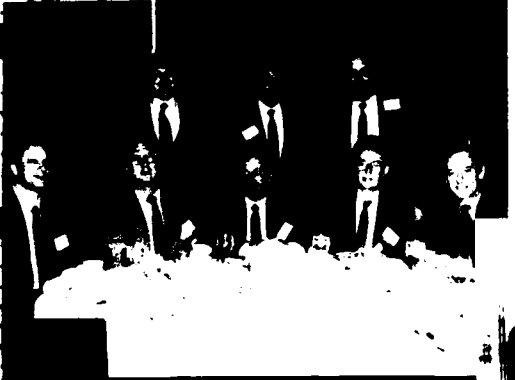
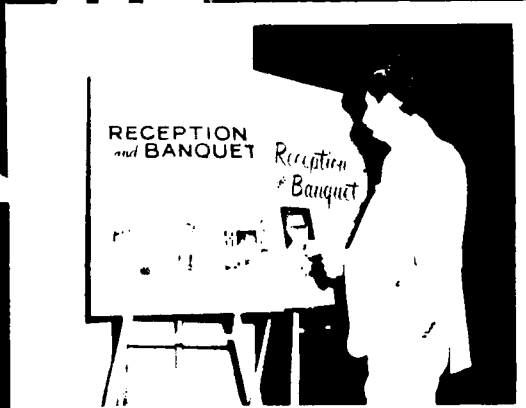
## Outstanding Technical Paper

- H. Lubars and J. A. Olszewski, General Cable Corp.—“Analysis of Structural Return Loss in CATV Coaxial Cable” 1968
- J. P. McCann, R. Sabia and B. Wargotz, Bell Laboratories—“Characterization of Filler and Insulation in Waterproof Cable” 1969
- D. E. Setzer and A. S. Windeler, Bell Laboratories—“A Low Capacitance Cable for the T2 Digital Transmission Line” 1970
- R. Lyenger, R. McClean and T. McManus, Bell Northern Research—“An Advanced Multi-Unit Coaxial Cable for Toll PCM Systems” 1971
- J. B. Howard, Bell Laboratories—“Stabilization Problems with Low Density Polyethylene Insulations” 1972
- Dr. H. Martin, Kabelmetal—“High Power Radio Frequency Coaxial Cables, Their Design and Rating” 1973
- D. Doty, AMP Inc.—“Mass Wire Insulation Displacing Termination of Flat Cable” 1974
- T. S. Choo, Dow Chemical U.S.A.—“Corrosion Studies on Shielding Materials for Underground Telephone Cables” 1975
- N. J. Cogelia, Bell Telephone Laboratories and G. K. Lavoie and J. F. Glahn, US Department of Interior—“Rodent Biting Pressure and Chemical Action and Their Effects on Wire and Cable Sheath” 1976
- Thomas K. McManus, Northern Telecom Canada Ltd. and R. Beveridge, Saskatchewan Telecommunications, Canada—“A New Generation of Filled Core Cable” 1977
- Fumio Suzuki, Shizuyoshi Sato, Akinori Mori and Yoichi Suzuki; Sumitomo Electric Industries, Ltd., Japan—“Microcoaxial Cables Insulated with Highly Expanded Polyethylene By Chemical Blowing Method” 1978
- S. Masaki, Y. Yamazaki and T. Ideguchi, Nippon Telegraph and Telephone Public Corporation, Japan—“New Aluminum Sheath Cable Used for Electromagnetic Shielding” 1979
- P. Kish and Y. LeBorgne, Northern Telecom Canada Limited, Montreal, Canada—“General Crosstalk Model For Paired Communication Cables” 1980
- C. J. Arroyo, N. J. Cogelia, Bell Laboratories, and R. J. Darsey, Western Electric—“Thermal Behavior of Experimental Plenum Cable Sheaths Determined in a Radiant Heat Chamber” 1981
- R. H. Whiteley, Raychem Ltd.—“A Comprehensive Small Scale Smoke Test” 1982

## Best Presentation

- N. Dean, B.I.C.C.—“The Development of Fully Filled Cables for Distribution Network”
- J. D. Kirk, Alberta Government Telephones—“Progress and Pitfalls of Rural Buried Cable”
- Dr. O. Leuchs, Kable and Metalwerke—“A New Self-Extinguishing Hydrogen Chloride Binding PVC Jacketing Compound for Cables”
- S. Nordblad, Telefonaktiebolaget L. M. Ericsson—“Multi-Paired Cable of Nonlayer Design for Low Capacitance Unbalance Telecommunications Network”
- N. Kojima, Nippon Telegraph and Telephone—“New Type Paired Cable for High Speed PCM Transmission”
- S. Kaufman, Bell Laboratories—“Reclamation of Water-Logged Buried PIC Telephone Cable”
- R. J. Oakley, Northern Electric Co., Ltd.—“A Study into Paired Cable Crosstalk”
- G. H. Webster, Bell Laboratories—“Material Savings by Design in Exchange and Trunk Telephone Cable”
- J. E. Wimsey, United States Air Force—“The Bare Base Electrical Systems”
- Michael DeLucia, Naval Ship Research and Development Center—“Highly Fire-Retardant Navy Shipboard Cable”
- William L. Schmacher, AMP Inc.—“Design Considerations for Single Fiber Connector”
- Richard C. Mondello, Bell Labs.—“Design and Manufacture of an Experimental Lightguide Cable For Undersea Transmission Systems”
- I. Wadehra, IBM Corporation—“Performance of Polyvinyl Chloride Communication Cables in Modified Steiner Tunnel Test”
- J. J. Refi, Bell Laboratories—“Mean Power Sum Far-End Crosstalk of PIC Cables as a Function of Average Twist Helix Angle”
- G. S. Anderson, Belden Corporation—“Installation of Fiber Optic Cable on 457 Meter Tower”
- A. Yoshizawa, The Furukawa Electric Co., Ltd.—“Structure and Characteristics of Cables for Robots”

CANDID SCENES AT 31st IWCS





## CONTRIBUTORS

**Alacave-Alambres y Cables Venezolanos C.A.**  
 Caracas, Venezuela  
**Albany International Corp.**  
 Chatham, NY  
**Alcan Canada Products Ltd., Wire & Cable-Bracebridge Works**  
 Ontario, Canada  
**Allied Corporation Allied Fibers & Plastics Company**  
 Morristown, NJ  
**Alpha Wire Corporation**  
 Elizabeth, NJ  
**American Hoechst Corp.**  
 Somerville, NJ  
**AMP Inc.**  
 Harrisburg, PA  
**Anaconda-Ericsson Inc.**  
 Bohemia, NY  
**ARCO Aluminum Company**  
 Louisville, KY  
**ARCO Chemical Company**  
 Philadelphia, PA  
**Arvey Corporation**  
 Cedar Grove, NJ  
**Associated Lead Inc.**  
 Philadelphia, PA  
**ATC (PTY) Limited**  
 Brits, Tranvaal, South Africa  
**Austral Standard Cables Pty. Ltd.**  
 Clayton, Victoria, Australia  
**Badische Corporation**  
 Williamsburg, VA  
**Barcel Wire & Cable Corp.**  
 Irvine, CA  
**Beacon Reel Co.**  
 Beacon Falls, CT  
**Belden Corporation**  
 Technical Research Center, Geneva, IL  
**Bell Canada H. Q. Engineering-Technology Development**  
 Toronto, Ont., Canada  
**Bengamin/Clarke Assoc., Inc.**  
 Kensington, MD  
**Berkshire Electric Cable Co.**  
 Leeds, MA  
**Berk-Tek, Inc.**  
 Reading, PA  
**BICC Telecommunication Cables Limited**  
 Prescot, Merseyside L34 5SZ, England  
**Boston Insulated Wire & Cable Co. Ltd.**  
 Hamilton, Ontario, Canada  
**Brand-Rex Company**  
 Willimantic, CT  
**Breen Color Concentrates, Inc.**  
 Lambertville, NJ  
**The Bridge Mfg. Company**  
 Enfield, CT  
**Burgess Pigment Co.**  
 Sanderville, GA  
**Cables de Comunicaciones, S.A.**  
 Zaragoza, Spain  
**Camden Wire Co., Inc.**  
 Camden, NY  
**Canada Wire and Cable Ltd.**  
 Winnipeg, Manitoba, Canada  
**Capscan, Cable Company**  
 Adelphia, NJ  
**Carlew Chemicals Ltd.**  
 Montreal, Quebec, Canada  
**R.E. Carroll, Inc.**  
 Trenton, NJ

**Cary Chemical Corp.**  
 Leominster, MA  
**Cary Chemicals Inc.**  
 Edison, NJ  
**CasChem, Inc.**  
 Bayonne, NJ  
**Celwave Technologies, Inc.**  
 Claremont, NC  
**Chase & Sons, Inc.**  
 Randolph, MA  
**Chromatics, Inc.**  
 Duncan, SC  
**C-I-L Inc.**  
 Brampton, Ontario, Canada  
**Colorant, AB**  
 Knivsta, Sweden  
**Colorite Plastics Co.**  
 Ridgefield, NJ  
**Commonwealth Telephone Co.**  
 Dallas, PA  
**Comm/Scope Company**  
 Catawba, NC  
**Communications Technology Corp.**  
 Los Angeles, CA  
**Conoco Chemicals Co.**  
 Saddlebrook, NJ  
**Delphi Wire and Cable**  
 Folcroft, PA  
**Dow-Chemical USA**  
 Midland, MI  
**Dow Corning Corporation**  
 Midland, MI  
**E. I. du Pont de Nemours & Co., Inc.**  
 Wilmington, DE  
**Dussek Campbell Ltd.**  
 United Kingdom  
**Eagle-Pitcher Industries, Inc.**  
 Cincinnati, OH  
**Eastman Chemical Products, Inc.**  
 Kingsport, TN  
**The Electric Wire & Cable Co. of Israel Ltd.**  
 Haifa, Israel  
**Electrical Conductors, Inc.**  
 No. Chicago, IL  
**Electronic Systems Divisions**  
**Geosource Inc.**  
 Houston, TX  
**Ensign-Bickford Industries, Inc.**  
 Simsbury, CT  
**EnviroStrand, Inc.**  
 Leominster, MA  
**ESSEX GROUP**  
 Decatur, IL  
**EXMET Corporation**  
 Bridgeport, CT  
**Facile Technologies Inc.**  
 Paterson, NJ  
**Firer BV**  
 The Netherlands  
**Formulabs Industrial Inks Inc.**  
 Escondido, CA  
**Franklin Plastics Corp.**  
 Kearny, NJ  
**Gavitt Wire and Cable Co., Inc.**  
 Brookfield, MA  
**Gem Gravure Co., Inc.**  
 West Hanover, MA  
**General Cable Company Fiber Optics Div.**  
 Edison, NJ

**General Electric Company Silicone Products Division**  
 Waterford, NY  
**Georgia-Pacific Corporation**  
 Fairfield, NJ  
**W.L. Gore & Associates**  
 Newark, DE  
**Great Lakes Chemical Corporation**  
 West Lafayette, IN  
**Habla Cable Inc.**  
 Ronkonkoma, NY  
**Harbour Industries, Inc.**  
 Shelburne, VT  
**High Voltage Engineering Corp.**  
 Burlington, MA  
**Hitachi Cable America Inc.**  
 New York, NY  
**Hong Kong Telephone Co. Ltd.**  
 Hong Kong  
**Hudson Wire Company**  
 Ossining, NY  
**Independent Cable, Inc.**  
 Hudson, MA  
**International Wire Products Company**  
 Wyckoff, NJ  
**I.T.T. Electro-Optical Products Div.**  
 Roanoke, VA  
**ITT Surprenant Division**  
 Clinton, MA  
**J-Sil Silicones**  
 Corporate Office, Weatherford, TX  
**Judd Wire Div., HVE**  
 Turner Falls, MA  
**Jydsk Telefon A/S**  
 Tranbjerg, Denmark  
**Kable Tapes Ltd.**  
 Manitoba, Canada  
**Kaliflex Div., Kalex Chem Products**  
 Brooklyn, NY  
**Kennrich Petrochemicals, Inc.**  
 Bayonne, NJ  
**Lamart Corp.**  
 Clifton, NJ  
**Laribee Wire Mfg. Co., Inc.**  
 Jordan, NY  
**Lignes Telegraphiques et Telephoniques Documenta-  
 tion Technique**  
 Sainte Honorine, France  
**LONZA Inc.**  
 Fair Lawn, NJ  
**J.J. Lowe Associates-Tapes & Reel Div.**  
 Bedford Hills, NY  
**Lynn Plastics Corporation**  
 Lynn, MA  
**Mallefer Company**  
 South Hadley, MA  
**Major Wire Co., Inc.**  
 Chicopee, MA  
**Manning Paper Company, Div. Hammermill Paper Co.**  
 Green Island, NY  
**Micro-Tek Corp.**  
 Cinnaminson, NJ  
**Mid-Continent Telephone**  
 Hudson, OH  
**K. Miller Tool & Mfg. Co., Inc.**  
 West Springfield, MA  
**Monsanto Polymer Products Co.**  
 St. Louis, MO  
**The Montgomery Co.**  
 Windsor Locks, CT  
**Montrose Products Company**  
 Auburn, MA

**Mossberg Industries**  
 Cumberland, RI  
**Neptco**  
 Pawtucket, RI  
**Nesor Alloy Corporation**  
 West Caldwell, NJ  
**The New Brunswick Telephone Co. Ltd.**  
 Canada  
**NFK KABEL B.V.**  
 The Netherlands  
**Nippon Telegraph & Telephone Public Corporation**  
 Japan  
**Nokia, Inc.**  
 Atlanta, GA  
**Nonotuck Manufacturing Co.**  
 South Hadley, MA  
**North Anson Reel Co.**  
 North Anson, ME  
**Northern Telecom Canada Limited**  
 Lachine, Quebec  
**OKI Electric Cable Co., Ltd.**  
 Kawasaki-shi, Japan  
**The Okonite Company**  
 Ramsey, NJ  
**Olin Corporation**  
 Stamford, CT  
**Omya, Inc.**  
 Proctor, VT  
**The Ore & Chemical Corporation, A Subsidiary of  
 Metallgesellschaft AG**  
 New York, NY  
**Pennwalt Corp.**  
 Philadelphia, PA  
**PENRECO**  
 Butler, PA  
**Pfizer Inc.**  
 Easton, PA  
**Phalo Corporation**  
 Shrewsbury, MA  
**Phelps Dodge**  
 White Plains, NY  
**Phillips Cables Ltd.**  
 Vancouver, B.C. Canada  
**Radiation Dynamics, Inc.**  
 Melville, L.I. NY  
**Railway Systems Design, Inc.**  
 Wilmington, DE  
**Reichhold Chemicals, Inc.**  
 Hackettstown, NJ  
**Reliance Comm/Tec**  
 Chicago, IL  
**Rhone-Poulenc Inc.**  
 Monmouth Junction, NJ  
**Raychem Corporation**  
 Menlo Park, CA  
**David W. Riley Consultant Extrusion Engineers**  
 Plainfield, NJ  
**Rilsan Corporation**  
 Glen Rock, NJ  
**The Rockbestos Company**  
 Wallingford, CT  
**Santech, Inc.**  
 Toronto, Ontario, Canada  
**Saytech, Inc.**  
 Sayreville, NJ  
**Shell Chemical Company**  
 Houston, TX  
**Siecor Corporation**  
 Hickory, NC  
**Siemens AG**  
 Munich, Germany

**Simplex Wire and Cable Company**  
 Portsmouth, NH  
**Societe Anonyme de Telecommunications**  
 Paris, France  
**Solem Industries, Inc.**  
 Norcross, GA  
**Soltex Polymer Corporation**  
 Houston, TX  
**Standard Electrica, S.A.**  
 Maliano (Santander) Spain  
**Sumitomo Electric Industries, Ltd.**  
 Yokohama, Japan  
**Sun Refining and Marketing Company**  
 Philadelphia, PA  
**The Swiss Insulating Works Ltd.**  
 Breitenbach/Switzerland  
**Syncro Machine Company**  
 Perth Amboy, NJ  
**Synthetic Products Company Sympro-Ware**  
 Dispersions  
 Stratford, CT  
**Taconic Plastics Ltd.**  
 Petersburg, NY  
**Tamaqua Cable Products Corp.**  
 Schuylkill Haven, PA  
**Telecom Australia**  
 Melbourne, Australia  
**Telecommunications Products Dept./**  
**Coming Glass Works**  
 Coming, NY  
**Teledyne Farris Engineering**  
 Palisades Park, NJ  
**Teledyne Thermatics**  
 Elm City, NC  
**Telephone Cables Ltd.**  
 Dagenham, Essex, England

**Tenneco Polymers, Inc.**  
 Houston, TX  
**Tensolite Co. Div. of Carlisle Corp.**  
 Buchanan, NY  
**Thermax Wire Corp.**  
 Flushing, NY  
**Thiokol**  
 Seabrook, TX  
**3M Company**  
 St. Paul, MN  
**Times Fiber Communications, Inc.**  
 Wallingford, CT  
**Topedo Wire & Strip, Inc.**  
 Pittsfield, PA  
**Trea Industries Inc.**  
 North Kingston, RI  
**USE Industries, Ltd.**  
 Tokyo, Japan  
**Union Carbide Corporation**  
 Danbury, CT  
**Valtec**  
 West Boylston, MA  
**Weber & Scher Mfg. Co. Inc.**  
 Newark, NJ  
**Whitemore Wire & Cable Corp.**  
 North Hollywood, CA  
**Wilson-Fiberfil International**  
 Neshanic Station, NJ  
**Wyre Wynd Inc.**  
 Jewett City, CT  
**Wyrough and Loser, Inc.**  
 Trenton, NJ  
**Zumbach Electronics Corp.**  
 Elmsford, NY  
**Mohawk Wire & Cable Co.**  
 Leominster, MA  
**Norsk Hydro Polymers Ltd.**  
 England

# TABLE OF CONTENTS

Document contains papers on the following topics

**TUESDAY, NOVEMBER 15, 1983—9:30 AM-12:00 PM**

## Hunterdon and Cumberland Rooms

**Greeting:** Mr. Theodore Pfeiffer, Technical Director, US Army Communications-Electronics Command, Fort Monmouth, N.J.

### SESSION I: CURRENT TRENDS IN LOCAL AREA NETWORKS

**Chairperson:** Eugene Riley, Anaconda-Ericsson, Inc.

#### Panel Members:

Mr. Greg Barnicoat, Senior Product Engineer, Ericsson Information Systems, Stockholm, Sweden

Mr. Hank Dorris, District Manager, Systems Standards, A.T.&T. Information Systems, Morristown, New Jersey

Dr. Del Hanson, Section Manager, Fiber Optics Products, Hewlett Packard, Palo Alto, California

Dr. Rick Jones, Director of Engineering, Siecor FiberLAN, Raleigh, North Carolina

**TUESDAY, NOVEMBER 15, 1983—2:00-5:00 PM**

## Hunterdon Room

### SESSION II: DESIGN & TESTING

**Chairperson:** George Webster, Bell Laboratories

Use of Plain Copper Conductors in Lieu of Tinned-Copper for Internal Cables—*B. T. de Boer* and *K. G. Mottram*, Telecom Australia, Victoria, Australia..... 2

Development of Copper-Coated Aluminum Shielded Wire—*H. Saen* and *A. Mori*, Sumitomo Electric Industries, Ltd., Tochigiken, Japan..... 9

Aluminum Foil Shield Effectiveness as it Applies to Twisted Pair Cable Construction—*M. Lombardo*, Department of the Army, Tobyhanna Army Depot, Tobyhanna, Pennsylvania... 17

Unbalanced Digital Crosstalk in Balanced Twisted Pair Inside Wiring Cable—*D. P. Woodard, Jr.*, Bell Laboratories, Norcross, Georgia..... 24

Design and Characteristics of Radiating Pair Cable—*N. Tago*, *H. Satani*, *Y. Miyamoto*, and *Y. Amano*, Sumitomo Electric Industries, Ltd., Yokohama, Japan..... 30

Quality Rating Method for Cable Transmission Parameters—*P. A. Link*, Bell Telephone Laboratories, Holmdel, New Jersey..... 37

**TUESDAY, NOVEMBER 15, 1983—2:00-5:00 PM**

## Gloucester Room

### SESSION III: FIBER OPTIC APPLICATIONS & TERMINATIONS

**Chairperson:** John Tompson, Nokia, Inc.

Bell System Lightguide Cable Interconnection Equipment, Central Office to Customer Premises—*M. R. Gotthardt*, Bell Laboratories, Norcross, Georgia..... 45

Termination of Cylindrical Grooved Optical Cables—*A. Bouvard*, *J. P. Hulin*, *M. deVecchis*, L.T.T., Conflans Ste Honorine, Cedex, France, and *R. Poulson*, Raychem, Cedex, France..... 49

Field Trial of Composite Fiber-Optic Overhead Ground Wire—*S. Kubota*, *H. Kawahira* and *T. Nakajima*, Tokyo Electric Power Co., Inc., Tokyo, Japan, and *Y. Kitayama*, *Y. Saito*, *I. Matsubara*, Sumitomo Electric Industries, Ltd., Yokohama, Japan... 54

Factory Splicing of Optical Waveguide Fiber—*D. L. Taylor*, Corning Glass Works, Corning, New York..... 63

Fabrication and Evaluation of High Density Multi Fiber Plastic Connector—*S. Tachigami*, *A. Ohtake*, *T. Hayashi*, *T. Iso*, and *T. Shirasawa*, The Furukawa Electric Company, Ltd., Chiba, Japan..... 70

Lead Making for Improved Continuous-Flow Manufacturing Systems—*P. Heintzman*, AMP Inc., Harrisburg, Pennsylvania..... 76

**WEDNESDAY, NOVEMBER 16, 1983—9:00 AM-12:00 PM**

## Hunterdon Room

### SESSION IV: MATERIALS

**Chairperson:** Andrew Dunin, DuPont Canada

Longitudinal Waterblocking Performance of Conductive and Nonconductive Swellable Nonwovens—*B. J. Nieuwhof* and *R. A. de Vrieze*, Firet bv Veenendaal, Holland..... 86

Evaluation of Adhesive Materials for Bonded Sheath Cable Designs—*A. C. Levy* and *B. J. Overton*, Bell Laboratories, Norcross, Georgia 88

New Data on Long Term Stabilisation of Polyethylene for Telecommunication Wire Insulation—*F. K. Meyer* and *H. Linhart*, Ciba-Geigy Ltd., Basle, Switzerland..... 94

**Behaviour of Four Non-Migratory Antioxidants in Solid Polyethylene Insulation—H. J. Ruddell, D. J. Adams, P. Latoszynski, and B. deBoer, Telecom Australia, Melbourne, Vic., Australia** ..... 104

**Equipment and Design Changes in Extrusion of Foamed Fluoropolymer Resins—S. K. Randa, M. A. Carlson and D. P. Reifschneider, E. I. DuPont DeNemours & Co., Inc., Wilmington, Delaware** ..... 111

**Foamable PVDF Fluoroplastic for Wire and Cable Applications—R. L. Pecsok and O. R. Odhner, Pennwalt Corporation, King of Prussia, Pennsylvania** ..... 119

**WEDNESDAY, NOVEMBER 16, 1983—9:00 AM-12:00 PM**

**Gloucester Room**

**SESSION V: FIBER OPTIC CABLE DESIGN I**

**Chairperson: Joseph P. McCann, US Army CECOM, Ft. Monmouth**

**Development of Composite Fiber-Optic Electric-Power Umbilical Cable and Optical Feedthrough for Deep Ocean Mining—T. Mitsui, T. Gomi, T. Itoh, S. Ushitani and M. Yamaguchi, Sumitomo Electric Industries, Ltd., Osaka, Japan** ..... 125

**Analysis of Excess Attenuation in Optical Fibers Subjected to Low Temperatures—J. P. Garmon, Georgia Institute of Technology, Atlanta, Georgia** ..... 134

**Buckling of Optical Fibers within Elastomers Used in an Embedded-Core Cable Structure—L. L. Blyler, Jr., C. Gleniewski, X. Quan, and H. Ghoneim, Bell Laboratories, Murray Hill, New Jersey** ..... 144

**Design Aspects of Loose Buffer Tube Fiber Optic Cables—R. L. Ohlhaber, Belden Corporation, Geneva, Illinois** ..... 151

**Non-Metallic Optical Cable with Optical Fiber Catenary for Long Span Aerial Application—E. Hayasaka, F. Ohtsuka, and M. Monma, The Tohoku Electric Power Co., Inc., Sendai, Japan; H. Horima, T. Nakatani, and M. Nakaseko, Sumitomo Electric Industries, Ltd., Yokohama, Japan; and N. Abe, Kitanihon Electric Wire Co., Sendai, Japan** ..... 155

**Non-Metallic Long Span Optical Fiber Aerial Cable for the Use at 1.3  $\mu$ m—H. G. Haag and P. E. Zamzow, AEG-Telefunken Kabelwerke AG Rheydt, Monchengladbach, Federal Republic of Germany** ..... 167

**WEDNESDAY, NOVEMBER 16, 1983—2:00-5:00 PM**

**Hunterdon Room**

**SESSION VI: MATERIALS II**

**Chairperson: James Tyler, Essex Group**

**New Silicone Rubber Cable Insulation Promises Circuit Integrity, Low Toxicity, Low Smoke and Low Flame Spread in Flaming Environments—M. Cabey, Dow Corning Corporation, Midland, Michigan** ..... 175

**A Polytetrafluoroethylene Insulated Cable for High Temperature Oxygen Aerospace Applications—A. T. Sheppard, Martin Marietta Corp., New Orleans, Louisiana, and R. G. Webber, George C. Marshall Space Flight Center, Alabama** ..... 183

**Development of Flame Retardant, Low Aggressivity Cables—J. R. I. Bury and B. A. Cranfield, Standard Telecommunication Laboratories Ltd., Essex, England** ..... 193

**Low-Smoke, Halogenfree Ship-Offshore/Onshore Cables with Improved Flame Retardance and Fire Resistance—J. R. Pedersen, T. Holte and E. Johansen, Standard Telefon og Kabelfabrik A/S, Oslo, Norway** ..... 200

**Versatile Five Barrier Systems for Telephone Cable—R. H. Keith, D. G. Dahms and R. R. Licht, 3M Company, St. Paul, Minnesota** ..... 206

**WEDNESDAY, NOVEMBER 16, 1983—2:00-5:00 PM**

**Gloucester Room**

**SESSION VII: FIBER OPTICS CABLE DESIGN II**

**Chairperson: Paul Dobson, Valtec Corporation**

**Cylindrical V-Grooved Nonmetallic Optical Fiber Cable—M. DeVecchis, J. P. Demey, J. P. Hulin, J. Personne, and J. C. Staath, L.T.T. Conflans Ste Cedex, France** ..... 215

**Design and Test Results of Optical Fiber Units for Submarine Cable—H. Yamamoto, K. Mochizuki, Y. Namihira, and Y. Niino, Kokusai Denshin Denwa Company, Ltd., Tokyo, Japan** ..... 220

**Metal-Free Cylindrical V-Grooved Optical Cable—G. LeNoane, CNET, Lannion, France; C. Audoux and P. Cheron, Silec, Montereau, France; and B. Missout, SAT, Paris, France** ..... 228

**Design, Fabrication and Testing of a Rugedized Fiber Optic Cable—H. L. Blumsack, P. J. Dobson, D. Hurwitz and I. D. Aggarwal, Valtec, West Boylston, Massachusetts** ..... 236

**A Rodent and Lightning Protective Sheath for Fiber Optic Cables—***W. C. L. Weinraub and D. D. Davis*, Bell Telephone Laboratories, Norcross, Georgia, and *M. D. Kinard*, Western Electric Company, Norcross, Georgia. . . . . 243

**THURSDAY, NOVEMBER 17, 1983—9:00 AM-12:00 PM**

**Hunterdon Room**

**SESSION VIII: APPLICATIONS AND LOCAL AREA NETWORKS;**

**Chairperson:** John Brazee, Cook Electric Company

**A Radically New Approach to the Installation of Optical Fibers; Using the Viscous Flow of Air—***S. A. Cassidy and M. H. Reeve*, British Telecom, Ipswich, England. . . . . 250

**Material Composites for Multimedia Communications Cable—***G. L. Grune*, IBM Corporation, Research Triangle Park, North Carolina. . . . . 255

**Design of a Twisted Pair Cable for a Token Passing Local Area Network—***P. Abramson*, IBM Corporation, Research Triangle Park, North Carolina. . . . . 268

**Measurement of the Characteristic Impedance of Balanced Twisted Pairs Using Scattering Parameters—***R. B. Hobgood*, IBM Corporation, Research Triangle Park, North Carolina. . . . . 271

**Design/Process Optimization of Paired Computer Interconnecting Cable for Local Area Networks—***E. D. Laing*, Siecor Corporation, Hickory, North Carolina. . . . . 277

**Evaluation of Foam-Skin Cables for Aerial Applications—***G. Samuelson*, Anaconda-Ericsson, Inc., Overland Park, Kansas. . . . . 281

**THURSDAY, NOVEMBER 17, 1983—9:00 AM-12:00 PM**

**Gloucester Room**

**SESSION IX: SINGLE MODE FIBER AND APPLICATIONS;**

**Chairperson:** William Chervenak, Corning Glass Works

**A Practical Single-Mode System, 50KM at 140 MBIT/S—***M. J. Gibson*, BICC Telecommunications Cables Ltd., Prescot, England; *P. Morris*, Plessey Telecommunications Ltd., Nottingham, England, and *A. Carter*, Plessey Research (Caswell) Ltd., Towcester, England. 287

**Performance Characteristics of Vad Single Mode Fibers in Mass Production Basis—***H. Sato, H. Kanamori, N. Yoshioka, M. Kyoto, M. Nishimura, S. Suzuki, M. Watanabe, S. Kato and T. Kuwahara*, Sumitomo Electric Industries, Ltd., Yokohama, Japan. . . . . 294

**Recent Developments in Mini-Unit Cable—***D. O. Lawrence and P. R. Bark*, Siecor Corporation, Hickory, North Carolina. . . . . 301

**Realization, Laying and Splicing of a Monomode Optical Fiber Cable with Low Losses at 1.55 —***D. Boscher, B. Nonclercq, A. LeBoutet*, CNET, Lannion, France, and *B. Missout*, SAT, Paris, France. . . . . 308

**A Field Splicing System for Single-Mode Optical Fiber—***G. K. Pacey, R. Neumann, and H. Lukas*, Bell Northern Research, Ottawa, Canada. . . . . 316

**Optical and Mechanical Properties of Single-Mode Cables at 1300 nm—***S. In't Veld, D. Roland, D. Hurwitz, P. Prideaux and I. D. Aggarwal*, Valtec, West Boylston, Massachusetts. . . . . 323

**THURSDAY, NOVEMBER 17, 1983—2:00-5:00 PM**

**Hunterdon Room**

**SESSION X: FIRE, SMOKE AND TOXICITY; *and — 1983***

**Chairperson:** Austin Wetherell, Underwriters Laboratories

**A New Engineering Approach for Cable in Fire Situations Using Halogenated Polymers—***J. R. Hoover, A. L. Moran, J. G. DiPinto, D. H. Lutz, D. B. Allen, E. I. DuPont De Nemours & Co.*, Wilmington, Delaware; *G. C. Sweet*, Du Pont (U.K.) Ltd., Herts, England, and *J. O. Punderson*, Consultant, Marietta, Ohio. . . . . 330

**Characteristics of Heat and Flame Resistant Optical Fiber Cables—***Y. Kikuchi, A. Mogi, T. Kobayashi, N. Nisono, T. Murayama, and Y. Sugawara*, Fujikura Ltd., Chiba-ken, Japan. . . 348

**Cable Fire Studies Using the Ohio State University Release Rate Apparatus—***W. Pocock*, David Taylor Naval Ship R&D Center, Annapolis, Maryland, and *John Geremia*, U.S. Naval Academy, Annapolis, Maryland. . . . . 354

**Circuit Transmission Integrity of Plenum Cables in a Developing Fire Scenario—***C. J. Arroyo and T. P. Bursh*, Bell Laboratories, Norcross, Georgia. . . . . 372

**Large Scale Fire Test of Cables Installed in Tunnels—***H. Ishihara, M. Miwa, K. Kuratani, and J. Sawada*, Nippon Telegraph & Telephone Public Corp., Tokyo, Japan. . . . . 381

Overall Safety of Cable and Wiring Materials—*F. B. Clarke, I. Benjamin and P. DiNenno*, Benjamin/Clarke Associates, Inc., Kensington, Maryland..... 390

**THURSDAY, NOVEMBER 17, 1983—2:00-5:30 PM**

**Gloucester Room**

**SESSION XI: FIBER OPTICS CHARACTERIZATION AND TESTING**

**Chairperson:** Robert Depp, Defense Electronics Supply Center, DESC

Fracture Mechanics Evaluation of the Static Fatigue Life of Optical Fibers in Bending—*D. V. Nelson*, Stanford University, Stanford, California, and *V. Fentress*, Raychem Corporation, Menlo Park, California..... 399

Computerized Optical Fiber Characterization—*W. L. S. Mathu*, NKF Kabel B.V., Waddinxveen, The Netherlands..... 407

Remote Ended Time Domain Bandwidth Measurements on Installed Regenerator Sections of Multimode Optical Fiber Cable in the British Telecom Network—*S. Ahmad* and *B. W. Allen*, British Telecom, Wembley, United Kingdom..... 414

Development of Short-Distance Optical Transmission Cords—*M. Yuto, K. Hayashi, H. Mukunashi* and *S. Iguchi*, Sumitomo Electric Industries, Ltd., Yokohama, Japan..... 424

Thermal Properties of Loose Tube Secondary Coated Optical Fibers Experimentally Discussed by a Relative Light Pulse Delay Technique—*H. Damsgard*, NKT, A/S Nordiske Kabel, Copenhagen, Denmark..... 429

Breakout Cables for Short Haul Fiber Optic Systems—*F. T. McDuffee*, Phalo/O.S.D., Manchester, New Hampshire..... 436

AD P 002526

USE OF PLAIN COPPER CONDUCTORS IN LIEU  
OF TINNED-COPPER FOR INTERNAL CABLES

B.T. de Boer

K.G. Mottram

Telecom Australia  
Melbourne,  
Australia.

ABSTRACT

In line with most Telephone Operating Administrations, Telecom Australia has specified and used tinned-copper conductors, with PVC insulation and sheathing, for most internal cabling within telephone exchanges and subscribers' buildings. Following some reported problems associated with solderability, an investigation showed that the current production tinned conductors in Australia were inadequately specified; however, the excellent performance of plain copper prompted a more detailed investigation which revealed that plain copper conductors (i.e., no tinning) were suitable for all current applications of internal cable. The study covered soldering, wire wrapping, and insulation displacement terminations. As a result of this work, Telecom Australia has adopted plain copper as the standard for internal cables. This decision has resulted in both an improved performance in comparison with the previous tinned conductors (particularly in relation to solderability) and a substantial cable cost reduction.

INTRODUCTION

Telecom Australia, like most Telephone Operating Administrations, has specified and used tinned-copper conductors for internal cables. Much of the reason for the use of tinned conductors can be traced back to the use of rubber insulation. Among the chemicals added to rubber to modify its properties was sulphur, and as sulphur readily attacks copper, it was necessary to provide copper conductors with a protective coating. The coating had to be readily applicable to copper wire, be corrosion resistant to sulphur, and be readily solderable. Tin had these properties and was probably originally applied to the copper wire by hot dipping, resulting in a reasonably generous coating thickness. With the change to PVC insulation, the tin coating on internal cable conductors was retained, presumably to maintain solderability. The tin coating is now commonly applied by electroplating, and at least on products supplied to Telecom Australia, is very thin, averaging about 2  $\mu\text{m}$  thickness on conductors of 0.4 mm diameter. The tinning specification requirements are stipulated in AS 1574<sup>1</sup>.

Following some reported problems associated with solderability of tinned conductors, an investigation was conducted using both tinned-copper and plain copper wires from current production cable.

SOLDERABILITY EVALUATION

The evaluation of solderability was performed using an extensive range of tinned-copper and plain copper wires from Australian manufacturers. Solderability was assessed according to Clause 2.8 of AS 1099 2 Ta Soldering<sup>2</sup>. An activated flux, as specified in Clause 2.8.2.3, was used for the solderability tests. (This flux was 25 percent by mass of colophony, 75 percent by mass of 2-propanol (isopropanol) with the addition of diethylammonium chloride to an amount 0.5 percent chloride. An activated flux was chosen because Telecom Australia uses activated resin-cored solder to AS 1834<sup>3</sup> for general electrical component soldering operations). The principle of the test method is to measure the time elapsing between the moment a wire bisects a molten solder globule and that when the solder flows around, covering and wetting the wire. The shorter this period of time, the better the solderability of the wire. Immediately prior to each solderability test, the PVC insulation was stripped from each metallic wire. Ten samples from each wire designation were tested for solderability, and all quoted results are the average of these 10 individual measurements.

The initial solderability evaluations were conducted in December 1976 and May 1977 on wires in the "as received" condition (i.e., cable manufactured within the previous twelve months). Since the growth of intermetallic compounds<sup>4-10</sup> was suspected as the cause of solderability problems, solderability tests were also performed on samples of the tinned-copper wire, without insulation, which were artificially aged according to AS 1099 2 Ba Dry Heat<sup>2</sup> (16 hours dry heat at a temperature of 155°C). In 1980, further samples of insulated wire from the original spools were again tested for solderability. These results represent approximately three years natural ageing in a mild laboratory environment, and again the insulation was stripped just prior to solderability testing.

Typical results of this solderability testing on many hundreds of samples are given in Table 1. The tests indicate that, on freshly stripping the PVC insulation, all plain copper wires soldered readily even after three years' natural ageing. Tinned-copper wires also generally soldered readily, although they exhibited larger variability with occasional relatively high values. Natural ageing for three years had little effect on tinned-copper wire.

TABLE 1. SOLDERABILITY EVALUATION OF  
TINNED-COPPER AND PLAIN COPPER CONDUCTORS

Designation Insulation Colour	Conductor Type	Soldering Time - (second)					
		As received 1977		Naturally Aged (approx. 3 years)		Artificially Aged	
		Mean	SD	Mean	SD	Mean	SD
Cable Sample Number 1							
Brown	plain copper	0.11	0.01	0.28	0.06		
Red	" "	0.12	0.01	0.37	0.09		
Orange	" "	0.12	0.01	0.31	0.06		
Green	" "	0.11	0.01	0.37	0.07		
Blue	" "	0.11	0.01	0.32	0.08		
Slate	" "	0.11	0.01	0.28	0.05		
White	" "	0.11	0.01	0.24	0.06		
Cable Sample Number 2	tinned-copper						
Orange	" "	0.38	0.07	0.28	0.07	7.1	5.1
Green	" "	0.39	0.06	0.45	0.13	12.8	5.4
Blue	" "	0.30	0.05	0.37	0.07	2.2	2.3
White	" "	0.33	0.14	0.29	0.05	6.4	3.9
Brown	" "	0.39	0.11	0.38	0.06	11.7	7.6
Slate	" "	0.37	0.11	0.29	0.07	8.0	3.7
Blue/White	" "	0.46	0.13	0.31	0.05	12.2	13.3
Cable Sample Number 3	tinned-copper						
Red	" "	0.44	0.11	1.01	0.52	67.4(a)	20.8
Orange	" "	1.08	1.17	0.96	0.41	44.1(b)	12.1
Green	" "	0.39	0.11	0.76	0.29	32.6(c)	23.1
Blue	" "	1.05	0.56	1.23	0.70	40.3(c)	34.4
White	" "	0.45	0.18	0.94	0.49	49.5(d)	21.3
Black	" "	0.44	0.11	0.34	0.06	14.9(e)	12.0
(a) Average of 6 samples; other 4 failed to solder in 100 seconds (b) Average of 7 samples; other 3 failed to solder in 100 seconds (c) Average of 8 samples; other 2 failed to solder in 100 seconds (d) Average of 5 samples; other 5 failed to solder in 100 seconds (e) Average of 9 samples; other 1 failed to solder in 100 seconds							

Note SD = Standard Deviation

The artificially aged wires exhibited generally poor solderability and some wires became unsolderable.

#### METALLOGRAPHIC EXAMINATION

Cross-sections of a number of tinned-copper wires were prepared for metallographic examination. The examination revealed that circumferentially and longitudinally the tin coating was very uneven with typical thickness values between 0.5  $\mu$ m and 3.0  $\mu$ m. With the difficult-to-solder samples, diffusion had occurred between the copper base and the tin coating to form a copper-tin intermetallic compound. In cases where wires were unsolderable, the tin coating was completely consumed and only an intermetallic compound remained. Thwaites<sup>4</sup>, Bernier<sup>5</sup>, MacKay<sup>6</sup>, Billot<sup>7</sup>

and others all refer to solderability problems with the establishment and growth of copper-tin intermetallic compounds which occur during manufacture and ageing of tinned-copper conductors.

AS 1099 2 Ta allows for an artificial ageing test to assess susceptibility of tinned-copper wires to the growth of intermetallic compounds. In regard to artificial ageing, Ochs<sup>8</sup> considers that ageing of four hours at a temperature of 155°C is equivalent to three years' natural storage. This contrasts with the AS 1099 2 Ta requirement of 16 hours at 155°C, and supports our experience that the ageing requirement of AS 1099 2 Ta is far too severe, since it would normally be expected that wires would be terminated within three years of manufacture.

## RECOMMENDATIONS FROM SOLDERABILITY STUDY

From our results, and from the literature, it is evident that there is a potential problem with respect to solderability of tin-coated copper wires. With thin tin coatings (less than 2  $\mu\text{m}$ ) there is the risk that, either in manufacture and/or storage, the tin coating can be consumed by diffusion between the copper base and the tin coating to form difficult-to-solder copper-tin intermetallic compounds. Perhaps not unexpectedly, various investigators have recommended different values to reduce this risk. For long-term retention of solderability, the following authors have recommended these minimum coating values:

Bader and Baker <sup>9</sup>	: 2.5 $\mu\text{m}$ solder, 5 $\mu\text{m}$ tin
Bernier <sup>5</sup>	: 5 $\mu\text{m}$ tin
Cavanaugh GW and Lanagan J <sup>10</sup>	: 7 $\mu\text{m}$ solder
Billot and others <sup>7</sup>	: 2.5 $\mu\text{m}$ tin
Thwaites <sup>4</sup>	: 8 $\mu\text{m}$ tin or solder

On the other hand, our results indicated that freshly stripped plain copper wire soldered as well, if not better, than tinned-copper wire. It was therefore quite possible that a superior performance could be achieved with plain copper wire, whilst at the same time, a substantial cost saving could be realised by the elimination of the tinning requirement.

A number of other factors, however, needed to be examined prior to any full-scale changeover to plain copper conductors. These included the evaluation of plain copper against other termination practices (i.e., wire wrapping and insulation displacement connections), and the evaluation of all terminating practices, particularly solderability, after short-term ageing (usually less than six months) with insulation removed. This requirement results from the existing practices within Telecom Australia and some support industries, of pre-preparing and stripping wire harnesses for later mass installation.

The following criteria were therefore established to assess the suitability of plain copper wires for general use for internal cables:

- Since it is considered that wires will be terminated within 5 to 5 years after manufacture, the terminating performance of aged (3 to 5 years) and freshly stripped conductors must be guaranteed.
- Since at times wires prepared for terminating are left stripped of insulation for up to six months prior to installation, the terminating ability must be adequate under these conditions.
- Terminations and joints using plain copper wires must be shown to be completely suitable or at least equivalent to those made using tinned-copper wire.

For soldered terminations, the requirement of performance after ageing for freshly stripped conductors was satisfied by the previous evaluation given in Table 1. The requirements of (b) and (c) required further evaluation.

## WIRE WRAPPING WITH PLAIN COPPER CONDUCTORS

To evaluate the performance of wire-wrap terminations, samples of plain copper and tinned-copper conductors were tested against the requirement of Telecom Australia Specification 1305<sup>11</sup>. This Specification was basically derived from IEC Publication 352. Brass posts 1.2 mm square, with maximum corner radii of 0.075 mm, and electroplated with 6  $\mu\text{m}$  of tin, were used in the tests. Plain copper and tinned-copper conductors of 0.40 mm diameter were used in the evaluation for comparison. The post dimensions, tin coating thicknesses, and diameters of the conductors were chosen as the most critical combination under the specification tolerances for material supplied to Telecom Australia. All joints were wrapped with an electrically operated Standard Pneumatic tool, model number 615 with a sleeve type 18840 432. Where unwrapping was required, a manually operated Gardiner tool 280 15 AA4 was used.

A range of mechanical, thermal and exposure tests, as specified in Telecom Australia Specification 1305, were conducted on the wire wraps. Each value quoted is the average of thirty individual tests. The details of the tests performed and the results obtained were as follows:

### Stripping Force

This test was conducted according to the requirements of Clause 4.3 of Telecom Australia Specification 1305. Using a forked tool, the force required to strip the wire turns off a post was measured. For the size of post and wire used, the specification requires a minimum force of 22 N. As the average for tinned-copper wire was 42 N, and for plain copper wire 30 N, both combinations were satisfactory.

### Vibration

Joints were vibrated according to the requirements of AS 1099 2 Fc<sup>2</sup>. This standard requires two hours vibration on three mutually perpendicular axes, with a frequency sweep from 10 to 500 Hz, and with the amplitude 0.75 mm peak or 10g, whichever is the greater. After vibration, the average change in resistance for the tinned-copper wires was 0.64 milliohm and for the plain copper was 0.11 milliohm.

### Damp Heat

Joints were exposed for 56 days at a temperature of 40°C at a relative humidity of 93% according to the conditions of AS 1099 2 Ca<sup>2</sup>. After exposure, the average change in resistance for the tinned-copper wires was 0.18 milliohm and for the plain copper was 0.33 milliohm.

### Hydrogen Sulphide Exposure

Joints were exposed for 21 days at a temperature of 25°C and a relative humidity of 75% with a hydrogen sulphide concentration of 10 ppm, according to the conditions of AS 1099 2 Kd<sup>2</sup>. After exposure, the average change in resistance for the tinned-copper wires was 0.56 milliohm and for the plain copper was 0.87 milliohm.

### Rapid Change of Temperature

Joints were subject to thermal shock by alternating between one hour at a temperature of -55°C and one hour at 125°C according to the requirements of AS 1099 2 Na<sup>2</sup>. After 25 cycles, the average change in resistance for the tinned-copper wires was 0.38 milliohm and for the plain copper was 0.32 milliohm.

### Stress Relaxation

Joints were exposed at a temperature of 125°C for a total of 1000 hours. The resistance changes observed are given in the following table.

TABLE 2. AVERAGE CHANGE IN WIRE-WRAP JOINT RESISTANCE ASSOCIATED WITH STRESS RELAXATION TEST

Wire Type	Average change in resistance (mΩ) for the following times				
	200 h	400 h	600 h	800 h	1000 h
Tinned-Copper	0.55	0.49	1.55	2.07	2.40
Plain Copper	0.35	0.88	1.08	1.04	1.30

(10 hours at 125°C approximates to 1 year at 20°C)

### Multiple Wrapping

The object of this test was to determine the effect on joint quality of consecutive wraps, each with a new wire on a single post. Multiple wraps are a common phenomenon in the real field environment. After 50 wraps, the joints were exposed to a hydrogen sulphide environment as specified above.

The results obtained were as follows :

TABLE 3. CHANGE IN WIRE-WRAP JOINT RESISTANCE AFTER MULTIPLE WRAPS

Condition	Joint resistance (milliohm)	
	Plain copper	Tinned-copper
1 wrap	3.96	3.67
50 wraps	4.67	4.20
50 wraps + H <sub>2</sub> S exposure	5.81	4.83

### Results from Wire-Wrap Evaluation

Wrapped joints made with plain copper and tinned-copper conductors were subjected to a range of tests, aimed at determining compliance with quality requirements for wrapped connections. Both types of wire were considered satisfactory in all the tests; neither type of wire was superior in all the tests. As a result of this evaluation, it was considered that wire-wrapped joints using plain copper conductors and tin-plated posts to Telecom Australia specifications, were completely satisfactory for field use.

### SOLDERABILITY PERFORMANCE OF EXPOSED PLAIN COPPER CONDUCTORS IN A TELEPHONE EXCHANGE ENVIRONMENT

To determine the effect on solderability of plain copper conductors left exposed without insulation, field experiments were established in four telephone exchanges in different parts of Australia.

Pre-stripped plain copper and tinned-copper wires of recent manufacture from two sources were exposed to the normal controlled exchange environment where the wiring harnesses would be stored prior to installation. The experimental sites were exchanges in Mackay, Port Kembla, Mildura and Port Pirie. See Figure 1. The sites were chosen because they offered a variety of atmospheric conditions due to climate and local industrial activity.

Samples were tested for solderability after exposure for two, four and six months, and results are given in Table 4. In addition, nine individual tinned-copper wires from the two manufacturers' cables (as received) were mounted for metallographic examination. Nearly all samples had some area of tin coating thinner than 0.5 µm; one wire had large areas with tin thickness less than 0.1 µm. The inter-metallic layer was approximately 0.4 µm thick and the average thickness of tin from all samples was 2.4 µm.

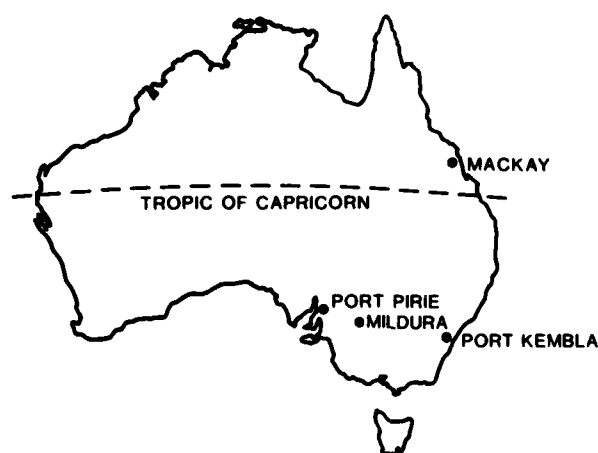


FIGURE 1. EXPOSURE SITES FOR SOLDERABILITY SAMPLES AT TELEPHONE EXCHANGES.

TABLE 4. SOLDERABILITY PERFORMANCE OF  
STRIPPED PLAIN COPPER AND TINNED-COPPER CONDUCTORS  
(0.40 mm) EXPOSED TO EXCHANGE ENVIRONMENT (AIR-CONDITIONED)

Sample Exposure Environment	Soldering Time (second)							
	Plain Copper Wire				Tinned-Copper Wire			
	Manufacturer Number 1		Manufacturer Number 2		Manufacturer Number 1		Manufacturer Number 2	
	Mean	SD	Mean	SD	Mean	SD	Mean	SD
As received	0.63	0.20	0.53	0.25	0.62	0.08	1.81	0.84
Six days air conditioned office	0.50	0.09	0.50	0.11	0.49	0.08	1.50	1.20
Mackay								
2 months	0.56	0.10	0.54	0.08	0.49	0.12	0.54	0.31
4 months	0.69	0.24	0.71	0.19	3.22	2.82	1.10	1.13
6 months	0.84	0.26	0.82	0.32	0.85	0.63	1.10	0.92
Port Kembla								
2 months	0.34	0.08	0.42	0.10	4.09	5.58	1.92	2.58
4 months	0.56	0.13	0.66	0.58	-	-	-	-
6 months	0.58	0.31	0.84	0.55	2.62	1.26	5.39	9.81
Mildura								
2 months	1.49	0.80	0.50	0.08	1.39	0.64	0.70	0.50
4 months	0.39	0.09	0.50	0.11	1.79	1.16	7.02	10.4
6 months	0.42	0.04	0.44	0.10	4.93	10.4	7.70	14.9
Port Pirie								
2 months	-	-	-	-	-	-	-	-
4 months	0.63	0.15	0.87	0.26	2.37	2.37	1.85	0.98
6 months	0.51	0.08	0.50	0.13	2.15	3.20	1.03	1.21

Note SD = Standard Deviation

From Table 4, it can be seen that all "as-received" samples soldered in a reasonable time, but tinned-copper wires from manufacturer number 2 were the poorest and showed greatest variability. All plain copper wires, exposed at the four sites, soldered readily and showed little variability even after six months exposure. The tinned-copper wires generally exhibited poorer solderability and much greater variability than the bare copper wires. Of the 220 plain copper wires exposed in the telephone exchanges, the longest soldering time was 3.58 s after two months exposure at Mildura. Of the 200 tinned-copper wires exposed in telephone exchanges, one became unsolderable, and three wires took between 30 s and 40 s to solder.

#### SOLDERABILITY PERFORMANCE OF EXPOSED PLAIN COPPER CONDUCTORS IN AN INDUSTRIAL ENVIRONMENT

A criticism of the previous evaluation was that the environment was too controlled, and in some cases may be far more severe. In particular, if plain copper was proposed for use by equipment manufacturers, who also used the practice of pre-stripping wire sometimes well in advance of

termination (particularly soldering), then the performance of plain-copper wires exposed without insulation in an industrial environment was required.

An additional set of field experiments was therefore undertaken with sites now chosen for realistic manufacturing environments. Two sites were established at equipment manufacturers' factories, whilst at the other two sites, the samples were sheltered, but freely exposed to outside air in highly industrialised areas.

Again the samples were tested for solderability after two, four and six months. The exposed conductors were also evaluated for wire-wrap performance, although the only test performed was initial joint resistance. The results of these evaluations are given in Table 5. As before, the solderability results are the average of ten values and wire-wrap results are the average of 30 measurements. Test procedures are as previously described.

TABLE 5. SOLDERABILITY AND WIRE-WRAP  
PERFORMANCE OF STRIPPED PLAIN COPPER AND TINNED-COPPER CONDUCTORS  
(0.40 mm) EXPOSED TO INDUSTRIAL ENVIRONMENT

EXPOSURE		SOLDERABILITY TIME (second)				WIRE-WRAP JOINT RESISTANCE (milliohm)			
Site	Time (month)	Plain Copper		Tinned-Copper		Plain Copper		Tinned-Copper	
		Mean	SD	Mean	SD	Mean	SD	Mean	SD
Factory Site Number 1	2	0.67	0.26	1.36	0.58	4.0	0.34	4.2	0.25
	4	0.84	0.37	1.23	0.64	4.0	0.40	3.9	0.32
	6	0.79	0.11	3.40	3.12	3.8	0.39	3.8	0.34
Factory Site Number 2	2	1.12	0.65	3.50*	7.30*	3.9	0.38	3.9	0.27
	4	0.46	0.18	1.15	0.60	4.0	0.38	3.8	0.28
	6	1.06	0.33	1.79	0.75	3.9	0.40	3.9	0.41
Field Site Number 1	2	0.72	0.32	1.00	0.57	3.0	0.51	3.7	0.25
	4	1.94	0.91	2.71	2.10	3.9	0.36	3.9	0.35
	6	3.23	2.27	25.01	22.20	3.8	0.41	3.8	0.42
Field Site Number 2	2	0.98	0.34	1.01	0.49	3.9	0.34	3.8	0.33
	4	1.03	0.38	1.04	0.51	3.9	0.36	3.9	0.31
	6	2.95	2.22	2.97	2.45	3.7	0.43	3.7	0.30

Note SD = Standard deviation

\* The average of 9 samples was 1.20 and the SD was 0.48. The tenth value was 24.24.

In relation to solderability, the results again indicated the good performance of plain copper conductors, even though in some cases significant tarnishing of the surface had occurred. Even after six months exposure, the plain copper conductors had reasonable solderability times, although some degradation in performance was obvious. Tinned-copper conductors showed generally poorer solderability and greater variability after ageing. In the case of Field Site Number 1, extensive degradation of solderability performance for tinned-copper was observed.

The results of this solderability evaluation were strongly supported by an independent study performed by Standard Telephones and Cables Pty. Ltd. who are a major equipment supplier to Telecom Australia. Samples of both tinned-copper and plain copper conductors, with insulation removed, were aged in a number of factory environments and were tested for solderability after two, four and six months. The testing was performed using a GEC Meniscograph Wetting Balance, and evaluations used both activated and non-activated flux. All solderability testing was carried out at a temperature of 250°C. The results correlated strongly with our own evaluation, and again clearly showed that plain copper wire was in all cases as good as, if not better than, the current production tinned-copper wire.

The evaluation of wire-wrap performance of the exposed plain copper and tinned-copper conductors

generally showed the insensitivity of this termination technique to the test conditions. Both conductor types showed no real change in joint resistance with conductor ageing time. This would be expected since the wire-wrap process by nature removes surface oxides, and whilst the intermetallic compounds are difficult to solder, they do not alter surface conductivity, or the ability to achieve the cold welding necessary for successful wire-wrap joints.

#### INSULATION DISPLACEMENT CONNECTIONS

Insulation displacement connection systems are now used extensively for terminating internal cables, and the use of these systems is expected to grow in future years. Extensive studies both world-wide and within Telecom Australia have resulted in the acceptance of this technique for jointing plain copper conductors in external cables. Successful experience now extends over many years. An investigation aimed at examining the performance of tinned-copper conductors with insulation displacement systems is currently proceeding within Telecom Australia.

### CONCLUSION

Following an investigation into solderability problems, it was found that current production tinned-copper conductors had tin coatings too thin to guarantee completely efficient solderability. Other investigators have reported this problem, and have recommended tin coating thicknesses significantly greater than were being provided by Australian manufacturers.

The investigation, however, indicated that the use of plain copper conductors may have been a suitable solution to the problem which would also achieve a significant cable cost saving.

Extensive studies were undertaken which resulted in the conclusion that plain copper conductors were entirely suitable as an alternative to tinned-copper conductors for internal cables. The studies covered solderability, wire-wrapping, and insulation displacement connections. Against significant popular belief, the studies also indicated that plain copper conductors, exposed without insulation in reasonable environments for periods up to six months, maintained satisfactory solderability with commonly used activated flux solders.

As a result of these investigations, Telecom Australia has adopted plain copper conductors as standard for internal cable and jumper wire designs. Although field experience with the new conductors extends for only six months, no problems or field dissatisfaction have been encountered.

The change to plain copper conductors for internal cables will have the following benefits :

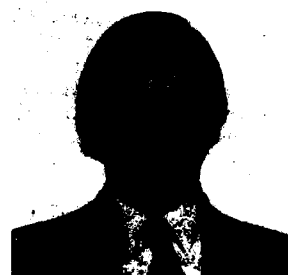
- (a) Improved solderability performance compared with previously inadequately specified tinned-copper conductors.
- (b) Reduced cable cost due to elimination of tinning requirements.

### REFERENCES

1. Australian Standard 1574-1975, "Copper and Copper Alloy Wire for General Electrical Purposes".
2. Australian Standard 1099-1982, "Basic Environmental Testing Procedures for Electronics and Telecommunication Purposes".
  - 2 Ba Dry heat test for electronic components
  - 2 Ca Damp heat, steady state
  - 2 Fc Vibration (sinusoidal)
  - 2 Kd Hydrogen sulphide test for contacts and connections
  - 2 Na Rapid change of temperature, two-chamber method
  - 2 Ta Soldering
3. Australian Standard 1834-1979, "Tin-Lead and Other Tin-Based Solder Alloys".
4. Thwaites C.J., "The Attainment of Reliability in Modern Soldering Techniques for Electronic Assemblies", International Metallurgical Reviews, Review 166, 1972, Volume 17, Page 12.
5. Bernier D., "Effect of Ageing on the Solderability of Various Plated Surfaces", Plating, 1974, September, Page 843.
6. Mackay C.A., "Aspects of Soldering", International Tin Research Institute Publication, Number 539, Page 5.
7. Billot M., Element S., Fouquet M.P. and Dhaussy J.C., "Ensuring Solderability in Electronic Components for Space Applications", Tin and its Uses, 1982, Number 131, Page 2.
8. Ochs L., "Solderability of Component Leads after Extended Storage and Accelerated Ageing Process", Siemens Components Report X (1975), Number 3, Page 94.
9. Bader W.G. and Baker R.G., "Solderability of Electrodeposited Solder and Tin Coatings after Extended Storage", Plating, 1973, March, Pages 245 to 246.
10. Cavanaugh G.W. and Lanagan J., "Solderability of Electrodeposits", Plating, 1970, March, Page 246.
11. Telecom Australia Specification 1305, "Quality Requirements for Wrapped Connections".

# ACKNOWLEDGEMENTS

Many people rendered valuable assistance in the design and conduct of the experiments and their help is gratefully acknowledged. Special acknowledgement is given to all the staff of the Metallurgy and Electrochemistry Section of the Research Laboratories and to staff of the Lines Construction Branch for help in the preparation of this paper. Thanks are also extended to Standard Telephones and Cables Pty. Ltd. and L.M. Ericsson Pty. Ltd. for their assistance and participation. The permission of the Chief General Manager, Telecom Australia, to publish this paper is acknowledged.



B.T. de Boer  
Cable Design and  
Specifications Section  
Lines Construction Branch  
Engineering Department  
Telecom Australia  
28/570 Bourke Street  
MELBOURNE Vic. 3000  
AUSTRALIA

Bob de Boer is Manager of the Cable Design and Specifications Section at Telecom Australia. He joined Telecom Australia in 1972 after graduating in Electrical Engineering from Monash University in Victoria. He has had extensive experience in the areas of telecommunication cable design, specifications and provisioning, as well as the installation of external plant.



K. G. Mottram  
Metallurgy and  
Electrochemistry Section  
Research Department  
Telecom Australia  
770 Blackburn Road  
CLAYTON VIC 3168  
AUSTRALIA

Ken Mottram graduated in Metallurgical Engineering from the Royal Melbourne Institute of Technology in 1948. In 1949, he joined the Research Laboratories of Telecom Australia. He has been involved in the investigation of a wide spectrum of problems concerning materials for telecommunication plant. He is now Section Head of the Metallurgy and Electrochemistry Section at Telecom Australia.

## DEVELOPMENT OF COPPER-COATED ALUMINUM-SHIELDED WIRE

H. Saen

A. Mori

Sumitomo Electric Industries, Ltd.

3-3 Satuki-Cho, Kanuma-Shi, Tochigi-Ken, 322 Japan

*The authors*  
Abstract

Aluminum-shielded wires are usually used in short lengths of about 200 millimeters in many electronic devices because of their easy termination. However, some problems have occurred in shield effect. We have found that this is due to the increase of contact resistance between the aluminum and the drain wire, which is caused by aluminum oxide. *that*

To overcome this problem, we developed a new shield tape composed of aluminum foil laminated with polyester film and having a copper layer over the aluminum face. The contact resistance between the shield tape and the drain wire could thus be reduced and was found to be very stable. A wire spirally wrapped and shielded with this new tape has very stable shield effect when subjected to a humid environment or H<sub>2</sub>S environment, even in short lengths of 100mm.

*This is the* We also developed a new construction for the spirally wrapped shield which is very useful and reliable for multi-conductor wires having individually insulated and shielded conductors.

1. Introduction

Many internal wiring materials used in electronic equipment such as audio components and video tape recorders are being thoroughly reviewed for the purpose of reducing weight and size. And, shielded wires, which are one kind of these materials, must be balanced both in terms of electrical properties and termination characteristics. When shielded wires are used in internal wiring, they are cut very short in wire lengths most 10 to 30 cm and a great number of them are used. So, easy termination characteristics of shielded wires are important from the point of view of cost reduction. The kinds of shielded wires usually used in internal wiring are: 1) Metal braid shielded wire, 2) spiral shielded wire (wire with a shield comprised of several tens of approxi-

mately 0.1mm diameter copper wires densely and spirally wrapped over the insulation and protected with a jacket), 3) aluminum shielded wire, and 4) conductive plastic shielded wire (using carbon-mixed polyvinyl chloride extruded on to the insulation as the shielding material).

Metal braid shielded wires have a very good shield effect but are very expensive and become costly in termination. Spiral shielded wires have a very good shield effect after metal braid shielded wires and are cheaper than metal braid shielded wires, but their termination characteristics don't satisfy requirements for internal wiring material. Next, conductive plastic shielded wires have very good termination characteristics because the terminations of this wire's shield are not necessary.

However, the range for which these wires can be used is limited, because these wires have the worst shield effects of all the wires. Lastly, aluminum shielded wires have generally been thought to have a shield effect nearly as good as that of spiral shielded wires and to have very good termination characteristics for the same reason as conductive plastic shielded wires. We can agree at the point that wires are completed. But, we found when aluminum shielded wires were exposed in the conditions of vibration and high moisture, these wire's shield effects were remarkably depressed. This is a very important defect, because all electronic equipment is necessarily exposed in these conditions during shipping, and portable types of video tape recorders and audio components

are exposed in the condition of vibration while they are carried around and are played in the unfavorable condition of electromagnetic interference. this depression of aluminum shielded wire is caused by the increase in contact resistance between the aluminum surface and the drain wire. To solve this problem, we recently developed a new type of aluminum shielded wire: a copper-coated aluminum shielded wire. This wire has a stable shield effect even in the various circumstances mentioned above because the shielding tape of this wire is coated with a thin copper layer on the aluminum face.

We also developed a new method of spirally wrapping aluminum shielding tape. In this new method, a part of the copper coated tape is folded back on to itself and then is spirally wrapped around the insulated conductor. This allows that multi-conductor wires with each conductor wrapped aluminum shielding tape are thin and can be terminated cheaply because the shield is removed with the jacket. The details of this new wire are described below.

## 2. Shielding tape construction

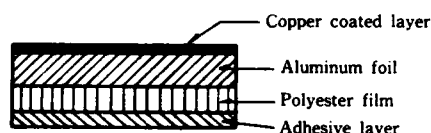


Fig.1 Copper-coated aluminum shielding tape

An ordinary aluminum shielding tape is constructed from an aluminum foil with thickness about  $10\text{ }\mu\text{m}$  and a plastic film which is made of polyester or polyvinyl chloride and is bonded with the aluminum foil to reinforce it, and an adhesive layer to bond the plastic film to the jacket of an aluminum shielded wire. The total thickness of this tape is 15 to  $40\text{ }\mu\text{m}$ . This thin tape can give flexibility to aluminum shielded wire that is required of internal wiring material. The advantages of using aluminum as shielding metal foil are that it is very thin, cheap, and has high resistance to cracking when bent. However, aluminum is

easily oxidized due to its inherent properties and its face has a oxidized layer of  $\text{Al}_2\text{O}_3$ . This layer makes aluminum's contact force (the force that is necessary to get a fixed contact resistance) increase. Due to this defect, the contact resistance between the aluminum face and a drain wire provided for contact with the aluminum surface for the shield grounding becomes unstable and greater. This makes the shield effect of an aluminum shielded wire depress remarkably. In order to solve this problem, we developed a new shielding tape that is very thinly coated with several hundreds Å of copper on the aluminum face of ordinary aluminum shielding tape as shown in Fig.1. We are producing this copper-coated aluminum shielding tape by vacuum deposition, and have also confirmed that coating by sputtering gets the same characteristics. A grounding drain wire contacts the aluminum face through a copper layer. This minimizes the contact force and stabilizes the contact resistance between the aluminum face and the grounding drain wire. As shown in Fig.2, the contact force of the aluminum foil is reduced by more than 50% by attaching the copper-coating layer.

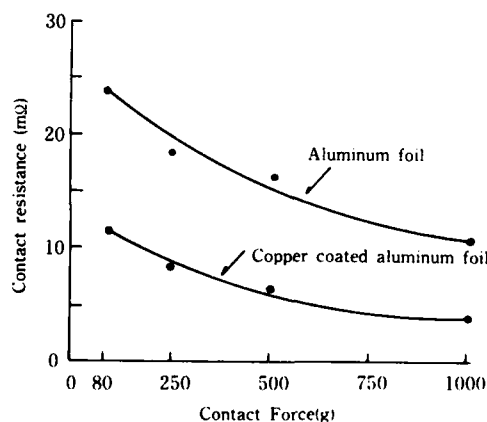


Fig.2 Contact force of aluminum foil.

Fig.3 shows the results of a test to observe the influence of oxidation upon contact resistance by leaving the shielding tape in a constant-humidity oven to promote oxidation on

the aluminum face. There is a large fluctuation in the contact resistance in the aluminum foil after the humidity test, with the measurements varying from 1 to 10 K $\Omega$  after the foil is subjected to a 60°C  $\times$  95% RH. environment for 48 hours. On the other hand, the value for the copper-coated aluminum foil is only 17 m $\Omega$ , indicating only a slight increase. Therefore, it is judged that the latter maintains good electrical characteristics over a long period of time, and, in particular, has reliable shielding effect.

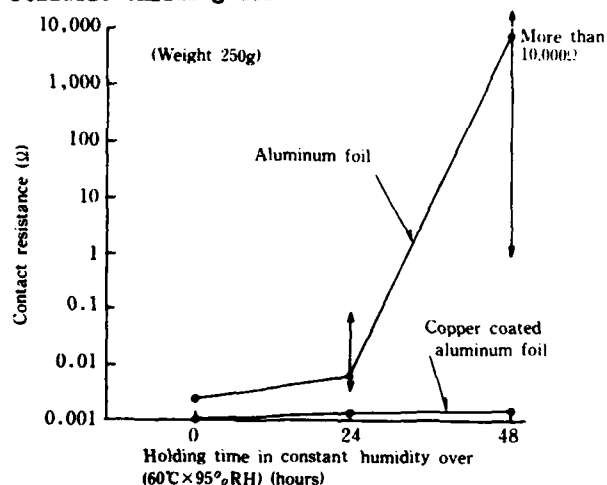


Fig.3 Contact resistance of aluminum foil after humidity test.

### 3. Shield effect of copper-coated aluminum shielded wire

#### 3-1. Contact resistance of drain wire

The shielding factor which represents the shielding effect is expressed by the following formula:

$$\lambda = 1 - \frac{K_0 j \omega L_s}{(j\omega + \frac{2R_s}{L}) + j \omega L_s} \quad (1)$$

Where,

- $\lambda$  : Shielding factor
- $K_0$  : Constant
- $\Gamma$  : Resistance of the shielding material
- $R_s$  : Contact resistance
- $L_s$  : Self-inductance of the shielding material
- $L$  : Length of the shielding material

As is clear from formula (1), the shielding factor is significantly affected by the contact resistance and the length of the shielding material.

The length of shielded wire used as internal wiring varies from 10 to 100cm, but the average length is from 20 to 30cm. From formula (1), it is obvious that such a short length makes it difficult to get high shield effect. Therefore, it is necessary to stabilize the contact resistance to a minimum value as much as possible.

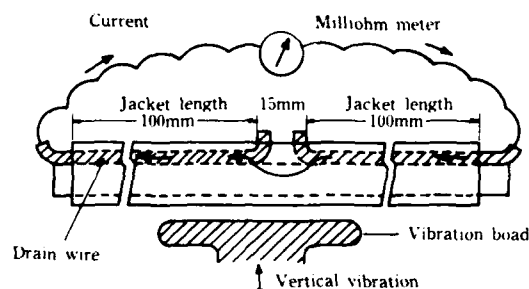


Fig.4 Simple measurement method of contact resistance

Fig.4 shows the simple measurement method of contact resistance of shielded wire with a grounding drain wire. Contact resistance including the resistance of the drain wire and the aluminum shielding foil is measured by a milliohm meter.

The same sample is then subjected to a 50-cycle vibration test using a vibration tester with a vibration amplitude of 1.5 mm, a vibration frequency varying from 10 to 55 to 10 again, with each cycle lasting 60 seconds. The contact resistances during and after the vibration test are measured.

This vibration test is significant in that the wire is often subjected to vibration during shipment, during picture taking in the case of portable video tape recorders, or while driving speakers in the case of the radio cassette tape recorders.

The results of a vibration test are shown

as original values in Table 1.

There is no variation due to vibration in the contact resistance, in the copper-coated aluminum shielded wire and its contact resistance remains quite stable as does the spiral shielded wire.

But the contact resistance of the aluminum shielded wire after the vibration test increases by approximately 100-fold from the value before the vibration test.

Next, the samples are left for 168 hours in a constant-humidity and temperature over at 60°C and 95 % RH, and then the values of contact resistance before during and after the vibration test are measured.

The result are shown as values after humidity test in Table 1.

The copper-coated shielded wire and the spiral shielded wire show approximately the same values before the vibration test, about a 4-fold increase over the original values.

However, the contact surface between the drain wire and the shield is cleaned during the vibration test, and the contact resistance is returned to the original level after the vibration test.

However, the surface oxidation of the aluminum shielded wire is promoted by humidity, and the contact resistance increased by as much as 1,000 fold or more after the vibration test.

And then, in the H<sub>2</sub>S atmosphere test, the samples are subjected to H<sub>2</sub>S atmosphere

for 48 hours and their contact resistances before, during and after the vibration test are measured.

The results are shown in the column "values after H<sub>2</sub>S environment test" in table 1.

The copper-coated aluminum shielded wire and the spiral shielded wire show approximately the same values before the vibration test, but the aluminum shielded wire shows an increase of approximately 10 to 100 fold over the values of the copper-coated aluminum shielded wire.

After the vibration test, the contact surface between the drain wire and the shield of the copper-coated aluminum shielded wire was cleaned and the contact resistance returned to approximately the original level before the vibration test.

In the case of the aluminum shielded wire, however, the aluminum surface was affected by H<sub>2</sub>S atmosphere and the contact resistance didn't return to the original level after the vibration test.

In fact, the contact resistance increased by as much as 100 fold over the original value.

The contact resistance values after the vibration test from Table 1 are shown graphically in Fig.5.

From the above results of several environmental tests, it is obvious that the copper coated aluminum shielded wire shows a more stable contact resistance than the aluminum

Table 1. Contact resistance after environmental tests.

(Unit: Ω)

Condition of environment Condition of measurement Wire sample	Original value			Value after humidity test			Value after H <sub>2</sub> S environment test		
	Value before vibration	Max. value in vibration test	Value after vibration test	Value before vibration	Max. value in vibration test	Value after vibration test	Value before vibration	Max. value in vibration test	Value after vibration test
Copper-coated aluminum shielded wire.	0.04	0.04	0.04	0.08	0.1	0.04	0.06	0.08	0.04
	0.05	0.05	0.05	0.16	0.2	0.05	0.15	0.12	0.06
Aluminum shielded wire.	0.05	1	0.2	0.1	more than 100	1.0	0.5	more than 100	9
	0.08	2.0	9.5	6.3		more than 100	7.0		more than 100
Spiral shielded wire.	0.01	0.01	0.01	0.02	0.02	0.01	0.02	0.02	0.01
	0.02	0.02	0.02	0.08	0.05	0.02	0.08	0.04	0.02

shielded wire.

Therefore, the copper-coated aluminum shielded wire necessarily can maintain the reliability of the shield effect over long terms, but the aluminum shielded wire cannot because the contact resistance is easily affected by atmosphere.

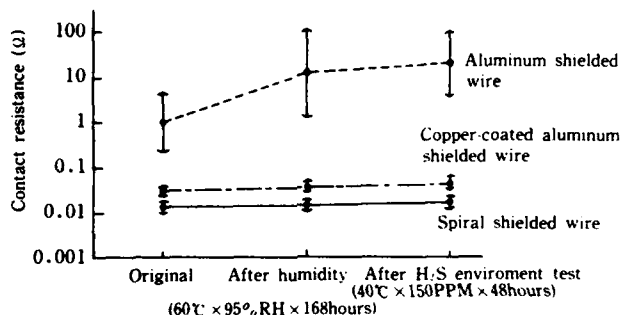


Fig.5 Contact resistance after vibration test following environment test

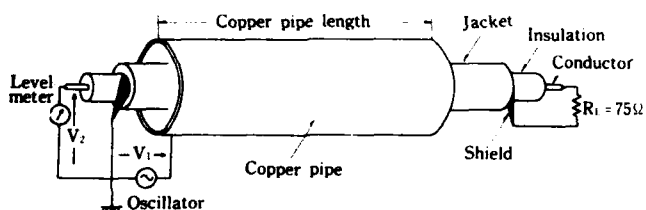


Fig.6 Measurement method of static shield effect

Fig.6 shows the method of measurement of the static shield effect of shielded wire. Electrostatic inductive voltage  $V_1$  is generated between the copper pipe and the shield. And then the voltage  $V_2$  induced between the conductor and the shield of which the shielded wire is terminated at the resistance 75 is measured. The static shield effect is then obtained by the following formula:

$$\text{Static shield effect} = -20 \log \left( \frac{V_2}{V_1} \right) \text{ dB}$$

The original values of the static shield effect for different shielded wires are shown in Fig.7.

The metal braid shielded wire shows the best

shield effect of all of them and the shield effect of the spiral shielded wire is next best.

There is only a slight difference of 2 to 3 dB in the original values between the copper-coated aluminum shielded wire and the aluminum shielded wire.

The shield effect of the conductive plastic wire depresses remarkably in comparison with other shielded wires, because the volume-inherent resistivity of the shielding material in the conductive plastic shielded wire, (which is  $10^{-10} \Omega \cdot \text{cm}$ ), is extremely large as compared to that of the metal shields, (which is only  $10^{-6} \Omega \cdot \text{cm}$ ).

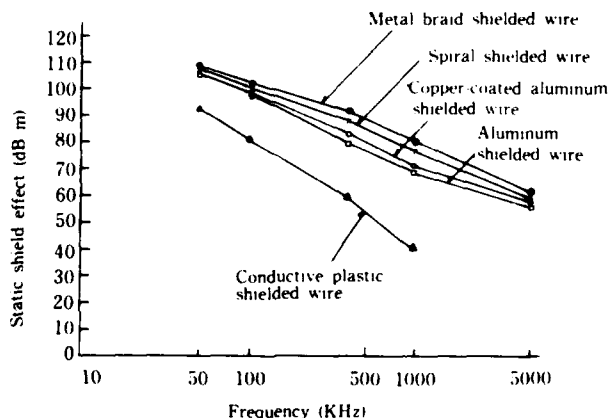


Fig.7. Frequency characteristics of static shield effect.

Fig.8 shows the static shield effect after leaving the samples in a  $60^\circ\text{C} \times 95\% \text{ RH}$  constant-humidity over for 30 days. The static shield effect of the copper-coated aluminum shielded wire as well as that of the spiral shielded wire is reduced by only 1 dB, while the static shield effect of the aluminum shielded wire is reduced by as much as 6 to 7 dB.

Such a result is closely related to the increase in the contact resistance after the humidity test as described in 3-1. It can be easily understood that the static effect of the aluminum shielded wire when using a short length in internal wiring will

depress more remarkably than the results of the humidity test show.

This is because the length in internal wiring - which is at most 10 to 30 cm - is shorter than the length in this test - which was 1 meter.

Also, the internal wiring materials are apt to suffer vibrations.

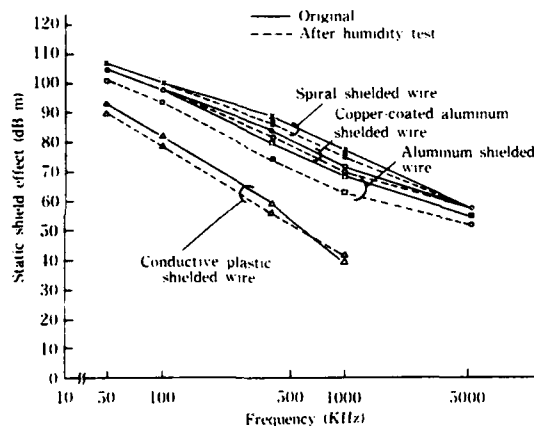


Fig. 8 Frequency characteristics of static shield effect after humidity test

Fig. 9 shows the static shield effect after the samples are left in a 100°C constant-temperature oven for 96 hours.

All shielded wires except the conductive plastic shielded wire show almost no change in the static shield effect.

The change of the conductive plastic shielded wire is due to the change of the volume-inherent resistivity.

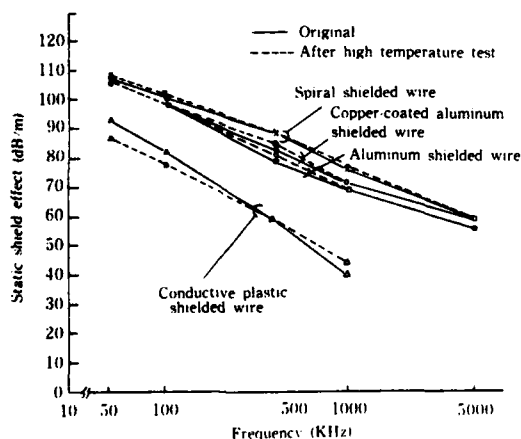


Fig. 9 Frequency characteristics of static shield effect after high temperature test

Fig. 10 shows the static shield effect after the bending test.

The test consists of ten bending cycles of  $\pm 90$  degrees at 5-cm intervals over 1.1m long wire sample.

Bending cannot be avoided during the fabrication of any shielded wire, but especially in the case of aluminum shielded wire there is always the possibility of the depression of the static shield effect by cracks in the aluminum foil.

As shown in Fig. 10, the static shield effects of copper-coated aluminum shielded wire aren't depressed by the bending test but rather are improved.

This is probably due to an increase in the contact pressure between the drain wire and the aluminum surface, causing a reduction in the contact resistance in the same degree.

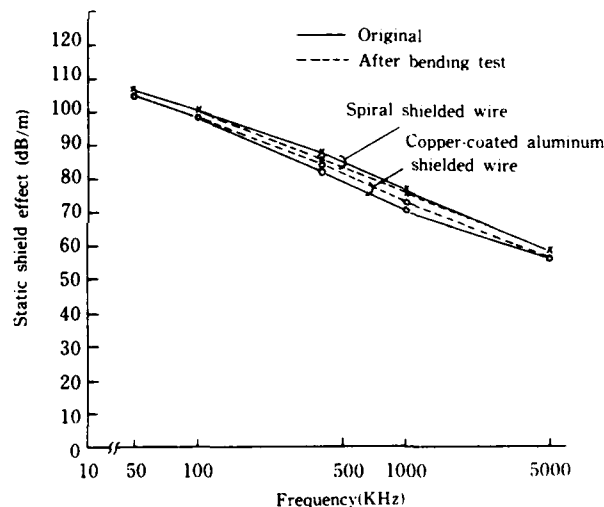


Fig. 10. Frequency characteristics of static shield effect after bending test

#### 4. Electrostatic noise voltage characteristics

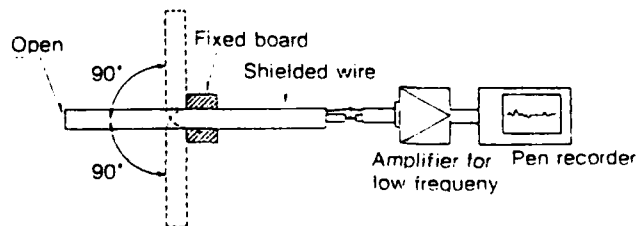


Fig. 11. Measurement method of electrostatic noise

Electrostatic noise voltage which is generated between the shield and the insulation during repeated  $\pm 90^\circ$ -degree bending of wire as shown in Fig.11 also is measured.

Fig.12 shows the result.

Both the aluminum shielded wires show almost the same levels of electrostatic noise voltage and lower levels of it than the spiral shielded wire.

This is the reason why aluminum shielding tape is bonded to the jacket of each aluminum shielded wire like the conductive plastic shielded wire and can not move independently

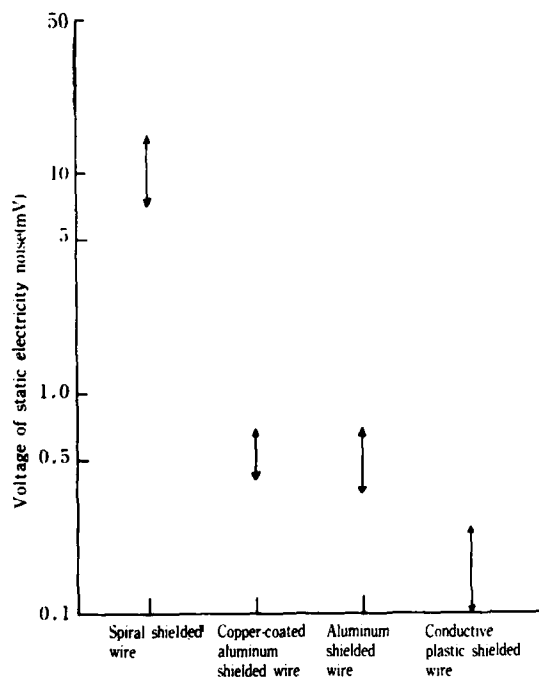


Fig.12. Characteristics of electrostatic noise

### 5. Construction of wire

We developed the independent wrapping method of aluminum shielding tape. Fig.13 shows the construction of two conductors each individually spirally wrapped with copper-coated aluminum shielded wire as an example of the application of this method. As in Fig.13, about 1.5mm of the edge of the copper-coated aluminum shielding tape is folded back on to the adhesive layer and

over-wrapped on the insulated conductor. Parts of the exposed copper layer can make contact with the drain wire and the shielding tape itself is bonded to the jacket by the exposed adhesive layer. Because of this adhesion, the shielding tape will be rejected at the same time as the jacket, making the separate termination of the shield unnecessary.

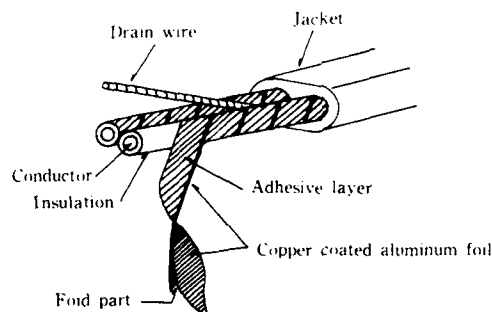


Fig. 13. construction of two conductors each spirally wrapped with copper-coated aluminum shielded wire

We developed three conductors and four conductors each with spirally wrapped copper-coated aluminum shielded wires as shown in Figures 14 and 15 using the tape-wrapping method noted above.

These wires are well suited to the internal wiring of narrow spaces because of their thin diameters and flexibility and are as easy to fabricate as two conductors each spirally wrapped with copper-coated aluminum shielded wire (Fig.13).

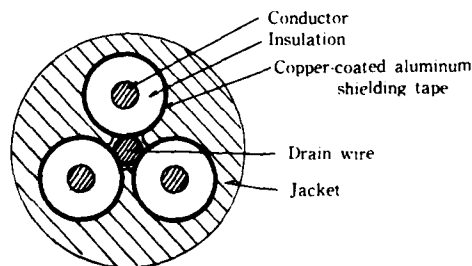


Fig.14 3-conductors each spirally wrapped with copper-coated aluminum shielded wire

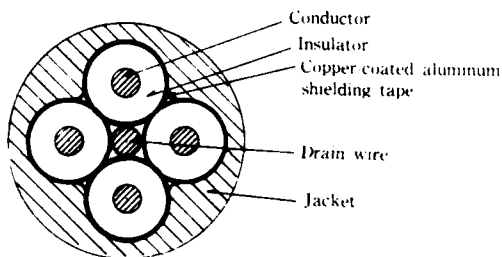


Fig.15 4-conductors each spirally wrapped with copper-coated aluminum shielded wire

#### 6. Conclusion

The copper-coated aluminum shielded wire has a reliable static shield effect over a long period of time like the spiral shielded wire, its static shield effect is very close to that of the spiral shielded wire, are the termination characteristics of this wire are as easy as those of other aluminum shielded wires.

There has never been a shielded wire with all of these characteristics.

After this, however, many kinds of copper-coated aluminum shielded wires (with a variety of conductor numbers, conductor sizes, insulation materials, etc.) are going to be used as internal wiring materials in electronic equipment thereby making possible greater lightening and miniaturization.



Haruo Saen

Haruo Saen was born in 1949 and received a B.S. degree in electrical engineering from Fukui University in 1972.

He joined Sumitomo Electric Industries, Ltd. in 1972, and has been engaged in design of wires used in electric equipment.

He is a senior engineer of Electronics Wire Division.



Akinori Mori

Akinori Mori was born in 1947 and received a B.S. degree in mechanical engineering from Kyushu University in 1970.

He joined Sumitomo Electric Industries, Ltd. in 1970, and has been engaged in manufacturing and design of wires used in electric equipment.

He is a senior engineer of Electronics Wire Division.

## ALUMINUM FOIL SHIELD EFFECTIVENESS FOR ELECTRONIC CABLES

MICHAEL R. LOMBARDO

PRODUCTION ENGINEERING DIVISION, TOBYHANNA ARMY DEPOT  
TOBYHANNA, PENNSYLVANIA 18466ABSTRACT

Historically, shielding of electronic cables has been expressed in terms of shield coverage. The numeric value used to delineate shield coverage corresponded to the actual area of the conductors covered by the cable shield.

Generally, the larger the percentage of coverage the greater the shield's effectiveness. Presently, with the advent of more sensitive, more sophisticated equipment 100% shield coverage has not been totally adequate. Shield effectiveness can be defined as the functional capability of a shield. The shield must prevent any external signal from entering the conductors and also prevent the conductors from radiating signals beyond the shield. Both parameters of this function are important, but not necessarily proportional. This problem of proportionality occurs primarily in the type cable described herein.

1. Introduction

Design engineers require a quantitative measurement to express shield effectiveness, and a technique which offers enough sensitivity to detect small ruptures in shielding. These problems in measurement are particularly apparent when examining aluminum foil shielded twisted pair cable which is operated in the balanced mode.

This project began as an effort to specify shielding parameters and requirements for aluminum foil shielded twisted balanced pair cable with an incorporated drain wire. This item is further described as individually shielded multi-pair cable. It is the intention of this paper to discuss problems with contemporary shield effectiveness measurement techniques. The discussion shall be limited to aluminum foil shields on twisted pair constructions.

Each technique yields valuable data and has inherent drawbacks. The data collected thus far fails to indicate conclusively that any one method can provide a sufficient view of the function known as shield effectiveness. Portions of this function are revealed by some tests and other portions by other methods. The indicated proportions and their relationship to each other will be found in the conclusions of the paper.

2. Project Outline

In the remainder of this paper, a brief review of the problem is given to establish a history necessary to provide a full understanding of the project. Initially, a development of the test requirements is used to show the parameters of shield effectiveness that were desirable. The cable type under consideration here is a multi-pair construction. Each pair consists of two insulated conductors and an uninsulated drain wire. The cable pair is covered by an aluminum foil shield which is insulated from other pair shields by a polyester backing. Conductors may be operated in the balanced or unbalanced mode. The drain wire is located beneath the shield throughout the cable. (Figure 1).

TYPICAL CABLE CONSTRUCTION

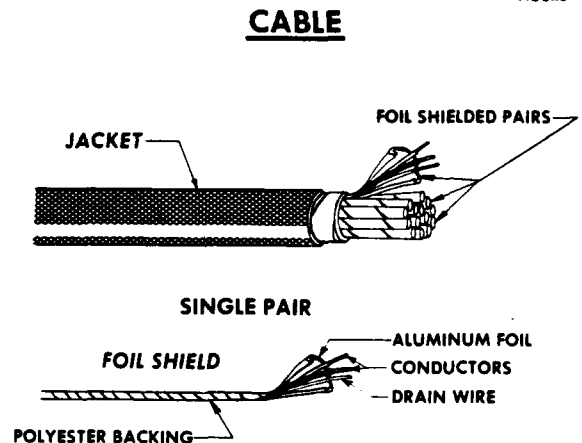


FIGURE #1

FIGURE 1

Testing problems were inherent due to the cable design. Terminating the drain wire and shield became major difficulties. The twisted pair construction disallowed many common test fixtures because of the two conductors and their twist length. Those fixtures would have interfered with the basic configuration of the cable.

Contemporary methods of measuring shield effectiveness are discussed in terms of their failure to meet the requirements of this project. Current test methods which were important to the development of the procedure to be presented are: (1) Shielded room measurement; (2) Braid shield enclosures; (3) Transfer impedance tests; (4) Absorbing clamps; (5) Crosstalk evaluation; (6) TEM cells; (7) Open site Antenna Range Tests; (8) Shield injection; and (9) Quadaxial test fixtures. These methods were incorporated with every form of tube, box or jig that could be imagined in order to achieve a test which would accommodate the cable and test to the established requirements. Early test data showed poor repeatability in all cases. None of the methods exhibited the necessary sensitivity to detect perforations in the foil shield. Due to the compounding of errors from test equipment and fixtures, the best accuracy was 3.8 db in a measurement scale of 120 db, or more than 3%. Further results of the test method investigations are expressed in the actual test development described herein as a solution to the aluminum foil shield effectiveness measurement problem. A discussion of the use of automatic test equipment is included to explain the gains in sensitivity and accuracy which were achieved by using a controller and net-work analyzer. A detailed description of the test method and test data is included as part of the body of this work. Due to the shift in interest from shield coverage to shield effectiveness, and the present concerns with signal loss from shielded cables, the emphasis on test types has changed. The electrical (EMC or RFI) tests and test data interpretations, are more important than the physical construction of this shield. Shielding requirements are more likely to be expressed in terms of signal attenuation rather than percent of coverage.

### 3. Test Method Requirements

General problems existed with tests involving this type cable. The foil shield and drain wire function as one unit. The shielding capability of the construction is related to the combined effect of these components. The drain wire functions more prominently at lower frequencies whereas the foil shield has more effect at higher frequencies. The trade off in shielding between these two components need not be expressed separately, but the method of terminating the foil shield and drain wire to the test fixture can change the measurements. The characteristic twist of the cabled pair leads to difficulties when a sample is positioned in a test fixture. The coiling or helix shape of the sample causes inaccurate readings when probes or pickups are passed along its length. Excess movement of a pair, after it has been separated from a cable, usually results in foil shield damage. If the foil becomes loosened from the conductors, contact between the drain wire and foil is lost.

The foil shield, itself, cannot be clamped or soldered to in any fashion which interferes with the cable construction. Dealing with most, or all of these problems was a factor in test method development. Test chambers with detector probes could not be used because of the associated physical mounting problems.

Nearly all the test fixtures used to measure shield effectiveness have been developed around coaxial cables with braided shields. A study of these test fixtures determined their unsuitability for the aluminum foil model which was to be tested. Basic differences in the foil shield design made it impossible to use most test fixtures which involved probes or pressure contact devices, other tests required soldered connections within the test fixture which were impossible because of the aluminum shield. Adapting or developing a test which had the sensitivity, accuracy and reliability necessary meant a new test procedure.

The shield effectiveness test was required to detect small ruptures in the cable specimen. In order to be considered sensitive enough, a test sample with a one-half inch slit in the foil shield must be detectable when the total test sample length is approximately 36 inches. Any test which would not show a perceptible difference in measurement under these conditions was rejected. In this way a concept was developed which showed the test requirements to be, "Total Shield Effectiveness" and "Localized Shield Effectiveness". The concept of Local Shield Effectiveness is to express or detect leaks or ruptures in a foil shield. The Total Shield Effectiveness of a cable measures an average over an entire test sample. Given certain conditions, the cable may be exceptional throughout its length - yet at one point along the length of the cable the shielding may be very poor. This was not acceptable, a measure with some "Localized" shielding indication as a component of the Total Shield Effectiveness was required.

The test also needed a high degree of repeatability. In open site antenna tests noise levels and measurement conditions may change daily, this does not allow for a quantitative numeric value to be established. This procedure cannot be used by different individuals at different locations with any degree of repeatability. This type of user repeatability and dependability proved to be an essential requirement. The ability to obtain repeatable results by any qualified individual was a prime requirement of this project.

Test accuracy for comparison of results under the conditions already described has become very important. The actual numeric accuracy of the test should be within one percent; this allows sensitivity and repeatability to be independent of the numeric accuracy of the test results.

Test reliability has been used as a means of controlling independent variables. By using every means to guarantee the results on a 100 percent schedule the validity of the procedure was increased tremendously.

The currently available data on the shielded pair cable was obtained by crosstalk measurements. Some of the variables involved in this method prevent a quantitative assessment of the shield effectiveness function. The pair alignment with regard to its adjacent pair is a large enough factor numerically to preclude statements regarding the foil shield's influence on the data. A test was needed to measure signal penetration with regard to the shield alone. When tests of the individual shields are compared to crosstalk data conclusions can be drawn concerning the shield to shield signal transference. Whereas the shield effectiveness data relates to only one shielded pair, crosstalk results relate to two pair and their cabled position.

Further questions concerning the foil shield included frequency range over which a shield type could perform and yield a required amount of attenuation. The test was expected to show differences in construction as they related to frequency range. Once again, the sensitivity of the test method was a crucial concern. If the generated data could not ascertain differences in construction, which are theoretically proven, the test sensitivity was not adequate.

#### 4. Test Method Investigated

Many types of tests were evaluated in terms of the requirements which were previously discussed. Original plans for the testing of the cable included the use of a shielded room. The cable was to be placed in the room with both ends routed out of the room from the inside. This approach was to provide isolation from spurious signals as well as protection from signals generated on and around the test equipment. The shielded room produced fields of its own and the signal strength within the room varied from point to point. Absorbing material was suggested as a means of controlling these problems, but it became apparent at that time that some sort of test fixture was necessary to control variables more closely.

The first test data was taken from a method using a braid as an overall shield. The test equipment was a tracking generator which was used to inject a signal onto the conductors. A spectrum analyzer acted as the receiver. The braided shield functioned as an exterior "circuit" shield and the pick-up for the spectrum analyzer. The circuit formed was triaxial and the cable was terminated in 75 ohms. The drain wire was soldered to the external braided shield to form a grounded circuit. The foil shield was placed around the braid. Contact between the cable foil shield and the outer braided "circuit" shield was accomplished by folding the foil shield over the braid and applying heat shrinkable tubing (Figure 2).

BRAIDED TEST FIXTURE  
SCHEMATIC DIAGRAM

FIGURE #2

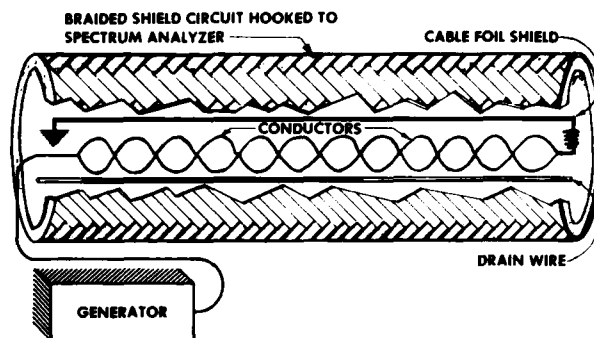


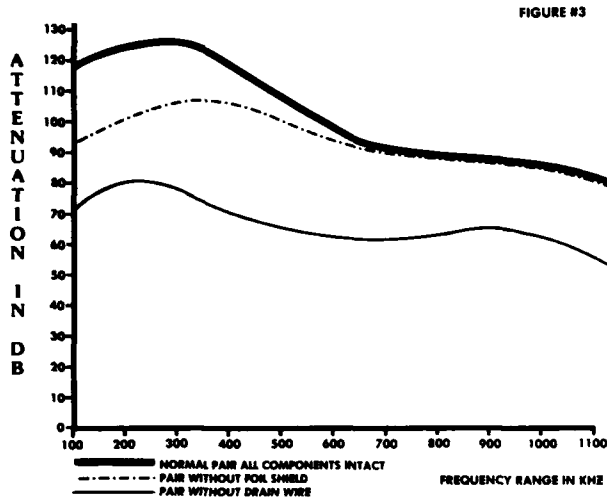
FIGURE 2

The principle involved the coupling of signal which had penetrated the foil shield and had been induced onto the external "braid" circuit. The test data generated by this procedure exhibited unreliable repeatability. The system was checked by substituting a solid copper tube for the cable foil shield. Reference plots showed that the braided outer circuit shield was initiating unwanted perturbations in and of itself. Because of the electrical interference generated, this approach was abandoned.

Surface transfer impedance was also explored as a means of determining the shield characteristics. This method would yield a measurement of the shield independent of the cable components and other associated cable shields. Results of the transfer impedance tests indicated that the drain wire played a predominant role in the shield configuration. Experiments were conducted with twisted pairs and a drain wire alone. The shield was carefully removed during these measurements.

In associated tests, the drain wire was removed and a pair tested with only the foil shield intact. The results clearly indicated the drain wires function in the shield's effectiveness. The data from these combined tests did not coincide. Measurements taken with the shield alone showed approximately 50% higher levels of emitted signal (Figure 3).

# SHIELD EFFECTIVENESS PLOT TRANSFER IMPEDANCE METHOD



The data collected from the tests, which involved the conductors and drain wire without the foil shield, showed increased levels of emitted signal of approximately 30% at 100 KHZ. The total change in attenuation as recorded in both test groups (drain wire, without shield-shield without drain wire) did not agree with the theoretical function of the shield components. The drain wire should have a greater influence on shielding at lower frequencies and the foil should show increased effectiveness at high frequencies. Graphs of the shield function of the drain wire effect, and foil effect, corresponding to frequency, showed an exaggerated drain wire contribution to the shielding function, and an understated aluminum foil contribution. It was later proved that the individual component resistance caused the measurement error. This was proved by substituting different drain wires which were the same gauge but different stranding. The change in shield effectiveness related exactly to the change in drain wire resistance. Due to these results, surface transfer impedance was not used to calculate shield effectiveness for aluminum foil shields. With proper consideration to individual component parameters, the discrepancies could be accounted for mathematically. The calculations proved too cumbersome for the required measurement statistics.

The absorbing clamp method of measuring shield effectiveness was not suitable because the gathered information could not be directly related to the overall sample length. The absorbing clamp makes measurements at one point along the sample.

A method to relate maximum and minimum reading was unsuccessful due to the inability to express these readings as some part of the sample length. Further work with the absorbing clamp showed the distance from the clamp to the sample to be critical. No acceptable means of controlling that distance could be found. Measurements made with the absorbing clamp were useful in detecting signal leakage at connector junctions. This information was helpful in developing contacts with sufficient attenuation to allow successful measurements at a later date.

Crosstalk tests were performed. The collected data although inconsistent, yielded valuable shield effectiveness information. The test results related one pair to another with reference to the pair shields. The most important concept here is that cabling and pair placement are variables that heavily influenced the test data. A measurement which provided data on one shield alone was necessary to express the function properly. A combination of crosstalk test data and shield effectiveness measurements would result in an overview of the shield function that would satisfy the requirements of the project.

Open site antenna tests conducted on test samples proved to be sensitive enough but lacked the repeatability necessary. Reference plots changed with ambient signal levels and test conditions. Ground references adversely affected test results. Open site antenna tests could not be conducted under sufficiently controlled conditions to establish absolute parameters. Although some of the data was double checked using this method, it could not be set forth as a procedure to be used industry-wide. In many instances where data seems to be conflicting, an open site antenna test can be used to confirm the results.

Shield injection is, in some respects, the inverse of the proposed technique. Although application of the signal to the conductors or shield should result in the same measurement the procedure is not proportional. Proof of the reciprocity is possible by adding an additional environmental shield over the signal shield. Differences between the two readings can be resolved mathematically.

Transverse electromagnetic cells or TEM Cells have great potential for performing EMC and RFI measurements. The cells versatility and accuracy did yield consistent repeatable data. Problems encountered were the mounting and terminating of samples in such a manner as not to disturb the foil shield. Sample movement related to placement in the cell proved to be undesirable. A special cell with incorporated test fixtures could have been developed to overcome these problems. Further investigation was not conducted because of the direction that research had already taken. It became apparent that a Quadraxial test fixture with characteristics similar to a TEM Cell would best meet the needs of this project. The fixture needed to be an expanded coaxial transmission line with specified propagation factors.

## 5. Test Method Description

The following system was used to test foil shielded pairs for shield effectiveness under conditions satisfying the aforementioned requirements. This procedure circumvents most, if not all, of the test and fixture problems encountered in other methods. Figure 4 is the electrical schematic for the test fixture used in the foil shield project.

QUADRAXIAL TEST FIXTURE  
SCHEMATIC DIAGRAM

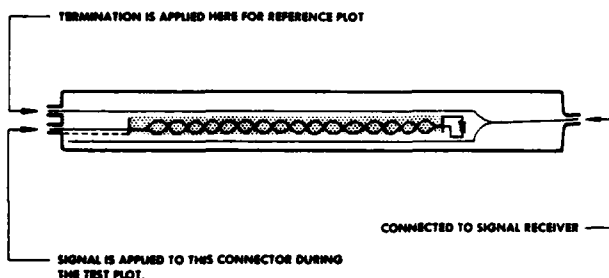
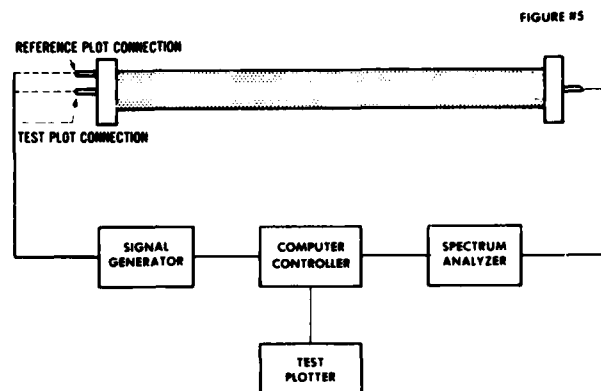


FIGURE 4

Samples were prepared with carefully controlled sample lengths. Connectors and junction shields were attached to the cable samples. Location of the samples within the test fixture was controlled by a plastic insert which allowed a minimum amount of sample movement without jeopardizing the foil shield by clamping it. The Quadraxial test fixture was connected to a computer controlled network analyzer, spectrum analyzer, and remotely programmed signal generator (Figure 5). Results were plotted automatically. A reference plot of the test set-up with the sample in place was the first operation in actual testing. The reference plot develops criterion such as resonance of the fixture which must remain the same and must fall into established limits (Figure 6). It has been shown that test results obtained from data with a 20 percent change in reference plot resonance produces unusable data. The most important aspect of the fixture resonance is the center frequency. The duration and amplitude are subject to variation without substantial effect on the test results. Using the reference plot as a reliability check is not to be misconstrued as a total or foolproof double check, it merely provides information to be used in relationship to the data received from the test sample.

TEST FIXTURE  
EQUIPMENT SET-UP



Note: When the test plot is being run the reference connector is terminated in 50.0 ohms.

FIGURE 5

QUADRAXIAL TEST FIXTURE  
REFERENCE PLOT

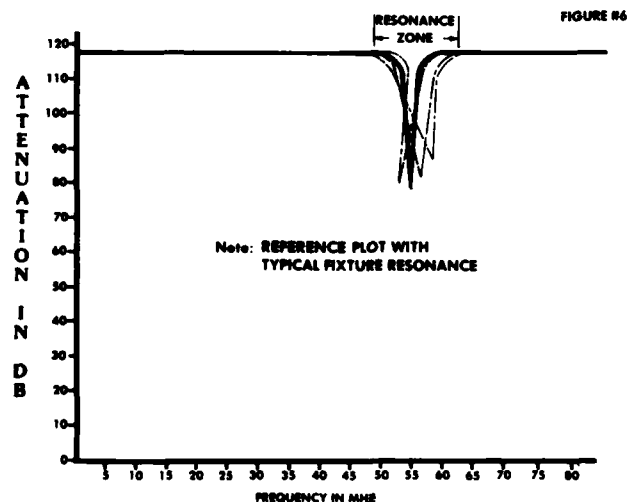


FIGURE 6

The information derived from the test plot and the reference plot must be correlated in order for the test run to be legitimate. The test fixture via the reference plot must exhibit a db level previously established by historical data. In most instances, the data produced in this project indicates a 117 db level plus or minus 1 db to be typical fixture attenuation at the time of test. Fixture resonance occurred between 50 and 60 MHZ in all cases. The amplitude of the fixture resonance points was randomly selected by a computer controller which established measurement points within stated frequency ranges. The average range was ten points per octave or sixty points per test. With the characteristic parameters of the reference plot and the proper test plot curve a measure of reliability can be established. Note, the test data curves express the same function of shield effectiveness in all cases. This characteristic curve is an expression of aluminum foil shield effectiveness as it relates to twisted pair cable (Figure 7).

## 6. Conclusion

The precise function of aluminum foil shielding on twisted pair cable can be expressed using automatic test equipment and a Quadraxial Test Fixture. Crosstalk data when compared to the shield effectiveness results will evaluate cabled pairs of this type. Information on individual shields when contrasted with pair to pair crosstalk data provides an overall view of the EMC or RFI capabilities of the complete cable. The correlation between points on the crosstalk graph and the shield effectiveness graph where their frequency ranges overlap show consistent ratios. Provided with all three groups of figures, shield effectiveness, crosstalk, and their related ratios design engineers can predict more closely their cable requirements.

Automatic test equipment played a large role in the development of this procedure. Manual tests of the same type were used in previous attempts to solve the shield measurement problem. The manual procedure introduced enough error and data variance to cause many of the test graphs to show unpredictable results. The automatic configuration allows comparison of test signals and test conditions before, during and after tests as an additional measure of reliability. Variables such as impedance and signal amplitudes were more easily controlled using this system.

The purpose of this paper has been to explain the development of this particular shield effectiveness test and show how it is related to the function of shield effectiveness in this type cable.

TYPICAL FOIL SHIELD  
FUNCTION

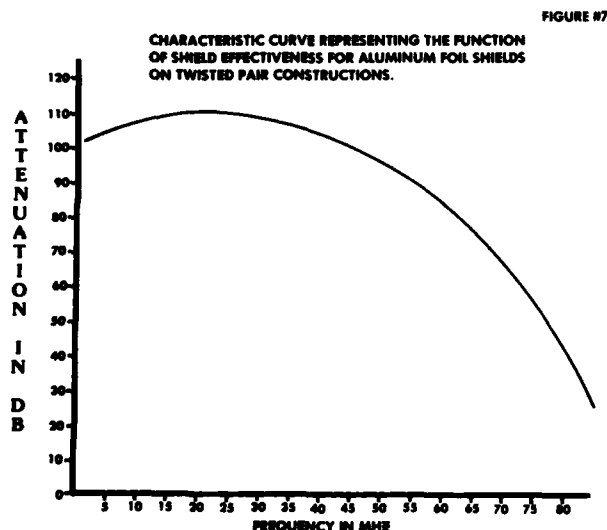


FIGURE #7

FIGURE 7

## REFERENCES

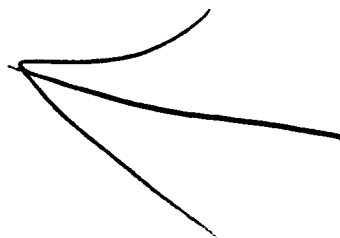
1. Bernhard E. Keiser, Principles of Electromagnetic Compatibility, Artech House, Inc., 1979.
2. Test Report By: Chris W. Carlson, "Test Project Report (No. 7891)". Elite Engineering Company, April 26, 1983.
3. Anatoly Tsaliovich, "Shielded Electronic Cables for EMI Protection", Innovator, Belden's Tech. Jour., pp. 22-35, published December 1982.

## ACKNOWLEDGEMENT

The author wishes to thank the people of the cable and wire industry for their helpful discussions and suggestions, all of which were invaluable. Thanks also to the many people who contributed their effort in preparing this paper.



Michael R. Lombardo is a Project Engineer for Tobyhanna Army Depot, Tobyhanna Pennsylvania. He is currently involved in Electronic Design and Development within the Project Design and Development Branch. Michael has been working in test analysis and testing for the past ten years. His main interests are electronic cable and transmission line.



# UNBALANCED DIGITAL CROSSTALK IN BALANCED, TWISTED PAIR, INSIDE WIRING CABLE

D. P. Woodard, Jr.

Bell Laboratories  
Norcross, Georgia 30071

## ABSTRACT

A model is derived that accurately predicts pulse crosstalk between two unbalanced circuits in a multipair cable. If pair integrity is maintained and single point grounding is observed, coupling is capacitive and increases directly with length. If unused conductors are allowed to float, coupling capacitance increases strongly, but predictably.

Based on this model, twisted pair inside wiring cables are capable of transmitting digital signals over longer distances and at greater rates than those recommended in industry standards.

## INTRODUCTION

Twisted pair inside wiring cables were designed to transmit balanced analog voice signals over comparatively short distances. For many years these cables, made mostly with 24 gauge conductors in various pair count sizes, have been used almost exclusively for this purpose. The cables are relatively inexpensive, and having been produced in quantity, their use is widespread. Major changes now occurring in customer-premise equipment, particularly the growth of digital networks, open questions concerning the performance of twisted pair cable when used in an unbalanced way. One of the most important parameters, of course, is crosstalk between contiguous, unbalanced cable pairs.

A large number of unbalanced digital circuit configurations exist. Two examples are shown in Figure 1. In 1(A) receiver currents return on separate leads to their originating generator grounds. Single point grounding at the generator ends reduces both ground potential differences and intercircuit common mode coupling. Further, if the signal and return leads are paired, mutual inductive coupling between circuits is also minimized and is approximately equal to that found between balanced pairs. In Figure 1(B) multiple receiver currents return on common leads; capacitive, inductive and common mode couplings are all likely and it is not possible to predict which will dominate.

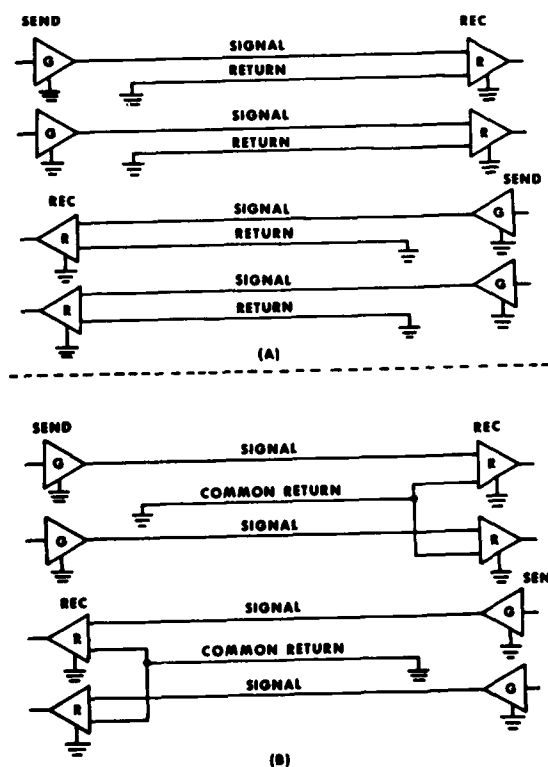


FIGURE 1

Figure 2 shows a similar mélange of possible configurations for one direction of transmission where almost any combination of coupling is possible.

## CAPACITANCE COUPLING MODEL

The arrangement of Figure 1(A) requires more conductors per circuit than other configurations; however, its performance is more predictable. The configuration is redrawn in Figure 3 for a more detailed look. Typically, nodes labeled  $T_1$  and  $T_2$  are two pair-conductors (perhaps tip conductors) coupled by  $C_C$ . The remaining conductor nodes,  $R_1$  and  $R_2$ , are common.  $C_a$  and  $C_b$  are the capacitances from  $T_1$  and  $T_2$  to ground.  $R_p$  is the series-parallel combination of conductor resistance and near and far end terminations if the conductors are short,

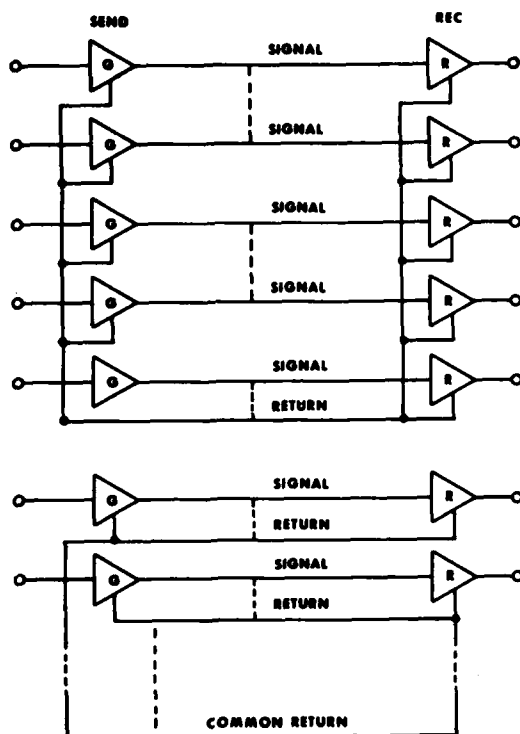
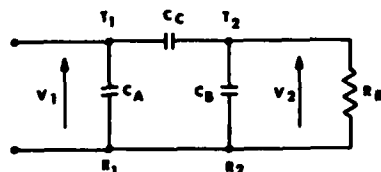


FIGURE 2



CROSSTALK EQUIVALENT CIRCUIT

FIGURE 3

or near end termination and characteristic impedance if the conductors are long.  $V_1(t)$  is the disturbing voltage;  $V_2(t)$  is the resulting disturbance which may be assumed at this point to occur at the near end.

The Laplace voltage transfer function between the two circuits is simply

$$\frac{V_2(s)}{V_1(s)} = \frac{C_C}{C_b + C_C} \left( \frac{s}{s+a} \right) \quad (1)$$

where

$$s = j\omega$$

and

$$a^{-1} = R_b(C_b + C_C).$$

If  $V_1(t)$  is a linear rise unit step,

$$V_1(t) = \frac{(t-t_0)}{t_0} u(t-t_0). \quad (2)$$

The disturbance transform is

$$V_2(s) = \frac{1}{at_0} \left( \frac{C_C}{C_b + C_C} \right) \left[ \frac{1}{s} - \frac{1}{s+a} \right] (1-e^{-st_0}) \quad (3)$$

with the inverse

$$V_2(t) = \frac{1}{at_0} \left( \frac{C_C}{C_b + C_C} \right) \left[ (1-e^{-at}) u(t) - (1-e^{-a(t-t_0)}) u(t-t_0) \right]. \quad (4)$$

Using representative parameters for 24 gauge PVC insulated twisted pairs

$$C_b = 30 \text{ pF/ft} \gg C_C$$

and

$$R_b = 100 \text{ ohms}$$

the network time constant  $a^{-1}$  is about 3 nsec/ft. For a wide range of input rise times and pair lengths, therefore, the normalized peak disturbance becomes

$$V_{2\text{max}} = \frac{R_b C_C}{t_0} \quad (5)$$

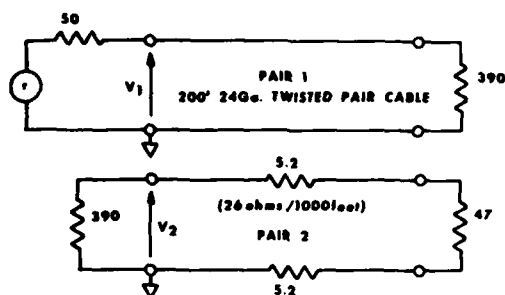
using Equation (2) and assuming  $(1-e^{-at}) = 1$ .

For 200 feet of inside wiring cable terminated and coupled as shown in Figure 4, we have the following near end crosstalk (NEXT) loss comparison for a range of rise times.

Table 1

Rise Time $t_0$ ( $\mu\text{sec}$ )	NEXT LOSS, dB	
	Measured	Calculated
10	63.2	63.3
20	68.6	69.3
30	72.0	72.8
40	74.2	75.3
50	76.7	77.3
70	79.2	80.2
100	83.7	83.3

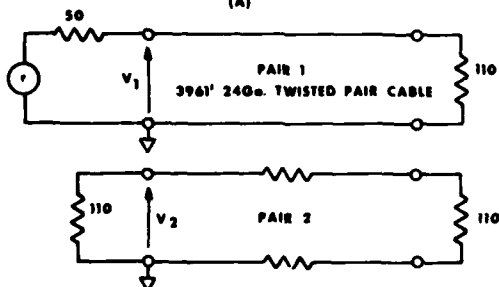
Comparison of Measured And Calculated  
Near End Crosstalk Loss For 200 Feet  
Twisted Pair 24 Gauge Cable



$$R_B = 50 \text{ ohms (390 IN PARALLEL WITH } 47 + 10.4)$$

$$C_C = 137 \text{ pF, } C_B = 6112 \text{ pF, } \alpha = 3.27 \times 10^6 \text{ sec}^{-1}$$

(A)



$$R_B = 110 \text{ IN PARALLEL WITH } |Z_0|$$

$$C_C = 20,340 \text{ pF WITH TERTIARY PAIRS FLOATING}$$

$$= 1,530 \text{ pF WITH TERTIARY PAIRS GROUNDING}$$

(B)

FIGURE 4

In this case measured NEXT =  $20 \log \frac{V_1(X=0)}{V_2(X=0)}$

and calculated NEXT =  $20 \log \left( \frac{R_B C_C}{\tau} \right)$ . The circuit terminations are somewhat arbitrary but typically might represent 50 ohm generators driving a load of 10 bridged, 4K receivers.

A much longer circuit is shown in Figure 4(B) for which we have the following results for two typical unbalanced pairs in a 25 pair cable.

Table 2

Rise time to, $\mu\text{sec}$	Tertiary Pairs					
	Grounded			Floating		
	NEXT, dB	$ Z_0 $		NEXT, dB	$ Z_0 $	
	Meas.	Calc.	$\Omega$	Meas.	Calc.	$\Omega$
10	48.0	48.0	34	22.6	22.5	56
20	47.4	47.5	110	23.7	23.7	155
40	52.8	52.8	130	29.3	29.3	176

Comparison of Measured and Calculated  
Near End Crosstalk Loss for 3961  
Feet Twisted Pair 24 Gauge Cable  
With 110 Ohm Terminations

Although the loads in this case incidentally approximate the characteristic impedance of a balanced pair, the values were chosen primarily for convenience. For the longer cable, NEXT depends on an apparent  $|Z_0|$  which is generally unknown. In this case impedances were calculated from NEXT measurements using initial arbitrary near end terminations and then using these  $|Z_0|$  to perform the 110 ohm NEXT calculations.

The state of the unused tertiary pairs has an important effect on NEXT loss. As shown in Table 2, NEXT loss decreases approximately 23 dB if the tertiary pairs are all allowed to float. This is a direct result of an increase in coupling capacitance  $C_C$ , Equation (5).

The model, Figure 3, does not distinguish between near end and far end (FEXT) crosstalk, which is not a consideration for the short length case. For the long line, Figure 4(B), however, the far end disturbance is observed to approximate a delayed, attenuated replication of the near end disturbance. This observation can be proven theoretically without difficulty.<sup>2</sup> Therefore, assuming equal pulse losses in both disturbed and disturbing circuits for the range of rise times, NEXT and equal level far end loss (ELFEXT) are equal. For the long line, both the 40  $\mu\text{sec}$  rise time step input and the resulting near end disturbance were both attenuated about 10 dB.

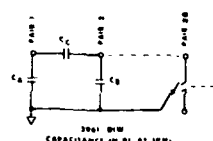
#### CAPACITANCE COUPLING

Since typical inside wiring cables generally have no metallic sheaths, capacitive coupling between two given unbalanced pairs is very sensitive to how the other pairs are used. The increase in  $C_C$  from the all-grounded to the all-floating tertiary state was implied by the sharp decrease in NEXT loss in Table 2. The increase in  $C_C$  is given explicitly in Table 3 which shows the cumulative effect on the three capacitances,  $C_A$ ,  $C_B$ ,  $C_C$ , of pairs 1 and 2 as pairs 3 through 25 are successively floated.  $C_C$  increases by more than an order of magnitude; ground capacitances  $C_A$  and  $C_B$  decrease by about 50%; mutual capacitance  $C_{mut}$  remains almost constant.

CUMULATIVE EFFECT OF FLOATING SUCCESSIVE PAIRS

Pair	$C_C$	$C_A$	$C_B$	$C_{mut}$
Floating				
All Grounded	12740	123760	119740	62774 pF
1	1561	123570	119730	62776
2	1573	123440	119730	62751
3	1660	123230	119580	62769
4	1689	123170	119540	62758
5	1722	123130	119440	62750
6	1756	122020	119370	62740
7	1841	122780	119240	62733
8	1903	122680	119100	62735
9	1986	122560	118730	62729
10	2082	122380	118470	62774
11	2231	122120	118030	62751
12	2404	121810	117500	62798
13	2600	121580	116430	62775
14	3113	120860	115260	62710
15	3795	120240	114860	62045
16	3929	119070	113400	62012
17	4756	117630	111370	61963
18	5365	115930	110620	61919
19	6716	113510	107210	61851
20	7820	110970	105140	61808
21	9568	108210	102280	61672
22	12899	97770	96560	61480
23	20170	79180	84740	60989

TABLE 3



If all ring conductors are grounded, capacitance changes that result from floating successive tip conductors are reduced considerably. Cumulative changes for this case are shown in Table 4. Coupling capacitance changes little if any, as the tip conductors are switched between ground and comparatively low impedance terminations. These data for 110 ohm terminations are given in Table 5. In this case only one tip at a time was switched between open, ground, and termination, all other tips being left grounded. As one would expect, a given  $C_c$  is affected differently by each of the tertiary tips.

CUMULATIVE EFFECT OF FLOATING SUCCESSIVE TIPS

Pairs Floating All Grounded	$C_c$ 1209	$C_a$ 123500	$C_b$ 119810	$C_{TOT}$ 22014 pf
3	1445	123420	118940	62014
4	1450	123390	118940	62012
5	1474	123250	118900	61992
6	1480	123240	118890	61993
7	1480	123240	118890	61993
8	1494	123230	118850	61994
9	1511	123200	118820	61996
10	1518	123190	118760	61985
11	1540	123170	118720	61992
12	1550	123140	118670	61982
13	1570	123130	118610	61984
14	1590	123100	118510	61971
15	1610	123070	118430	61963
16	1682	122950	118230	61954
17	1692	122880	118220	61944
18	1734	122800	118130	61941
19	1811	122650	117930	61933
20	1850	122460	117890	61916
21	1928	122320	117610	61907
22	1961	122240	117590	61881
23	1985	122000	117390	61862
24	2071	121660	117410	61820
25	2129	121390	117330	61792

TABLE 4

EFFECT OF OPENING, GROUNDING, AND TERMINATING TIP CONDUCTORS

All Tips	Open	$C_c$ Ground 1917	110 $\Omega$ Term. 1925
3	2017	1924	1925
4	1938	1925	1924
5	2020	1925	1925
6	1946	1925	1925
7	1953	1925	1925
8	1943	1925	1925
9	1978	1925	1925
10	1947	1924	1925
11	1905	1925	1925
12	1950	1924	1925
13	1952	1924	1924
14	1992	1924	1924
15	1968	1924	1925
16	2170	1923	1925
17	1937	1922	1923
18	2026	1922	1922
19	2142	1921	1922
20	2015	1920	1921
21	2166	1921	1920
22	1935	1921	1921
23	2014	1919	1921
24	2126	1918	1919
25	2014	1917	1918

TABLE 5

#### CALCULATION OF COUPLING CAPACITANCE CHANGE

Coupling capacitance between two unbalanced cabled circuits, therefore, is quite sensitive to the state of other circuits on conductors in the same sheath. Thus it is possible for the NEXT loss between two circuits to change in a dynamic way as other circuits are driven between high and low impedance effective terminations. As an advisable practice all unused conductors should be grounded, and terminating impedances should be kept as small as possible.

However, it is possible to predict coupling between circuits for a given configuration as

well as perturbations that result from configuration changes. The prediction assumes knowledge of all cable conductor to conductor capacitances. The procedure is outlined as follows.

For a system of  $n$  conductors, charges and potentials are related by the set of equations<sup>3</sup>

$$Q = K\phi \quad (6)$$

where  $Q$  and  $\phi$  are the  $(n \times 1)$  charge and potential vectors respectively and  $K$  is the  $(n \times n)$  capacitance coefficient matrix. The diagonal elements of  $K$ ,  $k_{11}, \dots, k_{nn}$ , are the conductor self capacitances, that is, the sum of all capacitances that connect node  $i$ , for example, to all other nodes including the ground node. The off-diagonal elements of  $K$ ,  $k_{ij}$ ,  $i \neq j$ , are the coefficients of induction, or simply the negatives of the coupling capacitances; in this case the capacitance is that between conductor  $i$  and conductor  $j$ . By assuming a sinusoidal potential variation and differentiating, Equation (6) becomes

$$I = j\omega KV \quad (7)$$

since

$$\frac{dq}{dt} = i(t) = Ie^{j\omega t} \quad \text{and} \quad \phi = Ve^{j\omega t}. \quad (8)$$

The first row of (7) is typical of the set

$$I_1 = j\omega [k_{11}V_1 + k_{12}V_2 + \dots + k_{1n}V_n] \quad (9)$$

from which we deduce, in general, that the capacitances from node to ground are

$$C_{i0} = \sum_{j=1}^n k_{ij}, \quad i = 1, n. \quad (10)$$

This is illustrated in Figure 5 where node voltages would be computed from Equation (7)

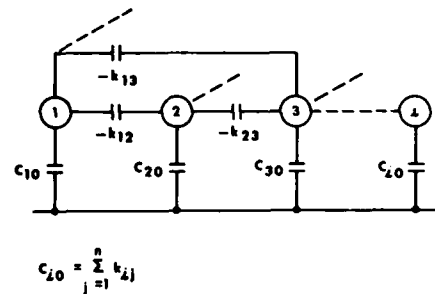


FIGURE 5

for unity input current to node i. The resulting equivalent circuit is shown in Figure 6 where a new, but unknown, coupling  $C'_{ij}$  now joins nodes i and j. Node capacitances to ground are node self capacitances,  $k_{ii}$  and  $k_{jj}$ , less  $C'_{ij}$ . Since the node voltages are known and related by simple voltage division, it follows that

$$V_j = \frac{V_i C'_{ij}}{k_{jj} - C'_{ij}} \approx \frac{V_i C'_{ij}}{k_{jj}} \quad (11)$$

since  $k_{jj} \gg C'_{ij}$ . Rearranging gives the new apparent coupling capacitance

$$C'_{ij} = \frac{V_j k_{jj}}{V_i} \quad (12)$$

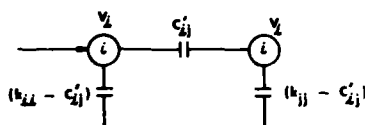


FIGURE 6

Since negligible current flows through  $C'_{ij}$  compared to that through  $(k_{ii} - C'_{ij})$ ,  $V_i$  is closely approximated by  $k_{ii}^{-1}$ . Therefore

$$C'_{ij} \approx k_{ii} k_{jj} V_j \quad (13)$$

In general, node self capacitances can be modified to show the effect of terminated tertiary.

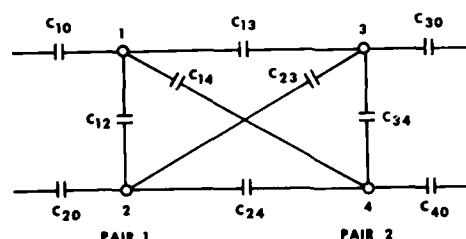
COMPARISON OF MEASURED AND CALCULATED COUPLING CAPACITANCES

Pairs Floating	$C_c$ pf Measured	$C_c$ pf Calculated
3	1561	1577
4	1573	1585
5	1660	1697
6	1689	1729
7	1722	1768
8	1756	1816
9	1861	1922
10	1903	1985
11	1986	2097
12	2062	2166
13	2231	2367

TABLE 6

Measured coupling capacitances from Table 3 are compared to calculated values, using this procedure, in Table 6.  $C_c$  is the capacitance between the tip conductors of pairs 1 and 2, beginning with no pairs floated and continuing with pairs 3 through 13 floated successively. The first calculated case requires inversion of a  $(2 \times 2)$  matrix; the last, a  $(24 \times 24)$ . Although the differences between measured and calculated capacitances increase with the number of floating pairs, corresponding crosstalk

losses using Equation (5) differ only by about 0.5 dB. Figure 7 shows one pair-to-pair combination of capacitances that were measured to permit the above predictions. There are 300 such combinations in a 25 pair cable.



10 CAPACITANCES BETWEEN 2 PAIRS AND GROUND FOR A TYPICAL MULTIPAIR CABLE

FIGURE 7

#### UNBALANCED DIGITAL TRANSMISSION CAPABILITY

Previous sections have described a pulse crosstalk model for multipair cable based on measurable capacitance. Pulse wave forms other than the linear rise time unit step can be used as easily with the model. Coupling between signal conductors increases directly as pulse rise time decreases and dramatically if unused tertiary conductors are allowed to float when the cable has no metallic sheath. Although this increase can be predicted, it is certainly more practical to avoid floating conductors and high impedance terminations. We will assume that the cable is not so misused in estimating its transmission capability based on crosstalk loss.

A cumulative probability distribution of 25 pair inside wiring cable coupling capacitance, elements  $C_{13}$ ,  $C_{14}$ ,  $C_{23}$  and  $C_{24}$  of Figure 7, is given in Figure 8. The truncated distribution indicates that about 20 percent of the conductor combinations are effectively shielded from each other by intervening tertiaries. But more importantly, the coupling between any two, non-paired signal conductors does not exceed 1.06 pf/foot for more than 5 percent of the pair combinations.

Using this value of  $C_c$  in Equation (5), assuming an effective impedance level ( $R_0$ ) of 50 ohms, a crosstalk loss objective of 20 dB, ten equal level in-phase disturbers (which means an additional 20 dB circuit separation), and a pulse bit width of  $3t_0$ , the relationship between length ( $l$ ) and bit rate ( $B$ ) is

$$l = \frac{67 \times 10^6}{B} \text{ feet.} \quad (14)$$

As a conservative estimate, therefore, we might well expect to transmit at 67 kilobits/second over 1000 feet of twisted pair cable.

COUPLING CAPACITANCE DISTRIBUTION 24 GA. IWC

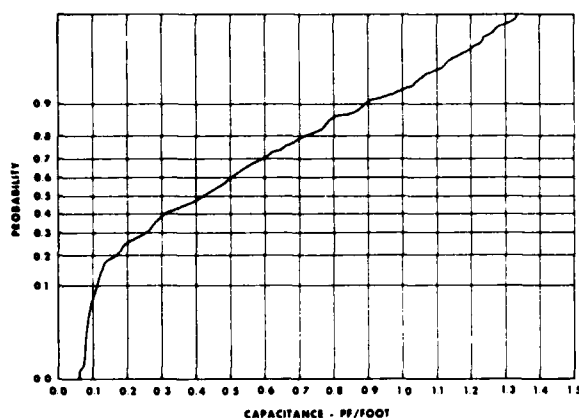


FIGURE 8

Equation (14) applies to a specific example and is not meant to define the rate/length capability of twisted pair inside wiring cable. In particular direct comparison of these results with other digital systems is inappropriate (T1 carrier is capable of transmitting 1.5 megabits/second with repeater spans of about 6000 feet) since both the transmission media and the system performance requirements may be distinctly different.

The mean, direct pair capacitance measured for the cable described in Figure 8 is 9.6 pf/ft with a standard deviation of about 1 pf/ft. Assuming therefore a maximum pair tipping capacitance of 13 pf/ft, the same coupling occurs between circuits when transmitting only 76 feet in opposite directions on both conductors of a single pair. Clearly, this is not a satisfactory solution; however the example illustrates the crosstalk penalty of using both conductors of a pair for full duplex operation or as separate circuits. In addition to maintaining pair integrity, other means for achieving a longer, usable cable length would include using a more efficient digital format as well as decreasing both the bit rate and the number of possible disturbers.

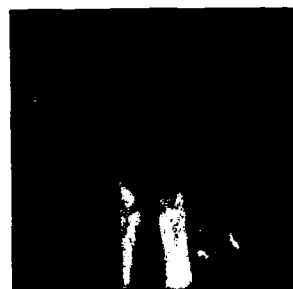
#### SUMMARY

A model has been developed that accurately predicts digital crosstalk between two unbalanced circuits in a multipair cable. Coupling is capacitive, increases directly with length and is sensitive, in a predictable way, to how the other conductors are used. A simple expression is given relating length and bit rate which can be modified easily to reflect one's own degree of conservatism.

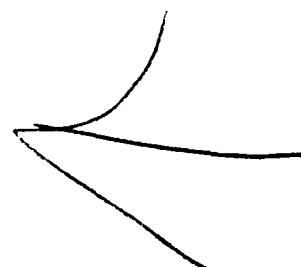
To minimize crosstalk for a given digital system and to improve performance of cabled digital circuits in general, it is important to maintain pair integrity, avoid multipoint circuit grounds and to ground unused pairs or terminate them with low impedances.

#### REFERENCES

1. Electronic Industries Association (EIA) Standard, RS-423-A, "Electrical Characteristics of Unbalanced Voltage Digital Interface Circuits," December 1978.
2. Transmission Systems for Communications, Bell Telephone Laboratories, Inc., Fourth Edition, p. 290, Western Electric Company, Inc., Winston-Salem, North Carolina.
3. Fields and Waves in Modern Radio, Ramo and Whinnery, Second Edition, p. 263, John Wiley and Sons, New York.



Dan Woodard is a Member of Technical Staff, Bell Laboratories, Norcross, Georgia.



## DESIGN AND CHARACTERISTICS OF RADIATING PAIR CABLE

N. Tago, H. Satani, Y. Miyamoto, Y. Amano

Sumitomo Electric Industries, Ltd.  
1, Taya-cho, Totsuka-ku, Yokohama, JapanAbstract

The radiation theory of sources located at a constant interval on a straight line is well known in the Leaky Wave Guide and the technique has been applied to the Leaky Coaxial Cable. In the Radiating Pair Cable (RPC), the technique is applied by twisting a cable pair at constant pitch and lay in the cable.

The expression of the radiation field of the RPC was derived and it showed that the RPC gave an optimum distribution of the source for radiation.

1. Introduction

There are several types of leaky cables now available as antennas for radio communication purposes. Generally, the electromagnetic fields provided by them are classified as follows: radiation field, surface wave propagating along the cable and induction field provided along the cable in TEM mode, etc. Table 1 shows the relation of field strength to distance from the cable and the usual operating frequency of these fields.

Table 1 Classification of electromagnetic field of leaky cables  
( $r$ : distance from cable,  $\alpha$ : constant)

Classification	Field strength	Operating frequency
Induction field	$\propto r^{-2}$	VLF ~ LF
Surface wave	$\propto r^{-1/2} e^{-\alpha r}$	HF ~ UHF
Radiation field	$\propto r^{-1/2}$	VHF ~ EHF

At an operating frequency of VHF or higher, radiating cables have the advantage that the coupling loss between them and an antenna several meters away can be 20 dB less than that of leaky cables creating surface waves. Therefore, one of the radiating cables, the leaky coaxial cable (LCX), has been providing an important function for operating VHF and UHF signals in radio communication systems such as railway radiotelephone systems or paging systems in buildings or factories.

However, the LCX suffers from handling difficulty due to its relatively large gauge. Hence,

there is a pressing demand for cables with a smaller gauge and weight that have radiation performance capabilities equivalent to those of the LCX. The radiating pair cable (RPC) has a simple structure consisting of a pair of insulated conductors, yet is capable of providing a radiation field as good as that of the LCX. This paper discusses the relationship of the cable structure to its characteristics in both theoretical and experimental terms.

2. Cable construction

Figure 1 shows an example of the RPC. Basically the cable consists of a pair of balanced conductors located at a constant distance  $D$ , twisted with a constant pitch  $P$ . The LCX, on the other hand, consists of a pair of coaxial conductors having slots located at a constant pitch  $P$  on the outer conductor.

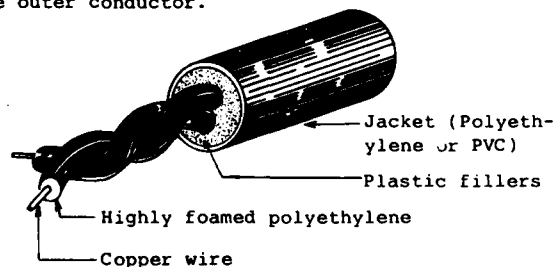


Figure 1 Construction of the Radiating Pair Cable

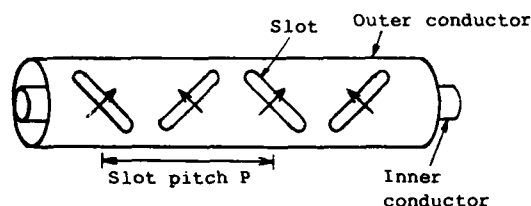
Both cables apply the same radiation principle that a periodic source distribution created by the conductor twisting or the slot arrangement provides an equiphase surface travelling away from the cable, and creates a radiation electromagnetic field (Figure 2, 3).

However, as far as the characteristics of the radiation source, with the exception of periodicity are concerned, the RPC differs from the LCX.

The slot cut on the outer conductor of the LCX diagonal to the axis of the cable generates electrical current in the azimuth direction of the cable and it provides a radiation source equivalent to that of a magnetic dipole antenna. Therefore, the LCX is considered to be an array antenna consisting of minute magnetic dipoles located at

a constant interval. On the other hand, the RPC is considered to consist of dipole antennas located contiguously and rotating their direction uniformly along the cable. These construction characteristics result in an advantage in the radiation characteristics of the RPC.

Leaky Coaxial Cable (LCX)



Radiating Pair Cable (RPC)

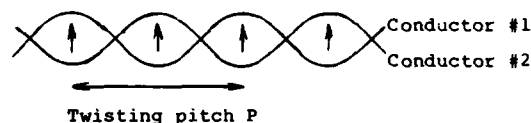


Figure 2 Basic construction of the LCX & the RPC  
(↑: Electric field)

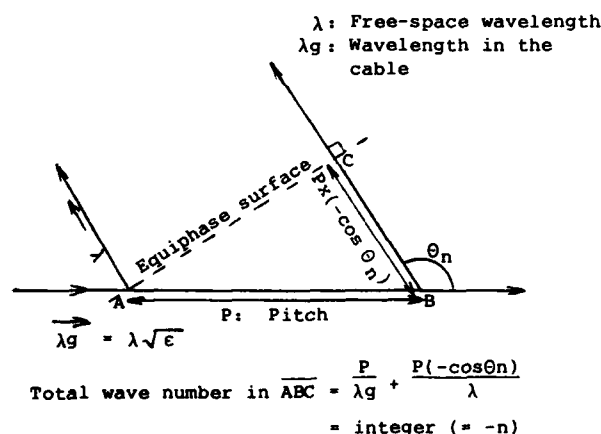


Figure 3 Equiphase surface due to the periodic source

### 3. Theoretical study of the radiation field

As known from the study of the characteristics of the LCX or from the leaky wave guide, the radiation from sources located at a constant interval along the cable forms an equiphase surface perpendicular to the direction of angle  $\theta_n$  in accordance with equation (1) (Figure 3).

$$-1 < \cos \theta_n = \sqrt{\epsilon} + \frac{n\lambda}{P} < 1 \quad (n = -1, -2, \dots) \dots (1)$$

where  $\epsilon$ : specific permittivity

It should be noted, by the way, that the radiation sources of the RPC are distributed contiguously; therefore, we shall now discuss the details of the radiation characteristics by deriving the expressions of the electromagnetic field.

First, we shall discuss the radiation field provided by the LCX, and then that provided by the RPC. We can obtain the expression for the field from the magnetic Herz-vector as follows:

$$\vec{E} = -j\omega\mu_0 \nabla \times \vec{\Pi}_m \dots (2)$$

$$\vec{\Pi}_m = \frac{1}{j4\pi\omega\mu_0} \int_{-\infty}^{+\infty} \vec{J}_m \frac{e^{-jkR}}{R} dz' \dots (3)$$

where  $\omega$ : angular frequency  
 $\mu_0$ : permeability of free-space  
 $k$ : phase constant of free-space  
 $\vec{J}_m$ : magnetic current =  $\oint \vec{n} \times \vec{E}_s dl$

$\vec{n}$ : normal vector on the outer conductor  
 $\vec{E}_s$ : electric field on the outer conductor  
 $\oint_C dl$ : circular integration along the outer conductor

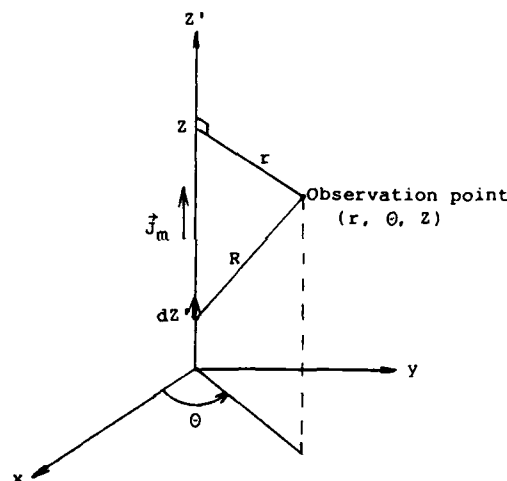


Figure 4 Coordinates (1)

The magnetic current  $\vec{J}_m$  is generated by the slots on the outer conductor of the LCX and is expressed by the delta-function due to the discontinuity of the slots. If there are  $N$  slots located at a minor interval  $P/N$  from each other and the groups of  $N$  slots are arranged at a major interval  $P$ , a particular component of  $\vec{J}_m$  can be expressed by developing the delta-function by Fourier-series as:

$$\vec{J}_m = e^{-j\beta z'} \sum_{n=-\infty}^{+\infty} e^{-j\frac{2\pi n z'}{P}} \sum_{l=1}^N \vec{J}_{ml} e^{-j\frac{2\pi n l}{N}} \dots (4)$$

where  $\vec{J}_{ml}$ : magnetic current at  $l$ th slot in the  $N$ -slots group  
 $\beta$ : phase constant in the cable

If we assume the magnetic current of the field component in azimuth direction  $E_\theta$ , which is the major component of the radiation field, is given by equation (4),  $E_\theta$  is obtained by (2), (3) as:

$$E_\theta = \sum_{n=-\infty}^{+\infty} \frac{j\zeta_n}{4} H_1^{(2)}(\zeta_n r) e^{-j\beta n z'} \sum_{\ell=1}^N J_{m\ell} e^{-j\frac{2\pi n}{N}\ell} \dots (5)$$

where  $\beta n = \beta + \frac{2\pi n}{P}$ ,  $\zeta_n = \sqrt{k^2 - \beta n^2}$ ,

$H_1^{(2)}$ : Hunkel function of the 2nd kind of the 1st order

When  $E_\theta$  provides a radiation field, the integer  $n$  must have -1 as its basic mode, or -2, -3, ... as its harmonic modes, and the frequency band is obtained as:

$$\frac{c}{P} \cdot \frac{n}{\sqrt{\epsilon+1}} < f < \frac{c}{P} \cdot \frac{n}{\sqrt{\epsilon-1}} \dots (1)'$$

(c: light velocity)

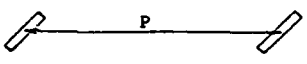
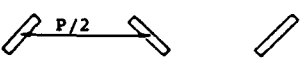
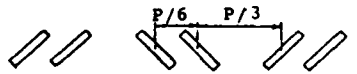
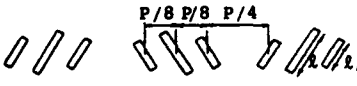
which is equivalent to (1)

From (1)', we can see that as the operating frequency becomes higher, the higher modes of  $n = -2, -3, \dots$  radiate and interfere with the basic mode due to the difference of their phase constants.

If we try to widen the operating frequency band by suppressing the higher modes, we must design the dimensions and the arrangement of the slots such that the term  $\sum_{\ell=1}^N J_{m\ell} e^{-j\frac{2\pi n}{N}\ell}$  in (5) is reduced to zero at  $n = -2, -3, \dots$  i.e. as the source intensity varies sinusoidally along the cable with a period of the major pitch.

Table 2 Typical slot arrangement and single mode frequency band of the LCX

$$(f_L = \frac{c}{P} \cdot \frac{1}{\sqrt{\epsilon+1}})$$

Slot arrangement	Single mode frequency band
 Single	$f_L < f < 2f_L$
 Zigzag	$f_L < f < 3f_L$
 6 division rectangular	$f_L < f < 4f_L$
 8 division sinusoidal	$f_L < f < 7f_L$

Thus the discontinuity of the radiation source of the LCX requires the reduction of higher harmonics of the delta-function for widening the frequency band. Table 2 shows typical slot arrangement of the LCX and the frequency band operating only in basic mode.

Next, we shall discuss the radiation field of the RPC. The expression of the field of the RPC can be obtained from the electric Herz-vector in place of the magnetic one of the LCX.

$$\vec{E} = \nabla(\nabla \cdot \vec{\Pi}_e) + k^2 \vec{\Pi}_e \dots (6)$$

$$\vec{\Pi}_e = \frac{1}{j4\pi\omega\epsilon_0} \left[ \int_{-\infty}^{\infty} \frac{e^{-jkR_1}}{R_1} ds_1 - \int_{-\infty}^{\infty} \frac{e^{-jkR_2}}{R_2} ds_2 \right] \dots (7)$$

where  $\epsilon_0$ : permittivity in free-space

$$I: I_0 e^{-j\beta z'}$$

(We assume  $I_0$  to be a constant in order to simplify the problem)

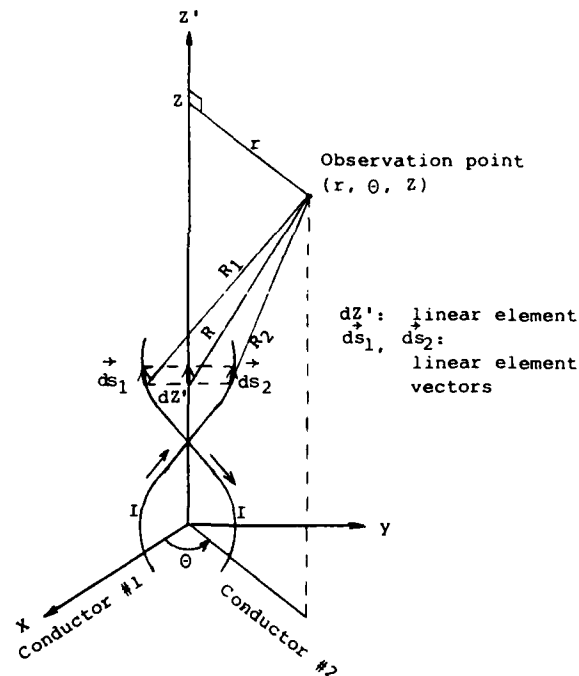


Fig. 5 Coordinates (2)

If the distance of conductors D is much smaller than wavelength  $\lambda$  and the distance between the cable and observation point R, (7) results as

$$\vec{H}_e = \frac{I_0}{j4\pi\omega\epsilon_0 P} \int_{-\infty}^{\infty} \left[ i\vec{z} \frac{r}{R^3} \cos\left(\frac{2\pi}{P}Z' - \theta\right) + \frac{i\vec{\theta}}{R} \cos\left(\frac{2\pi}{P}Z' - \theta\right) - \frac{i\vec{r}}{R} \sin\left(\frac{2\pi}{P}Z' - \theta\right) \right] e^{-j(kR + \beta Z')} dZ' \dots (8)$$

where  $i\vec{z}$ ,  $i\vec{\theta}$ ,  $i\vec{r}$ : unit vectors in the Z,  $\theta$ , r-direction

and (6) results as

$$E_z = -\frac{I_0 e^{-j(\beta Z + \theta)}}{4\omega\epsilon_0} \cdot \frac{D}{P} \zeta \beta H_1^{(2)}(\zeta r) \dots (9)-1$$

$$E_\theta = -\frac{I_0 e^{-j(\beta Z + \theta)}}{4\omega\epsilon_0} \cdot \frac{D}{P} k^2 H_0^{(2)}(\zeta r) \dots (9)-2$$

$$E_r = \frac{I_0 e^{-j(\beta Z + \theta)}}{4\omega\epsilon_0} \cdot \frac{D}{P} (\zeta^2 + k^2) H_0^{(2)}(\zeta r) \dots (9)-3$$

where  $\zeta = \sqrt{k^2 - \beta_{-1}^2}$ : phase constant in radial direction

$$\beta_{-1} = \beta + \frac{2\pi}{P}(-1)$$

$H_0^{(2)}$ : Hankel-function of the 2nd kind of the zero order

When we compare the field expression of the RPC (9) with that of the LCX (5), we see that there exist no higher modes of  $n = -2, -3, \dots$  and, that there exists only a single basic mode in the case of the RPC.

So the interference from the higher modes no longer occurs and the RPC requires no construction modification like that of the slot arrangement of the LCX to widen the frequency band.

This advantage is due to the source distribution of the RPC. When we compare the Herz-vector of the RPC (8) with that of the LCX (3), we see that the source distribution of the RPC corresponding to that of the LCX is

$$I_0 \frac{D}{P} \cos\left(\frac{2\pi}{P}Z' - \theta\right) e^{-j\beta Z'} \text{ and } I_0 \frac{D}{P} \cos\left(\frac{2\pi}{P}Z' - \theta\right) e^{-j\beta Z'} \dots (10)$$

which is a sinusoidal source distribution, an optimum one that has no higher harmonic. Such a source distribution of the RPC is related to its construction. Because the electric current source of the RPC is laid helically along the conductors, an azimuth component in a particular direction ( $\theta = \text{const.}$ ) is seen to vary sinusoidally along the cable.

The frequency band of a single mode of the RPC is equal to that of the basic mode.

$$f_L = \frac{c}{P\sqrt{\epsilon+1}} < f < \frac{c}{P\sqrt{\epsilon-1}} = f_H \dots (11)$$

Table 3 shows the frequency band widths calculated by (11) and those of the LCX in Table 2.

Table 3 Frequency band width of a single mode radiation

$$(f_L = \frac{c}{P\sqrt{\epsilon+1}})$$

Cable	Specific permittivity and slot arrangement etc.....	Frequency band width
RPC	$\epsilon = 4$ (Solid PVC insulation)	$2f_L$
	$\epsilon = 2.3$ (Solid PE insulation)	$4f_L$
	$\epsilon = 1.44$ (Highly foamed PE insulation)	$10f_L = \frac{2}{\sqrt{\epsilon-1}} f_L$
	$\epsilon = 1$ (Air insulation)	$\infty$
LCX	$\epsilon = 1.23$ , Single arrangement	$f_L$
	$\epsilon = 1.23$ , Zigzag arrangement	$2f_L$
	$\epsilon = 1.23$ , 6 division rectangular arrangement	$3f_L$
	$\epsilon = 1.23$ , 8 division sinusoidal arrangement	$6f_L$

The RPC can obtain a wider frequency band than the LCX by the use of a low-permittivity insulation.

#### 4. Radiation characteristics

##### 4.1 Frequency characteristics

The frequency characteristics of the radiation field strength can be calculated from equation (9). However, we shall calculate the coupling loss as a practical value in place of the field strength. The coupling loss  $C_L$  is defined by

$$C_L = -10 \log \frac{P_r}{P_t} = -10 \log \frac{\lambda^2 |G| |E|^2}{4\pi Z_0 I_0^2 Z} \dots (11)$$

where  $P_t$ : the power propagating along the cable  
 $P_r$ : the power received by an antenna  
 $G$ : the absolute gain of an antenna  
 $Z_0$ : free-space impedance  
 $Z$ : characteristic impedance of the cable

By the approximation  $|H_m(\zeta r)^{(2)}| = \sqrt{\frac{2}{\pi \zeta r}}$ , we can obtain the expression of coupling losses relating to azimuth and axial components  $E_\theta$ ,  $E_z$  of the electric field.

$$\begin{cases} C_{L\theta} = -10 \log_{10} \frac{GD^2}{8C^2 \epsilon \beta^2 P^2 Z Z_0 \zeta r} \dots (13)-1 \\ C_{Lz} = -10 \log_{10} \frac{GD^2}{32\pi \epsilon_0^2 P^2 Z Z_0 f^2 r} \dots (13)-2 \end{cases}$$

Next, we normalize the operating frequency  $f$  as

$$f_N = [f - (f_L + f_H)/2] / (f_H - f_L)$$

then (13)-1, (13)-2 are written as

$$\begin{cases} C_{L\theta} = 10 \log_{10} \sqrt{1-4f_N^2} + A\theta \dots (14)-1 \\ C_{Lz} = 10 \log_{10} \frac{f^2}{\sqrt{1-4f_N^2}} + AZ \dots (14)-2 \end{cases}$$

where  $A\theta$ ,  $AZ$ : constants

Numerical calculations and measured values of the trial cable are shown in Figures 6 and 7; The comparison between them shows good agreement. The trial cable corresponds to a lower-coupling-loss grade in the LCX, the coupling losses of which range between 50 dB and 80 dB in the case of 50 mm cable or between 60 dB and 80 dB in the case of the smaller diameters.

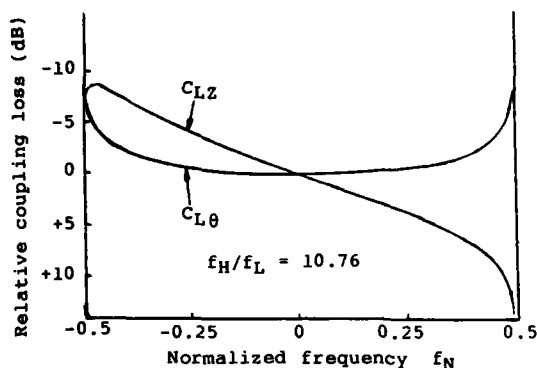


Figure 6 Frequency characteristics of coupling loss (calculation)

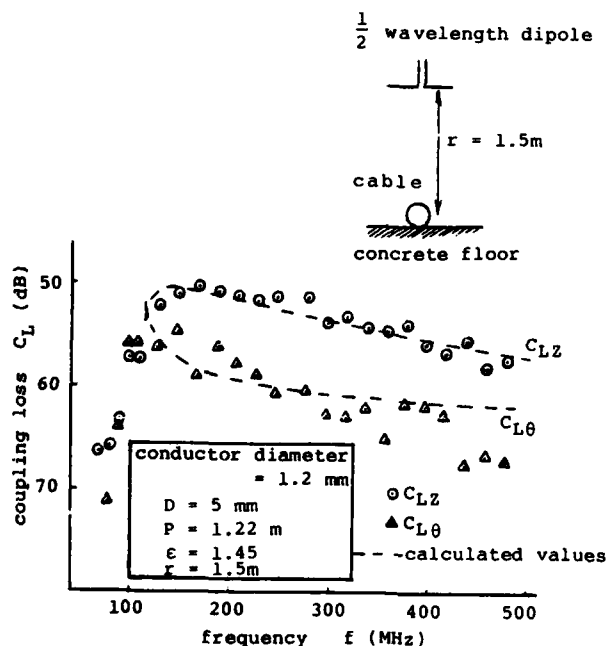


Figure 7 Frequency characteristics of coupling loss (measured)

#### 4.2 Attenuation in free-space

The radiation field of the RPC attenuates in free-space as does that of the LCX, which radiates on the basis of the same principle, i.e. the attenuation of the field strength is expressed by the Hunkel-function in (9), the magnitude of which is inversely proportional to the square root of the distance  $r$  if  $r$  is large enough. As shown in Figure 8, the trial cable provides a radiation field nearly proportional to  $r^{-1}$ . Therefore we can take a longer distance from an antenna to an RPC or an LCX than to other leaky cables such as a cable operating surface wave.

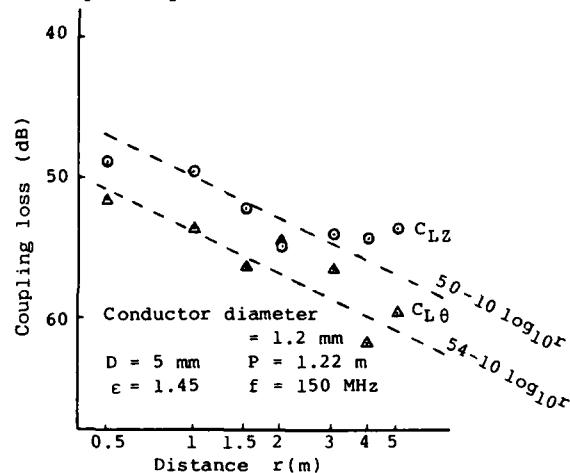


Figure 8 Attenuation in free-space

#### 4.3 Relation between cable dimensions and radiation characteristics

In the case of the LCX, we can design the relative radiation power by controlling the intensity or distribution of the source by varying the length or arrangement of the slots. In the case of the RPC, the radiation characteristics depend on the dimensions of the conductor interval  $D$  and the twisting pitch  $P$ .

##### (1) Conductor interval $D$

If the parameters except  $D$  are fixed, (13) is written as

$$C_{L\theta} \text{ or } C_{LZ} = -10 \log D^2 + A \dots\dots (16)$$

(A: constant)

and we see that the radiation power is proportional to the square of  $D$ . The result corresponds to the fact that the radiation power of the electrical dipole is proportional to square of  $D$ . The measured coupling loss relating to  $D$  is shown in Figure 9 and coincides with equation (16).

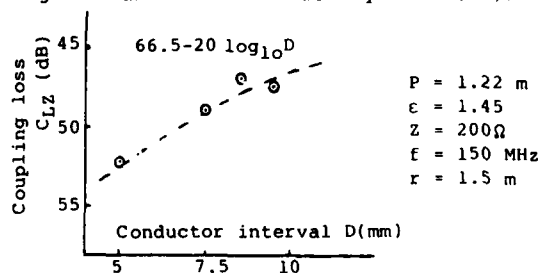


Figure 9 Coupling loss vs. conductor interval

## (2) Twisting pitch P

When we discuss the relation of the twisting pitch P to the radiation power, attention must be paid to the operating frequency because the pitch P determines the frequency band. If the parameters except the pitch P and the frequency f are fixed, equation (13) is written as

$$C_{L\theta} = 10 \log P + B_{\theta}(fP) + A_{\theta}' \quad \dots\dots\dots(17)-1$$

$$C_{LZ} = 10 \log P + B_Z(fP) + A_Z' \quad \dots\dots\dots(17)-2$$

where  $A_{\theta}'$ ,  $A_Z'$ : constants

$$B_{\theta}(fP) = 10 \log \frac{2\pi}{C} \sqrt{(fP)^2 - (\sqrt{\epsilon} fP - C)^2}$$

$$B_Z(fP) = 10 \log \frac{C}{2\pi \sqrt{(fP)^2 - (\sqrt{\epsilon} fP - C)^2}}$$

As shown in equation (11), the operating frequency band is inversely proportional to P, so we shall discuss the problem under the following condition.

$$f = V/P \quad (V: \text{constant}) \quad \dots\dots\dots(18)$$

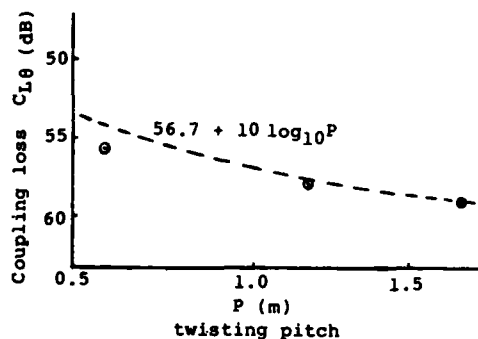
Then  $B_{\theta}$  and  $B_Z$  become constants, and (17)-1 and (17)-2 are written as

$$C_{L\theta} \text{ or } C_{LZ} = 10 \log P + A' \quad \dots\dots\dots(19)$$

( $A'$ : constant)

From equation (10) we see that the radiation power is inversely proportional to the twisting pitch P.

This result means that conductor twisting with pitch P in the RPC is equivalent to slot arranging with pitch P in the LCX. The measured coupling loss relating to P is shown in Figure 10 and coincides with equation (19).



D = 5 mm  
Conductor diameter = 1.2 mm  
 $\epsilon = 1.45$   
f.P = 272 MHz.m  
r = 1.5 m

Figure 10 Coupling loss vs. twisting pitch

## 5. Transmission loss

In addition to the radiation characteristics, the transmission loss should be discussed for the case of leaky cables. Since the RPC is not a shield-type cable like the LCX, it couples with the conductors outside more easily. This coupling causes the generation of the modes which propagate outside the cable and attenuate more greatly than does the original mode of the cable. Therefore, the transmission loss of the RPC increases greatly when installed along metallic bodies or a concrete floor. Besides, the increasing by radiation as occurs in any radiating cable and which is expressed in the form of the radiation resistance per unit length as

$$R_r = \frac{2\pi r |E|^2}{10^2 Z_0}$$

Figure 9 shows the transmission loss of the trial cable. We see from the figure that the influence of environment upon the transmission loss must be considered in the whole system design:

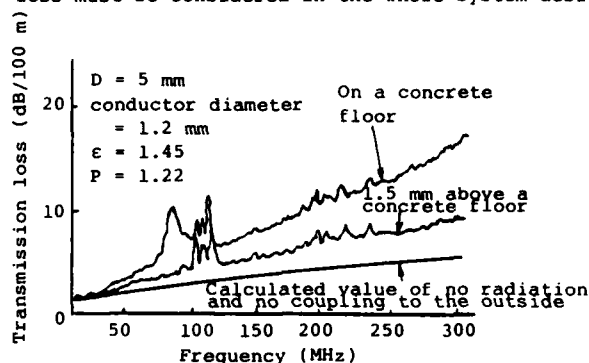


Figure 11 Transmission loss of the RPC

## 6. Conclusion

The trial cables were fabricated for use at a frequency band range of 120 ~ 300 MHz. They provide a low coupling loss and other characteristics as shown in Table 4. Since the cables are of the balanced type of 200Ω, the diagram of a basic system structure is as shown in Figure 12.

By making good use of its light weight and small diameter, the RPC cable may be applied in many kinds of systems, such as the wired-wireless telemonitoring of an electrocardiogram in a hospital.

Table 4 Dimension and electrical characteristics of the trial cables

Cable diameter (mm)	14	20
Cable weight (kg/m)	0.15	0.30
Conductor diameter (mm)	1.2	2.0
Conductor interval (mm)	5.0	8.5
Coupling loss at 150 MHz (dB)*	55	50
Transmission loss at 150 MHz (dB/100 m)	10	7
Characteristic impedance (Ω)	200	200

(\*) antenna:  $\frac{1}{4}$  wavelength dipole in azimuth direction 1.5 m apart

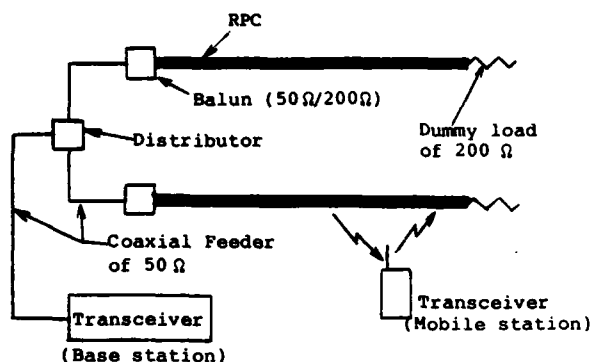


Figure 12 Diagram of the RPC system

#### References

- (1) N. Kurauchi et al.: "Wideband Leaky Coaxial Cables" Paper of IECE of Japan, Vol. 54-B No. 11, 1971



Noriyuki Tago  
Sumitomo Electric  
Industries, Ltd.  
1, Taya-cho, Totsuka-ku,  
Yokohama, Japan

Noriyuki Tago received a B.S. degree in Electronics and Communication Engineering from Waseda University in 1980. Then he joined Sumitomo Electric Industries, Ltd., and is at present in charge of development and designing of communication cables. He is a member of the Institute of Electronics & Communication Engineers of Japan.



Yoshio Miyamoto  
Sumitomo Electric  
Industries, Ltd.  
1, Taya-cho, Totsuka-ku,  
Yokohama, Japan

Yoshio Miyamoto received a B.S. degree in Electrical Communication Engineering from Osaka University in 1968. Then he joined Sumitomo Electric Industries, Ltd., and is now manager of Communication System Engineering Section, Communications Division. He is a member of the Institute of Electronics & Communication Engineers of Japan.



Hiroshi Satani  
Sumitomo Electric  
Industries, Ltd.  
1, Taya-cho, Totsuka-ku,  
Yokohama, Japan

Hiroshi Satani received a B.S. degree in Electrical Engineering from Himeji Institute of Technology in 1981. Then he joined Sumitomo Electric Industries, Ltd., and is at present in charge of industrial engineering of communication cables.



Yoshikazu Amano  
Sumitomo Electric  
Industries, Ltd.  
1, Taya-cho, Totsuka-ku,  
Yokohama, Japan

Yoshikazu Amano received a B.S. degree in Electrical Engineering from Osaka University in 1968. Then he joined Sumitomo Electric Industries, Ltd., and is now manager of Communication Cable Engineering Section, Communications Division. He is a member of the Institute of Electronics & Communication Engineers of Japan.

# NEW QUALITY ASSESSMENT PROCEDURE FOR EXCHANGE AREA CABLE TRANSMISSION PARAMETERS

P. Allen Link

Bell Telephone Laboratories  
Holmdel, N. J.

## ABSTRACT

To best represent the customers' needs, a method of evaluating the transmission quality of exchange area cable must have representative requirements, a statistically powerful method of evaluating the conformance of cables to the requirements and a means of combining the results in a fashion that reflects the end use of the product. The method described herein utilizes a requirement structure containing nominal and maximum requirements to define a desirable distribution for each parameter. The evaluation technique uses variables test data and a continuous, quadratic penalty function to measure how well the produced cable population is centered with respect to the nominal requirements and stays within the maximum levels. Finally a quality rating procedure combines the results for the parameters into "LOSS" and "NOISE" scoring classes that reflect the impact of deviations on the telephone company. The method provides for the best technical and economic representation of quality for the customer because it inspires the production of a very consistent, predictable media, provides the user with known quantities for precise engineering and application and evaluates the quality on the basis of how the product is used.

## INTRODUCTION

The transmission quality of exchange area cable is of primary importance to the telephone companies. Huge quantities of cable are installed each year with a trend towards more and more sophisticated services. Having a known, consistent, predictable media is necessary to be able to efficiently and accurately engineer and provide the circuits necessary for these services.

Consistent, predictable transmission parameters are achieved with good design and good process controls. However, knowing if the design and process have achieved and can maintain the quality needs of the customer requires an effective quality assessment procedure that reflects those needs.

The quality assessment approach described herein reflects the telephone companies needs by means of three contributing parts: a comprehensive requirement structure, a statistically powerful means of evaluating cable parameters to that structure

and a means of combining the individual results in a fashion that reflects the impact of deviations on the telephone company.

## REQUIREMENT STRUCTURE

The foundation for any good quality assessment procedure is a comprehensive set of technical requirements. The requirements are the reference points that define acceptable or unacceptable performance of the product. Thus it is important that both the levels specified for each parameter and the structure or manner in which each parameter is defined reflect how the product is used.

For exchange area cable, individual transmission parameters are typically specified in terms of cable average and individual pair or conductor requirements. The cable average requirement is important because it reflects the average contribution of the individual cable when spliced into an end-to-end circuit. The individual pair or conductor requirements are important from the standpoint of controlling variation within a cable. This minimizes unsatisfactory performance of individual circuits.

The important issue here is determining how best to use the cable average and individual levels to structure each requirement. One way is to specify only maximum levels. This structure anticipates that the cable average and individual pairs or conductors will always be somewhere at or below the maximum levels. This is not the best structure from the telephone companies viewpoint. The nature of the product going into the field should be more closely defined. A far superior structure is one that specifies nominal cable averages as well as maximum (and minimum) cable averages and individual pair or conductor levels for each transmission parameter. This is the general requirement structure used by Bell Laboratories.

Figure 1 illustrates the Bell System requirement structure for four basic transmission parameters and compares it to the REA structure for the same parameters. For mutual capacitance the Bell System and REA structures are essentially the same. Both have nominal levels, maximum cable average levels and individual pair levels. The REA has a minimum cable average for all cables while the Bell System has a minimum on pulp insulated cables only. For the other three characteristics, the REA specifies only maximum levels while the Bell System requirements include nominal levels. The individual

FIGURE 1

## COMPARISON OF CABLE REQUIREMENTS

CHARACTERISTIC	BELL REQUIREMENTS	REA REQUIREMENTS
MUTUAL CAPACITANCE	CABLE NOMINAL (83 nf/mi) CABLE MAX. AVG. (87 nf/mi) INDIV. PR. MAX. (1% > 92)	CABLE NOMINAL (83) CABLE MAX. AVG. (87) PR. RMS DEV. (3%)
CONDUCTOR RESISTANCE	CABLE NOMINAL INDIV. COND. MAX.	NONE INDIV. COND. MAX.
RESISTANCE UNBAL.	CABLE NOMINAL (1.1%) CABLE MAX. AVG. (1.5%) INDIV. PR. MAX. (5.0%)	NONE CABLE MAX. AVG. (1.5-2.0%) INDIV. PR. MAX. (4-5%)
CAPACITANCE UNBAL.	CABLE NOMINAL (105-120) CABLE MAX. AVG. (180-210) INDIV. PR. MAX. (1000)	NONE CABLE MAX. AVG. (175) INDIV. PR. MAX. (800)

values for Bell System and REA requirements are essentially the same for mutual capacitance and resistance unbalance. REA individual conductor resistance maximums are about 1.0 percent higher for 22 and 24 gauge and slightly higher for 26 gauge conductors. Bell System capacitance unbalance maximum levels are higher than REA levels. However, as this paper will show, the presence of a nominal requirement is more important to the customer.

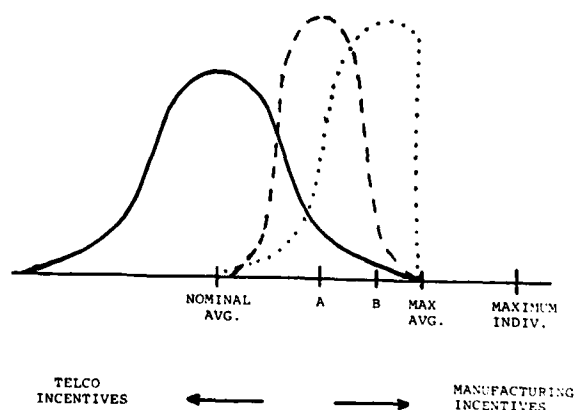
The specification of nominal levels and control to them result in important advantages for the telephone company. The nominal level provides a benchmark or central value for the population of manufactured cables and therefore reflects the ultimate transmission performance of concatenated cables in the field. For example, when numerous cable lengths of different resistances from a population centered at the nominal level are spliced together in the field, the individual end-to-end circuits will average the nominal level of resistance and have relatively small deviations from it. A quality program that controls the process to the nominal requirements helps to provide a consistent, uniform product with predictable transmission performance. This allows the telephone company to optimize its engineering and application of exchange area cable and therefore its costs.

Figure 2 illustrates why the adherence to nominal levels can be cost effective for the telephone company. The solid line distribution represents the desirable situation for any particular transmission parameter. The population of cables is centered around the nominal and essentially all cables are below the maximum cable average requirement. Circuits made by splicing together cables from this population will average the nominal level with only small deviations from it. The dashed-line distribution and the dotted-line distribution represent less desirable situations that can occur if transmission parameters are not controlled to nominal requirements. Both are the typical result of strong economic incentives for the supplier to save copper and plastic. In the dashed-line case, the supplier simply improves control of the process to decrease the spread in cable averages (less

process variation). In the dotted-line case, the supplier uses extensive inspection to screen out cables exceeding the maximum requirement. Of course, a combination of both situations is also possible. In each case, the average level of a parameter of the cable population and therefore the average level of end-to-end circuits can be significantly higher than the nominal level as indicated by the A and B levels on the chart.

In the undesirable cases described, the telephone company does not have a predictable number to use for engineering purposes. Without control to nominal levels the transmission parameters will most likely be somewhere between the nominal and maximum specified levels. If the telephone company engineers circuits to Bell System nominal levels, they have the risk of circuits not performing as expected. Without the nominal level and control to it, the level assumed for engineering can only be a guess.

Nominal cable average requirements are advantageous to the telephone companies for a number of additional reasons.

FIGURE 2  
ECONOMICS

1. The network now in existence has been designed using nominal cable requirements. Additions should be consistent with past cable transmission parameter levels or the value of the past investment is diluted.
2. Most equipment intended for use on the network has been designed assuming nominal levels for the cable.
3. Decreasing system margins make it more important for the telephone companies to know transmission parameter levels with more precision. For example, there has been an average 3 db deterioration in the noise environment since 1964. The deterioration is even more pronounced on long rural loops. Higher resistance design rules and the use of electronic telephone sets has added hundreds of ohms to loop resistances compared to past applications.

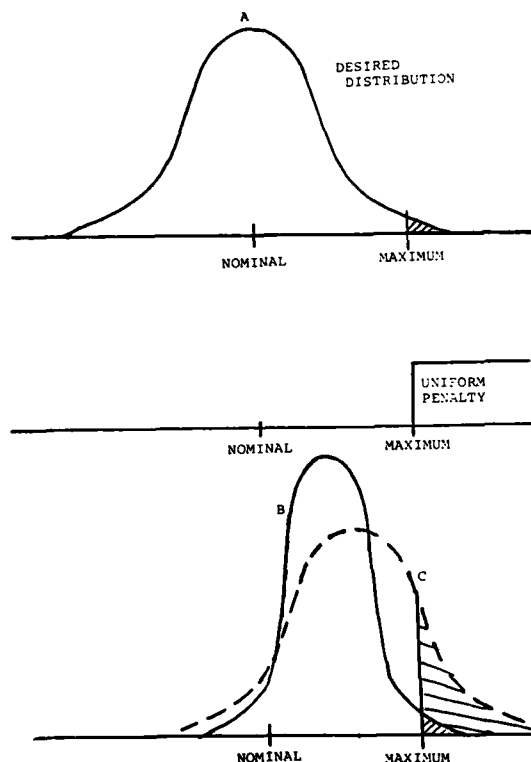
#### EVALUATION TECHNIQUE

The evaluation technique is the manner in which individual cable test results are compared to the requirement structure. It should make the comparison in a fashion that leads to an accurate picture of the quality of the cable population being shipped. At the same time, it should be statistically powerful so that a minimum amount of data is required to obtain the quality picture. Both objectives are achieved in this evaluation technique by use of cable average distributions, variables data and a continuous, quadratic penalty function.

The requirement structure contains both cable average and individual pair or conductor requirements. For quality assessment purposes, cable averages are better indicators of quality than individual pair or conductor readings from both a use and manufacturing viewpoints. As described in the previous section, splicing numerous cable lengths together in the field creates an averaging effect on end-to-end circuits. Because of this the cable average better reflects the contribution of an individual cable to the quality of field performance. A high individual pair in one cable length may not be noticed after splicing and it will add only a little to the average. Many high pairs will significantly shift the average and will affect field performance. During manufacturing, the individual conductors in a particular cable are taken from a stock that was manufactured over a period of time. Thus the collection of individual readings in the form of the cable average is a better indication of the overall cable manufacturing process than just the maximum individual readings.

Variables data are important to this evaluation technique because it provides statistical power and a measure of conformance of cable average distributions to the requirements. Figure 3 illustrates why it is best to use variables test results. The top distribution (A) is a desirable one since it is centered on the nominal level and has very little area over the maximum average requirement. The penalty function typically used with attributes

FIGURE 3  
EVALUATION TECHNIQUE



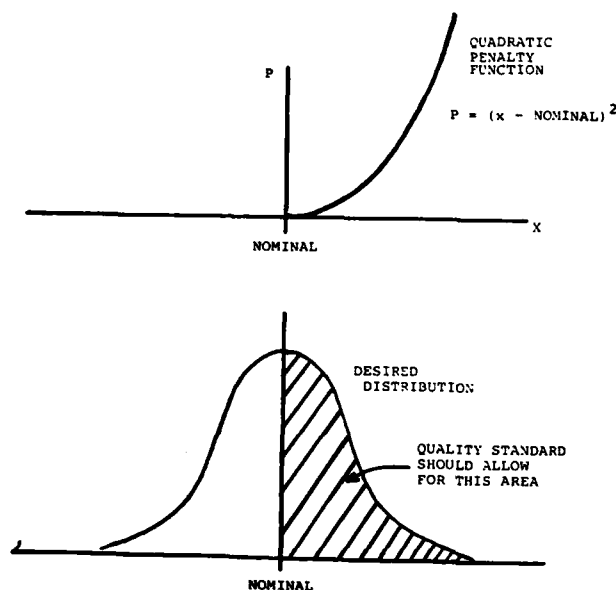
data is the uniform one directly below distribution A. It assesses a fixed number of penalty points for each cable that exceeds the maximum requirement. Since this is usually a very small percentage, the quality decision is often based on a few cables that exceed a maximum instead of the entire population. It has no sensitivity to the nominal level or where the great majority of cables are with respect to the nominal or maximum levels. It can determine the difference between distribution A and distribution C since there is a larger percentage of cables exceeding the maximum in C. However, it cannot distinguish between distributions A and B (or the three distributions in Figure 2) since the percentage exceeding the maximum requirement is the same for each. Notice that the center of the distributions and therefore the ultimate circuit performance can be quite different for distributions A, B and C.

The actual variables test results can be used to accurately evaluate the quality of the cable average distribution if the continuous quadratic penalty function, shown in Figure 4, is used. Each measured cable average is assessed a penalty according to its distance from the specified nominal requirement. The penalty is equal to the distance squared:  

$$\text{PENALTY} = (\text{MEASURED AVERAGE} - \text{NOMINAL})^2$$

This provides a very strong incentive for the

FIGURE 4  
EVALUATION TECHNIQUE



manufacturer to control the cable process at the nominal level. Small deviations are assessed little, but large deviations generate very large penalties.

The quadratic penalty function was chosen because it best represents the cost of having quality different from a distribution centered at the nominal. There is no added cost to the telephone company when cables are at the nominal. Also, the cost increase for small deviations from the nominal are small. But large deviations from the nominal can be quite expensive. Thus, if we use a Taylor Series expansion of a general cost function  $f(x)$ :

$$f(x) = f(x_0) + (x-x_0)f'(x_0) + \frac{1}{2} (x-x_0)^2 f''(x_0) + \dots$$

if  $f(x_0) = 0$

and  $f'(x_0) = 0$

Then  $f(x) = c(x-x_0)^2$

For purposes of this quality assessment procedure, it was decided to use a single sided penalty function instead of a double sided one. While a double sided function is possible, it becomes a bit more complicated mathematically and all manufacturing cost incentives tend to prevent excessive deviations below the nominal levels.

#### APPLICATION OF THE EVALUATION TECHNIQUE

How can one use the quadratic penalty function to determine the quality of the shipped cable population? The simplest method would be to add the penalty points for all cables sampled or measured. While this would provide a relative measure from one lot to another, it does not provide an understandable, intuitive result. A better method is to normalize the penalty points by means of a quality standard. Since the requirement structure defines a distribution centered at the nominal requirement, the right half of the distribution is expected to exceed the nominal. Therefore, penalty points must be expected for those cables exceeding the nominal level. As shown on the bottom of Figure 4, the average number of points expected per cable can be used as a quality standard. If the assessed level of points for each sampled (measured) cable is divided by the standard to form an index, we have a simple, understandable measure of how each cable contributes to the overall level of quality for the produced distribution. Thus for any single transmission parameter:

let  $x_i$  = observed parameter for cable  $i$

$$f(x_i) = \text{penalty function} = (x_i - \text{nominal})^2$$

$m$  = number of cables sampled

$$P_i = f(x_i) = \text{penalty assessment}$$

$y^*$  = quality standard or expected penalty for a cable from the desired distribution

For each  $x_i$  an index is formed

$$I_i = \frac{P_i}{y^*} = \text{index for cable } i$$

$$\bar{I} = \frac{1}{m} \sum_{i=1}^m I_i = \text{quality index for all cables tested}$$

$$s^2 = \frac{1}{m} \sum_{i=1}^m (I_i - \bar{I})^2 = \text{sampling variance for } \bar{I}$$

By the Central Limit Theorem,  $\bar{I}$  is distributed normal with mean  $\theta$  (the true index) and variance  $\sigma^2$  (the true sampling variance). This means that the quality index for each parameter is distributed normally regardless of the underlying distribution of the parameter. Being able to characterize the distribution of the index in this manner is quite helpful when and if any statistical tests are performed on the results.

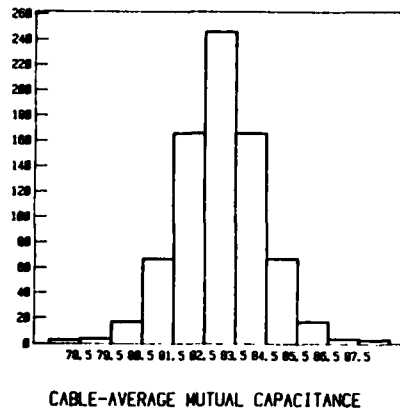
#### THE QUALITY STANDARD

The quality standard was described as the expected penalty assessment for a cable from the distribution defined by the requirement structure. Using

FIGURE 5

## THE QUALITY STANDARD

## • ACCEPTABLE DISTRIBUTION



the terminology of the previous section:

$$y^* = E(p_1 | \text{desired distribution}) = \frac{1}{2} \sigma^2$$

This calculates to be one half the variance of the desired distribution for any given parameter. Figure 5 illustrates how the quality standard is generated with a discrete example. The histogram shows a typical distribution for mutual capacitance in a well controlled process. The distribution is centered at the nominal (83nf/mile) and has approximately 0.3% of the cables exceeding the maximum of 87nf/mile. Since we are using a single sided penalty function, all cables (503 of them) at or below 83nf/mile receive zero penalty. However, 166 cables have averages that are one nf from the nominal. Each is assessed a penalty of  $(1)^2 = 1$  penalty point or 166 total. Sixty-seven cables have average capacitances two nf/mile from the nominal. Each of these is assessed  $(2)^2 = 4$  penalty points for a total of  $4 \times 67 = 268$ . And so on for all cables to the right of the nominal requirement. A total of 726 penalty points are expected for the 760 cables in the distribution. Thus the average penalty expected per cable is  $726/760 = 0.96$ . This is the quality standard. It is in close agreement with the theoretical standard (in the continuous case) of 0.98.

In this evaluation technique the quality standard is a direct calculation from the requirements. There is no judgement involved other than assuming a reasonably small tail of the distribution allowed to exceed the maximum requirement. Selecting 0.3% in this example does not mean we condone 0.3% defective in all situations. It is only deemed acceptable if the cable population for the parameter in question is centered at or below the nominal requirement. This ensures that the concat-

## • CALCULATE ASSESSMENT

$0 \times 503 =$	0
$[84 - 83]^2 \times 166 =$	166
$[85 - 83]^2 \times 67 =$	268
$[86 - 83]^2 \times 17 =$	153
$[87 - 83]^2 \times 4 =$	64
$[88 - 83]^2 \times 3 =$	75
TOTALS	760    726

$$726 / 760 = 0.96 \quad \text{QUALITY STANDARD}$$

## • IN THE CONTINUOUS CASE

$$\sigma = 1.4$$

$$\frac{\sigma^2}{2} = 0.98 \quad \text{QUALITY STANDARD}$$

tenated cables will be within limits.

QUALITY RATING STRUCTURE

Comparing the test results for a cable parameter with the appropriate quality standard provides an index that measures any individual cable against the expected penalty assessment. Adding the indices together for all cables tested in a given time period for a parameter provides an estimate (I) for how well the produced population compares to the desired distribution of cable averages. Given accurate requirements, this should reflect the ultimate performance of the cable with respect to that parameter.

At this point we must decide if the best measure of the cable quality is achieved by evaluating each parameter separately. Do the parameters best reflect customer use when evaluated independently? If parameters are combined, how should they be combined and with what relative weights? Theoretically it is easy to combine the normally distributed indices.

Let  $j = 1, 2, \dots, n$  parameters

$W_1, \dots, W_n$  = weights for the parameters

$\bar{I}_j$  = quality index for parameter  $j$

$S_j^2$  = sampling variance for  $\bar{I}_j$

then

$$\bar{I} = \sum_{j=1}^n W_j \bar{I}_j = \text{composite quality index}$$

$$y_n^2 = \sum_{j=1}^n w_j^2 s_j^2 = \text{composite sampling variance}$$

Evaluating the parameters separately achieves the best sensitivity to each parameter. Often this is difficult to administer and provides too detailed a picture. On the other hand, combining results can introduce masking of a problem with an individual parameter. Thus combinations must be made in a manner that minimizes the masking problem.

For exchange area cable, the four transmission parameters in Figure 1 are the key indicators of transmission quality. (D. C. conductor resistance, resistance unbalance, mutual capacitance and capacitance unbalance to ground.) There are four potentially feasible ways to evaluating transmission quality with these parameters.

1. each parameter evaluated separately
2. all parameters combined
3. unbalances combined and resistance and capacitance combined (noise and loss)
4. resistance parameters combined and capacitance parameters combined.

From the manufacturing viewpoint, options one and four are more sensitive to the process. Resistance and resistance unbalance are controlled by the wire drawing process while capacitance and capacitance unbalance are controlled by the insulating, cabling and jacketing processes. Evaluating the parameters in this manner would be most sensitive to an individual process change.

From a telephone company viewpoint, the best option is number three. Cable circuits are primarily engineered and installed on the basis of loss. Resistance alone determines how far the telephone company can go and still ring a telephone. However, resistance and capacitance together determine attenuation and therefore how well a signal will be transmitted. This also provides for a minimum of masking since some resistance and capacitance tradeoffs can be made without significantly affecting loss. Figures 6 and 7 illustrate the relative effects of conductor resistance (CR) and mutual capacitance (CM) on voice frequency loss with the other at nominal. Figures 8 and 9 provide the same comparison for carrier frequencies. The charts show that similar shifts in capacitance and resistance have the same relative effects on loss. Thus masking is minimized if these parameters are combined with a 50-50 weighting.

A similar situation holds for the combination of resistance unbalance and capacitance unbalance. Both affect noise and therefore telephone company maintenance costs. Figures 10 and 11 show the relative effects of the two unbalances on noise metallic. As in the loss category, similar changes in either parameter have the same relative effect on noise. Therefore, the combination is an accurate reflection of the effect of deviations on

the telephone company. Masking is minimized with a 50-50 weighting for the combination.

The loss-noise ratings are superior to the other options for a number of reasons. The primary reason is that it most accurately reflects the telephone company use of the product. Evaluating each parameter separately does not reflect possible tradeoffs. Evaluating all parameters together is insensitive to the loss and noise differences. Using the resistance/capacitance combinations (option 4) allows masking between parameters that do not affect the customer in the same way. For example, high conductor resistance could be masked by good resistance unbalance. One could have a noise-free circuit over which the signal cannot be transmitted due to high loss.

#### QUALITY RATING IMPLEMENTATION

The quality rating structure uses the results of the evaluation technique to generate quality indices for LOSS and for NOISE. What do these indices mean? The index for LOSS is an estimate of the conformance of the shipped cable population to the specified resistance and capacitance requirements. If the index is 2.0 it is an indication that the costs may be twice as much as at the quality standards. But the index is generated from a relatively small number of sampled cables from that population. There is sampling error to be considered. Since the indices are distributed normally, it is an easy task to perform a variety of statistical tests on the estimate (index). For example, using the index and the estimated sampling variance, one can perform a simple hypothesis test to determine if the index is statistically different from the desired level of 1.0. In the Bell System, the index and variance are analyzed using the Quality Measurement Plan which includes past results to obtain long-run quality estimates as well as estimates for the most recent time period (rating period) of data collection.

Sample sizes for this quality assessment procedure are calculated using a variety of inputs - including costs for field defects, costs for inspection, the probability of poor quality (based on past results), production levels and quality standard levels. For most processes, sample sizes between 25 and 50 cables per rating period provide very satisfactory sensitivity in the results.

#### CONCLUSIONS

The consistency and predictability of transmission media for present and future telephone company applications can be quite important. The telephone companies should be aware that there can be significant differences in the requirements from different cable suppliers. Also, even with the same requirement structure, there can be significant differences in the quality of the cables received. This paper has demonstrated that both a good requirement structure and an effective quality evaluation are necessary. Without specified nominal requirements and the quality tools to enforce them, the telephone companies cannot safely

FIGURE 6  
RESISTANCE EFFECT ON ATTENUATION

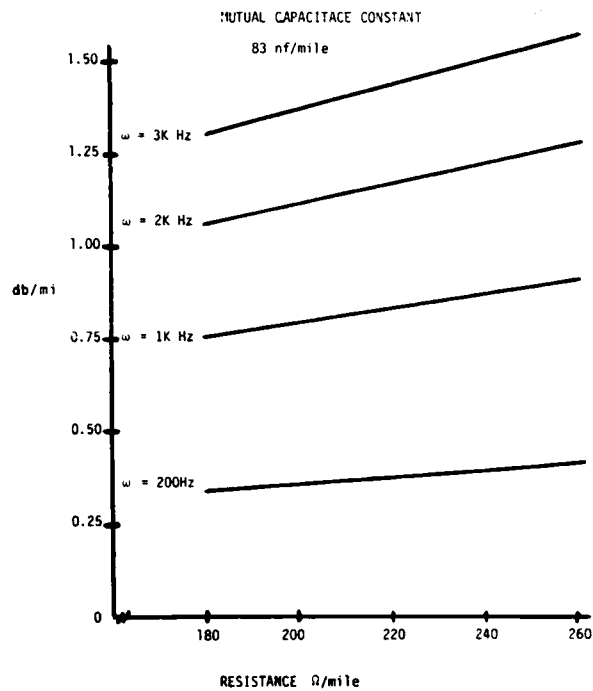


FIGURE 8  
RESISTANCE EFFECT ON ATTENUATION

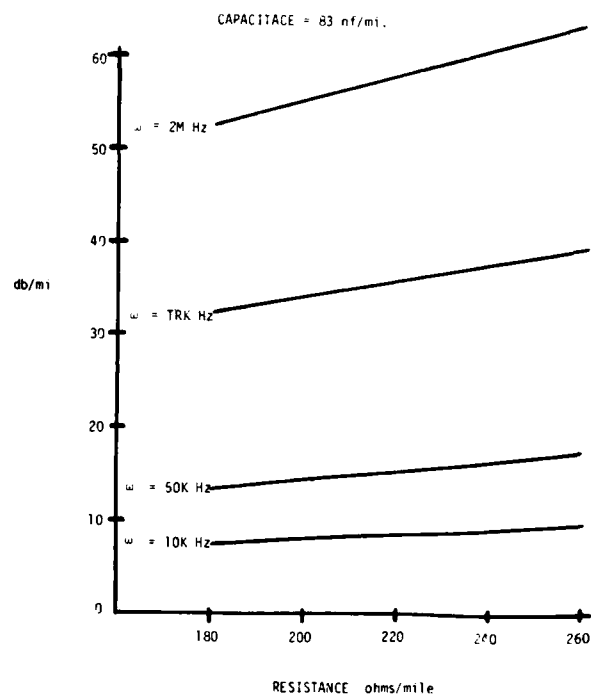


FIGURE 7  
CAPACITANCE EFFECT ON ATTENUATION

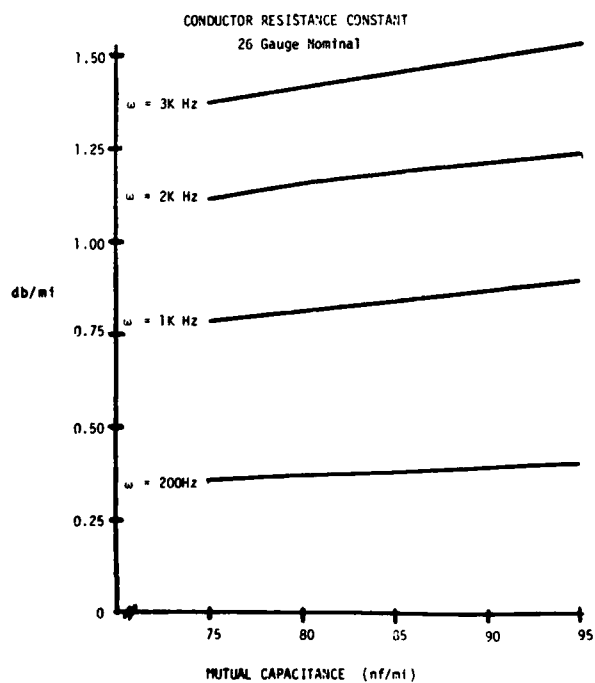


FIGURE 9  
CAPACITANCE EFFECT ON ATTENUATION

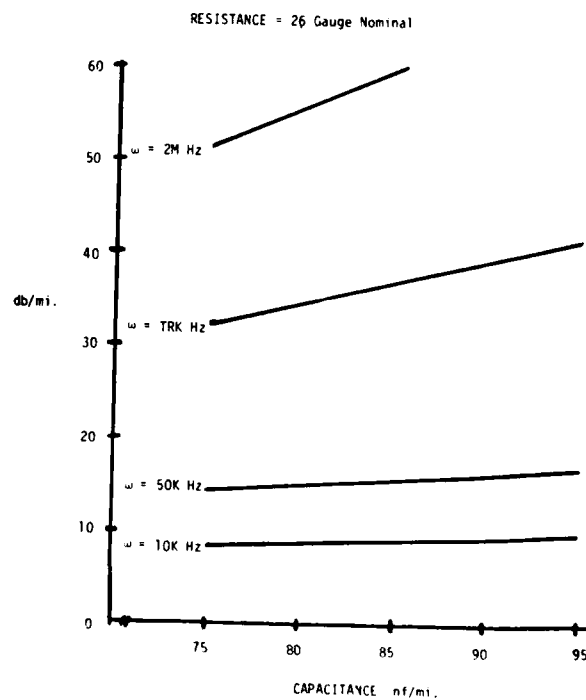


FIGURE 10

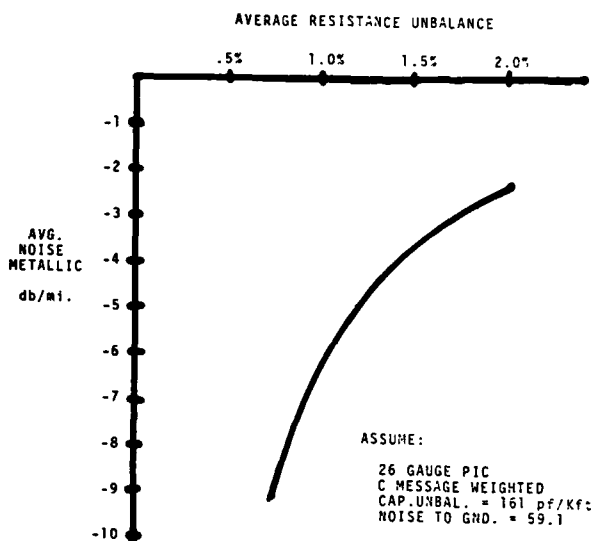
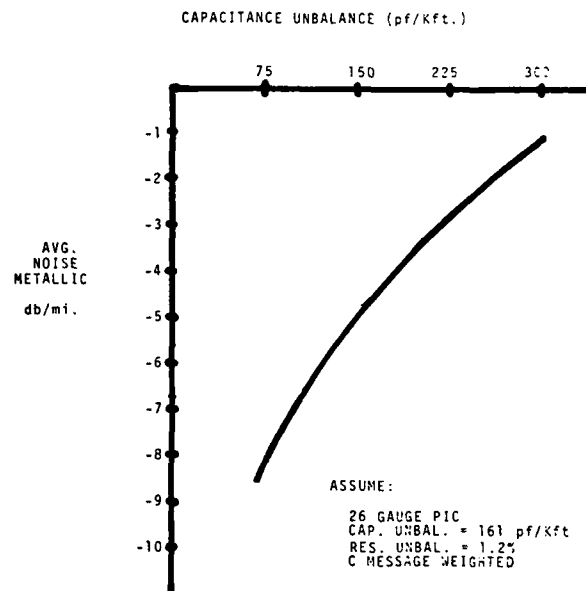
EFFECT OF RESISTANCE UNBALANCE ON NOISE

FIGURE 11

EFFECT OF CAPACITANCE UNBALANCE ON NOISE

assume values for transmission characteristics that will provide precise, economic engineering and use of cables. These same tools provide valuable information to suppliers concerning the adequacy of the manufacturing process.

ACKNOWLEDGEMENTS

The original concept and theory for this procedure was developed by M. S. Phadke. The theory was applied and developed into a viable procedure by P. E. Plsek. Ms. G. C. Miranda provided the analyses for the weighting factors.



P. Allen Link  
Bell Telephone Labs  
Crawford's Corner Road  
Holmdel, N. J. 07733

Mr. Link received a BSEE degree from Lafayette College in 1968 and an MS degree in Systems Engineering and Operations Research from the University of Pennsylvania in 1970. Since joining Bell Laboratories in 1968 he has been involved in the development of quality assurance procedures and standards for cable and wire, outside plant, lightguide, microwave radio, undersea cable, protection, PBX and digital carrier systems. Presently he is supervisor of the Transmission Systems Group of the Quality Assurance Technology Center.

BELL SYSTEM LIGHTGUIDE CABLE INTERCONNECTION EQUIPMENT,  
CENTRAL OFFICE TO CUSTOMER PREMISES

Manfred R. Gotthardt

Bell Laboratories  
Norcross, Georgia

ABSTRACT

Lightguide cable interconnection equipment furnishes the interface between outside plant and central office, remote terminal, or customer premises transmission equipment. Primarily, the interconnection equipment provides a convenient centralized access point for cabled optical fibers, lightguide cable sheath termination, and other functions such as; fiber organization, fiber storage, and the accommodation of splices and connectors.

Since the installation of the first Bell System lightwave system, several different types of interconnection equipment units have been developed. These provide an interconnection capability from the central office to customer premises. Described in this paper are the design approaches taken to develop this equipment and short descriptions of the units.

INTRODUCTION

Historically, interfacing with outside plant and the interconnecting of lines and trunks have been an integral part of common telephone systems. Main distributing frames, trunk span terminating frames, trunk distribution frames, etc., are all a necessary link in connecting to the "outside world". In today's lightwave systems, lightguide cable interconnecting equipment (units) provide the same basic connectivity to outside plant cables. The need for these units was established with the introduction of the first Bell System lightwave system.

Since 1979, numerous installations of lightguide cable interconnection equipment units have been made in the Bell System FT3, FT3C, and Fiber SLIC-96® lightwave digital transmission systems. Most recently, applications of these units in building distribution systems have also been accomplished.

From the beginning the overall guiding criteria applied to the development of this equipment were to achieve a high degree of flexibility, a high connector density, an uncomplicated working vehicle, and a minimum number of cabinet designs.

LIGHTGUIDE CABLE INTERCONNECTION EQUIPMENT -  
GENERAL

Lightguide cable interconnection equipment consists of a series of single cabinets, which may vary in size relative to their optical fiber organizing and storing functions and their single fiber cable interconnection capacities.

The main functions of this equipment are to:

- provide a convenient interface between outside plant and central office cabling
- provide a central test access point to outside plant optical fibers
- permit rapid rearrangement among transmission equipment and outside plant optical fibers
- provide transition hardware to fanout optical fibers from cabled fiber ribbon configurations
- provide for organized optical fiber slack and splice storage
- provide a single fiber cable interconnection panel.

Two cabinets designed to be used with ribbon-based cables have a modular optical fiber fanout unit to achieve a high connector density per cabinet size. The cabinets are as follows:

- A. Lightguide Cable Interconnection Terminal (LCIT), Figure 1.
- B. Lightguide Cable Interconnection Equipment (LCIE), Figure 2.

The fanout unit shown in Figure 3, is used with ribbon-based cables to fanout the fibers contained in the ribbons. The front face of a fanout unit contains twelve biconic connectors, each connector providing access to a fiber residing in the ribbon. Connection to the cable ribbon is accomplished through a short ribbon "lead" which is stored within the fanout unit.

Three cabinets designed for stranded cable applications use fiber slack and splice storage slide-out trays in place of fanouts. These three cabinets are:

- C. Lightguide Stranded Cable Interconnection Equipment (LSCIE), Figure 4.
- D. Lightguide Stranded Cable Interconnection Terminal (LSCIT), Figure 5.
- E. Lightguide Stranded Cable Interconnection Module (LSCIM), Figure 6.

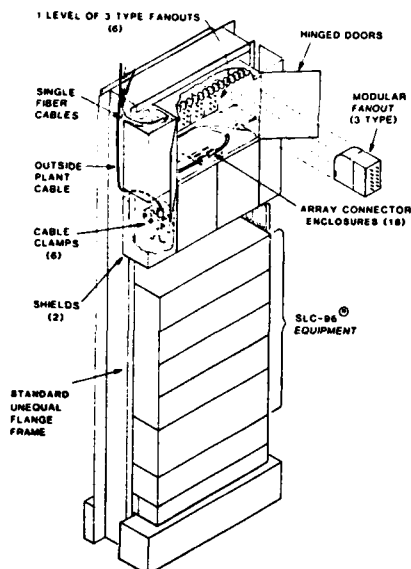


FIGURE 1. LIGHTGUIDE CABLE INTERCONNECTION TERMINAL (LCIT), 2 LCITs SHOWN

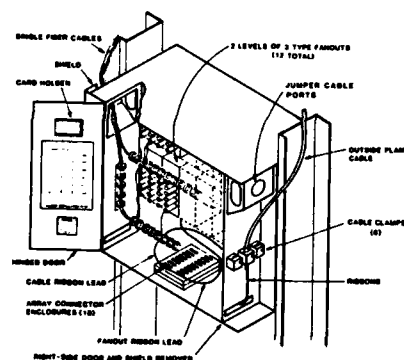


FIGURE 2. LIGHTGUIDE CABLE INTERCONNECTION EQUIPMENT (LCIE)

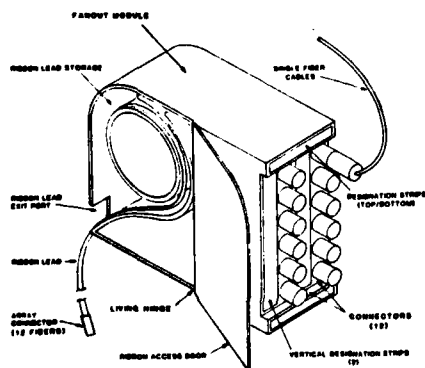


FIGURE 3. 3 TYPE FANOUT, LIGHTGUIDE (TYPICAL)

## DESCRIPTIONS OF THE CABINETS

### A. Lightguide Cable Interconnection Terminal (LCIT)

The Lightguide Cable Interconnection Terminal, refer to Figure 1, is a metal cabinet which may be frame mounted on a standard unequal flange frame, or wall mounted. It is optionally available in a front only cabinet access configuration or a central office mounting configuration with standard front and rear cabinet access.

Primarily designed for installations in controlled environments, i.e., Mini-huts, Maxi-huts, or Controlled Environmental Vaults, the LCIT can also be installed in outdoor Community Service Cabinets.

Six outside plant cables can be terminated in an LCIT of 11 inches in height, 21 inches in width, and 12 inches in depth. A total of six fanouts can be mounted corresponding to a total of six ribbons or seventy-two fiber connections. An eighteen position array connector storage platform provides six positions for fanout-to-cable ribbon connections, and twelve positions for cable ribbon-to-cable ribbon "splice throughs". The connectors (biconic sleeve type) mounted on the fanouts form the interconnection "array" for subsequent single fiber cable (jumper) connection.

### B. Lightguide Cable Interconnection Equipment (LCIE)

The Lightguide Cable Interconnection Equipment, refer to Figure 2, has the same general features as the LCIT but differs in vertical size and connection capacity. The height of the LCIE is 18 inches and provides for the interconnection of 144 fibers using 12 fanouts.

One LCIE and six Wavelength Division Multiplex (WDM) cabinets (a full 3 channel WDM, FT3C filter system) can be mounted on a single seven foot tall frame. Without WDM, up to a maximum of three LCIEs may be mounted on a single frame, providing an interconnection capacity of 432 fibers.

The LCIE uses the same array connector storage platform as the LCIT, but in this case twelve positions are used to connect fanout-to-cable ribbons and the other six positions are reserved for "splice throughs".

Exploded view diagram of a fiber optic patch panel assembly. The diagram shows the following components and their assembly relationships:

- STANDARD PATCH PANELS**: The main front panel of the assembly.
- WIRE LAMP**: A component on the left side of the panel.
- WIRE**: A component at the bottom left of the panel.
- JUMPER CABLE PORTS**: Ports on the back of the panel.
- JUMPERS**: Cables connecting the ports.
- DOWNHOLE REINFORCEMENT FOR CLAMP**: A reinforcement piece at the bottom right.
- OPTIONAL HYPERCONDUCTOR PANELS (SEE CONNECTIONS WIRE)**: An optional component at the bottom right.
- SLIDE OUT BRACE TRAY**: A tray at the bottom right.
- SPICES**: A component at the bottom right.
- FIBER**: A component at the bottom right.
- POWER SWITCH SLOT**: A slot at the bottom right.
- POWER SWITCH**: A switch at the bottom right.

Diagram illustrating the components of a cable splice tray assembly, showing the exploded view of the tray and its mounting hardware. The components are labeled as follows:

- OUTSIDE PLANT CABLES
- JUMPER CABLE PORTS
- CABLE CLAMP (10)
- PLASTIC SHIELDS
- TRAY ENTRY
- TRAY
- SPICES
- BLADE OUT SPICE TRAYS (10)
- DOOR REMOVED FOR CLARITY
- SPICE TRAY CONNECTION PANEL (11) CONNECTION SIDE
- TRAY ENTRY SLOT
- JAMPER

Diagram illustrating the rear view of the unit, showing cable connections and dimensions. Key components and labels include:

- OUTSIDE PLANT CABLES
- CABLE CLAMPS (1)
- FIBER ENTRY
- JUMPER CABLE PORTS
- FIBERS
- SPICES
- WAVE OUT SPICE TRAY (1)
- OPTIONAL INTERCONNECTION PANEL (SEE INSTRUCTIONS TOP)
- ONLY IF CONNECTIONS ARE SHOWN
- FOR DOWN DOOR REMOVED FOR CLARITY

Dimensions are indicated: 18" (width), 12" (depth), and 6" (height).

The module has a single slide out splice tray and an optional cable interconnection panel.

Up to four outside plant cables can be terminated whenever the module is installed on 23 inch or wider frames and up to two cables can be terminated on 19 inch frames.

An option to add two more splice trays to increase the module capacity to seventy-two splices is also available. This option is in lieu of the interconnection panel option.

The module's flexible and adaptable mounting arrangements along with its other attributes have already found application in building distribution systems as well as remote terminals.

#### SUMMARY

All the equipment designs provide exceptionally flexible mounting arrangements and qualify for international CCITT standard frame mounting. All cabinets feature adaptability and compactness.

With this equipment and associated splice closure apparatus optical fiber connectivity and accessibility is provided from the central office to the customer's premise.



Manfred R. Gotthardt is a Member of the Technical Staff, Lightguide Joining Group, Bell Labs, Norcross, Georgia, where he is responsible for the development of lightguide cable interconnection and distribution equipment used in central offices, repeater stations, remote terminal loop applications, and customer premises. His earlier work at Bell Labs consisted of designing circuits for Remote Line Concentrators, the Electronic Switching System #1 (ESS #1) Master Control Center, and writing and testing system maintenance programs for those systems. He was also involved in the installation and test of the initial ESS #1, and supervised the operational activities related to ESS#1 system laboratory models. He has a Bachelor of Science in Industry and Technology from Northern Illinois University (NIU), has done graduate work at NIU and Georgia State University, and has been granted two patents. He is a member of the IEEE.



## TERMINATION OF CYLINDRICAL GROOVED OPTICAL CABLES

A. BOUVARD\* - J.P. HULIN\* - M. de VECCHIS\* - W. POULSON\*\*

\*THOMSON C.S.F./L.T.T. - CONFLANS Ste HONORINE - France

\*\*RAYCHEM - CERGY PONTOISE - France

### ABSTRACT

A zero loss termination system adapted to cylindrical grooved (or slotted core) cables is described that provides individual protection of each fibre at a breakout point without the need to cut or splice the fibres.

Applications of this device are described, for example, the design of termination subassemblies (cable termination boxes, distribution frames, drop terminals) in the French wired city of BIARRITZ, cable splicing organization including high density cables and various subassemblies for videocommunication networks.

### INTRODUCTION

The cylindrical grooved (or slotted core) cables that have been developed from 1976 <sup>1 2 3</sup> are characterized by an easy access to the fibres located on the grooves at the periphery of the cylindrical unit.

In order to keep all the advantages of this cable design, in particular to avoid any remaining microbending effect on the fibres, primary coated fibres are directly used for the cable construction, without any further protection in intimate contact with the fibres. In particular, there is no secondary coating or buffering and no tubing of the fibres in the cable.

A further protection of the fibres is usually required at any termination or breakout point of the cables. Even if it is actually possible to use directly in these cases primary coated fibres, for example, inside a protective housing, it is much more convenient to add some protection to the fibres, that can avoid for example breakage due to contact with sharp edges. A good protection is given by small loose tubes protecting individual fibres.

This paper describes the termination device that carries out the change of structure (slotted core to individual loose tubes).

### DESCRIPTION OF THE DEVICE

The device is made by a holding cylinder in which the protective tubes are inserted, which is placed at the end of the unit. The cylinder and the tubes are blocked at the extremity of the unit by a heatshrinkable sleeve (figure 1).

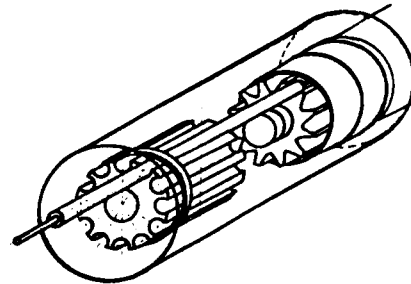


Figure 1 - Schematic of the termination device

In order to avoid the need to cut or splice the fibres at the breakout point, the protective tubes are slid over the fibres. The 10 tubes corresponding to the 10 fibres of a unit are placed at the same time. This can be done over a length up to few meters, either manually or by using some of the tools that have been developed for the mass splicing process adapted to the cable structure <sup>3 4</sup>.

Identification means are included for example color coding of the tubes.

### TECHNOLOGY

The design parameters of the ten fibre termination system were to provide a strong mechanical joint to the cable core at the breakout from the ten fibre unit. The joint had to be capable of withstanding both lateral and longitudinal stresses and shocks during handling. The initial length of protection required for the fibres was set 1.2 m. The termination should also withstand 160 hours of thermal cycling between - 20°C and + 60°C without measurable change in the fibre attenuation. In addition for economic reasons, it was necessary to minimise the component count and simplify installation to be compatible with available skills and installation training facilities.

The kit consists of four basic components. First a cylindrical thermal barrier in a radiation cross-linked modified polyolefine material which is aligned partly on the thermoplastic jacket of the cable and partly over the prestripped grooved core of the cable.

A high temperature polyvinylidene fluoride alignment barrel is then slid over the central steel strain bearing core of the 10-fibre unit butting against the core.

Mechanical protection for the fibres is provided by ten colour coded precision extruded protection tubes in an irradiation stabilized fluoropolymer, which are simultaneously slid over the primary coated fibres. The tubes are pushed home under the thermal barrier previously installed which thus provides additional protection at the critical transition point of the fibre from its path in the cable to the breakout direction parallel to the cable core.

The ten tubes are then clipped into the alignment barrel leaving only two mechanical joints to complete the termination.

These two joints are made simultaneously by a small one piece termination sleeve in irradiated polyolefin tube with Olefin co-polymer based thermoplastic adhesive inserts at each end. The termination sleeve is prepositioned on the cable before the previous steps and brought into position for the final installation so that one insert aligns with a recess in the alignment barrel, the other over the core of the cable.

Installation using a hot air temperature controlled pistol then shrinks the termination sleeve and fuses the adhesive inserts. The first insert joins the termination sleeve, fibre protection tubes and the alignment barrel. The second insert joins the same heat shrinkable termination sleeve to the protection tubes and to the grooved core.

The termination thus forms a thermally stable joint independant of longitudinal stress in the steel strength member of the cable. Increase of diameter is kept to less than 10 % compared with the cable unit. The use of colour coded protection tubes facilitates the identification of fibres. The basic design is easily adaptable to other configurations of slotted core cable.

The figure 2 shows the thermal barrier, the alignment barrel and the termination sleeve. The complete termination system is shown in figure 3.



Figure 2 - Main parts of the device



Figure 3 - Termination system

### APPLICATIONS

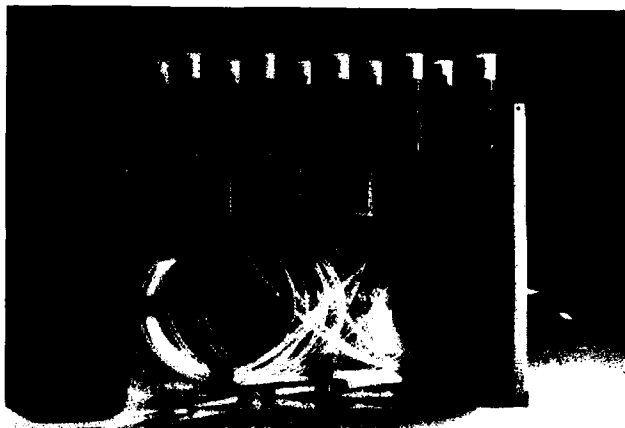
This device has been extensively used in the network of BIARRITZ, the French wired city. The optical distribution network has a star structure using 70-fibre feeder cables, 10-fibre distribution cables and 2-fibre optical drop cables. The drop terminals, which are installed on the outside or in the basement of apartment buildings, or at a suitable roadside points in individual housing areas, are located at the extremity of a distribution cable that contains a single 10 fibre slotted core unit. An inner box holds the termination system with loops accomodating slack individual fibres. These fibres are terminated by single fibre connectors for the connection to the 2 fibre drop cables. In that case, the connectors are adapted to the dimensions of the protective tube to provide continuous protection. Each drop terminal can serve up to 5 subscribers. The figure 4 shows a drop terminal.



Figure 4 - Drop terminal

The termination device and the corresponding 10 connectors are at first installed, and the inner box is closed. Then, subscribers are served when necessary by connecting a drop cable.

The same termination device is used for the distribution frame at the extremity of the 10 fibre units. The same basic concept is used to fan out the cable unit and to permit single fibre connections (figure 5).



**Figure 5 - Distribution frame**

The distribution frame are located in the side part of a standard SOTELEC 80 rack.

More generally, the same termination device has been used in any case where it was needed to change the structure from the 10-fibre unit to individually protected fibres. For high count fibre cables made by stranding several 10-fibre units together, each unit is terminated by this device.

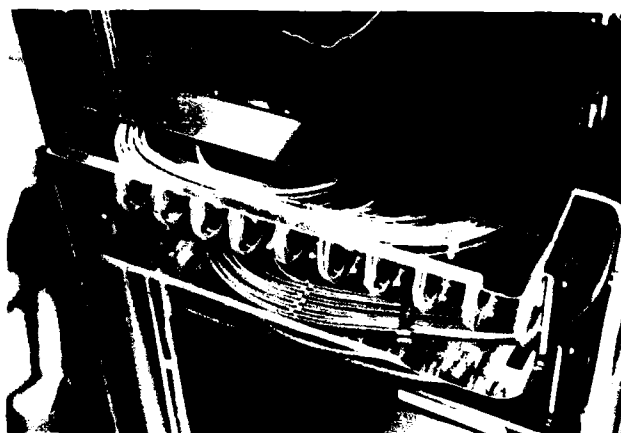
For example, a distribution frame accommodating 140 fibres in one rack giving a completely universal interconnection matrix has been developed. The 10 fibres of a unit are accommodated in a sliding box in which the lengths of monofibre patch cords needed for interconnection purposes are individually looped. The fanning out of the 10-fibre unit is made in the sliding box by using the termination device (figure 6) and the joining between individually protected fibres and single fibre patch cords is made by connectors mounted in the front wall of the sliding box (figure 7).

An other important application of this termination device is in the cable splicing. In the mass splicing process that has been developed for the slotted core cables<sup>4</sup>, a grooved support is used that has three main functions :

- protection of fibres,
- identification of fibres,
- precise positioning for the butt joint.

The first two functions can be performed by the termination device and the splicing of fibre is then done by any traditional individual process. This method can be used when the mass splicing process is not applicable for example with monomode fibres or in subscriber loop networks where rerouting may be required.

**10-fibre sliding box for distribution frame :**



**Figure 6**



**Figure 7**

The splice is made by using one organizer tray per cable unit. The cable unit is clamped at one corner of the organizer tray and a termination device is applied. The individual fibres are looped into the tray. This loop provides for subsequent recabling or rerouting.

The final splice is made by stacking the organizer trays. The cable units are looped between the trays. The overall protection is provided by a commercial splice closure. A 70-fibre cable splice is about 700 mm long and 220 mm in diameter (figure 8).



**Figure 8 - 70-fibre cable splice**

### CONCLUSION

A termination device adapted to slotted core cable has been described that provides individual protection of each fibre at a breakout point without the need to cut or splice the fibres. This device is used in various subassemblies of the network of BIARRITZ, the French wired city, such as distribution frames and drop terminals. An other possible application is in cable splicing.

### REFERENCES

- 1 G. LE NOANE :  
"Optical fibre cable and splicing technique"  
2th ECOC - PARIS - Sept. 1976 - pp. 247-252.
- 2 G. LE NOANE - M. de VECCHIS :  
"Further developments on compartmented fibre optic cable structure and associated splicing technique"  
IOOC - TOKYO - July 1977 - pp. 355-358.
- 3 M. de VECCHIS - J.P. HULIN - J.C. STAATH :  
"Ultra low loss cables using the cylindrical V-grooved structure"  
I.W.C.S. - CHERRY HILL - Nov. 1981 - pp. 228-235.
- 4 A. BOUVARD - J.P. HULIN :  
"Results on field operation of a mass splicing process"  
7th ECOC - COPENHAGEN - Sept. 1981 - paper 7.3.
- 5 R. FRANCOIS - M. TRIBOULET - M. DUPIRE -  
D. CAPOROSI - J.L. POPOVICS :  
"Optical fibres in subscriber loop networks"  
Commutation & Transmission - N° 2/3 - June 1982.



**Michel de VECCHIS** was born in 1946. He received his engineer degree from Ecole Nationale Supérieure des Télécommunications, PARIS, in 1969. He joined L.T.T. in 1970 and was first engaged in research and development work in the field of microwave components and sub-systems. From 1974, he worked on optical fibre cables and systems. He is now the technical manager of L.T.T. Cable Division.



**Jean Pierre HULIN** was born in 1946. He received his engineer degree from Ecole d'Electricité et de Mécanique Industrielle (Ecole Violet), PARIS, in 1971. After some years devoted to production of special purpose cables, he joined L.T.T. fibre optic group in 1977. He has been the head of optical fibre cable and splice group and is now the assistant technical manager of L.T.T. Cable Division.



**André BOUVARD** was born in 1945. He joined L.T.T. in 1968 and has been engaged in the mechanical problems of transmission equipments. He joined the fibre optic group in 1979 and has been in charge of splicing and connectorization problems. He is now responsible of the definition of industrial processes of L.T.T. Cable Division.



**William J. POULSON** was born in 1951. He received a B. Sc. (Eng.) degree from Imperial College of Science and Technology in LONDON, 1972. He has worked with instrumentation systems, microwave measurements, connectors, and is now responsible for the product design group and drawing office with RAYCHEMS EUROPEAN INTERCONNECTION DIVISION.

**THOMSON C.S.F./L.T.T.**  
**B.P. N° 5**  
**F 78702 CONFLANS STE HONORINE - France**  
**Phone : (33) 3.974.56.56**

**RAYCHEM**  
**2-4, Avenue de l'Eguillette**  
**Z.A. du Vert Galant**  
**F 95310 SAINT OUEEN L'AUMONE - France**  
**Phone : (33) 3. 037.92.12**



## FIELD TRIAL OF COMPOSITE FIBER-OPTIC OVERHEAD GROUND WIRE

S. Kubota  
H. Kawahira  
T. Nakajima

I. Matsubara  
Y. Saito  
Y. Kitayama

The Tokyo Electric Power Co., Inc.  
Tokyo, Japan

Sumitomo Electric Industries, Ltd.  
Yokohama, Japan

Abstract

A composite fiber-optic ground wire (OPGW), which provides additional communication capabilities for system protection and control of overhead power transmission systems has been developed. After laboratory tests, the OPGW was strung along a live power transmission line in a mountainous region and has been confirmed to have sufficient performance to establish a high-speed digital transmission network able to withstand actual conditions. The field trial line, constructed substantially by existing techniques, has proved that the new OPGW, accessories such as clamps and joint boxes, installation technique, and on-tower splicing method can be effectively utilized to produce a protection and control system with extremely stable characteristics.

1. Introduction

The stable, efficient operation of any electricity supply network requires a variety of reliable communication systems. However, in the case of conventional transmission systems, problems arise due to the limited bandwidth of metallic communication cables and their susceptibility to electromagnetic induction from power lines, high short-circuit currents, or lightning.

In contrast, optical fiber communication systems, which have progressed spectacularly in recent years, are well suited to power systems

because of their low transmission loss, wide bandwidth, interference immunity, small diameter, and so on. Composite fiber-optic overhead ground wires have been developed to aid in efficient, safe operation of electricity supply networks. Though the optical fiber cable combined with a ground wire is exposed to severe conditions such as wide temperature variations and large strain, a newly developed composite cable was confirmed by laboratory and field tests to have stable transmission characteristics under severe conditions.

In this paper, properties of our newly developed composite fiber-optic overhead ground wire and applications of the composite cable to an actual power transmission line are reported.

2. Composite Fiber-Optic Overhead Ground Wire (OPGW)2.1 OPGW System

In applying optical fibers to power transmission lines, a composite fiber-optic overhead ground wire (OPGW) and a self-supporting optical cable<sup>[1]</sup> were both considered to be suitable. However, OPGWs have superior mechanical properties, since the optical cable is housed in overhead ground wires and protected by them, and installation cost of OPGWs is lower compared to methods of manufacturing and installing power cables and optical cables separately. Figure 1 shows a typical overhead power transmission system with an OPGW. The OPGW is installed on the top of the towers between

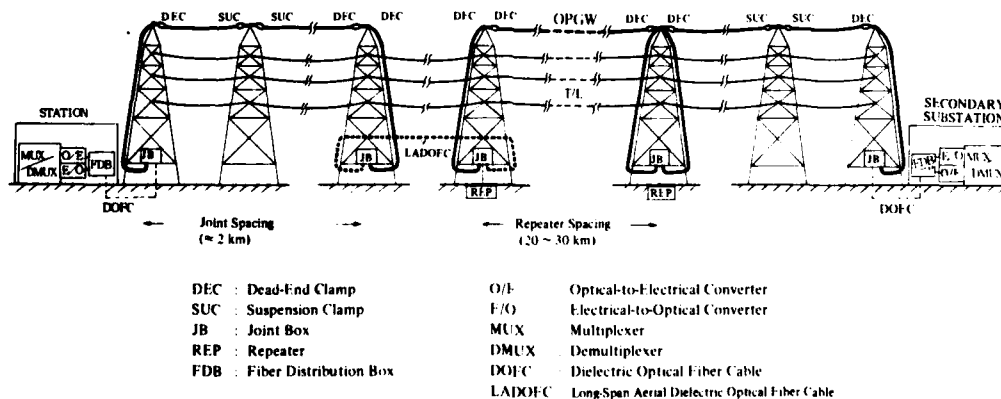


Fig. 1 Typical Transmission Line System with OPGW

a station and substation. In the terminal stations, optical communication equipment such as multiplexers (MUX), demultiplexers (DMUX), optical-to-electrical (O/E) and electrical-to-optical (E/O) converters, and fiber distribution boxes (FDB) are located. Multiplexed optical signals are transmitted via OPGWs jointed at the base of towers, and via dielectric optical fiber cables (DOFC) to the stations. At present, repeater spacing is around 20km for LED systems and 30km for LD systems.

## 2.2 Advantageous Features

In designing OPGWs, the following matters must be considered.

- (1) An OPGW should be compatible with the conventional overhead ground wire, i.e., it should have almost equal diameter, weight, tensile strength, and electric resistance.
- (2) The optical fibers should be protected from mechanical force during installation and clamping the OPGW.
- (3) The optical fibers must be stable under severe conditions in a wide temperature range.

Figure 2 shows the cross-sectional structure of two typical designs of OPGWs developed to satisfy the above requirements. An 80mm<sup>2</sup> OPGW was designed for high-voltage power transmission lines of 154kV and lower, and a 300mm<sup>2</sup> OPGW was designed for extra-high-voltage lines of 275kV or more. Optical fibers are manufactured by the VAD process; graded-index multimode fibers with a core diameter of 50 $\mu$ m, a cladding diameter of 125 $\mu$ m, and a refractive index difference  $\Delta = 1\%$ , or step-index single-mode fibers with a core diameter of  $\sim 9\mu$ m, a cladding diameter of 125 $\mu$ m, and a refractive index difference  $\Delta = \sim 0.3\%$  are used. In the following laboratory test and field trial, graded-index fibers were used. The strain level of the screening test of optical fibers during the manufacturing process was set at two times the value normally used, so failure probability of 1000km-long proof-tested optical fibers can be expected to be less than 1% over 30 years. Both types of OPGWs contain one optical fiber unit at the center of aluminum-clad steel wires. Each of four optical fibers is housed in a slack condition within a spiral groove of an aluminum spacer so as to give the fiber the desired mechanical properties to endure a standard installation method for conventional ground wires.

Figure 3 shows transmission loss increase against compression force for two typical structures of optical units, Al-sheathed cushion

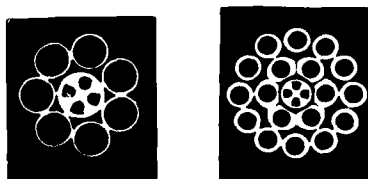


Fig. 2 Cross Sections of OPGWs  
(left: 80mm<sup>2</sup> OPGW, right: 300mm<sup>2</sup> OPGW)

type<sup>[2]</sup> and newly developed Al-sheathed Al-spacer type. In the Al-sheathed cushion type, optical fibers are protected with a cushion layer of Kevlar (aramid resin) and an aluminum tube with a thickness and outer diameter of 0.5mm and 4.5mm, respectively. But when compression force of above 100kg is applied to 5cm of such an optical unit, the transmission loss of the optical fiber starts increasing. On the other hand, the new design (with almost the same outer dia.) was confirmed to withstand compression force ten times that of the Al-sheathed cushion type and to provide rigid protection against lateral pressure.

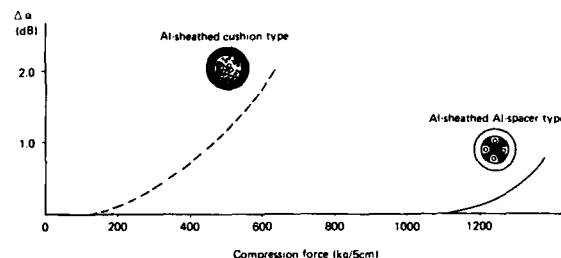


Fig. 3 Mechanical Strength Comparison Between Typical Constructions of Optical Units for OPGWs

Because the ground wire is exposed to high temperatures brought about by induction currents from adjacent power conductors, the resistance of the optical fiber to heat was increased by utilizing two kinds of heat-resistant coating materials, an inner layer of room-temperature-vulcanized silicone of 400 $\mu$ m outer diameter and an outer layer of fluorocarbon polymer of 700 $\mu$ m outer diameter.

Figure 4 shows temperature characteristics of heatproof optical fibers coated with fluorocarbon polymer and a conventional standard optical fiber coated with nylon. Two types of heatproof optical fibers were developed for OPGWs, both of which can withstand a wider temperature range compared with nylon-coated optical fibers. Type A is coated with standard-grade fluorocarbon polymer commercially called ETFE or Tefezel by du Pont and is able to withstand from -60°C to 250°C. Type B, coated with a higher grade fluorocarbon polymer commercially called Teflon PFA by du Pont, can withstand from -60°C up to 300°C.

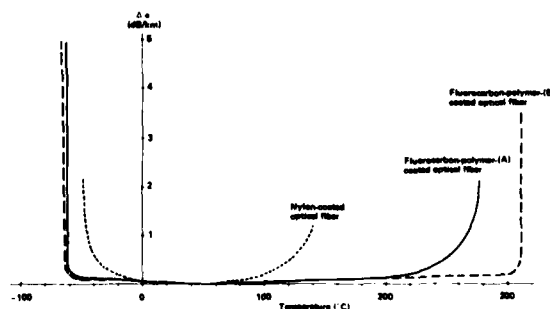


Fig. 4 Temperature Characteristics of Heat-Proof Optical Fibers

The table shows the structural specifications of two standard OPGWs. The 80mm<sup>2</sup> OPGW usually contains A-type heat-proof optical fibers, and thus the permissible operating temperature is from -50 to 100°C. The 300mm<sup>2</sup> OPGW usually contains B-type heat-proof optical fibers, and thus the permissible operating temperature is from -50 to 150°C. Furthermore, permissible peak temperatures of the two types of OPGWs, 80mm<sup>2</sup> and 300mm<sup>2</sup>, are 250°C and 300°C, respectively. Peak temperature means temporary increase of conductor temperature caused by short-circuit fault. Figure 5 shows both types of OPGWs.

Specifications of OPGWs

Description		Type	80 mm <sup>2</sup> OPGW	300 mm <sup>2</sup> OPGW
Optical Fiber	Relative Index Difference (%)	M.M.F.	1.0	
		S.M.F.	0.3	
	Core/Cladding Diameter (μm)	M.M.F.	50/125	
		S.M.F.	9/125	
	Buffer/Coat Diameter (mm)		0.4/0.7 (silicone resin/fluorocarbon polymer)	
Fiber Unit	Number of Fibers		4	
	Construction		Aluminum-sheathed helical-grooved aluminum spacer	
Ground wire	Wire of Outer Layer	Material	Aluminum-clad steel wire (IACS 23%)	
		Outer Dia. (mm)	3.8	4.3
	Number of Wires of Outer Layer		7	18
	Overall Diameter (mm)		12.4	21.1
	Weight (kg/km)		552	1264
Minimum Breaking Strength (kg)			9260	16440
Modulus of Elasticity (kg/mm <sup>2</sup> )			14600	10500
Thermal Coefficient (×10 <sup>-6</sup> /°C)			13	16
DC Resistance (Ω/km)			0.954	0.167
Operating Temperature (°C)			-50 to 100 (peak 250)	-50 to 150 (peak 300)

M.M.F.: graded-index multi-mode fiber  
S.M.F.: step-index single-mode fiber  
IACS: International annealed copper standard



Fig. 5 300mm<sup>2</sup> OPGW and 80mm<sup>2</sup> OPGW

## 2.3 Mechanical Characteristics of OPGWs

### 2.3.1 Stress-Strain-Creep Test

Figure 6 shows a stress-strain-creep curve of an 80mm<sup>2</sup> OPGW. Length of the OPGW under test was 16m, and gauge length was 5m. The tension was increased to and held for 30 minutes at 30% UTS (ultimate tensile strength) after being set at 8% UTS as an initial condition. After this holding time, the tension was reduced to the initial value, and like this the tension was changed between the initial value and high loads of 50% UTS with 1-hr hold and 70% UTS with 1-hr hold. Furthermore, the tension was increased to 85% UTS and reduced to 50% UTS. At this point, the measuring instruments were removed from the specimen, and then the tension was increased up to breaking point. During this test procedure, the transmission loss of the optical fiber and the elongation of the conductor were monitored continuously. The result of this test shows that the breaking point of the OPGW was 109% UTS and that no change in transmission loss occurred even at the breaking point with elongation of 1.5%.

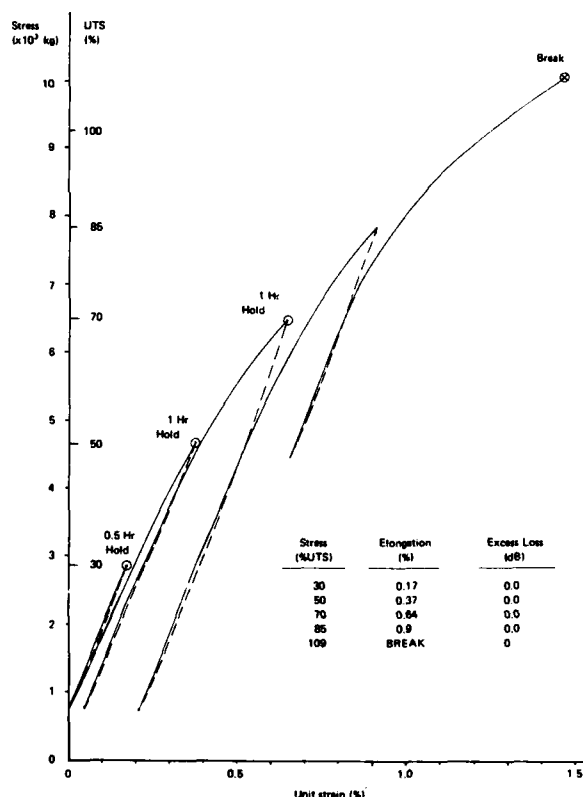


Fig. 6 Stress-Strain-Creep Curve for 80mm<sup>2</sup> OPGW

### 2.3.2 Vibration Test

To confirm the endurance capability of the OPGW and accessories against aeolian and turbulent vibration, a vibration test was conducted with the setup shown in Fig. 7. A 30m-long 80mm<sup>2</sup> OPGW was installed under tensile strength of 20% UTS. Four fibers were connected to each other in series in joint boxes, and transmission loss was measured by the cut-back method. At first, the OPGW was vibrated  $1.6 \times 10^7$  times under the condition simulating turbulent vibration (frequency: 10Hz, amplitude: 2mm). In series, it was vibrated  $5.1 \times 10^7$  times under the condition simulating aeolian vibration (40Hz, 2mm). During all series of vibration tests, no change in transmission loss was observed, and no trouble and no damage were found in any accessories, such as clamps and protective tube to protect the optical fiber unit.

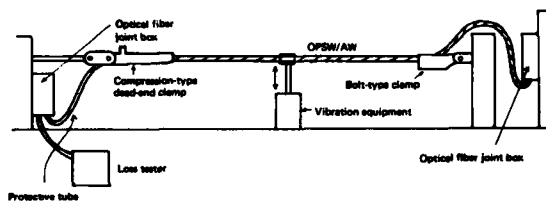


Fig. 7 Setup of Vibration Test

### 2.3.3 Creep Test

Creep of the OPGW was measured with the tension held at a constant value of 20% UTS utilizing a regulated tension loader. The measured value of the creep of an 80mm<sup>2</sup> OPGW after 1000 hours was 0.017%, the same level as with conventional ground wires.

### 2.3.4 Pulling-Through Pulley Test

A 15m-long 80mm<sup>2</sup> OPGW was bent around a 300mm-diameter pulley at a bending angle of 60 degrees at stringing sheave under tension of 1850kg (20% UTS). An approx. 15m section of the

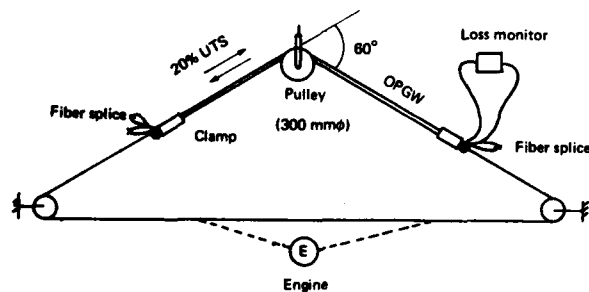


Fig. 8 Setup of Pulling-Through Pulley Test

OPGW was then pulled back and forth at that angle on the pulley for 20 cycles, and transmission loss was monitored. Figure 8 shows the test setup.

No change in transmission loss of the fiber was observed during this test. After 20 cycles of passing through the pulley, no changes in mechanical properties and structure of the OPGW, i.e., lay length of the aluminum-clad steel wires and outer diameter of the OPGW, was observed. The OPGW was confirmed to protect the optical fiber from the various stresses of bending, elongation, and compression resulting from the bending and pulling.

### 2.4 Temperature Characteristics of OPGWs

#### 2.4.1 Temperature Cycle Test

Cyclic temperature change between -25°C and 100°C was applied to a 500m-long optical fiber unit in a chamber. Figure 9 shows the result of this temperature cycle test. Change in transmission loss of a 2000m-long optical fiber including five fusion splices was less than 0.2 dB/km at wavelengths of both 0.85μm and 1.3μm. The heat-proof optical fiber with primary and secondary coats of room-temperature-vulcanized silicon and fluorocarbon-polymer, respectively, was confirmed from the test to withstand severe temperature condition on OPGW.

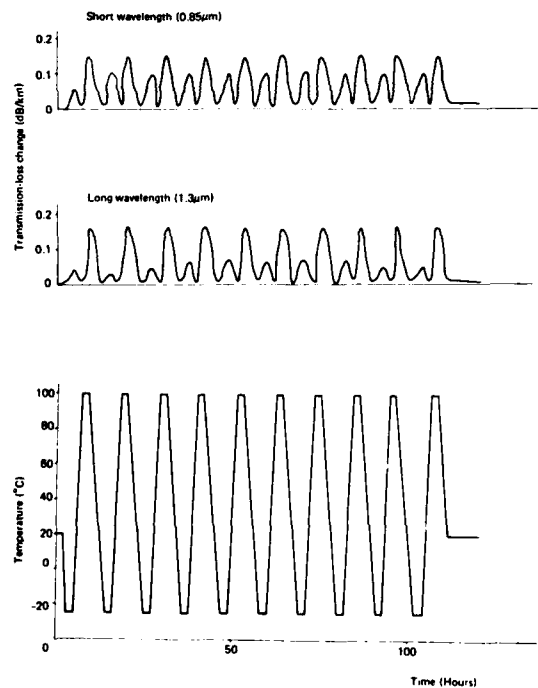


Fig. 9 Transmission Loss Change with Temperature

#### 2.4.2 Short-Circuit Test

In accidents of power transmission lines, high heat resistance of the optical fiber is required since the optical fiber is exposed to very high temperatures caused by fault current. Short-circuit current was applied repeatedly to a 40m-long 300mm<sup>2</sup> OPGW installed on a test bed with a stringing tension of 20% UTS to simulate fault current. The transmission loss and bit error of a 6.3Mb/s pseudo-random pulse signal were monitored through two 80m-optical fibers spliced in series. Figure 10 shows the changes in transmission loss of the optical fiber and temperature of the 300mm<sup>2</sup> OPGW. Alternating current of 25kA was applied to the OPGW for 0.75 seconds after the conductor temperature was raised and kept constant at 150°C by current. It was confirmed that temporary change in transmission loss of the optical fiber was less than 0.1 dB/km under high-temperature conditions around 300°C.

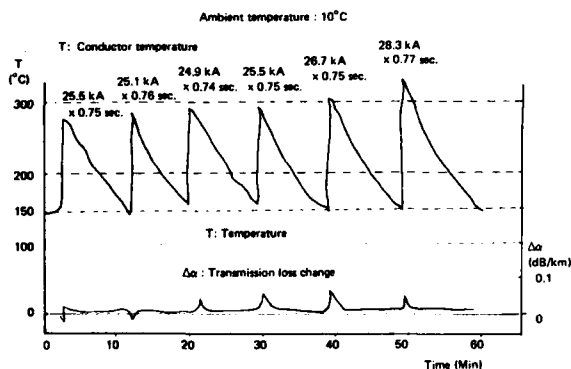


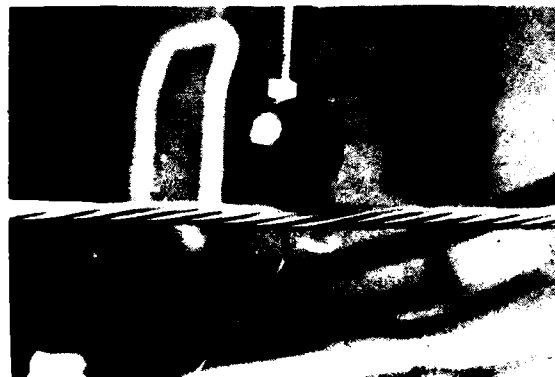
Fig. 10 Short Currents vs. Changes in Attenuation and Temperature for 300mm<sup>2</sup> OPGW

#### 2.4.3 Arc Discharge Test

Arc current was discharged from a carbon electrode to a midpoint on a 10m-long 80mm<sup>2</sup> OPGW to simulate a lightning strike and evaluate the effects of heat, shock stress, and arcing. Test conditions of the arc discharge were selected to produce a discharge energy corresponding to the maximum observed lightning energy in Japan. Discharge currents up to 8kA and discharge holding time of 0.04 second were used. In spite of smelting of the aluminum layers on the aluminum-clad steel shielding wires, no change in transmission loss of the optical fiber and no bit errors of 6.3Mb/s digital signals with pseudo-random sequence were observed at the instant of current discharge. Figure 11 shows a series of test scenes.

#### 2.5 Accessories for Installation

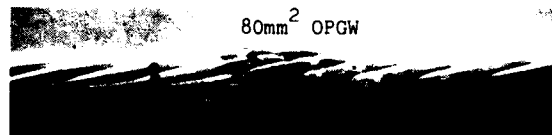
Cable accessories for installation, such as clamps and a straight wire joint, were designed with slight modifications rather than as completely new types. In the field trial, two types of dead-end clamps were utilized. Figure 12 and Figure 13 show a bolt-type and a compression-type dead-end clamp, respectively.



Before discharge



Discharging



After discharge

Fig. 11 Arc Discharge Test

The structure of each type of conventional dead-end clamp was slightly changed in order to achieve the gripping force for the OPGW and to protect the optical fibers during and after the clamping procedure. No significant change in transmission loss was observed during the fitting procedure of either type of dead-end clamp at both ends of the OPGW and during tensile test of up to 10,000kg. In addition, an existing dead-end clamp, i.e., a preformed armor grip, was also confirmed experimentally to be applicable to a newly developed OPGW without any modification, as shown in Figure 14. Since ground wires are ordinarily installed in overhead lines more than several hundred kilometers long, a number of midway connections are naturally required. To accomplish this purpose, a compact, long-term waterproof joint box and a mid-span joint have also been developed. Figure 15 shows a mid-span joint.

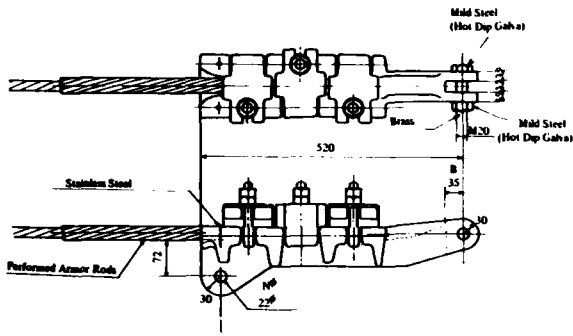


Fig. 12 Bolt-Type Dead-End Clamp

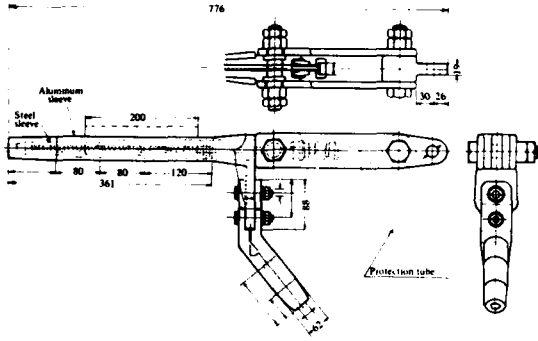


Fig. 13 Compression-Type Dead-End Clamp



Fig. 14 Tensile Test of Armor Grip

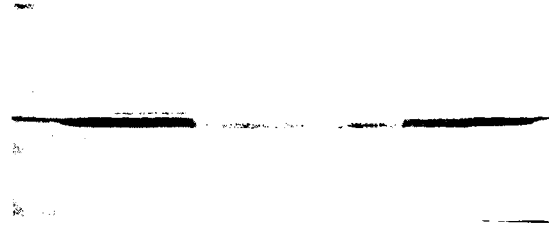


Fig. 15 Mid-Span Joint

### 3. Field Trial

Following the laboratory tests of the OPGWs, a field trial is in progress to confirm the long-term reliability in practical use. An 80mm<sup>2</sup> OPGW was installed in August 1982 on an actual power transmission line of the Tokyo Electric Power Company at a mountainous region of Tochigi prefecture north of Tokyo. Figure 16 shows the field trial route of the 80mm<sup>2</sup> OPGW. The installed OPGW is about 3km in total length. The optical fibers were fusion spliced in weatherproof joint boxes on the top of the towers at four intermediate joints (towers #5, #8, #10, and #11) and two terminal joints (towers #1 and #12). The OPGW was installed with no special precautions and was anchored utilizing two types of clamps. Bolt-type clamps were used at ten intermediate towers (four dead-end towers and six suspension towers). Compression-type clamps were also used at two terminal dead-end towers (#1 and #12). Observation sheds were built at both ends of the field trial line to accommodate equipment for monitoring optical transmission characteristics as well as natural environmental conditions. A nonmetallic loose-groove-spacer-type optical fiber cable<sup>[3]</sup> was installed between a joint box

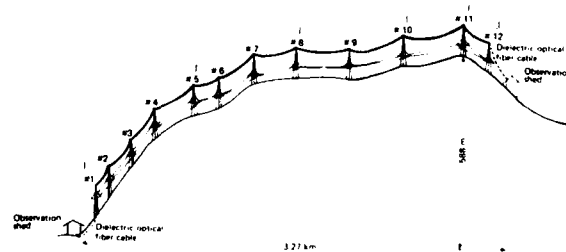


Fig. 16 Field Trial Route of 80mm<sup>2</sup> OPGW

on the top of the tower and a fiber distribution frame (PDF) in the observation sheds at each terminal to protect the electronic equipment in the shed from lightning surge current.

Figure 17 shows the observation system of the field trial. Two of the four optical fibers in the OPGW are spliced in the observation shed next to tower #12, and transmission loss as well as bit error rate for a 32Mb/s digital signal over the 6.5km-long optical fiber are monitored continuously. A digital telephone signal is transmitted over the third optical fiber between two observation sheds utilizing two-way communication or the two-wavelength division multiplex communication technique. The remaining optical fiber is used for collection of lightning surge signals picked up with detectors. Lightning surge current is detected by means of a current transformer and two types of sensors--light-emitting diodes (LED) and bismuth silicon oxide (BSO) sensors--installed on the top of towers #1 (BSO), #5 (LED), and #8 (LED).

The OPGW was installed along a steep mountain slope, with a local relief of about 600m. Normal erection procedures and equipment (e.g., a conventional tensioner and conventional pulleys) were successfully utilized. At the top of the tower, both OPGWs to be jointed were anchored with bolt-type dead-end clamps and fixed with a jumper clamp, and then were led directly into the joint box. All fiber splicing work were conducted in a standard procedure on scaffolds

constructed on the tops of the towers, and spliced optical fibers are housed within the joint box. In spite of the bad operating conditions at the top of the tower, such as wind, rain, and vibration, arc-fusion splicing was performed successfully. Average splicing loss of the total of 32 fusion splices was 0.045dB/splice (maximum measurement was 0.15dB/splice) and after installation, transmission loss measurements of the four optical fibers were 2.49 to 2.60dB/km at a short wavelength of 0.85 $\mu$ m and 0.65dB/km at a long wavelength.

Figure 18 shows a view of the top of the dead-end tower, and Figure 19 shows a view of the installed field trial line.



Fig. 18 View of Top of Tower

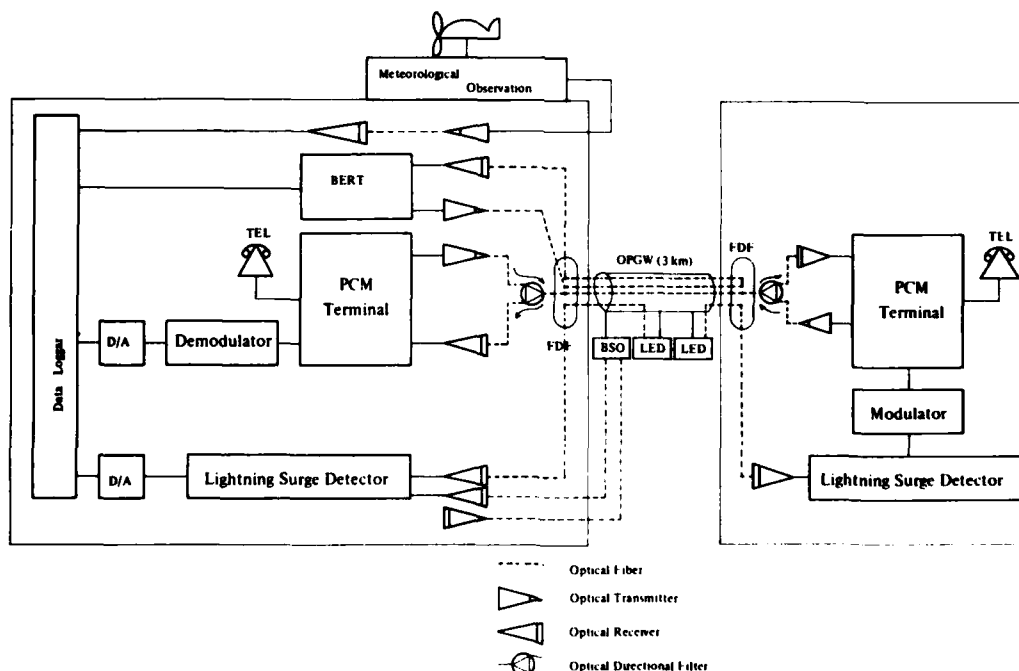


Fig. 17 Observation System of Field Trial

Figure 20 shows the field trial data: variations of transmission loss, temperature, and wind velocity. It has been confirmed from this field trial over one year that change in transmission loss of the optical fiber is less than  $\pm 0.2\text{dB}/6.5\text{km}$  and bit error rate for 32Mb/s digital signal (loss margin:  $\sim 2\text{dB}$ ) is less than  $10^{-9}$  under actual conditions, even when a lightning struck the OPGW, and the OPGW was proved to have adequate mechanical, electrical, and thermal properties to withstand harsh conditions in actual use.



Fig. 19 Installed Field Trial Line

#### 4. Conclusion

A composite fiber-optic ground wire has been developed. The OPGW was installed overhead on an actual power transmission line without any trouble and has been confirmed to have sufficient performance to establish a high-speed digital network able to withstand actual conditions. The field trial line has proved that the new OPGW can be effectively utilized to produce a protection and control system with extremely stable characteristics.

#### Reference

- [1] E. Hayakawa, F. Ohtsuka, M. Monma, H. Horima, T. Nakatani, K. Kuranobu, "Non-Metallic Optical Fiber Cable, Incorporating Fiber Reinforced Plastic Catenary for Aerial Application", I.O.O.C., 1983.
- [2] M. Igarashi, J. Yokoyama, H. Iwamura, N. Mori, I. Matsubara, Y. Saito, "Composite Fiber-Optic Overhead Ground Wire", Proc. of 29th I.W.C.S., 1980.
- [3] O. Ichikawa, K. Sakamoto, Y. Saito, "Development of Nonmetallic, Loose-Groove Spacer-Type Optical Fiber Cable", 31st I.W.C.S., 1982.

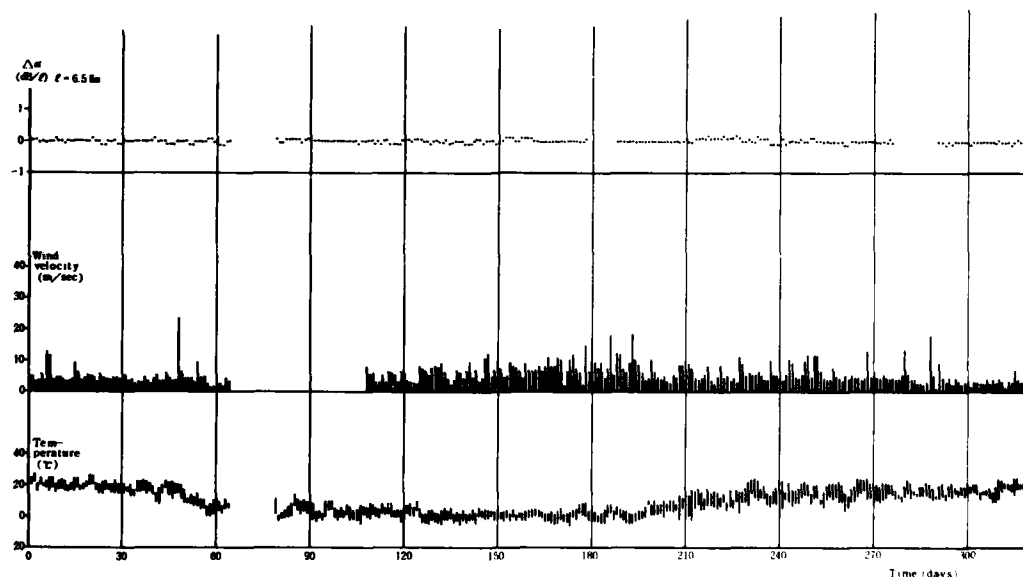


Fig. 20 Field Trial Data ( $l = 6.5\text{km}$ )



Simao Kubota  
The Tokyo Electric Power  
Co., Inc.  
1-3, 1-chome,  
Uchisaiwai-cho,  
Chiyoda-ku, Tokyo,  
Japan

Simao Kubota received the B.E. degree in electrical engineering from Shinshu Univ. in 1961. He joined the Tokyo Electric Power Co., Inc. in 1961, where he has been engaged in the section of electronic tele-communications. Mr. Kubota is now a chief researcher of Engineering Development Division in Engineering Research & Development Center, and a member of the Institute of Electronics and Communication Engineers of Japan.



Ichiro Matsubara  
Sumitomo Electric  
Industries, Ltd.  
1-3-12, Moto-Akasaka  
Minato-ku, Tokyo  
Japan

Ichiro Matsubara received the B.E. degree in electrical engineering from Kyoto Univ. in 1966. He then joined Sumitomo Electric Industries and has been engaged in design research and development of various kinds of cables and overhead power transmission lines. Mr. Matsubara is now a manager of Overhead Power Transmission Line Engineering Section, and a member of the Institute of Electric Engineers of Japan.



Hiroyoshi Kawahira  
The Tokyo Electric Power  
Co., Inc.  
2-4-1  
Nishi-Tsutsujigaoka,  
Chofu-City,  
Tokyo, Japan

Hiroyoshi Kawahira received his B.S. degrees in Electrical Engineering from Nippon Univ. He joined the Tokyo Electric Power Co., Inc. in 1962, where he has been engaged in the section of substation facilities. Mr. Kawahira is now a senior researcher of Power Engineering Division in the Engineering R & D Center.



Yasunori Saito  
Sumitomo Electric  
Industries, Ltd.  
1, Taya-cho,  
Totsuka-ku,  
Yokohama, Japan

Yasunori Saito received his B.S. degree in Electrical Communication Engineering from Tohoku Univ. in 1969. He then joined Sumitomo Electric Industries and has been engaged in research and development of high frequency transmission lines including fiber optics. Mr. Saito is a chief research associate of R & D Group, and a member of the Institute of Electronics & Communication Engineers of Japan.



Tatsuo Nakajima  
The Tokyo Electric Power  
Co., Inc.  
1-3, 1-chome,  
Uchisaiwai-cho,  
Chiyoda-ku, Tokyo,  
Japan

Tatsuo Nakajima received the B.E. degree in electrical engineering from Tokyo Univ. in 1961. He then joined the Tokyo Electric Power Co., Inc. and has been engaged in construction and maintenance of overhead transmission lines. Mr. Nakajima is now a deputy manager of Operation & Maintenance Department.



Yoshinobu Kitayama  
Sumitomo Electric  
Industries, Ltd.  
1, Taya-cho,  
Totsuka-ku,  
Yokohama, Japan

Yoshinobu Kitayama received his M.S. degree in Electrical Engineering from Kyoto Univ. in 1982. He then joined Sumitomo Electric Industries and has been engaged in research and development of optical fiber and cables. Mr. Kitayama is a member of Yokohama R & D Group, and a member of the Institute of Electronics & Communication Engineers of Japan.

## FACTORY SPLICING OF OPTICAL WAVEGUIDE FIBER

D. H. TAYLOR AND S. L. SAIKKONEN

CORNING GLASS WORKS  
CORNING, NEW YORK 14831ABSTRACT

The increasing need for longer and longer link lengths, and reclamation of shorter lengths, reinforce the continued need for permanent low loss joints between optical fibers. In support of this need, we have directed efforts toward the optimization of fusion splicing in a factory environment. The goal of the present work was to develop a process for the splicing of optical fibers utilizing standard arc fusion techniques. The resultant spliced fibers are to be indistinguishable from unspliced fiber with respect to fiber and coating geometries. In addition, the same stringent mechanical and environmental performance requirements must be met. Tests on a large number of factory splices will be discussed and performance results given.

INTRODUCTION

Arc fusion splicing of optical waveguide fiber is currently the most popular method of providing stable, reliable low-loss interconnection of multimode fiber in field installations. Although typical arc fusion splice losses may average between 0.1 to 0.2 dB using visual fiber end alignment methods, the repeatability of the process often requires considerable operator skill and consistency. Also, since field-type splices are usually supported and protected by relatively large reinforcement members, little emphasis is placed on the bare fiber tensile strength or geometric homogeneity of the fiber and coating across the spliced area. The purpose of this article is to present an arc fusion splicing process for reclamation of short fiber lengths and the creation of very long factory lengths. The factory splices shall meet the following criteria:

- Attenuation:  $\leq 0.2$  dB
- Strength:  $> 0.69$  GN/m<sup>2</sup> (100 KPSI)

- Coating Outside Diameter: same as nominal coating  $\pm 15$   $\mu$ m
- Coating Concentricity:  $\frac{\text{min. wall}}{\text{max. wall}} \geq 0.7$
- Fiber Cladding Diameter:  $125 \pm 3$   $\mu$ m

FIBER SELECTION

To consistently produce spliced fiber lengths meeting the 0.2 dB attenuation specification, it is necessary to match the fibers as closely as possible in numerical aperture and core diameter. This is facilitated by selecting fibers drawn from the same preform.

FIBER COATING REMOVAL

The coating on the 50/125 multimode fiber tested is a mechanically strippable UV-cured acrylate. Stripping is accomplished using a hand-held mechanical fiber stripping tool. This tool is similar in appearance and operation to a simple copper wire stripper but incorporates a precision laser drilled hole at the jaw closure point which minimizes mechanical damage to the bare fiber surface. This tool produces a clean, well defined coating termination.

Optical waveguide fiber loses approximately 30% of the initial tensile strength by removal of the protective coating, the method of removal, whether by chemical stripping using methylene chloride or by mechanical stripping using the forementioned tool is not a factor.

FIBER END CLEAVING

Close control of the fiber end angle and face condition has significant effect on the splice attenuation and geometry. Distortion of the core during fusion due to the flow of the core glass in a direction away from the point of first glass contact will contribute to splice losses in excess of 0.2 dB. This phenomena is minimized by limiting fiber end angle to

1° or less. To create a fused joint in which the cladding diameter is maintained with a  $\pm 3 \mu\text{m}$  specification in respect to the nominal cladding O.D., it is necessary to limit the included angle between the ends to be fused to  $< 2^\circ$ . Greater angles will produce a necked down region at the joint. In an attempt to minimize the exposure of the bare fiber to contamination and mechanical damage, the fiber is cleaved such that only 4 mm of fiber is exposed beyond the coating. Early experiments show that minimizing the length of exposed fiber yields significant gains in the spliced fiber tensile strength. See Figure 1. This is most likely attributable to the elimination of mechanical damage to the glass surface created by contact with mechanical clamps and vacuum chucks, or simply the reduction of glass surface area exposed to airborne contamination.<sup>1</sup>

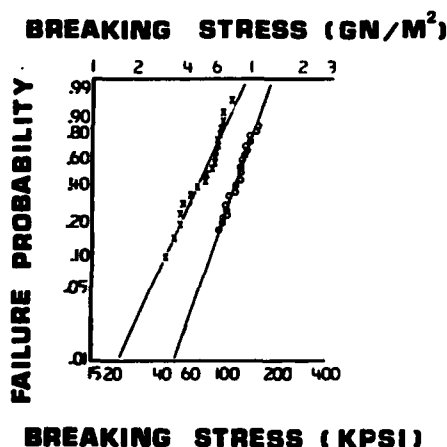


Fig. 1. Fusion spliced and acid etched 50/125 fibers. Left curve (X) total exposed glass length across splice is 127 mm. Right curve (O) total exposed glass length is 8 mm.

#### FIBER END ANGLE MEASUREMENT

Two methods of fiber end angle and condition measurement were tested. The first method utilizes a laser beam reflecting from the fiber end face onto a target. The target is marked with annular rings corresponding to progressively larger fiber end angles from the target center-point. The second method utilizes a laser beam diffracted through the sides of the fiber onto a calibrated rearviewing screen.<sup>2</sup> Although both methods will accurately measure to within  $\pm 4^\circ$ , the latter method is less prone to variations in operator interpretation of indicated end angle and condition.

#### FIBER END CLEANING

The degree of cleanliness of the bare fiber ends and the exposed cladding surface is critically important to the splice attenuation and strength respectively. Residual coating particles or other contamination at the fiber ends often create an air bubble or actually become an inclusion during fusion, thus providing high splice losses.<sup>3</sup> Any contamination on the cladding surface may become partially melted into the glass surface in the cooler regions of the fusion heat affected zone or may become nucleating sites for surface devitrification during fusion,<sup>4</sup> both being surface point defects resulting in poor fiber strength.<sup>1,5</sup> This theory is supported by the fact that a typical fusion spliced fiber fails in tension at a distance between 0.5 mm to 1 mm beyond the splice. This distance corresponds to the heat-affected zone along the fiber.

For the factory splicing process, the prepared fiber ends are cleaned in an ultrasonic bath using isopropyl alcohol. The exposed glass is then examined to insure no visible contamination is present.

#### FUSION SPLICING

The fusion splicer consists of two vacuum chucks, each independently adjustable on three axes, for supporting the fiber by the coating layer. Tungsten electrodes spaced at .86 mm are supplied by a power source incorporating arc current, time, and ramp controls. A stereoscopic microscope with a maximum power of 135X is used for viewing. The longitudinal (z) axis of one vacuum chuck is driven by a programmable stepping motor for driving the fiber ends together during the fusion cycle. Fiber core alignment is accomplished by manipulating lateral axes (x and y) vacuum chuck micropositioners while observing for the least attenuation step on an OTDR incorporating a high resolution real-time display.

For the 50/125 multimode fibers tested, the optimum pre-fusion and fusion currents are 14 mA and 17 mA respectively. A pre-fusion arc duration of one second in conjunction with a fiber end spacing of 100  $\mu\text{m}$  produces the best fiber end rounding. Prior to fusing, the fibers are positioned longitudinally such that the ends are as close together as possible without touching. The lateral axis positioners are then adjusted for best core alignment using the OTDR. The ends are then positioned to just touch each other. The fusion arc current is started, then at the moment the fiber ends begin to melt, the z axis drive is activated to compress the ends together. The duration of the

fusion arc current with respect to splice attenuation and tensile strength will be discussed below.

#### RESTRENGTHENING

Typical breakage of fusion spliced 50/125 fiber occurs at tensile loads of less than  $0.35 \text{ GN/m}^2$ . The fracture is normally located between 0.5 and 1 mm on either side of the splice interface. Thermal analysis of the breakage zone indicates thermal stresses of approximately  $0.03 \text{ GN/m}^2$ . Scanning electron micrographs and microprobe analysis of the break source does not indicate the presence of foreign material, therefore the loss of fiber strength during heating is thought to be surface devitrification initiated by the presence of surface contamination.<sup>4</sup> Since the fiber tensile strength can be directly related to the surface flaw depth, then an acid etching treatment of the spliced area to remove a specific amount of material was designed. Utilizing the relationship between flaw depth and applied stress at failure, shown in Figure 2,  $0.34 \text{ GN/m}^2$  corresponds to a flaw depth of 2.3 microns. An understanding of etch rates and crack tip rounding lead to an estimate that a minimum etch depth of 0.5 microns is required to increase the minimum strength from 0.34 to  $0.69 \text{ GN/m}^2$ . A two minute etch in a room temperature solution of 15%, by weight, ammonium bifluoride was chosen for this purpose (Figure 3).

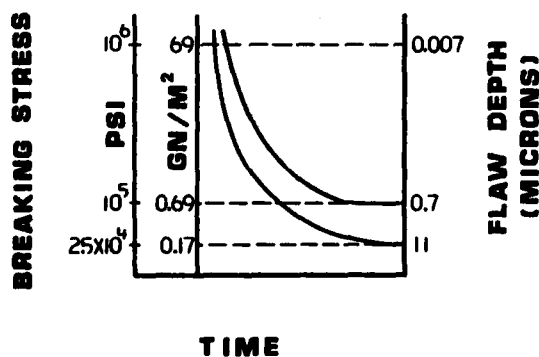


Fig. 2. Relationship Between Breaking Stress and Flaw Depth.

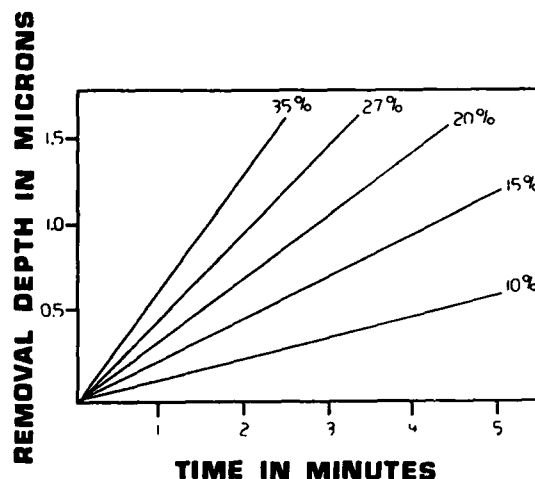


Fig. 3. Rate of Material Removed in Room Temperature Ammonium Bifluoride.

#### RECOATING

Recoating of the spliced area with a material of similar physical properties and with the same dimensional tolerance as the existing coating requires the implementation of a molding technique. A split stainless steel mold is used in which the mold cavity is the same diameter as the existing coating. The exposed fiber at the splice is automatically centered in the mold cavity by the existing coating on each side of the splice. With the mold closed, a UV curable coating is injected into the mold cavity, then cured by ultraviolet light.

#### MEASUREMENT TECHNIQUES

Splice attenuation and tensile testing are performed on each factory splice. Attenuation is measured using an OTDR at 820 nm wavelength. The step loss is measured from each end of the link then the two readings are averaged. This is necessary to eliminate the OTDR loss measurement error due to the concatenation of two fibers of different scattering coefficients.<sup>6</sup>

Tensile testing of the splice is accomplished by tensioning the spliced section between two mandrel-wrapped capstans. The splice is loaded at a 4% strain rate either to failure as done for testing purposes to determine ultimate strength, or up to  $0.69 \text{ GN/m}^2$  (100 kpsi), then released, which is the pass-fail criteria for the factory splice.

## STRENGTH OPTIMIZATION

Using the fiber preparation, handling, splicing and acid etching techniques described above to meet the factory splice specifications, it is found that the fusion arc duration and the amount of material removed by acid etching has the most pronounced effect on the tensile strength of the spliced fiber. Figure 4 indicates an optimum fusion time of 2.6 seconds and optimum acid etch time of between one and two minutes. Investigation of fusion times beyond 2.6 seconds yield tensile strengths less than those found in the optimum region.

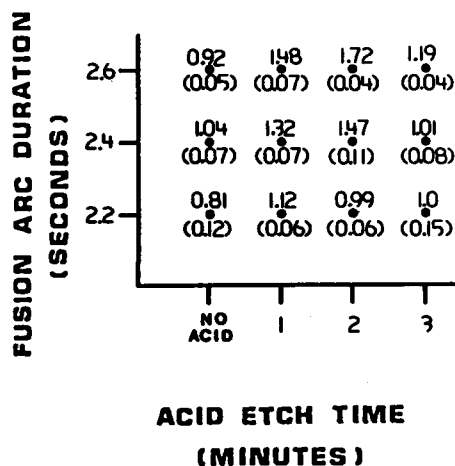


Fig. 4. Experimental Points for Median Splice Strength and Attenuation Values at a Constant Fusion Arc Current of 17 Milliamps and Constant Acid Concentration of 15% (wt.). Key: GN/m<sup>2</sup> dB

## EXPERIMENTAL DATA

The recoated, fusion spliced section of fiber must meet and perform to the same specifications as the unstripped, unspliced fiber.<sup>7,8</sup> Geometries, optical performance and protection ability of the recoat area for a series of spliced fibers have been evaluated.

### A. Geometry

Fusion spliced fiber must have the same diameter and geometry as the unspliced fiber. The recoated section should be nominal  $\pm 15\mu\text{m}$  in diameter and have a concentricity  $>0.7$ . Measurements on ten spliced and recoated fibers are shown in Table 1. Both parameters are well within the stated specifications.

TABLE 1

## RECOAT GEOMETRY (250 $\mu\text{m}$ Fiber)

Overall Diameter (Microns)	Concentricity	
	Minimum Thickness	Maximum Thickness
246	.93	
247	.91	
249	.89	
249	.92	
250	.92	
251	.90	
250	.94	
252	.86	
250	.91	
250	.88	

### B. Attenuation Discontinuity

The attenuation step at a splice joint as measured on an OTDR should be  $<0.2$  dB. The average value for 20 fusion spliced fibers is 0.055 dB. Figure 5 illustrates the cumulative distribution for the measured attenuation losses.

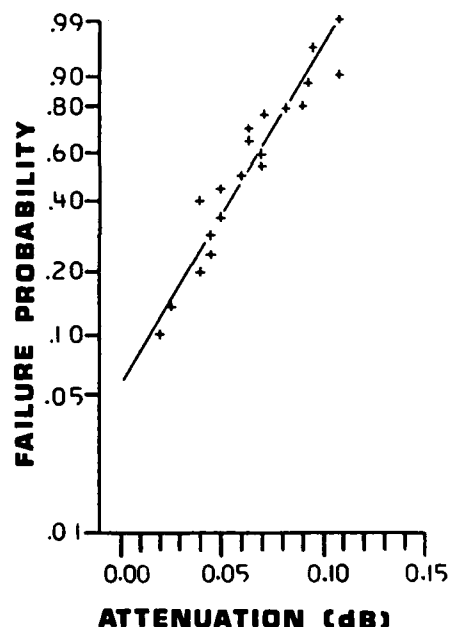


Fig. 5. Cumulative distribution for attenuation losses of spliced fibers.

### C. Strength

The specification of tensile strength requires the spliced section pass a proof stress of  $0.69 \text{ GN/m}^2$ . Average measured tensile strengths of 20 fusion spliced and recoated sections is  $1.55 \text{ GN/m}^2$ . A cumulative distribution of the 20 measured samples is shown in Figure 6.

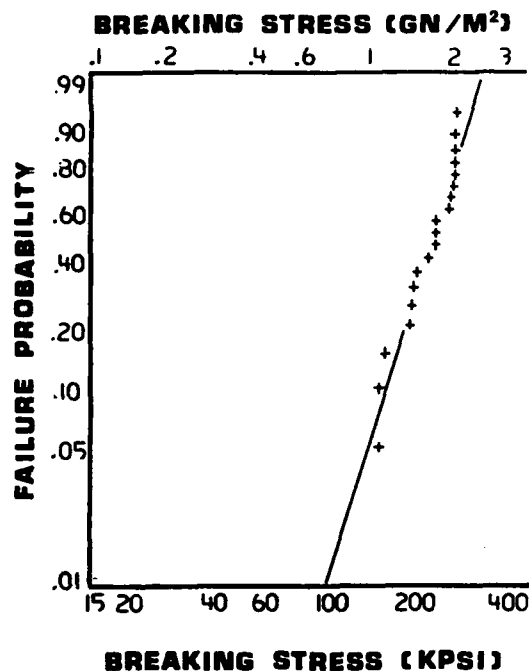


Fig. 6. Cumulative distribution for tensile strength of spliced fibers.

#### D. Abrasion Resistance

The material used to recoat the stripped and fusion spliced area should afford the fiber the same level of resistance to mechanical abrasion as the original coating. A measure of this resistance is done by tensioning the fiber and dropping sand on the recoat area until failure occurs. The average amount of sand required to cause catastrophic failure in 10 spliced and recoated sections is 50 kg. These results are comparable to the resistance demonstrated by the original UV-curable acrylate coatings.

#### E. Microbend Resistance

The increase in attenuation as measured on a fusion spliced and recoated section should not exceed that of an adjacent unspliced section. For this test, 1.635 m of fiber was placed upon 150 grit silicon carbide sandpaper and loaded with flat steel plates to induce microbending. A plot of attenuation versus load is shown in Figure 7. The maximum average attenuation was seen to be 0.89 dB. These results are comparable to the microbend resistance of the unspliced fiber.

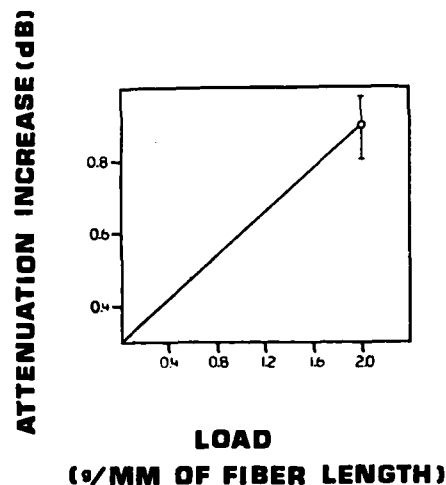


Fig. 7. Microbend Loss

#### F. Temperature Dependence

Average temperature dependence for fibers containing one fusion splice per length is shown in Figure 8. The maximum allowable change in attenuation of 0.2 dB/km, over the temperature range  $-60^{\circ}\text{C}$  to  $+85^{\circ}\text{C}$ , is easily met. In fact, the average measured increase is 0.06 dB/km.

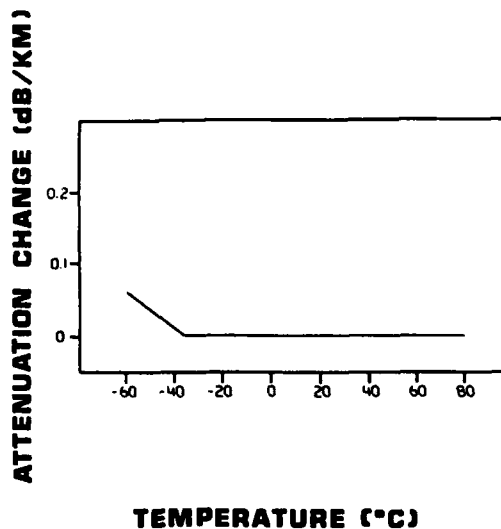


Fig. 8. Temperature Dependence

#### G. Environmental Results

Environmental test results for fibers containing one fusion spliced, recoated section per length are shown in Figure 9 through 12. In

all cases results are comparable with the performance of unspliced, UV-curable acrylate coated fibers.

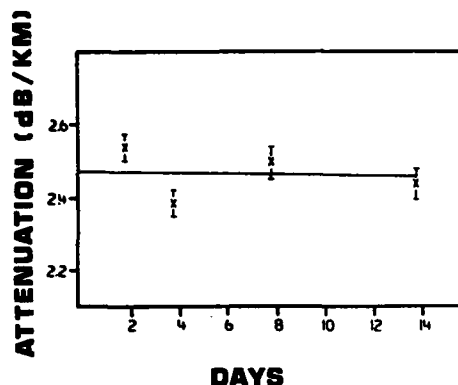


Fig. 9. Tap Water Soak at 20°C

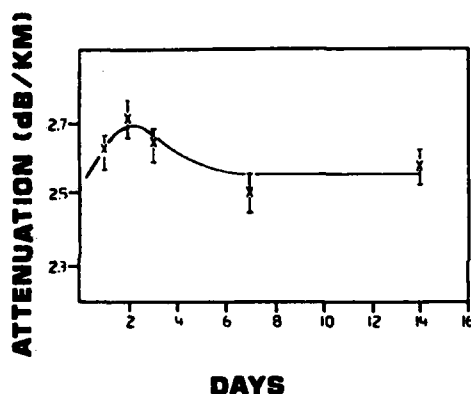


Fig. 10. Tap Water Soak at 65°C

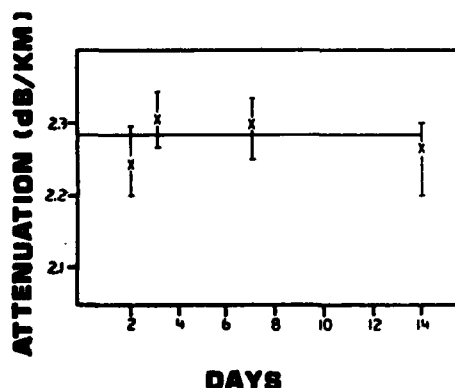


Fig. 11. Temperature Humidity Cycling. +65°C, 98% RH to -10°C, 4% RH

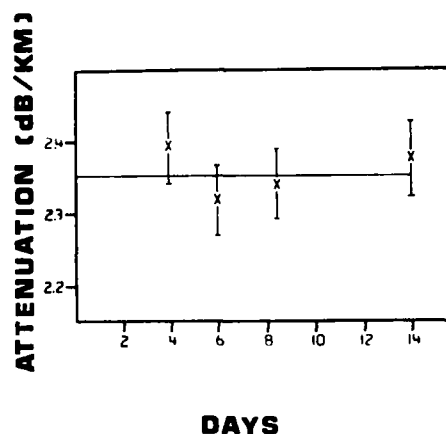


Fig. 12. Dry Heat Soak at 65°C

#### SUMMARY

Careful fiber handling and end preparation techniques are necessary in providing fusion spliced joints having low attenuation and high strength. Minimizing the amount of exposed glass in conjunction with an ultrasonic cleaning technique are required to minimize surface contaminants on the fiber cladding surface and the fiber ends prior to fusion splicing. Fiber end angles of  $<1^\circ$  are required to provide fusion splices meeting the attenuation and dimensional specifications with  $>90\%$  success. An acid etching process is used to increase the spliced fiber strength. The spliced area is recoated to the same geometric tolerances as the existing coating by using a split molding process.

In conclusion, fusion spliced and recoated fibers have demonstrated very good mechanical and environmental performance. They have performed well over wide temperature extremes and after exposure to various environments. Mechanical performance and protection afforded by the recoated section is of quality equivalent to that of unspliced fiber. Geometric and mechanical tolerances are the same as for unspliced fibers.

#### ACKNOWLEDGEMENTS

The authors would like to thank L. M. Jayne for his contributions from previous experimentation in arc fusion splicing. They also wish to express their appreciation to R. E. Porter for her experimental documentation and suggestions.

#### REFERENCES

1. Grisby, R., "Developments in Fusion Jointing of Optical Fibre", BICC, unpublished work.

2. Millar, C.A., "A Measurement Technique for Optical Fibre Break Angles", Optical and Quantum Electronics, 13 (1981), pp. 125-131.
3. Rondan, Fernandez B., Morales, A. Aguilar, "Optical and Mechanical Characteristics of Microflame Fusion Splicing of Optical Fiber", International Wire and Cable Symposium Proceedings, 1982.
4. Tabata, K., "On The Causes of The Surface Devitrification of Glasses", Researches of the Electrotechnical Laboratory, No. 165, 1926.
5. Hatakeyama, J., et al., "Mechanical Strength of Fusion Spliced Optical Fibres", Electron. Lett., 1978, 14, pp. 613-614.
6. Gentile, J., "Characterizing Optical Fibers with an OTDR", Electro-Optical Systems Design, April, 1981.
7. Eccleston, D. J., "Environmental Testing of Coated Optical Fibers", Wire Technology, May 1982, pp. 113-116.
8. Young, D. R., "Environmental Effects on Acrylate Coated Optical Fibers", International Wire and Cable Symposium Proceedings, 1981.

#### BIBLIOGRAPHY



Donna Taylor is currently Senior Mechanical Environmental Engineer at the Waveguide Product Engineering Laboratory of Corning Glass Works.

A graduate of Alfred University in Ceramic Science, she has worked in the areas of mechanical testing and developments of technical glasses and glass-ceramics in Corning Glass Works' Research and Development Laboratories.



Stuart Saikkonen has been working on all aspects of optical waveguide splicing for the past year. He is currently the project engineer for the Corning Glass Works' Factory Splicing program. He received his bachelor's degree in Mechanical Engineering from Rochester Institute of Technology in 1981.



## FABRICATION AND EVALUATION OF A HIGH DENSITY MULTI FIBER PLASTIC CONNECTOR

S. Tachigami, A. Ohtake, T. Hayashi, T. Iso, and T. Shirasawa

The Furukawa Electric Company, Ltd. Tokyo, Japan

## Summary

This connector is made by direct-molding a five-fiber tape using transfer-molding machine, so that it may be small in size, high in precision, low in cost, and easy to assemble. This connector has dimensions of 5 mm(t) x 13 mm(W) x 10 mm(L) and fiber space is 0.3 mm and alignment-hole space is 7 mm: five fibers of 0.125 mm in diameter and two alignment-holes of 1.4 mm in diameter are positioned in the line in the center of end face. The guide rod which is inserted in the alignment-hole has a diameter of 1.4 mm  $\pm$  0.5  $\mu$ m. The point to achieve ultra-precision molding was clarified as follows. The metal mold was machined by using sub-micron precision technique. That was designed so that the flow of molten resin might not disturb the alignment of fibers. The mold resin epoxy was selected as a mold resin from the view point of viscosity, shrinkage, tensile strength, adhesion to fibers and chemical resistance. We achieved a high precision direct-molding technique. The technique realized the axial offset of fibers and holes less than 2  $\mu$ m, with the result of alignment average insertion losses (150 connectors, namely 750 fibers) of 0.45 dB and the maximum of 0.8 dB without using index match.

## 1. Introduction

Realizations of multi fiber connectors are still very few — only a few examples have been reported so far. We have developed by direct-molding with plastics a multi fiber connector for a five-fiber tape<sup>(1)</sup> as shown in Fig. 1, which were

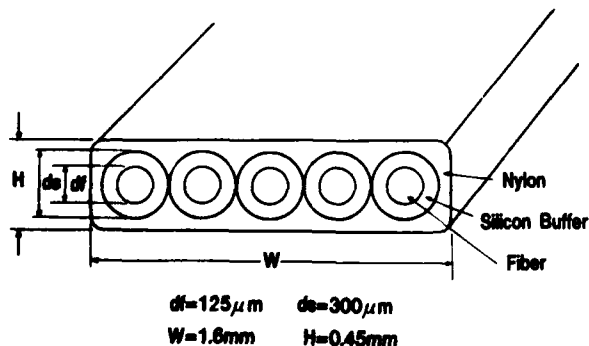


Fig. 1 Construction of Nylon extruded Five-fiber tape

reported previously. This time, a high fiber positioning accuracy within  $\pm 2 \mu$ m has been achieved along with a high insertion loss performance of 0.45 dB. Hereunder will be described the manufacturing aspects that have enabled a high positioning accuracy, and the characteristics of this connector.

The features of this connector are (1) a direct-molding type that permits assemble in the factory, (2) a low price expected because of a plastic molding, (3) a higher density, etc.

## 2. Construction and Manufacture of Connector

As reported previously<sup>(2)</sup>, this multi fiber plastic connector has a construction as shown in Fig. 2. The plug end face has dimensions

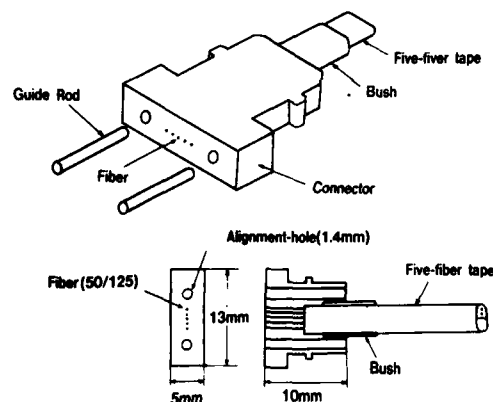


Fig. 2 Construction of Multi Fiber Plastic Connector

of 5 mm(t) x 13 mm(W), and 5 fibers are transfer-molded with a pitch of 0.3 mm transversely along the center line. On each side of the fibers, alignment-holes of  $\phi 1.4$  mm x 2 pcs are positioned, a distance of 7 mm apart. Precise insertion is accomplished by means of  $\phi 1.4$  mm guide rods of  $\pm 0.5 \mu$ m accuracy.

The points that have enabled ultra-precision molding are as follows. The outline of the metal mold is shown in Fig. 3. On the metal mold surface, the five fibers and the guide rods for molding are positioned with high precision.

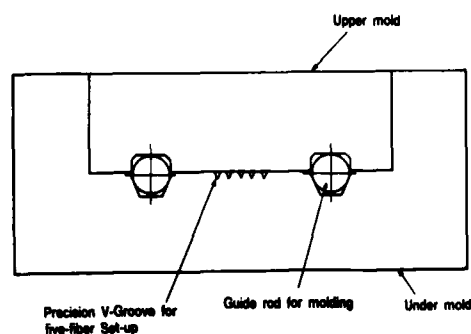


Fig. 3 Cross-section view of the metallic mold

The processing of the V-grooves was accomplished with a sub-micron accuracy. Also, a metal mold construction (positions of molding pins and especially fiber arrangement structure) free from the fluid effect of the molding material has been established. Rods of  $1.405 \text{ mm} \pm 0.5 \text{ }\mu\text{m}$  were used for molding.

As the molding material, a mold epoxy resin was adopted from the consideration for moldability. This resin has an optimal viscosity characteristic free from fiber breakage during molding, and also little forming shrinkage, high mechanical strength, excellent adhesion to fibers, and excellent chemical resistance. The typical physical properties of the mold epoxy resin used are shown in Table 1. The plug end face needs to be mirror-polished after molding. Polishing consists of two steps; a rough polish for 5 min., and a finishing polish for 5 min. respectively. Figure 4 shows the condition of the end face after completion of polishing. The finishing polish is lapped by using  $1 \text{ }\mu\text{m}$  aluminum oxide powder.

### 3. Results of Evaluation

#### 3.1 Dimensions

The multi fiber plastic connectors of this construction were made in quantity of 200 connectors (number of fibers  $n = 1000$ ). The alignment-hole diameters were measured with a  $1 \text{ }\mu\text{m}$ -step pin gauge in the range of  $1.399\text{--}1.403 \text{ mm}$  with a result that all were

Table 1 Properties of Epoxy Resin

Item	Unit	Data
Specific Gravity	—	1.8
Bending Strength	$\text{kg/mm}^2$	15
Modulus of Bending Elasticity	$\text{kg/mm}^2$	1400
Impact Strength	$\text{kg}\cdot\text{cm/cm}^2$	2
Water Absorbing	wt%	0.80
Expansion Coefficient	$1/^\circ\text{C}$	$2.0 \times 10^{-5}$
Mold Temperature	$^\circ\text{C}$	170 ~ 190
Mold Time	S	90 ~ 180
Mold Pressure	$\text{kg/cm}^2$	> 30
Mold Shrinkage	%	0.4

accurate to  $1.400 \pm 1 \text{ }\mu\text{m}$ . Next, the positions of the alignment-holes and the fiber center was checked. With the  $1.400 \text{ mm}$  rods fitted into the alignment holes, each position was measured in regard to x and y directions with a tool microscope, from which the center positions were calculated. The results showed an offset from the center line from a guide rod to another one of within  $\pm 1 \text{ }\mu\text{m}$  in the y direction. Also, the dimensional accuracies in the x direction were within  $0.300 \text{ mm} \pm 1 \text{ }\mu\text{m}$  in the pitches between the fibers, and within  $7 \text{ mm} \pm 2 \text{ }\mu\text{m}$  in the distance between the guide rods as designed for.

#### 3.2 Initial Characteristics

##### (1) Connecting loss

The connecting loss of multi fiber plastic connectors was measured with the measuring setup shown in Fig. 5. Guide rods of  $\phi 1.400 \text{ mm}$  were used, and an arbitrary sample was picked up from the moldings as a standard connector. The results of measurement are shown in Fig. 6. The fibers employed were GI fibers with a core-diameter of  $50 \text{ }\mu\text{m}$ , O.D.  $125 \text{ }\mu\text{m}$ ,  $\Delta = 1\%$  ( $\text{NA} = 0.23$ ). The average values for  $N = 150$  connectors (number of fibers  $n = 750$  cores) without using index match were satisfactory to show the average connecting loss



Fig. 4 Polished end face

of 0.45 dB and the maximum of 0.8 dB.

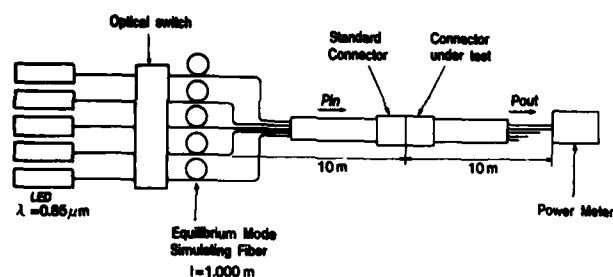


Fig. 5 Measurement Setup of Multi Fiber Plastic Connector

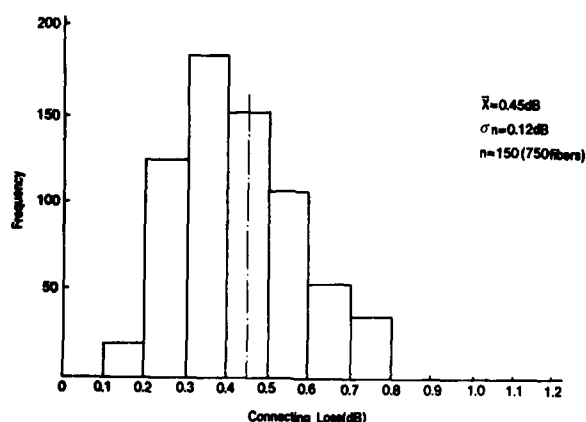


Fig. 6 Connecting Loss

## (2) Tensile strength

Figure 7 shows the measuring method. The breaking point was measured by stretching while monitoring the power, and by confirming the interruption of the light passage. The data of the initial value are shown in Fig. 8. The initial value was 8.1 kg.

## 3.3 Reliability Test

The conditions of the various reliability tests carried out are shown in Table 2.

### (1) Humidity test

The variations of dimensions were measured after exposing the sample in a 60°C x 95% relative humidity test chamber for 30 days. No change in the alignment-hole diameters was noticed, all staying at  $1.400 \text{ mm} \pm 1 \text{ } \mu\text{m}$ .

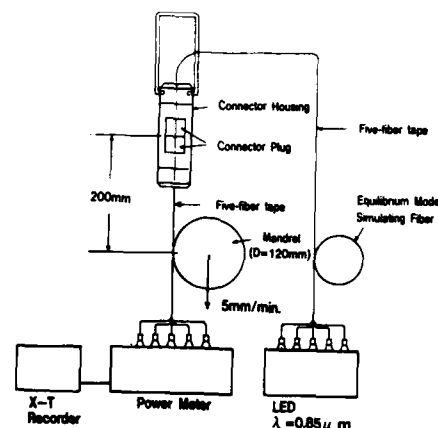


Fig. 7 Tensile test method

Table 2 Reliability Test Condition

Item	Condition	The Number of Samples	Estimation Method
Humidity	60°C x 95% RH	10 (5 Couples)	Dimensions, Loss Increase and Breaking Strength
Heat Cycle	-30°C ~ +60°C 4 Cycle/day	10 (5 Couples)	Loss Increase and Breaking Strength
High Temperature	80°C	10 (5 Couples)	
Low Temperature	-20°C	10 (5 Couples)	
Vibration	Frequency: 20Hz Amplitude: 1.5mm Direction: Longitudinal and Radius Time: 1 Hour	10 (5 Couples)	Loss Increase
Connecting and Disconnecting	500 Times	6 (1 Couples x 3)	

Further, the pitch between fibers in the x direction remained unchanged within  $0.300 \text{ mm} \pm 1 \text{ } \mu\text{m}$  after the humidity test. The distance between the center of alignment-holes showed an increase of  $3 \text{ } \mu\text{m}$  against the 7 mm pitch, i.e., an increase of  $1.5 \text{ } \mu\text{m}$  (0.04%) against the 3.5 mm pitch between the connector center position and the center of alignment-holes.

Further, there was no deviation from the center line from a guide rod to another one in the y direction, being within  $\pm 1 \text{ } \mu\text{m}$ . The tensile strength after the humidity test is shown in Fig. 8.

Five samples, each with connectors attached to both ends of 2 m-long five-fiber tape, were connected in series and subjected to 60°C x 95% R.H. x 30 days test, and the connecting loss was measured. The results of measurement are shown in Fig. 9. As a result, there was seen little change in the tensile strength and the connecting loss before and after the humidity test, thus proving the stable characteristic against the humidity heating.

## (2) Heat cycle test

Like the humidity test, five samples, each made of five-fiber tape with connectors attached to the both ends, were connected in series and subjected to a(-30° to + 60°) x 30 day test, and the connecting loss variation was measured. The results of measurement are shown in Fig. 9. Before and after the heat cycle, there was almost no connecting loss variation, thus proving satisfactory heat-cycle resistance characteristic of this multi fiber plastic connector. Furthermore, the samples whose heat-cycle was completed were subjected to a tension test by the measuring method shown in Fig. 7, and the tensile strength variation before and after the heat cycle was examined. The test results are shown in Fig. 8.

There was almost no change in the tensile strength before and after the heat cycle, thus proving satisfactory heat-cycle characteristic from the mechanical point of view.

## (3) High- and low- temperature tests

High- and low-temperature tests were performed with the same evaluation method as the humidity test. The testing conditions were 80°C x 30 days continuous for the high-temperature test and -20°C x 30 days continuous for the low-temperature test. The changes in the connecting loss and tensile strength before and after the tests are shown in Fig. 9 and Fig. 8. In either case, no change was recognized, proving that this connector has satisfactory high- and low-temperature characteristics.

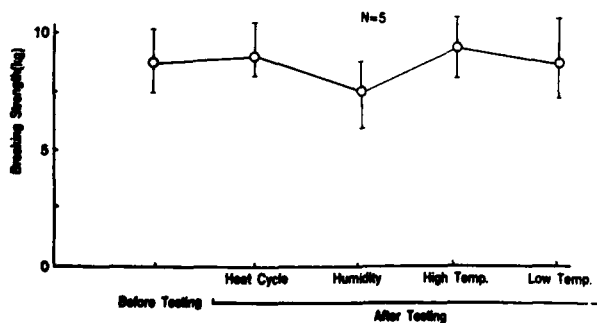


Fig. 8 Breaking strength change before and after reliability test

## (4) Vibration test

The same sample as in the humidity test was mounted on a vibration tester for a vibration test. The test conditions were frequency 20 Hz, total amplitude 1.5 mm, one hour vibration each in horizontal and vertical directions - 2 hours in total. The changes in the connecting loss after the test are shown in Fig. 9. Almost no change is seen, thus proving a stable property.

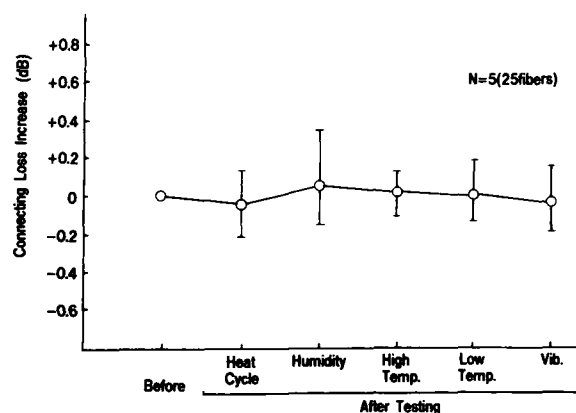


Fig. 9 Connecting loss change before and after reliability test

## (5) Repetitive connecting and disconnecting test

With connectors attached to both ends of 2 m-long five-fiber tape, the sample connectors were repeatedly connected and disconnected, and the connection loss was measured every 50 cycles with the measuring setup shown in Fig. 5.

The number of samples was  $n = 3$ . The results of connecting and disconnecting tests up to 500 cycles are shown in Fig. 10. The change in the connecting loss was within  $\pm 0.1$  dB, thus showing a stable characteristic. The diameters of the alignment-holes were measured after the 500 connecting and disconnecting tests with a result that no change in the alignment-holes diameters was noticed, thus proving a good wear-resistance property of this connector.

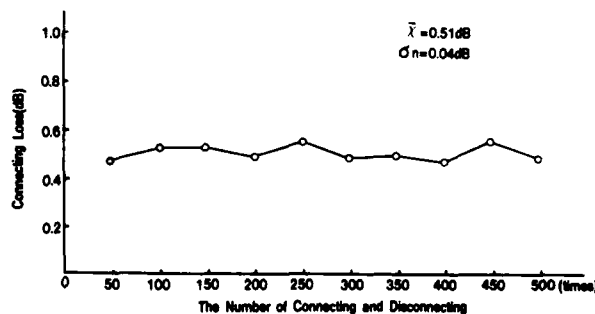


Fig. 10 Result of connecting and disconnecting test

#### 4. Conclusion

A multi fiber plastic connector has been developed by direct molding five-fiber tape through ultra-precision transfer-molding. Having satisfactory connection loss performance of 0.45 dB (without using index match) on an average, and a maximum 0.8 dB, this connector has stable characteristics also in such environmental tests as the humidity test and heat-cycle test as well as in various mechanical tests such as the repetitive connecting and disconnecting test. Far surpassing a single fiber connector in its density, this multi fiber plastic connector is highly effective as a terminal connector of multi fiber cables or multi fiber tapes, thus promising a wide application in future.

#### 5. Acknowledgement

We would like to express our appreciation to Mr. M. Azuma and Mr. S. Inao of R. & D. Dept. of Furukawa Electric Co., Ltd. for valuable guidance and advice in this development project, and further to Mr. S. Takagi and other members of Communication System Equipment Dept. of the same company for great assistance in the manufacture and evaluation of this multi fiber plastic connector.

#### 6. Literature

- (1) Y. Koyamada, S. Hatano, H. Shinohara, and F. Nihei, "A Study on High Density Optical Cables with a Great Many Fibers", IWCS, 1981.
- (2) M. Oda, M. Ogai, A. Ohtake, S. Tachigami, and K. Ohkubo, "Nylon Extruded Fiber Ribbon and its Connector", OFC, 1982.



Shigeru TACHIGAMI  
The Furukawa Electric Co.,  
Ltd.  
6 Yawata-Kaigan-Dori,  
Ichihara, Chiba, Japan

Mr. Tachigami graduated from Tohoku Univ. 1970 with a B. Sc. in mechanical engineering. Then he joined The Furukawa Electric Co., Ltd. and has been engaged in research and development to telephone cable and the accessories. He is presently engaged in research and development of accessories of optical fiber cable.

Mr. Tachigami is now an assistant manager of Fiber Optics Apparatus Group, Research & Development Department, Telecommunication Division. He is a member of the Institute of Electric Engineers of Japan.

Mr. Hayashi graduated from Kyoto Univ. 1981 with a B. Sc. in chemical engineering. Then he joined The Furukawa Electric Co., Ltd. and has been engaged in research and development of fiber optics apparatus.

Mr. Hayashi is now a staff engineer of Fiber Optics Apparatus Group, Research & Development Department, Telecommunication Division at The Furukawa Electric Co., Ltd. and a member of the Institute of Electronics and Communication Engineers of Japan.



Takaaki ISO  
The Furukawa Electric Co.,  
Ltd.  
6 Yawata-Kaigan-Dori,  
Ichihara, Chiba, Japan

Mr. Iso graduated from Nikko High-school 1962. Then he joined The Furukawa Electric Co., Ltd. and has been engaged in product of metallic cables, and is now in research and development of fiber optics apparatus.

Mr. Iso is now an engineer of Fiber Optics Apparatus Group, Research & Development Department, Telecommunication Division at The Furukawa Electric Co., Ltd.



Akihiro OTAKE  
The Furukawa Electric Co.,  
Ltd.  
6 Yawata-Kaigan-Dori,  
Ichihara, Chiba, Japan

Mr. Otake graduated from Tohoku Univ. 1974, and joined The Furukawa Electric Co., Ltd. in 1974 and has been engaged in development of coaxial cables, optical fiber cables, and now development of accessories of optical fiber cables.

Mr. Otake is now a staff engineer of Fiber Optics Apparatus Group, Research & Development Department, Telecommunication Division at The Furukawa Electric Co., Ltd. and a member of the Institute of Electronics and Communication Engineers of Japan.



Tohru SHIRASAWA  
The Furukawa Electric Co.,  
Ltd.  
6 Yawata-Kaigan-Dori,  
Ichihara, Chiba, Japan

Mr. Shirasawa graduated from Tokyo Institute of Technology 1977 with a M. Sc. in mechanical engineering. Then he joined the Furukawa Electric Co., Ltd. and has been engaged in design of productive plants at Plant Engineering Division.

Mr. Shirasawa is now a staff engineer of Machine Department of Plant & Facilities Division.



Takehiro HAYASHI  
The Furukawa Electric Co.,  
Ltd.  
6 Yawata-Kaigan-Dori,  
Ichihara, Chiba, Japan



AD-A136 749

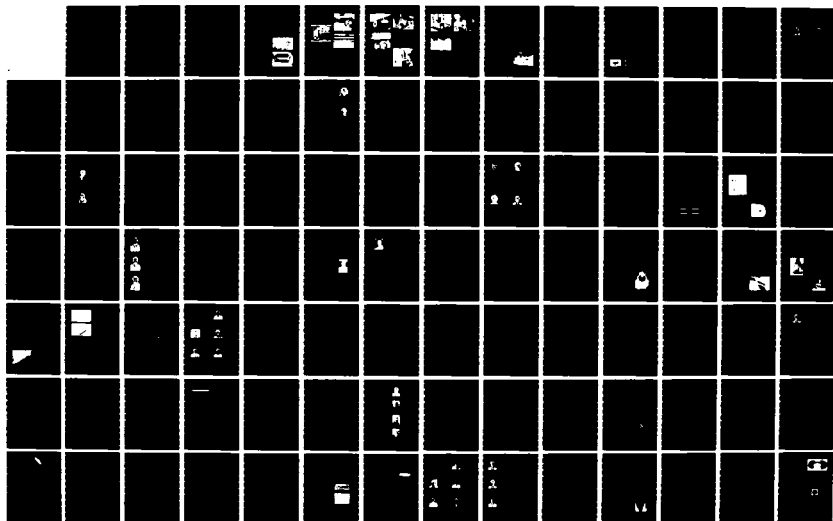
PROCEEDINGS OF THE INTERNATIONAL WIRE AND CABLE  
SYMPOSIUM (32ND) HELD AT (U) ARMY  
COMMUNICATIONS-ELECTRONICS COMMAND FORT MONMOUTH NJ  
17 NOV 83

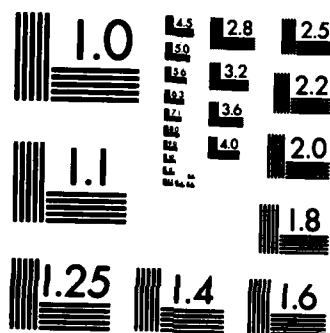
2/5

UNCLASSIFIED

F/G 5/2

NL





MICROCOPY RESOLUTION TEST CHART  
NATIONAL BUREAU OF STANDARDS-1963-A

## LEAD MAKING FOR IMPROVED CONTINUOUS-FLOW MANUFACTURING SYSTEMS

Paul Heintzman

AMP Incorporated

### ABSTRACT

The importance of the latest in connector technology, chip carriers, surface mounted devices, and high density interconnects not withstanding, the foreseeable future of most durable goods includes designs in which discrete wires play a significant role. As long as user operated electro-mechanical controls exist for widely spaced functional components such as motors, relays, and safety switches, discrete wiring harnesses will continue to be a major concern of original equipment manufacturers. Economy and productivity must be maintained in spite of competitive pressures which demand expanded product lines and carefully controlled component inventories, manufacturing schedules, and deliveries.

This paper explores some of the options available to answer these needs as they relate to discrete wiring and harnessing. Not only is available manufacturing hardware analyzed in terms of production capabilities but also in-house and vendor supply source alternatives are considered. The place of existing manufacturing technology, from hand operated bench machines to high-speed, high-volume automatic lead making equipment is discussed with respect to the most economical production applications. Included here is consideration of nondedicated automatic lead making machines with interchangeable tooling for the application of a variety of terminals in profitable intermediate volume runs.

### MANUFACTURING CHALLENGES TODAY

The latest fluctuations in economic conditions have pointed out quite clearly the vulnerability of domestic manufacturing to the whims of the economic climate and the fickleness of the American consumer. Ideally, a manufacturing system should be able to adjust almost instantaneously to any real or perceived change. The sooner adjustments can be made, the more likely a manufacturer is to be able to adjust product inventories to demands, thereby avoiding the financial setbacks of overstock or the loss of market share because sudden demand cannot be met.

The need to be flexible is no more apparent than it is in mature industries, typically white goods. In spite of the desire for flexibility, reality dictates the unlikelihood that an entire manufacturing production line can reach the ideal. However, production system improved only a

little, at a reasonable cost, might very well enhance the manufacturer's position in the market place. Moreover, if some element which improves one system can be used in another, then the advantages multiply.

A great deal has been said about the need for American manufacturers to update their production equipment to meet the needs of productivity. Unfortunately, the investment needed to accomplish this has been astronomical. Domestic production has limped along with outclassed methods because the necessary capital to update has not materialized. Indeed, available funds, especially in the white goods industries, of necessity have been channeled into minimizing the effect of shrinking sales.

Many manufacturers recognize that automation, or further automation, is likely to be the only possible course for survival. Again, the cost is often prohibitive. In many cases, not only is the price too high, but volumes of any one product line do not justify the investment for full automation. To reconcile costs and volumes, one possible answer could be automated equipment which is initially less expensive than presently available machines, and which has the flexibility to allow it to change quickly and be moved to another production area.

### DISCRETE WIRING IN THE MODERN WORLD

In spite of an apparent romance with "hi-tech" one simple fact remains: as far as anyone can see into the future, certain major industries will continue to use discrete wiring. The white goods industry is a good example. At least up to this point in time, no one has come up with an alternative when a satellite approach to the transmission of signals to components is a necessary design element of a product. This is especially true when only a few signal transmission lines are needed and when the component terminals are widely spaced. Essentially, what this means is that the newer techniques of mass termination of discrete wires and ribbon cable have limited application in some industries. The necessity of manufacturing single leads remains.

In the consumer products industry, as in others like it, the OEM has two choices for fulfilling his discrete wiring needs, in-house manufacture, or job-shop to a harness maker. In either case the economics are essentially the same. If the product or product lines are of only moderate volume, the expense of each finished unit will be affected to some degree by the cost of harness manufacture. So far nothing new.

Automatic equipment is available. If the manufacturer uses an in-house leadmaker, he must have sufficient volume to justify the equipment not only in terms of up-time, but also in terms of the changeover time needed to produce leads of a different configuration. The bottom line is, the single lead discrete wire is here to stay at least for a good while. Ways need to be found that will allow manufacturers to economically produce or economically purchase this component.

Ideally the manufacturer can maintain better control over the production of his finished product if all work is done in-house. If this is not possible, then a job-shop that can respond to his needs is the next most desirable alternative. Traditionally, one answer to this problem has been to go to foreign sources whose relatively inexpensive labor costs make purchasing medium quantities economically viable. As transportation costs have risen, the need for timely response to market demands has increased, and controlling inventories has become an essential of good management, foreign sourcing has become less desirable. Even when using local suppliers, purchasing medium quantities of a specific lead has become critical to the final cost of a finished product. A supplier incapable of responding quickly and reliably to a rush order leaves the manufacturer in the lurch.

In the past, economically rewarding harness manufacture depended heavily on productivity based on vast numbers of identical leads produced at great rates. Current markets demand greater product-line diversity, and smaller numbers of relatively short lived models. This trend is likely to dominate the future. Further, as associated technologies develop, manufacturers must be able to update products on very short notice. Undoubtedly, all these changes directly affect the harnesses used, and therefore, their manufacture.

To maintain productivity and competitive position, manufacturers must rely on manufacturing equipment that will adjust to their low- and medium-volume needs. Adjusting manufacturing techniques to accommodate high volume production equipment to lower volume use is impractical.

Productivity of harness making equipment can no longer be measured solely in terms of increased production runs over shorter time spans. Assuredly speed is important, but serious consideration must be given to the ability to produce low-to-medium volume runs and the ability to change quickly and efficiently to a different lead configuration for another low-to-medium volume run. Presently, automatic equipment that can fulfill this need and at the same time remain flexible in terms of lead and terminal type, simply isn't available.

Machine designers have long given up the idea of developing the perfect lead making machine. Theoretically, a machine that terminates an infinite variety of connectors on infinitely variable wire lengths, at incredible speeds is possible — indeed, some machines available today closely approach that ideal — but at what cost? And, when the time comes to change tooling (which is frequently necessary because of the wide disparity between terminal configurations used within one or more products) at what down-time cost? And what cost to dedicate a skilled operator?

While the ideal is not impossible, it is impractical from a cost standpoint. Obviously, some compromises must be made. By establishing those characteristics that cannot or should not be compromised, an outline of a practical machine can be established. To be an economic advantage, the capital investment necessary for the lease or purchase of such a machine must be significantly less than currently available high-speed automatic equipment. This only makes sense, but at the same time the newly designed equipment must be at least competitively priced in comparison to available lower volume machines while providing more capability.

Satisfying these requirements is not unlike a juggler's trying to balance on the end of a broomstick, items which share no truly similar physical characteristics.

#### ANALYSIS OF SPECIFIC NEEDS

A careful analysis of the lead making industry reveals that the overwhelming majority of terminals used in harness manufacture crimp single, solid or stranded, conductor wires to either open or closed barrel connectors which are delivered to the termination tooling in either end feed or side feed strip. While infinitely variable wire lengths, from miniscule to super length, are sometimes specified, need for leads less than 1 1/2" long and greater than 60" long, decreases with each increment in either direction.

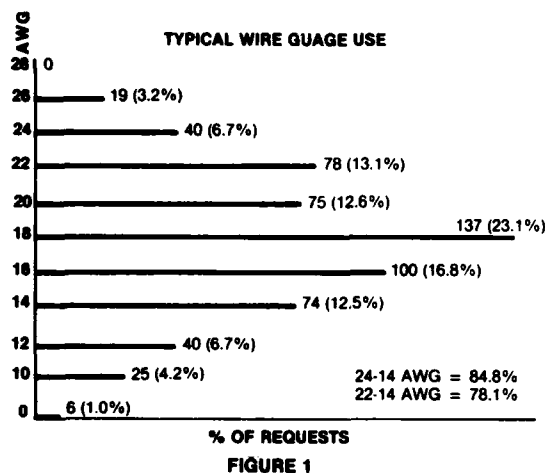
Research shows that creating a machine capable of terminating some of the more esoteric connectors such as gold wire splice or modular plugs on to unusually short or long leads, substantially increases machine cost. Keeping in mind that the proposed equipment is intended for moderate production runs, the likelihood is that manufacturers and harnessmakers who need the capability to terminate some of these more exotic terminals onto extremely short or long leads would likely find high-speed automatic machines to be more economically viable.

The primary thrust of the development of a new machine is to make automatic production equipment possible for production runs which have been, up to this point, handled by the most basic terminating equipment. Those who have justification for high-speed high-volume equipment may have little interest in a new machine. The new concept is intended to fill the present vacancy between the high-volume equipment and labor intensive low-volume nonautomatic equipment.

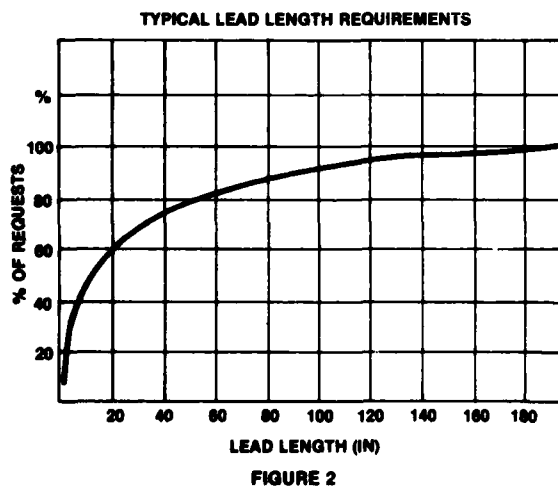
#### REQUIREMENTS

The shift in lead types, configurations and production runs have influenced perceived characteristics for mid-range machines. Surprisingly, high machine cycle rate is not a priority item for many industrial and data system manufacturers. This rate requirement would be adequately filled by a stable, reliable machine that produces 3000 to 4000 leads per hour *without* a full time operator in attendance. Ease of maintenance and quick changeover of wire and terminals are the high priority items since the average run between set-up ranges from about 300 to about 3000 leads.

In addition to simplicity of set up, simplicity of controls, and simplicity of operation, a machine of this sort should accommodate a wide variety of insulation types and a wide tolerance for wire diameter, limpness, or stiffness. Clear indications exist which show that almost 85% of harness leads fall between 24 AWG wire and 14 AWG wire with 23% being 18 AWG (Figure 1). The 24 to 14 AWG range should therefore fall within the machine's capability.



Along this same line, research shows that 80% of all lead lengths required by manufactures fall between 8" and just under 60" with a 3/32" to 1/2" strip length (Figure 2). For those occasions where longer leads are required, a simple double cycling function, at an understandably somewhat slower speed, would suffice. Sufficient need for single ended leads exists to make that capability an additional requirement.



### THE MACHINE: Making It Simple

As lead making equipment designs developed to meet the demand for expanded capabilities, machines, of necessity, increased in complexity and consequently increased in cost. To meet new production demands a concerted effort must be made to simplify. Through direct effort to uncomplicate, it is possible to create a

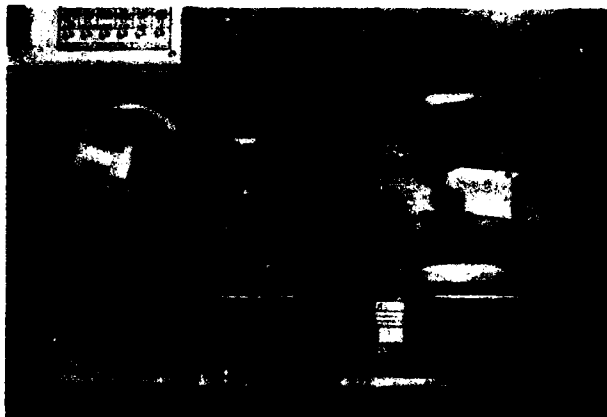
machine that not only does the job well, but also considerably reduces operator skill requirements.

The result of this research is the Economator lead making machine which attempts to fill the gap between labor intensive low production bench equipment and very high-speed automatic leadmakers. As such, it will handle 14-24 AWG stranded or solid wire for producing leads of 2 3/4" to 60". Little or no variation in lead length occurs. 2800 leads per hour for short leads and 2000 leads per hour for longer lengths are typical. At a slightly reduced rate, up to 120" leads can be made with an optional double stroke cycle.

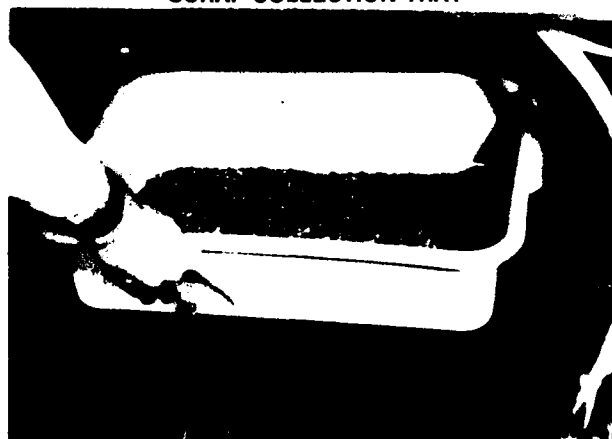
Simplicity of design and convenience of operation were principle design factors. With leveling legs retracted, the weight of the machine is transferred to casters which allow the machine to be relocated in various production areas.

Instead of standing idle, the Economator machine can be quickly changed over to produce leads for another production line. In this way, overall machine up-time increases. The base assembly includes storage for application tooling (Figure 3) and scrap collection trays (Figure 4). Modular sub-assembly units, attached to the base, perform individual functions. Modularization along with simplified tooling fixtures allows quick set-up and adjustment with minimum tools and skill.

### TOOLING STORAGE



**FIGURE 3**  
**SCRAP COLLECTION TRAY**



**FIGURE 4**

## Controls

Although the sequential machine cycle is directed by a programmable controller, operation of the machine is simplified through a straightforward control panel (Figure 5) which consists of an on/emergency stop button, a cycle jog button and a cycle stop button. A series of toggle switches control individual machine functions. The operator need only select the appropriate switch to check a function — no complicated keyboards or typed-in commands are necessary. The elimination of keyboard and CRT contribute to the machine's overall cost efficiency.

CONTROL PANEL

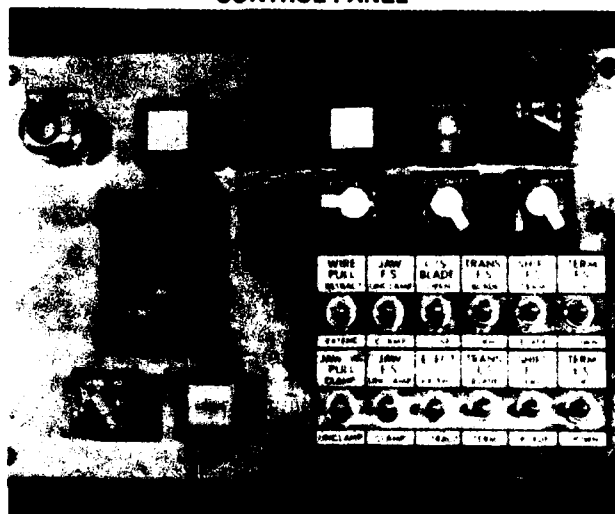


FIGURE 5

For single-ended termination, or nonterminated lead making, a selector switch can be set to de-activate either or both crimping units. Additional switches provide transfer shift motion to accommodate certain terminals and provide for an add-on wire marker.

The control panel includes a digital batch counter, and audible batch indicator. Emergency stop and jog switches are remotely located on the far side of the machine opposite the position normally occupied by the operator.

## Incoming Wire Preparation

Wire handling is equally simple. Once the wire in use has been removed, the replacement is fed through a dereeling unit (Figure 6) which includes an anti-back-up device and wire straightener. The wire is looped once around a constantly running capstan wheel so wire feed only occurs when the rail mounted wire-pull jaws grip the wire and move to the pre-set length. 24 to 14 AWG solid or stranded wire with insulation outside diameter of .235" to .040" are all within the machine's capability. Lead length changes are made by way of a simple adjustment handle (Figure 7) which is unlocked, slid along the scale to its new location and locked in place. A lighted marker makes set up simple and accurate.

WIRE DEREEING UNIT

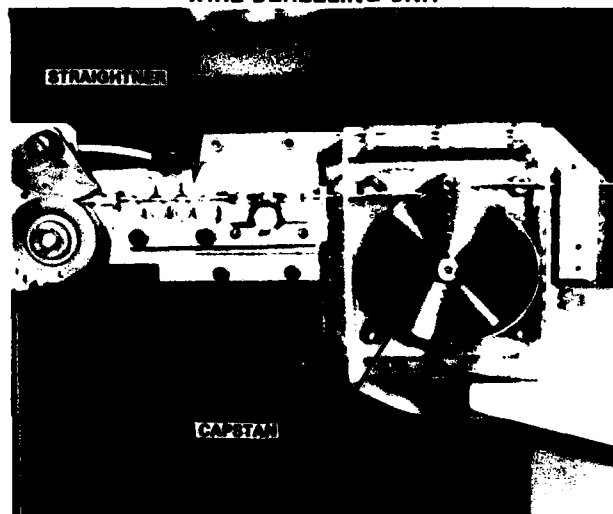


FIGURE 6

LEAD LENGTH ADJUSTER

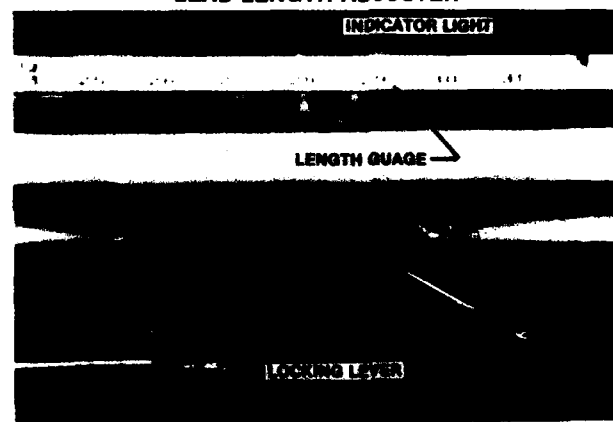


FIGURE 7

## Stripping Modules

Drawing on some existing technology, which has proven itself over time, some of the questions of reliability which often plague new designs are eliminated. For instance, the stripping blades common in the industry, incorporated into a new design achieves several advantages. First of all, they are readily available. Secondly, by using equally common holding fixtures, modules can be set up and inventoried (Figure 8) so they are available when needed for a changeover from one lead configuration to another. These modules are designed to allow positive placement and mounting with four set screws. Fine adjustment is made by manipulating a simple knob (Figure 9). Final fine adjustment of closing depth is accomplished with a simple self-locking knob. The strip blades are horizontally opposed which permits chips to fall freely into a collecting tray integrated into the machine.

### STRIPPING MODULES

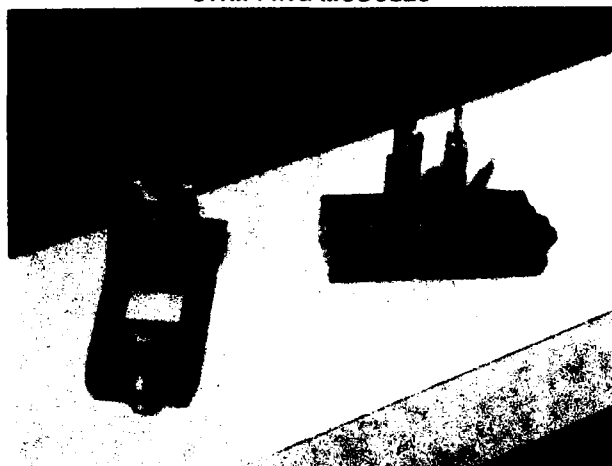


FIGURE 8

### ADJUSTMENT KNOBS

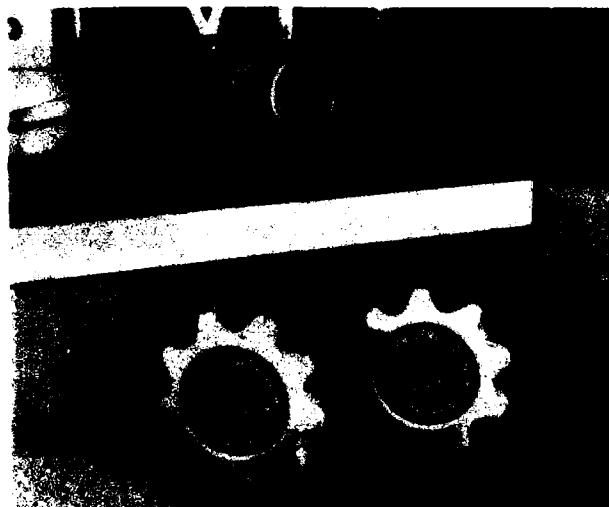


FIGURE 9

### Wire Handling

Two identical transfer units, one on the feed side for the forward end of the incoming wire and one on the eject side for the trailing end of the finished wire grip the respective ends just behind the stripping blades. The units, in one smooth motion, pull the wires back, stripping the insulation, transfer 45°, and push the wire into the appropriate terminating unit.

When closed barrel product is being run, the wire is transferred horizontally and pushed straight into the terminal. For open barrel terminals, a knob adjustment changes the wire transfer, bringing it in high. A simple tonking attachment (Figure 10) on the terminator pushes the wire down onto the terminal an instant before the final crimp. In either case, open or closed barrel terminals, precise positioning of the wire is adjusted with individual self-locking knobs.

### OPEN BARREL TERMINAL TONKING DEVICE

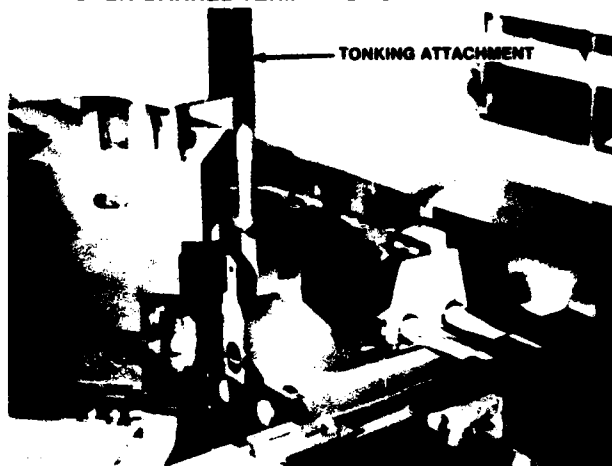


FIGURE 10

### Terminating Units and Applicators

The two terminating units (Figure 11), one on the incoming side and one on the trailing side use quick-change heavy duty applicators (Figure 12). These crimping devices are modularized, off-the-shelf items (Figure 13). No set up time is needed other than to remove the one mounted in the terminating unit, and to position the new one. The applicators are the same as those used on high-speed automatic equipment. Their proven performance under severest conditions make them the choice for longevity. This tooling is readily available in sufficient variety to allow termination of wires to almost any open or closed barrel terminal. In addition, the applicators allow adjustment for crimp height and crimp width so they in themselves contribute to the machine's flexibility by being individually adaptable to terminal variation within a family of connectors. The applicators' basic design allows adaptation to development of new terminals.

### TERMINATING UNITS



FIGURE 11

#### HEAVY DUTY MINI-APPLICATOR



FIGURE 12

#### APPLICATOR MODULES



FIGURE 13

#### Set-up Time

Since the terminator is mounted on an air bearing, the unit is easily rotated outward giving unencumbered access for applicator positioning and such minor adjustment as may be necessary. In addition, each terminating unit has a constantly rotating nylon brush (Figure 14) against which mounted terminals are run thereby assisting the dereeling process. Mounting hardware for the applicators eliminates the need for wrenches and sockets; control knobs accomplish fine adjustments. Overall set-up time is minimal.

Total change-over time including applicator, strip blades, product reels and wire is typically 20 minutes. This includes adjustments for strip depth and to the wire feed tube.

#### DEREELING BRUSH



FIGURE 14

The terminating units, with appropriate applicators will process end feed, side feed, open and closed barrel terminals. A split cycle feature eliminates cycle dwell characteristically present when a closed barrel terminal is being processed with mechanical cam-driven terminating equipment. The typical pause of these machines occurs when the tool descends to capture the terminal. The lead processing operation must wait for the terminal position before the wire can be pushed into the terminal. With split cycle operation, the press' sequential cycle is split so capturing the terminal occurs during wire preparation. Thus the terminal is ready to accept the wire without delay.

#### PERFORMANCE AND APPLIED COST

All the good ideas and innovative approaches in the world are wasted unless a machine of this type meets two important standards: versatile performance and cost effective operation. In terms of performance capability, the machine succeeds:

Functions: single lead measure, cut, strip, and terminate; none, one, or both ends.

Terminate: open or closed barrel, side or end feed.

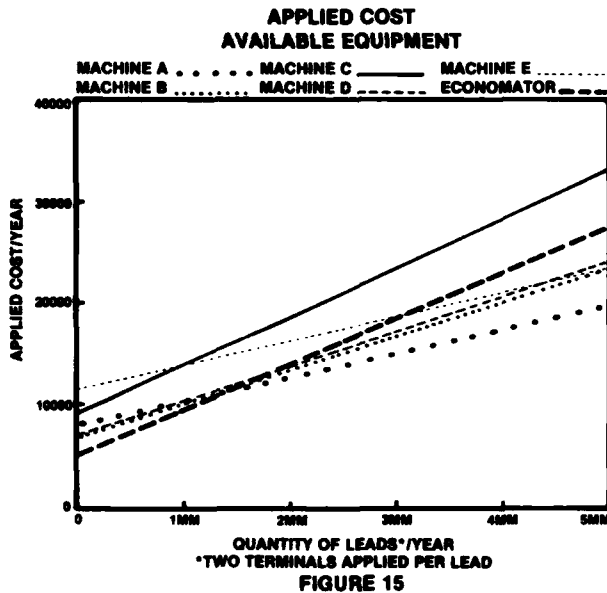
Wires: 24 to 14 AWG, stranded or solid; .040" to .235" insulation diameter of all material types.

Lead length: 2.5" to 60" with a tolerance of  $\pm .25\%$  and a minimum tolerance of  $\pm 1/32"$

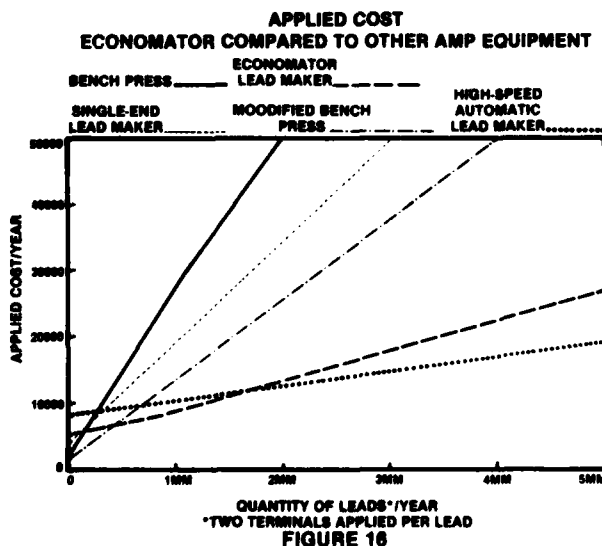
Strip length:  $1/8"$  to  $1/2"$ , with a tolerance of  $\pm 1/64"$ .

Typically, the Economotor machine completes 2800 leads per hour using closed barrel terminals, 2700 leads per hour using open barrel terminals, and 2000 leads per hour when working to maximum single stroke length. True this is a lower productivity level than high-speed automatic equipment, but the Economotor lead making machine is intended to operate at 60% of the cost of the high volume units.

Cost effective production is of course the determining factor. Keeping in mind that this machine is intended to fill a specific need, comparison to other equipment presently available shows that the Economator lead maker maintains a significant and consistent applied cost advantage when production quantities do not exceed 1.5 million leads per year (Figure 15). In many cases the other available machines lack some of the Economator machine's terminal handling capability.



In comparison to other methods of single lead manufacture, the Economator machine again stakes out an important range. From above 500,000 leads per year, and up to more than 1.5 million leads per year, the Economator lead maker provides a lower applied cost than any other method, including simple bench-mounted terminating equipment, single-end lead making machines, and high-volume automatic machines (Figure 16).



In addition, if the total up-time increase which results from this machine's quick change-over capability is considered, the Economator machine's cost effectiveness range shows applied cost advantage to 4 million leads per year. All applied cost figures for these comparisons are based upon, 1800 shift hours per year, 6" lead length, and a labor rate of \$12.00 per hour. All calculations consider terminating both ends of a lead; figures will vary as changes are made in the basic productivity model.

Finally, mention must be made of the steps that have been taken to ensure that the greatest overall up-time is possible. As a result of making this aspect a major consideration, the Economator lead making machine has shown a 40% increase in up-time over other comparable machines. The contributing factor here is the machine's inherent flexibility and the significant reduction in set-up time needed to change from one lead and terminal configuration to another.

## CONCLUSION

The degree of success with which American industries meet their production and market challenges are very closely tied to their ability to adopt efficient manufacturing methods. Component production is an important consideration, especially now that the necessity of quick response to change has become obvious. Efficient moderate production rate assembly equipment that can be easily retooled for a variety of purposes is a significant resource.

The Economator lead making machine has been specifically designed to help those who need to manufacture leads efficiently in moderate quantities. Manufacturers, whose primary business is lead production, will find this machine to be an advantage for economically satisfying smaller orders. OEM's, using the Economator machine, can have an in-house alternative to purchasing from outside vendors.

## AMP ECONOMATOR LEAD MAKER



# LONGITUDINAL WATERBLOCKING PERFORMANCE OF CONDUCTIVE AND NON CONDUCTIVE WATERSWELLABLE NONWOVENS

B.J. Nieuwhof

R. de Vrieze

FIRET bv, P.O.Box 45, 3900 AA VEENENDAAL, The Netherlands

## ABSTRACT

Since the introduction of plastic insulated cables for transport of energy and telecommunication networks, longitudinal water penetration has become a subject of major interest.

Besides already introduced systems like Aquablock, petrolatum filling, steel jackets etc. water expandable tapes offer a distinct solution to the so called longitudinal water ingress into the cable interstices. The tapes have been developed in cooperation with European cablemakers and a practical experience of three years is available now.

Power cables have been subjected to the French EDF test where water penetration during functioning of the cable has been measured. Besides measurements on the cable itself the lecture will propose a measurement method for swellable effectiveness and control.

Other phenomena regarding interaction between metallic screens and the tape, temperature and electrical resistivity and long term stability will be reported.

## INTRODUCTION

Since the introduction of plastic insulated telephone and power cables, longitudinal water penetration has become a subject of major interest to anyone exploiting such cables.

Buried cables especially have more opportunity to suffer from water penetration. Water treeing is a well known phenomenon in PE- and XLPE insulated power cables and a loss of capacity in telecommunication cables does not lead to an efficient usage of the investment in communication network. Obviously the restriction of the repair length in case of damage does not need any further comments.

As the problem of water penetration is not entirely from a recent date, more than one solution has been developed. Solutions like Aquablock, Teleflock, Petrol Jelly filling, filling compounds and bituminised papers have to be mentioned.

As far as radial water penetration is concerned, extruded metal shields and aluminium-plastic composites offer a perfect seal against water and water vapour unless the shield has been damaged by

an external event. An additional longitudinal water barrier will prevent the cable in this case for any further water ingress.

A solution to the longitudinal water ingress in power and telecommunication cables is the usage of a water expandable tape, well known as nonwoven "swellable tape". In spite of its youth it has already given proof of its effectiveness.

## NONWOVEN SWELLABLE TAPE

Starting the development of a swellable tape preferably based on a nonwoven web, the objectives for the R&D department were:

"Try to develop an efficient system to achieve a longitudinal water barrier in power and telecommunication cables, enabling the use of existing cable production techniques. The solution should offer not only convenience during cable production but also during splicing, terminating and repairs. In this respect the usefulness of nonwovens has to be considered".

Water penetration into a cable should be stopped as soon as it has reached the inner structure.

Therefore the following demands can be formulated:

- The barrier system should consist of two cooperating parts.
  1. expanding item
  2. porous substrate
- The expanding part should have a fast and high swelling response to water.
- The substrate may not restrict the wetting of the expandable part.
- The water barrier should remain in its place during production, transport and installation of the cable.

The usage of swellable powders applied loose in a cable had been tried out already. A powder has the advantage of filling up all the interstices but on the other hand it is not very convenient while handling.

So summarizing, the conclusion of incorporating a swellable powder into a porous substrate slitted into tape is obvious.

A nonwoven as substrate will offer the following advantages:

- Due to its porosity the penetrating water will be allowed to flow directly into the swellable powder of the tape. The swellable powder will start its expansion immediately.

Porosity also helps the cushioning between insulation and metal screens in a cable. Porous materials also offer a good adherence to carbon black in case of conductive tapes.

- The composition of fibres in a nonwoven tape must be adapted to the chemical, mechanical and thermal conditions in the cable. Therefore a swellable tape has to be made of polyester fibres offering an excellent thermal and chemical stability.

Mechanically the weight per unit area and the bonding agent used, will guarantee sufficient tensile strength for wrapping purposes.

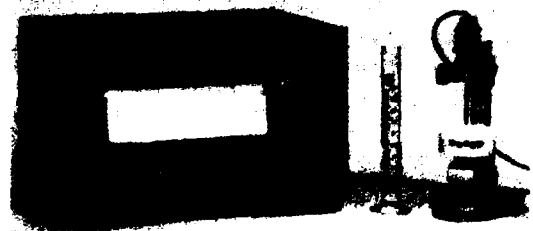
- Nonwoven technology gives access to laminating and sandwich techniques.
- The construction of a nonwoven swellable tape corresponds with the following description:
  - A porous nonwoven substrate mainly responsible for the mechanical strength.
  - On this substrate the swellable reactant is applied. This reactant is a synthetic water swellable powder with a specified particle geometry.
  - On top of the powder a covering nonwoven has been situated.

The whole system has been combined into a sandwich construction by means of a special production technique.

When semi-conductive substrates and covering nonwovens are taken, a semi-conductive swellable tape will be achieved. It will be obvious that the amount of swellable powder taken per unit area, will influence the volume of response to water penetrating into the cable.

#### CHARACTERISTICS OF SWELLABLE TAPE

In order to characterize the swellable properties of the tape, a special test has been developed.



A circular test specimen taken from the tape is situated with the swellable side up in a polyamide cup. A perforated ram is placed on top of the sample. By adding water the tape will start to expand and the dilatation of tape and ram are registered by a recorder. The results are plotted as shown in the following graph (Fig. 1)

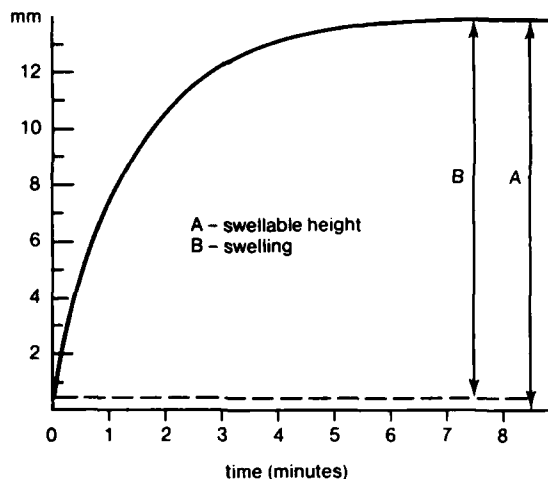


fig. 1 swellable height

As the concentration of ions solved in the water will affect the final swelling height, the test has to be carried out with distilled water.

The effect of ion concentration on the swellable height is shown in the following graph (Fig. 2)

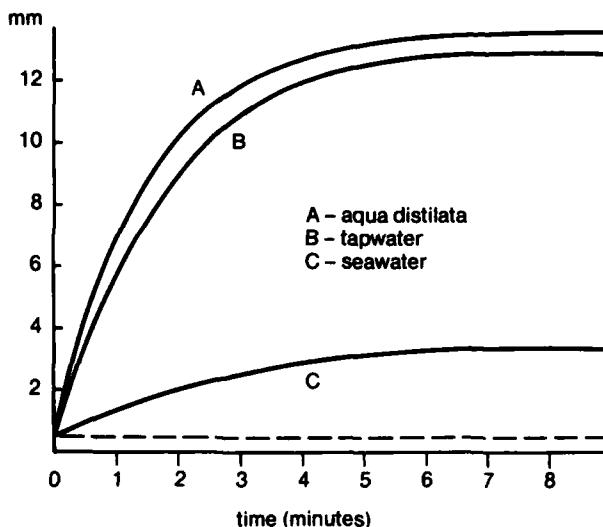


fig. 2 effect of ion concentration on swellable height

Finally there is some noticeable effect of pressure on the swellable tape. The jelly like powder acts as a sponge under pressure.

When it swells into the cable interstices it will not burst the cable jacket. The water inside the cable is blocked by means of the

- capillary counter pressure of the expanded gels
- the shear of the jelly like mass against the cable inside walls.

Of course the total effect of counter pressure depends on the cable geometry (free cross sectional area) and the swellable capacity of the tape chosen for the purpose.

Next graph shows the pressure sensitivity of a product with a swellable height of 3 millimeters. (Designed for telecommunication cables.)

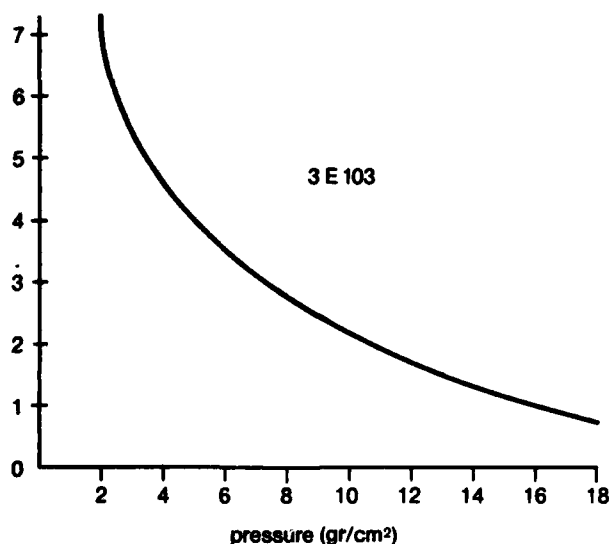


fig. 3 pressure sensitivity of swellable tape

#### APPLICATION REQUIREMENTS

During the 3 years of its existence, swellable tape had to face a lot of cable requirements such as:

##### - Temperature stability

As the temperature in the area of the screen might easily reach a height of 90 to 100°C for long periods, the tape has to be stable against this influence. There are two relevant tests to determine the performance of the tape.

##### 1. French EDF test: (Fig. 4)

The tape has to withstand the pressure of 80 millibar static watercolumn under the following conditions:

- 24 hours at room temperature
  - 4 hours heating up till 120°C conductor temperature
  - 4 hours cooling down to room temperature
- The cycle of the 4 hours heating and 4 hours cooling will be repeated 10 times.

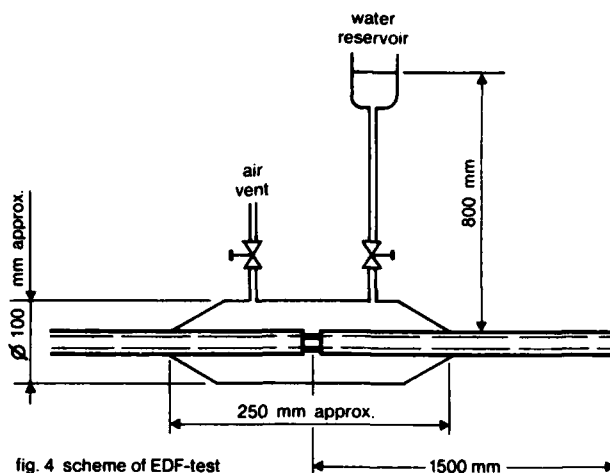


fig. 4 scheme of EDF-test

No water is allowed to break through on a distance of 1,5 meter from the entrance point of water penetration during the test.

Tests carried out with nonwoven swellable tapes did not show any failure even after a repeat of the test with the same specimen at 130°C and 135°C.

##### 2. Oven test: (Fig. 5)

Swellable powder has been exposed during 2 months to a temperature of 130°C. The powder will decrease in its capability to respond to water. If the original swellable height is 100%, only a decrease of max. 20% has been determined (see Fig. 5)

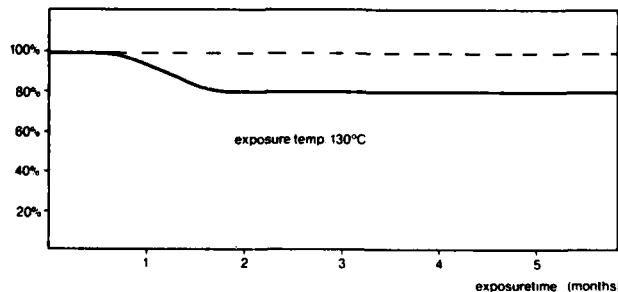


fig. 5 percentage of original swellable height

##### - Microbiological stability

As micro organisms, entering the cable together with the water, might attack the swellable system, synthetic systems are preferable.

##### - Corrosion of metallic screens

With aluminium and steel no corrosion has been discovered. In case the tape is used in contact with copper, a corrosion inhibitor will inhibit the reaction of copper with oxygen to produce copper oxide. This allows the choice of an organic acid containing swelling powder which would otherwise accelerate corrosion by forming copper complexes with the copper oxide. The search for corrosion inhibitors without health and environmental hazards must be carefully done.

- Applicability

The nature of the nonwoven enables longitudinal and helical application of the tape, due to its flexibility and smoothness. The high porosity provides heat barrier properties during the extrusion of the jacket and will protect thin conductors against the heat capacity of the extruded mass.

- Submarine applications

As said before, the swellable powder in the tape is sensitive to high ion concentrations. Therefore a tape for submarine cables has not been developed.

There are powders available which are less sensitive to this phenomenon. These powders can be chosen for submarine applications, however, to achieve an adequate height, more powder should be added into the tape.

- Viscosity breakdown

Not only the influence of ions is important. Amongst the swellable powders available there are some showing a substantial viscosity breakdown while in contact with water.

If this happens the effect of counter pressure built up by the powder will disappear after some time and the water front will penetrate further into the cable.

- Recuperative properties

Very important for power cables is the recuperative ability of the powder after having been wetted.

The effect with the powder used so far is the same as shown in fig. 5. So a 20% loss of swellable height has been found but the powder is still capable of swelling even after several test cycles.

#### APPLICATIONS

Power cables:

A radial water barrier in this cable is already achieved by its jacket, insulation and in some cases by means of an aluminium, lead or steel shield.

Longitudinal water barrier, however, has to be achieved mainly in the circumferential area where the metallic screen is applied. The geometric size of the interstices will determine the place and desired effectiveness of the barrier solution.

It will be clear that the waterblocking system may not have any influence on the normal function of the cable. Therefore if the tape has to be applied under the metallic screen, semi conductivity is a necessity, although there are some successful results with 50% overlapping swellable non conductive tape and conductive bedding tape.

A conductive bedding tape under the screen and a non conductive swellable tape wrapped over the screen has also been tried out successfully.

Choice between alternative solutions is usually on the basis of cost performance calculations.

Telecommunication cables:

As there is no demand for semi conductivity here, the tapes are used of course in the non conductive state.

Advantages mentioned for power cables are also valid for telephone cables. Petrol Jelly filling is widely used in the telephone cable industry. Swellable tape is by no means a replacement for this system but may be considered as a valuable additional against safeguard longitudinal water ingress. Especially in double jacketed cables swellable tape is applicable between the inner jacket and aluminium screen. There are constructions in the market where the tape is used in direct contact with the Petrol Jelly. One of the latest developments in this case is a swellable tape with one side laminated on a plain polyester film with specified electrical properties (e.g. 0.7 KV and 12 KV). All the swellable nonwovens are applicable helically as well as longitudinally.

#### CONCLUSION

Swellable tape has found its place already in power and telephone cables where longitudinal water penetration has to be avoided.

Although not every requirement can be met the balance sheet shows significant advantages proved by its application over the last 3 years in substantial amounts of cables.

It is still a barrier solution on its way to further perfection and therefore worth to be a subject of discussion from now on.

## LITERATURE

### Elektrizitätswirtschaft

Vol. 79 (1980) no. 26 page 1022 H. Kober  
Longitudinal water barrier in the screen area of  
a polymer insulated cable (German)

Vol. 80 (1981) no. 7 page 222 G. Hahne & H. Kober  
New constructions of power cables (German)

### Elektrotechnische Zeitschrift

Vol. 193 no. 4 February 1982 page 173-176  
G. Kammel & H. Sünderhauf  
Polymer insulated cables with longitudinal water  
barrier (German)



Ben Nieuwhof was born and educated in Zwolle, The Netherlands. After his study at the Groningen Institute of Technology, he attained his diploma in Chemical Engineering.

From 1962 he worked in the Dutch Chemical Industry where he was primarily involved in R&D projects. In 1968 he transferred to a marketing function where he worked on the development and market introduction of products of DSM designed for the plastics processing industry.

Currently he is the manager responsible for the product group "electrical applications" of FIRET bv in Veenendaal, The Netherlands, producer of nonwoven materials.



Roelf de Vrieze was born in Bandung Indonesia. He grew up in the Netherlands where he attained diplomas of the Dordrecht Institute of Technology in Chemical and Industrial Engineering.

Currently he is working as development engineer at FIRET bv in Veenendaal, The Netherlands, producer of nonwoven materials, where he is responsible for the development of cable wrapping materials.

As the designer of the water swellable nonwoven tapes, he maintains technical contacts with the R&D departments of cable industries.



EVALUATION OF ADHESIVE MATERIALS  
FOR BONDED SHEATH CABLE DESIGNS

A. C. Levy and B. J. Overton

Bell Laboratories  
Norcross, GeorgiaABSTRACT

Bonded sheath cable designs require bond stability over the wide range of environmental extremes experienced by the cable prior to, during and after installation. In order to select acceptable sheath bonding materials, short term laboratory tests were developed which would predict long term performance. These tests include one which predicts long term bond performance at high temperature in a pressurized environment, and one which correlates with low temperature buckling performance of the cable during installation. The effect of shield corrugations on bond strength is also discussed.

1.0 INTRODUCTION

A bonded sheath (polyethylene to steel) is used in telecommunications cable to prevent buckling of pressurized cable during installation<sup>1</sup>, particularly at low temperature; to reduce moisture diffusion<sup>2</sup>; and to limit corrosion<sup>2</sup> of the steel. The bonding of the outer polyethylene (PE) jacket to the steel during extrusion is accomplished by a polymer coating on the steel. To prevent buckling effectively, the bond must remain intact during storage of the pressurized cable as well as during installation. For the former case, high summer temperatures are critical, as solar heating can produce jacket temperatures in excess of 60°C (140°F).

This paper presents laboratory test methods which correlate with the performance of adhesive bonds in cable sheath:

- during low temperature installation where buckling is most likely to occur and
- during high temperature reel yard storage where long term pressurization can cause delamination.

The tests are described and data presented which illustrate their application.

2.0 EXPERIMENTAL

The evaluation of the bond strength capabilities of various materials has in the past cen-

tered around room temperature peel tests. Although room temperature testing is useful from a quality control standpoint, it does not address bond properties at the high and low temperature extremes critical to bonded sheath. The test methods described below are designed specifically for that purpose.

2.1 Low Temperature Buckling

Bond failure which occurs in cable buckling is related to high strain rate induced stress in peel and shear modes. For this reason, low temperature performance of materials in laboratory T-peel and lap shear tests should be a reasonable indicator of performance in cable.

2.1.1 T-Peel

The T-peel test method outlined below includes both flat and corrugated composites as shown in Figure 1. The composites were prepared by laminating 75 mil thick plaques of jacket grade polyethylene to coated steel in a laboratory press at a temperature and pressure designed to simulate cable-line extrusion conditions. One inch wide samples cut from these composites were tested in an Instron tensile tester at a crosshead rate of two inches per minute. An environmental chamber attachment was used to obtain temperatures other than ambient. The corrugated as well as flat configuration was chosen since the steel is corrugated in the cable geometry. The direction of peel with respect to the corrugations (Figure 1) was chosen both for uniformity of peel and to maximize shear loading at the corrugation walls.

2.1.2 Lap Shear

Lap shear tests inherently contain a peel as well as a shear component. The peel component results from bending which occurs as a result of the lap joint offset. To minimize the lap joint offset, the specimens shown in Figure 2 were prepared by bonding a thin (two mil) PE film between two layers of coated steel in a laboratory press (200°C, 10 psi, 30 seconds). Testing was done on an Instron at a crosshead rate of 0.05 in./min.

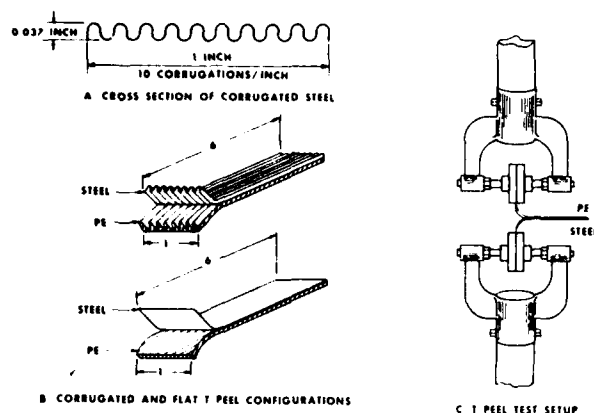


FIGURE 1. T PEEL TEST SPECIMENS AND SETUP.

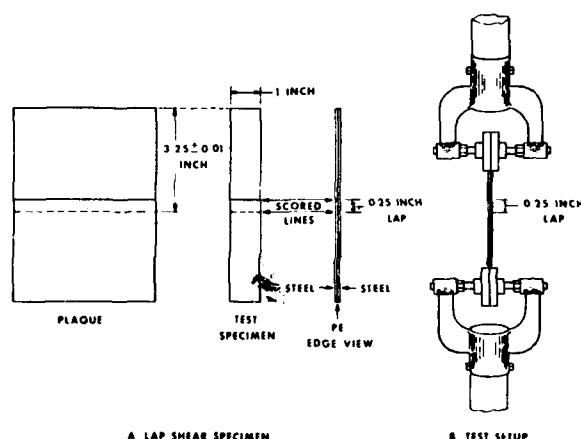


FIGURE 2. LAP SHEAR SPECIMEN DIAGRAM AND TEST SETUP

## 2.2 Pressure Induced Delamination

As previously noted, solar heating can significantly increase cable temperature above the ambient environment. If due to solar heating the bond strength drops too low, the pressure on the jacket/coated steel interface will cause the bond to delaminate in a peel mode.

The peel can be either longitudinal (along the cable) or circumferential (around the cable) depending on the nature of the initiation flaw as illustrated in Figure 3. A flaw might be introduced by incomplete corrugation fill, the presence of excess corrugating oils on the coated steel surface, flaws at the overlap seam of steel, or a variety of other conditions.

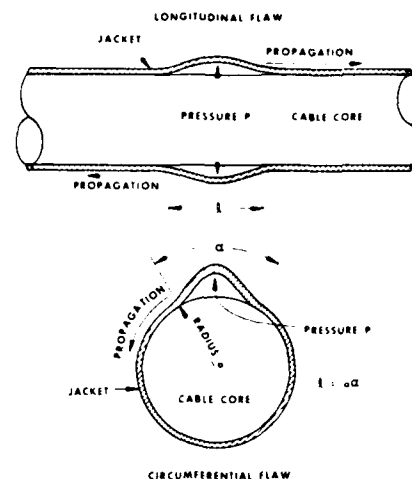


FIGURE 3. LONGITUDINAL AND CIRCUMFERENTIAL FLAWS IN BONDED SHEATH, CONSIDERED IN ANALYSIS OF CONSTANT LOAD PEEL DATA

The resistance of the bond to this type of environment can be determined by placing pressurized cable samples in an oven. However, one would like to be able to predict the performance capability of various materials analytically in the laboratory without the expense of manufacturing a cable.

One such laboratory method of simulating pressurization of the bond interface is the constant load peel test. In conjunction with time-temperature superposition principles, constant load data may be used to predict long term failure time for a bonded sheath system. The test and method of data treatment are described below.

A diagram of the constant load test apparatus is shown in Figure 4. It functions as follows. When the load is placed on the sample, clock 1 is activated. After peel initiates, a switch stops clock 1 and starts clock 2. After a given peel distance, switch 2 stops clock 2. In this manner, both the initiation time to peel,  $t_i$ , and the peel rate are read directly.

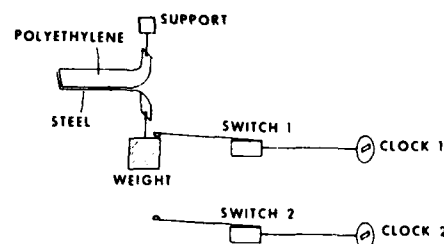


FIGURE 4. CONSTANT LOAD PEEL APPARATUS

The data obtained can be reasonably represented by

$$t_i/a_T = qP^{-m} \quad (1)$$

where  $P$  is the peel load,  $a_T$  is a temperature dependent shift factor such as that used in the time/temperature superposition of the mechanical properties of viscoelastic materials,<sup>3</sup> and  $q$  and  $m$  are constants characteristic of the material system being evaluated.

The values of  $q$  and  $m$  and  $a_T$  can be used to predict failure time in the cable if one can relate peel load in a flat geometry to the pressure in the cable. This relationship has been developed by Brockway<sup>4</sup> for both the longitudinal and circumferential peel modes shown in Figure 3.

For the longitudinal case

$$P_L = 0.98 p(l_0/2) \quad (2)$$

and for the circumferential case

$$P_C = pa \tan(0.5 l_0/a) \quad (3)$$

In the above equations,  $P_L$  and  $P_C$  are respectively the longitudinal and circumferential peel loads,  $p$  is the pressure in the cable,  $l_0$  is the flaw length and  $a$  is the cable radius. These equations can be substituted into equation (1) to give

$$t_i/a_T = q(0.98 p l_0/2)^{-m} \quad (4)$$

and

$$t_i/a_T = q(pa)^{-m} \tan^{-m}(0.5 l_0/a) \quad (5)$$

Using the above equations and a given flaw size, one can calculate  $t_i$  at a given temperature and pressure, by using the values of  $q$  and  $m$  characteristic of the material. Conversely, if a minimum  $t_i$  is required to survive the worst reel yard conditions, the maximum flaw size that can be tolerated and still meet this requirement can be calculated.

### 3.0 MATERIALS

Materials used in this study are either a 6.0 mil thick tin plated steel (TPS) or a 6.0 mil thick electrolytically chrome coated steel (ECCS), both coated with either a single layer (SL) of an ethylene-acrylic acid copolymer (EAA)<sup>2,5</sup> or a dual layer<sup>6</sup> (DL) of EAA and polyethylene (PE). The EAA is nominally a 5.5 melt index material containing 8% by weight acrylic acid. In the DL product, the EAA is next to the steel. The PE outer layer serves as the bonding surface for the cable jacket, usually a linear low density polyethylene (LLDPE). The advantage of the dual layer over the single layer is that the EAA/PE bond is formed under the ideal conditions of coextrusion rather than in cable manufacture where the

presence of corrugating oils and other manufacturing variables can degrade the bond. The outer layer PE to LLDPE bond is easier to form during jacketing than the EAA to LLDPE bond because of the greater chemical similarity of the former material pair.

Cables containing both SL and DL coated steel have been evaluated for low temperature buckling and high temperature bond delamination. Both coated steels were found to perform well with respect to buckling. However, at high temperature, the DL containing product is much the better of the two.

## 4.0 RESULTS

Data which illustrate the application of T peel, lap shear and constant load peel test methods are given below.

### 4.1 T-Peel Data

A typical T-peel profile of flat SL coated steel bonded to LLDPE is shown in Figure 5. High temperature as well as the critical low temperature data are included. The mode of bond failure at high and low temperature is predominantly at the adhesive/polyethylene interface. Room temperature failures occur at both the steel/adhesive and adhesive/polyethylene interfaces. The bond strength is very low in the 10°F temperature range.

The data in Figure 5 for corrugated, SL coated steel show a very high peel strength at low temperature, in contrast to the flat steel. This increase is much greater than the 15-20% increase in surface area caused by the geometry differences. Thus, the excellent low temperature buckling performance of cable containing SL steel can be attributed to the corrugated steel geometry. Finally, it should be noted that at temperatures above 120°F, there is no measurable corrugation effect.

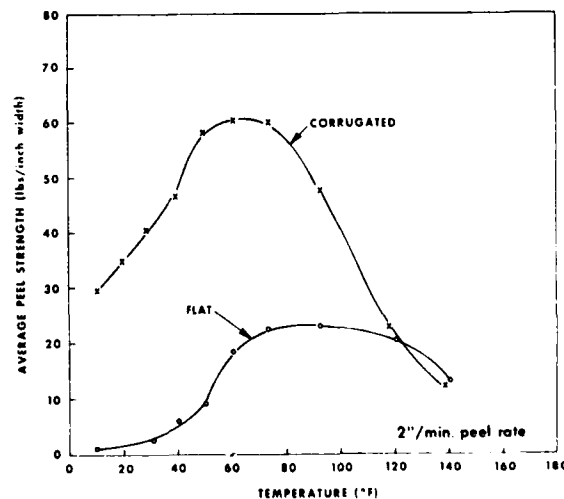


FIGURE 5. T PEEL STRENGTH OF FLAT AND CORRUGATED PLAQUES vs. TEMPERATURE. (SL COATED STEEL/LLDPE)

Bond strength data for flat, DL coated steel bonded to LLDPE are given in Table I along with similar results for the SL case. As can be seen, the 10°F value for DL coated steel is substantially higher than obtained with the SL material.

TABLE I

T-PEEL STRENGTH OF SL AND DL COATED ECCS BONDED TO LLDPE

Coating Type	Peel Strength (Pounds/Inch)			
	T F:	10	73	140
SL		1-4	18	12
DL		12	18	12

#### 4.2 Lap Shear Results

A possible explanation for the large corrugation effect shown in Figure 5 is that in the test configuration the adhesive is loaded partially in shear at the corrugation walls. In order to verify this hypothesis, lap shear tests were run on samples as shown in Figure 2. The data are given in Figure 6.

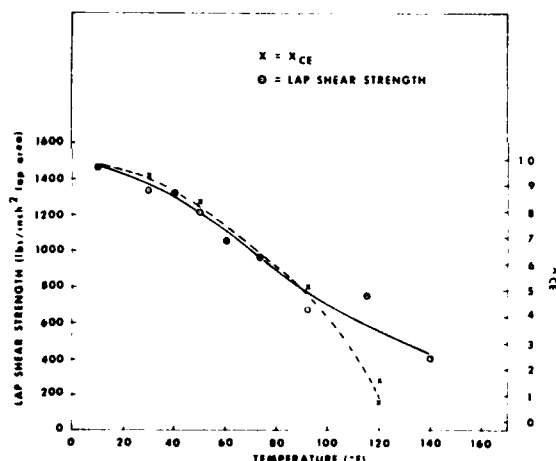


FIGURE 6. CORRUGATION EFFECT,  $X_{CE}$  AND LAP SHEAR STRENGTH vs. TEMPERATURE. (SL COATED STEEL/LLDPE)

The data show high values of lap shear strength at 10°F that decrease with increasing temperature. At 140°F, the decrease is about an order of magnitude. As a further comparison, one can calculate from the data in Figure 5 the fraction of the bond strength due to the corrugation effect,  $X_{CE}$ , over the test temperature range as

$$X_{CE} = \frac{\text{Corrugated Plaque Bond Strength} - \text{Flat Plaque Bond Strength}}{\text{Corrugated Plaque Bond Strength}}$$

These data are also plotted in Figure 6. As one might expect, the curves are similar in shape over the range where the corrugation effect is significant.

#### 4.3 Constant Load Peel Results

Whereas T-peel tests reflect the delamination resistance of bonded sheath undergoing high rates of strain, constant load peel data provide the basis to predict the bond life of pressurized sheath in the static, reel yard environment. The principles are illustrated below.

In order to correlate laboratory data with the previously described high temperature cable performance, both SL and DL coated steel were bonded to LLDPE, Figure 1, and tested in constant load peel at temperatures from 140 to 170°F. Flat steel was used because, as previously noted, there is no corrugation effect above 120°F, Figure 6. Representative data for the DL case are given in Table II. As can be seen, the peel rate is relatively fast once peel has initiated. Therefore, from a practical standpoint failure can be taken as the time,  $t_i$ , at which the peel initiates.

TABLE II

CONSTANT LOAD RESULTS  
DL COATED STEEL/LLDPE

T - °F	Loads-lbs	Initiation Time-Days	Peel Rate-Inches/Day
140	1	2.416	0.8
	2	0.398	13.9
	3	0.064	11.9

Data such as given in Table II and Figure 7 were used to calculate the q and m values, Equation (1), in Table III. The master curves from the data shift such as indicated in Figure 7 are shown in Figure 8.

TABLE III

VALUES OF q AND m FOR SL AND DL COATED STEEL/LLDPE

	q	m
SL Coated Steel	0.045	2.18
DL Coated Steel	0.287	3.03

The above results were used with Equations (2) and (4) to predict failure time in the cable as a function of flaw length. These data are given in Figure 9.

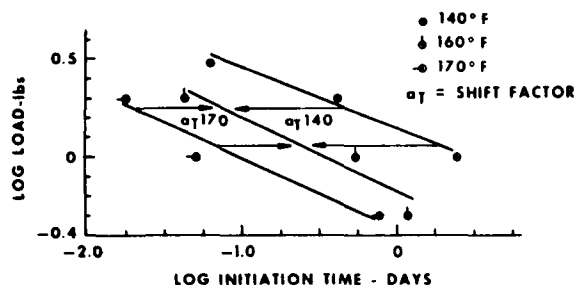


FIGURE 7. DATA SHIFT - INITIATION TIME  
DL COATED STEEL/LLDPE

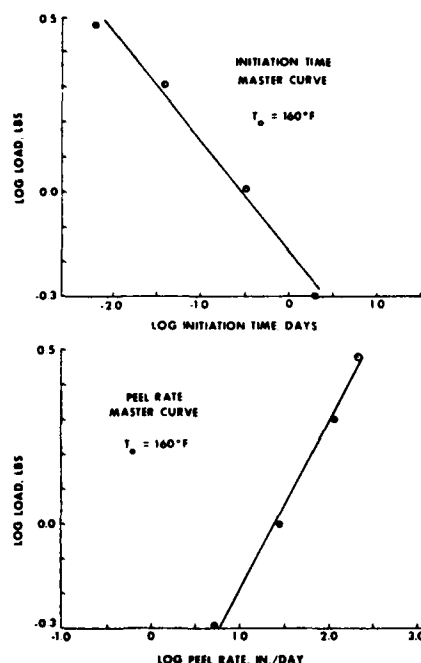


FIGURE 8. MASTER CURVES FOR INITIATION TIME AND  
PEEL RATE, DL COATED STEEL/LLDPE

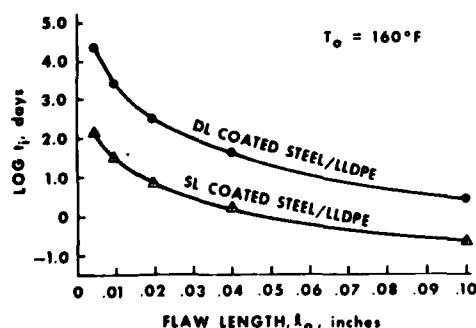


FIGURE 9. PREDICTED INITIATION TIME AS  
A FUNCTION OF FLAW LENGTH

A typical flaw size in bonded sheath is of the order of 0.02 inches.<sup>7</sup> The maximum flaw size as determined by examination of representative cables is approximately 0.04 inches.<sup>7</sup> Using these flaw sizes and Figure 9 one can determine the respective initiation times. These data are given in Table IV. The numbers for the SL and DL coated steel/LLDPE systems agree well with actual tests on cable.

TABLE IV

PEEL INITIATION TIME AT 160°F, 10 PSI

Material System	Initiation Time (Days)	
	Flaw Size (in)	
SL Coated Steel/ LLDPE	0.02	0.04
	10 <sup>3-14</sup> a	2
DL Coated Steel/ LLDPE	300 (>250) <sup>b</sup>	90

<sup>a</sup>Tests on cable with 0.026in. maximum flaw

<sup>b</sup>Flaw size <0.02 in., cable still on test

By this technique, the estimate of the equivalent time<sup>7</sup> at 160°F to simulate a worst case storage condition of one year is ~ 20 days. Based on a worst measured flaw of 0.04 inches, one would expect DL coated steel to survive storage under worst case conditions for more than four years.

## 5.0 CONCLUSIONS

The prior discussion illustrates how laboratory techniques can be used to determine the acceptability of adhesive materials for bonded sheath cable. In particular,

- T peel analysis of composites containing corrugated steel can be used to predict low temperature cable buckling performance and
- Constant load peel on flat composites can be used for determining the performance of bonding materials in cable in a high temperature, pressurized environment.

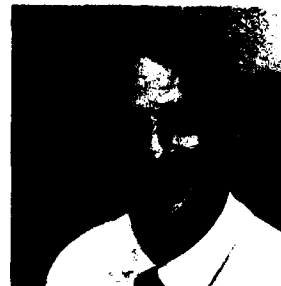
Additional conclusions can be drawn with respect to the mechanisms which contribute to low temperature bond strength and the relative performance of DL and SL coated steel. With regard to the former, T-peel and lap shear data indicate that shear loading at the corrugation walls is a significant contributor to low temperature bond strength. In the latter case, DL coated steel has been shown to offer superior bond performance relative to the SL product at both the low and high temperature environmental extremes.

#### ACKNOWLEDGEMENTS

The authors wish to thank the following people whose assistance was instrumental to this program: R. N. Binkley, R. J. Harmel, M. D. Kinard, D. W. Lemke, N. Levy, D. M. Mitchell and R. Sabia.

#### REFERENCES

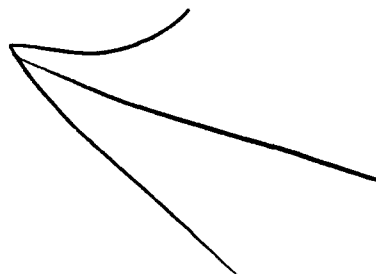
1. G. M. Yanizeski, E. L. Johnson and R. G. Schneider, Cable Sheath Buckling Studies and The Development of a Bonded Stalpeth Sheath, Proceedings of the International Wire and Cable Symposium, 1980.
2. G. E. Clock, G. A. Klumb and R. C. Mildner, "Adhesive Thermoplastic Polymers for the Wire and Cable Industry", "Proceedings of the Twelfth Wire and Cable Symposium," 1963.
3. J. D. Ferry, "Viscoelastic Properties of Polymers," Wiley, New York, 1970.
4. G. S. Brockway (Plastic Engineering Consultants) letter to B. J. Overton, (Bell Laboratories) July 6, 1981.
5. R. C. Mildner, U. S. Patent 3,681,515.
6. L. S. Scarola, U. S. Patent 4,132,857.
7. G. M. Yanizeski, unpublished data.



A. C. Levy is a graduate of the Georgia Institute of Technology (B.A., M.S., Ph.D.). He was employed by the Film and Fiber Division of E. I. DuPont prior to joining the Transmission Media Laboratory of Bell Telephone Laboratories in 1976. Since 1976 he has been active in the development of materials for conventional and lightguide cable applications.



B. J. Overton is a senior technical associate in the Chemical Engineering Group at Bell Labs in Atlanta. Since joining the Labs in 1978, he has been involved in the development and characterization of protective materials for lightguide and conventional cable.



NEW DATA ON LONG TERM STABILIZATION OF POLYETHYLENE  
FOR TELECOMMUNICATION WIRE INSULATION

Felix K. Meyer and Helmut Linhart

CIBA-GEIGY Ltd., Basle, Switzerland

ABSTRACT

Medium density polyethylene is widely used for the insulation of telecommunication wires. A lifetime of 40-50 years is generally desired. Thus the stabilization of the polyethylene in contact with copper is of prime importance. In this paper new data pertaining to the long term heat stabilization are presented. The loss of stabilizers as a function of time is examined and aging data on actual wires are shown. There is evidence that polyethylene stabilized with a combination of a sterically hindered phenolic antioxidant (pentaerythrityl tetrakis (3,5-di-*t*-butyl-4-hydroxyphenyl propionate)) and a copper deactivator (N,N'-bis (beta-3,5-di-*t*-butyl-4-hydroxyphenyl-propiono) hydrazide) has good chances of reaching the expected lifetime.

INTRODUCTION

Solid or cellular polyethylene is widely used for the insulation of telecommunication wires. Whereas high density polyethylene (HDPE) or polypropylene copolymers are generally employed for this application in North America, medium density polyethylenes (MDPE) with densities around 0.93 are now commonly used in Europe and many other parts of the world.

The insulation is generally expected to have a lifetime of 40 to 50 years. In contact with copper and at temperatures above room temperature, the polymers used cannot reach the expected lifetime without the addition of adequate heat stabilizers. Degradation is most critical in above

ground closures where peak temperatures up to 60°C may occur.

Until the early seventies, the stabilization system consisted primarily of a phenolic antioxidant. Upon realizing the importance of copper catalyzed degradation at the elevated temperatures occurring in above ground closures, a copper deactivator was included in the stabilizer formulation.<sup>1</sup>

In more recent times, early failures of solid polyethylene insulation connected in above ground closures were reported from Australia. According to Ruddlell and co-workers, Telecom (Australia), who investigated the problem,<sup>2,3</sup> the rapid depletion of the poorly soluble antioxidant AO-1 used at the time of manufacturing of the cables was the main reason for the premature failure. Furthermore, at that time, no copper deactivator was used. It also appears that there exists a close relationship between the concentration of titanium dioxide (TiO<sub>2</sub>) used for the pigmentation of the wires and the number of failures. This indeed suggests that the particular type of TiO<sub>2</sub> used at that time had a strongly adverse effect on the stability of polyethylene.

While investigating the failure of these cables,<sup>2,3</sup> the researchers at Telecom carried out various studies on other stabilizer systems. Based only on migration data, partly made in LDPE (density = 0.919, which is no longer used for telecommunication wire insulation), they questioned the

validity of various stabilizer systems and made certain recommendations.

In this paper, we present:

- a review on "stabilizer loss"
- migration studies on actual telecommunication wires
- influence of preconditioning at 60°C on the aging performance of cellular insulation
- aging data as a function of temperature for solid insulation.

#### LOSS OF STABILIZER

The quantity of a stabilizer migrating to the surface of a test specimen is often taken as a measure for the loss of the stabilizer. With such an approach, clearly only one aspect of stabilizer loss is being considered. The actual loss of a stabilizer as a function of time or during a given processing step may include the following:

- a) exuded stabilizer (crystallized on the surface or sublimated)
- b) oxidized stabilizer (for antioxidants)
- c) chemically transformed stabilizer (other than b)
- d) stabilizer bound to the polymer chain.

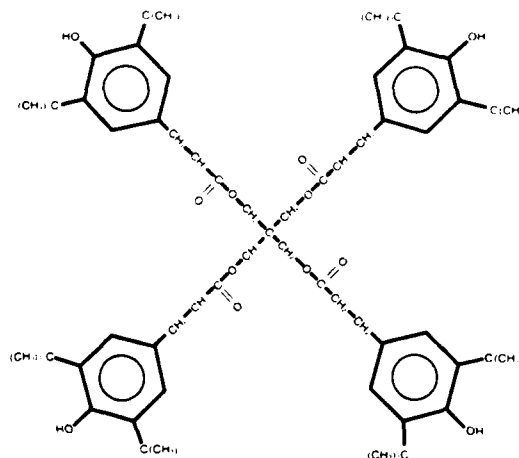
Of all the above, only the stabilizer crystallized on the surface can be easily analyzed. This is, indeed, the reason why exudation and loss are so often associated.

Most stabilizers used for polyolefins are stable up to 300°C. Therefore, the purely thermally induced transformations of the stabilizers will be neglected.

The specific analytical determination of oxidation products, of chemically transformed products and of stabilizer units possibly bound to the polymer chain is rather difficult, because of the very

low amounts of the various species to be determined.

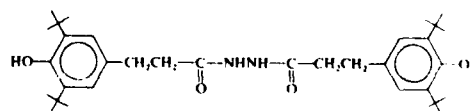
It follows that a positive approach, i.e. the determination of the stabilizer content still present in its original form in the sample, seems at first sight to be more reliable. The values obtained on loss of stabilizer in such a manner should be examined carefully when multifunctional stabilizers are involved. To clarify this point, let us take the following antioxidant:



AO-2

AO-2 has four sterically hindered phenolic groups all of which function as antioxidant. Partly oxidized AO-2 is still active as antioxidant, but will be considered as lost when analyzing for "unchanged" AO-2 in the polymer.

Similarly, if the following copper deactivator is considered:



MD-1

MD-1 comprises two antioxidant functions (sterically hindered phenolic group) and one metal chelating function (hydrazide). If one or two of the phenolic groups are oxidized, MD-1 still retains all its properties as copper deactivator, but will be considered as lost when analyzing for unchanged MD-1 in the polymer.

In view of the above, it becomes evident that performance data is practically the only means of providing a reliable information on the amount of active residual stabilizer left in the polymer.

#### EXUDATION OF STABILIZERS

As mentioned above, exudation studies are popular because of their convenience. Nevertheless, exudation data can be misleading if stabilizers with different volatilities are compared. A very volatile product may be considered as non-exuding because it will not accumulate on the surface of the test specimen. This becomes increasingly critical when exudation tests are carried out at elevated temperatures.<sup>2,3</sup> To be valid, the exudation data have to be supported in this instance by a material balance (which is nearly impossible when polyfunctional stabilizers are involved, see above).

Another aspect to be considered when comparing the migration of various stabilizers is the solubility of the stabilizer at the corresponding temperature. For a fair and meaningful comparison, initial concentrations should not exceed the solubility of the stabilizer. For example, the migration studies carried out at 60°C in ref. 3 showed only the exudation of the stabilizer in excess of its solubility. For AO-2, a solubility at 60°C of 750-800 ppm was determined (ref. 3, figure 6). The initial antioxidant concentration in the migration tests was 1000 ppm. As expected, an average AO-2 exudation of 20% after 35 days at

60°C was found (ref. 3, figure 4). Similarly for AO-1, a solubility of approx. 500 ppm was determined and the observed exudation was indeed approx. 50%. This is further supported by the fact that in most instances, no further increase in exuded stabilizer was found after 35 more days at 60°C. Thus, instead of obtaining some measure of the rate of depletion of the stabilizer as a function of time, the migration studies in ref. 3 confirmed only the already known solubility data for the additives involved.<sup>4</sup>

One way to overcome several of the problems related to the determination of the loss of stabilizer as discussed previously is working with radioactively labeled stabilizers. In this way the stabilizer concentration in the polymer can be followed as a function of time. Since this method does not discriminate between original, chemically transformed and oxidized stabilizer, a specific method has to be used to monitor the evolution of the original stabilizer.

Using Liquid Scintillation Counting, the concentration of AO-2 has been followed at room temperature in LDPE for up to 4 years (Fig 1) and in HDPE for up to 6 years (Fig 2).<sup>5</sup> Initial concentra-

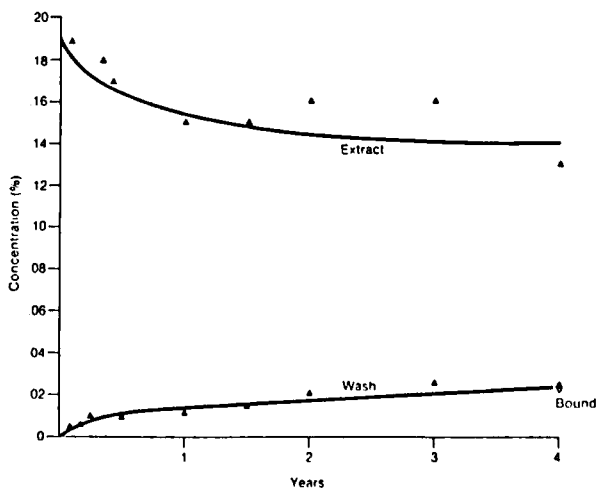


Figure 1: Exudation of <sup>14</sup>C labeled AO-2 from LDPE Plaques (0.6mm) as a function of time at Ambient Temperature.

tions of 2000 ppm were used; thus, in LDPE ( $d = 0.920$ ), certainly well above the solubility level. Despite this, Fig. 1 shows that after 4 years only about 200 ppm exuded to the surface. Another 200 ppm were found to be bound to the polymer. Here, the very low exudation originates from a very low diffusion coefficient,<sup>4</sup> related to the geometry of AO-2. Fig 2 shows that in HDPE ( $d = 0.952$ ) no migration of <sup>14</sup>C-labeled AO-2 could be detected after 6 years. Using liquid chromatography, it was also possible to determine that most of AO-2 was still in its original form.

The above data illustrate convincingly the effect of density on the exudation of AO-2 from polyethylene (see also ref. 6).

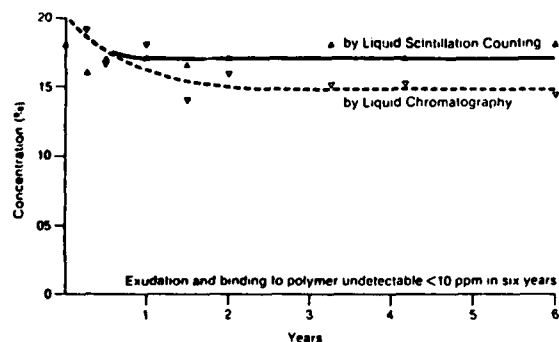


Figure 2: Exudation of <sup>14</sup>C-labeled AO-2 from HDPE Plaques (0.6mm) as a Function of Time at Ambient Temperature.

#### ANTIOXIDANT LOSS BEFORE PROCESSING

Seemingly high antioxidant depletion in the compound, stored for up to 3 years before processing, has been reported (approx. 50% loss, no indication concerning the initial concentration).<sup>3</sup> The depletion was related to migration. We have seen in the preceeding chapter that, for AO-2, exudation could certainly not have caused the reduction in antioxidant level. The decrease of AO-2 in its original form is due to its activity as antioxidant. Being a tetrafunctional antioxidant, the oxidation of one of the phenolic groups will reduce only one fourth of the antioxidative activity, yet still,

the molecule will be counted as lost. Again, direct comparison between various antioxidants with different numbers of active groups is misleading.

To illustrate further this effect, we are showing in Table I the residual AO-2 concentration in, and the corresponding heat stability of, polypropylene plaques after up to 15 years storage. Whereas the content of AO-2 in its original form diminishes substantially (~80% after 15 years), the corresponding oven-aging performance is much less affected.

Table I: RESIDUAL ANTIOXIDANT CONCENTRATION AND HEAT STABILITY OF POLYPROPYLENE PLAQUES (0.6mm) AFTER STORAGE<sup>a)</sup> FOR UP TO 15 YEARS<sup>b)</sup>.

Years Storage	Antioxidant <sup>c)</sup> Concentration	Hours to Failure at 150°C
0	0.16%	1290
1	0.13%	1090
5	0.09%	830
10	0.06%	1080
15	0.02%	770

a) ambient conditions b) taken from ref 5

c) AO-2

#### ANTIOXIDANT LOSS DURING PROCESSING

Except for volatile or thermally unstable products, antioxidant loss during processing is mainly caused by oxidation. Most antioxidants have at least some activity as processing stabilizers. Ruddell and co-workers<sup>3</sup> have shown very neatly that the loss of AO-2 during processing can be reduced significantly by the addition of a phosphonite (PS-1) acting as processing stabilizer (hydroperoxide decomposer). The beneficial contribution of a processing stabilizer towards oxidative degradation can also be derived from oxygen induction time measurements (Table II).

Table II: CONTRIBUTION OF PROCESSING STABILIZERS IN  
OXYGEN INDUCTION TIME TEST

Polymer: MDPE MFI = 0.2 d = 0.929

Formulation	OIT (minutes) at 220°C
without	1.5 - 2
0.1% PS-2	3.5
0.1% AO-2	9
0.1% AO-2 + 0.1% PS-2	14

#### LONG TERM HEAT STABILIZATION OF CELLULAR TELECOM- MUNICATION WIRE INSULATION

To test the relative performance of two stabilizer systems, based on AO-2 or on AO-3, in cellular telecommunication wire insulation, two commercial compounds were chosen. They were identical in every aspect except for the primary antioxidant. The insulation materials used in this study were medium density based (solid polymer density of 0.935).<sup>7</sup> They contained 0.1% MD-1 and an azodi-carbonamide blowing agent added at a concentration to obtain a nominal 35-40% expansion during the wire covering extrusion process. The extrusion melt temperature to optimize their expansion was between 205 and 210°C. Of each formulation white (TiO<sub>2</sub> pigmented) and blue (pigmented with TiO<sub>2</sub> and phthalocyanine blue) wires were produced on an industrial line. The conductor was a 0.5 mm copper wire and the insulation a cellular layer 0.125 mm thick. Preliminary investigations had shown that the performance of AO-2 was about twice that of AO-3.

First, we examined the influence of preconditioning at 60°C on the exudation of the stabilizers from the cellular insulation (Table III). No exudation was detected for any of the stabilizers up to 140 days. Table III shows also the change of the stabilizer content in the compound and in the

cables and also after preconditioning. A very significant drop in the concentration of unchanged antioxidant is observed during the industrial manufacturing of the cable. This is not surprising because the processing conditions (high temperature) are rather damaging to the polymer, thus consuming antioxidant. Furthermore, some interaction between the antioxidant and the foaming agent and its degradation products cannot be excluded.

The concentrations of unchanged antioxidants, both AO-2 and AO-3, and of unchanged metal-deactivator decrease significantly during preconditioning at 60°C. This is caused by further oxidation promoted by the cellular structure of the insulation (enhanced oxygen diffusion). After 140 days, the concentration of unchanged AO-3 left is very low, whereas AO-2 and MD-1 as such have virtually vanished. It should be kept in mind that AO-2 is tetrafunctional and, therefore, will be lost as such much faster than the bifunctional AO-3, which, in addition, was introduced at twice the initial concentration of AO-2. The decrease of the unchanged MD-1 concentration is most certainly related to the oxidation of one or two of its phenolic groups, leaving the metal chelating properties intact.

From the oven-aging data presented in Table IV, it is apparent that, despite the virtual absence of unchanged stabilizers after 140 days preconditioning at 60°C, there is abundant antioxidative power left. Preconditioning causes only a very small reduction of the aging performance. This can be related to the oxidation of the antioxidants during preconditioning. Table IV shows also clearly that AO-2 is at least twice as effective as AO-3. This ratio is not affected by preconditioning, in contrast to what one would expect based on the migration data published in ref. 2 and 3. The superiority of AO-2 over AO-3, taken alone or in combination with either MD-1 or MD-2 can also be observed in the oxygen induction time test (Table V).

Table III: INFLUENCE OF PRECONDITIONING AT 60°C ON THE EXUDATION OF STABILIZERS FROM CELLULAR TELECOMMUNICATION WIRE INSULATION

Cable Compound	Color	Stabilizer	Conc. in Compound %	Analyzed conc. in the cable			Analyzed in the wash after 70 days and 140 days
				Initial %	after 70 days %	after 140 days %	
A	white	AO-2	0.07	0.03	0.006	<0.005	all <0.005%
		MD-1	0.09	0.05	0.009	<0.005	
A	blue	AO-2	0.07	0.02	0.009	<0.005	
		MD-1	0.09	0.06	0.025	<0.005	
B	white	AO-3	0.2	0.11	0.05	0.03	all <0.005%
		MD-1	0.09	0.07	0.04	0.01	
B	blue	AO-3	0.2	0.13	0.08	0.05	
		MD-1	0.09	0.07	0.05	0.02	

Table IV: INFLUENCE OF PRECONDITIONING AT 60°C ON THE AGING PERFORMANCE\* OF CELLULAR TELECOMMUNICATION WIRE INSULATION

Cable Compound	Color	Stabilizer	Conc. in Compound	Days to failure at 105°C		
				initial	after 70 days at 60°C	after 140 days at 60°C
A	white	AO-2	0.07%	66	62	55
		MD-1	0.09%			
A	blue	AO-2	0.07%	65	67	59
		MD-1	0.09%			
B	white	AO-3	0.2%	63	63	57
		MD-1	0.09%			
B	blue	AO-3	0.2%	65	62	57
		MD-1	0.09%			

\* pig-tail test: days to appearance of visible cracks

Table V: OXYGEN INDUCTION TIMES OF VARIOUS STABILIZER SYSTEMS

Polymer: MDPE MFI=0.2 d=0.929

Formulation	OIT (minutes) at 220°C
0.1% AO-2	9
0.1% AO-2 + 0.1% MD-1	16
0.1% AO-2 + 0.1% MD-2	11
<hr/>	
0.1% AO-3	6.5
0.1% AO-3 + 0.1% MD-1	12
0.1% AO-3 + 0.1% MD-2	9

Trials are presently underway with solid wire insulation based on the same resins to determine the effect of the insulation's structure. Since the study yielded similar results for the white and the blue wires, only blue will be taken.

#### LONG TERM HEAT STABILIZATION OF SOLID TELECOMMUNICATION WIRE INSULATION

For time considerations, the effectiveness of a stabilizer system is frequently studied at high temperatures, just below the melting point of the polymer. It has been argued that the data obtained at these temperatures are irrelevant both because of possible changes in the energy of activation and because of the increased solubility of most stabilizers at these temperatures. To take into account the above limitations, we have studied the antioxidant system AO-2/MD-1 at temperatures between 70°C and 110°C. Actual wire samples were aged in a draft air oven. For these trials, a medium density polyethylene (density = 0.928 and mfi = 0.2 measured at 190°C/2.16 kg) was chosen. The wires with a TiO<sub>2</sub> pigmented insulation of 0.2 mm thickness and a copper core of 0.5 mm were produced on an industrial line (max. extrusion temperature 260°C).

Figure 3 shows the days to visible cracks (pig-tail test) as a function of temperature. The coordinates of the plot are the logarithm of time and the inverse of absolute temperature. Assuming a constant energy of activation, the projected lifetimes at 30°C are indicated.

These data show clearly the benefit to be derived from increasing the concentration of AO-2 from 250 ppm to 750 ppm in combination with 1000ppm MD-1. The lowest test temperature, 70°C, is certainly close enough to the most critical temperature of 60°C as proposed by the researchers at Telecom<sup>3</sup> based on their migration studies. It is also close enough to 30°C to allow fairly safe extrapolation. With the combination 750 ppm AO-2 and 1000 ppm MD-1, a lifetime for the insulation of 4 1/2 years is obtained if the cable is permanently maintained at 70°C. The projected lifetime of the same formulation at a constant 30°C operating temperature is over 80 years.

Telecommunication wires jointed in above ground closures will be exposed to elevated temperatures only part of the day and only for part of the year. During night time, temperatures will often fall below 30°C. Therefore, telecommunication wire insulation made of polyethylene stabilized with 750 ppm AO-2 and 1000 ppm MD-1 should withstand easily the expected lifetime of 40-50 years even in Australia.

#### ACKNOWLEDGEMENTS

We are indebted to K. Normanton and P. Francis of BXL Plastics for their cooperation and stimulating discussions. The contribution of experimental data from our colleagues F. Mutterer and A. Schmitter, CIBA-GEIGY (Basle) and P. Klemchuk and P.L. Horng, CIBA-GEIGY (Ardsley, N.Y.) is gratefully acknowledged.

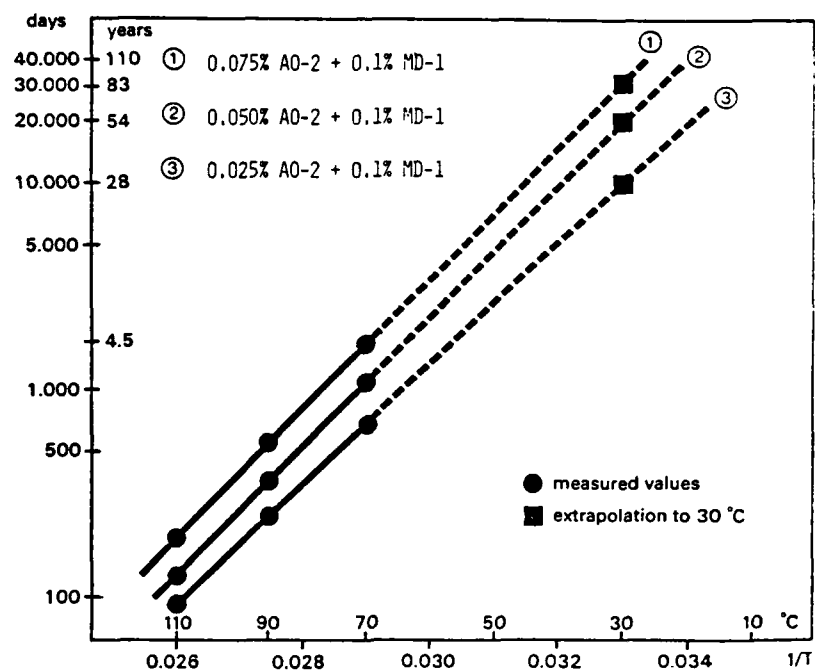


Figure 3: Heat Stability of Solid MDPE Telecommunication Wire Insulation as a Function of Temperature.

Oven-Aging: Pig-Tail Test (days to appearance of visible cracks)  
 Copper Conductor: Ø 0.5mm Insulation: 0.2 mm  
 Polyethylene: d = 0.928 MFI: 0.2

#### REFERENCES

1. H.M. Gilroy, Proc. 23rd Int. Wire & Cable Symp., 42 (1974)
2. H.J. Ruddell, D.J. Adams and B.A. Chisholm, Plastics in Telecommunication, 3rd Intl. Conf., London (1982)
3. B.L. Board and H.J. Ruddell, Proc. 31st Int. Wire & Cable Symp., (1982)
4. J.Y. Moisan, Eur. Polym. J. 16, 979 (1980)
5. P.P. Klemchuk and P.L. Horng, 25th Microsymposium, "Processing and Long Term Stabilities of Hydrocarbon Polymers", Prague (1983)
6. J.Y. Moisan, Eur. Polym. J. 16, 989 (1980)
7. British patent no. 1274645 or US patent no. 3645929

## APPENDIX I: CHEMICAL IDENTIFICATION OF STABILIZERS

Designation	Tradenames	Chemical Name
AO-1	SANTONOX R	4,4'thiobis(2-t-butyl-5-methylphenol)
AO-2	IRGANOX 1010	Pentaerythrityl-tetrakis-(3,5-di-t-butyl-4-hydroxyphenyl-propionate)
AO-3	NONOX WSP	2,2'-methylenebis(4-methyl-6-(1'-methylcyclohexyl)phenol)
PS-1	IRGAFOS P-EPQ	Tetrakis-(2,4-di-t-butyl-phenyl)-4,4'biphenylene diphosphonite
PS-2	IRGAFOS 168	Tris(2,4-di-t-butylphenyl)phosphite
MD-1	IRGANOX MD 1024	N,N'-bis(beta-3,5-di-t-butyl-4-hydroxyphenyl-propiono)hydrazide
MD-2	EASTMAN OABH	Oxalic acid-bis(benzylidene hydrazide)

## APPENDIX II: EXPERIMENTAL

### Analytical

The insulation was dissolved in chlorobenzene and AO-2 and MD-1 were determined via High Pressure Liquid Chromatography and AO-3 via Gas Chromatography. Exudation of stabilizer was checked by dipping the insulated wire into acetone for 3 minutes and subsequent analysis as above.

### Oxygen induction times (OIT)

OIT measurements were carried out at 220°C on a Mettler TA 2000 according to the IEC draft "Proposed method for testing copper-catalyzed oxidative degradation of polyolefins". Copper pans were used.

### Resistance to thermal aging

Ten cable samples of each formulation were aged in a draft air oven. Periodically, the samples were taken out of the oven and, after cooling, wound around a stainless steel rod of 1 mm diameter. The pig-tails were then examined for cracks using a magnifying glass. The data shown in this paper are the mean of the ten determinations (Standard deviation  $\pm 5\%$ ).



Felix K. Meyer graduated in 1976 as a Chemical Engineer from the Federal Institute of Technology, Lausanne and in 1979 he obtained his Ph. D. in Physical Chemistry. Before joining CIBA-GEIGY Ltd., Basle in 1981, he was post-doctoral fellow at Stanford University. At present he has world-wide responsibilities for the technical promotion of additives for polyolefins.



Helmut Linhart graduated in chemistry from Darmstadt Technical Institute (FRG) in 1958. He joined Enka-Glanzstoff AG and worked over 10 years in the research center for fiber polymer development. In 1969 Mr. Linhart joined CIBA-GEIGY Ltd. in Basle Switzerland as Group Leader in the Polymer Additive Department. In 1976 he was assigned special responsibilities for the development of, and technical service for, additives in polyolefins. In 1978, he was appointed Marketing Manager and since 1980 Head of Marketing and Application for the same product group.



# BEHAVIOUR OF FOUR NON-MIGRATORY ANTIOXIDANTS IN SOLID POLYETHYLENE INSULATION

H.J. Ruddell

D.J. Adams

P. Latoszynski

B.T. de Boer

Telecom Australia  
Melbourne,  
Australia

## ABSTRACT

An earlier investigation into premature cracking of solid polyethylene insulation of telecommunication cables in above-ground joints identified the cause as early depletion of antioxidant. A contributing factor was found to be the loss of antioxidant by migration. Consequently, antioxidants were sought with minimal migration from polyethylene at service temperatures up to 60°C. Tests conducted showed that four out of fourteen phenolic antioxidants investigated exhibited negligible migration, and were considered suitable for further examination. Large reaction losses, however, were found with all four antioxidants when used alone in the presence of copper, and this was not altered by the use of a secondary antioxidant. These losses were reduced to negligible proportions with only two of the antioxidants when used in combination with metal deactivators. As a result of this work, studies are in progress to determine the capability of these two stabilising systems to protect solid medium-density polyethylene for more than 40 years under adverse thermal conditions.

## INTRODUCTION

The premature embrittlement of solid, medium-density, polyethylene (MDPE) insulation of unfilled cable installed in Australia between 1965 and 1974 was reported<sup>1</sup> at the 31st IWCS. The degradation occurred only in the insulation from that section of cable from which the sheath had been removed for jointing, and only in joints installed in above-ground enclosures<sup>2</sup>. The early degradation of the polyethylene was shown to be caused by thermo-oxidation resulting from a number of competing and interacting factors. These were initial low levels of antioxidant, loss of antioxidant during processing, interaction between antioxidant and metal ions, high temperatures in jointing enclosures, and loss of antioxidant by migration.

Insufficient antioxidant, processing losses and reaction with metals associated with pigments and opacifiers were factors common to all the antioxidants, and were readily rectified by obvious means. Also, it has been found that the high temperatures, up to 60°C, experienced by the exposed insulation within the enclosures, could be substantially reduced by the use of white reflective covers. Loss by migration, however, varies according to specific properties of the antioxidant, in

particular, its solubility and diffusion in the polymer; hence correction of this factor required individual examination of each antioxidant in the polymer.

The migration of a number of additional antioxidants was therefore studied at various concentrations, either alone or in combination with a secondary antioxidant and/or metal deactivator. The aim was to establish at least two alternative stabilising systems of non-migratory components, capable of protecting MDPE against thermo-oxidation for a minimum of 40 years under existing operating conditions.

## STABILISER MIGRATION - EXAMINATION IN PLAQUES

Permanax WSP(PQ) was the only antioxidant covered in the previous paper<sup>1</sup> which showed negligible migration tendencies in low-density polyethylene (LDPE), as shown in Figure 1.

Since these results were published, work has been directed to investigating other proprietary stabilisers of the hindered phenolic type, a group well recognised for their excellent antioxidant and non-staining properties in polyethylene. Another advantage of this group to the Australian polymer and cable industry is that the concentration may be readily determined<sup>3</sup> in both unoxidised and oxidised polyethylene by high-performance liquid chromatography (HPLC) analysis.

Eight antioxidants were examined in unpigmented 0.5 mm thick LDPE plaques, in a similar manner to those antioxidants previously described<sup>1</sup>, at about 0.1% concentration in UCAL DFDL 6005 of density 919 kg/m<sup>3</sup> and MFI of 0.3 g/10 minutes. The results in Figure 2 show that only four antioxidants showed little or no tendency to migrate. Of these, three were products of Cyanamid International (USA), marketed under the trade name of "Cyanox", namely Cyanox 425, Cyanox 1790 and Cyanox 2246. (See Figure 13 for their chemical structures.) The other was the Ciba-Geigy product Irganox 1076 which was excluded from further investigation, since its low melting point of 52°C led to physical losses during polymer compounding.

A search for an alternative non-migratory metal deactivator to Eastman Inhibitor OABH was also conducted but without success. Uniroyal's Naugard XL-1, claimed to possess the dual property of both antioxidant and metal deactivator, exhibited

PERCENTAGE OF STABILISER MIGRATED TO SURFACE

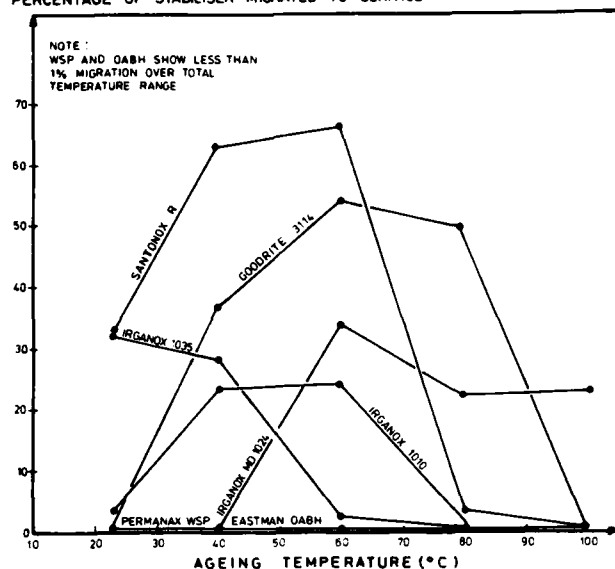


FIGURE 1. MIGRATION OF STABILISERS FROM LDPE PLAQUES AFTER AGEING FOR 28 DAYS AT VARIOUS TEMPERATURES<sup>1</sup>.

excessive migration from LDPE as shown in Figure 2, whilst UCDA 16, manufactured by Ube Industries Ltd., and Cyanamid's Cyanox 2379 were both withdrawn from the market for commercial reasons before examinations commenced.

#### STABILISER MIGRATION - EXAMINATION IN INSULATION

Consequently, of the fifteen stabilisers (Table 1) evaluated in the migration studies, the only four antioxidants considered worthy of further investigation in MDPE were Cyanox 425, Cyanox 1790, Cyanox 2246 and Permanax WSP(PQ). These were examined at various concentrations as the primary antioxidant in insulation extruded on to copper wire, either as the sole stabiliser, or in combination with the secondary antioxidant Sandostab P-EPQ (0.05%) and/or metal deactivator Eastman Inhibitor OABH (0.1%) or Irganox MD 1024 (0.1%). In all, 32 combinations of stabilised MDPE were extruded, under commercial operating conditions, as unpigmented solid insulation of radial thickness 0.32 mm on to 0.64 mm copper conductor wire. The MDPE had a density of 927 kg/m<sup>3</sup> and an MFI of 0.3 g/10 minutes.

Sufficient lengths of each of the insulated wires were prepared in such a manner as to enable residual stabiliser content, loss by migration, oxidation induction time (OIT), elongation at break, and dielectric dissipation factor ( $\tan \delta$ ) to be monitored subsequent to various ageing periods in air at temperatures of 23, 40, 60 and 80°C. Elongation at break and the value of  $\tan \delta$  are indicators of changes in physical and electrical properties, respectively, which occur over a long period of time. However, insufficient results have been accumulated to report these tests in this paper. The stabiliser content in the polymer bulk and the loss of stabiliser by migration were determined

PERCENTAGE OF STABILISER MIGRATED TO SURFACE

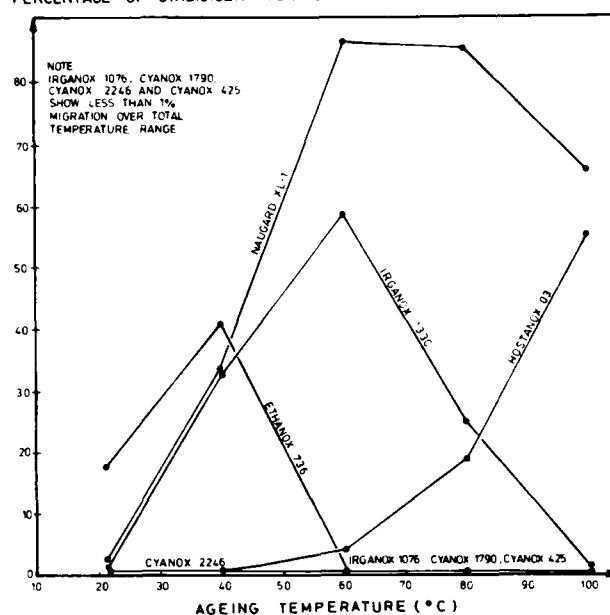


FIGURE 2. MIGRATION OF ADDITIONAL STABILISERS FROM LDPE PLAQUES AFTER AGEING FOR 28 DAYS AT VARIOUS TEMPERATURES.

on 4 m lengths of insulated wire, aged as coils with diameters of 60 mm. The stabiliser which migrated to the polymer surface after each ageing period was removed by dipping the coil in acetone, 30 times in 30 seconds, followed by an acetone wash, and finally a wipe of the uncoiled wire with cotton wool, wetted with a fresh amount of the same type of solvent. For determining migration of Eastman Inhibitor OABH, the same technique was used, except that the solvent was acetone containing 10% v/v dimethyl formamide. The stabiliser content in the combined "wash" was determined<sup>3</sup> by HPLC, and the quantity of stabiliser which had migrated was expressed as a percentage of the initial stabiliser content in the sample. The quantity of active stabiliser remaining in the polyethylene insulation was determined by stripping 2 m of insulation from the wiped sample, dissolving this insulation in toluene, precipitating the polyethylene out of solution with ethanol, and determining the stabiliser content in the filtered solution by HPLC. OITs, regarded<sup>4</sup> as a measure of the thermo-oxidative stability of a polymer, were determined on 15 mg samples of the same insulation aged for the HPLC determinations. The tests were conducted in aluminium pans at a temperature of 200°C in pure oxygen, introduced at 100 mL per minute, using a Dupont 910 DSC.

As anticipated from the preliminary work conducted on plaques, negligible migration occurred with any of the four antioxidants investigated when the polyethylene insulation was tested after the first ageing period of 28 days. The non-migratory behaviour was independent of ageing temperature (23° to 80°C), concentration of the antioxidant (0.07% to 0.23%) and the presence of a secondary antioxidant and/or metal deactivator.

### LOSS ON AGEING

A reduction in the quantity of active antioxidant, in the polyethylene insulation (independent of that due to migration) was observed after ageing for only 28 days at 40, 60 and 80°C, and, as shown in Figures 3 and 4, was alarmingly high. (Values given at 23°C are the initial values before ageing). Losses in Permanax WSP(PQ), Cyanox 425 and Cyanox 2246 averaged around 20%, 30% and 46% respectively at 60°C, and greater than 90% at 80°C. Cyanox 1790 performed the best of all four antioxidants. It, too, showed an average loss of 20% at 60°C, but only 31% at 80°C. The losses were independent of the initial concentration of the primary antioxidant and the presence of the secondary antioxidant Sandostab P-EPQ.

The magnitude of loss of antioxidant as determined by chromatographic HPLC analysis, was supported by thermal analysis OIT. This is shown in Figure 5 for Cyanox 2246 and Cyanox 1790. Similar correlations occurred for Permanox WSP(PQ) and Cyanox 425.

The losses in insulation aged at 60°C and at 80°C were also accompanied by a gross colour change in the insulation, going from a natural polyethylene appearance to an intense golden-yellow colour. The mechanical properties of the insulation, however, were unaffected, as shown by the retention of high values of elongation after ageing.

### EFFECT OF METAL DEACTIVATOR

The loss of antioxidant was arrested in insulation containing Permanax WSP(PQ) and Cyanox 1790, when a metal deactivator was included in the stabilising system. As shown in Figure 6, the presence of the metal deactivator, however, did not in any way diminish the losses of Cyanox 425 or Cyanox 2246 at any temperature over the 28 day ageing period of the test. The metal deactivator did, however, prevent discolouration occurring in any samples, indicating that no relationship exists between antioxidant loss and changing colour under the conditions of these tests. The results obtained were similar, regardless of whether the metal deactivator was Eastman Inhibitor OABH or Irganox MD 1024, or whether the secondary antioxidant Sandostab P-EPQ was present or absent.

The concentration of the metal deactivators in the presence of all four antioxidants remained reasonably stable, as shown in Figures 7 and 8. The exception is Irganox MD 1024 at temperatures above 60°C. Approximately 90% of the loss of Irganox MD 1024 which did occur was due to migration, as indicated in the data of Figure 1, and not due to other reactions discussed in this paper.

The effect of the metal deactivator in retarding the rate of antioxidant losses is more clearly illustrated in Figures 9 to 12 where the losses are shown after a period of ageing for 105 days at a temperature of 60°C.

CONCENTRATION OF PRIMARY ANTIOXIDANT (PERCENT)

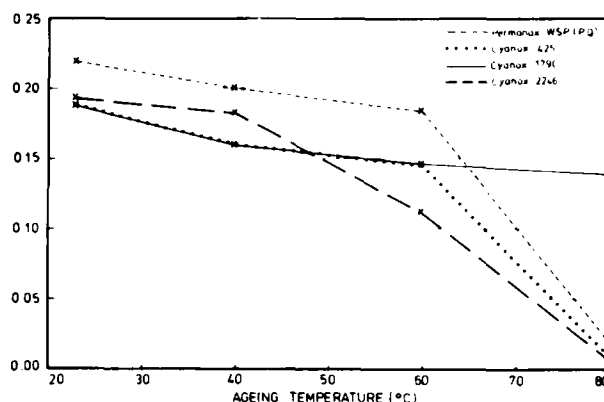


FIGURE 3. CONCENTRATION OF PRIMARY ANTIOXIDANT IN INSULATION AFTER AGEING FOR 28 DAYS AT VARIOUS TEMPERATURES.

CONCENTRATION OF PRIMARY ANTIOXIDANT (PERCENT)

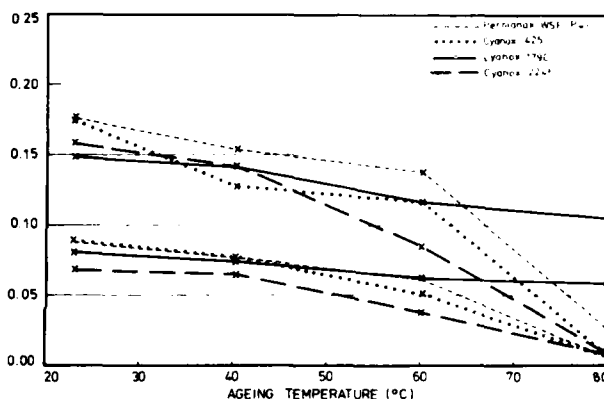


FIGURE 4. CONCENTRATION OF PRIMARY ANTIOXIDANT IN INSULATION ALSO CONTAINING THE SECONDARY ANTIOXIDANT SANDOSTAB P-EPQ AFTER AGEING FOR 28 DAYS AT VARIOUS TEMPERATURES.

PERCENTAGE OF INITIAL VALUE

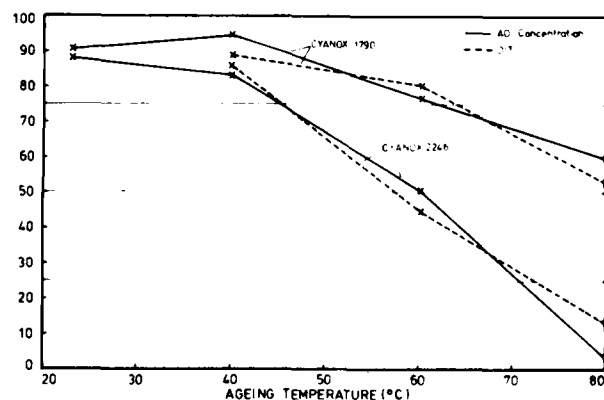


FIGURE 5. COMPARISONS OF CONCENTRATIONS OF ANTIOXIDANT AND OXYGEN INDUCTION TIME (OIT) IN INSULATION AFTER AGEING FOR 28 DAYS AT VARIOUS TEMPERATURES.

CONCENTRATION OF PRIMARY ANTIOXIDANT (PERCENT)

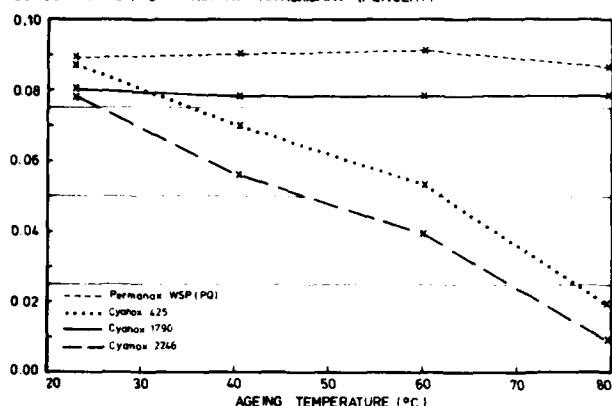


FIGURE 6. CONCENTRATION OF PRIMARY ANTIOXIDANT IN INSULATION CONTAINING A METAL DEACTIVATOR AND SECONDARY ANTIOXIDANT AFTER AGEING FOR 28 DAYS AT VARIOUS TEMPERATURES.

CONCENTRATION OF EASTMAN INHIBITOR OABH (PERCENT)

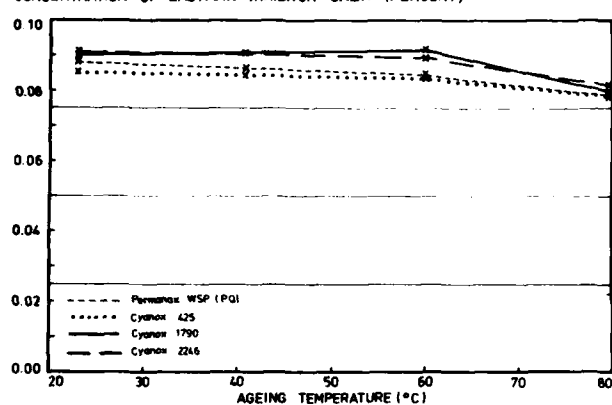


FIGURE 7. CONCENTRATION OF EASTMAN INHIBITOR OABH IN THE PRESENCE OF VARIOUS PRIMARY ANTIOXIDANTS IN INSULATION AFTER AGEING FOR 28 DAYS AT VARIOUS TEMPERATURES.

CONCENTRATION OF IRGANOX MD 1024 (PERCENT)

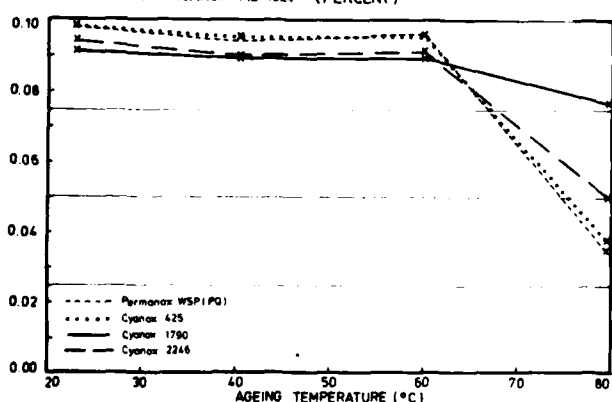


FIGURE 8. CONCENTRATION OF IRGANOX MD 1024 IN THE PRESENCE OF VARIOUS PRIMARY ANTIOXIDANTS IN INSULATION AFTER AGEING FOR 28 DAYS AT VARIOUS TEMPERATURES.

CONCENTRATION OF PERMANAX WSP(PQ) (PERCENT)

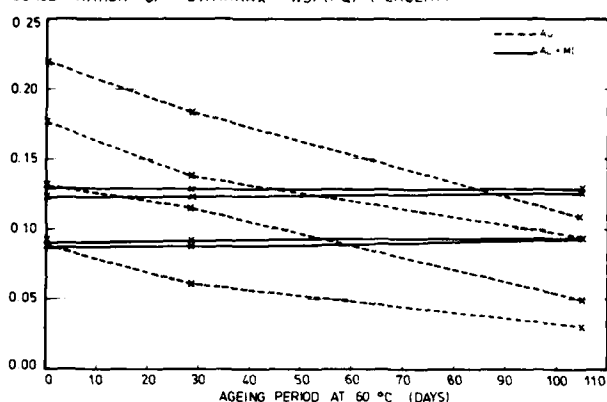


FIGURE 9. CONCENTRATION OF PERMANAX WSP(PQ) IN INSULATION METAL DEACTIVATED AND NON-DEACTIVATED SYSTEMS AFTER AGEING AT 60°C.

CONCENTRATION OF CYANOX 425 (PERCENT)

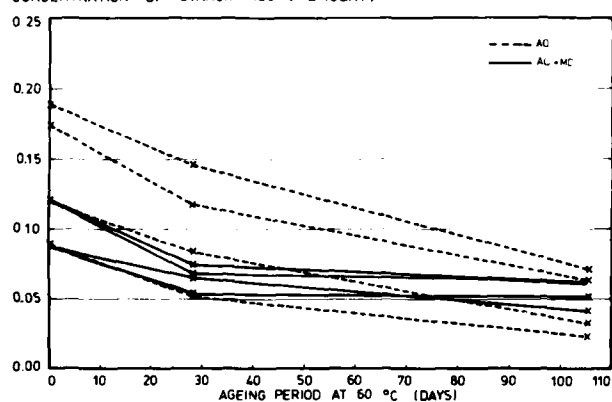


FIGURE 10. CONCENTRATION OF CYANOX 425 IN INSULATION METAL DEACTIVATED AND NON-DEACTIVATED SYSTEMS AFTER AGEING AT 60°C.

CONCENTRATION OF CYANOX 2246 (PERCENT)

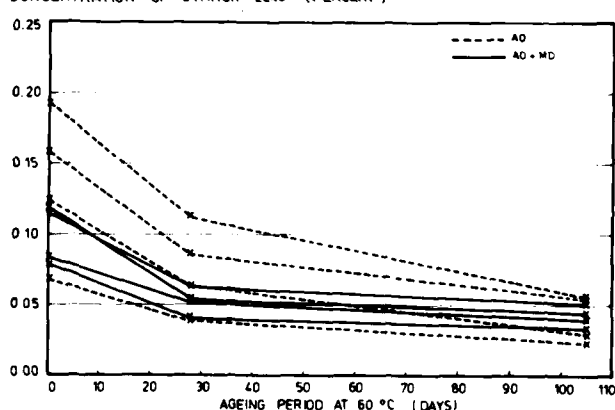


FIGURE 11. CONCENTRATION OF CYANOX 2246 IN INSULATION METAL DEACTIVATED AND NON-DEACTIVATED SYSTEMS AFTER AGEING AT 60°C.

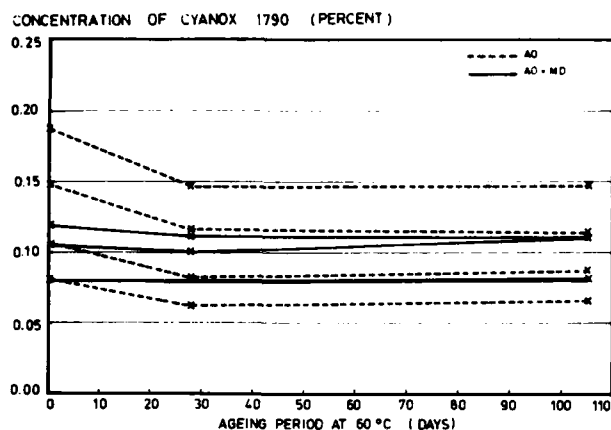


FIGURE 12. CONCENTRATION OF CYANOX 1790 IN INSULATION METAL DEACTIVATED AND NON-DEACTIVATED SYSTEMS AFTER AGEING AT 60°C.

Figure 9 shows that when the Permanax WSP(PQ) system was aged at 60°C at concentrations ranging between 0.08% and 0.22%, an average loss of around 20% of the initial value occurs during the first 28 days, and 56% after 105 days. However, when metal deactivators Eastman Inhibitor OABH or Irganox MD 1024 are included in the system, no apparent loss occurs over the entire ageing period of 105 days.

Figures 10 and 11 show that Cyanox 425 and Cyanox 2246 behave in a similar manner to each other. This behaviour can be expected from the similarity in their chemical structures, as illustrated in Figure 13. When used alone, a rapid loss of around 33% and 46% respectively occurred during the first 28 days, with a total loss of around 69% and 71% respectively for the total ageing period of 105 days. However, unlike the Permanax WSP(PQ) formulations, the metal deactivated systems still showed similar high losses of around 37% and 48% respectively, for the first 28 days, after which the rate of loss decreased to only a further 11% for the total 105 day period.

Figure 12 shows Cyanox 1790, when used without a metal deactivator, to show a similar rapid loss of approximately 20% as that of Permanax WSP(PQ) during the first 28 days of ageing but, unlike the others, exhibited no additional loss on further ageing. In the presence of Eastman Inhibitor OABH or Irganox MD 1024, Cyanox 1790 behaved similarly to Permanax WSP(PQ) in showing no detectable loss over the entire ageing period of 105 days at 60°C.

#### CONCLUSION

Our investigations have shown that each of the four phenolic types of antioxidants examined, namely Permanax WSP(PQ), Cyanox 425, Cyanox 2246 and Cyanox 1790, exhibit sufficient solubility in polyethylene of density 927 kg/m<sup>3</sup> so that, when the polyethylene containing these antioxidants was extruded as insulation on wire, negligible antioxidant was lost to the system by migration to the surface of the insulation.

However, large losses did occur, presumably through reactions dominated by copper catalysed thermal oxidation, with all four antioxidants, when used alone or with a secondary antioxidant. Cyanox 1790 performed much better than the other three, and this was considered to be due to the isocyanurate ring exerting some degree of metal deactivation.

When recognised metal deactivators, Eastman Inhibitor OABH or Irganox MD 1024, were included in the stabilising system, negligible antioxidant loss was observed in the systems containing Permanax WSP(PQ) and Cyanox 1790. The metal deactivators had little or no effect on the losses occurring during the first 28 days of ageing losses in the Cyanox 425 and Cyanox 2246 systems, but they did, however, exert a retarding influence on the amount of primary antioxidant lost as the ageing period progressed.

This suggests that reactions, other than those catalysed by metals, are occurring which Cyanox 425 and Cyanox 2246 alone are incapable of suppressing. The presence of the secondary antioxidant Sandostab P-EPQ was also ineffectual in retarding these reactions.

Permanax WSP(PQ) and Cyanox 1790, when used in combination with a metal deactivator, were the only two antioxidants to show acceptable stability at all temperatures for test periods up to 105 days. The question still remains, however, whether these systems are capable of protecting the polymer for 40 years in an environment with an average temperature of about 40°C, and if so, at what initial concentration. It is intended to extend the ageing periods up to several hundred days, whilst following changes in mechanical, electrical and chemical properties. The results, derived from these laboratory tests, will then be correlated with studies being conducted in field environments of high ambient temperatures. It is intended that these results will be reported at a later date.

#### ACKNOWLEDGEMENTS

Many people rendered valuable assistance in the design and conduct of the experiments and their help is gratefully acknowledged. Special acknowledgement is given to all the staff of the Polymer Section of the Research Laboratories for the development of the analytical techniques and the design and execution of the many experiments involved. Further acknowledgement is given to the staff of the Lines Construction Branch for help in the preparation of this paper. Thanks are also extended to ICI Australia Operations Pty. Ltd., Union Carbide Australia Ltd. and Austral Standard Cables Pty. Ltd. for their participation. The permission of the Chief General Manager, Telecom Australia, to publish this paper is acknowledged.

TABLE 1 CHEMICAL IDENTIFICATION OF STABILISERS

Trade Name	Manufacturer	Chemical Name
Santonox R	Monsanto Co.	4,4'-thiobis (6-tert-butyl-3-methylphenol)
Irganox 1010	Ciba-Geigy Ltd.	Tetrakis {methylene-3-(3',5'-di-tert-butyl-4'-hydroxyphenyl) propionate} methane
Irganox 1035	Ciba-Geigy Ltd.	2,2'-thiodiethyl-bis {3-(3,5-di-tert-butyl-4-hydroxyphenyl) propionate}
Irganox 1076	Ciba-Geigy Ltd.	Octadecyl-3-(3',5'-di-tert-butyl-4'-hydroxy-phenyl) propionate
*Irganox 1330	Ciba-Geigy Ltd.	1,3,5-trimethyl-2,4,6-tris (3',5'-di-tert-butyl-4'-hydroxybenzyl) benzene
+Permanax WSP(PQ)	Vulnax International Ltd.	2,2'-dihydroxy-3,3'-bis (1-methylcyclohexyl)-5,5'-diphenylmethane
Goodrite 3114	Goodrite Chemicals	Tris (3,5-di-tert-butyl-4-hydroxybenzyl) isocyanurate
Hostanox 03	Hoechst AG	Bis {3,3-bis (4'-hydroxy-3'-tert-butylphenyl) butyric acid} ethylene glycol ester
Ethanox 736	Ethyl Corporation	4,4'-thiobis (6-tert-butyl-2-methylphenol)
Cyanox 425	American Cyanamid Co.	2,2'-methylene-bis (4-ethyl-6-tert-butyl-phenol)
Cyanox 1790	American Cyanamid Co.	Tris (4-tert-butyl-3-hydroxy-2,6-dimethylbenzyl) isocyanurate
Cyanox 2246	American Cyanamid Co.	2,2'-methylene-bis (4-methyl-6-tert-butylphenol)
Naugard XL-1	Uniroyal Chemical Co.	2,2'-oxamido-bis-(ethyl-3-(3,5-di-tert-butyl-4-hydroxyphenyl) propionate}
Eastman Inhibitor OABH	Eastman Chemical Products Inc.	Oxalic acid - bis (benzylidene hydrazide)
Irganox MD 1024	Ciba-Geigy Ltd.	N,N'-bis {3-(3,5-di-tert-butyl-4-hydroxyphenyl) propionic acid} hydrazide
Sandostab P-EPQ	Sandoz Ltd.	Tetrakis (2,4-di-tert-butylphenyl) 4,4'-biphenylenediphosphonite

\* equivalent to Ethyl 330  
+ equivalent to Nonox WSP(PQ)

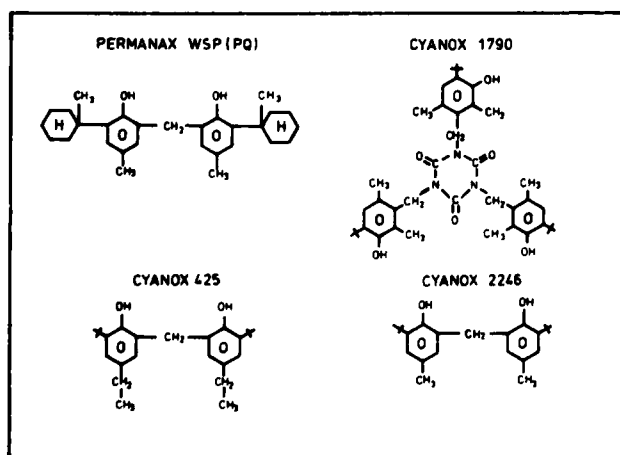


FIGURE 13. CHEMICAL STRUCTURE OF THE FOUR NON-MIGRATORY STABILISERS.

## REFERENCES

- 1 B.L. Board, H.J. Ruddell, Proc. 31st Int. Wire & Cable Symp., 300 (1982).
- 2 H.J. Ruddell, D.J. Adams, B.A. Chisholm, Plast. in Telecommun., 3rd Int. Conf., 8-1 (1982).
- 3 Australian Standard 1049-1983.
- 4 G.A. Schmidt, Proc. 26th Int. Wire & Cable Symp., 161 (1977).



H.J. Ruddell  
Polymer Section  
Research Laboratories  
Telecom Australia  
770 Blackburn Road  
CLAYTON Vic. 3168  
AUSTRALIA



P.R. Latoszynski  
Polymer Section  
Research Laboratories  
Telecom Australia  
770 Blackburn Road  
CLAYTON Vic. 3168  
AUSTRALIA

Hec Ruddell joined Telecom Australia Research Laboratories in 1955 as a Chemist after 19 years in private industry in the field of oils, general chemistry, rubbers, and plastic. In 1966 he was promoted to set up the Polymer Section which is responsible for the investigation, development and application of all plastics, rubbers and adhesives in communications equipment. He was actively associated with the early manufacture and installation of plastics cable, including the development and formulation of epoxy resins and the epoxy resin field pack, the design of joints, particularly those for multi-pair submarine cables laid off the coast of Queensland, and the recent developments in filled cable, optical fibres, and stabilisation of polyethylene. Mr Ruddell has been an Associate Member of The Plastics Institute of Australia since 1959, and was awarded a Fellowship of that Institute in 1982.

Peter Latoszynski joined Telecom Australia Research Laboratories in 1972 as a Technical Assistant with the Analytical Chemistry Group. He graduated in 1975 with a Diploma of Applied Science (Chemistry) from Footscray Institute of Technology (in Victoria), and in 1980 gained a Graduate Diploma of Analytical Chemistry from the Royal Melbourne Institute of Technology. In 1976 he joined the Polymer Section and is currently a Science 2 Chemist involved with the investigation into stabilisation of Polymers.



D.J. Adams  
Polymer Section  
Research Laboratories  
Telecom Australia  
770 Blackburn Road  
CLAYTON Vic. 3168  
AUSTRALIA



B.T. de Boer  
Cable Design and  
Specifications Section  
Lines Construction Branch  
Engineering Department  
Telecom Australia  
28/570 Bourke Street  
MELBOURNE Vic. 3000  
AUSTRALIA

David Adams joined Telecom Research Laboratories in 1972 after 3½ years in the Chemical Laboratory of the Naval Dockyards, Williamstown, Victoria. He graduated in 1975 with a Diploma of Applied Chemistry from the Footscray Institute of Technology (in Victoria). His interests in plastics include their weathering, stabilisation and flammability. He is currently a Senior Chemist.

Bob de Boer is Manager of the Cable Design and Specifications Section at Telecom Australia. He joined Telecom Australia in 1972 after graduating in Electrical Engineering from Monash University in Victoria. He has had extensive experience in the areas of telecommunication cable design, specifications and provisioning, as well as the installation of external plant.

## EQUIPMENT AND DESIGN CHANGES IN EXTRUSION OF FOAMED FLUOROPOLYMER RESINS

STUART K. RANDA, MARK A. CARLSON, AND DAVID P. REIFSCHNEIDER

E. I. DU PONT DE NEMOURS &amp; CO., INC.

Recent growth of computer networks has increased the market for foamed coaxial cables. To meet this need, the gas injection process for foaming of Teflon\* FEP and PFA fluorocarbon resins introduced in 1981 at the 30th Wire and Cable Symposium has been refined. Advances in die and extruder screw design have broadened capability from 500 CATV coaxial cable to miniature wire sizes. Increased processing speeds and higher core quality have been achieved.

These coaxial cables have a unique combination of properties that are maintained over a wide range of temperatures and signal frequencies. They have dielectric constants as low as 1.3 and low flame spread and smoke generation as tested to UL 910.

These cables are now widely used for high frequency signal transmission in compliance with the National Electric Code for installation without conduit in building air handling plenums. Military applications represent newer areas of interest with weight and space savings and high electrical quality.

The characteristics of several coaxial cables are reviewed.

FOAMED COAXIAL CABLE PROPERTIES

Foaming a dielectric material reduces the dielectric constant (DC) and dissipation factor (DF). This reduction in DC and DF in an assembled coaxial cable offers lower capacitance, lower attenuation, and higher velocity of propagation than solid dielectric core cables. These improved electrical properties offer better performance and the ability to optimize the cable design.

Cables of FEP and PFA resins can be made with void contents as high as 70% and dielectric constants as low as 1.3. Comparable cables of polyethylene, foamed to a dielectric constant of 1.5, do not have as low capacitance or as high velocity of propagation as does FEP or PFA foam. In addition, structural return loss in FEP and PFA coaxial cables can be controlled within the specifications of MIL-C-17 by careful regulation of extruder and capstan speeds and attention to reducing mechanically induced line speed variations.

\* Reg. U. S. Pat. Ofc. for Du Pont's Fluorocarbon resins.

Cores of FEP foam have twice the compressive strength of similar polyethylene foam cores, measuring the force required to compress the core by 25%. This simulates a situation where mechanical stress might disturb the electrical characteristic of a cable but not short it entirely.

To meet the capacitance, velocity, and attenuation requirements of the military specifications, with reasonable foam levels, only FEP and PFA are suitable. Other fluoropolymers with higher DC and DF would need to be foamed to much higher void levels.

DESIGNING FOAMED COAXIAL CABLES

Common cable design formulas can be used to predict foamed coaxial cable properties. Slight deviation from calculated values results from the use of stranded conductors and braided shields, but the relationships are satisfactory for approximation.

- Characteristic Impedance,  $Z_0$ , is given by:

$$Z_0 = \frac{138.2}{K} \log_{10} \frac{D}{d}$$

Where K = Dielectric Constant

D = Core O.D.

d = Conductor O.D.

- Capacitance is:

$$C = \frac{7.354 K}{\log_{10} \left( \frac{D}{d} \right)}$$

- Attenuation is:

$$A = \frac{.435}{Z_0} \left[ \frac{1}{d} + \frac{1}{D} \right] \sqrt{F} + 2.78 P \sqrt{K} F$$

Where F = Frequency, in Megahertz

P = Dissipation Factor

- Relative Velocity of Propagation, (%):

$$VP = \frac{100}{\sqrt{K}}$$

These equations show that low dielectric constant is the main factor in developing low capacitance and high velocity. In the attenuation calculation, the low dissipation factor of FEP and PFA results in cables having low signal loss.

The design criteria of a foamed coaxial cable of specific impedance (50, 75, or 93 ohm) can be satisfied by various conductor size, core diameter, and foam level (dielectric constant) combinations.

Two options are available in designing a foamed coaxial cable to replace a solid core:

1. Maintain the same core O.D., using a larger conductor.  
Result: Improved electrical properties: lower capacitance, higher velocity, lower attenuation.
2. Maintain the same conductor, but reduce the core O.D.  
Result: Reduced weight and size. Attenuation remains the same, but capacitance is lowered and velocity increased.

The first option may be preferred in many cases, because it offers the advantages of compatibility with existing connectors. New cable designs for specific applications could utilize the reduced weight and size advantages of the second option, but user and manufacturer interchange is necessary to develop satisfactory cable specifications.

Property measurements provide the best comparison of the improvement available from foamed cables. Table A shows a comparison of properties for RG-59 type cables, and Table B shows the same comparison for RG-11 type cables. These data are for foamed cables with the same core O.D. as solid constructions, but using a larger conductor. Significant improvements in capacitance, velocity, and attenuation are underlined.

**TABLE A**  
TYPICAL AVERAGE PROPERTIES (1) RG-59 TYPE COAXIAL CABLE

	Solid Core Polyethylene	Solid Core Teflon® FEP	Foam Core Teflon® FEP
Conductor O.D.	.025	.025	.032
Core O.D.	.146	.146	.146
Shield	95% B.C.	95% B.C.	Foil + 60% Al.
Jacket O.D.	.240	.215	.215
Weight lbs./1000 ft.	38	43	28 (2)
Capacitance, pf/ft.	21	19.5	<u>16.6</u>
Impedance, ohms	73	75	75
Attenuation dB/100 ft.			
50 MHz	2.4	2.2	<u>1.9</u>
100 MHz	3.4	3.4	<u>2.7</u>
200 MHz	4.9	5.1	<u>3.9</u>
300 MHz	6.1	6.4	<u>5.0</u>
400 MHz	7.1	7.6	<u>5.8</u>
Velocity of Propagation, %	66	69	<u>82</u>
Dielectric Constant	2.1	2.1	1.48

(1) Data courtesy of Nitamp Wires Inc. and Berk-Tek, Catalog information from Belden Corp., M/A COM Comm/Scope, Inc., and Times Fiber Communications Inc.

(2) Weight reduction due to foil and Al. shield. With 95% B.C. shield, weight is approximately 38 lbs./1000 ft.

**TABLE B**  
TYPICAL AVERAGE PROPERTIES (1) RG-11 TYPE COAXIAL CABLE

	Solid Core Polyethylene	Foam Core Teflon® FEP
Conductor O.D.	.048	.064
Core O.D.	.285	.285
Shield	95% B.C.	95% B.C.
Jacket O.D.	.405	.370
Weight, lbs./1000 ft.	95	93
Capacitance, pf/ft.	20.5	<u>16.5</u>
Impedance, ohms	75	75
Attenuation, dB/100 ft.		
50 MHz	1.3	<u>1.0</u>
100 MHz	2.0	<u>1.3</u>
200 MHz	2.9	<u>2.2</u>
300 MHz	3.6	<u>2.9</u>
400 MHz	4.2	<u>3.4</u>
Velocity of Propagation, %	66	<u>83</u>
Dielectric Constant	2.3	1.45

(1) Data courtesy of Nitamp Wires, Inc. and Berk-Tek. Catalog information from Belden Corp., Times Fiber Communications Inc.

If the option of reducing the core diameter is chosen, a smaller, lighter cable results with lower capacitance, higher velocity, but essentially the same attenuation. Table C shows the benefits of downsizing.

**TABLE C**  
TYPICAL AVERAGE PROPERTIES (1) RG-59 TYPE COAXIAL CABLE

	Solid Core FEP	Downsized Foam Core FEP
Conductor O.D.	.025	.025
Core O.D.	.146	<u>.116</u>
Shield	95% B.C.	95% B.C.
Jacket O.D.	.215	.180
Weight, lbs./1000 ft.	43	<u>25</u>
Capacitance, pf/ft.	19.5	<u>16.5</u>
Impedance, ohms	75	75
Attenuation, dB/100 ft.		
50 MHz	2.2	2.3
100 MHz	3.4	3.4
200 MHz	5.1	5.1
300 MHz	6.4	6.4
400 MHz	7.6	7.3
Velocity of Propagation, %	69	<u>82</u>
Dielectric Constant	2.1	1.48

(1) Data courtesy of Nitamp Wires Inc.

Coaxial cable with a .060 foamed core has been made as an alternate to RG-316, which uses a solid PTFE core. Properties have been measured and are shown in Table D. Again the advantages of lower capacitance, higher velocity, and lower attenuation result. This cable easily meets the requirements of MIL-C-17/113C.

**TABLE D**  
MEASURED PROPERTIES OF EXPERIMENTAL  
RG-316 TYPE COAXIAL CABLE (1)

	C-17/113C Spec.	FEP Foamed Core
Conductor O.D.	.0201	.025
Core O.D.	.060	.060
Capacitance, pf/ft.	32	<u>26</u>
Impedance, ohms	50	50
Attenuation, dB/100 ft.		
50 MHz	7.5	2.8
500 MHz	23	15
1.0 GHz	36	22
2.0 GHz	47	33
3.0 GHz	58	<u>42</u>
Velocity of Propagation, %	69.5	<u>83.9</u>
Dielectric Constant	2.10	1.42

(1) Measurements courtesy of Therman Inc. and Teledyne Thermatics.

Techniques for producing RG-62 coaxial core, an intermediate size core, at 30 ft./min. were introduced in the 1981 paper. The paper reviewed extruder and die design, supershear extrusion along with foam process instrumentation. This process uses Freon® 22 chlorodifluoromethane gas as a foaming agent. A number of manufacturers now utilize this process routinely to produce coaxial cable cores.

The newer techniques developed are now in use to achieve higher rates and involve the following process improvements:

- ### IMPROVED EXTRUDER SCREW DESIGN

This modification followed a basic melt pressure study of the extruder during RG-62 and RG-8 foam core production. In this study, the extruder barrel was drilled to accept melt pressure transducers at many points along the length of the screw, as shown in Figure 1A.

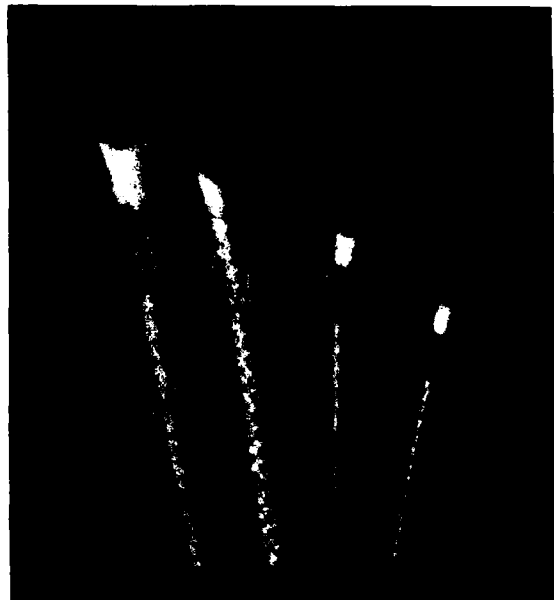
This fill variation could be monitored by the readings from the pressure transducers. Low pressure occurred when the section of the screw containing F-22 gas rotated under the transducer. The melt front being pushed forward by the screw flight indicated a higher pressure. Using a strip chart recorder, the percentage melt fill was determined from the ratio of the lengths of the pressure traces. As a result of this study, the melt fill in subsequent screw designs was increased to 50% by decreasing the channel depth in the gas zone.

International Wire &amp; Cable Symposium Proceedings 1983

The increased melt-to-barrel wall contact allows uniform conveying of molten resin through the extruder and stable RG-62 core production speeds of 100 ft./min. Figure 3 shows a typical cross section of a RG-62 core. The foam cells have a closed structure with diameter in the 3 to 8 mil range.

FIGURE 2

Foamed Coaxial Cables of FEP Resin



Additional process development work has been carried out to improve uniformity of larger coaxial cores such as RG-8, RG-11, etc. This was accomplished by better control of pumping zone melt pressure of the 50% melt fill screws.

PUMPING ZONE MELT PRESSURE

Extrusion Foaming RG-62 Coaxial Core

The basic extruder screw design with its five key zones is shown in Figure 1A. A threshold cross-head pressure of 1500 psi is required to achieve foamed cores having small closed cells. At this pressure, the pumping zone has at least one flight 100% filled with melt. This is shown in Figure 1B. This melt fill can be visually noted from a "shadow" line that becomes traced on the surface of the screw channels in normal use. Just one flight of pumping zone, 100% melt filled, allows extrusion of RG-62 coax cores at line speeds as high as 100 ft./min. Additional fill of this zone is required for production of the larger diameter cores.

Influence of Die Design on Melt Pressure

Streamlined dies and tips having a shallow cone angle and a smooth transition to a die land are also necessary to improve line speeds of RG-62 from 30 to 100 ft./min. Early dies included a cup-shape on the die orifice. Figure 4 shows typical crossheads with streamlined die and tip design. These larger annular opening dies allow the extruder screw to be run at higher speeds and develop the 1500 psi crosshead melt pressure needed for good foam cell formation.

Extruding Coaxial Cores Larger Than RG-62

The large opening dies needed for coaxial cables larger than RG-62 produce less melt pressure at low screw speeds, and consequently, less fill of the pumping zone.

To achieve high precision melt delivery required for larger coaxial cores, more pumping flights must be filled with melt. To accomplish this, higher melt pressure is needed directly in front of the screw. There are several ways to accomplish this.

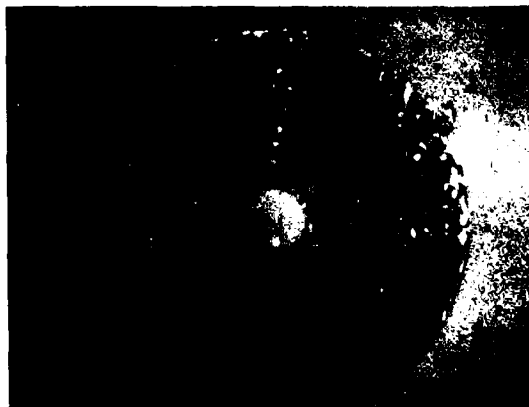
By design, approximately 85% of the pumping flight length is 100% filled with a 2500 psi upstream melt pressure as shown in Figure 1C. With these pumping flights filled, the extruder screw's uniformity in melt delivery is significantly improved allowing higher line speeds while producing large diameter coaxial cores to close diameter tolerances. This, of course, assumes that the extruder and capstan motors have the needed speed regulation. The limit of this procedure is that the melt pressure must not be allowed to increase to where melt would flood the gas zone.

FIGURE 3

Cross Sectional View

RG-62 Coaxial Core of FEP Resin

(Magnification 20X)



This limit is ~2800 psi on our 2 inch, 27.8 length to diameter screw. Should the injection zone flood, the F-22 gas could not enter the extruder barrel and foaming would cease. The absolute threshold pressure for back flooding the gas zone varies with specific screw size and features such as pumping zone depth and length.

Best operation is achieved using a melt pressure monitor near the tip of the screw. A rupture disc of 'Hastelloy' C, rated well below maximum barrel pressure, could be installed at this same point for equipment protection. In operation, the melt pressure in the pumping zone of the extruder screw can be raised using the following techniques:

- Increasing the screw RPM.
- Reducing temperature 10°F in the mixing torpedo of the screw.
- Use of restrictions to reduce melt flow such as:
  - ✓ a breaker plate and screens
  - ✓ a small bore adapter
  - ✓ a choke ring on the crosshead core tube
  - ✓ a moveable die tip to close the gap in the cone section of the die
  - ✓ small diameter dies having lower melt draw balance.

All of these listed modifications can generate the desired barrel melt pressures, but must be balanced with the pressure required at the die for good foaming.

Longer range, added control can be achieved through extruder screw design and proper balance of the pumping and metering channel depths. Such extruder screws would be designed for high speed production of a specific range of coaxial core sizes.

#### INJECTOR PROBE DESIGN AND FREON® 22 CONSUMPTION

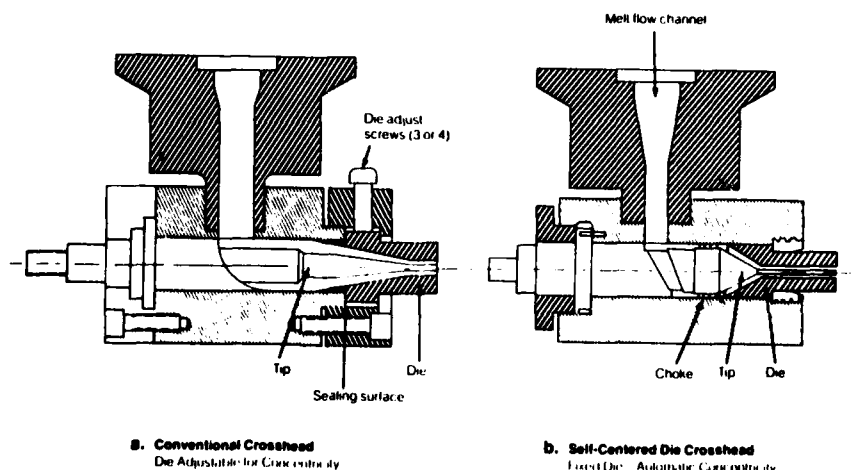
When screws with high melt fill in the gas zone are run at high speeds, the probe carrying F-22 gas into the extruder is wiped with melt much more frequently. To prevent melt plugging of the probe, it is important that the front flat face of the probe be as flush as possible with a line tangent to the extruder barrel wall. A small probe opening, between 8 and 18 mils in diameter, at the probe's face contacting the melt, has been used with good results. The high speed of gas flowing through such a small orifice allows the 3 mil barrel wall coating of molten FEP resin to be ruptured so the F-22 gas flows into the void space of the screw's gas zone during each turn of the screw.

Injector probes with tips having orifices as small as 4 mils in diameter limit the amount of gas entering the extruder, limiting production rates. If used, the extrusion rate must be slowed to balance resin throughout with the lower amount of gas being injected. A rotameter <sup>(2)</sup> in the gas injection line can be used to indicate intermittent gas flow or loss of flow.

The consumption of F-22 gas for foamed RG-62 at a coating speed of 70 ft./min. is about 0.2 weight per cent. This means every 500 lbs. RG-62 foam FEP requires one pound of F-22 gas. This information was obtained by weight loss measurement on small F-22 gas cylinders during an extrusion. The gas absorption of the molten FEP resin is dependent on the rate of extrusion. This means as the extruder screw conveys resin faster, less F-22 is absorbed by the melt. Increasing the pressure of the F-22 using the gas regulator increases gas absorption to maintain the desired foam void level.

FIGURE 4

#### TYPICAL CROSSHEADS AND STREAMLINED TOOLING



## DIE DESIGN

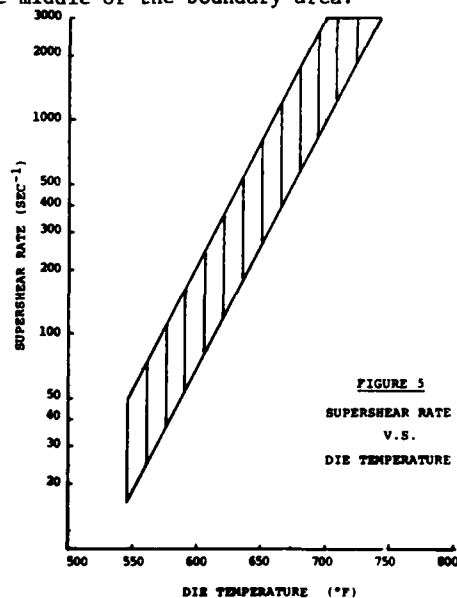
Tooling design requirements have been greatly simplified since introduction of this foaming process. High quality foamed cables can be made using both tubing and a pressure type set-ups. All major brands of self-centering or adjustable centering crossheads can be used with a wide range of cone angles and land lengths. The rheology properties of FEP and PFA permit this tooling flexibility.

The preferred tooling design uses single taper dies and tips with relatively short parallel lands. A schematic of this design is shown in Figure 4. Taper length and land length are kept the same on the dies and tips so tooling sets are interchangeable.

A variety of cable sizes have been produced using this new tooling design approach. Some of these cables include RG-6, RG-8, RG-11, RG-58, RG-59, RG-62, RG-316 and CATV 500. The flexibility of this design method permits the processor to handle present and future cable designs.

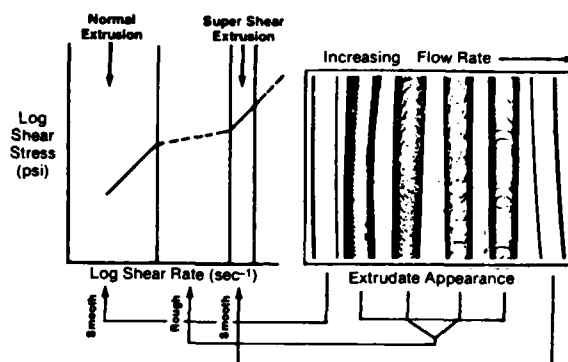
### TOOLING DESIGN CRITERIA

FEP and PFA coaxial cables are extruded in the supershear extrusion range. This is necessary to develop crosshead pressure and to reach practical rates. Supershear extrusion boundaries for FEP are shown in Figures 5 and 6. FEP processes best above shear rates of 200  $\text{sec}^{-1}$  and PFA above 600  $\text{sec}^{-1}$ . Extrusion is normally done in the middle of the boundary area.



Tooling is always sized based on the percent voids required for the coaxial cable. Included angles of the single taper may range from 30° to 100°. Land lengths may be varied between L/D ratios of 3:1 to 16:1. Draw down ratios are usually between 1:1 and 10:1 but may go as high as 20:1 for miniature cables. A draw ratio balance (DRB) close to 1 is desired but can be as low as 0.8 and still produce good quality cable cores.

Figure 6  
Rheology States of FEP Resin

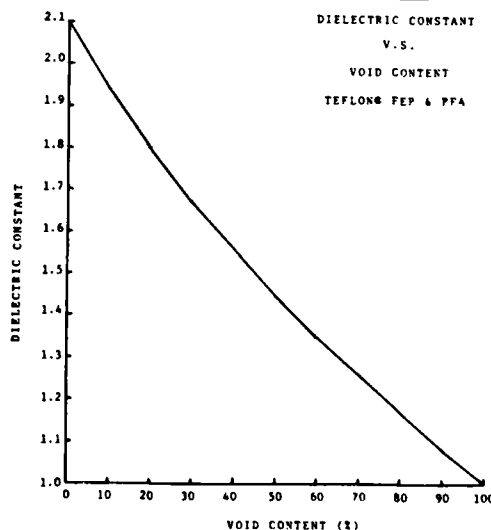


### DIE DESIGN STEPS

A step-by-step approach for foamed cable tooling design is given below. The required die diameter, tip diameter, draw down ratio (DDR), draw ratio balance (DRB) extrusion rate, line speed and die temperature can be calculated for a broad range of coaxial cables. Both tubing and pressure type tooling can be used but tubing is the preferred method.

- (1) Estimate the dielectric constant needed to meet cable electrical requirements.
- (2) Estimate the void content of the cable core using Figure 7 and the dielectric constant from Step 1.
- (3) Using the void content, calculate the un-foamed cable diameter using Equation I.
- (4) Estimate minimum tip O.D. by adding adequate vacuum clearance and the desired tip wall thickness to the conductor diameter.
- (5) Calculate die diameter at a DRB of 1 using Equation II.
- (6) Calculate the extrusion rate (pph) required to reach the supershear region using Equation III. (200  $\text{sec}^{-1}$  FEP, 600  $\text{sec}^{-1}$  PFA).
- (7) Calculate minimum line rate based on supershear extrusion rate using Equation IV.

FIGURE 7



The same design approach can be used for pressure tooling. Skip Steps 4, 5 and 6 and size the die based on the unfoamed diameter from Step 3. Calculate the minimum line rate to reach supershear using Equation V.

The required die temperature can be estimated using Figure 5. Figure 5 is based on melt rheometer data. Most crosshead die temperatures run 50-75°F below the rheometer temperature for good supershear. At 200 sec.<sup>-1</sup> most crosshead die temperatures will be around 580°F.

#### TOOLING DESIGN EQUATIONS

$$\text{Unfoamed Core Diameter } (d_{cu}) \quad (I)$$

$$d_{cu} = \left[ (d_{fd}^2 - d_{bc}^2) \times \left( 1 - \frac{2 \text{ voids}}{100} \right) + d_{cw}^2 \right]^{0.5}$$

$$\text{Die Diameter at DSB - 1 } (d_d) \quad (II)$$

$$d_d = (d_t \div d_{bc}) \times d_{cu}$$

$$\text{Supershear Extrusion Rate } (Q) \quad (III)$$

$$Q = \bar{S} \times P_m \times W \times \pi^2 \times 600$$

$$\text{Line Rate} \quad (IV)$$

$$\text{fpm} = \frac{Q}{\text{sp. gr.} \times 20.42 \times (d_{cu}^2 - d_{bc}^2)}$$

$$\text{Pressure Extrusion Shear Rate } (\dot{\gamma}) \quad (V)$$

$$\dot{\gamma} = \frac{5.38}{\pi} \left( \frac{Q_t - \frac{\pi V_w R_1^2}{\ln R_0/R_1} \left[ \frac{1}{2} \left( \frac{R_0^2}{R_1^2} - 1 \right) - \ln \frac{R_0}{R_1} \right]}{(R_0 + R_1) \times (R_0 - R_1)^2} \right) + \frac{V_w}{R_0 \ln R_0/R_1}$$

$d_d$ = die diameter	$Q$ = pph	$R_0$ = die radius
$d_t$ = tip diameter	$\bar{S}$ = shear rate (sec <sup>-1</sup> )	$R_1$ = conductor radius
$d_{fd}$ = foamed dielectric dia.	$P_m$ = melt density (lb./in. <sup>3</sup> )	$V_w$ = wire velocity (in./sec.)
$d_{cu}$ = coated wire diameter	$W$ = average die circumference	$Q_t$ = extrusion rate (in <sup>3</sup> /sec.)
$d_{bc}$ = bare conductor dia.	$\pi$ = annular die opening	

#### END USE APPLICATIONS

##### Commercial Uses

The National Electrical Code, since 1978, has permitted the use of low flame spread, low smoke producing cables, as tested by UL 910 to be installed without conduit in air handling plenum spaces above suspended ceilings of commercial buildings.

Applications for foamed FEP cables include:

- Direct computer interconnects
- Broadband and baseband computer networks
- Network drop cables
- C.C.T.V.
- Factory automation networks.

These cables are now specified by IBM Inc., Xerox Inc., Wang Laboratories Inc., and others for use with their systems when wiring is installed in air handling plenums.

#### Military Uses

Foamed coaxial cables of FEP offer advantages to military for the following reasons:

- Low flame spread and smoke give increased safety within aircraft and ships.
- High temperature rating.
- Resistance to degradation from any solvent, oil and fuel.
- High mechanical strength compared to conventional foam cables.

Most of the present MIL-C-17 coaxial cables can be designed and fabricated using foamed FEP. The options of improved electrical properties or reduced weight are apparent in their value.

In addition, cables can be designed in cooperation with cable manufacturers to optimize performance for specific requirements.

#### REFERENCES:

- (1) Extrusion Foaming of Coaxial Cables of Melt Fabricable Fluorocarbon Resins, Cherry Hill, New Jersey, November 18, 1981, S. K. Randa.
- (2) Brooks Instrument Division, Emerson Electric, Hatfield, PA 19940. Flow rate 0.02 to 2.12 liters/min. at 1 atmosphere and rated for the cylinder F-22 pressure.

#### ACKNOWLEDGEMENTS:

P. H. Squires, E. I. Du Pont: Assistance with screw design.

E. C. Suratt, E. I. Du Pont: Assistance with RG-8 coax core extrusion.

Y. Saito, Mitsui Fluorochemicals Co., Ltd.: Assistance with streamlined die design.

The Du Pont Company assumes no obligation or liability for any advice furnished by it, or for results obtained with respect to these products. All such advice is given and accepted at the buyer's risk. Du Pont warrants that the materials it sells do not infringe the claims of any United States patent; but no license is implied nor is any further patent warranty made.



STUART K.  
RANDA

Stuart K. Randa, Technical Consultant with Du Pont's Fluoropolymer Division, joined Du Pont in 1956 after earning a B.S. in Chemical Engineering from the University of Wisconsin. He has held positions in the Research, Sales and Manufacturing Divisions of the Polymer Products Department. His current responsibilities include process development and product application for Teflon® FEP, PFA and Tefzel® fluoropolymers.



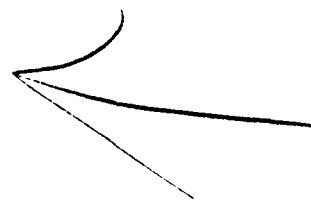
DAVID P.  
REIFSCHNEIDER

David P. Reifschneider, Technical Specialist with Du Pont Fluoropolymers Division, joined Du Pont in 1970 after earning a Bachelor of Electrical Engineering Degree at the University of Delaware. He has held positions in the Design and Construction Divisions of the Engineering Department, and in Sales, Market Development, and Marketing with the Polymer Products Department. He is presently responsible for electrical product applications for Teflon® FEP and PFA and Tefzel® fluoropolymers.



MARK A.  
CARLSON

Mark A. Carlson is a Technical Specialist with Du Pont's Fluoropolymer Division. Mark received a B.S. Degree in Chemical Engineering in 1977 from the South Dakota School of Mines and Technology. Mark has held process development and supervisory positions in the Manufacturing Division of the Polymer Products Department. His current responsibilities include process development and product application for Teflon® FEP, PFA and Tefzel® fluoropolymers.



## FOAMABLE PVDF FLUOROPLASTIC FOR WIRE AND CABLE APPLICATIONS

By R. L. Pecsok, O. R. Odhner

Pennwalt Corporation  
900 First Avenue  
King of Prussia, Pennsylvania 19406

ABSTRACT

A foamable polyvinylidene fluoride (PVDF) resin which meets the UL 910 flammability classification has been developed for wire and cable applications. The foamable PVDF composition is based on a chemical blowing agent system which is thermally activated during extrusion. Extrusion and wire coating conditions for the preparation of foamed PVDF insulation will be discussed. Electrical and mechanical properties of the foam insulation are presented with reference to the foam density and cell size.

INTRODUCTION

Usage of KYNAR<sup>(R)</sup> polyvinylidene fluoride in wire insulation and cable jacketing has grown recently because the relatively low flammability and smoke generation of KYNAR permits installation in plenum ductwork without the need for a costly conduit covering. Overall cost of KYNAR plenum wire and cable is thus competitive with less expensive insulation materials such as PVC which require conduit shrouding.

The inherently high dielectric constant of 8-10 for KYNAR renders it unsuitable for some applications, such as wire insulation in long length telephone cables, where a low dielectric constant is essential to minimize cross-talk interference. Typical PVC compounds which are currently used have dielectric constants in the 3 - 3.5 range. However, the dielectric constant of KYNAR can be reduced to a comparable level by foaming the material.

For a two component mixture, the Lictenecker Equation (1) expresses the total dielectric constant  $K'$  as a function of the components as follows:

$$\log K'_{12} = V_1 \log K'_1 + V_2 \log K'_2$$

$\log K'_{12}$  = dielectric constant of the mixture  
 $K'_1$  = dielectric constant of the component 1  
 $K'_2$  = dielectric constant of component 2  
 $V_1$  = volume fraction of 1  
 $V_2$  = volume fraction of 2

By incorporating a gas with a low dielectric constant (such as air where  $K' = 1.0$ ) into KYNAR, the dielectric constant of the foam structure is then directly proportional to the volume fraction of KYNAR. A KYNAR foam with 55% void content should have a dielectric constant in the range of 3.5 and would then be suitable for many wire insulation applications including long length telephone primaries.

There are basically two different ways to foam KYNAR by extrusion:

1. Chemical blowing agent - Thermally activated during extrusion.
2. Physical blowing agent - Direct gas injection during extrusion.

This work focuses on the chemical blowing agent approach because it is a simpler system and can be readily used on conventional wire extrusion equipment. Direct gas injection requires equipment modifications

including special screw/mixing designs, gas handling/metering, and possibly barrel porting. The melting point of KYNAR is low enough (about 160°C range) to enable compounding below the activation temperature of typical blowing agents.

#### MATERIALS

All work was conducted using KYNAR<sup>(R)</sup> Foam 468 a foamable PVDF compound developed by Pennwalt Corporation. KYNAR Foam 468 is specifically tailored for wire and cable extrusion. Let down of KYNAR Foam 468 is not necessary nor is the addition of nucleation agents. Rheology data is shown in Figure 1 and is typical of a medium viscosity commercial KYNAR 460 grade (rheology procedure described in Ref. 2). Foam activation is shown as a function of melt temperature in Figure 2 and is optimum in the 240 - 250°C range.

#### EXTRUSION AND WIRE COATING CONDITIONS

Extrusion equipment requirements for KYNAR Foam 468 are similar to those for unmodified KYNAR and no additional tooling or equipment modifications are needed. Extrusion of KYNAR requires streamlined flow channels to prevent melt stagnation and subsequent discoloration or decomposition. Typical wire extrusion setup and conditions for KYNAR Foam 468 are shown in Table 1. Conventional screw designs of 24 L/D, 3-5:1 compression ratio, with sharp or gradual transition zones are suitable. A high metering zone temperature is employed to activate the foaming agent. The metering zone is preferred for the activation because the heat transfer to the melt is more effective and uniform,

which leads to a more homogenous foam activation and cell structure in the end product. The crosshead should be designed to minimize abrupt internal pressure drops and prevent premature bubble growth inside the die. Ideally, all foam growth should occur just outside the die to minimize open cell formation (3,4). Typically dies with little or no land lengths are recommended for optimum foam structure (5). However, our experience with dies having moderate straight land lengths has been satisfactory, at least with small die orifices.

Typical of all foam wire operations, the quench rate, line speed, wire preheat, die tip temperature, and extrusion rpm have significant effects on the wall thickness, foam structure, and final properties. The qualitative effects of these variables are listed in Table 2 and must be adjusted according to the particular equipment setup and desired end product.

#### FOAMED WIRE INSULATION PROPERTIES

As discussed earlier, the foam structure, and hence properties, are highly dependent upon the processing conditions. KYNAR Foam 468 can be processed to yield foamed structures with integrity at a density as low as 0.3 g/cc compared to 1.76 g/cc for the unfoamed KYNAR. However, the dielectric strength decreases with a reduction in density as shown in Figure 3. Cell size also influences the dielectric strength behavior, where a reduction in cell size leads to a higher dielectric strength.

(Figure 3). For a given insulation thickness, the density and cell size must be adjusted to give a suitable dielectric strength which meets the product specifications. For example, a minimum density of .75 g/cc is needed for a 6 mil wall to pass the 2KV spark test as required for telephone wire insulation.

Properties for a thin wall (0.007 in.) foamed insulation of .80 g/cc are presented in Table 3. The insulation was processed using the equipment and conditions specified in Table 1. Properties for unfoamed KYNAR 460 are shown for comparison. The foamed insulation has a dielectric constant of 3.6, comparable to that of PVC primary insulation used in long length telephone cables.

As is typical of foams, the foamed KYNAR insulation exhibits improved flexibility as noted by the lower flexural modulus and strength. Tensile, and to a smaller extent, flexural strength decrease with decreasing density in a manner illustrated in Figure 4 (6). The mechanical, as well as the electrical properties, also depend on the cell size; however, for the range 0.0001 to 0.010-in cell size, most of the mechanical properties tend to depend mainly on the density.

A cable construction containing 24 pairs of KYNAR 468 foamed primaries covered with an unfoamed KYNAR 460 jacket passed the flame spread and smoke emission requirements of the modified Steiner Tunnel Test (UL910).

#### CONCLUSION

Processing and properties for KYNAR 468 foam insulation based on a chemical blowing agent have been successfully demonstrated. Electrical insulation properties of the foamed KYNAR are comparable to PVC materials.

#### REFERENCES

1. See ASTM D1673.
2. J. E. Dohany, K. N. Davis, and H. Stefanou, Proc. 24th Int. Wire and Cable Sym., (1975), pg. 340.
3. S. K. Randa, Proc. 30th Int. Wire and Cable Sym., (1981), pg. 1.
4. T. C. Hodgson, D. B. Carefoot, G. F. Gouthro, and S. M. Beach, Proc. 25th Int. Wire and Cable Sym., (1976), pg. 317.
5. R. S. Poklamba and Costa Rosis, Wire Journal International, 16 (6), (1983), pg. 58.
6. K. N. Davis, Pennwalt Corporation, Internal Report.



Roger L. Pecsok received his BS (1976) and MS (1978) in Macromolecular Science from Case Western Reserve University. In 1978 he joined the Film and Allied Products Division of the 3M Company. Since 1982 he has been a Senior Plastics Engineer in the Fluorochemicals Division of the Pennwalt Corporation working on the development of foamable PVDF compounds.



Oliver R. Odhner has been a Plastics Engineer in the Fluorochemicals Division of the Pennwalt Corporation since 1968. In 33 years of plastics R&D, he has been awarded six patents related to plastics applications. He has been active in technical committees of wire and cable associations. In addition to his present role in the development of KYNAR® PVDF foam, he was involved in early Navy research of rigid polyurethane foams, and was responsible at Container Corporation of America for development of one of the first polystyrene foam egg cartons.

#### ACKNOWLEDGMENT

We gratefully acknowledge Pennwalt Corporation for support and permission to publish this work. We also express gratitude to S. L. Moore, B. K. Leavitt, and R. H. Markowski for their assistance in various aspects of this work.

TABLE 1

EQUIPMENT AND PROCESS CONDITIONS FOR KYNAR 468 FOAM WIRE INSULATION

Extruder:	1", 24 L/D					
Screw:	1/3 Feed, 1/3 Transition, 1/3 Metering 3.5:1 Compression					
Screen Pack:	40/60/100					
Die Orifice:	0.028"					
Die Straight Land Length:	0.045"					
Conductor:	24 AWG Solid Copper					
Extruder Temperature Profile (°C):	B1	B2	B3	Gate	Cross head	Forming Die
	210	220	270	230	210	200
Screw RPM:	15					
Line Speed:	100 fpm					
Die-Water Bath Distance:	0.5"					

TABLE 2

GENERAL EFFECTS OF PROCESS VARIABLES ON KYNAR 468 FOAM STRUCTURE

Process Variables	Change	Responses		
		Density	Cell Size	Thickness
Line Speed	+	+	-	-
Die-Water Bath Distance	+	-	+	+
Extruder Speed	+	0	- (slight)	+
Wire Preheat Temp.	+	-	+	+
Mandrel Advance (In Die)	+	+	-	-

KEY: + Increase  
0 No significant change  
- Decrease

TABLE 3

TYPICAL PROPERTIES OF KYNAR 468 FOAMED WIRE INSULATION

Test Method	Pham PVDF (KYNAR 468)	Virgin PVDF (KYNAR 460)
Wall Thickness ( $\times 10^{-3}$ in)	7	7
Density (g/cc)	1.80	1.76
Void Content (%)	55	0
Avg. Cell Size ( $\times 10^{-3}$ in)	100x mag.	0.6 - 1.0
Tensile Modulus (kpsi)	ASTM D638	140
Tensile Break Strength (kpsi)	" D438	1.8
Tensile Break Elongation (%)	" D438	50-60
Flexural Modulus (kpsi)	" D790	135
Dielectric Constant 100 Hz	ASTM D1631	3.6
Dielectric Strength (V/mil)	" D149	560
Insulation Resistance (megohm-in)	" D1001	200-300

Figure 1  
Apparent Viscosity Vs Shear Rate for KYNAR 468 Foam

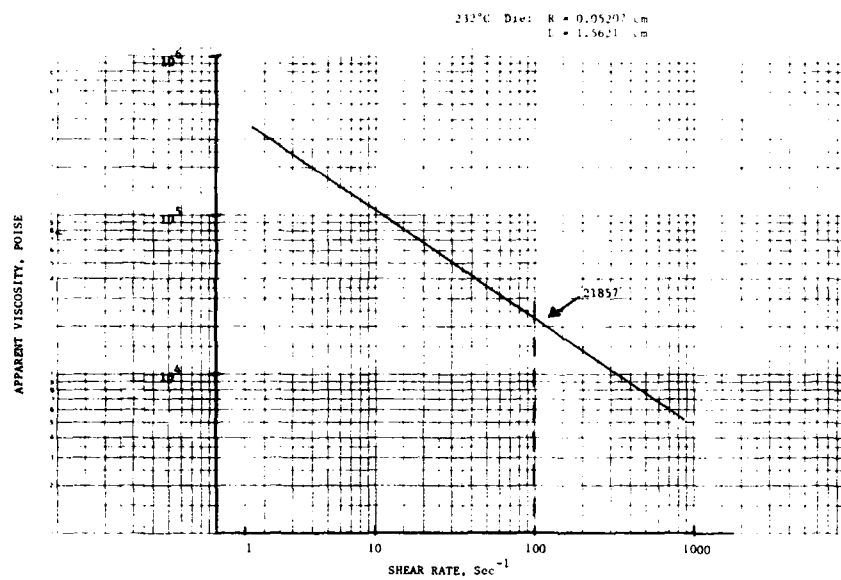


Figure 2  
Foam Activation: Density Vs Melt Temperature of KYNAR 468

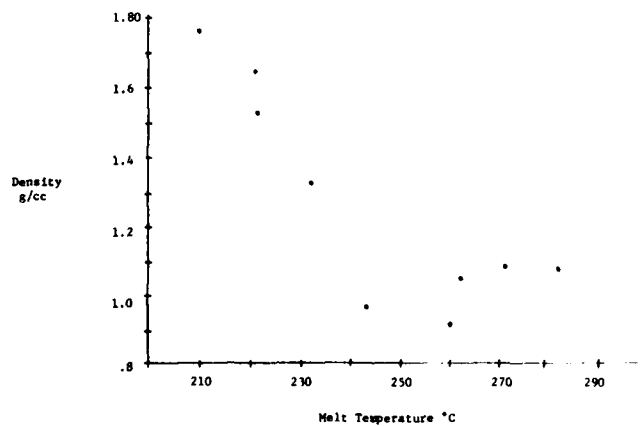


Figure 3  
KYNAR 468 Foam  
Dielectric Strength Vs Density

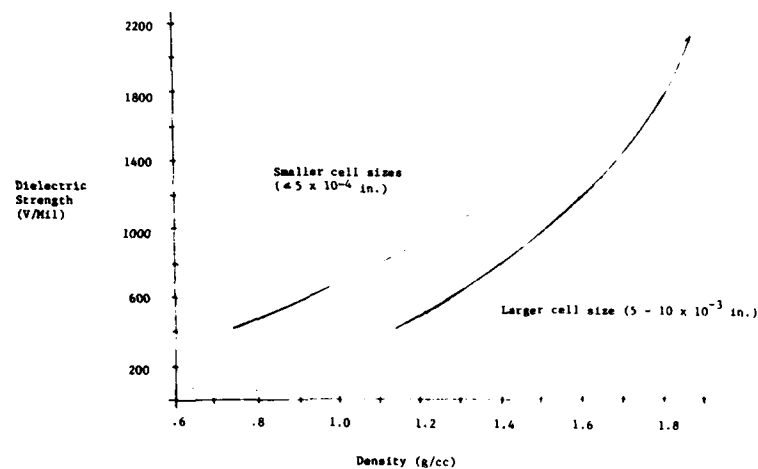
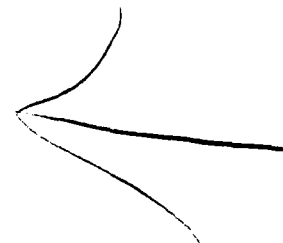
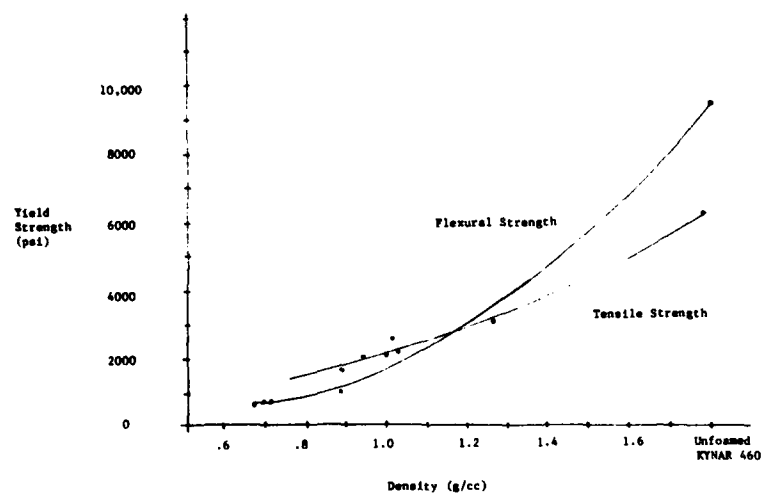


Figure 4  
KYNAR 468  
Tensile and Flexural Strength Vs Density



# DEVELOPMENT OF COMPOSITE FIBER-OPTIC ELECTRIC-POWER UMBILICAL CABLE AND OPTICAL FEEDTHROUGH FOR DEEP OCEAN MINING

T. Mitsui, T. Gomi, T. Itō, S. Ushitani, M. Yamaguchi

Sumitomo Electric Industries, Ltd., Osaka, Japan

## Summary

The development of mining systems for mineral resources from deep ocean floors is now progressing in many countries. In Japan, the Agency of Industrial Science and Technology, MITI, has conducted research and development for a manganese nodule mining system. In this project, it is planned to use a new composite fiber-optic electric-power umbilical cable for electrical power and control signal transmission from a main vessel to subsea equipment such as lifting pumps and collecting devices at about 5,000 meters' depth. The umbilical cable system is required to have good resistance to repetitive bending, twisting, and other external forces and to be able to withstand water pressure of up to 550kgf/cm<sup>2</sup> 5g cm.

A 100m-long sample umbilical cable, electrical connectors, and optical feedthroughs for this system have been developed and successfully passed mechanical, electrical, and optical tests.

## 1. Introduction

In the field of sea and seabed resource utilization, the focus of research is now shifting from oil drilling in shallow seas to the establishment of deep sea technology, such as the search for and mining of manganese nodules and other resources, or investigations into the activities of the earth itself, such as earthquakes. For this reason, it is expected that in the 1980's a large amount of various investigative data concerning the deep sea and the seabed will be required, such as video images, topographical measurements, changes in the seabed, analyses of seabed materials and gases, and investigations of ocean pollution, temperatures, and currents. In addition, it becomes necessary to supply reliable control signals and electrical energy from the surface of the sea to machines in the deep sea, such as boring equipment, mining equipment, unmanned submarine investigating devices, robots, etc.

In order to establish a transmission system suitable for handling large quantities of such data and energy between the deep sea and the sea surface, a lightweight, small-diameter composite fiber-optic electric-power umbilical cable, optical feedthroughs for passing the optical fiber cable into pres-

surized components such as data terminal boxes, electric connectors for power cables, and other components are necessary. In the research and development of a manganese nodule mining system, our firm has been engaged in the development of electrical control and data gathering systems.

In 1982, we conducted development of a composite fiber-optic electric-power umbilical cable of the 5,000m class, a waterproof-type optical feedthrough, and an electric connector able to withstand a pressure of 550kgf/cm<sup>2</sup>, and satisfactory actual performance was obtained, the details of which are given in this report. The newly developed umbilical cable has Kevlar armoring and contains one three-phase 6.6kV power line for motive supply, two single-phase 3.3kV power lines for measurement and control functions, and 26 optical fibers. The umbilical cable is lightweight and satisfactorily passed mechanical tests under conditions similar to those expected in actual use, such as repeated bending, twisting, and subjection to other external forces.

High-voltage electrical connectors for 6.6kV class and 3.3kV class, with the connector case filled with an insulating oil to balance the internal and external pressure of the case, were trially manufactured, and insulation resistances were measured under water pressure of up to 900kgf/cm<sup>2</sup> by a 1,000V megohmmeter. Resistance values were more than 2,000MΩ, satisfactory for actual use. Further, no problems with the electrical connectors were discovered when they were taken apart and analyzed after the tests.

Two kinds of optical feedthroughs with comparatively simple structures--one for four fibers and another for one fiber--were trially manufactured. Optical transmission losses were measured under water pressure of up to 900kgf/cm<sup>2</sup>, then under water pressure cycles from 0 to 600kgf/cm<sup>2</sup>. Increase of loss by the tests was small compared with the normal margin (3 to 5dB) for the design of optical transmission circuits. It was thus confirmed that the feedthroughs were suitable for actual use.

## 2. Composite Fiber-Optic Electric-Power Umbilical Cable

### 2.1 Design of Cable

Table 1 shows requirements for a composite fiber-optic electric-power umbilical cable.

Table 1 Requirements for composite umbilical cable

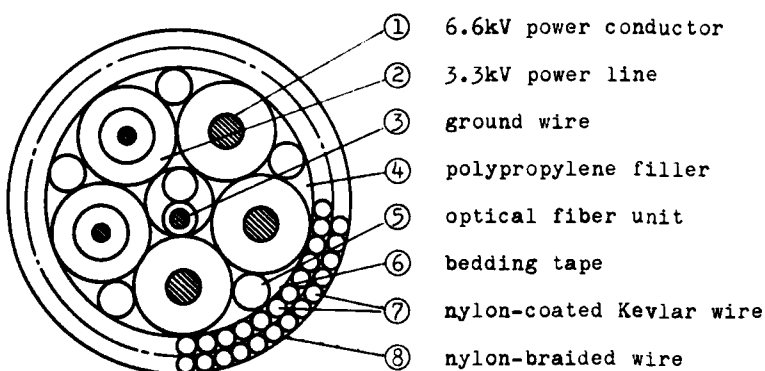
Cable length		6500m
Power line measurement and for motive supply	Voltage at receiving end	6000V
	Voltage drop	less than 10%
	Load	500kW
	Frequency	36 to 60Hz
Power line for measurement and control devices	Secondary voltage at receiving end	100 to 110V
	Load	3kVA
	Frequency	60Hz
Optical fiber	Core diameter	50 $\mu$ m
	Clad diameter	125 $\mu$ m
	NA (numerical aperture)	0.2
	Transmission bandwidth	more than 200MHz·km at 0.85 $\mu$ m
	Transmission loss	less than 3dB/km at 0.85 $\mu$ m

## 2.2 Structure of Cable

Figure 1 shows the cross section of the 100m-long cable trially manufactured, and Photo 1 shows its appearance.

### 1) Optical fiber units

In the optical fiber units, nylon-coated quartz optical fibers of 2mm outer diameter and nylon-coated Kevlar wires of the same diameter are stranded together, then covered by a low-density polyethylene sheath. Two 3-fiber, two 4-fiber, and two 6-fiber units were utilized, giving a total of 26 fibers.



outer diameter of cable: approx. 72mm

cable weight in air: approx. 4.1kgf/m

cable weight in water: approx. 0.5kgf/m

Fig. 1 Cross section of umbilical cable

### 2) Electric power lines

Since the cable must be light in weight, aluminum was selected for the conductors of the 6.6kV electric power line. In addition, when conductors were stranded, they were molded with a waterproof filler compound which hardens at room temperature to prevent insulation from being forced between the conductors due to high pressure. The three-phase 6.6kV (53A) power line is used to feed power to subsea equipment.

The two single-phase 3.3kV (1A) power lines are of coaxial structure so as to avoid making the outer diameter of the umbilical cable larger; they are used to feed power to measurement and control devices. The insulation of both types of power conductors is crosslinked polyethylene.

### 3) Ground wire

To prevent personnel on the mother ship from receiving electric shocks, a ground wire with a conductor wound by semiconductive tape was used. The same technique as used to avoid pressure collapse of the power conductors was used for the ground wire.

### 4) Armor wires

Since the armor wires must be high in tensile strength, light in weight, and anti-corrosive, the use of steel was not appropriate. FRP-type Kevlar wires impregnated with unsaturated polyester, which is convenient for handling in the manufacturing process, were used for optical fiber units and outer armor. Rod-type Kevlar, which has less elongation than rope type, was used in order to prevent elongation damage to the optical fibers. A 0.5mm-thick sheath of nylon 12 was applied to each Kevlar wire to increase its wear resistance.

Further, to prevent twisting, the outer armor wires are stranded in two contrahelical

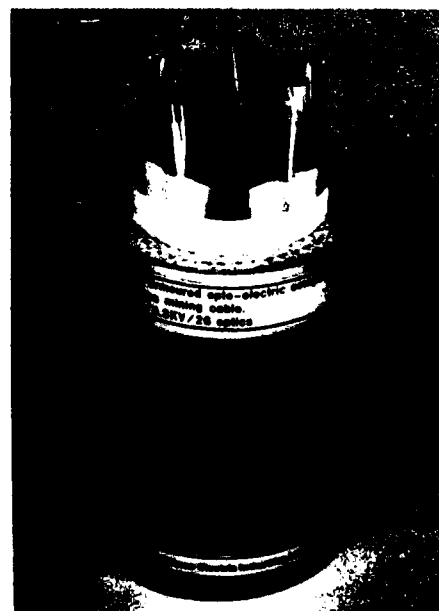


Photo 1 Composite fiber-optic electric-power umbilical cable

layers. In this cable, the Kevlar FRP wires were wound before being cured, and then the cable was drawn through a hot water basin for curing. In this way, the armor wires became like a coil spring set while the cable is in straight condition, with no residual stress, resulting in a cable with excellent conservation of shape.

### 2.3 Practical Performance Confirmation Tests

To confirm the required performance of this umbilical cable and load conditions at the time of use, performance tests were conducted to determine mechanical and optical transmission characteristics. Table 2 summarizes the test items.

#### 1) Flexible rigidity (EI) test

Results of the flexible rigidity (EI) test

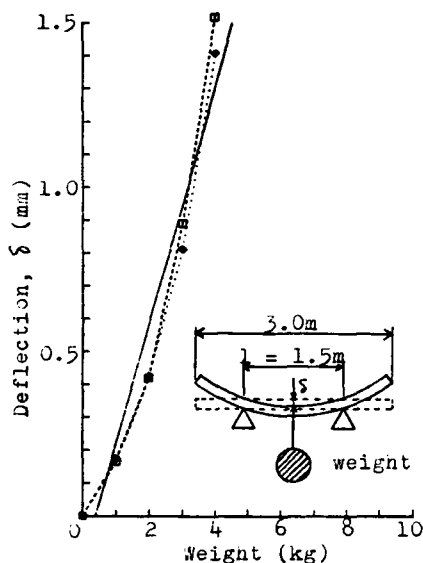


Fig. 2 Flexible rigidity

are given in Fig. 2. EI is equal to  $1.95 \times 10^4 \text{ kgf.cm}^2$ , and from this result it was confirmed that the umbilical cable is as flexible as ordinary electric power cable.

#### 2) Tensile tests and tensile breakdown test

The test results of elongation vs. tension, PD output (of one fiber from each unit) vs. tension, change of outer diameter vs. tension, twist angle vs. tension, and twist torque vs. tension are shown in Figs. 3 to 7, respectively. Concerning optical transmission characteristics, a simplified method was used to measure photodiode (PD) output voltage by attaching PDs and light-emitting diodes (LEDs) directly at both ends of one fiber from each unit. It was confirmed that elongation of the optical fibers was only 0.5% at a tension of 10 metric tons and, as shown in Fig. 4, that PD output was not significantly affected.

The sample after the tensile breakdown test is shown in Photo 2. We considered the breakage of armor wires as the breakdown of the umbilical cable. The breakdown tension is 41.7 metric tons, a value above the actual service tension. And when armor wires broke, both power conductors and optical fibers remained intact.

Table 2 Contents of test

Purpose	Item	Test conditions	Measured items
Evaluation of mechanical characteristics	Flexible rigidity (EI) test	Weight: 0 to 10kgf Cycles: 2	Weight (W), deflection ( $\delta$ ), span length (l), EI = $l^3 W / (48 \times \delta)$
	Tensile test	Tension: 0 to 10 metric tons Cycles: 3	Tension, elongation, outer diameter, twist angle, twist torque
	Tensile breakdown test	Tension: 0 till breakdown (41.7 metric tons)	Tension, optical transmission characteristics
	Repeated water pressure resistance test	Pressure pattern: shown in Fig. 8	Water pressure, time, dismantlement of samples
Evaluation of fatigue characteristics	Repeated bending test	Tension: 5 metric tons Sheave diameter: 1.5m Dynamic sidewall pressure: 6.7 metric tons/m Sheave groove radius: 26mm Movement quantity: $\pm 0.5m$ Cycles: 2,000	Tension, outer diameter, optical transmission characteristics
	Repeated bending and twisting test	Twist: Angle: $\pm 35^\circ$ Cycles: 20,000 Large bend: Angle: $\pm 15^\circ$ Cycles: 10,000 Small bend: Angle: $\pm 2.5^\circ$ Cycles: 266,000	Large bending cycle, optical transmission characteristics, check of breakage of power conductors, dismantlement of samples
Evaluation of electrical characteristics	Voltage withstand test	3.3kV class: 10kV x 10 min 6.6kV class: 18kV x 10 min	Voltage, time

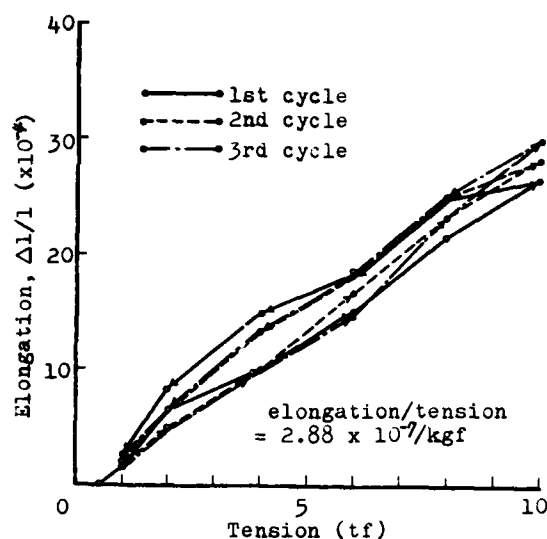


Fig. 3 Elongation vs. tension

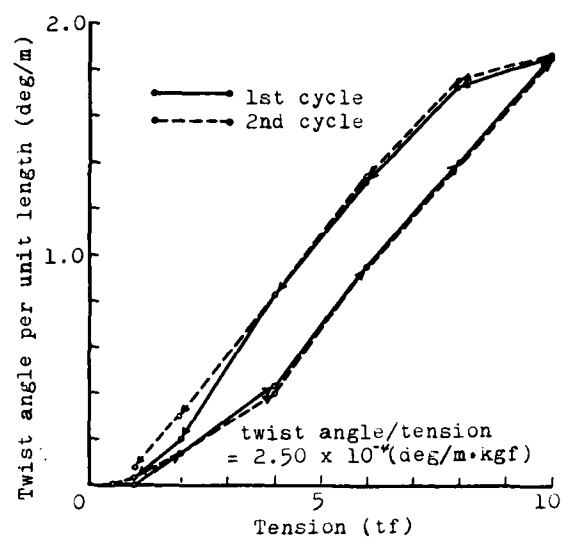


Fig. 6 Twist angle vs. tension

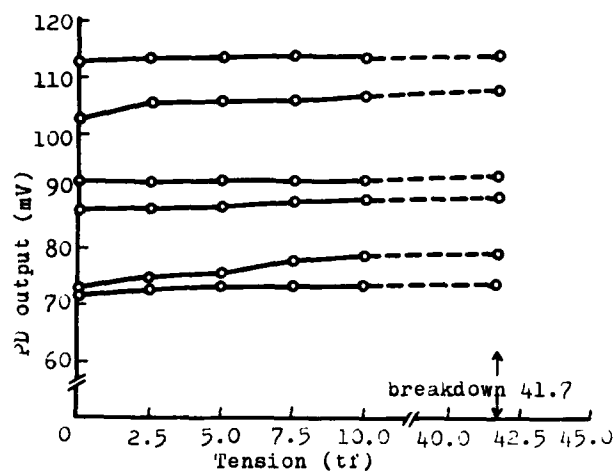


Fig. 4 Optical transmission vs. tension

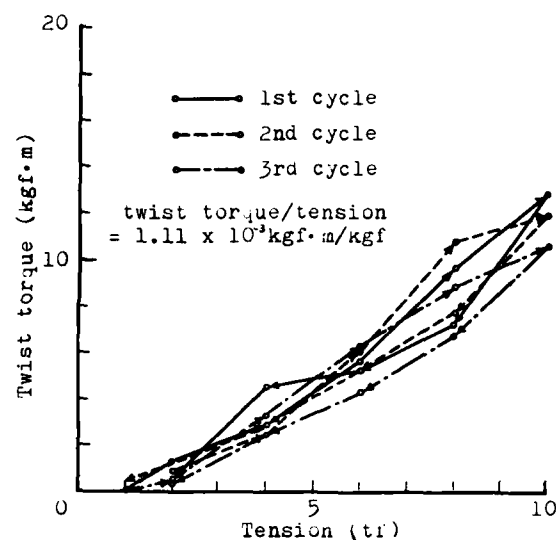


Fig. 7 Twist torque vs. tension

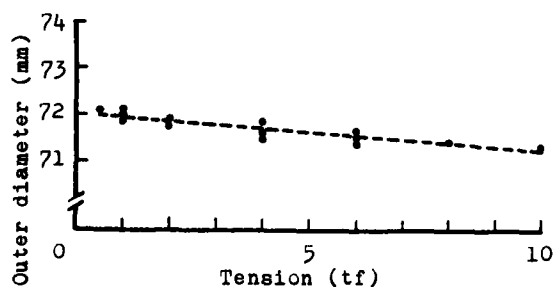


Fig. 5 Outer diameter vs. tension



Photo 2 Sample before (rear) after tensile breakdown test

### 3) Repeated water pressure resistance test

To test the umbilical cable's ability to withstand water pressure, individual power conductors of 1m length, with both ends water-proofed, were subjected to pressure of 0 to 900kgf/cm<sup>2</sup> (maximum) in the apparatus shown in Photo 3, with the pressure pattern shown in Fig. 8. No abnormalities were discovered when the conductors were dismantled.

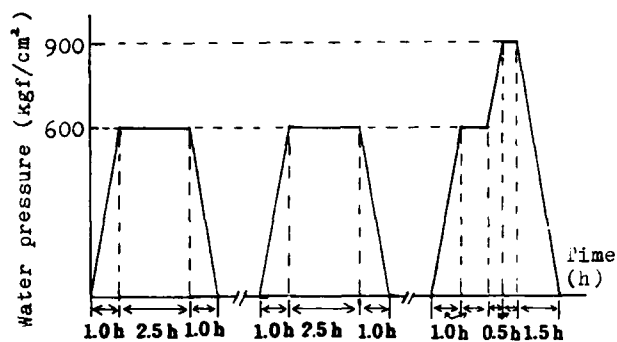


Fig. 8 Pressure pattern during repeated water pressure resistance test

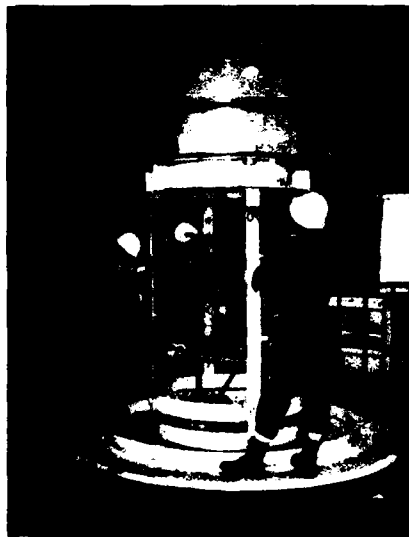


Photo 3 Repeated water pressure resistance test

### 4) Repeated bending test

Optical transmission characteristics of one fiber from each unit during 5,000 cycles of repeated bending are shown in Fig. 9. It was confirmed that transmission loss remained constant even after 5,000 bends at a dynamic side wall pressure of 6.7 metric tons/m. When the sample cable was dismantled after this test, everything was in good order except that the bedding tape had broken at the bending places.

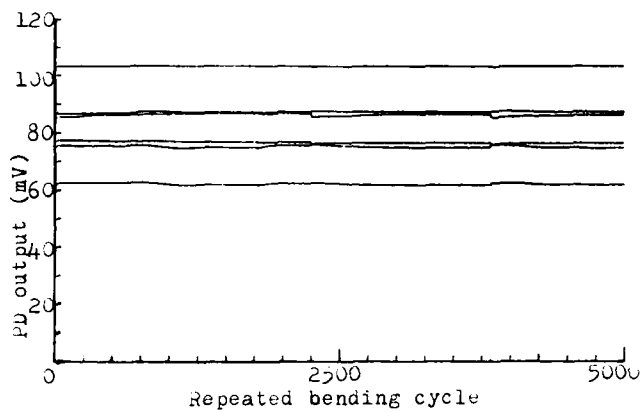


Fig. 9 Optical transmission vs. repeated bending

### 5) Repeated bending and twisting test

Our specially designed setup for the bending and twisting test is shown in Photo 4. Optical transmission characteristics of eight fibers (4-fiber optical transmission line  $\times$  2) subjected to 10,000 cycles of repeated large bending are shown in Fig. 10. It was confirmed that no large change in transmission loss occurred even during a complex mechanical test such as this. When the sample cable was dismantled after the test, everything was in good order. Intermittent testing of power conductors also revealed no problems.

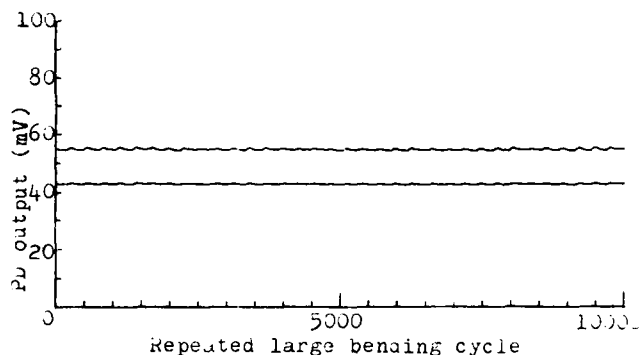


Fig. 10 Optical transmission vs. repeated bending and twisting



Photo 4 Setup for repeated bending and twisting test

#### 6) Voltage withstand test

A voltage withstand test of power conductors was conducted according to JIS-C-3005-8 (2) after the repeated bending test and repeated bending and twisting test, and the conductors passed successfully.

#### 3. Electrical Connectors

Since no high-voltage electrical connectors of 3.3kV (1A) and 6.6kV (53A) class were available, they had to be developed. The basic design concept was to use the following:

a) Dry connection (connecting and disconnecting in air)

b) Sealing with O ring and rubber gasket

We designed and manufactured two prototype connectors, one of 3.3kV class, the other of 6.6kV class. The mechanism of sealing is shown in Fig. 11. The connector case is filled with an insulating oil to balance the internal and external pressure of the case so that water does not enter through pressure barriers or seals. Photo 5 shows the prototype 6.6kV-class connector with a protective case.

To confirm the required performance of the two connectors, insulation resistance was measured with a 1,000V megohmmeter under the same water pressure pattern (max. 900kgf/cm<sup>2</sup>) as in the water pressure resistance test of power conductors, and it was found that both connectors had a good insulation resistance of over 2,000M $\Omega$ . When the sample connectors were dismantled after this test, everything was in good order.

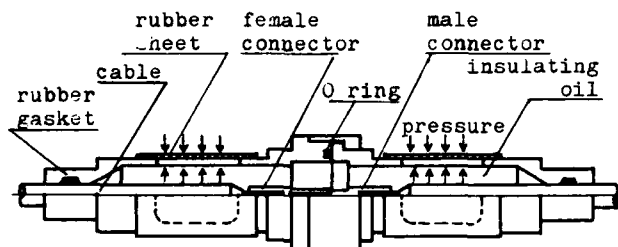


Fig. 11 Mechanism of sealing

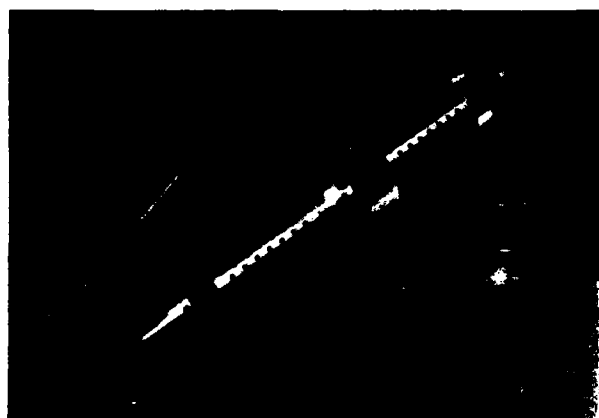


Photo 5 Prototype connector (6.6kV class)

#### 4. Optical Feedthroughs

##### 4.1 Structure

Data terminal boxes are normally kept at atmospheric pressure to ensure correct operation of electronic devices and circuits. Therefore, it was necessary to develop wall penetrations for optical fibers to feed them from high-pressure to low-pressure areas.

Injected resin seals were adopted for resistance to high pressure. The injected resin seal is used by drawing an optical fiber through a metal cylinder and filling the surroundings with hardened resin. The adhesion of the resin resists the high pressure. The newly developed optical feedthrough utilizes two types of resin injected in two steps. This double-seal structure improves the resistance to high pressure. As the resin is injected in a vacuum vessel and thus has no voids, the deformation of the resin caused by locally concentrated stress is prevented. The inside surface of the metal cylinder through which the optical fiber is drawn has screw threads so that the adhesion surface is larger, and the adhesion between the resin and the metal cylinder is thus also larger.

Figure 12 shows the structure of the pressure-resistant feedthrough for one optical fiber connected to a data terminal box. The optical fiber is drawn into the data terminal box through the feedthrough from the water outside and is connected with E/O or O/E converters. This optical feedthrough is inserted into a hole of the data terminal box and is tightened by a nut. The high-pressure side is protected by a shrinkable tube to prevent it from bending. Photo 6 shows the pressure-resistant feedthrough for one optical fiber, and Photo 7 for four optical fibers.

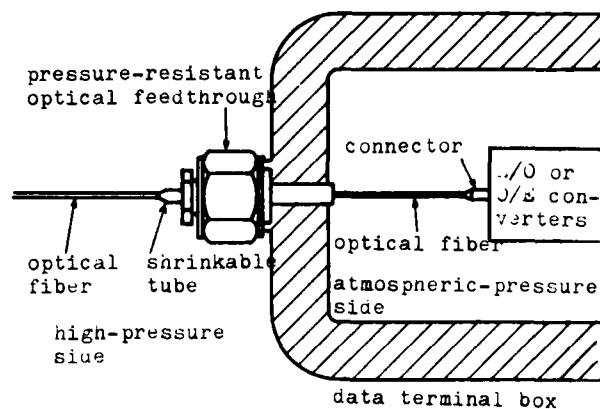


Fig. 12 Pressure-resistant optical feedthrough



Photo 6 Feedthrough for one optical fiber



Photo 7 Feedthrough for four optical fibers

## 4.2 Pressure Test

### 1) Test method

The optical transmission loss of the samples in high-pressure condition was measured in a pressure test, as shown in Fig. 13. One 1-fiber optical feedthrough was attached at each flange of the pressure test vessel, the optical fibers are connected with E/O or O/E converters, and the optical transmission loss while pressurized was measured. The 4-fiber optical feedthroughs were also tested by the same method. Test pressure was  $600\text{kgf/cm}^2$ , equivalent to that at 6,000m depth.

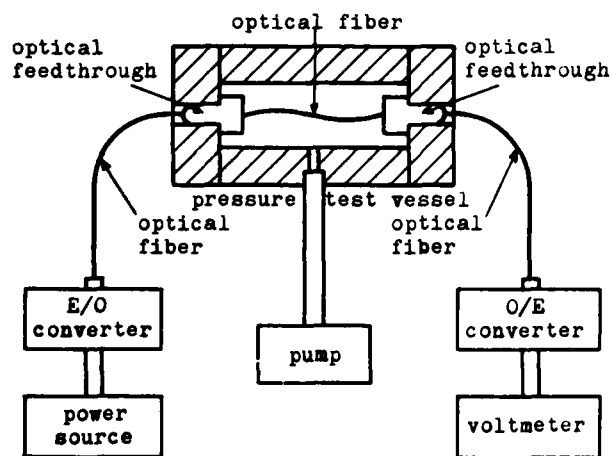


Fig. 13 Pressure test arrangement

### 2) Test items

The following tests were conducted:

- Pressure step test ( $0 \rightarrow 600\text{kgf/cm}^2$  at  $50\text{kgf/cm}^2$  intervals)
- Pressure cycle test ( $0 \rightarrow 600\text{kgf/cm}^2$ , 10 cycles)

Pressure patterns are shown in Figs. 14 and 15.

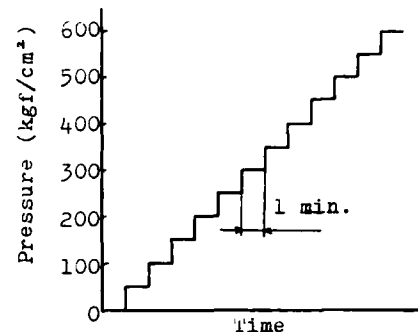


Fig. 14 Pressure pattern for step test

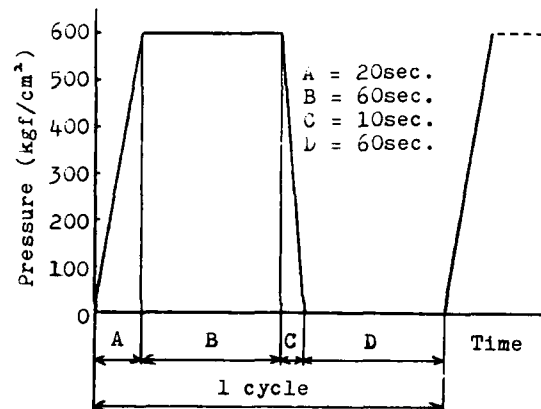


Fig. 15 Pressure pattern for cycle test

### 3) Test result

Figure 16 shows an example of the result of the pressure step test. As pressure increased, the optical transmission loss of the 4-fiber type increased, while that of the 1-fiber type remained constant. Figure 17 shows an example of the results of the pressure cycle test. The optical transmission loss at  $600\text{kgf/cm}^2$  increases with pressure for the 4-fiber type, but returns to the starting point when pressure returns to zero. Table 3 shows the results of a pressure test at  $600\text{kgf/cm}^2$ .

Figure 18 shows an example of the result of a pressure test at  $900\text{kgf/cm}^2$ . The optical transmission loss increases suddenly at a pressure of  $900\text{kgf/cm}^2$  for the 1-fiber type and at  $700\text{kgf/cm}^2$  for the 4-fiber type. But the optical transmission loss returns to normal when pressure drops to zero, so it has been confirmed that the optical feedthroughs and fibers are not damaged.

There is no problem for practical use because the increase of optical transmission loss with pressure is under 3 to 5dB, the normal amount of margin in design of optical transmission systems.

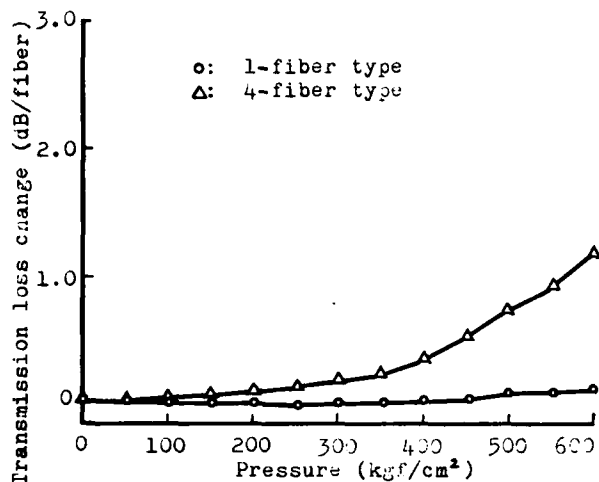


Fig. 16 Results of pressure step test

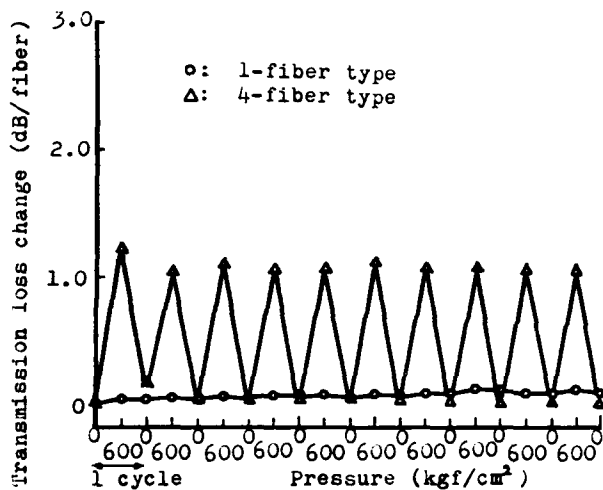


Fig. 17 Results of pressure cycle test

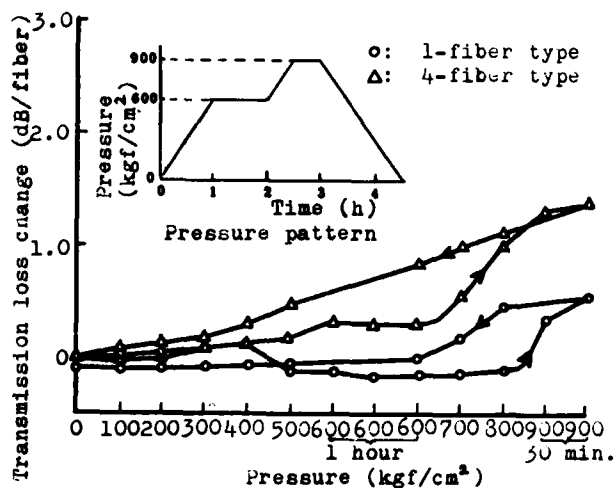


Fig. 18 Results of pressure test at 900kgf/cm²

Table 3 Increase of optical transmission loss (at 600kgf/cm²)

Test items Samples	Pressure step test	Pressure cycle test
1-fiber type	0.08 to 0.10 dB (3)	0.10 dB (1)
4-fiber type	0.5 to 1.3 dB (8)	0.3 to 1.2 dB (4)

( ): number of measurements

#### 4.3 Stress Analysis

Figures 19 and 20 show examples of analysis of deformation and stress lines by means of the finite element method for the 1-fiber feedthrough at a pressure of 600kgf/cm². As shown in Fig. 20, the deformation of resin injected in the metal cylinder is about 100µm for 600kgf/cm², which is in the allowable range.

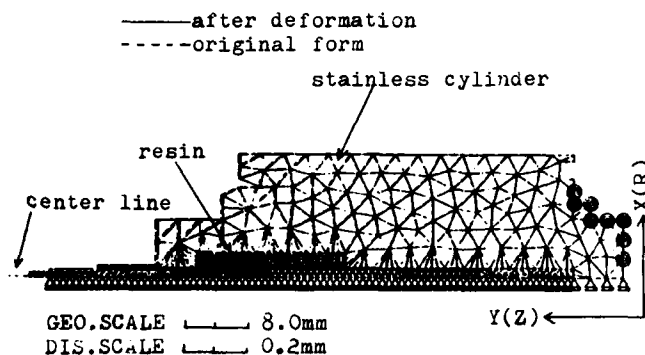


Fig. 19 Analytical results of deformation for optical feedthrough

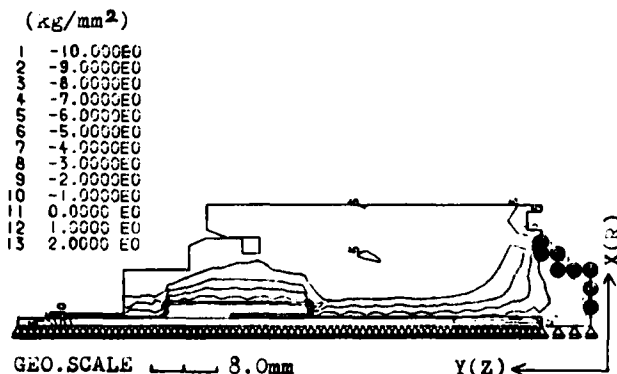


Fig. 20 Stress line diagram for optical feedthrough (R equistress line)

## 5. Conclusion

Elemental technologies for a composite fiber-optic electric-power umbilical cable, high-voltage electric connectors, and optical feedthroughs have been developed for use in deep-sea mining systems at depths of approx. 5,000m. The authors are confident that in the near future this technology, along with optical transmission circuits now under development, will contribute greatly to development of ocean resources.

## Reference

- 1) S. Ōtani, et al.: Newly Developed Optical Fiber/Power Composite Umbilical Cable for Deep-sea Unmanned Work Vehicle, the 30th International Wire & Cable Symposium, 1981



Tetsuji Itō  
Sumitomo Electric  
Industries, Ltd.  
1-3, Shimaya 1-chome,  
Konohana-ku, Osaka,  
Japan

Tetsuji Itō received B.S. and M.S. degrees in electrical engineering from Osaka University in 1975 and 1978, respectively, then joined Sumitomo Electric Industries, Ltd., where he is engaged in R & D of energy transmission. Mr. Itō is a member of the Institute of Electrical Engineers of Japan.



Tsutomu Mitsui  
Sumitomo Electric  
Industries, Ltd.  
1-3, Shimaya 1-chome,  
Konohana-ku, Osaka,  
Japan

Tsutomu Mitsui received B.S. and M.S. degrees in electrical engineering from Tokyo Institute of Technology in 1962 and 1964, respectively. He then joined Sumitomo Electric Industries, Ltd. and worked in the field of extra-high voltage oil-filled cables as a staff member in R & D and design section. At present, he is deputy manager of the Osaka R & D department, and a member of the Institute of Electrical Engineers of Japan.



Shigefumi Ushitani  
Sumitomo Electric  
Industries, Ltd.  
1-3, Shimaya 1-chome,  
Konohana-ku, Osaka,  
Japan

Shigefumi Ushitani received B.S. degree in mechanical engineering from Ehime University in 1977 and M.S. degree in mechanical engineering from Osaka University in 1979. He then joined Sumitomo Electric Industries, Ltd., where he is engaged in R & D of energy transmission. Mr. Ushitani is a member of the Japan Society of Mechanical Engineers.



Takeshi Gomi  
Sumitomo Electric  
Industries, Ltd.  
1-3, Shimaya 1-chome,  
Konohana-ku, Osaka,  
Japan

Takeshi Gomi received B.S. degree in electrical power engineering from Hokkaido University in 1963. He then joined Sumitomo Electric Industries, Ltd. and worked in the field of power cable engineering such as construction work, design of underground cables and transmission systems, and production of paper insulated power cables. After filling the role of chief research associate on development of opto-electric deep sea umbilical, he is now manager of Photonics Project Group of R & D group.



Masayoshi Yamaguchi  
Sumitomo Electric  
Industries, Ltd.  
1-3, Shimaya 1-chome,  
Konohana-ku, Osaka,  
Japan

Masayoshi Yamaguchi received B.S. and M.S. degrees from Osaka University in 1979 and 1981, respectively, then joined Sumitomo Electric Industries, Ltd., where he is engaged in R & D of energy transmission. Mr. Yamaguchi is a member of the Japan Society of Applied Physics.



# ANALYSIS OF EXCESS ATTENUATION IN OPTICAL FIBERS SUBJECTED TO LOW TEMPERATURES

Powers Garmon

Georgia Institute of Technology  
Engineering Experiment Station  
Atlanta, Georgia 30332

## Abstract

Optical fibers which exhibit a dual coating comprised of a low modulus inner layer and a high modulus outer layer at times display excessive attenuation increase at low temperatures. The excess loss may be attributed in part to forces exerted on the optical fiber by the polymer coatings as the temperature decreases, thereby resulting in fiber bending. Fiber bending may occur if the optical fiber assumes a spiral configuration within the low modulus primary coating due to thermal contraction of the secondary coating. Defects in fiber coatings, such as coating eccentricity, fluctuations in coating thickness, and voids between primary and secondary layers, may amplify excess attenuation as the fiber temperature decreases.

coating is sufficient to cause the optical fiber to buckle and assume a spiral configuration within the primary coating layer. Microbending loss at low temperatures may result from localized fluctuations in coating diameter, coating eccentricity, and void formation at the primary secondary coating interface. Moreover, a fiber which exhibits optical defects may amplify the effects of coating-related fiber bending.

Mathematical models are available which characterize excess attenuation as a function of fiber bending. By developing mathematical expressions for the several physical mechanisms which lead to fiber bending, the performance of optical fibers at low temperatures may be predicted and compared to previously reported results.

## 1.0 Introduction

Optical fiber cables of the tight construction class are typically comprised of polymer coated optical fibers stranded about a central strength member and enclosed by a tightly-fitted polymer jacket. Additional layers of strength members and plastic jacket may be added over the tight sub-cable. The optical fibers typically exhibit a two layer coating consisting of a low modulus primary coating and a high modulus secondary jacket. Although the coatings are designed to minimize microbending loss, at times excessive power loss is observed when the coated fibers and/or finished optical cable are subjected to low temperatures. Excess power loss in optical fibers may be caused by constant fiber curvature or by random, microscopic fiber bends.

Fiber coatings are responsible for several mechanisms which lead to fiber bending. Macroscopic fiber bends may occur at low temperatures if the axial compressive force exerted by the longitudinal contraction of the secondary

## 2.0 Fiber Bending Loss Theory

Excess loss in optical fibers may be caused by a constant fiber curvature bend or by random, nearly sinusoidal bends. The former excess loss mechanism is referred to as macrobending, while the latter is termed microbending. Power loss due to fiber macrobending is caused by a leakage process of the guided modes analogous to quantum mechanical tunneling through a potential barrier. Excess loss due to random fiber microbending is caused by coupling of power between guided modes and radiation modes.

Optical fibers subjected to macrobending lose power by radiation. For large radius of curvature bends the losses are negligible; however, at bends of a critical radius and below the losses become prohibitive. Constant fiber curvature losses therefore act like a switch. Gloge<sup>1</sup> has derived an expression which describes the aforementioned behavior. The fraction of modes lost in a constant curvature bend is expressed as

$$\frac{N_s - N_c}{N_s} = \frac{g + 2}{2g\Delta} \left[ \frac{2a}{\rho} + \left( \frac{3}{2n_0 k \rho} \right)^{2/3} \right], \quad (1)$$

where:

- $a$  = fiber core radius,
- $N_s$  = number of modes in a straight fiber,
- $N_c$  = number of modes in a curved fiber,
- $g$  = power law exponent,
- $\Delta$  = relative index difference,
- $n_0$  = cladding refractive index,
- $k$  =  $2\pi/\lambda$ ,
- $\rho$  = fiber bend radius.

A plot of fraction of modes lost to fiber bend radius is shown in Figure 1, where  $\Delta = 0.010$ ,  $a = 25 \times 10^{-6}$  m,  $g = 2$ , and  $\lambda = .85 \times 10^{-6}$  m. Significant mode loss is observed to occur for fiber bend radii of 50 mm or less.

Microscopic deviations of the optical fiber axis from the straight condition result in microbending loss for microbends of a specific spatial periodicity. Mode coupling causes power to be coupled from one mode to another. Ultimately, power is coupled from higher order modes to radiation modes and excess microbending loss is observed. Gloge<sup>2</sup> has shown that mode coupling occurs almost exclusively between adjacent modes. Significant mode coupling occurs if the fiber perturbation, or microbend, has Fourier components equal to the mode spacing  $\omega_c$ . For a graded, parabolic index fiber,  $\omega_c = \sqrt{2\Delta/a}$ . For  $\Delta = .01$  and  $a = 25 \times 10^{-6}$  m,  $\omega_c = 5.66 \times 10^3$  m<sup>-1</sup>, which corresponds to a spatial periodicity of approximately 1 mm. Thus fiber microbends with spatial periods near 1 mm are expected to contribute to mode coupling and resultant excess loss. Olshansky<sup>3</sup>, Marcuse<sup>4</sup>, and Gloge<sup>5</sup> have derived expressions for excess loss. The excess loss coefficient due to fiber microbending may be expressed as

$$\gamma = \frac{f C(\omega_c) 2^p}{\Delta}, \quad (2)$$

where:

- $f$  = numerical coefficient,
- $C(\omega_c)$  = curvature power spectrum,
- $p$  = positive integer,
- $\Delta$  = relative index difference.

The curvature power spectrum is defined

$$C(\omega) = \frac{1}{L} \left\langle \left| \int_0^L C(z) \exp(i\omega z) dz \right|^2 \right\rangle, \quad (3)$$

where  $C(z)$  is the curvature of the function  $y(z)$  which describes the shape of the microbend.

Gloge<sup>1</sup> assumed a microbend of the fiber axis can be represented by a sinusoidal ripple of length  $S$ , frequency  $\nu$ , and amplitude  $h$ . The waveguide is otherwise straight. The curvature function for the sine ripple is  $(2\pi\nu)^2 h \sin(2\pi\nu z)$  and the corresponding curvature power spectrum is  $[(2\pi\nu)^4 \langle h^2 \rangle S^2]/L$ . The excess loss coefficient derived by Olshansky may be expressed as  $[32\pi^4 f \nu^2 \langle h^2 \rangle]/\Delta a$ . The microbending attenuation  $\alpha$  is related to the excess loss coefficient  $\gamma$  by  $\alpha = 4.34 \delta L$ . Therefore, microbending attenuation as a function of microbend amplitude  $h$  is

$$\alpha = 2.7 \times 10^{11} \langle h^2 \rangle. \quad (4)$$

Thus, for graded index fibers with  $\Delta = 0.01$ ,  $a = 25 \times 10^{-6}$  m, and fiber radius  $b = 63 \times 10^{-6}$  m, fiber microbending results in noticeable excess loss if the spatial period for the microbend is approximately 1 mm and the microbend amplitude is of the order of  $1 \times 10^{-6}$  m.

### 3.0 Fiber Bending Loss Mechanisms

#### Fiber Macrobending Due to Axial Compressive Forces

Optical fibers coated with one or more plastic layers are subjected to a compressive strain when the temperature is lowered. The compressive strain is caused by the difference in thermal expansion coefficients between the optical fiber and the plastic coatings. A fiber will buckle when subjected to an axial load if the applied force is greater than or equal to a critical force. An expression which relates critical force to dimensional and material parameters for a bar embedded in an elastic medium has been derived by Timoshenko<sup>6</sup> and employed by Katsuyama<sup>7</sup> to study the effects of temperature on fiber buckling. The case of an optical fiber exhibiting a dual coating (low modulus primary coating and high modulus secondary coating) is similar to the problem solved by Timoshenko, since the optical fiber is embedded in an elastic primary coating, and an axial load is applied by the secondary coating when the temperature decreases. Katsuyama observed by means of optical microscopy the buckling of a metal wire jacketed with the aforementioned type of coatings and assumed that optical fibers may also buckle within the polymer coatings under certain conditions at low temperatures.

The critical force required to cause fiber buckling is

$$F_{CR} = r_F^2 \sqrt{\pi E_p E_F} \quad (5)$$

where

$$\begin{aligned} r_F &= \text{fiber radius,} \\ E_p &= \text{Young's modulus of primary coating} \\ E_F &= \text{Young's modulus of optical fiber.} \end{aligned}$$

The fiber can withstand some compressive strain without buckling, which is represented by

$$\epsilon_{CR}(T) = \sqrt{\frac{E_p(T)}{\pi E_F}} \quad (6)$$

The axial strain exhibited by the optical fiber due to thermal contraction of the secondary plastic coating is

$$\epsilon_T = (\alpha_S - \alpha_F) \int_{T_0}^T \frac{dT}{1 + \frac{E_F A_F}{E_S(T) A_S}} \quad (7)$$

Where  $\alpha_S$  and  $\alpha_F$  are thermal expansion coefficients of the secondary coating and fiber,  $E_S(T)$  is Young's modulus of the secondary coating as a function of temperature, and  $A_F$  and  $A_S$  are cross-sectional areas of the fiber and secondary coating, respectively. The strain difference  $\epsilon_D$  between the optical fiber and the secondary coating is determined from  $\epsilon_D = \epsilon_T - \epsilon_{CR}$ . For  $\epsilon_D$  greater than or equal to zero, fiber buckling will occur and the fiber may assume a helical configuration within the primary polymer coating. According to Timoshenko, the spiral pitch for the case of a buckled bar embedded in an elastic medium is

$$p = 2\pi r_F \sqrt{\frac{\pi E_F}{4 E_p(T)}} \quad (8)$$

The bending radius of a fiber in a helical configuration in terms of spiral pitch and strain difference is

$$\rho = \frac{p}{2\pi \sqrt{2 \epsilon_D}} = \frac{r_F}{\sqrt{2 \epsilon_D}} \sqrt{\frac{\pi E_F}{4 E_p(T)}} \quad (9)$$

For a known value of fiber bending radius,  $\rho$ , the effect on transmission loss can be obtained from Equation 1.

From Equations 6 and 7, the strain difference  $\epsilon_D$  between the optical fiber and secondary polymer coating is a function of primary and second coating

physical parameters. For given values of thermal coefficient of expansion, Young's modulus, and coating cross-sectional area, values for  $\epsilon_D$  may be generated for designated temperatures. Conditions favorable to fiber buckling and resulting power loss may thereby be determined. Some conditions which lead to fiber buckling due to low temperature exposure are demonstrated in Figure 2, which displays strain difference as a function of temperature for various coating property combinations. Whenever  $\epsilon_D$  is positive, fiber buckling will occur. The curves in Figure 2 were generated by assuming that Young's modulus for the primary coating can be represented as

$$E_p(T) = [1 + .001(T - 20^\circ\text{C})^{1.75}] E_p(20^\circ\text{C}) \quad (10)$$

and Young's modulus for the secondary coating as

$$E_S(T) = [1 + 0.0375(T - 20^\circ\text{C})] E_S(20^\circ\text{C}) \quad (11)$$

Furthermore, the jacketed fiber outer diameter for the dual coated fiber is 1.0 mm and the optical fiber diameter is .125 mm. The physical parameters considered for each of the curves in Figure 2 are given in Table 1. The data displayed in Figure 2 indicate that fiber buckling can be avoided for temperatures as low as  $-55^\circ\text{C}$  (curves C, D, and E) by choosing the proper combination of material and dimensional parameters such that  $\epsilon_D$  remains less than zero over the temperature range of interest. The importance of not allowing the strain difference to exceed zero is shown in Figure 3, where a plot of fiber bending radius versus strain difference is displayed. It is seen that fiber bend radius decreases very rapidly once  $\epsilon_D$  exhibits positive values. Small positive values of  $\epsilon_D$  will result in fiber bending radii of a magnitude predicted by Figure 1 to cause significant power loss.

#### Fiber Macro-bending Due to Jacket Eccentricity

The attenuation increase at low temperatures of optical fibers tightly jacketed with a single high modulus coating has been studied by Hillerich.<sup>8</sup> The effect of jacket eccentricity for fibers exhibiting a low modulus primary coating and a high modulus secondary jacket on power loss at low temperatures can be determined by considering that the radius of curvature of a fiber subjected to bending due to thermal contraction of the polymer coatings may be represented as

$$\frac{1}{R} = \frac{M}{EI} \quad (12)$$

where  $M$  corresponds to the sum of all bending moments and  $EI$  is the sum of all modulus-inertial terms. For an optical fiber with modulus  $E_F$  and radius  $r_F$ ; a primary coating of modulus  $E_P(T)$ , eccentricity  $\vec{e}_P$ , and primary jacket radius  $r_P$ ; and a secondary coating of modulus  $E_S(T)$ , eccentricity  $\vec{e}_S$ , and overall coated fiber radius  $r_S$ , the radius of curvature of an eccentrically coated fiber subjected to thermal contraction forces at low temperature is

$$\frac{1}{R(T)} = \frac{4 \epsilon_T E_S(T) r_S^2 (\vec{e}_P + \vec{e}_S)}{E_F r_F^4 + E_S(T) r_S^4} \quad (13)$$

The term  $\epsilon_T$  is the thermal strain exhibited by the coated fiber at a given temperature and may be calculated from Equation 7.

The use of conventional self-centering coating apparatus and concentricity monitors ensure that jacket eccentricity values are small. The effect of small eccentricity values is obtained from Equation 13 by employing Equations 7, 10, and 11, for the case where  $E_T = 4.7 \times 10^{-3}$ ,  $r_F = 6.3 \times 10^{-5}$  m,  $r_P = 1.5 \times 10^{-4}$  m,  $r_S = 5 \times 10^{-4}$  m,  $E_S(20^\circ\text{C}) = 1 \times 10^9$  N/m<sup>2</sup>,  $E_F = 7 \times 10^{10}$  N/m<sup>2</sup>,  $\vec{e}_P = 1.0 \times 10^{-5}$  m,  $\vec{e}_S = 5 \times 10^{-5}$  m and  $T = -55^\circ\text{C}$ , to obtain a constant curvature fiber bend radius of 220 mm. According to Figure 1, such a large fiber bend radius will not result in any significant optical power loss. Therefore, as long as coating eccentricity values are maintained within limits possible with conventional fiber coating technology, no appreciable macrobending is expected due to jacket eccentricity.

#### Fiber Microbending Due to Fluctuations in Coating Diameter

Fluctuations in optical fiber coating diameter may occur during application of either the primary or secondary fiber coating. The primary coating is applied during the fiber drawing process. It is possible for beading, or nearly sinusoidal ripples, to appear in the primary coating. Roe<sup>9</sup> has found that the beading of a primary coat on an optical fiber is a manifestation of the general phenomenon of liquid column instability first studied by Plateau and Rayleigh. The beading effect occurs while the coating is still in the liquid state, and ripples of from 1 to 5 mm in length are possible. The amplitude of the ripple is dependent upon material and

processing parameters, and under certain conditions may be large enough to cause excessive microbending loss.

The secondary plastic coating is typically applied by means of the extrusion process. Defects in the secondary coating occur when a ripple exists in the primary coating or when contaminant or improperly melted resin passes through the extruder tip. The spatial period of these localized defects range from one to five millimeters.

Since microbending theory, as presented in Section 2, predicts that attenuation increase may occur for microscopic fiber bends of spatial period of one millimeter, the aforementioned jacket defects may result in increasing excess power loss as the temperature is lowered and lateral forces are applied to the fiber. Microbending loss due to jacket defects can result from jacket eccentricity as well as lateral pressure from other cable elements when low temperatures are encountered.

The effect of a ripple in the primary coating combined with jacket eccentricity can be seen by considering the following situation. A sinusoidal ripple with an amplitude of  $25 \times 10^{-6}$  m is present in the primary coating whose nominal diameter is  $3 \times 10^{-4}$  m. The primary coating then exhibits diameters of  $2.5 \times 10^{-4}$  m,  $3.5 \times 10^{-4}$  m, and  $2.5 \times 10^{-4}$  m within the region of the ripple. Assume a primary coating eccentricity of  $1 \times 10^{-5}$  m and a secondary coating eccentricity of  $5 \times 10^{-5}$  m. When the fiber is subjected to low temperatures, thermal contraction of the secondary coating causes the fiber to conform to a curve of radius  $R(T)$ , except at the locations where ripples exist in the primary coating. At these points, the fiber curvature is modified by the presence of the ripple with the result that in the ripple zone, the fiber radius of curvature is increased. A fiber bend of microscopic amplitude results at the junction of constant fiber curvature and modified fiber curvature caused by the ripple. The magnitude of the fiber bend can be approximated by assuming that the deflection in the bend area is equal to the sums of the deflections in the regions of different radius of curvature. According to Timoshenko<sup>10</sup>, the deflection  $h$  of a fiber for a given radius of curvature  $R(T)$  is

$$h = \frac{(S/2)^2}{2R(T)} \quad (14)$$

where  $S$  is an arc length of approximately one millimeter. By employing Equation 13, microbend deflection amplitudes may be determined as a function of temperature. For  $T = -55^\circ\text{C}$ , the radius of curvature of the fiber at all points except where ripples exist is .22 m. Within the coating defect zone, a larger radius of curvature exists and is assumed to be .4 m. The magnitude of the fiber deflection over the one millimeter spatial period is, from Equation 14,  $8 \times 10^{-7}$  m. Since two such microbends are possible for a single ripple in the primary coating, the microbending loss caused by the ripple at  $-55^\circ\text{C}$  is, from Equation 4, equal to 0.35 dB.

If several defects exist per kilometer, a significant excess loss may be attributed to the existence of the ripples. If, the amplitude of the fiber deflection is less than that assumed in the above example, no measurable excess loss may be observed if the optical fiber is screened prior to cabling by exposure to low temperatures. However, when the fiber is incorporated into a cable of tight construction, thermal contraction of the cable jacket may result in lateral forces being applied to the region of the coating defect and may be of a magnitude sufficient to result in microbends of amplitude which result in prohibitively high excess loss. When a fiber exhibiting a defect of the dimensions stated above is subjected to a lateral force due to the thermal contraction of the cable jacket, the secondary coating hump of  $2.5 \times 10^{-5}$  m amplitude is pressed into the fiber. The low modulus primary coating is able to buffer the effect of the hump to some extent. The ability of a primary coating to provide a buffer for secondary coating defects has been studied by Hanson.<sup>11</sup> If the low modulus primary coating is able to buffer the fiber from the  $2.5 \times 10^{-5}$  m hump such that a fiber microbend of  $1 \times 10^{-6}$  m amplitude occurs, the resulting excess loss attributable to the coating defect is 0.54 db. However, if a  $3 \times 10^{-6}$  m fiber deflection should occur, the corresponding excess loss per defect is 4.9 db.

Large microbend amplitudes are especially likely if the primary coating modulus increases significantly at low temperatures, since its ability to provide a buffering action against defects is minimized. Should the primary coating pass through the glass transition temperature, a rather rapid transition from low to high microbend amplitude could occur with a resulting high rate of

increase in excess loss being exhibited by the fiber.

#### Fiber Bending Due to Void Formation at the Primary-Secondary Coating Interface

The high modulus secondary coating may be applied to the primary-coated fiber by means of melt extrusion. Improper processing conditions may lead to the formation of occasional voids along the length of the fiber at the primary-secondary coating interface.

Rokunoke<sup>12</sup> observed voids between the fiber and extruded polymer jacket. He postulated that when the extrudate is quenched too rapidly, the surface layer solidifies while the interior of the jacket is still in the molten state. The density difference between the molten state and the solid surface layer creates voids.

The effect of void formation between polymer layers may be determined by assuming that numerous voids of different lengths and amplitudes are symmetrically configured at random locations along the length of the fiber. When the fiber is subjected to low temperatures, the secondary jacket contracts and applies an axially compressive force to the primary coated fiber. If the applied force exceeds some critical value, the primary coated fiber will buckle within the void. If the fiber deflection exceeds the void height, the primary coated fiber will be forced against the inner wall of the secondary coating resulting in fiber microbends.

Timoshenko<sup>13</sup> has analyzed the problem of a bar with both ends built in, which is similar to the void problem stated above. The critical compressive force for which fiber buckling within the void will occur is

$$F_{CR} = \frac{4\pi^2 E_F I_F}{l^2} \quad (15)$$

where  $l$  is the length of the void. If the applied force equals  $F_{CR}$ , a full wave deflection will occur with an amplitude

$$d = \frac{l}{2} (1 - \epsilon_D) \tan \theta \quad (16)$$

where  $\theta$  is the angle subtended by the deflection and  $\epsilon_D$  is the strain difference defined earlier. The critical strain of a fiber segment enveloped by a void is dependent upon void length, as is the critical force. This length dependence is displayed in Figure 4. Also shown in Figure 4 is the thermal strain term defined by Equation 7. Since fiber buckling occurs for  $\epsilon_T - \epsilon_{CR} > 0$ , the case depicted in Figure 4, for  $E_g(20^\circ\text{C}) =$

$5 \times 10^8 \text{ N/m}^2$ ,  $\alpha_s = 1 \times 10^{-4} \text{ }^\circ\text{C}^{-1}$ ,  
 $r_p = 1.5 \times 10^{-4} \text{ m}$ , and  $r_s = 5.0 \times 10^{-4} \text{ m}$ ,  
 indicates that fiber buckling may occur at  $0^\circ\text{C}$  for voids of 10 mm length; whereas, if void lengths are less than 4 mm long, fiber buckling will not occur until the temperature is lowered to  $-45^\circ\text{C}$ .

The deflection amplitude at  $T = -45^\circ\text{C}$  for voids of 4 mm length is from Equation 16,  $28 \times 10^{-6} \text{ m}$ . For a void height of  $25 \times 10^{-6} \text{ m}$ , the primary coated fiber will be pressed against the inner wall of the secondary coating and microbending will occur. At  $T = -50^\circ\text{C}$ , a deflection amplitude of  $54 \times 10^{-6} \text{ m}$  is obtained which results in more severe microbending. The magnitude of the microbending loss at  $T = -45^\circ\text{C}$  for a void of 4 mm length and  $25 \times 10^{-6} \text{ m}$  height is, from Equation 4, .15 dB; whereas, a loss of 1.1 dB is predicted at  $T = -50^\circ\text{C}$ . The microbend amplitudes for the above calculations were obtained from geometrical considerations and are  $0.5 \times 10^{-6} \text{ m}$  and  $2 \times 10^{-6} \text{ m}$ , respectively. Therefore, a fiber with voids less than or equal to 4 mm in length may perform well until a critical temperature is reached and then prohibitive loss will be observed.

#### 4.0 Conclusion

Excess attenuation at low temperatures has been attributed to the following fiber bending mechanisms: fiber macrobending due to thermal contraction of the secondary coating, and fiber microbending due to ripples in the primary coating, bumps in the secondary coating, eccentric coatings, and void formation at the primary-secondary coating interface. The predicted types of behavior for fibers subjected to the above bending mechanisms are presented in Figure 5. These curves are in agreement with experimental results obtained by Kopstein.<sup>14</sup> All of the curves pertain to parabolic graded index multimode fibers exhibiting a composite coating comprised of a low modulus inner layer and a high modulus outer jacket.

Curve A of Figure 5 represents the case where the axial compressive force applied by the contraction of the secondary coating is sufficient to cause fiber buckling at  $-40^\circ\text{C}$ . Excellent transmission performance is predicted until the onset of fiber buckling at  $-40^\circ\text{C}$ , after which catastrophic excess loss is predicted.

The behavior of fibers which display ripples in the primary coating is depicted by Curves B and C. Curve B

represents the case where five ripples of moderate dimensions exist in a one kilometer length of fiber; whereas, Curve C demonstrates the result of the primary coating exhibiting a glass transition temperature of  $-45^\circ\text{C}$ .

The effect of void formation between the primary and secondary coatings is shown by Curve D. Prohibitive excess loss is predicted when the fiber buckles within the void and is pressed against the inner wall of the secondary coating.

In order to eliminate or significantly reduce the effects of the aforementioned bending loss mechanisms associated with optical fiber coatings, a combination of proper material selection, optimum coating dimensions, and process control must be practised. If properly chosen coatings are applied under controlled conditions to optical fibers which exhibit acceptable optical parameters, high performance, on a high yield basis, at low temperatures is expected.

#### References

1. D. Gloge, "Bending Loss in Multimode Fibers with Graded and Ungraded Core Index," Applied Optics 11, pp. 2506-2512, 1972.
2. D. Gloge, "Optical Power Flow in Multimode Fibers," Bell System Technical Journal 51, p. 1767, 1972.
3. R. Olshansky, "Mode Coupling Effects in Graded Index Optical Fibers," Applied Optics 14, pp. 935-944, 1975.
4. D. Marcuse, "Loss and Impulse Response of a Parabolic Index Fiber with Random Bends," Bell System Technical Journal 52, p. 1423, 1973.
5. D. Gloge, "Optical-Fiber Packaging and Its Influence on Fiber Straightness and Loss," Bell System Technical Journal, 54, p. 245-262, 1975.
6. S. Timoshenko, Theory of Elastic Stability, First Edition, McGraw Hill, pp. 108-112, 1936.
7. Y. Katsuyama, Y. Mitsunaga, Y. Ishida, and K. Ishihara, "Transmission Loss of Coated Single-mode Fiber at Low Temperatures," Applied Optics 19, 24, pp. 4200-4205, 1980.
8. B. Hillerich, D. Palmer, P. Shlang, "Criteria for the Jacketing of Optical Fibers," Proc. of Third Europ. Conf. on Opt. Commun. (Munich) p. 86, 1977.
9. R. Roe, "Wetting of Fire Wires and Fibers by a Liquid Film," J. Colloid Interface Sci 50, No. 1 pp. 70-79, 1975.
10. S. Timoshenko, Elements of Strength of Materials, Second Edition, D. Van Nostrand Co., Inc. p. 122, 1940.

11. E. Hanson, "Origin of Temperature Dependence of Microbending Attenuation in Fiber Optic Cables," Fiber and Integrated Optics 3, pp. 113-148, 1980.
12. M. Rokunohe, T. Shinteni, M. Yajima, A. Utsumi, "Stability of Transmission Properties of Optical Fiber Cables," Proc. Second Europ Conf. on Optical Fiber Commun (Paris), pp. 183-189, 1976.
13. S. Timoshenko, Theory of Elastic Stability, First Edition, McGraw Hill, p. 67, 1936.
14. R. Kopstein, "Ultra Low Loss Optical Fiber Cable Assemblies," Research and Development Technical Report - CORADCOM-78-2922-3, February, 1981.

Table I. Physical Parameters for Figure 2

Curve No.	$E_p$ (20° C) ( $\times 10^6$ N/m <sup>2</sup> )	$E_s$ (20° C) ( $\times 10^9$ N/m <sup>2</sup> )	$\alpha_s$ ( $\times 10^{-4}$ °C <sup>-1</sup> )	$r_p$ (mm)	$r_s$ (mm)
A	1.0	0.5	2.0	150	500
B	1.0	1.0	1.0	150	500
C	1.0	0.5	1.0	150	500
D	1.0	0.5	1.0	200	500
E	3.5	0.5	1.0	150	500

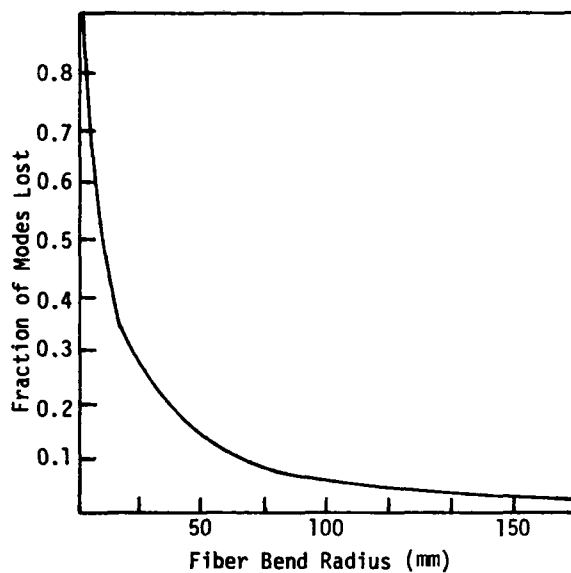


Figure 1. Fraction of modes lost as a function of fiber bend radius.

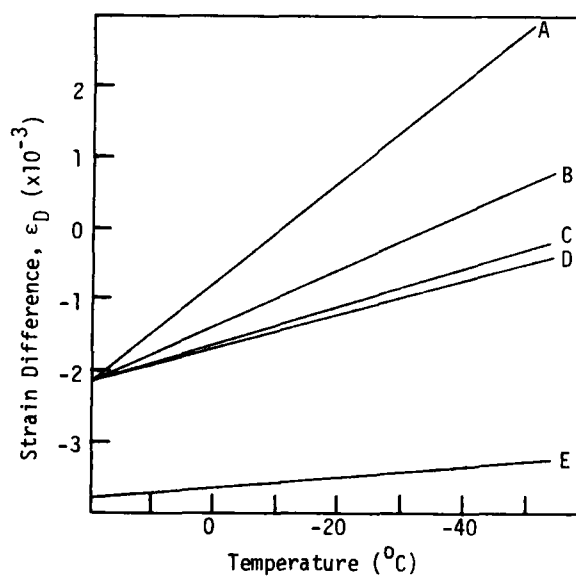


Figure 2. Strain difference as a function of fiber temperature.

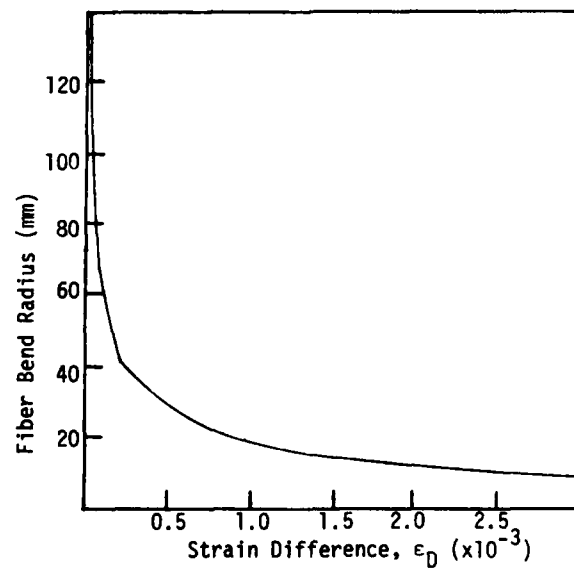


Figure 3. Fiber bend radius as a function of strain difference.

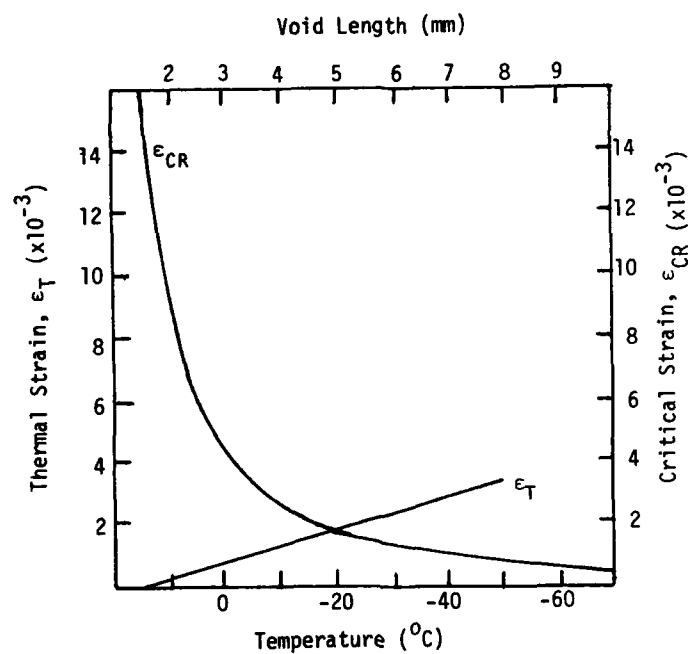


Figure 4. Critical parameters for predicting fiber buckling in voids between primary and secondary coatings.

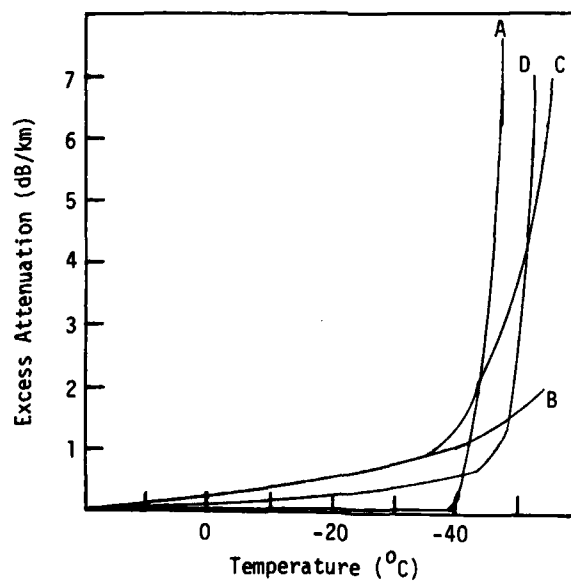
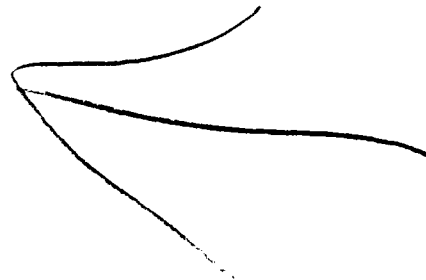


Figure 5. Predicted fiber performance at low temperatures.



Powers Garmon is a Senior Research Scientist at the Georgia Institute of Technology Engineering Experiment Station. He received a B.S. degree in physics in 1970 from Berry College and was granted a Ph.D. degree in physics in 1976 from Clemson University. Prior to his work at Georgia Tech, he was an Assistant Professor of Physics at Auburn University, a materials engineer at Superior Cable Corporation, and a project engineer at ITT-EOPD. His current research interests include high speed signal processing, optical power coupling, and optical fiber sensor development.



# Buckling of Optical Fibers Within Elastomers Used in an Embedded-Core Cable Structure

by

L. L. Blyler, Jr., C. Gieniewski, X. Quan and H. Ghoneim

Bell Laboratories  
Murray Hill, N.J. 07974

## Summary

Optical fibers must be packaged in cable structures such that transmission losses due to microbending are minimized. In an embedded-core cable structure, the fibers are helically stranded within a core consisting of a central strength member surrounded by a low modulus elastomeric buffer in which the fibers are embedded. Excess losses due to fiber buckling within the elastomer may be incurred with this structure as a result of axial compressive loading of the fibers during cable bending. An experimental technique has been developed to evaluate the tendency of an optical fiber to buckle within the elastomer of an embedded core cable. The technique utilizes a sample in which a coated fiber is molded into a sandwich structure. The tendency to buckle is shown to be strongly related to the modulus of the elastomer; high modulus elastomers provide buckling stability. The adhesive and frictional forces between the fiber coating and the elastomer are also obtained with the sandwich specimen. Adhesive failure and fiber slippage are shown to be compressive strain relief mechanisms with certain elastomers. In addition, a mechanism of fiber failure due to localized buckling is observed within high modulus, highly adherent elastomers when fibers are subjected to large compressive strains ( $>3\%$ ).

Greater than

## INTRODUCTION

Optical fibers must be packaged in cable structures such that transmission losses due to microbending are minimized. One cable structure which has been successfully used is the "embedded core" design,<sup>1</sup> shown schematically in Figure 1. In this cable structure, the fibers reside in a core consisting of a central steel wire surrounded by a low modulus elastomer in which the fibers are embedded. The fibers are stranded about the core axis and are each individually enveloped by the elastomer which provides a buffer layer for microbending resistance. The resistance to lateral fiber deformation afforded by the elastomer is an important factor in this embedded core structure. The elastomer must stabilize the fiber such that it will not buckle under axial compressive loading encountered during normal bending of the core. This factor is especially important if the adhesive or frictional forces between the fiber coating and the elastomer are sufficiently high to prevent strain averaging by axial movement of the fiber between the tensile and compressive sides of its helical path.

In consideration of the foregoing effects, we undertook an experimental investigation to determine the buckling resistance provided by a number of thermoplastic elastomers of differing mechanical properties which might be candidates as embedding materials. Additionally, we investigated the adhesive and frictional characteristics of these materials in contact with a coated fiber.

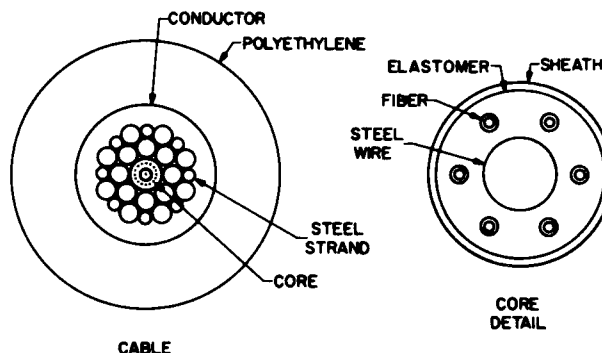


Figure 1: Embedded core submarine lightguide cable

## EXPERIMENTAL

### Elastomeric Materials and Their Properties

The elastomeric materials used in the optical fiber buckling experiments included block copolymers of styrene/butadiene/styrene (SBS) and styrene/ethylene-butene/styrene (SEBS), segmented polyurethanes (PU), and a segmented polyether-ester copolymer (PES). They are described in Table I. Tensile properties of the materials were measured with an Instron tensile testing machine at a constant crosshead movement of 0.5 cm per minute using 5 cm long test specimens. The tests were carried out at about 23°C and 58% relative humidity. Modulus-strain data are shown in Figure 2. The optical fiber used in these studies was coated with a ultraviolet (UV)-cured epoxy acrylate,<sup>2</sup> dyed red for better visibility when embedded in the elastomers. The cladding diameter of the fiber was 125  $\mu\text{m}$  and the diameter of the coated fiber was about 260  $\mu\text{m}$ .

### Method of Embedding Optical Fiber in Elastomers

The optical fiber was embedded between two equally thick sheets of a given elastomer by compression molding at about 165°C in a frame mold. This was done in two stages. In the first stage, two 15.2x7.6x0.041 cm plaques of the elastomer were obtained from one frame mold. Next, lengths of the optical fiber were symmetrically positioned between the two plaques in a 0.082 cm deep frame mold and compression molded again. The fiber ends were led out from the mold through grooves provided at the opposing sides of the frame with the fiber axis passing through the middle of the mold.

TABLE I

Properties of Elastomers Used in the Fiber-Buckling Experiments

Elastomers	Polymer Type	Appearance	Secant Tensile Modulus at 1% Strain, MPa	Shore Hardness at 23°C	Specific Gravity at 23°C
A	SEBS	transparent	0.97	35A	0.90
B	SEBS	transparent	2.14	45A	0.90
C	SEBS	transparent	4.97	55A	0.90
D	SEBS	Natural White	6.41	60A	1.20
E	PU	transparent	11.0	80A	1.10
F	SBS	Natural White	16.6	75A	1.01
G	PU	transparent	20.0	87A	1.12
H	PU	transparent	20.7	42D	1.13
I	PES	semi-transparent	51.7	40D	1.17

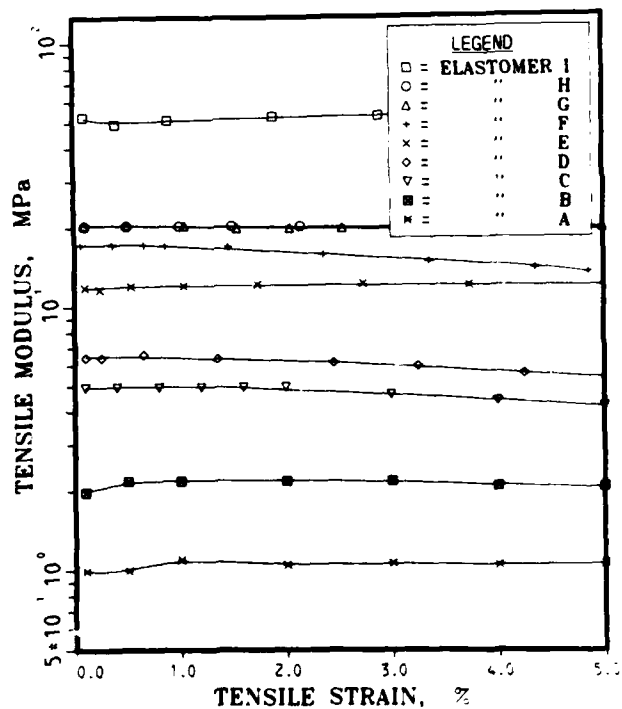


Figure 2: Modulus vs. strain of elastomers tested at  $10\% \text{ min}^{-1}$  and  $23^\circ\text{C}$ .

In the second stage one side of the elastomer sandwich containing the embedded fibers was molded against an elastic, high-modulus substrate to which the elastomer plaque adhere well (see Figure 3). The use of such a substrate is crucial to the success of the buckling experiment, as will be made clear later. Commercial  $254\text{-}\mu\text{m}$  poly(ethylene terephthalate) (PET) film was found to be an excellent substrate material for this purpose. Its semitransparency allows one to observe the optical fiber during the buckling experiments. The film has a high tensile modulus, it can be bent elastically to curvatures of small diameter, and it adheres well to the elastomers studied.

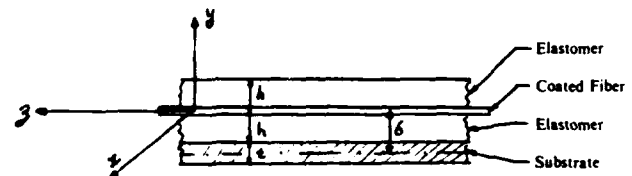


Figure 3: Elastomer sandwich containing embedded fibers.

### Measurements of Adhesion and Friction

The adhesion and friction between the elastomers and the fiber coating were measured by pulling the coated fiber out of the elastomer sandwich with an Instron tensile testing machine at 23°C and 58% relative humidity. Strips, 6-cm long by 1.27-cm wide, with the fiber oriented in the long direction of the strip, midway between its edges, were cut from the elastomer plaques and used as test specimens. A convenient length of fiber for gripping purposes was left extended beyond one end of the specimen. The fiber was then broken within the elastomer using the tip of a razor blade at a predetermined position and the specimen was positioned in the rubber coated grips of the Instron machine. One grip held the elastomer sandwich, the other grip held the extended end of the fiber, with the cut fiber end in the elastomer located between the grips. A pulling force was applied to the fiber at a constant Instron crosshead movement of 0.5 cm per minute. The technique is shown schematically in Figure 4.

This method provides a means of measuring the adhesive and frictional forces between the fiber coating and its embedding elastomer. A typical trace of force vs. fiber pullout distance is shown in Figure 5. The peak force represents adhesive failure, and the rest of the trace represents the dynamic friction between the fiber coating and the elastomer as the fiber is pulled out at a constant rate.

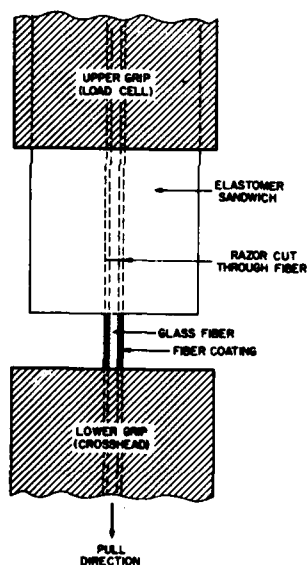


Figure 4: Measurement of adhesive and dynamic frictional stresses.

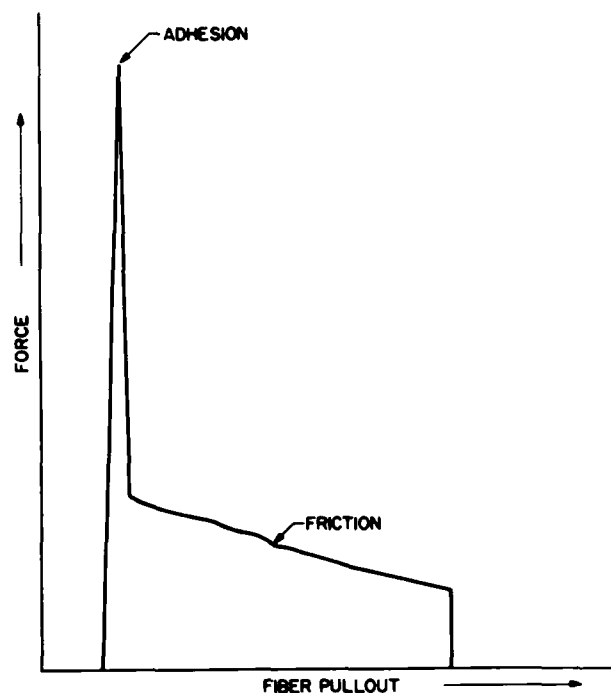


Figure 5: Force vs. fiber pullout trace

### Fiber Buckling Experiments

The fiber-buckling experiments were carried out by bending the sandwich structures consisting of the hard, elastic PET substrate overmolded with the various elastomers containing the embedded fibers. Bending of the sandwich structures was done over stainless steel forms having circular curvatures of known radii such that the embedded fibers were put into compression (see Figure 6). The fiber buckling was observed through the PET substrate and the elastomer, under low magnification. Buckling resulted in a sinusoidal path of the fiber with a discernible buckling period and amplitude (see Figure 7). The periods and amplitudes were measured with the aid of a millimeter scale attached to the forms or to the PET substrate.

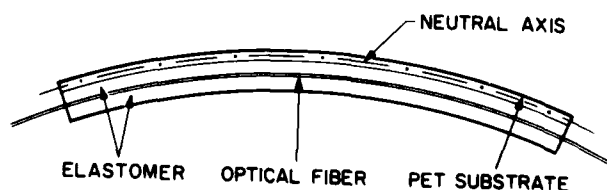


Figure 6: Bending of sandwich structure

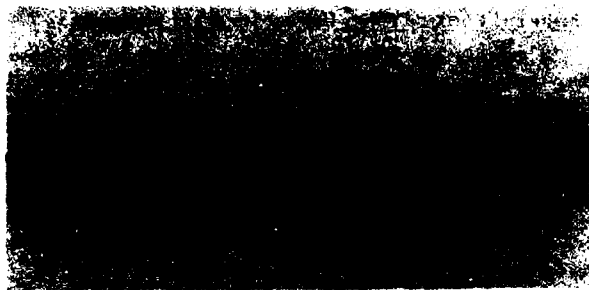


Figure 7: Buckling of optical fiber within elastomeric medium.

## RESULTS AND DISCUSSION

### Fiber Buckling Phenomenon

Because the modulus of the PET substrate sheet is two or more orders of magnitude higher than that of each of the elastomers studied, the neutral bending plane of the sandwich remains very close to the central plane of the PET sheet during bending. Referring to Figure 3, the distance  $\delta$  from the neutral plane to the fiber axis is given by:

$$\delta = \frac{t}{2} \frac{(2h+t)}{(t+2h\gamma)} \quad (1)$$

where  $\gamma = E_1/E_2$

$E_1$  = tensile modulus of the elastomer

$E_2$  = tensile modulus of the PET sheet

$h$  = distance from the surface of the PET sheet to the fiber

$t$  = thickness of the PET sheet.

Using an elastomer whose modulus approaches the modulus of the PET sheet would shift the neutral plane position toward the fiber axis. In our experiments the largest shift occurs with the stiffest embedding elastomer we used, Sample I. The modulus of PET is about  $3.7 \times 10^3$  MPa and that of Sample I is about  $5.17 \times 10^1$  MPa. For this combination the shift in neutral-plane position toward the fiber axis is calculated to be only 0.0023 cm, about 4% of the total distance. This very small shift was neglected in our fiber buckling experiments.

### Relationship of Elastomer Modulus to Fiber Buckling

The experimentally obtained relationship between the modulus of the embedding elastomers and the radius of curvature at the onset of fiber buckling is displayed in Figure 8. It is evident that elastomers with high moduli provide high resistance to fiber buckling. It is felt that an embedding medium with a high modulus helps to stabilize the fiber by providing lateral support. In fact when the highest modulus elastomer (Sample I) was used as the embedding medium, buckling was not observed even at a radius of curvature of 0.8 cm. The lowest modulus elastomer, Sample A, exhibited fiber buckling at a radius of about 40 cm. These observations are consistent with theoretical predictions for beams on elastic foundations.<sup>3</sup>

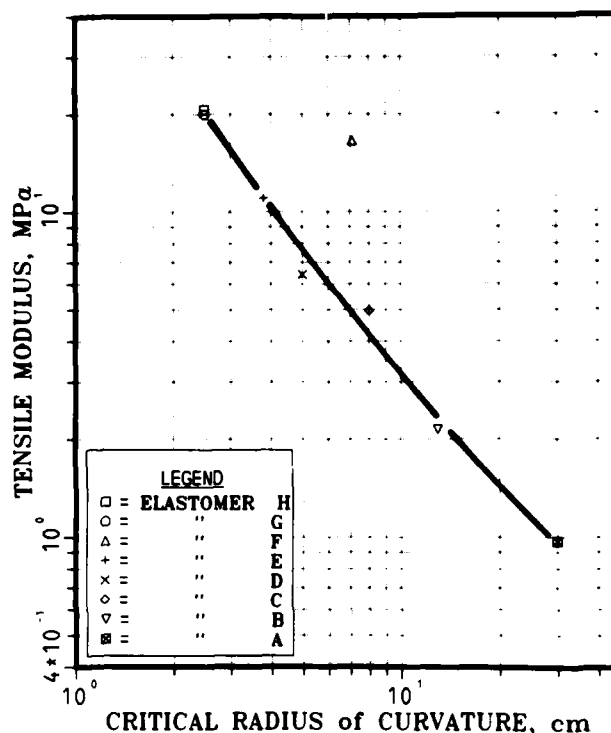


Figure 8: Modulus vs critical radius of curvature for buckling.

In these experiments care was taken to insure that the fiber coating was adhered to the elastomer in all the samples used to determine the critical bending radii. The sandwich was never bent such that the fiber was put into tension, which would stress the adhesive bond prior to the buckling experiments. Similarly the bond between the elastomer and the PET substrate was maintained. Lack of sufficient adherence of the elastomers to the PET substrate would result in uncontrolled neutral axis position shifts in the fiber buckling experiments. Under these conditions and neglecting any shear or other deformations induced in the elastomer by the stressed fiber, the critical compressive strain,  $\epsilon_c$ , in the fiber at the onset of buckling may be calculated according to

$$\epsilon_c = \frac{\delta}{\rho_c} \quad (2)$$

where  $\rho_c$  is the critical radius of curvature. The critical compressive strain is plotted as a function of elastomer modulus in Figure 9 and varies from approximately 0.2% for sample A to about 2% for samples G and H.

The fiber buckling periods and amplitudes were also measured during the buckling experiments. The buckling periods were almost constant along the fiber axis for a particular elastomer, but varied in length from 2 to 6 mm in different elastomers. The experimental results summarized in Table II show that the longer sinusoidal periods were associated with elastomers in which the fiber buckling occurred most readily, i.e., elastomers with low moduli. These observations are also consistent with theory.<sup>3</sup>

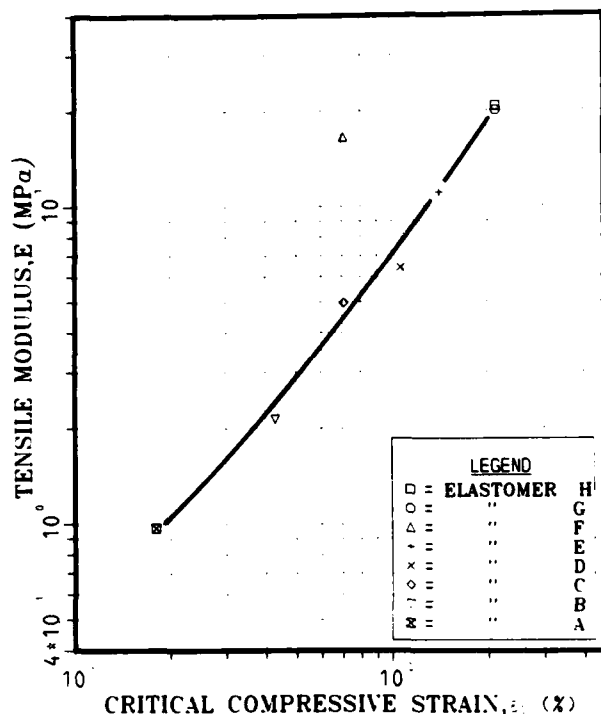


Figure 9: Modulus vs. critical compressive strain.

The buckling amplitudes followed a similar relationship. In all elastomers tested, except Sample I, the fiber buckling amplitudes were small at the onset of buckling, on the order of 0.1 to 0.2 mm. Upon further bending over smaller radii, the amplitudes first increased, then remained constant in the stiffer elastomers until the fibers broke. In the softer elastomers under the same bending conditions, the amplitudes increased, passed through a maximum reaching about 1 mm, then decreased and became nonuniform, presumably due to the loss of adhesion and subsequent fiber slippage.

#### Adhesive and Frictional Forces Between Fibers and Elastomers

The adhesive and frictional shear stresses between the coated fibers and the embedding elastomers are listed in Table II. Significant in these data are the low adhesion values obtained for the SEBS elastomers. In contrast, the adhesion of the PU elastomers to the fiber coating was exceptionally high. Typically the adhesion between the PU elastomer and fiber coating was so strong that adhesive failure occurred at the coating-glass interface. As a result we estimate the adhesive failure stress between the coating and the glass fiber to be 17 MPa. Dynamic friction between the elastomer and coating could not be measured for this case.

#### Relationship of Fiber Buckling to Adhesion and Frictional Forces

Within the sandwich structure used in these experiments it was observed that fiber buckling did not occur when the adhesive or frictional forces between the fiber coating and the elastomer were low. Under these conditions, the fiber moved freely (slipped) in the elastomer when the sandwich structure was bent. This effect was readily observed while experimenting with SEBS elastomers. When the 15 cm long samples were bent, fiber buckling was observed only in the middle portion of the samples. At the ends the fiber overcame all adhesive and frictional resistance and moved within the elastomer, thereby relieving the compressive strain. After the samples were bent several times at different radii, fiber buckling could be induced in the middle part of the specimen only upon sudden bending. On holding the sample in the bend configuration, fiber buckling gradually disappeared. These experiments show that in the absence of adhesion, sufficiently high frictional forces must be present to prevent slipping, and that buckling disappears when the frictional forces are overcome and the fiber translates axially.

As discussed earlier, when fibers are stranded around a central strength member and embedded in an elastomer in a cable core, fiber buckling may occur on the compression side of the core during cable bending. On the other hand, the tensile and compressive forces generated along the fiber by core bending may be sufficient to break the adhesive bond between the coating and the elastomer and to overcome the frictional forces resisting fiber translation. If this occurs, strain averaging along the lay length of the fiber is possible and buckling may be averted. This has been detected in a steel-reinforced lightguide cable sheath where the steel reinforcing wires are able to slip and relieve the strain due to bending by averaging the compressive and tensile sides of a lay length.<sup>4</sup>

TABLE II  
Summary of Experimental Results on Buckling of Optical Fibers

Elastomer	Radius at Onset of Buckling, cm	Buckling period, mm	Amplitude Range, mm	Sandwich Radius at Which Fiber Broke, cm	Adhesive-Failure Stress Between Elastomer and Fiber Coating, MPa $\times 10^2$	Dynamic Frictional Stress Between Elastomer and Fiber Coating, MPa $\times 10^2$
A	40-30	6	0.2-1.0	<0.8	17.6-19.6	7.8-9.8
B	15-13	5	0.2-1.0	<0.8	27.5-29.4	12.7-14.7
C	10-8	5	0.2-1.0	<0.8	29.4-39.2	11.8-17.7
D	8-5	5	0.2-1.0	<0.8	28.4-42.2	7.8-9.8
E	4.5-3.8	3	0.1-0.5	1-0.8	>883	N.A.
F	9-7	4	0.2-1.0	1-0.8	74.5-136	9.8-39.2
G	3-2.5	2	0.1-0.2	1.4-0.8	>1049	N.A.
H	3-2.5	2	0.1-0.3	1-0.8	>1020	N.A.
I	None	None	None	1.8-1.4	922	324-451

It is possible to estimate the tensile and compressive strain distribution along a fiber in a cable core of known geometry subjected to bending by following the analysis of Lutchansky.<sup>5</sup> From this calculation, the shear stress distribution along the coating-elastomer interface may be determined and compared with the adhesive failure and frictional stresses determined in the experiments described herein. The analysis, presented in the next section, shows that the shear stress is nonuniformly distributed along the fiber and that bending in different planes may be required to completely break all adhesive bonds. However, while the adhesive failure mechanism might serve to alleviate fiber buckling, it might also provide a path for water ingress from the ends of the cable.

#### Calculations of Compressive Strains and Shear Stresses on Fibers in an Embedded Core Structure.

According to Luchanski<sup>5</sup> the length of a differential element of a fiber of negligible thickness helically stranded about a cylinder (or core) is

$$ds_c = \sqrt{R^2 + k^2} d\theta \quad (3)$$

where  $R$  = cylinder radius

$k = \ell/2\pi$

$\ell$  = lay length

$\theta$  = cylindrical coordinate

When the core is bent with a radius of curvature,  $\rho$ , the differential element length becomes, approximately

$$ds_T \approx \sqrt{R^2 + k^2} d\theta + \frac{k^2 R \cos\theta d\theta}{\rho \sqrt{R^2 + k^2}} \quad (4)$$

where  $\theta = 0$  is taken where the fiber crosses the outermost radius of the bent core. If we assume the fiber is bonded to the core and there are no deformations in the core caused by interaction with the fiber (a worst case assumption), then the tensile strain,  $\epsilon$ , in the fiber due to core bending is given by

$$\epsilon(\theta) = \frac{k^2 R \cos \theta}{\rho [R^2 + k^2]} \quad (5)$$

Note that the strain is zero at  $\theta = \pm 90^\circ$  and alternates between tension and compression. Also the quantity  $k^2/(R^2 + k^2) = \cos^2 \alpha$ , where  $\alpha$  is known as the lay angle.

Next consider the equilibrium of a fiber element of differential length  $ds_T$  in a cable core subjected to bending, as depicted in Figure 10. The fiber has radius,  $r_f$ , while the fiber coating has radius,  $r_c$ . In accord with eq. (5) a nonuniform tensile stress distribution,  $\sigma$ , occurs along the fiber which is compensated by a shear stress distribution,  $\tau$ , at the coating surface. Only the tensile stress in the glass fiber is considered because the fiber modulus is nearly two orders of magnitude higher than the coating modulus.

From Figure 10 a force balance (neglecting fiber curvature) gives

$$\tau = \frac{r_f^2}{2r_c} \frac{d\sigma}{ds_T} \quad (6)$$

Since  $\sigma = E_f \epsilon$ , where  $E_f$  is the tensile modulus of the glass fiber, we have

$$\tau = \frac{r_f^2}{2r_c} E_f \frac{d\epsilon}{ds_T} \quad (7)$$

Combining eqs. 4, 5 and 7 with the approximation  $ds_T \approx \sqrt{R^2 + k^2} d\theta$  and carrying out the differentiation yields

$$\tau = \frac{r_f^2}{2r_c} E_f \frac{k^2 R \sin \theta}{\rho [R^2 + k^2]^{3/2}} = \frac{r_f^2}{2r_c} E_f \frac{1}{\rho} \cos^2 \alpha \sin \alpha \sin \theta. \quad (8)$$

Note that the shear stress is zero at  $\theta = 0^\circ$  or  $180^\circ$ , and is maximum at  $\theta = \pm 90^\circ$ , the points at which the tensile stress in the fiber is zero. This result implies that when the cable is bent to a radius of curvature which is sufficient to cause adhesive failure between the fiber coating and the core elastomer, the failure should occur locally. It may be necessary to bend the cable in different planes to effect complete adhesive failure.

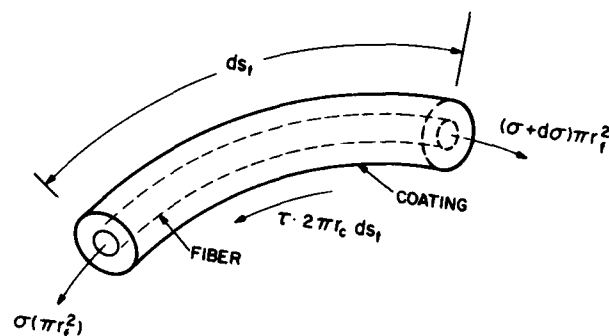


Figure 10: Force equilibrium on embedded fiber element during cable bending.

#### Breaking of Fiber on Bending To Small Radii

Optical fibers embedded in the stiffer elastomers broke during bending of the sandwich structure around curvatures of small radius. The radii at which fibers broke in a particular elastomer are given in Table II. Breakage appeared to be associated with the tendency to buckle locally with very small bending radii at a weak point in the elastomer medium. In PES and PU elastomers this local buckling occurred at a sandwich radius of about 0.8 to 1.4 cm at which point the fiber compressive strains are estimated to be 3.5 to 6.5%. Fiber breaks occurred at intervals of 1 to 2.5 cm along the fiber axis with an audible shattering and the fiber ends at the breaks were pulverized. This effect was also observed in the SBS sample, but the distance between the fiber breaks was about 2 to 3 cm. Optical fibers embedded in the soft SEBS elastomers did not break on bending around a radius of 0.8 cm. At this radius, the fiber moved freely (slipped) within the SEBS and followed the curvature without failure. We did not use smaller radius forms because the 0.8-cm radius bends already resulted in stresses that exceeded the elastic limit of the PET substrate sheets.

## SUMMARY AND CONCLUSIONS

1. A very strong relationship exists between the modulus of the elastomer and the critical radius of curvature (or critical compressive strain in the fiber) at the onset of buckling. In the lowest modulus elastomer tested (sample A,  $E = 0.97$  MPa) buckling occurs at an estimated fiber compressive strain of 0.18% whereas in the highest modulus elastomer (Sample I,  $E = 51.7$  MPa) no buckling is observed at estimated compressive strains approaching 7%. The high modulus elastomers stabilize the fiber by inhibiting lateral deformation.
2. The adhesion and frictional stresses between the coated fiber and the elastomers studied varied widely. The PU elastomers exhibited very high adhesion to the coated fiber, while the SEBS elastomers exhibited low adhesion.
3. A mechanism of fiber failure was observed when the sandwich structure was bent with small radii of curvature. The effect occurs in high modulus elastomers which have strong adhesion to the fiber coating. In these cases, the buckling or slipping modes of compressive strain relief are unavailable to the fiber. As a result high compressive strains in the fiber, estimated to be 3 to 7%, cause highly localized, sudden buckling. These buckles have extremely small radii of curvature resulting in very large tensile strains on the fiber. The fiber breaks immediately with considerable fragmentation and an audible sound.

## ACKNOWLEDGMENTS

The authors wish to thank M. R. Santana for his valuable guidance and suggestions concerning the analysis of results obtained in this work. In addition we appreciate the efforts of M. R. Santana, E. Scalco and R. D. Tuminaro who critically reviewed the manuscript.

## REFERENCES

- [1] R. F. Gleason, R. C. Mondello, B. W. Fellows and D. A. Hatfield, "Design and Manufacture of an Experimental Lightguide Cable for Undersea Transmission Systems," Proc. 27th Int. Wire and Cable Symposium, (CORADCOM, Fort Monmouth, NJ), Cherry Hill, NJ, November 16, 1978, pp. 385-9.
- [2] U. C. Paek and C. M. Shroeder, "Calculation of Photopolymerization Energy Required for Optical Fiber Coating," Appl. Opt., 20, 1230 (1981).
- [3] S. Timoshenko and J. M. Gere, *Theory of Elastic Stability*, McGraw-Hill, New York, N.Y., 1961, pp. 94-8.
- [4] M. R. Santana and G. M. Yanizeski, "Bending Performance of Fiber-Optic Cable Sheaths: Application of New Apparatus and Techniques", J. Mech. Design, 104 578 (1982).
- [5] M. Lutchansky, "Axial Stresses in Armor Wires of Bent Submarine Cables," J. Eng. for Ind., 687 (1969).



Lee L. Blyler, Jr. is a supervisor of the Plastics Applied Research, Properties and Processing Group at Bell Laboratories, Murray Hill, New Jersey. He received his PhD degree in Aerospace and Mechanical Sciences from Princeton University in 1966. He joined Bell Laboratories in 1965 and has carried on work in polymer rheology and processing and optical fiber coating.



Czeslaw Gieniewski undertook undergraduate studies in chemistry at Derby and District College of Technology in Derby, England and received a B.Sc. degree in chemistry from Upsala College in 1956. He has also taken graduate studies at the Polytechnic Institute of New York and at Seton Hall University. He joined Bell Laboratories in 1958 and carried on work in several areas of polymer materials research and development.



Xina Quan received SM and SB degrees in chemical engineering from MIT and is currently a doctoral candidate at Princeton University working on interfacial studies of polymer blend and copolymers. She is a member of the Plastics Research and Development Department at Bell Laboratories and since 1980 has developed polymer formulations for various telecommunications applications.



Hany Ghoneim received his PhD degree in Mechanics and Materials Science from Rutgers University in 1982. He joined Bell Laboratories in a post-doctoral position in September 1981 and has been involved in modeling of polymer mechanics.

## Design Aspects of Loose Buffer Tube Fiber Optics Cable

Ronald L. Ohlhaber

Belden  
2000 S. Batavia Ave.  
Geneva, IL 60134

The theory and operation of cables which employ loose buffer tubes to contain optical fibers will be discussed. These cables permit tradeoffs between physical strength, temperature range and structural dimensions. Specific examples show how the materials and cable construction can be controlled to yield the desired performance.

## INTRODUCTION

Loose buffer tube fiber optic cable construction has now been employed for a number of years and the resulting cables have performed successfully under wide variety of conditions. Critical to many applications has been the excellent performance properties of these cables with respect to their low or non-existent change in optical attenuation when subjected to high tensile forces or wide temperature ranges. The ability to perform in any set of conditions can be related back to the basic cable design and construction.

Understanding of a loose buffer tube cable's performance requires knowledge of the many parameters associated with the cable construction. Earlier papers have described and explained many of the basic properties, however, they typically did not address in detail some of the design tradeoffs such as relationship between buffer tube dimensions and fiber types.<sup>1-4</sup>

This paper presents cable models for various physical constructions and includes experimental tests, plus the associated tradeoffs possible. The ranges for excess fiber and related attenuation will be obtained from elementary cable models based on a straight buffer tube and when the tube is in a cable helix. This analysis will further permit predictions of the lowest temperature at which a cable can operate successfully. While this paper presents results for multi-mode optical fibers, the physical analysis is also applicable in part to cables which contain single mode fibers.

## PHYSICAL CABLE MODEL

## Buffer Tube Operation

Before discussing a single or a multifiber cable, analysis of the fiber and its immediate containment element, the buffer tube, will form the basis for understanding of more complex structures. It is the interaction of the fiber with the tube that produces the limits of cable performance. For most multimode fibers, the forces that the fiber experiences result in an increased attenuation due to microbending. The degree of microbending is a function of the relative change in length

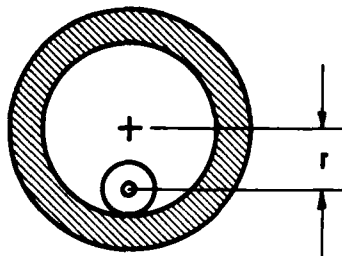


Table 1. Fiber inside a buffer tube.

between the fiber and that of the buffer tube. Also of consequence is the frictional forces between the fiber and tube.

It is also known that as the tube contracts or expands due to changes in temperature, the fiber must move into a curved path or take the form of a helix inside the tube. Therefore, the amount of excess fiber or fiber shortage becomes the governing criterion for operation. In addition, the inner buffer tube surface should be extremely smooth and the fiber to tube coefficient of friction very low.

The fiber and tube relationships for optical transmission depends on the type of fiber, its outer diameter, the tube inner diameter, and the coefficient of friction. To define the space available for the fiber inside the tube, a radius  $r$ , between the center of the tube and the fiber center can be employed. This radius as indicated in Figure 1, is established by taking one half the difference of the tube inner diameter and the fiber outer coating diameter. The  $r$  values for various tube and fiber combinations are given in Table 1.

Table 1. Fiber and tube dimensions

Tube I.D.	Fiber O.D.	$r$	Diameter Ratio
1.2 mm	0.5 mm	0.35 mm	2.4
1.2	0.25	0.475	4.8
1.0	0.5	0.25	2.0
1.0	0.25	0.375	4.0

In addition to the coated outer diameter of the fiber, the fiber's core, cladding, and refractive index difference, all contribute to its microbending sensitivity. By using studies such as Stueflotten's, it is possible to relate the amount of excess fiber length in the tube to the induced optical attenuation for various fiber outer diameter to tube inner diameter combinations<sup>5</sup>. Figure 2 shows one set of such relationships

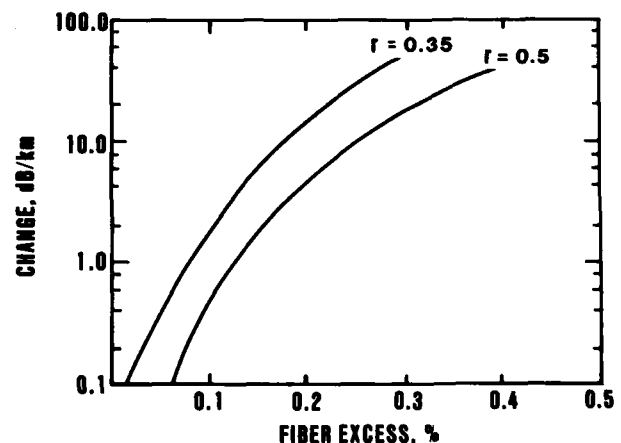


Figure 2. Induced fiber attenuation as a function of excess fiber length.

for typical multimode 50 micron core, 125 micron clad, graded index fibers. For these combinations it is assumed that there is an extremely low coefficient of friction between the fiber and the inner tube wall. As can be seen, the fiber attenuation increases rapidly once the excess reaches about 0.2%. A general model guideline for the case of the 250 micron O.D. 50/125 micron fiber in 1.2mm I.D. buffer tube, is to employ a 0.5 dB/km attenuation increase for 0.1% fiber excess and a 4 dB/km increase for 0.2% excess.

To confirm such a model it is possible to temperature cycle a tubed fiber. However, this usually requires that the tube be in a coil or on a reel. The effect of the coiled tube gives the fiber an additional degree in freedom of moving from the inner to the outer inside wall of the tube. This, in effect, produces a range of temperatures over which the fiber experiences virtually no forces. This range is established by the difference in and expansion coefficient between the tube and fiber, and the coil radius.

To obtain consistent results, the initial length of the fiber to that of the tube must be known. This length difference is termed the initial excess, IE, and is established during the manufacturing process. Figure 3 shows the ranges of temperatures that can be obtained for various radii tube coils with an expansion coefficient difference of 5 E-5/°C, when starting with a 0.1% initial excess at 20°C and a tube I.D. to fiber diameter ratio of 4.8.

To account for the condition of tube expansion with respect to the fiber during high temperatures an identical model could be used to indicate increased attenuation when the fiber has been pulled tight to a given percentage against the inner tube wall. This is the dashed portion of the curve in Figure 3. Due to the high temperatures

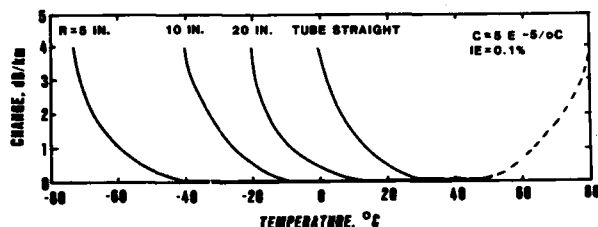


Figure 3. Induced loss for a 50/125/250 fiber inside a buffer tube coiled at various radii, R.

predicted, the upper limit is often impossible to achieve. Also, the exact response of a fiber to tension in a smooth tube has not been fully predicted. It is usually a state that is advantageous to avoid and is often prevented from occurring by the cable structural elements.

#### Cable Operation

When the buffer tube containing the fiber becomes part of a cable, two additional factors must be considered. They are the effective change in expansion coefficient of the tube due to other elements such as the cable strength members and jacket. Also the helix formed when the buffer tube is stranded around a central member must be considered for certain constructions.

The expansion coefficient of the overall cable structure depends not only on the coefficients of the various materials, but also on Young's modulus for each material. For example, in a cable with a large steel strength member, the resulting expansion coefficient may be close to that of steel. A simple model for combined materials yields the following relationship for the resulting expansion coefficient.

$$C = \frac{C_1 A_1 Y_1 + C_2 A_2 Y_2}{A_1 Y_1 + A_2 Y_2}$$

Where  $C_1$  and  $C_2$  are individual material coefficients,  $Y_1$  and  $Y_2$  are the associated Young's moduli, and  $A_1$  and  $A_2$  are the cross sectional areas.

For single fiber cable where the buffer tube is longitudinally combined with some strength member and outer jacket, the performance is similar to that of the buffer tube alone modified by the cable expansion

coefficient. Here again the resulting cable is typically tested in a coil and the effect of the coil radius must be considered in obtaining an accurate estimate for a linearly deployed cable. The solid curves of Figure 4 show the predicted results for one such structure where the cable consists of a Kevlar\* strength member and an outer PVC jacket when in a coil of radius 10 in. and also straight. For this cable, the negative coefficient of the Kevlar restricts its expansion at elevated temperatures and therefore reduces the induced attenuation change. A reduction in the initial fiber excess from 0.1% to 0.0% at 20°C, also shifts the cable operating range by approximately 20°C as shown by the dashed curve. A positive increase in the initial fiber excess of 0.1% would have produced a corresponding shift in the operation range toward higher temperatures.

The model for Figure 4 assumes that there is an initial excess of 0.1% in the fiber length when the temperature is 20°C. With an overall

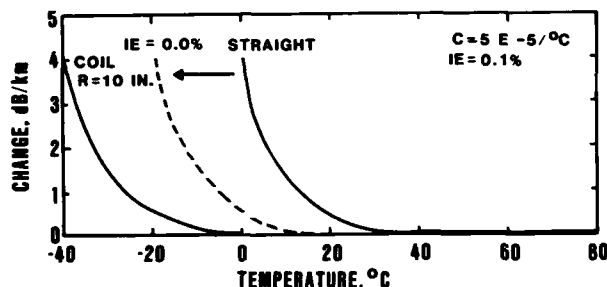


Figure 4. Model single fiber cable in straight or coiled form. Dashed curve shows response when changing from 0.1 to 0.0% fiber excess.

expansion coefficient of 5 E-5/°C, the cable quickly produces a fiber excess of 0.2% when the temperature decreases by 20°. While the initial 0.1% excess limits the lower temperature performance, it also permits some cable elongation without any load being applied to the fiber. Such elongation must be considered since it usually occurs when the cable is pulled during installation.

In reality, the elongation during installation may far exceed the 0.1% and actually stretch the fiber to some amount of its proof test value. The specified value for fiber or cable elongation will depend on an individual cable design. However, the long term fiber stress should be zero or some small percentage of the proof test value.

The single fiber cable construction identifies some of the unique properties which must be analyzed when working with optical cable design. For example, a cable with Kevlar for a strength element may structurally break at a pulling force of 1000 lbs. However, to reach this failure point, the Kevlar will elongate approximately 2.4%. This means that for an elongation of only 0.3%, a force of 125 lbs. need be applied. Such loading may occur during installation. This indicates the relationship between the amount of excess fiber in the buffer tube, and the resulting temperature range can vary substantially for a single fiber cable when installed with a residual stress.

Multifiber cables where the buffer tubes are stranded around a central member require employment of all the prior considerations, plus the fiber's have an additional range of freedom due to the helical configuration of the tubes. To analyze such cables, the additional amount of cable expansion or contraction before the fiber accumulates excess or is pulled tight in its tube must be determined. One method is to consider the additional change of length in terms of a relative excess, RE, available for the fiber. This range can be computed from the geometrical radius of the tube helix, RH, and the lay length, along with the tube and fiber dimensions. Figure 5 shows the relative excess values obtained for various cables with different helix radii and fibers with a 0.25 and 0.5 mm outer diameter.

The amount of relative fiber excess can further be related to the change in cable length due to temperature variations or tensile loading. It can be considered the percent change of length in the cable over which the fiber's attenuation is not affected by an accumulation or shortage of fiber in the buffer tube. When considering temperature alone

\*Trademark of DuPont

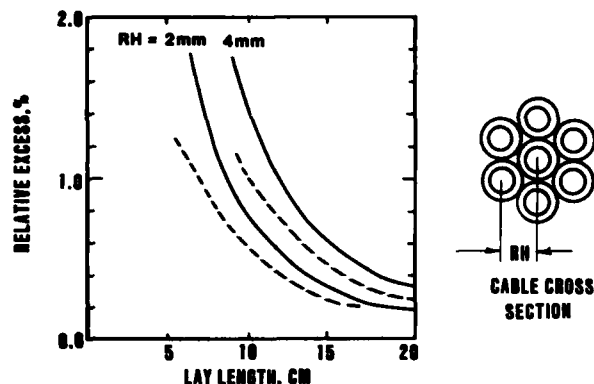


Figure 5. Relative excess for fiber in buffer tubes with various lay lengths. Solid curves indicate performance for a cable with a helix radius of 2 or 4 mm and tube I.D. to fiber O.D. ratio of 4.8. Changing fiber O.D. from 0.25 to 0.5mm results in shift to dashed curves.

the cable can expand and contract over this range. Consequently, this temperature range,  $TR$ , is then a function of the cables expansion coefficient,  $C$ , and related by  $TR = RE/C$ . Figure 6 indicates some of the range possible for cables with various expansion coefficients.

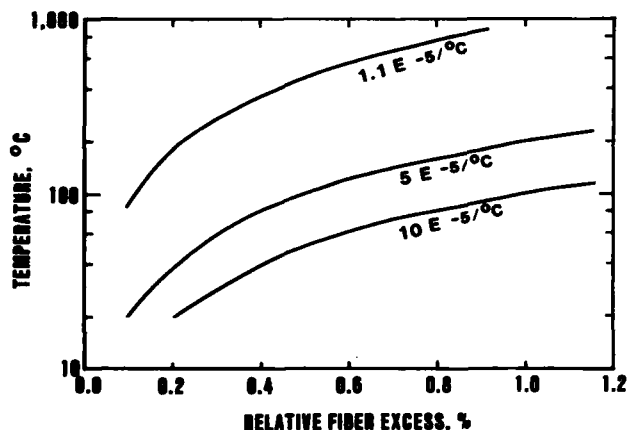


Figure 6. Temperature range for various cable expansion coefficients with a given relative excess.

While the relative excess can lead to a temperature range, the location of such a range for operation is also crucial. For a buffer tube with no excess fiber, the amount of apparent excess due to its cabling is not generally the same for contraction as for its expansion. In addition by varying the initial excess fiber in the tube the temperature range can be shifted. The magnitude of this shift is dependent on the total cables expansion coefficient.

Calculations for a six fiber cable using the relative excess for cable contraction when the temperature is reduced show the results in Figure 7. Here the change in fiber attenuation is obtained by determining the temperature where the cable has reduced its length so that the fiber experiences an actual excess in the buffer tube resulting in microbending loss. The sets of curves show the difference obtainable with two fiber sizes in the same cable construction. Also the change in low end temperature is evident for tubes starting with 0.1 and 0.2% initial excess fiber length. For this cable design, the high end temperature exceeds the 80°C limit.

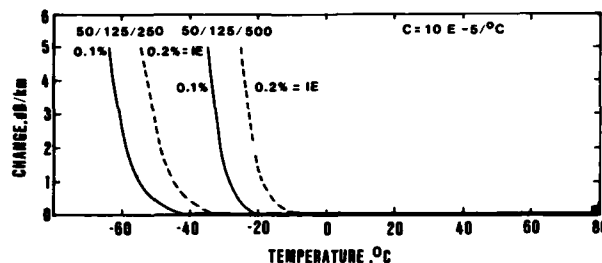


Figure 7. Six fiber cable design performance for two fiber sizes. Buffer tube lay length is 7.6 cm and the helix radius 2mm. Curves show range for either 0.1 or 0.2% initial excess.

Through such considerations it is possible to analyze a variety of cable constructions. As a summary, Table 2 presents the cable and fiber properties which may be required. While the prior discussion was based primarily on the graded index 50/125 coated multimode fiber, the method can be applied to other fiber types and sizes, when their interaction with the buffer tube is known. In addition, since microbending induced attenuation is approximately constant at optical wavelengths from 850 to 1,500 nm in graded index fibers, the results pertain to numerous potential applications.

Table 2. Cable Design Factors

1. Buffer Tube and Fiber
  - 1.1 Expansion coefficients
  - 1.2 Fiber bending sensitivity
    - Core and cladding diameters
    - Core to cladding ratio
    - Refractive index profile
    - Outer coating material
  - 1.3 Fiber to tube friction
  - 1.4 Initial excess fiber in tube
  - 1.5 Tube coil radius when testing
2. Additional Cable Parameters
  - 2.1 Buffer tube helix radius
  - 2.2 Tube helix lay length
  - 2.3 Expansion coefficient
  - 2.4 Tensile elongation limits
  - 2.5 Shrinkage

## EXPERIMENTAL RESULTS

The low temperature response for a fiber in a coiled buffer tube with an expansion coefficient on the order of  $7 E-5/°C$  is the solid curve in Figure 8. Also shown are two theoretical curves for fiber in tubes

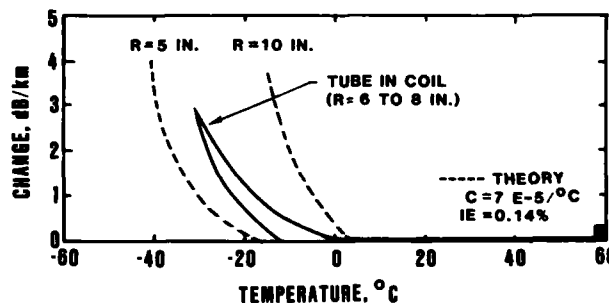


Figure 8. Temperature induced attenuation for a 50/125/250 fiber in a coiled buffer tube.

with coils of smaller and larger radii. All results are for a 50/125/250 micron fiber in a 1.2 mm I.D. low friction tube where there is 0.14% excess fiber in the tube at 20°C.

For six buffer tubes cabled around a central member, a number of cable materials and operational properties are possible. Figure 9 shows the results for three such cable combinations. Here excellent performance from +80 to -55°C is possible by employing a central fiberglass epoxy rod. Similar results are also obtainable with steel central elements. In all cases, the same graded index 50/125 fiber and same 1.2 mm I.D. buffer tubes with a 7.6 cm lay length and 2 mm helix radius were employed.

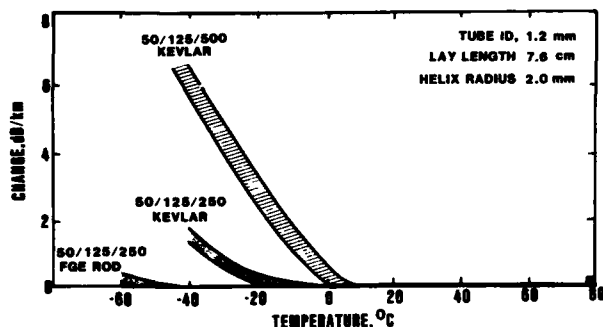


Figure 9. Experimental data for six fiber cables which have different size fibers and strength member materials.

The remaining two curves show the effect of changing the fiber outer coating dimensions. As expected, the smaller 250 micron O.D. fiber cable had about a 25 to 30°C lower temperature range with respect to the 500 micron O.D. fiber. Both these cables have limited cold temperature performance due to the Kevlar central element permitting a relatively high level of contraction. For high temperatures the performance is similar for all cables and an 80°C upper temperature is easily achievable.

For these cables the buffer tubes started with fiber excess values of over 0.1%. If the initial excess was decreased to zero or a negative value, the temperature range will be shifted to lower levels by approximately 10°C for each 0.1% change. Such changes toward negative excess must be analyzed, since consideration must also be given to the elongation which occurs when the cable is under tension during installation. The amount of safe tension for a cable requires calculation of the elongation when at its maximum installation temperature and then relating this value to the effective tension produced on the fibers.

## CONCLUSION

The design of fiber optic cables containing loose buffer tubes or any loose containment arrangement can be guided by the use of calculations which predict the physical forces and resulting configuration of the fiber. For buffer tube confinement, the movement of the fiber when it experiences a condition where it is pressed to the tube wall results in a rapid increase in attenuation. The conditions for such a case are usually produced when the cable and tube contracts, so that the fiber has passed through a region of relative freedom to a state where 0.2% or more effective excess has accumulated.

To predict performance ranges and associated physical properties requires the use of both the buffer tube geometry plus the use of the materials structural moduli, and expansion coefficients. In addition, the manufacturing parameters such as the initial amount of excess fiber in the tube at a given temperature must be carefully controlled to 0.1% if the desired temperature range is to be achieved. While many parameters must be considered for good cable design, a careful choice will lead to cables which have adequate temperature ranges and suitable limits for installation.

## REFERENCES

1. T.F. Lehman, R.K. Birkhead, and D.W. Williams, Proceedings FOC-81 East, March 24-26, pg. 87, 1981
2. M.M. Rahman, H.K. Eastwood, P. Rivett, and M. Herrera, Proc. 29th. International Wire and Cable Symposium, pg. 386, 1980.
3. U. Oestreich, G. Feidler, P.R. Bark, and D.O. Lawrence, Proc. 29th International Wire and Cable Symposium, pg. 394, 1980.
4. G.S. Anderson, Proc. 30th International Wire and Cable Symposium, pg. 127, 1981.
5. S. Stuefflotten, Applied Optics, 21, pg. 4300 (1982).



Ronald Ohlhaber received a B.S. Degree in Physics from Loyola University and a M.S. Degree, also in Physics, from Depaul University in 1965. He is presently the Product Development Manager for Fiber Optics located at Belden's Technical Research Center in Geneva, Illinois. Prior to joining Belden, he was engaged in fiber optic and electro-optic research as a staff member at IIT Research Institute and also worked in similar areas for the Government and Industry.

## NON-METALLIC OPTICAL CABLE WITH OPTICAL FIBER CATENARY FOR LONG SPAN AERIAL APPLICATION

E. HAYASAKA\*, F. OHTSUKA\*, M. MONMA\*, S. OHIRA\*  
 H. HORIMA\*\*, K. YAMASHITA\*\*, M. DAZAI\*\*, N. ABE\*\*\*

\* THE TOHOKU ELECTRIC POWER CO., INC. 3-7-1, ICHIBAN-CHO, SENDAI 980, JAPAN  
 \*\* SUMITOMO ELECTRIC INDUSTRIES, LTD. 1, TAYA, TOTSUKA-KU, YOKOHAMA 244, JAPAN  
 \*\*\* KITANIHON ELECTRIC WIRE CO., LTD. 1-2-1, KORIYAMA, SENDAI 982, JAPAN

Abstract

A non-metallic prehanger type self-supporting optical fiber cable with optical fiber catenary was developed and is considered to have a long-term operating capability under high tension and abnormal freak weather conditions. The non-metallic optical fiber cable is intended to be extremely effective for long span aerial cable mounting on all types of overhead poles and power transmission towers. Moreover, this type of cable has particular resistance to the accumulation and forming of ice or snow on the cable sheath which was observed during field test investigations.

1. Introduction

Ever since the advent of optical fiber cable, the electric power utilities which have early focussed attention to its superior features of low loss, wide bandwidth and non-inductivity have promoted positively the introduction of optical fiber cable to line of practical use. Although the overhead installation of these optical cables was principally conducted on power distribution lines which involve little restriction with respect to construction, when studying the construction of long distance optical transmission line that aims for the comprehensive communication network of the future, the utilization of overhead power transmission line of higher stability as transmission route can be considered as suitable. Thereby, the development of optical fiber/ground wire composite cable (OPGW) that contains the optical fiber in the ground wire was conducted (1).

In conducting the application of OPGW to existing power transmission line, there is the restriction relevant to works such as the operation of shutting down power supply. And to stretch around the optical fiber cable thoroughly utilizing the power transmission line, the method of installing optical fiber cable on power transmission steel towers that enables further flexibility of compatibility can be considered. Against such method, in case that the self-support type optical fiber cable used in practice for power distribution line is installed on power transmission steel towers, the following problems can be newly considered. Thereby, the application in reality was not conducted.

- (1) Because of using metal for suspension wire, insulation is difficult. And in the case of contacting the conductor of power transmission line, there is the fear of producing ground fault.
- (2) Because of the long span, there is the need to increase the size of suspension wire. Thereby the need arises to modify the steel towers.
- (3) Induced voltage is produced in the metal part of suspension wire offering the anxiety for securing the safety in conjunction with construction and maintenance.

In view of the above, the development of non-metallic optical fiber cable for long span that does not use at all metal in the cable composite was strongly called for.

Due to the background mentioned above, using FRP (Fiber Glass Reinforced Plastic) for the suspension wire, the non-metallic self-support type optical fiber cable used for installation on long span steel towers which has fully taken advantage of small diameter, light weight and insulation merit which are the essential features of optical fiber cable was developed this time.

Herein, the authors wish to deal with the design, manufacture, the result of evaluating the characteristics of non-metallic optical fiber cable for long span developed this time and the installation of such optical fiber cable as well as to report that the perspective was obtained for the application of this cable to practical use line.

2. Outline of non-metallic optical fiber cable for long span (2) (3)2.1 The target of development of cable

The following content can be considered as the characteristic requested in the optical fiber cable used for installation on steel towers.

- (1) From the viewpoint of securing the safety relevant to construction and maintenance, the non-metallic composition using no metal at all in the optical fiber cable composite must be assured.
- (2) In the stringent environment of installation on steel towers, the characteristics of optical

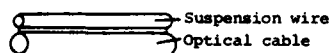
fiber cable must be guaranteed over a long period of time.

- (3) The mechanical strength of the optical fiber cable must be large and its installation works must be possible to be conducted readily.
- (4) Being of light weight and small diameter, the construction difficult to permit accretion of snow must be incorporated.
- (5) The construction must be simple permitting readily the manufacture.

The target was set to develop the non-metallic optical fiber cable for long span that satisfies the requirements mentioned above.

## 2.2 Design concept of optical fiber cable

When studying the non-metallic overhead optical fiber cable following the design concept of self-support type optical fiber cable using steel wire for the suspension wire, the composition of type SSD (8-figure type), type SSF (lashing type) and type SSS (stranding type) respectively shown in Fig. 1 (a) ~ (c) can be considered first. As the material of suspension wire against such cable, although FRP or Kevlar® rod provided with high Young's Modulus is assured for practical use, the Young's Modulus of these non-metallic rod is some  $1/4 \sim 1/3$  being small compared to Young's Modulus of steel wire. Therefore to guarantee the long life of optical fiber cable, tension applied on the optical fiber cable must be restricted as small as possible. Also to realize the installation condition (tension and sag) being the same as that of self-support type optical fiber cable using the suspension wire of steel wire, FRP or Kevlar® rod provided with the outer diameter of some 2 fold compared to steel wire size must be used. Thereby, outer diameter of optical fiber cable increases, the wind pressure load thereby increases, the flexibility of optical fiber cable drops hence resulting in the increase of cable cost. Thus the cable becomes impractical for use. To solve these problems, pursuing the means of absorbing the elongation of optical fiber cable and studying the cable construction that prevents the increase of suspension wire size, the non-metallic self-supporting optical fiber cable that ensures the practical use was successfully developed.



(a) Type SSD (8-figure type)



(b) Type SSF (Lashing type)



(c) Type SSS (Stranding type)

Fig. 1  
Drawing showing  
the construction  
of self-support  
type optical  
fiber cable

Figure 2 shows the design conceptional drawing of non-metallic optical fiber cable for long span developed this time. The suspension wire constituted by FRP rod or the like is arranged in parallel with the round type non-metallic optical fiber cable. And the suspension wire and optical fiber cable are fixed by plastic connection piece at locations each with a constant spacing. Thereby the so-called pre-hanger formation (4) is arranged for which the development has been pushed forward by the group centering the Tohoku Electric Power Co., Inc. In this formation, the design is conducted to have the optical fiber cable form the catenary configuration against the suspension wire between the plastic connection pieces. As the result, the fiber cable itself is arranged to be longer by some 0.5% compared to the suspension wire. In this cable, until the suspension wire elongates over some 0.5%, the optical fiber cable does not sense the elongation, and then the optical fiber becomes subjected to strain following the elongation of the suspension wire. This means that Young's Modulus of FRP suspension wire equivalently becomes larger by 3 to 4 times in a small elongation of less than 1%. Thereby, despite using FRP rod for the suspension wire, without increasing the outer diameter of optical fiber cable in comparison with the optical fiber cable using the conventional steel wire for the suspension wire, the design of non-metallic overhead optical fiber cable provided with small diameter, light weight and ample tension was made possible.

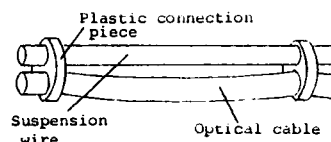


Fig. 2 Appearance of non-metallic optical fiber cable for long span

As the deformation of cable shown in Fig. 2, the construction of non-metallic optical fiber cable shown in Fig. 3(a) or (b) which is similar to the SSS configuration shown in Fig. 1(c) can be considered as the objective of reducing the wind pressure load. Figure 3(a) is such that against the optical fiber cable itself provided with the spacing  $P$  of plastic connection piece, the optical fiber cable is twisted for  $180^\circ$  at the location of  $1/2 P$  where fixation is made by the plastic connection piece. At the condition twisted as such, design is conducted so that slackness likewise exists in the optical fiber cable for some 0.5% in comparison with the suspension wire. Although Fig. 3(b) is of the design based in the same concept, in contrast with Fig. 3(a) in which twist of optical fiber cable is available in one direction of S or Z direction, Fig. 3(b) has the reversing twist of SZ conducted. Nonetheless, in such twisted configuration of cable, since the optical fiber cable sustains a substantial squeezing force near the location where the suspension wire and optical fiber cable cross each other by the cable passing along pulley explained later, there is the need of adopting a very strong optical

fiber cable mechanically.

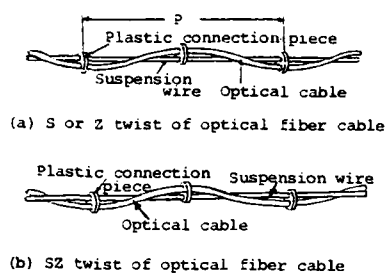


Fig. 3 Drawing showing the appearance of non-metallic optical fiber cable for long span similar to SSS

### 2.3 Design of suspension wire size and sag rate of optical fiber cable

Although FRP or Kevlar® rod can be considered for the suspension wire as mentioned previously, from the viewpoint of readiness of connection with the dead-end clamp and cost, FRP rod was chosen for the suspension wire. Furthermore, in order that, the tension imposed on FRP rod at the worst wind pressure load condition anticipated in the environment of installation becomes less than 40% of its break-down tension, the size of FRP rod was chosen. This tension corresponding to 40% corresponds to FRP creepage of  $0.1\%/10^4$  hours permitting as well to secure the factor of safety of over 2.5 of the optical fiber cable. On this occasion, although the maximum allowable elongation of optical fiber cable under the worst load condition was defined as 0.2% herein, the sag rate of the optical fiber cable itself is set so that the elongation becomes less than this 0.2%. In the optical fiber cable designed as such, the long period life not only for FRP but also for optical fiber cable becomes to be guaranteed. Now let us put the above-mentioned in order. As regards the optical fiber cable of the type developed this time, by choosing suitably the suspension wire size and sag rate of optical fiber cable from the parameters relevant to construction, the optical fiber cable that permits the installation with little tension in case dip can be taken fully is designed. On the contrary, design is conducted for the optical fiber cable of little dip in case the strength of steel tower is large. Thus, complying with the condition of power transmission line, the optimum performance of optical fiber cable can be expected to realize readily.

In the case of setting the FRP size and sag rate of optical fiber cable itself against a variety of span for the outer diameter of optical fiber cable itself set as 9.5mm and its weight set as 60kg/km, the result of calculating tension and dip of the respective temperatures at the load condition of no wind and no snow accretion, is shown in Table 1. Also the physical constants of FRP used then are summarized in Table 2.

Table 1 Result of calculation of installation parameters

Span of steel towers (m)	300	400	500	600	700
FRP suspension wire size (mm)	5	8	10	10	12
Sag rate of fiber cable itself (%)	2.5	2.5	2.7	2.5	2.7
Factor of safety of fiber cable	over 2.5	over 2.5	over 2.5	over 2.5	over 2.5
At times					
without the					
load of					
wind and					
snow					
accretion					
-20°C					
dip (m)	4.82	2.33	3.31	5.04	1.23
tension(kg)	431	493	708	405	2,288
+10°C					
dip (m)	5.06	2.42	5.11	5.39	2.28
tension(kg)	411	459	710	366	2,232
-20°C					
dip (m)	5.31	2.52	5.43	6.15	2.24
tension(kg)	392	426	742	329	2,174
+40°C					
dip (m)	5.36	2.63	5.65	6.42	2.40
tension(kg)	375	473	755	304	2,123
-60°C					
dip (m)	5.31	2.74	5.39	6.71	2.47
tension(kg)	358	460	729	281	2,068

Table 2 Physical properties of FRP rod

Items	Physical property value
Young's Modulus (kg/mm)	4,800
Maximum elongation (%)	2.2 ~ 2.3
Bending strength (kg/160mm)	135
Compression strength (kg/cm)	306
Thermal expansion coefficient (1/°C)	$2.0 \times 10^{-6}$

### 2.4 Design is concrete of optical fiber cable

With the premise set to install on power transmission steel towers provided with the span of some 300m, 5 kinds of non-metallic optical fiber cable as shown in Table 3 were designed and manufactured. The respective cables of No. 1 ~ No. 3 are such that their optical fiber cable core is jointly installed with the suspension wire and only the construction of optical fiber cable core itself differs. The spacer constructions applied to the optical fiber cable core of No. 2 and No. 3 are the optical fiber cable construction developed by Sumitomo Electric Industries, Ltd. (6) (7). The presence of its superior transmission characteristics and mechanical characteristics is reported. Although the construction of optical fiber cable core of No. 4 and No. 5 is the same as that shown in No. 2 cable, as shown in Table 3, the optical fiber cable core is twisted only in one direction for 180° for every fixed interval or twisted alternately. Since this optical fiber cable is not exposed to high temperature environment, the 0.9mm standard nylon coated fiber with core diameter 50µm, cladding diameter 125µm and silica type graded index of refractive index difference of 1% can be normally applied intact. FRP rod of 8mm is used for the suspension wire and black polyethylene (PE) jacket is applied to protect against UV radiation. Although the spacing of PE connection piece was designed for 500mm, this spacing was determined with consideration given to installation and aesthetic appearance. Nonetheless, the degree of freedom for design is

retained. The sag rate of the optical fiber cable itself against the suspension wire was set as 0.5%. Outer diameter of respective cables is 10mm and height is 21.5mm. Also the weight is some 0.19kg/m. Thermal expansion linear coefficient is  $7.67 \times 10^{-6}$  1/°C. Based on the characteristic evaluation result against respective cables, the features of the respective cables are described in Table 3. Photo 1 shows the appearance of grooved-spacer type 8-fiber cable (S) and Photo 2 shows its side appearance.

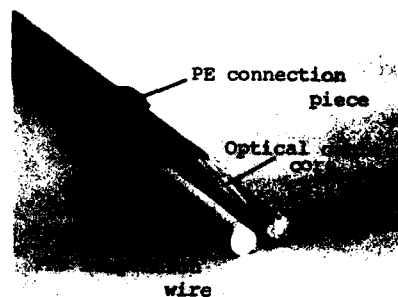


Photo 1  
Appearance of  
grooved-spacer  
type 8-fiber  
cable (S)

Table 3 Design in concrete of cable and its features

No.	Cable type	Manu- fac- ture length	Cross sectional construction of cable	Side face construction of cable	Features of cable
1	Stranded type 4-fiber cable(S)	1,000		 Suspension wire and cable itself are jointly in- stalled.	Manufacture of cable is very easy. Attachment of cable slackness is easy. Design of small diameter and multi-fiber is very easy. Cable itself is little soft mechanically. At extremely low temperature, loss temperature character- istic poses problem.
2	Tape- spacer type 4-fiber cable(S)	800		 Suspension wire and cable itself are jointly in- stalled.	Manufacture of cable itself is very easy. Attachment of cable slackness is easy. Design of small diameter and multi-fiber is somewhat difficult. Mechanical strength of cable itself is large. Loss temperature character- istic is stable.
3	Grooved- spacer type 8-fiber cable(S)	150		 Suspension wire and cable itself are jointly in- stalled.	Manufacture of cable itself is easy. Attachment of cable slackness is easy. Design of small diameter and multi-fiber is easy. Mechanical strength of cable itself is very large. Loss temperature character- istic is stable.
4	Tape- spacer type 4-fiber cable(T)	300		 Cable itself is twisted 180° in one direction for every fixed interval.	Manufacture of cable itself is easy. Twisting of cable is rather difficult. Crossing point of cable and suspension wire is likely to sustain mechanical damage. Loss temperature character- istic is stable.
5	Tape- spacer type 4-fiber cable(S2)	300		 Cable itself is twisted 180° in left and right alternately for every fixed interval.	Manufacture of cable itself is easy. Twisting of cable is rather difficult. Crossing point of cable and suspension wire is likely to sustain mechanical damage. Loss temperature character- istic is stable.

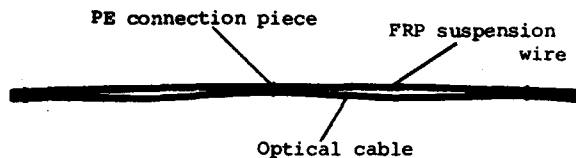


Photo 2 Side appearance of newly developed non-metallic optical cable

### 3. Characteristics of cable

5 kinds of cables shown in Table 3 were manufactured and evaluation of transmission and a variety of mechanical properties was conducted. Thereby the characteristics of non-metallic optical fiber cable for long span were grasped. The VAD fibers that possess superior transmission characteristics (8) were used for the manufacture. The authors herein wish to report mainly on the stranded type and the tape-spacer type optical fiber cables.

#### 3.1 Variation of transmission loss between the respective manufacturing processes

The transmission loss between the respective manufacturing processes was measured at both short and long wavelengths. The result of measurement is shown in Fig. 4. By integrating the suspension wire and cable itself by PE connection pieces and by forming the periodic catenary of the cable itself between those PE connection pieces, the manufacture of stable cable without deteriorating, especially the transmission characteristics was ascertained even after the process that applies reversing twist to the cable itself.

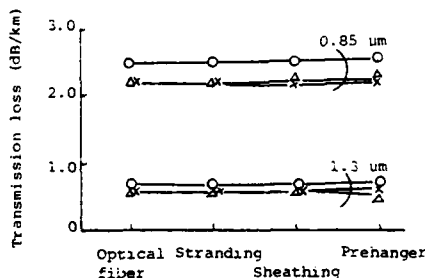


Fig. 4 Result of measuring transmission loss during manufacturing processes

whereas, in the above drawing,

- : Stranded type 4-fiber cable (S)
- △ : Tape-spacer type 4-fiber cable (S)
- × : Tape-spacer type 4-fiber cable (SZ)

#### 3.2 Temperature characteristics of transmission loss

Holding the cable in the temperature controlled chamber, the variation of transmission loss in the temperature range of  $-30^{\circ}\text{C}$  ~  $+60^{\circ}\text{C}$  was investigated using LED light source with the emitting wavelength

of  $0.85\mu\text{m}$ . Temperature was let to change as  $+20^{\circ}\text{C}$  +  $-30^{\circ}\text{C}$  +  $+60^{\circ}\text{C}$  +  $+20^{\circ}\text{C}$  and the variation of light output level during the above temperature change was continually recorded. The result of measurement for the tape-spacer type 4-fiber cable (S) and (SZ) is shown in Fig. 5. Despite the existence of periodic catenary of cable or twist, both cables had the loss variation maintained within  $\pm 0.1\text{dB/km}$  and their characteristics were very stable. This result indicated no problem in the application to extremely low temperature district.

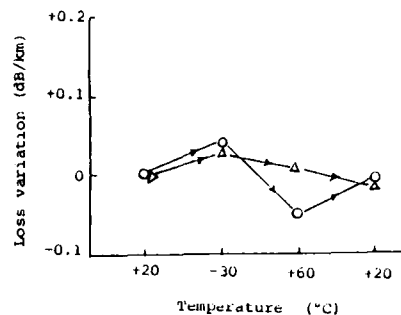


Fig. 5 Result of measuring the transmission loss-temperature variation

whereas, in the above drawing,

- : Tape-spacer type 4-fiber cable (S)
  - △ : Tape-spacer type 4-fiber cable (SZ)
- Measuring wavelength :  $0.85\mu\text{m}$

### 3.3 Physical properties of optical fiber cable

#### 3.3.1 Mechanical properties of optical fiber cable

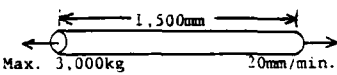
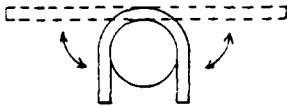
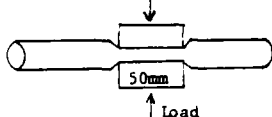
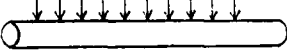
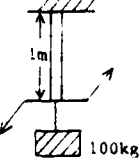
Although the mechanical properties of short length optical fiber cable was investigated first, since marked difference of properties was not made available between the stranded type cable and the spacer type cable, the respective items of mechanical tests conducted against the stranded-type 4-fiber cable (S) and their results are summarized in Table 4. Although all of these tests adopted the stringent conditions close to the limit tests, the deterioration of properties posing a problem in particular was unable to be recognized.

Assuming a very stringent case of installation condition, the stringent squeezing tests for long length (9) as shown in Fig. 6 imposing bending and squeezing force on the cable under high tension were conducted. By having the other end of optical fiber turned back and connected thus forming a loop, the variation of light output level was measured continually during the tests in the measuring cot. The result of measurement for both cables of the tape-spacer type 4-fiber cable (S) and (SZ) is shown in Table 5. Despite the very stringent test conditions applied to the tape-spacer type 4-fiber cable (S), the substantial mechanical strengths were verified to be provided. Such superior properties are greatly due to the special construction such as that by the sag existing in the cable itself, tension applies only on the suspension wire when the cable

passes along pulley with almost no tension applied on the cable itself. On the other hand, in the tape-spacer type 4-fiber cable (SZ), there was a substantial loss variation during the test and the loss did not restore to the original level even after completing the test. This is because a substantial external force applies on the cable at the location where the suspension wire crosses with the cable itself. Therefore against such formation of

the cable being reversed and twisted, it can be considered that there is the need to apply a very robust construction like the construction of the grooved-spacer type 8-fiber cable (S) shown in No. 3 of Table 3. Figure 7 shows the situation of the variation of light output level during the test of 200kg tension. Also it was found that during the installation for both cables, twist of cable was difficult to arise.

Table 4 Mechanical test results of stranded type 4-fiber cable (S)

No.	Test item	Test condition	Test results
1	Tension	 <ol style="list-style-type: none"> <li>Distance between standard points: 1,500mm</li> <li>Pulling speed: 20 mm/min.</li> <li>No. of samples: 3</li> </ol>	<p>No variation of loss of fiber against tension of 3,000 kg.</p> <p>Elongation of FRP suspension wire</p> <p>1,500 kg - 0.6 %</p> <p>3,000 kg - 1.3 %</p>
2	Bending	 <ol style="list-style-type: none"> <li>Mandrel diameter: 500, 800, 1,000 mm</li> <li>No. of times of bending: 10 times of reciprocating bending</li> <li>No. of samples: respectively 2</li> </ol>	No variation of loss against respective mandrel diameters.
3	Compression	 <ol style="list-style-type: none"> <li>Flat plate compressed: 50 x 50 mm</li> <li>Compressive load: Max. 700 kg</li> <li>No. of samples: 3</li> </ol>	No variation of loss up to the compressive load of maximum 700 kg/50 mm.
4	Impact	 <ol style="list-style-type: none"> <li>Impact load: 1 kg, 2 kg, 3 kg</li> <li>Height (drop): 1 m</li> <li>Impact body: metal body of 25 mm</li> <li>Location of drop: 10 different location</li> <li>No. of sample: each one</li> </ol>	Loss variation is less than 0.05 dB even against the impact of 3 kg x 1 m.
5	Torsion	 <ol style="list-style-type: none"> <li>Sample length: 1 m</li> <li>Load: 100 kg</li> <li>Torsional angle: 720°/m</li> <li>No. of sample: 2</li> </ol>	No variation of loss.

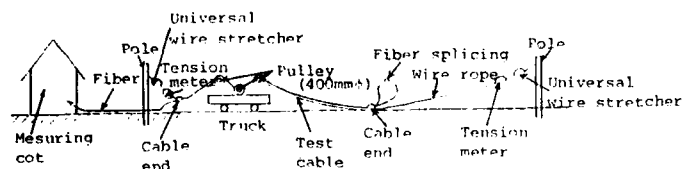


Fig. 6 Method of long length squeezing test

In the above drawing,

Moving speed of truck : some 7 m/min.  
Length of test cable : some 120 m  
Tension : 200kg, 300kg, 400kg

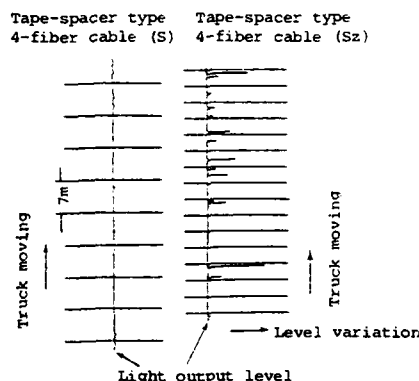


Fig. 7 Light output situation of level variation during long length squeezing test (tension 200kg)

±29mm was applied on the middle part. On this occasion, strain gauge was provided on the suspension wire and the strain applied to the cable was measured.

## (2) Test result

Strain applied to the suspension wire was  $1,600 \times 10^{-6}$  being fairly large. Although the vibration of  $10^7$  cycles was applied to this strain, there was no break not only for the FRP suspension wire but also for the optical fibers. Thus the test by this vibrational no. of cycles was let to complete for good. From this test result, it can be admitted that the vibration fatigue is difficult to arise in non-metallic optical fiber cable compared to the overhead power transmission conductor.

## (2) Measurement of wind induced noise

### (1) Testing method

Applying the predetermined wind velocity to the stranded-type 4-fiber cable (S), the wind induced noise produced was collected by microphone and the noise meter output was subjected to frequency analysis using the 1/3 octave analyzer.

### (2) Test result

Figure 8 shows the test result. In this drawing, the measured data of wind induced noise of ACSR 120mm<sup>2</sup> is shown for comparison. In case wind is blown vertically to both suspension wire and cable itself of the stranded-type 4-fiber cable (S), prominence of wind induced noise was unable to be recognized at the

Table 5 Result of long length squeezing test

### 3.3.2 Vibration characteristics of optical fiber cable

To grasp the vibration characteristics of optical cable in the practical use of non-metallic optical fiber cable used for installing on long span steel towers is very important subject. The result of measuring the vibrational fatigue characteristics, wind induced noise and energy absorbed is explained herein.

#### (1) Vibrational fatigue characteristics

##### (1) Testing method

The 3.9m-long stranded-type 4-fiber cable (S) with the epoxy putty type dead-end clamps described hereafter was set on the vertical type vibration testing machine. 1 ton of load was applied on the dead-end clamp. And the locations of 1m respectively from the middle part of test piece held vertically were fixed and the vibration of 5.5 Hz

Cable type	Test length (m)	Fiber loop No.	Fiber loop length (m)	Tension (kg)	Situation of light output level during test	Loss variation when completing test (dB)	No. of twists of cable (times)
Tape-spacer type 4-fiber cable (S)	100	1	200	200	A slight pulse-like loss variation is available.	-0.03	0
		2			"	0	
		1		300	"	+0.02	0
		2			"	+0.02	
		1		400	"	0	0
		2			"	+0.01	
Tape-spacer type 4-fiber cable (Sz)	120	1	240	200	A fairly large pulse-like loss variation is available.	+0.02	0
		2			"	+0.08	
		1		300	A very large pulse-like loss variation is available.	+0.27	0
		2			"	+0.10	
		1		400	"	+0.38	0
		2			"	+0.07	

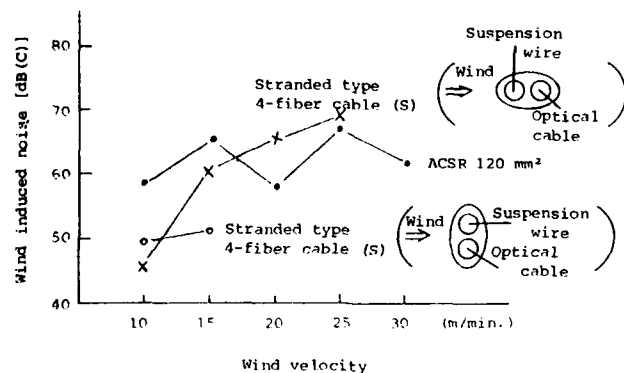


Fig. 8 Result of measuring wind induced noise

wind velocity of over 20m/min. In the case of wind blowing in parallel, suspension wire collided with the cable itself due to the reverse flow effect (wake induced vibration) of wind. And the occurrence of its collision noise was clarified. Even then, the wind noise level was not so great. Also if considering that the possibility of maintaining the suspension wire and cable itself in parallel against the wind direction is little in practice, no occurrence of wind induced noise can be considered all the more.

### (3) Measurement of energy dissipated

#### ① Testing method

The tape-spacer type 4-fiber cable (S) was strung for 150m with the tension of 370kg. And in the measuring setup shown in Fig. 9, the middle part was applied with vibration using the vibration applying machine and the measurement of energy dissipated for the respective frequency bands was conducted. Figure 10 shows the result of measurement. Compared to the energy dissipated of ACSR 120mm², although it was the same in the neighborhood of  $f=10\text{Hz}$ , the energy dissipated was found to be larger for some 2 ~ 10 fold at over  $f=20\text{Hz}$ . Although Fig. 10 shows the measured result of energy dissipated of OPGW 80mm; energy dissipated of non-metallic optical fiber cable was still higher for a few fold at over  $f=20\text{Hz}$ .

This cable construction was Bate damper construction and the entire span can be deemed as damper. Therefore the occurrence of aeolian vibration which poses a problem can be considered difficult.

## 4. Installation of non-metallic optical fiber cable for long span

### 4.1 Method of installation

The study of the method of installation of non-metallic optical fiber cable for long span was implemented by using the existing method of installation and tools as far as possible.

#### 4.1.1 Method of cable stringing

From the result of evaluating the mechanical properties of non-metallic optical fiber cable, the study result as described below was obtained.

- ① Cable stringing can be conducted by roughly the same method as the conventional wire stringing method of power transmission line. Since the non-metallic optical fiber cable is light in weight, the tension at the time of cable stringing is permitted to be fairly small compared to the conductor stringing tension of overhead power transmission line. Therefore the application to long length optical fiber cable is possible also.
- ② The standard pulley used in the power transmission line construction of 450mm diameter can be used intact.

#### 4.1.2 Cable tensioning method

As regards the cable tensioning method at the time of temporary anchoring at the steel tower, the grip for self-supporting cable as shown in Fig. 11 used for the installation works of self-support type communication cable was studied because the come-along used in the usual power transmission line works cannot be used due to the construction of non-metallic optical fiber cable for long span. The result of evaluating the gripping force of the grip used for self-supporting cable had the gripping force of over 1 ton evaluated. Thus, it was verified to permit the application to the temporary anchoring operation of non-metallic optical fiber cable for long span.

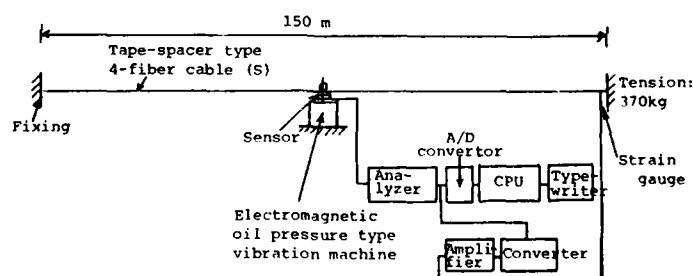


Fig. 9 Measuring setup of energy dissipated

### 4.2 Development of dead-end clamp

As regards the dead-end clamp for FRP suspension wire of non-metallic optical fiber cable for long span, 2 kinds viz., epoxy putty type clamp and mechanical type clamp were studied. Thereby the perspective for practical use was obtained. The following was set forth as the target of developing the clamp used for non-metallic optical fiber cable for long span.

- ① To secure the anchoring strength of over 2 fold of the estimated maximum tension in use (factor of safety is over 2).
- ② To provide sufficient vibration resistive characteristics (no. of vibrations 10Hz, vibration angle  $\pm 25^\circ$ , no drop of clamping force even for

③ Light in weight and easy for handling.

- ① FRP suspension wire
- ② Taper grabbing metalware
- ③ Taper suppressing metalware
- ④ Tightening metalware

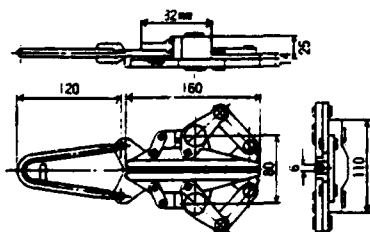
Figure 1 is a log-log plot showing the relationship between Dissipated Power (W) on the y-axis and Amplitude (p-p, mm) on the x-axis. The y-axis ranges from 0.01 to 100 W, and the x-axis ranges from 0.5 to 100 mm. Two sets of curves are shown, representing different cable types and tensions. The upper set of curves is for a 'Tape-spacer 4-fiber cable (S)' with a tension of 370 kg, and the lower set is for an 'OPGW 30mm²' with a tension of 1.85 ton. Each set contains curves for frequencies of 3.2 Hz, 19.5 Hz, 30 Hz, 40.2 Hz, 49.5 Hz, and 59.5 Hz. The curves show that dissipated power increases with both amplitude and frequency.

Frequency (Hz)	Tape-spacer 4-fiber cable (S) (Tension: 370 kg)			OPGW 30mm² (Tension: 1.85 ton)		
	Amplitude (mm)	Dissipated Power (W)	Amplitude (mm)	Dissipated Power (W)	Amplitude (mm)	Dissipated Power (W)
3.2	100	2.5	100	0.01	0.5	0.5
19.5	50	10	50	0.01	0.05	0.05
30	30	20	30	0.01	0.02	0.02
40.2	20	50	20	0.01	0.01	0.01
49.5	10	100	10	0.01	0.01	0.01
59.5	5	100	5	0.01	0.01	0.01

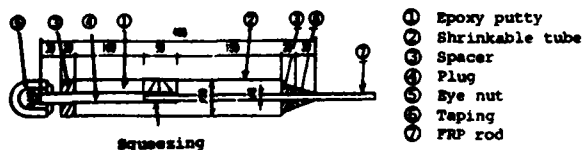
**Fig. 10 Result of measuring energy dissipated**



Photo 3 Appearance of epoxy putty type clamp



**Fig. 11 Construction of the grip for self-supporting cable**



**Fig. 12 Construction of epoxy putty type clamp**



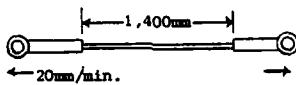
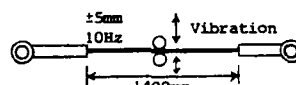
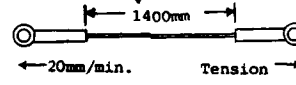
Photo 4 Appearance of mechanical type clamp

### 4.3 Field test

Stranded - type 4-fiber cable (S) of 650m was installed on 2 spans of steel towers of Nagaoka Test Line of the Tohoku Electric Power Co., Inc. (span distance, 300m and 313m) complying with the installation condition of Table 1 and field test was launched from December 1982. In the cable stringing works at that time, because of 2 spans being short, especially the pulley was not used but the winch was used

with persons arranged so that the cable does not touch the ground surface. Because of the light weight of cable, the works of both cable stringing and tensioning were completed without problem in a relatively easy manner.

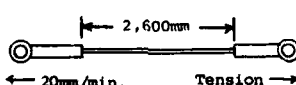
Table 6 Epoxy putty type clamp's properties

Test item		Test condition	Test result
Initial tensile strength			4,100 kg ~ 5,000 kg (n = 3) FRP break: 1 FRP slip out: 2
Tensile strength after vibration test	No. of times of vibrations: $10^7$ times		4,000 kg ~ 4,200 kg (n = 2) FRP break: 1 FRP slip out: 1
	No. of times of vibrations: $4 \times 10^7$ times		4,250 kg (n = 1) FRP slip out: 1

Stranded type 4-fiber cable (S)

Photo 5 View of field test

Table 7 Mechanical type clamp's properties

Test item		Test condition	Test result
Initial tensile strength	Taper grip metalware length L: 50 mm		3,200 kg ~ 3,250 kg (n = 2) FRP slip out: 2
	Taper grip metalware length L: 70 mm		4,130 kg ~ 4,200 kg (n = 2) FRP break: 1 FRP slip out: 1
	Taper grip metalware length L: 100 mm		4,750 kg ~ 5,000 kg (n = 4) FRP break: 2 No break: 2

From the time of completing the installation of cable, observation of snow accretion, monitoring and recording of tension variation, temperature variation and transmission loss of optical fiber cable were conducted continually. However until the present (end of July 1983), the transmission characteristics is extremely stable against snow and temperature variation. Photo 5 shows the situation of installation at the field site of non-metallic optical fiber cable for long span.

##### 5. Conclusion

The non-metallic optical fiber cable ensured for practical use for installing on long span steel towers was developed. The presence of superior transmission and mechanical characteristics was verified from the result of evaluating the characteristics of this cable. Developing 2 kinds of small type clamps, the installation method was found

that the conventional construction method of power transmission line can be applied intact. Stringing the cable at the field site, demonstration test is continuing. Although 8 months have passed, the transmission characteristics are very stable.

The perspective was obtained that the non-metallic optical fiber cable developed this time will become the powerful means of long distance optical fiber communication utilizing power transmission line.

##### References

- (1) S. Kubota, H. Kawahira, T. Nakajima, I. Matsubara, Y. Saito and T. Nakano, "Field Trial of Composite Fiber-Optic Overhead Ground Wire", Fourth International Conference on Integrated Optics and Optical Fiber Communication (IOOC'83), Tokyo, June, 1983.
- (2) E. Hayasaka, M. Maeda, H. Horima, T. Nakatani, T. Kumakura and N. Abe, "Non-Metallic Optical Fiber Cable Incorporating Fiber Reinforced Plastic Catenary for Aerial Application", IOOC'83, Tokyo, June, 1983.
- (3) E. Hayasaka, M. Maeda, F. Otsuka, H. Horima, K. Kuranobu, T. Nakatani, A. Kurosawa and T. Omori, "Development of Non-Metallic Optical Fiber Cable for Long Span Aerial Use", IECE Japan, CS83-54, June, 1983.
- (4) E. Hayasaka, S. Ohira, M. Monma, A. Kurosaka, T. Ohmori and M. Abe, "Development of Snow Accretion Resistant Self-Supported Optical Fiber Cable", IECE Japan, CS83-53, June, 1983.
- (5) Kyoka Plastic, Vol.25, No.3, 1979 (in Japanese).
- (6) S. Yonechi, H. Horima, S. Tanaka and K. Ishihara, "Application of Spacer Forming Technique to

Communication Cables", IWCS, 1980.

- (7) O. Ichikawa, K. Sakamoto, Y. Saitoh, "Development of Nonmetallic, Loose-Groove Spacer-Type Optical Fiber Cable", IWCS, 1982.
- (8) M. Nishimura, H. Horima, O. Nishi, H. Yokota, S. Suzuki and M. Iwazaki, "Application of VAD Fiber Cable to Commercial Fiber Optic Transmission System (FOTS)", IWCS, 1982.
- (9) Y. Kameo, H. Horima, S. Tanaka, Y. Ishida and Y. Koyamada, "Jelly-Filled Optical Fiber Cable", IWCS, 1981.



Masaki Monma  
The Tohoku Electric  
Power Co., Inc.  
7-1, 3-chome,  
Ichibancho,  
Sendai, Japan

Masaki Monma was born in 1935. He joined the Tohoku Electric Power Co., Inc., and has been engaged in the section of communication & electrics engineering. He is now a staff manager of the Electrical Engineering Department of the Tohoku Electric Power Co., Inc., and a member of the Institute of Electronics & Communication Engineers of Japan.



Eiji Hayasaka  
The Tohoku Electric  
Power Co., Inc.  
7-1, 3-chome,  
Ichibancho,  
Sendai, Japan

Eiji Hayasaka was born in 1950. He joined the Tohoku Electric Power Co., Inc. and has been engaged in the section of communication & electronics engineering. He is now an engineer of the Integrated Communication Network Development Office of the Tohoku Electric Power Co., Inc., and a member of the Institute of Electronics & Communication Engineers of Japan.



Sakari Ohira  
The Tohoku Electric  
Power Co., Inc.  
7-1, 3-chome,  
Ichibancho,  
Sendai, Japan

Sakari Ohira was born in 1941. He joined the Tohoku Electric Power Co., Inc., and has been engaged in the section of communication & electronics engineering. He is now a senior staff member of the Integrated Communication Network Development Office of the Tohoku Electric Power Co., Inc., and a member of the Institute of Electronics & Communication Engineers of Japan.



Fujio Ohtsuka  
The Tohoku Electric  
Power Co., Inc.  
7-1, 3-chome,  
Ichibancho,  
Sendai, Japan

Fujio Ohtsuka was born in 1931. He joined the Tohoku Electric Power Co., Inc. and has been engaged in the investigation and design of telecommunication systems for the electric power utilities. He is now a chief manager of the Integrated Communication Network Development Office of the Tohoku Electric Power Co., Inc., and a member of the Institute of Electrical Engineers of Japan.



Hiroaki Horima  
Sumitomo Electric  
Industries, Ltd.  
1, Taya-cho,  
Totsuka-ku, Yokohama  
Japan

Hiroaki Horima was born in 1947 and received the M.S. degree from Osaka University in 1972. He joined Sumitomo Electric Industries, Ltd. in 1972. and has been engaged in research and development of multi-pair communication cables, CATV coaxial cables and optical fiber cables. He is a senior engineer of Fiber Optics Division of Sumitomo Electric Industries, Ltd., and is a member of the Institute of Electronics and Communications Engineers of Japan.



Katsumi Yamashita  
Sumitomo Electric  
Industries, Ltd.  
1, Taya-cho,  
Totsuka-ku, Yokohama  
Japan

Katsumi Yamashita was born in 1942 and received the B.E. degree from Kanagawa University in 1970. He joined Sumitomo Electric Industries, Ltd. in 1958, and has been engaged in development and design of accessories for communication cables.



Masahiko Dazai  
Sumitomo Electric  
Industries, Ltd.  
1, Taya-cho,  
Totsuka-ku, Yokohama  
Japan

Masahiko Dazai was born in 1955 and received the M.S. degree from Tohoku University in 1982. He joined Sumitomo Electric Industries, Ltd. in 1982, and has been engaged in research and development of optical fiber cables. He is a member of the Institute of Electrical and Communications Engineers of Japan.



Noboru Abe  
Kitanihon Electric  
Wire Co., Ltd.  
1-2-1, Koriyama,  
Sendai 982,  
Japan

Noboru Abe received the B.E. degree in electrical engineering from Tohoku University in 1957. He then joined Kitanihon Electric Wire Co., Ltd. and engaged in research and development of communication cables, power cables and distribution wires. He is now a general manager of Product Division.



Non-metallic Long Span Aerial Cable with Optical Fibres for the Use at 1.3  $\mu\text{m}$ 

Helmut G. Haag, Peter E. Zamzow

AEG-TELEFUNKEN KABELWERKE AG, Rheydt, Mönchengladbach  
Federal Republic of Germany

For the use in overhead power lines the application of fully dielectric optical fibre cables is very useful. It is shown, that it is possible to construct long-span aerial cables for spanwidths of up to 1000 m. First results in test installations with graded index and single mode fibres at 850 and 1300 nm are reported. From these results estimations for system designs are derivated.

#### Introduction

For telecommunication purposes of electric power companies aerial cables with metallic armouring and copper conductors as self-supporting aerial cables and as suspension cables are used since many years.

First attempts with optical fibres are also done with metallic armoured cables. After these first experiences and some discussions with the power companies it became obvious, that a light, metal-free long span aerial cable with optical fibres meets the requirements of many users, especially in updating existing lines. The problems of laying and jointing must not require more qualified personal than expected for conventional aerial cables. Moreover, the high security requirements of the power companies to their power lines and equipments must not be diminished.

AEG-KABEL has developped a metal-free self-supporting long span aerial cable

for graded index and single mode fibres for spanwidth up to 1000 m. A report on first experiences in pilot projects is given.

#### Use of optical fibres at power companies

The electrical power companies need for steering and supervision of their network and for the recording and transmission of measuring data telecommunication transmission networks. For telephony and plant supervision telecommunication pathes with increased bandwidths will be needed in the future.

In introducing digitalisation at power companies, too, the optical fibre as transmission medium is preferable. Moreover the optical fibre as a dielectric transmission medium is not influenced by high voltages. First test systems have been realized with metallic armoured optical fibre cores /1,2/. In other systems metal-free optical fibre cables are lashed to a separate suspension wire in 2 - 50 m intervals /3/. These positive first experiences with optical fibres in the net of power companies led to optimised requirements. Optical fibre cables as metal-free self-supporting long-span aerial cables fulfill these requirements. In this context the aerial cables must be able to carry the additional loads by ice and wind given by national and international standards and may have no greater sag than the other ropes on the poles. In analysing the overhead po-

wer lines net and its information flow it becomes obvious, that normally on 110/220 kV lines 2 and 34 Mbit/sec are sufficient. For this purpose graded index fibres are appropriate. Depending on the used wavelengths up to 30 km could be covered without regenerators. On 380 kV lines normally connected to the European meshed net 140 Mbit/sec systems should be used to transmit up to 1920 digital channels. In this case by the long link lengths and the high bit rates the use of single mode fibres is advantageous. A block diagram (figure 1) shows the optical fibre use in the different networks of the electric power companies.

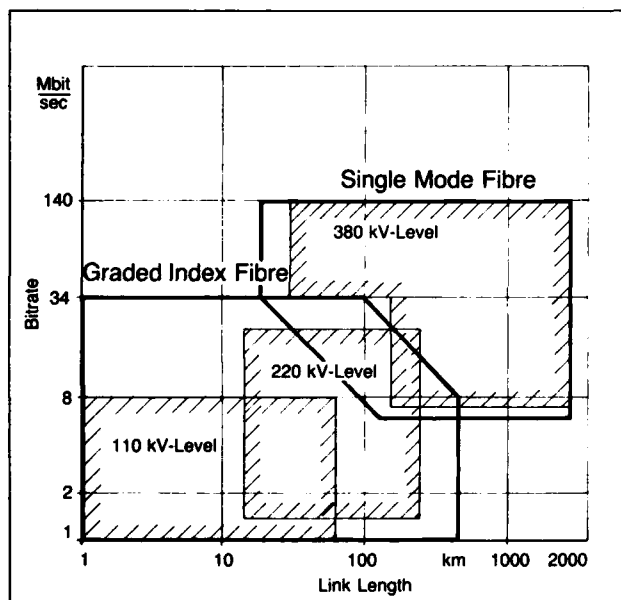


Fig. 1 Use of digital systems on optical fibres in the different levels of the electric power distribution network

Because it is not possible to carry electric energy for regenerator feeding in optical aerial cables the regenerator sections must be as long as possible. This will be reached by low fibre attenuation and, as few splices are possible, this means large single lengths of cables.

On the other hand the cable construction must be rigid enough, that environmental conditions by wind, ice, heat and vibration may influence the attenuation as less as possible.

#### Cable Concept

Because of these aerial cables are installed on high-tension poles the requirements on these cables are mainly effected from these circumstances.

A secure and universal solution is only reached, if the aerial cable is fully dielectric and self-supporting from pole to pole. The laying should be done with the same equipment as used for the ropes.

This means, that the light-weighted aerial cables (250 kg/km) with an outer diameter of 15 mm has to carry, following the VDE-standards, an ice-load of 650 kg/km. To avoid, that these cables under these conditions have greater sag than the 5 - 6 times heavier conductor ropes which carry only slightly higher ice-loading, they have

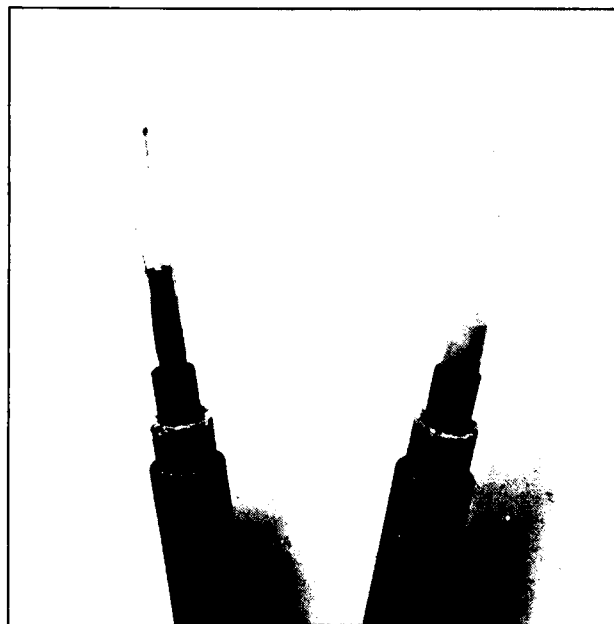


Fig. 2 Metal-free longspan aerial cable with one layer armouring

be suspended at 40°C much tighter than the conductor ropes.

Also for wind-loading the same standards as for conductor ropes are valid. At a cable diameter of 15 mm and 500 m span width the windloading at a wind speed of 30 m/sec reaches 4.35 kN. Then the cable hangs in an angle of more than 70°C to the vertical axis.

All these stresses may not effect in elongation and lateral forces the fibre itself, not to increase the attenuation nor to decrease the life-time. The fibre excess length is chosen as the best compromise between high efforts to the armouring and excess length of the fibre.

#### Cable Construction

The aerial cables consist of a fibre containing core and concentric armouring together with a protective outer sheath (figure 2).

As armouring fibre reinforced plastics (FRP) are chosen. The breaking strain for this material is about  $1200 \text{ N/mm}^2$  at a breaking elongation of 3 %. Our investigation has shown, that the Young modulus of the chosen FRP is not influenced by humidity. Moreover, temperature cycling between -30 and +70°C under bending strain of  $560 \text{ N/mm}^2$  shows no decrease of the Young modulus. But to protect the FRP from mechanical destroy at the spirals and against UV-radiation a black polyethylene sheath covers the armouring.

Because of the fully dielectric cable is hanging in high electric fields between the conductor ropes and is joined to earth potential at the poles high requirements are obvious to the surface resistance, the voltage strength, and the creep current strength.

The fibre containing cable core consists for 2 and 4 fibre aerial cable out of a plastic tube in which the fibres are wound around a soft helix. For higher-count fibre cables around a core 6 tubes containing 1 or 2 loose buffered fibres are stranded. The pitch length and the wall thickness of the tubes are chosen in such a way, that the required excess length is achieved by the movement of the fibres in the tube between inner and outer wall (figure 3).

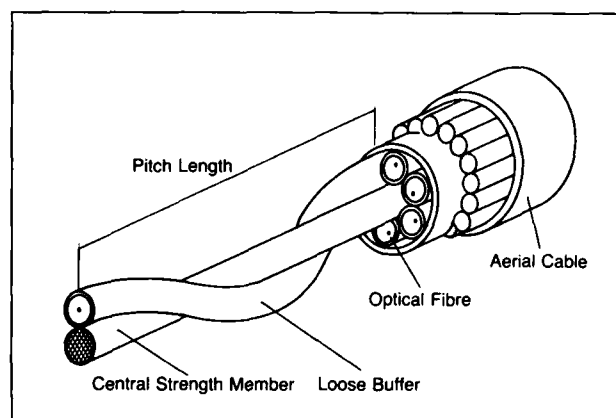


Fig. 3 Principle of layer stranding to achieve the required fibre excess length

#### Cable Characteristics

The main characteristics of the cable are the transmission characteristics during fabrication and under stresses during and after installation. Moreover, the mechanical and electrical behaviour and correlation between cable and fixing spirals are of main importance.

By adequate choose of material and machine parameters the attenuation behaviour during cabling is fully controlled, so that during fabrication no measurable change is observed. This is underlined by the fact, that also the bandwidth of the fibre is independent of the cabling stage. For a 6-

fibre cable in loose tube construction and double layer armouring figure 4 shows the attenuation behaviour during cabling.

Step of Fabrication \ Fibre No.	Attenuation at 1300 nm [dB/km]					
	1	2	3	4	5	6
Fibre Delivery	0,8	1,0	0,7	0,8	0,9	0,6
Buffered Fibre	0,9	0,8	0,7	0,8	1,0	0,6
Cable Core	0,8	0,9	0,9	0,8	1,0	0,65
Finished Cable	0,9	0,9	0,7	0,7	0,8	0,7

Fig. 4 Fibre attenuation at 1300 nm during cable manufacturing of a 6 graded index fibres double layer aerial cable.

On a 20 m sample we carried out vibration test. After  $2 \times 10^7$  cycles at a frequency of 24 Hz no change could be observed. In the test the cable was loaded with 8 kN. The swinging angle reached about 40 minutes which is twice the angle as normally used for vibration tests.

The stress/elongation test shows strictly Hook's behaviour up to the breaking point (fig. 5). Up to the maximum permissible force which is reached at  $-5^\circ\text{C}$  plus ice-loading the attenuation stays constant. This was measured at a 450 m sample in our test field. The attenuation behaviour over a temperature shows down to  $-30^\circ\text{C}$  only a small attenuation increase of 0.2 dB/km. Up to temperatures of  $60^\circ\text{C}$  no measurable attenuation changes were observed (figure 6).

For a double layer armoured construction the resulting torsion at mean pulling force, this means the pulling force with which the sample is loaded during laying in maximum reached 5 turns/100 m. Also for the 1-layer armoured cable which is in principle more sensitive to torsion under tension the torsion is controlled and compensated by the cable structure itself.

For gripping the cable by spirals at the

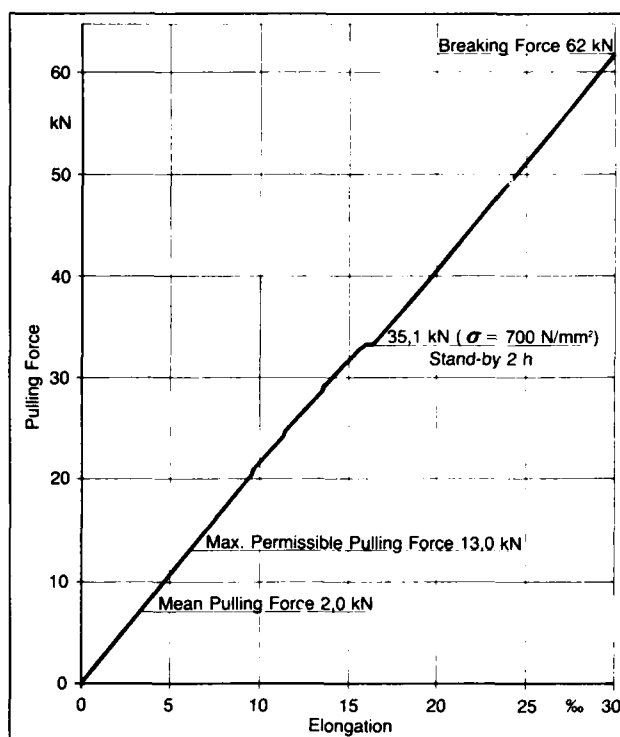


Fig. 5 Stress/elongation diagram of a one layer armoured metalfree aerial cable.

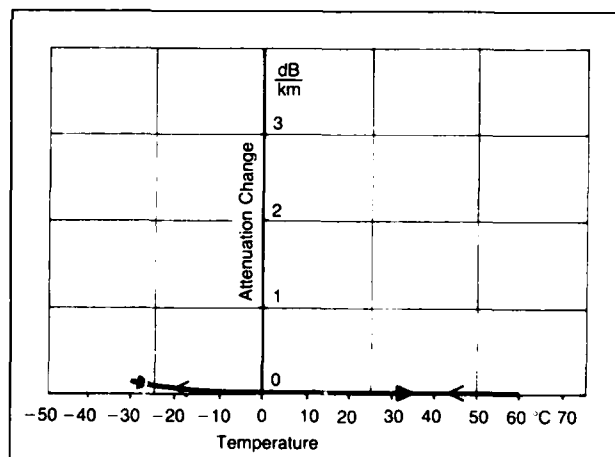


Fig. 6 Temperature dependence of the attenuation of graded index fibres at 850 nm in a non-metallic aerial cable.

poles the polyethylene sheath is not removed from the cable to avoid damage of the FRP by spirals and long-term UV-radiation and also to avoid water penetration.

Therefore the interaction between spiral

and polyethylene sheath is an important point. By the chosen spirals, polyethylene, and the sheath thickness for temperatures up to 60°C no slippage is observed during installation and service.

For the here presented cables figure 7 shows the construction and the mechanical behaviour at which no decrease of the transmission characteristics occurs.

Cable Type Parameter	One Layer Armouring		Double Layer Armouring	
	Central Basic Element	Stranded Buffers	Central Basic Element	Stranded Buffers
No. of Fibres	2-4	2-12	2-4	2-12
Cable Diameter [mm]	15,6	15,6	19,6	19,6
Cable Weight [kg/km]	225	235	365	375
Max. Span Width [m]	700	700	1000	1000
Temperature Range [°C]	-30 ÷ + 70	-30 ÷ + 70	-30 ÷ + 70	-30 ÷ + 70
Attenuation [dB/km]				
GI 850 nm	3,0	3,0	3,0	3,0
1300 nm	1,0	1,0	1,0	1,0
SM 1300 nm	0,7	0,7	0,7	0,7

Fig. 7 Constructional, mechanical and transmission characteristics of self-supporting non-metallic aerial cables.

#### Optical Fibre

The graded index fibres used in these experiments follow the CCITT recommendation and have an attenuation at 850 nm below 3 dB/km and at 1300 nm below 1 dB/km. The bandwidth reaches up to 800 MHzkm /4/. The used single mode fibres go along with the CCITT proposals and have a matched cladding (fig. 8). The attenuation at 1300 nm lies below 0.7 dB/km.

By the fact that the fibres in an aerial cable may be exposed to some lateral forces by the high mechanical loading on the cables it is necessary, that the microbending sensitivity of the fibre is reduced by an appropriate primary coating /5/.

We do this by a double layer primary coating. Over a first soft layer a second hard layer is applied. By an optimum com-

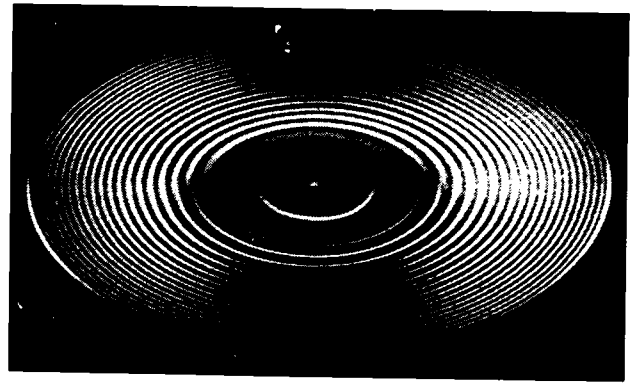


Fig. 8 Scanning electron microscope image of a single mode fibre

bination of dimension and hardness of the two materials a high breaking force of 63 N with a standard deviation of only 3 N and low microbending sensitivity.

The quality of the primary coating is controlled by a screen test with 10 N. The Weibull plot of 120 samples of 1 m length shows figure 9. These two facts achieve also for 4 km fibre length less than 1 % fai-

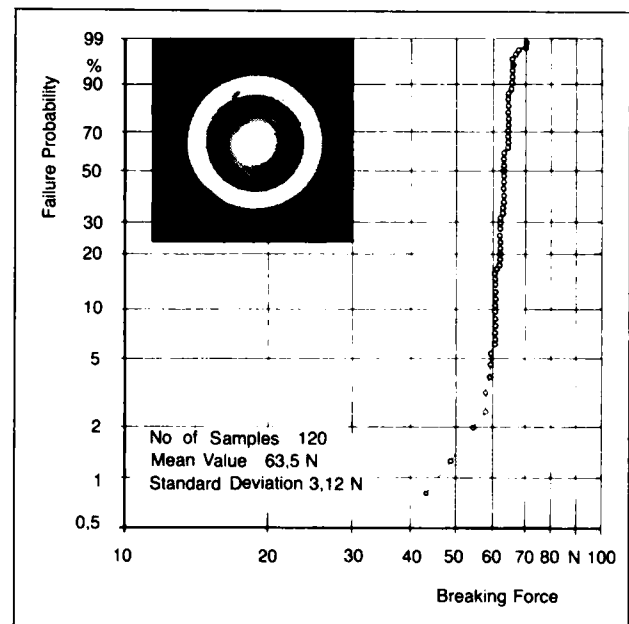


Fig. 9 Strength of a double layer coated graded index fibre 50/125 µm with 250 µm outer diameter (gauge length 1 m)

AD-A136 749	PROCEEDINGS OF THE INTERNATIONAL WIRE AND CABLE SYMPOSIUM (32ND) HELD AT... (U) ARMY COMMUNICATIONS-ELECTRONICS COMMAND FORT MONMOUTH NJ
UNCLASSIFIED	17 NOV 83 F/G 5/2

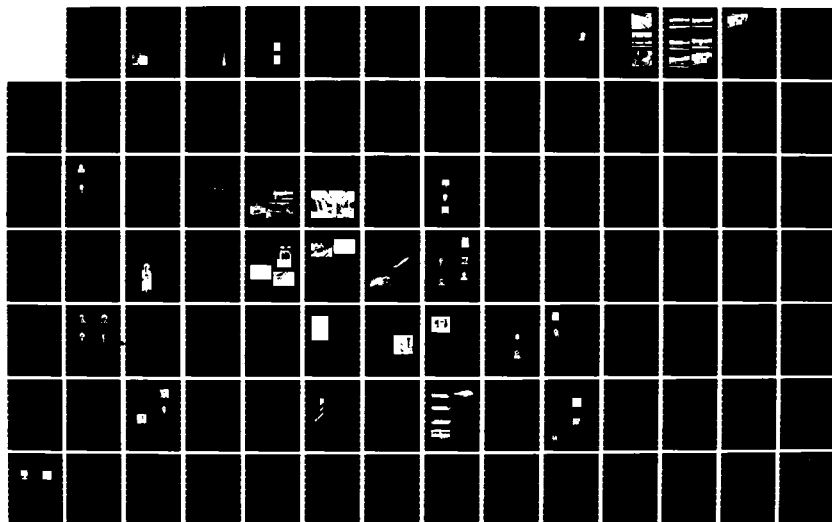
PROCEEDINGS OF THE INTERNATIONAL WIRE AND CABLE  
SYMPOSIUM (32ND) HELD AT... (U) ARMY  
COMMUNICATIONS-ELECTRONICS COMMAND FORT MONMOUTH NJ  
17 NOV 83 F/G 5/2

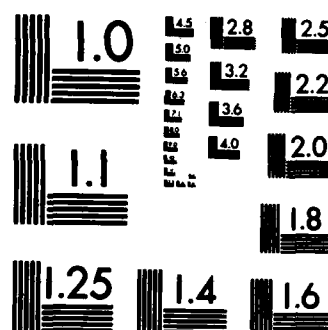
345

UNCLASSIFIED 17 NOV 83

F/G 5/2

NL





MICROCOPY RESOLUTION TEST CHART  
NATIONAL BUREAU OF STANDARDS-1963-A

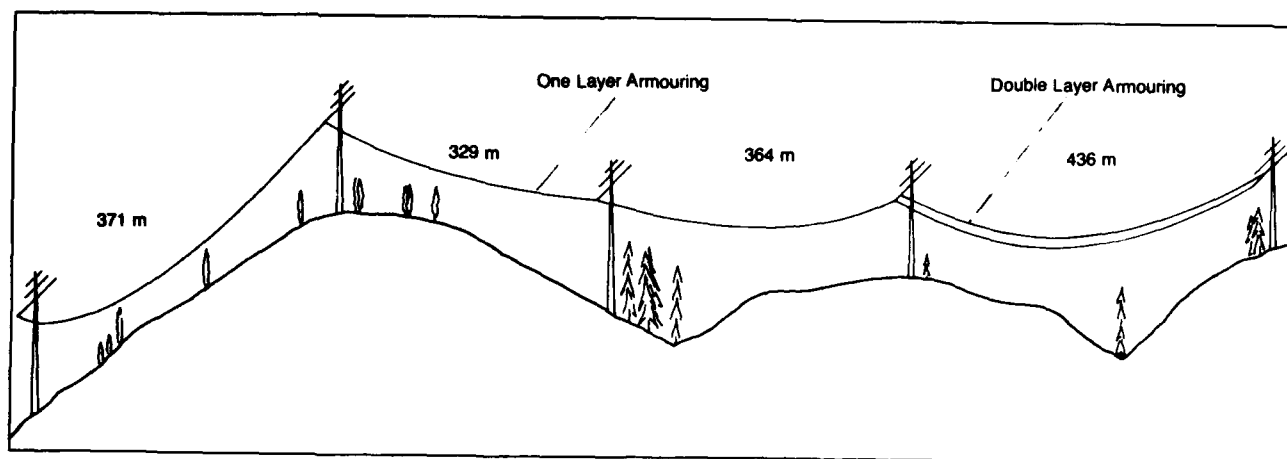


Fig. 10 Test link for a non-metallic long span optical fibre aerial cable in the German highlands.

ture probability if the stress in the fibres is kept below 3 N in the cable itself.

#### Projects

Our first metal-free supporting long span aerial cable with optical fibres we installed in early november 1982 in the German highlands on a 1600 m link in the 110/220/380 kV - net with spanwidth up to 435 m with a single layer armoured aerial cable with 1 basic element over 4 fields in a single length. As reference over the 435 m field a double layer armoured aerial cable was installed. The link and the poles show figures 10 and 11. The two 2-

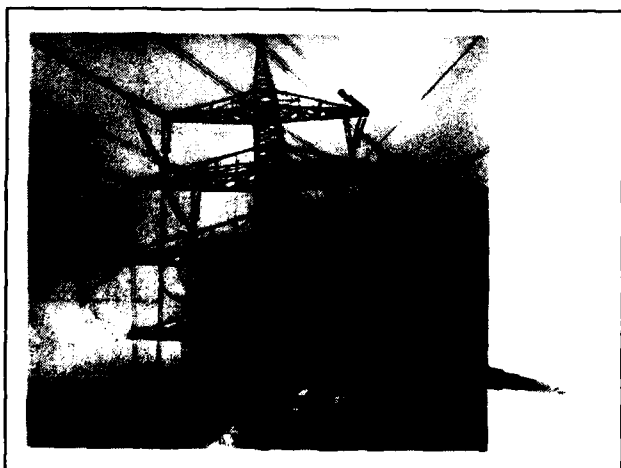


Fig. 11 Pole of the 110/220/380 kV link with a non-metallic aerial cable.

fibre aerialcables were linked over a 4-fibre earth cable of 500 m length to the next switching station. At this point the fibres were terminated by connectors. From this station the transmission measurements were done.

The fibres were spliced at the link end in 10 m height by arc fusion splicing. The splice attenuation was only 0.2 dB/splice. The splice boxes were derivated and adopted to the fibre splices from conventional jointing boxes /6/.

As observed during the installation also in the following control measurements the attenuation stays unchanged. To control the temperature dependent attenuation we undertook long-term measurements at lower temperatures (0 - 20°C) and extreme high temperatures (15 to 40°C). As shown in figure 12 no temperature dependent attenuation change was measured. Also hard windloading during a thunderstorm shows no measurable attenuation change (figure 12 outer left).

The measurements of the sag show no temperature independent sag change which could be correlated to a slippage of the cable in spirals.

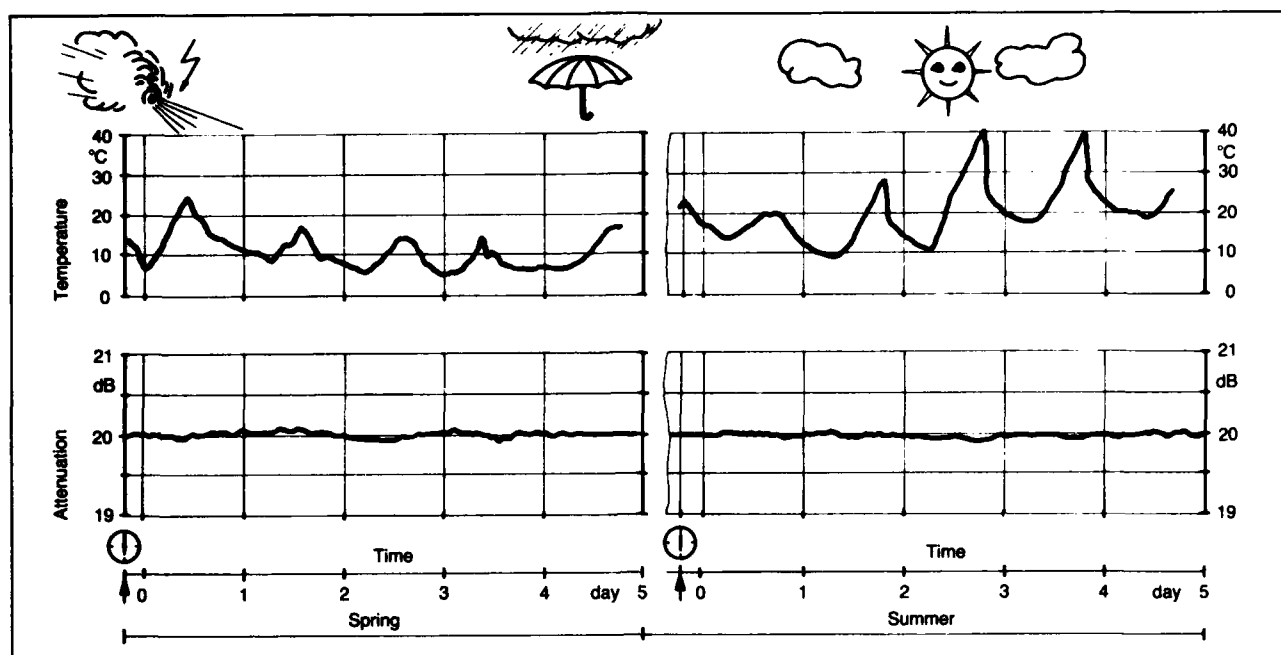


Fig. 12 Longterm attenuation (850 nm) of a non-metallic aerial cable measured in spring (left) and summer (right); link length 4.4 km including 2 connectors and 5 splices

For the next project a valley-crossing with a free span width of 995 m a second layer-armoured cable in single buffered construction was fabricated. This cable contains besides graded index fibres also 2 single mode fibres. The cross-section of the cable shows figure 13.

During the fabrication neither the graded index fibres nor the single mode fibres show any measurable attenuation change at 1300 nm. The experience on laying and the achieved results will be reported on the symposium.

Such long-span field efforts make planning work difficult with respect to sag and swinging. The planning has to verify, that under all possible temperature-, ice- and windloadings no touch between aerial cable and conductor rope will occur. To realize these conditions the cable will be installed with a sag of 93 m at 40°C.

#### Outlook

The undertaken cable system development activities and the test installation in systems led to realistic planning informations for overhead lines with metal-free,

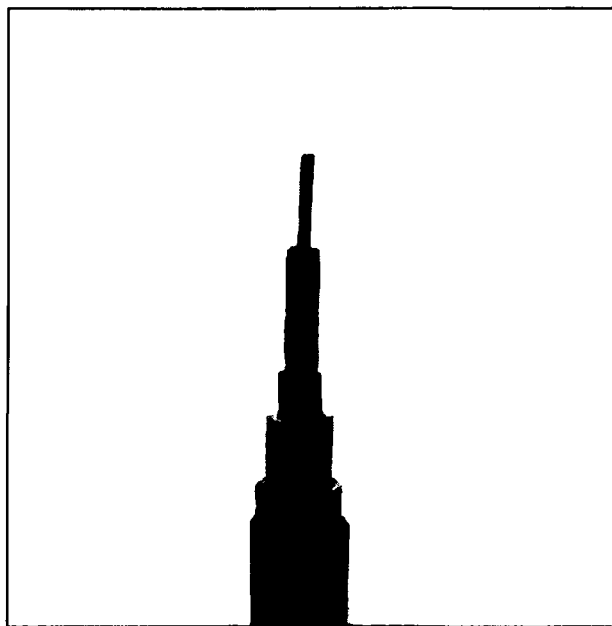


Fig. 13 Make-up of the combined graded index/single mode fibre cable for 995 m spanwidth.

self-supporting optical fibre aerial cables. Single and double layer FRP-armoured aerial cables are available together with the appropriate spirals. The cable core may consist of central basic elements with large inner diameter for 2 - 4 fibres or stranded tubes with 1 or 2 fibres for cables with up to 12 fibres.

The results have shown, that graded index fibres at 850 and 1300 nm as well as single mode fibres at 1300 nm could be cabled and installed without additional losses. Out of the long-term results we could minimize the environmental margin to a few 1/10 dB/km for all given cases.

A splice attenuation of 0.2 dB could be realized even in poles. The used production principle allows the fabrication of long cable lengths adapted to the expected application to yet as few splices as possible in the whole link.

Out of the requirements of the system users for control data and telephony in such network 2 Mbit/sec systems are sufficient. In this case the system planning could calculate with 50 respectively 40 dB at 850 respectively 1300 nm for the system attenuation on graded index fibres.

In the European link systems also higher data streams are possible. For 140 Mbit/sec systems single mode fibres at 1300 nm with system attenuation of 30 dB are appropriate.

#### References

- /1/ Haag, H., G. Thönnessen, Selbsttragendes Luftkabel mit Lichtwellenleitern für eine 220 kV-Freileitungsstrecke; Elektrizitätswirtschaft 80 (1981) 26, pp. 967 - 973.
- /2/ Benndorf H., et al., Fiber-Optic

System for Transmission of Information on High Voltage Overhead Power Lines CIGRE (1980), 35 - 09, pp. 1-12

- /3/ Möhle, K., D. Speck, Der Einsatz der Lichtwellenleitertechnik zur Informationsübertragung im Mittelspannungsnetz der Neckarwerke Elektrizitätsversorgung AG; Elektrizitätswirtschaft 82 (1983) 1/2, pp. 25 - 29
- /4/ Huber P., et al., Properties of Fibres Drawn from uncollapsed VCVD-Preforms  
Proc. 9th ECOC, Cannes, 1982, pp.
- /5/ Jostan I. L., Strength of Optical Fibres when Exposed to Moisture or water  
Cost 208/7, 20.04.82, Ipswich/GB, "Workshop on Fibre Strength and Reliability"
- /6/ Zielinski, H.G., S. Klinger, Fibre Optical Coupling Techniques and Cable Accessories  
Wiss. Ber. AEG-TELEFUNKEN 53 (1980) 1-2, pp. 34 - 41

Helmut G. Haag (Speaker)  
AEG-KABEL  
Optical Fibre Division  
Mönchengladbach, West-Germany

He was born in 1948. He received his Dipl.-Phys. degree from the University Stuttgart and joined AEG-KABEL in 1975. After being engaged in several fields of coaxial cable development, he is now responsible for development and production of optical fibre cables.

Peter E. Zamzow  
AEG-KABEL  
Optical Fibre Division  
Mönchengladbach, West-Germany

He was born in 1940. After finishing his postgraduate studies in telecommunication cables at Munich and Graz as Dipl.-Ing., he joined AEG-KABEL in 1970. He has been engaged in development and production of telecommunication cables. Since 1980 he is head of the fibre optic division in AEG-KABEL and became in 1982 senior engineer.

## NEW SILICONE RUBBER CABLE INSULATION PROMISES CIRCUIT INTEGRITY, IN FLAMING ENVIRONMENT

Melvin A. Cabey

Dow Corning Corporation

## SUMMARY

To provide an improved alternative to fluoropolymers and other halogenated materials used for insulation of most plenum cables, a project was undertaken to develop silicone elastomers which would meet Steiner Tunnel Test criteria. Equally important, the project aimed to retain the long-recognized ability of silicone elastomers to form a non-conductive ash when burned. The new material resulting from this project provides improved flame retardancy and lower smoke density, without sacrificing the best flame environment properties of earlier silicone rubbers. It does not melt, flow or drip, and burns to form a ceramic that clings to the conductors. This nonconductive ceramic has enough strength to remain in place during and after burning, thus providing insulation between adjacent conductors to assure circuit integrity.

inal mechanical and electrical properties over a temperature range of -60 to 250°C. Figure 2 shows the electrical properties of a typical silicone rubber as a function of temperature. Silicone rubber also retains properties after heat aging, even when the properties are measured at elevated temperatures.

This ability to function despite prolonged exposure to high temperatures has led to wide application of silicone rubber as electrical insulation in a variety of appliances. The list includes toasters, space heaters, radiant ovens, microwave ovens, and electrical ranges. The fact that silicone rubber is the standard insulation for OEM automotive ignition wire in the United States indicates a high degree of resistance to impulse voltages. Its use as a jacket material on much ignition wire confirms its ability to withstand mechanical stress and abuse in a harsh environment.

## INTRODUCTION

Silicone rubber has been used as wire and cable insulation since the early 1950s. Since that time, the mechanical, electrical and fire retardant properties of silicone rubber have undergone constant improvement. Today's silicone elastomers are better and more cost effective than ever. Figure 1 shows the improvements in tensile strength and elongation that have been made over the last 30 years. As shown in Table I, silicone rubber also has excellent electrical properties.

Temperature

A major reason for the use of silicone rubber wire and cable insulation is its wide service temperature range. Typically, organic elastomers designed for high temperature service become brittle at moderately low temperatures, and those compounded for low temperature application become unserviceable at moderately high temperatures. In contrast, silicone elastomers retain most of their orig-

In 1980 Murray reported new silicone rubber technology which further improved the heat aging stability of silicone rubber.<sup>1</sup> Products based on this new technology meet UL 62 requirements for retention of 75 percent of original elongation after 60 days at 210°C. One of these products also achieves a V-0 rating when tested according to the small specimen section of UL 94.

Circuit Continuity

One of the reasons that the U.S. Navy has used silicone rubber for shipboard wire and cable insulation for nearly 30 years is the material's ability to maintain circuit continuity while, and after, burning. Being thermosetting, it does not melt. Rather, it forms a nonconductive ash with sufficient mechanical strength to continue to function as an electrical insulator and maintain circuit continuity.

A simple test of the electrical integrity of cable materials in fire exposes

the cable to the flame of a Fisher laboratory burner. Test criteria is the length of time electrical continuity is maintained. In 1978 Lipowitz reported that fire retardant silicone rubber insulated cable maintained continuity for more than 30 minutes exposure to the burner whereas polyvinylchloride and a certain fluorocarbon insulation lost their insulating ability within 3 minutes or less.<sup>2</sup>

In another test Noble used portions of cables that had been exposed for one hour to the 70,000 Btu/min. ribbon gas burner specified in IEEE Standard 383 for cables used in nuclear power plants.<sup>3</sup> Cables were bent around a 12-inch diameter mandrel, reverse bent around another mandrel and tested for electrical resistance and AC-dielectric withstand strength at 1000 and 4000 volts. Table II gives the resistance range of six samples each of three different cables and the number of samples passing the dielectric strength test.

In tests conducted by Baltimore Gas and Electric Co., silicone rubber insulated cable remained operable after being subjected to a severe oil fire.<sup>4</sup> The tests indicated that by maintaining electrical continuity, silicone rubber insulated cable would permit orderly shutdowns in case of a fire and in some cases replacement of the cable might even be deferred. Concluding that these advantages far outweigh the premium price of the cable, the company uses the silicone insulated cable for control, instrumentation and power circuits up to 600 volts.

As good as they are, however, previous silicone rubber wire and cable insulations were not designed for plenum cable installations.

#### NATIONAL ELECTRICAL CODE FOR PLENUM CABLE

Because of concern about fires being spread by flammable cable insulation through the space above dropped ceilings which also act as air return plenums, the National Electrical Code in 1975 specified that electrical cable installed in ceiling plenums be enclosed in metal conduit. The type of cable installed in these plenums includes communications cables for telephone, intercoms, computer terminals and video screens, security system cable for fire and burglar alarms and closed-circuit video surveillance. Although these are all essentially low voltage systems presenting no particular fire hazard themselves, the presence of flammable electrical insulation could spread a fire originating from another source, generating smoke and toxic and corrosive gases in the process.

The National Electrical Code is only an advisory document, but it has a great influence on local codes. Many municipalities adopt it without exception. Some municipalities, New York and Los Angeles for example, while using it as a guide, enact more stringent regulations.

In 1978 the Code pertaining to plenum cable was modified to permit "listed" exceptions to the conduit requirement. In 1981 Underwriters Laboratories issued UL 910, "Standard for Test Method for Fire and Smoke Characteristics of Cables Used in Air-Handling Spaces." This Standard establishes the criteria under which such products as "Telephone Cables (WYRZ)", "Power-Limited Circuit Cable Classified for Fire and Smoke Characteristics" (QPMR) and "Power Limited Fire-Protective Signalling Cable Classified for Fire and Smoke Characteristics" (HNIW) can be used without being enclosed in conduit.

In essence this Standard requires that smoke from burning cable exhibit optical densities of 0.5 or less and maximum flame-spread distances of 5 feet or less when tested in a modified Steiner tunnel test.<sup>5,6</sup> In this test, ASTM E-84 (UL 723), 25 ft. lengths of cable are placed in a cable rack located in the tunnel. Two gas burners, each producing 5000 Btu/min., located beneath one end of the rack, expose the first 4.5 feet of the specimens to flame. Air is introduced at the flame end of the tunnel at a constant, controlled velocity of 240 feet per minute. Test duration is 20 minutes.

At the time that the National Electrical Code for plenum cable was modified in 1978 to permit exceptions to cable installation in metal conduit, there was no silicone rubber that would pass this test. However, considering the other benefits of silicone rubber in a fire environment, especially its ability to maintain circuit integrity while burning and its inherently low evolution of toxic gases, it was felt that if a material meeting NEC plenum cable requirements could be developed, it would provide the electrical wire and cable industry with a superior insulating material.

#### NEW SILICONE RUBBER TECHNOLOGY

Development work to produce such a material began in earnest in 1980. Table III shows the progressive improvement of flame retardance and smoke generation in tests used to screen materials before subjecting them to the Steiner tunnel test. The improvement over non-flame-retardant silicone rubber is

substantial. NRS smoke density has been reduced by a factor of ten or more and limiting oxygen index has been increased by more than 50 percent. ASTM E162-67 is a more severe test than UL 94. It provides an indication of surface flammability by combining a radiant heat energy source with a flame source. The numerical index is a combination of the flame spread factor and the heat evolution factor. When tested according to this standard, the new material exhibits a very low flame spread and heat flux factor.

### Steiner Tunnel Tests

A number of preliminary tests have been conducted in the Steiner tunnel. These tests indicate that properly formulated silicone rubber can pass the classification requirements of UL 910. The history of these tests, shown in Table IV, shows steady improvement in both flame propagation and smoke density.

The illustrations provide a record of a succession of tests. Figure 3 shows the cable in place in the cable rack prior to testing. Figure 4 shows the cable in the Steiner tunnel after the burn. Note the white ash and dust of the flame affected areas. The fact that there was no dripping of molten material is evident. In fact, cleaning the tunnel following the test was simply a matter of blowing away the amorphous silica ash. Figure 5, a close-up of the charred cable, reinforces this observation.

Figures 6 through 10 show the post-test condition of cutaway sections of one cable at varying distances from the flame end of the rack. The section of cable in Figure 6 was only four inches from the jets of the gas burners. The silicone rubber insulation burned, but the nonconductive ceramic still adheres to the conductor. Note the circumferential cracks formed by shrinkage as the material was fired. Electrical tests, described later, showed this section to be effectively insulated although oxidation of the copper conductor had increased its electrical resistance. Figures 7 and 8 show sections of cable located 9 inches and three feet respectively from the burner end of the rack. Again the ceramic adheres to and insulates the conductors. At four feet from the burners, less cracking from ceramification is evident (Figure 9). At nine feet from the burners the cable is unaffected by the flame and is completely flexible (Figure 10).

A series of tests were conducted to demonstrate the electrical continuity of burned cable. Figure 11 shows a Variac and a light bulb connected to one pair of a 25-pair cable taken from the first five feet of the Steiner tunnel after the burn. An adjacent

pair is connected to an ohmmeter to determine whether leakage would occur.

In Figure 11, note that the Variac switch is off, the light bulb is not lit, and the ohmmeter reads zero. In figure 12, the Variac switch is on, energizing the pair to 105 volts (three or four times its rated voltage), and lighting the bulb. The ohmmeter continues to register zero, indicating no leakage current.

### POTENTIAL FUTURE STANDARDS

As a result of a number of recent disastrous fires in hotels and office buildings, increasing concern is being expressed today over the toxicity of smoke and gases produced when plastic materials burn.<sup>7</sup> A recent article, Rebecca Lewis of Chemical & Engineering News points out that the Center for Fire Research, a part of the National Bureau of Standards, reports that 80 percent of fire deaths result from smoke or gas inhalation. Also, the U.S. National Fire Protection Association has reported "an apparent increase in fire fighter casualties from smoke inhalation." Fires appear to develop faster and produce heavier and more irritating smoke than in the past.

dards will likely include smoke toxicity as well as smoke density and flame spread criteria. It has been reported that the State of New York may adopt a test developed by Dr. Yves C. Alarie for comparing smoke toxicity of different materials as a standard for rating all building materials and furnishings.

### Products of Silicone Combustion

Dr. Lipowitz produced a model for combustion of low volatility polydimethylsiloxanes including silicone rubbers (Figure 13). Volatile cyclic dimethylsiloxanes are produced above 350°C and undergo combustion in the gas phase. Feedback of energy from the flame pyrolyzes more cyclics. Simultaneous oxidation produces oxidized silica ash on the surface and a partially oxidized gel beneath. These layers tend to shield the material beneath from the flame. Assuming an excess of oxygen, combustion products are carbon dioxide, water and amorphous silica.

Lipowitz also points out that the actual products of combustion depend on the fuel-to-air ratio. Depending on this ratio, the products of polydimethylsiloxane combustion may be water, carbon dioxide, amorphous silica,

and small amounts of nitrous oxide, hydrogen, carbon monoxide, carbon, silicon monoxide and silicon nitride.

In some types of service the corrosiveness of smoke and gases may be of great concern. In copper mirror corrosion tests (ASTM D-2671) silicone rubber vapors were the least corrosive to copper of the wire and cable insulating materials tested (8).

Many organic materials use halogenated flame retardants. These often increase the rate of smoke generation, toxicity and corrosiveness. In contrast, flame retarded silicone rubbers produce smoke having lower optical density than conventional silicone stocks (Table V).

### CONCLUSIONS

A new silicone rubber insulation is designed for wire and cable classified under UL 910 for use without conduit in air handling spaces. It has essentially the same mechanical and electrical properties as silicone rubbers presently used in the electrical wire and cable industry. The silicone rubber uses no halogenated flame retardant additives. This contrasts with fire-retardant organic polymers which may contain up to 50 percent by weight of heavy-smoke-producing halogenated materials.

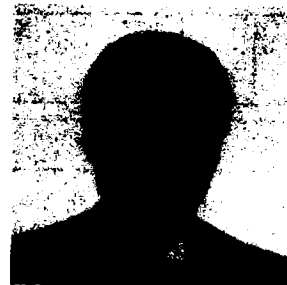
In addition to low smoke density and negligible flame spread, the new rubber preserves electrical circuit integrity during and after burning. While burning, it does not melt or produce any messy and potentially hazardous droplets. Finally, its gaseous products of combustion are very low in toxicity, especially when compared to those of fire-retardant organic rubber insulating materials.

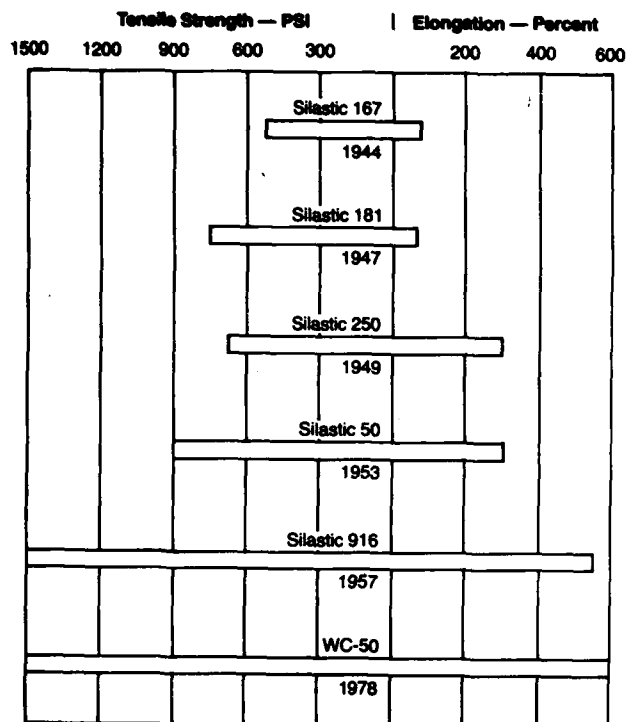
### REFERENCES

1. Dams, M.J and Murray, M.C., New Technology Improves Heat-Aging Stability of Silicone Rubber for Wire and Cable Insulation, International Rubber Conference, Nuremburg, W. Germany, September 24-26, 1980.
2. Lipowitz, J., Combustion, Flammability and Fire Hazard Properties of Silicones Publication NMAB-342, National Academy Sciences, Washington, D.C., 1978.
3. Noble, M.G., Off. Plastic Caoutch., 22: 693, 1975.
4. Allison, W.W., Planning Electric Cable Systems to Minimize Fire Loss, Plant Engineering, January 19, 1978.
5. Parker, W.J., An Investigation of the Fire Environment in the ASTM E-84 Tunnel Test, NBS Technical Note 945, National Bureau of Standards, Washington, D.C., August 1977.
6. Standard for Test Method for Fire and Smoke Characteristics of Cables Used in Air-Handling Spaces, UL 910, Underwrite Laboratories, Inc., Northbrook, IL, May 1982.
7. Rawls, R.L., Fire Hazards of Plastics Spark Heated Debate, Chemical & Engineering News, January 3, 1983.
8. Robertson, J.W., Paper C74 207-7, IEEE Winter Meeting, New York, NY, January 1974.

Melvin A. Cabey is a Technical Service and Development Representative at Dow Corning Corporation. For the last three years he has specialized in silicone materials for the wire and cable market. Previously, for five years, he had developed fluorosilicone elastomers for the aerospace and automotive markets. He is a graduate of Western New England College with a B.S. degree in chemistry, and also holds an MBA degree from Central Michigan University.

The author wishes to acknowledge help from Robert S. Bloor in the preparation of this paper.





**Figure 1. Major improvements in the physical strength of silicone rubber.**

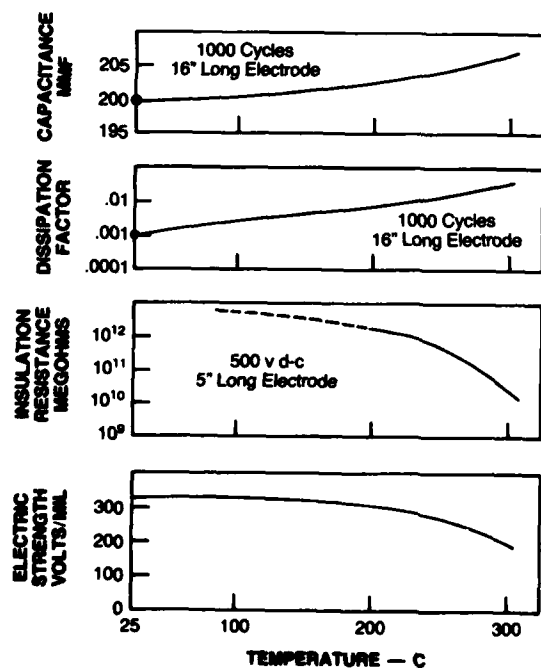


Figure 2. Dielectric properties of silicone rubber as a function of temperature.



Figure 3. Cables in place for Steiner tunnel test, UL 910.

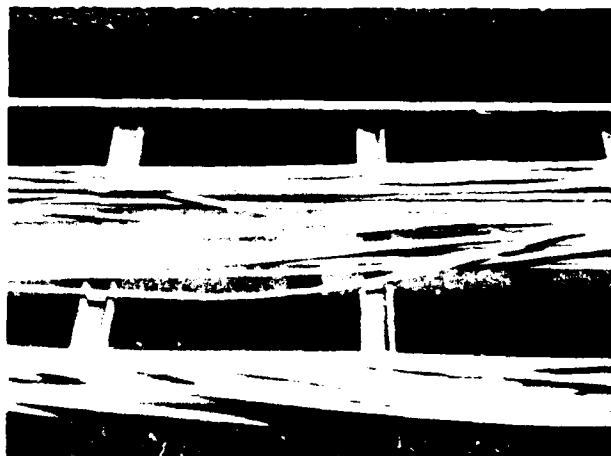


Figure 4. Cable after the test. Note absence of molten drops of material.



Figure 5. Close-up of cable after tunnel testing.

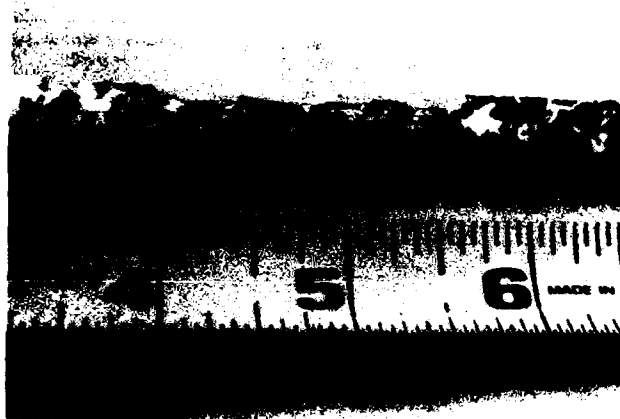


Figure 6. Portion of cable located only 4 inches from burner end during test with jacket cut away. Conductors are now protected by ceramic.



Figure 9. Cutaway of cable located 4 feet from burner end shows less cracking from shrinkage caused by ceramification.



Figure 7. Cut away portion of cable 9 inches from burner end during test.



Figure 10. Cable 9 feet from burner end is completely flexible.



Figure 8. Portion of cable 3 feet from burner end during test.



Figure 11. Electrical test for circuit continuity and current leakage of burned cable. Variac is off.

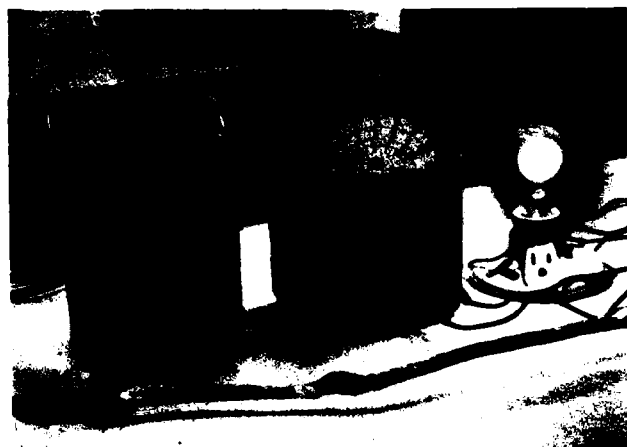


Figure 12. Same circuit as in Fig. 11. Variac is on, energizing the circuit to 105 volts (more than three times its rated voltage).

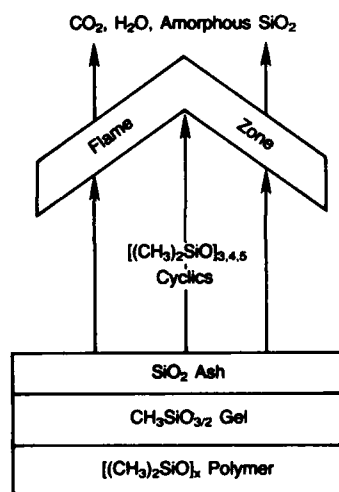


Figure 13. Model for burning of low volatility polydimethylsiloxanes.

TABLE I. Electrical Properties of Silicone Rubber

Dielectric Strength (Volts/mil)	
Single Thickness = 0.030" =	675
0.070" =	500
0.100" =	450
Dissipation Factor	
10 <sup>2</sup> Hz	0.002
10 <sup>5</sup> Hz	0.002
10 megahz	0.010
Volume Resistivity (ohm-cm)	2.01 x 10 <sup>15</sup>
Dielectric Constant	
10 <sup>2</sup> Hz	3.0

TABLE II. Electrical Data for Six Cable Samples After Fire Test<sup>a</sup>

Cable	Insulation	Insulation Resistance (Mohm/1000 ft.)		Dielectric Withstand Strength <sup>b</sup>	
		After Roasting	After Bending	1000V	4000V
A	Silicone	29-252	30-300	6	5
B	Silicone	0.9-144	0.2-135	6	0
C	Silicone	5-135	8-126	6	3

<sup>a</sup>From reference 3

<sup>b</sup>Number passing of six samples tested

TABLE III. Fire and Smoke Properties of Silicone Rubbers

Material	NBS Optical Density, D <sub>94</sub> (flaming)	T <sub>16</sub> <sup>*</sup>	UL 94 Rating	L.O.I.	ASTM E162-67 Flame Spread Index
Conventional Silicone	436	1.2	None	28	46.98
Early Flame Retardant Silicone	119	1.5	V-1	35	24.8
Improved Flame Retardant Silicone	75	1.8	V-0	40	11.63
New Material	30	2.5	V-0	45	7.65

\*T<sub>16</sub> = Time to 75% Light Transmission.

TABLE IV. Flame Retardant Silicone Rubber Wire and Cable Insulation

	I	II	III	IV	V	VI
Construction	24 AWG 8 Pair	22 AWG 2 Pair	22 AWG 2 Pair	24 AWG 4 Pair	22 AWG 2 Pair	24 AWG 25 Pair
Primary Insulation Thickness, in.	0.015	0.015	0.015	0.015	0.015	0.010
Jacket Thickness, in.	0.025	0.025	0.025	0.030-0.050	0.025	0.025
Jacket O.D.	0.450	0.195	0.195	0.540	0.200	0.400
Number of 25-ft. cable lengths tested	18	52	52	18	51	26
Flame Spread, ft.	25	17	19	14.5	10	3
Smoke Density	>1.0	0.56	0.92	0.40	0.17	0.200

TABLE V. NBS Smoke Chamber (Flaming) Data for Silicone Rubber (3.3-mm Thickness)

Sample	Dm	T16 (min.)	Gas Analysis			
			CH <sub>4</sub> (ppm)	CO (ppm)	HC (ppm)	CO <sub>2</sub> %
Me <sub>2</sub> Rubber	436	1.2	None	130	48	1.36
Me <sub>2</sub> Rubber (flame retarded)	119	1.5	220	160	279	1.09
PhMe Rubber (flame retarded)	70	1.9	320	150	217	1.06
New Materials (flame retarded)	30	2.5	300	125	205	1.05

# A POLYTETRAFLUOROETHYLENE INSULATED CABLE FOR HIGH TEMPERATURE OXYGEN AEROSPACE APPLICATIONS

Alvin T. Sheppard  
Materials Engineering  
Martin Marietta Aerospace  
New Orleans, LA

Robert G. Webber  
NASA  
Marshall Space Flight Center  
Huntsville, AL

## ABSTRACT

For electrical cables to function and survive in the severe high temperature oxygen environment that will be experienced in the External Tanks of the Space Shuttle, extreme cleanliness and material purity is required. Through work accomplished under NASA Contract Number 8-30300 and sponsored by the George C. Marshall Space Flight Center, Huntsville, Alabama, a flexible light weight cable has been developed for use in pure oxygen at worst case temperatures of -190 to +260 degrees Centigrade and pressures as high as 44 pounds per square inch absolute. A comprehensive series of tests were performed on cables manufactured to the best commercial practices in order to establish the basic guidelines for control of build configuration as well as each material used in construction of the cable.

## Introduction

The Space Shuttle External Tanks were designed with the intent to utilize existing "State-of-the-Art" materials wherever possible since the tanks are to be the first mass produced hardware assembly to be used in aerospace applications. After an intensive evaluation of available wire and cable in use for high temperature applications, polytetrafluoroethylene (PTFE) insulated wire and cables were selected to be used in the oxygen tank for flexibility, high temperature capability, demonstrated oxygen compatibility and availability. This selection was based on history extending as far back as January, 1960 in the Journal of "Teflon" where insulated wires had been tested to temperatures as high as 450 degrees Centigrade for 15 minutes without failure or degradation. The material has accumulated an impressive record of aerospace uses in high temperature and pressure applications for seals, coatings liners as well as wire insulation in intimate contact with hydrogen, oxygen and exotic propellants as reported in JSC-02681.

The physical and thermal properties are shown in Figure 1 and Table I.

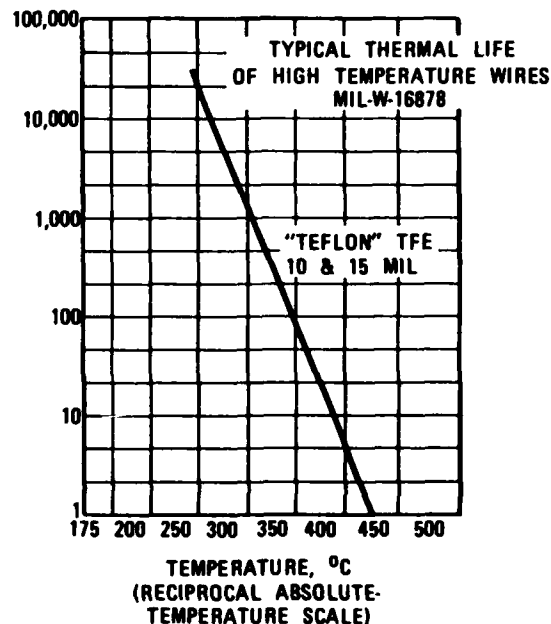


FIGURE 1- THERMAL LIFE CHARACTERISTICS FOR TFE FLUOROCARBON RESIN IN AIR

Thermal life charts for dielectric material serve to indicate whether assigned temperature ratings will result in satisfactory life under anticipated conditions. The amount of time an insulated wire can be expected to operate at any temperature can be estimated by regression analysis of experimental data by extrapolating the plot of time (log scale) versus temperature (reciprocal of absolute temperature scale). The resulting chart is usually a straight line which is comparable with the time-temperature function of a first order chemical reaction rate below critically higher temperature where the material begins to melt, gel or suffer rapid chemical decomposition. Temperature ratings for the wires covered herein are based on this characteristic, assuming a life of 20,000 hours under average or normal service conditions. Under conditions where the dielectric is subjected to higher than normal loads or mechanical stress, either the thermal life will be shortened or the wire must be operated at less than the assigned rating.

Conversely, although not recommended for general practice, the possibility exists that wires may be operated at higher than rated temperature either when a reduced life expectancy is acceptable or under conditions of virtually no load or mechanical stress upon the dielectric.

The unique combination of chemical and physical properties of PTFE results as a consequence of its true fluorocarbon structure. The unusual structure leads to a material which displays an almost universal chemical inertness; complete insolubility in all known solvents below 300 degrees Centigrade; excellent high heat resistance; and unsurpassed electrical characteristics including a low dielectric loss, a low dielectric

constant and high dielectric strength. Furthermore, PTFE does not embrittle at very high or at very low temperatures.

#### APPROACH

A preliminary wire/cable specification was prepared at the onset of the effort to assure known and like characteristics of test specimens. This specification was based on existing aerospace wire and cable specifications, 40M39513 and 40M39526 for standard electrical test characteristics, materials and configuration controls.

Table 1. Properties of Polytetrafluoroethylene

PHYSICAL, ELECTRICAL AND ENVIRONMENTAL	
PROPERTIES	TYPICAL VALUES
Specific Gravity	2.15
Tensile Strength, (p.s.i.)	4000
Elongation, (%)	300
Modulus of Elasticity in Tension, (p.s.i.)	$0.58 \times 10^5$
Thermal Conductivity ( $\text{cal sec}^{-1} \text{cm}^{-1} \text{°C}^{-1}$ )	$6 \times 10^{-4}$
Specific Heat* ( $\text{cal gm}^{-1} \text{°C}^{-1}$ )	0.25
Thermal Expansion, ( $\text{°C}^{-1}$ )	$10 \times 10^{-6}$
Continuous Use Temperature ( $\text{°C}$ ), 20,000 hrs	260
Melt Temperature ( $\text{°C}$ )	327
Low Temperature Limit ( $\text{°C}$ )	Near -273
Flammability*	Non-Flammable
Flammability, Oxygen Autoignition ( $\text{°C}$ )	491
Weight Loss (%/Hr.) 425°C	0.15
Dielectric Constant	2.1
Dissipation Factor	.0002
Volume Resistivity ( $\text{ohm-cm}$ )	$10^{18}$
Corona Resistance	Fair
Offgassing (TORR) 27°C	$5 \times 10^{-16}$
100°C	$5 \times 10^{-12}$
Cold Flow and Cut Through	Fair
Ultraviolet Radiation	Excellent
Nuclear Radiation (in presence of air)	Poor
Electrical-Mechanical Stress Cracking	Excellent
Chemical-Mechanical Stress Cracking	Excellent

\*Above 690°C the decomposition products will burn in air, but the resin will not support combustion once heat is removed. Combustion products are mainly carbon dioxide and hydrogen fluoride, with small amounts of carbon tetrafluoride.

Qualifying tests of the finished cable were performed for oxygen system usage in accordance with the following schedule:

1. Flamability and oxygen compatibility tests:

a. General

All materials considered for use in a manned spacecraft including the materials of the spacecraft, stowed equipment of experiments are evaluated for flammability, odor and offgassing characteristics in accordance with NASA Hand Book (NHB) 8060.1. Specimens of materials in the configuration intended for use are to be subjected to each applicable test in their most hazardous use environment. For oxygen tank wiring, the "worst case" flight conditions (3A-AOA) are shown in Figure 2.

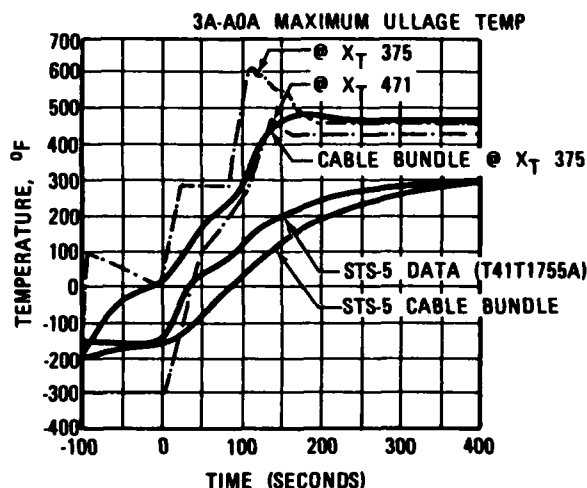


FIGURE 2 - CABLE BUNDLE, 3A-AOA MAXIMUM LO2 ULLAGE TEMPERATURE

b. Test Conditions vs. Operating Environment 3A-AOA

Parameters	Operating	Test
Oxygen (%)	100	100
Pressure (Psia)	20 to 36.7	40 to 44
Temperature (°C)	-184 to +241	+255 to +265
Flow Rate (CFM)	10 (Turbulent)	0 (Stagnant)
Current (Amp)	0.130 (Maximum)	25 to 50
Exposure Time	8 Minutes (Flight)	As Required
Open Flame	None	20 - 30 Seconds
Flame Temp. (°C)	-----	+1800 to +2200

c. Test Description

Test # 1

Specimen supported vertically in test chamber. It is subjected to open flame applied to low end of specimen for 20 to 30 seconds. Ignitor supplies a flame temperature of +1800 to +2200°C. To be acceptable, material must be self-extinguishing within 6 inches after ignition.

Test # 4

Specimen supported horizontally in test chamber. Current is supplied to a shorted pair of conductors in one cable in increments of 5 amperes per minute until conductor fuses or insulation ignites. To be acceptable, specimen must be non-combustible.

Test # 13

A minimum of 20 specimens cut to 11/16 inches to length are subjected to ambient oxygen mechanical impact tests at 10 Kg-m (72 ft. lbs.). To be acceptable, there can be no audible explosion, no flash, or visual evidence of burning such as char or major discoloration as a result of the impact.

2. Strippability and handling of wire and cable:

- Stripping techniques - mechanical, thermal.
- Protection against fraying and particulation.
- Personnel safety.

### 3. Crimpability:

- a. Connector terminations
- b. Splices and methods of splice protection.

### 4. Cryogenic Exposure Tests:

- a. Immerse in liquid nitrogen (-196 degrees Centigrade), mandrel test, visual inspection, electrical insulation test.
- b. Heat cycle to +316 degrees Centigrade, shock by immersion in liquid nitrogen and repeat item a tests.

### 5. Physical and Electrical Characterization:

- a. Physical properties of insulation.
- b. Insulation shrinkage.
- c. Dielectric strength and insulation resistance.
- d. Effect of moisture on dielectric strength, insulation resistance and mandrel tests.

### 6. Completed harness assembly tests:

- a. Contamination - particles generated (including oxygen cleaning).
- b. Clamping supports.
- c. Splices, as applicable.
- d. Connector termination and backshell support.
- e. Protective coatings or other insulations.

Upon completion of the qualifying tests, the preliminary Martin Marietta specification, STM E300 was finalized to reflect changes found to be necessary from the results of the tests. Processes and procedures were implemented for wire and cable preparation, termination, cleaning and handling to assure oxygen compatibility would be maintained throughout assembly and installation in the finished flight vehicle.

### TESTING

The initial PTFE insulated cables, subjected to oxygen flammability testing, ignited and burned all of the specimen insulation. However, there was no self-ignition and all other tests indicated acceptable results for the intended application. At this point in the program a complete evaluation of oxygen tank system was performed to determine if a flame hazard exists. The final result of the hazards analysis is presented in Table 2.

Table 2. Worst Case Point  
Level Sensor Circuit Analysis

1. Type of Failure - Fire.
2. Fuel Source - Polytetrafluoroethylene Insulation.
3. Ignition Source - Electrical Current or Mechanical Impact.
  - a. 5 to 9 amperes will ignite insulation providing 18 of 19 strands of conductor are cut in shorted configuration.
  - b. Impact sensitive materials not permitted inside tank.
4. Modes of Failure\* - Current (Sequential)
  - a. Single Failure - 18 of 19 strands of conductor severed on positive input wire. Current=130 Milliampere.
  - b. Second Failure - positive input wire shorts to ET Body. Current=150 Milliampere.
  - c. Seventh Failure - short circuits across three resistors and three transistors. Current=550 Milliampere.
  - d. Eighth Failure - failure of voltage regulator in a short circuit mode. Current=7.5 amperes continuously (for 9 amperes for 3 seconds) if two main power busses are at same voltage level such that they conduct equally.

\*Note: All failures must be "fail shorted" not open, or a "failed voltage regulator with balanced power busses".

In continuing tests, a glass fiber sleeve was placed over each of the test cables. The sleeves were of thin diameter Beta glass fiber strands which were braided into a tight construction in order to provide maximum cable surface coverage with minimum particulate contamination generation during flight usage. Sleeving wall thicknesses were selected to range from 0.013 to 0.016 inch with overall diameters sized to slip easily over the cables during harness fabrication.

The addition of glass fiber sleeves required special cleaning and handling procedures to meet the environmental cleanliness limits for oxygen propellant systems:

#### Cleanliness Limits:

No particles larger than 1000 microns.  
Non-volatile residue shall not exceed one milligram per square foot of surface area.

#### Cleaning Procedure:

The assembled harness is flushed by three separate washes of a clean azeotrope of trichlorotrifluoroethane with approximately 50% methylene chloride in order to remove organic contaminants including nonvolatile residue.

After flushing, the assembly is washed and tested for particulate and nonvolatile residue using clean trichlorotrifluoroethane. Sampling is taken from each wash until particle count produces no particles in excess of 1000 microns and nonvolatile residue is less than one milligram per square foot.

This cleaning method has been found to be adequate to remove residual flammable hydrocarbon such as silicones, oils and starches from the outside cable surfaces as verified by infrared spectrographic tests. The solvents have low boiling points which prevent entrapment and will not burn or ignite when exposed to flame.

With the glass fiber sleeves, external ignition of test specimens met the program requirements by self extinguishing within the allowed dimensions although the electrical ignition tests continued to fail at the fusing current levels. Since

failure of electrical ignition specimens imposed the requirement to perform harness configuration flammability testing, each cable lot was subjected to configuration tests. Under normal flight operating configurations, these specimens could not be electrically ignited during the flame tests and the glass fiber sleeved cables were found to be acceptable for the first External Tanks where benign operating environments would be experienced. See Figure 2, STS-5 Data.

For light weight rapid production improvements, attempts were made to obtain the oxygen cable with factory installed glass fiber sleeving.

Flammability tests on this configuration produced the first observed drip, spark and flare burning affects to be reported on PTFE materials. A reevaluation of previous cable lots resulted in establishing degree of flammability and identified differing flame characteristics from different manufacturer's cable lots. With the consent of the suppliers, each of the cable lot configurations were submitted to Dupont for evaluation. A generalized summary of Dupont's findings is shown in Table 3 along with flammability ratings.

Table 3. Evaluation of Cable Specimens

Sample Designation	Number of Conductors	Insulation Thickness	Filler Number	Yarn % PTFE	Jacket Thickness	Rating Flame
1	3	0.0103	3	9.3	0.014	1
2	3	0.0095	3	20	0.014	4
3	2	0.0106	2	16.6	0.012	3
4	2	0.0108	2	7.1	0.014	2

Flame Rating 1 is worst, 4 is best construction.  
Sample #2 had tightest jacket construction and contained greatest percentage of PTFE in filler yarn.  
Sample #4 had loosest construction with easily separated jacket tapes and lowest content of PTFE in filler yarn.

All of these samples met the electrical and material requirements of the controlling Military and NASA specifications to which they were supplied. All of the samples indicated entrapped flammable hydrocarbons in jackets and extruded conductor insulation by tests performed at Martin Marietta Michoud Division.

Because PTFE materials from suppliers other than Dupont had been used in the cable constructions and because different "Teflon" TFE base resins had been introduced by Dupont for the extruded

insulation, an investigation into the basic manufacturing processes and materials began. The preliminary results of this continuing study are presented in Figs. 3 and 4.

FIGURE 3- AVAILABLE PTFE MATERIALS

TEFLON*	DESCRIPTION	MAJOR USES
"Teflon" 1	General Purpose Powder for Molding and Extr.	Gaskets, Seals
"Teflon" 5	Special Molding Powder	Sheet and Rod
"Teflon" 6, 6C,	Granulated for Cylinders	Skived Tape and
6A	Special Powder for Compounding	Molded Shapes
"Teflon" 7, 7A	and Extr.	Thin Wall Tubing
7C	Special Powder for Void-Free Molding	Wire Coat, Tape
"Teflon" 8, 8A	General Purpose Powder	Molded Sheets,
"Teflon" 9, 9A,	High Melt Viscosity	Tape, Wire Wrap,
9B, 9C	Granular Form, High Resistance to charge factor	Tubing
"Teflon" 30, 30B	Aqueous Dispersion for Dip Coating	Replaces "Teflon" 1
"Teflon" 41BX	Aqueous Dispersion for Compounding	Ram Extruded
"Teflon" 62, 64	Special Powder for Extrusion	Special Usage
		Impregnation of
		Glass Cloth
		Electronic Comp.
		Wire coating, jacketing, tubing

\*Dupont Trademark

FIGURE 4- OTHER SUPPLIERS OF POLYTETRAFLUOROETHYLENE\*

Allied Chemical Corporation supplies G18, G80, G83 and G700	Halon (Trademark)
American Hoechst supplies TF1100, TF1620, TF1640, TF1665, TF2053 and TF2071	Hostaflon (Trademark)
Carborundum Company supplies WR-25	EKKCEL (Trademark)
ICI and ICI Americas, Inc. supplies CD1, CD4, CD123-CD126, CD509, G3, G161, G163, G201, G256, G306-G308, G401 and GP1	Fluon (Trademark)
LNP Corporation supplies 139 and 158	Polycomp (Trademark)
Montedison supplies 139 and 158	Algoflon (Trademark)

\*As of information compiled to end of 1980.

The various material control specifications (ASTM D1457-81a, AMS 3651C, L-P-403C and MIL-P-22241B) do not provide adequate material requirements for PTFE applications in aerospace oxygen environments since these documents do not exclude copolymers or cross mixing of fluorinated hydrocarbons so long as the basic characteristics listed in the governing specification are met. In process, extrusion and sintering of the materials, development toward easier handling, forming and better yield of finished product have tended to lower the flame resistance of the PTFE materials in oxygen environments without affecting characteristics in air. Spectrographic evaluation (Fig. 5) of the PTFE insulation on the finished cables from all suppliers of the oxygen system cables indicated the presence of varying amounts of flammable hydrocarbons entrapped in the PTFE structure. These hydrocarbons were traced back to be extrusion aids which had been used in billet forming for modified ram extrusion. The extrusion aid recommended in the modified process is a liquid organic wetting agent, such as naphtha. This agent is supposed to volatilize during the extrusion and sintering operation (371 to 399 degrees Centigrade). However, the extruded material tends to form a gas tight seal entrapping small amounts of the extrusion aid within the structure and air circulated heat (tunnel ovens) cannot volatilize or otherwise remove it from the insulation. In review of this method, a non-flammable wetting agent was sought to replace the existing extrusion aids and permit the modified processes to still be used.

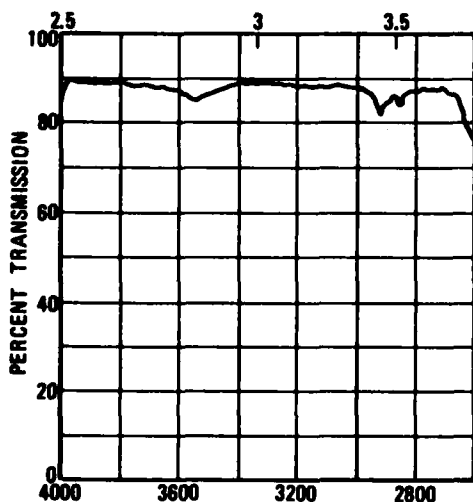


FIGURE 5 - INFRARED SCANNING SPECTROGRAPH SHOWING PRESENCE OF FLAMMABLE HYDROCARBONS

After chemical reaction and production environmental impact (OSHA) studies, perchloroethylene was selected as the best candidate for a

non-flammable extrusion aid since it had a history of use in fractionation tests of PTFE resin powders under ASTM D1456-81a and is presently used in industrial applications for dry-cleaning. Quirk Wire Company, Incorporated, of West Brookfield, Massachusetts, was contacted and agreed to fabricate wire and cable samples using the suggested nonflammable extrusion aid. Test specimens examined using infrared scanning spectrography indicated clean PTFE (See Figure 6).

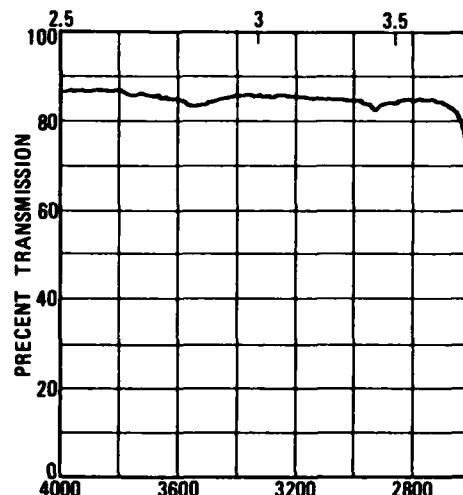


FIGURE 6 - INFRARED SCANNING SPECTROGRAPH OF "CLEAN" PTFE

Upon the successful completion of qualifying electrical and spectrographic testing, cable specimens were submitted to MSFC for oxygen flammability testing. Special attention was given to test configuration, position in test chamber, environmental temperature and equipment controls. A video tape recorder and camera was included for these tests. Using "worst-case" test electrical ignition specimens under close observation from initiation to completion, visual evidence of overheating was noted before current was applied for test. One thermocouple had been placed above the center of the test bundle and upon the application of fusion current, the bundle ignited and burned propagating to the thermocouple insulation leading to a connector and associated power wiring within the chamber which burned vigorously. As a result of this test, the chamber heaters were repositioned to minimize radiant heating affects and two thermocouples were positioned near the test specimens to more properly monitor environment. One thermocouple was placed near point of specimen ignition with the other placed to monitor heat affects (See Figures 7 and 8).

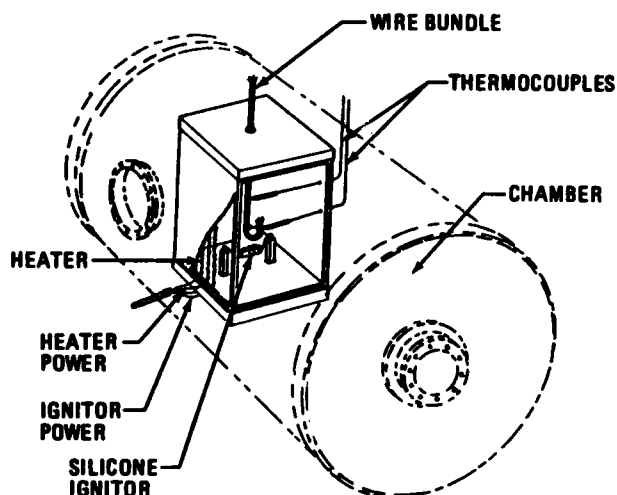


FIGURE 7 - TEST NUMBER 1 - UPWARD PROPAGATION

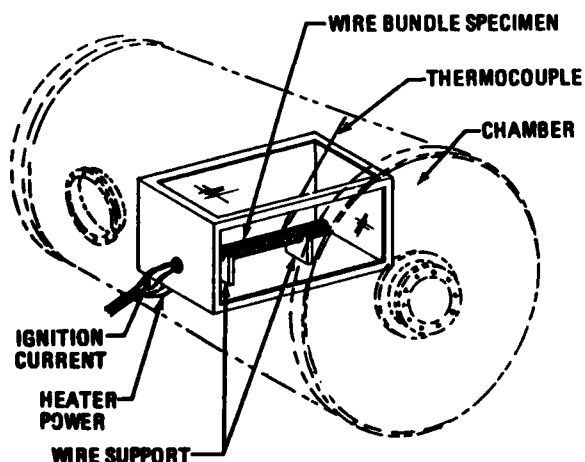


FIGURE 8 - TEST NUMBER 4 - ELECTRICAL OVERLOAD TEST

Utilizing these testing techniques, it was determined that position of specimen within the chamber was critical to the test. If the point of ignition was not heated to the "worst-case" temperature, the specimen would not ignite even though the remainder of the specimen was at that temperature. By repositioning such that the test specimen was within the test temperature envelope, the specimen would ignite and propagate because a high heat spike would be generated upward around the surface of the tested specimen (tunnel effect), Fig. 9

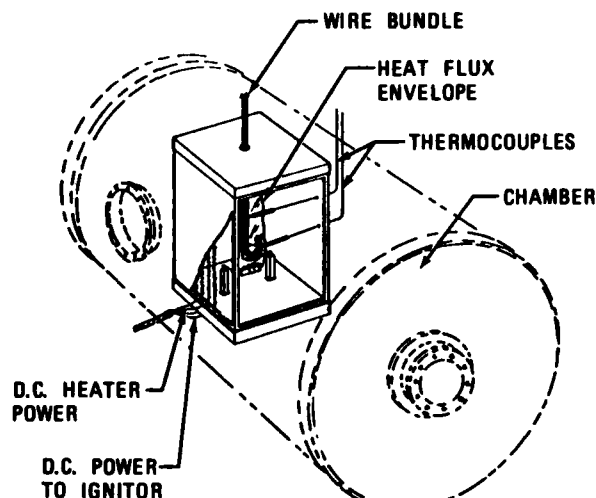


FIGURE 9 - TEST NUMBER 1 - FLAME IGNITOR SHOWING IGNITION HEAT FLUX OVER SPECIMEN

With the better definition of the heat environment experienced in the test chamber, controls were introduced to provide proper sample position and heat application from specimen to specimen so that comparisons of test results could be relied upon as true indicators of specimen flammability.

In conjunction with the test hardware modifications, test specimen configuration was revised to more closely simulate the harness configuration of the flight hardware. The glass fiber sleeve was increased in thickness from 0.016 to 0.032 inches with an added requirement that the sleeve must fit snugly over each cable.

#### CONCLUSIONS

As a result of these studies, two lots of cable manufactured to the latest requirements have been tested and found satisfactory for flight usage. Although the cables can still be ignited and some traces of flammable hydrocarbons have been noted during flammability tests, the product can be rated non propagating within the oxygen environment. Efforts will continue to improve and upgrade the cable to the best possible configuration for aerospace applications in oxygen. The basic differences between the oxygen cable and those manufactured to Military Specification Requirements as determined through the work accomplished in this study are:

1. Jacket tapes of the cable must be tightly wrapped and sintered (melted) to seal the construction into an airtight, watertight

configuration. The volatile additives in the unsintered tapes must be removed during sintering. Air tightness serves to restrict the flow of flammable gases in the configuration when ignited and provides more bulk by close contact to help prevent flame propagation.

2. Filler yarns to be used in the cable must be constructed and coated such that they do not introduce paths through which flammable gases may flow upon ignition of the cable and contain no volatiles to assist propagation.
3. Fiberglass cable sleeves must be of tight weave or braid construction of a thickness sufficient to prevent cross propagation between cables should ignition occur. The sleeve must fit snugly to the cable to prevent the flow of flammable gases between the cable surface and the sleeve. This serves as added bulk to limit heat transfer and restrict flame propagation.
4. All materials of construction must be free of volatile hydrocarbons. Entrapped pockets of gases will be released upon ignition to flare and produce high heat spots across cables in the harness resulting in flame propagation. Where possible, non flammable solvents, wetting agents or other additives should be used in processing the base resin materials.

5. Use only the materials which have been tested and approved for the application. Substitution of an unknown off-the-shelf product may result in catastrophic failures either by material characteristics or by unacceptable processing.

Martin Marietta Corporation's process specification STM E300-2 has been expanded to document the complete requirements for acceptable materials, methods of processing, cleaning and testing for the fabrication of oxygen compatible cables. Presently, there is one qualified supplier to this specification.

Materials used in the cable construction are listed below:

#### Cable Description:

The cable consists of two 20 AWG conductors cabled together with two 0.034 inch diameter glass fiber fillers with a left hand lay of 8 to 16 times the diameter of the multiple. The essentially circular configuration is then wrapped tightly with one sintered PTFE tape (50% overlap) and cross wrapped with two unsintered tapes. The wrapped configuration is then sintered at high heat to melt the outside tapes into an airtight, watertight seal about the cable. See Fig. 10.

#### FIGURE 10 - HEAT SINTERING PTFE

In 1981, ASTM D1457 was revised to change the sintering procedure for Type III resins by a Note A to Table 3 of ASTM D1457-81a:

"Procedure A has been specified in previous issues of Specification D1457 for Type III resins. For improved precision Procedure B should be used."

	<u>A</u>	<u>B</u>
Initial Temp. °F	716 ± 10	554
Rate of Heating °F/h	NA	216 ± 18
Hold Temp. °F	716 ± 10	716 ± 10
Hold Time, Min	30 ± 2, -0	30 ± 2, -0
Cooling Rate °F/h	132 ± 9	108 ± 9
Final or Second Hold Temp. °F	572 ± 10	561 ± 10
Second Hold Time, Min.	NA	24 ± 0.5, -0
Period to Room Temp. Min. h	1/2	1/2

Volatilization Temperature of Naptha ranges from 200 to 575°F.

TFE sintering temperature range is 700 to 750°F.  
melt temp. 621°F.

#### Materials:

##### Conductors:

Each conductor consists of 19 strands of 32 AWG nickel coated copper wires overlaid with extruded Dupont T-64 "Teflon" insulation (10 mils thickness). The insulation is formed using perchloroethylene as the extruding aid.

##### Fillers:

The fillers are formed of glass fiber strands in accordance with MIL-Y-1140, form 2, Class C, impregnated with 12% by weight (minimum) of PTFE. The dispersion coat is ICI-AD1 which is an emulsion of PTFE, Triton Soap in

approximately 6% water. The coated fibers are subjected to several heat passes to remove traces of the soap and any starch binder which may be present in the fibers.

#### Sintered Tape:

The tape is skived from ram extruded billets which are sintered. Allied G80 PTFE (a granular powder) is used for this application with no extruding aid present.

#### Calendared Tapes:

The unsintered outside tapes are formed by calendaring from billets of ICI CD651 PTFE. The billets are compression molded using a purified kerosene as the extrusion aid, so this wetting agent must be removed by sintering and other cleaning processes during cable manufacture

#### Comments:

From infrared scanning tests, specimens of the cable constructed from materials listed indicated very low hydrocarbon content. However, during flammability tests in oxygen, spot flame and propagation has shown that not all of the flammable hydrocarbons have been removed from the outside tapes.

ALVIN T. SHEPPARD  
Senior Materials Engineer  
Department 3516  
Martin Marietta Corp.  
P. O. box 29304  
New Orleans, LA 70189

Mr. Sheppard is presently the responsible electrical materials and process engineer for the Space Shuttle External Tanks. His experience includes engineering support for electrical materials and process specifications in such programs as Titan, Skylab and Viking at Martin Marietta, as well as design, research, development and implementation of test instrumentation for Cryogenic, Exotic and Solid propellant fuel systems used during the Gemini, Saturn and Apollo programs at Rocketdyne.

As a design improvement, attempts will be made to obtain calendared tapes made from billets formed using perchloroethylene as the extrusion aid and fillers having 20 to 25% by weight of PTFE for better bulk and sealing.

#### Acknowledgements:

A tremendous amount of technical support was provided by George C. Marshall Manned Space Flight Center Materials and Processes Laboratory in the resolution of oxygen system electrical cable problems and without the fullest cooperation of the following suppliers, the task could not have been accomplished:

Champlain Cable Corporation, Winooski, Vermont  
DeWal Industries, Incorporated, Saunderstown, Rhode Island  
Dodge Fluorglas, Oak Industries, Hoosick Falls, New York  
E. I. DuPont De Nemours and Company, Plastic Products and Resins Department, Wilmington, Delaware  
Imperial Wire and Cable, Newton, Pennsylvania  
Teledyne Thermatics, Elm City, North Carolina  
Tensolite Insulated Wire Company, Buchanan, New York  
Wirecraft Products, West Brookfield, Massachusetts

ROBERT G. WEBBER  
Materials Engineering  
Department EH 32  
George C. Marshall Space Flight Center  
Huntsville, Ala 35812

Mr. Webber is currently involved in research on the chemical reactivity of non-metallic materials in oxygen rich environments for aerospace application. His experience includes specialized studies on the strain rate properties of speciality metals and oxygen compatibility testing of non-metallic materials. He is a member of the American Society for the Testing of Materials Committee G04 on Compatibility and Sensitivity of Materials in Oxygen Enriched Atmospheres and is performing graduate work in mechanical engineering at the University of Alabama in Huntsville.

## DEVELOPMENT OF FLAME RETARDANT, LOW AGGRESSIVITY CABLES

J.R. Bury and B.A. Cranfield

Standard Telecommunication Laboratories Ltd.,  
Harlow, Essex, CM17 9NA, England.Summary

The construction of a fire retardant, low aggressivity cable may, depending upon the severity of application, require four components based on polymers-insulation, fire barrier tape, bedding and sheath. A number of high performance polymers have been evaluated as insulation materials, whilst STC have developed a range of bedding and sheathing materials, both thermoplastic and crosslinkable, to meet the exacting requirements of industrial and military users.

Introduction

During the past few years it has become increasingly apparent that flame retardant polymers and compounds are becoming essential components of wires, cables and associated electrical equipment. This realisation derives from the increasing recognition of the hazards to people, property and equipment from cables involved in fires. Early development work to improve the performance of cable insulation and sheathing was directed towards reducing flammability and increasing resistance to fire propagation. Halogenated polymers and flame retardant additives proved reasonably effective. However, whilst cables are rarely the cause of a fire, their behaviour when subjected to a fire environment has continued to give rise to a concern which has been sharply focused by the devastating results of some recent fires in which such materials have been present. This concern has led to an urgent reappraisal of the specifications governing the use of these products, with particular attention being paid to the evolution of smoke, corrosive and toxic gases. The cable industry in Europe has responded to the challenge and STC has made a major contribution to the development, characterisation and use of low aggressivity polymers and compounds for insulation and sheathing applications. These materials, in addition to possessing good flame retardance are characterised by their low evolution of smoke and aggressive fumes when exposed to fire.

New Specification Philosophy

The trend towards low fire risk cables, now accelerating throughout Western Europe, is evident in a wide range of specifications originating from many industrial and military sectors. In general, specification requirements may be segregated into

two groups. The first group concerns low fire risk requirements common to all sectors and includes:-

- i) a high level of resistance to ignition and flame propagation;
- ii) low smoke evolution;
- iii) low acid gas evolution;
- iv) low toxic gas evolution;
- v) low heat of combustion.

Requirements (iii) and (iv) preclude the use of halogenated materials.

The second group comprises requirements relevant only to certain sectors and includes:-

- i) oil resistance - cables are often used in aggressive environments where resistance to a number of oils and fluids is of paramount importance, for example in mass transport locomotive wiring, oil and petrochemical industries, shipboard and aircraft wiring.
- ii) abrasion resistance - many installation practices and operation techniques require a high degree of abrasion resistance, for example for pulling through crowded or non-linear cable ducts and when using robot handling techniques.
- iii) radiation resistance - for the nuclear power industry.
- iv) maintenance of circuit integrity - for control and emergency circuits in, for example, aircraft and major industrial complexes.

Thermoplastic materials can in many cases meet the specification requirements but it is sometimes necessary to crosslink the cable materials in order to achieve the appropriate combination of properties.

Test Procedures on Materials

Classifying flammability is a complex matter since many factors are involved in the propensity of a given material to ignition and burning. Test results will depend, for example, upon the shape and orientation of the sample, the ambient temperature, the temperature of impinging gases and the shape of the test chamber. For the purposes of providing an initial separation of non-runners from possible contenders, we have found the following fire related tests to be useful:

### Oxygen Index (OI)

The volume proportion of oxygen in an oxygen/nitrogen mixture passing through the test chamber at a fixed rate of flow is adjusted until sustained combustion of the ignited specimen is just possible. The test specification employed is BS 2782 Method 141B.

### Temperature Index (TI)

The temperature at which sustained combustion of the ignited specimen is just possible at an oxygen concentration of 20.8% (i.e. the oxygen concentration in the atmosphere). This test has greater relevance than the OI test to the probability of a material sustaining combustion in a fire, when the ambient temperature is high. There is no ASTM, BS or ISO specification covering this test.

### Smoke Generation

In accordance with ASTM E-662 a specimen of the material under test is exposed to radiant heat (smouldering combustion) or to a group of propane burners (flaming combustion) in an NBS Smoke Chamber. Smoke evolution is monitored by recording the optical density of the chamber atmosphere during the test. The maximum optical density and the time to reach this value are noted.

### Acid Gas Evolution

The specimen is pyrolysed in air and the gases evolved are collected in water. The strength of the acid solution thus formed is determined and used to calculate the quantity of acid gas generated. This test is specified in draft IEC 754 and VDE 0472.

### Toxicity Rating

A sample of known weight is pyrolysed at about 1000°C in a given volume of air. After burning the gases evolved are analysed for specific constituents e.g. HCl, HCN, CO, CO<sub>2</sub>. This test is specified in UK Ministry of Defence Specification NES 713. The definition of 'Toxicity' as such is an extremely complex and controversial matter.

### Heat of Combustion

This is determined in accordance with VDE 0472.

### Materials Evaluation and Development

#### Insulation

The choice of insulation material for a low fire risk cable is influenced by a number of conflicting parameters which require to be optimised to give the appropriate combination of properties.

The material must have suitable dielectric characteristics. However, the quality of insulation should suit the application: underspecifying leads to unsatisfactory performance, while over-specifying may result in an unduly expensive

product. Physical and mechanical properties are also significant: cables and wires must be capable of performing for many years, even in hostile environments. Finally the material should be flame retardant, not evolve aggressive fumes, and it should generate minimal smoke. The requirement for materials satisfying these conditions has resulted in the development of several halogen-free, flame retardant polymers and compounds: their key properties are summarized in the last three columns of Table 1.

Table 1 : Key Properties of Insulation Materials

Properties	Typical PVC	Typical PE	Noryl	Ultem	PEEK
Specific Gravity	1.4	0.95	1.05	1.07	1.30
Ultimate Tensile Strength (MPa)	20	15	40	120	100
Elongation at Break (%)	300	500	250	150	200
Oxygen Index (%)	30	17	30	47	30
Temperature Index (°C)	220	N/A	300	330	325
Smoke Generation	High	Medium	Medium	V.Low	V.Low
Relative Permittivity	4-5	2.3	2.6	3.1	3.0
Max. Operating Temp. (°C)	100	80	100	200	200

These new materials include:-

Noryl - modified polyphenylene oxides, manufactured by General Electric Plastics, and specially formulated for use as wire insulation.<sup>1</sup> These materials combine good mechanical, electrical and flame retardant properties.

Victrex PEEK - polyetheretherketone, an ICI developed high performance thermoplastic polymer suitable for extrusion. We have found that it possesses an impressive range of properties including exceptional heat resistance, extremely low acid gas and smoke evolution, high strength and outstanding chemical and fluid resistance. Crystallinity to a level of about 40% can be achieved. PEEK requires processing temperatures in the range 370°-400°C, with the use of high temperature extruders.

Ultem - an amorphous polyetherimide from General Electric Plastics provides many of the features of PEEK, but the existing grades are not so good in respect of solvent resistance, being soluble for example in some chlorinated hydrocarbons. Slightly lower extrusion temperatures, however, can be used and the material is less expensive.

It may be noted here that some common non-flame retardant insulation materials may, in certain applications, be used in combination with protective tapes, low fire risk bedding and sheathing materials. EPR and polyethylene, for example, have found use in the nuclear power industry as insulations where their excellent dielectric properties are useful.

#### Protective Tapes

It is often necessary to interpose a helically or longitudinally applied tape between the

insulated conductors and the cable sheath. Polymeric tapes are used to maintain strand geometry and for unit identification, while metal tapes provide armouring protection, electrical screening, and a moisture barrier. Cables intended for use in high fire risk environments sometimes require a fire barrier layer beneath the fire retardant sheath. Materials at present available for this layer are not extrudable and are therefore applied in tape form.

Metallic tapes such as steel and aluminium, have excellent fire barrier characteristics but make the construction rather rigid. Two classes of fire barrier material may be considered if greater flexibility is required:-

- i) Inorganic materials such as asbestos and glass fibre, both of which are available in various forms, including mica impregnated glass fibre.
- ii) Polymeric organic materials (e.g. polyimide and polyaramid), which derive their high temperature resistance from the stabilizing effect of their high aromatic content on the polymer structure.

We have evaluated a number of potential tape materials and have identified suitable products for use in a wide range of cable constructions.

In the future, it is possible that PEEK film, either directly extruded or skived from moulded blocks, could have application as a protective tape.

#### Sheathing

The foregoing insulation and taping materials are generally unsuitable for sheathing applications, except where extremely arduous environments must be tolerated and where, therefore, material cost is not a selection criterion. For cable sheathing, the greater material volume usage usually demands a less expensive product. Flexibility is of greater importance whilst insulation resistance and high speed processing capability are of less consequence.

With these factors in mind, a survey of the vast range of polymer types presently marketed will reveal that no readily available polymer possesses the desired combination of characteristics for a low fire risk sheathing material. Therefore, a flame retardant additive must be combined with a polymer or blend of polymers in order to achieve these characteristics. A quantification of some of the important mechanical and fire related properties which have been set as target values is shown in the first column of Table 2.

Our developments have concentrated on combining the flexibility and mechanical integrity of inexpensive polyolefin copolymers with the fire retardant, low aggressivity and mechanical reinforcement properties of certain types of filler. We have found that several such copolymers are capable of accepting filler loadings in excess of 50% by weight to give extrudable, flexible, mechanically robust products with excellent flame

retardant properties. In some cases the reduction in extensibility which often accompanies the loading of polymer with filler can be partially offset by the addition of a coupling agent. Thus the components of a typical low fire risk sheathing formulation could be:-

Polymer - We have found that ethylene copolymers such as EPR, EPDM, EMA, EEA, EBA and EVA, singly or in combination, are all candidate materials for this application. Careful attention, however, must be paid to the grade of polymer selected, since only certain grades, characterised by the comonomer content and by the melt flow index, have been found suitable.

Filler - The most suitable filler has been established as alumina trihydrate. This filler releases 30% by weight of water vapour in the temperature range 160°C-260°C, an action which is endothermic, so that local heat is absorbed, in addition to the water vapour acting to reduce the local oxygen concentration and to suppress ignition.

As in the case of polymer selection, strict attention must be paid to the choice of filler grade, especially to particle size and distribution. Some suppliers of alumina trihydrate are currently offering surface treated grades with the claim that improved mechanical properties in compounds may be achieved.

Figure 1 indicates the dependence of OI on the filler content.

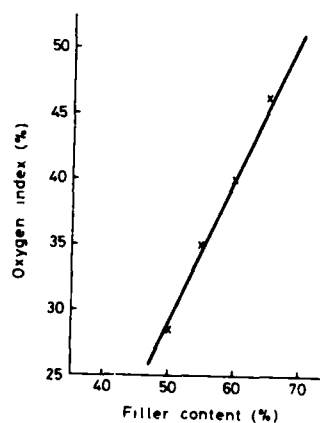


Fig.1 Oxygen index / filler content

We have briefly examined the properties of compounds utilising other water containing fillers such as magnesium hydroxide. We see no advantage at present in switching to materials which are less readily available than alumina trihydrate. It is possible that certain combinations of these two

fillers could offer advantages in some property areas but this aspect has not been studied methodically.

**Coupling Agent** - The most readily available classes of coupling agents are the titanates and the silanes; from among the wide range of these products available we have been able to select grades which give valuable improvements in mechanical properties over the equivalent untreated compound.

**Antioxidant** - A wide choice of antioxidants is available, the main selection criteria being long term compatibility with the compound and non-interference with the action of the coupling agent if this is present.

**Plasticiser** - Some formulations employing high viscosity base polymers require plasticisation as an aid to compounding and extrusion.

The result of these considerations has been the development of a family of sheathing compounds covering a wide range of flame retardant and mechanical characteristics so that the optimum product may be selected for a desired application. The basic characteristics of three thermoplastic compounds are shown in Table 2.

Table 2 : Characteristics of STC Thermoplastic Sheathing Compounds

Properties	Target Values	Typical PVC	4/7L	4/7	4/7M
Specific Gravity	-	1.40	1.45	1.50	1.59
Ultimate Tensile Strength (MPa)	10	15	7	8	10
Elongation at Break (%)	150	250	250	200	140
Oxygen Index (%)	35	32	35	40	46
Temperature Index (°C)	260	220	260	280	280+
Smoke:					
Flaming Mode (D <sub>m</sub> )	100	200		80	
Smouldering Mode (D <sub>m</sub> )	200	400		150	
Toxicity Rating	<5	>10		<1	

It is seen that these compounds are characterised by excellent OI, TI, low smoke and acid gas evolution and good mechanical properties. Moreover, where improvements in operating temperature, tensile strength, abrasion and fluid resistance are required we have found that these compounds are amenable to crosslinking.

It is convenient at this stage to briefly review the three crosslinking processes now available to the cable maker. They are:-

**Peroxide Crosslinking** - Thermal decomposition of peroxide, generally incorporated into the polymer at a level of 1-3%, is achieved by passing the cable through a heated, pressurised tube immediately after extrusion. The decomposition process provides highly active free radicals which interact with the polymer chains to produce

crosslinks.

**Electron Beam Crosslinking** - Cables are irradiated by a beam of high energy electrons accelerated by a high voltage generator. The cables are traversed under the beam several times to ensure even penetration. The electrons release hydrogen ions from the polymer chains thereby producing free radicals which combine to form a crosslinked structure.

**Water Crosslinking** - For this process, a silane grafted polymer is required. The crosslinking process is carried out separately from extrusion by immersion of the finished cable in either hot water or steam. Water initiates the crosslinking reaction, the rate of which increases with temperature. The capital cost of equipment for this process is very low and this factor constitutes a major advantage to cable companies who are considering entry to the crosslinked materials market for the first time. As examples of crosslinking times at 70°C (the maximum safe crosslinking temperature of ethylene copolymers in order to avoid deformation), a 2 mm thick sheath would require 48 hours, whilst a 5 mm thick sheath would require about 120 hours. Despite these apparent advantages, however, a high OI processable product of this type is not yet available. The only commercially available product of which we are aware has an OI of 29. The problems associated with increasing the filler loading in order to raise the OI are, firstly, that the product becomes difficult to process and secondly that surface moisture on the filler can promote premature crosslinking. We are currently looking at ways to overcome these problems in order to make available a processable product with an OI of at least 35 and a reasonable shelf life.

Although crosslinking introduces an additional production step, the use of crosslinked polymers offers substantial advantages for the more demanding applications. Electron beam radiation is the preferred method of crosslinking because fine control of the product properties is readily achieved by control of the radiation dose on a standard compound. Peroxide crosslinking, on the other hand, requires a specific compound containing a particular peroxide concentration for each combination of final properties. Furthermore inhomogeneity of product properties will result if the dispersion of the low level of peroxide is inadequate. An additional benefit of radiation crosslinking is that slightly higher break elongation values can be obtained for a specific ultimate tensile strength, compared with peroxide crosslinking.

Figures 2 and 3 compare crosslinking methods with respect to elongation at break.

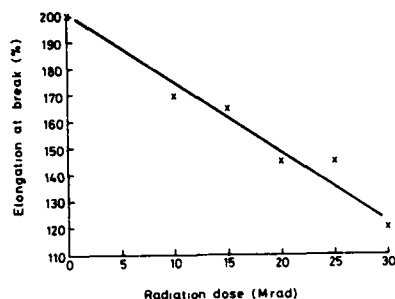


Fig. 2 Elongation at break / radiation dose

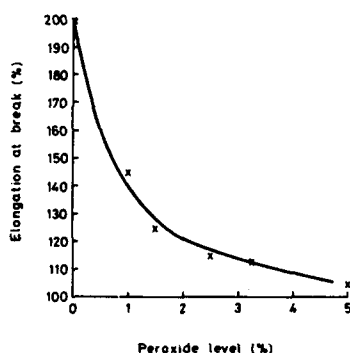


Fig. 3 Elongation at break / peroxide level

The properties of some crosslinked compounds developed by STC are shown in Table 3.

Particular attention has been paid in the design of the compounds shown in Tables 2 and 3 to ease of compounding and extrusion. No special equipment is required for compounding, both batch internal mixers and continuous twin-screw compounders having been used successfully. The melt viscosity of the compounds is somewhat higher than that of a typical PVC compound but extrusion experience has shown that these compounds can be processed on standard extruders, and we have found that a low compression PVC screw is satisfactory.

Bedding compounds have been developed using the same components as the sheathing compounds and

Table 3 : Characteristics of STC Crosslinked Sheathing Compounds

PROPERTY	4/7 Radiation crosslinked	5/2 Radiation crosslinked	6/5 Peroxide crosslinked
<b>Physical</b>			
Density (g/cm <sup>3</sup> )	1.50	1.44	1.43
<b>Mechanical</b> (BS 6746)			
Tensile Strength at Yield (MPa)	17	11	12
Elongation at Yield (%)	140	130	190
Ultimate Tensile Strength (MPa)	15	10	11
Elongation at Break (%)	180	230	270
<b>Thermal</b> (BS 6746)			
Heat Shock (°C)	150	150	150
Cold Bend (°C)	-40	-40	-40
Cold Impact (°C)	-40	-40	-40
<b>Ageing</b> (10 days at 100°C)			
Ultimate Tensile Strength (MPa)	16.5	13.5	12
Elongation at Break (%)	150	210	230
<b>Electrical</b> (BS 6746)			
Wet Insulation Resistance k(MΩ.km)	1	2	3
Relative Permittivity	2.85	6.2	3.0
<b>Flammability</b>			
Oxygen Index (BS 2782, 141B)	40	31	33
Temperature Index	280	280	260
Smoke -			
flaming mode (D <sub>m</sub> /minutes)	80/8	60/33	90/10
smouldering mode (D <sub>m</sub> /minutes)	150/10	60/20	180/15
Toxicity Index (NES 713)	0.6	0.2	0.6

4/7 = Standard compound

5/2 = Oil resistant compound

6/5 = Special flexible compound

may have the same formulation. If even higher flame resistance is required, this can be achieved by raising the filler content. Although mechanical properties will suffer there is often little or no mechanical requirement for this application. OI values in excess of 50 have been achieved.

#### Cable Design Concepts

A low fire risk cable must, of course, carry out its primary function of signal or power transmission and it must also be capable of withstanding the rigors of installation and operating conditions. Hence the need for a range of materials for insulation, tapes and sheaths. As previously mentioned many cable designs utilise polyethylene or EPR insulations and rely on the tapes and sheathing materials to provide the necessary degree of flame retardance. For more demanding applications the insulation materials themselves will have to be changed. Under no circumstances will STC Low Fire Risk Cables use low fire risk sheathing materials in conjunction with halogenated insulation materials.

#### Test Procedures on Cables

Numerous standards, both national and international, exist for fire tests on cables and cable bundles. These often involve the testing of substantial cable samples in large oven type enclosures. The key features of some of the more commonly used tests are shown in Table 4.

STC Low Fire Risk cables have been successfully tested to IEC 332 - Part 3 (category A) and in the LTE 3-metre smoke cube.

Table 4 : Fire Tests on Cables and Cable Bundles

STANDARD	DESCRIPTION OF STANDARD	TESTING DEVICE	DURATION (mins)	SPECIMEN	TEST CRITERION
BSA	BSA 111	Balston gas burner	10 Mins.	Single cable	Fire propagation
BSA	BSA 111 modified	BSA 111 STC 111 methane flame, 10 Mins.	10 Mins.	Cables in horizontal plane	Flame spread and smoke evolution
BSA	BSA 111	Industrial refrigerated sprays	10 Mins.	Parallel cables in horizontal plane	Smoke emission
BSA	BSA 111	10 litres of ethanol in fuel tray at base of burner	Complete burning of ethanol	No. of vertical cables depends on weight of non-metallic material	Extent of fire damage
BSA	BSA 111	Radiant heater plates at 100°C	Vertical cables, 1 m long, total of 10 kg/m non-metallic material		Extent of fire damage
International	IEC 701	Tube type gas burner at 100°C with operating voltage applied	3 hours	Single cable, horizontal	Fire resistance with voltage applied to cable (no failure of 3A Fuse)
International	IEC 701	Balston gas burner	10-40 Mins.	1 m vertical cables, number depending on weight of non-metallic material	Self-extinction and flame spread

#### Areas of Exploitation

The materials evaluated and developed are being increasingly accepted in a wide range of communication, control and power cable applications in which flame retardancy is an essential requirement. Each of these application areas has a specific operating environment, but with the wide range of materials at our disposal we are able to select the optimum combination to meet the application requirements. Some of the major exploitation areas currently being accessed include the following:-

##### Mass Transport

It is especially important to use low fire risk cables with low smoke characteristics for underground railway tunnels since visibility and orientation would otherwise be severely impaired. London Transport now specify low fire risk materials for all types of cables used in the underground system. They have also been instrumental in the development of a suitable smoke chamber for cable testing. Commonly known as the 3-metre cube test it is often specified by other industrial cable users and may well be adopted by IEC.

##### Military Applications

The UK Ministry of Defence is currently rewriting specifications for shipboard wiring to preclude the use of halogenated materials. This application area is particularly arduous for sheathing materials requiring a high degree of resistance to a range of very aggressive fluids including fuel and lubricating oils. A specially formulated STC compound is currently undergoing approval testing for this application.

#### Nuclear Environments

Several application areas are currently under consideration. Firstly, it is anticipated that a pressure water reactor will be built in the UK in the near future which will utilise low fire risk materials for all cable applications. Secondly, the CERN organisation in France and Switzerland is currently building a new storage ring for the LEP project. Our sheathing material Standard 4/7 has been fully approved and is also being used by other cable manufacturers to supply cables outside the STC range of products. Lastly, a special superscreened cable using high performance insulation and sheath has been produced jointly with UKAEA at Winfrith Heath.

#### Other Exploitation Areas

Other applications under consideration or at an early stage of development include use in telephone exchanges, public buildings, offshore oil, automotive and industrial complexes. Furthermore, successful penetration into certain cable related areas is underway, for example as outer covering for special aerial feeder coaxial cables and as the insulation in flexible conduit systems.

#### Conclusions

A range of low fire risk materials has been developed which are halogen-free and exhibit low smoke, low acid gas and low toxicity characteristics when burning.

The cable designer has a choice of various insulation, tape, bedding and sheathing materials and can select from these on the basis of performance and cost. The materials range from the high cost, high performance insulations to sheathing compounds with similar cost/properties structure to PVC.

All preferred insulation, bedding and sheathing materials are extrudable using conventional equipment. No costly tape insulating processes are required and as none of the materials evolve corrosive fumes during processing there is no necessity for special metals for extruder barrels and screws.

The compound development work carried out by STC will be continued both to improve the existing grades and also to increase the range to include an improved dielectric material for use as a low cost insulation for low voltage power cables. Further work is also being carried out to produce a silane grafted polymer which can be compounded to give higher OI values than are currently available.

#### Reference

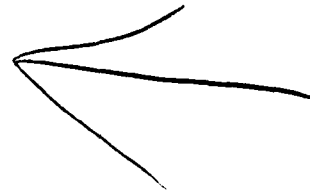
1. H. de Munck, J.R. Bury, W.E. Simpson and J.A. Devoldere: "A New Non-halogenated Flame Retardant Wire Insulation Based on Polyphenylene Oxide"; Proceedings of the 29th International Wire and Cable Symposium, Cherry Hill, 18-20 November 1980, pp. 268-276



J.R. Bury joined STL in 1967 and is at present Manager of the Polymer Processing and Application Department, working on the development of new materials and techniques for wire and cable applications. He is a member of the Royal Society of Chemistry and the Plastics and Rubber Institute.



Brian Cranfield graduated from the South Bank Polytechnic, London in 1965 with a degree in Chemical Technology, specialising in Polymer Technology. He joined the STL polymer laboratory in the following year and is now Manager of the Polymer Science and Technology Department, concerned with the characterisation of polymer structure and properties, and with the development and characterisation of new materials and processes for wire and cable applications. He is a member of the Royal Society of Chemistry and the Plastics and Rubber Institute.



# LOW-SMOKE, HALOGENFREE SHIP-OFFSHORE/ONSHORE CABLES WITH IMPROVED FLAME RETARDANCE AND FIRE RESISTANCE

J. R. Pedersen, T. A. Holte and E. Johansen

Standard Telefon og Kabelfabrik A/S  
OSLO NORWAY

## Abstract

Cables with improved fire-resistance and flame-retardance have been developed. They will continue to function at least 3 hours even at temperatures up to 1000°C and do not propagate fire when tested according to IEC 332 part 3 1982<sup>1</sup>, category A.

Made with halogenfree materials they give off no corrosive gases and very little visible smoke in cases of fire.

Cables are made for power, signal and instrument installations in hospitals, high rise buildings, railroad cars, subways, on board ship, oil rigs and oil production platforms. The offshore cables are specially constructed to withstand the rugged climatic conditions in the North Sea area.

## Introduction

The production in the North Sea oil fields together with new cable specifications in late 1970 from the Norwegian Navy, were deciding factors in our determination to improve the range of existing ship- and offshore cables.

Cables with excellent flameretardant properties have for some time been made with the traditional, halogen-containing materials such as PVC, PCP, CSP and fluoroplastics. They do not propagate fire even under the most severe test conditions.

Halogen containing materials have, however, some adverse fire-technical properties. When exposed to fire they develop heavy, black smoke and form toxic and corrosive gases.

This can prove to be a safety hazard not only in that smoke and choking gases can cause panic in a fire situation, but also hinder fire fighting procedures.

Furthermore, the cost of cleaning up, restoring structures, and replacing corrosion sensitive equipment and other secondary damages after a fire are usually much higher than the initial cost of damage from the fire itself. Attempts by us and others to reduce these affects of halogenated materials have resulted in only marginal improvements. Thus the task of developing a new "safety cable" became an important one.

The breakthrough came with the introduction in 1981 of the newer high oxygen index halogenfree (HF) materials based on EPDM and EVA.

At the same time the emphasis on safety and fire integrity had increased the demand for fire resistant cables.

In Norway the Navy and the Coast Guard were the first customers to order HF cables to be operable in and after a fire as defined in IEC 331<sup>2</sup>.

Fire resistant HF cables have since 1981 continually been supplied to the new oil rigs in the North Sea.

Taking the possibility of a hydrocarbon (HC) fire into consideration the newly developed cables discussed in this paper have been tested not only according to IEC 331<sup>2</sup>. In a qualification test the cables, mounted in a tray, are tested at 950-1000°C at rated voltage for 25 min. exposed to mechanical impacts and a salt water spray at intervals the last 20 min.

## Cable materials

The development of suitable flame-retardant HF cable materials has been concentrated on olefinopolymers, including EPDM and EVA.

To get the desired flameretardant properties formulations with aluminium trihydrate (ATH) were chosen, but some compositions can also include other inorganic fillers containing water of crystallization.

With ATH used as the flameretardant in a polyolefincopolymer system, the composition of a sheathing compound is as follows:

EVA	wt%:	35
ATH	" :	57
Smoke suppressant	" :	2
Lubricants	" :	2
Processing aids	" :	2
Peroxide/TAC	" :	2

The materials were mixed in a two stage process on a Banbury 3D, dropped on a 2-roll mill and granulated. The insulating and sheathing processes were carried out on conventional rubber extrusion lines.

The mechanical properties of these materials satisfy the requirements in the relevant cable specifications. For the HF sheath, the tensile strength is 11 MPa (1600 PSI), the tensile elongation 150% and the oxygen index above 30.

The elongation at rupture for the sheathing material is to some extent sacrificed to achieve an oxygen index high enough to pass the stringent flame propagation tests discussed later. Experience has shown that this does not adversely effect the handling or installation of the cables.

The HF cables have been approved by the Norske Veritas.

Table 1.

Typical properties of crosslinked HF materials

Properties	Insulation		Bedding	Outer sheath		
	Requirem. IEC 92-3	HF material	HF material	Requirem. IEC 92-3	HF material	CSP typical
TS MPa	>4.2	5.5	>2.0	10	11	12
PSI	>600	800	>290	1450	1600	1740
EB %	>200	200	100	300	150	450
LOI ASTM D 2863	-	>24	>40	-	30	>32
Corrosivity VDE 0742 part 813	VDE					
a) pH	>3.5	3.86	4.28	-	3.96	1.94
b) conductivity $\mu$ S	<100	52.2	27.5	-	57.3	5590
Arapahoe ASTM D 4100-82	-	4	4	-	3	10

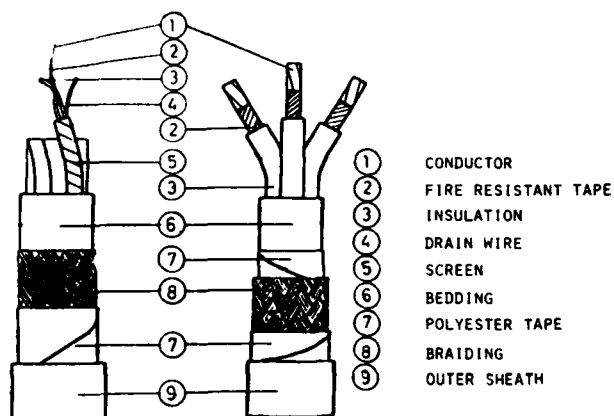
### Cable construction

The cables discussed in this paper are all of similar construction.

Important parameters are the high temperature performance of the materials like swelling, gas generation etc. Important to avoid kinking of the conductors is also the braid angle, especially on some of the smaller dimensions with copper conductors from 0.5 to 2.5 mm<sup>2</sup>.

Figure 1

Power- pair- and multiconductor cables for ship and offshore installations



## Fire testing of cables

In order to establish overall acceptable fire properties the following series of tests on cables, are used

IEC 331 <sup>2</sup>	fire integrity
IEC 331 "STK modified" <sup>3</sup>	" "
IEC 332-3 <sup>1</sup> 1982	fire propagation categories A, B, C
IEC 332-1	flame retardancy
London Transport 3 m cube <sup>4</sup>	smoke development

### IEC 331 "STK modified"

The STK fire integrity<sup>3</sup> test was developed to demonstrate that the cable cleated to a ladder or tray, will keep functioning in a fire. A mechanical impact and saline water spray procedure is introduced to simulate a real fire situation. Parts of this test is taken from the Belgian norm C 30-004<sup>5</sup>.

Four lengths of cable mounted with stainless steel tape, one single length and three in a bunch. Five lengths are used if test is to include an optical fibre.

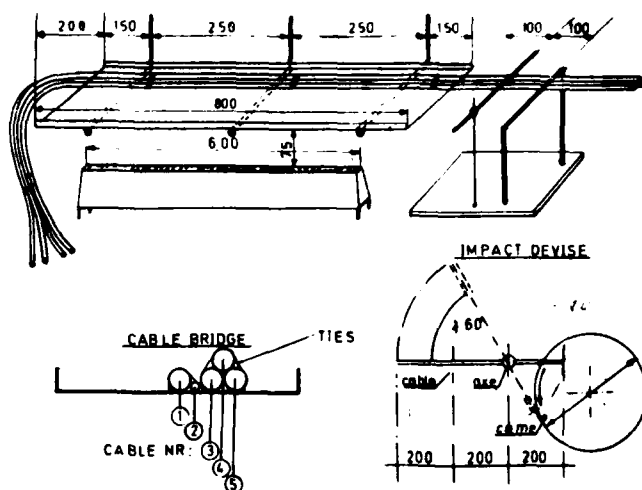
The cables are tested at 950-1000°C for 25 min. at rated voltage.

The first 5 min, ignition of cables

the next 10 min, 3% salt water spray every second minute for half a minute at a rate of 0.2 l/min

the final 10 min, impact by a steel rod every ½ minute.

Figure 3 CABLE INTEGRITY TEST

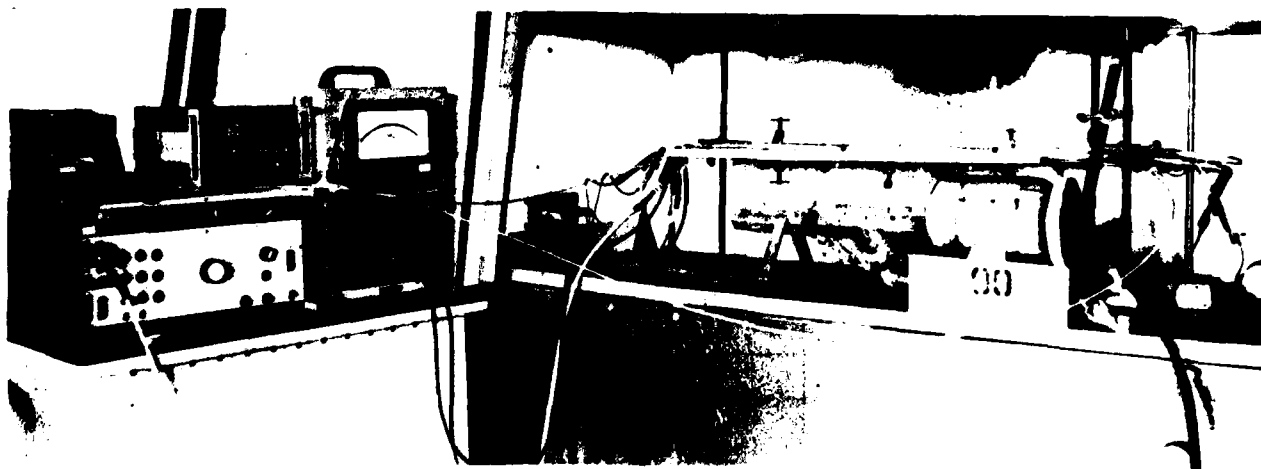


The power cables have passed the test if rated voltage does not cause a short circuit.

Figure 4 The mounting of cables with stainless steel tape.



Figure 2 Test set-up IEC 331 - "STK modified"<sup>3</sup>



For pair-, multiconductor signal- and fibreoptical cables the following properties are monitored every 5 min. during the 25 min. test.

#### Test schedule of cable

The cables are tested as follows

Cable 1, rated voltage

Cable 2, optical fibre. Loss in dB

Cable 3, mutual capacitance, pF

Cable 4, earth-capacitance unbalance, pF

Cable 5, insulation resistance, M $\Omega$

See figure 3 for cable location.

The cables have passed the test if,

- insulation resistance during the whole test is above 1 M $\Omega$
- the increase of capacitance is less than 50% on the total length
- the earth capacitance unbalance is less than 10% of the mutual capacitance
- for the optical fibre the excess loss in dB, is acceptable. The value is at present under discussion.

Table 2. Results pair cable

250V 1x2x0.75mm<sup>2</sup> at 950-1000°C

Time (min.)	Ins.resist. (M $\Omega$ )	Mutual- cap. (pF)	Earth cap. unbalance (pF)
0	10·10 <sup>6</sup>	132	0
5	10·10 <sup>6</sup>	138	-1
15	3·10 <sup>6</sup>	134	+16
25	3·10 <sup>6</sup>	90	+16

#### Fire propagation testing

The IEC 332-3, 1982<sup>1</sup> was developed to check fire propagation of bunched cables under realistic and controllable conditions. The dimensions of the test chamber, the heat loss through the oven walls, the air flow, the burner and the energy input are specified. From six points in the test oven the temp.-profile is recorded by the use of a datalogger. Reproducible results are obtained. See fig. 6.

Figure 5 STK facilities for testing fire properties of cables



In fig. 5, the oven with the door open, is shown the result of a category A test on a halogenfree fire resistant power cable, 3x2,5mm<sup>2</sup>. Cable lengths (38) 3,5 m long were mounted on a ladder to give 7 litres of organic (inflammable) material per m height on the ladder.

Ignition time 40 min, ribbon burner, 70000 BTU as described in IEC 332-3<sup>1</sup>. The cables were damaged up to only 1/4 of the total height.

#### Smoke testing

Comparative tests carried out on cables with halogen containing and HF materials clearly show the advantage of the last type. Within IEC the 3 m cube test<sup>4</sup> is now being discussed as the most relevant smoke test. Here cable samples are being burned, the smoke collected and the density measured as a function of time. An important parameter is the visibility distance, the distance over which it is necessary to have visibility to see an EXIT sign.

Table 3.

#### Fire properties of HF cables

Power cables	IEC 332-3 1982			IEC 331 3 hrs 800°C	IEC 331 - STK mod 25 min - 1000°C
	Cat A	Cat B	Cat C		
750 V	pass	pass	pass	pass	pass
6 kV	pass	pass	pass	pass	not tested
15 kV	fail	pass	pass	not tested	not tested
Pair-, multiconductor cables					
250 V	pass	pass	pass	pass	pass
All cables were tested at rated voltage					
Fibre optical cable				tested <sup>x)</sup>	tested <sup>x)</sup>
x) requirements are under discussion.					

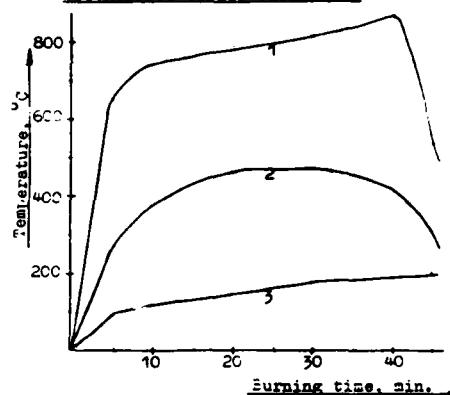
#### Conclusion

Halogenfree power- pair- multiconductor- and fibre-optical cables with much improved flameretardant- and fire-resistant properties are now available. The cables pass the IEC 332-3 category A flamepropagation test except for the 15 kV cable with crosslinked PE insulation that pass category B. Requirements for the optical fibre cables have not been set, but they stay in operation for at least 25 min. The cables with improved fire resistance pass IEC 331<sup>2</sup> and the much tougher STK fire integrity test.

It is our belief that as an increased number of users realize the many safety advantages of halogenfree cables, their acceptance and application will increase drastically.

Figure 6

Temperature as a function of time in the IEC 332-3 oven.  
Halogenfree cable, category A



1. Temperature at the burner height
2. " 1,5 m from floor
3. " 3,5 m " "

#### Acknowledgements

The authors wish to express their thanks and acknowledge the contributions of Mr. H. P. Dalby, Mr. S. Henriksen, Mr. I. Granheim, Mr. H. Thomassen and Mr. A. Hassel, in materials development, cable construction and testing.

## References

1. IEC 332 part 3 1982  
IEC Central Office 1 Rue de Varembe, Geneva, Switzerland
2. IEC 331 IEC Central Office 1 Rue de Varembe, Geneva, Switzerland
3. IEC 331 "STK modified" STK-KTL-TR-83/15  
Standard Telefon og Kabelfabrik A/S, P.B. 60 Økern, Oslo 5, Norway
4. 3 m cube test, London Transport Research Laboratory, 55 Broadway, London SW 1
5. Belgian norm, C 30-004  
Institut Belge De Normalisation  
Avenue de la Braban Conne 29, 1040 Brucelles



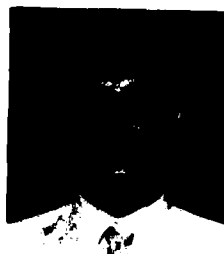
T. A. Holte

Graduated from the Technical University of Delft, Netherlands in 1956 with a Master of Science Degree in Electrical Engineering. Joined STK in 1956 as a test engineer in the High Voltage Laboratory. Head of the Power Cable Installation Department for 7 years and is at present in charge of the Technical Department.



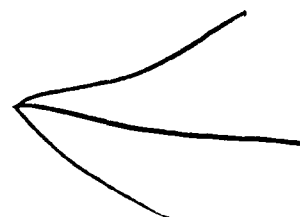
J. R. Pedersen

A 1955 graduate of Stockholm Tekniska Institut and 1960-63 part time studies at Stevens Institute of Technology, 11 years as a research chemist with CRL, Allied Chemical Co. Joined STK in 1969 and is at present in charge of materials development and 1 kV cable design.



E. Johansen

As an Engineer of Oslo Ingeniørhøgskole he joined Standard Telefon og Kabelfabrik A/S in 1980, and is now working in the Technical Department of the Power Cable Division.



## VERSATILE FIRE BARRIER SYSTEMS FOR TELEPHONE CABLE

Roger H. Keith\*, Douglas G. Dahms\*, Richard R. Licht<sup>+</sup>\*TelComm Products Lab/3M Ceramic Materials Dept/3M  
St. Paul, Minn.ABSTRACT

Fire barriers prevent smoke and fire spread along and between cables, through walls and floors, and protect critical conductors and equipment from heat. New flexible intumescent materials expand up to 10 times when heated, are versatile and easy to install in sealing fire-rated floor and wall penetrations. Telephone cables have large insulator/metal ratios and may have slack or oval jacketing, making older limited expansion materials ineffective. Strict design for specific cables and cable densities is obsolete; reactive foaming chemicals are not needed for an effective seal. Fire-expanding hydrated silicate particles are incorporated in a neoprene matrix yielding environmental protection for tough, flexible board, sheet, tape, caulk, putty, and foam rubber products. Penetration kits from these materials have been underwriter tested. Their UL ratings are compared with rubber blocks, foaming resins, and compressed washer devices. Traditional telecraft skills and tools install and adapt the new material to many cable types. Ease, simplicity, speed, and sureness of installation entry, and reentry/reseal are related to the fire hazard window of cable, fiber, or coax additions.

INTRODUCTION

Fire barriers are employed to fill openings around cables which penetrate walls and floors, and prevent the spread of flame and smoke from one area to another in the event of fire. They also resist water battering from fire hoses, but do not necessarily protect the cables themselves from the fire, although many materials which make good fire barriers also can be used as cable or equipment protective coverings. In order to work effectively, a fire barrier must not only resist the fire itself, but must also retain an effective seal around a cable which may not be fire resistant, and may be softened, melted, or in flame itself. The fire barrier must not only keep the hot gases and flames from penetrating the wall or floor opening, but must also provide the proper thermal properties to prevent conduction of heat down the cable, causing separate ignition of cable insulation on the opposite side of the barrier.

DESIGN VARIABLES

Many factors contribute to the behavior of a particular cable for fire conditions<sup>1-5</sup>. In particular, the conductor type, size, and insulation, percent fill of the penetration, and floor or wall thickness affect performance: It is easier to firestop a cable with aluminum conductors of small gauge with a high melting or refractory insulation, through a thick, normal density floor or wall, than a similar cable with copper large gauge conductors in a low melting insulation and jacket, through a thin low density concrete floor or wall. The greater the number of cables passing through the penetration, the more difficult it is to provide an effective firestop.

Copper conductors are difficult to firestop, being outperformed in power cabling by similar aluminum installations by almost a factor of two. Aluminum will melt off at a lower temperature. This cuts off the major source of heat transfer through the wall which can cause ignition of cabling on the opposite wall face.

For a given cable type, smaller conductors have less cross section, and thus conduct less heat. For example, a 300 MCM cable reaches 650°F (343°C) in 100 minutes while a 2/C/16 AWG will not reach that temperature in 180 minutes during a fire test.

The "F" rating is affected by the material of the insulation and jacketing. As heat is conducted through the penetration by the cable conductors, low flashpoint materials will fail first: Polyethylene and polyvinyl chloride insulation will have the poorer durability than silicone rubber or mineral-filled cable.

The percent fill is a measure of the number of cables in a penetration, expressed as the total cross sectional area of cabling, compared to the total open area of the infilled penetration as 100 percent. The higher percent fill, the more heat is conducted through the penetration, lowering the T rating. Round cables, tightly packed, achieve about 40 percent fill on a measured percent fill basis.

The type of floor or wall concrete and its thickness will affect fire performance and T ratings. Lightweight concrete testing is more severe than tests on normal density materials. The thicker the floor and the higher its density, the

more cooling capacity and conductivity the floor offers to the system. For example, a 2 1/2" (64mm) floor will stay at 212°F (100°C) for 1 hour during a fire test, but a 4 1/2" (114mm) floor will maintain that temperature for 3 hours.

Telephone cables present an especially difficult problem for fire barrier design, not only because of their extensive use of polyethylene which is flammable and thermoplastic at relatively low temperatures, but also for the high ratio of insulation to conductor cross section. This ratio is critical to the efficiency of the seal or amount of leakage which may occur around a heated cable for a given fire barrier design and material. A cable with a high ratio of metal to insulation will have little shrinkage and many barrier systems may work, whereas as small gauge telephone cables require a high performance barrier material, and clever designs which can expand in fire conditions to take up the large insulation area and exert additional pressure to exclude fire spread through extrusion or thermoplastic melt and drip. Slack jacketing and oval outlines typical of many inside plant cables make the problems of a tight sealing barrier design even more formidable. Similar problems have existed in sealing to plastic pipe and until recently this service required thermal release of metal sprung compression collars<sup>6</sup> to aid the limited swell of even the best available materials.

#### PREVIOUS DESIGNS

##### Cements and Grouts

Portland cement, plaster, and other castable refractories have been used to fill openings around cables and other utilities with varying success, shown in Figure 1. Although installations may use traditional contractor skills, the results are poor

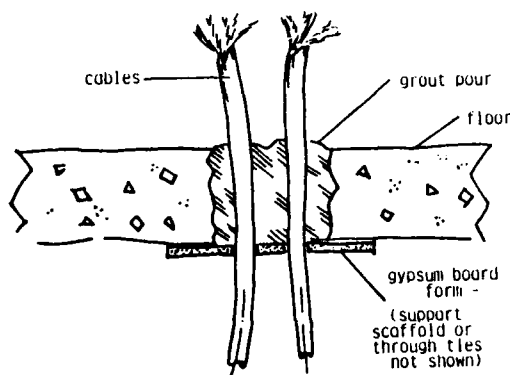


FIGURE 1. CEMENT AND GROUT POURS

unless fireproof tubular conduit penetrations are used in accord with precisely specified sealing methods. Although cementing can be made to work well with water pipe penetrations for example, these systems do not work where a melting, shrinking, or inflammable jacket can pull away from the cement upon application of heat. They require craft skills which are outside normal telephone

installation experience, and may require extensive or special pouring forms and scaffolding, particularly if a high ceiling or large opening is to be sealed. These traditional difficulties have resulted in a view that the securing of a fire barrier is nearly impossible during the time when cables are placed or added, and that the building owner must restore his floor or wall fire integrity, not as the work progresses, but rather when the job is complete, or more frequently some days or weeks later when a separate grouting contractor can perform the work.

Unfortunately, this leaves an installation unprotected at the time when accidents are most frequent during remodeling or construction, as well as extending the risk for some time afterwards. In the frequent refurbishing of highrise premises, an almost continuous violation of fire integrity can result if timetabling is not rigorous. Impact chipping and jackhammering are frequently needed to make inspection or new work openings.

##### Clamped Rubber Blocks

Several systems are available in which shaped rubber blocks firmly fit cables penetrating a wall or floor, and are placed in groups in a surrounding metal frame which holds them securely<sup>7,8</sup>. This type of system is shown in Figure 2, and it requires a

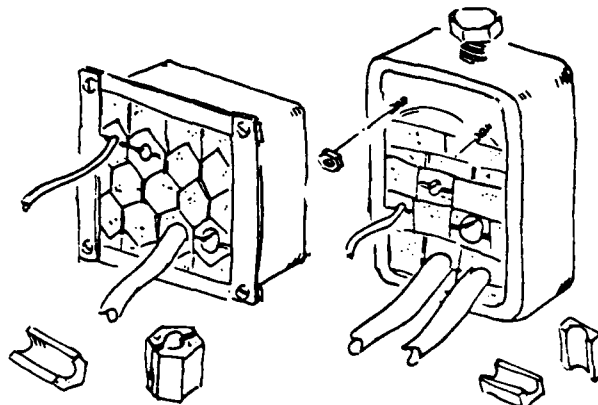


FIGURE 2. SHAPED RUBBER CLAMP BLOCKS

stock of many kinds of rubber blocks to fit each individual cable size. Blank blocks are used to fill spaces reserved for future additions or required by cable density limitations, and addition of a new cable requires specification, ordering and fitting of its proper block. This type of barrier relies on clamping pressure to take up a large part of the sealing requirements as prestressing, since the dense rubber blocks do not expand sufficiently to take up large insulation/conductor ratios or high conductor densities efficiently. A structural restraining frame, wedges, and jackscrews are often employed to get a high clamping stress. This tight seal is frequently employed in cable penetrations through watertight bulkheads aboard ship where weight and cost is relatively unimportant and exceptional pressure tightness in ordinary service may be even more critical than fire performance characteristics.

### Compressed Washer Pokethroughs

Mechanical force is used to compress washers of fire expanding rubber in a typical floor monument pokethrough which leads wiring up from a floor duct. A steel conduit tube carries the cables to an outlet housing, and this is tightly bound to the floor by prestress of the washers, shown in Figure 3. This type of design is sometimes used as a wall penetration, and if used to clamp directly on an elastic cable sheath, must be fitted precisely to the number and types of cables to be protected.

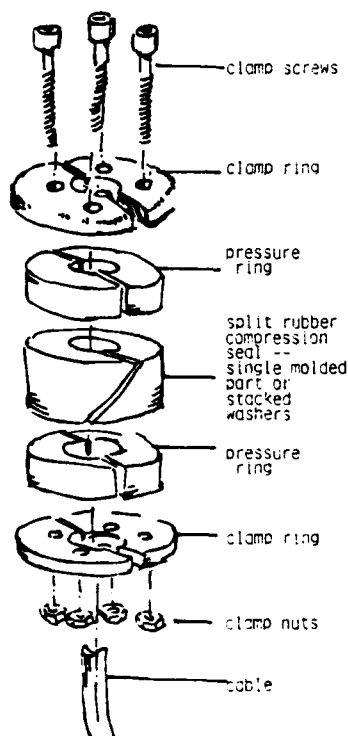


FIGURE 3. COMPRESSED WASHER PENETRATION

These devices work well in relatively smooth round penetrations, but require a secondary preparation for a rough opening. They cannot be easily adapted to non-circular openings, and must be rebuilt or replaced if cables to be clamped are changed or added.

### Chemical Foam

Liquid systems which react to form an expanding syrup are available to seal cables at wall and floor penetrations. Two reactive materials are mixed by the user in a mixing cartridge or a foaming machine, to give a silicone foam which expands to 3 times its original volume, within a work life of 13 minutes to 15 seconds in the range from 32° to 122°F (0 to 50°C). A fire-resistant foam board and packing materials are used to dam the syrup in place until it is completely set. The material is flexible and easily cut to add or change cabling, after which it is sealed with more foam. Surfaces should be free of oil, grease, wax,

rust, scale, dirt, or other contamination and a test is recommended to see if cure inhibition may be a problem at the foam interface. The degree of foaming is a function of the method and vigor of mixing as well as the amount of confinement of the foam, and a small amount of hydrogen gas is given off during foam expansion.

### FLEXIBLE INTUMESCENT MATERIALS

Flexible sheeting with a large fire expansion fills the need for a material which can be easily cut with shears or lineman's snips, and incorporated into devices using that large expansion to give exceptional versatility and performance. In a typical formulation, particles of hydrated silicate are completely enclosed in a neoprene rubber matrix, protecting them from extremes in both wet and dry conditions, and yielding a tough, flexible material<sup>9</sup>. In fire service, the fire barrier material expands quickly to seal openings, squeezes and displaces thermoplastic materials, and forms a strong char which is an efficient heat barrier and resists dislodgement by fire hose pressure<sup>10</sup>.

Swell ratios are reliable and far in excess of what has been available until now. Table I shows properties of this material; Figures 4 and 5 show test apparatus for determining temperature rise during fire exposure, and typical results.

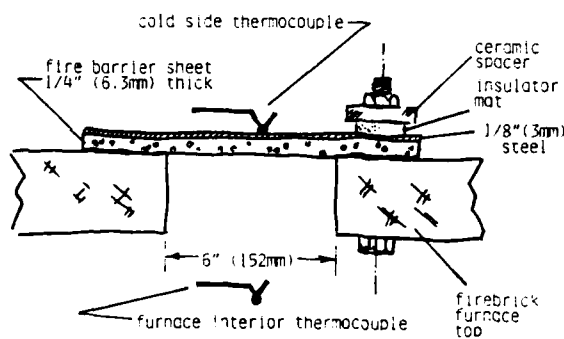


FIGURE 4. TEMPERATURE RISE APPARATUS

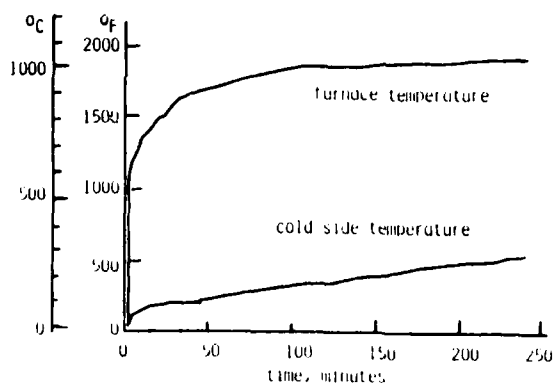


FIGURE 5. TEMPERATURE RISE RESULTS

The material can not only be formed into a thick sheet, but it can also be used as a thin tape. When the sheet is laminated to an aluminum foil, wire screen, or steel plate, the fire barrier sheet is constrained so nearly all its expansion in fire conditions is directed along the thickness axis of the material. This effect is shown in Figure 6,

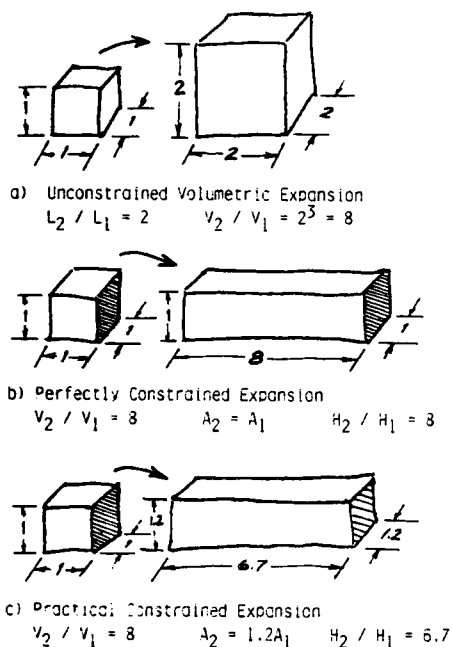


FIGURE 6. EFFECTS OF DIRECTED EXPANSION

and allows not only directed but also amplified intumescent expansion, since the entire volume expansion is confined to a single axis. The large swell results in a large thickness increase, whereas complicated individual rigid compartmented honeycomb constructions<sup>11</sup> were formerly needed to obtain effective action.

This fire barrier material has reasonably good heat conductivity before fire exposure, so it is a logical material to enclose fire sensitive priority equipment and services with little derating due to normal service heat buildup. This contrasts with the excellent protective thermal insulating properties during and after fire exposure which causes swelling.

Related formulations of silicate particles in caulk and putty matrixes give a family of seal construction materials with similar properties and advantages, and a sponge neoprene rubber pad with about 70 percent void volume adds further versatility.

#### Intumescent Sheet Devices

Fire barrier sheets have been fabricated into several designs of kits to seal cable penetrations through round and rectangular openings. A design for round openings<sup>12</sup> is shown in Figure 7. The

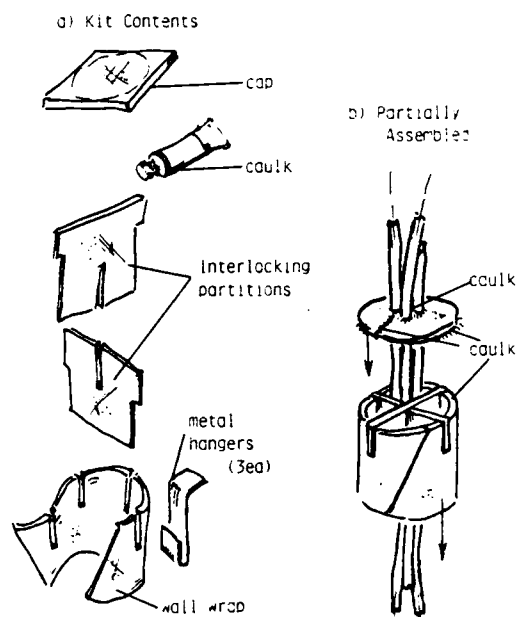


FIGURE 7. ROUND PENETRATION KIT

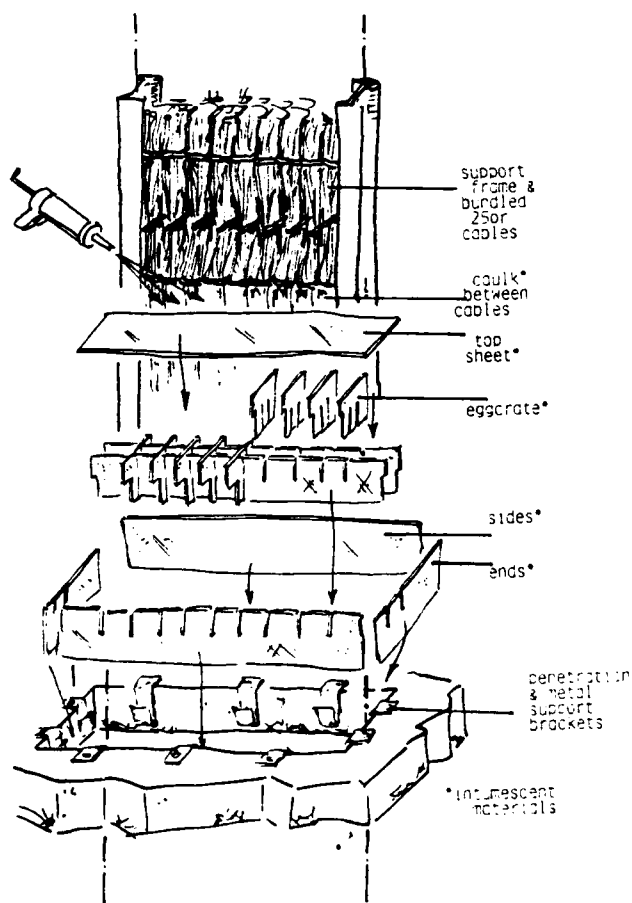


FIGURE 8. RECTANGULAR PENETRATION KIT

girth wrapper is slipped into the wall or floor, an x-interlocking grid is placed around the cables, lids are cut to fit the cables with lineman's snips, and caulked or puttied in place with the related fire barrier materials. The rectangular penetration is similar, and uses a rectangular grid and covers, shown in Figure 8.

Still another form of rectangular penetration uses vertically hanging "cards" in place of a grid, as shown in Figure 9. The cables will seal well in

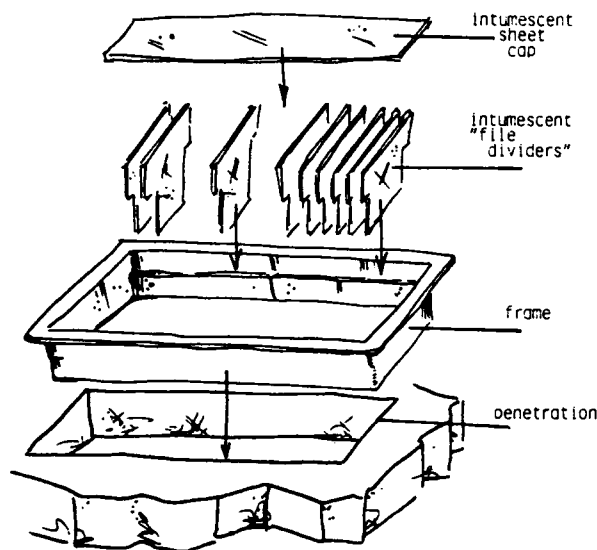


FIGURE 9. HANGING CARD RISER CABLE PENETRATION

all these designs, whether in very low or very high packing densities, and addition or replacement of cabling services is easily and quickly accomplished using simple shears, and no special ordering or specification of fitted parts is needed.

#### COMPARITIVE PERFORMANCE

Ratings of fire service of various barrier systems are compared in Table II, according to Underwriters' Laboratory tests. The superiority of intumescent sheet kits is especially evident in the variety of services, density variation of cable packing, extreme minimum wall and floor thickness which can be accommodated, and versatility of use that their ratings cover.

#### EMERGING APPLICATIONS

These materials are ideally suited for retrofitting and upgrading protection for riser cables in customer premises and central offices. Additional material forms incorporating mica swelling agents and endothermic<sup>13</sup> materials which actually use a chemical reaction to absorb the heat of a fire are two product forms being developed, and used to make a protective firebreak<sup>14</sup> for polyethylene jacketed central office riser cables at splice cases, shown in Figure 10.

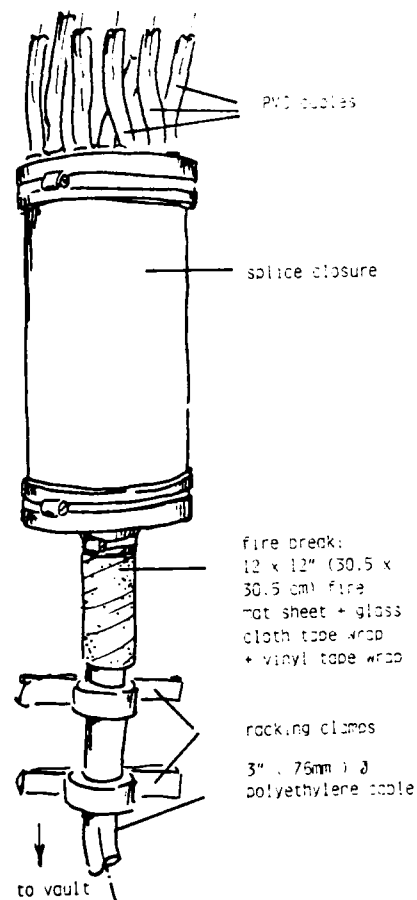


FIGURE 10. SPLICE CLOSURE FIRE BREAK

The simplicity of application of intumescent sheet materials and their kits recommends these and other new systems for retrofitting and upgrading of protection in existing central offices, highrise and other commercial installations. Hotel and central office fires have given visibility to the need for rapid and easy firestopping, especially while construction or alterations are still in progress. The increasing addition of data cabling: copper pair, coax, and fibers makes versatility and rapid restoration of firestopping a frequent and timely concern. Telephone apparatus and cable is seldom the cause of fire<sup>15</sup>, but can cause its spread if not properly blocked at firewalls. The telecraft "friendliness" of intumescent sheet and its application provides a way in which operating company, interconnect, or private contractor can provide a real benefit of instantaneous firestopping security as an integral part of their installation service.

# REFERENCES

1. Kautman, S., et al "Large Scale Fire Tests of Building Riser Cables" Int. Wire & Cable Symp. Proc. 1982, pp. 411ff.
2. Whiteley, R. H., "A Comprehensive Small Scale Smoke Test" Int. Wire & Cable Symp. Proc. 1982 pp. 427ff.
3. Lupton, E.C., et al, "Some differences noted in the Flammability of Wire Construction Between Testing at Room Temperature and at Elevated Temperature" Int. Wire & Cable Symp. Proc. 1975
4. Gouldson, E.J., et al, "Fire Hazard Evaluation of Cable and Materials" Int. Wire & Cable Symp. Proc. 1975
5. Lee, J. L., et al, "Indexing Method for Cable Classification Using the FM Laboratory Scales Combustibility Apparatus" Intl. Wire & Cable Symp. Proc. 1980 pp. 235ff.
6. Dolder, R. "Fire Retardant Partitioning for Openings for Plastic Pipe Lines" U.S. Patent 4,307,546
7. Anon, "Beehives Inhibit Fires" Electronics & Power (UK) V. 29 No. 7/8 p. 537, July/August, 1983.
8. Brattberg, N., "Pressure-Tight Packing Assembly for Conductors Passing Through a Wall" U.S. Patent 2,732,226
9. Langer, R., et al, "Intumescent Fire Retardant Composites" U.S. Patent 4,273,879
10. Anon, "Report on Intumescent Material", File R8399 Proj. 77NK10917 Underwriters' Laboratories, February, 1979.
11. Miguel, A.S., et al, "Intumescent Material - Honeycomb Thermal Barrier" U.S. Patent 4,299,872
12. Fleming, P.B., et al, "Fire Barrier Device" U.S. Patent 4,364,210.
13. Daroga, M., et al, "Flame Barrier" U.S. Patent 4,286,013
14. Anon, "Closure Flammability Tests" Par. 5.53 of Cable Entrance Splice Closures Bell Tech Ref. Pub 55006 Issue 1, October, 1981
15. Hill, S. "Communications Systems Installation and the Fire Problem" Building Industry Consult. Serv. Wkshp. U.Ky, 1981.

TABLE I. NEW INTUMESCENT SHEET PROPERTIES

Activation	250°F (120°C.)	
Expansion begins	350°F (175°C.)	
Expansion is significant	5 to 11 times	
Multi-directional free expansion	typical 8 times	
Weight loss	25%	
Expanded char strength	500 psi	
Refractory temperature	1740°F (950°C.)	
Dielectric strength: (ASTM D-149) sheet as supplied	242 volts/mil average	
	200 volts/mil minimum	
Flame Spread:		18.88
ASTM E-84		
Fuel contribution:		0
ASTM E-84		
Smoke Development:		231
ASTM E-84		
Hardness:		
	55 to 70 Shore A.	
Compression set:		
	25% maximum (ASTM D-395 Method B)	
Color:		
	As supplied - brown; char - black.	
Thermal conductivity (K):		
• Of the sheet (ASTMD-1518-64) without aluminum foil:	• Of the char (BTU/in/hr/ft <sup>2</sup> /°F.)	
(BTU/in/hr/ft <sup>2</sup> /°F.)	0.32 @ 75°F.	
1.56 @ 95°F.	0.51 @ 613°F.	
1.81 @ 148°F.	0.66 @ 1130°F.	
Comparisons at 70°F:	Comparisons at 75°F:	
Silicone 1.56	Vermiculite 0.47	
Chloroprene 1.32	Mineral wool (loose) 0.28	
Mica products 2.68-4.8	Fiberglass (loose) 0.28	
	Styrofoam 0.22	

Humidity Conditioning		Resistivity (ASTM D-257) 500 VDC for one minute			
Temperature	Relative Humidity	Volume Res. (ohm-cm)	Surface Res. (ohm-cm)		
75°	20%	4.9 x 10 <sup>10</sup>	1.8 x 10 <sup>11</sup>		
75°	50%	3.6 x 10 <sup>10</sup>	2.0 x 10 <sup>11</sup>		
75°	75%	4.7 x 10 <sup>10</sup>	1.5 x 10 <sup>11</sup>		
75°	90%	4.5 x 10 <sup>10</sup>	1.0 x 10 <sup>11</sup>		
Atmospheric Conditioning		After Exposure			
Test Condition	Temperature	Humidity	Time	Elastic Properties	Nominal Expansion
Air conditioned room	22°C.	—	—	excellent	8 times
Oven	87°C.	—	90 days	very good	5 times
Humidity chamber	32°C.	95%	90 days	very good	10 times
Water immersion	22°C.	—	60 days	good	10 times
Floor wax and stripper	22°C.	dip	120 days	excellent	10 times
Gasoline	22°C.	soak	60 days	fair	5 times
Methyl alcohol	22°C.	soak	60 days	good	4 times
Weatherometer QUV		ASTM 53-77	2,650 hours	excellent	12 times
Weatherometer XW		ASTM G-23-69	1,640 hours	fair	10 times

**TABLE IIA: THROUGH-PENETRATION FIRESTOP DEVICES: U.L. CLASSIFICATIONS**

Material, Type	Thickness (minimum) Wall Floor	Penetration Size Maximum	Penetration Items	% Fill (max)	Fire Ratings F, hr T, hr	
Intumescent						
FPS	8"	6-1/2"	6"	6"-ABS/PVC Pipe	One Pipe 3	3
FP	8"	6-1/2"	6"	3" Steel Pipe	One Pipe 3	3
Intumescent						
5902	7-5/8"	2-1/2-4-1/2*	10"Ø	Metal Pipe	75%	1-3 0
5902R	7-5/8"	4-1/2"	10"x20"	Multiple Metal Pipe	----	3 0
5904	7-5/8"	4-1/2"	10"Ø	Plastic Pipe 4"D.	One Pipe 1-3	0-3
5904R	7-5/8"	2-1/2-4-1/2*	8"x16"	3/C #2awg PE/PVC	30%	1-3 0-3
5904R	7-5/8"	6"	10"x20"	25pr Tel Cables in Tray	52%	3 1
5904R	7-5/8"	4-1/2"	10"x20"	25pr Tel Cables in Tray	52%	2 1
Rubber Blocks						
TWF-6	7-5/8"	6-1/2	21-1/4"x13-1/2"	300 MCM PVC	6%	2-3 N.D.
TWF-10	7-5/8"	6-1/2	21-1/4"x13-1/2"	1/2 Conduct	6%	2-3 N.D.
Rubber Blocks						
RGB-2	7-5/8"	4"	10-17/64x7-1/32"	250 MCM	6%	3 N.D.
RGB-6	7-5/8"	4"	10-17/64x7-1/32"	Sch. 40 Pipe	----	3 N.D.
Rubber Blocks						
RGB-2	7-5/8"	4"	4-11/32x5-1/2"	Sch. 40 Pipe	----	3 N.D.
RGB4x2	7-5/8"	4"	10-17/64x7-1/32"	250 MCM PVC	6%	3 N.D.
Rubber Blocks						
CAFS	7-5/8"	3*	8"Ø	3/C 2 awg PVC	6%	3 N.D.
CFSI	7-5/8"	3*	8"Ø	Sch. 40 Pipe 6"Ø	One Pipe 3	N.D.

N.D. - Not determined \* - Light weight concrete

**TABLE IIB: FILL VOID OR CAVITY SYSTEMS: U.L. CLASSIFICATIONS**

System and UL Number	Minimum Thickness in Wall Floor	Maximum Penetration Size	Maximum Cable Size	% Fill	Minimum Depth of System	Number of Components	Rating F hr T hr	
Silicone Foam								
1	8"	--	4"Ø	----	9-5/8"	3	2	N.D.
2	8"	--	12"x30"	40*	8-5/8"	3	2	N.D.
3	8"	--	6"Ø	40	8-5/8"	3	2	N.D.
4	8"	--	4"	40	8-5/8"	3	2	N.D.
Silicone Foam								
5	8"	--	48"x48"	40*	8-5/8"	3	2	N.D.
6	8"	--	16"x16"	10	7-5/8"	3	2	N.D.
7	8"	--	16"x16"	5	7-5/8"	3	2	N.D.
8	8"	8"	16"x16"	----	7-5/8"	3	2	N.D.
9	8"	--	16"x16"	--	7-5/8"	3	2	N.D.
Silicone Foam								
10	12"	12"	30"x30"	23	14"	3	3	N.D.
11	12"	12"	6"Ø	20	11-1/2"	2	3	N.D.
12	12"	12"	44 ft <sup>2</sup>	20	8"	3	3	N.D.
13	12"	12"	10"Ø	----	12"	2	3	N.D.
14	12"	12"	10"Ø	--	8"	2	2	N.D.
15	12"	--	6"Ø	8	9-3/4"	2	2	N.D.
16	12"	--	10"Ø	--	9"	2	3	N.D.
17	12"	--	6"Ø	17.5	5-9"	2	3	N.D.
18	12"	--	24"x48"	23	12"	3	3	N.D.

TABLE IIB: FILL VOID OR CAVITY SYSTEMS: U.L. CLASSIFICATIONS (Continued)

System and UL Number	Minimum Thickness in Wall	Floor	Maximum Penetration Size	Maximum Cable Size	% Fill	Minimum Depth of System	Number of Components	Rating F hr	T hr
Silicone Foam									
19	8"	8"	32 in <sup>2</sup>	----	--	6"	3	2	N.D.
20	8"	8"	30"x3"	----	--	7-1/2"	1	2	N.D.
21	8"	8"	8"Ø	12C 14 awg	4	6-3/4"	2	2	N.D.
22	8"	8"	64 in <sup>2</sup>	----	--	8-1/2"	3	2	N.D.
Silicone Foam									
23	12"	12"	45 ft <sup>2</sup>	7/C-12 awg	33	13"	2	3	N.D.
Silicone Foam									
24	8"-13"	8-13"	192 in <sup>2</sup>	350 MCM	2.7	8"-13"	3	2&3	N.D.
25	8"	8"	192 in <sup>2</sup>	350 MCM	2.7	4"	2-3	2&3	N.D.
26	8"-13"	8"-13"	192 in <sup>2</sup>	350 MCM	39*	8"-13"	3	2&3	N.D.
27	8"	8"	192 in <sup>2</sup>	350 MCM	39*	6"	3	2&3	N.D.
28	13"	13"	384 in <sup>2</sup>	300 MCM (7/C)	8 (39)	8"-13"	3	2&3	N.D.
29	8"	8"	384 in <sup>2</sup>	350 MCM 2 Hr	39*	7"	3	2&3	N.D.
30	8"-13"	8"-13"	575 in <sup>2</sup>	350 MCM/3C 2awg	39*	8"-13"	3	2&3	N.D.
31	8"	8"	6"Ø	----	--	8"	3	3	N.D.
32	8"	8"	6"Ø	350 MCM	10.4	5"	3	3	N.D.
Intumescent Caulk and Putty									
33	8"	--	2Ø	350 MCM	59	4"	1	3	1/2-2
Batts and Mastic									
34	8"	6-1/2"	9ft <sup>2</sup>	2/0 awg	39*	6-1/2-8"	4	3	N.D.
35	8"	6-1/2"	12"Ø	----	--	10-1/2"	4	3	1"
Fiber and Mastic									
36	6"	6"	392 in <sup>2</sup>	Blank	--	5"	4	3	3
37	6"	6"	10"Ø	Pipe	--	5"	4	3	1/2-1
38	6"	6"	10"Ø	3/C 2 awg	20	5"	4	3	1/2
Pillows									
39	10"	10"	32"x40"	10 awg (Larger)	34*(20)	20"	2	3	3
Fiber and Mortar									
40	10"	10"	40"x72"	1/0 awg	39*	10"(34")	3	3	3
41	8"	6.5"	24"x36"	2 awg	39*	6.5(30.5)	3	3	1,2,3
Pillows									
42	8"	6.5"	24"x36"	300 MCM 2 awg	36(39)*	23.5"	2	3	1-1/2
Putty									
43	8"	6.5"	10"Ø	500 MCM	17	10"(12")	1	3	3
Fiber and Mortar									
44	8"	6.5	4"Ø	24 Pr Tel	16	20"(26")	2	3	3
45	8"	6.5"	1"x2"	24 Pr Tel	25	24"	3	3	2
Fiber and Mortar and Mastic									
46	8"	6.5"	4"Ø	300 MCM	11	20"	3	3	1-1/2-3
Fiber System									
47	8"	6.5"	45"x48"	Blank	--	6-1/2"-8"	1	3	3
Boot and 2 Part Putty									
48	--	6.5"	6"Ø	Steel Pipe	--	10"	2	3	2
Intumescent Caulk and Putty									
49	7-5/8"	2-1/2"	8"Ø	7/C 12 awg	42.9	1"-3 1/2"	2	3	0-3

TABLE IIB: FILL VOID OR CAVITY SYSTEMS: U.L. CLASSIFICATIONS (Continued)

System and UL Number	Minimum Thickness in		Maximum Penetration Size	Maximum Cable Size	% Fill	Minimum Depth of System	Number of Components	Rating F hr T hr	
Fiber and Mastic									
50	6"	6"	392 in <sup>2</sup>	3/C 2 awg	30*	5"	4	3	0-3
51	6"	6"	392 in <sup>2</sup>	300 MCM	30*	5"	4	1	1
52	6"	6"	10"Ø	6" Pipe	--	5"	4	1	3/4-1
53	6"	6"	392 in <sup>2</sup>	300 MCM	30*	5"	4	1	1
54	6"	6"	10"Ø	Blank	--	5"	4	1	1
Putty									
55	8"	8"	4"Ø	Blank	--	6"	1	1	3/4
56	8"	8"	4"Ø	300 MCM	39*	8"	2	1	1
Putty									
57	8"	8"	16 ft <sup>2</sup>	300 MCM	39*	12"(42")	4	3	N.D.
58	8"	8"	6"Ø	300 MCM	7	12"(42")	4	3	N.D.
59	8"	8"	10"Ø	Pipe	--	12"	2	3	N.D.
60	8"	8"	400 in <sup>2</sup>	300 MCM	1.8	8"(32")	4	3	N.D.

N.D. - Not Determined

\* - Percent fill of cable tray, not penetration

(A1) - Aluminum Conductor

Depths in parentheses for mastic paint on cable



Douglas G. Dahms is the Project Leader for the Maintenance and Rehabilitation Section of 3M's TelComm Products Division Laboratory. He joined 3M's Electrical Group in 1973 after studying chemistry at the College of St. Thomas and the University of Minnesota. Mr. Dahms has held various technical positions in Manufacturing Technology, Product Assurance, and Process Engineering of TelComm Products/3M. His present responsibility covers the research and development of both mechanical and chemical products directed toward the maintenance and rehabilitation sector of the telecommunications industry.

Roger H. Keith is a Senior Specialist in 3M's TelComm Products Laboratory, Cable Accessories and Maintenance and Rehabilitation Products. He is a member of Sigma Xi, Tau Beta Pi, past chairman of the Twin Cities AIChE, and a member of the American Welding Society national committee on Ventilation Safety and Health. He holds a BChE from the University of Dayton, did graduate work at U of Cincinnati and received his Ohio P.E. in 1962. Before coming to 3M he was with the University of Dayton Research Institute, where his duties included instrument design for fire testing at FAA's aircraft crash test facility.

Richard R. Licht is a Product Development Supervisor in 3M's Ceramic Materials Department, Interam<sup>®</sup> and Fire Barrier products. He holds a B.S. in chemistry from the University of Wisconsin at River Falls. He is a member of the Industry Advisory Committee on Through Penetration Firestop.

## CYLINDRICAL V-GROOVED NON METALLIC OPTICAL FIBRE CABLE

M. de VECCHIS - J.P. DEMEY - J.P. HULIN - J. PERSONNE - J.C. STAATH

THOMSON C.S.F./L.T.T. - CONFLANS Ste HONORINE - France

## ABSTRACT

The manufacturing process of a non metallic cylindrical grooved (or slotted core) cable is described. The results obtained show that the behaviour of the cable is basically the same as one using metallic strength member with an even better temperature stability.

Testing methods used for the cables are presented particularly concerning temperature stability and elongation tests.

The results on cable production are given, showing the high quality level of this new cable.

## INTRODUCTION

The cylindrical grooved (or slotted core) structure has been previously described in various papers <sup>1 2 3</sup>. The cable unit consists of a grooved core (figure 1) into which fibres are fitted loosely and untensioned with a slight excess length. The cylindrical core is reinforced by a central strength member to endow the whole assembly with the appropriate mechanical and thermal properties. The grooves have a pitch either continuous or alternate.

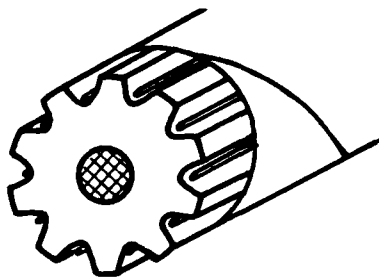


Figure 1 - Structure of cable unit

It has been shown that the type of material used for the central strength member is very important considering thermal and mechanical properties of the composite material of the core and these last two parameters are essential for the cable design <sup>4 5 6</sup>.

The first experiments and the production of these cables have started using a steel strength member <sup>6</sup>.

However, as it may be required for some applications to avoid the use of metallic parts on optical cables, we have designed cables using the same basic

structure in which all metallic parts are replaced by dielectric ones.

## DESIGN CONSIDERATIONS

The first step is to replace the metallic central strength member by a dielectric one without losing on mechanical and thermal stability of the core.

It has been shown that the thermal behaviour of the cable unit must be carefully investigated because it is used as a guidance for the selection of materials and cable parameters <sup>6 7</sup>.

The mechanical behaviour of the unit is also very important due to its influence on the mechanical parameters of the complete cable and the need of a sufficient stability for stranding and sheathing operations.

The two parameters have been considered as the basic selection criteria for the dielectric strength member and the related testing methods are described below.

In some applications, for example protection of buried cables against lightning, cables have been used with dielectric units and outer metallic reinforcement parts that could be easily earth place to place. However in that case, it is better to have a fully dielectric cable and in some other cases any metallic part in the cable is strictly prohibited for example for non detectable military cables.

Then, the second step is to design a fully dielectric cable incorporating non metallic unit according to the above considerations.

The selection of reinforcement dielectric member made for the first step becomes very helpful and the same type of material can be used for the design of outer protections.

## DESIGN OF THE UNIT

The goal was to reach performances at least similar to those of a standard unit with a steel strength member. We have considered two types of unit for this study.

The first one is very similar to our standard unit. The diameter of the rod is the same (4 mm) and the diameter of the strength member has been slightly increased (from 1 mm to 1.3 mm) to partially compensate

the difference on YOUNG's modulus (for the selected material the YOUNG's modulus is between 5000 and 5500 daN/mm<sup>2</sup>).

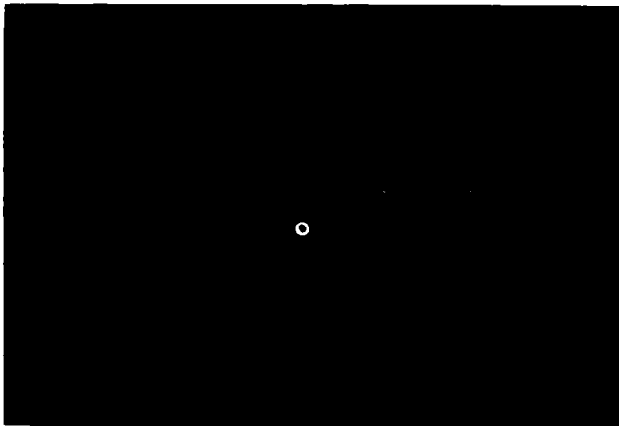
The second one has a 6.5 mm diameter and the strength member diameter is 2.7 mm.

We have tested various types of strength members differing by the materials and the technology of production. Some one have been rejected due to non satisfactory behaviour for example aramide fibre yarns that give a good tension stability but a poor compression behaviour.

As the rod is made by extruding plastic around the strength member, we have been very cautious about the high temperature stability of the strength member in order to avoid gas exhaustions from the strength member in the extruder head. The adherence parameters of the extruded plastic on the strength member have also been carefully investigated as they strongly influence mechanical and thermal behaviour of the composite material of the rod. Considering that point, the direct extrusion of the grooved rod has been preferred to the machining of the grooves previously described <sup>6</sup> as being less sensitive to adherence variations.

We have selected a strength member made from glass fibres that has a temperature expansion coefficient similar to that of the optical fibres.

Various cable unit have been made of the two types. For the first type ( $\varnothing$  4 mm), we have made units with 4 and 10 grooves (figure 2).



**Figure 2** - Grooved unit

For the second type ( $\varnothing$  6.5 mm), we have made units with 10 grooves. In all cases, the results have been satisfactory and are given below in more details.

#### TESTING METHODS

The two main tests for selection of the strength member are, as above indicated, the thermal stability and the mechanical behaviour.

For testing the thermal stability, we use a large climatic chamber in which large diameter reels ( $\varnothing$  2.2 m) can be accommodated (figure 3). The unit or the cable is wound in one layer and the tension is released before the test. Furthermore, the thermal inertia of the reel is reduced by holes (figure 4). We have verified that the stability of cable temperature inside the climatic room is better than 0.1°C. A smaller climatic chamber is used to regulate the temperature of electronic equipments, in particular sources and detectors.



**Figure 3** - Climatic chamber



**Figure 4** - Reel for climatic tests

The mechanical behaviour is checked on a 45 m long tensile strength testing bench in which a part of a long length of cable can be submitted to tension while monitoring its length variation. When a longer length has to be tested, transfer devices (i.e. pulleys) can be used.

For example, tests has been made with tension applied on 225 meters in the center of a 1 km long cable. The various parts of the unit (or cable) are clamped at the extremities of the bench by a multiple winding on a chuck drum. Three hydraulic jacks enable to tensile test units or cables from 0 to 2000 kg (figure 5).



Figure 5 - Tensile test bench

These two test equipments are fully programmable and computer controlled and it is possible in both cases to monitor in parallel the attenuation of 40 fibres at 0.85  $\mu$ m and 10 fibres at 1.3  $\mu$ m.

### RESULTS OBTAINED

Using these two tests for the selection of materials and manufacturing parameters in order to be sure that fibres are free from microbending constraints <sup>6</sup>, we have verified that, as it is the case for units with a steel strength member, the attenuation of fibres is always reduced during the cabling process, for the same reason as explained in <sup>3</sup> to <sup>6</sup>.

The figure 6 shows the cross section of a complete cable made by using a 10 grooves 4 mm diameter unit protected by a polyethylene sheath with 2-glass fibre reinforcements.

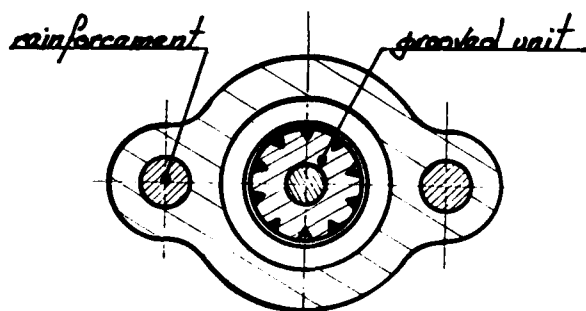


Figure 6 - Cross section of the 10 fibre cable

The figure 7 shows a picture of the cable. The glass fibre reinforcements of the sheath have been calculated to give tensile characteristics similar to those of 0.9 mm thick corrugated aluminium sheath. The figure 8 shows

the comparison of the two measured characteristics (elongation vs.tension).



Figure 7 - 10 fibre cable for duct

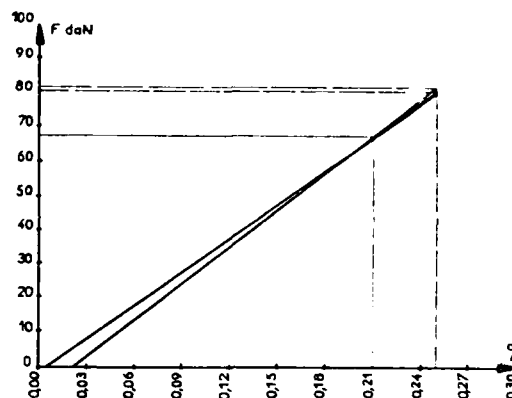


Figure 8  
Tensile characteristics of Al. sheath  
and glass fibre reinforcements

The results obtained on this cable are given on the table below for a 2.500 m long 6 fibre cable which has been laid in normal PVC ducts.

Fibre number	Attenuation (dB/km) at 0.85 $\mu$ m		
	Fibre on reel	Cable	Cable in duct
1	2.9	2.6	2.5
2	2.8	2.4	2.5
3	3.1	2.5	2.5
4	3.0	2.8	2.9
5	2.7	2.6	2.5
6	2.8	2.7	2.7
Average	2.9	2.6	2.6

The thermal behaviour of this cable (attenuation variation vs. temperature) is given on figure 9. It appears that the attenuation variation is lower than 0.2 dB/km for a temperature range of  $-35^{\circ}\text{C}$ ,  $+70^{\circ}\text{C}$ .

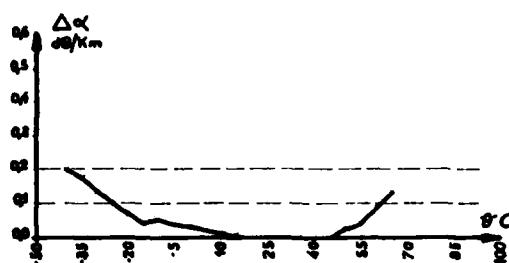


Figure 9 - Thermal characteristic

A small field cable has been manufactured by using a 4 mm unit and an external plastic sheath without reinforcement (figure 10).

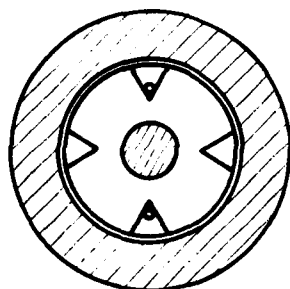


Figure 10 - Cross section of the field cable

The thermal stability of this cable is similar to the previous one. The same type of structure has been used with a 6.5 mm unit (figure 11).



Figure 11 - Cable using a 6.5 mm unit

The figure 12 shows the mechanical behaviour of this cable and gives attenuation variation vs. elongation.

We have manufactured cables by stranding with a central strength member 4 mm units to obtain 30, 50 and 60 fibre cables. The figure 13 shows the 60 fibre cable.

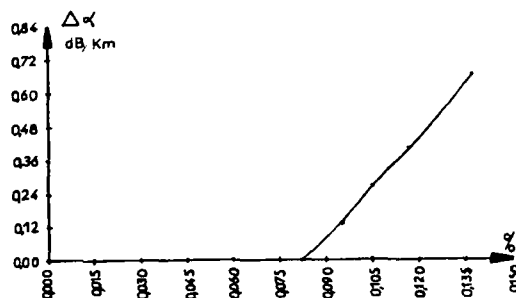


Figure 12 - Tensile characteristic

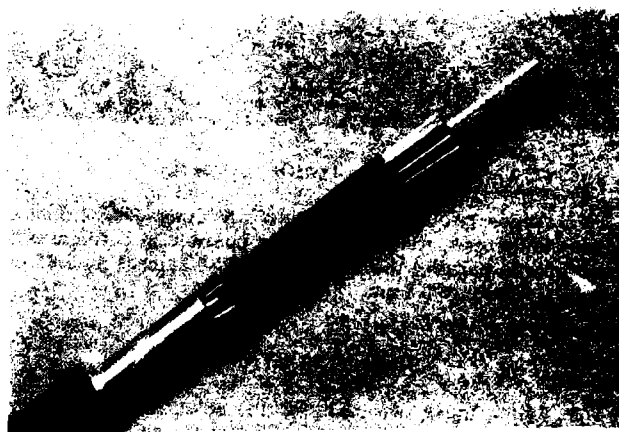


Figure 13 - 60 fibre non metallic cable

## CONCLUSION

It has been demonstrated that the cylindrical grooved structure can be used successfully for non metallic cables. Such cables are suitable for short or long links especially in severe environment and have excellent transmission loss stability with multimode or monomode fibres. They are now in industrial production and the first links have been delivered. For example, a 30 km long 10 fibre (1.3  $\mu\text{m}$ ) repeater less link has been delivered to the French Army.

## REFERENCES

- 1 G. LE NOANE :  
"Optical fibre cable and splicing technique"  
2th ECOC - PARIS - Sept. 1976 - pp. 247-252.
- 2 G. LE NOANE - M. de VECCHIS :  
"Further developments on compartmented fibre optic cable structure and associated splicing technique"  
IOOC - TOKYO - July 1977 - pp. 355-358.

- 3 G. LE NOANE - M. de VECCHIS - J.P. HULIN :  
"Experimental results of cylindrical V-grooved structure optical cables laid in duct and spliced"  
4th ECOC - GENOVA - Sept. 1978 - pp. 218-223.
- 4 M. de VECCHIS - J.P. HULIN - J.C. STAATH :  
"Design of low loss thermal stable optical cables using a cylindrical V-grooved structure"  
IOOC - SAN FRANCISCO - April 1981 - pp. 4-6.
- 5 G. LE NOANE :  
"Optical fibre cable"  
I.T.U. Telecom. J. - Vol. 48 - Nov. 1981 - pp. 649-656.
- 6 M. de VECCHIS - J.P. HULIN - J.C. STAATH :  
"Ultra low loss cables using the cylindrical V-grooved structure"  
I.W.C.S. - CHERRY HILL - Nov. 1981 - pp. 228-235.
- 7 D. BOSCHER - B. NONCLERCQ :  
"Ultra low loss optical fibre cable design and characterization"  
7th ECOC - COPENHAGEN - Sept. 1981 - paper 12-5



**Jean Pierre HULIN** was born in 1946. He received his engineer degree from Ecole d'Electricité et de Mécanique Industrielle (Ecole Violet), PARIS, in 1971. After some years devoted to production of special purpose cables, he joined L.T.T. fibre optic group in 1977. He has been the head of optical fibre cable and splice group and is now the assistant technical manager of L.T.T. Cable Division.



**Michel de VECCHIS** was born in 1946. He received his engineer degree from Ecole Nationale Supérieure des Télécommunications, PARIS, in 1969. He joined L.T.T. in 1970 and was first engaged in research and development work in the field of microwave components and sub-systems. From 1974, he worked on optical fibre cables and systems. He is now the technical manager of L.T.T. Cable Division.



**J. PERSONNE** was born in 1947. He received his engineer degree from Ecole Spéciale de Mécanique et d'Electricité, PARIS, in 1970. He joined L.T.T. in 1971 where he was first in charge of control process and studies for classical cables. Since 1971, he is in charge of theoretical studies on optical cables.



**J.C. STAATH** was born in 1947. He received his engineer degree from Ecole Nationale Supérieure de l'Electronique et de ses Applications, CERGY, in 1972. He has been with L.T.T. from 1974 for research and development on long distance communication cables. He joined fibre optic group in 1980 as staff engineer for optical cables and is now in charge of testing methods on cables.



**J.P. DEMEY** was born in 1953. He received his engineer degree from Ecole Nationale d'Ingénieurs de METZ in 1976. He joined L.T.T. in 1977 and worked for research and development on copper and optical cables. He is now in charge of development and materials problems.

**THOMSON C.S.F./L.T.T.**  
B.P. N° 5  
F 78702 CONFLANS STE HONORINE - France  
Phone : (33) 3.974.56.56



## DESIGN AND TEST RESULTS OF OPTICAL FIBER UNITS FOR OPTICAL SUBMARINE CABLE

H.YAMAMOTO K.MOCHIZUKI Y.NAMIHIRA Y.NIIRO

KOKUSAI DENSHIN DENWA Co.,LTD.(KDD)  
3-2 Nishishinjuku 2-Chome,Shinjuku-Ku, Tokyo,JAPANSummary

This paper describes the design and test results of two types of optical fiber units for optical submarine cables.

One is an embedded-into-silicone-rubber type optical fiber unit. The optical loss change is very small under various test conditions as microbending is hard to occur in this fiber unit. For example, the temperature coefficient was about 0.2 m dB/km/°C. The manufacturing results of 30 km continuous length of this type unit are also described.

The other fiber unit has a strain relaxing effect as each fiber is surrounded with an extremely soft silicone gel and a hard nylon jacket, and these six fibers are stranded. The strain relaxing effect will contribute toward reducing the required screening level of optical fibers used in optical submarine cables. About 0.2 % strain relaxing effect was obtained in our experimentally manufactured optical fiber unit. It will be expected that the required screening level will be reduced about 0.6 %.

1. Introduction

The demand for international telecommunications are increasing with the advent of new services such as data transmission and video communications along with usual telephone and telegraph services. Consequently, submarine cable systems with larger capacity are required. However, there are many problems in realizing these using conventional coaxial cables from technical and economical view points, and also it is difficult to make them suitable for digital transmission.

On the other hand, rapid progress has been made recently in the development of 1.3  $\mu$ m monomode fibers which have many advantages such as low loss, large bandwidth and small diameter. Long repeater spacing and large capacity submarine cable systems with small diameter cables can be expected with 1.3  $\mu$ m monomode fibers.

Recently various optical submarine cable structures have been proposed and developed in several countries.(1)-(5) It is common in all of these cable structures that an optical fiber unit( An assembly of plural optical fibers) is installed in the cable center and anti-hydraulic

pressure layer, strength member layer, humidity protection layer and insulation layer are arranged over the optical fiber unit to protect it from various external forces and humidity permeation.

The most important point for realizing highly reliable optical submarine cables is how to protect the mechanical properties of fine optical fibers from the severe undersea environment for a long period. Thus to design and examine the optical fiber unit is important.

The design requirements for optical fiber units are clarified and two types of optical fiber units are proposed. And test results of experimentally manufactured units are also reported in this paper.

2. Optical Submarine Cables

Optical submarine cables will be handled under severe mechanical conditions because they are installed into deep sea by cable ship. For example, maximum sea depth for a transoceanic submarine cable is 8,000 m, which is equivalent to 800 kg/cm<sup>2</sup> hydraulic pressure. Also several tons of tensile force will be loaded on submarine cables under cable installation work. Optical submarine cables must be stable under these severe conditions.

The typical design requirements for a transoceanic optical submarine cable are shown in Table 1, and an optical submarine cable structure, which is thought over these requirements, is shown in Figure 1. A distinctive feature of this cable is that a small diameter, thick-walled aluminum pipe is constructed by assembling three pieces of fan-shaped aluminum wire over the optical fiber unit, so a long length of cable can be manufactured easily. Optical fiber units which are examined in this paper are used in this optical submarine cable.

3. Requirements for Optical Fiber Units<sup>(6)</sup>3.1 Optical Fibers

Table 2 shows specifications of optical fibers used in an optical submarine cable. These values are chosen to use optical fibers as monomode transmission at 1.3  $\mu$ m.

### 3.2 Outer Diameter

Optical submarine cables will be subjected to large tensile force fluctuations during cable installation work or cable recovery work for repair, and will be expanded and contracted repeatedly. If optical fiber units and cables are not unified, they will move independently. The optical fiber units may be subjected to larger strain than cables locally and optical fibers may be broken. Thus it is important to unify optical fiber units and cables.

In order to unify optical fiber units and cables we chose a method that the outer diameter of optical fiber unit was made a little smaller than three divided aluminum pipe, and adhesive materials were filled between the unit and the aluminum pipe. Accordingly the outer diameter of optical fiber unit is fixed a little smaller than the inner diameter of three divided aluminum pipe.

### 3.3 Fiber Strength

Figure 2 shows Tension-Strain characteristics of the optical submarine cable shown in Figure 1. This figure shows that cable elongation strain will be 0.3-0.4 % at cable installation into deep sea, and 0.6-0.7 % at cable recovery from the deep sea for about 2 days. Also, residual strain will be 0.1 % after cable installation. Optical fiber units will be subjected to those strains because optical fiber units and cables are unified. Required strength of optical fibers used in an optical submarine cable must be decided taking into account the above-mentioned strain and time factor because optical fibers have static fatigue properties. Screening tests will be carried out to insure required strength of optical fibers. Figure 3 shows the required screening test level and fiber strain. From this figure, the required screening test level will be determined at 2 % strain for optical fibers used in an optical submarine cable.

### 3.4 Water Propagation

A break in an optical submarine cable will be exposed to high hydraulic pressure if cable failure occurs. If there are vacancies in the cross section of an optical submarine cable, water propagation will occur to the axial direction of cable. And strength of optical fibers may decrease in the water-propagated submarine cable. So the cross section of optical submarine cables should be filled up to prevent water propagation at cable failure occurrence. Accordingly, optical fiber units have to be filled up with plastics.

### 3.5 Hydraulic Pressure

The inside diameter of the aluminum pipe will be reduced about 10  $\mu$ m when an optical submarine cable is installed at 8,000 m sea depth.<sup>(7)</sup> Then the optical fiber unit will be subjected to inner pressure increase because there is no vacancy in the cable to prevent water propagation at cable failure occurrence.

The degree of inner pressure increase will be different with filling materials, but plastic materials will ordinarily be used to fill up the vacancies, and the degree of inner pressure increase will be less than 10 % of outer hydraulic pressure which is placed on the cable.

### 3.6 Optical Fiber Splices

The unit length of optical fiber units will be about 30-50 km. However, it will be difficult to manufacture such long and continuous-length optical fibers so that transmission characteristics and mechanical properties of those optical fibers are satisfied. Thus it is important to develop a compact protection method for a fiber splice point and accommodate it into the optical fiber unit. Fiber strength at the splice points are required to pass through 2 % elongation strain because they are included in the optical fiber units.

### 3.7 Minimum Bending Radius

The minimum permissible bending radius of optical submarine cables is 1 m, which is determined from the cable laying machinery of the cable ship. This bending radius does not affect on the transmission characteristics of optical fiber unit. However, tail cable will be used at the cable coupling which is used to join the optical submarine cable and optical repeater, and the minimum radius of tail cable is 30 mm. Thus the minimum permissible bending radius of optical fiber units is 30 mm, because optical fiber units pass through the tail cable at the cable coupling.

## 4. Optical Fiber Unit Design

According to design requirements, two types of optical fiber units are designed and experimentally manufactured.

Figure 4 shows one of the optical fiber units (Type 1 Unit) in which six coated optical fibers are stranded around a central tension member and embedded into silicone rubber. Nylon coated optical fibers are used because of stability of transmission characteristics and ease of handling at cable termination. An outer diameter of coating nylon is chosen at 0.6 mm so that the outer diameter of optical fiber units will not be large. Silicone rubber is selected for filling materials of the optical fiber unit because of its buffer effect and ease of separation of optical fibers at cable termination. Transmission characteristics of optical fibers will be stable because microbending will be hard to occur in this type of optical fiber unit.

Figure 5 shows another type of optical fiber unit (Type 2 Unit) in which each primary coated optical fiber is surrounded with an extremely soft silicone gel and hard nylon jacket, and these six fibers are stranded around a central tension member.<sup>(8)</sup> Space between the central tension member and the six nylon jacketed fibers and also the outside of them are filled with plastics to prevent water propagation.

A strain relaxing effect will be attained in this optical fiber unit as the optical fibers sink in the silicone gel layer to the center of the fiber unit when the optical fiber unit is elongated. The amount (U) by which the optical fiber sinks in the silicone gel layer is expressed by Equation (1).

$$U = -\frac{2 \cdot \epsilon_u \cdot E \cdot A}{\pi \cdot E_s \cdot r \left[ 1 + \left( \frac{P}{2\pi r} \right)^2 \right]} \ln \frac{a}{D} \quad \text{----- (1)}$$

where,

- $\epsilon_u$  ; Strain of optical fiber unit
- E ; Young's modulus of optical fiber
- A ; Cross sectional area of optical fiber
- $E_s$  ; Young's modulus of silicone gel
- r ; Pitch radius of optical fiber
- P ; Stranding pitch
- a ; Radius of optical fiber
- D ; Thickness of silicone gel

The elongation strain of optical fibers is expressed by Equation (2).

$$\epsilon_f = \frac{\sqrt{P^2(1 + \epsilon_u)^2 + (2\pi(r-x))^2}}{\sqrt{P^2 + (2\pi r)^2}} - 1 \quad \text{----- (2)}$$

$$x = \begin{cases} U & \text{---}(U \leq D) \\ D & \text{---}(U > D) \end{cases}$$

The difference between optical fiber unit strain and optical fiber strain is the strain relaxing effect. If more strain relaxing effect is required, it is necessary to thicken the silicone gel layer or shorten the stranding pitch. If a thick silicone gel layer is adopted, the cable diameter will be large and if a short stranding pitch is adopted, the bending radius becomes small. As a result, bending loss increases and manufacturing speed decreases. From these points design parameters of this type optical fiber unit were chosen as shown in Table 3. The strain relaxing effect is expected to be about 0.2 % with the design parameters and a 0.2 % strain relaxing effect will decrease the required screening test level for optical fibers about 0.6 %, so the yielding rate of optical fibers will increase. Furthermore, an optical submarine cable which has used this type fiber unit will be highly reliable because optical fibers will not be subjected to residual cable strain.

## 5. Test Results of Type 1 Unit

### 5.1 Loss Change During Manufacturing

Figure 6 shows an example of transmission loss change at 1.3  $\mu$ m during manufacturing processes of a 10 km optical fiber unit. The transmission loss change during each manufacturing process was less than 0.03 dB/km.

### 5.2 Temperature Characteristics

Figure 7 and Figure 8 show the results of temperature test which was conducted by using a

30 km cabled optical fiber unit. Transmission loss change with temperature is shown in Figure 7. The temperature coefficient of optical fiber loss was 0.2 m dB/km/°C. Fiber strain change with temperature is shown in Figure 8. The thermal expansion coefficient was  $1.94 \times 10^{-3}$  %/°C. According to those results, the transmission loss will be decreased and optical fibers will be subjected to compressive strain in the laid optical submarine cable because of temperature difference between sea bottom and factory condition.

Another test was conducted by using a 80 m optical fiber unit at low temperature region down to -60 °C and loss change was measured with loop back of six fibers in the unit. The loss change with looped back 480 m optical fiber was less than 0.01 dB.

### 5.3 Aging Characteristics

Type 1 optical fiber unit has been aged at the room temperature condition from just after unit manufacturing. Aging characteristics of optical fiber unit transmission loss is shown in Figure 9. In this figure solid line shows the spectral loss characteristics just after the unit manufacturing and dotted line shows the spectral loss characteristics aged after 15 months. Loss change was not observed during 15 months aging time.

### 5.4 Loss-Hydraulic Pressure Characteristics

Hydraulic pressure test was conducted by using 150 m optical fiber unit up to 50 kg/cm<sup>2</sup> and loss change was measured with loop back of five fibers in the unit. The loss change was about 5 m dB/km at 50 kg/cm<sup>2</sup>. Another hydraulic pressure test was conducted by using 200 m cabled optical fiber unit up to 800 kg/cm<sup>2</sup>, and loss change was measured with loop back of four fibers in the cable. The loss change was less than 5 m dB/km at 800 kg/cm<sup>2</sup>.

### 5.5 Bending Characteristics

Figure 10 shows loss change with bending. Six optical fibers were looped back and 300 mm length of optical fiber unit were bent in this bending test. Three pieces of optical fiber units were evaluated. The average value of fiber parameters of six fibers in each optical fiber unit is shown in this figure. According to this test result, a minimum permissible bending radius is less than 30 mm at the tail cable.

### 5.6 Loss-Elongation Characteristics

An elongation test was conducted by using a 80 m long optical fiber unit and loss change was measured with loop back of six fibers in the unit. The loss change with looped back 480 m optical fiber was less than 0.01 dB during three times of elongation tests up to 1 % strain and restoring operation. After this test, this unit has been kept with 0.5 % elongation strain for 12 hours and loss change was less than 0.01 dB.

## 5.7 30 km Continuous Length Fiber Unit

A 30 km continuous-length optical fiber unit was successfully manufactured at 1981. Each fiber used in this optical fiber unit had 1 to 3 splice points. The protection structure of splice point was small, so the outer diameter of the optical fiber unit at the splice point was not large compared with the ordinary fiber unit diameter. All fibers and splice points were passed through a 1.0 % strain screening test. Transmission loss of the six optical fibers in this fiber unit was 0.5 - 0.56 dB/km at 1.3  $\mu$ m which included splice loss. This 30 km optical fiber unit was cabled and installed in the sea as a part of the first sea trial system.<sup>(9)</sup>

## 6. Test Results of Type 2 Unit

### 6.1 Loss Change during Manufacturing

In the experimental manufacturing of 2 km length Type 2 optical fiber unit, the loss change was 0.02-0.1 dB/km at 1.3  $\mu$ m during manufacturing processes.

### 6.2 Strain Relaxing Effect

Figure 12 shows the relation between optical fiber strain and optical fiber unit strain. The dotted line shows experimental results and the solid line shows the calculated values. The strain-relaxing effect was measured using a 15 m length optical fiber unit. Fiber elongation was measured using the phase delay method and measuring accuracy was less than 0.01 %. The discrepancy between calculated value and experimental value at the low strain area will be caused by elasticity of the silicone gel. The experimental optical fiber unit has about 0.2 % strain relaxing effect. Also, this figure shows that the strain of optical fibers became the same as the original strain when tension was released.

## 7. Conclusion

The requirements for optical fiber units used in optical submarine cables are clarified in this paper and two types of optical fiber units are proposed and evaluated under various test conditions.

The structure of embedded-into-silicone rubber type optical fiber unit ( Type 1 ) is stable under various test conditions. But high strength fibers passed through a 2 % screening test must be used, so the problem of how to obtain long fibers with such high strength has to be solved.

On the other hand, about 0.2 % strain relaxing effect will be attained with the other optical fiber unit ( Type 2 ). But there are some problems to be solved with this type fiber unit, for example, how to insure uniformity of the strain relaxing effect along the fiber unit, and how to improve the productivity of the fiber unit. It is also important to select appropriate materials for this type fiber unit to keep the strain relaxing effect for a long period.

Recently, many efforts have been made to obtain high-strength optical fibers, and high-strength and long length optical fibers will be expected.<sup>(10),(11)</sup> Thus the Type 1 optical fiber unit is desirable from the view point of long term stability of transmission characteristics.

## Acknowledgement

The authors would like to thank Drs. H.Kaji, H.Teramura, K.Amano, and C.Ota for their encouragement and M.Nunokawa, Dr. K.Tatekura for their discussion. They also wish to acknowledge Nippon Telegraph & Telephone Public Corporation for their co-operation, and to thank Furukawa Electric Co. LTD., Sumitomo Industries LTD., Fujikura Cable Works LTD. for their manufacturing of experimental optical fiber units.

## Reference

- (1) K.Amano, "Undersea Cable Technology" IEEE Trans. MTT-30, No 4, pp 543-550, April, 1982.
- (2) R.F.Gleason, R.C.mondello, B.W.Fellows, D.A.Hadfield, "Design and Manufacture of an Experimental Lightwave Cable for Undersea Transmission Systems", 27th I.W.C.S, pp 385-389, Nov., 1978.
- (3) P.Wortington, "Installation of Trial Optical Fiber Cable Designed for Transoceanic Submarine Cable Telecommunications Systems" 29th I.W.C.S, pp 410-417, Nov., 1980.
- (4) G.Le Noane, M.Leneir, "Submarine Optical Fiber Cable Development in France", I.C.C 82, 7D.4, June, 1982.
- (5) H.Fukutomi, N.Kojima, F.Ashiya, Y.Negishi, "Submarine Optical Fiber Cable Development", I.C.C 82, 7D.1, June, 1982.
- (6) H.Yamamoto, Y.Ejiri, K.Tatekura, M.Nunokawa, Y.Niuro, "Design and Experimental Models of Fiber Unit for Optical Submarine Cable" I.E.C.E Japan CS-81-27, May, 1981.
- (7) Y.Ejiri, M.Nunokawa, K.furusawa, Y.Niuro, "Design and Test Results of An Optical-Fiber Submarine Cable", 31st I.W.C.S, Nov., 1982.
- (8) H.Yamamoto, Y.Namihira, Y.Niuro, "An Optical Fiber Unit for Optical Submarine Cable", Electronics Letters, vol 19, No 4, pp 215-216, Feb. 17, 1983.
- (9) K.Amano, Y.Niuro, K.Furusawa, M.Nunokawa, H.Wakabayashi, "50km, Two-Repeater Sea Trial of Optical-Fibre Submarine Cable System", Electronics Letters, Vol 18, No 22, PP 952-953, Oct. 28, 1982.
- (10) D.L.Brownlow, F.V.Dimarcello, A.C.Hart, Jr R.Huff, "High Strength Multikilometer Light guides for Undersea Applications", 8th E.C.O.C, postdeadline paper, 1982.
- (11) S.Sakaguchi, M.Nakahara, Y.Tajima, "Drawing of High-Strength Long Length Fibers", I.O.O.C 83, 29-A4-5, June, 1983.

Table 1 Design requirements for optical-fiber submarine cable

Items	Objectives
Maximum Sea Depth	8,000m
Maximum Water Pressure	800 kg/cm <sup>2</sup>
Tensile Strength	≥8ton
Cable Modulus	≥19km
Sinking Velocity	≥1,000m/h
Allowable Minimum Bending Radius	≤1m
Number of Fibers	Max. 6
Maximum Power	±10KV
Feed Voltage	±10KV
DC Resistance	≤0.5Ω/km

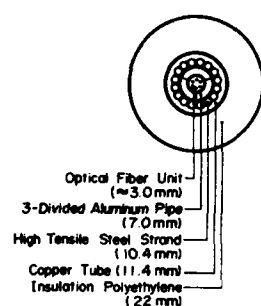


Fig 1 Cross section of an optical submarine cable

Table 2. Specifications of optical fiber

Items	Objective values
core diameter (μm)	9μm (nominal value)
clad diameter (μm)	125μm ± 2.4%
Δ (%)	0.25 - 0.35 %
cutoff wave length (μm)	1.10 - 1.28μm
Loss (dB/km) at 1.3μm	≤0.5 dB/km
proof strain (%)	2.0 %

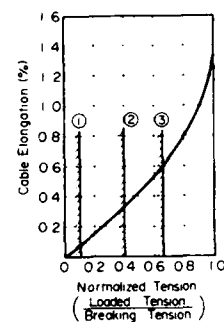


Fig 2 Tension-strain characteristics of optical submarine cable

- ① Residual tension
- ② Installation into deep sea
- ③ Recover from deep sea

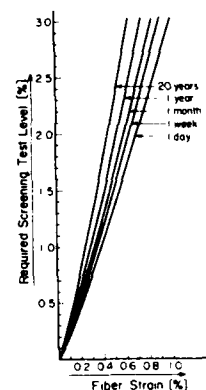


Fig 3 Relation between fiber strain and required screening test level

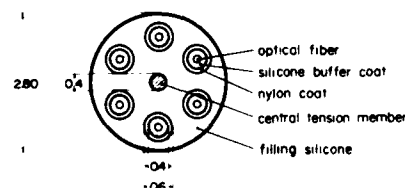


Fig 4 Cross section of embedded-into-silicone rubber type optical fiber unit (Type I)

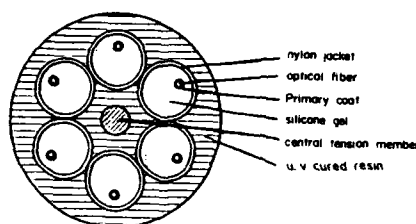


Fig 5 Cross section of optical fiber unit with strain relaxing effect (Type 2)

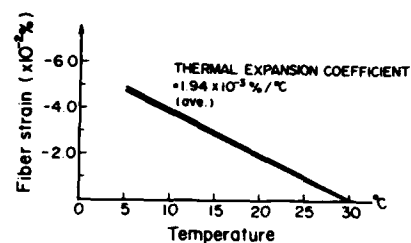


Fig 8 Fiber strain-temperature characteristics of cabled optical fiber unit (Type 1)

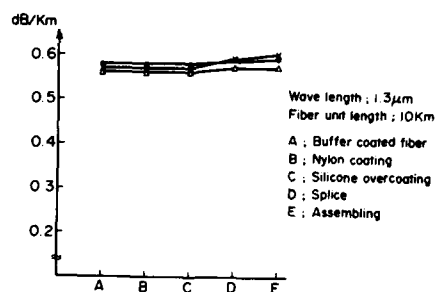


Fig 6 Loss change during optical fiber unit manufacturing processes (Type 1)

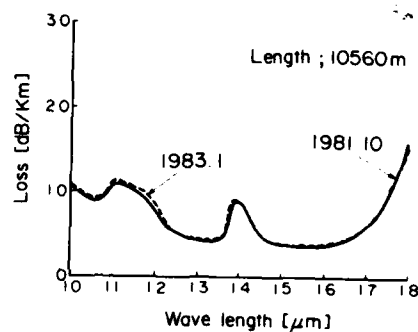


Fig 9 Spectral loss aging characteristics (Type 1)

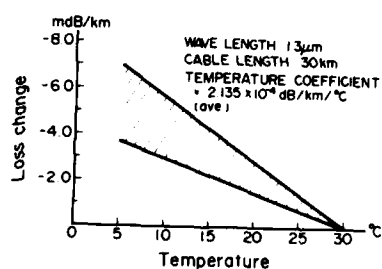


Fig 7 Loss-Temperature characteristics of cabled optical fiber unit (Type 1)

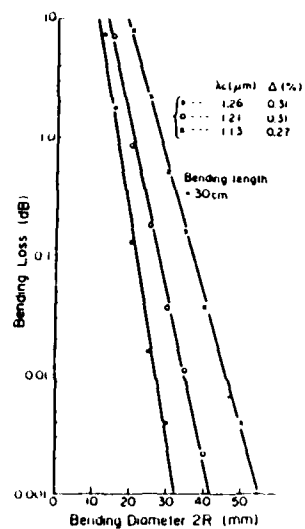


Fig 10 Bending loss characteristics of optical fiber unit (Type 1)

Table 3. Design parameters of optical fiber unit with strain relaxing effect

Optical fiber outer diameter (monomode)	0.125 (mm)
Primary coating outer diameter	0.250 (mm)
Silicone gel outer diameter	1.00 (mm)
Nylon coating outer diameter	1.20 (mm)
Central tension member outer diameter	0.40 (mm)
Optical fiber unit outer diameter	3.75 (mm)
Stranding pitch	90 (mm)

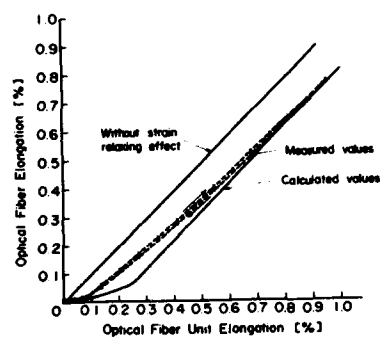


Fig 11 Relation between fiber strain and optical fiber unit strain (Type 2)



Hitoshi Yamamoto received his B.S. in 1971 and M.S. in 1973 in Communication Engineering from Osaka University. He joined KDD Laboratories and engaged in the development of repeaters for coaxial submarine cable systems. Recently he has been engaged in the development of optical submarine cables, especially optical fiber unit design.



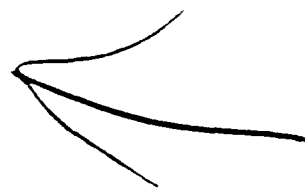
Kiyohumi Mochizuki received the B.S. degree in electronic engineering from Yamanashi University, in 1973, and the M.S. degree from Osaka University in 1975. From 1978 to 1979 he studied at Southampton University. In 1979 he joined KDD Laboratories and has been engaged in research on dispersion and polarization characteristics in single-mode optical fibers.



Yoshinori Namihiro received the B.S. degree from Ryukyu University in 1973, and the M.S and Ph.D. degrees, both in electrical communication engineering, from Tohoku University, in 1976 and 1979, respectively. He joined KDD laboratories and has been engaged in research on dispersion and polarization in single-mode fibers under thermal stress and some external forces.



Yasuhiko Niino received his B.S. degree in electrical communication from Musashi Institute of Technology in 1964. After graduation he joined KDD. He has been engaged in the development of submarine coaxial cable systems. He is presently managing a group with responsibilities for development of optical fiber submarine cable systems in KDD.



## METAL-FREE CYLINDRICAL V-GROOVED OPTICAL CABLE

G. LE NOANE\* - C. AUDOUX\*\* - P. CHERON\*\* - B. MISSOUT\*\*\*

\* : CNET-LANNION - Route de Trégastel - 22301 LANNION - FRANCE  
 \*\* : SILEC - Rue de Varennes - 77130 MONTEREAU - FRANCE  
 \*\*\* : SAT-Direction Technique Câbles - 41 rue Cantagrel-75013 PARIS - FRANCE

ABSTRACT

→ The V-grooved cylindrical optical cable design is particularly suitable to obtain very low loss optical cables. From experience of this structure, metal-free optical cables have been manufactured.

After a brief description of the V-grooved cylindrical structure, non metallic materials which can be used as reinforcement are described.

Composition, mechanical and optical properties of metal-free V-grooved cylindrical cables are given.

The purpose of metal-free optical cables, i.e. cables without any conducting material, is :

- to insure a good insulation between the ends of a link,
- to avoid any degradation of the cable and connected equipments by electromagnetic inductions : lightning, wandering currents.

That is the reason why metal-free V-grooved rod cables have been designed.

2. - V-GROOVED ROD CABLE DESIGN

A 10-fiber V-grooved rod cable consists of :

- a cylindrical rod with 10 helicoidal grooves receiving the fibers. This rod is manufactured by extrusion on a central strength member; this member is generally a stainless steel strand or a galvanized steel strand,
- an outer sheathing consisting of an aluminum tube or a steel tube, surrounded with a high density polyethylene jacket.

The jacket is tied to the aluminum tube by a pitch coat or to the steel tube by sticking with a copolymer (ethylene/acrylic acid).

The purposes of the central strength member are :

- to make easier the extrusion of the V-grooved cable. The helicoidal grooves are manufactured with a rotating die. The die induces on the plastic materials and therefore on the central member a twisting effort. Then the member should have a high twisting modulus to obtain the extrusion with a good regularity,
- to insert the fibers into the grooves longer than the groove itself. The excess length is depending on the type of the cable. It is achieved by pulling the rod during the laying of the fiber in the groove. The excess length is obtained as the pulling is released.
- to reduce the thermal expansion of the assembly grooved rod plus central strength member as a whole.

1. - INTRODUCTION

The V-grooved optical fiber cable design is currently used in FRANCE (1), (2).

At the present time 20,000 fiber kilometers have been layed in FRANCE and are operating without any problem. For instance the BIARRITZ city network has been completed with more than 10,000 kilometers of fibers layed (3).

The V-grooved optical cable design has many advantages in comparison with other designs (tube design) :

- 10-fiber modules
- low volume
- easiness and reliability of manufacturing
- mass splicing easiness.

This design has good optical and mechanical characteristics.

For instance, a 60 daN force can be applied to this cable during pulling in duct without any stress on the fibers. The attenuation change in the fibers is less than 0.1 dB between -40°C and + 50°C.

The relationship giving the thermal expansion is :

$$\alpha = \frac{\sum E_i S_i \alpha_i}{\sum E_i S_i}$$

$\alpha$  = thermal expansion coefficient of the assembly

$E_i$  = Young's modulus of each component

$S_i$  = surface of each component

$\alpha_i$  = thermal expansion coefficient of each component.

Then, the central strength member should have a high Young's modulus and a low thermal expansion coefficient.

The cable outer sheath should have the peculiar property :

- to protect the cable during the laying, avoiding any irreversible elongation; then it should have a high crushing strength and a high tensile strength;

- to possess a low thermal expansion coefficient, in order to protect the fibers from large temperature changes.

Then the outer sheath strength member should also have a high Young's modulus and a low thermal expansion coefficient.

### 3. - METAL-FREE STRENGTH MATERIAL PROPERTIES

Material requirements of strength members have been described in the last paragraph. A peculiar study has been made on following materials :

- glass fibers,
- aromatic polyamide fibers,
- drawn thermoplastic fibers.

#### 3.1.- Material description

##### 3.1.1. Glass fiber materials

Two glass fiber families can be supplied on the market : "sillionne" and "Verranne".

"Sillionne" is made of unbroken fibers, and "Verranne" is made of tuft fiber parts stranded. "Sillionne" has a much higher tensile strength than "Verranne".

Fibers can be made of :

- E glass (borosilicate)
- or - S glass (aluminosilicate).

Young's modulus of S glass is 18% higher than E glass, but is less used in reinforced plastics.

S glass is more expensive than E glass.

"Sillionne" is sold as roving (parallel fiber tuft) or as stranded and twisted textile threads. Threads can be glued by rubber latex impregnation.

Rigid shapes with 60 to 80 % glass can be obtained by pultrusion, i.e. by drawing a polyester or an epoxy resin impregnated roving out of a heated die. These shapes have a low thermal expansion coefficient, high tensile and buckling strengths.

#### 3.1.2. Aromatic polyamide fiber materials

Aromatic polyamide fibers are known as KEVLAR (registered trademark DU PONT). They can be purchased as roving, strands or ropes. They generally are impregnated with a flexible polyurethane to improve abrasion resistance.

Due to the properties of components, it seems difficult to get rigid pultruded shapes with required physical properties.

#### 3.1.3. Drawn thermoplastic monofibers

Fibers drawn from polypropylene, high density polyethylene, polyester or polyamide have higher mechanic properties than the material itself.

Drawing ratio is from 6 to 12. Drawing temperature is depending upon the material. An annealing is performed to reach a good dimensional stability.

Drawn polyamide monofibers are the most usual on the market.

Some companies have developed polyester (5) and low density polyethylene (6) for their own applications.

Unfortunately, all those fibers have low Young's modulus.

#### 3.2.- Material properties

Properties of materials described in the last paragraph are compared with properties of steel in table 1.

Glass fibers have a lower Young's modulus, but a lower thermal expansion coefficient than steel which is generally used. Then it seems possible to use glass fibers as strength members in optical fiber cables.

Plastic monofibers have a very low Young's modulus.

Materials	Density g/cm <sup>3</sup>	Young's modulus 10 <sup>3</sup> dan/mm <sup>2</sup>	Linear thermal coefficient 10 <sup>-7</sup> 1/K
Steel	7,86	20	130
E glass fiber	2,54	7,3	8
S glass fiber	2,48	8,6	8
Kevlar 49	1,45	13	- 20 (★)
Kevlar 29	1,44	6	- 20 (★)
Monofiber :			
-polyester	1,38	1,5	-
-LDPE	0,96-0,98	1,6	-
-polyamide		0,19	

(★) residual constraint materials.

TABLE 1

Composite materials, the components of which are in the above table, have been implemented. Their diameter went from 1.2 to 1.5 mm. Their mechanical properties and manufacturability as V-grooved rod central strength member have been studied.

Young's modulus and residual elongation after a 0.2 % elongation of those composite materials are described in table 2.

Descrip- tion	Mate- rials	Dia- meter mm	Young's modulus 10 <sup>3</sup> daN/ mm <sup>2</sup>	Residual elongation after a 0.2% elon- gation, %
Stainless steel strand	Stainless steel	1.2	17	0
Impregnated glass roving strand	glass/ polyure- thane	1.22	2.85	0.023
Impregnated glass roving	glass/ polyester	1.35	5.95	0
KEVLAR 29 roving strand	KEVLAR 29/ polyure- thane	1.5	3.4	0.015
KEVLAR 29 rope	"	1.4	3.0	0.022
KEVLAR 49 roving strand	KEVLAR 49/ polyure- thane	1.35	4.55	0.024
KEVLAR 49 rope	"	1.35	4.5	0.025
Drawn poly- amide mono- fiber	polyamide	1.2	0.2	0.1

TABLE 2

### 3.3.- Implementation

Composite materials described in the above table have been implemented as central strength member of V-grooved rods. Logged parameters are diameter, pitch and profile of grooves.

Stranded or rope composite materials do not yield a regular groove pitch. Torsion modulus is too low, and the rod can be rotated by the rotating die. Moreover longitudinal compression strength is too low to avoid thermoplastic (polyolefine) shrinkage during cooling. Then diameter changes are occurring.

The composite glass/polyester rod, more rigid, is the only material enabling a good grooved rod quality. This material has the best Young's modulus, a zero residual elongation and a low thermal expansion coefficient. For this reason it has been selected as a strength member in metal-free cables.

## 4. - METAL-FREE CABLE IMPLEMENTATION

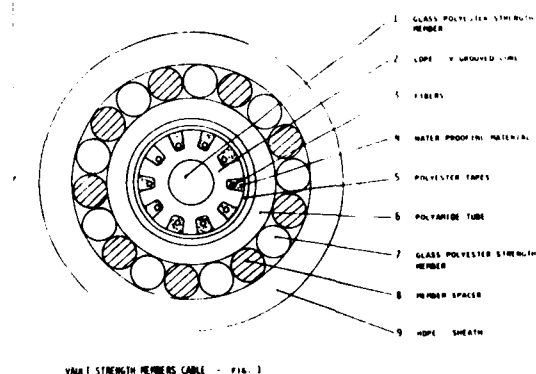
### 4.1.- Cable design

Two cable designs can be implemented :

- in the first one, the rod central strength member has the same dimensions as the metal cable,
- in the other design, the central rod has a larger central strength member, therefore the outer sheath needs no strength member.

#### 4.1.1. "Vault structure" strength member cable

A cable has been implemented with the composite glass polyester rods described in the last paragraph. Cable parts are (fig. 1 and 1-1) :

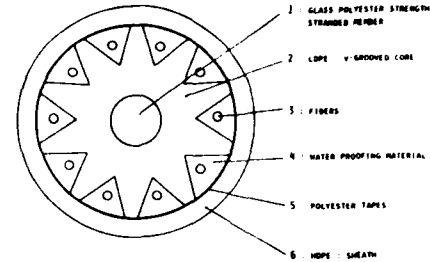


VAULT STRENGTH MEMBERS CABLE - FIG. 1

- FIG. 1 -

#### 4.1.2. Reinforced central strength member cable

Cable parts are (fig. 2) :



REINFORCED CENTRAL STRENGTH MEMBER CABLE : FIG. 2

- FIG. 2 -

- a 10-groove polypropylene rod : the 6 mm diameter rod is extruded on a central strength member made of a 6 glass polyester, 0,86 mm diameter fiber strand. Grooves are filled with a water proofing material.

- an outer protective sheath :
  - . high density polyethylene
  - . 1.5 mm thick.

#### 4.2.- Manufacturing

##### 4.2.1. Vault structure cable

The V-grooved rod manufacturing machine has been described in a previous communication (4). It is an extruding machine with a rotating die. The central strength member speed and the rotating die speed have to be monitored to keep a constant helix pitch. During manufacturing, groove pitch and diameter are continuously recorded.

The cabling machine used to lay the fibers into the grooved rod has been described in the same communication (4).

A special machine has been designed for the outer armour of the cable, consisting of glass polyester rods clamped between a polyamide tube and the outer sheath.

If no special care had been taken, the cabling of the vault on the central rod would have introduced constraints on the rod, changing the overlength of the fibers, and therefore the temperature range of the cable.

- FIG. 1.1 -

- a 10-groove L.D.P.E. rod : the 4 mm diameter rod is extruded on a 1.6 mm diameter glass polyester strength member. Grooves are filled with a water proofing material.

- a polyamide tube which is loosely extruded on the V-grooved rod :

- . outer diameter 6,3 mm
- . inner diameter 5 mm

- a 350 mm pitch helicoidal vault consisting of sixteen 1.3 mm diameter rods :

- . 6 polyamide filling rods
- . 10 glass/polyester composite rods

- a polyester ribbon on the vault.

- an outer protective sheath :
  - . high density polyethylene
  - . 1.35 mm thick.

The outer cable diameter is 12.2 mm.

The vault configuration, consisting of joined rods, is clamped between the inner tube and the outer sheath. It protects the cable against crushing.

A special machine has been implemented in order to avoid these difficulties.

It has been used for the manufacturing of lengths of 10-fiber cables.

Mechanical and thermal tests were performed on these lengths (see 5 below)

#### 4.2.2. Reinforced central strength member cable

The manufacturing of the V-grooved rod is the same as previously. Optical fibers are layed in to the grooves through a special process, to adjust the proper overlength of fibers. Therefore, no constraints are introduced on the fibers, due to temperature or cable pulling.

All measurements are made on four 50/125 graded index fibers in the cable. Results are given in table 3 and fig. 3.

FIBER N°	20° C attenuation, dB/km		Changes in attenuation at - 40°C dB/km		Changes in attenuation at +50°C dB/km	
	in the rod	after sheathing	in the rod	after sheathing	in the rod	after sheathing
1	2.5	2.5	+0.02	+0.03	0	0
2	2.5	2.5	+0.02	+0.02	0	0
3	2.5	2.5	0	+0.03	+0.03	0
4	3.0	3	0	0	0	0

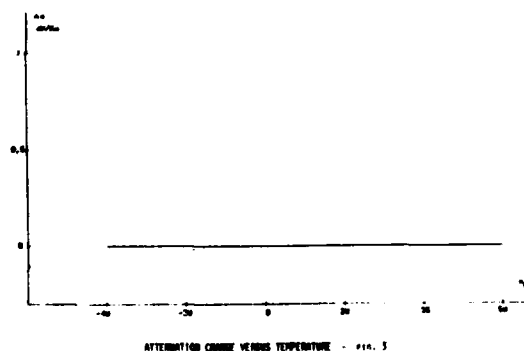
### 5. - METAL-FREE CABLE CHARACTERISTICS

The results gathered in this communication are related to the vault structure metal-free cable. Characterization of the reinforced central strength member cable is still on progress.

#### 5.1.- Optical characteristics

20° C attenuation is measured by retrodiffusion at 0.85  $\mu$ m.

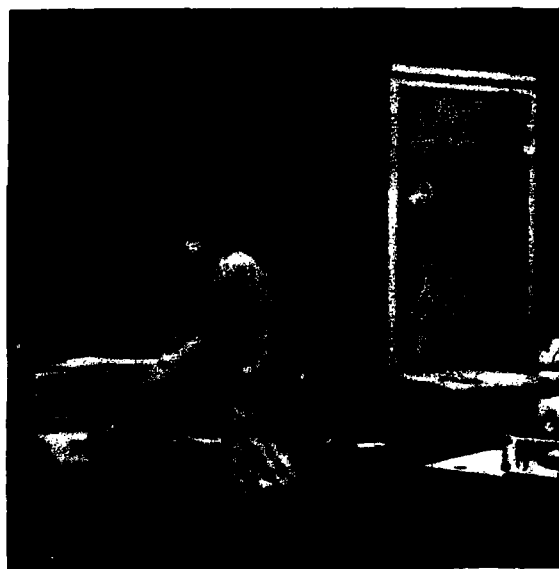
-40°C and +50°C attenuation change is measured by the insertion loss method. The cable is loosely wound without any constraint round a 2 meter diameter drum (fig. 3-2). Light emitter stability is better than 0.05 dB per 24 hours. Figure 3-1 shows the measurement bench.



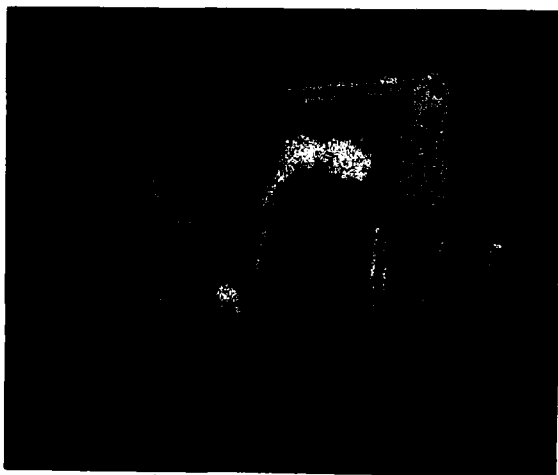
- FIG. 3 -

T A B L E 3

Thermal range of the cable is greater than - 40°C/+ 50° C.



- FIG. 3.1 -



- FIG. 3.2 -

## 5.2.- Mechanical characteristics

### 5.2.1. Pulling test

#### 5.2.1.1. Test description :

A 600 meter cable is pulled on 300 meters with a winch between two pulling wheels.

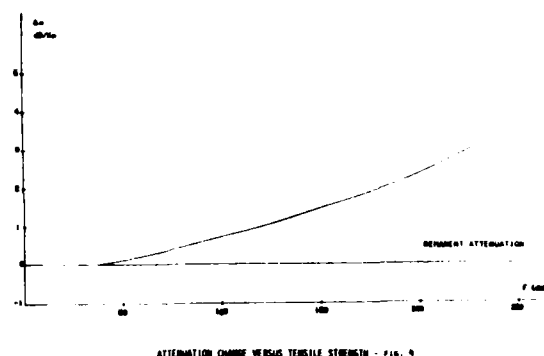
Attenuation is measured by the insertion loss method. The pulling force is measured with a constraint gauge.

The force is applied by 0.5 hour steps. Each step is followed by a zero force time, to measure residual elongation and attenuation. Then the next step is applied with an increase of 10 daN.

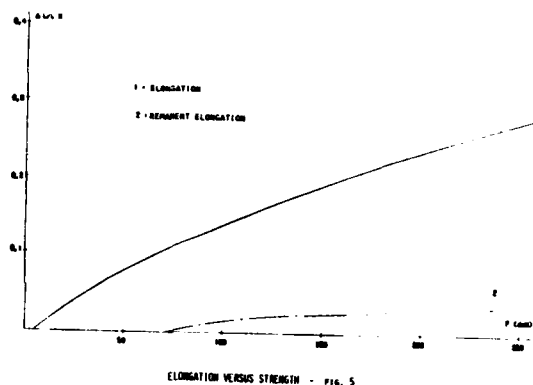
#### 5.2.1.2. Results :

Figure 4 shows attenuation changes and residual attenuation versus the applied force.

Figure 5 shows elongation changes and residual elongation versus the applied force.



- FIG. 4 -



- FIG. 5 -

The glass polyester central strength member cable has a higher tensile strength than the standard steel central strength member cable.

The glass polyester elasticity is better than steel elasticity, then we can pull on the cable with a 250 daN force with less than 0.1 dB/km residual elongation.

### 5.2.2. Crushing strength

#### 5.2.2.1. Test performed :

A compression force is applied to the cable, perpendicularly to the axis, with a cylindrical 0.5 mm diameter key. The force is measured with a dynamometer. The key is drawn nearer to the cable at 1 mm per minute speed. Attenuation is measured by the insertion loss method.

The force corresponding to 0.1 dB/km attenuation increase is logged.

#### 5.2.2.2. Results :

Measurements have been performed on :

- the metal-free cable,
- a corrugated steel screen cable (steel is 0.15 mm thick).

The 0.1 dB/km residual attenuation load is 200 daN for the metal-free cable and only 100 daN for the metallic standard cable.

Vault structure cables have a better crushing resistance than steel cables.

#### 6. - CONCLUSION

A vault structure metal-free cable has been designed and implemented. Optical and mechanical properties are excellent. The strength member material is a glass polyester compound which characteristics (Young's modulus, elasticity and temperature coefficient) are convenient for an optical fiber cable strength member.

A reinforced central strength member metal-free cable has been designed and implemented. Characterization of this cable is on progress.

Both structures will be compared on manufacturing and price parameters.

Both cable structures are compatible with :

- great length mechanical laying techniques,
- lubricants like the micro-ball method implemented by the CNET (9),
- flat mass splicing, which is generally used in FRANCE for cable splicing (8).

#### REFERENCES

- (1) - Optical fiber cable and splicing techniques  
G. LE NOANE - 2nd ECOC (1976) - p. 247 - 256.
- (2) - Optical fiber cables using V-grooved cylindrical units : High performance cables - D. BOSCHER, G. LE NOANE, B. NONCLERC, A. ZAGANIARIS - Fiber and integrated optics, Vol.4 n° 1, p. 67-93.
- (3) - BIARRITZ, la ville câblée par fibres optiques - M. DUPIRE, B. MARC, A.de PANAFIEU 8th ECOC (1982) ) p.504-509.
- (4) - Low-loss optical fiber cable design and manufacture - D. BOSCHER, B. MISSOUT, P. CHERON - 30th IWCS 1981 - p. 139-146.
- (5) - Câbles à fibres optiques - R.E.J. BASKETT, S.G. FORD - Revue des Télécommunications n° 52/1, 1977, p.55-60.
- (6) - Realizing the potential of high modulus polymers. I.M.WARD, A.G. GIBSON - Plastics design and processing - December 1981 - p. 45-48.
- (7) - Local network fiber optic cables - D. BOSCHER, G. LE NOANE, B. NONCLERC - I.C.C. 83 BOSTON - Session C III-6.
- (8) - Flat mass splicing process for cylindrical V-grooved cables - R. DELEBECQUE - E. CHAZELAS - D. BOSCHER - 31st IWCS 1982 - p. 178-184.
- (9) - Manufacture, laying and splicing of monomode optical fiber cables with low losses at 1.55  $\mu$ m - D. BOSCHER, B. NONCLERC, M. LE BOUTET, B. MISSOUT - 32nd IWCS 1983.



Georges LE NOANE  
Centre National d'Etudes  
des Télécommunications  
LANNION - (France)

Georges LE NOANE graduates from the "Ecole Nationale Supérieure des Arts et Métiers" in 1969. He is nine years experienced in optical fiber cable and splices design. As manager of the optical fiber and cable department at CNET, his responsibilities include studies of multimode fibers, pulling and coating techniques, mechanical strength and ageing of fibers, optical cables, splices, connectors design and characterization.



Philippe CHERON  
SILEC  
Département :  
Câbles Téléphoniques  
MONTEREAU - (France)

Philippe CHERON graduated from the "Institut National des Sciences Appliquées" of LYON in 1973. He is presently working on the development and evaluation of optical fiber cables at the Telephone cable division of SILEC company.



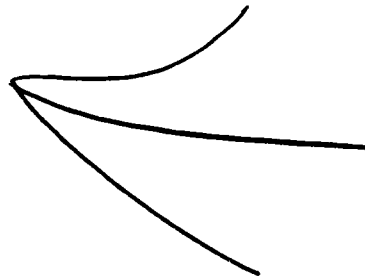
Christian AUDOUX  
S I L E C  
Département : Recherches  
et Développement  
MONTEREAU - FRANCE

Christian AUDOUX graduated from the "Ecole Nationale Supérieure de Chimie" of CLERMONT-FERRAND, in 1966. He is working on materials for cables specially for optical cables.



Bernard MISSOUT  
Société Anonyme des  
Télécommunications  
Département "Câbles"  
PARIS - FRANCE

Bernard MISSOUT graduated from the "Ecole Nationale Supérieure des Arts et Métiers" in 1971. He is presently in charge of special cable machines development and studies particularly about fiber optical cables, at the cable division of SAT company.



## DESIGN, FABRICATION AND TESTING OF A RUGGEDIZED FIBEROPTIC CABLE

H. L. Blumsack, P. J. Dobson, D. Hurwitz, I. D. Aggarwal

Valtec, A Subsidiary of U. S. Philips Corp.  
West Boylston, Massachusetts 01583Introduction

The implementation of optical fiber cables in military applications has been relatively slow because very stringent environmental and mechanical requirements are imposed on those cables. For example, field deployment in a tactical environment requires a light weight, all dielectric cable which can be operated at temperatures as low as  $-55^{\circ}\text{C}$  and be able to withstand several hundred impacts of 1 N-m at temperatures as high as  $+85^{\circ}\text{C}$ . It is very difficult to achieve satisfactory performance under these conditions since most plastic materials contract at low temperatures, which results in increased optical loss; and they soften at high temperatures, which results in reduced impact resistance.

This paper presents the design and manufacture of a small size, lightweight, all dielectric cable suitable for easy deployment and recovery in cross-country terrain. Intended as the data and communication link between a battlefield radio station and a jeep-mounted radio system, the cable is composed of two optical fibers twisted together, around which are applied two contrahelically wound layers of Kevlar yarns, an inner jacket, two more contrahelical layers of Kevlar yarns, followed by an outer jacket.

This cable was required to exhibit less than 6 dB/km attenuation and greater than 400 MHz-km bandwidth at 850 nm over a temperature range of  $-55^{\circ}\text{C}$  to  $+68^{\circ}\text{C}$ . The cable also was required to weigh less than 50 lbs./km so that it would be light enough for one-man carry. Further, it was required to withstand 400 lb. tensile load, and 200 impacts of 1 N-m at  $+85^{\circ}\text{C}$ ; and not fail optically under 400 psi compression and the formation of ice around it.

Discussion

Development of such a cable becomes a matrix of tradeoffs, inasmuch as the quick and easy improvement of one performance parameter compromises one or more of the others. For example, a more rugged cable is not the smallest, or the lightest. Most of the tradeoffs

were more complex; and, in order to evaluate their impact, the referenced analytical models were used to characterize every cable feature.

Generally, the most troublesome feature to achieve in optical cables is negligible increase of attenuation at low temperatures. This is due to the phenomenon known as microbending, which causes the fiber to have excess optical loss.

In a cable structure, plastic and polymer materials are applied around the glass fibers to package them and to provide protection from the environment. Unfortunately, plastics have more than  $10^3$  times larger coefficients of thermal expansion than glass. At low temperatures this results in longitudinal compressive stress being imposed on the fiber which can cause the fiber to buckle out of its nominally straight lay in the form of microbends.

The amount of longitudinal compressive strain to which the fiber in this cable is subjected can be calculated by

$$\left(\frac{\Delta L}{L}\right)_t = \left[ \frac{E_G A_G \alpha_G + \sum E_n A_n \alpha_n}{E_G A_G - \sum E_n A_n} \right] \Delta t$$

where  $\frac{\Delta L}{L}_t$  is the strain at the lowest operating temperature.

$E_G$  = Young's Modulus of fiber core.

$A_G$  = the cross section of area of fiber core.

$E_n$  = the Young's Modulus of surrounding material.

$A_n$  = the cross sectional area of surrounding material.

$\alpha_G$  = the coefficient of expansion of fiber

$\alpha_n$  = the coefficient of expansion of surrounding material.

$\Delta t$  = temperature change from when first the cable has been finished to the lowest operating temperature.

The values of both Young's Modulus and the coefficient of thermal expansion change with temperature. For the purpose of this study, it was assumed that they remained constant with temperature.

In this cable  $\frac{\Delta L}{L}$  is approximately  $15 \times 10^{-3}$  per degree  $^{\circ}\text{C}$ .

The compressive force generated by contraction is given by

$$F = EA \alpha \Delta t$$

Thus, when cable of this general configuration would be subjected to a change from room temperature, say  $20^{\circ}\text{C}$ , to  $-55^{\circ}\text{C}$ , it would exert a force of 139 lbs. attempting to contract it 1.13%. The cable design, and the techniques of manufacturing it, had to overcome that phenomenon.

Normally, a steel wire or dielectric rod is placed longitudinally in the cable to inhibit cable contraction at low temperature. However, two performance requirements prevented their inclusion. One, the cable must be all dielectric so that it is immune from electromagnetic fields. Second, the cable must be easily handleable and have no preferential direction of bend so that pay-out and retrieval can be accomplished easily. The latter would not be possible unless the fibers were stranded around a central member. Since there are only two fibers, there is no center.

Hence, it became necessary to evaluate all materials which are applied around the glass fibers for their contribution to microbending loss.

Two layers of UV curable acrylate are coated directly onto the fiber as part of the drawing operation. This coating protects the glass surface from foreign substances and physical abuse.

A computer model was developed based on a paper by Gloge<sup>(2)</sup>. The model shows that multiple layers inhibit microbending losses more effectively than single coatings and that further improvement can be made by choosing materials by reason of modulus and optimizing the thickness of each layer. To determine the thickness of each layer applied around the optical fibers, the finite element method was used to analyze the internal stress produced in the fiber when the cable is under longitudinal compressive loads.

Further processing of the fibers includes color coding for individual identification of each fiber and buffering.

The glass fibers are insulated, to some extent, from microbends by a buffering layer which is applied around the individual fibers in a cable. The buffer also provides a physical package enabling the fiber to be handled during subsequent processing of the cable and termination. There are, essentially, two types of buffering, namely tight buffering and loose tube buffering.

Tight buffering is the concept of applying a plastic jacket directly onto the polymer coated glass fiber.

Loose tube buffering is the concept of placing the fiber inside a gel-filled tube having an inner diameter large enough to allow the fiber to move freely within it. Thus, the fiber is decoupled from cable strain. While multifiber telecommunication cables can take advantage of the loose tube concept, it would not be suitable for this particular cable for many reasons. One, inclusion of the buffer tubes would cause both the cable diameter and its weight to be greater than allowed by specification. Also, field cables are payed-out and retrieved repeatedly. If the fibers were contained within loose tubes, there is a possibility that after repeated deployment the fibers could become gathered in one or more places along the length of the tube; and, such gathering could result in buckling of the fiber if not in fiber breakage. It must be noted that hundreds of cables with loose tube buffered fibers have been reeled, unreeling, and reeled-up again many times without any deleterious effects. Even so, those cables were designed without concern for a lifetime of that kind of service. Additionally, in a crush situation, the tube may collapse beyond its yield point so any increased optical loss would not be reversible and the cable might be no longer serviceable.

Therefore, the tightly buffered concept was used for this cable. Fibers used in the first attempt to produce this cable had 50  $\mu\text{m}$  core, 125  $\mu\text{m}$  cladding, and 400  $\mu\text{m}$  UV cured coating. They were the high quality fibers normally used in telecommunication cables. In addition, the fibers were tightly buffered with Hytrel. Those fibers did not achieve the desired optical performance of less than 2 dB/km increase at  $-55^{\circ}\text{C}$ . There are several factors which contributed to that increase. Most prominent is the fact that tightly buffered fibers also are susceptible to microbending losses. In that prototype, the loss was due to contraction of the plastic buffer itself at cold temperatures. When the buffer contracts, it microbends the fiber which, in turn, causes significant signal loss. It is known that the susceptibility of a fiber to induced attenuation decreases as numerical aperture (N.A.) increases.

Olshansky<sup>(1)</sup> describes the relationship

among the parameters of a step index fiber by the following:

$$\alpha_b = \frac{c r_c^4}{\Delta^3},$$

where

$$c = 0.9 p \frac{h^2}{b^6} \left( \frac{E_m}{E_G} \right)^{3/2}$$

$\alpha_b$  = distortion loss

$r_c$  = core radius

$b$  = fiber diameter

$\Delta$  = relative index difference

$$1 - \frac{n_{\text{clad}}}{n_{\text{core}}}$$

$h$  = effective rms bump height

$p$  = number of bumps per unit length

$E_m$  = modulus of encapsulating material

$E_G$  = modulus of fiber core

While it is recognized that this equation was not developed for application to graded index fiber, empirical data shows it to be qualitatively correct. Figure 1 shows the relationship of microbending sensitivity to fiber N.A. The vertical axis is merely an arbitrary reference number for sensitivity. A value of one was assigned to Valtec's standard 50  $\mu\text{m}$  core/125  $\mu\text{m}$  clad telecommunication quality fiber which has well understood performance.

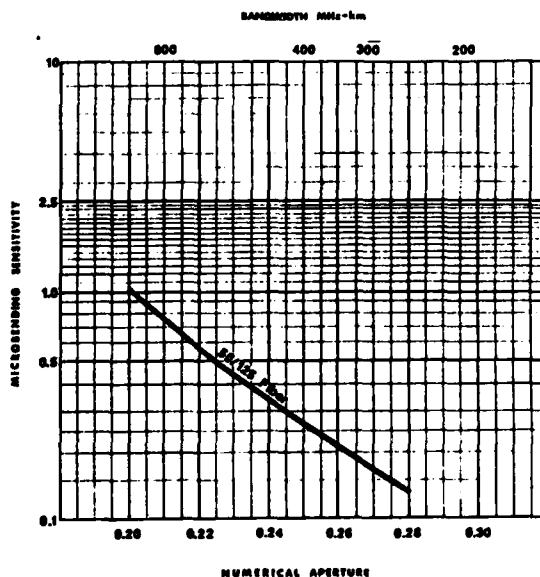


Figure 1

This chart, as well as results of test cables, indicated that standard production

fibers used for telecommunication cables would not be suitable for tactical type applications and that higher N.A. fibers were needed. Optimum results are obtained with fibers of  $0.22 \pm 0.02$  N.A.

### Cable Design

The cable comprises two fibers twisted together. A range of lay length was calculated by establishing a level of stress which the fiber would be allowed to endure. Cables were evaluated with various lay lengths between 3/4 inch and 3-1/2 inches. Shorter lays would induce too much bending stress due to stranding even though there would be less stress due to cable strain, while longer lays would induce less bending stress but more stress due to cable strain and cable bending. It was determined that lay lengths shorter than 1-1/2 inches could introduce microbending loss.

An inner jacket is extruded over the cabled core. It packages the fibers and provides a buffer layer between the fiber and Kevlar strength member. The material is polyurethane.

Here, too, choices had to be made. There are two dissimilar urethane polymers. Ester based urethanes can hydrolyze in water, so this jacket utilizes an ether based compound which is not susceptible to hydrolysis. Polyurethane was chosen for this application because of its resistance to abrasion by the Kevlar, as well as its modulus, low temperature flexibility and fungus resistance.

The strength member is composed of layers of Kevlar 49 yarns served over the inner jacket. Kevlar 49 was chosen primarily because it is dielectric; but also, it exhibits a high strength-to-weight ratio, and low elongation. The lay length has been calculated to ensure that when the cable is subjected to a tensile load, the Kevlar and not the optical fibers, takes the load. The strength member limits cable elongation to less than 1% when the cable is subjected to 400 lb. tensile load. In addition, a feature of the design allows the cable to elongate without pulling the fibers out of an attached connector.

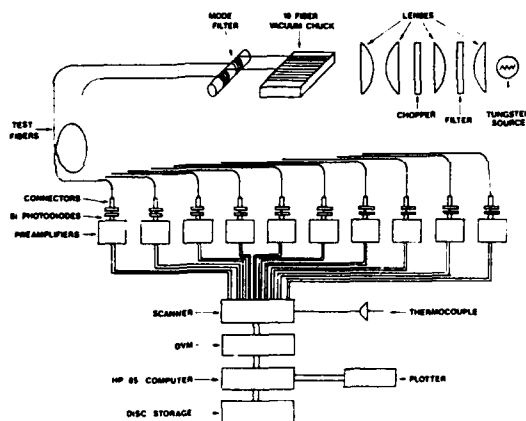
An outer jacket is extruded over the Kevlar strength member. While it also is polyether based urethane, it is a slightly different compound than the inner jacket. This compound was chosen for its toughness (cut, tear, puncture, and abrasion resistance), low temperature flexibility, and excellent stability under varied environmental conditions.

Unique techniques and elaborate process control systems are employed to manufacture this cable. It is most important that there is the proper amount of excess fiber relative to jacket and that the relationship remains proper when the cable is strained by both tensile and contraction forces.

## Tests and Results

Prototypes of each candidate construction were made and tested extensively both optically and mechanically under a variety of environmental conditions. In all, prototypes of twenty different designs were produced and tested. Mechanical tests of specimens were conducted on equipment designed in accordance with MIL-STD-1678. The equipment and/or reels of cable can be placed inside our laboratory or inside our environmental chamber, which is capable of holding temperatures between  $-55^{\circ}\text{C}$  to  $+85^{\circ}\text{C}$ .

A special test facility, shown in Figure 2, is utilized to measure attenuation continuously during the environmental tests. Known at Valtec as the Delta Optical Power Measurement System (DOPS), it incorporates a light source, chopper, monochromatic filter and lenses which couple light into one end of both fibers simultaneously. The far ends of the fiber are coupled to photodiodes which are connected to a DVM. System control, data acquisition and analysis are performed by an HP-85 computer.



Delta Optical Power Measurement System

Figure 2

The following describes some of the tests and test results:

Attenuation versus tension tests were performed in accordance with DOD-STD-1678, Method 3010 on the apparatus shown in Fig. 3. At 400 lbs. load, cable elongation was approximately 0.75% and the average increase attenuation was only 0.04 dB/km.

Samples of cable with 5 kg mass suspended were subjected to 2000 cycles of bending around a 1 inch diameter mandrel at room temperature in accordance with MIL-STD-1678, Method 2010.

None of the fibers showed an attenuation increase greater than 0.5 dB/km.

Samples of cable with 2.3 kg mass suspended were conditioned at  $-55^{\circ}\text{C}$  for 20 hours, then while at that temperature were wrapped six times around a 2.75 inch diameter mandrel as described by MIL-STD-1678, Method 2020. None of the fibers showed attenuation increase greater than 0.2 dB/km.

Samples of cable with 10 kg mass suspended survived 2000 cycles of combined twist-bend around a 1 inch diameter mandrel at room temperature in accordance with MIL-STD-1678, Method 2060.

Samples of cable conditioned at  $+85^{\circ}\text{C}$  survived 200 impacts of N-m as prescribed by MIL-STD-1678, Method 2030. Other samples survived the same impacts at  $+25^{\circ}\text{C}$ ; and, still others survived at  $-55^{\circ}\text{C}$ .

Cables were temperature cycled from  $-55^{\circ}\text{C}$  to  $+85^{\circ}\text{C}$  in accordance with MIL-STD-1678, Method 4010. There was no measurable increase of attenuation at high temperatures; there was an average of 0.8 dB/km increase at  $-55^{\circ}\text{C}$ . This was considerably better than the 2.0 dB/km allowed.

The data presented in Figures 4 through 7 show that optical fiber cables can be manufactured to withstand rugged field conditions without significant mechanical degradation and exhibit stable optical performance over a wide range of temperatures. This is achieved by appropriate selection of fiber, polymer coating materials, buffering, strength members and jacket compounds; and, combining them properly.

## Summary

A ruggedized, all dielectric, field deployable cable has been designed, manufactured, and rigorously tested to assure compliance with the severe requirements of military field conditions. The following performance was achieved:

1. Optical attenuation less than 6 dB/km from  $-55^{\circ}\text{C}$  to  $+68^{\circ}\text{C}$ .
2. Impact resistance of at least 200 times with 1 N-m at  $-55^{\circ}\text{C}$  to  $+85^{\circ}\text{C}$ .
3. Pulling strength of at least 400 lbs.
4. Compression withstand of at least 400 psi.
5. Cyclic flex capability of at least 1000 cycles around 1 inch mandrel.
6. Twist/bend capability of at least 2000 cycles around 1 inch mandrel.
7. Cable weight less than 50 lbs./km.

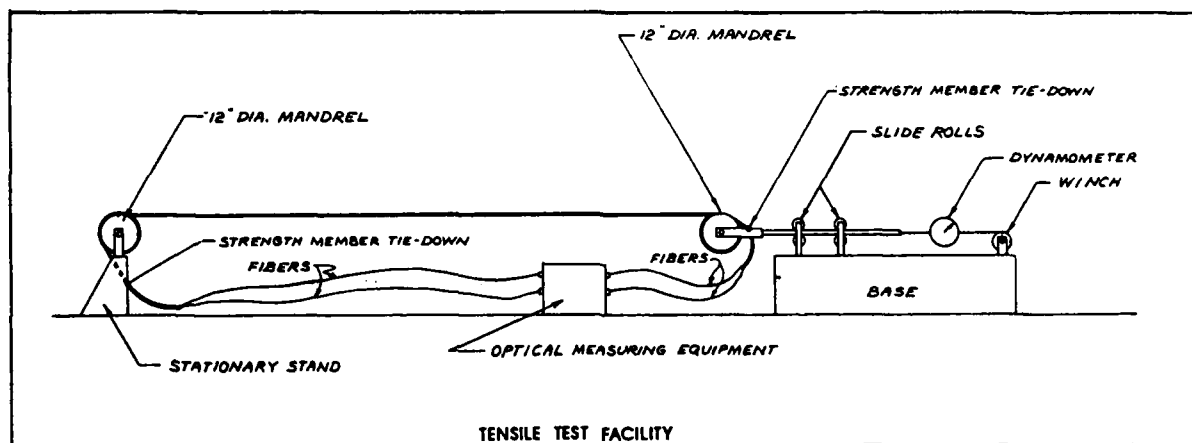


Figure 3

Physical Test Results

Parameter	Units	Requirement	Results by Sample		
			1	2	3
Number of Fibers	Fiber	2	2	2	2
Fiber Identification	Color	Red/White	Red/White	Red/White	Red/White
Fiber Dimension					
Core	μm	50 ± 4	51.4/50.0	50.6/51.8	49.3/48.7
Clad	μm	125 ± 4	123.8/123.2	123.9/124.3	125.8/125.4
Concentricity	%	96, min.	99.7/99.2	99.7/99.3	99.4/99.0
Buffer	μm	550 ± 50	572.5/583.3	593.4/592.9	581.3/589.1
Cable diameter	Inch	0.190 ± 0.015	0.198	0.196	0.196
Cable Weight	lbs/km	50.0, max.	47.5	48.9	45.9
Tensile Strength	% Strain	1.0, max.	0.74	0.75	0.75
	@ 400 lbs. Increase Attn., db	0.96, max.	0.01/0.13	0.02/0	0.05/0.03

Figure 4

Optical Test Results

Parameter	Units	Requirement	Results by Sample		
			1	2	3
Operating Wavelength	nm	850 ± 30	850	850	850
Numerical Aperture		0.18 ± 0.04	0.214/0.210	0.214/0.212	0.210/0.219
Fiber Bandwidth	MHz-km	400, min.	653/667	774/776	1213/1188
Fiber Attn. @ 20-25°C	db/km	6.0, max.	3.7/4.3	3.1/3.5	3.2/3.8

Figure 5

### Mechanical Test Results

Parameter	Units	Requirement	Results by Sample		
			1	2	3
Precondition of Samples	Hours	48	48	48	48
Cyclic Flex - 1000 Cycles Around 1 in. Mandrel with 5 kg Load	Increased Attn., dB	0.96, max.	0.54/0.52	0.15/0.15	0.02/0.03
Cold Bend - 6 Wraps Around 1.75 in. Mandrel with 2.3 kg Load @ -55°C	Increased Attn., dB	0.96, max.	0.1/0.2	0.2/0.1	0.2/0
Twist/Bend - 2000 Cycles Around 1 in. Mandrel with 10 kg Load		Survive		No Broken Fibers	
Impact - 200 Times with 1.0 N-m @ -55°C, @ +25°C, @ +85°C		Survive		No Broken Fibers	
Compression					
After 400 psi Attn., dB/km	Increased	1.51, max.	0.07/0.13	0/0	0.01/0.02
Under 100 psi Attn., dB/km	Increased	1.51, max.	0.8/0.7	0.9/0.8	0.9/0.5

Figure 6

### Environmental Test Results

Parameter	Units	Requirement	Results by Sample		
			1	2	3
Precondition of Samples	Hours	48	48	48	48
Temperature Cycle -55°C to +68°C	Change Attn., dB/km	2.0, max.	0.32-0.12 1.10-0.73	0.41-0.09 0.64-0.12	0.53-0.06 0.66-0.08
Humidity, 95% @ 65°C dB/km	Change Attn.,	2.0, max.	0.22/0.20	0.18/0.18	0.22/0.20
Ice Crush dB/km	Change Attn.,	2.0, max.	-0.2/0.1	0/0	0/0.1

Figure 7

While the cable described herein was designed specifically to meet the requirements of one program, it might be suitable in other military applications, local area or campus systems, data installations and the like. More importantly, it is felt that the concepts, technology, and experience can be applied to each unique set of requirements.

#### References

1. R. Olshansky, "Distortion Losses in Cabled Optical Fibers", Applied Optics, Vol. 14, No. 1, January, 1975
2. D. Gloge, "Optical Fiber Packaging and Its Influence on Fiber Straightness and Losses", Bell System Technical Journal, pp 245-262, February, 1975

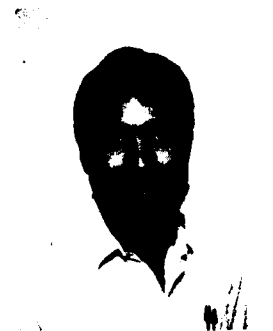
HARVEY L. BLUMSACK was graduated with a BSE from Lowell Technological Institute, 1960, MA Ed from Salem State College, 1972, CGS in Management from Boston University, 1980. He has 23 years experience in cable application and design, and joined Valtec in 1981 where he is currently Manager of Cable Engineering.



PAUL J. DOBSON was graduated from USAF Electronics School, USAF Institute, and Capitol Radio Institute. He has 6 years experience in design and manufacture of fiberoptic cable. Paul has co-authored several papers relating to fiberoptic technology, and has two patents pending. He joined Valtec in 1968 where is is currently Senior Staff Engineer.



ISHMAR D. AGGARWAL received his Ph.D. in Materials Science from Catholic University in Washington, D.C. in 1974. He is currently Vice-President of Research and Development at Valtec.



DAN HURWITZ received his B.S. in Ceramic Science from Penn State University in 1977. He is currently the Environmental Test Engineer for Valtec, responsible for testing and evaluating environmental effects on optical fibers and cables.



## A Rodent and Lightning Protective Sheath for Fiber Optic Cables

W. C. L. Weinraub and D. D. Davis

Bell Laboratories  
Norcross, Georgia 30071

M. D. Kinard

Western Electric  
Norcross, Georgia 30071ABSTRACT

A new protective sheath design for fiber optic cables has been developed. It features corrugated and longitudinally applied metal members with a plastic jacket in an adhesively bonded construction. The use of conventional corrugation tools and longitudinal application in a single pass results in low cost and high line speeds. Tests have shown this sheath to be rodent proof, to have exceptionally high lightning-withstand capability, and in general, to be very rugged mechanically, without compromising cable handling qualities or optical performance. This design is used as a protective oversheath for ribbon core cables and as a primary sheath for stranded core cables. It is recommended for buried and aerial applications, particularly where rodent and lightning resistance is essential. It is also recommended as a general mechanical protection and in buried submarine application.

INTRODUCTION

The placing of telephone cables in the air or the burying of them directly in the ground subjects them to a wide variety of hazards. Given the extent of the outside plant, over time, almost any imaginable hazard can occur. By providing protection from the statistically most significant hazards, repair costs and lost revenues can be greatly reduced but the return must be weighed against the cost of protecting the system. Given the small, comparatively fragile nature of fiber optic cables relative to their capacity and revenue contribution, taking extra pains to protect them from chewing vermin, lightning stroke, mechanical abrasion and crushing can pay off handsomely. However, since every foot of cable at risk must be so protected, the cost per foot of the protection must be kept as low as possible or the capital overhead can negate any savings in maintenance and repair expenses.

Since the above mentioned mechanical hazards do not occur separately, but correlate naturally as a function of buried or aerial installation, we have elected to pursue the development of a single protective system design capable of meeting the broad design objectives of good overall protection at low cost rather than tailor a design to each use.

THE RODENT PROBLEM

Attack by chewing vermin has been a continuing concern for all utilities who must bury their transmission medium in the ground or suspend it in the air. In general, over large areas of the country, gopher attack on buried cable and squirrel attack on aerial cable are statistically the most significant hazards. Gophers are found in about 60% of the continental U.S.<sup>1</sup> Given the size, strength and chewing kinematics of gopher species, cables below about 0.75 inches in diameter are subject to far more severe attack than larger cables in that the animals can bite directly down on them.<sup>2</sup> On cables above this size only a scraping or raking action takes place. On cables exceeding about 2.1 inches in diameter, gopher attack is rarely observed.<sup>3</sup> In biting, gophers have been shown to exert pressures up to 18,000 psi. It has been found, not surprisingly that, with limited exceptions, the only way to protect directly exposed cables is to wrap them in a metallic layer.<sup>4,5</sup> Cogelia et al., as a result of extensive cage testing, have developed merit indices to rate various metals, based on laboratory hardness and ductility measurements.<sup>4</sup> Of the materials tested although several materials gave good results, in standard cage exposure tests to pocket gophers, *Geomys bursarius*, only low carbon steel at least .006 inch thick and AISI 304 stainless at least .003 inch thick have given 100% protection on buried wire below the 0.75 inch critical size range.

For cables well above the critical size limit (0.75 inch), the use of longitudinally applied corrugated metal strip has proven a sufficient protection. However, in smaller sizes, particularly for buried wire in the 0.2-0.4 inch range, the presence of a longitudinally lapped seam has led to failures and helically applied tape armors have proven superior.<sup>6</sup> Since our cables fall into an intermediate range 0.5-0.8 inches, the fate of longitudinal layers was uncertain. Helical taping, however, is a slow, expensive process with too high a scrap rate for efficient use on lightguide cable. Longitudinal construction, if suitable from a performance standpoint, would be economically preferable from a manufacturing perspective.

In buried cables, the use of longitudinally appliedterneplate (tin coated carbon steel) has occasionally led to long term failures even in cables larger than 0.75 inch. In such cases

chewing or scraping results in a violation of the plastic jacket, exposing the underlying steel. Once exposed, the steel - which withstands the initial attack, corrodes readily rendering it ineffective as a general mechanical protection and against any subsequent gopher attack. Gophers are territorial animals which range over a home plot and may repeatedly return to areas or burrows previously occupied.<sup>1</sup> Secondary attack is therefore a common occurrence. It was felt that this problem could be countered by the use of a corrosion resistant barrier such as stainless steel.

It was further hypothesized that if adhesive bonding between a stainless steel tape and a plastic jacket could be achieved, the use of corrugated, roll-formed, longitudinally applied construction would better be able to withstand rodent attack, even on cables in the critical size range. The presence of adhesive bonding between jacket and a steel armor layer has been shown to be of considerable advantage with respect to buckling and kinking resistance in copper cables.<sup>7</sup> In addition, because it adds considerable annular mechanical support to the rolled-tube geometry of the steel, bonding would improve crush resistance and tend to hold the lapped seam shut, overcoming a major concern for rodent resistance. Finally, bonding would prevent the wholesale removal of plastic jacket in sheets or strips, necessitating its removal laboriously from each element of area, greatly increasing the work involved to violate the sheath and thus further impeding the progress of the chewing hordes.

#### THE LIGHTNING PROBLEM

Cable damage due to lightning strike is a constant concern to operating companies. This is true of buried as well as aerial cables. Although it was once believed that buried cables would be shielded from the harmful effects of lightning strikes, this has not proven to be the case. There are two primary mechanisms by which lightning strikes to earth can cause damage to buried cables. The first is thermal, causing burning, charring, and melting of the sheath components by the heating effects of the arc and of the lightning current being carried to ground by the metallic members of the core or sheath. The second is mechanical, causing crushing and distortion of the sheath. This latter results from an explosive impact, sometimes called the steamhammer effect, which is caused by the instantaneous vaporization of water in the earth in the lightning channel to the cable.

While fiber optic cables do not employ metallic conductors for transmission, metallic strength members are commonly used in the sheath. This renders them susceptible to lightning strike. Fiber optic cables with all-dielectric sheaths are available, but they are expensive to manufacture and present problems in locating them once installed. In addition, these cables have poor resistance to rodent attack, calling for very expensive protection

measures. Generally, all dielectric route construction has proven to be of limited application. In metal bearing cables, since it is desirable to keep lightning current from arcing into the cable core where the fibers would be damaged, a robust, highly conductive, protective oversheath which would preferentially carry surge currents seems to be a logical means of minimizing lightning damage. Heating damage to a fiber optic cable at the lightning strike point results from the high temperature arc to the metal. Additional heating of the sheath occurs due to  $I^2R$  power as the lightning current flows down the sheath.<sup>8</sup> This second form of heating may be minimized by selecting a metallic oversheath with high conductivity, thus allowing the lightning current to flow to ground without causing as much burning of the sheath. For this reason, a corrugated aluminum or copper tape was included as the primary conductive element of the oversheath. The conductivity of this layer in conjunction with the corrugated stainless steel bonded to the jacket, which provides increased crush resistance and minimizes damage from the steamhammer effect, could be expected to provide excellent lightning protection.

#### THE MECHANICAL PROTECTION PROBLEM

The necessity of protecting the "core" of a communication cable has long been recognized for copper cables. It is perhaps even more critical for a fiber optic cable due to its large signal density and the fragility of the glass fibers.

All of the normal mechanical hazards exist for a fiber optic cable: Abrasion and crushing are possible when placing cables in aerial, buried or underground plant. Unreeling, feeding over sheaves, coiling and bending, and other normal handling present the possibility of sheath kinking or buckling. Any of these hazards could violate the sheath integrity, leading to immediate damage to the fiber core or long term degradation in the environment.

Reference was made in the section on rodents to the protective capabilities of a sheath utilizing corrugated roll-formed stainless steel adhesively bonded to a polyethylene jacket. This concept is very similar to a number of sheaths and oversheaths existing in the copper cable area. These sheaths have a history of providing good mechanical protection during placing and throughout the life of the cable. They are robust enough to provide abrasion and crush resistance and flexible enough to handle well without kinking or buckling. The logic of extending the copper cable sheaths design concepts in an upgraded form to fiber optic cables will be discussed in detail below.

#### SHEATH DEVELOPMENT

The predecessor of our new design was the Rodent Tape oversheath for multimode fiber optic cable. It was conceived and developed as rodent and light mechanical protection. The

design comprised two spirally wrapped servings of stainless steel tape (Figure 1). It offered excellent protection from rodent attack and some mechanical protection but had two serious shortcomings: The sheath was expensive since its complex sheathing machinery resulted in low line speeds and taping and jacketing had to be done in two separate operations. A more serious problem lay in its relatively poor lightning protection. The stainless steel members have a fairly low conductivity, which gives rise to increased ohmic heating due to lightning current.

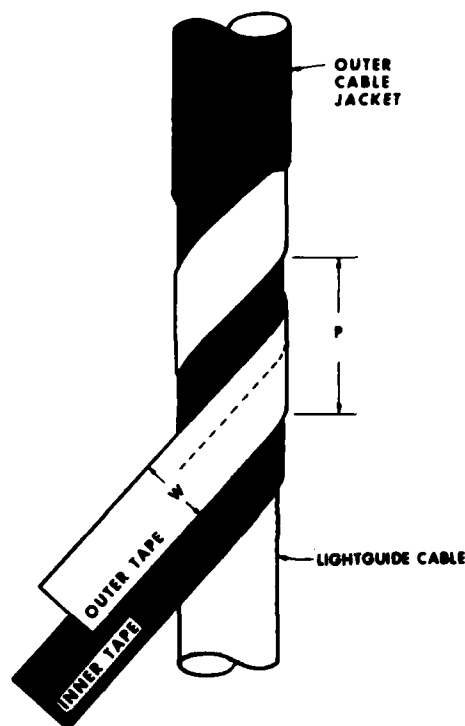


Figure 1 - Rodent Tape Oversheath

The shortcomings of the Rodent Tape oversheath are avoided in copper cables by the ASP sheath. It offers protection from mechanical damage, electromagnetic interference, and lightning. Its cost is quite low since it is applied in a single pass at high line speeds utilizing simple machinery. It is important to note that its resistance to rodent attack is only fair, much less secure than the Rodent Tape oversheath.

We undertook to design a new protective sheath incorporating the best of the ASP sheath concepts with the best features of the Rodent Tape oversheath. The new sheath, which was called B-Oversheath according to our design sequence, would maintain good rodent and mechanical protection while adding a lightning protection capability. It would retain the cable handling and corrosion resistance characteristics of the Rodent Tape, while achieving the mechanical durability of bonded ASP construction.

A prototype design calling for a corrugated stainless steel, rolled-tube armor, adhesively bonded to a polyethylene jacket seemed to constitute a promising line of investigation as a means of rodent resistance and general mechanical protection. The use of this construction, if proven successful, could be expected to yield a substantial reduction in cost over helical taping. Inquiry showed, however, that no adhesive system and laminating process capable of bonding stainless steel to polyethylene jacketing compounds existed in the industry at large. Further, although corrugating and roll forming of aluminum and carbon steels were established processes, the extension of the process to stainless steel was untried. The pursuit and development of a bonded stainless construction then fell to us.

The construction of the B-Oversheath is shown in Figure 2 and detailed below:

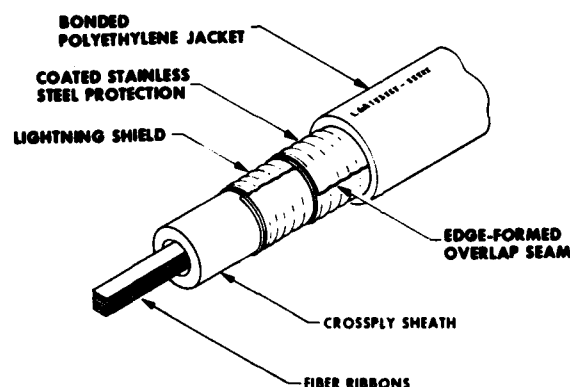


Figure 2 - B Oversheath

- Conductive Inner Shield: A conductive inner shield, borrowed from the ASP concept, is the primary mechanism for achieving lightning protection. A copper tape is the preferred shield, based on its high conductivity and inherent corrosion resistance. Coated aluminum has been used as an alternate to the copper.
- Corrosion Resistant Outer Shield: A high strength metal sheath member is needed for mechanical protection and good handling characteristics. A stainless steel tape was chosen because of its excellent corrosion resistance and demonstrated good rodent protection. The alloy chosen is a common engineering material and has been found compatible with existing metal forming equipment and techniques.
- Corrugated Metals: Corrugating the metal sheath members increases the flexibility of the sheath construction in longitudinal bending and, more significantly, greatly

increases the radial modulus of the metal members. This stiffening of the sheath promotes crush and impact resistance. It has been analytically and experimentally shown that buckling performance and crush resistance increase with the ratio of radial modulus to longitudinal modulus.<sup>7</sup> This is shown schematically in Figure 3, below:

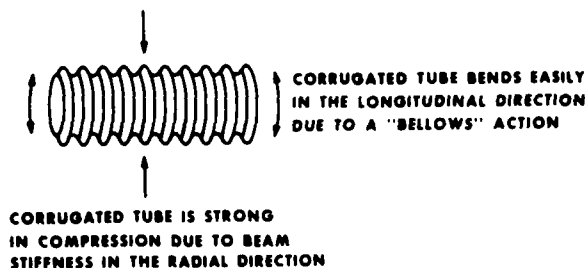


Figure 3 - Forces on a Corrugated Tube

- **Bonded Construction:** The B-Oversheath is another in the Bonded Sheath family.<sup>7</sup> The outer metal member, stainless steel in this case, is adhesively bonded to the polyethylene jacket. As in other bonded sheaths, the bonding creates a steel/jacket composite. Such sheaths exhibit excellent kinking and buckling characteristics. This bonding also increases structural integrity for resistance to crushing, impact, plowing, etc. As discussed in the Rodent Section, the bonded construction drastically increases the difficulty of removal when a rodent gnaws the jacket from the cable.

Special adhesive systems are required to bond stainless steel to polyethylene. No such adhesive systems were or are currently available commercially. The passivity of the stainless steel surface, which is the source of its corrosion resistance, makes adhesive bonding difficult. Western Electric Company has developed an adhesive/application system for this sheath.

- **Cable Jacket:** The B-Oversheath uses linear low density polyethylene or medium density polyethylene for the outer jacket. All of the compounds used are common cable industry materials, exhibiting good flexibility, environmental stress crack resistance, abrasion resistance, and notch accommodation. The jacket is extruded onto the cable in the same pass as the metal application.

The B-Oversheath was originally conceived as a second generation oversheath for multimode fiber optic cable having a crossply primary sheath. Although the first commercial

production of this sheath variant was a submarine armor application, the bulk of the commercial orders have been for rodent and lightning protection, as planned. A second, but potentially very important application for this sheath is as a primary sheath on stranded fiber optic cables both single and multimode. This variant is expected to become a mainstay commercial offering for aerial and buried applications.

#### RODENT TEST PROCEDURES AND RESULTS

In general, gophers are very consistent chewers animal-to-animal and day-to-day, spending about 10% of their time in active gnawing behavior.<sup>1</sup> Squirrel chewing is more idiosyncratic. An energetic squirrel can do far more damage than any gopher, but lazy animals may ignore a specimen entirely. Standard caged rodent exposure tests for wire and cable have been developed as a result of a collaborative study between the U.S. Fish and Wildlife Service and Bell Laboratories.<sup>4</sup> The gopher test, which simulates an encounter with a horizontal cable in a burrow, presents the cable specimen on the far side of a cage divider with a 2 x 2 inch hole in it. This test has proven very successful in predicting subsequent field performance of buried wire and cable. The squirrel test, in which the specimen impedes the animals access to a nest box in its cage has proven less reliable as a predictor. In both cases, test duration is seven days. A standard test series exposes 10 specimens but may use fewer animals repetitively.

Specimens of three oversheathed cables, all 0.73 inch in overall diameter, were subjected to the seven day cage exposure to rocky mountain pocket gophers, *G. bursarius*, and fox squirrels, *Sciurus niger*. In the first, the oversheath elements were applied without bonding the jacket. The second had a fully bonded jacket. The third included an adhesively sealed overlap seam. In all cases, the specimens were oriented to maximize the animal's access to the lap seam. Figures 4 - 6 show the results of these tests, while Figure 7 shows some typical examples of gopher attack on an all-dielectric cable (severed in 48 hours) and an unprotected steel-reinforced cable of the type used as the core for the experimental oversheaths. Figure 8 shows what an active squirrel can do to an unprotected cable. The results showed that, for the trial cables, in all cases the outer plastic was removed but no animal succeeded in penetrating the steel armor or in gaining entry to the core by lifting the overlapped seam. In 60 individual test exposures, there were no failures. However, the degree to which the seam was disturbed clearly declined with both seam sealing and jacket bonding showing that they provided a considerable added performance margin. Clearly, this

design area gives highly successful protection against chewing rodents.

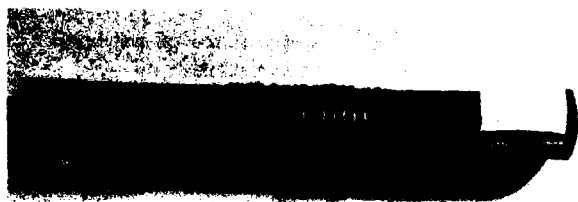


Figure 4 - Unbonded Jacket, No Seam Sealing, Typical Gopher Attack



Figure 5 - Bonded Jacket, No Seam Sealing Typical Gopher Attack



Figure 6 - Bonded Jacket, Seam Sealing, Severe Gopher Attack

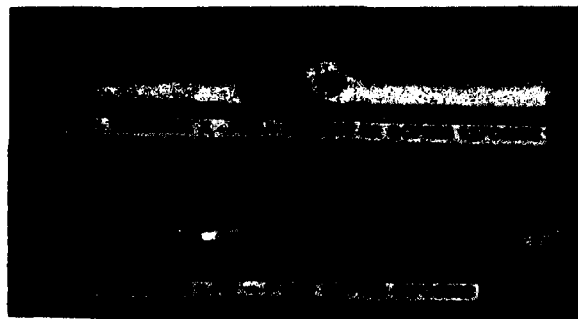


Figure 7 - All-Dielectric Cable, Gopher Attack

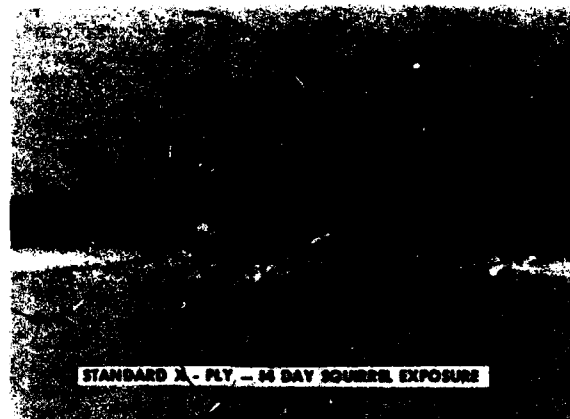


Figure 8 - Cross-Ply Cable, Squirrel Attack

#### LIGHTNING TEST PROCEDURES AND RESULTS

In order to prepare the cable samples for testing, each was cut to a length of four feet and one end was stripped for a few inches to expose all metallic members of the sheath and oversheath. All of the metallic members were secured to a 4 inch by 4 inch steel plate. To approximate the conditions present when a stroke occurs in the middle of a long cable span, the end of the core tube was potted in epoxy to insure that the fibers would not be pulled into the tube on the impact of the lightning. For testing, the sample is buried vertically in a heavy sand-filled test box with the metal end plate resting on the ground plate in the bottom of the box. The test box contains a 2 ft. cube or sand. A discharge electrode is situated about 1 inch from the sample, and a small hole is drilled in the jacket down to the stainless steel to ensure that the discharge current goes directly to the metallic sheath rather than travelling down the outside of the jacket to the ground plate. The sand in the box was kept wet to provide a relatively constant specific gravity.

The surge generator/wave shaping circuit is shown in Figure 9. For the smaller peak current discharges, 10  $\mu\text{F}$  of capacitance was used. A curved aluminum bar connecting the capacitor bank switch to the test fixture acted as an inductor to provide a longer action integral. For peak currents above 90 kiloamperes, the same circuit was used, but with 20  $\mu\text{F}$  of capacitance.

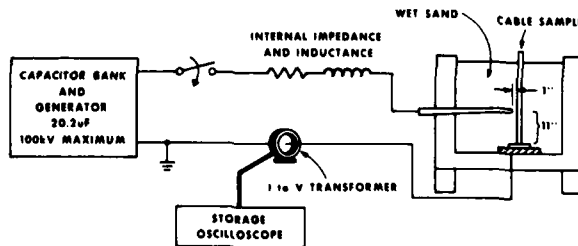


Figure 9 - Test Circuit

Sixteen cable samples were tested at various peak current levels. Nine of the samples contained a corrugated 8 mil aluminum layer underneath a layer of corrugated stainless steel, and seven of the samples contained a layer of corrugated 6 mil copper underneath the stainless steel.

The aluminum shielded cables were subjected to spark discharge current peaks ranging from 33 kA to 100 kA. All of these samples showed evidence of sheath crushing, although the level of crushing was moderate for the lower current levels. Each sample had a hole melted in the stainless steel at the discharge point, while all samples tested at 40 kA and above exhibited holes melted in the aluminum as well. Arcing sometimes occurred to the outer layer of wires of the crossply sheath in the higher current level tests. There was some arcing to the inner layer of wires in samples tested at peak currents greater than 60 kA. No fibers were damaged in any of these samples.

The samples containing a corrugated copper shield under the stainless steel were tested at peak current levels of 60 kA to 195 kA. As in the aluminum shielded samples, holes were melted in the stainless steel at the discharge point. However, holes were not melted in the copper. Slight melting and even minor splitting of the copper due to impact was evident in the samples tested at very high peak current levels (greater than 120 kA), but no hole was formed. In addition, arcing to the crossply wires occurred only at very high peak currents.

Since no fibers were damaged in any of these samples, it is difficult to quantify the damage levels, particularly to compare the copper and aluminum shielded samples. However, it may be noted that the degree of physical damage in copper shielded sample tested at 60 kA looked very similar to that in the aluminum shielded sample tested at 33 kA.

#### EFFECT OF MATERIAL PROPERTIES ON LIGHTNING PERFORMANCE

The high crush resistance of the corrugated stainless steel layer of the B-Oversheath is an effective protection against damage due to the steamhammer effect. For protection against heating damage, several material properties are important. High conductivity minimizes  $I^2R$  heating, of course. However, melting of the metal layers at the point of strike is due primarily to heat transferred in the arc itself. In this regard, the material's specific heat and density determine its resistance to thermal damage. Copper holds a clear advantage over aluminum in terms of its conductivity, but it also proves to be superior in the amount of heat it can absorb without melting or vaporizing. Equation 1 below shows a formula for

calculating the amount of energy necessary to melt a given volume of material.

$$E/V \propto C_p \rho (T_m - T_A) + h_{sf} \rho \quad (1)$$

where:  $E$  = Energy  
 $V$  = Volume  
 $T_m$  = Melting temperature of material  
 $T_A$  = Ambient temperature  
 $C_p$  = Specific heat of material  
 $\rho$  = Density of material  
 $h_{sf}$  = Latent heat of fusion of material

If we apply this equation to both aluminum and copper, we find that almost twice as much energy is required per unit volume to melt copper as opposed to aluminum. This is consistent with observations of the cable samples subjected to high current spark discharges.

#### LIGHTNING DAMAGE FORECASTS

In the past, lightning testing and field studies have been primarily concerned with buried coaxial cables. The primary damage mechanism in these cables is crushing of the coax tubes. Lightning simulations by spark discharge tests such as those conducted on our fiber optic cables indicate that damage occurs to the tubes at peak current levels exceeding 60 kA. Field trouble rate data have been compiled for coaxial cables, and these data have been used to generate a curve which predicts the trouble rates per sheath mile as a function of soil resistivity and average number of thunderstorm days.

Some work has been done to extrapolate curves for other peak current damage threshold levels.<sup>9</sup> If we apply these extrapolated curves to our protected fiber optic cables, vanishingly small trouble rates are predicted. For instance, in an area with 80 thunderstorm days per year and a soil resistivity of 500 meter-ohms, such as conditions found in high lightning areas of Florida, one may expect on the order of 1.2 troubles/year per 1000 sheath miles on a cable which withstands a 100 kA surge discharge. Similarly a cable which withstands 195 kA without service affecting damage corresponds to a trouble rate of 0.8 troubles/year per 1000 sheath miles. These results are extensively extrapolated and should not be regarded as precise predictions. However, even significant departures from these predicted rates indicate very low trouble rates. This is supported by statistics of direct earth strokes. Only .017% of the recorded earth strokes exceed 200 kA. Thus, we feel confident in asserting a very high level of protection against lightning damage for this design.

#### CONCLUSION

A highly successful protective sheath system for fiber optic cables has been developed.

This design combines a highly conductive layer and a corrosion-resistant mechanically rugged shell. In laboratory testing this design has shown negligible vulnerability to both rodents and high current spark discharge. It is now being produced as an oversheath on ribbon cables and also as a primary sheath on stranded cables.

#### ACKNOWLEDGEMENTS

The authors wish to acknowledge the assistance and advice of the following persons in the development of the sheath design, in the manufacture of experimental cables, and in the preparation of this paper: R. N. Binkley, W. D. Bohannon, N. J. Cogelia, A. S. Hamilton, M. J. Swiderski, D. E. West, and R. N. Williams.

#### REFERENCES

1. E. R. Hall and K. R. Kelson, "The Mammals of North America," Ronald Press Company, New York, March, 1956.
2. N. J. Cogelia, Bell Telephone Laboratories, Private Communication.
3. R. A. Connolly and N. J. Cogelia, "The Gopher and Buried Cable," Bell Telephone Laboratories RECORD, April, 1970.
4. N. J. Cogelia, G. K. LaVoie, and T. F. Glahn, "Rodent Biting Pressure and Chewing Action and Their Effects on Wire and Cable Sheath," Proceedings of the 25th International Wire and Cable Symposium, 1976.
5. R. A. Connolly, Bell Telephone Laboratories Internal Document, October 29, 1968.
6. L. F. O'Neill, Jr. and W. C. Reed, Bell Telephone Laboratories Internal Document, May 12, 1982.
7. G. M. Yanizeski, E. L. Johnson, and R. G. Schneider, "Cable Sheath Buckling Studies and the Development of a Bonded Stalpeth Sheath," Twenty-ninth International Wire and Cable Symposium, 1980.
8. The International Telegraph and Telephone Consultative Committee, "The Protection of Telecommunication Lines and Equipment Against Lightning Discharges," The International Telecommunication Union, 1974.
9. L. Levey, Bell Telephone Laboratories, Unpublished Work.



William C. L. Weinraub  
Bell Laboratories  
2000 N. E. Expressway  
Norcross, Georgia 30071

Mr. Weinraub is a Member of the Technical Staff at Bell Laboratories, Norcross, Georgia. His current responsibilities include design of mechanical protection for fiber optic cables. He received a Bachelor of Science degree in Geology from Yale University in 1971 and a Master of Science in Mechanical Engineering from the University of Massachusetts in 1980. He has a background in Brittle Fracture Mechanics, and has worked as a blacksmith.



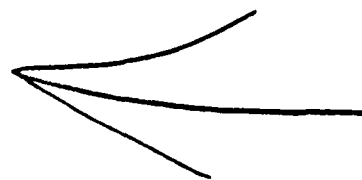
Donald D. Davis, Jr.  
Bell Laboratories  
2000 N. E. Expressway  
Norcross, Georgia 30071

Mr. Davis is a Member of the Technical Staff at Bell Laboratories, Norcross, Georgia. His current responsibilities include testing and measurements of paired cables as well as testing mechanically protected fiber optic cables. Mr. Davis received a Bachelor of Science degree in Electrical Engineering from North Carolina State University in 1980 and Master of Science degree in Electric Engineering from the Georgia Institute of Technology in 1981. He has a background in communications and optics.



Michael D. Kinard  
Western Electric Company  
2000 N. E. Expressway  
Norcross, Georgia 30071

Mr. Kinard is a Development Engineer at the Western Electric Company Cable and Wire Product Engineering Control Center in Norcross, Georgia. He received a Bachelor of Science in Mechanical Engineering from Old Dominion University in 1974. He joined Western Electric in 1979 and is currently responsible for cable sheath design and development. He has a background in power plant design and overhaul, and in thermal and heat transfer analysis.



# A RADICALLY NEW APPROACH TO THE INSTALLATION OF OPTICAL FIBRE USING THE VISCOUS FLOW OF AIR

S A Cassidy, M H Reeve

British Telecommunications Research Laboratories,  
Martlesham Heath, Ipswich, Suffolk, England

## ABSTRACT

The small size and weight of optical fibres makes it possible to install them into cable bores using compressed air. Units consisting of several fibres in a small package are drawn into the bores by the viscous flow of the air. These units can be routed through various sizes of pre-installed empty cable without need for fibre joints, as and when they are needed. The distributed nature of the drag force along the fibre length avoids the large end stress associated with traditional cable drawing, particularly on tortuous routes.

The empty cable can be made cheaply and installed without due care and the fibre unit would be a standard item to be used in any size of cable.

A fibre unit 2.5 mm in diameter containing 10 fibres and weighing 3g/m has been installed into a cable with seven 6 mm bores along a length of 325 m using 40 psi of air pressure. 50 psi was sufficient to install 140 m in an internal route including 16 right angled bends and 15 m of upward vertical length. [The maximum stress was ~ 100 gf.]

## Installation Details

The equipment needed for an installation is shown in fig 1. The rubber wheels are driven under a constant torque just high enough to overcome the effect of the pressure drop along the air-sealing hypodermic tube, and to feed the fibre unit off the drum. Subsequently the air flowing down the cable bore carries the fibre unit along the route.

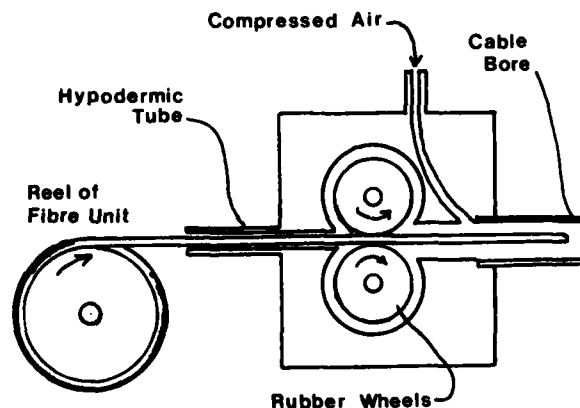


Fig. 1

In order to predict the maximum achievable lengths and the routes in which it is feasible to use this technique, and to investigate the possibility of optimizing parameters such as sizes, materials and pressures, some analysis of the forces involved is necessary.

## Analysis of Forces

The drag force can be split into two parts, a hydrostatic or floatation force, due to the simple pressure drop along the bore, and a purely viscous component due to the frictional shear force at the surface of the fibre unit.

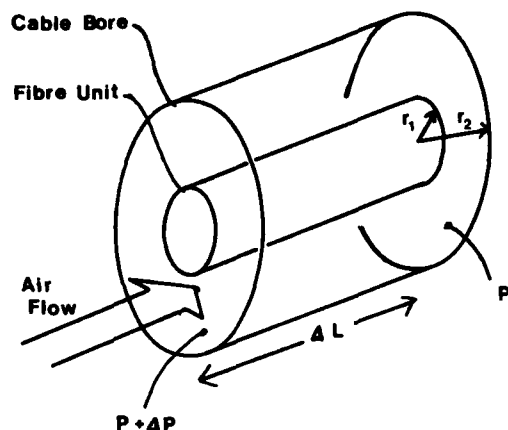


Fig.2

The hydrostatic force is the result of displacing the volume of the fibre unit in a pressure gradient and is equal to the product of the volume and the gradient.

$$F = \frac{\Delta P}{\Delta L} \pi r_1^2 \Delta L$$

With the symbols as defined in fig 2. Thus the hydrostatic force per unit length is

$$\frac{\Delta P}{\Delta L} \pi r_1^2$$

The viscous force is due to the force imbalance on the annulus of gas in fig 2. The force on the annulus at pressure  $P + \Delta P$  is greater than that on the annulus at pressure  $P$ . The force difference is thus

$$\pi(r_2^2 - r_1^2) \Delta P$$

and the force per unit length is

$$\frac{\Delta P}{\Delta L} \pi(r_2^2 - r_1^2)$$

This force is balanced by the shear reaction around the bore and fibre unit surfaces and by the acceleration of the gas. The latter effect can easily be shown to be small for these pressures and flow rates. How this viscous shear force is distributed between the surface of the bore and the surface of the fibre unit will depend on the nature of the flow.

Flow Rate vs Air Pressure  
in 170 m of 7mm Bore

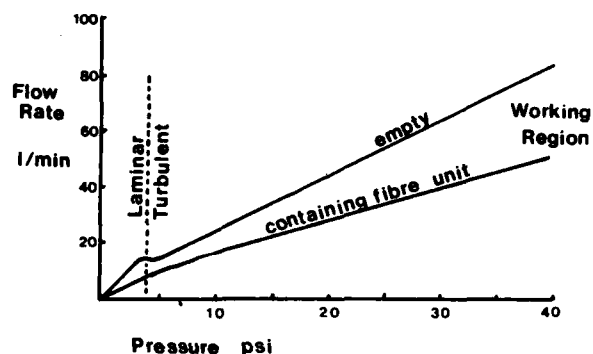


Fig.3

In the region we are working, as can be seen from fig 3 the flow is very turbulent and so it seems reasonable to assume that the highly random movement of the gas radially spreads the shear force equally over all of the surfaces wetted by the gas. The fibre unit then has a share proportional to its share of the total surface.

$$\text{Proportion of total surface of fibre unit} = \frac{r_1}{r_1 + r_2}$$

Thus the fibre unit share of the viscous part of the drag force is

$$\frac{\Delta P}{\Delta L} \pi(r_2^2 - r_1^2) \frac{r_1}{r_1 + r_2} = \frac{\Delta P}{\Delta L} \pi r_1(r_2 - r_1)$$

Adding this to the hydrostatic component gives the total force per unit length

$$\frac{\Delta P}{\Delta L} \pi r_1 r_2$$

#### Measurements

As an installation proceeds, and the length subject to friction and drag force increases, the amount by which the drag force exceeds the friction will increase and be measurable as a tension at the installation end. To measure this the apparatus in fig 4 was used.

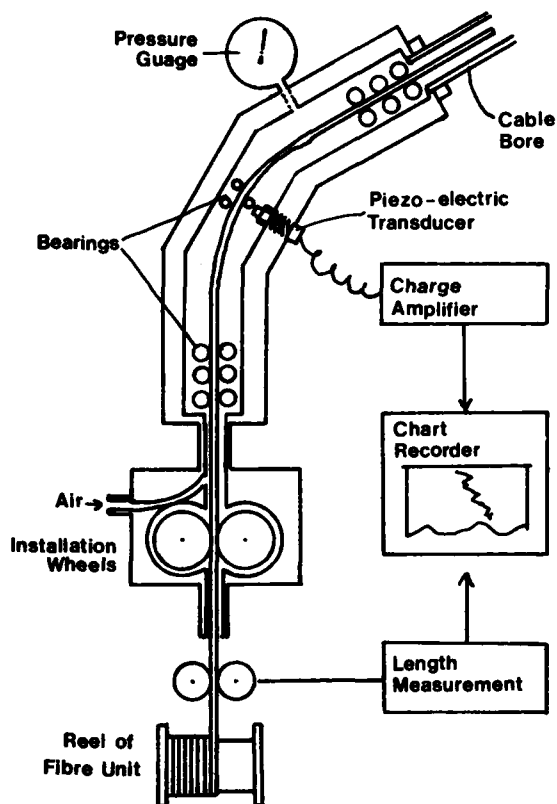


Fig.4

The fibre unit runs first over a piezo electric force transducer before continuing down the cable bore. Bearings at the entry and exit of the force measuring head prevent movement of the unit from effecting the transducer, thus allowing axial tension only to be measured. Any tension in the fibre unit is measurable as a force on the transducer.

Some results for different pressures and cable bore diameters are given below (fig 5). The theoretical lines show the difference between the expected increase in drag as the installed length increases and the increase in friction as the length increases.

It will be noted that the predictions agree well at the ends of the installations, but differ, appreciably for the small bore sizes, in shape from the measured tensions. This is because we have used a constant  $\Delta P/\Delta L$  (total pressure used  $\div$  total bore length) in the calculations, ie a linear pressure gradient down the bore, whereas the partial filling of the bore by the fibre unit causes a larger pressure drop along the partially installed length, and thus a larger than expected drag force in the first stages of the installation. This effect is obviously exaggerated when the fibre unit fills a larger

proportion of the bore area.

Using the now well known<sup>1</sup> technique of optical phase delay, a fibre strain measurement was performed on an installation using one of 10 fibres in a unit 2.5 mm in diameter weighing 3g/m. The installation was carried out using a 7 mm bore at 80 psi. The strain vs installation length is shown in Fig 6. At the end of a 200 m run, the fibre strain was 0.022%, in keeping with the strains measured mechanically.

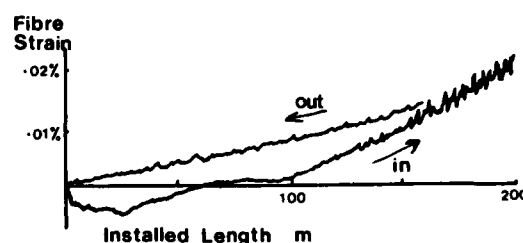


Fig.6

#### CONCLUSION

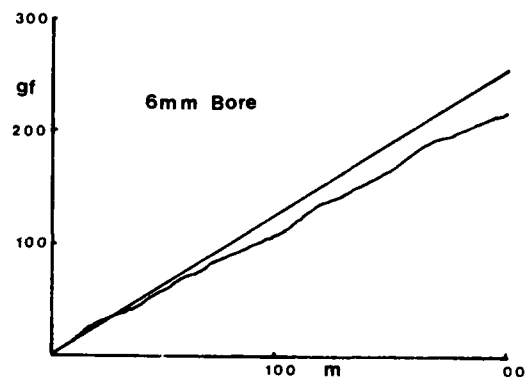
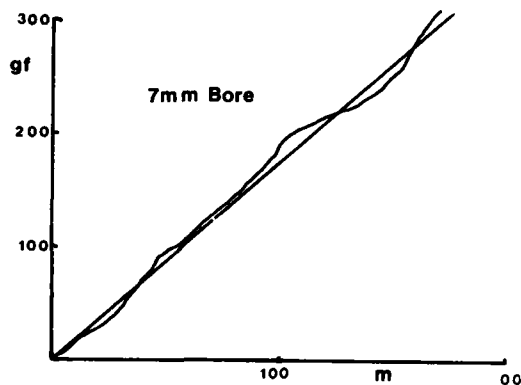
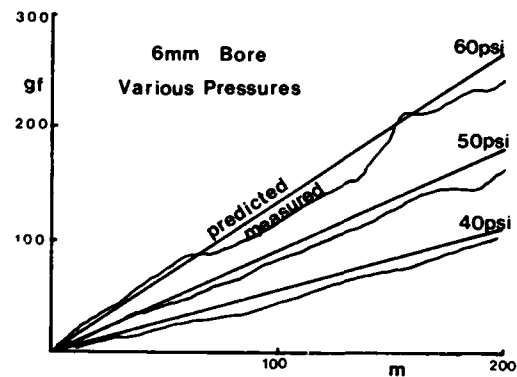
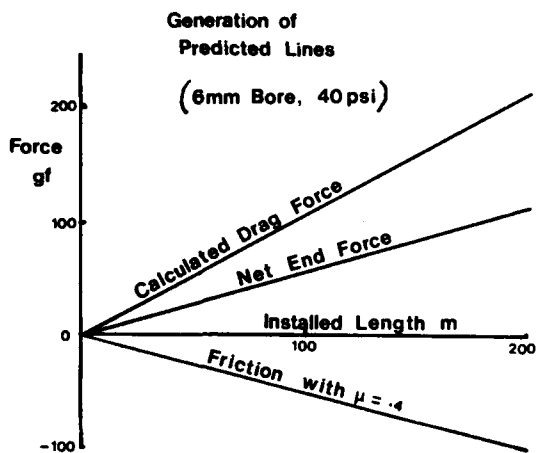
We have demonstrated a technique for installing optical fibres using the viscous flow of air. The applications for this technique lie in difficult internal routes such as data links and links inside exchanges, difficult high capacity external routes, ie local wideband distribution systems and possibly in the cheap junction network.

In these applications the installation risk and capital cost are greatly reduced. The possibility of routing from cable to cable using sets of installation wheels running in tandem avoids the need for large numbers of fibre joints. The route capacity can also be increased in line with demand.

Our measurements and calculations show that with the compressors already available on the UK cabling vehicles, 300 m is achievable and up to 1000 m in good routes, using 6 mm bores.

#### ACKNOWLEDGEMENTS

The authors would like to thank R J Bates, S J Page, P Townley and R Kashyap for their help with measurements, C J Todd for discussions and the Director of British Telecommunications Research Laboratories for permission to publish this work.



60 psi

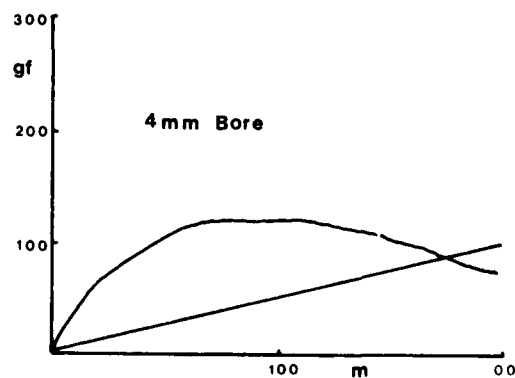
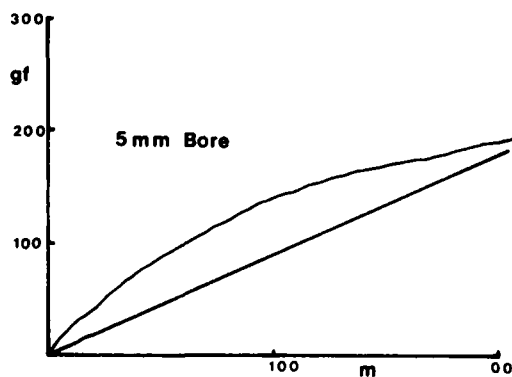


Fig. 5

#### REFERENCE

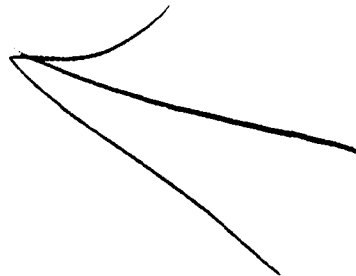
- 1 "Single-ended fibre strain and length measurement in frequency domain", R Kashyap, M H Reeve, Electronics Letters, 16, 18, 28 Aug 1980 p 689-690.



Stephen Cassidy graduated from Oxford University in 1980 with a degree in Natural Sciences. Since joining British Telecom Research Laboratories, he has worked on various aspects of optical cable research. These have included studies of fibre strain during several coating and cable fabrication processes, and in cable installation.



Michael Reeve graduated from Durham university in 1973 with a degree in applied physics and joined the British Telecommunications (then Post Office) Research Department at Martlesham in Suffolk. He has worked on a number of aspects of optical fibre communications including fibre scattering and mode cut-offs, fibre strength and cabling. He is currently head of a group concerned with optical cable research.



## MATERIAL REQUIREMENTS FOR MULTIMEDIA COMMUNICATIONS CABLE

G. L. Grune

IBM Corp.  
Polymers Group (E79)  
Research Triangle Park, N. C. 27709

*Abstract*

Recently, much interest and investigation have taken place within the communications industry concerning local area networks (LANs). With this interest arose an opportunity for a newly designed multimedia cable with materials never before used within the same construction. These cables will allow a user to send and receive information from a variety of equipments. All compounds and composites are expected to meet more severe physical, mechanical and chemical testing than previous communications cables. The properties and materials studied for these cables must meet not only flammability requirements, but also must sustain minimum performance requirements during their 15-30 year lives. Eight cable designs are currently being studied for materials selection including outdoor and indoor/outdoor types. Finally, the issue of toxic gases emission if the cable composite were to burn is considered and discussed.

One goal of this study was to list materials currently used for the construction of the multimedia communications cable and consider alternate materials which could be used to improve electrical, physical and chemical properties as well as flammability and toxicity concerns. Also important is the need to address the fifteen to thirty (15-30) year life specification during which the cables must sustain minimum performance criteria. For this requirement to have any meaning, the cable materials must also maintain minimum physical and chemical stability standards during the same fifteen to thirty (15-30) year period.

*Introduction*

Historically, the word "plenum" comes from the stoics meaning the "whole of space regarded as being filled with matter"<sup>1</sup>. This may not be the best method to describe the present day use of the word plenum for indoor cables, which is now better described as the return air space above a suspended ceiling or below a raised floor. Until 1975, the National Electric Code (NEC) required that all cables installed in a plenum be enclosed in a metallic raceway or conduit or metal sheathed cables without conduit. Exceptions to the conduit requirement, which became accepted in 1975, included communications, power limited and fire alarm cables. Until only recently, however, has there been an approved U.L. (Underwriters Laboratories) test showing such cables as having "adequate" fire resistant and low smoke producing characteristics. The cables described in this report have been classified as "Power Limited Circuit Cable, Class 2", and are communications cables.

The cost reductions associated with installation of plenum cables instead of installation of non-plenum cables which require PVC jackets inside of metallic conduit become obvious. If a plenum cable can be constructed which will burn less than, or equal to, a PVC cable within a metal conduit and cost less than the non-plenum cable, it will also serve the purpose of reducing field installation time and cost. Wadehra<sup>2</sup> and others have estimated the cost of installed conduit, including materials and labor, to exceed \$2.00/ft. As the cost of labor increases, the price of conduit will become prohibitive and as more local building codes allow the use of plenum materials, the sight of cable contained within conduit will be found only in older buildings.

The design of the non-plenum cable, however, was still essential in meeting the needs of areas where plenum materials are not yet accepted. The section on the design of non-plenum cables will parallel that of the section on plenum cables and will focus on the multimedia composite cables currently under development, containing three voice grade media (VGM) telephone wires, two data grade (DGM) communication wires and two single optical fiber units (OFM), (3-2-2). With the exception of the indoor/outdoor, outdoor and office media cables, the other designs include the same materials and constructions but to a lesser extent.

*1. The Design of Non-Plenum Composite Cables**1.1 Non-Plenum Jacket Design of Composite Communications Cables*

Figure 1 shows the design of the 3-2-2 non-plenum version of the communications cable which is to be manufactured. The design includes an outer jacket of PVC, (polyvinyl chloride) black in color, with a nominal wall thickness of .899 mm and a minimum wall thickness of .762 mm. No maximum wall thicknesses for the indoor cables have been specified, but the obvious understanding is that the jacket thickness must not interfere with the cable flexibility.

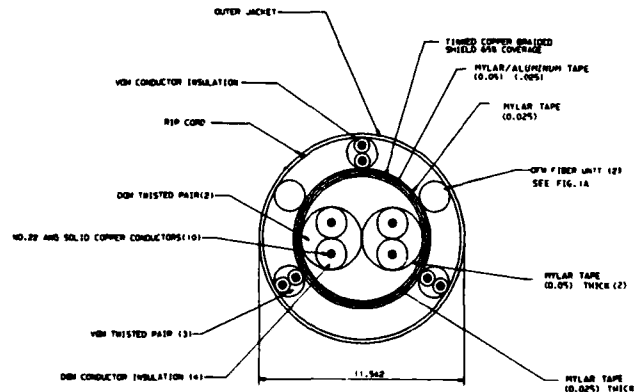


Figure 1  
Drawings for 3-2-2 Non-Plenum Cable

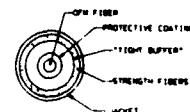


Figure 1A  
OFM Fiber Unit

Each of the base resins provided by PVC suppliers are compounded by the various cable vendors. The compounding is normally a proprietary process and allows the cable vendor flexibility in formulating a benefit-cost type compound in terms of physical properties and prohibitive expense.

A typical flexible compound consists of 50% PVC, 25% plasticizer and 25% other additives. The incorporation of more than one plasticizer is usually required to obtain the desired combination of properties. For example, phthalates impart high dielectric strength, adipates and sebacates improve cold bending properties and phosphates improve flame retardance.

Initial EDX analysis (energy-dispersive x-ray) of sample PVC jackets indicates only the presence of lead salts, used as stabilizers needed to counteract the tendency of vinyl compounds to degrade when exposed for prolonged periods to temperatures in the upper end of the useful range (+75°C), and Ca- which is part of the CaCO<sub>3</sub> filler compounds used to stretch the more expensive PVC resin and add some toughness. No doubt, adipates and/or sebacates are being used to improve the cold bend properties required by an IBM specification (-55°C). Additives including the following modifiers may be added:

Lubricants - such as stearic acid to improve surface appearance or increase extrusion speed.

Fillers - such as special clays - added toughness.

Carbon black - to retard UV degradation and make compound semi-conductive.

Pigment - for color.

Fungicide - to control fungus growth.

The typical properties of the base PVC resin are listed in Table 1.

Table 1

<i>PVC Electrical Insulation - Typical Formulation and Properties</i>	
<i>Formulation</i>	<i>Parts By Weight</i>
PVC - Resin	100
Di (2-ethylhexyl) phthalate	55
Basic white lead carbonate	10
Electrical grade clay	10
Paraffin wax (160-165°)	0.5
<i>Physical Characteristics</i>	
Specific gravity	1.32
Tensile strength, psi	2700
Ultimate elongation, %	310
Hardness, shore A-2	85
<i>Electrical Characteristics</i>	
Dielectric strength, volts/mil	880
Dielectric constant	
60 cycles, 27°C	6.7
1000 cycles, 27°C	5.9
Power factor	
60 cycles, 27°C	0.044
1000 cycles, 27°C	0.065

Some of the cable suppliers have the capability of irradiating polymers with gamma radiation which creates free radicals that help to form a network of cross-linked polymer chains. This irradiation enhances mechanical strength, abrasion and cut-through resistance as well as temperature resistance. It is possible that some PVC jacketed compounds being used for the non-plenum cables will be cross-linked by radiation.

PVC has been the preferred material for jacketing indoor telephone cables for over fifty (50) years and REA (Rural Electrification Association) specification PE-220 requires PVC raw material and compounding properties shown in Table 2 and reported in REA PE 220.

Table 2

<i>Typical Compounding Formulations For PVC Cable Jacketing</i>		
	<i>Percent</i>	
	<i>Outdoor Use</i>	<i>Indoor Use</i>
PVC*	46.0	52.0
n-octyl n-decyl-o-phthalate	32.0	-
Di-2-ethylhexyl o-phthalate	-	27.9
Basic Lead Carbonate	3.0	-
Clay	9.0	-
Calcium Carbonate	9.0	17.0
Carbon Black (Channel Black)**	1.0	-
Basic Lead Silicate	-	3.0 Tribase E MacGregor 670
LDPE	-	0.1
Total	100	100

\* Resin GP-5-00003 in accordance with ASTM D1755-66

\*\* For colors other than black a minimum of 3% rutile Titanium Dioxide should be added in place of the carbon black.

A concern raised during the design of these cables was and remains the stability of jacket materials under various exposures levels including: ultraviolet degradation (UV), ozone expose (O<sub>3</sub>) and temperature extremes. Special attention will be given to using "sunlight-resistant" PVC as listed in U.L. subject 1277.

The requirements of NEC Article 725 according to U.L. subject 13 Appendix A, which are to be used for LAN cables, refers only to the jacketed cable in the finished, compounded form including anti-oxidants, UV stabilizers, plasticizers, color pigments and other extrusion additions to the "raw" PVC resin. These final property requirements by U.L. are more concerned with temperature ratings and flammability than anything else. The Subject 13 document specifies jacket thickness, cable armor, cold bend test, deformation test, heat shock test, vertical flame test, dielectric voltage withstand, and allows as optional the IEEE 383 flame test and a spark test. Again, it should be noticed that the U.L. requirements are specified for the finished cable - not the raw materials specified by the R.E.A. Both organizational documents were considered before writing the final specifications for the newly designed communications cable.

A major difference found when comparing PVC compounds of one wire and cable producer to that of another producer of PVC jacketed cable are the types of plasticizers used to improve flexibility, volatility, processing and stability. Phthalates, adipates, azelates, trimellitates, maleates, fumarates, and polymeric plasticizers of high molecular weight esters and epoxies can all be used to formulate the desired compound.

Also of concern are the flame retardants, antioxidants and UV light stabilizers used in the PVC jacketed insulation. As partially shown in Table 2, many different substances are used to retard the many mechanisms of degradation that PVC can undergo including:

Dehydrochlorination  
Oxidation  
Chain scission  
Cross-linking

The substances used to prevent these degradation mechanisms should act in the following way:

— As HCL acceptors — (Dehydrochlorination prevents further dehydrochlorination)

- Radical scavenger — Radicals result in chain scission cross-linking and oxidation
- Compatibility — Incompatibility can detract from stabilizer effectiveness and the inherent chemical and physical properties of PVC

Not just any combination of these stabilizers would be useful due to possible chemical incompatibility, but new formulations are constantly being tried. In the case of  $\text{Sb}_2\text{O}_3$ , a synergistic effect with the inherently halogenated PVC causes an unusually high LOI and thus better flame retardant PVC. More information on the synergistic effects of  $\text{Sb}_2\text{O}_3$  are detailed in a discussion by Touval<sup>3</sup>. Table 3 lists the type of additives and the intended use of these stabilizers, which could be included in the PVC compound used for the LAN cable construction.

Table 3

PVC Stabilizers		
UV Light Absorbers	Heat Stabilizers	Anti-Oxidants
Carbon Black		
2-Hydroxy-4-Methoxy Benzophenone	Basic lead Chlorosilicate	Dibasic lead Phosphate
2, 2-Dihydroxy-4-Methoxy Benzophenone	Sulfate complex	
2-Hydroxy-4-n-Octoxybenzophenone	Lead-Barium-Calcium complex	Alumina Trihydrate
2-(2-Hydroxy-5-5-Octylphenyl)-Benzophenone		
Dibasic lead phosphate ( $2\text{-PbO-PbHPO}_3 \cdot \frac{1}{2}\text{H}_2\text{O}$ )	Antimony Trioxide ( $\text{Sb}_2\text{O}_3$ )	Zinc Borate Hindered-phenols
$\text{TiO}_2$	Dibasic lead Phthalate	Amines
		Distearylthiodi-Propionate
	Dibasic lead Stearate	
	Dibasic Lead Phosphate	

IR and EDX analyses of a PVC jacketing compound supplied by one of the vendors are shown in Figures 2 and 3. The infrared scan reveals that the PVC is plasticized and the EDX analysis confirms the use of lead salts for heat stabilization, titanium dioxide for oxidation inhibition, and  $\text{CaCO}_3$  for filler.

### 1.2 Non-Plenum Voice Grade Media (VGM) Insulation

Directly underneath the PVC sheath of the 3-2-2 non-plenum cable the first three pairs of conductors are voice grade media (VGM) or telephone wire. The primary insulation which will be used for the wire is either solid, flame retarded polyethylene or polypropylene needed to meet the stringent electrical requirements imposed on these conductors. The electrical requirements imposed are listed in Table 4 which was taken directly from the new LAN cable specification. The major reason that polyolefins were selected for the telephone wire insulators is that attenuation specifications

could not be guaranteed due to the inherent dissipation factor @ 1MHz of 0.06-0.10 for PVC versus that of .0002-.0003 for most polyethylene and polypropylene compositions. It is because of the expressed need for these electrical properties that many specification problems have occurred. Because the PE-71 specification was intended for PVC insulators, the chemical, physical, electrical and color requirements were written for PVC - not polyethylene. This prompted the need for another type of PE material currently under development. The heat-stabilized, flame-retarded, cross-linked polyethylene which at least one cable vendor will employ for the cable, is a compound similar to the one which has been developed since 1959. The composition was released in a U.S. Department of Commerce Institute for Applied Technology document.<sup>4</sup>

Table 4

VGM Mechanical and Electrical Requirements	
Mechanical: VGM Wire	
VGM: Conductors	
Material:	Commercially Pure Fully Annealed Copper per ASTM-B3-74
No. of Conductor Pairs	3
Wire Size	No. 22 AWG (Solid)
Diameter	$0.643 \pm 3\%$
D. C. Resistance	$\leq 17.4 \text{ OHMS}/304.8\text{M} @ 20^\circ\text{C} \pm 1^\circ\text{C}$ per Conductor
VGM: Conductor Insulation	
Material:	Cross-linked Solid Polyethylene With Flame Retardant
Wall Thickness	$0.34 \pm 0.10$
Wire Diameter Including Insulation	$1.32 \pm 0.20$
VGM: Pair Assembly (3 Pairs)	
Color Code:	Pair No. 1 { White/Blue Pair No. 2 { White/Orange Pair No. 3 { White/Green Mark or stripe each wire with the color of its mate
Lay (Twist)	
Electrical: VGM Pairs	
Characteristic Impedance	$600 @ 1000 \pm 15\% \text{ HERTZ}$
Attenuation	$6.2 \text{ NOM } 7.13 \text{ MAX DB/Km} @ 150 \text{ KHZ}$
Crosstalk	Near End Crosstalk (NEXT.) Between any VGM Pair to any other VGM Pair must be more negative than $-33\text{DB}$ from 3.0 to 5.0 Megahertz for length of 0.5 Kilometers or greater.
Mutual Capacitance	$52 \pm 4 \text{ pf/m} @ 1000 \pm 100 \text{ HZ}$ (Measured with Shield Floating)

The low density, high molecular weight, non-linear polyethylene can be cross-linked by either chemical or ionizing radition techniques with a resulting compound which exhibits basically the same characteristics. Radiation cross-linking changes the thermoplastic into a three-dime

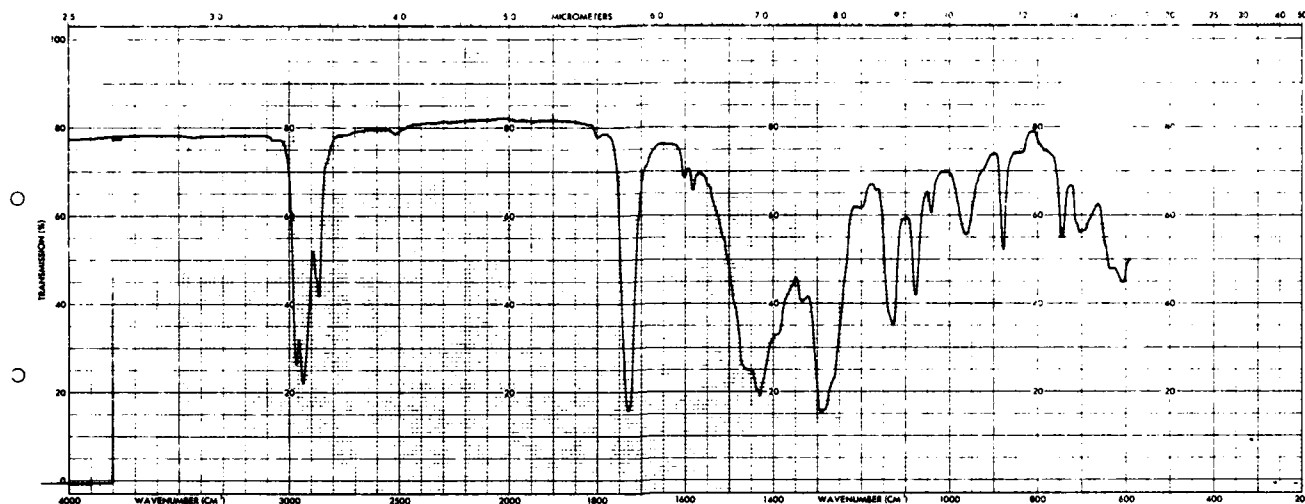


Figure 2  
IR Scan of Plasticized PVC Jacket

OUTSIDE CABLE JACKET (PVC)

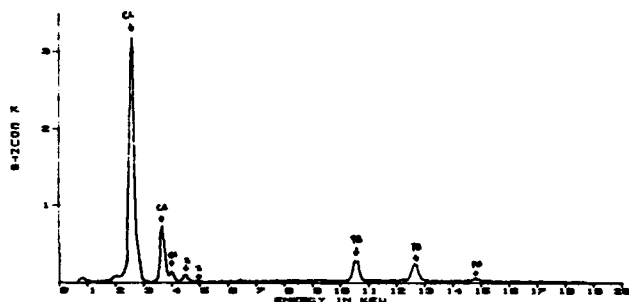


Figure 3  
EDX of Plasticized PVC Jacket

network with rubber-like elasticity at temperatures above the crystalline melting range. To permit operation at elevated temperatures, a three-dimensional gel aids in adding strength to prevent physical damage. Protection against oxidation is accomplished by the addition of low-volatility heat stabilizers. Prior to irradiation, PE was flame retarded by the addition of antimony trioxide  $Sb_2O_3$  and chlorinated hydrocarbons. This system was completely unsatisfactory for an insulation to be radiation cross-linked and used at elevated temperatures because of the instability of the carbon-chlorine bond to both radiation and heat.

To understand the nature of a cross-linked polyolefin insulation, a visualization of the molecular structure of polyethylene before and after cross-linking has been achieved is necessary. Figure 4(a) illustrates the representation of the molecular structure of base resin PE. Figure 4(b) is a representation of the molecular structure after exposure to high energy penetrating radiation causes a chemical change resulting in the cross-linking of molecules into a three dimensional structure with the cross-links shown in heavy black lines.

Due to the unique classification of the cable (U.L. listed as Power Limited Circuit Cable, class 2), it has been difficult to decide upon the property requirements of both the raw material and the finished form polyethylene and polypropylene insulators. REA, PE-22 states specifically that:

"The colored polyethylene material applied over the conductors shall meet the requirements of REA specification PE-200, 'Polyethylene Raw Material' for high density polyethylene insulating grade material, Appendix C."

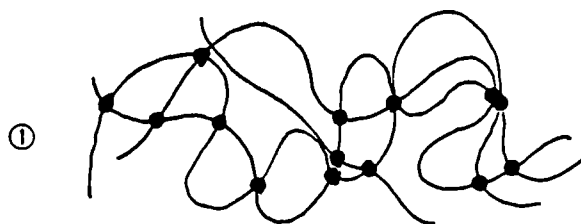


Figure 4a  
Molecular Structure of Pre Radiation Cured Polyethylene

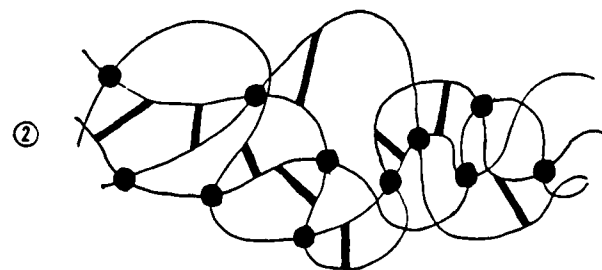


Figure 4b  
Molecular Structure of Post Radiation Cured Polyethylene

However, this specification is in direct conflict with the low density resin being supplied for the VGM insulators by at least one cable vendor. The finished wire insulation requirements for both polyethylene and the crystalline propylene/ethylene copolymer are stated in REA PE-22. IPCEA (International Power and Cable Engineering Association) standard-61-402 also lists properties for polyethylene primary insulation. U.L. Subject 13 Appendix A strictly imposes physical property requirements for PVC insulation and jacket or "other acceptable compounds". Obviously, the imposition of property standards for the VGM insulation has been troublesome due to the nature of existing cable standards.

Cable manufacturers are trying several insulation formulations including the propylene-ethylene copolymer (commonly referred to as propylene). The advantages of synthesizing this copolymer include the fact that polypropylene has the lowest density of all thermoplastics with a specific gravity of  $0.91 \text{ gm/cm}^3$ , a low coefficient of friction equal to nylon (0.12) and high resistance to environmental stress cracking. In addition, there

are no known solvents for polypropylene at room temperature and thus it offers better resistance than PE at higher temperatures. The disadvantage is that the brittleness temperature ( $\sim T_g$ ) is about  $+8^\circ\text{C}$  and this necessitates using a PE ( $T_g -55^\circ\text{C}$ ) blended copolymer. The brittleness temperature of  $-15^\circ\text{C}$  for crystalline PE/PP retains many of the best properties of both high density polyethylene and crystalline polypropylene and has been accepted as an alternate material by REA in PE-22, 23 and 38. At concentrations of 20% or less, polyethylene contributes low temperature toughness without sacrificing significantly the physical and high temperature properties of polypropylene.

Chemical analysis of a typical cross-linked, flame retardant PE compound meeting U.L. VW-1 Flammability Requirements, was performed and yielded some interesting results. Figure 5 shows the IR scan for the solid PE insulation on the VGM wire which was taken by vapor-extraction on to a glass plate. The compound could not be dissolved due to the high percentage of cross-links.

Next, a differential scanning calorimetry (Figure 6) measurement was made on a sample of the same polymer and revealed three (3) distinct endotherms. A softening pt. temperature at approximately  $88^\circ\text{C}$  which indicated the presence of vinyl acetate (plasticizer) was confirmed by the solvent extraction (with acetone) IR scan seen in Figure 5. The melting endotherm ( $T_m$ ) at  $119^\circ\text{C}$  confirmed the fact that the PE was cross-linked. Finally, at first a somewhat puzzling endotherm at  $231^\circ\text{C}$  indicated (after viewing computer-library matched IR spectra) what seemed to be the presence of BTDA (3, 3', 4, 4' - Benzaphenone tetracarboxylic dianhydride). Finally, the EDX analysis (qualitative) of Figure 7 verifies the presence of brominated flame retardants which react synergistically with  $\text{Sb}_2\text{O}_3$ , antioxidants containing titanium ( $\text{TiO}_2$  and other titanium oxides), and the use of  $\text{CaCO}_3$  filler.

### 1.3 Non-Plenum Optic Fiber Media (OFM) Insulation

As shown in Figure 1, also placed directly under the PVC jacketing of the 3-2-2 non-plenum cable design with the three VGM wires are two single optic fiber media units (OFM). A separate figure (1A) displays the construction of the single optic fiber units which will be identical in composition except for the color of the outer jacketing. One unit is proposed to be colored orange and the other black, both having an outer diameter of  $2.8 \pm 0.3 \text{ mm}$ .

Beginning with the construction of the OFM unit from the outside to the inside core (as is being done for the overall cable construction), the jacketing material has been one of much concern. Currently, one cable

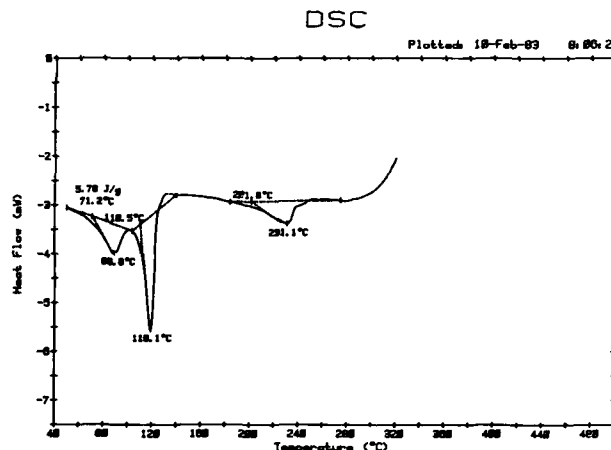


Figure 6  
DSC of Cross-linked Polyethylene

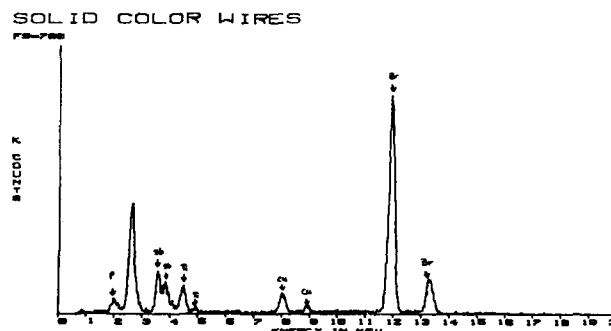


Figure 7  
EDX Analysis of Cross-linked Polyethylene Compound

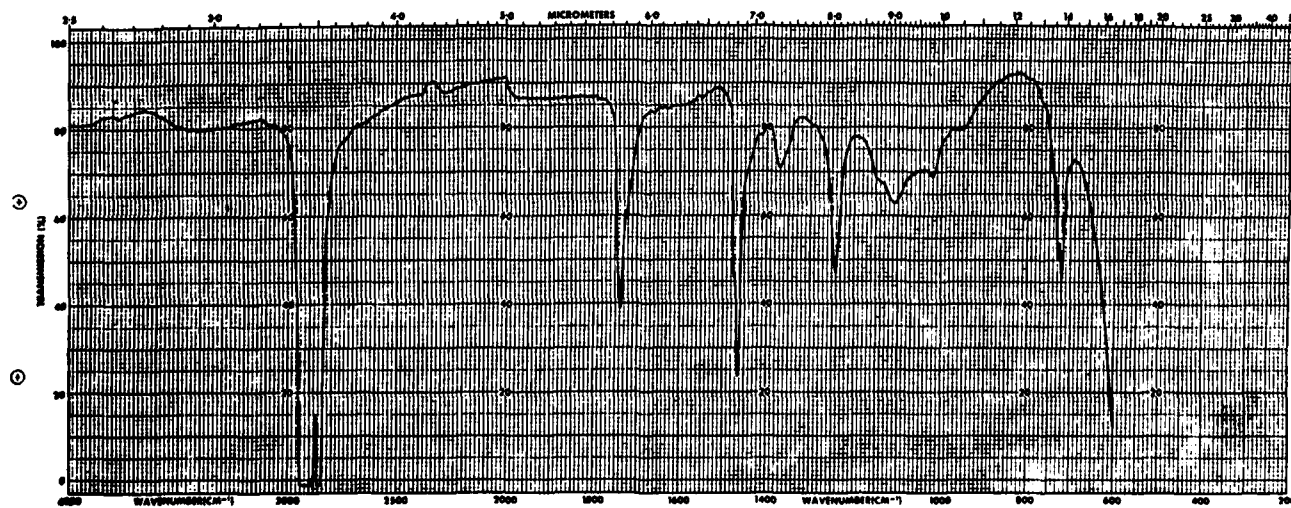


Figure 5  
IR Scan of Cross-linked Polyethylene

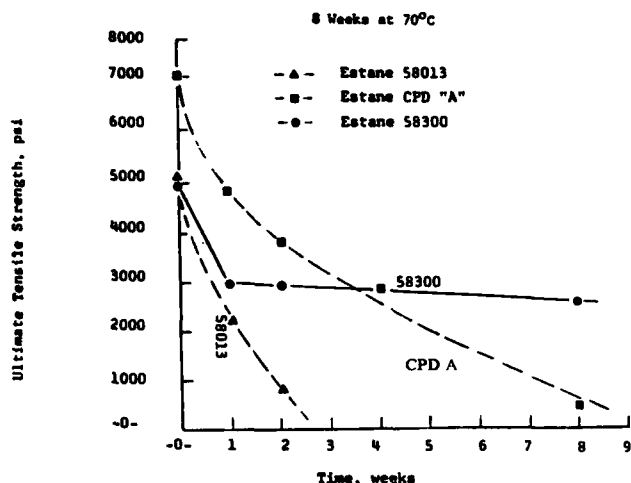


Figure 8  
Water Resistance of Estane Compounds

manufacturer uses a polyurethane compound, of a proprietary nature, which is sold by B. F. Goodrich under the tradename of Estane 58202. This estane is formulated from prepolymers of either methylene-diphenyl isocyanate (MDI) or toluene diisocyanate (TDI) and a reaction with a polyether based glycol. The polyether based glycol urethanes are usually selected over polyester based polyurethanes where end-use applications include the need for hydrolytic stability, low temperature flexibility and fungus resistance. An indoor/outdoor fiberoptic cable, in the same LAN cable family, is also slated to use the same polyurethane formulation. The reasoning which is behind using the same urethane formulation for jacketing as for the single fiber units is due to the unique nature of various chemical compositions of these urethanes and the fact that other formulations require diversely different extrusion conditions. To change these extrusion conditions during manufacture of a single cable is time consuming and costly to the cable vendor. The fact that these different formulations require unique extrusion conditions is documented well in a B. F. Goodrich Technical Service Bulletin<sup>5</sup> which contains viscosity vs. shear rate plots, the curves of which vary greatly.

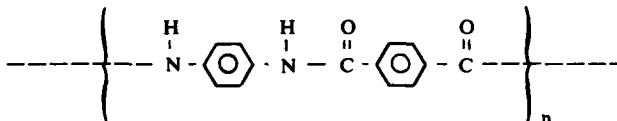
Two conditions, moisture and water stability, are of great concern due to the ability of H<sub>2</sub>O to penetrate fused SiO<sub>2</sub> (the 'glass' for optic fibers) and cause attenuation fluctuation - and due to the fact that urethanes have been known to chemically decompose in moist environments. Figure 5 indicates that some newer polyurethane formulations are more hydrolytically stable.

In all, it must at this point be concluded that there are some PVC compounds which will meet the requirements of the outer jacket for the OFM single fiber units and until such time that field experience indicates the same longevity capabilities of polyurethanes as with PVC, the selection of materials to be used for this application should be carefully considered.

Directly underneath the OFM jacketing, Figure 1A indicates the use of strength fibers which are of "sufficient strength to protect the optic (SiO<sub>2</sub>) fiber during pulling". To date, most cable vendors are using Kevlar 49 fibers as strength members because of their excellent tensile, elongation and modulus properties. These fibers also act as a buffer between the optic fiber cladding and the OFM outer jacket. The chemical, physical and mechanical properties of Kevlar 49, 1420 Denier (a measure of thickness and weight) fiber are well understood and documented. Kevlar 49 has almost twice the stiffness of glass fibers at approximately half the weight, as well as better stress fatigue and vibration (i.e. damping properties). In terms of tensile strength, modulus and weight, Kevlar is obviously superior to steel for the applicator. Another important comparison is resistance to creep at 50% ultimate breaking strength of Kevlar 49 with other fibers.

This may be the single most important property indicating the need for Kevlar 49 in the OFM single unit application.

Kevlar has excellent thermal stability - not showing any strength deterioration until reaching approximately 350°F, and it will not melt, but it will carbonize at 800°F. No embrittlement or degradation of Kevlar properties at temperatures as low as -320°F occur, and very important to optic fiber construction is the fact that almost no shrinkage occurs in the upper and lower temperature extremes. Some susceptibility of the aramid bonds to Florida sunlight, has been documented. The chemical composition of Kevlar is that of a continuous "liquid-crystal" polymer which derives its amazing strength and modulus from the fact that the molecules are aligned in one direction in a solution of sulfuric acid (anisotropic solution). The molecules which become aligned are polyamides of the general structure shown below:



and exhibit "rod-like" geometry which allows for the possibility of the high degree of molecular orientation.

Proceeding toward the inner glass core, a tight buffer surrounds the inner optic fiber cladding which is applied at the receiving cable vendor. This tight buffer, which is mechanically strippable, and has a diameter of  $0.9 \pm 0.05$  mm, is usually composed of a heat-stabilized, polyester-based elastomer which chemically exists as a block copolymer of short chain diol terephthalate and long chain polyether diol terephthalate. It can be extruded over the acrylate cladding of the SiO<sub>2</sub> fiber at melt temperatures ranging from 200°C - 250°C, and is especially formulated for prolonged exposure to temperatures exceeding 120°C and less than -40°C. Some formulations are known for flexibility and impact and creep resistance which are consistent with the properties of Kevlar 49 and polyurethanes - the materials which surround the polyester elastomer. Many varied antioxidants and plasticizers can be added to this polyester formulation depending on the particular requirements.

The last layers of protection afforded the optic fiber used by the U.S. cable vendors consist of UV cured highly cross-linked acrylates. The initial coating "A" and the second layer "B" withstand a 50K psi proof test, and a 100K psi proof stress, respectively. Extensive environmental testing is outlined in a paper by Eccleston<sup>6</sup>. All the testing focuses on the change in fiber attenuation which occurs after the period of time designated. Unfortunately, no data on any of the proprietary polymer coatings is available. Figure 1A refers to the acrylates as "protective coatings" which are applied onto the SiO<sub>2</sub> fiber in two steps - first, "A", followed by fiber cooling and then coating "B" is applied. The coating (referring to both) shall be a non-conductive material and mechanically strippable. The fused SiO<sub>2</sub> glass without the proper coating application would withstand a 100K psi proof test 100% of the time as depicted in Figure 9 from Quan and Gulati<sup>7</sup>. The fused SiO<sub>2</sub> glass fiber characteristics are not discussed in this paper.

#### 1.4 Non-Plenum Film Usage

Still proceeding from the external jacket of the 3-2-2 non-plenum cable to the core, directly under the 3 pair 22 AWG solid copper VGM (telephone wire) and 2 pair OFM fiber units lies a polyester film or tape of  $0.025 \pm .003$  mm thickness followed by a tinned copper braided shield with 65% coverage using 34-36 AWG wires. The tinned coating on the copper is to be  $\geq 0.8$  mm and is used to retard corrosion. The shield is also used to guard against EMI (electromagnetic interference) with the foamed DGM (digital grade media) pairs and to help protect from VGM "ringing voltage" interruption. Next, a layer of aluminum backed polyester film overlapped a minimum of 25% with a thickness of  $.05 \pm .025$  mm and aluminum backing of  $.025 \pm .002$  mm is used to help protect the DGM

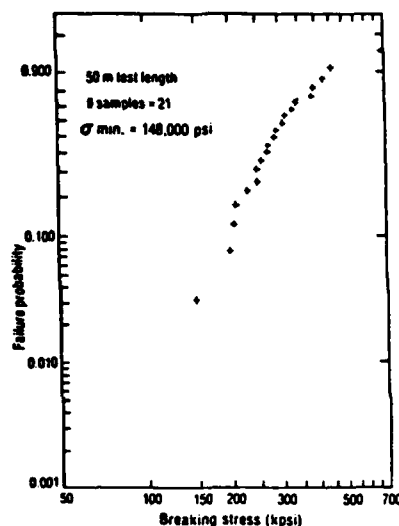


Figure 9  
Weibull Distribution of Failure Probability  
of Acrylate Coated Glass Fibers<sup>7</sup>

core from both electrical and environmental changes. The fourth layer of film around the inner core (see Figure 1A) is again a polyester tape which is  $.05 \pm .005$  mm in thickness. The final two layers which surround the dual inner core foamed DGM conductors also consist of the same polyester film wrapper - both having  $.025 \pm .003$  mm thicknesses.

As can be discerned from the above discussion, there is a considerable amount of polyester film which may be used in the construction of the cable. Estimates of up to 2 lbs. of PET tape/1000 ft. will be used for the non-plenum design. Polyester film has a very non-absorbant nature, but when heated in a humid atmosphere, especially in the presence of alkalis, the film will degrade chemically and physically - eventually becoming unsuitable for use. The major portion of PET (polyethylene terephthalate) film is biaxially oriented, which can significantly affect the physical and chemical stability of the film. This orientation usually begins to "relax" after a shelf-life of six (6) months to one (1) year. The effect of this orientation on PET properties is depicted in Table 5 below.

Table 5

Properties of PET Films		
	Extruded	Oriented
Modulus, $10^3$ PSI	310	800
Tensile strength, $10^3$ PSI	7.7	20-35
Tear strength, gm/mil	45	25
Maximum use temp. °F	165	300

The .05 mm polyester films specified in the cable construction constitute using 1 mil. (.0001 inch) thick wrappings, which, as can be seen in Table 5 above, means the only parameter of concern when orienting the PET is the tear strength. This should only be important during cable installation. Surprisingly, the properties of 5-7.5 mil thick aluminum backed PET film do not exceed those of the biaxially oriented PET without any backing with the fortunate exception of tear strength.

### 1.5 Non-Plenum DGM Insulation

The last two pairs of conductors, which comprise the dual inner core of the 3-2-2 non-plenum cable are termed DGM (digital grade media) twisted pairs. These two pair are to be insulated with low density, cross-linked foamed PE or any other material allowing the DGM pair, "when measured with all other insulated conductors and the shield grounded, to have an insulation resistance of not less than 16,000 megaohm-kilometers at  $23 \pm 1^\circ\text{C}$ ". This measurement should be made with a DC potential between 100 and 550 volts applied for no longer than one minute. Although impossible for the single DGM wires to meet the U.L. VW-1 requirements, - the cable with the outer jacket removed and the shield in place must pass U.L. VW-1.

The individual solid wire size has been specified at No. 22 AWG which constitutes a copper conductor diameter of  $.643 \pm 3\%$  mm with a D.C. resistance  $\sim 17.4$  ohms/304.8 m at  $20 \pm 1^\circ\text{C}$ . The foamed insulation wall thickness specification is most lenient, currently specified at  $0.825 \text{ mm} \pm 20\%$  with the wire diameter including insulation specified at  $2.3 \pm 0.3$  mm. The color markings for the DGM wires, a continuing subject of controversy with this design, requires natural colors on all four DGM wires: one pair having a red striped and green striped wire, the other pair having an orange striped and black striped wire. The method of striping has also been controversial, currently requiring single, helical stripes which are to complete a  $360^\circ$  rotation at  $\leq 25$  intervals.

The first foamed or "cellular" polyethylenes were made in Britain for the Canadian telephone companies which were looking for improvement in signal reliability and economy. Cellular PE (or PP) is achieved either by injecting nitrogen into molten polymer or by compounding with chemical blowing agents. The extruded foam has voids or cells which reduce the dielectric constant of the material toward that of air (1.0). The decreased dielectric constant allows for decreasing signal loss. Since 1971, a low-medium density cellular polyethylene with fine, uniform and non-inter connecting cell structure with a denser layer accumulating at the outer surface of the insulation, has been on the market.

Currently, no physical or chemical property specifications exist for the foamed insulation. The insulation currently being used is an expandable, low density polyethylene compound specifically designed to provide a density between  $0.40 - 0.48 \text{ g/cm}^3$  when completely foamed with a gas volume of 50-55%. The supplied resin contains a temperature sensitive blowing agent which allows the cable vendor to use the same extrusion equipment as is used for the solid PE insulation - no gas injection into the extruder is required. For optimum results, the melt extrusion temperatures should remain in the  $138-160^\circ\text{C}$  range (high for most polyethylenes). Specific processing conditions will vary based on the cable vendor's equipment. Striping of the natural (white appearance) colored foamed PE is easily accomplished by band marking with the appropriate dyes while reheating the foamed PE insulation.

In all, several problems can be foreseen involving the foamed insulation. Degradation due to moisture, UV or ozone exposure has not been documented; therefore, the ability to retard these exposures for a sustained period of time remains questionable, and further research in this area is warranted.

## II. 3-2-2 Plenum Cable Design for LAN

### 2.1 Plenum Outer Jacket Design

This second section parallels that of section 1 (3-2-2 non-plenum cable design) and because of the flammability requirements (U.L. 910 which is discussed next) would include mostly a discussion of the fluoropolymers which E.I. DuPont de Nemours and Co. of Wilmington, Delaware, markets for wire and cable applications.

Although other fluoropolymers have been approved by U.L. for meeting U.L. 910, there exists no polymer more compatible for cable jacketing than FEP (fluorinated ethylene propylene) primarily for its optimum electrical, thermal, moisture resistance, chemical inertness, and flexibility in frigid temperature environments. Other fluorocarbons which have been

tried and initially discarded for 3-2-2 plenum cable jacketing include: Kynar (vinylidene fluoride - too stiff; TFE (tetrafluoroethylene) - too difficult to extrude; and Halar (ethylene-chlorotri-fluoroethylene copolymer) - questionable flammability results when used in certain thicknesses.

The jacket is to be black pigmented in color and have the same nominal wall thickness of .889 mm and minimum wall thickness of .762 mm as the 3-2-2 non-plenum PVC jacket. Again, as with the PVC jacket, no maximum wall thickness was indicated with the understanding that cable flexibility is an important parameter.

To ensure against corrosion of metals due to molten FEP, the same tinned copper braided shielding is used for the 3-2-2 plenum cable construction. Also, to ensure against an extraordinary amount of inert fillers being added to pure FEP resin in the dry hopper prior to extrusion as a cable jacket, U.L. lists minimum acceptable properties for FEP after extrusion. These property requirements are listed in U.L. 62, U.L. 83 and U.L. Subject 13, Appendix B - Table 3. Also listed in U.L. Subject 13, Appendix B are the "minimum acceptable average thickness" and the "minimum acceptable thickness at any point" for the diameter of the assembly under a cable jacket using FEP (or PVC). These requirements are listed in Table 5 of this report and show where the LAN cable requirements originated. It will be the recommendation of the IBM-RTP Materials Lab to adopt the U.L. Subject 13, Appendix B (Table 5) requirements for FEP insulation.

Table 5

Required Jacket Thicknesses for U.L. Subject 13 Appendix A		
Jacket Thicknesses		
Diameter of Cable under Jacket or Armor in Inches	Minimum Average Thickness - Inches	Minimum Thickness at Any Point - Inches
0 - 0.700	0.030	0.024
0.701 - 1.000	0.060	0.048
1.001 - 1.500	0.080	0.064
1.501 and larger	0.110	0.088

## 2.2 Plenum VGM Insulation

Paralleling the Section 1.2 discussion of non-plenum VGM insulation, the plenum 22 AWG VGM conductors are allowed less insulation thickness due to the fantastic electrical properties of FEP. It is because of the electrical properties of FEP, in fact, that the choice of using another solid fluoropolymer is limited.

One question to be answered about the FEP, a copolymer of fluoroethylene and hexafluoro-propylene, is its resistance to decomposition at high temperatures. Although less stable than other fluorinated polymers, no severe decomposition begins below 370 °C.

A final concern, which will be addressed in more detail in the appropriate section, is that the VGM wire pairs must be colored white/blue, white/orange, and white/green - with the white conductor striped the color of the solid colored insulator. In the flame retardant polyethylene compounds needed for non-plenum VGM wires, fillers are a necessity, but for the plenum version, color pigmentation of the FEP is the only requirement which disallows the use of virgin resin. Data collected illustrates the amount of color concentrate used by one cable vendor, the amount of pigment loading in the color concentrate, and how the FEP color concentrates vary in tensile properties according to color. Inspection of the data indicates that tensile properties show that both the blue and green color concentrates have substantially reduced elongation compared to virgin resin. How this will affect the ability of the plenum VGM telephone wire to meet the minimum acceptable ultimate elongation specified in U.L. Subject 13 and also meet the minimum acceptable insulation thicknesses in the same U.L. document along with the REA color requirements, to be discussed, remains an important issue to be resolved.

## 2.3 Plenum OFM Insulation

Currently, the exact same single optic fiber unit construction in terms of material and dimensional requirements is specified for the plenum cable as for the non-plenum cable with the single exception of the outer jacket. This jacket was extruded from Kynar by at least one cable vendor but with little success due to fiber optic attenuation losses. The next candidate for plenum construction was a copolymer of ethylene - tetrafluoroethylene.

Seven conductor 12 AWG wire insulated and jacketed with this copolymer has passed the stringent IEEE 383 tray flame test possibly indicating that this material used in the plenum construction will not interfere with passing the U.L. 910 tunnel test. The possible problems associated with using ETFE include the extrusion of the polymer at 270 °C over the remaining core materials (rated far below this temperature) discussed in Section 1.3 and the same problems associated with coloring the ETFE black and orange as for FEP.

## 2.4 Plenum Film Usage

The current drawings for plenum cables call for the same polyester films to be used as for the non-plenum construction. Although the possibility that these films will be used in a plenum construction (several plenum cables using mylar tape have passed the U.L. 910 test) exists, several problems with using polyester tape have occurred and others are foreseen. One cable, which was sent to IBM-RTP for qualification exhibited "fused" polyester tape over the DGM pairs; apparently from the extrusion temperatures required for FEP jacketing.

One cable vendor has already tried the use of a glass tape material which would be wrapped around the tinned copper braided shielding to act as a heat shield for the remainder of the cable. Several manufacturers of inorganic tapes have products which could accomplish this task economically.

## 2.5 Plenum DGM Insulation

Foaming FEP for wire insulation has been a practiced process since 1964. Only recently, however, has the making of cellular PFA (a copolymer having a tetrafluoroethylene backbone with a fully fluorinated alkoxy side chain) been possible. A current example of a cable using foamed PFA extrudate is the RG 62 coaxial cable made for IBM and other computer manufacturers. It was the intent of LAN cable designers to meet, at the least, the same electrical requirements of RG-62 with both the plenum and non-plenum DGM twisted pair conductors.

Currently, the insulation wall thickness ( $.825 \pm 20\%$  mm) and overall wire diameter, including insulation ( $2.3 \pm 0.3$  mm) are specified exactly the same for the plenum DGM as for the non-plenum DGM conductors. With the superior electrical properties of cellular PFA (compared with cellular PE) over a higher frequency range, it may be possible to reduce these insulation thickness requirements. PFA and FEP both have the same resin electrical properties (dissipation factor =  $.0002$  at  $10^2$  Hz) and when expanded into a cellular structure having 60% void content, both exhibit a dielectric constant of approximately 1.3. (Typical value for cellular PE = 1.5).

Only the military standards for wire and cable seem to address material requirements for PFA, although U.L. may be in the process of writing some finished wire or cable material specification. (For U.L. 83 or 62, etc., no update as of July, 1979).

## III. Flammability, Toxicity and Color Requirements and Concerns for LAN Wire and Cable

### 3.1 Flammability Requirements for Non-Plenum Cable

Without a better U.L. standard than currently exists for non-plenum wire and cable than the U.L. VW-1 (vertical wire) flame test, it was decided to make this test the minimum standard for the LAN cable. This is the most severe non-plenum wire test which U.L. currently imposes and it is specified in several U.L. documents (such as U.L. 83, 62, 44 and Subject 758) as well as being referred to in several others. The verticle test

was required, rather than the horizontal flame tests, due to the fact that in several instances, the cable will be installed in a verticle manner (inside the wiring closet and from the ceiling to the office).

The U.L. VW-1 test configuration is shown in Figure 10. The critical criteria for the single conductor wire allows: no flaming for longer than sixty (60) seconds after any of the five (5) applications of the flame; no more than 25% of the indicator flag to be damaged and no flaming particles which ignite the cotton.

This test is required for individual conductors and single optic fiber units in the non-plenum cable construction. One exception includes the office cable, which must meet VW-1 requirements with the outer jacket construction only, due to the fact that no single conductors will be outside of the jacket during installation and the entire cable assembly will be connected with the jacket remaining. The other exception (aside from the outdoor cable) is that the non-plenum DGM wires are currently not required to meet VW-1. The main reason, other than the fact that these will always be connected during installation, is that the foamed PE conductors are currently incapable of meeting this flammability requirement.

The problems associated with using this test as the sole flammability criteria for non-plenum cables include the fact that the DGM wires can not pass the flammability requirements and that the IEEE 383 flame test for cable represents the most severe accepted flammability test for non-plenum applications.

ESSENTIAL DIMENSIONS FOR VERTICAL WIRE FLAME TEST

Proportions suggested for clarity of detail

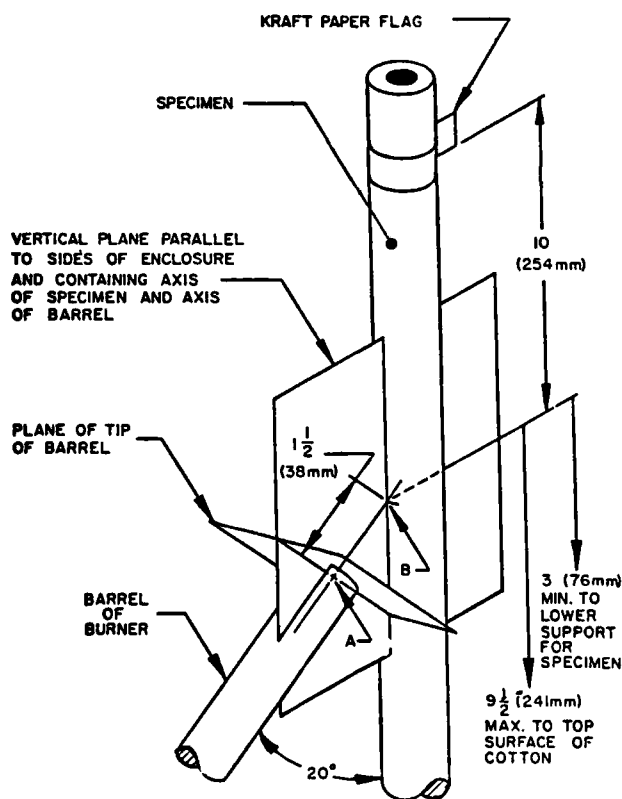


Figure 10  
Underwriters Laboratory VW-1 Test Configuration

### 3.2 Flammability Requirements for Plenum Cables

Prior to 1978, there were no test methods available for measuring the flammability performance of fluoropolymer insulated cables (cables outside of metal conduit to be used in a plenum area). The test that had been used for over twenty (20) years to determine flame spread and smoke characteristics of interior building materials was the ASTM-E-84 Steiner Tunnel Test, but it was not suitable for testing cables. Modification of the Tunnel Test was made by installing a simulated cable tray which would hold the cables for testing. This provided an effective way of measuring the cables' smoke emission and flame spread. It is this modification which the Underwriters Laboratories has adopted and listed in the November 20, 1980 issued U.L. 910 "Test Method for Fire and Smoke Characteristics of Cables". It is also this test which is required for the IBM LAN plenum cables. There is a generally accepted opinion in the field of fire safety that this is a very severe test.

Dr. Inder Wadehra<sup>2</sup> has published a report indicating that properly spaced PVC insulated cables are capable of meeting the 4' flame spread and optical density peak of 0.50 requirements specified by U.L. 910. Unfortunately, currently U.L. requires that the cables not be spaced. Due to the crowding of the cables in the tray, the important consideration becomes the fuel value (or Limiting Oxygen Index - LOI) of the materials used in cable jacketing and wire insulation. The advantages of using fluorocarbons becomes obvious when viewing the values listed in Tables 6 and 7. In fact, the only practical materials which meet the U.L. 910 criteria are the fluorocarbons listed in Table 6 - the major producer being E. I. Du Pont de Nemours, U.S.A. Other materials considered for building plenum cables are being considered and are discussed in the appropriate section.

Table 6

Limiting Oxygen Index (LOI) for Polymers			
$\text{Limiting Oxygen Index (LOI)} = \frac{(O_2)}{(O_2) + (N_2)} \times 100$			
Oxygen Indices of Polymers			
Polymer	LOI	Polymer	LOI
Polyformaldehyde	15	Polysiloxane	24.5
Poly(ethylene oxide)	15	Polycarbonate	27
Poly(methyl methacrylate)	17	Nomex	28.5
Polyacrylonitrile	18	Poly(phenylene oxide)	29
Polyethylene	18	Polysulfone	30
Polypropylene	18	Phenolic Resin	35
Polyisoprene	18.5	Neoprene	40
Polybutadiene	18.5	Polybenzimidazole	41.5
Polystyrene	18.5	Poly(vinyl chloride)	42
Cellulose	19	Poly(vinylidene fluoride)	44
Poly(ethylene terephthalate)	21	Poly(vinylidene chloride)	60
Poly(vinyl alcohol)	22	Carbon	60
Nylon-6,6	23	Polytetrafluoroethylene	95

Table 7

<i>Fuel Value of Various Polymers Compared With Oil, Coal and Wood</i>		
<i>Fuel Values of Various Materials*</i>		
<i>Fuels</i>	<i>Heat Contributed</i>	
Fuel Oil	41.9 MJ/kg	18,000 BTU/LB
Coal	23.3-32.6 MJ/kg	10-14,000 BTU/LB
Wood	18.6-23.3 MJ/kg	8-10,000 BTU/LB
<i>Insulating Materials</i>		
Polyethylene	46.5 MJ/kg	20,000 BTU/LB
PVC	20.9-30.2 MJ/kg	9-13,000 BTU/LB
Rubber	23.3-32.6 MJ/kg	10-14,000 BTU/LB
Fluorocarbons	5.1 MJ/kg	2,200 BTU/LB

\*Per ASTM D-240 and ASTM D-2015 heat of combustion tests

### 3.3 Toxicity Concerns for LAN Cable

The different number of materials which will be used for these communication cables, most of which were documented here, if involved in a fire, would create some combination of toxic gases. The most common off-gas which is produced in a fire - carbon monoxide - would also be evolved from the polyethylene and polypropylene insulation and fillers used in these cables.

Also worrisome are the toxic volatiles produced from the combustion of PVC and the fluorocarbons during either flaming combustion or non-flaming degradation. Even more alarming is the fact that the approach to making polyolefins flame retardant is by adding halogenated compounds (such as chlorine and bromine) which, when exposed to flames, can give off more toxic fumes than the virgin material.

For PVC, much data exists both from real life situations and from laboratory tests, that suggest PVC is no more harmful than burning wood, in an actual fire. There are, however, conflicting laboratory data which suggest that the evolution of HCL from PVC could be severe enough to cause human fatality. An analysis of volatile products from the pyrolysis of PVC is given by Einhorn and Grunnet<sup>8</sup>. Another important concern during the combustion of PVC is the evolution of dark, smoldering smoke, which is always given off from the extrudable grade of material. Some successful attempts have been made to control the evolution of smoke for rigid (moldable) PVC. The necessity of plasticizer additions in the wire and cable grades of PVC make the possibility of creating a smokeless cable compound a twenty year old dream.

Other materials used in the construction of the LAN cable, including polyester tapes and elastomers, polyurethane jacketing, and UV cured acrylates would all give off toxic gases in the event of a fire. Einhorn<sup>9</sup> points out the various products evolved during combustion of these and other plastics and suggests that research of the toxicological aspects of pyrolysis and combustion during fire exposure has lagged so far behind other aspects concerning flammability characteristics of materials, that a fair assessment of the toxic hazards cannot be adequately described.

With the recent increased use of fluorocarbons due to the new NEC regulation allowing cables to be installed outside of conduit, a real concern has been expressed about the possibility of fluorinated hydrocarbon off-gasses produced in a fire where such cables have been installed. This concern has been heightened by the recent (June, 1982) release of the NBS Protocol<sup>10</sup> which depicts PTFE (polytetrafluoro ethylene) - a fluorocarbon - as being 2-3 orders of magnitude, more toxic than any other polymer tested or than Douglas Fir. The toxicity data are for rats exposed to fumes from these materials which were propagated during both flaming and non-flaming combustion. Efforts to refute the NBS data such as suggesting that in a more "accurate fire scenario" such as in the presence of a methane or acetylene flame (over 2000°F) the fluorocarbon materials give off less

harmful fumes than other polymers, are in progress. The problem is that no one can predict what conditions are prevalent in a given fire. To predict what fire hazard either plenum or non-plenum cables present is nearly impossible without re-creation of the specific fire in question. Two criteria which cable producers should strive for are that:

1. The cables do not help to propagate the fire; and
2. The cables do not toxicologically endanger the lives of workers who inhabit areas which are served by these cables.

At this point, not enough scientific evidence supports the second part of this criteria due to the use of fluorocarbon insulation for wire and cable. Also, no known toxicity test which will specify cables as being environmentally safe currently exists.

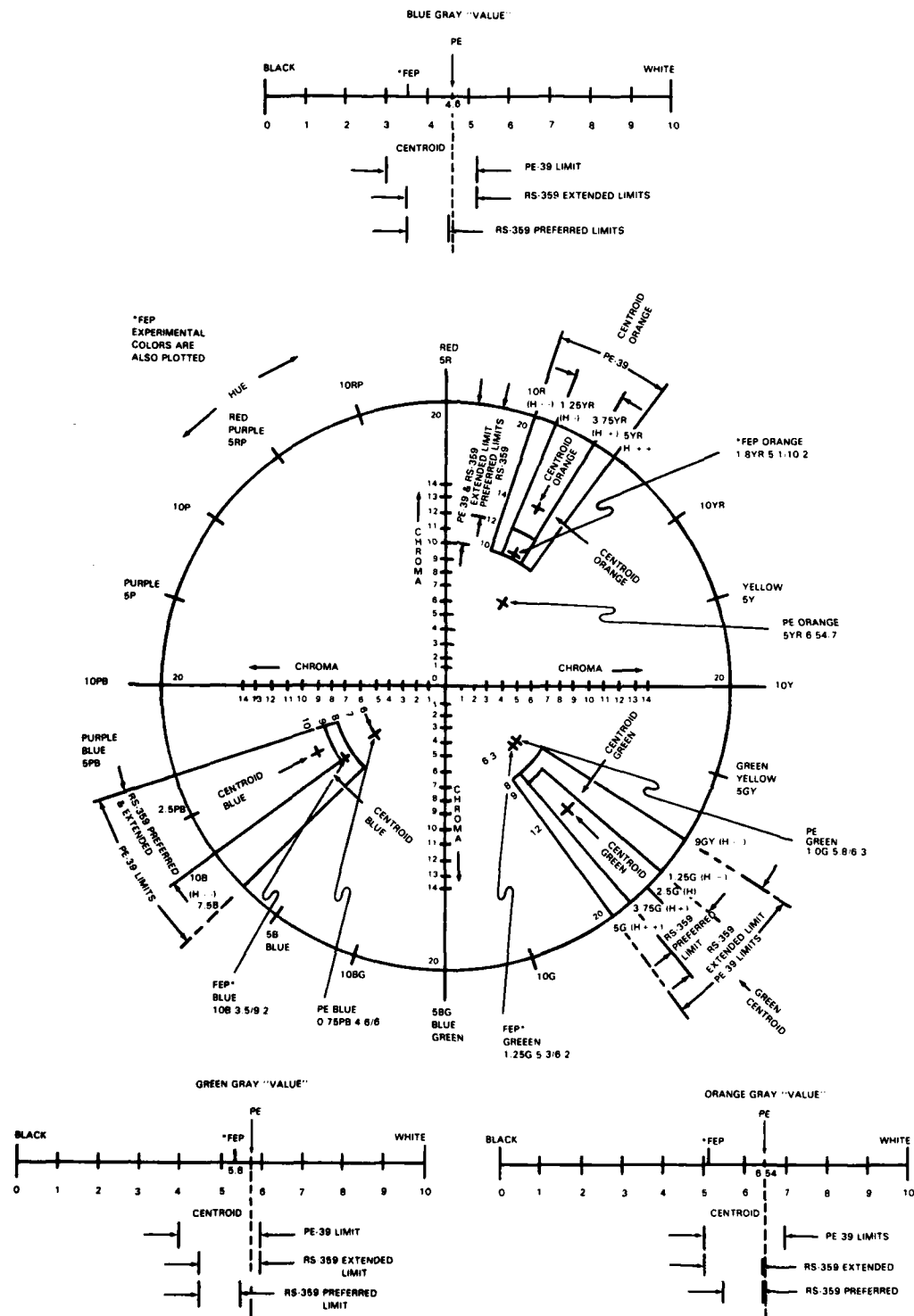
### 3.4 Color Requirements for Multimedia Communications Cable

The color requirements for this cable are important for both the plenum and non-plenum VGM (telephone) wires. Historically, the Bell System, which has used primarily twenty-five (25) pair PVC insulated telephone wires, has met the requirements of EIA (Electronic Industries Association) RS-359. This color standard gives values for two different color systems - Munsell and CIE. The REA (Rural Electrification Association) has taken the RS-359 color requirements and written a specification (using only the Munsell color system) which is incorporated in the PE-39 document.

The problem which IBM has with meeting the REA, PE-39 specification - which is less stringent than EIA RS-359 - is that no PVC insulation is used for indoor telephone wire for this new cable. However, in striving to meet the same flammability and physical property requirements as for PVC insulated conductors, the flame retardants ( $\text{Sb}_2\text{O}_3$ ) and antioxidants ( $\text{TiO}_2$ ) added to the cross-linked polyethylene severely dulled the colors. The white slurries of  $\text{TiO}_2$  and  $\text{Sb}_2\text{O}_3$  reacted with the 1% loading of color pigments in such a way as to lessen the intensity of the blue, green and orange colored insulation. Coloring PVC compounds does not present the same problems.

For fluorinated ethylene-propylene (FEP) resins, the color requirements of PE-39 also present a problem. The color pigment concentration levels previously discussed and used to make color concentrates supplied to cable vendors are currently insufficient. The new method includes adding more color pigment to the color chips, thus using higher loading concentrations in the final insulation. This procedure, however, may still adversely affect physical and electrical properties of FEP. Even with the new method, color plaques of FEP submitted to the IBM-RTP Materials Lab, which were using a Hunter Labscan computer, still did not meet the REA PE-39 color requirements. This data and data from the cross-linked, flame retarded PE are plotted on the Munsell color wheel in Figure 11. Close inspection of Figure 11 shows that only the green FEP meets the REA PE-39 color specifications. All PE plaques missed meeting the requirements due to the low chroma value which is a measure of the color intensity. Until the cable vendors along with the color pellet suppliers approach the color problem in the same vein as DuPont - by adding more pigment to the color pellet - it will be difficult to adjust the chroma value for flame retarded polyolefins. A cooperative effort by one supplier resulted in PE color plaques with 3 and 4% color loading which meet PE-39 requirements, but the physical and flammable properties of their compound are more severely reduced than the reductions seen for DuPont's FEP.

In order to convert from the CIE to the Munsell color system, a software program has been obtained from Dr. Fred Billmeyer's group at Rensselaer Polytechnic Institute (Troy, NY). Further efforts to achieve the color requirements for both PE and FEP insulated VGM conductors, including looking at inking and dyeing procedures, are currently underway at IBM-RTP, as well as within the cable industry. As new colored insulation samples are obtained, an effort to quantify the values of the new colors will be made and documented.



**Figure 11**  
**Munsell Color Wheel**  
**Polyethylene (PE) Telephone Wire Insulation Color Plot Compared to:**

- EIA-RS-359 Preferred Limits
- EIA-RS-359 Extended Limits
- REA-PE-39 Limits

#### IV. Summary of Composite Cable Design

##### 4.1 Fifteen (15) Year Cable Aging Criteria

The current design criteria for the LAN cable includes at least a 15-year life requirement. This specification is considered to mean that the cables must maintain their minimum electrical requirements for at least 15-years with no field failures. No specified test exists for measuring the life expectancy of the LAN cables described in this paper.

There are two methods of evaluating the accelerated aging of the cable. The first method involves testing of the important individual materials which are used in the composite cable design. The second method involves accelerated aging of the entire cable. It is much simpler to test the individual materials than the entire cable due to the fact that polymer interactions (for example, PVC plasticizer which may bleed into the PE insulated VGM) may take place during the accelerated aging process. In determining the aging "program" which a material should be subjected to, it is important to realize what primary mechanism of degradation exists. For polyethylenes, these mechanisms are well understood and documented.<sup>11</sup> For fluorocarbons, the mechanisms of aging and its effects on the thermal, chemical, environmental and electrical stability are well understood.<sup>12</sup> For PVC, however, the study of accelerated aging becomes more complex as the amount of plasticizer and additives, which compose the PVC compound, increase. Sometimes, one mechanism of degradation for PVC will be predominant initially and, eventually, some other mechanism will be the major cause of further deterioration.

Dakin<sup>13</sup> and<sup>14</sup>, in at least two papers, was the first to establish application of aging theory. He did this by developing a theoretical basis for determining the deterioration of electrical insulation. This involved the assumptions that the magnitude of a physical property is a function of time and temperature.

Several fluorocarbons and polyethylene insulations have been life-tested under various conditions using various end of life data points. Of special concern for these communications cables are:

1. The PVC jacketed compounds
2. The solid and foamed PE and PP/PE compounds
3. The foamed fluorocarbon materials

During the past several months, thermal-life data for some of the insulation materials used for these cables has been collected. More life testing data for other possible plenum and non-plenum materials is currently being generated at IBM-RTP, by a detailed aging study of all the cable materials discussed herewithin. The results of this 1-1 1/2 yr. study, designed to measure the kinetic rate of degradation, using tensile strength, elongation and insulation resistance as the physical test parameters, will be detailed in a future report.

##### 4.2 Outdoor and Indoor/Outdoor LAN Cable Designs

Sections 1 and 2 of this report detailed the choice of materials used for the 3-2-2 non-plenum and 3-2-2 plenum cable designs. The reader should realize (see Figure 12) that LAN cables 3-2-0, 0-2-2 and the Type 1 0-2-0 are constructed almost identically to the 3-2-2 cables and are not further discussed for that reason.

Still there exists an outdoor 0-2-0 cable, an 0-0-2 fiber optic cable, and an 0-2-0 office cable in the proposed LAN family. The design of these three cables are found in Figure 12.

Other materials which should be considered to upgrade the flammability and toxicity standards of the LAN non-plenum cable, would be to use either mica or even ceramic tape around the foamed DGM and solid VGM wire pairs. This would enhance the ability of the materials to sustain their physical and electrical integrity over the 15-year cable life as well as providing a flame and toxic retardant barrier. As other non-plenum materials are suggested and become available, new design strategies will be discussed.

The plenum cable allows for the area of greatest cost reduction. The raw resin costs of fluoropolymers varies from \$6.50-18.00/lb currently, with the price not expected to decrease. The basic need is to supply the cable industry with a non-flammable, non-toxic cable jacket and insulation

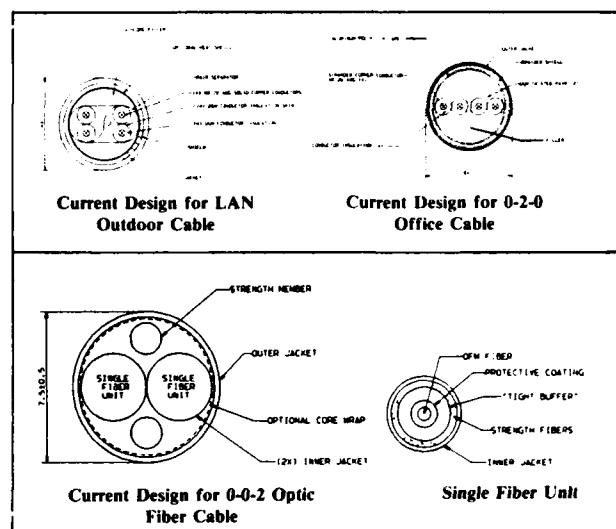


Figure 12

capable of withstanding U.L. 910 Steiner Tunnel Test requirements. It is the conjecture of the IBM-RTP Materials Lab that a LAN cable using polyethylene insulators in a plenum construction is feasible if inorganic materials are utilized as the flame and toxic retardant jacket and shielding. Western Electric and DuPont have already developed a "B" plenum cable using 25 pair PVC (24 AWG) insulated telephone wires wrapped in a glass core which is then surrounded by a single layer of polyimide tape. Over the polyimide is a corrugated aluminum shield with another layer of polyimide over the aluminum shield to provide abrasion resistance. A similar construction, using low cost inorganic materials with PE conductors is envisioned for the new LAN system. A cost comparison summary based on materials which would provide the necessary flammability and toxicity requirements is found in Table 8.

Table 8

Cost Comparison of Materials Under Consideration For Plenum Cable		
Composition	Temperature Rating	Approx. Cost/Ft.
1. Ultem Tape (polyetherimide)	500° - 600°C	\$ 0.05/Ft.
2. Cotronics 390 Ultratemp (ceramic tape)	up to 3000°F	\$ 0.12/Ft.
3. Cotronics 395 Thermeez (ceramic sleeving)	1100°F	\$ 0.17/Ft.
4. 3M's Nextel (ceramic cloth)	3500°F	\$ 1.06/Ft.
5. GE's Gemax (Mica tape)	1000-1500 °F	\$ 0.10/Ft.
6. Siltemp (Glass cloth)	2500-3000 °F	\$ 0.44/Ft.
7. DuPont's FEP (Extruded Teflon)	800-1200°F	\$ 0.35-0.55/Ft.

Summarizing, the concerns of the Materials Lab at IBM-RTP about LAN cable materials selection have been addressed in this report. Such problems as: plasticizers used in PVC jacketing, thermal and other environmental aging processes, upgrading of the U.L. VW-1 test, finding cheaper and better materials to meet the U.L. 910 test requirements, the color matching with REA standards for VGM pairs, and the need for a U.L. standard for fiber optics, still exist. To resolve some immediate concerns, a risk assessment is being performed with regard to cable materials and life expectancy.

#### References

1. *The American Heritage Dictionary*, William Morris, Editor, Houghton Mifflin Co., New York, NY, 1970, p. 1007.
2. Wadehra, Inderjit, *The Performance of Polyvinyl Chloride Communication Cables in Modified Steiner Tunnel Test*, International Wire and Cable Symposium Proceedings, Nov. 1979.
3. Touval, Irv, *Antimony Oxide: Synergism in Flame Retardants*, Plastics Compounding, Sept./Oct., 1982. Reprinted in An M&T Chemicals Report - Rahway, NJ.
4. Cook, Paul M., *An Evaluation of Heat Stability, Flame-Retarded, Cross-linked Polyolefins for Electronic Wire and Cable Applications*, Raychem Corp., Redwood City Calif., Processed for Defense Documentation Center, Defense Supply Agency, U.S. Dept. of Commerce, Inst. of Appl. Tech., Dec., 1959.
5. Technical Service Bulletin TSR 73-83 TF-46, "Extrusion of Estane Thermoplastic Polyurethanes", 1973, B.F. Goodrich Corp.
6. Eccleston, D. J., "Environmental Testing of UV-Cured Acrylate Coated Fibers", Telecommunications Products Dept., Corning Glass Works, Corning, N.Y.
7. Quan, Frederic and Gulati, "The ABC's of Glass Fiber Strength", *The Wire Journal*, Jan., 1980.
8. Einhorn and Grunnet, "The Physiological and Toxicological Aspects of Degradation Products During the Combustion of PVC Polymers", in *Flammability of Solid Polymer Cable Dielectrics*, EPRI Publication TPS 77-738, Pala Alta, Calif., Nov., 1979, pp. 3.1-3.48.
9. Einhorn, I. N., "Physiological and Toxicology Aspects of Smoke Produced During the Combustion of Polymeric Materials", *Environmental Health Perspectives*, Vol. 11, pp. 163-189, 1975.
10. Levin, Fowell, Paabo, Stolte, Maker and Birky, M., "Further Development of a Test Method for the Assessment of the Acute Inhalation Toxicity of Combustion Products", U. S. Dept. of Commerce, NBS, Wash., DC, pp. 1-134, June 1982.
11. Gilroy, H. M. and Howard, J. B., "Some Observations on Long-Term Behavior of Stabilized Polyethylene", *Polym. Engr. and Sci*, Vol. 15, No. 4, pp. 268-271, Apr., 1975.
12. Bro, M. I., McCane, D. I., Allen, D. B., and Reed, J. C., "Perfluoroalkoxy Fluorocarbon Resin Properties Relating to Electrical and Electronic Applications", presented at 29th International Wire and Cable Symposium, Cherry Hill, NJ, Nov., 1980.
13. Dakin, T. W., "Electrical Insulation Deterioration Treated as a Chemical Phenomenon", *Transactions AIEE* 67, 1948, pp. 113-118.
14. Dakin, T. W., "Electrical Insulation Deterioration", *Electro-Technology* 66(6), Dec., 1960, pp. 123-130.



G. L. Grune  
IBM Corp.  
Polymers Group (E79)  
Research Triangle Park, N. C. 27709

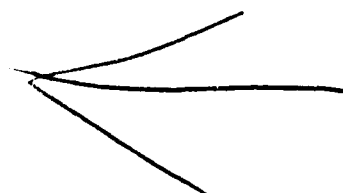
#### About the Author

Guerry L. Grune obtained his B.S.M.E. from Duke University, 1978 (graduation with distinction) with a double major (A.B.) in Chemistry the same year. After working for Fiber Industries Incorporated, a subsidiary of Celanese and ICI of Great Britain, from 1978-1980 in the polyester filament and liquid crystal high modulus organic fiber groups, he returned to graduate school at the University of Massachusetts. There, he obtained his M.S.Ch.E. (1982) from the Departments of Chemical Engineering and Polymer Science and Engineering working under Dr. Robert W. Lenz in the area of thermotropic liquid crystals. Upon finishing his M.S. degree requirements in May, 1982, he joined the IBM-Raleigh Materials Laboratory, and has been associated with materials selection and development for LAN cable, fiber optics and the connector systems which will be used for the project.

#### Acknowledgments

I would like to thank the following people for helping make this paper possible:

- Ken Bedard (Brand-Rex Co.) — Non-Plenum Cable Data
- Charles Butz (DuPont) — Fluoropolymer Data
- Ron Crouch (Brand-Rex Co.) — Non-Plenum Cable Data
- Gail Gardner (IBM) — Typing
- Les Hilliard (IBM) — IR, and DSC Analysis
- Benton Hobgood (IBM) — LAN Electrical Specifications
- Al Overby (IBM) LAN Specifications
- Lou Roberts (Brand-Rex Co.) — Non-Plenum Cable Data
- Michael See (IBM) — Optic Fibers
- Charles Sloop, III (IBM) — EDX Analysis
- Leonard Stumbough (IBM) — LAN Specifications
- Dr. I. Wadehra (IBM) — Fire Regulations
- Rosa Walker (IBM) — Figures and Tables



AD-A136 749

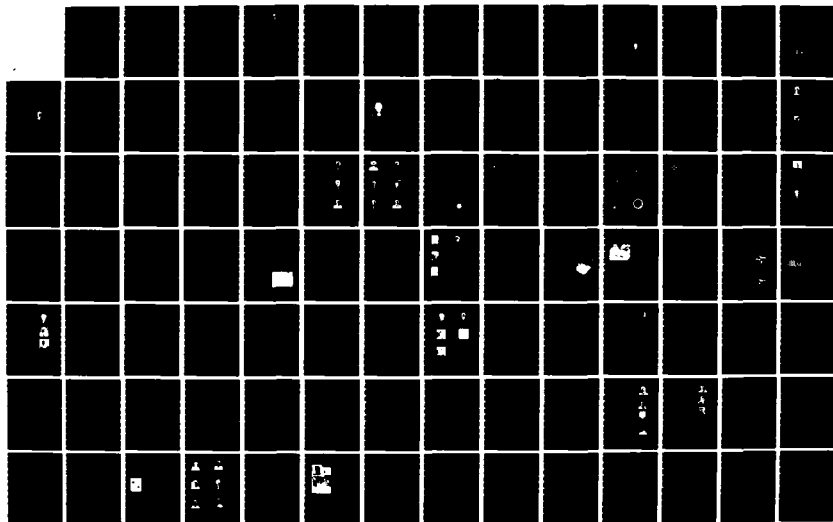
PROCEEDINGS OF THE INTERNATIONAL WIRE AND CABLE  
SYMPOSIUM (32ND) HELD AT... (U) ARMY  
COMMUNICATIONS-ELECTRONICS COMMAND FORT MONMOUTH NJ  
17 NOV 83

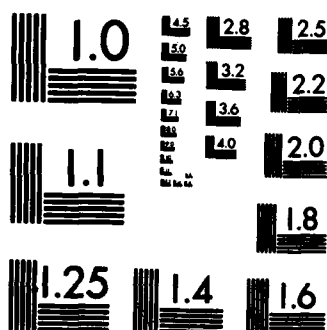
4/5

UNCLASSIFIED

F/G 5/2

NL





MICROCOPY RESOLUTION TEST CHART  
NATIONAL BUREAU OF STANDARDS-1963-A

## DESIGN OF A TWISTED PAIR CABLE FOR A TOKEN PASSING LOCAL AREA NETWORK

Paul Abramson

IBM Corporation  
Research Triangle Park, NC

## ABSTRACT

The proposed IBM Local Area Network architecture required a cable consisting of two twisted pairs. The paper describes the design and construction of a cable to meet the required parameters of "attenuation", "crosstalk" and "characteristic impedance". The cable which resulted from this design has been characterized from 10 kHz to 20 MHz, and is capable of sustaining both low and high speed data transmission over this entire frequency spectrum. Detailed curves showing the major parameters as a function of frequency for typical samples are presented. In addition, versions of the cable have been designed to meet U.L. requirements for both plenum and non-plenum use.

## INTRODUCTION

The cable which is the subject of this paper is a proposed design consisting of two high quality twisted pairs of solid #22 gauge wire, for potential use in a new "Local Area Network" system.

The particular Local Area Network system under consideration is of the "Token Passing Ring" variety. Figure 1 is a simplified system schematic of this network showing a number of terminals connected together in a ring allowing complete peer-to-peer communication. A special bit pattern called a "free token" travels around the ring from terminal to terminal. When a terminal wishes to send a message to another terminal or device which is connected to the ring, it waits until the "free token" arrives. It then changes the bit pattern to "busy", places the address of the terminal to which it wishes to communicate on to the line, and then transmits the message. Since this message is accompanied by a "busy token", it travels around the ring without interference, being repeated by every terminal on the ring. When it reaches the addressed terminal the message is read and repeated so that the original message returns to the sender, where it is removed from the ring and the "busy token" is replaced by a "free token".

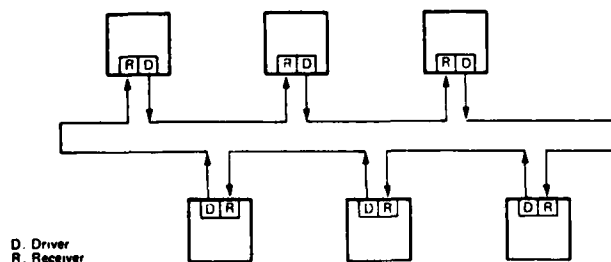


Figure 1  
Ring Topology

This "token ring" architecture as well as other types of architectures which allow only one user at a time to use the transmission facilities calls for a relatively high data rate in order to minimize the waiting time for access

to the line. In the system under consideration, a data rate in the megabit range has been determined to be required.

This brief description of the "token ring" architecture has been presented in order to show its impact on the major requirements of the cable, which is the subject of this paper.

In order for a cable to be suitable for this application, there is a fundamental requirement for two twisted pairs, as we are dealing with a ring architecture, which calls for an input line and an output line at each terminal on the ring. In addition, there are three major parameters which must be considered. These are attenuation, crosstalk, and characteristic impedance.

As was just mentioned, the data rate is high, in the megabit range. Since, as is well known, attenuation of a twisted pair increases with frequency it is extremely important that attenuation be kept low so as to allow for long unrepeated runs.

Near-End Crosstalk (NEXT) is the second parameter of prime importance since as figure 1 shows, each terminal has an input and output line in the same cable. This places a large burden on the crosstalk specification, since an incoming data signal which may be considerably attenuated after a long run, is adjacent to a freshly repeated signal which is at full power and could interfere with the incoming signal. A cable with poor crosstalk would therefore greatly limit the distance between terminals.

The final parameter, characteristic impedance, is required to be closely controlled since at the high data rate any mismatch between interconnected cables would produce undesirable reflections. The final cable design is primarily a result of an engineering combination of these three parameters.

One additional point should be mentioned at this time pertaining to shielding. The proposed cable must meet the new FCC specifications regarding the radiation of electrical noise. It also should reject ambient electrical noise which could cause errors in the data. These two requirements call for rather substantial shielding.

## CABLE CONSTRUCTION

Figure 2 shows a cross section of the cable outlining many of the construction details. The primaries consist of two twisted pairs of #22 gauge untinned copper wire. The insulation consists of foamed polyethylene or polypropylene with a 50% blow. A foamed dielectric is used to produce a low capacitance cable capable of carrying the megabit rates for which it is intended. In order to achieve high immunity to common-mode noise, as well as very low crosstalk, it is of utmost importance that very good pair balance be maintained. One method is to run single primary wire without color, since it has been found that the addition of different color chips change the dielectric constant of the insulation. Identification of the four different wires in the two pairs is accomplished by color stripping. The two pairs are twisted with different lay lengths also to reduce crosstalk.

The two twisted pairs are laid parallel to each other in the cable producing a rather flat cable without any filler. This also reduces crosstalk, since the pairs do not nest into each other, and facilitates printing on the outer jacket. Around the twisted pairs is an aluminum mylar shield with the aluminum facing out. Around this shield is a braided, tinned copper shield

with 65% coverage. No drain wire is required, since the aluminum touches the braid for shield grounding. A black PVC outer jacket surrounds the entire cable.

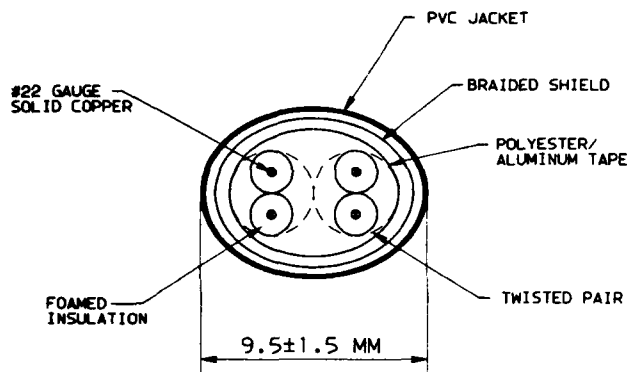


Figure 2  
Cable Construction

#### ATTENUATION

As mentioned earlier, attenuation is a very important parameter of this cable. The specification for attenuation is 22 db/km max. at 4 MHz with the attenuation curve to generally follow the square-root-law. This law states that the attenuation should double for every four-fold increase in frequency. Consequently, there is also a specification that the attenuation at 16 MHz should be less than 45 db/km. Figure 3 shows a curve of attenuation vs. frequency for a typical cable. The measurements were taken in the balanced mode with transformer baluns at each end of the twisted pair.

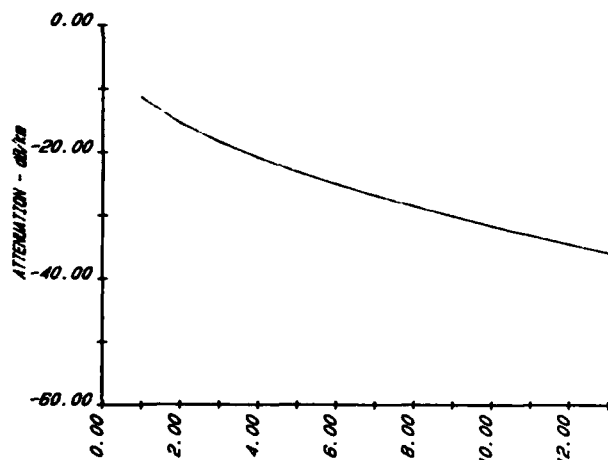


Figure 3  
Attenuation Vs. Frequency

#### CHARACTERISTIC IMPEDANCE

Another parameter of importance in the cable is the characteristic impedance. This parameter is also measured in the balanced mode using the method of "S" parameters. This method is described in detail by another paper entitled "Measurement of the Characteristic Impedance of Balanced Twisted Pairs Using Scattering Parameter" also presented at this Symposium. The specification for characteristic impedance is 150 ohms  $\pm$  10%. This value was arrived at as a compromise between cable diameter

and attenuation. Figure 4 shows a curve of characteristic impedance vs. frequency for the typical cable.

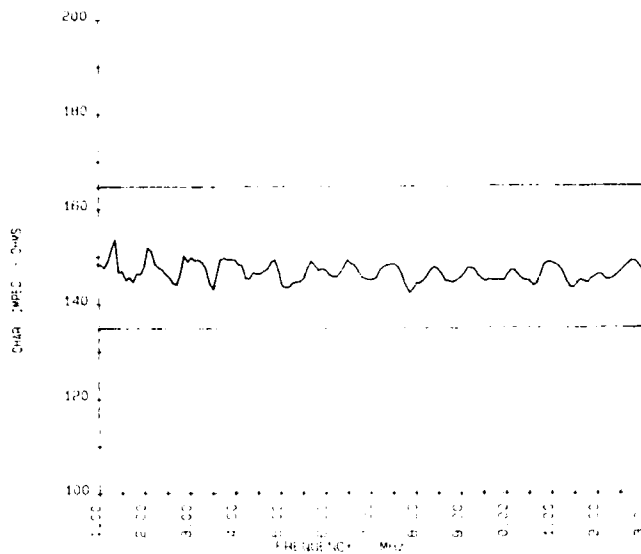


Figure 4  
Impedance Vs. Frequency

#### NEAR END CROSSTALK (NEXT)

As mentioned earlier, near-end-crosstalk, along with attenuation is the determining factor in calculating the maximum unrepeated length for a cable run. The major factors in obtaining good crosstalk is pair balance and twist. The actual plot of NEXT vs. frequency is never a smooth curve, and is therefore specified as a worst value in a given frequency range. As with the other parameters, this is also measured in the balanced mode. The proposed specification for this cable is that the NEXT should be less than -58 db from each of the pairs to the other measured between 3 to 5 MHz.

Figure 5 shows a plot of NEXT from 1 to 13 MHz.

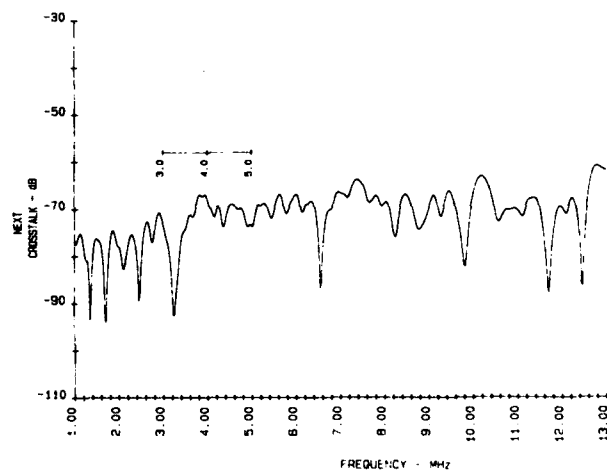


Figure 5  
Crosstalk Vs. Frequency

#### U.L. CONSIDERATIONS AND PLENUM CABLE

The cable described above was designed to meet U.L. requirements for listing as a "Power Limited Class 2 Circuits Application" cable by meeting N.E.C. Article 725 according to U.L. Subject 13 Appendix A. In addition, the cable is required to meet the V.W.1 flame test with and without the PVC outer jacket.

A second version of this cable was designed for plenum use which is to be U.L. classified as fire resistant and low smoke according to N.E.C. Article 725 2(b) exception and U.L. Article 910. This cable has the same electrical specifications, but is constructed using foamed Teflon as the wire insulation, and has a Teflon outer jacket. This plenum cable is to pass the Steiner Tunnel Test.



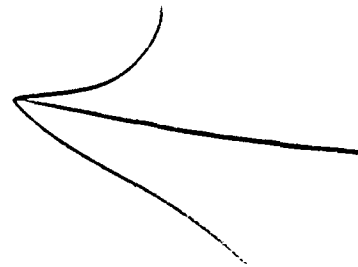
#### ABOUT THE AUTHOR

Paul Abramson is a senior engineer in transmission technology development at IBM, Research Triangle Park.

Since joining IBM in 1960, he has worked in the area of factory automation, data transmission, portable terminals, and special projects concerned with contactless connectors and porcelain-on-steel PC boards.

Before coming to IBM, he worked on military data transmission at RCA and Reeves Instrument.

Mr. Abramson holds a BEE from City College of New York and has done extensive work at Columbia University in electrical engineering and computer science.



# MEASUREMENT OF THE CHARACTERISTIC IMPEDANCE OF BALANCED TWISTED PAIRS USING SCATTERING PARAMETERS

R. Benton Hobgood

IBM Corporation  
Research Triangle Park, NC

## ABSTRACT

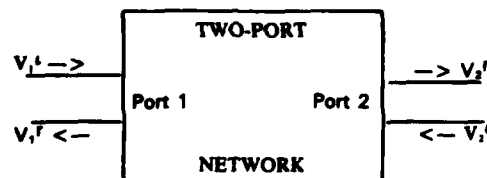
The concept of scattering parameters has previously been used to describe the behavior of circuit networks in an effort to predict their behavior under varied external conditions. This paper describes the use of scattering parameters to lump an impedance test setup, including connectors, cables, baluns, and even internal test equipment circuitry into one two-port network. Scattering parameters are then derived to describe the behavior of that network at one port as a function of varying loads that may be connected at the other port. After the network is characterized, the cable impedance is calculated from corrected short and open circuited cable impedance measurements. The basic theory of scattering parameters and their application to this procedure are described, and equations are presented which are used to implement this method. A brief description of a computer program that was written to accomplish this procedure is included. Sample plots of the impedance of balanced cables which have been produced by the program are also presented.

## INTRODUCTION

The performance of twisted-pair cable is dependent upon the proper termination of that cable in its operating system, especially with data rates that extend into the megabit range. To properly terminate a twisted-pair, the characteristic impedance the pair will present to the transmission system must be known under conditions as close to actual operation as possible. Since twisted-pair cables are normally driven with balanced signals, and practically all readily available test equipment for measuring impedance is single-ended in nature, a method for measuring the characteristic impedance of a twisted-pair cable in a balanced condition is needed. The method outlined in this paper allows the cable to be measured in a balanced condition by measuring the short and open circuit impedances using a balun (BALanced-to-UNbalanced transformer) to provide a balanced signal from the test equipment. The characterization of the test setup (including the balun) is accomplished using Scattering parameters. These S parameters describe the behavior of the setup as a function of any test load that may be present at the test port; therefore, they may be used to offset the effect of the balun on the measurement result.

## THEORY

S parameters outline the relationship of traveling waves in a multi-port network. A two-port network may be represented as follows:



$$V_1^r = S_{11}V_1^i + S_{12}V_2^t \quad (1)$$

$$V_2^r = S_{21}V_1^i + S_{22}V_2^t \quad (2)$$

If equations (1) and (2) are solved simultaneously for  $V_1^r$  in terms of  $V_1^i$ , the following is obtained:

$$V_1^r = (S_{11} + \frac{S_{12}S_{21}*(V_2^t/V_2^r)}{1 - S_{22}*(V_2^t/V_2^r)})*V_1^i$$

$$V_1^r = S_{11} + \frac{S_{12}S_{21}*(V_2^t/V_2^r)}{1 - S_{22}*(V_2^t/V_2^r)} \quad (3)$$

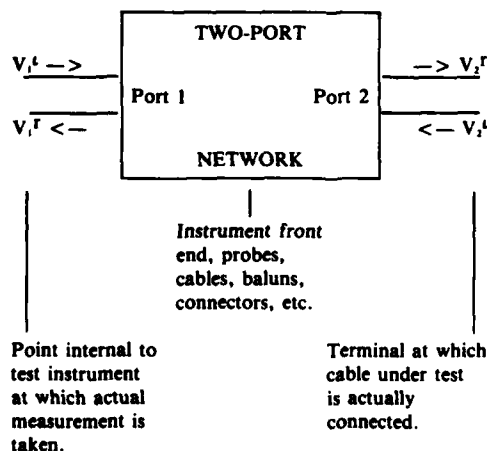
If  $V_1^r/V_1^i = \rho_{input}$  and  $V_2^t/V_2^r = \rho_{load}$  then:

$$\rho_{input} = S_{11} + \frac{S_{12}S_{21}*\rho_{load}}{1 - S_{22}*\rho_{load}} \quad (4)$$

where  $\rho_{input}$  is the reflection coefficient the test setup presents to the actual measurement point, and  $\rho_{load}$  is the reflection coefficient presented by the load to the test setup.

## APPLICATION

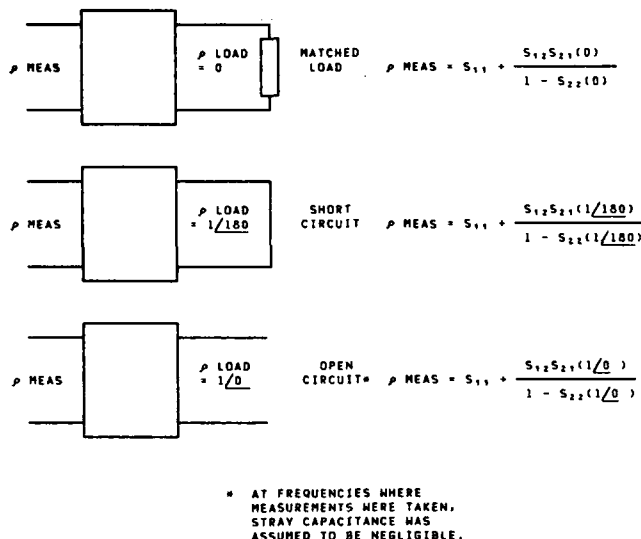
The test setup may be equated to the two-port network in the following manner:



If the S parameters for the network are found, they may be used to calculate the actual load seen at port 2 based on a measurement taken at port 1. Note that the components within this network must behave in

a linear manner over a range of loads from a short circuit to an open circuit if the derived S parameters are to describe the total network's behavior accurately.

The next task is to determine the S parameters for the test setup. Equation (4) has three variables related to the test setup. They are  $S_{11}$ ,  $S_{22}$ , and the product  $S_{12} \cdot S_{21}$ . To obtain them, three conditions must be measured. Each condition, along with the partially completed equation (4), is illustrated in Figure 1.



**Figure 1**  
Measurement of Three Known Conditions  
to Determine S Parameters

For each condition, the measured value of  $\rho$  is substituted for  $\rho_{\text{input}}$  in the appropriate equation. There are now three equations and three unknowns ( $S_{11}$ ,  $S_{22}$ , and  $S_{12} \cdot S_{21}$ ). If these equations are solved simultaneously, the following relations are found for the three unknowns:

$$S_{11} = \rho_{\text{match}} \quad (5)$$

$$S_{22} = \frac{2 \cdot \rho_{\text{match}} - \rho_{\text{short}} - \rho_{\text{open}}}{\rho_{\text{short}} - \rho_{\text{open}}} \quad (6)$$

$$S_{12} \cdot S_{21} = (\rho_{\text{match}} - \rho_{\text{short}}) \cdot (1 - S_{22}) \quad (7)$$

From these equations, the three unknowns (S parameters for the test setup) may be found.

Now that the S parameters are known, equation (4) may be used to describe the actual  $\rho$  presented by the cable under test as a function of the measured  $\rho$ . When equation (4) is solved for  $\rho_{\text{load}}$ :

$$\rho_{\text{load}} = \frac{\rho_{\text{meas}} - S_{11}}{S_{22}(\rho_{\text{meas}} - S_{11}) + S_{12}S_{21}} \quad (8)$$

where  $S_{11}$ ,  $S_{22}$ , and  $S_{12}S_{21}$  are known. Now  $\rho_{\text{load}}$  (actual load at the test port) may be found from the value of  $\rho_{\text{meas}}$  (measured reflection coefficient).

At this point, we have an equation which relates the actual reflection coefficient presented by a load to the measured value of the reflection coefficient which consists of the actual load combined with the effects of the test setup, including the balun. Therefore, as long as the network is linear, the actual reflection coefficient of the load may be calculated from

the reflection coefficient measured through the test setup.

The next step is to convert readings from the measuring device to reflection coefficients and convert calculated values of reflection coefficients to the desired impedances. The method depends on the type of equipment used. If an instrument such as a vector impedance meter is used (readings obtained directly in impedance: magnitude and angle), the impedance readings must always be converted to an equivalent reflection coefficient before being substituted into any of the equations. If the output impedance of the balun is chosen as the reference impedance ( $Z(o)$ ), the following equation may be used:

$$\rho_{\text{meas}} = \frac{Z_{\text{meas}} - Z(o)}{Z_{\text{meas}} + Z(o)} \quad (9)$$

Once the calculated or "actual" reflection coefficient is obtained, the impedance may then be found using the same reference impedance ( $Z(o)$ ) and the reciprocal equation:

$$Z_{\text{actual}} = Z(o) \cdot \frac{(1 + \rho_{\text{load}})}{(1 - \rho_{\text{load}})} \quad (10)$$

If an instrument such as a network analyzer is used where the reflected wave may be measured in terms of the incident wave by a relative measurement (usually in dB), the following equation may be used to convert the measured value "M" to the equivalent reflection coefficient (The measured value is in dB. The associated phase angle becomes the phase of the reflection coefficient.)

$$\rho_{\text{meas}} = \text{inverse-log} (M/20) \quad (11)$$

After the "actual" reflection coefficient is obtained, the "actual" impedance may be found using equation (10) stated previously.

The only task remaining is to take the calculated open and short circuit impedance measurements for a cable and obtain the geometric mean to find the characteristic impedance as follows:

$$Z(o) = \sqrt{Z(\text{sc}) \cdot Z(\text{oc})} \quad (12)$$

## EXAMPLE

A sample calculation demonstrating the derivation of the S parameters and the measurement of a 250-meter length of cable is shown below. The cable is suppose to exhibit a nominal impedance of 150 ohms. All measurements were taken using a vector impedance meter and a balun whose balanced output impedance is 50 ohms. The following measurements were taken directly from the impedance meter readout:

$$Z(\text{match}) = 49.8 \Omega \angle 2.0$$

$$Z(\text{short}) = 11.8 \Omega \angle 77.0$$

$$Z(\text{open}) = 189 \Omega \angle -79.0$$

$$Z(\text{cable-short}) = 83.1 \Omega \angle -49.0$$

$$Z(\text{cable-open}) = 181 \Omega \angle -19.0$$

Measurements are first converted to reflection coefficients using equation (9):

$$\rho(\text{match}) = \frac{49.8 \angle 2.0 - 50 \angle 0}{49.8 \angle 2.0 + 50 \angle 0}$$

$$= .0176 \angle -96.5$$

$$\rho(\text{short}) = .9040 \angle 154.0$$

$$\rho(\text{open}) = .9097 \angle -29.2$$

$$\rho(\text{cable-shorted}) = .5159 \angle -54.9$$

$$\rho(\text{cable-open}) = .5886 \angle -11.0$$

Next, using equations (5), (6), and (7), the S parameters for the test setup are calculated:

$$S_{11} = \rho_{\text{match}}$$

$$= .0176 \angle -96.5$$

$$S_{22} = \frac{2\rho_{\text{match}} - \rho_{\text{short}} - \rho_{\text{open}}}{\rho_{\text{short}} - \rho_{\text{open}}}$$

$$= \frac{(2(.0176 \angle -96.5) - .9040 \angle 154.0 - .9097 \angle -89.2)/(.9040 \angle 154.0 - .9097 \angle -89.2)}$$

$$= .0107 \angle -111$$

$$S_{12} \cdot S_{21} = (\rho_{\text{match}} - \rho_{\text{short}})(1 - S_{22})$$

$$= (.0176 \angle -96.5 - .9040 \angle 154.0) \cdot (1 - .0107 \angle -111)$$

$$= .9066 \angle -27.6$$

Now that the S parameters have been found, equation (8) may be used to determine the actual reflection coefficient of the load from the measured value. For the Z(cable-shorted) measurement:

$$\begin{aligned} \rho_{\text{load}} &= \frac{\rho_{\text{meas}} - S_{11}}{S_{22}(\rho_{\text{meas}} - S_{11}) + S_{12}S_{21}} \\ &= \frac{(.5159 \angle -54.9 - .0176 \angle -96.5)}{(.0107 \angle -111)(.5159 \angle -54.9 - .0176 \angle -96.5) + .9066 \angle -27.6} \\ &= 0.5623 \angle -28.4 \end{aligned}$$

For the open circuit measurement:

$$\rho_{\text{load}} = 0.6341 \angle 16.7$$

Equation (10) is then used to convert the two reflection coefficients to impedances. First the short circuit cable impedance:

$$\begin{aligned} Z_{\text{actual}} &= Z(o) \cdot \frac{(1 + \rho_{\text{load}})}{(1 - \rho_{\text{load}})} \\ &= 50 \cdot \frac{1 + .5623 \angle -28.4}{1 - .5623 \angle -28.4} \\ &= 132.8 \angle -38.0 \end{aligned}$$

Using the same equation for the open circuit impedance:

$$Z_{\text{actual}} = 186.8 \angle 31.4$$

The last step is to find the geometric mean of the two impedances using equation (12):

$$\begin{aligned} Z(o) &= \sqrt{Z(\text{sc}) \cdot Z(\text{oc})} \\ &= \sqrt{132.8 \angle -38.0 \cdot 186.8 \angle 31.4} \\ &= 157.5 \angle -3.3 \end{aligned}$$

## IMPLEMENTATION

A computer driven network analyzer system was used to implement the method. The system consisted of an analyzer, a frequency synthesizer, a directional coupler, a balun, a desk-top computer, and a plotter. The analyzer measures reflection coefficients directly by using the directional coupler to compare the magnitude and phase of incident and reflected voltages. A diagram of the setup is shown in Figure 2.

A program was written for the desk-top computer that selects measurement frequencies for the synthesizer, reads and stores measured data from the analyzer, performs the calculations required to determine the S parameters and actual short circuit, open circuit, and characteristic impedances, and finally plots the results on a chart of impedance versus frequency. A flow chart of the program is shown in Figure 3.

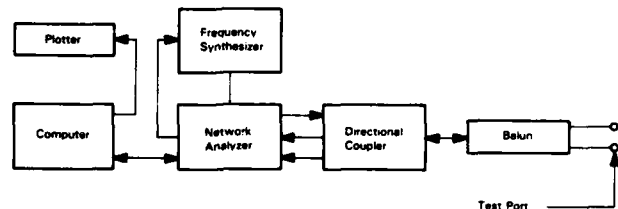


Figure 2  
Diagram of Equipment Connection

## RESULTS

Several plots produced from measurements using the network analyzer setup have been included to indicate typical results using this measurement method. All of these plots indicate the magnitude of the resultant impedance only. Figure 4 plots the results of measurements of several carbon resistors, giving an indication of the reliability of the measurements. Accuracy of the method with the network analyzer setup is generally within 2% for measurement of impedances between 10 ohms and 1000 ohms. A listing of the plotted measurements for these carbon resistors indicate results that are within 1% of the actual values (which is the tolerance of the resistors used).

Figure 5 is a plot of the impedance of a short length of cable in a balanced and unbalanced condition. Note the difference in measured values. This difference becomes even more pronounced with longer lengths. Figure 6 illustrates a typical plot of relatively consistent twisted-pair whose nominal impedance is specified at 150 ohms. Pairs that are less consistent in their physical parameters may exhibit variances from nominal that are significantly greater. Figure 7 is a plot of the results of measurements on 110 ohm twinaxial cable and 93 ohm coaxial cable. As one might expect, the impedance of coaxial cable is more consistent with frequency than that of a twisted-pair construction.

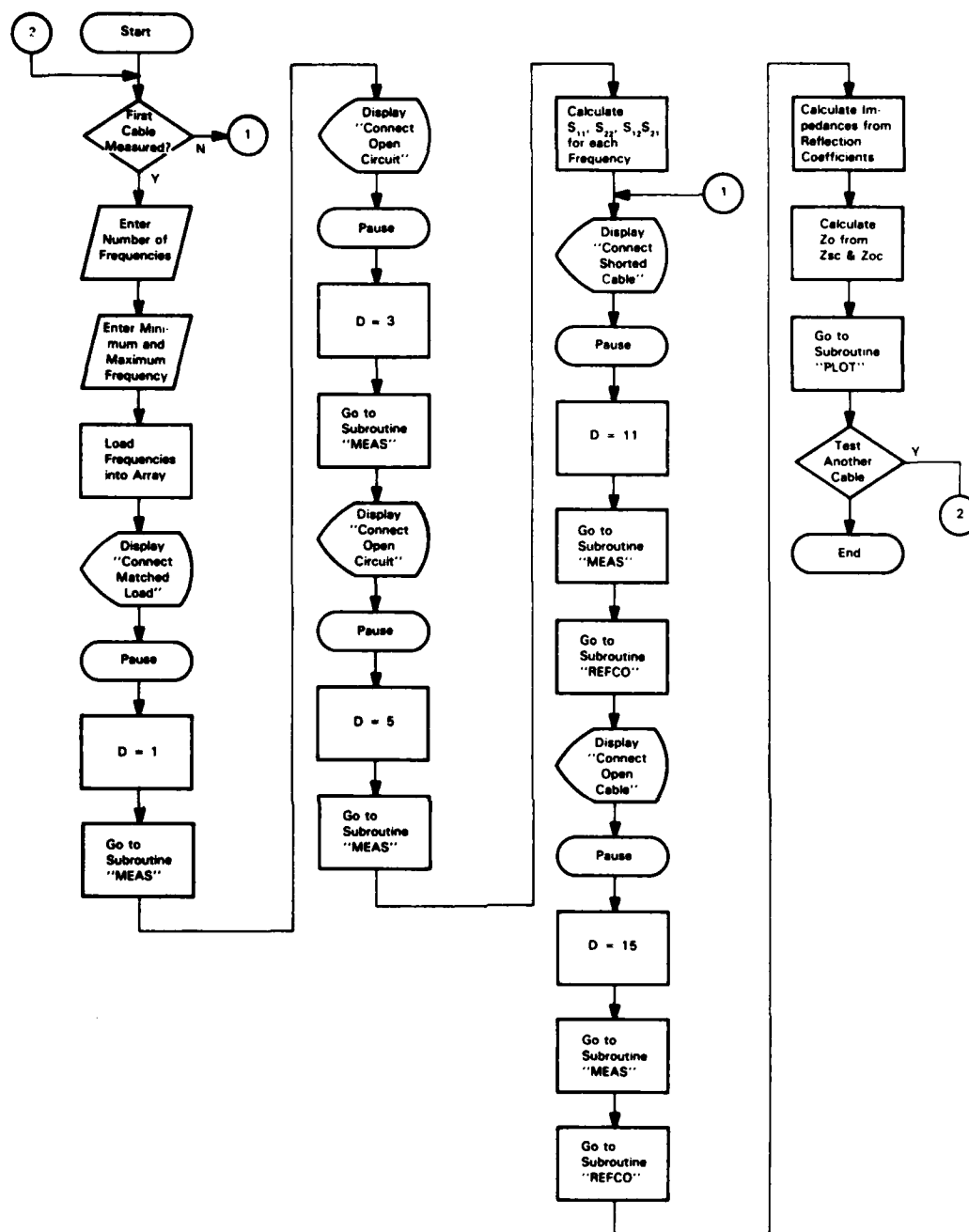
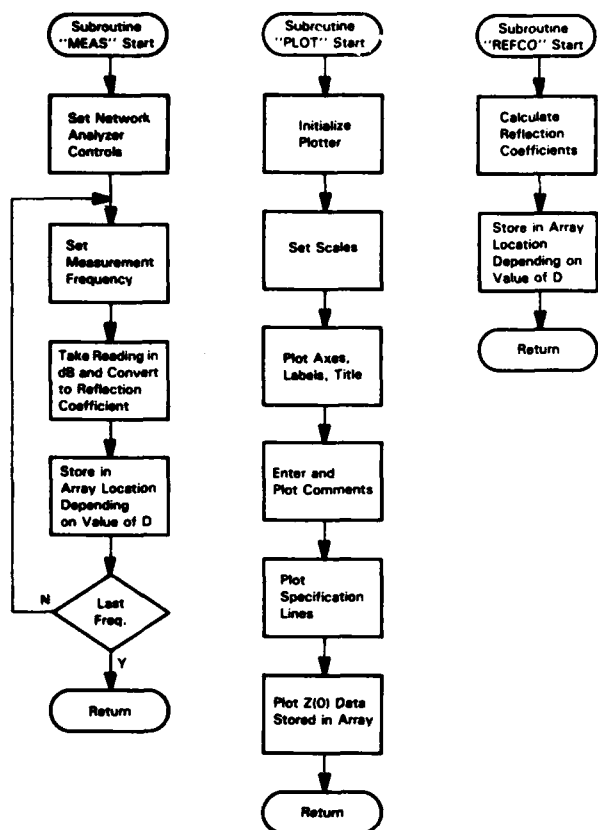
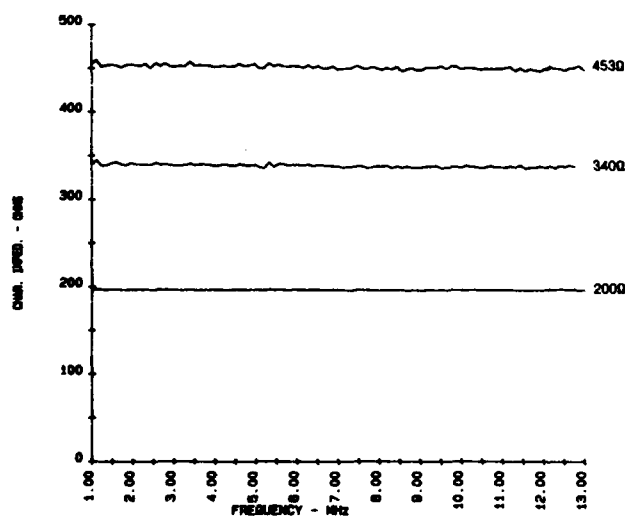


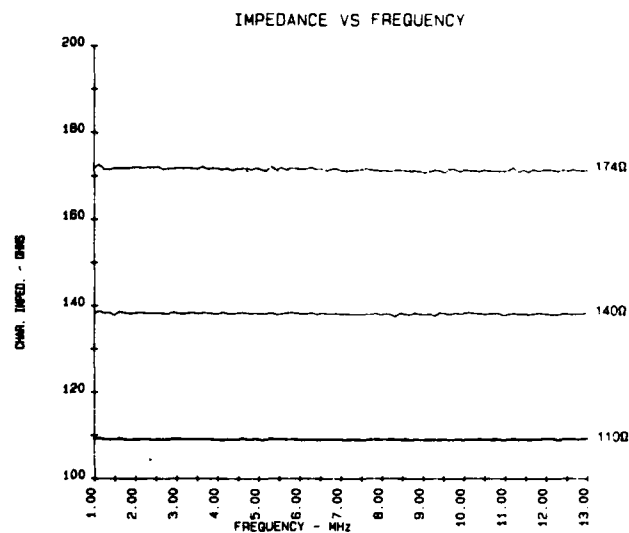
Figure 3A  
Flow Chart for Network Analyzer Program



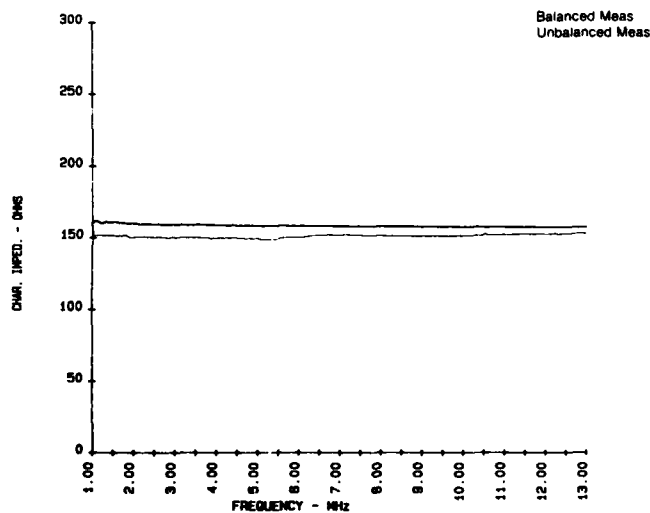
**Figure 3B**  
Flow Chart for Network Analyzer Program



**Figure 4(A)**  
Plot of Resistance Measurements



**Figure 4(B)**  
Plot of Resistance Measurements



**Figure 5**  
Plot of Balanced Vs Unbalanced Measurements

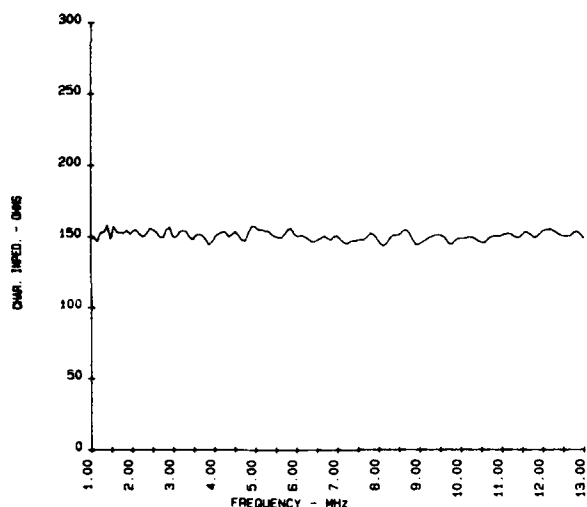


Figure 6  
Plot of 150Ω Twisted-Pair Cable

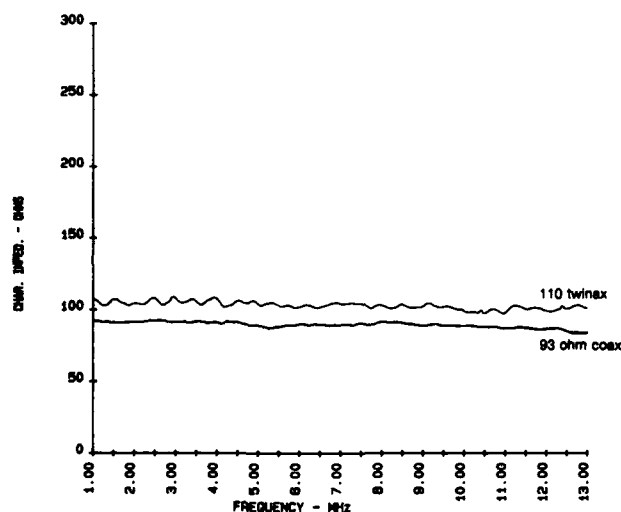


Figure 7  
Plot of Twimax and Coax Cable

## CONCLUSIONS

With continually increasing data rates, the control of the impedance of a cable, especially at frequencies corresponding to these higher transmission speeds, becomes increasingly important. The ability to measure the characteristic impedance of a cable accurately in a manner similar to the actual operating condition is a significant advantage in predicting cable behavior within a system. Also, a graphic representation of this impedance as a function of frequency is another way of judging the quality and consistency of any twisted-pair construction. The method and implementation outlined in this paper will allow both a balanced measurement and a plot of impedance versus frequency to be achieved. In addition, since the use of S parameters compensates for the effects of the entire measuring system, this method may be extended to compensate for other unavoidable effects such as long connecting cables, connectors and switching relays. The only requirements are a good quality balun and a programmable calculator for single frequency measurements, or a computer driven test setup with plotter for a full plot of impedance versus frequency.

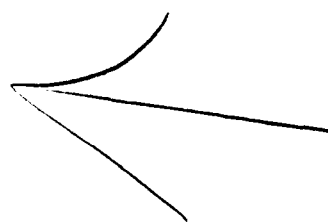
## REFERENCES

1. "An Explicit Solution for the Scattering Parameters of a Linear Two-Port Measured with an Imperfect Test Set", W. Kruppa and K. F. Sodomsky, *IEEE Transactions on Microwave Theory and Techniques*, Volume MTT-19, January, 1971, pages 122-123.
2. *Electromagnetics*, John Krauss and Keith Carver, copyright 1973 by McGraw-Hill, Inc.
3. *Microwave Theory and Measurements*, Irving Kosow, Editor, copyright 1962 by Prentice Hall, pages 7-18, 24-40.
4. "RF Network Analyzer Basic Measurements", *Hewlett Packard Application Note 219*, November, 1978.
5. *Transmission Lines for Communications*, C. W. Davidson, copyright 1978 by Halsted Press.



R. B. Hobgood  
IBM Corporation  
DG75/B061  
P.O. Box 12195  
Research Triangle Park, NC 27709

Benton Hobgood graduated with a B. S. degree in Electrical Engineering from North Carolina State University in 1977. He was employed by Carolina Power & Light Co. in Radio Engineering for 4 years before coming to IBM in 1981. Since joining IBM, he had been involved in the development of twisted-pair cables for local area networks.



# DESIGN/PROCESS OPTIMIZATION OF PAIRED COMPUTER INTERCONNECTING CABLE FOR LOCAL AREA NETWORKS

E. D. Laing

Siecor Corporation  
Hickory, North Carolina

## ABSTRACT

Recent renewed interest in paired, shielded cable for the interconnection of computers, their associated peripherals and other data handling equipment has given rise to a variety of specialized cable designs utilizing low mutual capacitance, balanced pairs to achieve the required high frequency transmission performance. Of particular concern in these designs is the near-end crosstalk interference between pairs in a common shield. The frequencies of operation are such that near-end crosstalk can be a dominant, limiting factor in system performance; hence, multi-pair cables used in such systems must be designed to minimize this parameter and manufacturing processes carefully controlled to achieve the design objectives.

This paper describes a particular cable design which provides the required high frequency transmission properties and at the same time, yields significantly enhanced near-end crosstalk performance properties. The technique for fabricating this cable is simple yet effective and results in improved production efficiencies when compared to more conventional processes used in the manufacture of such cables.

## Background

Computers, their associated peripherals and other data handling equipment in local area networks are typically interconnected by coaxial type cables. Coaxial cables are preferred because of their inherent good high frequency performance characteristics and ease of connection access. However, depending upon the architecture and topology selected for a given network, coaxial cable may present certain disadvantages which can be overcome with paired, shielded cable. Consider the following:

- Coaxial cable is an unbalanced medium and as such, is susceptible to common-mode noise. This refers to external signals which are picked up by both circuit conductors, i.e., the center conductor and the shield. Due to the different impedances to ground of the two, dissimilar potentials will be induced in the two, the net result giving rise to a circulating "noise" current. If on the other hand, the cable consists of a well-balanced twisted pair, the noise signal affects both wires equally.

If the pair is terminated in a balanced receiver or transformer, there will be little or no net noise signal to circulate in the circuit.

- To minimize the effects of external electromagnetic radiation, a grounded shield must surround the circuit conductors. Since the shield of a coaxial cable is part of the working circuit, grounding it can actually introduce noise. The shield on twisted pair cable is isolated from the working circuits, hence the cable is immune to this mode of noise entry.

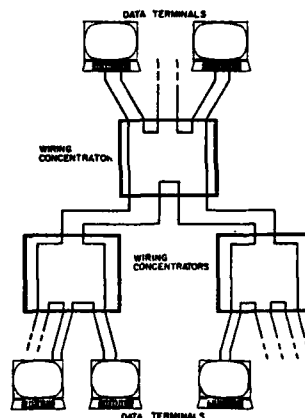


Figure 1

- If a ring topology such as shown in Figure 1 is to be implemented using baseband signalling, each terminal device requires two transmission paths to a wiring concentrator with provision for simultaneous transmission over each. With coaxial cable, two separate cables would be required. With shielded, paired cable, the two circuits can be provided under one sheath resulting in a simpler, less costly installation. Even more important, because of the simultaneous reception/transmission occurring at the terminal, a severe near-end crosstalk problem exists. Well balanced twisted pairs with predetermined good crosstalk characteristics tend to minimize this problem. In the ring topology shown in Figure 1, a single circuit is all that is required to interconnect the wiring concentrators; however, two are usually provided, the first serving as a redundant, backup circuit or an extra circuit for future expansion of the

network where multiple rings between concentrators may be implemented. Again, a two pair cable is an obvious advantage for this purpose.

All of the aforementioned disadvantages of coaxial cable could be overcome with optical fiber cable; however, for low bandwidth applications (10 MHz and below) and typical distances of less than one Km, optical systems are still more expensive than copper cable systems. Optical systems require more expertise in splicing and terminating and because they are relatively new, potential users hesitate to specify them.

The signalling method also has a bearing on the cable to be used in a given network. Currently, two signalling methods are used, broadband and baseband. In broadband signalling, the data signal is used to modulate a carrier (frequency modulation) and the modulated carrier applied to the cable. Since the FM carriers used are typically in the 50-100 MHz range, twisted pair cables are severely limited by attenuation and therefore coaxial cables must be used. In baseband signalling, the data signal is applied directly to the cable and since the effective frequencies of the data signals are typically in the 1 to 10 MHz range, shielded, twisted pair cable can be used effectively in these systems. Obviously, baseband signalling systems are less expensive due to the elimination of the FM modulation electronics. Other factors such as greater reliability, availability and ease with which a ring topology can be implemented and serviced make the baseband system more attractive to the system designer. From the foregoing general discussion, one can appreciate the potential for paired cable in the current local area network market. The choice of transmission medium is still dependent upon the network design being engineered to achieve optimum balance between present installed cost, efficiency and effectiveness of the data handling process and making provision for future growth. At least one major computer system manufacturer, for economic and other reasons mentioned above, has embarked on a full scale switch to paired cable supplemented by fiber optic cable for current and future system installations. The cable designs required for this purpose, although generally following conventional practice, are quite specialized and involve very stringent physical and electrical performance characteristics.

#### Cable Design

To achieve the required transmission characteristics for use in the 1 to 10 MHz range and in lengths up to 1 Km without repeaters, the cable utilizes 22 AWG, low mutual capacitance pairs. The version of current interest is designed for a characteristic impedance of 150 ohms @ 4 MHz, a value which represents an engineering trade-off between acceptable cable size and cost and reasonable attenuation. The insulation is a foamed, low dielectric constant material to achieve an optimum insulated conductor diameter-to-mutual capacitance ratio. The insulated conductors are paired and assembled

into a core, shielded with an aluminum/polyester foil followed by a copper wire braid and plastic jacket overall. Two versions are required, one utilizing fluoropolymer materials for plenum use, the other utilizing polyethylene and polyvinyl chloride for non-plenum applications (Figure 2).

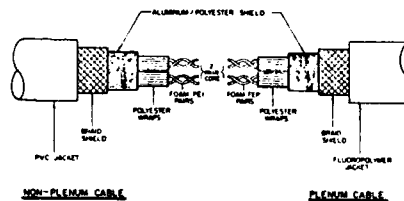


Figure 2

In these designs, pair balance is critically important to minimize common-mode noise pick-up, the generation of internal noise, and to reduce crosstalk between pairs. This dictates close tolerances on the insulation thickness and preferably, continuous monitoring and/or automatic control of the insulating process. Subsequent processes must also be closely controlled to carry this balance through to the finished product. As previously mentioned, near-end crosstalk interference (NEXT) in these cables is a most serious consideration and as one would expect, at the frequencies being considered and with pairs lying adjacent in a common shield, is one of the most difficult parameters to control. NEXT is reduced by utilizing relatively short pair lays with twist ratios chosen to minimize inductive and capacitive coupling between the pairs. In one version of these cables, the pairs were also individually wrapped with polyester tape to increase the degree of physical separation between them, a feature which tends to improve crosstalk performance. This design although adequate, was complicated from a manufacturing standpoint due to the multiplicity of operations involved, was expensive and extremely process sensitive.

#### The New Design

An improved design utilizing a longitudinally-applied internal screen (Figure 3) to isolate the individual pairs from each other has been developed.

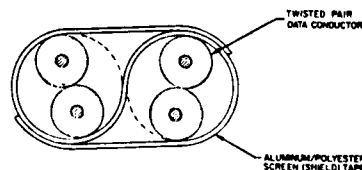


Figure 3

The screen, a modified version of the type used in telecommunications cable, is applied so that it passes between and around the pairs providing total isolation between them. The screen tape used is a standard aluminum foil/polyester laminate regularly used for shielding purposes. No other tapes are required over the individual pairs or over the two pair core as in previous designs. The screen tape also serves as the metallic shield tape required directly under the braid wire shield. The necessary electrical contact between the metallic shield tape and the copper wire braid shield is provided by the bare aluminum foil which is facing outward over approximately one half the periphery of the screened core. (The other half is of course, insulated from the braid by the polyester backing on the screen tape.)

#### Fabricating the New Design

The process for manufacturing the screened cable utilizes the same basic principle as originally developed for internally-screened telecommunications cable. The two pairs are positioned laterally on either side of the screen tape and the three elements drawn through a forming tool. The forming tool consists of a metal plate with two circular holes and an extended "S"-shaped aperture large enough to accommodate the tape, centered between the holes. This device positions the pairs and forces the screen tape to begin folding around them. Uniform tension on the tape is essential to ensure the correct folding action takes place in the forming tool. A series of progressively smaller polishing dies immediately after the forming tool serve to complete the folding action of the outer edges of the tape around the pairs such that the tape overlaps itself on diametrically opposite sides of the two pair core. The overlaps are important to ensure maximum electrical isolation between the pairs is achieved. Figure 4 illustrates schematically how the tape forming takes place.

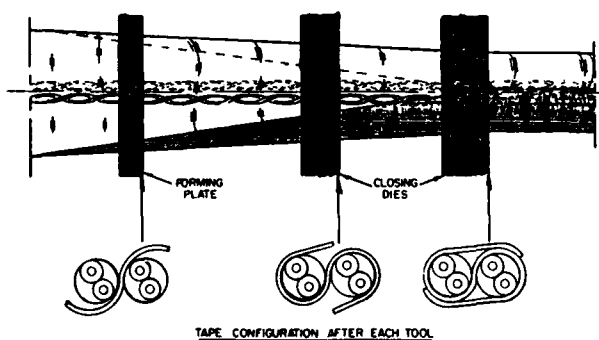


Figure 4

A copper wire braid is then applied over the screened core in the normal manner to lock the screen tape in place and complete the shielding process.

In order to maintain equivalent attenuation and characteristic impedance in the cable with the addition of the screen, a slight adjustment of the insulation wall thickness is necessary. The fact that the shield now effectively surrounds and is in closer proximity to the working pairs causes an increase in mutual capacitance and consequently, an increase in attenuation and a decrease in characteristic impedance. Increasing the insulated conductor diameter approximately 6% is adequate to reestablish nominal attenuation and characteristic impedance while still meeting the prescribed DOD tolerance, a factor of concern for connectorization. In the completed cable, this increased dimension is nicely compensated for by the elimination of pair and core wrap tapes so that the overall cable diameter is roughly the same as the multi-taped version. Cable appearance and handling characteristics are not appreciably affected by the addition of the screen tape. Figure 5 lists a number of physical tests which these cables are required to withstand without incurring out-of-spec changes in electrical performance. The screened cable easily meets

TESTS (ON COMPLETED CABLE)	REQUIREMENTS
Tensile Strength - Force of 60 lbs applied to a 330 foot length and held for 1 minute.	On completion of each test, all electrical parameters must still be within the original specified tolerance limits.
Compression - Force of 100 lbs applied between two 4 inch wide steel plates for 1 minute.	
Flex - 20 cycles through 180° about a mandrel of the same radius as the specified minimum bend radius.	
Impact - Ten hits of 3.5 ft-lbs force applied at 1/4 inch intervals along the cable using a 7 lb weight dropped a distance of 6 inches.	
Bend - 5 consecutive pulls applied to an approximate 1 foot section of cable around a 90° bend under tensile load of 60 lbs (Minimum radius of bend - 3 inches for non-plenum cable, 6 inches for plenum cable).	

Figure 5 - Physical Requirements for 2 Data Pair Cables

all of these prescribed test requirements with equivalent or better performance than the previous cable designs.

#### Advantages of the New Design

The screen tape in this design eliminates the need for the aluminum/polyester tape under the braid shield as well as all other tape wraps used to improve near-end crosstalk. Compared with multi-taped, unscreened cable, the new design yields a NEXT improvement in the order of 30% while significantly reducing manufacturing costs. Figure 6 shows typical NEXT response versus frequency for screened and unscreened cable.

This NEXT improvement realized with the screened design can provide added benefits to system performance in the way of enhanced common-mode noise rejection.

In general, the screened cable provides an additional bonus of better electrical stability over the frequency spectrum of interest. Both NEXT and characteristic impedance show less drastic fluctuations with frequency than

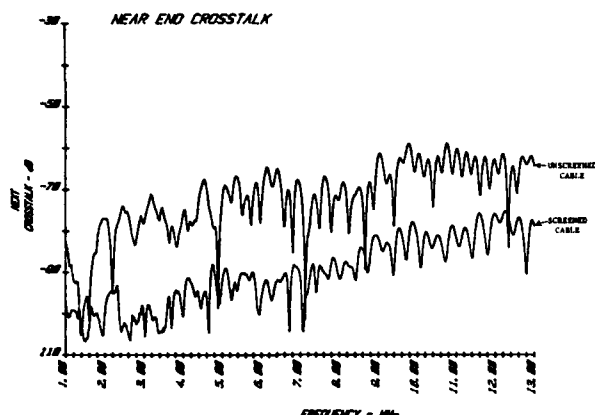


Figure 6

unscreened cable types. Figure 7 shows typical characteristic impedance versus frequency traces for screened and unscreened cable. Reference to Figures 6 and 7 then illustrates the above mentioned improved stability achieved with screened cable.

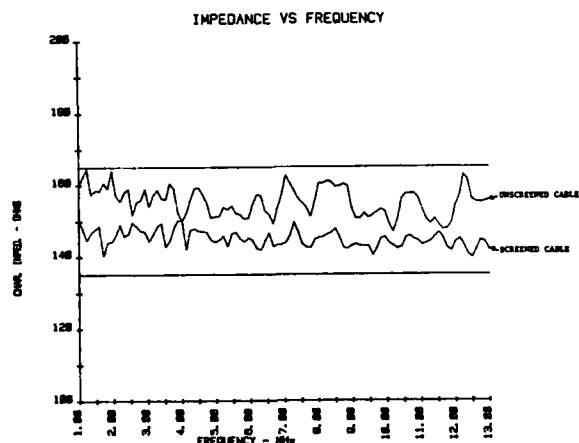


Figure 7

Compared to the multi-taped versions, screened cable is simpler and easier to terminate, an advantage which is reflected in substantial installation cost savings.

#### Summary

The performance, ease of application and cost of shielded, paired cables make them viable alternatives to coaxial cables for data terminal/computer interconnections where moderate data transmission speeds, baseband signalling and moderate distances are involved. The paired cables used in these applications require well

balanced pairs with extremely good near-end crosstalk characteristics. A novel screened cable design has been developed which is relatively simple to manufacture and provides enhanced near-end crosstalk performance and good electrical stability over the frequency spectrum required for low/medium speed data transmission. Compared to multi-taped core data cables, screened cables are simpler and easier to terminate thereby providing greater economy of installation.

#### References

1. Matching the Media to Local Network Requirements - P. Abramson and Franc E. Noel, Data Communications, July 1983.
2. The Impact of Fiber Optics on Local Area Networks - D. Jay Cunningham, Telephony, January 3, 1983.
3. Multipair Cable Shielding for PCM Transmission - W. L. Roberts and F. N. Wilkenloh, 19th. International Wire and Cable Symposium, December 1970.



Edwin D. Laing  
Siecor Corporation  
Hickory, North Carolina  
28601

Ed Laing is Product Engineering Manager in the Research and Development group at Siecor. He is a 1959 graduate of Ryerson Polytech., Toronto, Canada and has been involved in the telecommunications cable manufacturing industry for the past 24 years. He is a member of the Insulated Cable Engineers Association, Inc. and a member of the Association of Professional Engineers of the Province of Manitoba, Canada.

## EVALUATION OF FOAM-SKIN CABLES FOR AERIAL APPLICATIONS

Gene R. Samuelson

Anaconda Wire and Cable Company  
Overland Park, Kansas 66204ABSTRACT

Since the introduction of foam-skin filled cables, there has been considerable discussion within the Industry, both pro and con, regarding the acceptability of foam-skin filled cables for aerial application. This paper reports on results obtained from a study undertaken to evaluate the changes in transmission properties of such cables in a simulated aerial environment.

Cable samples produced by six cable manufacturers using conventional, high-temperature drip-resistant filling compounds with a petrolatum base were subjected to temperature cycling from -40°F to 140°F. Transmission parameters were measured at 1, 150 and 772 kHz and compared to initial values. A solid polypropylene insulated filled cable was included for reference.

The results show that foam-skin petrolatum based filled cables exhibit stable electrical characteristics when exposed to cycled temperature extremes.

INTRODUCTIONHistorical Background

The idea of cellular insulation was first patented in England in 1930<sup>1</sup> and field trials were installed there in the early 1950's. Filled cellular field trials were made in the mid-1960's when moisture problems with air-core plastic cable became evident.<sup>2</sup> With the rapid acceptance in England, the cellular technology emigrated to Canada in the late 1960's.

Manufacturers in the U.S.A. were slow to accept cellular, due to reservations about processing and long-term performance characteristics.<sup>3</sup> Instead, solid plastic insulated, jelly-filled cables

were developed in the same period. Then the world-wide oil shortage in the early 70's forced a reassessment which made filled cellular cable much more attractive.<sup>4</sup> The oil shortage caused a reduction in the supply of polyolefins which made manufacturers look more intensely at ways to reduce cable sizes and conserve insulating, filling and jacketing materials. The answer, of course, was to change to cellular insulation.

A modified version of this straight cellular insulation was introduced in 1975, which involved extruding a "skin" of solid material over the cellular inner core of insulation - hence, foam-skin cable.

Testing Background

From the beginning, much concern has been expressed about the long term stability of cellular (foam) and foam-skin cables. The primary focus of this concern was the possibility of the migration of filling compound into the cell structure of the insulation, and the resulting effect on transmission characteristics. Of equal importance was the strength and longevity of the insulation system in combination with the filling compound.

Tests have been conducted using temperature cycling, long-term temperature aging and water immersion to examine both single and cabled conductors for changes in weight, dimensions, strength, elongation and electrical characteristics. It has been found that the filling compound can definitely migrate into the foam insulation<sup>5,6,7,8,9</sup>, but that the migration process is resisted by the viscosity and molecular weight distribution of the base oil of the filling compound, the permeability of the insulation and a small cell size.<sup>7,9,10,11</sup> Consequently, the design of the insulation/filling compound system is critical to the long-term stability of the cable. That design has improved significantly over the past decade.

The mechanism of filler migration involves a gradual expansion of the insulation followed (some say accompanied) by a filling of the cells. This causes an initial reduction in capacitance as the conductors separate with expansion. Some portion (or all) of this reduction is gained back as the cells fill. Concern has been expressed about a reduction in waterproofness as the air in the cells is displaced into the conductor interstices. Tenzer and Olszewski<sup>11</sup> have made the interesting and logical observation that the displaced air would "remain as small discontinuous bubbles", which, of course, would not permit water ingress and maintain the watertight integrity of the filled cable design.

By far the most popular method of aging test samples is through high temperature soaking - usually at 60° to 70°C to accelerate any filler migration or insulation deterioration. The soaking medium could be air or water or filling compound. The medium did not appear to have an impact on the test findings in the papers reviewed.

High/low temperature cycling was suggested by Molleda<sup>12</sup> as a good way to investigate insulation cracking, which he saw as a major long-term problem for aerial installations. Beach<sup>13</sup> suggested that temperature cycling produces the same effects as high temperature aging and that core temperatures of cables installed aerially can be expected in the 50° to 60°C range.

It has been suggested by several investigators<sup>6,7,13,14,15</sup> that filler migration has no major effect on cable stability, that the long-term electrical characteristics of a properly designed filled foam skin cable remain well within useful limits.

## EXPERIMENTAL RESULTS

### Objectives

This study investigated the electrical performance of filled cables with foam skin insulation after exposure to temperature cycling, simulating the extremes cables would be expected to experience in an aerial environment. It was expected that the electrical characteristics of the samples would remain functionally stable throughout the test period.

Additionally, foam skin cable samples from six different manufacturers were included with a solid polypropylene insulated filled cable to compare the stability of the foam skin products with this standard construction.

All investigations were made with the final objective of recommending filled foam-skin cable for aerial applications.

### Test Procedures

The samples tested environmentally were 35 feet long with 25 pairs of 22 gauge conductors. The tests involved one standard solid polypropylene insulated sample and six foam-skin samples, all with high-temperature drip-resistant petrolatum-based filling compounds. The physical characteristics of the foam skin samples are shown in Table 1.

Table 1

Dimensional Range of Foam-Skin Samples

Dimension	Low	High
Skin Thickness (mils)	2.0	3.3
Diameter over Dielectric (mils)	44.3	47.6
Core Wrap Thickness (mils)	2.9	7.0
Core Diameter (inches)	.430	.448

The temperature cycled samples were coiled loosely and cycled from -40°C (-40°F) to +60°C (140°F) for approximately four cycles a day, with a 2-hour soak at each extreme to ensure the whole sample reached the test temperature. Five pairs from each sample were tested at ambient (68°F) as a reference, and then after 50 cycles, were returned to ambient for 24 hours and tested again. Measurements included loop resistance, inductance, capacitance and conductance at 1 kHz, 150 kHz and 772 kHz. The tests were repeated after 100, 150, 250 and 350 temperature cycles.

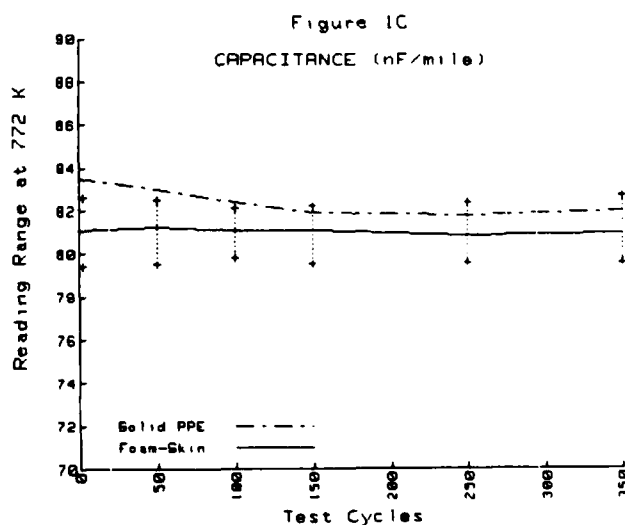
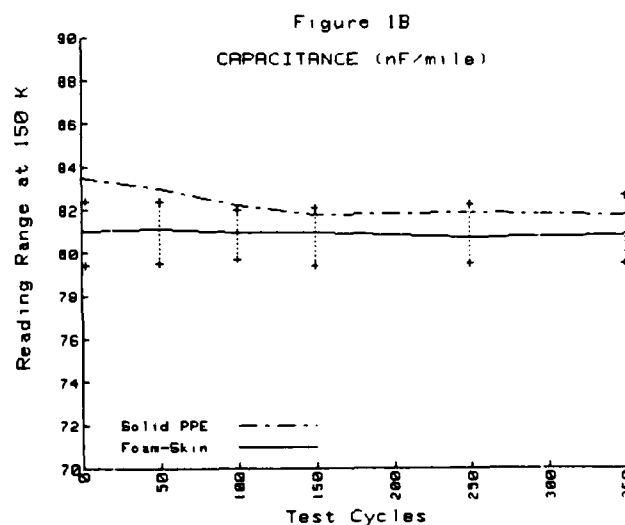
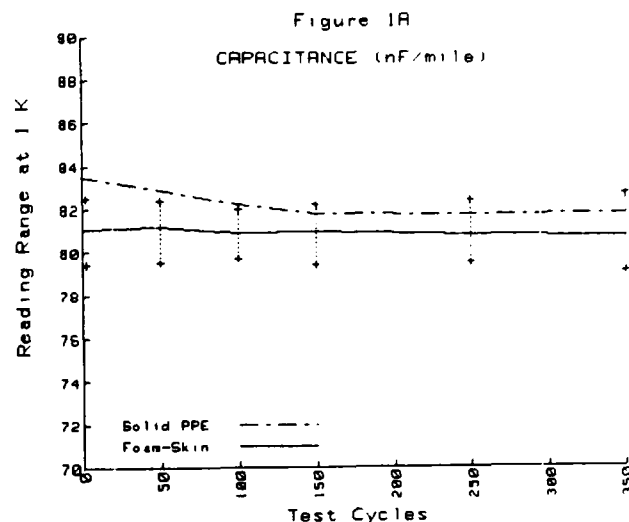
## Results

Once the measurements were taken, the data was processed to produce normalized primary and secondary parameters, of which capacitance, attenuation and impedance are considered most important for this study. Capacitance was chosen as the design parameter which would be most obviously affected by changes induced by filler migration. Attenuation and impedance were included as indices of operational behavior of the cables, especially at the higher frequencies. Table 2 shows the calculated values, but the data was also plotted (Figures 1A through 3C), which reveals more clearly the comparisons of interest.

The plots depict the average values for the standard solid polypropylene insulated sample compared to the composite average for all six foam-skin samples. Also included in the plots was the range of foam-skin values at each data point.

The capacitance plots (Figures 1A, 1B and 1C), at the three test frequencies, reveal the composite foam skin average to be very flat over the 350 cycles, while the solid PPE sample exhibits a slight reduction in capacitance through 150 cycles, then a leveling off at about 2% below its initial value. A possible explanation could be that the solid insulation absorbed some filling compound with the cycling process and expanded to an equilibrium condition. The expansion of insulation would separate the paired copper conductors, causing a reduction in mutual capacitance. When the expansion stopped, the change in capacitance also stopped, indicating that the solid insulated sample had effectively "aged" at 150 cycles and had stabilized.

It would be logical to expect that foam skin samples would be affected by the same migration mechanism within the same 150 test cycles. If the foam skin did, in fact, absorb filling compound and expand (as has been found to happen in other investigations<sup>5,6,7,8,9</sup>), some other factor must have offset the capacitance reduction that would accompany expansion of the conductor insulation. If the cells filled with migrating oils at the same time the insulation matrix was absorbing those same oils and expanding, the displacement of air cells from near the conductors out into the interstices would cause an offsetting increase in mutual capacitance.<sup>5</sup> That offset could cause the foam skin capacitance to remain stable even when the physical changes were occurring.



The attenuation plots (Figures 2A, 2B and 2C) again show the composite foam skin average to be very flat. At 1000 Hz, the solid sample exhibited the same initial reduction and subsequent stabilization characteristic as it did for capacitance. However, at the higher frequencies, the plots for the solid insulated sample were flat and lower than the foam skin plot. The lower attenuation levels at the higher frequencies may be explained by the fact that the foam skin conductors are smaller than their solid counterparts, and, therefore, the paired conductors would be closer together. At higher frequencies, skin and proximity effects would increase attenuation values of foam skin conductors over those for the larger solid conductors, and would also tend to override the impact of capacitance variations on attenuation observed at 1000 Hz.

Figure 2A

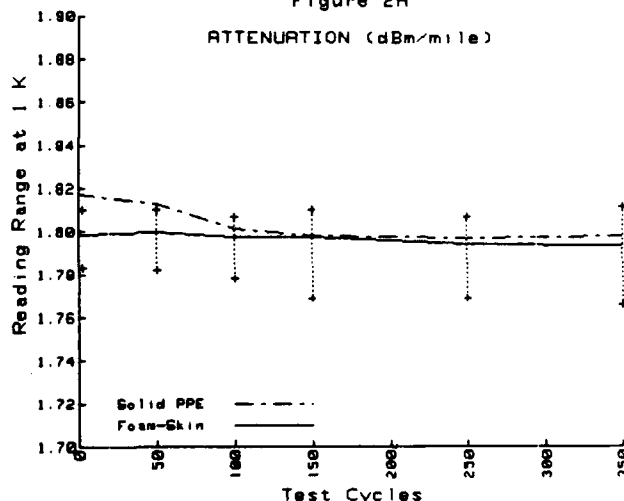


Figure 2B

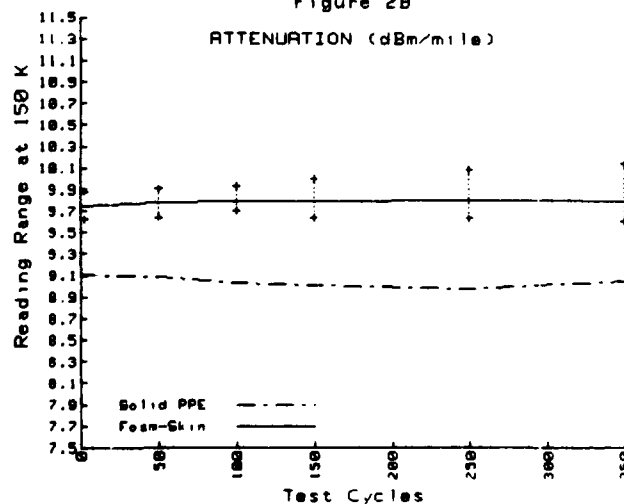
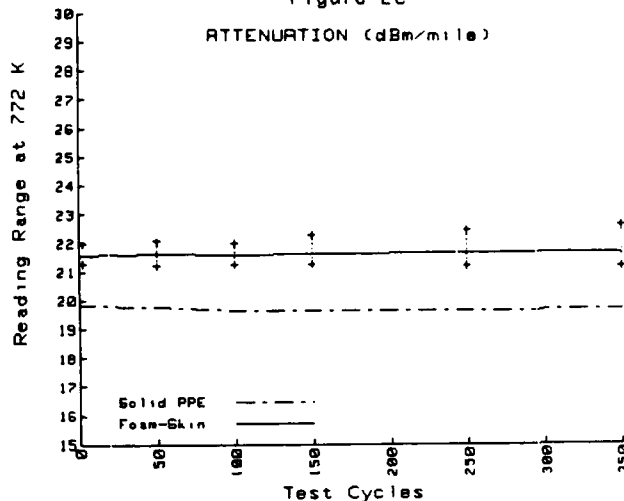


Figure 2C



The impedance plots (Figures 3A, 3B and 3C) for the foam-skin composite average impedances were also very flat. The solid insulated sample exhibited a slightly increasing trend from the initial values, reaching a stable level at near 150 test cycles. This agrees closely with the changes in the capacitance data and may be explained by the inverse relationship of capacitance and characteristic impedance in the transmission line formulas. The difference in impedance levels between the solid and foam-skin data can be attributed to conductor size, as with the above analysis for attenuation.

Figure 3A

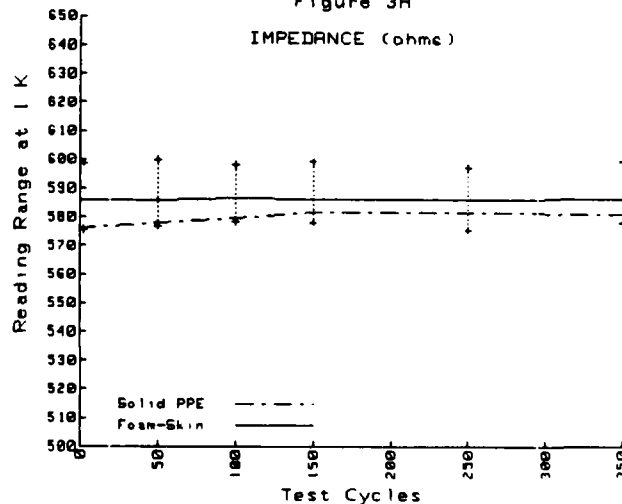


Figure 3B  
IMPEDANCE (ohms)

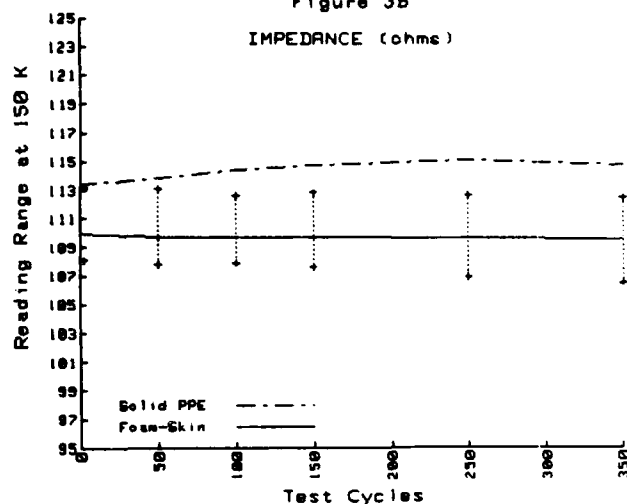
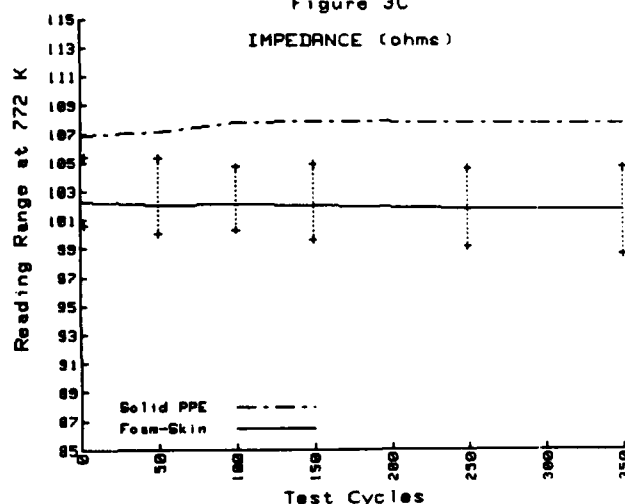


Figure 3C

IMPEDANCE (ohms)



### CONCLUSIONS

In reviewing past investigations into the long-term stability of petrolatum-based filled foam and foam skin cable in aerial installations, much support can be found in laboratory testing at elevated temperatures and in field trials. The results of this study sustain that trend, demonstrating additionally, with the six different manufacturers represented, that the industry can produce high-temperature drip-resistant petrolatum-based filled foam-skin cables which exhibit stable electrical characteristics when exposed to the temperature fluctuations of aerial installations. This and past studies demonstrate that foam-skin cables filled with petrolatum-based filling compound are appropriate for aerial installations.

### Acknowledgements

Appreciation is due to D. Butler for the many measurements performed and to E.W. Riley for consultation.

### References

1. Windeler, A.S. "Polyethylene Insulated Telephone Cable", Bell System Technical Journal, Volume 32, 1953.
2. Dean, N.S. "The Development of Fully-Filled Cables for the Telephone Distribution Network", 17th Annual Wire and Cable Symposium, 1968.
3. Metcalf, E.D. "Cellular Insulation as an Answer to Material Conservation", 23rd IWCS, 1973.
4. Metcalf, E.D. "New Developments in Filled Cables", Anaconda Engineering Bulletin EB52-0, 1977.
5. Gouldson, E.J. Farago, M., Baxter, G.D. "Foam-Skin, a Composite Expanded Insulation for Use in Telephone Cables", 21st IWCS, 1972.
6. Verne, S., Pinching, A.A., Haggard, J.M.R. "Long-Term Stability of Fully Filled Cables", 22nd IWCS, 1973.
7. Pritchett, J., Mather, E.L., Verne, S. "Fully-Filled Telephone Cable with Cellular Polyethylene Insulation After 10 Years Service", 24th IWCS, 1975.
8. Eoll, C.K. "The Aging of Filled Cable with Cellular Insulation", 27th IWCS, 1978.
9. Mangaraj, D., Biskeborn, M.C. Kiss, K.D. "The Effect of Filling Compound Migration on Cellular Insulation", 27th IWCS, 1978.
10. Foord, S.G. "Compatibility Problems in Filled Cellular Polyolefin Insulated Telephone Cables", 22nd IWCS, 1973.
11. Tenzer, M. and Olszewski, J.A. "Analysis of Long Term Stability of Expanded Insulations in Filled Cables", 28th IWCS, 1979.
12. Molleda, L.M. and Used, E. "Filled Cable for Aerial Installation", 25th IWCS, 1976.

13. Beach, S.M., Bullock, K.R. and Cretney, D.F. "The Properties of Cellular Polyethylene Insulated Filled Communication Cable and Its Increasing Use", 24th IWCS, 1975.

14. Parker, R.D. and Tarwater, R.W. "Analysis of the Long Term Performance of Expanded Insulation in Waterproof Cable", 30th IWCS, 1981.

15. Garmon, J.P. and Davis, L.E. "A Comparison of the Properties of Foam and Foam-Skin Insulation in Filled Cables", 28th IWCS, 1979.



Gene Samuelson is a Senior Electrical Engineer in charge of the Electrical Laboratory at the Telecommunications Product Engineering Center for the Anaconda Wire and Cable Company. He received his B.S.E.E. degree from Iowa State University at Ames, Iowa in 1969. He served the U.S. Navy as a Civil Engineer Corps Officer and worked with Bendix Corporation in Kansas City as a Test Equipment Engineer, before accepting his current position.

TABLE 2

		CAPACITANCE (nF/mile)					
Designation	Freq	REF	50	Test Cycles			
				100	150	250	350
PPE SOLID at	1 K	83.50	82.90	82.20	81.80	81.70	81.80
FS MAX at	1 K	82.50	82.20	81.80	82.00	82.20	82.50
FS AVG at	1 K	81.85	81.17	80.92	80.95	80.78	80.73
FS MIN at	1 K	79.40	79.70	79.90	79.60	79.70	79.30
FS Sigma at	1 K	1.195	1.015	.8200	.9566	1.032	1.176
PPE SOLID at	150 K	83.50	83.00	82.20	81.80	81.90	81.80
FS MAX at	150 K	82.40	82.20	81.80	81.90	82.10	82.50
FS AVG at	150 K	80.90	81.12	80.93	80.93	80.75	80.82
FS MIN at	150 K	79.40	79.70	79.90	79.60	79.70	79.70
FS Sigma at	150 K	1.179	.9980	.7967	.9004	.9247	1.068
PPE SOLID at	772 K	83.50	83.00	82.40	81.90	81.80	82.00
FS MAX at	772 K	82.60	82.30	81.90	82.00	82.20	82.50
FS AVG at	772 K	81.00	81.22	81.05	81.05	80.82	80.95
FS MIN at	772 K	79.40	79.70	80.00	79.70	79.80	79.80
FS Sigma at	772 K	1.230	1.050	.8118	.9094	.9663	1.060
		ATTENUATION (dBa/mile)					
Designation	Freq	REF	50	Test Cycles			
				100	150	250	350
PPE SOLID at	1 K	1.817	1.813	1.801	1.790	1.797	1.790
FS MAX at	1 K	1.810	1.800	1.805	1.800	1.805	1.810
FS AVG at	1 K	1.798	1.800	1.798	1.798	1.794	1.794
FS MIN at	1 K	1.783	1.784	1.780	1.771	1.771	1.768
FS Sigma at	1 K	.0091	.0094	.0093	.0134	.0123	.0143
PPE SOLID at	150 K	9.104	9.090	9.030	9.013	8.975	9.049
FS MAX at	150 K	9.003	9.067	9.097	9.964	10.05	10.11
FS AVG at	150 K	9.740	9.776	9.792	9.792	9.798	9.798
FS MIN at	150 K	9.619	9.670	9.741	9.673	9.670	9.648
FS Sigma at	150 K	.0957	.0772	.0609	.1010	.1312	.1599
PPE SOLID at	772 K	19.82	19.70	19.65	19.65	19.68	19.70
FS MAX at	772 K	21.96	21.93	21.80	22.10	22.32	22.49
FS AVG at	772 K	21.56	21.65	21.62	21.66	21.68	21.70
FS MIN at	772 K	21.27	21.36	21.42	21.44	21.37	21.35
FS Sigma at	772 K	.2026	.2424	.1960	.2911	.3442	.4127
		IMPEDANCE (ohms)					
Designation	Freq	REF	50	Test Cycles			
				100	150	250	350
PPE SOLID at	1 K	575.8	576.1	579.8	581.8	581.6	581.4
FS MAX at	1 K	590.0	590.5	596.0	597.0	596.0	590.4
FS AVG at	1 K	586.1	585.8	586.7	586.4	586.3	586.0
FS MIN at	1 K	575.6	578.4	579.8	579.7	577.2	580.1
FS Sigma at	1 K	9.255	8.569	7.665	7.763	8.020	8.145
PPE SOLID at	150 K	113.4	113.0	114.4	114.7	115.1	114.7
FS MAX at	150 K	113.2	112.0	112.3	112.5	112.3	112.1
FS AVG at	150 K	110.0	109.7	109.7	109.7	109.6	109.5
FS MIN at	150 K	100.1	100.1	100.2	107.9	107.2	106.0
FS Sigma at	150 K	1.925	1.725	1.551	1.606	1.704	1.763
PPE SOLID at	772 K	106.9	107.1	107.0	107.9	107.0	107.0
FS MAX at	772 K	105.4	105.0	104.4	104.6	104.3	104.4
FS AVG at	772 K	102.3	102.0	102.1	102.0	101.0	101.0
FS MIN at	772 K	100.6	100.3	100.6	99.90	99.40	98.90
FS Sigma at	772 K	1.077	1.700	1.450	1.659	1.665	1.036

## A PRACTICAL SINGLE-MODE SYSTEM, 50 km AT 140 Mbit/s

M.J. GIBSON

P. MORRIS

A. CARTER

BICC, PRESCOT

PLESSEY  
NOTTINGHAMPLESSEY  
(CASWELL)ABSTRACT

This paper gives details of a fully engineered single-mode optical fibre system between Liverpool and Preston, England. The installation of cable will start in September 1983 and be completed in December 1983 with the line equipment following shortly afterwards with the complete system ready for service in early 1984. This contract was undertaken as a commercial venture. Its completion will show that single-mode systems are ready for inclusion in trunk telecommunications networks with a minimum of special treatment. The cable, which contains eight step-index fibres, will be laid in standard ducts with an average joint spacing approaching 2 km. The fibres are to be spliced using a specially developed arc welder which automatically aligns the fibres and attains a low average splice loss. A fibre cutter is used which can consistently achieve fibre end-angles of less than  $0.5^\circ$ . The 140 Mbit/s line equipment includes single-mode stripe lasers and PIN-FET detector modules operating at 1300 nm. From the available power ratio given by these devices equipment margins are subtracted, for variation of the devices with temperature and time and for equipment imperfections, which gives a gross cable budget including maintenance allowances. This budget will allow the operation of the system without an intermediate repeater.

INTRODUCTION

The single-mode system being installed between Liverpool and Preston, England (Fig.1) will be one of the first of its type in the world. Single-mode systems are rapidly becoming a standard part of the trunk telecommunications network in the U.K. and the completion of this route will demonstrate the arrival of these systems as a practical reality.

Telecommunications traffic will be intercepted at Ormskirk, roughly half-way along the route but it is intended to couple the two halves temporarily to evaluate the system's performance, without regeneration, over the full 50 km. The information gained from this exercise will show what are the practical limits to the length of current systems.

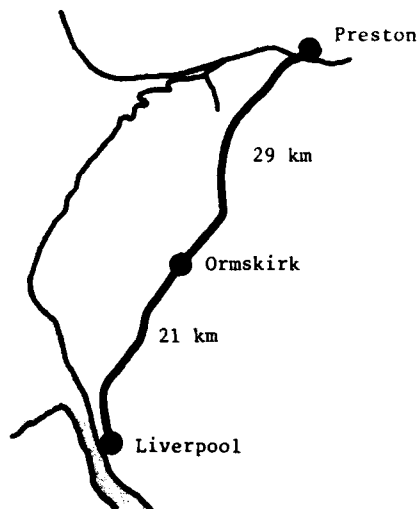


Figure 1. Cable Route.

CABLE DESIGN

The cable consists of eight fibres loosely laid in tubes and six insulated copper conductors stranded around an insulated steel strength member. Paper tapes are then wrapped around this structure and a polyethylene sheath and aluminium moisture barrier applied over the tapes (Fig.2).

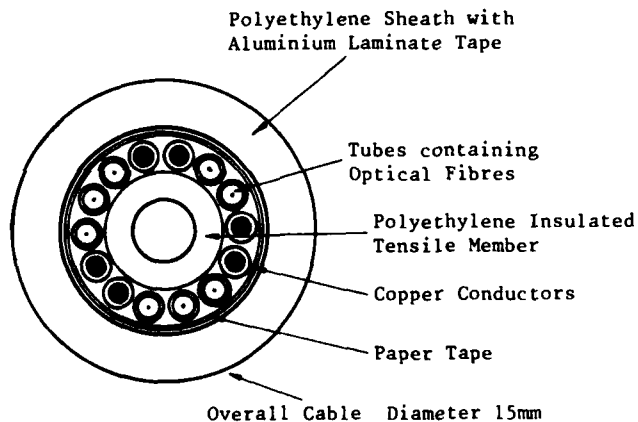


Figure 2. Cable Cross Section.

This design gives the fibre protection from strain which can cause microbending and affect the fibres long-term mechanical properties. The strain margin which gives this protection is determined by the tube size and the lay length. The margin is designed to be 0.8% which means that during installation the fibre undergoes no strain until the cable strain exceeds this figure. A further amount of strain is permitted to reach the fibre during installation but it is carefully ensured this is not exceeded.

The size of the central steel tensile member is determined by the cable weight. Its strength is such that even when the cable is subjected to a maximum installation tension equal to three times the cable weight per kilometre the fibre is not excessively strained. The weight of the cable is 214 kg/km so tensions in excess of 6000 Newtons could be used.

The copper pairs are used for the provision of pressure alarms and engineering speaker circuits.

The whole of the cable sub-system is designed to be pressurised with a constant head system.

#### SINGLE MODE FIBRE

The single-mode fibres have been produced by the outside vapour deposition process. The fibre consists of a germania-doped silica core surrounded by a pure silica deposited cladding whose outside diameter is 125  $\mu\text{m}$ . The fibre is coated to a diameter of 250  $\mu\text{m}$  with UV-cured acrylate resin which is mechanically strippable. During manufacture the fibre is proof tested to a level which determines what are the acceptable levels of strain during and after its installation.

When describing single-mode it is usual to discuss the mode field radius rather than the core size which is relatively difficult to measure. The mode field radius or spot size is dependent on design of the fibre, i.e. its refractive index profile, and the wavelength of measurement. These fibres have a spot size of 5  $\mu\text{m}$  at the nominal operating wavelength of 1300 nm (Fig.3).

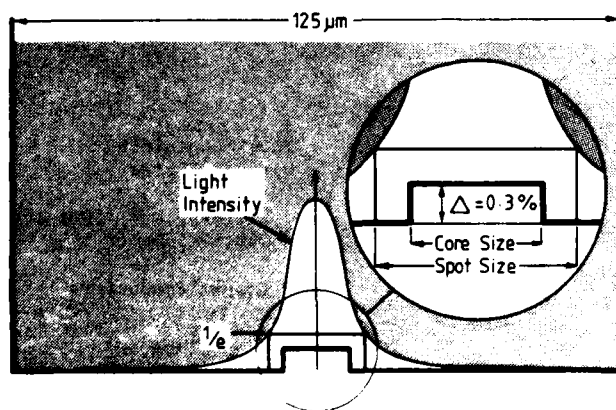


Figure 3. Core and Spot Size.

A significant amount of the light travels in the cladding region adjacent to the core and for this reason the quality of this inner cladding is very important. The diameter of this region is about 60  $\mu\text{m}$ .

The core size and refractive index difference ( $\Delta$ ) have been carefully chosen to strike a balance between low splice losses and low bending losses while still producing a wavelength of zero dispersion that is compatible with the intended operational wavelength. A large spot size is desirable for good splicing losses but this means having a low refractive index difference which gives rise to higher bending losses. The waveguide dispersion which is adjusted to balance material dispersion at the zero dispersion wavelength is a function of the refractive index profile so this must be taken into account to give adequately low values over the range of operational wavelengths. The balance achieved means that no bending loss is observable in these fibres as in the 1300 nm region due to the bends imposed upon them by cabling and jointing. Furthermore it has been shown that adequately low splice losses of about 0.2 dB can be readily achieved.

The dispersion in the operational wavelength region which is specified to be 1275 to 1325 nm is well below the required 6 ps/km/nm.

The attenuation of all fibres used on this route is below 0.5 dB/km.

#### CABLE ROUTE

The cable route between Liverpool-Preston was previously occupied by a large coaxial cable which has been removed and the ducts renovated or rebuilt where necessary. A detailed summary was made of the route in order to enable an accurate cable allocation to be made and so minimise wastage. Manhole to manhole distances were logged and those unsuitable for jointing noted. The figures from the survey were entered into a computer programme which produced a matrix of the possible lengths of cable that could be installed. Once the manufactured lengths from the factory were known these could be matched to make the most efficient use of the available cable.

#### CABLE ALLOCATION

Detailed information of the cable route was taken from large scale maps of the cable route and directly logged into a computer programme which after taking into account bends, gradients and duct conditions, estimated the required pulling in tension to install the cable between the jointing points already determined in the survey. The length was curtailed whenever the maximum manufactured cable length (2.2 km) or the maximum allowed tension (4500 Newtons) were exceeded.

In straight sections it was predicted that lengths well beyond 2 km could be cabled in one haul. This computer programme has not been verified in practice but it is intended to install and monitor several lengths to determine its accuracy.

Using this programme only as a rough guide cables have been allocated to the whole route and give a planned average joint spacing of 1.9 km.

#### CABLE INSTALLATION

Installation of these optical fibre cables requires little special equipment. The cable is drawn in with a rope attached to the cable via a mechanical safety linkage and swivel (Fig. 4). The former contains a pin which is designed to shear at 4500 Newtons and so prevent excessive tension being applied to the cable while the swivel protects the cable from torsion. This equipment has a diameter slightly greater than the cable and so effectively clears the path. It is clamped to the central steel member of the cable which takes all the load and the whole assembly is sealed with a heatshrink sleeve.

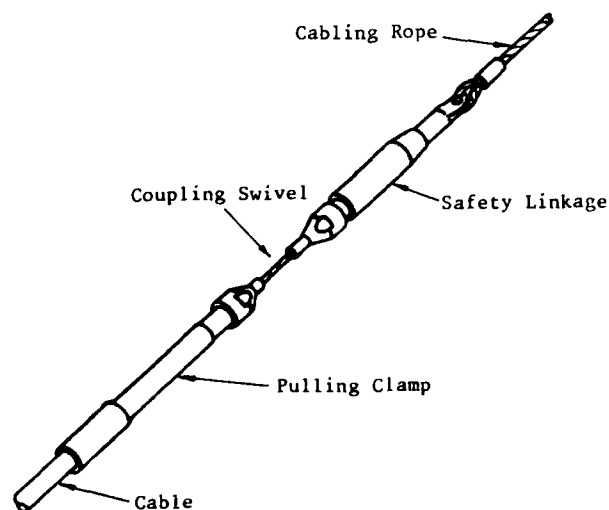


Figure 4. Cable Pulling-In Arrangement.

Particular care must be taken that the cable is not pulled round sharp bends under tensions and where this would occur the cable is pulled out, fletted and drawn in again. Where necessary light hand pulling on the sheath is carried out but the maximum recommended tension is 300 Newtons.

During installation some lengths will be drawn in with an active drawrope which will monitor the installation tension throughout the operation. The rope, which contains copper wires, takes readings from a strain gauge, located at the safety linkage,

to the winch where they are logged into a computer. These will be compared with the predicted tensions and used to improve the computer model.

After installation each cable is pressurised until it is jointed in order to provide some protection and warning of any damage to the sheath.

#### CABLE AND FIBRE JOINTING

The cable closure is formed by injection welding polyethylene end-caps to the sheath of the cables. A 100 mm diameter polyethylene sheath is welded to the end caps in order to complete the closure. Inside the closure is held the chassis which forms the framework to hold the fibre splices and conductor joints (Fig. 5). A external contactor is fitted to the alternate joints and wired to the pressure alarm circuit. A 3 to 4 metre loop of cable is left on either side of the joint for maintenance purposes.

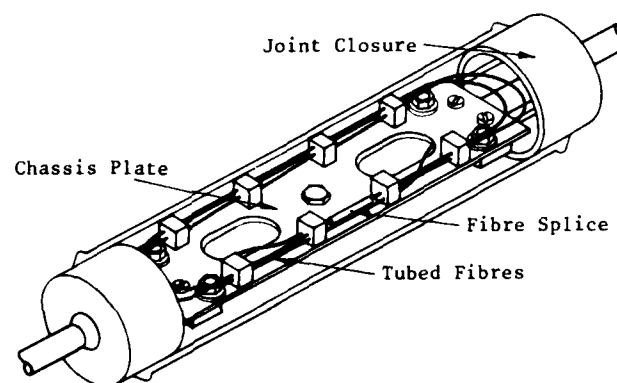


Figure 5. Joint.

The jointing is performed on a specially designed work bench upon which the monomode fibre welder and joint closure are mounted. This bench can be fitted to the manhole furniture if jointing takes place inside a manhole or surface box or can be free standing for jointing above a manhole. About 2 metres of cable is stripped down and this amount of tubed fibre can be looped inside the joint meaning that several attempts can be made at jointing fibres and there is easy movement of the completed splice between the welder and the joint. The copper conductors are jointed on the underside of the chassis and the electrical continuity of the moisture barrier and steel tensile member are maintained.

The fibres are spliced using a microprocessor controlled electric arc welder. The tube is cut back to expose the coated fibre and the coating is removed from 75 mm of fibre which is then cleaved. The fibre is curved slightly under tension and nicked with a diamond cutter. This causes a crack to propagate across the fibre and yield an almost perfectly perpendicular surface free from chips or hackle. It is essential that the angle of the fibre end-face is no more than 0.5° since this will give

a poor splice. The cutter used is capable of this most of the time but care must be taken to detect the occasional poor end. This is either detected visually using the welder microscope or by the failure to make a good splice. The only solution is to recut the end.

After cutting both fibres they are held in V-grooves on the welder and roughly aligned by sight using stepper motors while the fibres are only a short distance apart. Accurate alignment is accomplished automatically by monitoring and optimising the light through the fibres. Light is injected on one side about 20 mm from the end of a fibre and detected at the same distance on the other side. The fibres are then butted together manually before the automatic welding sequence begins.

The fibres are then separated a short distance and given a short pre-fusion arc after which the fibres are pushed together during the main fusion arc's operation and over-fed a precisely controlled amount. The completed weld is checked for its quality visually and, while data is being gathered, its attenuation will also be monitored using the cut-back technique.

Once the jointer is satisfied with the weld it is carefully transferred to the front of the welder where the weld is placed in an aluminium channel which grips the tubing on either side of the splices and gives complete mechanical protection. After potting the assembly is transferred to the joint closure where the excess tubing is carefully coiled and clipped to the chassis before the aluminium splice housing is clipped in place on the centre of the chassis.

Experience so far shows that the optical jointing part of the operation can be completed in a period of less than three hours. If this is accomplished the whole joint may be completed in one day but it is prudent to allow up to two days because of the time taken in setting up a normal joint in manholes on busy roads or in wet conditions.

#### CABLE TERMINATIONS

The cable termination unit or racksplitter is a factory made unit which is jointed to the main route cable in exchanges. This joint is a standard joint and requires no special treatment. The unit consists of a length of 8 fibre cable which runs from the termination joint to a resin block which is mounted above the equipment rack position. The resin block contains no fibre joints and is used to gas seal the cable and as a mechanical support where the 8 single fibre leads are split from the main cable (Fig. 6). Separate electrical wires are also brought out here. The single fibre leads are re-inforced PVC tubes in which the fibre runs loosely to the connectors. The leads are four metres long and ensure full interchangeability of all fibres.

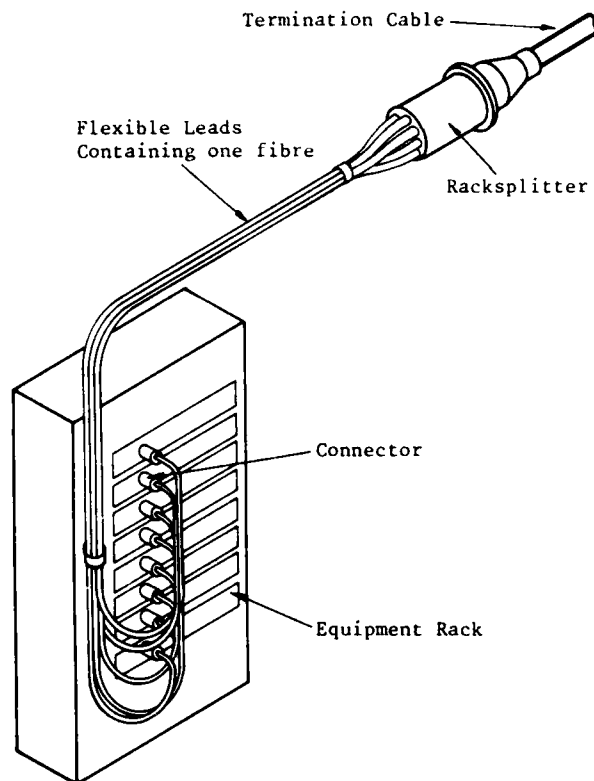


Figure 6. Termination Arrangement.

The optical connectors are high performance precision ferrules plugs which give a loss of less than 1 dB. In order to minimise connector losses a cable containing 8 fibres with a very low average spot concentricity error was chosen to use in the manufacture of the racksplitters.

#### CABLE SUB-SYSTEM PERFORMANCE

The two main criteria for judging the performance of optical fibres are their attenuation and dispersion. The latter is a function of the fibre design and manufacture, operating linewidth and length. These factors are out of the hands of the cable manufacturer once the fibre is received. It is therefore of much more concern to minimise attenuation by careful cable design and manufacturing, jointing and termination.

Increase in attenuation due to cable manufacture and installation is undetectable so that the fibre attenuation as received is that as installed. Jointing losses depend upon the intrinsic losses which depend upon the fibre and

extrinsic losses which depend upon how well the splice is made. By careful control of both these factors an average joint loss of less than 0.2 dB has been attained. This means a cable sub-system budget can be compiled as shown in Table 1.

	dB
Fibre Loss (0.45 dB/km)	22.5
Splice Losses	4.5
Connector Losses	1.5
TOTAL CABLE LOSS	28.5

Table 1  
Estimated Losses for a 50 km Cable Section

A computer simulation of the contribution made by spot concentricity error predicted that its contribution to splice loss would have a maximum average value of 0.02 dB when the fibres are simply aligned visually with no use of power monitoring.

Since the attenuation will vary with wavelength in the range 1275 to 1325 nm which is the operating window some account must be taken of this effect. In our experience this variation has a average swing of 0.4dB/km between the highest value at 1275 nm and the lowest value around 1310 nm.

Dispersion also varies with wavelength and to ensure it stays within the systems budget for 50 km at 140 Mbit/s the dispersion must be less than 4 ps/km/nm on average. This figure relies heavily on the actual operational wavelength but should be met comfortably within the operational wavelength range.

#### OPTOELECTRONIC DEVICES

The optoelectronic devices perform a crucial role in the overall link operation. The laser diode source must be stable, reliable, capable of fast modulation and launch significant optical power into the monomode fibre. The detector must be reliable and highly sensitive to the incoming radiation. Taken together, the laser launch power and receiver sensitivity define the gross allowable loss budget of the system.

#### THE LASER SOURCE MODULE

Both source and detector elements are fabricated in the compound semi-conductor GaInAsP lattice matched onto InP substrates. This material can be grown for emission at any wavelength between 0.95 and 1.65  $\mu\text{m}$ ; in this case 1.3  $\mu\text{m}$  is chosen to match the loss and dispersion minima of the fibre.

High performance double heterostructure stripe geometry laser chips are utilised in this system (1); such devices can couple power levels of over 1 mW into the fibre and have optical switching times of less than 1.5 ns. Lasing threshold current is typically 120 mA-150 mA, with a differential slope efficiency of 30% per facet above threshold.

The laser chip is mounted in an optical module which efficiently couples the light from the laser into the fibre. Typically 20 mA current pulses are required to give the normal peak optical power of -2 dBm or 630  $\mu\text{W}$ . Also contained within the module are thermo-electric coolers, which are necessary to stabilise the chip temperature near 25°C even with a case temperature of 65°C, and a photodiode which monitors the rear facet output of the laser for control purposes.

#### THE PIN-FET DETECTOR MODULES

The PIN detector photodiodes are grown with a bandgap corresponding to 1.65  $\mu\text{m}$ , giving a device with a high responsivity between 1 and 1.65  $\mu\text{m}$ , which can be used in either current 1.3  $\mu\text{m}$  or future 'third window' systems at 1.55  $\mu\text{m}$ .

The PIN detector diodes are packaged in a hybrid assembly with a GaAs FET preamplifier ('PIN-FET'). This configuration gives a very low input capacitance together with low noise amplification, resulting in a very high sensitivity receiver. Module construction is fully hermetic and epoxy free for high stability and reliability. The receivers are specified to tolerate optical power levels as low as -44 dBm (RZ) for a  $10^{-9}$  bit error rate at the coded line rate for 140 Mbs PCM transmission.

#### OPTICAL LINE EQUIPMENT

##### LINE TERMINAL EQUIPMENT (LTE)

The terminal equipment consists of 7 cards and 2 power supply units housed in one 8V.U. shelf of the British Telecom equipment practice TEPIE. A further 4V.U. shelf is used for cable access and ventilation.

The transmit path consists of 3 cards, 2 of which perform the function of C.M.I. decoding, scrambling, 5B6B encoding and data rate changing and a third card containing the transmit optical

interface. This card contains the laser, its driver, and the circuitry required for controlling the laser temperature, threshold current and mean power output along with their associated alarm and protection circuits. These alarms and the output of the on-board line error monitor may be taken to an optional line supervisory system which uses the optical fibre as a telemetry path for the precise location of intermediate regenerator faults on multi regenerator systems.

The receive path again consists of 3 cards, 2 of which perform the inverse function of the transmit side with the addition of jitter reduction. The third card is the receive optical interface which contains a PIN/FET detector to detect the incoming light, an equaliser, clock extraction, data threshold detection and retiming circuitry. This card also contains a line error monitor which again feeds the optical supervisory system.

The remaining card in the LTE is the alarm card which collects together the error and fault signals from the logic cards, displays them and drives station alarm buses. The laser alarms are displayed separately on the transmit optical interface, this allows for full alarm facilities at intermediate repeater stations which utilises 2 transmit interface cards and 2 receive interface cards interconnected to form a bi-directional regenerator.

Further options which may be fitted to the LTE are recorder and telemetry cards. The recorder enables detailed logging of system performance via a digital interface to the CCITT V28 (R5232) standard. The telemetry card exploits redundancy in the line code to provide a terminal to terminal 64 kb/s ancillary data link.

#### SYSTEM PERFORMANCE

The system has been designed to operate with an error rate of better than 1 in  $10^9$ . The system budget is shown in Table 2.

Mean Transmitted Output Power	-6 dBm
Receiver Sensitivity for 1 in $10^9$	-44 dBm
Gross System Budget	38 dB
Allowance for Temperature Ageing and Production Tolerance	6 dB
Cable Attenuation and Connector Loss	32 dB

Table 2  
Optical System Power Budget

From this budget it is apparent that there is no additional operating margin and therefore this distance represents the maximum which is practically realisable at present. Greater distances could be achieved if the transmitted output power were to be increased, however this would incur optical safety problems. The present system meets Class 1 Laser product limits with the exception of certain multiple failures.

#### REFERENCE

- (1) "A comparison of simple stripe geometry and advanced structure 1.3  $\mu$ m GaInAsP lasers for 140 Mb/s Monomode Optical Communication Systems" A.C. Carter et al, European Conference on Optical Communication, Cannes 1982.



M.J. Gibson,  
BICC Telecommunication Cables Limited,  
P.O. Box 1,  
PRESCOT,  
Merseyside,  
L34 5SZ.

Michael Gibson is a Senior Systems Engineer with BICC Telecommunication Cables Limited where he has worked since 1977. He has been involved in the design and development of optical fibre components and more recently in the engineering of optical fibre systems, specializing in single-mode systems. He graduated with an Honours degree in Physics at Imperial College, London University.

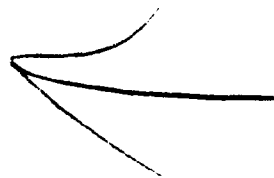
A. Carter,  
Allen Clarke Research Centre,  
Plessey Research (Caswell) Limited,  
Caswell,  
TOWCESTER,  
Northants.  
NN12 8EQ.

In 1973 he received the Honours degree in Physics from the University of Oxford at which he continued as a post-graduate student, researching the infra-red properties of impurities in semiconductors, receiving the D. Phil. degree in 1977. Since then he has been employed at Plessey Research (Caswell) Limited researching into optoelectronic devices for fibre optic communications, including LEDs, lasers and monolithic integrated devices. He has also been extensively involved in the design of electronic circuits for fibre optic equipment, including transimpedance receivers, LED drivers and stabilised laser transmitters.



P. Morris,  
Plessey Telecommunications Limited,  
Beeston,  
NOTTINGHAM,  
NG9 1LA.

Joined the Transmission Division of Plessey in 1970 working on 24 and 30 channel PCM multiplexing and signalling equipment. In 1975 he moved to the copper line system development group and in 1978 took charge of the optical fibre line system development. He is presently the manager responsible for digital optical line systems development at Beeston.



## PERFORMANCE CHARACTERISTICS OF VAD SINGLE MODE FIBERS IN MASS PRODUCTION BASIS

H. Sato, H. Kanamori, N. Yoshioka, M. Kyoto, M. Nishimura,  
S. Suzuki, M. Watanabe, S. Kato, T. Kuwahara

Sumitomo Electric Industries, Ltd.  
1, Taya-cho, Totsuka-ku, Yokohama 244, Japan

Abstract

The results of investigations on the VAD single mode fibers, fabricated in mass production basis, are presented. In performance characteristics of the VAD single mode fibers operated at  $1.3\mu\text{m}$ , the low transmission loss could be achieved by improvements on the VAD process and dehydration process. The median and minimum of the transmission losses of the single mode fibers were  $0.42\text{dB/km}$  and  $0.32\text{dB/km}$  at  $1.3\mu\text{m}$ , respectively. Satisfactory properties were also obtained for the other characteristics, cut-off wavelength, spot size, dispersion, and fiber geometrical parameters. These results are chiefly attributed to the successful developments of the high reproducibility of the VAD preforms with a sufficient longitudinal uniformity. The length dependences on transmission characteristics of long-spliced single mode fibers are also discussed, and the additive properties of transmission loss and dispersion are confirmed.

1. Introduction

Single mode fibers are attractive transmission media for long-repeater-section and high-bit-rate communications. Therefore, many efforts have been focused on improving the production process of those fibers, and fabrications of them have been already established successfully through several methods such as VAD<sup>[1]</sup>, MCVD<sup>[2]</sup>, OVD<sup>[3]</sup>, and PCVD<sup>[4]</sup> in the research and development stages or trial production. Especially, the VAD method has made a dramatic progress within a late few years and obtained satisfactory productivity and performance characteristics. Furthermore, this method shows us the possibilities of continuous operation and high-speed synthesis of porous soot preforms. However, still now, enough knowledge can not be obtained about the performance of the mass produced VAD fibers. This report presents some performance characteristics of those fibers.

2. Preform and fiber fabrication

Porous soot preforms for the VAD single mode fibers were synthesized by oxyhydrogen flame. For

the purpose of constructing a single mode structure, thin core soot of  $\text{SiO}_2\text{-GeO}_2$  and thick cladding soot of  $\text{SiO}_2$  were formed simultaneously by multiple burners through which the raw materials were fed with combustion gases. The outer diameter of soot preform was about  $100\text{mm}$ . The ratio of synthesized cladding diameter to core diameter of the transparent glass rod was around 8.0. The schematic diagram of the VAD process is shown in Fig. 1.

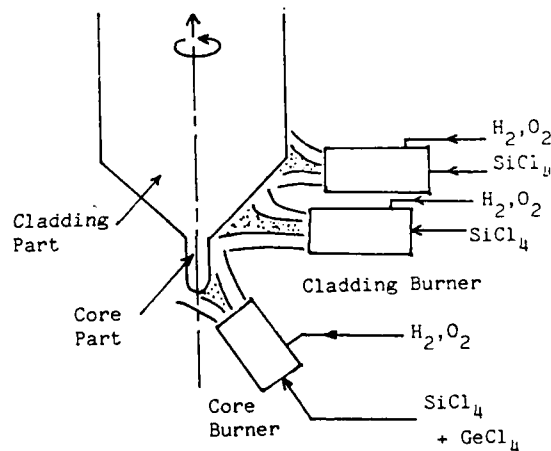


Fig. 1 Schematic diagram of VAD process

The soots preforms were dehydrated and sintered into glass rods. The rods were elongated into thinner rods and jacketted with silica tube so as to satisfy a specification. Fibers were drawn from a silica-jacketted preform and coated by silicone resin primarily and by nylon secondarily. The fiber structure is shown in Fig. 2.

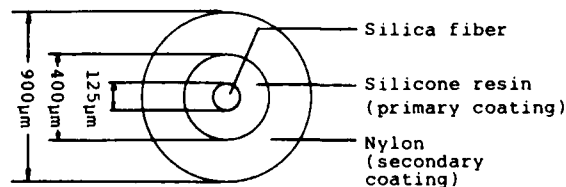


Fig. 2 Structure of doubly coated optical fiber

A typical refractive index profile of the preform is shown in Fig. 3. The refractive index difference was 0.3%.

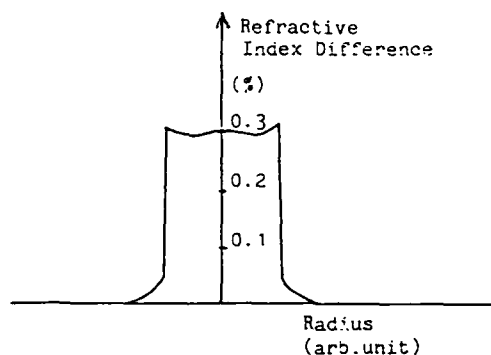


Fig. 3 Refractive index profile of a VAD single mode fiber

### 3. Measurements

Fiber parameters were measured by the following methods:

- (i) A transmission loss was measured by using a cut-back reference method.
- (ii) A cut-off wavelength was measured by bend measurements on a 2m length of fiber.
- (iii) A refractive index profile was measured by using an interference microscope or a preform analyzer.
- (iv) A spot size was measured by using NFP or FFP technique.
- (v) A chromatic dispersion was measured by using a fiber Raman laser.
- (vi) Geometrical parameters were measured by using microscope with a electrical micrometer.

### 4. Performance characteristics of single mode fibers

In order to realize the longer repeater section of more than 20km and the higher bit-rate transmission of more than 400Mb/s, the following characteristics are required for single mode fibers:

- (1) Low transmission loss
- (2) Small tolerance in cut-off wavelengths
- (3) Small tolerance in spot sizes
- (4) Small core eccentricity
- (5) Low dispersion

In this section, the good achievements concerning the above five items are discussed for the single mode fibers.

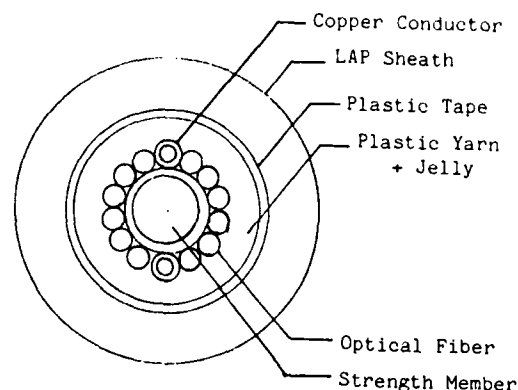


Fig. 4 Structure of layer type cable

And the transmission characteristics of long spliced single mode fibers which are embedded in the layer type cable shown in Fig. 4 are discussed.

#### (1) Transmission loss

The high reproducibility of low loss VAD single mode fibers was realized by two remarkable progresses. One was the progress of dehydration technique. And the other progress was made on the synthesizing technique. By this technique cladding layer could be thick enough to prevent the OH contamination from jacketing silica tubes. Fig. 5 shows the composite plots of spectral loss curves of 65 fibers. The residual OH absorption loss at  $1.39\mu\text{m}$  was 1.0dB/km on the average. Fig. 6 shows the distribution of transmission loss at  $1.3\mu\text{m}$  for randomly sampled 1500km VAD secondary coated fibers. The medium and minimum loss were 0.42dB/km and 0.32dB/km, respectively. This minimum loss was the same as the value estimated by Rayleigh scattering loss.

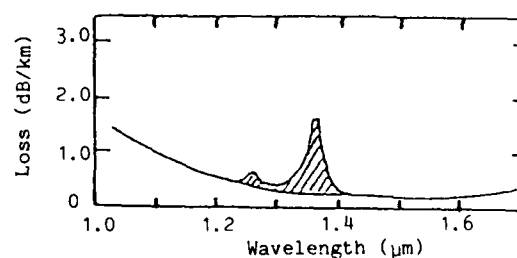


Fig. 5 Spectral loss curves of 65 fibers

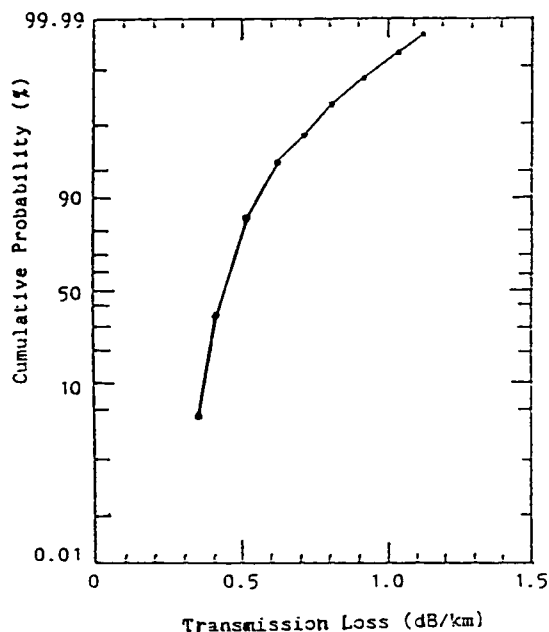


Fig. 6 Distribution of transmission loss at  $1.3\mu\text{m}$  of secondary coated fibers

## (2) Cut-off wavelength

A cut-off wavelength of single mode fibers depends mainly on core diameter and refractive index difference. The specified refractive index differences were obtained by a precise control of raw materials flow rates. The distribution of the cut-off wavelengths for randomly sampled 1500km VAD secondary coated fibers is shown in Fig. 7. This figure illustrates a normal distribution centered at  $1.19\mu\text{m}$ .

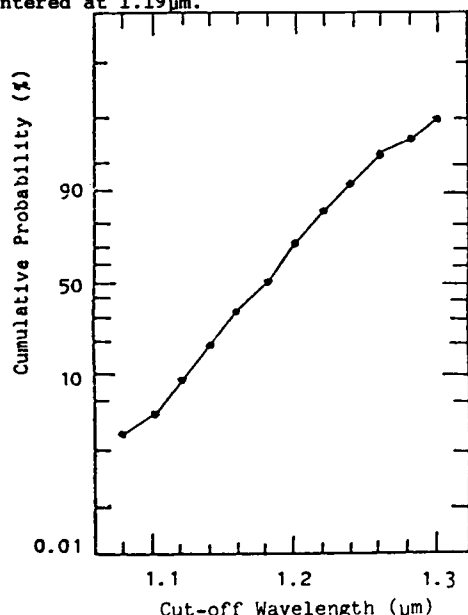


Fig. 7 Distribution of cut-off wavelength of secondary coated fibers

## (3) Spot size

The spot size of single mode fibers depends mainly on refractive index difference. In order to adjust the spot size, it is important to control precisely the flow rate of the raw material in the VAD process. The distribution of the spot size for the randomly sampled 1500km VAD secondary coated fibers is shown in Fig. 8.

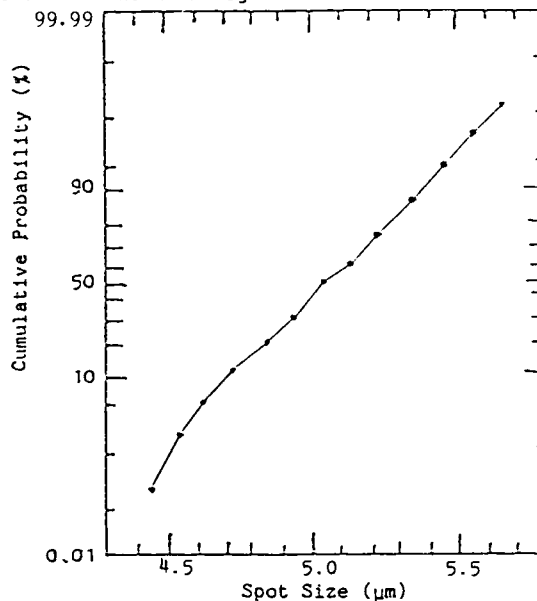


Fig. 8 Distribution of spot size of secondary coated fibers

## (4) Fiber geometrical parameter

The measured values of the cladding diameter and core ellipticity of the fibers perfectly met to the general specifications of those parameters which were  $125\pm 3\mu\text{m}$  and less than 10%, respectively. The core eccentricity of the VAD fiber is mainly dependent on the clearance between the VAD glass rod and the inner wall of the silica tube. The reduction of the clearance has been achieved by the improvements on silica tube jacketing technique. Fig. 9 shows the distribution of the core eccentricity for the randomly sampled 1500km VAD secondary coated fibers.

## (5) Dispersion characteristics

A measurement of the dispersion characteristics by fiber Raman laser is shown in Fig. 10. The zero dispersion wavelength depends on both spot size and cut-off wavelength. In order to obtain the lower dispersion, it is important to design the fiber specification appropriately.

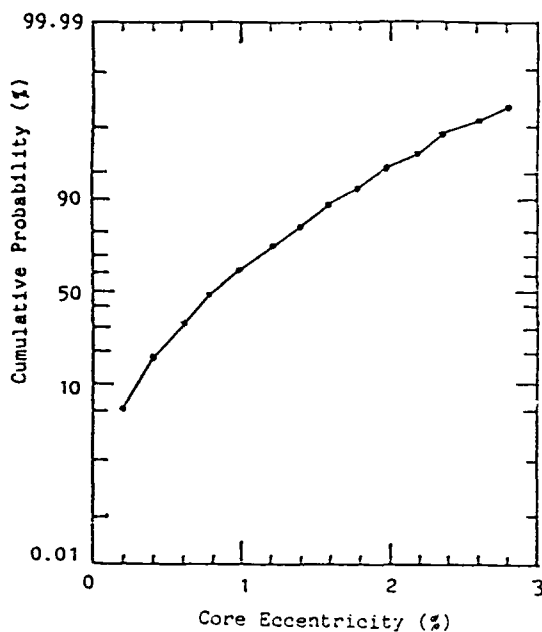


Fig. 9 Distribution of core eccentricity  
Core eccentricity is defined as follows:

$$\text{Core Eccentricity} = \frac{\sqrt{(t_1 - t_2)^2 + (s_1 - s_2)^2}}{\text{outer diameter (125}\mu\text{m)}} \times 100(\%)$$

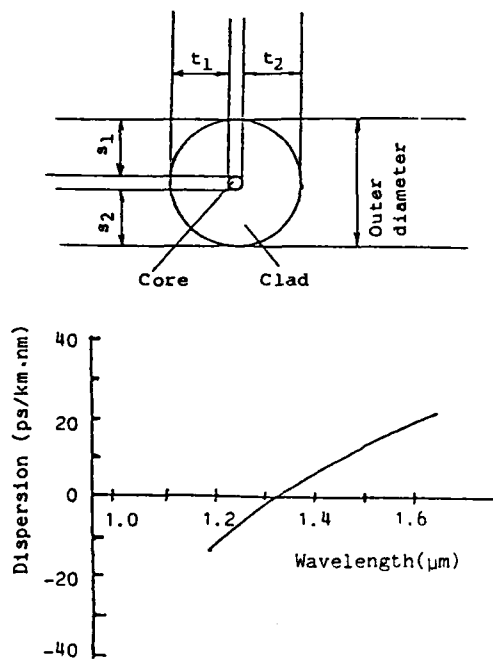


Fig. 10 Measurement of dispersion characteristics

Histogram of the zero dispersion wavelength is shown in Fig. 11

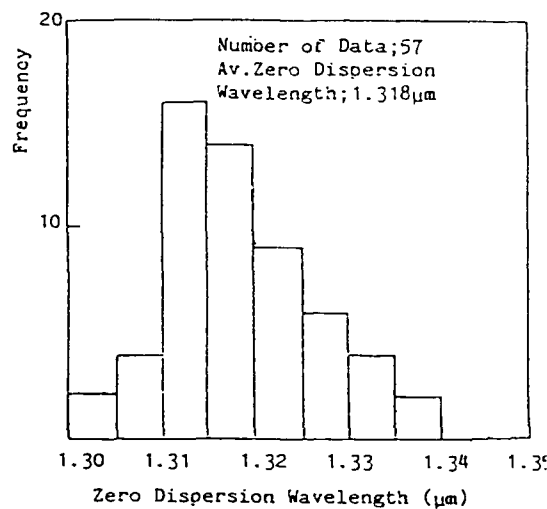


Fig. 11 Histogram of zero dispersion wavelength

#### (6) Transmission characteristics of long spliced fiber

In order to confirm the additive properties of the transmission losses and dispersions, we constructed long spliced single mode fiber links using the selected fibers which are embedded in two 2km-length cables. A cable structure is described in Fig. 4. The transmission losses in each manufacturing process are shown in Table 1. It is found that the intrinsic transmission losses of the VAD single mode fibers are not impaired after cabling process. Fig. 12 (a) shows the measured results on

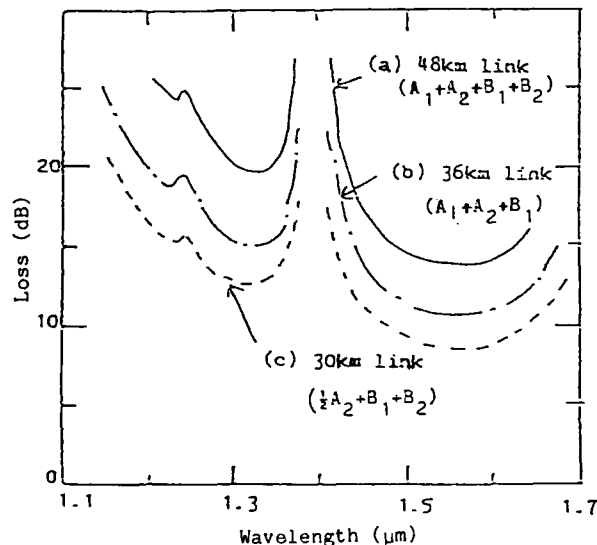


Fig. 12 Spectral loss curves of 48km link(a), 36km link(b) and 30km link(c)

the spectral loss curve of 48km link. The transmission losses including splicing losses at 23 points were 20.0dB/48km at 1.3 $\mu$ m and 14.0dB/48km at 1.55 $\mu$ m. Fig. 12 (b) shows the spectral loss curve of 36km link. The losses of 15.2dB/36km at 1.3 $\mu$ m and 10.6dB/36km at 1.55 $\mu$ m were measured. Because the average splicing loss was 0.075dB/1 splice, the loss of 48km link was estimated to be 19.7dB by summing the losses of 24 fibers shown in Table 1 and measured splicing losses. Therefore, it can be concluded that the transmission loss shown a sufficient additive property in the case of single mode fibers.

The chromatic dispersion was also investigated. The chromatic dispersions of the selected 24 secondary coated fibers before cabling are shown in Table 2. After cabling, six 2km-unit-length fibers are spliced into four pieces of 12km long links. The measured chromatic dispersions of the fibers are also shown in Table 2.

In a 48km spliced fibers link, the measured dispersion by LD direct modulation is 2.13ps/km $\cdot$ nm, which is in good agreement with the average dispersion of 24 fibers (2.21ps/km $\cdot$ nm) on taking measuring accuracy in account. Therefore, it can be concluded that the chromatic dispersion characteristics show an additive property and can be expressed as the following equation

$$\bar{D} = \frac{\sum D_i \cdot l_i}{\sum l_i}$$

where  $\bar{D}$ : Dispersion of a long spliced fiber  
 $D_i$ : Dispersion of i-th fiber  
 $l_i$ : Length of i-th fiber

Table 1 Transmission losses of the selected 24 secondary coated fibers before and after cabling

Cable	Fiber No.	before cabling	after cabling
A	1	0.34	0.44
	2	0.38	0.45
	3	0.35	0.35
	4	0.36	0.35
	5	0.33	0.39
	6	0.38	0.38
	7	0.33	0.35
	8	0.55	0.55
	9	0.36	0.35
	10	0.40	0.47
	11	0.39	0.42
	12	0.35	0.34
	Average	0.38	0.40
B	1	0.36	0.36
	2	0.35	0.33
	3	0.35	0.35
	4	0.41	0.35
	5	0.32	0.34
	6	0.35	0.31
	7	0.34	0.33
	8	0.38	0.34
	9	0.43	0.38
	10	0.38	0.37
	11	0.35	0.33
	12	0.39	0.37
	Average	0.37	0.35

The zero dispersion wavelengths are shown in Table 3. The average zero dispersion wavelength (1.314 $\mu$ m) is also in agreement with the average value (1.314 $\mu$ m) calculated from the zero dispersion wavelengths of original long fibers from which the 2km-unit-length of fibers in the cables were obtained.

Table 2 Dispersions of the selected 24 secondary coated fibers before cabling and 4 links after cabling.

(ps/km $\cdot$ nm, at 1.29 $\mu$ m)

Cable	Fiber No.	before cabling	after cabling
A	1	2.1	2.30
	2	2.2	
	3	2.2	
	4	1.6	
	5	2.5	2.20
	6	2.7	
	7	2.1	
	8	1.9	
	9	2.6	
	10	2.7	
	11	2.1	
	12	2.1	
	Average	2.23	2.25
B	1	2.1	2.20
	2	2.6	
	3	2.2	
	4	1.6	
	5	1.6	1.89
	6	2.1	
	7	2.1	
	8	2.5	
	9	2.5	
	10	2.7	
	11	2.1	
	12	2.1	
	Average	2.18	2.05

Table 3 Zero dispersion wavelengths of spliced fiber links

Name of 12-km spliced fiber	Zero dispersion wavelength ( $\mu$ m)
A <sub>1</sub>	1.316
A <sub>2</sub>	1.315
B <sub>1</sub>	1.315
B <sub>2</sub>	1.311
Average	1.314

## 5. Conclusion

The improvements of the VAD single mode fibers at the research and development stages have been successfully applied to the mass-producing of the single mode fibers. Consequently, it was proved that the mass-produced VAD single mode fibers had satisfactory transmission characteristics for a practical use. The VAD method is the most promising technique for a great demand for optical fiber cables in the near future.

## References

- [1] M. Hoshikawa et al., "Current status of VAD fiber: Process and Performance" 27A2-3 '83 IOOC
- [2] J. Irven et al., "Single mode fiber reproducibility" Proceedings of 7th IOOC '81
- [3] G.E. Berkey et al., "Single-mode fibers by the OVD process" Technical digest of OFC '82
- [4] Bachmann et al., "Recent Progress in the Preparation of GI-and SM-fibres by means of the PCVD process" Post-deadline paper Technical Digest of '83 IOOC



Hisao Sato  
Sumitomo Electric  
Industries, Ltd.  
1, Taya-cho, Totsuka-ku,  
Yokohama, Japan

Hisao Sato was born in 1953 and received a M.S. degree from Tokyo University in 1979. He joined Sumitomo Electric Industries, Ltd. in 1979, and has been engaged in research and development of optical fiber fabrication. He is an engineer of optical fiber plant of optical division, and is a member of Chemical Society of Japan.



Hiroo Kanamori  
Sumitomo Electric  
Industries, Ltd.  
1, Taya-cho, Totsuka-ku,  
Yokohama, Japan

Hiroo Kanamori was born in 1956 and received a M.S. degree from Tokyo Institute of Technology in 1981. He joined Sumitomo Electric Industries, Ltd. in 1981 and has been engaged in research and development of optical fiber fabrication. He is a member of the Physical Society of Japan.



Naoki Yoshioka  
Sumitomo Electric  
Industries, Ltd.  
1, Taya-cho, Totsuka-ku  
Yokohama, Japan

Naoki Yoshioka was born in 1950 and received a M.S. degree from Osaka University in 1975. He joined Sumitomo Electric Industries, Ltd. in 1975, and has been engaged in research and development of optical fiber fabrication. He is a member of a Institute of Electronics and Communication Engineers of Japan.



Michihisa Kyoto  
Sumitomo Electric  
Industries, Ltd.  
1, Taya-cho, Totsuka-ku,  
Yokohama, Japan

Michihisa Kyoto was born in 1949 and received M.S. in 1975 in Kyoto University. He joined Sumitomo Electric Industries, Ltd. in 1978, and has been engaged in research and development of optical fiber fabrication. He is a member of Chemical Society of Japan



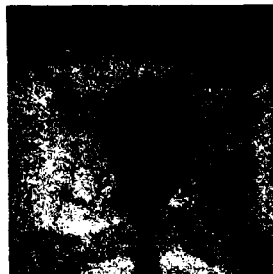
Minoru Watanabe  
Sumitomo Electric  
Industries, Ltd.  
1, Taya-cho, Totsuka-ku,  
Yokohama, Japan

Minoru Watanabe was born in 1946 and received a Ph.D. degrees in chemistry from Kyoto University in 1977. He joined Sumitomo Electric Industries, Ltd. in 1977, and has been engaged in research and development of optical fiber fabrication. He is a senior engineer of Yokohama Research and Development Department and is a member of the Institute of Electronics and Communication Engineers of Japan, the chemical Society of Japan, the Japan Society of Applied Physics and the Ceramic Society of Japan.



Masayuki Nishimura  
Sumitomo Electric  
Industries, Ltd.  
1, Taya-cho, Totsuka-ku,  
Yokohama, Japan

Masayuki Nishimura was born in 1956 and received a M.S. degree from Tokyo University in 1981. He joined Sumitomo Electric Industries, Ltd. in 1981, and has been engaged in research and development of optical fiber characterization. He is a member of the Institute of Electronics and Communication Engineers of Japan.



Shuji Kato  
Sumitomo Electric  
Industries, Ltd.  
1, Taya-cho, Totsuka-ku,  
Yokohama, Japan

Shuji Kato was born in 1948 and received the B.E. degree from Tokyo University in 1971. He joined Sumitomo Electric Industries, Ltd. in 1971, and has been engaged in the fiber optic engineering. He is now a senior engineer of Fiber Optics Division and is a member of the Institute of Electronics and Communications Engineers of Japan.



Shuzo Suzuki  
Sumitomo Electric  
Industries, Ltd.  
1, Taya-cho, Totsuka-ku  
Yokohama, Japan

Shuzo Suzuki received a M.S. in 1972 from Tokyo University. He joined Sumitomo Electric Industries, Ltd. in 1972, and has been engaged in research and development of optical fiber and cable. He is a member of the Institute of Electronics and Communication Engineers of Japan.



Toru Kuwahara  
Sumitomo Electric  
Industries, Ltd.  
1, Taya-cho, Totsuka-ku,  
Yokohama, Japan

Toru Kuwahara was born in 1948 and received a M.S. degree from Tohoku University in 1973. He joined Sumitomo Electric Industries, Ltd. in 1973, and has been engaged in research and development of superconducting cables millimeter waveguides, and optical fibers. He is a senior engineer of optical fiber plant of fiber optics division and is a member of the Institute of Electronics and Communications Engineers of Japan.



## RECENT DEVELOPMENTS IN MINI-UNIT CABLE

Mr. Derek Lawrence  
Dr. Peter Bark

Siecor Corporation  
Hickory, NC

The Mini-Bundle™ cable design was introduced two years ago as a high fiber density design. Data was presented on developmental cables and a first installation.<sup>1,2</sup> Since that time more than 30,000 km of fiber has been cabled using the design. Applications have included duct, aerial and direct buried as well as special designs including underwater. Performance data obtained in the field and in the lab are reported for these cables of various designs. Splicing procedures are addressed. The extension of the design to single mode fibers is described and the versatility is demonstrated by examples of special cables.

#### Introduction

The number of fiber optic cable installations has exploded over the last couple of years. The selection of cable designs has been based on cable performance, ease of manufacture, long lifetime expectancy and ease of installation. One additional factor, which is now emerging due to the large volume and widespread installations, is the area of cable design versatility and universality.

It is necessary to have cable design concepts which are versatile in the following areas:

- 1) Wide range of fiber counts
- 2) Various fiber types
- 3) All-dielectric possibility
- 4) Variable tensile ratings
- 5) Armored sheath options

At the same time it is a major advantage if the above versatility can be achieved with a single universal design concept. The Mini-Bundle cable is such a design. In particular, this design provides an all-dielectric option and single mode capability. Other high fiber count cable designs have been found unsuitable for single-mode fibers and necessitated the development of a very different design. Similarly, the all-dielectric versions have not been readily achievable. This has led to the undesirable situation of very different cable designs for single-mode versus multi-mode cables and all-dielectric versus metal containing cables. Mini-Bundle cable offers the

major advantage that only one basic set of procedures is necessary to install and splice the cable no matter which of the various options are required. The hardware remains basically the same and craftspeople only have to learn one technique. This should be recognized as a major factor by operating companies as the volume increases.

#### Basic Cable Design

The Mini-Bundle design is an extension of the well-proven loose buffer design principle.<sup>1</sup> The major advantages of the design in the area of fiber stress/strain and transmission stability are well documented.<sup>2,3</sup> In this design multiple fibers, each with an acrylate coating of 250  $\mu$ m are arrayed together loosely inside a plastic buffer tube (Figure 1). The tube is filled with a special moisture-resistant compound. The required number of these mini-unit buffer tubes are stranded around a central anti-buckling element of steel or fiberglass epoxy. A composite sheath of tensile reinforcing material and plastic jacket complete the construction. An additional steel tape armor and outer jacket can provide additional mechanical protection if required (Figure 2). The number of fibers per tube can be varied over a wide range (up to 12). The tube size itself can also be optimized.

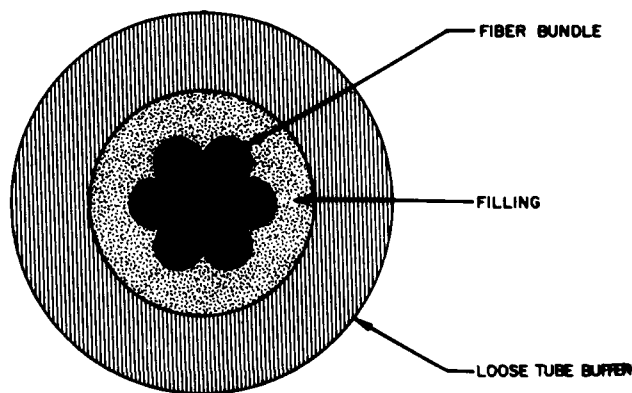


FIGURE 1: MINI-UNIT BUFFER TUBE

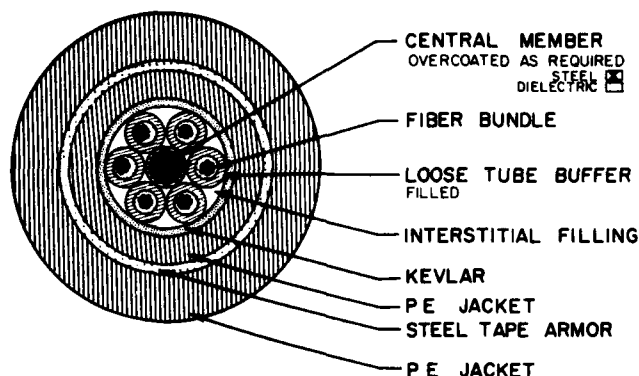


FIGURE 2: 36-FIBER MINI-BUNDLE CABLE  
DOUBLE JACKET - STEEL TAPE ARMOR

The performance of the Mini-Bundle cable design is well predictable from the following basic equations:

- (i) Fiber bending stress  $\sigma$

$$\sigma = E \frac{d_f}{2R}$$

$E$  = Young's Modulus Glass

$d_f$  = Fiber diameter

$R$  = Fiber bend radius

The minimum fiber bend radius is determined from the allowable bending stress.

- (ii) Buffer stranding pitch  $P$

$$P = \sqrt{2\pi^2 D' \left( R - \frac{D'}{2} \right)}$$

$D'$  = Pitch circle diameter (for buffer tube).

- (iii) Tension/contraction window  $\epsilon_t/\epsilon_c$

Solving

$$P^2(\epsilon^2 - 2\epsilon) = \pi^2 W(2D' \pm W) = 0$$

$W$  = Fiber to buffer tube clearance

- (iv) Tensile Behavior

$$\epsilon_{c'} = \epsilon_s + \epsilon_c + \epsilon_f$$

$\epsilon_{c'}$  = Cable elongation (Total)

$\epsilon_s$  = Cable construction stretch

$\epsilon_f$  = Fiber elongation (allowable)

$\epsilon_c$  = Tensile window

$$\epsilon_f + \epsilon_c = \frac{L}{\sum_{m=1}^n E_m A_m}$$

$E_m$  = Young's Modulus of Material  $m$   
 $A_m$  = Cross Section of Material  $m$

- (v) Temperature Behavior

$$\Delta T = \frac{\epsilon_c}{\alpha_1 + \frac{\alpha_2 - \alpha_1}{1 + \left( \frac{E_1 A_1}{E_2 A_2} \right)}}$$

$\Delta T$  = Temperature change

$\alpha$  = Temperature coefficient of material  
(e.g.,  $\alpha_1$  = central member,  
 $\alpha_2$  = cable plastics)

Precisely controlled manufacturing processes enable the theoretical behavior to be translated into actual cable performance. Typical cable specifications are shown in Figure 3.

FIBERS (TYPICAL)	36	48	72	144
*WEIGHT (KG/KM)	135/215	170/255	260/355	310/425
*MAX DIAMETER (MM)	13.5/16	15/17.5	18.5/21	20.5/22.5

OPERATING TEMPERATURE (°C)	-40 to +70 Aerial -30 to +60 Underground
TENSILE DURING INSTALLATION (N)	1300, 2700 Standard Up to 6500 Optional
*BEND RADIUS (MM) FREE INSTALLATION	100/200 200/200
*CRUSH RESISTANCE (TYPICAL)	600/750 N/CN
*IMPACT RESISTANCE (TYPICAL)	50 x 3 Nm/200 x 5 Nm
*FLEX RESISTANCE (TYPICAL)	1000/100

\*NOTE: SINGLE JACKET/DOUBLE JACKET - STEEL TAPE ARMORED

FIGURE 3: SIECOR MINI-BUNDLE CABLE  
SPECIFICATIONS (TYPICAL)

### Testing

An extensive test program has been undertaken to initially fully characterize the cable design and performance and, on an on-going basis, to confirm the performance of Mini-Bundle cables. The mechanical properties of tensile, crush, impact and flexing together with high and low temperature performance are confirmed on a sampling basis for production cables.

The increasing volume of product and larger fiber counts have necessitated the development of multiple-fiber computer controlled measurement equipment. The equipment is shown in Figure 4. Each transmitter block consists of eight LED's and eight v-groove fiber holders to launch the light into the fiber. The receiver blocks are similar with a photodiode replacing the LED. Special mandrels are provided to allow steady state conditions to be achieved by a multiple turn mandrel wrap for each fiber. The

transmitter and receiver blocks are connected to a switching module with a power level indicator. The computer controls the switching modules through an interface bus. The output devices for the computer are a CRT, a digital plotter and a teletype printer.

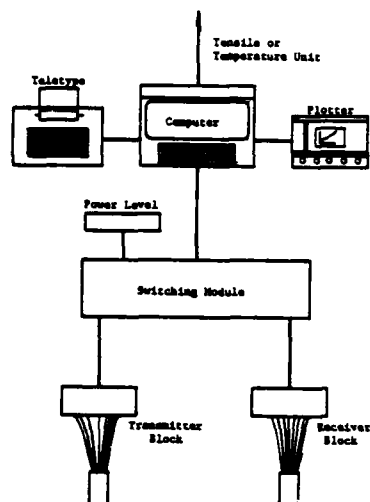


FIGURE 4: COMPUTER CONTROLLED MEASUREMENT SYSTEM

The computer is connected with an interface bus to the piece of test equipment to be controlled. In most cases this is either the temperature chamber or the long length tensile tester (Figure 5). With appropriate software, once the test has been set up, the entire procedure is computer controlled. Extensive temperature cycling of cable can be achieved with an output as shown in Figure 6A. Similarly, tensile test results are obtained as in Figure 6B.

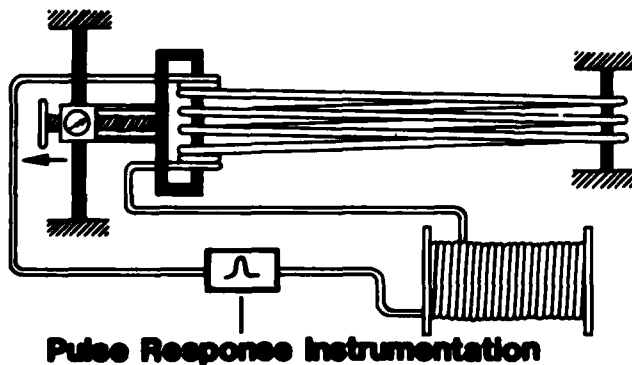


FIGURE 5: LONG LENGTH TENSILE TESTER

WAVELENGTH: 875 NM		FIBER		$\Delta\alpha$ IN DB/KM	
TEST TEMP IN °C: 23 -30 60		1°C		-30 60	
1	0.1	0.1	0.1	0.1	0.1
2	0.2	0.2	0.2	0.2	0.2
3	0.0	0.1	0.1	0.1	0.1
4	-0.1	0.2	-0.1	-0.1	-0.1
5	-0.1	0.2	0.0	0.0	0.0
6	0.0	0.3	0.0	0.0	0.0
7	0.1	0.1	0.2	0.2	0.2
8	0.0	0.3	0.1	0.1	0.1

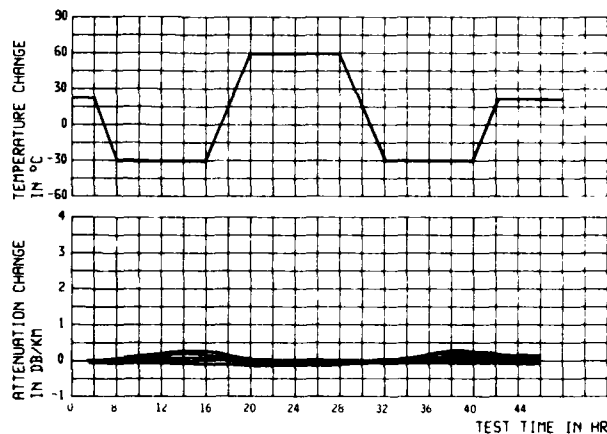


FIGURE 6A: TYPICAL TEMPERATURE RESULTS

GAUGE LENGTH: 6 X 21 = 126 M		FIBER		$\Delta\alpha_{avg}$	$\Delta\alpha_{f=0}$
TENSION VELOCITY: .20		1		-0.1	0.0 DB/KM
WAVELENGTH: 875 NM		2		-0.1	-0.0 DB/KM
STRAIN OF CABLE/FIBER		3		-0.1	0.0 DB/KM
$\epsilon_c (F=0.5 \text{ Fmax}) = 0.167$		4		0.2	0.0 DB/KM
$\epsilon_c (F=1.0 \text{ Fmax}) = 0.301$		5		0.0	-0.1 DB/KM
$\epsilon_c (F=0.5 \text{ Fmax}) = 0.101 \times 1000M$		6		-0.2	-0.0 DB/KM
$\epsilon_c (F=0) = 0.050$		8		0.0	-0.0 DB/KM
$F (L_p=0.330) = M$				0.2	-0.0 DB/KM
$\epsilon_c (F=1.0 \text{ Fmax}) = M$					
$\epsilon_c (F=0) = M$					

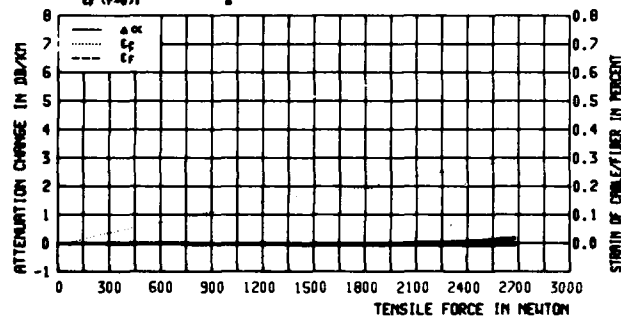


FIGURE 6B: TYPICAL TENSILE RESULTS

### Field Experience

In the last two years more than 30,000 fiber kilometers in cable have been manufactured for over 20 different installations. Cable has been installed and is successfully operating in all geographical areas of the country using all installation methods. Fiber counts most commonly from 24 to 72 have been installed, spliced and put into operation. Duct, aerial, direct buried, trenched and vertical installations have all been successfully implemented.

Mini-Bundle cable has required no special handling techniques beyond compliance to the tensile and minimum bend radius specifications. Standard tensile ratings of 2700N (600 lbs.) are normal. Handling of 2-3 km continuous lengths

is routine. The tensile ratings are conservative and in certain circumstances it has been necessary to exceed the rating significantly and no fiber degradation was observed.

The splicing of Mini-Bundle cable using the fusion process has proven to be a fast and efficient method. A special splice tray (Figure 7) enables the fibers to be handled individually. The buffer tube is terminated upon entry into the tray. Excess fiber loops allow for future splice remakes in the unlikely event that they are necessary. The splice region itself is fully protected in the plastic module which is filled with an RTV silicone. The splice trays when completed are conveniently accommodated in a universal thermoplastic enclosure which may be filled with a re-enterable encapsulant as necessary.

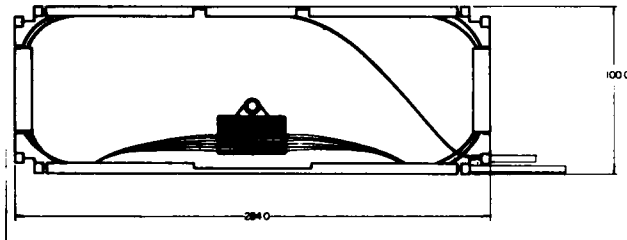


FIGURE 7: SPLICE TRAY

Several installations have involved very low loss cables with installed and spliced attenuations in the region of 1 dB/km at 1300 nm.

#### Options

The versatility of the design has been demonstrated with the development of several options.

An all-dielectric version of the product involves the substitution of a fiberglass-epoxy rod for the central steel wire normally used (Figure 8). Additional Kevlar reinforcing is utilized to maintain capability and specifications equal to the steel-containing version. No measurable diameter change is observed.

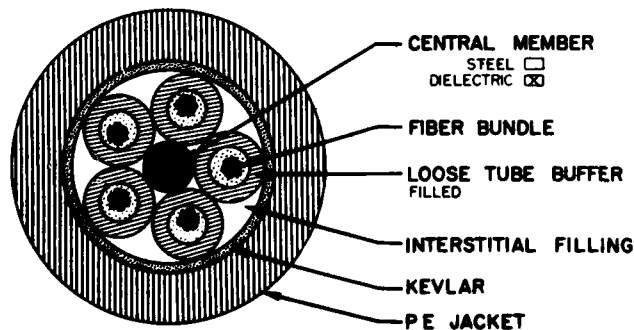


FIGURE 8: 30-FIBER MINI-BUNDLE CABLE ALL-DIELECTRIC

A teflon/steel tape armor (Figure 9) sheath over an inner jacket has been developed to provide extra protection to cable subjected to steam. Limited cable surface exposure to steam temperatures of up to 150°C is possible with this construction.

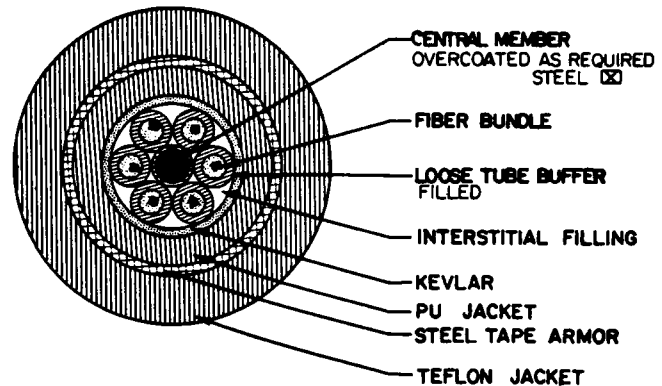


FIGURE 9: 36-FIBER MINI-BUNDLE CABLE STEAM RESISTANT

A cost-reduced underwater cable has been manufactured for river and lake crossings to supplement land based systems (Figure 10). The construction involves less expensive materials than the submarine cable previously reported on.<sup>1</sup>

A two-by-two version of the Mini-Bundle cable design has been developed using 500 µm coated fibers instead of the normal 250 µm coating (Figure 11). The large buffer tubes are stranded in a quad configuration with two anti-buckling elements. The unique application of this cable required that the coated fibers be accessed in the middle of the cable. The buffer tubes had to be removed for a short section without damaging or breaking the fibers which necessitated a special tool. A discrete plug is then applied around the fibers to provide a gas block.

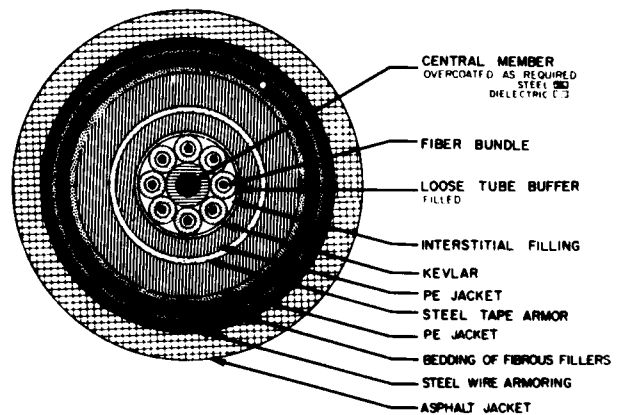


FIGURE 10: 48-FIBER MINI-BUNDLE CABLE UNDERWATER DESIGN

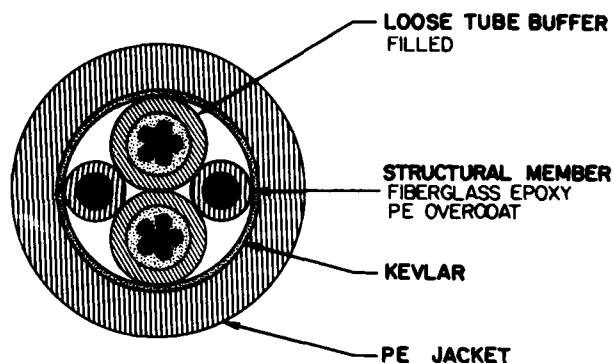


FIGURE 11: 12-FIBER MINI-BUNDLE CABLE  
TWO-BY-TWO DESIGN

#### Single-Mode Applications

The universality of the Mini-Bundle cable design has enabled the large data base gained with multi-mode cables to be used as a foundation for the adaptation to high fiber count, long length single-mode cables.

Several different fiber designs have been evaluated in experimental cables including the two shown in Figure 12.

	<u>Fiber Type A</u>	<u>Fiber Type B</u>
$\lambda$ Cut Off	1100 nm	1100 - 1270 nm
RID	0.4%	$0.3\% \pm 0.5\%$
Core Radius	$3.7 \mu\text{m}$	$4.35 \pm 0.65 \mu\text{m}$

FIGURE 12: SINGLE MODE FIBER DESIGNS EVALUATED

A 26-fiber cable was manufactured using fiber type A. From three to six fibers were assembled in each buffer tube and six buffer tubes were stranded together to form the core. A standard single jacket/Kevlar sheath completed the construction. Attenuation measurements at each stage during manufacturing showed no change. Spectral attenuation measurements of fibers before and after cabling are tabulated in Figure 13. Even in the 1600 nm range there is no evidence of microbending. Temperature tests down to  $-30^\circ\text{C}$  were carried out with no change in attenuation measurable at 1300 nm.

#### ROOM TEMPERATURE ATTENUATION (dB/km)

		<u>Average</u>	<u>2<math>\sigma</math></u>
1200 nm	cable	0.55	0.08
	fiber	0.63	0.11
1300 nm	cable	0.43	0.08
	fiber	0.51	0.06
1500 nm	cable	0.30	0.08
	fiber	0.36	0.05
1600 nm	cable	0.27	0.07
	fiber	0.32	0.06

#### ATTENUATION (dB/km @1300 nm)

	<u>Average</u>	<u>2<math>\sigma</math></u>
Room Temperature	.51	.04
$-20^\circ\text{C}$	.49	.04
$-30^\circ\text{C}$	.52	.03
$+60^\circ\text{C}$	.50	.04

FIGURE 13: EXPERIMENTAL CABLING OF  
SINGLE-MODE FIBERS

The type B fibers shown in Figure 12 have emerged as a standard. In order to confirm that these fibers have appropriate specifications a special five tube cable was manufactured. Eight fibers in the cable were in compliance with the type B specifications. Five additional fibers were deliberately selected to have both a lower cut-off wavelength and a lower refractive index difference than the specifications for type B allows (i.e.,  $<1100 \text{ nm}$  and  $<0.25\%$ ). With this combination the fibers are most sensitive to microbending effects. The results for the cable are shown in Figure 14. The 1300 nm measurements show little or no difference between the eight type B fibers and the 5 low  $\Delta$  - low  $\lambda_c$  fibers at room temperature and at the  $-30^\circ\text{C}$  and  $+60^\circ\text{C}$  extremes. At 1525 nm there is also no measurable difference at room temperature and at  $+60^\circ\text{C}$ . However, at  $-30^\circ\text{C}$  there is some evidence of the microbending edge for the low  $\Delta$ /low  $\lambda_c$  fibers. The type B fibers do not show the same susceptibility. This confirms the importance of the correct selection of the fiber specifications.

The results presented above confirmed the performance of Mini-Bundle cable designs for single-mode fibers. Large scale manufacturing of high fiber count single-mode cables has begun. To date approximately 5000 km of fiber has been cabled in the 40-50 fiber designs as shown in Figure 15. The cables include a twisted pair and have steel tape armoring for extra protection. Cable lengths up to 3 km have readily been manufactured. Some initial cabling results are summarized in Figure 16. In some cables a few

multi-mode fibers are included for special control/communication purposes.

#### TYPE B FIBERS

##### ADB/KM @1300 NM

	AVE	$\sigma$	MAX	MIN
Cable (23°C)	-.03	.04	+.01	-.12
-30°C	+.01	.01	+.02	-.01
+60°C	-.01	.01	+.01	-.03

##### ADB/KM @ 1525 NM

	AVE	$\sigma$	MAX	MIN
Cable (23°C)	-.05	.04	0	-.11
-30°C	+.01	.03	+.05	+.01
+60°C	-.01	.03	+.01	-.05

#### NOTE: AVE FIBER LOSS

@1300 NM	.53 dB/km	( $\sigma$ = .08 dB/km)
@1525 nm	.38 dB/km	( $\sigma$ = .06 dB/km)

#### LOW $\Delta$ - LOW $\lambda_c$ FIBERS

##### ADB/KM @1300 NM

	AVE	$\sigma$	MAX	MIN
Cable (23°C)	-.02	.03	+.01	-.05
-30°C	+.01	.02	+.02	-.03
+60°C	-.01	.02	+.01	-.02

##### ADB/KM @1525 NM

	AVE	$\sigma$	MAX	MIN
Cable (23°C)	-.13	.09	-.01	-.23
-30°C	+.11	.07	+.21	+.07
+60°C	+.02	.05	+.09	-.01

FIGURE 14: CABLE RESULTS TO CONFIRM FIBER SPECIFICATIONS

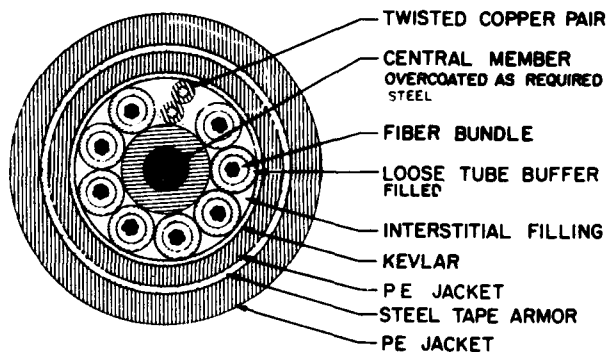


FIGURE 15: MINI-BUNDLE CABLE SINGLE-MODE 40-50 FIBER

The very low losses and low pulse dispersion have enabled transmission over long distances (35 km) and high bit rates (405 Mbits) to be demonstrated. Large scale field installations are underway utilizing this technological capability.

- ATTENUATION  
0.46 DB/KM at 1300 NM  
0.042  $\sigma$
- LONG LENGTH TENSILE TEST  
0.30% CABLE STRAIN AT 3000 N (660#)  
0.0 DB/KM AT 1300 & 1525 NM
- IMPACT  
100 x 3 NM  
NO FIBER BREAK
- CYCLIC FLEX  
>1000 AT 4 X CABLE OD  
170 N TENSION  
NO FIBER BREAK
- CRUSH  
NO  $\Delta$ DB >250 N/CM  
NO RESIDUAL  $\Delta$ DB 750 N/CM

FIGURE 16: INITIAL SINGLE-MODE CABLING RESULTS

#### Conclusions

The Mini-Bundle cable design has proven to be a versatile and universal concept for high fiber count cables. Substantial field experience has been gained and confirmed the results obtained during test programs. Both multi-mode and single-mode fibers can be cabled without impairment to their transmission parameters. The basic concept can be optimized to suit the particular application by appropriate sheath design, central member type and tensile reinforcement.

#### References

1. P. R. Bark, H. M. Liertz, U. Oestreich, G. H. Zeidler. High Fiber Count Cables of the Mini-Bundle™ Design, 30th IWCS 1981, Cherry Hill, NJ, pp. 255-258.
2. P. R. Bark, U. Oestreich, G. H. Zeidler. Stress-Strain Behavior of Optical Fiber Cable, 28th IWCS 1979, Cherry Hill, NJ, pp. 385-390.
3. P. R. Bark, U. Oestreich, G. H. Zeidler. Fiber Optic Cable Design, Testing and Installation Experiences, 27th IWCS 1978, Cherry Hill, NJ, pp. 379-384.



Peter R. Bark

Siemens AG  
Kistlerhofstrasse 174A  
Munich, West Germany

Peter Bark holds a Bachelor of Science degree from the Technical University at Munich. He also received his doctorate in engineering from the same institution in the field of molecular beam physics. He has been employed by Siemens AG in Munich, West Germany, since 1971, in several positions in the telecommunications cable field. His principal assignments were in the field of developing optical cables, interconnecting hardware and subsystems. From 1977 to 1983 Peter Bark was vice-president for Siecor Corporation responsible for engineering and manufacturing. He currently holds a senior management position with Siemens.



Derek O. Lawrence

Siecor Corporation  
610 Siecor Park  
Hickory, NC 28603-0610

Derek Lawrence graduated from the City University, London, with a degree in Communications Engineering. He has been involved in the cable industry since 1970 and from 1975 has worked in optical fiber cable engineering, manufacturing and development. Since 1979 he has been with Siecor Corporation and is currently Engineering Manager.



# MANUFACTURE, LAYING AND SPLICING OF MONOMODE OPTICAL FIBER CABLES WITH LOW LOSSES, AT 1.55 $\mu\text{m}$ .

D. BOSCHER \* - B. NONCLERCQ \* - A. LE BOUTET \* - B. MISSOUT \*\*

\* : CNET-LANNION B-Route de Trégastel - 22301 LANNION - FRANCE  
\*\* : SAT-Direction Technique Câbles-41 rue Cantagrel-75013 PARIS-FRANCE

## ABSTRACT

The use of monomode fibers with losses between 0.3 dB/km and 0.4 dB/km at 1.55  $\mu\text{m}$  has made it necessary to design a cable structure which does not add to the losses of these fibers.

The cylindrical V-grooved rod design protects the fiber from any stress and preserves its initial characteristics prior to cabling, even at 1.55  $\mu\text{m}$ . This technology has made it possible to direct efforts towards the installation of 40 kilometer repeaterless links operating at bit rates of approximately 1 Gbit/s.

This article first sets out to describe the structure of the 10-fiber cable and its manufacture. To minimize splice losses, it was decided to manufacture particularly long cable sections (2500 and 5000 meters).

The second part of this article is devoted to the installation procedures for the different cable sections comprising a link between two cities in western France. Special pulling techniques were adopted to avoid applying excessive stress on the cables.

The on-the-field splicing procedure of this fiber cable featuring the use of a <sup>carbon dioxide</sup> laser welding technique is then described.

Lastly, results of measurements made over this link are presented and analyzed.

## 1 - INTRODUCTION

Fiber optic telecommunications systems are now entering the installation phase. While early field trials seem to be directed towards broadband distribution local applications, the introduction of new services and interactive distribution will require that long-distance high rate links be installed over the next years to come. With this evolution in mind, it appears vital to begin field testing this type of link characterized by a very high transmission rate and extremely long repeater sections. The study and development programs that we have undertaken, are devoted to meeting these future needs.

## 2 - GENERAL DESCRIPTION OF THE PROJECT

In long-distance projects using 1.3  $\mu\text{m}$  multimode fibers elaborated a few years ago, performance targets were necessarily limited :

- digital rate : 140 Mbit/s
- repeater section length : 20 km.

In multimode fibers, these rate and band-pass characteristics are limited by band-pass concatenation problems. While in special laboratory links, the most well adapted fibers may be selected for achieving specific objectives, it is absolutely unthinkable to proceed in the same manner with commercial links where cost, maintenance and installation factors are of vital importance.

As monomode fibers have considerably progressed over the last few years, the use of 1.3  $\mu\text{m}$  or 1.55  $\mu\text{m}$  fibers has become feasible. Despite rate limitations caused in particular by fiber material dispersion and laser rapid modulation difficulties, rather ambitious links are currently being envisioned.

In an effort to test the operational characteristics of the various elements comprising a top-performance long-distance link, the CNET decided to install 11 kilometers of monomode fiber cable on a real scale. Using the loop-back technique, this stretch of cable allows links up to 110 kilometers in length to be tested. The initial targets are :

- 45 kilometers without any repeaters
- 560 Mbit/s
- two multiplexed sections (1.52  $\mu\text{m}$  and 1.56  $\mu\text{m}$ ).

Should these targets appear somewhat reserved in comparison with recent publications (1) (2), it should be noted that :

- this is not a laboratory experiment but a field trial involving a pre-jointed link fitted with its prototype terminal equipment
- the characteristic of this link may be fully maintained for future commercially used installations.

Using this same transmission line, systems operating at 1.7 Gbit/s over the same distance are scheduled to be trial-tested in the spring of 1984. A 100-kilometer link using heterodyne techniques shall be trial-tested by 1986.

## 3 - FIBER CHARACTERISTICS

Two parameters limiting repeater sections are to be considered for determining targets :

- fiber attenuation
- fiber dispersion (material and waveguide).

It was decided to use 1.55  $\mu\text{m}$  fibers with minimum attenuation (individually or in cable assem-

bly) to the detriment of material dispersion which would probably limit the link maximum digital rate. A few tests were conducted using 1.55  $\mu\text{m}$  fibers with a zero dispersion factor. However, during the manufacturing phase of the cables for this link, this technology had not been sufficiently debugged to guarantee the transmission quality required.

The fiber characteristics adopted were as follows :

outer diameter : 125  $\mu\text{m}$   
 mean spot size : 10 to 11  $\mu\text{m}$   
 loss at 1.55  $\mu\text{m}$  : 0.4 dB/km  
 total dispersion : 15 ps/nm.km

The fibers were provided by different suppliers:  
 - C.L.T.O. (the major part)  
 - Marcoussis Laboratory  
 - CNET (a few)

MCVD technology was used. The mean attenuation at 1.50  $\mu\text{m}$  over the 117 kilometers of fibers used in this project (fibers mounted on drum) was 0.37 dB/km.

The Wo measurements were performed by the suppliers using the VAL method (Variable Aperture Launch) and remade by the CNET using the Near Field Scanning method. These two methods yielded almost identical results as shown in Figure 1.

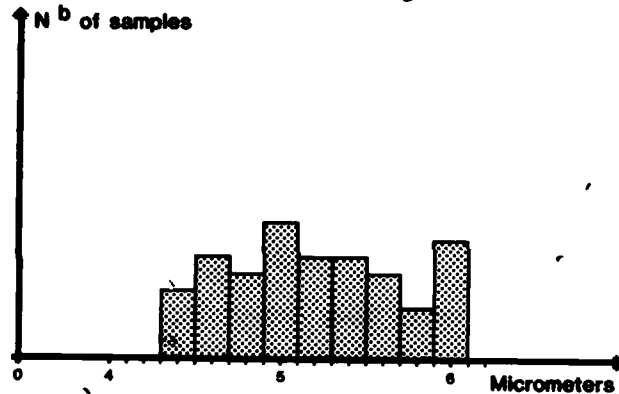


Fig. 1 - WO MEASUREMENTS OVER MONOMODE FIBERS ON LANNION-PERROS LINK

#### 4 - CABLE DESIGN

Previous publications have already fully developed the multiple advantages of the fiber cables with a cylindrical V-grooved rod :

- modularity
- fine mechanical and thermal behaviour
- the ease with which this cable can be series produced and therefore, its relatively low cost price
- its excellent transmission parameters achieved due to the total absence of stress on the fibers.

This last feature which is quite remarkable compared to other technologies used for multimode fibers plays a decisive role in the design concept of long-wavelength monomode fiber cables.

Certain cable assemblies known to cause additional losses are not suitable for use with very low loss monomode fibers (5) (6).

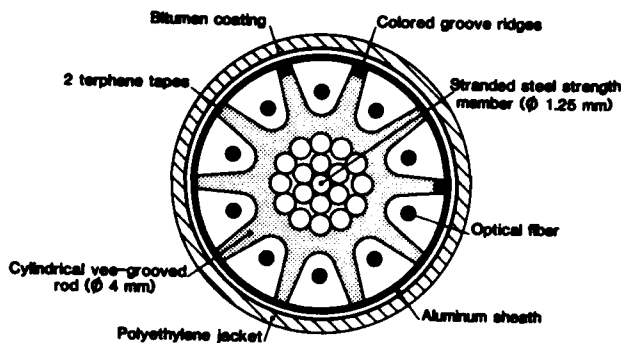


Fig. 2 - FIBER OPTICAL CABLE

The structure of the monomode fiber cable (fig. 2) used over the link is almost identical to that of the multimode fiber cables. It consists of a 10-grooved cylindrical rod (three groove ridges are colored to facilitate fiber locating) made in polypropylene extruded over a steel central strength member. A welded aluminum sheath ensures the mechanical protection of the cable. It is coated with an extruded layer of bitumen followed by a high density polyethylene jacket. The cable outside diameter is approximately 10.4 mm.

#### 5 - CABLE MANUFACTURE AND RESULTS OBTAINED

With a cable mean attenuation of 0.3 dB/km, it was decided to manufacture and lay long cable sections in order to decrease the effects of splices on the overall link losses.

Despite recent publications mentioning excellent laboratory results in splicing monomode fibers, considerably different results are obtained when jointing these same cables in the field. The splicing of fibers having inevitably different geometrical characteristics results in additional losses of a few decibels. Such losses soon become prejudicial to the overall link transmission quality when there is an excessive amount of splices.

The manufacturing process for cylindrical V-grooved fiber cables may be broken down into four main operations :

- extrusion of the V-grooved rod
- insertion of fibers into the rod
- application of the aluminum sheath
- application of the plastic jacket (bitumen coating + HDPE).

##### . Cylindrical V-Grooved Rod Extrusion

The extrusion of the grooved rod involves a single operation requiring a die with a profile

corresponding to that of the rod to be obtained. This die rotates such that the rod grooves are helically formed. The groove pitch is determined by the line travel speed/die rotation speed ratio. During this same operation, three groove ridges are coloured differently (Fig. 2) in order to facilitate subsequent fiber locating following their insertion into the rod. This operation is performed at a rate of 50 m/min. The extruded rod is coiled down into a drum with a 7500 m capacity.

#### Fiber Insertion in the Cylindrical V-Grooved Rod

Fiber insertion is performed using a rotating pay-off which is also used in the making of multi-mode fiber cables. A control unit adjusts the pay-off rotation speed so that the fiber insertion machine pitch is the same as the actual rod's groove pitch. During this operation, two plastic tapes applied to the rod thereby fixing the fibers securely in their grooves. This machine enables fiber

cable to be assembled 7500 meter in length.

#### Cable Metal Sheath

##### - Characteristics :

- . annealed A5 aluminum
- . thickness : 0.7 mm
- . outside diameter : 7.5 mm

This sheath is obtained by forming and welding an aluminum strip longitudinally.

##### - Sheathing weld line

The machine used has been developed by SAT. Its main characteristics are :

- . high frequency welding ~ 450 kHz
- . maximum HF generator power output : 90 kW
- . weld current delivered via an induction coil
- . weld speed > 100 m/min.

##### - Weld line drawing (fig. 3)

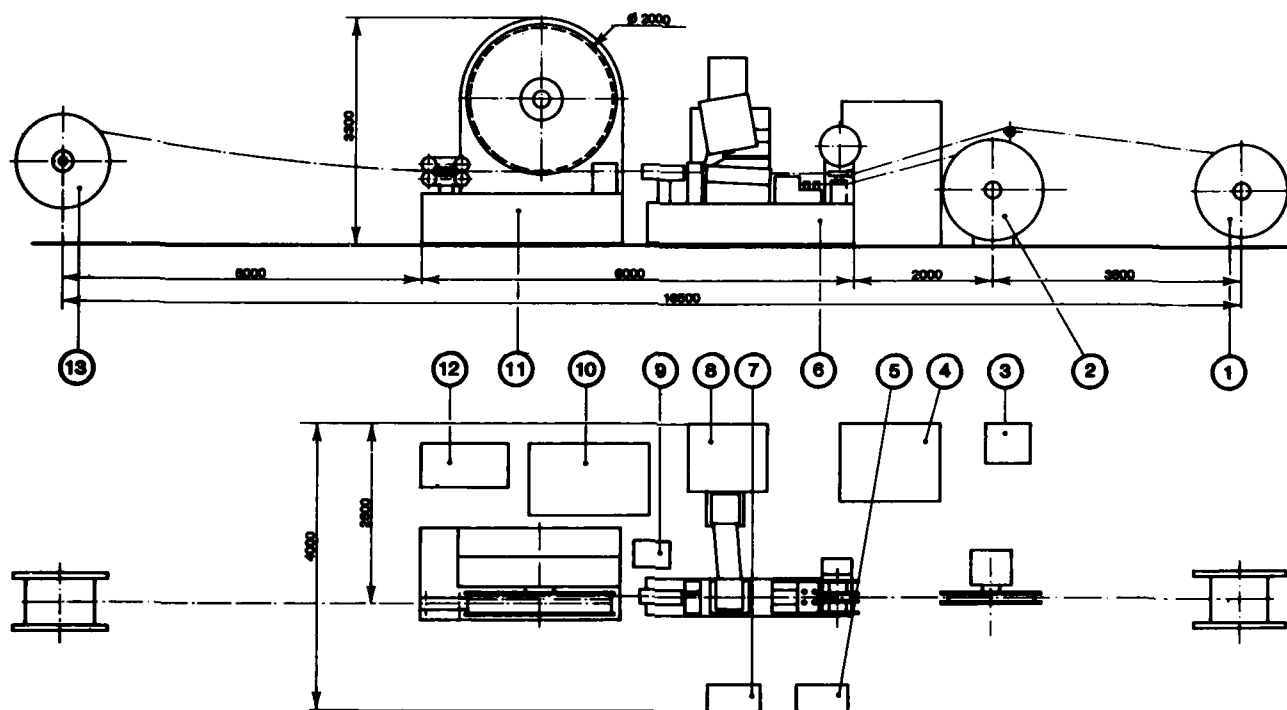


Fig. 3 - SMALL DIAMETER METAL SHEATHING LINE  
WITH HIGH FREQUENCY WELDING EQUIPMENT

- |  |   |
|--|---|
| 1. Cable pay-off stand                           | 7. Control console                                      |
| 2. Aluminum strip pay-off stand                  | 8. Oscillator cabinet                                   |
| 3. Auto-transformer                              | 9. Sheath cooler liquid motopump and tank               |
| 4. Power cabinet                                 | 10. Heat exchanger for the HF welding current generator |
| 5. Weld quality test bench                       | 11. Pulling capstan                                     |
| 6. Mill for forming and welding the metal sheath | 12. Electrical unit cabinet                             |
|  | 13. Cable take-up stand.                                |

#### - Aluminum sheath welding

The maximum length of aluminum sheath which may be welded using this weld machine is contingent on the aluminum strip lengths available on the market (standard length : 1500 meters).

During the manufacture of the cable sheaths, it was necessary to butt-weld the aluminum strips. One of these cables measured 5000 meters in length.

This operation was carried out using a butt-welding machine including :

- . a strip pay-off
- . a TIG butt-welding machine
- . a high-capacity strip take-up.

#### . Cable Manufacture

Following a few tests evaluating the feasibility and quality of long cable sections, four different cables were made by SAT with the following lengths :

- . one measuring 1200 meters long
- . two measuring 2500 meters long
- . one measuring 5000 meters long

The manufacturing operations for the above occurred smoothly, thereby demonstrating that long cable section lengths constitute a viable industrial solution.

#### . Tests

These cables were measured at  $1.50 \mu\text{m}$ . The values obtained over the cables in comparison with those obtained with fibers wound on drums are provided in the histogram in Figure 4.

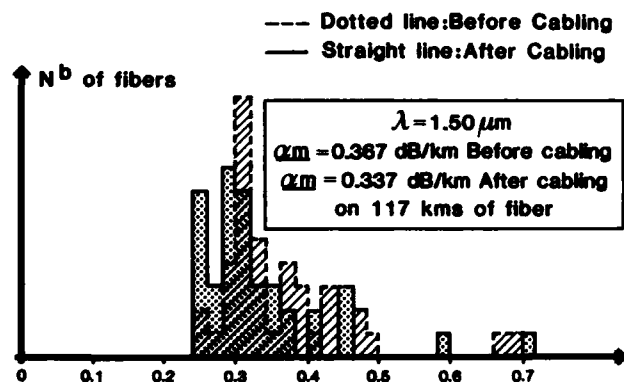


Fig. 4 - HISTOGRAM OF ATTENUATION AT  $1.50 \mu\text{m}$  BEFORE AND AFTER CABLING OF LANNION-PERROS LINK

Note the decrease in attenuation following cable assembly as in the case for multimode fibers. One of the 2500 meter cables comprising the link underwent thermal testing between  $-30^\circ\text{C}$  and  $+55^\circ\text{C}$ .

There is no appreciable variation in attenuation in this temperature range.

#### 6 - CABLE LAYING

Four cable sections were installed in ducts between Lannion and Perros-Guirec, two cities which are located in Brittany near the CNET laboratories. The configuration of this link is given in Figure 5.

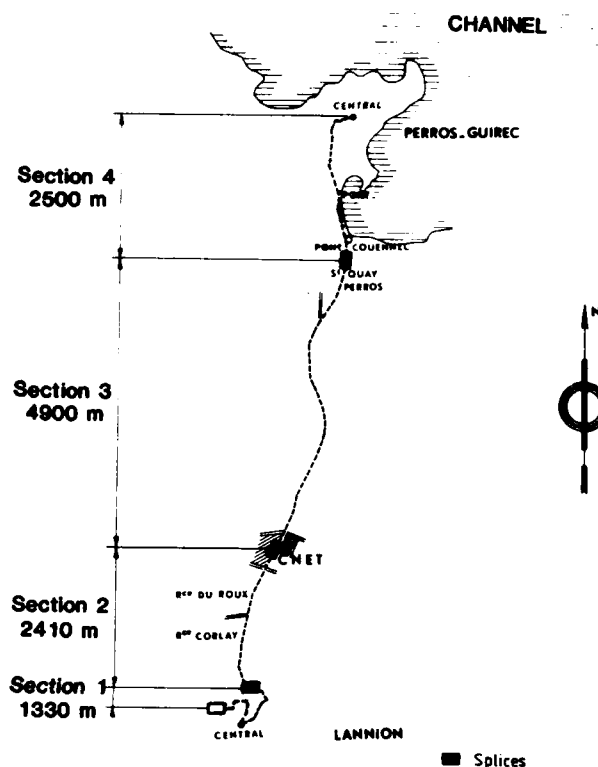


Fig. 5 - MONOMODE LINK LANNION-PERROS

The new "micro-ball" technique was used for laying these cables and in particular, for the 5000-meter cable section. These nylon micro-balls measuring 0.2 to 0.4 mm in diameter adhere to the cable and duct, thus allowing the cable to roll instead of slide over the duct walls. This results in a substantial improvement in the friction factor and a strong decrease in the pulling force required.

During this laying operation, a winch line was used with a maximum pulling force of 60 daN.

Figure 6 illustrates the force recorded during the laying of the 5000-meter cable section for which intermediate pull-through equipment was used.

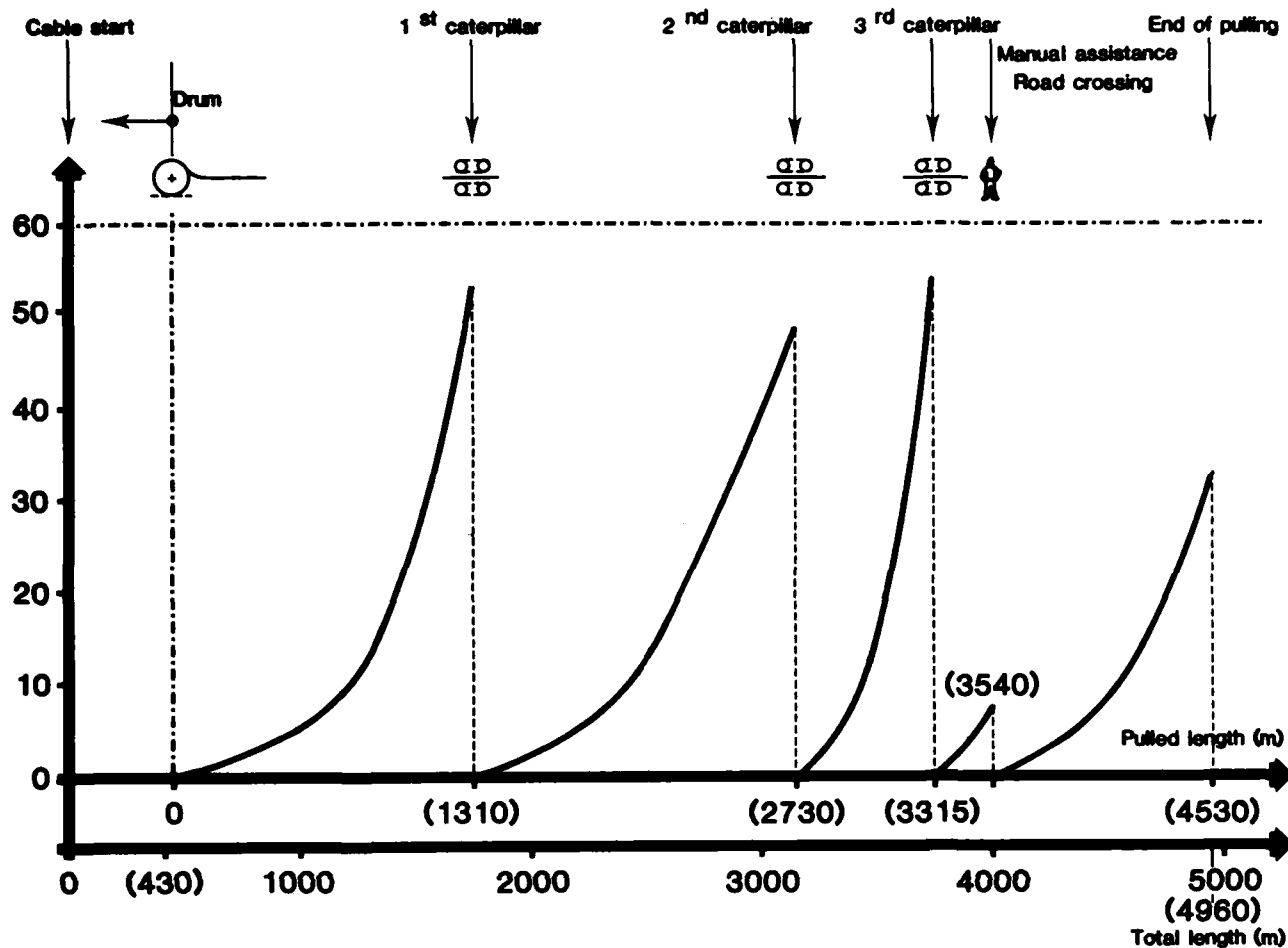


Fig. 6 - PULLING LOAD APPLIED TO THE 5000-METER CABLE

- Description of the Intermediate Pull-through

Operating characteristics :

- . pulling force : 100 daN max  
(for 10-fiber cables : force set at 60 daN)
- . speed : > 100 m/min
- . travel direction : any.

Technical description :

- . a caterpillar-type pull-through system is used
- . made of light material and driven by an hydraulic engine weighing 32 kg.

This equipment is therefore easily installed on site. Figure 7 provides a picture of the pull-through equipment.

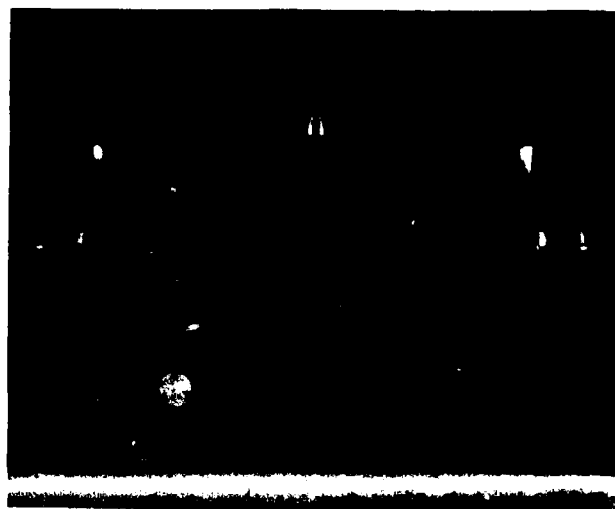


Fig. 7 PULLING CATERPILLAR

- the pull-through hydraulic engine is fed by a power feed system including :
  - a thermal engine driving a high pressure oil pump
  - a regulator system enabling operation at constant pressure. Therefore, a constant tension is applied to the cable. This pressure may be adjusted to vary the pulling load exerted on the cable.

Figure 8 illustrates the hydraulic drive system of this caterpillar.

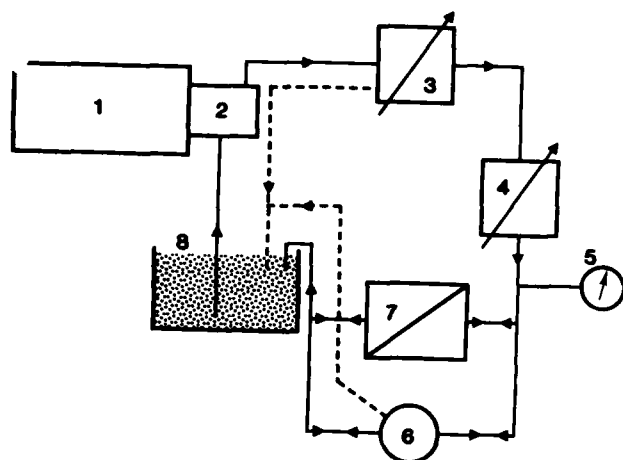


Fig. 8 - PULLING CATERPILLAR HYDRAULIC CIRCUIT

1. Thermal engine
2. High pressure oil pump
3. Maximum rate adjustment
4. Maximum pressure adjustment
5. Control gauge
6. Hydraulic Engine
7. Travel direction switching system
8. Oil reservoir

#### - Performance Characteristics Following Laying

Following cable installation, the fiber attenuation over the various cable sections remained unchanged.

#### 7 - SPLICING

A weld system using a CO<sub>2</sub> laser was developed for this operation. The CO<sub>2</sub> laser technique was selected for monomode fiber welding over conventional flame or arc welding techniques. Reliability studies had proved that this means of heating fibers yielded a weld joint with a considerably better mechanical resistance.

Flame fusion $\bar{\sigma}$	Arc fusion $\bar{\sigma}$	Laser CO <sub>2</sub> fusion $\bar{\sigma}$
0.8 ± 20% 15% $\sigma_i$	1.4 ± 25% 25% $\sigma_i$	2.2 ± 20% 40% $\sigma_i$

Fig. 9 - MECHANICAL PERFORMANCE OF VARIOUS FUSION SPLICES ON MULTIMODE FIBER OF INITIAL STRENGTH  $\sigma_i = 5.5$  GPa

The table in Figure 9 demonstrates that a breakage resistance approximately three times higher is achieved with the CO<sub>2</sub> laser than with flame welding.

Splicing on site is performed through dynamic optimization of the power input (figure 10).

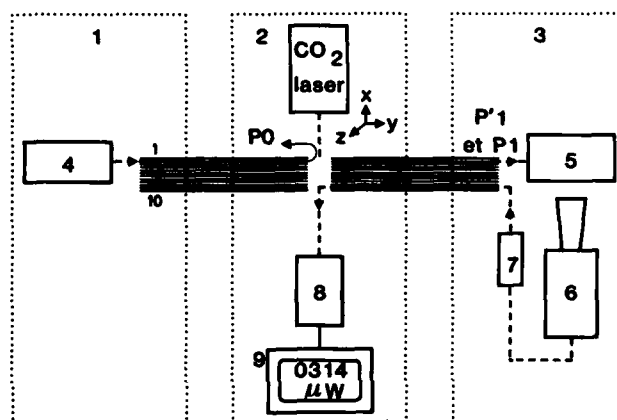


Fig. 10 - CO<sub>2</sub> LASER SPLICING SYSTEM

1. Link termination station
2. Intermediate chamber
3. Intermediate chamber
4. 1.5 μm laser emitter
5. 1.5 μm laser receiver
6. Television camera
7. TV signal transmitter
8. TV signal receiver
9. TV screen

An emitter with a stabilized power output injects light over the fiber to be spliced. The power received is  $P_0$ . The fibers to be jointed are placed face to face using a micro-displacement system until a maximum terminal power output is achieved ( $P'_1$ ). The value of  $P'_1$  is sent via a video system over one of the unspliced fibers of the cable.

$P_1$  is the power received following welding. The loss of the splice is therefore :

$$\alpha = 10 \log \frac{P_0}{P_1} - \alpha_{\text{fibers}}$$

The tenth fiber is spliced without loss optimization. Figure 11 gives the histogram of the splice attenuation values.

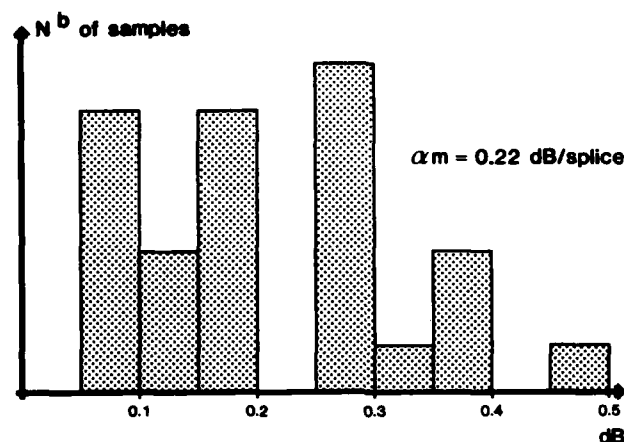


Fig. 11 - SPLICE ATTENUATION OVER THE LANNION-PERROS MONOMODE LINK (1.5  $\mu$ m)

The mean result obtained (0.22 dB) may appear high in comparison to results obtained on identical fibers in laboratory conditions. The dispersion of  $\alpha$  measured over these fibers (Fig. 1) explains this result for the most part.

#### 8 - LINK FINAL RESULTS

As the cables were not cut at the two link terminating stations, the total length of the link is 11.8 km. This allows 47.2 km of cables to be looped with an overall attenuation of 18.1 dB. The mean attenuation for this spliced, duct monomode link is therefore 0.38 dB/km at 1.50  $\mu$ m.

Terminal systems are currently being installed and the available band pass over the link is being evaluated with respect to the laser spectrum width. The first results obtained at the time of writing this article, attest that the objective of the first phase of this project (560 Mbit/s) has been reached.

#### 9 - CONCLUSION

Following conclusive field trials involving cable assembly and installation of multimode optical fibers using the cylindrical V-grooved rod concept, the first monomode link at 1.55  $\mu$ m has been manufactured and installed using this same technology. The results obtained demonstrate that monomode fibers constitute an excellent medium for long distance links. With the initial phase of this project almost completed, we are now preparing to increase to a rate of 1.7 Gbit/s over 45 km of this same link by next spring. This will constitute the first step towards the construction of the long distance, high rate links of tomorrow.

#### ACKNOWLEDGEMENT

We would like to express a special thanks to Mr Pecot's team who was responsible for the pulling of the cables comprising this link.

#### REFERENCES

- (1) 84 km transmission experiment at 1 Gbit/s using a 1.55  $\mu$ m mode stabilized laser  
Linke and Al 100C 83 Tokyo
- (2) Transmission experiment over 134 km of single mode fiber at 445.8 Mb/s  
Ichihashi, Nagai, Miya 100C 83 Tokyo
- (3) Optical fiber cables using V-grooved cylindrical units : high performance cables  
D. Boscher, G. Le Noane, B. Nonclercq, A. Zaganiaris  
Fiber and Integrated Optics Vol 4 N° 1 1982
- (4) Low Loss optical fiber cable and manufacture  
D. Boscher, B. Missout, P. Chéron  
IWCS Cherry Hill 1981
- (5) Single mode optical fibre microbending loss in a loose tube coating  
Hornung, Reeves Electronics Letters  
October 1981
- (6) Transmission characteristics of a cabled and jointed 30 km monomode optical fiber link  
B.P. Nelsen Electronics Letters  
October 1981
- (7) Low loss single mode fiber splices using ultraviolet curable cement  
C. Miller 100C 83 Tokyo
- (8) Optical fibers and cables for public telecommunications  
N. Kojima 100C 83 Tokyo
- (9) Local network fiber optic cables  
D. Boscher, G. Le Noane, B. Nonclercq  
ICC 83 Boston - Session C III-6



Daniel BOSCHER  
C N E T  
ROC/FCO-LANNION  
France

Daniel BOSCHER graduated from the "Ecole Nationale Supérieure des Arts et Métiers" in 1973. He joined the French Post Office in 1973. Since 1979, he is deputy manager of the optical fibers and cables department at CNET.



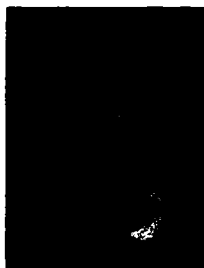
Bernard MISSOUT  
Société Anonyme de  
Télécommunications  
Direction Technique Câbles  
Paris - France

Bernard MISSOUT graduated from the "Ecole Nationale Supérieure des Arts et Métiers" in 1971. He is presently in charge of special cable machines development and studies particularly about fiber optical cables, at the cable division of SAT Company.



Bernard NONCLERCQ  
C N E T  
ROC/FCO-LANNION  
France

Bernard NONCLERCQ graduated from the "Ecole Nationale d'Ingénieurs" of BELFORT in 1971. He joined the CNET in 1978, where he is now in charge of studies concerning optical fiber cables.



Alain LE BOUTET  
C N E T  
ROC/FCO-LANNION  
France

Alain LE BOUTET received his Dipl. Ing. degree from the "Institut Industriel du Nord" in 1971, and his Dipl. Ing. degree in Electronics from the "Ecole Supérieure d'Electricité" in 1973. He then joined the CNET, where he was engaged in digital transmission systems. He joined the Fiber Optics Group in 1980, being now in charge of the measurement laboratory. With his team, he performs all the qualification tests on monomode installed links.



## A FIELD SPLICING SYSTEM FOR SINGLE-MODE OPTICAL FIBER

G. Pacey, R. Neumann, H. Lukas

Bell-Northern Research  
Ottawa, Ontario, CanadaABSTRACT

This paper discusses a field splicing system for single-mode optical fiber. The system consists of a specialized single-mode fusion splicing set and an optical power monitoring system used to assist in aligning the fibers. The prerequisites for fusion splicing of single-mode fiber are discussed. The fusion equipment and optical power monitoring system are described in detail and their operation is discussed. Finally, the performance of system is reported.

INTRODUCTION

The significantly greater bandwidth of single-mode fiber offers substantial advantages over conventional multimode fiber as a transmission medium for long-haul telecommunications systems. Single-mode fibers, however, pose increased difficulty for interconnection because of their significantly smaller cores. Particularly when used in long reach systems, with fiber attenuation in the order of 0.5 dB/km, low loss splices are essential to maximize system reach.

The need for tighter controls on core-to-core alignment and the more sophisticated fusion techniques required have prompted the development of specialized equipment. This paper discusses the prerequisites of single-mode fusion splicing, describes the design of a practical, field useable single-mode fusion set and an optical power monitoring system used to assist in the alignment of the fibers. Finally, the performance of and experience with the equipment is discussed.

FUSION SPLICING OF SINGLE-MODE FIBER

Splicing of single-mode fiber requires significantly better control of fiber-to-fiber alignment and more sophisticated fusion techniques than does splicing of multi-mode fiber.

Typically, single-mode fibers have core diameters in the order of 10  $\mu\text{m}$  or less versus 50  $\mu\text{m}$  for multimode fiber. Hence, more accurate alignment is required if low loss splices are to be achieved. Figure 1 shows empirical results of a comparative test of splice loss versus absolute transverse offset for typical single-mode and multimode fibers and demonstrates the greater sensitivity of the former in terms of transverse offset.

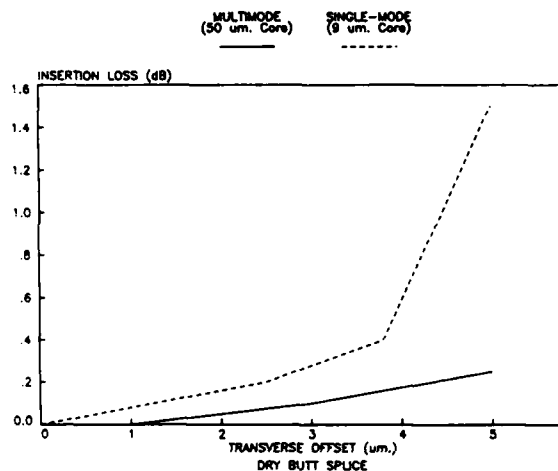


Figure 1: Graph of Single and Multimode Splice Loss vs Transverse Offset

Because of this greater sensitivity, methods which utilize the fiber cladding surfaces to align the fibers are inadequate. Differences in cladding diameter and core eccentricity will introduce unacceptable misalignment. Since the cores of the fibers cannot practically be aligned by direct visual observation, it is necessary to use alternative methods. The approach which optimized both the compatibility with the craftsman and the splice loss was to monitor the level of optical power transmitted or lost at the splice as a means of tracking the relative alignment of the fibers within a manipulative mechanism.

Sensitivity to angular misalignment is also more significant for single-mode fibers. Because the optical power is constrained to travel within one mode only, no potential exists for mode conversion at the splice due to angular differences in the cores. Hence, the core axes must be aligned to within less than  $\frac{1}{2}^\circ$  in order not to appreciably increase the splice loss.

Additional considerations are also required for the fusion process itself. Multimode fiber can tolerate a relatively significant amount of distortion at the splice and still provide low losses. The smaller core of single-mode fiber, however, is much more easily distorted due to localized tilt, transverse offset, necking and bulging of the cores within the region of the fused interface.

Fusion distortion results from an excess or irregular flow of the molten glass during the process of heating. A number of factors are important in minimizing distortion.

#### (1) Electrode Gap

Narrow electrode gaps are desirable for single-mode fibers so as to restrict the heated area as much as possible to the fiber-to-fiber interface only. Gaps of 0.5 mm are required as compared to typical multimode gaps in the order of 1.5 mm to 2.0 mm.

#### (2) Arc Current and Duration

Arc intensity, as determined by arc current, should be just sufficient to soften the glass so as to obtain a sound joint while avoiding excessive fluidity. Arc duration also controls the glass flow. A long duration arc contributes to distortion and allows time for surface tension to realign the fibers such that their claddings rather than their cores become concentric. The narrow acceptable range of arc current and duration requires an accurately controlled arc to guarantee uniform conditions from splice to splice.

#### (3) Fiber Push

Pushing of the fiber ends together during heating eliminates necking caused by the void of material which results from imperfectly cleaved endfaces. Pushing also assists in the achievement of more physically sound splices. The optimum amount of push is that which eliminates necking. Over pushing will result in distortion due to bulging of the cores.

#### (4) Cleave Quality

Fiber end cleaves must be of good quality, show less than  $1^\circ$  of angle, have flat surfaces without waves or excess hackle, and be free from burrs or chips. Poor cleave quality contributes to distortion as the glass flow will be excessive to fill the void between the unmatched ends. Poor cleaves may also cause a lateral shifting of the cores as they approach each other.

#### (5) Prefusion

Prefusion (i.e., heating prior to contact of the fiber endfaces) reduces the risk of bubble formation by helping to eliminate imperfections which can entrap air during the glass flow period.

#### Fusion Set Design

A fusion set designed with the above prerequisites in mind and specifically for use in the field is shown in Figure 2. It is a portable, self-contained instrument

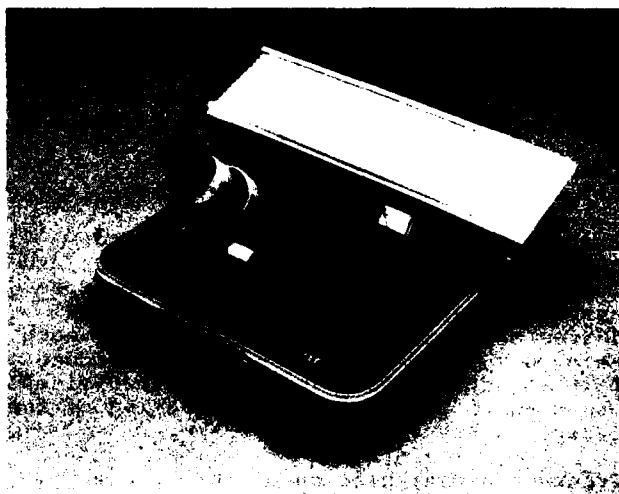


Figure 2: Fusion Set for Single-Mode Fiber

packaged in a ruggedized FRP case. It can be powered from a number of sources, including: 100, 120, 220, 240 volts AC, 50 - 60 Hz; external 12 volts DC (e.g., battery, service vehicle); and internal batteries for which a self-contained charger operating from the AC voltages is provided. The set utilizes a specialized fusion head and electronically controlled high performance arc supply/control circuit.

## 1. Fusion Head

The fusion head is shown in Figure 3. It provides a number of functions including: fiber holders and manipulators, sequencing functions for the fusion cycle, and an integrated splice package installation fixture.

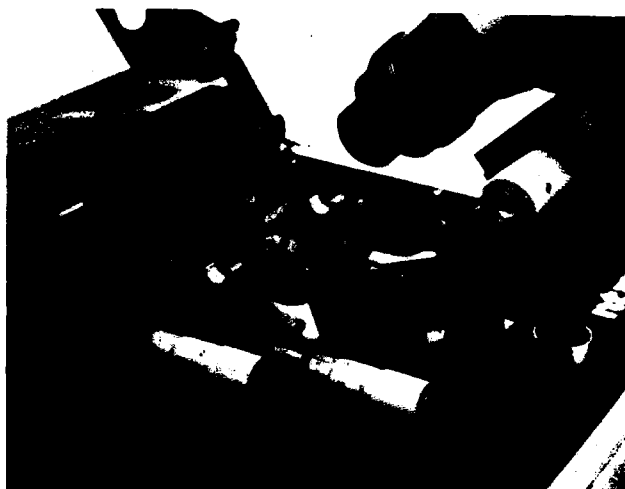


Figure 3: Single-Mode Fiber Fusion Head

### (i) Fiber Clamping and Manipulation

Two vee-groove blocks with associated clamps are utilized to hold the fibers and locate them with respect to the electrode assembly. In order to achieve the high degree of angular alignment required, each vee-groove block set is made as a matched pair and specialized low force fiber clamps are used to provide accurate seating of the fibers in the vee-grooves.

Transverse manipulation of the fibers relative to each other for the purpose of aligning their cores is provided by means of a unique cantilever and micrometer mechanism shown schematically in Figure 4. The left vee-groove block is mounted on a single structural member which, by nature of its geometric design provides for two cantilever spring elements. These elements provide for movement of the fiber holder in two mutually perpendicular axes via separate micrometer heads which use precision gear and eccentric mechanisms to achieve the high degree of resolution required. This design approach allows a much more compact and rigid structure than that which can be built up by means of conventional micrometer stages. In addition, the absence of separate pivotable elements and slides show superior tracking and hysteresis characteristics.

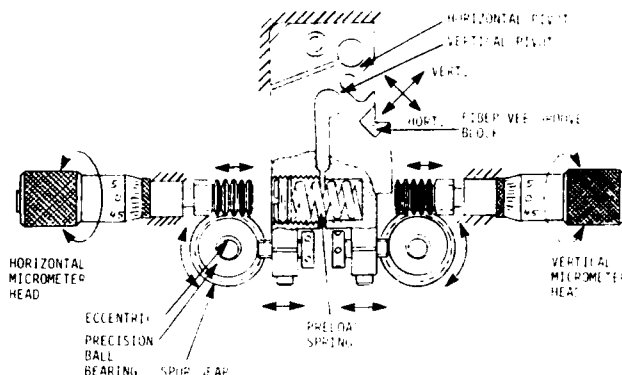


Figure 4: Principle of Cantilever Manipulators

### (ii) Fusion Sequencing

A motorized mechanism is utilized to control axial movements of the right hand fiber and to initiate the fusion arc at the appropriate time in the sequence. The right hand fiber clamp is mounted on a pivoted arm operated by the motor mechanism. The arm assembly is used to automatically set a gap of approximately 10  $\mu$ m between the fiber ends such that the fibers can be laterally manipulated without interference or scuffing of the fiber faces. The same mechanism also

provides for a controlled push of the held fiber towards the other fiber during the application of heat so as to eliminate necking at the splice. A control knob on the arm allows for adjustment of the amount of push.

The motor mechanism is also used to operate a mirror located beneath the fiber pair. The mirror, orientated at 45° to the fibers, provides a view of the vertical alignment of the fiber ends. Hence, both horizontal and vertical views of the fiber can be seen simultaneously in the microscope.

### (iii) Protective Splice Package Installation Fixture

The fusion head incorporates an installation fixture for a protective splice package of the type used for the multimode system<sup>1</sup>. See Figure 5. Transfer arms are provided to assist the operator in transferring the fused fibers to the installation fixture and for accurate registration of the splice into the package. A pressure arm ensures adequate closing pressure is applied to the package.

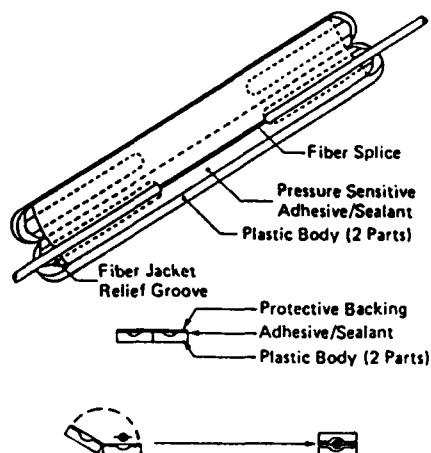


Figure 5: Protective Splice Package

## 2. Arc Supply/Control Circuit

A solid state arc supply and control circuit is used to provide maximum performance stability, compactness and reliability.

Arc current is monitored by a sensing circuit and feedback loop so that arc stability is maintained to within better than  $\pm 2\%$ . A 100 position control allows for a linear setting of the current over the range of 16 mA to 22 mA. A similar control allows for setting of arc duration over the range of 0.5 sec to 3.0 sec with a repeatability of better than  $\pm 0.1$  sec.

The control circuit also monitors the charge condition of the set's internal battery to ensure optimum fusion conditions. Several battery monitors are built into the circuit. A panel mounted LED indicator notifies the operator of the need to recharge. Failure to do so within a limited number of additional fusion cycles results in the arc being disabled before degradation of performance occurs.

The set can be operated from the external sources regardless of the state of charge of the internal battery. In excess of 125 fusion splice cycles are available when the battery is fully charged.

## 3. Fiber Viewing

A monocular zoom microscope (30x to 120x) is provided to assist the operator in accurate placement of the fibers with respect to the electrodes, inspection of the fiber cleave quality and in the course visual alignment of the fiber pair.

## 4. Fiber Organizer Bracket

A mounting bracket for the fiber organizer tray used in the splice closure<sup>1</sup> is provided on the console mounted at the back of the fusion set. This significantly increases the convenience of loading and accessibility to the splices in the tray and helps to minimize snagging of the fiber during handling.

## Splicing Operation

1. The fibers are prepared and loaded into the fusion set head and butted together.
2. The SET/FUSE button is pushed once upon which the right hand fiber will withdraw slightly to form a small gap between the fiber end faces in preparation for manipulation.
3. The fibers are coarsely aligned in the vertical (with assistance of the mirror) and horizontal planes by means of the appropriate micrometer heads.
4. Utilizing the optical power monitoring system, the fiber cores are brought into optimum alignment by the micrometer heads.
5. The SET/FUSE button is pushed a second time, and the operations discussed previously, to produce a "low loss" splice are performed automatically.
6. A splice package is placed into the installation fixture and the protective strip removed to expose the sealant/adhesive.
7. The fiber is moved by means of the transfer arms to the splice package.
8. The splice package is closed, and sealed by means of the pressure arm. Finally, the packaged splice is removed and placed into the organizer tray.

## Optical Monitoring System

In order to obtain the precise fiber alignment required for a low loss single-mode splice, some form of feedback is necessary to enable the splicer to optimize the fiber core alignment.

This involves injecting light into the fiber upstream of the splice point, detecting it in the fiber downstream of the splice point, and providing the splicer with a visual reading of the level of the downstream light level. The configuration employed for the optical monitoring is shown in Figure 6.

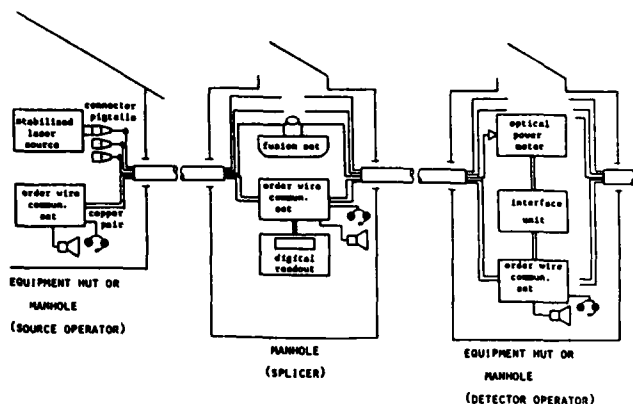


Figure 6: Principle of Remote Monitoring System

The laser shown in the figure injects a stable light level into each fiber of the upstream cable in turn, via detachable optical connectors. This light is coupled into the downstream fiber when the two fibers are butted together in the fusion splicer and is measured by the optical power meter at the far end of the downstream fiber. An electrical signal, proportional to the level measured by the power meter, is fed back to the splicer over a copper pair in the optical cable, or over the cable's metallic sheath and strength member by the Interface, Order Wire and Display unit shown. As well as providing a feedback signal for the splicer, the equipment allows voice communication between the splicer and the equipment operators at the upstream and downstream fiber ends.

A major consideration in the design of the optical monitoring system is the maximum range over which it must work. For single-mode high bit rate systems, a length of 40 km (20 dB optical loss) or more is quite likely. A laser light source and simple power meter provide sufficient sensitivity to monitor over 40 km of fiber plus the initial high loss of the joint before alignment.

The sensitivity of the monitoring system permits fiber alignment to be peaked to an accuracy of a few 100th's of a dB, sufficiently small not to add to the final splice loss.

Because of the potential noise pickup to be expected along 40 km of copper cable, in urban or industrial areas. The Interface unit converts the power meter signal into a high level frequency modulated audio tone. The tone is fed back to the splice location by the Orderwire units, where the Display unit demodulates it to produce a reading proportional to the original power meter reading.

To enable two way voice communications over a 40 km copper pair, a special order wire unit was designed which transmits voice and/or the FM audio tone.

Figure 7 shows prototypes of the optical monitoring system. All equipment is powered by rechargeable batteries and is housed in rugged carrying cases. The system has been used in the field since early 1983 and is performing well.

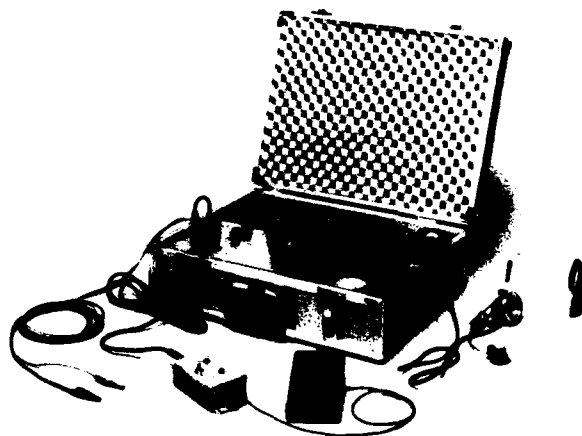
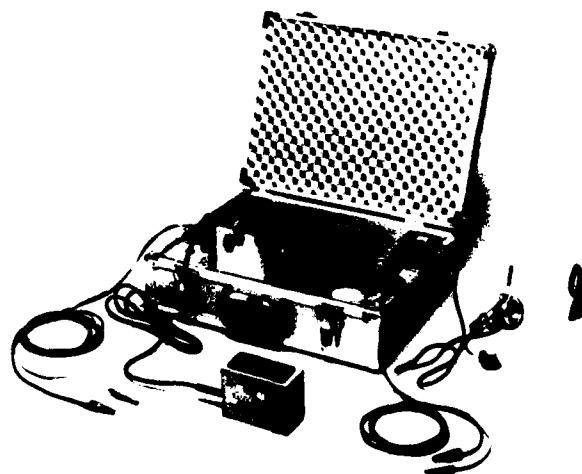


Figure 7: Upper: Detector, Interface and Communications Equipment  
Lower: Readout and Communications Equipment



## Performance

Figure 8 shows laboratory test data for splice insertion loss of the single-mode fusion set. For the purposes of the test a highly stable laser diode source of 1300 nm was used to launch into approximately 2 Km of fiber. The test fiber was of a depressed cladding construction with a core diameter of 9  $\mu$ m. Insertion loss was measured by first taking a reference reading of the optical power in the unbroken link after which the fiber was broken and rejoined by a splice. After splicing, a new power reading was taken and compared to the reference power reading to derive insertion loss. Splicing was conducted within a few meters of the source.

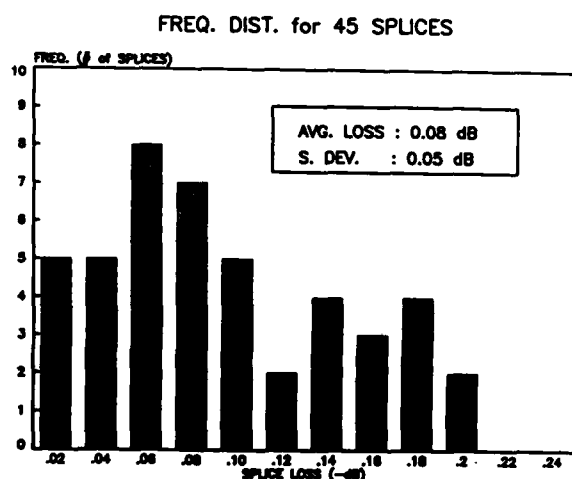


Figure 8: Graph of Insertion Loss Splice Results

Figure 9 shows test data for splice loss of field concatenated fibers using the single-mode fusion set and remote optical power monitoring system described. The test data shown is an estimated splice loss which was derived as the link was concatenated by taking the difference between measured link attenuations and factory measured fiber attenuations. Measurement accuracy for this test is estimated to be  $\pm 0.05$  dB.

Figures 8 and 9 indicate that comparable splice losses were achieved for both the field splices and the laboratory insertion loss tests. The slightly higher average field splice loss can be attributed to measurement accuracy and differences in core geometry and optical properties between the fibers of the concatenated link.

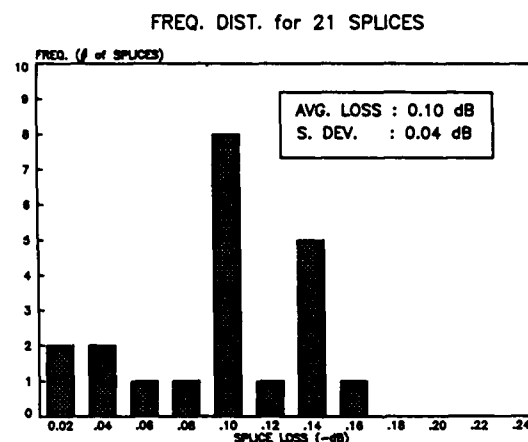


Figure 9: Graph of Concatenated Field Splice Loss Results

## Conclusion

A single-mode fusion splicing system, designed especially for field use, has been developed. The system consists of a specialized fusion set and remote optical power monitoring and communication equipment. Experience in using the system has shown that splices with an average loss of 0.10 dB or less can be achieved in both laboratory and field environments.

## References

1. G.K. Pacey and J.R. Scott, "A Splicing System for Optical Fiber Cables", 30th IWCS, Cherry Hill, New Jersey, Nov. 1981.

## Biographies

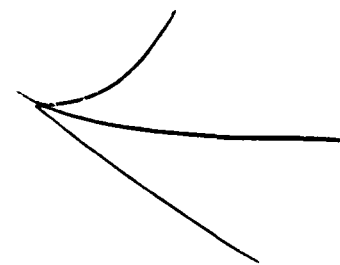
G.K. (Grant) Pacey graduated as a Mechanical Technologist from the Northern College of Applied Arts and Technology in Kirkland Lake Ontario in 1969. Grant completed his B.A.Sc in Mechanical Engineering at Queen's University, Kingston, Ontario in 1972 and his M.B.A. at the University of Ottawa, Ottawa, Ontario in 1981. He joined Bell-Northern Research in 1973 and has worked in the design of terminal equipment, electronic packaging, mechanical development and testing. During the last six years he has been involved in the development of connection technology for fiber systems. Grant is a member of the Association of Professional Engineers of Ontario.



Rick Neumann received his B.Sc. from the University of Manitoba in 1969, and his M.A.Sc. from the University of Toronto in 1974, both in Electrical Engineering. Since joining Bell-Northern Research in 1976, he has worked on digital microwave radio systems, on the design of fiber optic repeaters, and, for the past three years, on the measurement methods and electro-optical equipment needed for the field installation and testing of fiber optic cables.



Helmut Lukas completed his toolmaker's training in West Germany. A mechanical designer with many years of experience, he has been involved with numerous telecommunications product developments including connector blocks, splice closure, coaxial cable splicing, and a special project involving the development of a hydraulic prosthetic arm. For the past 9 years Helmut has been associated with the development of optical fiber connection technology.



## OPTICAL AND MECHANICAL PROPERTIES OF SINGLE-MODE CABLES @ 1300 nm

S. H. in't Veld, P. H. Prideaux, I. D. Aggarwal, D. Hurwitz, D. Roland

Valtec, A Subsidiary of U. S. Philips Corp.  
West Boylston, Massachusetts 01583Abstract

Single-mode fibers were produced by the MCVD process with losses as low as 0.40 dB/km at 1.3  $\mu$ m. Loose tube cables were made using these fibers without any loss penalty for a temperature range of -30°C to +70°C. The cables made with these single-mode fibers withstood 600 lbs. pulling and 8.75 N-m impact tests. Concatenation of these fibers using elastomeric splices showed an average splice loss of 0.11 dB. Measurement of optical loss and chromatic dispersion on the concatenated links indicated an average end to end loss of 0.54 dB/km and a linear addition of dispersion. Predictions of concatenated dispersion using the ESI parameters of the individual fibers showed excellent agreement with actual measurements.

Introduction

Single-mode fiber cables offer extremely low optical loss and nearly zero dispersion in the 1.3 micron region of the optical spectrum. They are ideally suited for long distance, high data rate applications such as telephone trunking. Due to their low optical loss and high bandwidth, unrepeaters links in excess of 35 km can be achieved using single-mode fiber cable. The design of single-mode fiber cable must include not only the mechanical design of the cable but also the design of the optical fiber. Optical fibers are designed to minimize the total attenuation and chromatic dispersion for the final optical system. To achieve a high performance optical system, tradeoffs must be made during the design of the fiber and cable. This paper presents some of the results from fiber and cable design efforts. A discussion of single-mode fiber properties will be given first, followed by a description of the Valtec ChannelMax™ cable.

Fiber Design

## A. ESI Description of Single-Mode Fibers

The single-mode behavior in optical fibers is achieved by restricting the diameter of the fiber core to typically less than 10 microns

and limiting the relative refractive index difference between the core and cladding glasses to less than 0.5%.

One of the most common refractive index profiles used for single-mode fibers is the step index profile. Extensive theoretical work has been done on the perfect step index profile. Unfortunately, real single-mode fibers never have perfect step refractive index profiles due to dopant diffusion and volatilization. However, fibers with these real refractive index profiles can be accurately approximated by an equivalent step index or ESI profile<sup>(1)</sup>.

The ESI profile can be determined from measurements of the fiber's mode field pattern. The mode field of the fiber and an ESI fiber can both be approximated by a Gaussian function. The 1/e width of the mode profile is known as the mode spot size. The ESI profile for a fiber will produce the same mode spot size as the actual fiber.

The ESI profile is specified in terms of an equivalent step index core radius,  $a_s$ , and an equivalent step refractive index difference,  $\Delta_s$ . From these parameters it is possible to calculate splice loss, microbending loss, and chromatic dispersion. For the remainder of this paper the fibers will be specified in terms of their ESI parameters or their spot size at 1.3 microns.

## B. Loss Considerations

The optical loss of a single-mode fiber is the sum of three major components. These components are fiber loss, microbending loss, and splice loss.

## 1. Fiber Loss

The major loss mechanisms in optical fibers are attributed to Rayleigh scattering and the absorption due to impurities. Rayleigh scattering is inversely proportional to the fourth power of the source wavelength. Although this scattering loss cannot be totally eliminated it can be minimized by choosing a

transmission wavelength in the 1200 to 1600 nm region. Scattering loss is also directly proportional to the concentration of the germania dopant in the SiO<sub>2</sub> core glass. Therefore, a low germania doped fiber has lower scattering attenuation. The absorption loss due to metal impurities is most predominant at shorter wavelengths and can successfully be eliminated by raw material purification. The most significant absorption loss in the 1200 to 1600 nm wavelength region is due to OH<sup>-</sup> impurities in the core of the fiber. For example, one ppm of OH<sup>-</sup> will produce an absorption loss of about 50 dB/km at 1.39  $\mu$ m wavelength which tails off towards 1.3  $\mu$ m. It is obvious that low OH<sup>-</sup> fibers are needed for operation in the 1300 nm region.

## 2. Microbending Loss

Microbending loss results from power coupling from the guided fundamental mode of the fiber to radiation modes. This coupling takes place when the fiber axis is bent randomly in a high spatial frequency. Such bending can occur during packaging of the fiber during the cabling process.

The microbending loss of a single-mode fiber is a function of the fundamental mode spot size,  $\omega$ . Fibers with large spot sizes are extremely sensitive to microbending. It is therefore desirable to design the fiber to have as small a spot size as possible to minimize microbending loss. The microbending loss can be expressed by the relation (2)

$$L_m = 2.15 \times 10^{-4} \omega^6 \lambda^{-4} L_{nm} \quad (\text{dB/km}). \quad [1]$$

Where  $\omega$  is the spot size and  $L_{nm}$  is the microbending loss of a 50 micron core, 0.20 N.A. multimode fiber subjected to the same microbending conditions. Note that the microbending loss follows a  $\omega^6$  dependence and hence small changes in spot size can have a drastic effect on the microbending loss.

## 3. Splice Loss

Ultimately the fibers will have to be spliced together to form the final link. For a cable with an average fiber loss of 0.4 to 0.6 dB/km, splice losses in excess of 0.2 dB per splice will drastically reduce the unrepeated distance which can be achieved. It is therefore extremely important that the fiber be designed such that splice loss be minimized.

Splice loss is due mainly to axial misalignment of the fiber cores. Splicing techniques which rely on aligning the outside surface of the fibers require extremely tight tolerances on core to outside surface concentricity. Offsets on the order of one micron can produce significant splice loss.

To minimize splice loss, it is desirable to have a large spot size. The splice loss in dB due to axial misalignment is given by (3).

$$L_s = \frac{10}{\ln 10} \left( \frac{d}{\omega} \right)^2 \quad (\text{dB}) \quad [2]$$

Where  $d$  is the axial misalignment of the fiber cores. It is obvious that minimizing optical loss involves making tradeoffs between the different sources of loss. It is advantageous to have a large spot size to minimize both Rayleigh scattering and splicing loss whereas minimizing microbending loss requires a small spot size. In addition, as will be described in the next section, the spot size plays a significant role in the chromatic dispersion.

## C. Chromatic Dispersion

Chromatic dispersion is due to both material and waveguide effects. In a strict sense these components cannot be completely separated; however, for the purposes of this paper the total dispersion will be considered as simply being the sum of material and waveguide dispersion.

### 1. Material Dispersion

Material dispersion is a property of the chemical composition of the core and cladding glasses of the fiber. The dominant material dispersion is that of the fiber core since most of the optical power is contained within this region. The material dispersion of pure silica has a zero crossing at a wavelength of approximately 1.28 microns. The addition of germania to the glass shifts this zero crossing to longer wavelengths. The amount of shift is a function of the concentration of dopant. To maximize the information capacity of the fiber, it is required that the fiber be operated at its zero dispersion wavelength. In practice, it is sufficient to operate within 10 to 20 nm of the zero dispersion wavelength. The effect of adding waveguide dispersion is to shift the zero crossing wavelength to even longer wavelengths than that due to material dispersion alone. Therefore, both waveguide and material dispersion must be minimized for a total dispersion which is nearly zero at 1.3 microns.

### 2. Waveguide Dispersion

A simple algebraic equation can be obtained for waveguide dispersion from the spectral dependence of mode spot size (4). The parameters used in the equation are the ESI core radius and the cutoff wavelength of the LP<sub>11</sub> mode. The waveguide dispersion in ps/nm-km is given by

$$D_w = -231.6 \frac{\lambda}{\omega^2} \left( \frac{\lambda}{\omega} \frac{d\omega}{d\lambda} - \frac{1}{2} \right) \quad (\text{ps/nm-km}) \quad [3]$$

The wavelength dependence of spot size can be obtained from the relation [3]

$$\frac{\omega}{a_s} = 0.65 + 0.434 \left( \frac{\lambda}{\lambda_c} \right)^{3/2} + 0.012 \left( \frac{\lambda}{\lambda_c} \right)^6 \quad [4]$$

where

$$\lambda_c = 2\pi a_s n_1 \quad 2\Delta_s / 2.405 \quad (\mu\text{m}) \quad [5]$$

where  $n_1$  is the refractive index of the core glass (1.46).

The effect of decreasing the fiber core size, which corresponds to decreasing the spot size, is to increase the waveguide dispersion. As a result, the zero dispersion wavelength of the total dispersion will shift towards longer wavelengths. Since the zero material dispersion of germania doped silica is typically greater than 1.3 microns, the addition of waveguide dispersion moves the zero dispersion wavelength further away from the operating wavelength of 1.3 microns. It is therefore desirable to have a large core size to minimize the chromatic dispersion at 1.3 microns.

#### D. Optimum Design

Based on the preceding sections, the following requirements can be stated

1. Small spot size to minimize microbending loss.
2. Large spot size to minimize splicing loss, Rayleigh scattering loss, and chromatic dispersion at 1.3 microns.
3. Minimum germania concentration in the core of the fiber to minimize Rayleigh scattering and material dispersion.

To achieve objective 3, a depressed cladding design has been adopted. This design allows lower germania concentrations to be used in the core of the fiber by depositing a cladding region which has a refractive index which is lower than that of pure silica. By using this design a reduction of approximately 0.05 dB/km in Rayleigh scattering loss as well as a decrease of approximately 10 to 20 nm in the zero dispersion wavelength can be achieved as compared to the equivalent matched cladding design.

A tradeoff must be made to achieve objectives 1 and 2. If an average axial offset of 0.5 microns is assumed and an upper bound of 0.10 dB per splice is allowed due to axial misalignment, then from equation [2] the minimum spot size is 3.3 microns. This spot size, however, would produce enough waveguide dispersion to shift the zero dispersion wavelength to approximately 1.34 microns. What must be done, then, is to design the fiber to have as large a spot size as possible without incurring excessive microbending loss during the cabling process.

By performing microbending tests as well as cabling experiments using fibers with different spot sizes, it was found that a spot size of approximately 4.5 microns at a wavelength of 1.3 microns gave the best tradeoff between microbending loss and chromatic dispersion. This spot size corresponds to ESI parameters of  $a_s = 3.9 \mu\text{m}$  and  $\Delta_s = 0.33\%$ . A typical preform refractive index profile of this type of fiber is shown in Figure 1.

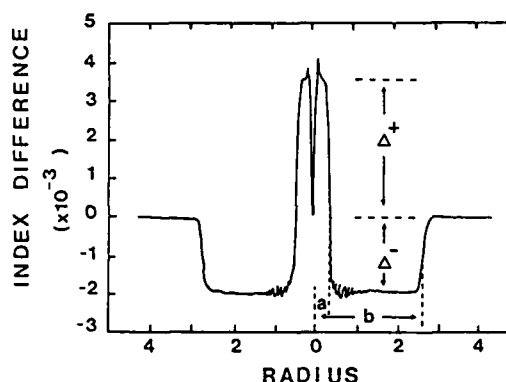


Fig. 1. Typical preform refractive index profile

#### Cable Design

An optical fiber cable must be designed such that the optical fibers it contains are protected from the environment. The fibers must be protected from the high tensile forces which are required to pull the cable into place. They must also be protected from abrasion and crushing loads. One of the most important characteristics of an optical fiber cable is its ability to withstand large variations in temperature without subjecting the optical fibers to strain which would cause a drastic increase in the optical loss. This temperature immunity is achieved by stranding the fibers around a central strength member in a helical manner. The actual pitch or lay length of the stranding, along with the coefficients of thermal expansion of the materials used in the cable, determine the temperature extremes at which the cable can operate. A short lay length is desirable for a cable which will be subjected to large temperature variations. However, the lay length cannot be made extremely small or the lifetime of the fibers will be reduced.

Along with these technical requirements is the requirement that the cost of the cable be minimized. A commonly used cable design is the loose tube design in which each fiber channel is contained within a primary tube and stranded around a central strength member. The Valtec ChannelMax™ design is also a loose tube design; however, it does not require an individual primary tube for each fiber channel. By

TABLE I  
Average Fiber Parameters

$\lambda_c$ (microns)	$a_s$ (microns)	$\Delta s$ (%)	$\omega_c$ 1.3 (microns)	$\lambda_o$ (microns)
1.212	3.90	0.33	4.44	1.313

TABLE II  
VALTEC SINGLE MODE CABLE

Total Number of Fiber: 24

Total Number of Tube: 4

Channel No.	Loss at Different Process Stage in dB/Km at 1300 nm			Loss Difference Cable - Fiber (dB/Km)	Loss at -30°C at 1300 nm (dB/Km)	Loss Difference (-30°C)-(Room Temp) (dB/Km)
	Fiber	Tube	Cable			
1	.51	.57	.57	.06	.57	0
2	.41	.45	.40	-.01	.48	.08
3	.39	.37	.40	.01	.45	.05
4	.43	.38	.37	-.06	.43	.06
5	.45	.48	.42	-.03	.46	.04
6	.41	.35	.41	0	.41	0
7	.41	.44	.42	.01	.43	.01
8	.43	.36	.38	-.05	.45	.07
9	.43	.39	.44	.01	.46	.02
10	.42	.43	.44	.02	.48	.04
11	.44	.43	.41	-.03	.40	-.01
12	.43	.42	.40	-.01	.38	-.02
13	.39	.42	.56	.17	.45	-.11
14	.44	.42	.44	0	.51	.07
15	.46	.46	.46	0	.52	.06
16	.43	.42	.44	.01	.44	0
17	.35	.55	.39	.04	.42	.03
18	.44	.40	.49	.05	.45	-.04
19	.50	.57	.49	-.01	.61	.12
20	.36	.35	.39	.03	.44	.05
21	.40	.46	.46	.06	.48	.02
22	.46	.48	.50	.04	.39	-.11
23	.40	.39	.41	.01	.39	-.02
24	.40	.45	.46	.06	.39	-.07
Average	.43	.44	.44	.01	.45	.01

color coding and stranding six fibers around each other, they can be contained within a single primary tube. A 24 fiber cable then only requires four primary tubes. As a result, the cost of materials for the cable has been reduced without sacrificing performance.

The ChannelMax<sup>TM</sup> cable design is shown in Figure 2. The cable is designed to accommodate up to 6 primary tubes. In cases where less than six primary tubes are used filler tubes are included. Each of the primary tubes is gel filled. The six tubes are stranded around a polyurethane covered steel strength member. The steel member can be designed such that the cable can withstand 600 lbs. of pulling tension without inducing any significant tension to the optical fibers. The stranded tubes are held in place with a polyester binder tape. A polyethylene outer jacket is extruded over the cable after the binder tape has been applied.

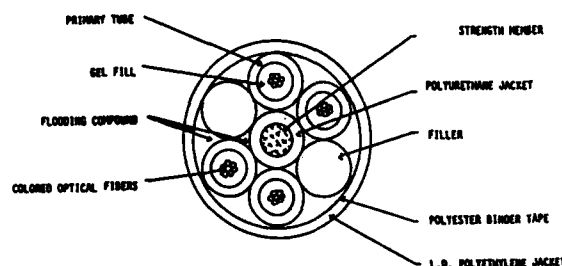


Fig. 2. 24 Fiber ChannelMax

### Optical Performance

#### A. Optical Loss

A 24 fiber ChannelMax<sup>TM</sup> cable was fabricated using single-mode fiber of the depressed cladding design. The average fiber parameters are given in Table I. Table II summarizes the optical loss of the cable at 1.3 microns both during the cable construction as well as during the environmental testing. The average optical loss of the finished cable at 1.3 microns was 0.44 dB/km. The average cabling induced loss at this wavelength was only 0.01 dB/km. This indicates that using the present fiber and cable designs, fiber can be cabled with virtually no loss penalty.

The performance of the cable at low temperatures was determined by subjecting the cable to a temperature of -30°C. At this temperature a 0.01 dB/km increase in optical loss was observed. Based on these results, it can be concluded that this cable design can be used in environments with low temperature extremes down to -30°C without any appreciable increase in optical loss. The optical loss of the cable was also tested under impact, crush, tensile load, cold bend and cyclic flex testing. The results of these tests are given in Table III.

Since this cable was to be used for system testing, the fiber channels were spliced together to give concatenated links of 2.027, 4.054, 6.081, 12.162, and 24.324 km. The splicing was performed using elastomeric splices. The average splice losses for each concatenated channel is given in Table III. The total average splice loss of all the channels was 0.11 dB. With these low splice losses as well as the low loss of the fiber cable, the total end to end loss averaged 0.54 dB/km. This low optical loss translates into an unrepeated span of approximately 45 km for a system with a total span loss of 25 dB.

TABLE III

Summary of Optical Loss After Splicing

Length (km)	Loss (dB)	Norm. Loss (dB/km)	Avg. Splice Loss (dB)
4.054	2.20	0.54	0.08
6.081	3.40	0.56	0.12
12.162	6.20	0.51	0.05
24.324	12.90	0.53	0.17

#### B. Dispersion

The chromatic dispersion of these concatenated links was measured using a single pass Raman laser system (5). The results are summarized in Table IV. There is no indication of anything other than a purely additive law for total dispersion. The average zero dispersion wavelength of all the fiber used in the cable was 1.313 microns. The average dispersion value at 1.3 microns was -1.0 ps/nm-km. This is almost exactly what was measured on the concatenated links.

Figure 3 is a plot of the dispersion components as well as the total dispersion of the 24 km channel. The figure also includes the predicted dispersion using a model developed at Valtec. The prediction was made using the average fiber parameters of the fibers used in the 24 km channel. The solid line is the predicted dispersion and the circles are measured points. The agreement is excellent throughout the 1.0 to 1.6 micron region.

Based on these results, it is clear that unlike multimode fiber, single-mode fiber bandwidth can be calculated precisely from the dispersion values of the individual fibers which make up the concatenated link. In addition, it is possible to predict the dispersion of the total link based on a model which does not require dispersion measurements on each of the fibers which make up the link.

TABLE IV  
Dispersion Results for the Concatenated Fiber

Length (km)	$\lambda_0$ (microns)	D @ 1.3 (ps/nm-km)
2.027	1.310	-0.8
4.054	1.311	-0.9
6.081	1.313	-1.1
12.162	1.313	-1.1
24.324	1.312	-1.0

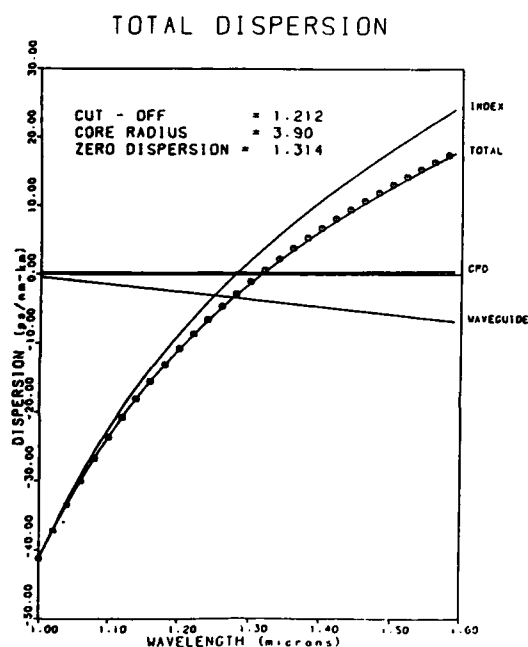


Fig. 3. Chromatic dispersion components and the total dispersion measured on the 24 km link and the prediction using the average ESI parameters

#### Conclusion

The design of a single-mode fiber cable has been reviewed with an emphasis on an optimum design to minimize total optical loss and chromatic dispersion. The results from measurements on a 24 fiber ChannelMax<sup>TM</sup> cable were presented. There was no significant increase in optical loss of the fiber due to the cabling process. The average optical loss of the cabled fiber at 1.3 microns was 0.44 dB/km. Environmental testing indicated that virtually no increase in optical loss occurred when the

cable was subjected to a temperature of -30°C. The fiber was spliced into concatenated links of various lengths with an average splice loss of 0.11 dB using an elastomeric splice. Dispersion measurements on each of these links confirmed that single-mode fiber chromatic dispersion is purely additive as predicted by theory. Average end to end loss of the cable including splices was 0.54 dB/km.

#### REFERENCES

1. H. Matsumura, and T. Suganuma, "Normalization of single-mode fibers having an arbitrary index profile", Appl. Opt., Vol. 19, No. 18, pp 3151-3158, 1980
2. L. Jeunhomme, "Single-mode fiber design for long haul transmission", IEEE J. Quantum. Electron., Vol QE-18, pp. 727-732, 1982
3. D. Marcuse, "Loss analysis of single-mode fiber splices", Bell Syst. Tech. J., Vol. 56, pp 703-718, 1977
4. P. Sansonetti, "Modal dispersion in single-mode fibres: simple approximation issued from mode spot size spectral behavior", Electron. Lett., Vol. 18, No. 15, pp 647-648, 1982
5. L. G. Cohen, and C. Lin, "A universal fiber-optic measurements system based on a near-IR Raman laser", IEEE J. Quant. Electron., QE-14, pp 855-859, 1978



STEVEN van't VELD received a M.S. degree in Mechanical Engineering at the Delft University of Technology, The Netherlands, in 1976. He joined NKF Kabel BV in 1978 as a development engineer in the Fibre Optics Group. In 1982 he came to Valtec where presently his function is Manager of Cable R&D.



DAN HURWITZ received his B.S. in Ceramic Science from Penn State University in 1977. He is currently the Environmental Test Engineer for Valtec, responsible for testing and evaluating environmental effects on optical fibers and cables.



PETER H. PRIDEAUX has a BA degree in Chemistry, and MS degree in Ceramics and earned a Ph.D in Ceramics in 1978 from Alfred University, Alfred, NY. He came to Valtec in 1980 and is presently Director of Optical Fiber Research & Development.



DAVID ROLAND received an Associate of Science in Laser and Electro-optics Technology at Springfield Technical Community College, Springfield, MA. He joined Valtec in 1980 and is presently with the Optical R&D Measurement Group.



ISHWAR D. AGGARWAL received his Ph.D. in Materials Science from Catholic University in Washington, D.C. in 1974. He is currently Vice-President of Research and Development at Valtec.



A NEW ENGINEERING APPROACH FOR CABLE  
IN FIRE SITUATIONS USING HALOGENATED POLYMERS

J. R. Hoover (Speaker), A. L. Moran, G. C. Sweet, D. B. Allen,  
J. G. DiPinto, D. H. Lutz and J. O. Punderson\*

Polymer Products Department  
E. I. Du Pont de Nemours & Co., Inc.  
Wilmington, Delaware

Abstract

All organic materials will burn and give off combustion products. Toxicity and corrosion are not inherent properties of a material; they depend upon the combustability of a material and the conditions and dynamics of a fire. Therefore, those properties which permit moderation or elimination of the fire itself should be identified and controlled.

Recently, undifferentiated toxicity and corrosion concerns have developed about halogenated polymers as a generic class.

This paper reviews fire science and toxicology considerations affecting materials selection and cable design options. It also examines the merits of performance specifications combined with a hazard analysis and materials engineering approach.

The objective is to identify the fire hazards associated with all materials and end products. The methodology ranks the risks as they occur in the fire sequence. The goal is to reduce the risk in the order and the magnitude of the threats imposed by the fire.

Introduction

Over the last 50 years, hundreds of millions of pounds of high performance halogenated polymers have been used to satisfy the high standards and critical requirements of the wire and cable industry. Their beneficial characteristics and reliable performance are widely recognized.

Recently, undifferentiated toxicity and corrosion concerns have developed about halogenated polymers as a generic class. Attempts have been made to completely exclude all types from some end uses based solely on chemical composition. This has often been done without thorough and meaningful assessment of the fire hazards associated with their use or with the use of alternate materials.

\*Consultant in Fire Standards. Formerly with  
E. I. duPont deNemours.

This paper reviews fire science and toxicology considerations affecting materials selection and cable design options. It also examines the merits of performance specifications combined with materials engineering versus the generic class exclusion approach.

The engineering approach attempts to identify the fire hazards associated with all materials and end products. The methodology is to rank the risks as they occur in the fire sequence. The goal of the approach is to reduce the risks in the order and the magnitude of the threats imposed by the fire.

A comprehensive perspective is provided for cable manufacturers, specifiers, regulators and end users. The objective is to optimize cable performance in a fire situation while retaining or improving the more traditional properties affecting day-to-day performance and long life durability.

The various classes of halogenated polymers are distinctly different in halogen content, thermal stability, flame retardancy, toxic effects, pyrolysate corrosivity and smoke generation. Key comparisons are shown.

Some polymers can incorporate a wide range of fillers and modifiers to minimize various fire hazards while optimizing mechanical and electrical properties. Information is included to show how halogenated polymers can meet critical performance specifications written for nonhalogen materials.

Fire Environment Effects

The direct effects on equipment, structures, and people are a function of the fire frequency, its overall magnitude, and proximity to the actual flames and main combustion sources. These direct effects often pose the greatest and most immediate threats to life and property.

Fire safety engineering, however, must also consider the indirect effects like convective heat, carbon monoxide, carbon dioxide, oxygen depletion, smoke generation, and acid gas evolution (Fig. 1).

(Figure 1)

#### Effects of Fire on Equipment, Structures and People

The direct effects are a function of:

- Fire Frequency
- Fire Magnitude
- Flame Exposure

The indirect effects are due to:

- Heat
- CO/CO<sub>2</sub>
- Smoke/Soot
- Acid Gases
- Water
- Fire Fighting Media

A number of primary and secondary concerns from the indirect fire effects are seen here in Figure 2. As a rule, all organic materials will burn and give off combustion products. The radiant and conductive heat itself can contribute to major structural damage, while the convective drafts from the fire can transfer the effluents far beyond the initial fire sources.

Actual fire fatality studies by the NFPA; Halpin, Zikira & Terrill; and others have concluded that carbon monoxide is often the highest volume and most commonly lethal toxicant, not (halogen) acid gases.<sup>12,13 & 14</sup> The heat from the fire also contributes to the lethality of the environment.

(Figure 2)

#### Indirect Effects Caused By Fire

Product	Concerns	
	Primary	Secondary
Heat	Deformation Deterioration Oxidation Death	Convective Transfer of Effluents Hyperthermia
CO/CO <sub>2</sub>	Suffocation	Disorientation
Smoke/Soot	Contamination	Clean-up Damage
Acid Gas	Corrosion	Clean-up Damage
Water	Soak Damage	Clean-up Damage
Fire Fighters	Mechanical Access	Clean-up Damage

Smoke and corrosion are only two aspects of fire destructiveness. They must be considered in relation to combustibility factors influencing whether or not fires occur and enlarge. In other words, it would be a very dangerous course to allow corrosion or smoke concerns to justify sacrifice in combustibility properties of cable materials, possibly bringing about larger numbers of fires and more extensive fires. Water soak and the conduct of the fire-fighters can also be sources of damage, though these are certainly justified in efforts to extinguish the fire.

A logical approach is needed to better understand the complexity of a fire and deal with the wide range of possible effects, concerns, and compromises in choosing and regulating materials used.

#### Total Fire Hazard Approach

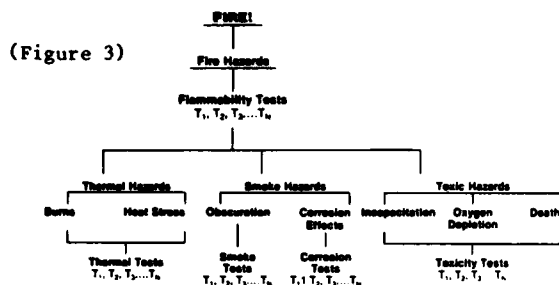
In a December, 1982 report to the NFPA,<sup>7</sup> the "Committee on the Toxicity of the Products of Combustion" reviewed extensive research on the toxicity issue, and other related fire hazard characteristics of materials. They concluded that toxicity tests alone are not adequate to judge toxic hazards and rank materials. The conditions in the fire environment affect the nature of the hazards that develop. The Committee therefore proposed that material performance characteristics and parameters of the overall system or environment must be considered in making meaningful hazard assessments.

It was recommended that some form of fire model using material performance characteristics determined in standard tests, in conjunction with system parameters, is needed to determine the nature of the fire environment and its threat to building occupants. Work on mathematical fire models is progressing but comprehensive hazard assessments may be some years away.

The Committee felt this subject was exceedingly complex and considered it inappropriate to recommend any specific hazard assessments techniques at this time. However, some of the following premises were considered. They are shown below, not as recommendations, but to illustrate the potential difficulties of equating specific laboratory combustion and toxicity test data to the real fire performance of materials:

- 1) The potential fire hazard of a product is given by the degree to which the product reduces the time available for escape, or decreases the time for a hazardous situation to develop.
- 2) The immediate threat to life safety in a fire situation is given by exposure conditions expressed as a concentration versus time relationship for heat, visible smoke, and toxic gases.
- 3) These concentration-time relationships in a fire system are functions of a) the rates of release of heat, visible smoke, and toxic gases for all materials exposed to the fire environment, b) their rates of transport within the system, and c) their rates of removal from the system by venting and absorption.
- 4) Total release rates of heat, visible smoke and toxic gases from a material are functions of the surface area exposed, the flame spread rate, and the release rates per unit area of the material. The latter quantities are dependent on exposure conditions and can be determined independent of the system in which the material is found.

5) Exposure conditions which determine release rates of a material can be related to the system characteristics, material configuration, and material location appropriate to the particular fire scenario being considered."



To recapitulate, Figure 3 lists the fire hazards of greatest topical concern to material selection today. There are many hazards associated with fire and numerous tests that can be used to judge some aspects of material performance under laboratory conditions.

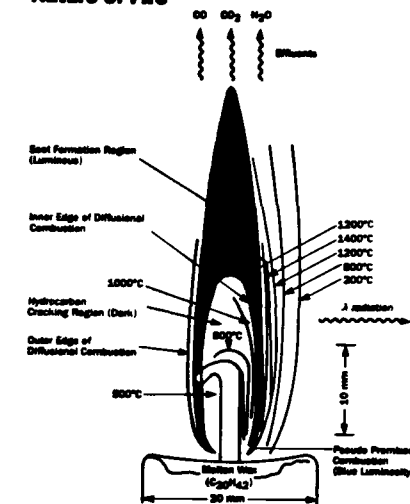
It is important to distinguish between a single "flammability test," of which there are many; and the total "fire hazard" which may be only partially characterized by any single flammability test. Hazard assessment includes flammability, the various ways it can be characterized, and other factors, conditions and interactions posed by the environment.

Furthermore, some types of hazards are sequentially dependent upon others. The toxicity and smoke hazards and corrosion effects depend upon the combustibility of materials and the conditions and dynamics of the fire. Materials more resistant to ignition, combustion and fire propagation usually produce lower smoke and toxicity hazards than materials which burn more readily and add to the risk of large scale fire development. Specific laboratory tests do not determine hazard. Such tests have a limited ability to predict the actual hazards and effects of a fire situation.

Programs to reduce or eliminate any one particular hazard should carefully consider the interactive effects on associated hazards, especially the flame hazard.

Fires are hazardous. All aspects of all hazards must be considered when selecting materials, designing cables or developing specifications. The following sections will examine each of the major hazards in more detail.

## Nature of Fire



Microstructure of candle flame, a vaporizing high molecular weight solid.

Ref. 1980 PRC Study

(Figure 4)

The terminology of physical chemistry and its application to fire science can be perplexing. The simplest fire model is an isolated flame on a solid substrate. A burning candle provides just such a model to help develop an understanding of the combustion mechanisms (Fig. 4).

The wax first melts, vaporizes above the wick and encounters oxygen. On ignition, oxidation occurs in a complex series of chemical reactions. The inner part of the flame contains insufficient oxygen for complete combustion and chemical reduction of carbon occurs to form soot and thus smoke. In a well designed candle, further oxidation reactions occur as the gases flow upwards and almost all the fuel is converted to carbon dioxide and water with a little carbon monoxide.

With the wide varieties and combinations of materials used on cables today, the reactions are far from simple and inevitably smoke, carbon monoxide, and a range of other effluents are produced. There are wide varieties of polymers and compounding ingredients that can reduce smoke and alter the type, amount and sequence of other effluents produced.

In the case of the candle the solid fuel behaves simply. It melts uniformly, vaporizing and burning evenly with pilot fuel supplied by the wick. In the case of polymers, decomposition must occur by first heating to a temperature which will break up and gasify the polymer network. The pyrolyzed gases evolved will then take part in the oxidative combustion process upon ignition.

Again, in the simple case, the candle wick is all important because it supplies a steady source of fuel. Wick surface effects like diameter, length and roughness are important. A candle without a wick will not sustain combustion under normal circumstances. Furthermore, if there were insufficient heat available by conduction, convection and radiation to melt the wax in the wick, the flame would also go out. Heat flux and the radiative feedback influence the rate of further fuel gas production.

This is an important principle. Many materials will not sustain a flame in isolation. For example, a log of wood goes out in isolation but a pile of logs burn steadily. Those with fireplaces know that the number of logs, their arrangement, location on the grate, damper draft setting and level of ashes under the grate all affect the fire. The principle is that there are strong interactive effects between burning objects in close proximity and with their surroundings. Each will sustain the other by providing sufficient heat and a combustion source.

It is thus important to remember that a single cable run may well appear flame resistant but would support combustion when bunched together with other cables to form a larger fuel and heat source. This principle is applied in specification procedures for bunched cables, which will be referred to again.

Combustion is a process of sequential steps. The five essential stages of the burning process are listed in Figure 5.

(Figure 5)

#### Stages of Fire

Stage 1	Heating
Stage 2	Decomposition
Stage 3	Ignition
Stage 4	Combustion
Stage 5	Propagation

Each of these stages is of course dependent upon the previous stage having taken place. It is important here to consider what constitutes flame resistance and the effect of flame retardants on organic polymers. Each stage is analyzed in turn:

Stage One is moderated by materials which can increase the specific heat of the compound. Inorganic hydrates are used since they absorb energy during dehydration. Such materials are often incorporated into polymers to improve initial flame resistance. In particular, they are used with polymers which do not have basic flame resistance; for example, nonhalogenated polymers.

However, such fillers are not regenerative and may not have long lasting effects at high temperatures or in the subsequent stages of the burning process, since they can be quickly exhausted under intense heat. Alumina hydrate ( $\text{Al}_2\text{O}_3 \cdot 3\text{H}_2\text{O}$ ) begins to lose water of hydration around  $220^\circ\text{C}$ , with much more rapid and complete loss at  $310^\circ\text{C}$ . Remember that boundary temperatures in a simple candle flame range from  $200^\circ\text{C}$  to  $1200^\circ\text{C}$ . Very high filler loadings ( $>200$  pph) are required with many nonhalogen polymers to optimize flame retardancy.

#### Stage 1 - Heating

Increase Specific Heat Eg. - Inorganic Hydrate Addition

\*\*\*

Stage Two is affected by materials which increase the decomposition temperature of the polymer. Fluorine, which forms an extremely strong bond with carbon, is very effective in decreasing the onset of decomposition. Thus fluorinated polymers are flame resistant in that they are difficult to ignite. Fluoroelastomers and perfluoroplastics commonly have a limiting oxygen index approaching 100.

Chlorine is also effective to some extent at this stage. Its bond energy is higher than bromine or iodine in this respect.

Phosphorous compounds and other additives are also effective in Stage Two. They function by forming a char residue thus depriving the access of oxygen to combustible material. Phosphorous also inhibits polymer chain scission, and promotes dehydration and other elimination reactions in oxygenated polymers. References (8) and (10) provide further background on this subject.

#### Stage 2 - Decomposition

- Inhibit with Polymers Containing - Fluorine  
- Chlorine
- Add Phosphorous Containing Compounds

\*\*\*

Stage Three and Stage Four reactions, both in the gaseous and condensed phases, are inhibited strongly by the halogens chlorine and bromine. The halogen mechanism is chemically regenerative within the flame boundaries, the Stage 1 hydrated filler system is not.

In the gaseous phase, redirection or termination of the chemical reactions occur. The physical effect of the heavy halogens on inhibiting oxygen access and heat occurs in the condensed phase. It is postulated that halogenation to form polymeric residues can also occur, which then form carbon. Hence, the high level of smoke associated with burning PVC.

In general, chlorinated polymers contain an excess of chlorine and so there is much scope for reduction of chlorine and the associated hydrogen chloride gas, in practical compounds. The goal would be to reduce the toxic hazards and corrosion effects without starving the inhibition reaction and increasing the flame hazard.

### Stages 3 and 4 - Ignition and Combustion

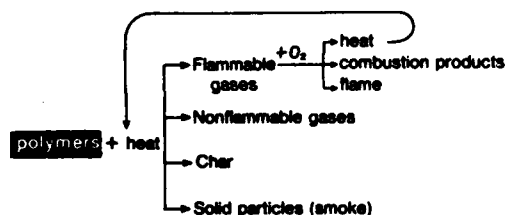
- Inhibited by Chlorine and Bromine
- Interruption of Flame Chemistry
- Formation of Noncombustible Residue

Earlier references were made to the false assumptions that may be drawn from the flame resistance of a single cable tested in isolation. This also applies to any laboratory test on a small specimen. The propagation of a fire is directly related to the total heat mass available. If net heat loss to the surroundings is greater than net heat gain from combustion then the fire will not propagate. At this point the reactions occurring in the ignition and combustion stages (i.e., Stages 3 and 4 of the individual components of the total mass) control the situation. To prevent propagation (Stage 5) continual inhibition of the oxidative flame chemistry is important. This is accomplished by evolution of hydrogen halide from the polymer which acts in a regenerative fashion to interrupt the free radical chain reaction chemistry.

Figures 6, 7 and 8, by D. Culverhouse<sup>8</sup>, illustrate the physics and chemistry of gas phase polymer combustion and the mechanism by which halogen interferes with the flaming process.

(Figure 6 - Ref. 8)

### Polymer Thermal Decomposition



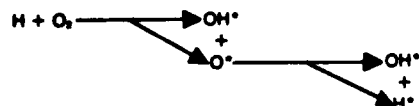
(Figure 7 - Ref. 8)

### Flame Chemistry Reactions

#### 1. Exothermic chain propagation



#### 2. Chain branching



\*Free radicals

(Figure 8 - Ref. 8)

### Halogen Gas Chain Chemistry Inhibition

#### 3. Chain Inhibition



#### 4. Re-generation of HX



X = Halogen (Cl, Br or I)

R = Alkane

Relative effectiveness of halogens →

I Br Cl F

\*Free radicals

From the foregoing it is our opinion that the presence of a halogen in the fire zone is of paramount importance to control propagation. Although the onset of decomposition can be reduced by the addition of inorganic hydrates, it should be kept in mind that after the heat sink effect has been exhausted there is nothing to inhibit the subsequent oxidation reactions from occurring. The degree to which this is important depends very much on the intensity of the fire and the type of cable construction. For example armouring in the design will itself act as a heat sink.

To demonstrate these points two cable compounds were compared, with the results shown in Figure 9.

(Figure 9)

### Flame Propagation Laboratory Versus Simulated Service Tests

	CSM + 25 PWR Clay	EPDM + 180 PWR Aluminum Hydrate
LOI	33	34
VWI—Lab Test	Pass	Pass
IEEE 383 Bunched Cable Test	Pass	Fail

The compound on the left, was based on CSM, and the other based on EPDM, which has no halogen in its composition.

The EPDM contained 180 parts of inorganic hydrate filler and the CSM was compounded for normal toughness, fluid resistance and long term durability.

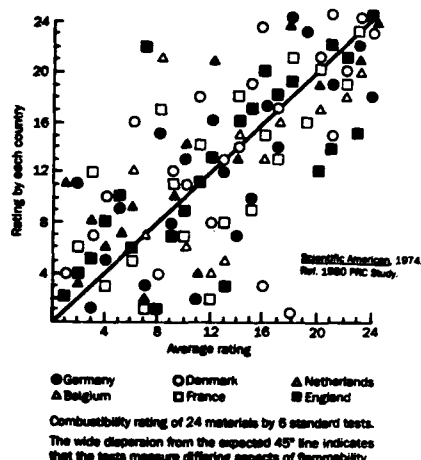
Although both had similar limiting oxygen index numbers and passed a single vertical wire test, the chlorinated polymer alone passed a bunched cable test. IEEE 383 is an American test procedure. (IEC 332-3 is the European test method for bunched cable testing and may replace the more well known CEST test.)

It is believed that in this severe test, the hydrate filler in the EPDM was used up in absorbing initial heat energy, and thereafter only char residues were available to prevent further propagation. In other words, the net heat absorbed by the filler system was less than the heat gain from the combustion process and fire environment.

Finally, just to put the question of combustibility into perspective, Figure 10 shows the complete lack of correlation between the ratings of 24 construction materials by six standard small scale tests. The conclusion from this evaluation is that each test measures some different aspect of flammability; no one test completely characterizes the total flammability hazard.

(Figure 10 - Ref. 7)

#### Small Scale Tests



#### Smoke Hazards<sup>15</sup>

This subject is of course extremely important where fires can take place in areas of difficult access or exit. Smoke can cause disorientation for persons trying to escape and also make fire fighting difficult.

(Figure 11a)

Specific Optical Density	CSM Smoke		EPDM Smoke
	Standard	Suppressed	
Flaming	695	219	91
Smouldering	450	302	570
Limiting O <sub>2</sub> Index	32	34	26
Smoke Index (NES 518 Method)	110	37	—

Much work has been done in order to reduce the smoke evolution of CSM cable sheathing compounds. By the addition of smoke suppressant materials to CSM, smoke generation can be reduced significantly as shown in Figure 11a.

Comparisons are obtained by tests carried out with an NBS smoke chamber. Note the reduction in specific optical density from 695 to 219 in the flaming mode for the smoke suppressed compound compared with standard. A similar reduction is observed in the smouldering mode. EPDM is much better in the flaming mode. The absence of a halogen type flame inhibition mechanism makes it a much more efficient fuel source. Note that in the smouldering mode EPDM is actually much higher in smoke density. In any case the much lower LOI of EPDM would indicate poor flame resistance.

The UK Admiralty, in their ships specification, have proposed a "smoke index." The CSM smoke suppressed compound shows a significant improvement when tested to this method, from 110 to 37.

Figure 11b shows some data obtained with PVC. PVC compounds are generally difficult to smoke suppress, particularly when low acid evolution is also required and retention of essential flame resistance desirable. However, much work is taking place to improve PVC in this regard.

Another way of looking at this is to measure the smoke density over the first four minutes of burning to produce a Smoke Obscuration Number. This penalizes materials which produce smoke in the early stages of a fire. The PVC compound takes about the same time to reach maximum smoke density as the unmodified CSM compound but the smoke density in the early critical stage of the fire is shown by the high SON<sub>4</sub>. The smoke suppressed CSM is clearly an improvement over the PVC cable compound tested.

#### PVC Versus CSM—Smoke Evolution

(Figure 11b)

	Standard CSM	PVC	Suppressed CSM
Smoke Obscuration Number	568	704	183
Time to Maximum Smoke Density	8	9	12

[Smoke Obscuration = Density at (1 + 2 + 3 + 4) Minutes]  
(No. SON<sub>4</sub>)

#### Corrosion Effects

The potential for corrosion is one of the elements in determining the hazard of smoke. This aspect, of course, is important for cables which are in close proximity to delicate electronic equipment as well as other components susceptible to service loss by corrosive attack.

Any method designed to reduce acid gas evolution to address toxicity concerns will also reduce the potential corrosivity.

The German VDE Specification Committee and latterly an IEC working group, have proposed that corrosivity can be conveniently measured by pH and conductivity tests. The pyrolysate of a burnt sampler is passed into solution and these measurements taken. Figure 11c shows the pH and conductivity of solutions prepared from a range of polymers.

(Figure 11c)

#### Corrosivity

	pH	Conductivity (Ω CM <sup>-1</sup> )
PVC	1.8	5600
Polychloroprene	2.0	4500
CSM Standard	1.9	3000
Chlorinated Polyolefin	2.7	3000
LDPE	5.0	20
EPDM	5.0	60
EVA	4.0	75
Low Acid/Low Smoke CSM	4.05	46
VDE Spec Proposed	4	100

The more acidic materials produce, as expected, a lower pH value and higher conductivity value. The bottom of Figure 11c shows results for a low acid CSM compound and the proposed specification values. There should be no difficulty in meeting these specification values consistently with such a material.

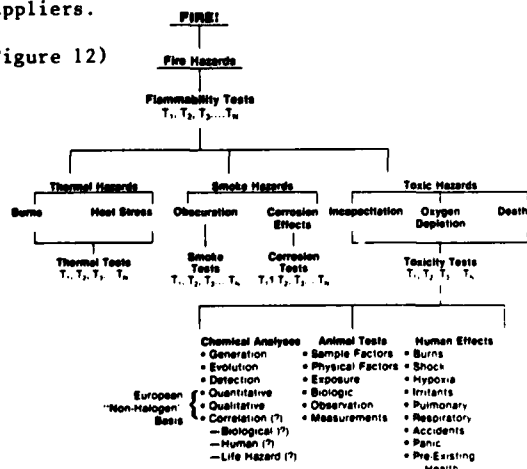
This approach to defining potential corrosive effects shares the same limitations of many other laboratory tests - i.e., in an effort to provide convenience and reproducibility for the experimentalist, tests are devised which may bear no relationship to the corrosive atmosphere generated in an actual fire situation. The dissolution of pyrolosates and subsequent measure of the behavior of the solution assumes a standard fire as well as equivalent transport properties of the evolved gases, neither of which should be assumed for a dynamic event such as a fire.

#### Toxic Hazards

There are an abundance of references on this subject. The vast majority of fire fatalities have always been the result of smoke inhalation. Statistical data show this to be the case independent of the fuel source, for smoke, the major killer, is an unavoidable consequence of fire. Inhalation of hot air is responsible for many fatalities. Experimental fires in building structures have shown that minimum survival concentrations of oxygen, or maximum survival breathing temperatures were reached before any toxic gases attained a lethal concentration. The National Fire Protection Association has developed the position that current small scale laboratory tests are not appropriate to assess the total toxic hazard of burning materials.

Figure 12 is similar to Figure 3 but with a listing of the historical toxicity issues that developed in Europe in the early 1970's. This lead to the generic exclusion of many materials based on their chemical composition and not on the basis of their actual performance in a fire. A broad reconsideration of the risks posed by this practice is underway among many end users, regulators, cable manufacturers and material suppliers.

(Figure 12)



All organic materials will produce carbon dioxide and carbon monoxide when burned. As previously mentioned, in the example of the candle, carbon monoxide is produced in real fires due to incomplete combustion. This gas ranks first as a cause of fire deaths because it is always present in uncontrolled fires. The NFPA again states that CO is always present in the lungs of fire victims.

Figure 13 gives some idea of the effect of carbon monoxide on human beings. Note that at 3000 ppm death can occur in 30 minutes.

A similar chart is shown for carbon dioxide (Fig. 14).

(Figure 13 - Ref. 7)

#### Response of Humans to Various Concentrations of Carbon Monoxide

Concentration, ppm	Symptoms
200	Headache after 2 to 3 hours, collapse after 4 to 5 hours
400	Distinct poisoning, frontal headache, and nausea after 1 to 2 hours, collapse after 2 hours, death after 3 to 4 hours
800	Collapse after 1 hour, death after 2 hours
1000 (0.1%)	Difficulty in ambulation, death after 2 hours
1500	Death after 1 hour
3000	Death after 30 minutes
8000	Immediate death by suffocation
12,800	Unconsciousness after 2 to 3 breaths, death in 1 to 3 minutes

Ref. Flammability Handbook for Plastics # 1982

(Figure 14 - Ref. 7)

#### Response of Humans to Various Concentrations of Carbon Dioxide

Concentration, ppm	Symptoms
250 to 350	Normal concentration in air
18,000	Ventilation increased by 50 percent
25,000	Ventilation increased by 100 percent
40,000	Ventilation increased by 300 percent, headache, weakness
80,000 (8%)	Dizziness, stupor, unconsciousness
120,000	Immediate unconsciousness, death in minutes
200,000	Narcosis, immediate unconsciousness, death by suffocation

Ref. Flammability Handbook for Plastics # 1982

The Toxicity Index assessment is carried out by assigning a toxicity rating to various gases that are likely to be produced during burning of cable materials. Some of these are shown in Figure 15. These numbers are then divided into a unit volume of each gas collected, to give an index figure. The summation of all the individual indices provides the final index for the material.

(Figure 15)

**Toxicity Index, REF NES 713**  
**Toxicity Rating—Concentration Considered Lethal After 30 Minutes**

Carbon Dioxide	100,000 ppm
Carbon Monoxide	4,000 ppm
Hydrogen Chloride	500 ppm
Sulphur Dioxide	400 ppm

Index of Each Gas =  $\frac{\text{Volume of Gas Produced During Pyrolysis}}{\text{Toxicity Rating}}$

Figure 16 demonstrates how this approach can be applied to CSM, using the MOD British Ministry of Defense test and calculation methods.

(Figure 16) **CSM—Evolution of Gases**

	Standard Sheath		Low Acid Sheath	
	Gas Volume	Index	Gas Volume	Index
H Cl	2780	5.55	280	0.57
SO <sub>2</sub>	230	0.58	178	0.45
CO	2260	0.57	1510	0.38
CO <sub>2</sub>	38200	0.38	40370	0.40
Total Index		7.08		1.80

NES 713 Calls for 5 Maximum

The left hand column of figures applies to a standard type of CSM compound which has not been compounded for reduced acid gas emission. The figures on the right are obtained for a specially designed cable jacket compound.

One can see the significant reduction in HCl gas emission that can be achieved. This allows CSM to meet the maximum allowable NES 713 index of 5. The actual percentage of acid gas evolved from such a compound is in the region of 0.5%.

The level of carbon monoxide evolved from these compounds is similar. Hence the index is controlled entirely by the level of HCl.

The same approach has been applied to PVC in order to reduce the acid gas level evolved during burning. However, the levels of acid reducing filler required for PVC have a significant effect on final flame resistance.

The approach utilized under NES713 provides two benefits: 1) it is a convenient method of deriving a number which can be used to rate materials; and 2) it avoids the use of test animals.

However, these benefits may be outweighed by its possible limitations. Like so many laboratory tests, it assumes a standard fire or a standard level of combustibility, which fails to credit a material's resistance to burning. Furthermore, it includes only those toxicants identified analytically - it does not account for those products of combustion that are not looked for. Finally, it fails the test of regulatory equity - it is based on composition, and does not measure the interaction of combustible materials with a realistic fire environment or a dynamic fire sequence.

Finally, to round off this section on toxicity, the results of some animal exposure tests carried out for NASA, by the University of San Francisco, are shown in Figure 17.

(Figure 17) **Relative Toxicity of Various Materials (NASA USF Procedure B)**

	Time to Death (Mins)
Polychloroprene	25
CSM	21
EPDM	21
NBR	19
Polyethylene	17
ABS	16.5
PVC	16.5
Polyamide	14
Food and Packaging	
Mashed Potatoes	11
Sugar	15
Spaghetti	20
Egg Carton	28

The NASA tests show the relative toxicity of various materials selected from the references. It is a sobering thought that in spite of all the efforts that have gone into the subject of burning cables, mashed potatoes or spaghetti are apparently more toxic under these test conditions than PVC, CSP, CPE or polychloroprene, all of which are halogenated.

Toxicity testing attempts to determine the physiologic response and actions of the principal life or health threatening factors present in fires. The objective in animal testing is to define the exposure/response relationship to evaluate the potential human health effects. The goal is to establish some margin of exposure safety for humans. Figure 18 lists just some of the many factors involved in animal inhalation toxicity testing.

(Figure 18 - Ref. 7)

#### **Factors Involved in Combustion Toxicity Testing Laboratory Animals**

- A. Sample Factors**
  - Size (weight, surface area)
  - Structure (powder, strips, block, sheet)
  - Position in furnace
  - Configuration: surface area to volume
  - Mode of decomposition
- B. Physical Factors**
  - Temperature rise
  - Heat Flux
  - Chamber dimensions, shape, materials of construction, lining
  - Length, volumes, and inner surfaces of connecting tubes, venting
  - Recycling, dilution or flow rate of combustion gases
- C. Exposure**
  - Dynamic or static chamber operation
  - Concentrations of combustion products
  - Nonflaming or flaming combustion
  - Head-only or whole body exposure
  - Duration of exposure
  - Ambient O<sub>2</sub> and CO<sub>2</sub>
  - Ambient humidity
  - Airflow rate through system in dynamic chamber operation

(Figure 18 - Ref.7)

- D. Biologic**  
 Species (rat, mouse, rabbit, etc.)  
 Sex, reproductive cycle  
 Animal care practices  
 Diet, food and water intake  
 Housing and caging facilities  
 Pre-exposure clinical observations  
 Pre-conditioning in neurophysiological tests  
 Quarantine  
 Activity or exercise
- E. Observations/Measurements on Animals**  
 Mortality, LC<sub>50</sub>  
 Immediate and delayed deaths  
 Neurophysiologic data EC<sub>50</sub> time to incapacitation  
 Body weight changes post exposure  
 Signs of eye and nose irritation, during and post-exposure  
 Evidence of recovery in post-exposure survivors  
 Diet consumption  
 Water intake  
 Urinary output  
 Urine osmolality, enzymes (LDH)  
 Blood chemistry, COHB, pH, pO<sub>2</sub>, pCO<sub>2</sub>, enzymes, e.g. transaminase, LDH, alkaline phosphatase  
 Blood pressure  
 Cardiovascular functions: EKG, heart rate  
 Pulmonary functions: respiratory rate, diffusional, mechanical, ventilatory measurements, lung macrophage response  
 Necropsy  
 Organ weights  
 Histopathology

Ref. 1980 PRC Study

The primary purpose of toxicity testing is to develop information on the human hazards to health and life from the perspective of the total fire scenario. Figure 19 lists the three main classifications of fire deaths compiled by the National Materials Advisory Board of the National Academy of Sciences. This further corresponds with previous references to carbon monoxide and heat as the most common cause of immediate fire deaths.

(Figure 19) **Smoke and Toxicity Human Considerations**

Category	Comments
Thermal	Aggravated by ventilation
Direct burns	Responsible for most prolonged hospitalization
General hyperthermia or shock	A significant factor in fire fighting
Chemical	Qualitatively and quantitatively influenced by ventilation
Conditions producing hypoxia	Chief cause of death, particularly carbon monoxide
carbon monoxide hydrogen cyanide oxygen deficiency	
Irritant gases and vapors	Delay egress, cause post-exposure respiratory complications
sensory pulmonary general respiratory irritants	
Smoke particulates	Decrease visibility; enhance toxic effect of adsorbed gases and vapors
Miscellaneous gases and vapors	
Exhaustive	Statistics relatively scarce
Panic, emotional stress	Often difficult to determine
Accidents, falls, other trauma	
Additive strain from preexisting health conditions	Significant particularly in older persons

## Laboratory Testing

5,16

Ref. 1980 PRC Study

The six European tests ranking the flammability of twenty-four building materials (Fig. 10) correlated so poorly that there is doubt of their utility, despite the reproducibility within the respective methods.

Stanford Research conducted an opinion study in 1977 among leading fire researchers to determine a) the state of understanding of fire and b) the ability to measure individual fire events. Figure 20/21 summarizes those results under eight categories. Figure 22 shows the many small scale tests under the same eight categories that were developed and are used today.

(Figure 20/21 - Ref. 7)

## Small Scale Tests Fire Events/Phenomena/Effects

	State of the Art*	
	Level of Understanding	Capability of Measurement
<b>1. Preignition</b>		
Softening and melting	8	9
Crosslinking	3	2
Dehydration	4	7
Pyrolysis	3	6
Char formation	2	8
Natural intumescence	4	5
<b>2. Ignition</b>		
Sustained/transient	8	10
Glowing/flaming	7	10
Spontaneous/remote heating	6	10
Piloted/flame heating	7	8
Radiation/convection	6	9
<b>3. Spread</b>		
Geometry	7	8
Orientation	6	7
Permeability	5	6
Thermal properties	10	10
Radiant augmentation	7	8
Forced convection	4	5
Transient burning	3	4
<b>4. Penetration/Endurance</b>		
Ablation	4	8
Char depth	7	9
Steady burning	7	10
Boundary transport	6	7
Thermal properties	10	10
Chemical/physical change	5	6

	State of the Art*	
	Level of Understanding	Capability of Measurement
<b>5. Heat Release</b>		
Burning rate (mass burning)	7	9
Surface spread	6	8
Heat feedback	4	8
Geometry	3	7
Orientation	2	8
Radiant augmentation	5	8
<b>6. Fuel Contribution</b>		
Pyrolysis	4	8
Smoldering	2	8
Flaming	2	8
Single-stage combustion	?	?
Two-stage combustion	?	?
<b>7. Smoke Production</b>		
Material composition	5	7
Toxic potential	3	5
Mass burning	5	7
Heat release	3	7
Smoke conversion potential	?	?
Geometry	2	7
<b>8. Flashover Potential</b>		
Enclosure geometry	6	7
Ventilation	7	8
Fuel bed (geometry, compactness, and such)	?	?
Single-stage combustion	?	?
Two-stage combustion	?	?

\*Scale of 0 to 10, with 10 as the highest level of understanding and capability. Question marks indicate that not enough is known about the phenomena to make a reasonable judgment.

Ref. 1980 PRC Study

(Figure 22 - Ref. 7)

### Small Scale Tests Some Currently Available Test Methods

	Adequacy Judgment*			
	Rationality of Design**	Realism of Simulation	Pertinence of Measurement	Quantitativeness of Measurement
<b>1. Preignition Tests</b>				
TGA/DTA	4	2	9	9
Pyrolysis	6	1	10	8
<b>2. Ignition Tests</b>				
Pill, Cigarette, Bolt	0	9-10	8-9	3
Satchkin Test				
ASTM E-136	2	2	3	2
Roof Covering				
ASTM E-108	2	10	8	6
Schlyter	7	4	6	6
Arc/Hotwire	1	8	8	3
Heat Release Rate				
Calorimeter (HRRC)	9	6	8	8
LOI ASTM D-2863	8	1	1	9
<b>3. Spread Test</b>				
Steiner Tunnel				
ASTM E-84	6	7	8	6
Radiant Panel				
ASTM D-162	9	7	8	7
Small Scale Tests D-635, D-1692	2	3	4	2
Corner Test	7	8	4	1

	Adequacy Judgment*			
	Rationality of Design**	Realism of Simulation	Pertinence of Measurement	Quantitativeness of Measurement
<b>4. Endurance</b>				
Standard T(t)				
E-119, E-152	2	6-8	7	5
Bureau of Mines penetration	1	1	3	1
Air duct Test				
UL-181	2	4	6	5
Pipe Insulation Test	2	8	9	10
<b>5. Heat Release Rate</b>				
HRRC	9	6	10	9
Bomb				
Calorimetry	1	0	3	10
NBS Potential Heat	8	6	7	9
<b>6. Fuel Contribution</b>				
ASTM E-84	5	7	6	5
<b>7. Smoke Production</b>				
NBS/AMINCO Chamber	7	4	8	9
R&H XP2				
ASTM D-2843	2	3	6	2
<b>8. Flashover Potential</b>				
Dutch Flashover Test	3	5	7	6

\*Scale of 0 to 10 with 10 the highest level

\*\*Pertaining to scalability, extrapolatability, versatility

Ref. 1980 PRC Study

The tests discussed in this presentation are small-scale tests. During the past few years small-scale fire tests of all types have come under considerable criticism because of the growing evidence they are not good predictors of actual fire performance, and the quoting of small-scale test data can be misleading to regulatory officials and the public.

Still, large-scale tests are costly and time-consuming, and some type of philosophy is needed on the relevant roles of both large- and small-scale tests.

There appears to be a developing consensus on the following:

- A) Small-scale tests are useful, and indeed essential, for guidance of research programs for development of new materials and products in the laboratory.
- B) The best test methods for judging materials acceptability and for public fire-safety standards are based on large-scale, end-use simulations related to realistic fire scenarios. End-use simulations requires an actual cable or end-use configuration rather than a small specimen of materials.

A list of the relevant fire parameters for large-scale "realistic" scenario performance is shown in Figure 23. Large scale tests are difficult and costly undertakings, but the efforts must be balanced against benefits of improved human safety and property protection.

(Figure 23 - Ref. 7)

### **Large Scale Tests Relevant Fire Situation Parameters**

#### **A. Materials Description**

Chemical composition  
Porosity  
Density  
Heat of combustion  
Heat of vaporization  
Rate of heat release vs. irradiance  
Heat capacity  
Thermal conductivity  
Moisture content  
Thickness  
Surface temperature during flaming combustion  
Surface temperature during glowing or smoldering combustion  
Surface flame spread rate vs. irradiance  
Stoichiometric air (or oxygen) requirement  
Composition of expected combustion products  
Toxicity of combustion products and fuel vapors  
Particle size and number (smoke)  
Emissivity of flame

#### **B. Material Ensemble Description**

Thickness and depth of material components  
Exposed surface areas  
Physical design of composites  
Shape details  
Expected orientation of "fuel bed" with respect to ignition sources  
Vertical and horizontal distances between items of fuel  
Heat sinks and sources

Procedural guidance of requirements and test specifications for large-scale fire hazard testing of electro technical products are given in Section 6 of the International Electrotechnical Commission IEC Standard Publication 695-1-1 (1982), Part 1, entitled Fire Hazard Testing. A sequential logic decision tree is also included for requirements and specifications.

The following section (6.1 Procedure) was reproduced by permission of the International Electrotechnical Commission, which retains the copy right. . .

#### **"6.1 Procedure (From IEC Standard 695-1-1 [1982] Part 1)**

- a) Establish the need for a test, its type and identify the main objectives.
- b) Examine the known existing and recommended test procedures developed for a similar purpose and their possible suitability and shortcomings.
- c) Collect as much background information as possible on the fire aspects to which the tests can be related and take into account the relevant scope and significance of the existing test procedures.
- d) If an existing test procedure appears suitable, check its provisions against the following features:
  - Environmental conditions: in practice, simplifications become necessary but the conditions finally adopted should bear as much relationship as possible to the environment which is being modelled.
  - Realistic examination: the validity of the test data is related to the manner of use and installation of the product and its association with other products.
  - Discrimination: those properties and characteristics of the test procedure which are of interest should be checked for their sensitivity, reproducibility and repeatability.
  - Expression of results: the test results shall be given in easily understood terms giving a fully objective description. All indefinite (subjective) phraseology should be avoided.
- e) If a new test procedure is to be developed, quantify the essential features as listed above. Further important features are the purpose of the test, the limitations of the test, the use of the information it provides, and the ease of operation.
- f) Specify acceptance criteria appropriate to the resistance to ignition and propagation of fire of the tested item.

- g) Undertake an investigation of the proposed test procedure and study its ability to meet the objectives.
- h) Prepare the standard for the test method including the relevant information on its field of application, its limitations and reservations, and on the use of the test results obtained. Make reference in the standard to a recommended test procedure wherever possible."

(Figure 24) An Engineering Approach

**Fire damage is a multifactor problem requiring a total systems approach.**

**Main Considerations**

- Building or Structure Design
- Fire Detection Equipment
- Fire Control Systems
- Materials Selection
- Education
- Attitude and Conduct

It can be concluded that fire damage is a multi-factor problem, requiring a "total systems" engineering approach.

Fundamental considerations (in Fig. 24) include:

- The design of the building, or structure.
- Fire detection and warning equipment.
- Fire control systems like water sprinklers or Halon® extinguishing agents.
- Materials selection and total fire hazard considerations.
- The education of people on fire prevention and safety.
- . . . and their subsequent attitude and conduct in a fire.

Du Pont Polymer Products Department expertise is primarily in the areas of material development and evaluation. The rest of this paper will deal with only those considerations.

(Figure 25) **Materials Selection**  
**The "Halogen-Free" Question**

**What are the facts?**

Post-fire corrosion is a problem in many end-use sectors.

**What are possible approaches to a solution?**

1. Generic-Class Exclusion...
2. Engineering...  
Priority/Risk/  
Performance Evaluations

With the Materials Selection consideration comes the "Halogen Free" question (Fig. 25). As one consequence to examine, "halogen free" or "nonhalogen" generic designations have been proposed for some end-use specifications as an expedient means of reducing certain corrosion hazards.

**What are the facts?**

Post-fire corrosion is a problem in many end-use sectors, but it is just one of many fire hazards encountered.

The implication or sometimes the direct conclusion drawn is that "nonhalogen" constructions are required to obtain satisfactory fire hazard reductions or that halogenated materials should be completely avoided for certain applications.

What are the possible approaches to solve the corrosion hazard problem?

- 1) The Generic Class Exclusion eliminates halogenated materials all together; no matter what their properties and characteristics are.
- 2) The Engineering Approach sets priorities, defines risks and establishes performance evaluations.

Let's examine the halogen exclusion approach in more detail.

(Figure 26) **Generic-Class Exclusion Approach**  
**I.e. Get rid of Halogens**

- Compromises many essential qualities in trade-off
- May increase fire frequency and size
- Corrosion damage may decrease while overall fire damage increases
- Not only Halogen acids are corrosive...

N	→ NO <sub>2</sub>	→ HNO <sub>2</sub>	NITROUS
S	→ SO <sub>2</sub>	→ H <sub>2</sub> SO <sub>3</sub>	SULFUROUS
C	→ CO <sub>2</sub>	→ H <sub>2</sub> CO <sub>3</sub>	CARBONIC
H/C	→ (HCO)	→ HCOOH	FORMIC
H	→ (OH)	→ H <sub>2</sub> O	WATER
P	→ (PO <sub>x</sub> )	→ H <sub>3</sub> PO <sub>2</sub>	PHOSPHOROUS

Materials should be judged by end-use performance not solely by chemical content

Excluding halogenated polymers can compromise many essential day-to-day end use performance qualities in the tradeoff (Figs. 26, 27 & 30).

Fires may increase in frequency and size if combustibility is compromised.

Corrosion damage may decrease, but overall fire damage may increase.

Other corrosive acids may be formed, depending upon the type of nonhalogen materials present and the conditions of the fire.

Materials should be judged on end-use performance, not solely by chemical content.

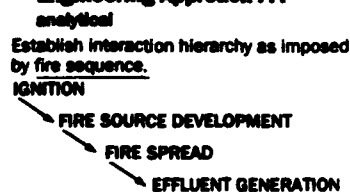
(Figure 27) **Generic-Class Exclusion Approach**  
continued...

- Halogen acids are not identical in corrosive effect on metals and concrete, etc.  
HF ≠ HCl ≠ HBr ≠ HI
- The amount of Halogen acid evolved varies with materials and composition chemistry.  
CSM ≠ PCP ≠ PVC ≠ TFE

Halogen acids have a well documented and very beneficial role in gas-phase fire inhibition.

Furthermore, even the various halogen acids are not identical in corrosive effect on metals, concrete and other construction materials. The amount and type of halogen acid evolved varies with materials, composition chemistry, thermal stability, as well as with time and temperature exposure conditions. Halogen acids have a well-documented and very beneficial role in gas-phase fire inhibition as explained in Figures 6, 7 & 8.

(Figure 28) **Engineering Approach...**

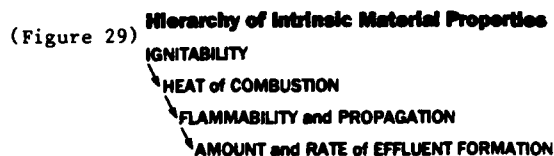


The development, spread and character of the fire determines the composition of the off-gases.

The Engineering Approach goes beyond fire effects and looks at the role of materials in each step of the fire sequence (Fig. 28).

The ignition, development and spread of the fire affects the nature and composition of the off-gases.

A material producing corrosive effluents should not always be assumed to increase risks to life and property. Just the opposite may be true if it is more resistant to ignition and burns less readily.



**Important Engineering Factors**

- Full-scale fire dynamics: IEEE-383
- Minimizing ignition and sustained combustibility
  - Short term heat-flux with hydrated fillers
  - Longer term gas-phase with halogen acids
- Reducing fuel sources and mass factors
- Reductions in corrosion and indirect effects without compromises in combustibility
- Retaining day-to-day safety and reliability

Keeping the applicability of laboratory test data in perspective the fire sequence can be examined from a materials viewpoint, translating the sequence into measurable material properties. These laboratory properties go from ignitability to measuring the amount and rate of effluent formation (Fig. 29). These properties can assist in material choices to optimize the cable constructions, but they are not predictions of end product performance.

The most important engineering factors include:

- o Keeping full scale, real life fire dynamics in mind with cable tests like IEEE-383 and others by UL, IEC, Factory Mutual, etc.

The two basic phenomena important in minimizing material ignition and sustained combustibility are again reviewed as engineering factors in the fire sequence context:

- A) Water from hydrated fillers does initially reduce the flame heatflux and cable combustibility. These fillers are commonly used in both halogenated and nonhalogenated polymers. However, water of hydration and its fire-limiting effects can be exhausted very quickly under intense flames. The nonhalogen polymer itself can then become a fuel source for the fire. A less fugitive inhibitor is needed.
- B) The evolution of halogen acids from PCP, CSM, TFE and other halogenated polymers can provide continuing gas-phase fire inhibition by interrupting the free-radical flame chemistry. Halogen acids have a very beneficial role to play in moderating or counteracting the central problem: the fire itself.

Other important engineering factors include<sup>11</sup>:

- o Configurations in the cabling systems and conditions of, and interactions with, the environment.
- o . . . spacing, ventilation, adjacent component ignition, electrical continuity, etc.
- o Reducing fuel sources and the amount of burnable material.

- Reducing corrosion without compromising combustibility . . . and retaining traditional safety and reliability.
- Considering the heat dissipating character of metallic armour, shields and braids.
- Utilizing blends, composites and laminates of materials with varying fire hazard profiles . . . this could include optimum choices of halogen and nonhalogen polymers.

No matter what is done to improve the burning characteristics of a compound, the cable still has to perform its major function - that is to transmit electrical power safely and reliably for many years in a variety of aggressive environments.

(Figure 30)

### Two Engineering Requirements of Cable Jackets:

#### 1. Day-to-Day Functionality

- Physical Strength
- Oil Resistance
- Ozone and Weather Resistance
- Heat Resistance
- Abrasion and Tear Resistance
- Low Temperature Flexibility
- Long Service Experience

#### 2. Fire Considerations

- Flame Retardancy
- Toxicity
- Corrosivity
- Smoke Evolution

Recent  
End-User  
Concerns

Halogenated polymers have for many years provided good service and performance. It has been shown that they have an equally important, if not critical role, to play in a fire situation. It has also been shown that there are methods available to cope with more recent concerns, namely the problem of the various hazards associated with fire exposure.

In our opinion, of the general purpose halogenated polymers available, CSM and PCP give the best overall balance of properties. These include their proven range of mechanical properties, resistance to a wide range of environments, plus reduced flame propagation. In addition, they can be compounded to meet the justified demands of the end user for a cable jacket meeting these more stringent environmental and safety needs (Fig. 30).

(Figure 31)

### CSM — Hydrogen Chloride Evolution

	General Purpose Vulcanizate	Low Acid Evolution Vulcanizate
HCl Evolution — Sample Heated 5.5°C/Minute to a Maximum of 500°C		
Beginning, °C	300	—
Peak, °C	310	—
Ending, °C	405	—
Amt. Evolved, mg/gm	88	0
% of Theoretical*	63	0
HCl Evolution — Pyrolysis at 820°C to 850°C		
% of Theoretical*	69	19

\*Theoretical assumes all of chlorine evolved as HCl and that HYPALON® 40 could yield 36% of its weight as HCl.

In Figure 31, a general purpose CSM vulcanizate is compared with one compounded for low acid gas evolution with an acid accepting filler. In one test, HCl evolution is measured during the heating of a sample from room temperature to 500°C, raising the temperature 5.5°C per minute. In the other test, HCl evolution is measured after pyrolysis of the sample at a temperature in the range of 820°C to 850°C. The results show a striking difference with both compounds. Hydrochloric acid evolution is cut to zero in the case of the 500°C test and reduced by 75% to 80% in the case of the pyrolysis test at 820°C to 850°C.

(Figure 32)

### CSM — Cable Jacket Compounds

	Typical Cable Jacket <sup>1</sup>	Low Acid Evolution Cable Jacket <sup>1</sup>	Original NES-518 Specification
Limited Oxygen Index — LOI	30	29.8	29 min.
Toxicity Index <sup>2</sup> (see footnote)	11	2.8	5 max.
Smoke Index <sup>3</sup>	110	37.6	20 max.
Acid Gas Content of Smoke <sup>4</sup> (cm <sup>3</sup> /10 m)	3025	50.4	100 max.
Congo Red Test min. to pH3 @ 200°C	11	>60	—

<sup>1</sup>These results are based on laboratory tests under controlled conditions and do not reflect performance under actual fire conditions.

<sup>2</sup>Tested to the requirements of British Naval Engineering STD 713; however, this test may not fully characterize all aspects of real life-scale combustion toxicity. See following charts for additional information.

<sup>3</sup>Tested to the requirements of British Naval Engineering STD 711.

<sup>4</sup>Tested according to the Toxicity Index Results of the British Naval Engineering STD 713, the March 1982 revision now specifies no halogens.

As noted before, the toxicity index is not based on a material's performance in fire. It should not be used as a full measure of toxic hazard.

Again, a typical CSM cable jacket compound is compared with one designed for low acid gas evolution (Fig. 32). Limited oxygen index is very similar for the two materials. Other British MOD NES tests which include toxicity index, smoke index, and acid gas content of smoke all show a definite advantage for the low acid evolution cable jacket. Smoke acid gas was reduced by a factor of 60 X or 6,000%. The Congo Red Test measures minutes to achieve an off-gas pH of 3 at 200°C in hermetically sealed glass tubes containing cable material samples. Ironically, this test was originally devised to separate halogenated materials from nonhalogen ones!

There appears to be considerable latitude in optimizing properties between acid gas evolution and other important requirements.

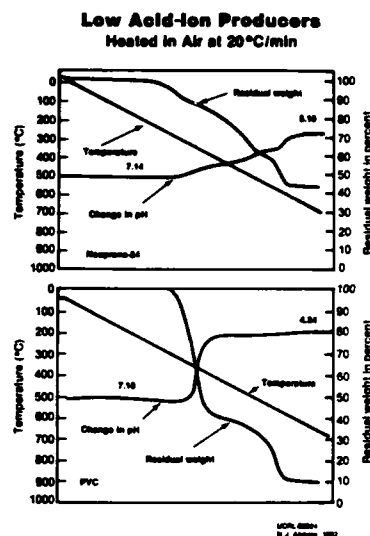
A low acid (0.5%) CSM jacketed cable (36mm dia.) has met the flame retardancy requirements of IEC 332-3, class B. Tests are underway for a class A rating. A 5% acid jacketed construction does meet class A. This construction includes three cores X 70MM<sup>2</sup>, nonflame retardant EPR insulation. It was 36mm in diameter and was tested without armour.

The Lawrence Livermore National Laboratory, under contract to the U.S. Dept. of Energy, has also developed some very interesting laboratory testing procedures. The first parts of the research were directed at fundamental analysis of the basic processes at work in the thermal degradation patterns of representative wire and cable materials. The subsequent program stages were to develop data applicable to prediction of fire-risk parameters for: contemporary zone models of fire growth and smoke motion, large experimental energy facilities, and ultimately new power-generating plants.

Thermograms and acid-ion production curves are shown (Fig. 33) for PVC versus an acid stabilized neoprene 84 composition. The neoprene composition incorporates a calcium carbonate (CaCO<sub>3</sub>) acid acceptor, similar to the "Low Acid Evolution" CSM composition shown in Figure 32. Additive stabilized compounds show a much more gradual degradation pattern resulting in a lower amount and slower rate of acid ion and volatile effluent generation over the temperature range studied.

It should be noted that the decomposition chemistry and physics of these polymers is more complex than discussed here, and highly dependent on composition and testing variables. Reference (17) provides a very thorough analysis. It is also possible that the performance of both the PVC and neoprene can be improved still further for the conditions represented by these tests.

(Figure 33 - Ref. 17)



### Summary

Halogenated plastics and elastomers should not be ruled out as a class in writing cable material specifications. Rather, such specifications should include end-use performance requirements which are necessary for the application involved.

Halogenated elastomers such as PCP and CSM are versatile materials which can be compounded to give low acid evolution as well as a wide variety of other critical properties. It is this versatility which has allowed these materials to be used so successfully over the years in a wide variety of wire and cable applications.

### Conclusions

(Figure 34)

### Fire Safety Issues

Influences	Technology
• Technical	• Cable Engineering
• Commercial	• Materials
• Regulatory	• Fire Science
• Political	• Toxicology

Toxicologists, fire scientists, material chemists, cable engineers and the academic community have mounted a major effort on fire safety. It is gratifying that these professions are beginning to have an impact on the commercial, regulatory and political influences as well.

Fires are hazardous events that threaten life and property. Full scale characterizations of those hazards must then be considered in: choosing materials, optimizing their compositions and measuring their responses to a particular fire scenario. The total hazard assessment is also important for designing cables, establishing specifications, certifying for use, and in establishing end-use regulations.

Small laboratory tests alone give an incomplete (or misleading) projection of actual use behavior. Performance testing in large-scale (installation) simulations are decidedly more effective than regulatory exclusions of generic materials based on chemical composition or small-scale laboratory test results with limited real life predictability.

#### Acknowledgements

The authors wish to thank the Du Pont Company for supporting extensive research on all aspects of material technology, fire hazard analysis, and overall fire safety. Appreciation is also due to the many fine customers of our products who share our concern and work hard to develop safer end products with the latest materials and technology.

Recognition should also go to the many electrical industry end users, specifiers, certifiers and regulators who are developing real life installation simulations that ultimately will provide improved safety for people and greater protection of property.

Finally, the background knowledge published by the References and the academic community greatly helps to increase the level of collective awareness and understanding of the issues and challenges we all face together.

#### REFERENCES

1. Final Report of the Products Research Committee - Fire Research on Cellular Plastics, April 1980, Library of Congress Catalogue 80-83306 USA.
2. Flammability Handbook for Plastics, Third Edition, by Carlos J. Hilado, Technomic Publishing Co., 1982.
3. Flame Resistance of Neoprene\* and Hypalon\* - McCormack. Rubber Age 1971.
4. Halogenated Elastomers : Versatile Cable Jacket Materials, Hoover, Moran; Whitlock, Elastomerics, March 1982.
5. A Closer Look at Cause and Effect in Fire Fatalities - John Punderson, Fire and Materials, Volume 5. No. 1, 1981.
6. Weatherley, J. W., 4th BEAMA/ERA Conference May 1982, London.
7. Report of the Committee on the Toxicity of the Products of Combustion to the National Fire Protection Association, USA. December 1982.
8. Compounding Rubber For Fire Resistance, D. Culverhouse, Rubber World (European Edition), April 1983.
9. Engineering Approach to Fire Damage, T. J. O'Neill, informal presentation, February 1981.
10. New Materials For Cable Sheathing, D. E. M. Ness and R. M. Black, Electronics & Power, October 1982.
11. Fire Hazard Testing, IEC Standard, Publications 695-1-1, 695-1-2 and 695-3-1, 1982, Bureau Central de la Commission Electrotechnique Internationale, 3 Rue de Varembe, Geneve, Suisse.
12. PVC - Its Characteristics In Fire Situations, D. L. Kent and H. F. van der Voort, Report, July 1, 1981 (Carlen Corp.).
13. A Fire Fatality Study, B. Halpin, E. Radford, R. Fisher and Y. Caplan, Fire Journal, May 1975.
14. Smoke and Carbon Monoxide Poisoning In Fire Victims, B. Zikria, G. Weston, A. Chadoff and J. Ferrier, Journal of Trauma, Vol. 12, No. 8, 1972.
15. OFFSHORE CABLES - The Role of Different Classes of Elastomers In The Fire Situation, G. C. Sweet, Presentation, PRI-Rubber In Offshore Engineering Conference, London, April 1983.
16. Cables For Hazardous Environments, Z. Bonikowski, Electronics & Power, April 1983.
17. Thermal Degradation of Cable and Wire Insulations, N. Alvares, A. Lipoka - Quinn, H. Hasegawa, Lawrence Livermore National Laboratory. UCRL-86924, November 1982.
18. Release Rate Calorimetry of PVC Compounds Containing Antimony Oxide and Iron Oxide, E. D. Nelson and S. Kaufman, Bell Laboratories, Norcross Ga., presented at the 7th International Conference on Fire Safety, Jan. 11, 1982.

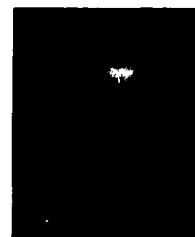
James R. Hoover received his BS degree in Math and Physical Science from the Pennsylvania State University in 1969. He joined the Chestnut Run Technical Service Laboratory in the Elastomers Department of Du Pont in 1969. Jim is currently Manager of Wire and Cable Industry Marketing Programs for Neoprene, Hypalon®, Nordel®, Vamac®, Hytrel®, Alathon®, and Keldax® in the Polymer Products Department. Previous positions in Du Pont included New Business Analysis and Development Manager for ELD/R&D, Hypalon® Product Manager, and professional positions in sales, manufacturing and research within the current Elastomers Division. Jim is a member of Sigma Xi, The ACS Rubber Division and has co-authored wire and cable related articles in *Elastomerics* and *Rubber World*.



Albert L. Moran has a BS degree in Chemistry from Fordham University and an M.B.A. from Indiana University. He joined the Du Pont Company in 1952 and has spent his entire career on technical service and development activities involving synthetic elastomers. He is currently Technical Service Manager for Hypalon®, Nordel®, Vamac® and the Electrical Industry at the Du Pont Chestnut Run Laboratories. Al has authored many technical papers and bulletins and has co-authored articles appearing recently in *Elastomerics* and *Rubber World*.



Gerry A. Sweet is a Qualified Associate of the Institute of Plastics and Rubber Industry since 1962. He has 30 years experience in the rubber industry; the last 15 were with Du Pont based at the Technical Service Laboratory in Hemel Hemstead, England. From 1977 until 1983 he was manager of the Specialty Rubber Products Group. Currently he is Market Development Coordinator for the Electrical and Petroleum Market Industries in the UK.



David B. Allen is a native of Chicago and completed secondary schooling there. Dave graduated in 1949 from Georgetown University, Washington, D.C., with BS in Chemistry. He performed graduate work at Northwestern University in Marketing prior to serving in U.S. Army, Chemical Corps. Dave joined Du Pont in 1954 after leaving the Army. His present assignment as Senior Development Specialist involves development of new markets and uses for wire and cable made from fluoropolymers in the Fluoropolymers Division of the Polymer Products Department. Dave is a member of several wire and cable committees namely:

- Society of Automotive Engineers (Aerospace Council) A2H Subcommittee on Wire and Cable.
- NEMA High Temperature Wire Section Technical Committee.
- EIA (Electronics Industry Assoc.) C83.3 Committee on Coaxial Cable for MIL-C-17.
- Underwriters' Laboratories Ad Hoc Committee on Large Scale Fire Testing.
- Co-author of several papers presented at Wire and Cable Symposia over last few years.



Joseph G. DiPinto has a degree in Chemical Engineering from the University of Notre Dame. He has been employed by the Du Pont Company for 30 years. Joe has 25 years experience in Elastomers technology, including polymer development, process technology, applications development and customer service. Presently he is Manager of Product Technology in the Fluoropolymers Division of Du Pont's Polymer Products Department.



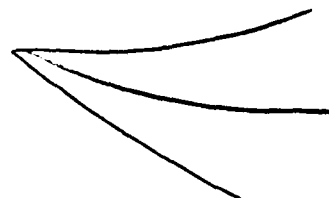
Donald H. Lutz received his BS in Biochemistry from the Pennsylvania State University in 1952. Prior to joining Du Pont Company in 1954, Don was employed at Firestone Tire and Rubber Company. Since 1954, Don has had various assignments in sales and market development dealing with the wire and cable industry. Currently, as a Senior Market Development Specialist in the Fluoropolymers Division of the Polymer Products Department, he is specializing in expanding the market base for high performance fluoropolymer insulated cable within the aerospace and military electronics industries.



John O. Punderson received the BSc degree in Chemistry and Physics from the University of Chicago and the PhD degree in Organic Chemistry from the University of Minnesota. For the past 30 years he has engaged in research for E. I. du Pont de Nemours Co. Inc., currently in the Polymer Products Department at Parkersburg, West Virginia.



Dr. Punderson is a member of several scientific societies and standards organizations. He has authored patents and publications in a number of fields with main emphasis on applications of polymers under extreme conditions of electrical, thermal, radiation and fire exposure. He has chaired or participated in ten committees on fire safety and combustion toxicology within the International Standards Organization, International Electrotechnical Commission, Institute of Electrical and Electronics Engineers, American Society for Testing and Materials, Society of the Plastics Industry, and Federal Aviation Administration SAFER Committee. Within Du Pont, Dr. Punderson has also taught a course on problem analysis and decision-making.



# CHARACTERISTICS OF HEAT AND FLAME RESISTANT OPTICAL FIBER CABLES

Y. Kikuchi, A. Mogi, T. Kobayashi, N. Misono  
T. Murayama, Y. Sugawara.

Fujikura Ltd.  
1440 Mutsuzaki, Sakura, Chiba, 285, Japan

*fiber-reinforced-plastic*

## Abstract

Flame resistant and flame retardant properties of various types of optical cables are investigated.

As a result of the tests, <sup>the authors</sup> we conclude that it is not suitable to employ the conventional 3-layer coating construction because of the weakness of thermoplastic resin coated fiber at a high temperature.

By adopting the heat resistant FRP jacketing on optical fibers, the authors have succeeded in the development of a flame resistant optical fiber cable.

Furthermore this optical cable has the noninductive characteristics due to the nonmetallic construction. The cable is light in weight and small in diameter and still has the sufficient mechanical properties.

Therefore, this type of cable is promising a flame resistant optical cable for uses in severe environments such as high temperature up to 800°C half an hour.

## 1. Introduction

Recently optical fiber cables have been applied to various environments which require special properties different from those of conventional optical cables.

The optical cables, used for environments such as power plants, chemical plants, tunnels, buildings and so on, should have heat and flame resistance to keep safe the telecommunication systems even in a emergency like a fire.

The transmission characteristics of fibers at a high temperature was reported. (1)(2) It indicated the necessity of protecting technique for keeping the mechanical strength of fibers at high temperatures.

First, the flame resistance of optical cables was investigated by changing cable structures, sheaths and coating and jacketing materials on fibers.

It has been found that a cable with heat resistant fiber-reinforced-plastic (FRP) jacketed fibers has good flame resistance.

## 2. Flame resistant cable

### 2.1 Design requirements

Basic design requirements for flame resistant cables are as follows.

- The cable should be easily handled and easily installed with the same manner of conventional optical fiber cables.
- Under normal conditions, it should have good transmission characteristics
- In a flame, it can keep good transmission characteristics during several ten minutes (e.g. 800°C \* 30 minutes). (3), (4)
- It should satisfy a flame retardant property such as IEEE-383.

### 2.2 Flame resistant property of the optical fiber cables

At first, flame resistant properties of unit type optical cables were investigated for optical fiber cables designed by considering, at least, heat resistance and flame retardance.

Fig. 1 shows a unit construction. The fibers have 3 layers of coverings. The surface of the fiber is protected by a primary coating. The second layer is silicone rubber. Taking the heat resistance into consideration, fluorine contained polymer was selected for the outermost jacketing. Kynol® is used as the unit buffer layer on the fiber strand. Kynol® is one of the best flame resistant materials. A polyimide tape was wrapped on the unit core. Unit diameter is 4.0mm. Figs. 2, 3 and 4 show the investigated sheath constructions. Each cable employs flame retardant PVC, for the outermost cable sheath.

Flame resistant property was investigated for three types of optical fiber cables mentioned above. The test method of flame resistance satisfies Regulation No.7 of Fire Defence Agency of Japan (FDAJ) "Testing Standard of Fire-Proof Cables".

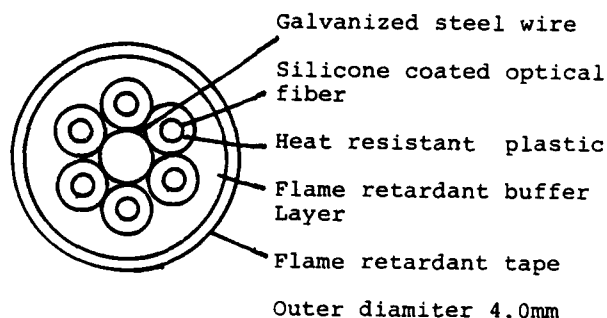


Fig.1 Optical fiber unit

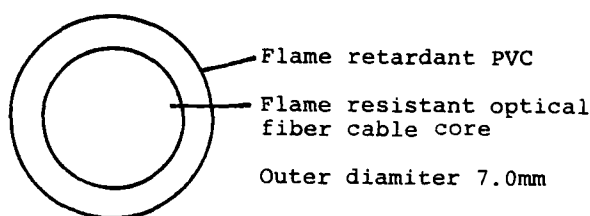


Fig.2 PVC sheath (A)

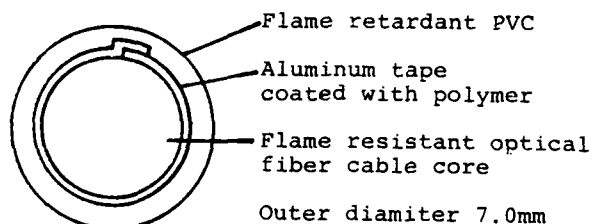


Fig.3 Laminated aluminum PVC sheath (B)

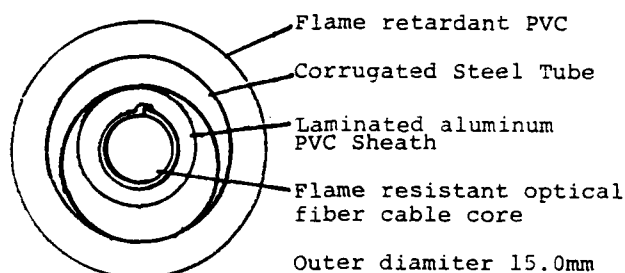


Fig.4 Corrugated steel tube armoured PVC sheath (C)

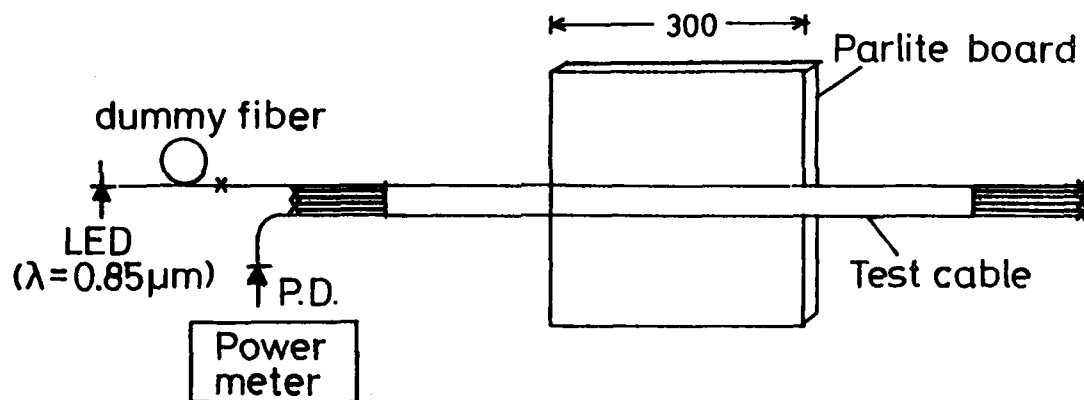


Fig.5 Measuring set-up

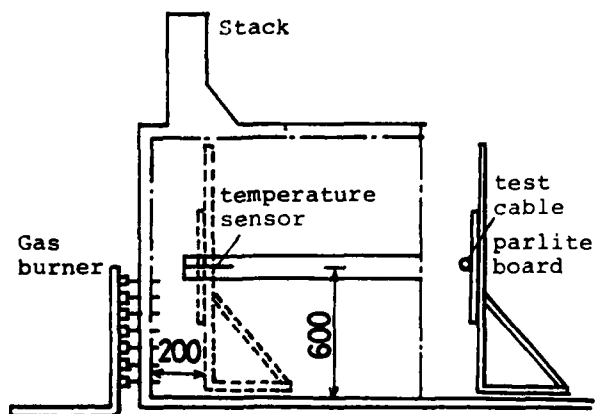


Fig.6 Equipment of flame resistant test

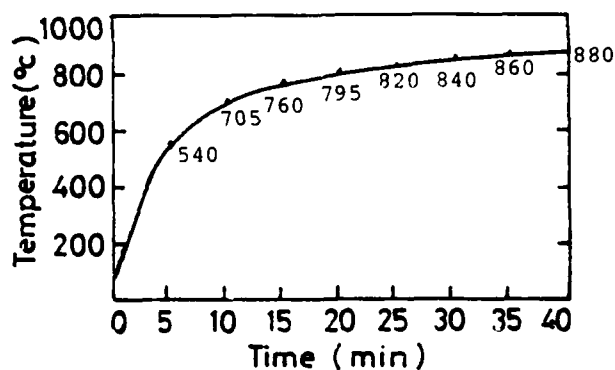


Fig.7 JIS A 1304 heating temperature curve

The test procedure is as follows; cables on test were fixed straight on a parlite board as shown in Fig. 5. Fig.6 shows a furnace compatible to Specification JIS A 1305. The temperature in the furnace is controlled according to JIS A 1304 heating temperature curve. (See Fig.7) This curve simulates a normal temperature change in a fire.

The measurement was done for 30 minutes and optical loss change was continuously monitored. The measuring set-up is shown in Fig.5. After the flame resistance tests, the appearance of the cables was examined in detail.

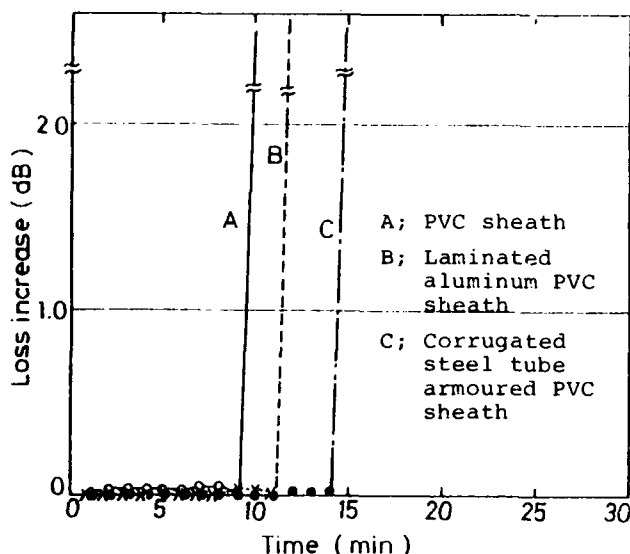


Fig.8 Comparative data of optical loss increase during examination of various types of optical cables

The test results are shown in Fig.8. It was found that the three cables could not satisfy the flame resistant condition mentioned previously, and optical losses of these cables rapidly increased after 10 to 15 minutes from the beginning of heating. In two tested cables; one is the cable with PVC sheath, and the other with a laminated aluminum PVC sheath; the materials except for optical fibers and steel wires burnt out or were carbonized. Aluminum was melted, too. Silicone rubber was decomposed completely. In the case of corrugated steel armoured cable, though it had been expected to withstand the fire, the results were the same as the former two. It was considered that optical fibers had broken in the flame resistance test, because the protective effect of coating materials disappeared at high temperatures.

As a result, it has been concluded that a metal sheath is not sufficient to protect fibers from flames. The following items should be taken into account in order to improve the flame resistance properties.

- (1) Employment of an adiabatic layer like a flame resistant tape to shield optical fiber strand from heating and fire
- (2) Employment of thermosetting plastics as the secondary jacketing material which can protect fiber surface even at high temperatures
- (3) Employment of the material for the unit buffer layer which can reduce the external force to optical fibers even at high temperatures

The unit construction was designed on the bases of the items mentioned above.

## 2.3 Materials of optical fiber unit

### 2.3.1 Secondary jacketing on coated fibers

FRP is thought to be appropriate as a hard shell which protects an optical fiber even in a fire. (5) Heat resistance of FRP jacketed fibers were examined. The heat resistance of FRP depends on that of the binder resin. Two types of FRP jacketed fibers were prepared. One is a fiber jacketed with conventional FRP and the other is a fiber jacketed with the heat resistant FRP which have been newly developed. The fibers were evaluated by measuring the number of broken fibers on the bending-heating test. Table.1 shows the results. The heat resistant FRP samples were not broken and did not show any residual bending after heated and with simultaneously bent 450mm in radius at 300°C for five hours. On the other hand all the conventional FRP samples broke under the same condition. As a result it is found that the newly developed FRP jacketed fiber has heat resistance even under bending due to cabling and the cable installation.

Table 1 Heat resistant property of FRP optical fibers

	bending radius (mm)	number of broken fibers after heating at 200°C for 20 minutes
A	150	6/10
	200	4/10
B	150	0/10
	200	0/10

A; conventional FRP optical fibers  
B; heat resistant FRP optical fibers

Next, the temperature dependence of optical losses were investigated for the two types of FRP jacketed fibers. Each 300m long fiber was coiled with 900mm dia. and put into an oven. The optical loss change was continuously monitored with the temperature up to 400°C. Fig.9 shows the results. While the loss of the conventional FRP jacketed fiber was increased drastically at about 300°C, the loss increase of the heat resistant FRP jacketed one was small. The reasons for the different loss characteristics are that many bucklings occurred in the conventional FRP, but that no visible change was observed in the heat resistant FRP.

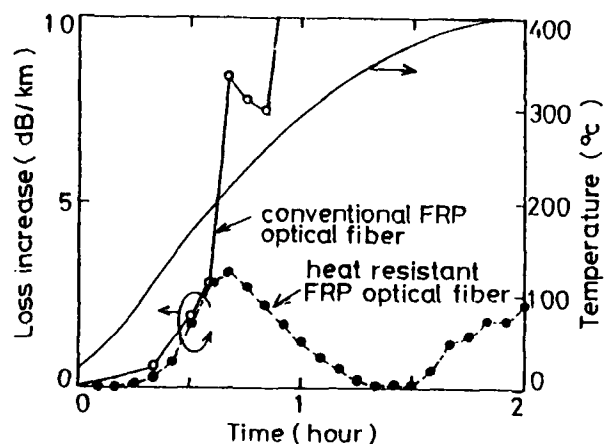


Fig.9 Optical loss increase of FRP optical fibers by heating

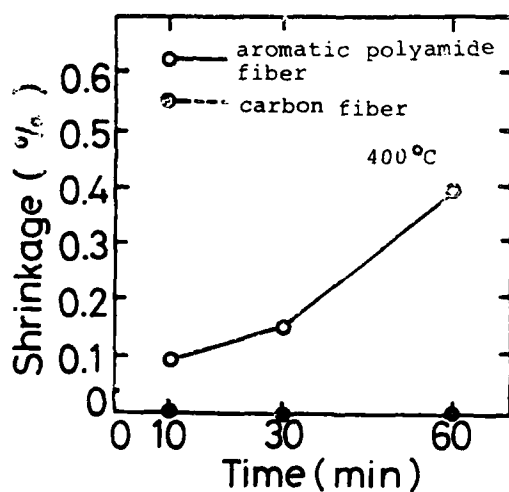


Fig.10 Shrinkage of plastic fibers after heating at 400°C

### 2.3.2 Buffer materials of unit

Buffer materials of a unit are required to be heat-resistant, flame retardant and unshrinkable at high temperature. Aromatic polyamide fiber and carbon fiber were chosen as suitable buffering materials of fiber unit and their heat shrinkages were studied. Fig.10 shows the result. No change was observed up to 400°C for carbon fibers. But for aromatic polyamide fibers 0.4% shrinkage was observed at 400°C. Moreover, no degradation was observed for carbon fibers in properties such as tensile strength and Young's modulus.

As a result, carbon fibers have been proved to be an appropriate material for the buffer of a flame resistant optical fiber cable.

### 3. Cable structure

The structure of a flame resistant optical fiber cable is shown in Fig 11. Heat resistant FRP jacketed fibers are stranded around a central member.

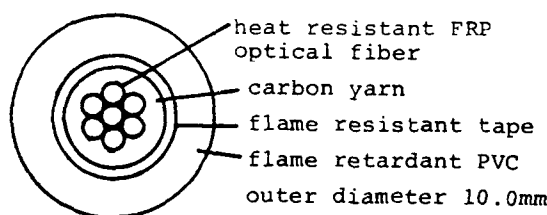


Fig.11 Newly developed a flame resistant optical cable

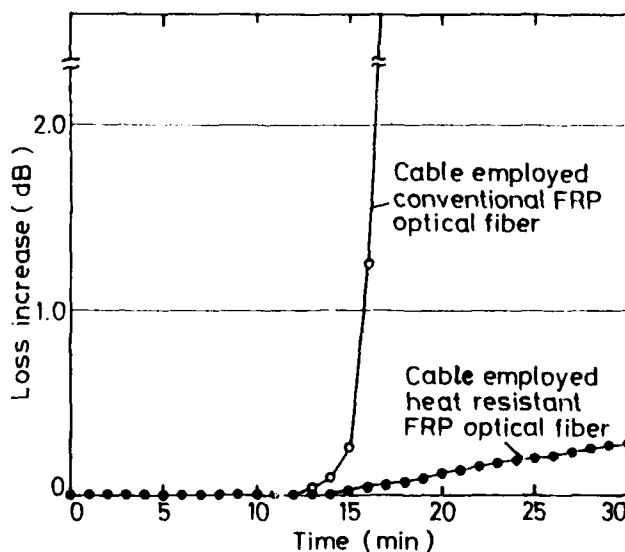


Fig.12 Flame resistant property of the cables employed FRP optical fiber

The cable core is wrapped with flame resistant tapes. The cable diameter is 10 mm. The flame resistant properties of the cable is shown in Fig.12, where the cable is compared with that composed of conventional FRP jacketed fiber. In the flame resistant cable, no remarkable loss increase was observed for half an hour at 800°C. The cable was taken to pieces and, as expected, the optical fiber had been protected in spite of carbonizing of FRP.

The cable also showed good property in vertical tray flame test (VTFT) specified in IEEE Std. 383. (See Photo.1)

Table 2 shows the characteristics of the newly developed flame resistant optical cable. The cable is light in weight and small in diameter and still has sufficient mechanical properties. Furthermore this optical cable has the noninductive characteristics due to the nonmetallic construction.

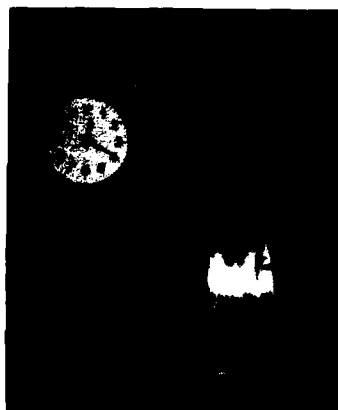


Photo. 1 IEEE 383 flame test

Table 2 Characteristics of the cable

optical fiber	graded-index doped silica fiber
core dia. (μm)	50
cladding dia. (μm)	125
FRP jacket dia. (mm)	1.0
NA	0.2
Tensile strength member	FRP
Approx. cable dia.	10
Approx. cable weight (kg/km)	90
Fiber attenuation (dB/km at 0.85μm)	3.0(nominal)
Tensile strength (kg)	50 (maximum)
Bending radius (mm)	100 (minimum)
Vertical tray flame test	passing of IEEE-383

#### 4. Conclusion

The flame resistance and flame retardant properties of optical fiber cables have been studied. As a result, the application of the heat resistant FRP is effective for realization of a flame resistant optical cable. The newly developed flame resistant with heat resistant FRP fibers passes the flame resistant test of JIS A 1304, half an hour at 800°C, without loss increase through the test.

#### 5. References

- (1) R. Yamauchi, et al., "Transmission characteristics of heated optical fibers" IOOC'81 Technical Digest 110 (1981)
- (2) T. Shiota, et al., "Spectral loss characteristics of hermetic coated fiber at high temperature" to be appeared at 9th ECOC (1983)
- (3) N. Asakawa, et al., "Development of inorganic material insulated flexible triaxial cable for FBR" 30th IWCS Proceedings 286 (1981)
- (4) K. Yoshioka, et al., "Flame resistant communication cable with lead screen tape coated with polymer" 29th IWCS Proceedings 240 (1980)
- (5) K. Fuse, et al., "Some excellent properties of new optical cables with FRP optical fibers" 30th IWCS Proceedings 147 (1981)



Yoshio Kikuchi

Fujikura Ltd.

1440 Mutsuzaki,  
Sakura, Chiba, 285,  
Japan

Yoshio Kikuchi was born in 1955 and graduated from Tohoku University with a M.E. degree in telecommunication engineering in 1980. He joined Fujikura Ltd. in 1980 and has been engaged in research and development of optical cable. He is now an engineer of optical fiber and cable section and a member of IECE of Japan.



Nobuyuki Misono

Fujikura Ltd.  
Sakura, Chiba, 285,  
Japan

Nobuyuki Misono was born in 1949. He joined Fujikura Ltd. after his graduation from Chiba University in 1973 and has been engaged in research and development of the metallic cables and optical cable. He is now an engineer of optical fiber and cable section and a member of the IECE of Japan.



Akio Mogi

Fujikura Ltd.

1440 Mutsuzaki,  
Sakura, Chiba, 285,  
Japan

Akio Mogi was born in 1946. He joined Fujikura Ltd. after his graduation from Haneda Institute High School in 1967 and has been engaged in research and development of the metallic cables and optical cable. He is now an engineer of optical fiber and cable section and a member of the IECE of Japan.



Toshiaki Murayama

Fujikura Ltd.

1440 Mutsuzaki,  
Sakura, Chiba, 285,  
Japan

Toshiaki Murayama was born in 1953 and graduated from Chiba University with a B.E. degree in physics in 1978. He joined Fujikura Ltd. in 1982 and has been engaged in research and development of optical cable. He is now an engineer of optical fiber and cable section and a member of the IECE of Japan.



Toshiaki Kobayashi

Fujikura Ltd.

1440 Mutsuzaki,  
Sakura, Chiba, 285,  
Japan

Toshiaki Kobayashi was born in 1947. He joined Fujikura Ltd. after his graduation from Tohoku University in 1971 and has been engaged in research and development of the metallic cables and optical cable. He is now an engineer of optical fiber and cable section and a member of the IECE of Japan.



Yasuyuki Sugawara

Fujikura Ltd.

1440 Mutsuzaki,  
Sakura, Chiba, 285,  
Japan

Yasuyuki Sugawara was born in 1947 and graduated from Tohoku University with a B.E. degree in telecommunication engineering in 1969. He joined Fujikura Ltd. 1969 and has been engaged in research and development of metallic cables and optical cables. He is now an assistant chief engineer of optical fiber and cable section and a member of IECE of Japan.

AD P002574

CABLE FIRE STUDIES USING THE OHIO STATE UNIVERSITY  
RELEASE RATE APPARATUS

Walter Pocock

David Taylor Naval Ship Research  
and Development Center  
Annapolis, MD

Abstract

The work reported here, carried out under the Navy's Ship Damage Control Program, was part of an evaluation of the Ohio State University release rate apparatus (rra), to determine its suitability for establishing smoke and flammability standards for shipboard cables. As a first step, a study was made of the relationship between four basic parameters and burning and smoke-generation of test cables in the rra. A statistical method was used in designing the test program and analyzing results. Eighteen cable types, made from two sets of materials, were used. The study showed the effect of heat flux on smoke and heat release rates to be pronounced, as expected; of cable diameter, moderate; of the ratio of volume of copper to total cable volume, slight; and of cable spacing, not significant. The study supports the concept that heat and smoke release rate data taken over a range of heat fluxes provide a better basis for predicting relative performance of cables in a real fire than do test methods in which heat flux is not controlled. The statistical method used here is believed to be an excellent procedure for similar studies in the future.

Introduction

The ongoing Cable Fire Studies task at the David Taylor Naval Ship Research and Development Center (DTNSRDC), Annapolis, MD., is a part of the Navy's Ship Damage Control Program, under the sponsorship of the Naval Sea Systems Command. The overall objective of the Cable Fire Studies task is to develop realistic standards of flammability, smoke, and corrosive products of combustion\* for shipboard electrical cables, in order to make optimum use of advancing technology of low-flammability and low-smoking cables. A segment of the task is an evaluation of the Ohio State University release rate apparatus (rra) as a tool for setting and monitoring such standards. As part of the evaluation, a study was made in the rra of the relationship between four basic parameters--heat flux, cable diameter the ratio of copper to combustibles in the cable, and cable spacing--and the burning and smoke-generating characteristics of the cable tested. The method and results of that study and some conclusions drawn from the results are the subject of this paper.

John Geremia

U.S. Naval Academy  
Annapolis, MD

Background

A previous IWCS paper<sup>1</sup> summarized the Navy's shipboard cable fire problem and described work carried out as the first segment of the Cable Fire Studies Task at DTNSRDC. This work was directed toward upgrading flammability requirements under MIL-C-915E, the Navy's principal specification for shipboard cables. An important result of that work was the incorporation of the IEEE-383 vertical tray flame propagation test<sup>2</sup> into MIL-C-915E.

The next objective of the Navy's Cable Fire Studies task, to develop smoke standards, led to a consideration of the OSU release rate apparatus (rra) for measuring smoke generation rates from burning cables. The rra had been developed about 10 years previously by Dr. Edwin Smith in the Chemical Engineering Department of OSU. Its use for obtaining fire data on cables has been reported at IWC symposia<sup>4,5</sup> and elsewhere<sup>6</sup>. It is also the subject of a proposed ASTM Standard Method,<sup>7</sup> which is expected to be officially adopted during the present calendar year. A survey of smoke-measuring methods in current use indicated the rra to be the device most likely to fill all the Navy's requirements in setting and monitoring smoke standards for cables. It was also apparent that it might be used as well for measuring corrosive and toxic products of combustion and for improved flammability measurements, as compared to the IEEE-383 test.

An important feature of the rra is that it measures burning and smoke generation over a range of heat flux values, such as occur in a real fire. Release rate data taken at various heat fluxes are therefore believed to provide a more realistic basis for predicting comparative behavior of several different cables in a real fire than other test methods, such as vertical tray flame propagation tests, in which there is no controlled variation in heat flux.

It was decided from these various considerations to make an evaluation of the rra as a test tool for Navy cables. In order to set standards, an understanding of what factors affect burning and smoke generation of cables, and what the effects are, was considered essential. For this reason, the basic parameter study was undertaken as the first step in the evaluation of the rra. The procedures and results of that study will now be presented.

\*Toxic products of combustion are being considered separately from that task.

### Description of Release Rate Apparatus

Figure 1 is a photograph of the rra used at DTNSRDC. Figure 2 is a diagram showing its essential parts. The following features of the rra are not shown in Figure 2:



Figure 1. Release rate apparatus  
(front of unit is on the right)

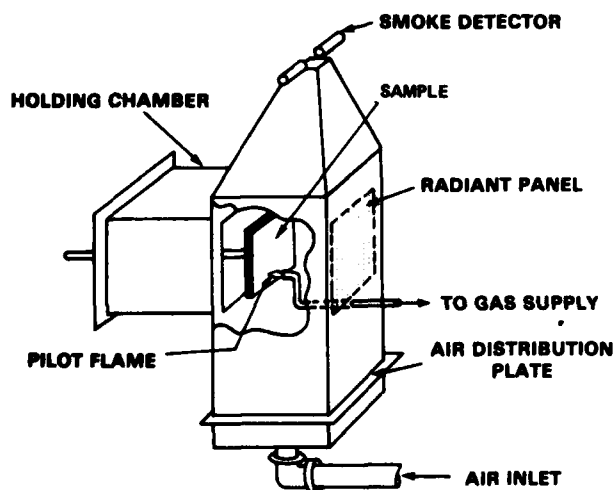


Figure 2. Release rate apparatus showing  
essential parts (front of unit is on left)

1. A branching off of the main air supply, which diverts a part of the total air flow to the upper portion of the unit, above the burn site.

2. The upper pilot burner, which ignites unburned volatile products from the sample.

3. A set of "radiation doors" that close off the holding chamber from the main burn chamber and protect the sample from the radiant heaters while it is in the holding chamber.

Other details of the construction and operation of the rra are given in the proposed ASTM Standard.<sup>7</sup> The principle and method of operation are as follows: The sample of combustible material, in this case, short segments of cable, is mounted as shown in Figure 2 (details of the cable segments are not illustrated in the figure). The sample is simultaneously subjected to heat from the radiant heaters, at a heat flux (heat intensity) that can be varied from 0 to 6 W/cm<sup>2</sup>, the upper limit of 6 having been estimated to be about the maximum likely to be found in an actual shipboard fire. Air is simultaneously moved past the sample at a controlled rate. If the heat flux is sufficiently high, the radiated heat decomposes and volatilizes the combustible material in the sample, and the pilot flame impinging on the sample surface causes ignition. The sample may also be run without the pilot flame, in which case the volatilized products may ignite spontaneously, particularly at a high heat flux. At a low heat flux, the sample may smolder without burning. The smoke detector measures optical density of the exiting smoke-laden air, from which the smoke release rate is calculated. The heat release rate of the sample is calculated from the difference between the inlet and outlet air temperatures (at the known air flow rate), corrected for thermal inertia (absorption of heat by the walls and other masses of the rra), minus the known heat input from the radiant heaters.

### Selection of Basic Parameters for Study

The following are major factors believed to affect the manner of burning and smoke generation of cables:

1. Magnitude of heat flux.
2. Nature of combustible materials in the cable.
3. Surface area of combustible material; initially, the cable jacketing, exposed to the heat source.
4. Thickness of combustible material exposed to heat.
5. Mass and surface area of copper in contact with combustible material.
6. Rate of oxygen delivery to the burning surface.

From a consideration of these factors, the following parameters were selected as the most important for study:

- heat flux (Factor 1)
- cable materials (Factor 2)
- cable diameter (relates to Factors 3 and 4)
- ratio of copper to combustible material (relates to Factors 4 and 5)
- spacing between individual cables in a group (relates to Factors 3 and 6)

## Development of Test Plan

### Approach

The approach decided upon involved a series of test runs in the rra at varying heat fluxes (h), with cables of different materials, diameters (d), and copper ratios (r) and using varying spacings (s) between individual lengths of cable in the test runs. In each run, heat and smoke data would be collected simultaneously on the cable sample. In order to obtain the maximum amount of useful information from a minimum number of test runs, a statistical method would be used in the planning of the test program and analysis of the data.

### Statistical strategy

The combinations of d, r, s, and h to be used in the individual test runs constituted the test strategy. The strategy selected was the Box-Behnken plan.<sup>8</sup> If only three independent variables were involved, say d, r, and s, this statistical plan could be represented on a 3-dimensional space, i.e., a cube. Each variable forms one of the three orthogonal axes, and the length of each axis represents the operating range of its corresponding variable. The combinations of d, r, and s would be obtained by selecting points from the center of each edge and the center point of the cube. Reference 8 shows how the 3-dimensional plan can be extrapolated to four or more independent variables. The result, for this study, was a series of 27 test runs involving combinations of the lowest, highest, and mid-point values of d, r, s, and h. The specific combinations used will be shown in a later section along with results of the test runs. A property of the statistical plan, known as blocking, required that each series of 27 test runs be performed in groups, or blocks, of nine runs each, and the order of carrying out the test runs was randomized within each block.

### Values of parameters d and r from shipboard cable information

In order to determine appropriate ranges of values of cable diameter (d) and ratio of copper to combustible materials (r) to be investigated, an analysis was made of data provided by the Naval Sea Systems Command. This was a compilation of linear footages of each type of cable on each of three Navy ships, two destroyers and a nuclear submarine. It was found convenient to define the parameter r as the ratio of the volume of copper to the overall cable volume (equal to cross-sectional area of copper/total cross-sectional area of cable). The results of the analysis indicated the appropriate ranges of values for the laboratory study to be about 0.4 to 2.2 inches for d and 0.03 to 0.3 (dimensionless) for r. The actual values decided upon (see discussion below) were set approximately at the low and high ends and mid-points of these ranges.

### Cable materials

It was decided to use two sets of cable

materials, one a low-flammability system consisting of a flame-retardant polyvinyl chloride (PVC) with flame-retardant silicone rubber insulation and filler; and the other a high-flammability system consisting of a standard PVC jacket per MIL-C-915E and non-flame-retardant silicone rubber insulation and filler. The low flammability cables would meet the flame-propagation requirement of Amendment 2 to MIL-C-915E (IEEE-383 test), and the high-flammability cables would not. In accordance with the statistical plan, 27 test runs, comprising the required combinations of d, r, s, and h, would be made with each materials system.

### Values of parameters h and s

Heat flux. Values of heat flux for the study were established after the low-flammability cables had been received. The lowest of the three values was set at 2 W/cm<sup>2</sup>, slightly higher than the minimum heat flux required to ignite the least-ignitable of all the cables. The high value was set at 6 W/cm<sup>2</sup>, the maximum expected in a shipboard fire, based on opinions obtained independently from several fire-technology specialists. The middle value was then set at the midpoint, 4 W/cm<sup>2</sup>.

Spacing of cables. The three values decided upon were: 1/2 d (cable diameter), the standard spacing used in the IEEE-383 test; 1/4 d; and 0 (cables packed tightly together).

### Design and Procurement of Test Cables

The eighteen test cables used were manufactured to specification for this study. Design and procurement of the cables were initiated concurrently with the development of the test plan. The desired cable designs were based on a 3 X 3 matrix in accordance with the statistical plan, representing nine cable types for each set of cable materials used. Each cable type is a combination of one value each of d and r. Five of the nine cable types were found among the standard MIL-C-915E designs, and the remaining four were special designs made by using standard MIL-C-915E components in non-standard configurations. Table 1 lists the cable types procured and the specified dimensional tolerances of each. The terms d<sub>1</sub>, d<sub>2</sub>, and d<sub>3</sub> designate the low, middle, and high values of d, respectively, and similarly for r<sub>1</sub>, r<sub>2</sub>, and r<sub>3</sub>. Figure 3 shows the limits of the values of d and r for each cable type, resulting from the dimensional tolerances, superimposed over the ideal limits of the statistical plan. As can be seen, it was not possible to obtain the exact values desired; consequently, values were taken as close as practicable, since the statistical plan is not sensitive to small excursions such as those in Figure 3. It was especially important that each of the major combustible materials, jacketing, conductor insulation, and filler, be as nearly identical as possible from one cable to another within each of the two materials systems. Otherwise, effects on burning and smoke due to unintentional differences in materials could obscure the effects coming from the basic parameters being studied. This problem was minimized by having all 18 cables produced by a single

Table 1. Details of test cables

Cable numbers		Cable type	Configuration (per MIL-C-915E)	Overall cable diameter, inches		Value of r, ratio copper vol/cable vol	
low flammability	high flammability			minimum	maximum	minimum	maximum
1	10	$d_1 r_1$	Non-standard; one std. 14(7) conductor	0.500	0.540	0.049	0.057
2	11	$d_1 r_2$	Std. SSGU-50, except for slight deviation in diameter	0.520	0.562	0.155	0.181
3	12	$d_1 r_3$	Non-standard; like SSGU-50, except for smaller diameter	0.416	0.450	0.242	0.284
4	13	$d_2 r_1$	Non-standard; three std. 23(7) conductors	1.249	1.350	0.038	0.044
5	14	$d_2 r_2$	Std. DSGU-100	1.079	1.167	0.145	0.170
6	15	$d_2 r_3$	Std. FSGU-150	1.503	1.625	0.239	0.279
7	16	$d_3 r_1$	Non-standard; three std. 75(37) conductors	2.109	2.280	0.044	0.051
8	17	$d_3 r_2$	Std. 5KVTSGU-250	2.054	2.220	0.152	0.178
9	18	$d_3 r_3$	Std. TSGU-400	2.038	2.293	0.256	0.299

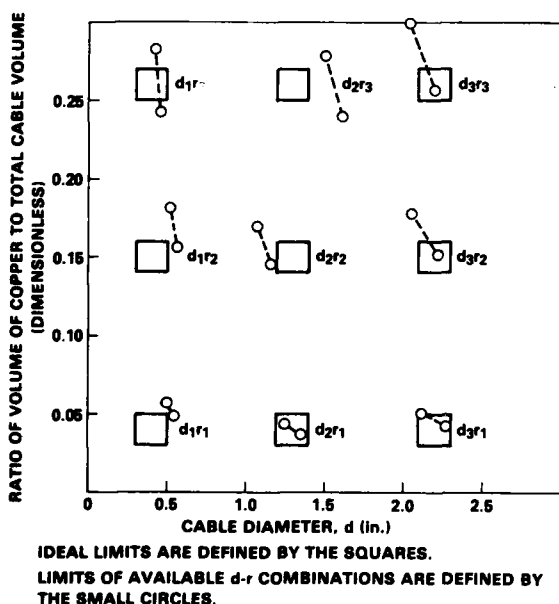


Figure 3. Limits of d and r of cable samples vs. ideal matrix

manufacturer and by giving special attention to the materials specifications. The statistical analysis of the data later on indicated that there were no significant effects of this type.

#### Laboratory Procedures

##### Dimensional measurements of test cables

Three samples of each of the 18 cables, taken from near the beginning of the reel, were used for measuring cable diameter (d) and copper ratio (r). After the first series of runs were made in the rra, additional sets of three samples each were

taken from farther along the reels and the measurements of d and r repeated. In all cases, d and r were within the values specified in Table 1. Variations in d and r were never greater than 5% and 10%, respectively, from one sample piece of a particular cable to another. The averages of the three values of d and r were used in the statistical analysis and appear in the data tables further on.

##### Release rate apparatus (rra)

Standard procedures outlined in the proposed ASTM method<sup>7</sup> were used, with the following exceptions:

1. The air flow through the unit was  $0.045 \pm 0.001$  kg/s ( $0.099 \pm 0.002$  lb/s), about 5% less than the standard value.
2. A special sample holder, 3 1/4 in. deep to accommodate the larger size cables, but otherwise of standard design, was used.
3. The length of a test run was set at 30 minutes. The smallest diameter cables usually burned up completely within this time, even at the lowest heat flux, whereas the largest diameter cables did not, even at the highest heat flux.

##### Recording of data and computer calculations

Data from the rra were recorded every 5 seconds on magnetic tape, using an Esterline-Angus data acquisition system, and were recorded simultaneously on a Hewlett-Packard Model 7100B strip chart recorder in order to monitor the test runs graphically. Data were transferred from the magnetic tape to disks, and calculations were made on a PDP-11 minicomputer. The basic quantities calculated were heat release and smoke release rates at each 5-second interval of the test run. From these, various other quantities could be calculated, such as heat release and smoke release rates per unit area of exposed cable at any given time, and total heat and smoke release per unit area, up to any given time in the run.

### Blank runs

To reduce errors in heat release measurements due to thermal inertia effects, a series of blank runs was made prior to the normal test runs. These were carried out with no cable samples in the sample holder, at the three heat fluxes used in the study, 2, 4, and 6 W/cm<sup>2</sup>. The resultant heat release data (close to zero in all cases) were incorporated into the computer program as blank run corrections applied to the calculations of the test runs.

### First 54 Test Runs

A series of 27 runs of low-flammability cables was carried out in the rra in accordance with the statistical plan. As explained earlier, this involved performing the 27 runs in groups, or blocks, of nine runs each, following randomized sequences within each block. Corresponding runs were then made with the high-flammability cables, using different random sequences within the blocks.

### Results of runs 1 through 54

Figure 4 is a reproduction of the strip chart of a typical run. The indicated run number, 1004, is the code designation for run 4 in the data acquisition system and the computer. The heights of the heat and smoke curves at any given time during the run represent, but are not linearly proportional to, the heat release and smoke release rates, respectively. Similarly, the areas under the curves up to any given time represent the total quantity of heat and smoke released up to that time. In order to relate the burning and smoke-generating characteristics of the cables to the basic parameters  $d$ ,  $r$ ,  $s$ , and  $h$ , it was necessary to simplify the voluminous data of the heat and smoke release curves. After preliminary statistical analyses, three quantities were selected as the most significant indicators, for the purposes of this study, of the burning and smoke-generating characteristics of the cables. These

are designated RHRAM, HRA5, and SRT/HRT.\* Briefly, RHRAM is a basic characteristic of the heat release curve which indicates the contribution of the combustible cable material to the fire once burning has gotten under way. HRA5 further characterizes the heat release curve, particularly with respect to ignitability of the cable.

A comparison of the smoke and heat release curves for most of the 54 runs indicates that smoke generation is closely tied to heat release, e.g., as seen in Figure 4. An examination of the quantities SRRAM and SRA5 for the low-flammability cables showed smoke release rates to vary with the basic parameters  $h$ ,  $d$ ,  $r$ , and  $s$ , in a manner very similar to heat release rates, as expected. These same relationships were not discerned with the high-flammability cables, but not necessarily because the relationships do not exist. They may exist but were not detected, since the magnitude of random variations in the smoke readings was much greater with the high flammability than with the low-flammability cables. It was decided to use the ratio SRT/HRT to characterize the smoke-generating property of the cables. This quantity simplifies the smoke data, in light of the apparent close relationship between smoke generation and heat release, since it is a measure of the tendency of a particular cable to produce smoke at a given intensity of burning.

The values of RHRAM, HRA5, and SRT/HRT and the basic parameters  $d$ ,  $r$ ,  $s$ , and  $h$  for runs 1 through 54 are given in Tables 2 and 3. For convenience, two additional quantities, SRAT and HRAT, are included. Note that  $SRAT/HRAT = SRT/HRT$ . In each table, the second through the fifth columns show the combinations of values of  $d$ ,  $r$ ,  $s$ , and  $h$  used in each test run. Runs 1-9 constitute the first block of runs in the statistical plan, 10-18 the second, and 19-27 the third. The randomized sequences in which the runs were carried out within each block are not shown here.

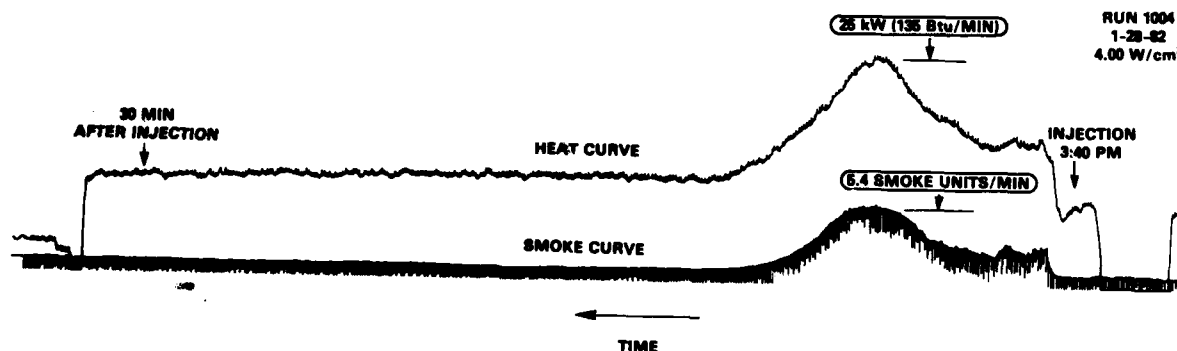


Figure 4. Strip chart curves of test run no. 4

\*See abbreviations and definitions at end of text.

Table 2. Summary of data, release rate apparatus runs 1 through 27,  
low-flammability cables

Run	Cable type	d (in.)	r (dimensionless)	s (fraction of cable diameter)	h (W/cm <sup>2</sup> )	Heat Data			Smoke Data	
						RHRAM (kW/m <sup>2</sup> )	HRA5 (MJ/m <sup>2</sup> )	HRAT (MJ/m <sup>2</sup> )	SRAT (smoke units/m <sup>2</sup> )	SRT/HRT (smoke units/MJ)
1	d3r3	2.089	0.299	1/4	4.0	79.4	12.0	105	1670	16
2	d3r1	2.215	0.047	1/4	4.0	75.7	10.9	107	1610	15
3	d1r1	0.544	0.049	1/4	4.0	137	15.7	77.0	2280	30
4	d1r3	0.425	0.272	1/4	4.0	122	16.1	56.1	1050	19
5	d2r2	1.138	0.153	1/2	6.0	137	21.3	140	4330	31
6	d2r2	1.138	0.153	1/2	2.0	112	0.0	97.6	750	8
7	d2r2	1.138	0.153	0	6.0	139	19.9	142	4280	30
8	d2r2	1.138	0.153	0	2.0	98	-1.1*	79.2	600	8
9	d2r2	1.138	0.153	1/4	4.0	130	15.3	154	3260	21
10	d3r2	2.201	0.155	1/4	6.0	92.9	14.3	122	4260	35
11	d3r2	2.201	0.155	1/4	2.0	61.3	0.0	35.6	250	7
12	d1r2	0.531	0.175	1/4	6.0	130	20.9	68.5	2460	36
13	d1r2	0.531	0.175	1/4	2.0	91.4	2.0	73.0	920	13
14	d2r3	1.568	0.258	1/2	4.0	121	16.1	163	2700	17
15	d2r3	1.568	0.258	0	4.0	109	14.3	149	2940	20
16	d2r1	1.320	0.040	1/2	4.0	110	17.0	162	4210	26
17	d2r1	1.320	0.040	0	4.0	93.1	14.0	137	2980	22
18	d2r2	1.138	0.153	1/4	4.0	128	16.7	149	**	**
19	d3r2	2.201	0.155	1/2	4.0	84.2	13.7	119	2400	21
20	d3r2	2.201	0.155	0	4.0	74.1	14.0	104	1960	19
21	d1r2	0.531	0.175	1/2	4.0	143	15.5	66.2	1350	20
22	d1r2	0.531	0.175	0	4.0	91.7	12.1	58.2	1520	26
23	d2r3	1.568	0.258	1/4	6.0	130	19.0	172	4770	28
24	d2r3	1.568	0.258	1/4	2.0	89.8	-2.8*	61.3	450	7
25	d2r1	1.320	0.040	1/4	6.0	117	20.3	170	5270	31
26	d2r1	1.320	0.040	1/4	2.0	66.6	-2.4*	62.0	580	9
27	d2r2	1.138	0.153	1/4	4.0	129	16.5	151	3240	22

\*See text for explanation of negative values.

\*\*Error in smoke photometer; data not valid.

Table 3. Summary of data, release rate apparatus runs 28 through 54  
high-flammability cables

Run	Cable type	d (in.)	r (dimensionless)	s (fraction of cable diameter)	h (W/cm <sup>2</sup> )	Heat data			Smoke data	
						RHRAM (kW/m <sup>2</sup> )	HRA5 (MJ/m <sup>2</sup> )	HRAT (MJ/m <sup>2</sup> )	SRAT (smoke units/m <sup>2</sup> )	SRT/HRT (smoke units/MJ)
28	d3r3	2.145	0.274	1/4	4.0	121	26.4	156	4080	26
29	d3r1	2.261	0.045	1/4	4.0	117	27.3	129	2700	21
30	d1r1	0.540	0.049	1/4	4.0	142	29.6	90.1	2650	29
31	d1r3	0.441	0.255	1/4	4.0	128	28.6	54.9	1770	32
32	d2r2	1.130	0.157	1/2	6.0	204	40.4	142	4710	33
33	d2r2	1.130	0.157	1/2	2.0	158	27.7	188	2440	13
34	d2r2	1.130	0.157	0	6.0	166	33.5	156	4430	28
35	d2r2	1.130	0.157	0	2.0	147	25.2	185	2400	13
36	d2r2	1.130	0.157	1/4	4.0	163	32.7	151	3740	25
37	d3r2	2.194	0.156	1/4	6.0	127	30.3	171	5510	32
38	d3r2	2.194	0.156	1/4	2.0	111	19.5	139	1770	13
39	d1r2	0.536	0.174	1/4	6.0	146	31.5	78.8	2430	31
40	d1r2	0.536	0.174	1/4	2.0	104	16.6	74.7	1150	15
41	d2r3	1.565	0.259	1/2	4.0	161	31.8	206	5130	25
42	d2r3	1.565	0.259	0	4.0	197	34.8	208	5210	25
43	d2r1	1.308	0.041	1/2	4.0	120	29.8	167	5410	33
44	d2r1	1.308	0.041	0	4.0	120	27.6	156	4280	27
45	d2r2	1.130	0.157	1/4	4.0	195	37.0	151	4020	27
46	d3r2	2.194	0.156	1/2	4.0	134	30.4	192	5150	27
47	d3r2	2.194	0.156	0	4.0	143	33.7	170	4520	27
48	d1r2	0.536	0.174	1/2	4.0	133	28.0	73.6	2050	28
49	d1r2	0.536	0.174	0	4.0	123	25.1	78.7	2210	28
50	d2r3	1.565	0.259	1/4	6.0	163	37.9	190	5500	29
51	d2r3	1.565	0.259	1/4	2.0	156	23.2	188	2130	11
52	d2r1	1.308	0.041	1/4	6.0	143	32.6	171	5980	35
53	d2r1	1.308	0.041	1/4	2.0	108	21.9	149	2110	14
54	d2r2	1.130	0.157	1/4	4.0	160	33.0	157	4270	27

Negative values of HRA5 occur in runs 8, 24, and 26 because the time to ignition of the cable sample is relatively long in those runs. Prior to ignition, the sample absorbs a measurable amount of heat from the radiant heaters (negative heat release), while giving off no significant amount of heat due to its own combustion. Heat evolution does in fact result from burning of the cable in the immediate vicinity of the pilot flame during this time, but this is low in magnitude. Ignition occurs when burning spreads beyond this region. In the three runs cited, the time to ignition was sufficiently long that the negative heat exceeded the positive in the first 5 minutes after injection of the cable sample. This can be seen in the heat release curve of run 26, Figure 5. Note that the height of the heat curve is lower during most of the 5 minutes after injection than just prior to injection, indicating negative heat release. Run 53, Figure 6, is shown for comparison. All conditions of run 53 are the same as those of 26 except that high- rather than low-flammability cable was used. Here, ignition occurred very quickly after injection, and HRA5 is substantially positive.

#### Statistical analysis of the data

The data of Tables 2 and 3 were fit by a least squares method to give six equations of the form

$$y = b_0 + b_1 D + b_2 R + b_3 S + b_4 H + b_{12} DR + b_{13} DS + b_{14} DH + b_{23} RS + b_{24} RH + b_{34} SH + b_{11} D^2 + b_{22} R^2 + b_{33} S^2 + b_{44} H^2,$$

in which y is RHRAM, HRA5, or SRT/HRT for either the low- or high-flammability cables, and

$$D = \frac{d - \bar{d}}{\hat{\sigma}_d}$$

$$R = \frac{r - \bar{r}}{\hat{\sigma}_r}$$

$$S = \frac{s - \bar{s}}{\hat{\sigma}_s}$$

$$H = \frac{h - \bar{h}}{\hat{\sigma}_h}$$

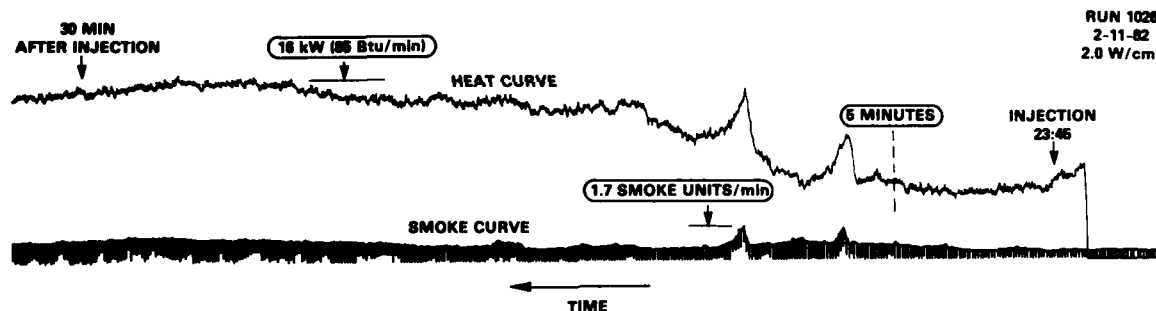


Figure 5. Strip chart curves of test run 26. Heat release curve shows negative HRA5

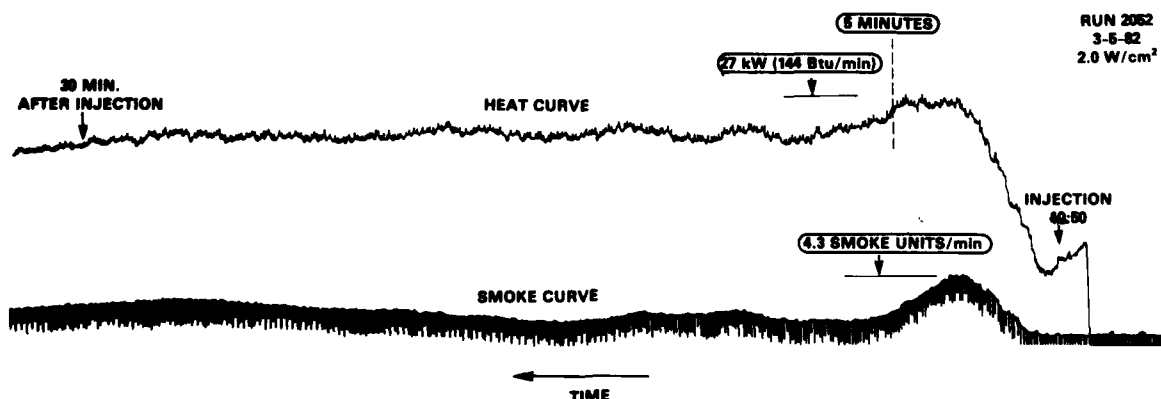


Figure 6. Strip chart curves of test run 53. Heat release curve shows positive HRA5

$\bar{d}$  = mean value of  $d$  for 27 test runs, and similarly for  $r$ ,  $s$ , and  $h$

$\hat{\sigma}_d$  = standard deviation of  $d$  for 27 test runs and similarly for  $\hat{\sigma}_r$ , etc.

(Note: the symbol  $\hat{\sigma}$  is used instead of  $s$  for standard deviation to avoid confusion with the  $s$  used for cable spacing.)

The term  $b_0$  is a constant which is different for each of the six equations. Each "beta coefficient",  $b_1$ ,  $b_2$ , etc., is a measure of the sensitivity of  $y$  to the independent variable or combination of variables associated with that coefficient. Thus, the larger the beta coefficient, the greater the sensitivity of  $y$  to the corresponding independent variable(s).

Cross terms, such as  $b_{12}DR$ , are mathematical representations of interactive (synergistic or antisnergistic) effects between the two independent variables, e.g.,  $d$  and  $r$ .

As a first step in the analysis of each equation, it is necessary to distinguish significant effects from random error scatter. This was done, following the Box Behnken method, by calculating random error and comparing it with the beta coefficient for each term of the equation other than  $b_0$ . The practical interpretation of the numerical results of this process is summarized in Table 4. Any variable which shows no significance may be dropped from the equation, and this was done in the analysis. Note that the cable spacing,  $s$ , was not found to be significant in any of the six equations. A possible explanation for this unexpected result is given further on.

Table 4. Effect of independent variables on RHRAM, HRA5, and SRT/HRT

Dependent variable	Parameters having a significant effect on the indicated dependent variable	
	low-flammability cables	high-flammability cables
RHRAM	$h, d$	$h, d, r$
HRA5	$h$	$h, d$
SRT/HRT	$h$	$h$

Further interpretation of each equation was achieved by plotting  $y$  versus the independent variable(s). When two variables were significant, i.e.,  $h$  and  $d$  for RHRAM of the low-flammability and for HRA5 of the high-flammability cables, a contour plot was executed on a plane of those two variables as shown in Figure 7. Where three variables were significant, i.e.,  $h$ ,  $d$ , and  $r$  for RHRAM of the high-flammability cables, contour plots were run as before at low, middle, and high values of  $r$ .

The significant relationships found between the dependent variables RHRAM, HRA5, and SRT/HRT and the basic parameters,  $d$ ,  $r$ , and  $h$  are plotted in Figures 8 through 16. Each curve represents

the most probable relationship between the indicated dependent variable and  $d$ ,  $r$ , or  $h$  ( $s$  was found to have no significant effect). Numbers in parentheses are run numbers from which the data points came.

Note that a given curve is not necessarily the best fit to the data points plotted with that curve. This is because each curve is a segment of a 5-dimensional surface which is a plot of the equation  $y = f(d, r, s, h)$ , where  $y$  is either RHRAM, HRA5, or SRT/HRT. Each 5-dimensional surface itself is the least-squares (statistically best) fit of all 27 data points from either runs 1-27 or 28-54, involving all 4 independent variables  $d$ ,  $r$ ,  $s$ , and  $h$ . Individual segments of the six 5-dimensional surfaces, the curves of Figures 8-16, are thus not necessarily the best statistical fits to just those data points closely associated with each individual segment. This does not apply to the curves of Figures 15 and 16 and the lower curve of Figure 13, since in these cases all 27 data points were plotted with the curves.

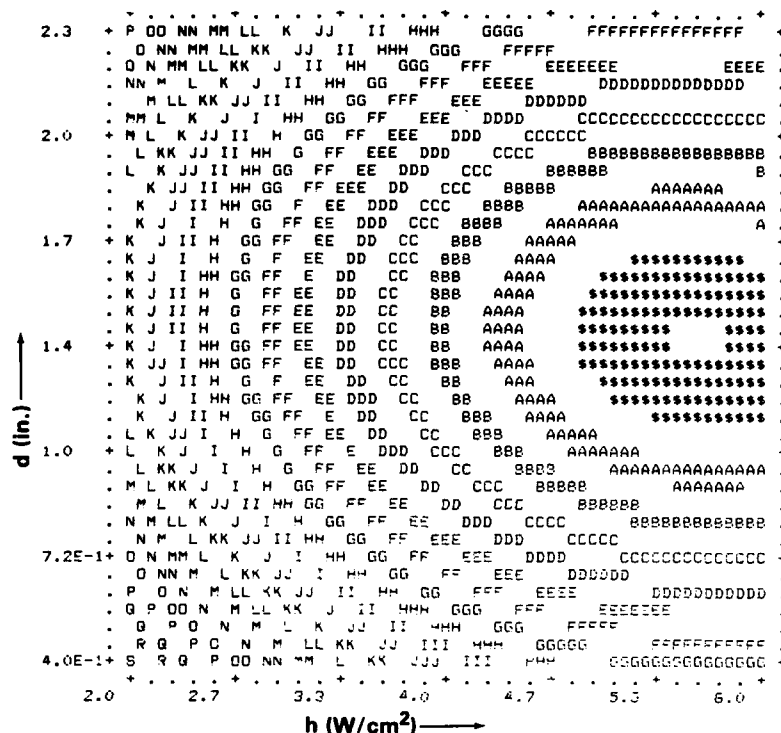
Figures 8-16 should be examined with reference to Table 4, since the curves are meant to show the magnitude of the effects indicated in the table to be significant.

The uncertainty limits shown on the graphs for the individual curves were calculated by the method of Abernathy et al.<sup>9</sup>

#### Additional Test Runs

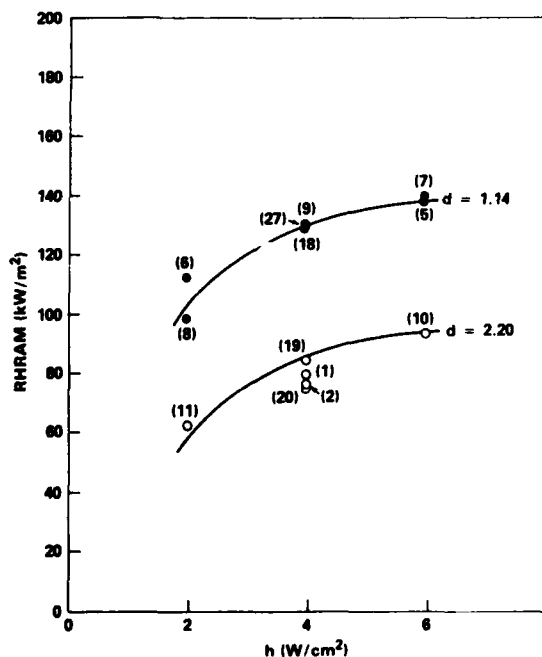
As part of an effort to find a simple correlation between rra heat release data and the IEEE-383 flame propagation test,<sup>2</sup> a series of IEEE-383 tests were made on some of the cables used in runs 1-54. Those tests will not be discussed in any detail in this paper. However, there appeared to be a correlation between the IEEE-383 test results and the quantity HRA5, at 2 W/cm<sup>2</sup>. In order to check the rra data in the apparent correlation, a second series of test runs was made in the rra on the same cables as in runs 1-54, but at a constant heat flux of 2 W/cm<sup>2</sup>. The Box-Behnken method was again used in planning the tests and analyzing the data, this time with a 3-dimensional matrix of the independent variables  $d$ ,  $r$ , and  $s$ . The test conditions and the results of these test runs are given in Tables 5 and 6. Runs 74 through 76 and 96 through 98 are duplicates of runs 13, 6, 11, 40, 33, and 38, respectively. Runs 99 through 104 are duplicates of runs 55, 68, 94, 86, 90, and 83, respectively, and were made because of difficulties with the smoke photometer or other problems in the later runs. It will be noted that there are many more replicates in runs 54-104 than in 1-54. This is not because this was required by the Box-Behnken plan, but because it was desired to further reinforce the data at 2 W/cm<sup>2</sup>. Tables 7 and 8 summarize the data from the replicated runs and show the reproducibility of readings from one replicated run to another.

Negative values of HRA5 are due to absorption of heat by the cable sample prior to ignition, as previously explained for runs 8, 24, and 26 (Table 2). Note that negative values occur only with low-flammability cables.



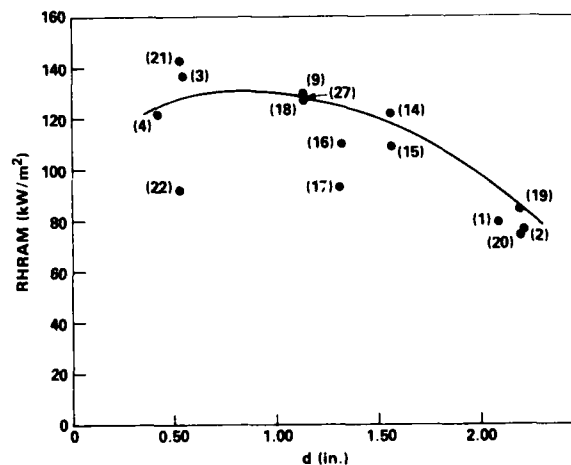
NOTE: IN THIS PLOT,  $\Phi$  = 3500 Btu/min-m<sup>2</sup> (= 61.6 kW/m<sup>2</sup>)  
 A = 3400  
 B = 3300, ETC.

Figure 7. Contour plot of RHRAM vs. h and d



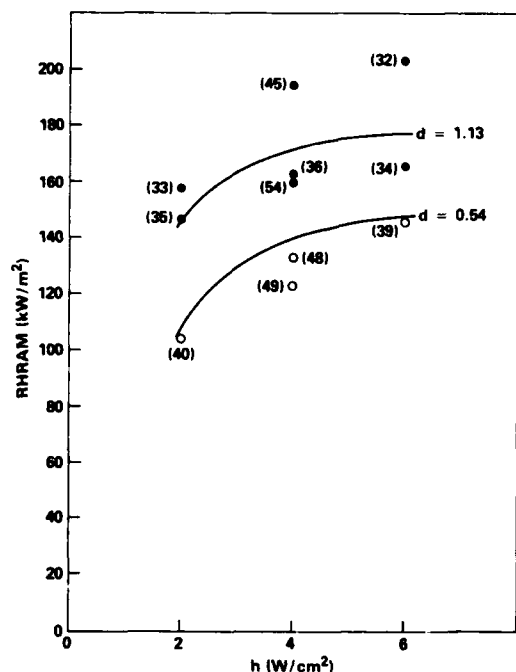
NOTE: UNCERTAINTY LIMITS AT 95% CONFIDENCE LEVEL  
 (11 DEGREES OF FREEDOM)  
 CENTER POINT:  $\pm 8$  kW/m<sup>2</sup>  
 EXTREMES:  $\pm 15$  kW/m<sup>2</sup>

Figure 8. RHRAM vs. h, low-flammability cable.



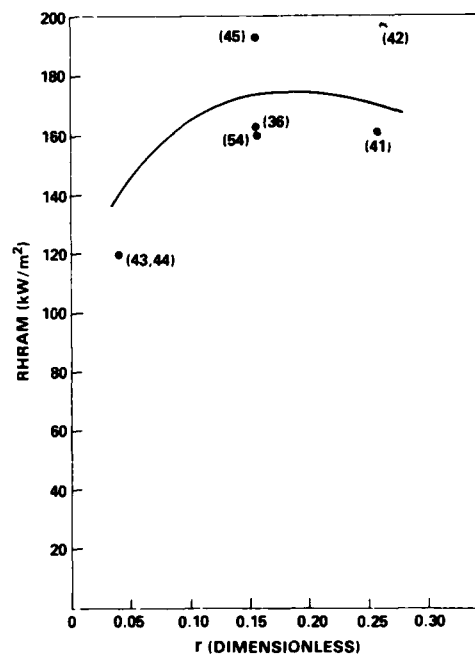
NOTES: 1. CURVE IS FOR  $h = 4.0$  W/cm<sup>2</sup>  
 2. UNCERTAINTY LIMITS AT 95% CONFIDENCE LEVEL  
 (11 DEGREES OF FREEDOM)  
 CENTER POINT:  $\pm 8$  kW/m<sup>2</sup>  
 EXTREMES:  $\pm 15$  kW/m<sup>2</sup>

Figure 9. RHRAM vs. d, low-flammability cables



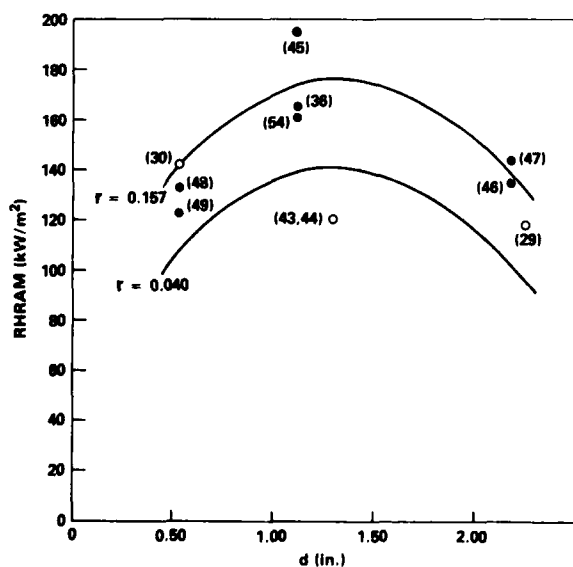
NOTES: 1. CURVES ARE FOR  $r = 0.16$  AT TWO VALUES OF  $d$   
 2. UNCERTAINTY LIMITS AT 95% CONFIDENCE LEVEL (11 DEGREES OF FREEDOM)  
 CENTER POINT:  $\pm 13 \text{ kW/m}^2$   
 EXTREMES:  $\pm 25 \text{ kW/m}^2$

Figure 10. RHRAM vs.  $h$ , high-flammability cables



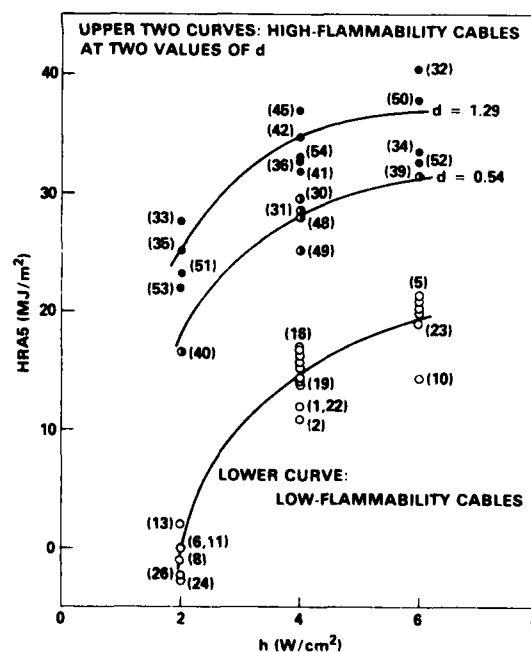
NOTES: 1. CURVE IS FOR  $h = 4.0 \text{ W/cm}^2$  AND  $d = 1.31 \text{ in.}$   
 2. UNCERTAINTY LIMITS AT 95% CONFIDENCE LEVEL (11 DEGREES OF FREEDOM)  
 CENTER POINT:  $\pm 13 \text{ kW/m}^2$   
 EXTREMES:  $\pm 25 \text{ kW/m}^2$

Figure 12. RHRAM vs.  $r$ , high-flammability cables



NOTES: 1. CURVES ARE FOR  $h = 4.0 \text{ W/cm}^2$  AT TWO VALUES OF  $r$   
 2. UNCERTAINTY LIMITS AT 95% CONFIDENCE LEVEL (11 DEGREES OF FREEDOM)  
 CENTER POINT:  $\pm 13 \text{ kW/m}^2$   
 EXTREMES:  $\pm 25 \text{ kW/m}^2$

Figure 11. RHRAM vs.  $d$ , high-flammability cables



NOTE: UNCERTAINTY LIMITS AT 95% CONFIDENCE LEVEL (11 DEGREES OF FREEDOM)  
 LOW FLAM. HIGH FLAM.  
 CENTER POINT:  $\pm 1.2 \text{ MJ/m}^2$   $\pm 2.1 \text{ MJ/m}^2$   
 EXTREMES:  $\pm 2.4 \text{ MJ/m}^2$   $\pm 3.9 \text{ MJ/m}^2$

Figure 13. HRA5 vs.  $h$

AD-A136 749

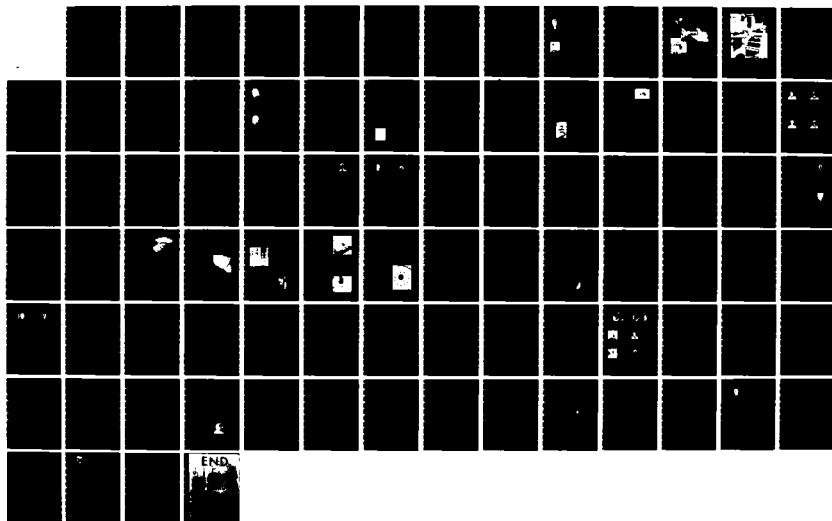
PROCEEDINGS OF THE INTERNATIONAL WIRE AND CABLE  
SYMPOSIUM (32ND) HELD AT (U) ARMY  
COMMUNICATIONS-ELECTRONICS COMMAND FORT MONMOUTH NJ  
17 NOV 83

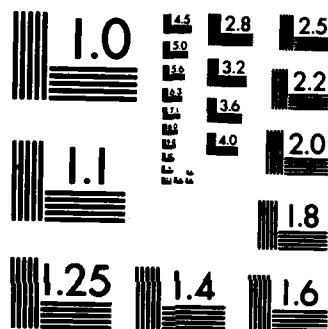
5/5

UNCLASSIFIED

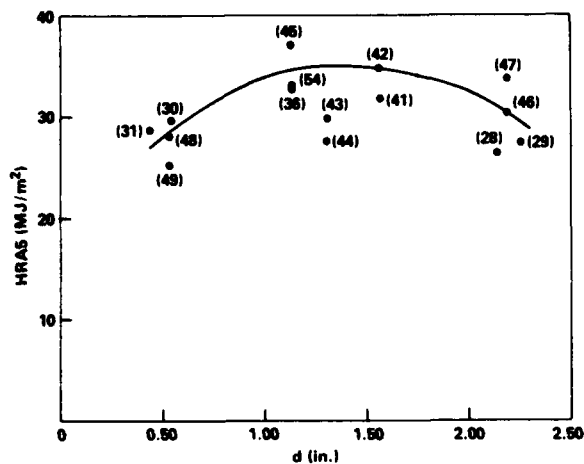
F/G 5/2

NL



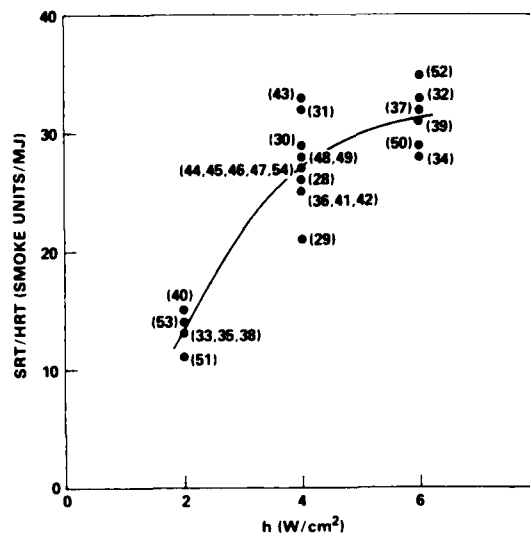


MICROCOPY RESOLUTION TEST CHART  
NATIONAL BUREAU OF STANDARDS-1963-A



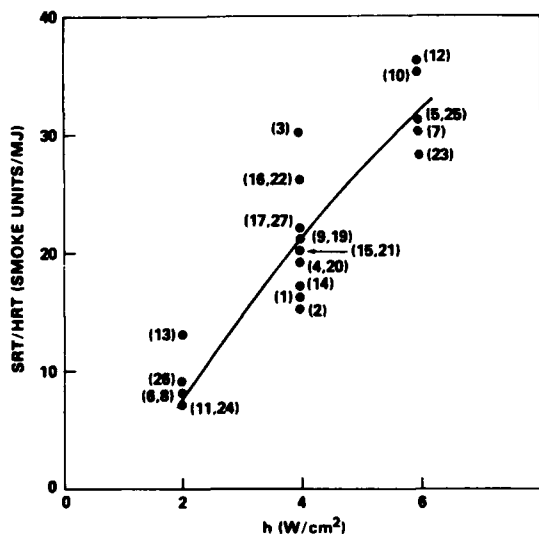
NOTES: 1. CURVE IS FOR  $h = 4.0 \text{ W/cm}^2$   
 2. UNCERTAINTY LIMITS AT 95% CONFIDENCE LEVEL  
 (11 DEGREES OF FREEDOM)  
 CENTER POINT:  $2.1 \text{ MJ/m}^2$   
 EXTREMES:  $3.9 \text{ MJ/m}^2$

Figure 14. HRA5 vs. d, high-flammability cables



NOTE: UNCERTAINTY LIMITS AT 95% CONFIDENCE LEVEL  
 (11 DEGREES OF FREEDOM)  
 CENTER POINT:  $\pm 4 \text{ SMOKE UNITS/MJ}$   
 EXTREMES:  $\pm 7 \text{ SMOKE UNITS/MJ}$

Figure 16. SRT/HRT vs. h, high-flammability cables



NOTE: UNCERTAINTY LIMITS AT 95% CONFIDENCE LEVEL  
 (11 DEGREES OF FREEDOM)  
 CENTER POINT:  $\pm 5 \text{ SMOKE UNITS/MJ}$   
 EXTREMES:  $\pm 7 \text{ SMOKE UNITS/MJ}$

Figure 15. SRT/HRT vs. h, low-flammability cables

The results of runs 54-104 are important not only in reinforcing the data of runs 1-54, but also in that they confirm the validity of the statistical method. Table 9 shows which of the independent variables d, r, and s have a significant effect on

the three dependent variables. Leaving out h, which is not a variable in this second series of runs, we find these relationships to be the same as were observed in runs 1-54 (Table 4). In Figure 17, curves b-b and d-d represent the estimated relationship between RHRAM and d for the low- and high-flammability cables, respectively, derived from the statistical analysis of runs 55-104. Curves a-a and c-c are corresponding results from runs 1-54. Note that curves a-a and c-c were obtained not from the  $2 \text{ W/cm}^2$  data alone, in the first series of runs, but from the total statistical analysis of runs 1-27 and 28-54. Figure 18 makes a similar comparison of HRA5 versus d for high-flammability cables. The corresponding comparisons of values of HRA5 for low-flammability cables and of SRT/HRT are given in tabular form, Tables 10 and 11, rather than being plotted, since in these cases the dependent variables do not show any significant dependence on d, r, or s (cf. Table 9).

#### Discussion

##### General comments on rra

Experience with the release rate apparatus in this study has shown it to be operationally a practical and convenient laboratory tool. The reproducibilities of the heat and smoke measurements are comparable to those of other flammability tests, such as vertical tray flame propagation tests; and smoke tests, such as the National Bureau of Standards smoke chamber method.<sup>10,11</sup>

Table 5. Summary of data, release rate apparatus runs 55 through 76, 99 and 100, low-flammability cables, at 2 W/cm<sup>2</sup>

Run	Cable type	d (in.)	r (dimensionless)	s (fraction of cable diameter)	Heat data			Smoke data	
					RHRAM (kW/m <sup>2</sup> )	HRA5 (MJ/m <sup>2</sup> )	HRAT (MJ/m <sup>2</sup> )	SRAT (smoke units/m <sup>2</sup> )	SRT/HRT (smoke units/MJ)
55	d3r3	2.085	0.299	1/4	55.0	-1.5	29.1	10	0
56	d3r1	2.238	0.047	1/4	55.8	0.0	48.5	350	7
57	d1r3	0.440	0.272	1/4	90.2	-0.6	50.1	600	12
58	d1r1	0.535	0.049	1/4	101	-0.6	75.3	1480	20
59	d3r2	2.201	0.155	1/2	64.3	-1.6	35.3	180	5
60	d3r2	2.201	0.155	0	54.9	-0.5	46.3	320	7
61	d1r2	0.531	0.175	1/2	84.4	1.6	60.9	800	13
62	d1r2	0.531	0.175	0	66.2	-2.4	44.4	630	14
63	d2r3	1.568	0.258	1/2	109	-1.6	93.3	870	9
64	d2r3	1.568	0.258	0	67.4	-1.8	57.4	290	5
65	d2r1	1.320	0.040	1/2	83.8	-0.6	76.2	370	5
66	d2r1	1.320	0.040	0	63.3	0.7	59.3	530	9
67	d2r2	1.097	0.153	1/4	106	-2.9	77.9	620	8
68	d2r2	1.097	0.153	1/4	112	-1.7	84.4	*	*
69	d2r2	1.097	0.153	1/4	96.7	-1.8	86.9	690	8
70	d3r3	2.085	0.299	1/4	63.4	-1.2	21.2	320	15
71	d3r1	2.238	0.047	1/4	37.9	-0.8	33.5	330	10
72	d1r2	0.531	0.175	1/2	88.3	1.4	66.2	890	13
73	d1r2	0.531	0.175	0	68.9	-2.0	50.6	680	13
74	d1r2	0.531	0.175	1/4	89.3	0.5	66.8	720	11
75	d2r2	1.097	0.153	1/2	115	0.5	123	1270	10
76	d3r2	2.201	0.155	1/4	47.0	-1.3	29.8	0	0
99	d3r3	2.085	0.299	1/4	51.3	0.2	25.0	0	0
100	d2r2	1.097	0.153	1/4	105	-0.4	92.1	510	6

\*Error in smoke photometer; data not valid.

Table 6. Summary of data, release rate apparatus runs 77 through 98 and 101 through 104, high-flammability cables, at 2 W/cm<sup>2</sup>

Run	Cable type	d (in.)	r (dimensionless)	s (fraction of cable diameter)	Heat data			Smoke data	
					RHRAM (kW/m <sup>2</sup> )	HRA5 (MJ/m <sup>2</sup> )	HRAT (MJ/m <sup>2</sup> )	SRAT (smoke units/m <sup>2</sup> )	SRT/HRT (smoke units/MJ)
77	d3r3	2.137	0.274	1/4	125	23.6	156	1950	13
78	d3r1	2.186	0.045	1/4	124	21.4	140	1570	11
79	d1r3	0.448	0.255	1/4	90.1	16.4	51.5	1280	25
80	d1r1	0.541	0.049	1/4	128	24.9	87.1	1810	21
81	d3r2	2.194	0.156	1/2	131	24.4	162	2630	16
82	d3r2	2.194	0.156	0	138	24.0	185	2570	14
83	d1r2	0.536	0.174	1/2	131	21.2	92.3	*	*
84	d1r2	0.536	0.174	0	92.2	14.4	88.0	1060	12
85	d2r3	1.565	0.259	1/2	147	29.3	190	2460	13
86	d2r3	1.565	0.259	0	150	24.5	183	*	*
87	d2r1	1.308	0.041	1/2	130	25.1	130	1750	13
88	d2r1	1.308	0.041	0	113	21.5	135	1830	14
89	d2r2	1.128	0.157	1/4	137	25.4	180	2580	14
90	d2r2	1.128	0.157	1/4	135	26.3	170	*	*
91	d2r2	1.128	0.157	1/4	149	24.5	174	2600	15
92	d3r3	2.137	0.274	1/4	102	20.1	130	1110	9
93	d3r1	2.186	0.045	1/4	135	21.3	140	1860	13
94	d1r2	0.536	0.174	1/2	122	20.8	82.6	*	*
95	d1r2	0.536	0.174	0	84.9	13.6	79.5	970	12
96	d1r2	0.536	0.174	1/4	99.5	17.3	86.9	1310	15
97	d2r2	1.128	0.157	1/2	171	30.6	182	2710	15
98	d3r2	2.194	0.156	1/4	119	20.1	133	1280	10
101	d1r2	0.536	0.174	1/2	124	19.8	79.6	940	12
102	d2r3	1.565	0.259	0	138	24.5	182	2130	12
103	d2r2	1.128	0.157	1/4	140	28.8	181	1990	11
104	d1r2	0.536	0.174	1/2	110	17.6	73.9	1540	21

\*Error in smoke photometer; data not valid.

Table 7. Reproducibility of measurements, low-flammability cables  
(replicated runs only)

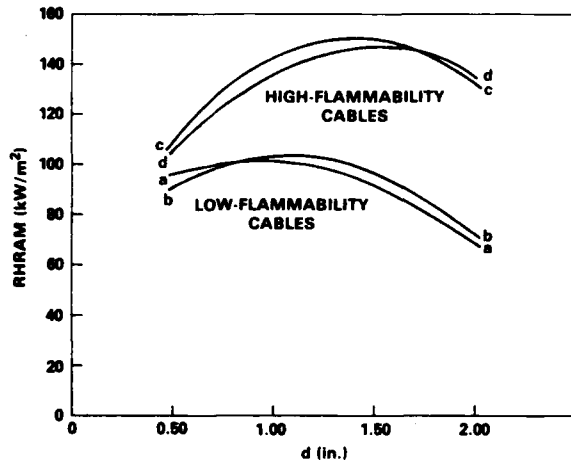
Run	RHRAM (kW/m <sup>2</sup> )			HRA5 (MJ/m <sup>2</sup> )			SRAT (smoke units/m <sup>2</sup> )		
	Individual Values	Mean	Standard Deviation	Individual Values	Mean	Standard Deviation	Individual Values	Mean	Standard Deviation
9	130	129	±1.0	15.3	16.2	±0.8	3260	3250	±10
18	128			16.7			----		
27	129			16.5			3240		
55	55.0	56.6	±6.2	-1.5	-0.8	±0.9	10	110	±180
70	63.4			-1.2			320		
99	51.3			0.2			0		
56	55.8	46.9	±12.7	0.0	-0.4	±0.6	350	340	±10
71	37.9			-0.8			330		
61	84.4	86.4	±2.8	1.6	1.5	±0.1	800	850	±60
72	88.3			1.4			890		
62	66.2	67.6	±1.9	-2.4	-2.2	±0.3	630	660	±40
73	68.9			-2.0			680		
67	106	105	±6.3	-2.9	-1.7	±1.0	620	610	±90
68	112			-1.7			----		
69	96.7			-1.8			690		
100	105			-0.4			510		
13	91.4	90.4	±1.5	2.0	1.3	±1.1	920	820	±140
74	89.3			0.5			720		
6	113	114	±1.4	0.0	0.3	±0.4	750	1010	±370
75	115			0.5			1270		
11	61.3	54.2	±10.1	0.0	-0.7	±0.9	250	130	±180
76	47.0			-1.3			0		

Table 8. Reproducibility of measurements, high-flammability cables  
(replicated runs only)

Run	RHRAM (kW/m <sup>2</sup> )			HRA5 (MJ/m <sup>2</sup> )			SRAT (smoke units/m <sup>2</sup> )		
	Individual Values	Mean	Standard Deviation	Individual Values	Mean	Standard Deviation	Individual Values	Mean	Standard Deviation
36	163	173	±19	32.7	34.2	±2.4	3740	4010	±270
45	195			37.0			4020		
54	160			33.0			4270		
77	125	114	±16	23.6	21.9	±2.5	1950	1530	±590
92	102			20.1			1110		
78	124	130	±8	21.4	21.4	±0.1	1570	1720	±210
93	135			21.3			1860		
83	131	122	±9	21.2	19.9	±1.6	----	1240	±420
94	122			20.8			----		
101	124			19.8			940		
104	110			17.6			1540		
84	92.2	88.6	±5.2	14.4	14.0	±0.6	1060	1020	±60
95	84.9			13.6			970		
89	137	140	±6	25.4	26.3	±1.9	2580	2390	±350
90	135			26.3			----		
91	149			24.5			2600		
103	140			28.8			1990		
40	104	102	±3	16.6	17.0	±0.5	1150	1230	±110
96	99.5			17.3			1310		
33	158	165	±9	27.7	29.2	±2.1	2440	2580	±190
97	171			30.6			2710		
38	111	115	±6	19.5	19.8	±0.4	1770	1530	±350
98	119			20.1			1280		

Table 9. Effect of basic parameters on RHRAM, HRA5, and SRT/HRT at a heat flux of 2 W/cm<sup>2</sup>

Dependent variables	Parameters having a significant effect on the indicated dependent variable	
	low-flammability cables	high-flammability cables
RHRAM	d	d, r
HRA5	-	d
SRT/HRT	-	-



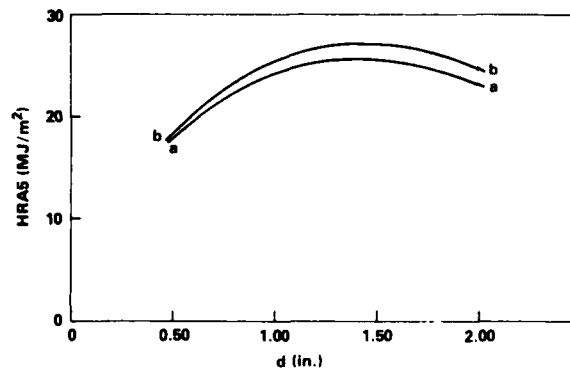
NOTES:

1. CURVE a-a IS FROM RUNS 1-27  
CURVE b-b IS FROM RUNS 55-76, 99, 100  
CURVE c-c IS FROM RUNS 28-54  
CURVE d-d IS FROM RUNS 77-98, 101-104
2. UNCERTAINTY LIMITS AT 95% CONFIDENCE LEVEL  
LOW FLAM. (13 DEGREES OF FREEDOM) CENTER POINT:  $\pm 7 \text{ kW/m}^2$   
EXTREMES:  $\pm 17 \text{ kW/m}^2$   
HIGH FLAM. (15 DEGREES OF FREEDOM)  $\pm 11 \text{ kW/m}^2$   
 $\pm 25 \text{ kW/m}^2$

Figure 17. RHRAM vs. d at 2 W/cm<sup>2</sup>, comparison of values, runs 1-54 with runs 55-104

#### Statistical method

As previously explained, the object in using the Box-Behnken statistical plan was to obtain a maximum amount of information from a minimum number of measurements. The results of the study indicate that this was reasonably well achieved. The validity of the statistical method is demonstrated by the close agreement in the results of the statistical analyses at 2 W/cm<sup>2</sup> between the two series of test runs (runs 1-54 and 55-104). This can be seen in Tables 4 and 9 and in Figures 17 and 18. A feature of the plan explained earlier is its ability to measure interactive effects between independent variables, indicated by cross terms of the equation for y. It is important to note that the statistical analysis revealed no significant interactive effects in this study. The results of the study suggest that the Box-Behnken plan could be used in similar investigations in which it is desired to measure the effects of several independent variables on one or more specific fire parameters of cables. The stability of the plan and therefore



- NOTES: 1. CURVE a-a IS FROM RUNS 28-54  
CURVE b-b IS FROM RUNS 77-98, 101-104  
2. UNCERTAINTY LIMITS AT 95% CONFIDENCE LEVEL (15 DEGREES OF FREEDOM)  
CENTER POINT:  $\pm 1.8 \text{ MJ/m}^2$   
EXTREMES:  $\pm 4.7 \text{ MJ/m}^2$

Figure 18. HRA5 vs. d at 2 W/cm<sup>2</sup>, comparison of values, runs 28-54 with runs 77-98 and 101-104, high-flammability cables

Table 10. HRA5 at 2 W/cm<sup>2</sup>, comparison of values from the two series of runs, low-flammability cables

Runs	HRA5 (MJ/m <sup>2</sup> )		
	range	mean	standard deviation
6, 8, 11, 13, 24, 26	-2.8 to +2.0	-0.7	$\pm 1.8$
55-76, 99, 100	-2.9 to +1.6	-0.7	$\pm 1.2$

Table 11. SRT/HRT at 2 W/cm<sup>2</sup>, comparison of values from the two series of test runs

Runs	SRT/HRT (smoke units/MJ)		
	range	mean	standard deviation
<u>low-flammability cables</u>			
6, 8, 11, 13, 24, 26	7 to 13	8.7	$\pm 2.3$
55 through 76 99, 100	0 to 20	8.7	$\pm 5.0$
<u>high-flammability cables</u>			
33, 35, 38, 40 51, 53	11 to 15	13.2	$\pm 1.3$
77 through 98 101 through 104	9 to 25	14.1	$\pm 3.8$

the reliability of the results can be improved by the replication of individual data points.

#### Observed effects of basic parameters on burning and smoke generation

The effect of increasing heat flux on the rate of burning was significant, as expected (Figures 8, 10, and 13). With regard to smoke generation (Figures 15 and 16), it might have been predicted that, although the smoke generation rate would increase with increasing heat flux, the ratio of smoke to heat release would decrease. One could argue that since smoke consists of unburned, but burnable, decomposition products, an increase in heat flux would cause more complete combustion, producing less smoke in relation to the amount of heat released. The curves of Figures 15 and 16 show just the opposite, i.e., the ratio of smoke to heat released increases. Obviously, in this heat flux range, the rate of decomposition of the cable materials is increasing faster than the rate of combustion. It must also be considered that a part of the smoke is a decomposition product of the silicone rubber, silica ( $\text{SiO}_2$ ), a semiopaque material that is fully oxidized and not subject to being rendered invisible by further combustion. The curves of Figures 15 and 16 show a downward bend (this is relatively small, but definite, in Figure 15), which indicates that if the heat flux continued to increase, SRT/HRT would eventually level off and then possibly decrease.

The observed variations in flammability with cable diameter for both the low- and high-flammability cables are plausible, although the decrease in both RHRAM (Figures 9, 11, and 17) and HRA5 (Figures 14 and 18) toward the lower values of  $d$  was not anticipated. This effect is probably the result of a limited fuel supply; i.e., the intensity of burning that develops in a given time period is limited by the relatively small amount of combustible material in the smaller diameter cables. The decrease in RHRAM and HRA5 toward the larger diameters is believed to be due to the increasing mass of material, which becomes more difficult to ignite and burn. The result of these two effects is the occurrence of maximum values of RHRAM and HRA5, representing the worst-case condition of burning, which occurs at a diameter between 0.75 and 1.0 inch for the low-flammability, and 1.25 to 1.50 inches for the high-flammability cables.

The observed effects of the remaining two variables,  $r$  and  $s$ , were unanticipated. Variations in  $r$  were expected to have a much greater effect on burning, and in the opposite direction to that shown in Figure 12. This latter result can not be explained at this point, but in any case, the effect of  $r$  is slight. The magnitude of the cable spacing,  $s$ , was found to have no significant effect on any of the dependent variables. As set forth earlier, spacing was expected to be a significant parameter, because it affects both the total cable surface exposed to the radiant heat and the rate of replenishment of oxygen at the burning surface. It is concluded from the observed results that the backing and walls of the

sample holder form a stagnant pocket that limits the influence of both of these factors. From the experience gained in this study, it appears logical in future rra measurements to eliminate spacing as a variable by standardizing it, say, at one-half the cable diameter, as in the IEEE-383 flame propagation test.

#### Overall significance of the rra data

It is not the intent of this presentation to come to any final conclusions on the use of the rra in cable fire and smoke measurements. Inasmuch as the Navy's evaluation of the rra is still in progress, no attempt will be made to recommend or describe a specific procedure for setting flammability or smoke standards; however, some general observations and suggestions will be made.

This study corroborates an appraisal made earlier: that flammability and smoke measurements carried out over a range of heat fluxes provide a more realistic basis for predicting the relative behavior of different cables in a real fire, than do test procedures that do not allow for controlled variations in heat flux. Two examples will be given to support this view:

**Flame propagation.** It was mentioned previously that an apparent correlation had been found between heat release data and the IEEE-383 flame propagation test. Briefly, the high-flammability cables, all of which had a value of HRA5 substantially above 0, when run at  $2 \text{ W/cm}^2$  (cf. Figure 13), consistently failed the IEEE-383 test, while the low-flammability cables having a value of HRA5 at or near 0, consistently passed. In these two groups of cables, those that passed the IEEE-383 test will clearly be more resistant to a fire of moderate severity than those that failed. However, in a group of cables of varying materials and/or constructions, all of which pass the IEEE-383 test, it is difficult if not impossible to predict from the IEEE-383 test results what their relative performance would be under more severe fire conditions. Release rate data, like that of Figures 8, 10, and 13, give a more complete picture of burning characteristics of a cable, from which one can venture real-fire predictions with greater confidence.

**Smoke measurement.** Smoke generation tests carried out at a single, relatively low heat flux are also subject to a limitation in the amount of useful information they provide. This can be illustrated by comparing the values of SRAT of test runs 8 (Table 2) and 35 (Table 3). These two cables were of the same size and configuration, and both were run at  $2 \text{ W/cm}^2$ . At that heat flux, the low flammability cable, having a value of SRAT of 600 (run 8) is a much lower smoking cable than the high-flammability one, having a value of 2400 (run 35). However, in runs 7 and 34, at the higher heat flux of  $6 \text{ W/cm}^2$ , the values are nearly the same for the low- and high-flammability cables, 4280 and 4430, respectively. A similar relationship is seen in runs 5, 6, 32, and 33; 10, 11, 37, and 38; 23, 24, 50, and 51; and 25, 26, 52, and 53. Thus, measurements made over a

wide range of heat fluxes give a more realistic picture of the smoke-generating properties of a cable and therefore provide a better basis for predicting its relative performance in a real fire than those made at a single, low heat flux.

In attempting to set flammability standards for cables, it must be recognized that the relating of test methods to real-fire situations is still to a large extent a matter of subjective judgement and "educated guesses." Using heat release data to model established test procedures such as vertical tray flame propagation tests<sup>10</sup> and the Steiner tunnel test<sup>5</sup>, or attempting to find a simple empirical correlation between rra data and the IEEE-383 test, as mentioned above, are probably constructive steps, in that the fire tests referred to have been widely accepted for some time. However, these approaches do not seem to make the best use of the potential of the release rate data. Another possible approach for setting cable flammability standards with the rra would be to use state-of-the-art cables as a norm. Heat release measurements would be made on the standard cable, and from these data, allowed maximum values for cables to be subjected to qualification tests would be established. These would be values of RHRAM and HRA5 (and/or other quantities taken from the heat release rate curves), that would be equal to, or less (more stringent) than, those of the norm. For example, if the low-flammability cables of the present study were the norm, then maximum values of HRA5 and RHRAM could be set at a single value or at several values of heat flux, based on curves like those of Figures 13 and 8. The requirements could be made more stringent simply by decreasing the allowed maximum values of HRA5 and RHRAM (and/or other heat release quantities) at the specified value or values of heat flux. The results of this study indicate that test results obtained on a cable of a given size and construction and made from a given combination of combustible materials could be applied to a range of cables of different sizes and configurations made from the same materials, with relatively small corrections being made for variations in cable diameter.

In attempting to set smoke standards for cables from release rate data, one can use a more quantitative approach, with less subjective judgement, than with flammability standards. This is because smoke generation is measured by light obscuration, which can be related more directly to real-fire situations. Simply stated, the laboratory data can be extrapolated in an approximately quantitative manner to a real fire, as on a ship, by comparing the surface area of cable involved in the fire, the volume of the space in which the smoke is dissipated, and the optical path through the smoke, between the laboratory and real-fire conditions. An estimate must be made of the expected heat-flux range in the real fire.

One final point that should be made is that for the Navy's purpose, the question of whether the rra can be used for setting smoke standards for shipboard cables may hinge on the sensitivity of the apparatus in measuring smoke; i.e., can the lowest smoke-generation values that will ultimately

be required in cables to solve the shipboard smoke problem be measured with the required accuracy in the release rate apparatus? DTNSRDC is now dealing with this question.

### Conclusions

1. The release rate apparatus is an operationally practical and convenient laboratory tool. Reproducibilities of rra measurements are comparable to those of other flammability and smoke tests in current use.

2. The Box-Behnken statistical plan is an effective method for providing a maximum of information from a given number of measurements. An important feature of the plan is its ability to measure interactive effects between independent variables. No such effects were found in this study. The results of the study suggest that this statistical strategy would be an excellent procedure for similar studies in the future, with either the rra or other fire test methods.

3. The study showed the effect of heat flux on heat and smoke release rates in the rra to be pronounced, as expected; of cable diameter, moderate; of the ratio of cross-sectional area of copper to total cable cross-sectional area, slight; and of cable spacing, not significant.

4. The study supports the concept that heat and smoke release rate measurements, made over a range of heat fluxes, provide a better basis for predicting relative performance of cables in a real fire than do test procedures that do not include controlled variations in heat flux.

5. A possible approach to setting flammability and smoke standards for cables using release rate data is suggested. It is noted that the potential application of the rra by the Navy for this purpose may hinge on the ability of the apparatus to measure low smoke release rates accurately.

### Abbreviations and Definitions

d	cable diameter (in)
h	heat flux - quantity of heat transmitted through a unit cross-sectional area or impinging on a unit surface area per unit of time (W/cm <sup>2</sup> )
heat release rate	the rate at which heat is emitted from a burning material (kW)
HRA5	total quantity of heat released per unit area of cable surface exposed to radiant heat in the first 5 minutes of a test run in the rra (MJ/m <sup>2</sup> )
HRAT	total quantity of heat released per unit area of cable surface exposed to radiant heat during a 30-minute test run in the rra (MJ/m <sup>2</sup> )

MJ/m <sup>2</sup>	megajoules per square meter (= 0.0113 X Btu/ft <sup>2</sup> )
NBS	National Bureau of Standards
OSU	Ohio State University
PVC	polyvinyl chloride
r	ratio of volume of copper to total cable volume in a given length of cable; equal to ratio of cross-sectional area of copper to cross-sectional area of cable (dimensionless)
RHRAM	maximum heat release rate per unit area of cable surface exposed to radiant heat during a 30-minute test run in the rra (kW/m <sup>2</sup> )
rra	release rate apparatus developed at Ohio State University
s	spacing between adjacent cables in rra or IEEE-383 test (fraction of the cable diameter)
smoke release rate	the rate at which smoke is emitted from a burning material (smoke units/min)
smoke unit	defined by the equation $D = k \times c \times L$ , where D is optical density (absorbance) (dimensionless); c is the smoke density; L is the length of the optical path (m); and k is the absorption coefficient. One smoke unit/m <sup>3</sup> is defined as the smoke density that will give a value of $D = 1$ , when $L = 1$ m and $k = 1$
SRA5	total quantity of smoke released per unit area of cable surface exposed to radiant heat during the first 5 minutes of a test run in the rra (smoke units/m <sup>2</sup> )
SRAT	total quantity of smoke released per unit area of cable surface exposed to radiant heat during a 30-minute test run in the rra (smoke units/m <sup>2</sup> )
SRRAM	maximum smoke release rate per unit area of cable surface exposed to radiant heat during a 30-minute run in the rra (smoke units/min-m <sup>2</sup> )

SRT/HRT ratio of total smoke to total heat released during a 30-minute test run in the rra (smoke units/MJ)

#### References

1. De Lucia, M.A., "Highly Fire-Retardant Navy Shipboard Cables," Proceedings of the 25th International Wire and Cable Symposium, Nov 1976
2. IEEE Standard 383, "IEEE Standard for Qualifying Class 1E Electric Cables and Field Splices for Nuclear Power Generating Stations," section 2.1.5
3. Smith, E.E., "Measurement of Heat, Smoke, and Toxic Gas Release", Fire Technology, Vol. 8, No. 3, Aug 1972
4. Gouldson, E.J., G.R. Woollerton, and J.A. Checkland, "Fire Hazard Evaluation of Cables and Materials", Proceedings of the 24th International Wire and Cable Symposium, Nov 1975
5. Gouldson, E.J., G.R. Woollerton, E.E. Smith and H.C. Hershey, "The Evaluation of Communications Cable Flammability Using the Release Rate Apparatus", Proceedings of the 26th International Wire and Cable Symposium, Nov 1977
6. Woollerton, G.R., "The Use of Release Rate Tests to Evaluate Flammability of Communications Cable," Journal of Fire and Flammability Vol. 9, Jul 1978
7. "Standard Method for Heat and Visible Smoke Release Rates for Materials and Products," proposed ASTM standard, ASTM Task Group E5.21.30
8. Box, G.E.P. and D.W. Behnken, "Some New Three-Level Designs for the Study of Quantitative Variables", Technometrics, Vol. 2, No. 4, Nov 1960
9. Abernathy, et al, "Handbook, Uncertainty in Gas Turbine Measurements", Arnold Engineering Development Center, technical report AEDC-TR-73-5, Feb 1973
10. Smith, E.E. and Woollerton, G.R., "Mathematical Model of Flame Spread through Grouped Vertical Cables Using Release Rate Data", Journal of Fire and Flammability, Vol. 12, Jan 1981, Table 3
11. Sparkes, C.J., J.J. Kracklauer, and R.E. Legg, "Interlaboratory Evaluation and Correlation Studies with the Arapahoe and NBS Smoke Chambers", Proceedings of the 26th International Wire and Cable Symposium, Nov 1977

#### Acknowledgements

The authors wish to thank the David Taylor Naval Ship Research and Development Center and the Naval Sea Systems Command for permission to publish the information presented here.



Walter Pocock  
Code 2713  
David Taylor Naval Ship  
R&D Center  
Annapolis, MD 21402

Walter Pocock received a bachelor's degree in chemical engineering from Johns Hopkins University in 1943 and a master's degree in chemistry from Columbia University in 1947. He is a registered professional engineer in Maryland. Since joining the Marine Engineering Laboratory (now DTNSRDC) in 1967, he has worked on various problems in the Navy's Deep Ocean Technology Program; on carbon brush wear problems, and, since 1980, on the ship-board cable fire problem.



John Geremia  
Mechanical Engineering  
Department, Mail Stop  
11C  
U.S. Naval Academy  
Annapolis, MD 21402

John Geremia received a B.S. in chemical engineering from Columbia University in 1961, and M.S. and Ph.D. degrees in mechanical engineering from Georgetown University in 1964 and 1970, respectively. He has served as a consultant to private industry and various government agencies in several fields, including fire safety. At present he is a member of the Mechanical Engineering faculty of the U.S. Naval Academy, where his duties include teaching and research.



# Circuit Transmission Integrity of Plenum Cables in a Developing Fire Scenario

C. J. Arroyo and T. P. Bursh

Bell Laboratories  
Norcross, Georgia

## ABSTRACT

This paper presents the preliminary results of a new test program designed to measure the circuit transmission integrity of various cable designs in a fire scenario. Cables are subjected to a novel yet simple circuit integrity measuring technique, while a localized heat source - simulating the intensity of a developing fire scenario - is applied to the cable. While this investigation only monitored changes in mutual and direct capacitance and capacitance-to-ground, other transmission parameters can be measured as well.

The importance of this new test method is that cables can be rapidly tested, analyzed and redesigned to withstand increasing fire intensities. Cables designed to withstand these extreme temperature environments should survive long enough to energize a fire alarm system, provide voice communication to various locations or effect an orderly shutdown of plant, as part of an energy and safety control PBX.

## INTRODUCTION

The circuit integrity of communication cables in a fire environment is of importance in hotels, commercial buildings, residences, nuclear power plants, ships, aircraft, mass transit systems or wherever individuals are in distress due to fire. One telephone systems manufacturer advertises<sup>1</sup> that, "A simple telephone call during hotel fires could save lives," but what if that call doesn't go through? In the past what have been described as circuit integrity tests<sup>2-5</sup> have, with few exceptions, been go-no/go type experiments that detect shorted circuits within a cable but do not assess the ability of a cable to perform its communication function during the time from initial fire exposure to the short circuit condition.

For example, a recent cable fire test was performed in a London Transport<sup>6</sup> disused tunnel (Figure 1). Circuit integrity (time to short circuit) of one heavily insulated and jacketed multi-pair cable was reported to be at least twenty minutes. It is not clear from this test what the optimum cable design materials should be for a particular fire scenario. It is clear

that a need exists for a laboratory test method that provides reproducible circuit integrity experiments to evaluate cable and wire materials designed to withstand high temperatures.

In this report the integrity of a circuit will be defined as the quality and/or state of maintaining a functioning electrical transmission network. Using this definition, 'circuit transmission integrity' of communication cables fails when intelligible communication ceases, i.e., when the cable fails to transmit intelligible signals.

## TEST PROCEDURE

To determine a test procedure three questions need to be addressed. How is circuit transmission integrity measured, what is an appropriate fire scenario, and what are the possible failure modes?

### A. Circuit Transmission Integrity Measurement

A literature search indicated that there does not exist a standard test that measures a cable or wire's circuit transmission integrity with temperature increase up to the point of material thermal degradation. Therefore, cables were placed inside the Radiant Heat Chamber (RHC)<sup>7</sup> and connected to measuring equipment that recorded changes in electrical transmission parameters with increasing temperature. The preliminary experiment described in this report measured mutual and direct capacitance and capacitance to ground for each cable pair. Capacitance was monitored because an increase in mutual capacitance with temperature increases the attenuation and degrades voice band transmission. More extensive measurements could have been performed but the rapid RHC thermal rise time and the number of pairs monitored put restrictions on the number of measured variables per test. Therefore one end of the cable was connected to an HP 4275A LCR Meter, a Model 6584-H Dual Programmable Twinaxial Switching System, and an HP 9845B computer. The other cable end was directed through the Radiant Heat Chamber and subjected to increasing temperatures monitored by a HP6940B Multiprogrammer. The instrumentation set-up (minus the HP6940B)<sup>8</sup> is shown pictorially in Figure 2.

POLYIMIDE HEAT BARRIER IMPROVES  
LONDON TRANSPORT SIGNAL CABLE



**FIGURE 1**

In a multipair cable, shown schematically in Figure 3, the two wires of a pair are surrounded by other pairs to form an electrostatic shield of effective diameter  $D$ . The shield in this case is neither solid nor perfectly cylindrical, but extensive research has shown that a pair in a multipair telephone cable closely approaches an ideal balanced shielded pair.

The mutual capacitance of an ideal balanced shielded pair can be obtained analytically in terms of pair geometry and the dielectric properties of the material with the rigorous mathematical expression:<sup>6</sup>

$$C_M = \frac{.01944 \epsilon}{\log_{10} \left( \frac{2S}{d} \right) \left[ \frac{1-(S/D)^2}{1+(S/D)^2} \right] - 0.1086 \delta_{12}} \mu F/mile \quad (1)$$

where  $S$ ,  $d$  and  $D$  are shown in Figure 3 and  $\delta_{12}$  is a function of  $S$ ,  $d$  and  $D$ . The effective dielectric constant  $\epsilon$  is not easily determined since it depends on the dielectric constants of both the insulating material and the air or filling compound present, which are themselves functions of frequency and temperature. For a given geometry:



**FIGURE 2. RADIANT HEAT CHAMBER - CIRCUIT (TRANSMISSION) INTEGRITY TEST APPARATUS**

$$C_M = K \epsilon$$

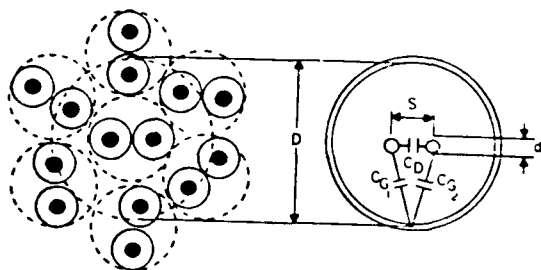
and

$$K = \frac{C_M}{\epsilon}$$

where K represents the geometric parameters found in Figure 3 and Equation 1.

(2)

Therefore, by monitoring the mutual capacitance,  $C_M$ , the behavior of the effective dielectric constant with increasing temperature can be monitored. This will be shown experimentally as cables insulated with materials having constant dielectric constant with increasing temperature exhibit a constant  $C_M$ , and cables insulated with materials having increasing dielectric constant for increasing



MULTIPAIR CABLE GEOMETRY  
FIGURE 3

temperatures exhibit increasing  $C_M$ . Also, the behavior of the geometry factor  $K$  will be demonstrated.

Cable transmission quality was not measured directly in this experiment since that parameter is dependent upon the particular transmission system applied to the cable. For our purposes, mutual capacitance was chosen as the measure of circuit transmission integrity since cable transmission can be expected to degrade as mutual capacitance increases.

#### B. Selection of a Fire Scenario

A fire scenario is defined as the staging of a fire test that simulates the intensity of a particular fire. Fire intensity is expressed in three modes: an incipient mode measures ease of ignition; a developing mode measures surface flammability; and a fully developed mode measures a structure's fire endurance.

In evaluating different cable fire tests it was determined that the Radiant Heat Chamber (RHC) functions in all three fire modes. First, in a steady state mode, cables tested in the RHC can be evaluated for ease of ignition or incipient stage. Second, in a transient mode the chamber subjects an individual cable to the intensity of a developing fire which measures a cable's surface flammability. In fact, the correlation between the RHC and the Steiner Tunnel UL 910 "Test Method for Fire and Smoke Characteristics of Cables," recognized as the standard measurement of cable surface flammability, has a coefficient of .78 for numerous cable designs evaluated at Bell Labs. Finally, the RHC can subject an individual cable to the same time vs. temperature curve as of a fully developed fire. It should be understood that a developed fire measures a structure's fire endurance and gives hourly ratings for the ability of components such as walls and floors to contain a fire. Cables are not evaluated in a fully developed fire mode such as the ASTM E119, "Fire Tests of Building Construction and Materials." Cables are only used when cable penetration fire stops are being rated as in IEEE 634, "Standard Cable Penetration Fire Stop Qualification Tests," since the cable's fuel load contributes to the time and intensity of the flashover condition. This conflagration type fire test rep-

resents a worst case condition, and cables are not presently designed nor expected to survive these conditions.

In our study, it was decided that the cables would be subjected to a developing fire scenario in the RHC which subjects a six inch length of cable to a temperature rate of rise of approximately 130°F/min. for 10 minutes. The results could then be correlated to a cable's performance in the UL 910 Steiner Tunnel test.

#### C. Possible Cable Failure Modes

As mentioned previously, one of the novel features of the circuit transmission integrity test is the concept of defining cable failure in terms of transmission parameters, e.g., mutual capacitance. As also mentioned, however, since the definition of transmission failure depends upon the transmission system in use, we have chosen not to define an arbitrary level of mutual capacitance increase as a failure criterion. Rather, we have chosen to monitor and record mutual capacitance until the point of a conventional conductor fault.

When cables are subjected to fire, only four internal conductor faults can occur, namely; ground, open, short or cross. Of the seven cables tested, only two had metallic sheath layers. Both of these used inorganic core wraps, which did not decompose under the temperature limits of the experiment. Therefore, a ground fault was unlikely, because conductors did not contact the metallic sheath layer. An open fault was not possible because test temperatures did not exceed 1300°F (copper melts at 1980°F), and visual inspection confirmed this. In this experiment only a short-between a pair's tip and ring - or a cross - contact with a conductor of another pair - are possible faults. Measurements to distinguish between a short or cross were not performed because the time of fault occurrence was of greater importance. However, in future tests resistance measurements can be performed to differentiate between these two faults.

#### CABLES TESTED

All cables tested were 25 pair, 24 AWG inside wiring or plenum cables. Cable samples were 7 feet long, although only 6" of the sample were within the RHC. Table 1 lists the cable type, jacket, shield, core wrap, insulation type, typical insulation dielectric constant, and fault initiation temperature (i.e., temperature at which discontinuity occurs). Of the five cables tested, cables 3 through 5 are UL classified plenum cables. The all PVC cable 1 is not permitted in plenum areas without metal conduits, so this cable represents the worst case. The experimental polyimide laminate cable 2 was tested solely for reference.

#### RESULTS

All electrical measurements were conducted at a frequency of 1 KHz. The results were plot-

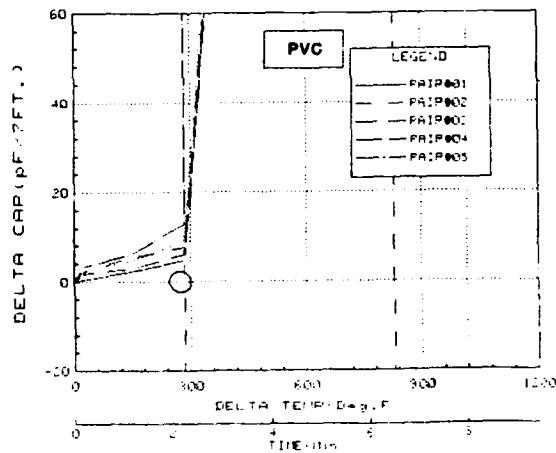
TABLE I

## Cable Constructions

Cable No.	Type	Jacket	Shield	Core Wrap	Insulation	Insulation Dielectric Constant* $\epsilon_i$	Initial Fault Temp. °F
1	All PVC Cable	PVC	-	-	PVC	3.8	285
2	Polyimide Laminate	Polyimide	1 mil Aluminum	60 mil Inorganic	PVC	3.8	540
3	Exp. Plenum Cable	Fluoropolymer	-	Compressible organic bound w/coated inorganic	PVC	3.8	360
4	B Plenum Cable	Polyimide	8 mil Aluminum	1 mil Polyimide 30 mil Glass	PVC	3.8	580
5	FEP	FEP	-	Coated inorganic	FEP	2.1	600

\*At room temperature.  
FEP - Fluorocarbon Resin

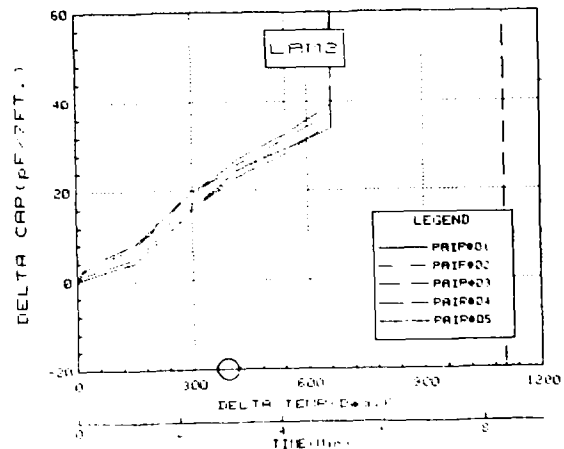
ted five pairs to a graph, as shown in Figure 4. (For each cable one typical five-pair graph will be shown.) The graphs plot each pair's increase in mutual capacitance,  $\Delta C_M$ , in pF/7 ft., versus increasing jacket temperature,  $\Delta T$ , in °F, and the elapsed time interval. Insulation temperatures measured in previous RHC reports<sup>7</sup> were not recorded because all conductors were being monitored for capacitance. However, from previous tests the softening or melt region of the particular insulation, at the corresponding jacket temperature, is represented by a circle on the abscissa. Faults are indicated by a discontinuity in the curve. Although all four component capacitances were measured for each cable, only  $C_M$  will be presented, as it will be shown (for B Plenum cable) that the components of  $C_M$  are related up until faults initiate.



$\Delta C_M$  VERSUS  $\Delta$ TEMPERATURE  
PVC CABLE  
FIGURE 4

A) PVC Cable - This cable consists of PVC jacket and insulation. Figure 4 shows the increase in  $C_M$  with increasing temperature up to the development of faults at 285°F and an average time of 2.25 minutes. At a rate of temperature rise of 130°F/minute, the PVC insulation doesn't exhibit a melt phase, but goes directly from a solid to a carbonaceous char.

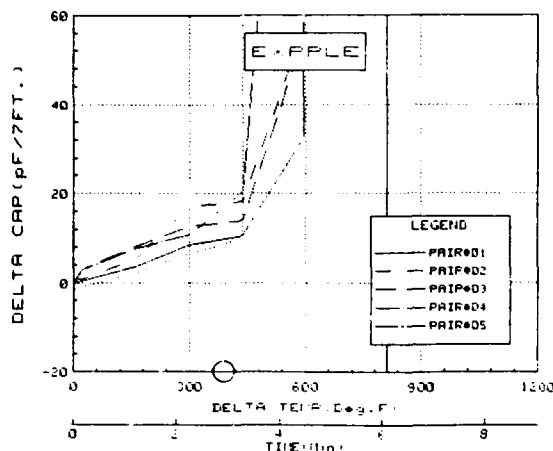
B) Experimental Polyimide Laminate Cable - This cable consists of a PVC insulated core, 60 mil inorganic core wrap, a helical wrap of 1 mil aluminum foil/1 mil polyimide laminate, and a helical outer 1 mil polyimide jacket. As seen in Figure 5 faults occur at a temperature of 540°F at an average time of 4.17 minutes. The  $C_M$  measurement beyond the melt region is a measure of the effects of the char formed around the conductors and the interaxial spacing. The uniformity of results is explained by a snug yet



$\Delta C_M$  VERSUS  $\Delta$ TEMPERATURE  
EXPERIMENTAL LAMINATE CABLE  
FIGURE 5

resilient core wrap that allows PVC char formation but restrains conductor movement due to charring. In other words, since the core geometry is restrained,  $K$  (equation 2) is held relatively constant and  $C_M$  increases with  $\epsilon$ . This point will be examined further in the case of B Plenum cable. This laminate cable design, by thermally protecting the PVC conductors, doubles the fault temperature/time occurrence as compared to the all PVC cable.

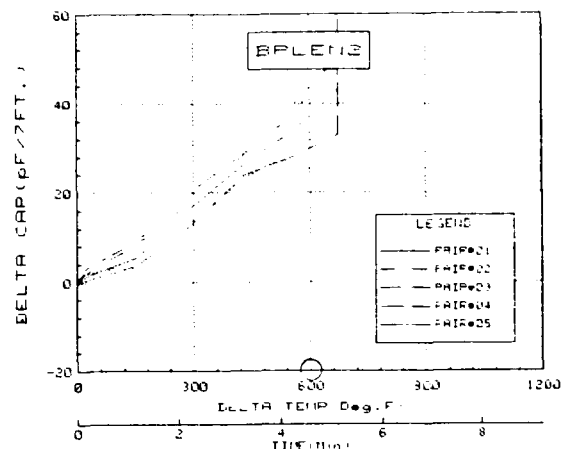
**C) Experimental Non-Shielded Plenum Cable - EXPPLE** - This cable consists of a PVC insulated core, a compressible organic core wrap bound with a coated inorganic wrap, and a fluoropolymer jacket. This design has passed the UL 910 cable fire test. As shown in Figure 6, faults



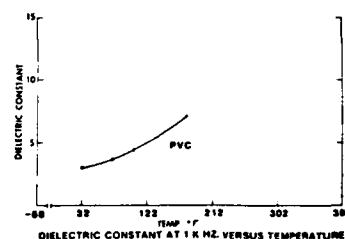
$\Delta C_M$  VERSUS  $\Delta$ TEMPERATURE  
EXPERIMENTAL NON-SHIELDED PLENUM CABLE  
FIGURE 6

develop at a temperature of 360°F around three minutes. Although this design is sufficiently low in smoke and flame spread to be classified by UL, it developed faults 100°F and one minute earlier than the previous laminated design which failed the UL test. Therefore, plenum cables which pass the UL 910 test should not be assumed to have superior circuit integrity. Redesigning and taking advantage of each cable's strengths would undoubtedly result in a better design.

**D) B Plenum Cable** - B Plenum cable consists of a PVC insulated core, 30 mil glass plus 1 mil polyimide tape core wrap, 8 mil corrugated wrap, 8 mil corrugated aluminum and double polyimide tape jacket. As shown in Figure 7A, B Plenum cable, UL classified for its fire and smoke resistant properties, shows better performance than the PVC and EXPPLE cables, but comparable results to the experimental laminate design (Figure 5). The difference between the B Plenum and the laminate design is in the metal thickness and 1 mil polyimide plus 30 mils inorganic core wrap. The initial temperature to fault was 580°F at about 4.75 minutes.



$\Delta C_M$  VERSUS  $\Delta$ TEMPERATURE



B PLENUM CABLE  
FIGURE 7A

At this point insulation dielectric constant vs. temperature curves (lower portion of Figure 7A) will be introduced to examine the relationship between mutual capacitance,  $C_M$ , and effective dielectric constant,  $\epsilon$ , introduced in equation 4. Figure 7A shows the rise in dielectric constant of PVC with temperature, similar to the rise in  $C_M$  of the four previous PVC insulated cables tested. It should be noted that the dielectric constant temperature range corresponds to the mutual capacitance temperature range up to the melt or softening point. Since present dielectric constant measuring techniques do not allow measuring above the polymer melting point, what is demonstrated in Figures 5 through 7A is the measurement of  $C_M$  which is a function of  $\epsilon$  (if  $K$  is constant), for these cables above the PVC melt region. This measuring ability will become more important when monitoring the next material.

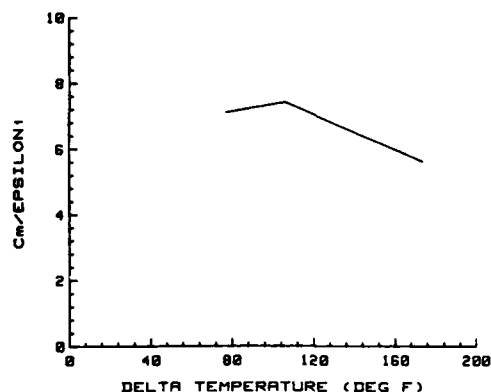
$C_M$  can also be used to determine the relative geometric changes during the test using equation (2) if one assumes

$$K = \frac{C_M}{\epsilon} \quad (2)$$

that the temperature dependence of the effective dielectric constant is identical to that of the insulation's dielectric constant,  $\epsilon_i$ .

By plotting  $C_M/\epsilon_i$  versus temperature in Figure 7B, the effects of material dielectric changes are normalized and the geometry factor K can be examined. Figure 7B shows an initial upward movement corresponding to a PVC softening phase where conductors could move closer together. The subsequent downward trajectory indicates conductors are moving further apart with increasing temperature, corresponding to the charring of PVC.

The ability to communicate via these cables was not measured in this test, however, it has been demonstrated that a rapid rise in temperature increases the cable's mutual capacitance. Since conductor resistance also increases with temperature, it can be shown that if conductor movement is minimal, degradation of voice band transmission occurs with increased attenuation.

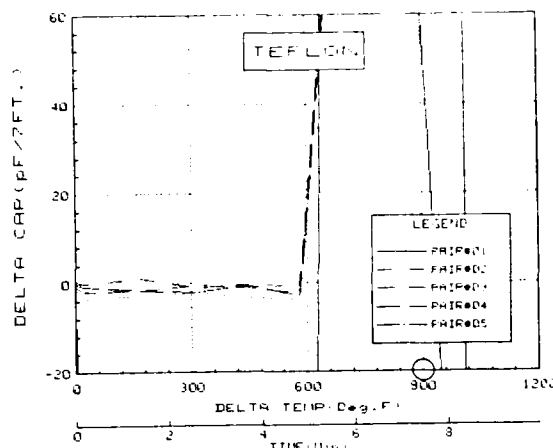


GEOMETRY FACTOR K vs DELTA TEMPERATURE FOR B PLENUM  
FIGURE 7B

NOTE: THIS CURVE IS TYPICAL OF ALL PVC INSULATED CABLES

E) FEP Plenum Cable consists of FEP insulated core and jacket with a coated inorganic core wrap. FEP conductors also exhibit stable  $C_M$  values in Figure 8 and a stable  $2.1 \epsilon_i$  value over a broad temperature range. FEP is the only cable material tested that, at elevated temperatures, remains molten until going into a gas phase in this simulated developing fire mode. The molten FEP insulation is retained within its core wrap. If this cable had a different core wrap, the FEP insulation would flow away from the conductors and faults would occur sooner. This construction illustrates the importance of core wraps in fire resistant cable design.

What is unusual is that faults occur at ~600°F jacket temperature before the insulation melts (487°F), which occurs when the jacket is at a temperature of 925°F, as indicated by the circle in Figure 8. One possible explanation is related to the fact that the cable ends are not restrained horizontally (see Figure 2). Therefore, as the FEP jacket melts, the weight of the cable outside the RHC applies a tensile and bending load on the cable core forcing the conductors within the RHC closer together.

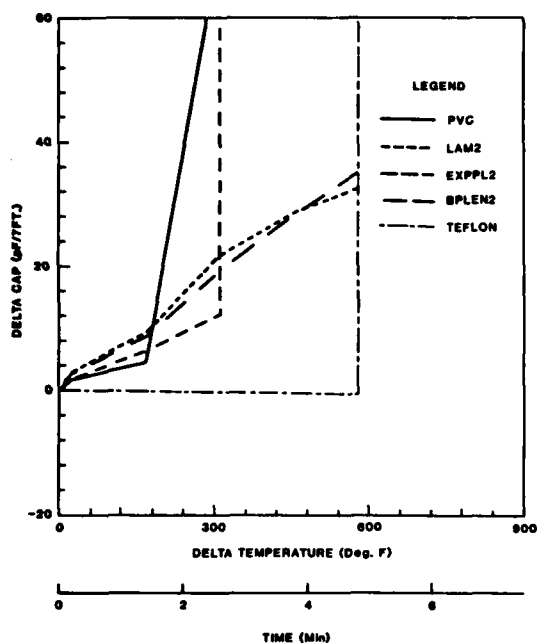


TEFLON CABLE  
FIGURE 8

Although all cables were similarly tested, this buckling effect in FEP is a phenomena not observed with the other cables tested. Apparently, the other tested materials remain structurally more rigid at elevated temperatures than FEP, which is the only high temperature material tested that melts instead of charring in a developing fire mode. Visual observations after UL910 tests agree with these observations. Although this might be considered a worst case condition, it indicates that the thermo-physical characteristics of fire resistant jackets, as well as their method of mounting or restraint, affect the performance of even the best dielectric insulating materials.

#### DISCUSSION OF TEST RESULTS

The higher temperatures required to develop faults in B Plenum cable as opposed to PVC cables are shown from average results of all 25 pair cables tested in Figure 9. This graph demonstrates the ability of extending a PVC cable's circuit transmission integrity an average of 300°F and 3.5 minutes in a developing fire scenario. This was possible by selecting thermal barriers in the form of high temperature jackets, core wraps and a metallic shield over PVC insulated conductors. The difference between the laminated (Lam 2) polyimide cable and the experimental (EXPPLE) plenum design demonstrates that cables which pass the UL910 test with low smoke and flame spread do not guarantee superior circuit transmission integrity performance.



AVERAGE RESULTS OF ALL 25 PAIRS FOR EACH CABLE TESTED  
FIGURE 9

#### DISCUSSION AND CONCLUSION

It should be emphasized that this test method has been designed to duplicate a developing fire scenario where, for example, flames have spread to the ceiling, broken through a ceiling tile, and impinge directly on a cable. If structural support members collapse, cable movement is expected and faults would occur sooner. However, a structural collapse implies a flashover condition and, as described earlier, cables are neither designed nor expected to be functional under such conditions.

A novel Radiant Heat Chamber-Circuit Transmission Integrity test has been designed that measures a cable's change in capacitance vs. temperature rise in a developing fire scenario. Although this report only measured capacitance, the other primary constants, resistance, inductance, and conductance can be measured. It is believed that this is the first thermal-dielectric failure mechanism test of wire insulation to measure and analyze cable transmission performance in a controlled fire scenario. Cables designed to withstand these extreme environments could survive long enough to energize a fire alarm system, provide voice communication to various locations and/or effect an orderly shutdown of a plant as part of an energy and safety control PBX.

#### ACKNOWLEDGEMENTS

The authors wish to express appreciation for the contributions made by D. P. Woodard, Jr., N. J. Cogelia, J. T. Loadholt, and especially W. C. Reed in the preparation of this paper.

#### REFERENCES

1. "A Simple Telephone Call During Hotel Fires Could Save Lives," S. T. Churchill, Total Systems, Inc. Telephony Journal, April 12, 1982.
2. "Fire Damage Data Analysis as Related to Current Testing Practices for Nuclear Power Applications," J. Klevan, et. al., Brookhaven National Laboratory, Upton, N.Y., October, 1977.
3. "Performance of Fluoropolymer Wire and Cable Insulation in Large Scale Tests for Flammability, Smoke, Corrosive Off-Gases and Circuit Integrity," E. W. Fasig, et. al., 26th International Wire and Cable Symposium, Cherry Hill, N.J., November, 1977.
4. "The Evaluation of Communication Cable Flammability Using the Release Rate Apparatus," E. J. Gouldson, et. al., 26th International Wire and Cable Symposium, Cherry Hill, N.J., November, 1977.
5. "A Study of Damagability of Electrical Cables in Simulated Fire Environments," EPRI NP-1767, Prepared by Factory Mutual Research Corp., March 1981.
6. "Polyimide Heat Barrier," Rubber and Plastic Fire and Flammability Bulletin, June/July 1982.
7. "Thermal Behavior of Experimental Plenum Cable Sheaths Determined in a Radiant Heat Chamber," C. J. Arroyo, N. J. Cogelia, R. J. Darsey, 30th International Wire and Cable Symposium, Cherry Hill, N.J.
8. "Shielded Pair of Wires," E. I. Green, H. E. Curtis and S. P. Mead, U.S. Patent No. 2,034,032, March 17, 1936.



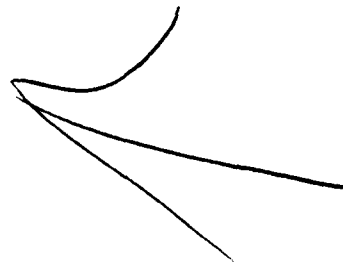
Talmage P. Bursh  
Bell Laboratories  
Norcross, GA 30071

Talmage P. Bursh is a member of Technical Staff at Bell Laboratories in Norcross, Georgia. His current assignment in the Lightguide Applications and Systems Group involves the engineering of loop feeder lightguide. Previous assignments have included transmission media characterization and shielding effectiveness measurements. He received his B.S.E.E. from Southern University and M.S.E.E. from Georgia Institute of Technology and he is a member of I.E.E.E. and Eta Kappa Nu.



C. John Arroyo  
Bell Laboratories  
Norcross, Ga. 30071

C. John Arroyo joined Bell Laboratories in 1969 after receiving his A.A.S. Degree in Mechanical Technology from New York City Community College. Since 1972 he has worked in Fire Research Technology and is presently a member of the Wire Media Group engaged in fire resistant cable concepts.



## LARGE SCALE FIRE TEST OF CABLE INSTALLED IN TUNNELS

H. Ishihara, M. Miwa, K. Kuratani, J. Sawada

Nippon Telegraph & Telephone Public Corp.  
Tokyo, JapanAbstract

A fire prevention system for telephone exchange offices in the case of tunnel accidents is presented.

Cables installed in tunnels have the potential of spreading fire from tunnels to buildings when a fire breaks out. In order to reduce this possibility, the Fire Service Law requires that cables installed in tunnels have sufficient fire resistance to prevent them from spreading fire from tunnels to buildings.

Fire tests are conducted as the initial task in developing a test method for determining structural details. These tests provide data on the flame propagation characteristics of tunnel cables in a simulated fireproof wall between tunnels and buildings. Fireproof wall design is based on information obtained from field surveys. Newly developed systems have already been introduced in telephone exchange offices, which have required fireproof walls to protect against fire spreading.

1. Introduction

NTT has already constructed about 300 kms of cable tunnels. Cables installed in tunnels have the potential to spread fire from tunnels to buildings in the case of tunnel accidents. The Fire Service Law requires that cables installed in tunnels have sufficient fire resistance to prevent burning from spreading from tunnels to buildings.

In NTT, a fire experienced at the Asahikawa-Toko Local Office was caused by cables installed in a tunnel catching fire. We have also heard about similar problem at the New York Telephone Company's Second Avenue Switching Center.

In order to solve this problem, those cable tunnels are systematically managed and they are constantly monitored by electronic sensors. Such fire prevention systems include;

- 1) Fireproof wall.
- 2) Fire resistant cables used between sensors and equipments.
- 3) Speakers and guidance lamps for emergency exit.

- 4) Fire sensors and combustible gas sensors.

Especially, the following factors about fireproof wall are considered.<sup>2)</sup>

- a) Sufficiently fire-resistant cables to prevent fire from spreading through the holes of fireproof walls.
- b) Sufficiently air-tightness to confine fire in a cable riser space.
- c) Sufficiently flexibility to meet cable installation and removal requirements (adopting fireproof blocks made of ceramic fiber with a rack frame structure).

Fire tests were conducted as the initial task in developing a test method for determining structure details. Using a large ignition source, the burning of combustibles within a fireproof wall without fire stops was simulated. It was found that some types have the potential of spreading fire from tunnels to buildings, where others employing newer fire-resistant materials did not show the same propensity to propagate fire. Furthermore, the new system completely satisfied the requirements for fire-resistance and air-tightness.

This paper presents an explanation of the fireproof wall characteristics and fire tests.

2. Purposes and Requirements of Fireproof Wall

Fireproof walls, a component of the fire prevention system in cable tunnels as shown in Fig.1, are partitions which have sufficient protection against fire. Fireproof walls have the following two purposes.

- 1) To prevent fires in cable tunnels from spreading to offices.
- 2) To improve the efficiency of the halon gas extinguisher system in the cable riser space.

The requirements to satisfy these purposes are as follows.

- 1) Sufficient fireproof property to prevent fire in the cable tunnel from entering the telephone office.
- 2) Sufficient air-tightness to prevent halon gas from spreading to the cable tunnel.

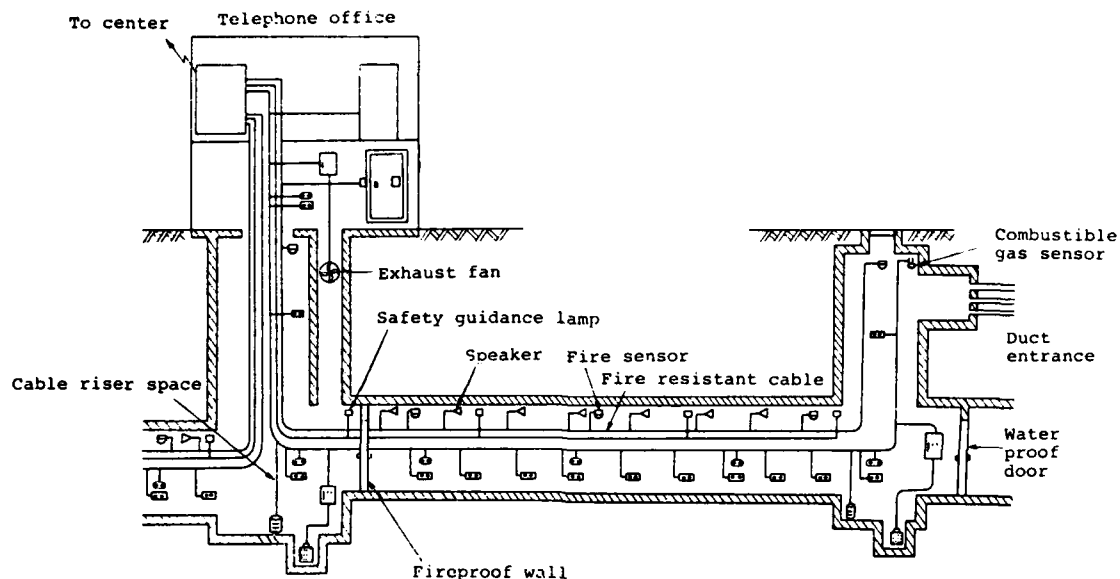


Fig.1 Fire prevention system in cable tunnel

- 3) Sufficient flexibility to meet cable installation and removal requirements.
- 4) Sufficient anti-corrosion to prevent long term deterioration in performance in the cable tunnel.

### 3. Fireproof Wall Structure

#### 3.1 Outline

The fireproof wall consists of three parts; (1) the cable entry area, (2) the door and (3) the wall as shown in Fig.2. The cable entry area is the most important.

As a result of investigation to determine the best structure, taking the necessary fireproof wall conditions into consideration, mainly fire prevention and easy construction, the best structure is that of setting up fireproof blocks on a shelf. An outline and the purpose of the equipment, which is used in the cable entry area, is shown in Fig.3. Photo.1 shows the situation of the fireproof wall.



Photo.1 Situation of fireproof wall

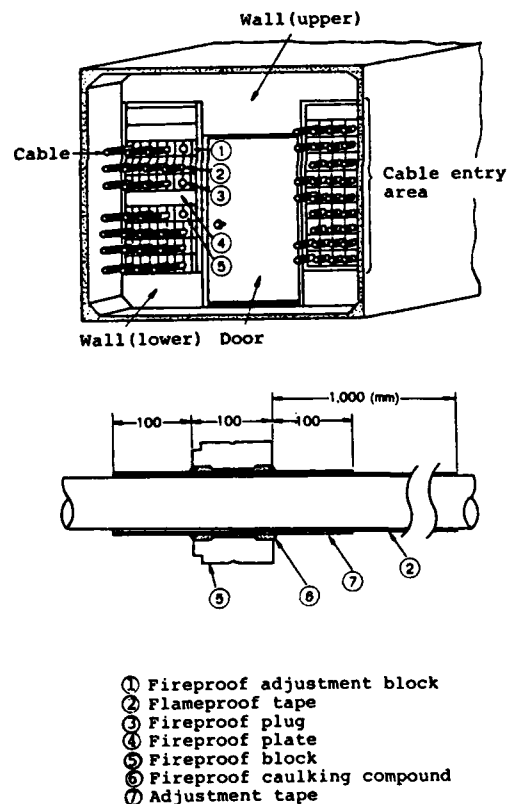
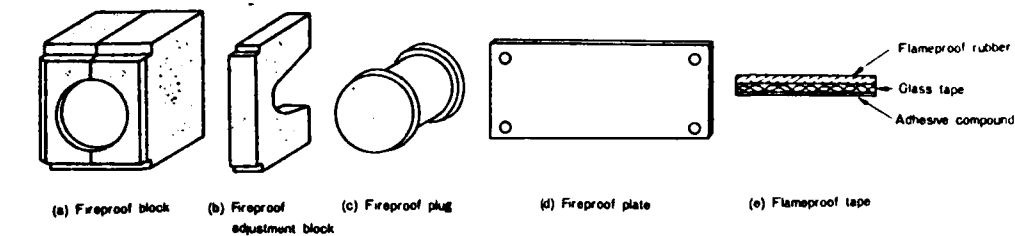


Fig.2 Fireproof wall outline



Name	Main Material	Purpose
(a) Fireproof block	<ul style="list-style-type: none"> <li>• Ceramic fiber</li> <li>• Aluminum cement</li> <li>• Silica etc.</li> </ul>	<ul style="list-style-type: none"> <li>• To hold the cables</li> <li>• To maintain fireproofness</li> </ul>
(b) Fireproof adjustment block		<ul style="list-style-type: none"> <li>• To adjust the space in the rack frame</li> </ul>
(c) Fireproof plug		<ul style="list-style-type: none"> <li>• To block the cable hole in a fireproof block</li> </ul>
(d) Fireproof plate	<ul style="list-style-type: none"> <li>• Steel plate</li> </ul>	<ul style="list-style-type: none"> <li>• To block the space in the rack frame when no cables are installed</li> </ul>
(e) Flameproof tape	<ul style="list-style-type: none"> <li>• Glass tape</li> <li>• Flameproof rubber etc.</li> </ul>	<ul style="list-style-type: none"> <li>• To prevent cables fire caused by radiant heat from the steel plate</li> </ul>

Fig.3 Equipment outline used in the cable entry area

### 3.2 Inquiry of Fireproof Structure in Cable Entry Area

To decide the best structure of cable entry area, NTT has investigated the various method. Various kinds of structures had been investigated as shown in Fig.4.

- 1) (Reinforced concrete wall + mortar)-structure.
- 2) (Fireproof plates + caulking)-structure.
- 3) (Flameproof material + steel plates)-structure.
- 4) (Spinkler + steel plates)-structure.
- 5) (Fireproof blocks + rack frame)-structure.

NTT has estimated fireproof, air-tightness, anti-corrosion and flexibility to meet cables. Consequently, NTT has confirmed that (fireproof blocks + rack frame)-structure is the most suitable.

### 3.3 Inquiry of Fireproof Block

The fireproof blocks must meet the following basic requirements.

- 1) Fireproof property enough to endure 2-hour heat (1010°C°).
- 2) Sufficient strength to support and handle cables.
- 3) Sufficient waterproofing (durability).
- 4) Economy.
- 5) Sufficient workability.

Concerning the fireproof, 2-hour heat test, the most suitable material for fireproof blocks is not metal and plastic, but ceramic.

Ceramics are classified according to fiber structure and granular structure. Fig.5 indicates the useful temperature ranges of various ceramics. As a result, NTT confirmed that the optimum material

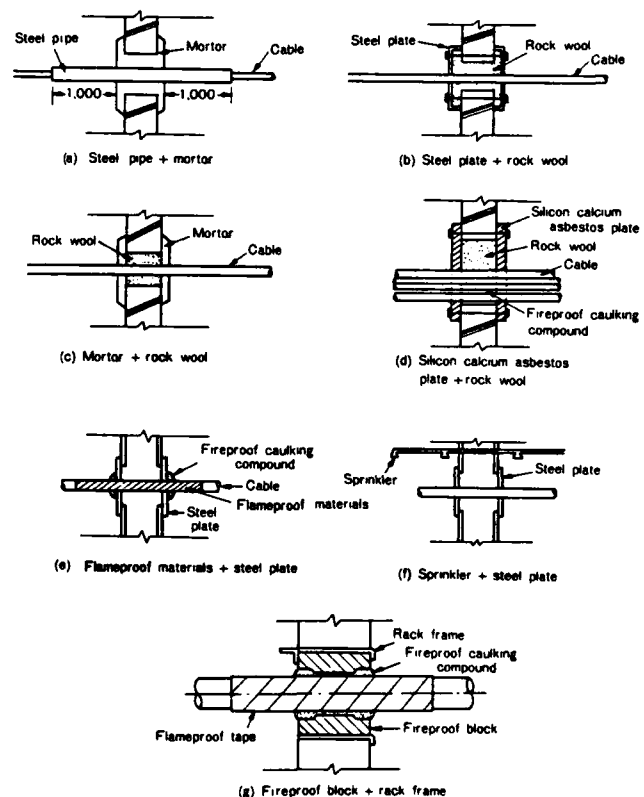


Fig.4 Various fireproof structures in cable entry area

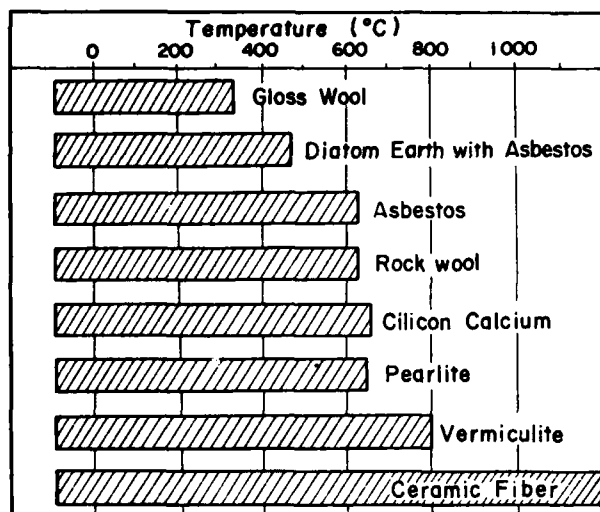


Fig.5 Useful temperature ranges of various ceramics

consists of ceramic fiber with organic and inorganic binders. The fireproof block thickness (10cm) is adopted to suppress the surface temperature to lower than 260°C by results of fireproof tests as shown in Fig.6.

\* NTT has adopted 2-hour heat fireproofing as prescribed in Japan Industrial Standard (JIS) A 1304. This is based on critical results of fire tests in cable tunnels.

### 3.4 Flameproof Tape

At NTT, most cables in the cable tunnels are sheathed by polyethylene. Consequently, even if a fire in the cable tunnel is contained by the fireproof wall, cables in the riser space have a possibility of catching fire given the high atmosphere temperature, cable droop and distension.

Cable droop occurs because the fire in the cable tunnel increases the radiant heat through the fireproof wall causing the cable to sag and allowing fire to spread through the fireproof block.

Cable distension, which has been confirmed by fire tests as shown in Fig.7 and Photo.2, occurs as follows;

- 1) The cable surface temperature in the cable riser space increases due to the radiant heat and heat conduction.
- 2) Combustible gas is generated in the cable from polyethylene, then distends the cable sheath.

3) Under critical conditions, the cable might burst and gas might spread.

Therefore, NTT has adopted flameproof tape which provides flameproofing and additional strength. However, it takes much time to apply the tape, especially in existing cable tunnels, and the cost for tape adoption has been carefully considered.

## 4. Results

In order to investigate characteristics of the fireproof wall, several tests were conducted at the Tsukuba Telecommunication Construction Engineering Center and the Japan Testing Center for Construction Materials.

### 4.1 Fire Test in the Cable Tunnel Model

To confirm the characteristics of cable fires, fire tests with the flameproof tape were conducted with the system as shown in Fig.7. The inside of cable tunnel during fire tests is as shown in Photo.2, and the results are shown in Fig.8.

These results show that the temperature in the cable tunnel can reach a maximum value of about 900°C and that more

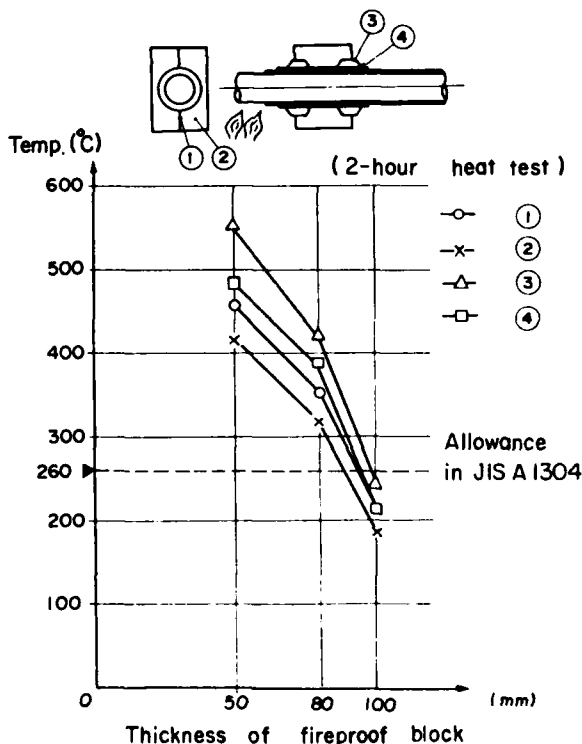


Fig.6 The correlation between temperature and thickness

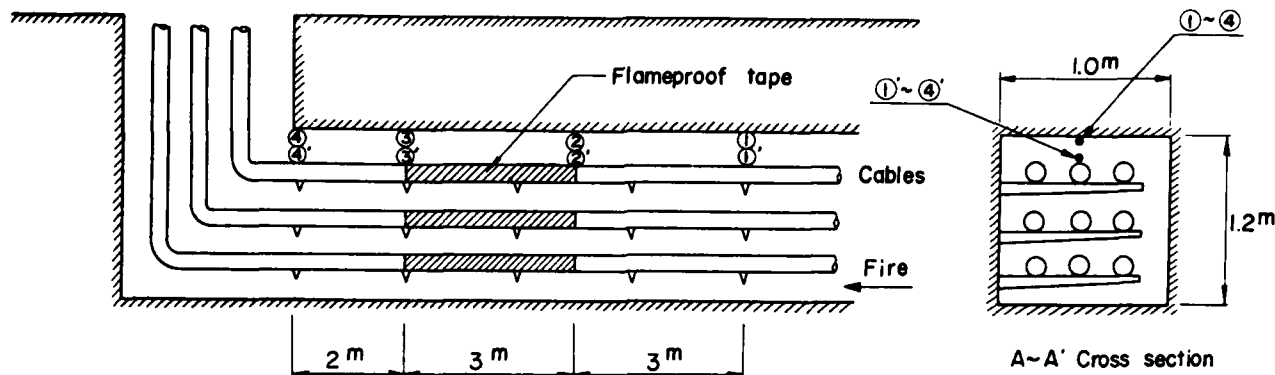
than 3m of flameproof tape can be useful for fire prevention in the cable tunnel under windless condition. However, tape construction cost is high, and in the case of an actual fire, strong winds from heat convection might occur. Therefore, NTT has minimized the use of flameproof tape and utilized it only as one aspect of the total fire prevention system in the cable tunnel.

#### 4.2 Fireproofing Test

The fireproofing test on the cable en-

try area was conducted using a twelve piece of cable fixed model. Test results showed that fire did not spread from one side of the model to the other after several 2-hour heat tests.

On the other hand, the radiant heat from steel doors and walls was a very large factor. Total fireproofing tests were performed at the Japan Testing Center for Construction Material, using a model whose size is the full scale square cable tunnel No.2 (2,450mm width  $\times$  2,250mm height) with forty cables in the cable



○ : Measured point

Fig.7 Fire test facility - simulated cable tunnel



Photo.2 The inside of cable tunnel during a fire test

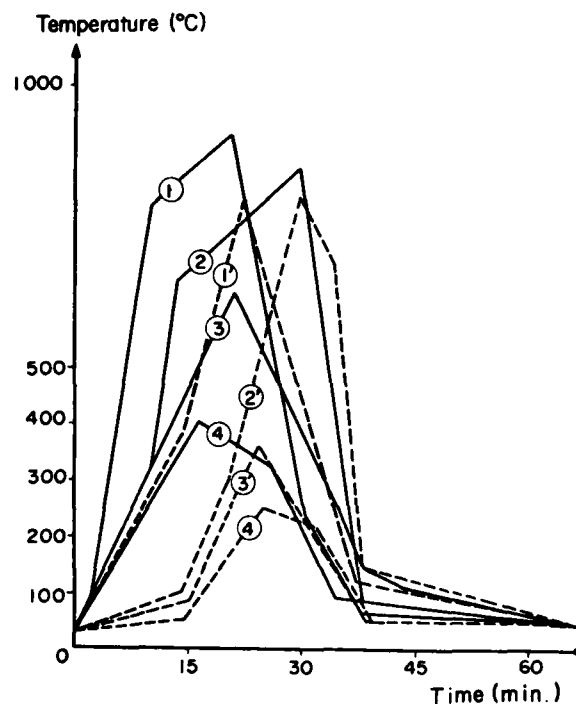


Fig.8 Variations of temperature - flameproof tape

entry area. Each cable was wrapped by flameproof tape. The test results are shown in Fig.9 and Fig.10 and the facility simulated fireproof wall is shown in Photo.3. Although the atmosphere temperature and the cable surface temperature increased due to radiant heat from the steel, fire did not spread from one side to the other through the fireproof wall during the 2-hour heat test. Judging from the results, NTT confirmed that the fireproof wall had sufficient fireproofing properties.

#### 4.3 Air-Tightness Test

Air leakage value through the fireproof wall (2,450mm width  $\times$  2,250mm height) was  $1.52\text{m}^3/\text{m}^2\cdot\text{min}$  at 2mm Aq. ( $0.35\text{m}^3/\text{m}^2\cdot\text{min}$  through the door plus  $1.17\text{m}^3/\text{m}^2\cdot\text{min}$  through the cable entry area). The air-tightness



Photo.3 Fire test facility - simulated fireproof wall

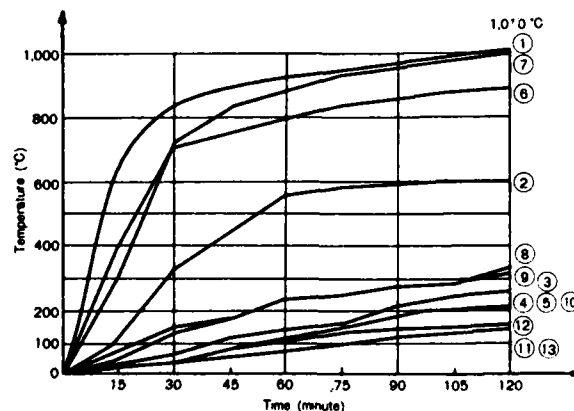
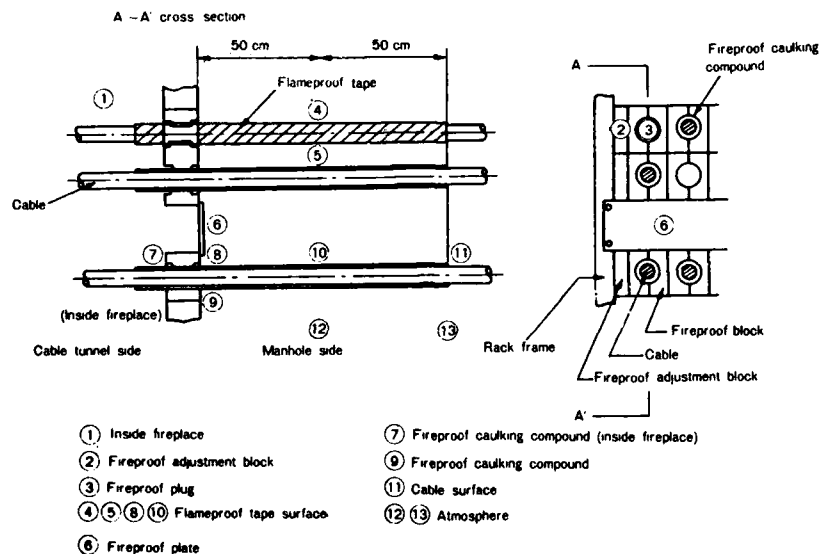


Fig.9 Variations of temperature - fireproof wall

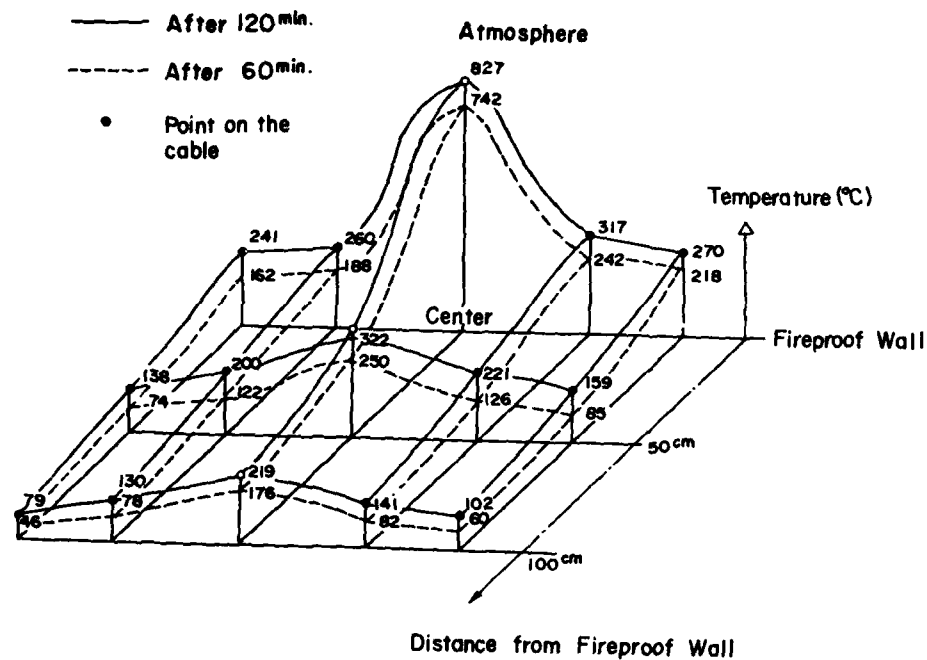


Fig.10 Temperature distribution

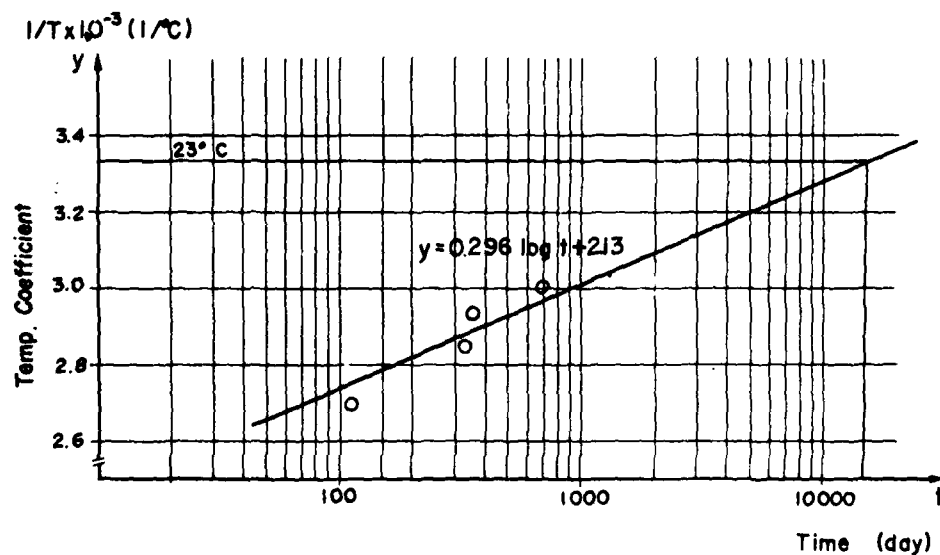


Fig.11 Accelerated durability test results

test results satisfied the standard air leakage value from a dampa—less than  $5\text{m}^3/\text{m}^2\cdot\text{min}$  at  $2\text{mm Aq}$ —as prescribed in the public notice from Japan's Ministry of Construction.

- 2) M.Miwa, M.Fukushika and J.Sawada, "Fire Wall in Cable Tunnel", J.T.R., vol 24, No1, 1982.

#### 4.4 Durability Test

It was confirmed that fireproof block qualities, such as its shape, strength and waterproofness, did not deteriorate after being immersed in sea water or water which contained cement.

With respect to flameproof tape, the life was estimated by accelerated durability tests. Tests were conducted under the condition of 100% moisture at  $60^\circ\text{C}$ ,  $70^\circ\text{C}$ ,  $80^\circ\text{C}$  and  $90^\circ\text{C}$ . The time at which the tensile strength of tapes became  $10\text{kgf}/\text{cm}$  was applied to estimate the life with an Arrhenius-plot. Fig.11 shows the result of life estimation and the useful flame-tape life is confirmed to be about 36 years under conditions of 100% moisture at  $23^\circ\text{C}$ .

#### 4.5 Cable Installation and Removal

The fireproof wall adopts the bolt connection construction method in order to facilitate cable installation and removal. Practically workability tests confirmed that the structure had no construction problems.

### 5. Conclusion

Since 1978, NTT has investigated the use of fireproof walls as one component of total fire prevention systems in cable tunnels, and has performed several tests to confirm the characteristics of the fireproof walls. Test results showed that the fireproof wall was sufficiently fireproof and that it was suitable to protect exchange offices from fires. The fireproof wall was introduced in main telephone exchange offices after standardization in 1982.

### 6. Acknowledgment

The authors wish to thank the manufacturing people, the people in Tsukuba Telecommunication Construction Engineering Center and colleagues in NTT who have been associated with this development project.

### Reference

- 1) H. Takashima and T.Uenoya, "Cable Tunnel Management System" J.T.R., vol 23, No.4, 1981.



Hiroshi Ishihara  
Engineering Bureau,  
NTT  
1-6 Uchisaiwai-cho  
1-chome, Chiyoda-ku  
Tokyo; Japan 100

Mr. Ishihara, General Manager of Outside Plant Division, NTT's Engineering Bureau, is now engaged in developmental research planning on whole telecommunication outside plants, cables, telephone poles, pipes and so on.

He is a member of the Institute of Electronics & Communications of Japan.



Mitsuhiro Miwa  
Engineering Bureau,  
NTT  
1-6 Uchisaiwai-cho  
1-chome, Chiyoda-ku  
Tokyo; Japan 100

Mr. Miwa, Senior Staff Engineer of NTT's Engineering Bureau, is now engaged in developmental research on cable tunnels, manholes, pipes, vehicles and so on.

He is a member of the Japan Society of Civil Engineers.



Kouichi Kuratani  
Engineering Bureau,  
NTT  
1-6 Uchisaiwai-cho  
1-chome, Chiyoda-ku  
Tokyo; Japan 100

Mr. Kuratani, Staff Engineer of NTT's Engineering Bureau, is now engaged in developmental research on cable tunnels, manholes, pipes, vehicles and so on.

He is a member of the Japan Society of Civil Engineers.



Jun Sawada  
Engineering Bureau,  
NTT  
1-6 Uchisaiwai-cho  
1-chome, Chiyoda-ku  
Tokyo; Japan 100

Mr. Sawada, Engineer of NTT's Engineering Bureau, is now engaged in developmental research on cable tunnels, manholes, pipes, vehicles and so on.

He is a member of the Japan Society of Civil Engineers.



## OVERALL FIRE SAFETY OF CABLE AND WIRING MATERIALS: PART I

Frederic B. Clarke, III, Irwin A. Benjamin and Philip J. DiNenno

Benjamin/Clarke Associates, Inc. of Kensington, Maryland

Small-scale tests for flammability are inadequate to predict fire performance in full-scale fires. Ignition resistance and flame spread measured by existing standard tests must be supplemented if overall cable fire hazard is to be assessed. Additional relevant data are provided by determining material behavior at elevated heat flux levels typical of those expected in room fires. In addition, computer-based room fire models are used to predict the full-scale conditions which cable materials may experience. This information can then be combined to provide a quantitative estimate of the contribution of cable materials to overall fire hazard. Hazard aspects include circuit integrity, structural fire spread, smoke generation and smoke toxicity.

BACKGROUNDINTRODUCTION

Despite tremendous advances made in polymer technology the fire performance of synthetic materials remains a source of concern to producers and users alike. In part, this concern springs from the chemical nature of most synthetics: carbon-based and combustible. The problem has been made more acute, moreover, by the fact that the design of relevant fire test procedures has, until recently, been almost totally empirical. In the 1970's, the entire field of fire testing received renewed regulatory and technical scrutiny, because of increased recognition that laboratory-scale tests often failed to predict the level of hazard in real fires.

Many commonly-used fire tests were developed before many of the subtleties of the fire problem were appreciated;

it is thus no surprise that the data they provide is often a poor match with what is needed. Tests were designed to mimic an envisioned set of fire conditions. When actual conditions differ from those of the test it is often difficult to predict performance. This discrepancy prompted investigators to focus on the environment in which a material was burning as well as on the material itself. Radiative heat transfer, the fluid mechanics associated with room fires and smoke behavior are some of the aspects of fire behavior which must be considered in addition to material flammability measurements. In addition, for life safety considerations the toxicity of the smoke may also be important.

The purpose of this paper is to examine how some of these parameters influence the outcome of cable fires. At the same time, it will become apparent that the relationship between fire phenomena is complex, and an overall estimate of hazard cannot be made by evaluation of test data alone.

GENERAL THEORY

Although wire and cable constructions may vary considerably, once they are involved in a fire the mechanics of the flaming process are the same. The actual combustion zone lies above the surface of the cable insulation, where fuel vapors, driven from the combustible substrate by heat radiated from the flame, combine with oxygen. In the intuitively obvious case, a fire can sustain itself only if the portion of the energy liberated in the flame which is returned to the fuel bed generates an equivalent amount of fuel vapor. Otherwise,

the fire will go out, sooner or later. However, if the solid fuel receives heat from some external source, the amount required from the flame is less, and stable burning can occur with less energy demands on the flame. This fact explains why a fire, once ignited, may go out if it is in a large room, yet burn vigorously if it is in a small one. The smaller room captures and returns a greater fraction of the fire's heat to the sample surface, and this dividend in energy feedback allows steady-state burning to occur.

The same principles apply to ignition. Ignition can occur only after the sample surface is hot enough so that the rate of fuel vapor production is sufficient to generate a combustible mixture of fuel and air above the surface. Thus, the minimum rate of energy transfer to the surface which will result in sustained ignition is one which will raise the temperature to the necessary fuel vapor production rate. If increasing amounts of energy are supplied to the surface beyond the minimum needed, the surface temperature will increase only slightly; most of the additional energy supplied is carried away from the surface by a increase in the amount of fuel being vaporized. The situation is analogous to the melting of an ice cube with a sun lamp: turning up the power of the lamp does not raise the surface temperature of the ice but merely causes more ice to melt per unit time.

This fact is important in trying to predict what will occur when a material is exposed to fire when the only information available is how readily the material will ignite. Figure 1 shows the burning rate per unit area, measured by rate of heat release, as a function of radiant energy supplied to the surface from an external source for a series of synthetic materials. Note that the ranking of materials at 1 watt/cm<sup>2</sup> is not the same as that for 4 watt/cm<sup>2</sup>. Common organic materials ignite at radiant energy levels near 2 watt/cm<sup>2</sup> while thermal exposures in a developing room fire can exceed 6 watt/cm<sup>2</sup> on the floor and walls, and in excess of 12 watt/cm<sup>2</sup> near the ceiling. Hence, measurements at more than one flux level may be appropriate, depending on the use for which the material envisioned.

## FIRE HAZARD ANALYSIS

### CABLE FIRE SCENARIOS

The use of a material, and the foreseeable circumstances of its fire involvement, constitute the fire scenarios relevant to a particular application. While there are in general thousands of conceivable fire scenarios, those important in wire and cable applications are but a small subset of the total. For example, resistance to ignition by a dropped cigarette, an extremely important fire property for mattresses and upholstered furniture, is but of relatively little interest in most cable applications. One would expect commonly-used insulation constructions to perform well in such a scenario.

For the purpose of this discussion, it is assumed that existing cable insulation/jacketing constructions have been designed to resist ignition from a small source, such as a match or bunsen burner. However, the previous section should have demonstrated that such performance provides very little information on how a material will behave on exposure to higher heat flux. As was pointed out, energy can be imposed on a cable array in substantial quantities from a fire burning in the same room, even if the fire and the target are well-separated. This is due to the fact that a layer of hot fire gases forms below the ceiling and above the fire plume. The depth of the layer, and to some extent its temperature, are determined by the fire size and the geometry of the vents through which the fire receives air and exhausts smoke. It is radiation from the hot layer, rather than from the fire plume, which dominates heat transfer in the room. Figure 2 illustrates this state of affairs. Cold air enters the room mass flow rate,  $\dot{m}$ , is entrained in the fire plume, and becomes part of the hot gas layer. The depth and temperature of the hot layer,  $z$ , are essentially the same throughout. Most of the heat felt by the target is due to  $q$ , the radiant flux from the hot layer, rather than from the flame. It is instructive to determine the size

of fire needed before  $\dot{q}$  becomes sufficiently large that ignition of remote objects is possible.

Figure 3 shows the radiant flux to the floor as a function of fire size (kW) for a 10 x 15 x 8 ft room with a standard doorway, and gypsum board walls (1). In order to provide some perspective, typical heat outputs of several different kinds of fires are shown on the curve. A burning trash barrel, typically a fire of about 150 kW, provides only a few hundredths watt/cm<sup>2</sup>. However, a 2-ft diameter pool of burning gasoline or fuel oil, produces heat at the rate of 1 megawatt in a room of this size. Such heat output provides an appreciable radiant flux to the floor. Thus, it is appropriate to inquire into the behavior of cable under conditions of relatively high radiant flux. If fuel spills, or alternatively the advent of some other large fire, can be envisioned.

#### CABLE FIRE PROPERTIES

There are several recognized fire tests for cable construction, two of the best known being IEEE 383 and UL 910. Both of these test expose cables to relatively severe fire conditions, but in neither case is the dynamic thermal environment easy to characterize under test conditions. At Factory Mutual Research Corporation, Dr. Tewarson has designed an apparatus which can provide a wide range of imposed radiant flux (2). Ignition properties, heat release and mass loss data can then be determined as functions of imposed flux, and this permits one to carry out the kind of analysis discussed here.

For example, Tewarson has determined the imposed flux necessary to ignite various cable constructions under piloted ignition conditions (3). Piloted ignition is where a spark igniter or small flame is placed close to the surface. Ignition will generally occur at lower fluxes for piloted ignition than for unpiloted, simply because the energy to heat the combustion gases to ignition is supplied by another source instead of the imposed flux. The data obtained are shown in Table 1. As can be seen, different cable materials show a substantial difference in ignition propensity. In spite of this, all of the cable samples tested pass IEEE 383.

The question to be answered then is whether differences in performance in the Factory Mutual test portend any differences in actual fires.

#### FIRE HAZARD ANALYSIS OF CABLES

A complete examination of cable fire hazard proceeds in the following steps:

1. Identification of relevant scenarios leading to fire involvement of cables;
2. Characterizing quantitatively the thermal conditions of cable exposure, the flow of combustion gases out of the fire compartment and the movement of smoke through other parts of the building;
3. Determining the cable's contribution to the growth of the fire and the composition of the smoke;
4. Evaluating the effects of cable involvement on continued operation of electrical systems, building fire resistance and life safety.

In this paper, attention will be limited to the scenario previously discussed -- the development of a fire which does not initially start in the cable, but which offers the possibility of secondary cable involvement. Until recently, the only way to determine the thermal conditions of such a fire would have been by actual measurements. However, high-quality mathematical models are now available which permit a relatively accurate estimate of such conditions if the characteristics of the burning fuel and the room are known. The model used in this study is a modification of one developed by Emmons and his associates at Harvard (4). The model provides a relatively complete mathematical description of the time history of temperature, ventilation flows, radiant flux and energy output throughout the room. It is computationally complex, requiring a relatively large computer to

carry out calculations in a conveniently short time period. The computer employer was a HP-9000 system which expanded disk capability.

The fuel chosen was a slab of polyurethane foam, comparable in size to a mattress; the room geometry is that described in the previous section. The fire growth rate was calculated based on ignition of the mattress by a small source such as a match or piece of paper. The real-life scenario which this might represent is the accidental ignition of a large block of polyurethane in a storeroom, where the storeroom door is left open. Figure 4 shows the fire size in kilowatts as a function of time. The fire growth curve shows typical s-shaped behavior. The early slow-growth phase is followed by a steep increase in fire size as radiative feedback from the hot upper layer becomes significant. Finally, as the fire approaches a megawatt in size, it begins to be limited by the amount of available fuel.

The results of this computation can be used to describe the thermal environment of cable passing through the storeroom. For ease of illustration it is assumed that the cable tray is installed horizontally near the floor, and that the area of exposed cable surface is approximately 1 sq. meter, although the analysis does not depend on these simplifications. As the fire grows, the radiative heat transfer to the cable bed increases to the point where ignition of the cable must be considered, with attendant effects on operation of the buildings' electrical systems. If ignition does occur, the energy contributed by the cable may increase the severity of the fire. This in turn could have an effect on the time to failure of compartment walls, and it will certainly increase the rate of smoke production. Each of these aspects of hazard will be examined in turn.

**CIRCUIT INTEGRITY** Figure 5 graphs the radiant flux to a horizontal floor-mounted target for the exposure fire and shows the levels of flux necessary to ignite selected cable samples whose ignition times are shown in Table 1. One would therefore expect sample 1 to ignite at approximately 300 seconds, samples 2 and 3 at around 500 seconds, and sample 6 somewhat above 800 seconds. Assuming (perhaps

incorrectly) that none of the samples tested retain circuit integrity very long after ignition, this approach also allows one to determine the minimum time to circuit failure in such a fire.

**CABLE EFFECT ON FIRE BUILDUP** Once the cable bed is ignited, its burning rate will contribute to the intensity of the fire. Determining the degree of contribution requires, as before, either a series of full-scale measurements or a predictive mechanism whereby the fire due to the cable can be integrated with the effects of the exposure fire. This integration can be accomplished using the model, providing the that release rate and ignition temperature of the irradiated target are specified. The ignition temperature can be approximated from the ignition flux measurements of Table 1. For purposes of comparison, it was assumed that all cable samples had the same heat release rate -- 250 kw. Figure 6 shows the upper room temperature, i.e., the temperature of the hot gas layer, as a function of time for fires involving the foam alone, and cable samples 1, 2, 3 and 6. As can be seen, Cable 1, 2 and 3 contributed substantially to fire severity\*. Whether or not the increased temperatures due to burning of the cable would have any important effect on the fire endurance of the surroundings depends on their makeup. The somewhat elevated temperature for 5-10 minutes would probably be unimportant if the storeroom walls are concrete, rated at 2 hours (by ASTM E-119), but could be quite significant if the walls are of lightweight construction, rated at, say, 30 minutes.

**CABLE EFFECTS ON SMOKE PRODUCTION** If the storeroom fire exhausts all of its combustion products into a large volume, such as a building atrium, the large space catches,

---

\* Under modeled conditions, cable 6 did not ignite during the 1000 second test period and therefore did not contribute to the fire.

---

holds and mixes all of the smoke produced, so that the smoke to which a person in the atrium is exposed consists of contributions from each burning material. The fraction of the total smoke obscuration which is attributable to each material is:

$$x_i = k_i M_i$$

where  $M_i$  is the total mass burned of component  $i$ . The proportionality constant  $k_i$  is different for each material, but in comparison to the differences in  $M$ , it may not be significant. For example, note from Figure 6 that the foam in the storeroom scenario will have burned for over 5 minutes before any cable material start producing enough smoke in a 1000 m<sup>2</sup> space so that occupants cannot see across the room. Table 2 shows the mass fraction of total smoke which is due respectively to the foam and the cables at various times after ignition in each fire. The contribution of the cable never exceeds 13% of the total smoke, thus, even if cables could be made out of smokeless material the best one could hope for in this scenario is to reduce obscuration by 13% over what it would be from the foam burning alone under similar thermal conditions.

There is, however, a variant to the so-called room-filling case, which is the exposure of building occupants to the smoke as it comes from the room. This can in principle occur in a hallway outside the postulated storeroom, but realistically, it must be sufficiently far from the fire that hazards from heat do not swamp those from smoke. The relative contribution of the cable to the makeup of the smoke at any instant is proportional to the relative mass loss rates of the cable and the foam owing to the relative amounts of foam and cable material present in the scenario under discussion, the largest ratio this value can have is 2:5, i.e., the cable contributes a maximum of 2/7 of the smoke mass. This assumes no difference in the fuel properties of the foam material and the cable material. If the cable material burns more slowly than the foam material, its relative contribution would be less. Thus, for the cable to contribute substantially to the smoke from this fire, it must be far smokier, pound for pound, than the fuel for the exposure fire.

The significance of contributions to smoke toxicity can be addressed by the same approach. However, more data on the burning materials are needed before results of this consequence can be obtained. Such a study will comprise Part 2 of this series of papers.

#### SUMMARY AND CONCLUSIONS

The purpose of this work was to show that cable fires, like most others, are difficult to characterize under all circumstances on the basis of existing fire tests. Indeed, scenarios of cable fire exposure can readily be envisioned in which performance measurements of a more fundamental type are necessary. In the case at hand, data obtained by the Factory Mutual Flammability Apparatus were required in order to predict whether cable will be involved in a fire. In addition, one needs a relatively detailed picture of fire buildup in the absence of the cable before it is possible to predict how cable itself will contribute to hazard. This study has employed a sophisticated room fire model, the so-called Harvard model, to provide the necessary information, since actual measurements on full-scale fires are difficult to obtain. The most significant conclusions are:

1. It is possible to predict the minimum times to circuit failure for cable exposed to a developing fire, even when the cables themselves are not initially ignited.
2. If the fire endurance properties of the structural components near the fire are known, it is possible to determine if the presence of cable will increase the likelihood of local structural failure and thus the spread of fire into adjacent rooms.
3. Cables which meet IEEE 363 are resistant to ignition from small sources and require a significant fire exposure before they become involved. In most such cases the smoke coming from the cable will constitute a relatively small fraction of the total smoke produced. Thus, there is limited

opportunity to reduce significantly the overall degree of smoke obscuration by addressing solely the smoke development properties of the cable materials.

4. Smoke toxicity, like smoke obscuration, depends in such cases on the properties of all of the smoke produced. Hence, an evaluation of toxic hazard requires this same kind of integrated approach. Dependence on small-scale toxicity information alone is inappropriate.

#### REFERENCES

1. Quintiere, J., and McCaffrey, B., "The Burning of Wood and Plastic Cribs in an Enclosure: Vol. I", National Bureau of Standards U.S., NBSIR 80-2054 (1980).
2. Tewarson, A. and Pion, R., "A Laboratory-Scale Test Method for the Measurement of Flammability Parameters", Factory Mutual Research, Norwood MA, Technical Report 22524 (October, 1977).
3. Tewarson, A., Lee, J. and Pion, R., "Categorization of Cable Flammability. Part I: Laboratory Evaluation of Cable Flammability Parameters.", Factory Mutual Research Corporation, Report Prepared for Electrical Power Research Institute, No. NP 1200, Part 1, October, 1979.
4. c.f. Emmons, H., "The Prediction of Fire in Buildings," 17th Symposium (International) on Combustion, The Combustion Institute, Pittsburgh, PA (1978).



FREDERIC B. CLARKE, III, Ph.D.  
Benjamin/Clarke Associates, Inc.  
10605 Concord St., Suite 501  
Kensington, MD 20895

Frederic Clarke is President of Benjamin/Clarke Associates, Inc., a firm specializing in the characterization and analysis of fire safety problems. Until fall, 1981 he was Director of the Center for Fire Research, National Bureau of Standards and Science Advisor to the United States Fire Administration. Previously, he served as legislative assistant to Senator John Culver (D.-Iowa), and as staff assistant to Congressman Jim Wright (D.-Texas), the House Majority Leader. Education: A. B., Chemistry, Washington University, St. Louis; A.M., Ph.D, Physical Chemistry, Harvard University.

#### Education and Honors

A.B., Washington University, 1966  
A.M., 1968, Ph.D., 1971 Harvard University (Physical-organic Chemistry)  
National Science Foundation  
Predoctoral Fellow at Harvard, 1966-69  
Congressional Fellow, 1976-77  
Phi Beta Kappa, Sigma Xi



IRWIN A. BENJAMIN, P.E.  
Benjamin/Clarke Associates, Inc.  
10605 Concord St., Suite 501  
Kensington, MD 20895

Irwin Benjamin is Vice President of Benjamin/Clarke Associates, Inc., a firm specializing in the characterization and analysis of fire safety problems. Until fall, 1981, he worked in fire research at the National Bureau of Standards, where he was Chief of the Fire Safety Engineering Division, Center for Fire Research. In that capacity, he planned and coordinated research on fire growth and fire behavior; supervised the development of systems for evaluating fire risk in buildings; the extension of analytical fire modeling to the solution of code problems; the development of a toxicity protocol for screening materials; the development of new methods of more cost effective fire protection systems; and the initiation of cost-benefit analysis to the application of alternate fire protection systems.

#### Education and Awards

B.S. Civil Engineering, Illinois  
Institute of Technology  
M.S. Structural Design, Kansas State  
University  
Graduate, Federal Executive Institute  
Department of Commerce Silver Medal  
Chi Epsilon Honorary Society



PHILIP J. DINUNNO, P.E.  
Benjamin/Clarke Associates, Inc.  
10605 Concord St., Suite 501  
Kensington, MD 20895

Philip DiNunno is a fire protection engineer with Benjamin/Clarke Associates Inc. He is primarily involved with the application of mathematical fire modeling to the evaluation of fire safety problems. DiNunno has worked for five years as a consulting engineer in fire protection, specializing in applying research results, and utilizing models for the evaluation of fire protection problems.  
Education:

B.S., Fire Protection Engineering,  
University of Maryland

TABLE 1

CRITICAL HEAT FLUX AND IGNITION TEMPERATURES  
FOR CABLE SAMPLES -- FACTORY MUTUAL  
FLAMMABILITY APPARATUS

CABLE SAMPLE	MINIMUM RADIANT HEAT FLUX FOR PILOTED IGNITION(W/CM <sup>2</sup> )	IGNITION TEMPERATURE (CALCULATED)(°C)
1	1.4	430
2	2.2	520
3	2.2	520
4	2.5	540
5	2.5	540
6	3.4	730

TABLE 2

FRACTION OF TOTAL SMOKE DUE TO BURNING OF  
FOAM AND CABLE AT VARIOUS TIMES IN THE FIRE

SMOKE SOURCE	FRACTION OF TOTAL SMOKE AT:			
	300 SEC	500 SEC	700 SEC	900 SEC
FOAM ALONE	1.0	1.0	1.0	1.0
FOAM + CABLE 1	1.0 0	.93 .07	.89 .11	.87 .13
FOAM + CABLE 2	1.0 0	1.0 0	.93 .07	.90 .10

FIG. 1: BURNING BEHAVIOR OF VARIOUS MATERIALS AS A FUNCTION OF EXTERNAL FLUX (WATTS/SQ CM)

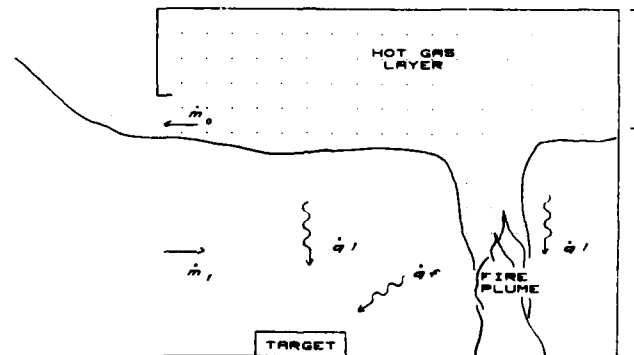
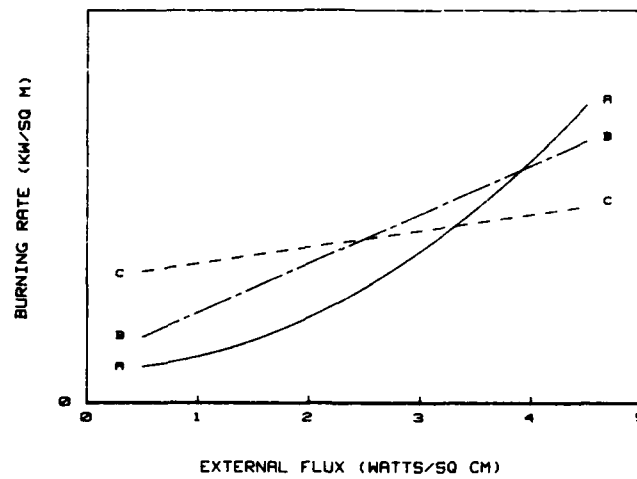


FIG. 2: 2-ZONE SCHEMATIC OF FIRE BURNING IN AN ENCLOSURE, DOORWAY AT LEFT

FIG.3: RADIANT FLUX VS. BURNING RATE

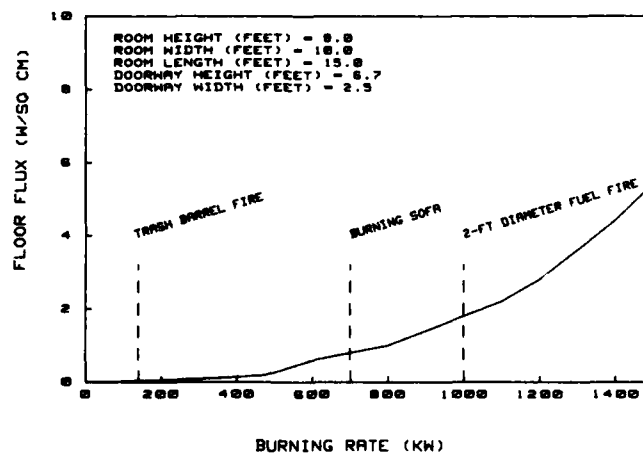


FIG. 4: HEAT RELEASE RATE AS A FUNCTION OF TIME

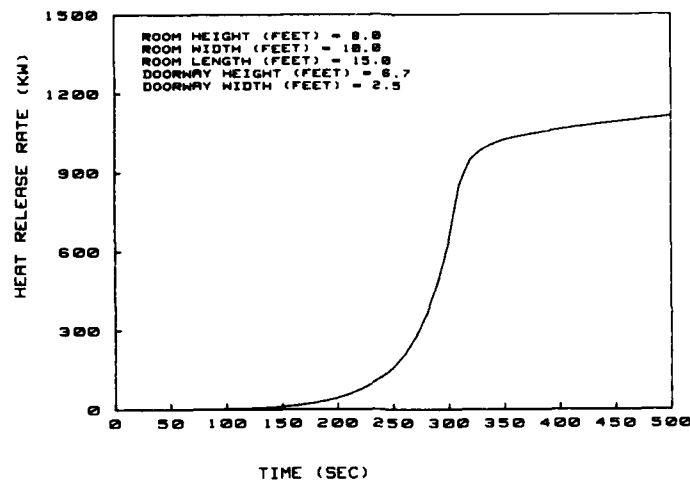


FIG. 5: RADIANT FLUX TO A HORIZONTAL TARGET AS A FUNCTION OF TIME

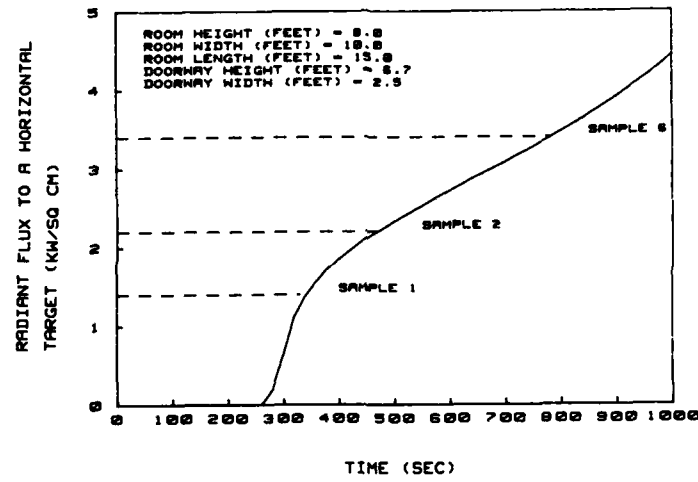
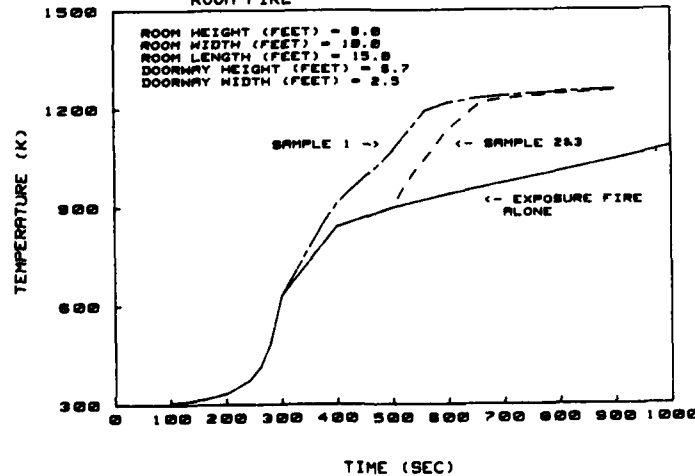


FIG. 6: UPPER ROOM TEMPERATURE AS A FUNCTION OF TIME: CABLE SAMPLES EXPOSED TO A DEVELOPING ROOM FIRE



## FRACTURE MECHANICS EVALUATION OF THE STATIC FATIGUE LIFE OF OPTICAL FIBERS IN BENDING

Drew V. Nelson\*    Vernon A. Fentress\*\*

\* Stanford University

\*\* Raychem Corporation

Abstract

Methods for predicting the time-dependent strength (static fatigue) of optical fibers using principles of fracture mechanics have been developed over the past few years. Previous fracture mechanics evaluations of optical fibers reported in the literature have generally considered the case of applied uniform tension.

In many applications, fibers are in bending. This paper uses stress intensity factors for semi-circular surface flaws in a round bar subjected to tension or bending to generate relations between fiber proof-stress level, applied stress and expected lifetimes. The factors are taken as a function of instantaneous crack depth during stress corrosion growth. Application of the results to the design of fiber optic organizer/closures is discussed.

where,  $a$  = crack depth (or length)

$\sigma$  = applied stress (calculated as if no crack were present)

$Y$  = a dimensionless factor dependent on the type of crack, specimen geometry, type of loading and ratio of crack depth to specimen size.

Typical results of such stress corrosion crack growth tests are shown schematically in Figure 1. For many glasses, over a wide range of applied  $K_I$ ,

$$da/dt = AK_I^n \quad (2)$$

where  $A$  and  $n$  are empirically fitted constants.

At a critical value of  $K_I$ , designated the fracture toughness  $K_{IC}$ , unstable growth occurs and fracture follows quickly. A threshold value of  $K_I$ , designated  $K_{Ith}$ , below which no growth should occur, may also exist, but this is still a matter of some uncertainty.

Introduction

It has been established<sup>1,2</sup> that the long-term static strength of glass products, including optical fibers, is governed primarily by stress corrosion cracking originating from microscopic surface flaws present from the time of fabrication. This failure mode has often been termed "static fatigue". To generate static fatigue data for glass products, the traditional approach has been to subject specimens to different stress levels and observe corresponding times to fracture. Since static fatigue is controlled largely by the rate at which initial flaws grow to a critical size for fracture, linear elastic fracture mechanics (LEFM) analyses and testing<sup>3-5</sup> have been performed more recently in an effort to improve both the understanding of the phenomenon as well as life prediction capabilities. Tests have consisted of loading to fixed stress levels relatively large specimens (e.g., microscope slides) containing cracks of a known size, then observing stress corrosion crack growth rate,  $da/dt$ , and plotting it against the Mode I stress intensity factor,  $K_I$ . This factor is of the form

$$K_I = Y\sigma\sqrt{a} \quad (1)$$

A number of authors<sup>2-4</sup> have shown that by substituting Equation (2) into Equation (1) and integrating the result between initial and critical flaw sizes, the life predicted for a given applied stress agrees well with conventional static fatigue data. In the case of optical fibers, it is currently impractical to monitor stress corrosion crack growth rate directly due to the small fiber diameter and small size of cracks. However,  $A$  and  $n$  can be inferred from traditional static fatigue data by matching crack growth life predicted by LEFM methods.

A commonly used approach for assuring adequate static fatigue life of optical fibers as well as other glass products involves proof-stressing<sup>6-8</sup>. Fibers which survive a given proof-stress level are "guaranteed" not to have any initial flaws deeper than the value determined by setting Equation (1) equal to  $K_{IC}$  and solving for depth for a given proof-stress level. Since much, if not most, of the scatter in static fatigue behavior of fibers which have not been proof-stressed is due to variability from fiber-to-fiber in largest initial flaw sizes, then proof-stressing, by virtue of establishing a "worst case" initial flaw size, also leads to predictions of time-to-failure which should represent conservative minimum values.

## Role of Tension Versus Bending

Most of the static fatigue data for optical fibers have been generated under uniform tension loading; crack growth analyses have been conducted for that loading case as well. In many actual situations, fibers are loaded in bending. An example is a fiber organizer. Several authors<sup>9-10</sup> have proposed that the static fatigue life in bending should be significantly longer than that in tension for the same stress level, based on probabilistic considerations. In bending, much of the volume<sup>9</sup> or surface area<sup>10</sup> containing microflaws is exposed to stress levels considerably smaller than in uniform tension (for the same maximum stress level), thus leading to a lower probability of causing failure. Moreover, half of the surface area (or volume) is under compression in bending, and no crack growth and fracture should occur there since cracks generally require tension for growth.

In addition to probabilistic considerations, another factor which could lead to a longer life in bending relative to tension (or alternatively, higher allowable bending stress for the same life), is the rate of stress corrosion crack growth. In applied tension, a crack grows through a uniform stress field, whereas in bending it grows through a declining gradient, which should cause a slower rate relative to uniform stress. Previous LEFM evaluations<sup>2</sup> of crack growth in optical fibers have assumed a semi-circular surface flaw and taken the value of  $Y$  in Equation (1) for that type of flaw in a large plate subjected to uniform tension. The  $Y$  value is often also taken as a constant and assumed to remain so during crack growth, a good approximation when an initial surface flaw is small compared to fiber diameter and when the amount of growth to the point of fracture is also small. However,  $Y$  is in fact a function of crack depth and also differs substantially for bending and for tension. As a crack grows through uniform tension  $Y$  increases, while the opposite occurs for bending. Also, the value of  $Y$  is different for surface flaws in plates than in round specimens. These considerations and their consequences on predicted crack growth lives in proof-stressed optical fibers will be examined in subsequent sections.

## Prediction of Fiber Life

In order to estimate the life of proof-stressed fibers, assuming it to be governed by stress corrosion cracking, the following items are needed:

- A stress intensity relation as in Equation (1);
- crack growth rate data, preferably expressed in a form such as Equation (2);
- fracture toughness,  $K_{IC}$ ;
- values of initial flaw sizes based on proof-stress levels.

Fracture toughness values<sup>11</sup> for most glasses fall in the range of 0.7 to 1.0 MPa $\sqrt{m}$ . For fused silica, as used in optical fibers,  $K_{IC}$  has been reported as 0.75 MPa $\sqrt{m}$  and 0.79 MPa $\sqrt{m}$ , a small variation. The following evaluation will use a value of 0.75 MPa $\sqrt{m}$ . Both references 2 and 12 recommend use of  $n = 17$  in Equation (2) for optical fibers, based on dynamic fatigue data. There is a wide variation of  $n$  values reported in the literature, depending on fiber coating, test conditions, etc.; but use of  $n = 17$  is thought to be on the conservative side. Corresponding values of  $A$  in Equation (2) were obtained from an empirical relation<sup>9</sup> derived from optical fiber static fatigue data (in units of GPa - seconds):

$$\log A = 3.289n - 10.05 \quad (3)$$

Stress intensity factors for two cases were used in the evaluation. The first case, denoted A, is a semi-circular surface flaw in a plate subjected to either tension or bending. See Figure 2. The  $K_I$  factor for a surface flaw varies with location around the crack front, generally reaching a maximum at the crack center (point of greatest depth) or at the crack tips on the surface (depending on the ratio of crack depth to surface length). Values of normalized  $K_I$  computed by finite elements<sup>13</sup> for case A at both crack center and at the tips are shown in Figure 3 as a function of normalized crack depth. Linear approximations to the finite element points are given by:

## Uniform Tension - Case A

### Crack Center

$$Y = \frac{K_I}{\sigma\sqrt{a}} = 1.24 + 0.45 \left(\frac{a}{D}\right) \quad (4)$$

### Crack Tips

$$Y = \frac{K_I}{\sigma\sqrt{a}} = 1.16 + 0.15 \left(\frac{a}{D}\right) \quad (5)$$

## Bending - Case A

### Crack Center

$$Y = \frac{K_I}{\sigma\sqrt{a}} = 1.24 - 0.15 \left(\frac{a}{D}\right) \quad (6)$$

### Crack Tips

$$Y = \frac{K_I}{\sigma\sqrt{a}} = 1.16 - 1.58 \left(\frac{a}{D}\right) \quad (7)$$

where  $D$  is fiber diameter. Note that the values for bending and tension at a given location on the crack front converge for very small crack depth, as should be expected. Note also that in Equations (4) and (6),  $Y$  is 1.24 for small crack depth, in agreement with the constant used previously in the literature<sup>2</sup>.

The second case considered, denoted by B, is a semi-circular surface flaw in a round bar subjected to uniform tension or bending, a better approximation to the situation in an optical fiber. Values of normalized  $K_I$  computed by finite elements<sup>14</sup> are shown in Figure 4. Only values at the crack center were reported in Reference 14. The Y factors bear a nearly linear relation with crack depth and are given by:

#### Uniform Tension - Case B

$$Y = \frac{K_I}{\sigma\sqrt{a}} = 0.80 + 1.62 \left(\frac{a}{D}\right) \quad (8)$$

#### Bending - Case B

$$Y = \frac{K_I}{\sigma\sqrt{a}} = 0.80 - 0.62 \left(\frac{a}{D}\right) \quad (9)$$

The lower values of Y for Case B relative to Case A are attributed to the influence of surface curvature. The following evaluation will also assume that a semi-circular crack shape is maintained during growth.

To compute maximum initial flaw size,  $a_i$ , which could exist after proof-stressing to a given level, Equation (4), (5) or (8) was set equal to  $K_{IC}$  and solved for  $a$ , depending on the case being analyzed. (It was assumed that proof-stressing is done in tension.) To determine final crack size at fracture,  $a_f$ , for a given applied service stress level, the appropriate equation for the case being analyzed [from Equations (4) through (9)] was set equal to  $K_{IC}$  and solved for  $a$ .

For a given proof-stress level and corresponding  $a_i$ , lives for the different  $K_I$  factors were determined by substituting each factor into Equation (2), then separating variables ( $a$  and  $t$ ) and numerically integrating between  $a_i$  and the  $a_f$  values corresponding to a number of different applied stress levels.

### Results

Lifetime predictions are shown in Figures 5 through 8. For Case A (plate) with applied uniform tension, there was a negligible difference between lifetimes predicted using  $K_I$  values at crack center or at crack tips; thus, only predictions based on surface values are shown in Figure 5. The lack of difference is, at first glance, somewhat surprising in view of the difference in  $K_I$  factors. However, the maximum initial flaw size after proof-stressing is larger for Equation 5 than for Equation 4, tending to compensate for the influence of lower Y in subsequent growth computations.

Figure 6 shows predicted lives for Case A with applied bending. When  $K_I$  at crack center is used, lives are somewhat longer than when  $K_I$  at crack tip is used, with the difference diminishing at higher applied stress levels. The difference in Y factors [Equations (6) and (7)] is substantial as a function of crack depth.

However, most of the crack growth life is consumed at small crack sizes where the difference in Y factors is reduced. By the time cracks are large enough for a significant difference in Y factors to exist, cracks are growing so rapidly that relatively little life is left, and thus, the difference in predictions is minimized. Comparison of the results in Figure 5 and 6 also shows that, at most, roughly a factor of two increase in life is predicted in bending versus tension for a given applied stress level. The difference in allowable stress levels between tension and bending to attain a given life is negligible. Again, the apparent reason for lack of a more pronounced difference in lives in bending versus tension is due to cracks spending most of their life at small sizes where differences in Y factors in bending and in tension are small.

Figure 7 shows predicted lives for Case B (round bar) with applied uniform tension. Only  $K_I$  factors at crack center were available for making these predictions. Compared to Case A with uniform tension, lives are somewhat longer, but not to the extent that one might expect from the substantial difference in Y factors. However, the initial flaw sizes after proof-stressing are larger for Case B than A, thus causing substantially equal  $K_I$  factors for subsequent growth.

Figure 8 shows predicted lives for Case B with applied bending. Again, only  $K_I$  factors at crack center were available for making these predictions. Also shown for comparison in this figure are lives for Case A with uniform tension. The combination of lower Y values in Case B due to a circular cross-section and the influence of the bending stress gradient results in substantially greater lives compared to Case A, even though initial crack sizes after proof-stressing are larger in Case B. For example, with a proof-stress level of 50 ksi (345 MPa) and applied stress of 20 ksi (138 MPa), the life for Case B, bending, is about twenty times longer than for Case A, tension. Comparison of the results of Figures 7 and 8 (both for Case B and both having the same initial crack sizes after proof-stressing) reveals the influence of the difference in Y factors with crack depth for tension and bending. It is likely that comparable difference in lives between tension and bending for Case A (Figures 5 and 6) were not seen because both initial and final crack sizes were smaller than in Case B, thus minimizing the influence of differences in Y factors with depth.

### Applications

The methods used in the splicing and subsequent storage of the optical fiber splice and fiber slack in the fiber optic organizer/closure will, to a large extent, determine the life expectancy and service quality of the fiber optic channel during service. In this applications section we will examine the potential impact of the data presented here on the organization and installation of fibers in the fiber optic organizer/closure.

To accomplish this we must first convert the results presented in Figures 6 and 8, fiber life as a function of stress, to fiber life as a function of bend radius, using the relationship

$$\sigma = Er/R$$

where  $E$  = Young's Modulus 71.70 GPa ( $10.4 \times 10^6$  psi)  
 $r$  = Fiber radius (62.5  $\mu$ m for multimode fibers)

$\sigma$  = Bending stress at radius  $r$ .  
 $R$  = Fiber bend radius.

Figure 9 shows the data of Figures 6 and 8 in terms of the bend radii necessary to produce the stress values of Figures 6 and 8. The dotted lines show the data of Case A (glassplate) in bending, while the solid lines represent Case B (glass rod) in bending. For the 345 MPa (50,000 psi) proof-stress fiber the reduction in allowable minimum bending radius is potentially 8 percent. For the 517 MPa (75,000 psi) fiber the reduction is 9 percent. For the 690 MPa (100,000 psi) and 1380 MPa (200,000 psi) fiber the reduction is 7 percent and 8 percent, respectively. The possible reduction in case/organizer cross-sections is equivalent to these differences.

#### Benefits for the Flat Plate Organizer

The traditional mode of fiber organization is by wrapping the fiber slack on a flat plate organizer. Figure 10 shows a typical flat plate organizer complete with harnessing straps by which the locus of the stored fiber is controlled. In an efficiently filled flat plate organizer/closure the organizer portion has flat plate organizers stacked to form a square or rectangular cross-section nestled close to the inner wall of the closure (like a square inscribed in a circle).

What is the result of applying the results of this analysis to flat plate organizer design? Specifically, for a 345 MPa (50,000 psi) proof tested fiber, fracture data generated for Case A in bending indicates a 38mm bend radius is necessary for a 40 year life. Data generated for Case B in bending yields a lower result of 34.5mm. This reduction could be significant for the flat plate organizer of Figure 10, as the larger the loop necessary to fit the straps, the more difficult it is to produce the correct size loop using an arbitrary length of fiber slack. The cross-section of the organizer/closure could be reduced a corresponding amount.

#### Benefits for the Mandrel-Wrap Organizer

Another approach for organizing fibers is the mandrel-wrap organizer. An example of this device is shown in Figure 11. The difference between this and flat plate organizers is that the fiber is placed in a flexible envelope or on a flexible sheet which is wrapped over a round mandrel, instead of being layed on a flat plate.

The advantage of the mandrel-wrap organizer is that the installation of a round assembly of spirally wrapped fiber sheets or envelopes into a round closure is potentially space saving as compared to inserting a square assembly of flat plates into a round closure. The necessity of separating fibers onto individual sheets or envelopes avoids the inter-fiber tangling associated with flat plate organizers.

The designer of the mandrel-wrap organizer must solve the problem of fiber microbending associated with wrapped layers pressing on the installed fibers. The bend radius correlations proposed here could be beneficial for the mandrel wrap organizer. This device has the same fiber wrapping problem as the flat plate organizer; that is, the larger the installed loop, the more difficult it is to store random fiber lengths. Smaller fiber loop requirements could somewhat ease the installed loop restrictions, as well as reduce organizer/closure cross-sections.

#### Benefits for Organizer/Closure Weight

The weight of the mechanical-type organizer/closure is particularly sensitive to fiber bend radius changes. Figure 12 graphs a survey of the weight per unit length of mechanical organizer/closures on the market.

A hypothetical closure of 150mm in diameter reduced 9 percent in diameter to 136mm would experience a 25 percent decrease in weight per unit length. Similar large weight reductions can be attained for various other diameters.

#### Conclusions

1. From a stress corrosion crack growth rate viewpoint, optical fibers in bending are predicted to have longer lives than those subjected to uniform tension loading. The increase in life depends on proof-stress and applied stress levels and is most pronounced when the  $K_I$  factor for a round bar is used.
2. Significant decreases in fiber optic organizer/closure cross sections can result from reductions in allowable fiber bend radius obtained through use of  $K_I$  factors for round bars. The reductions are on the order of 8-9 percent for a 40 year life compared to use of  $K_I$  factors for surface flaws in plates subjected to bending.
3. Even greater reductions in organizer/closure weight per unit length are possible. These reductions can be as much as 25 percent.

## References

1. Adams, R. and McMillan, P.W., "Review - Static Fatigue in Glass", J. Materials Science, Vol. 12, 1977, p. 643.
2. Kalish, D., Key, P., Kurkjian, C., Tariyal, B., and Wang, T., "Fiber Characterization - Mechanical", Chapter 12 in Optical Fiber Telecommunications, Academic Press, New York, N.Y., 1979.
3. Wiederhorn, S. and Bolz, L., "Stress Corrosion and Static Fatigue of Glass", J. Amer. Ceram. Soc., Vol. 53, No. 10, 1970, p. 543.
4. Ritter, J., and Meisel, J., "Strength and Failure Predictions for Glass and Ceramics", J. Amer. Ceram. Soc., Vol. 59, No. 11-12, 1976, p. 478.
5. Wachtman, J.B., Jr., "Highlights of Progress in the Science of Fracture of Ceramics and Glass", J. Amer. Ceram. Soc., Vol. 57, No. 12, Dec. 1974, pp. 509-519.
6. Wiederhorn, S., "Prevention of Failure in Glass by Proof-Testing", J. Amer. Ceram. Soc., Vol. 56, No. 4, 1973, p. 227.
7. Love, R., "The Strength of Optical Waveguide Fibers", SPIE Fibers and Integrated Optics, Vol. 77, 1976, p. 69.
8. Gulati, S.T., "Strength and Static Fatigue of Optical Fibers", Corning Glass Works, Corning, New York.
9. Patel, P., Chandan, H. and Kalish, D., "Failure Probability of Optical Fibers in Bending", International Wire and Cable Symposium Proceedings, 1981, p. 37.
10. Evans, A. and Jones, R., "Evaluation of a Fundamental Approach for the Statistical Analysis of Fracture", J. American Ceram. Soc., Vol. 61, No. 3-4, 1978, p. 156.
11. Wiederhorn, S.M., "Fracture Surface Energy of Glasses", J. Amer. Ceram. Soc., Vol. 52, No. 2, 1969, p. 95.
12. Helfenstine, J. and Quan, F., "Optical Fiber Strength/Fatigue Experiments", Corning Glass Works, Corning, NY.
13. Newman, J.C. and Raju, I.S., "Analysis of Surface Cracks in Finite Plates Under Tension of Bending Loads", NASA Technical Paper 1578, December, 1979.
14. Salah el din, A.S. and Lovegrove, J.M., "Stress Intensity Factors for Fatigue Cracking of Round Bars", International J. Fatigue, July 1981, p. 117.



Drew V. Nelson  
Mechanical Engineering Department  
Stanford University  
Stanford, California 94305

Drew Nelson is an Associate Professor of Mechanical Engineering at Stanford University, where he received his B.S. (1968), M.S. (1970), and Ph.D. (1978) degrees. He has seven years of industrial experience, including four with General Electric. His teaching and research involve fatigue, fracture mechanics, experimental stress analysis, non-destructive evaluation of materials, and mechanical design. He is a member of ASME, SESA, ASTM and SAE, and is an Officer of the Committees on Fatigue in the latter two societies.



Vernon A. Fentress  
Telecommunications Division  
Raychem Corporation  
Menlo Park, California 94025

Vernon Fentress received his Bachelor of Science degree in Mechanical Engineering from Carnegie Institute of Technology (now Carnegie-Mellon University) in 1966 and his Master of Science degree in Mechanical Engineering from Syracuse University in 1968. He joined Raychem Corporation in 1979 after several years with the Western Electric Wire and Cable Division in Atlanta, Georgia. He has been involved in fiber optics at Raychem since 1981 and is currently employed as a group leader in fiber optics for the Telecommunications Division of Raychem.

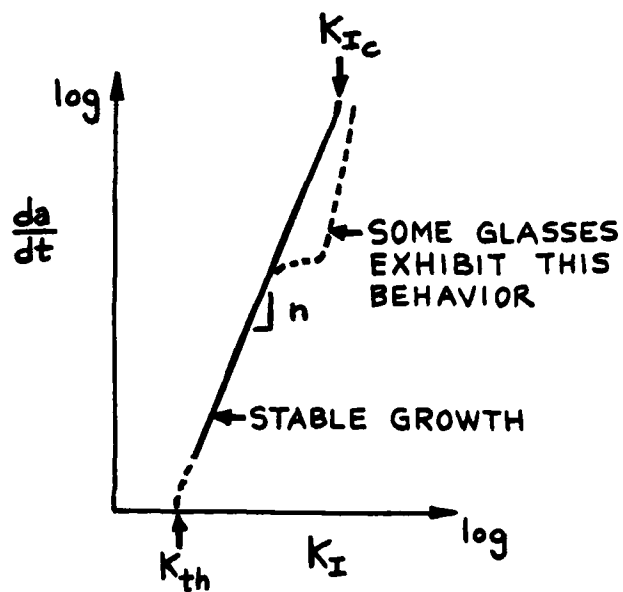


Fig. 1 - Schematic of stress corrosion crack growth rate behavior in glass

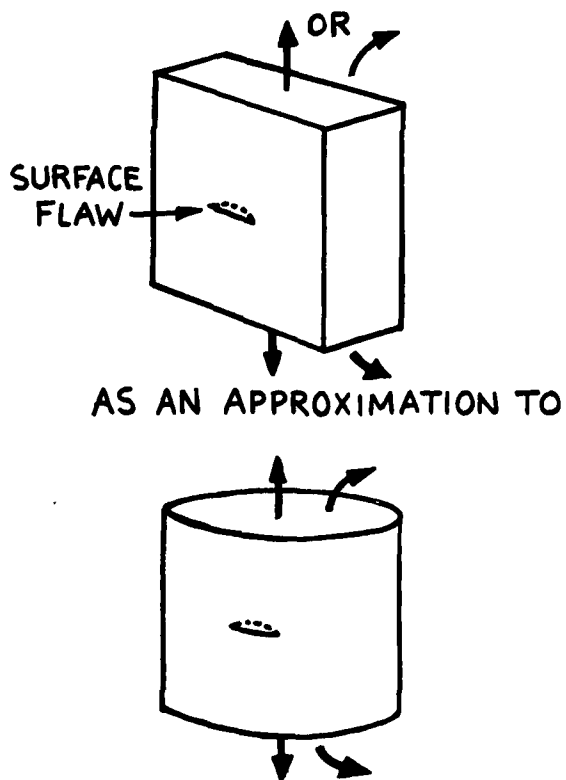


Fig. 2 - Plate surface flaw approximation to a surface flaw in a fiber

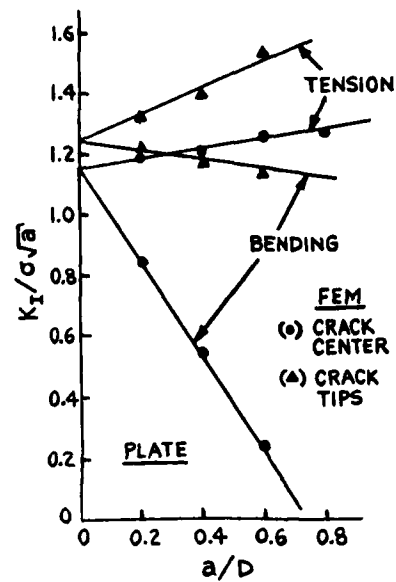


Fig. 3 - Normalized stress intensity factors vs. normalized crack depth for a semi-circular surface flaw in a plate

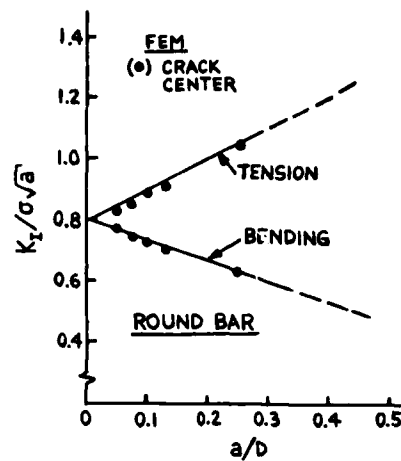


Fig. 4 - Normalized stress intensity factors vs. normalized crack depth for a semi-circular surface flaw in a round bar

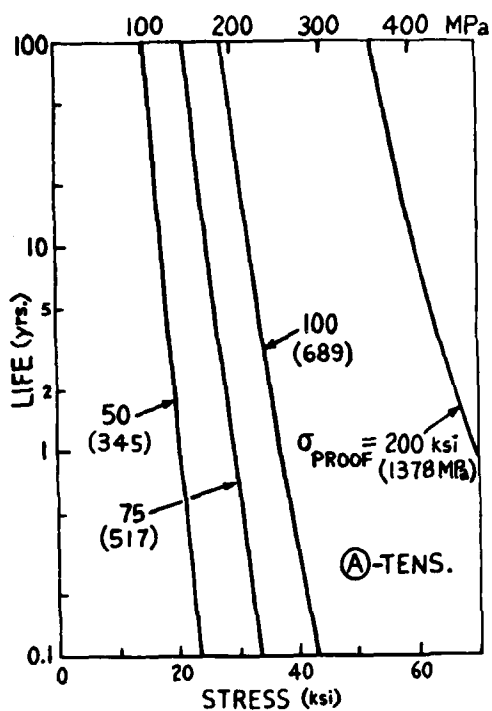


Fig. 5 - Predicted fiber lifetime using the stress intensity factor for a semi-circular surface flaw in a plate subjected to uniform tension

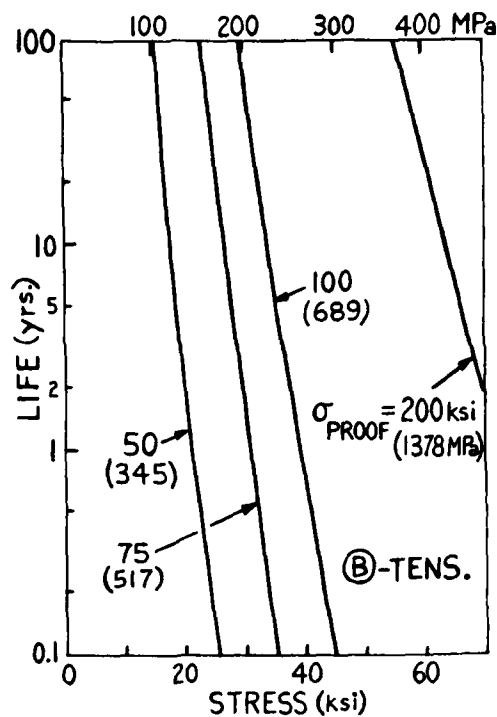


Fig. 7 - Predicted fiber lifetime using the stress intensity factor for a semi-circular surface flaw in a round bar subjected to uniform tension

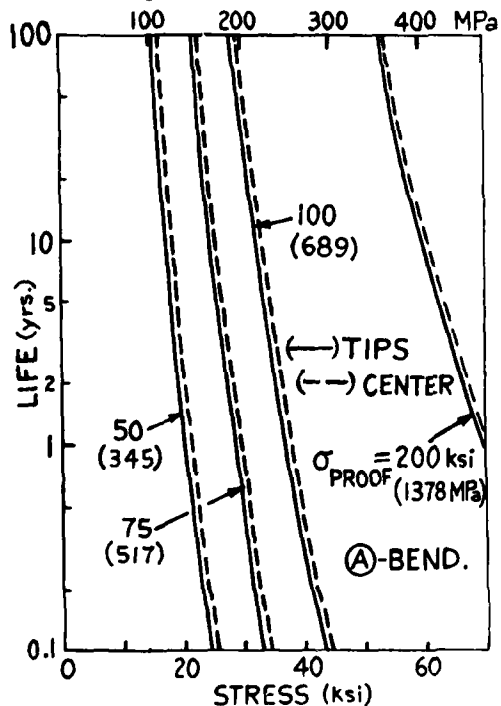


Fig. 6 - Predicted fiber lifetime using the stress intensity factors for a semi-circular surface flaw in a plate subjected to bending

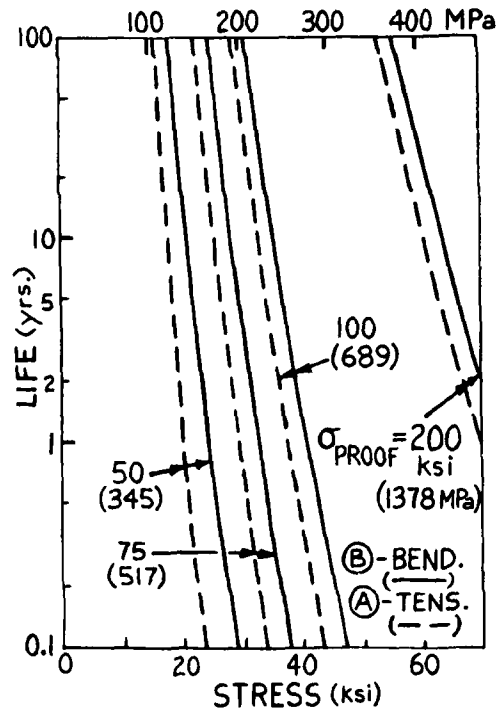


Fig. 8 - Predicted fiber lifetime using the stress intensity factor for a semi-circular surface flaw in a round bar subjected to bending

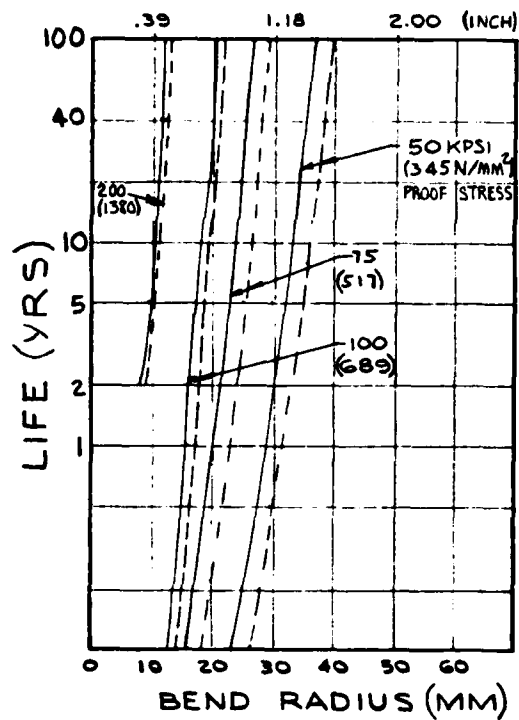


Fig. 9 - Predicted fiber lifetime as a function of fiber bending radius comparing Case A and B for bending

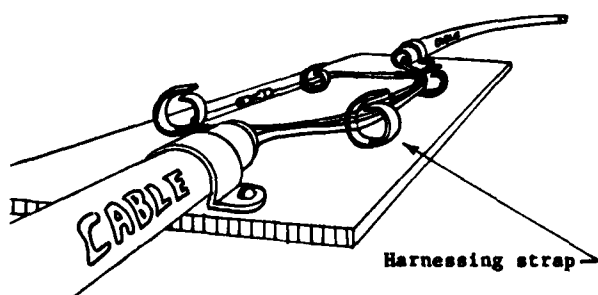


Fig. 10 - Flat plate organizer



Fig. 11 - Mandrel wrap organizer

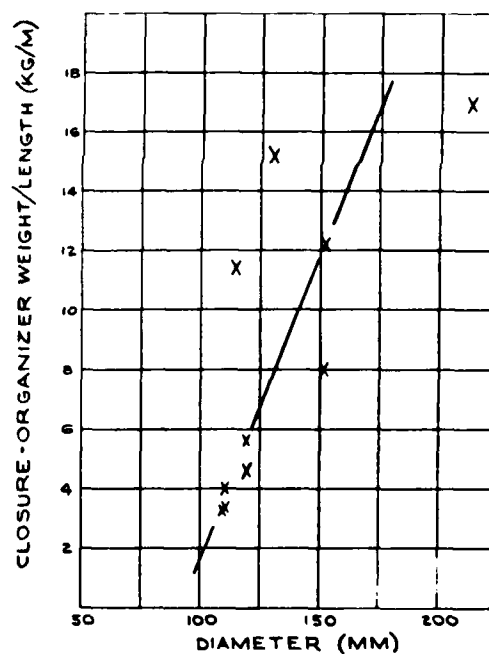


Fig. 12 - Mechanical organizer/closure weight per unit length as a function of diameter for ten commercial designs

## COMPUTERISED OPTICAL FIBRE CHARACTERISATION

Wim L.S. Malhu

NKF Kabel B.V., Waddinxveen, The Netherlands.

1. Abstract

In order to handle large amounts of optical fibre in cable manufacturing a computerised characterisation system was developed. With this system a low skilled operator can perform complete fibre characterisations with a cycle time of less than 5 minutes at a low cost level.

This paper describes the integral design of the system with a strong emphasis on accuracy, reduction of measurement costs, flexibility and ease of operation in a normal cable manufacturing environment. The system is capable of measuring attenuation, bandwidth and effective numerical aperture (choice of 8 wavelengths), length and backscattering of a 12 fibre cable in two consecutive measurement cycles (initial and cut back).

was designed which can operate at high speed in the normal cable factory environment, operated by low skilled operators without special experience in optical fibre measurements.

fig. 1 measurement room

2. Introduction

With the increase of the production volume of fibre optic cables a strong need was felt for an extension of the optical measurement capability. Previously all fibre characterisations had to be performed manually on a number of different equipment sets. Due to the reduction in fibre cost, the cost of optical measurements is no longer negligible in the total cable price. For these reasons the decision was taken to completely renew the production measurement sets. In order to obtain a cost effective solution an integrated set

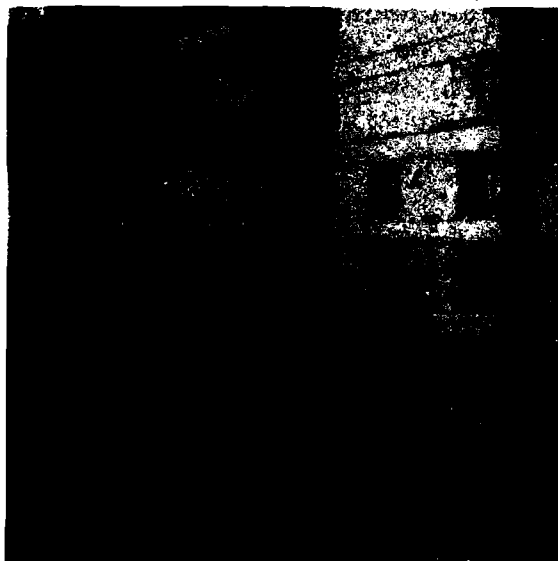
3. System specifications

The system is designed to cover all standard measurements during the production of optical cables with standard 50/125  $\mu\text{m}$  graded index fibres. The measurement program, which is specified per fibre, is a selection out of the following measurements:

- attenuation, bandwidth and effective numerical aperture for 8 possible wavelengths
- length measurement
- backscattering at 850 nm

All measurement and production data are stored in a data base, providing the life history of each fibre. The measurement time for a cable approval test (attenuation bandwidth at 850 and 1300 nm, length measurement and backscattering) on multifibre cables is less than 5 minutes per fibre.

fig. 2 measurement equipment



#### 4. Hardware

##### 4.1. Hardware concepts

To optimise measurement cycle time the following hardware design concepts were used:

1. Laser transmitters were used for all measurements, which gives an improvement of the S/N ratio.
2. Direct fibre to fibre couplings are used on both transmitter and receiver sides, which gives the advantage of wavelength independent optimum coupling positions. Therefore all transmitter and receiver interfaces are optical fibres, which can be located in a small (0.5 mm radius) area. Switching between transmitters

or receivers can be achieved quickly and without reoptimisation of the fibre's position. The gap between the fibres in the fibre to fibre coupling is controlled by an endface detection system with 1  $\mu$ m accuracy, which corresponds with the 1  $\mu$ m resolution of the step-motor driven translators for X,Y and Z positioning.

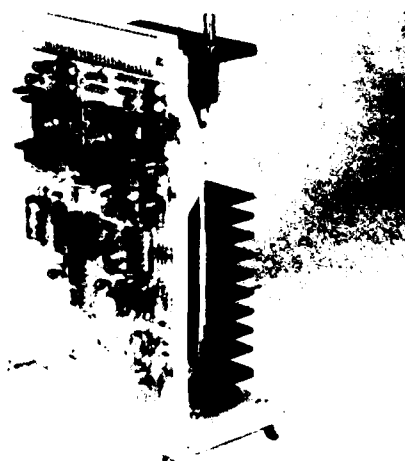
3. Designed as a cable oriented measurement system, it performs a measurement cycle on up to 12 fibres, leaving the operator free for a substantially longer time between initial and cut back measurements. During the measurement cycles the operator is free to prepare new fibres and cables.
4. Up to 12 fibres can be held in a 12-fold clamping device with precision vacuum chucks. All fibres will have a very small radial offset position, so very fast optimisation of the fibre coupling is performed.

#### 4.2. Hardware design

##### 4.2.1. Laser transmitters

Special plug-in laser transmitters were developed for use in

fig. 3 laser transmitter



attenuation bandwidth and effective numerical aperture measurements.

The lasers are temperature stabilised within  $0.02^{\circ}\text{C}$  by a thermoelectric cooling/heating circuit. Each transmitter has three remotely controlled modes:

- a. standby mode in which state only the temperature stabilisation is operational.
- b. CW mode with a 1 kHz sinusoidal modulation controlled by a wideband optical feedback circuit. With a multimode laser a stability of better than 0.05 dB is obtained over a 1 hour period. This mode is used for attenuation and numerical aperture measurements.
- c. pulsed mode for bandwidth measurements in which the laser is directly coupled to a pulse generator.

The transmitter contains an error circuit which generates an interrupt to the computer system when control of temperature or modulation is lost. A mode scrambler, consisting of a combination of step and graded index fibres, is integrated with the laser transmitter. The transmitter is rackmounted using high quality PC (physical contact) type connectors. Due to the spherical endfaces of the connectors the fibres make physical contact. In this way Fresnel reflections are overcome (low loss, low modal noise).

#### 4.2.2 Coupling system

The coupling systems on transmitter and receiver sides are mechanically the same. They consist of:

- a. translator stages
- b. endface detection system
- c. interface to transmitter/receiver
- d. 12 fold vacuum chuck.

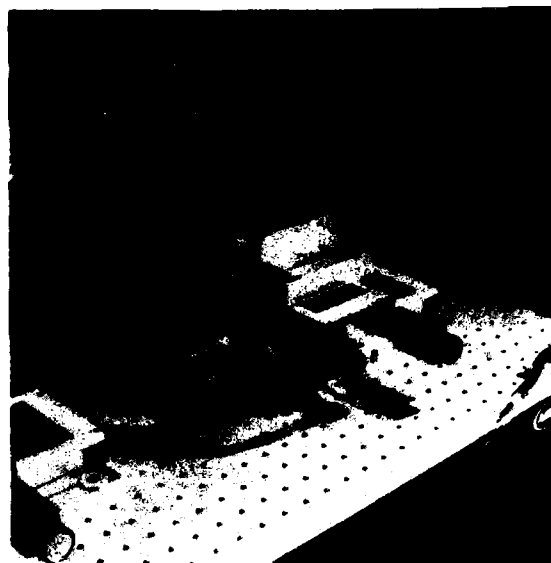


fig. 4 coupling system

#### The endface detection system

consists of two aligned 50  $\mu\text{m}$  core fibres with an endface separation of approx. 6 mm. The system measures the power transfer between these two fibres in a 30-40  $\mu\text{m}$  beam. By interrupting this beam with the fibre to be measured, the endface can be found with a  $\pm 1$   $\mu\text{m}$  accuracy. The initial increase of the power transfer when approaching with the fibre is due to reflection at the mirror-like endface of this fibre.

fig. 5 endface detection system



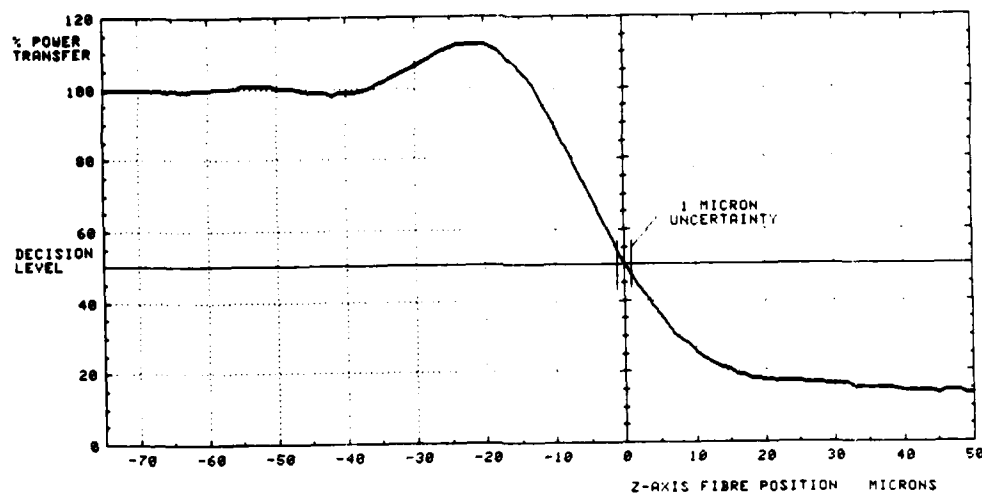


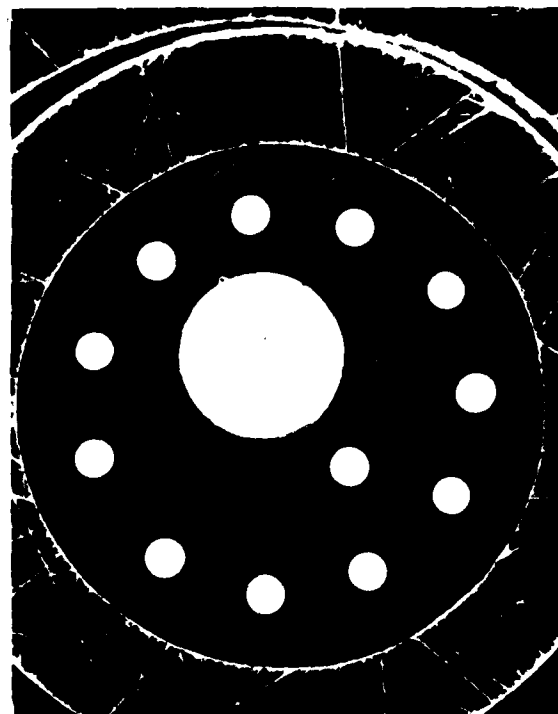
fig. 6 power transfer of endface detection system

The interface to the transmitter/receiver is a polished endface of a bundle of fibres contained in an injection needle. At the transmitter side this bundle consists of 12 50/125  $\mu\text{m}$  GI fibres, and a large core step index fibre for service and testing.

To obtain optimal connection at the receiver side, the fibres within the bundle are individually matched to the detectors. The intermediate distances between the fibres in the interfaces are measured once and stored in the computer system. Having optimised on any transmitter/receiver all other fibres can be found without reoptimisation of the fibre's position.

In order to avoid reflection problems the interface to the transmitters is wetted with a drop of glycerine.

fig. 7 transmitter interface



### Vacuum chucks

A measurement program can be executed on 1-12 fibres. Up to 12 fibres can be installed in the vacuum chucks, which enables a high precision alignment of the fibres in their radial direction. The largest uncertainty of the radial position is due to the variation of the fibre coating which is not stripped from the fibre before starting the measurement. Minor variations are due to coating eccentricity and to imperfect alignment of the vacuum groove and the Z-axis translator (approx.  $0.1^0$ ). Tests have shown a reproducibility of the fibre's position to better than 5  $\mu\text{m}$  in X direction and to better than 25  $\mu\text{m}$  in Y direction.

<u>radial offset (<math>\mu\text{m}</math>)</u>	X	Y
coating thickness	0	20
coating exc.	2	2
lateral var.( $\pm 1.5\text{mm}$ )	3	3
total	5	25

### Software design

To obtain a flexible, easy maintainable measurement system the software is highly structured and complementary to the hardware. All procedures are specified in reference tables for each measurement, transmitter and receiver. Small additional programs perform the actual read-out of measurement data and the data processing. The measurement system is connected to a fibre quality data base system in which quality and production data of each fibre are stored. Fast and easy retrieval of data on each fibre, cable order etc. is possible as well as production monitoring over a period of time.

## 5.1 Measurement cycle

In a measurement cycle three phases can be distinguished.

1. initialisation in which the fibre's identity is defined and a measurement tasklist is generated per fibre.
2. measurement in which the tasklist of each fibre is executed in a pre and a post cutback cycle.
3. data processing, again the tasklist is executed. Measurement data are calculated and stored in a data base file.

The three phases of a measurement cycle may overlap a subsequent measurement cycle, so during a measurement the data of a previous cycle may be processed and the tasklist for the next cycle may be generated.

### 5.1.1. Initialisation program

In the initialisation phase the operator may specify a fibre identity and an additional production code for each fibre position (1-12).

The program will then search the data-base for a prescribed measurement program for these fibres. When no program is specified the operator can specify one, or even generate a measurement by measurement tasklist for each set of fibres.

In this phase fibres can be also added or deleted from the data base, or updated (formation of bundles, cables etc). Also new measurement programs may be generated and/or assigned to a set of fibres.

### 5.1.2. Measurement program

The measurement program will execute the tasklist generated by the initialisation program. Each measurement (64 before cut back, 64 after cut back) is described in a measurement reference table by a transmitter, a receiver and a data processing program. Each transmitter (1-32) is described in a transmitter reference table by its position on the interface, its wavelength and, to switch it on, an equipment setting (address + command string).

Each receiver (1-16) is described in a receiver reference table by its position on the interface, a number of equipment settings and a readout program name.

The actual measurement data is obtained by the readout program and stored in an output file for the data processing program. The measurement program itself will perform the switching on and off of the transmitter and receiver, the positioning and optimisation of the fibres and guarding the measurement integrity of the fibres.

### 5.1.3 Data processing

The data processing program will execute the tasklist in combination with the output file of the measurement program. Each measurement has a specified data processing procedure which calculates the fibre data and stores it in the data base.

### 5.2 Additional software

Additional software has been written to update reference tables and to recalibrate the fixed positions in the system (service and maintenance). Fibre data can be extracted from the data-base with standard QUERY programs and may be printed on standard customer or internal forms.

## 6.

### Conclusions & Future aspects

This system has proven that large volume optical fibre high quality measurements are possible in a standard cable factory environment at a low cost level. In the near future the system will be extended to cover single mode fibre measurements as well.

NKF Optical Fibre Communication  
Waddinxveen Holland

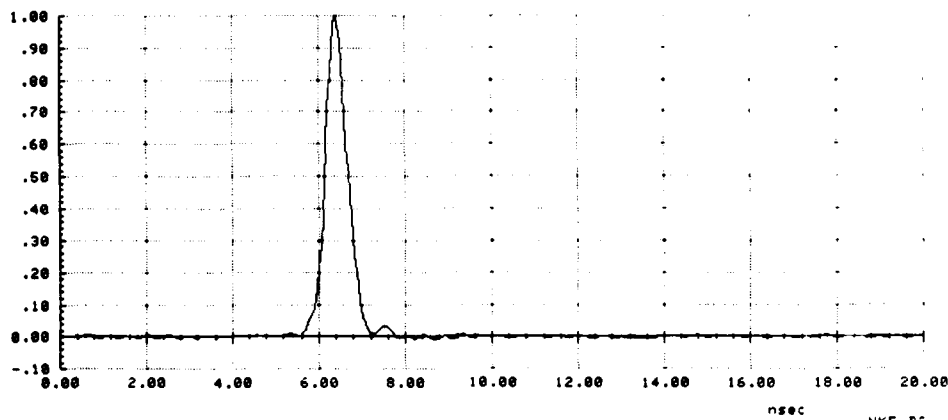
Date : 16-08-83  
Production code : 4  
Order : 3003905  
Cable : 1  
Article : 80029910

Fibre  
1 2083

Wavelength nm	Attenuation dB/km	Eff. NA	Gammafactor	Bandwidth MHz*km <sup>0.75</sup>	Disp. 10% nsec	Gauss Bw. MHz*km <sup>0.75</sup>
845	2.39			857	1.063	686

Backscattering : attenuation - 1.78 dB/km  
length - 1102 mtr.

845nm



NKF B1

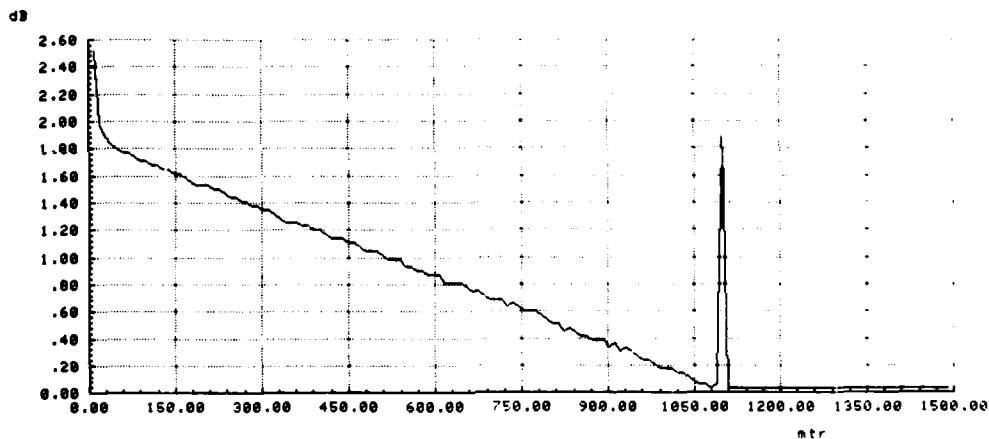
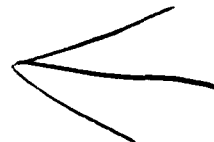


fig. 9 sample protocol

Wim L.S. Mathu was born in 1952 in Delft.  
After graduating from the Higher Technical College of Rotterdam in 1973, he joined NKF KABEL B.V., a member of the Philips Group, on a part-time basis, working on cable modelling and PCM measurement techniques.  
After obtaining a degree in electrical engineering from Delft University of Technology in 1980, he transferred to the Fibre Optics Development Group, where he is currently responsible for the development of optical fibre measuring equipment.



# REMOTE-ENDED TIME DOMAIN BANDWIDTH MEASUREMENTS ON INSTALLED REGENERATOR SECTIONS OF MULTIMODE OPTICAL FIBRE CABLE IN THE BRITISH TELECOM NETWORK

S Ahmad & B W Allen

British Telecom, Trunk and Junction Engineering Section, LLS3.4.2  
Carlton House, Carlton Avenue East, Wembley, England, HA9 8QH

## Summary

The measurement of bandwidth of multimode optical fibres is an established technique. It has normally been made on drums of fibre in the laboratory and on installed fibres where the distant-ends have been looped. In these cases both ends of the fibre are available at one location. This paper describes a technique developed for making time domain bandwidth measurements when both ends of the fibre are separated ie at two locations as in a telecommunication system. In the UK early systems had regenerator sections of up to 10 km long and 30 dB optical loss. The method described in the paper enables easy synchronisation of the transmitter and receiver of the measurement system over these sections. A comparison of results obtained for fibre on drum when tested with ends adjacent and when simulating ends remote is discussed. Measurements made on part of the British Telecom network of installed optical fibre cables are described and the uncertainties involved in these measurements are discussed.

## Introduction

Currently British Telecom are installing multimode optical fibre systems in the trunk and junction network. Much discussion has taken place about a suitable reference test method for the measurement of bandwidth of multimode optical fibres. Proposals have been put forward at the CCITT for measurements in the time domain<sup>[1]</sup> and the frequency domain<sup>[2]</sup>. The proposal put forward by British Telecom was for a time domain measurement<sup>[1]</sup>.

The time domain measurement requires precise synchronisation between the send and receive equipments and is essentially for measurements on drums of fibre, where few problems are presented. A time domain measurement on an installed regenerator section is more difficult since the send and receive equipments are separated by several kilometres.

The first generation of British Telecom optical fibre systems, operating at transmission rates between 8 and 140 Mbit/s, function with regenerator section lengths of approximately

10 km (30 dB attenuation).<sup>[3]</sup> The initial requirement was therefore for a measurement system to evaluate the bandwidths over at least 10 km of fibre.

A suitable technique for making remote-ended bandwidth measurements was required. This paper describes a technique developed which uses a second fibre as a synchronising link between the transmit and receive equipments. The technique was first proven in the laboratory by making conventional measurements on a drum of fibre (near-end) and then remeasuring the same fibre when simulating as a regenerator section (remote-ended). Results from these measurements are discussed in the paper.

Measurements were also made, using the technique developed, on installed fibres in the British Telecom Network.

Some of the results from these measurements are also given.

A brief resume of the measurement in the time domain is given below.

## The Time Domain Measurement<sup>[1]</sup>

The bandwidth of a multimode fibre is limited principally by two factors, mode dispersion and material dispersion. Material dispersion is a function of the linewidth of the light source. Since, in the measurements described the source is a laser, which has a narrow line width (2-4 nm), the effects of material dispersion can be ignored. Mode dispersion occurs because multimode fibres support many modes of propagation (500-1000 modes) and each mode has a different propagation velocity. If a short pulse is launched into the fibre then the variations due to the propagation times of the different modes will result in the pulse spreading as it propagates down the fibre. This will give an output pulse which is wider than the pulse launched into the fibre.

Time domain measurements are usually performed by launching a train of sub-nanosecond pulses  $g_1(t)$  into the fibre under test. The output pulses  $g_2(t)$  are detected at the far end of the fibre.

The fibre under test is then cut back, without disturbing the launch condition, and the transmitted pulses  $g_1(t)$  detected. The pulse waveforms are then transformed into the frequency domain by Fourier transform, giving  $G_1(\omega)$  and  $G_2(\omega)$ . The transfer function  $H(\omega)$  of the fibre can then be readily calculated from:-

$$H(\omega) = \frac{G_2(\omega)}{G_1(\omega)}$$

Amplitude and phase information are both available and in addition the impulse response can be obtained from the inverse transformation of  $H(\omega)$ .

The main problem with the time domain is that precise triggering of the sampling oscilloscope used at the receive-end is required. On a "drum" measurement this is overcome by the use of electrical links (having negligible jitter) between the pulse generator and (a) trigger pulse input to the oscilloscope and (b) the pulse input to the laser.

A schematic of the test equipment for conventional measurements of fibre on drum is shown in Fig 1.

#### Remote-Ended Measurement Considerations

On a practical regenerator section of an optical fibre route the two ends of the fibre are several kilometres apart.

One method of measurement is to "loop" the fibres at the distant-end and then to measure as for fibre on drum. This method suffers from:-

(a) the almost impossible task of detecting the test pulse, on long links, owing to the high value of loop attenuation.

(b) the difficulty of determining the bandwidth of individual fibres from the response of the looped fibres.

Another method is to trigger the oscilloscope at the remote-end with the incoming test pulse. However with the attenuation of the fibre over long links and the form of these pulses, which are very narrow and have low energy content the measurement becomes impracticable. This difficulty can be overcome by using a wider pulse for trigger purposes, however such a pulse is not suitable as a test pulse.

A solution can be achieved by using two pulses, a short pulse as a test pulse, and a long pulse for triggering (synchronising) the oscilloscope.

The methods considered for transmitting the trigger and test pulses were:-

(a) To couple the two lasers into the fibre under test with a suitable time difference between the two pulses. This requires the use of an optical coupler which reduces the transmitted pulse levels and complicates the launch conditions.

and (b) To use two fibres; ie in addition to the fibre under test, to use a control fibre to transmit the trigger pulse.

Method (b) was adopted.

#### Test Equipment

A schematic of the test equipment configured for remote-end bandwidth measurement is shown in Fig 2.

The test equipment is based on a commercially available waveform processing system<sup>41</sup> (this consists of a digitising sampling oscilloscope and a desk top computer) and suitable lasers and receivers.

The test pulse laser is a single heterostructure Gallium Arsenide type with a peak wavelength of 908 nm. The output pulse from this laser (Fig 3) has a rise time of 300 ps and a pulse width (FWHM) of 500 ps.

The trigger pulse laser is a multiheterostructure Gallium Aluminium Arsenide type with a peak wavelength of 850 nm. The output pulse from this laser (Fig 4) has a rise time of 1 ns and a pulse width (-50%) of <80 ns.

The optical receivers use ultra fast silicon avalanche photodiodes and are available commercially. These receivers have a radiant responsivity (1 MHz 50Ω  $R_L$ ) of 250 V/W and a -3 dB bandwidth of 1 MHz-2500 MHz.

#### Receive End Equipment

In Fig 2 Items (2), (3), (4), (5), (7) and (8) form the receive end equipment. The laser producing the long pulse (8) is triggered from the timing generator (4). This trigger is also delayed via a low jitter (<100 ps) digital delay generator to provide a trigger for the oscilloscope (3). The delay of the digital delay generator being approximately the combined delays of the control fibre and fibre under test.

At the receive end the incoming test pulse is detected by the APD receiver (2) and displayed on the sampling oscilloscope (3). The received signal is now available for processing using the mini-computer (8).

#### Transmit End Equipment

Items (1), (6) and (9) in Fig 2 form the transmit end equipment.

APD receiver (9) converts the long pulse from the laser into an electrical pulse suitable for the regenerator (6).

A schematic of the pulse regenerator is shown in Fig 5. It consists essentially of a commercially available trigger recogniser and pulse generator. The trigger recogniser has a sensitivity of 10 mV to 2 V (p to p 50%) in the frequency range d.c. to 1 GHz.

The pulse generator provides a 400 mV step output with a rise time of less than 1 ns to trigger the short pulse laser (1) used to generate the test signal. A passive delay line in the regenerator between the output of the trigger recogniser and the pulse generator allows the laser trigger pulse to be viewed on an oscilloscope. The pulse generator in the regenerator is wired as a repeater and works at the clock frequency of the timing generator (4).

#### Laboratory Measurements

Before remote-ended bandwidth measurements could be made in the field, it was necessary to prove the technique.

This was achieved by making measurements in the laboratory on a drum of fibre (near-end) and then remeasuring the same fibre simulated as a regenerator section (remote-end).

By making these measurements in the laboratory it was possible to set up the laser launch conditions on the test fibre and to change the measurement configuration from the near-end (Fig 6) to remote-end (Fig 2) without changing the launch conditions. It was also possible to trigger the laser in the same manner for both near-end and remote-end measurements by using the pulse regenerator (6) as configured in Figs 2 and 6.

Under these circumstances no additional measurement uncertainty due to the change of launch conditions or triggering of the short pulse laser was introduced when comparing the two methods.

Two drums of 50/125  $\mu$ m multimode optical fibre cable each with ten fibres were used for method evaluation purposes. The individual fibres within the cable on each drum were fusion jointed to produce two 4 km lengths of fibre on each drum. The fibre ends were then terminated with an optical fibre connector adopted by British Telecom for system usage.

The cable on one of the drums was used as the control fibre and the cable on the other drum as the fibre under test. Near-end measurements were made to detect a fibre output pulse with the equipment arranged as shown in Fig 6. The received pulse (near-end) was acquired, and signal averaging applied using the oscilloscope so that any errors due to random noise and any time jitter present on the system were minimised.

Without disturbing the launch conditions into the fibre, the equipment was rearranged as shown in Fig 2 and the receive pulse (remote-end) was then processed in the same manner as for near-end measurement.

The reference input pulse to the fibre was then obtained in the conventional manner by cutback, using the system connector as the cutback point.

This procedure was repeated for five sets of measurements on 4 km and 8 km lengths of fibre. 8 km lengths were achieved by joining the 4 km lengths with system connectors.

The results obtained are shown in Figs 7 and 8.

The laboratory measurements thus showed the feasibility of this technique of bandwidth measurement with the ends of fibre remote.

#### Field Measurements

The practicality of measurement was demonstrated on a British Telecom Proprietary Optical Line System. The route installed for a 8 Mbits digital system consisted of two sections.

(a) 8.8 km with an attenuation of 28 dB.

(b) 11 km with an attenuation of 32 dB.

The equipment was arranged as shown in Fig 2. The measurement was performed as for fibre on drum (remote-ended) with one exception, ie separate APD's were used for the receive pulse and the reference pulse into the fibre.

The response of the two APD receivers (2) and (9) were set up to be the same using the short pulse laser (1) before the fibre under test was measured. This response was checked after the measurement.

By aligning the two receivers it was possible to use the APD receiver (9) at the transmit-end for the "cut back" when making measurements on the fibre under test. To enable this another oscilloscope was used (not shown in Fig 2). Measurements were made on four fibres on each section of the cable route.

The results obtained were processed by the mini-computer (7) and are shown in Figs 9 and 10.

#### Discussion of Results and Measurement Uncertainties

The results were processed using FFT<sup>[5]</sup> techniques and the transfer function of the fibre computed. The software<sup>[6][7]</sup> provided by the manufacturer of the mini-computer was adapted for use for the remote-end measurements.

The prime causes of measurement uncertainties<sup>8)</sup> in a time domain bandwidth measurement are due to the following:

- (a) launch conditions
- (b) random noise
- (c) quantisation noise (in the sampling system)
- (d) time jitter
- (e) frequency resolution (due to the finite time window used for observing the signal).

Items (b) and (c) can be minimised by signal averaging and (d) can be minimised by careful selection of equipment with low jitter characteristics.

A complete analysis of measurement uncertainties in the time domain using a digital processing oscilloscope for signal acquisition is given in [9] and [10]. Various methods exist for the stabilisation of launch into a fibre. The method adopted in the measurement described was a restricted launch into the test lead<sup>1)</sup>.

All these measurement uncertainties apply equally to the near-ended and remote-ended measurements. It can be seen from Fig 7 that the spread of measurements in any pair of near/remote-ended measurements is small compared to the overall spread due to the change in launch conditions.

Fig 8 shows that the % error (with reference to the near-end measurement) of the remote-ended measurement is far less than the % error obtained from signal processing using a time window giving a 10 MHz frequency resolution.

#### Conclusions

A method and equipment for making time domain bandwidth measurements on connectorised regenerator sections of optical fibre cable has been described.

The method described requires an additional fibre as a control fibre for synchronisation between the receive and transmit equipments.

Since optical fibre cables in the British Telecom network are multi-fibre cables of eight fibres or more, an additional fibre is always available at the time of measurement for synchronisation purposes.

No significant measurement uncertainties have been introduced by the method described over and above those normally associated with a time domain bandwidth measurement.

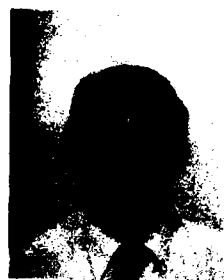
The feasibility of making measurements on installed cables with a practicable equipment has been demonstrated.

#### Acknowledgement

The authors are grateful to the Director Transmission Department, Local Line Services, British Telecom for permission to publish this paper.

#### References

- 1 CCITT Period 1981-1984: STUDY GROUP XV - CONTRIBUTION NO. 90 - Reference Test Method for Bandwidth.
- 2 CCITT Period 1981-1984: STUDY GROUP XV - CONTRIBUTION NO. 73 - Comments on the Reference Test Method of Baseband Amplitude Response. Source: Nippon Telegraph and Telephone.
- 3 R D Martin-Royle, G N Bennett Optical Fibre Transmission Systems in the British Telecom Network: An Overview. British Telecom Engineering Volume 1 Page 190.
- 4 "WP 1310 Signal Processing System" Tektronix Inc.
- 5 R W Ramirez "The FFT: Fundamentals and Concepts" Tektronix Inc.
- 6 C Flatau "Software for Computer-Controlled Measurement Systems" Tektronix Inc.
- 7 C Flatau "Measuring Complete Transmission Characteristics of Optical Fibres with Tektronix Signal Processing System". Tektronix Inc.
- 8 C Flatau "A Review of Error Reduction Methods for Optical Fibre Transmission Measurements". Technical Note TN-004 Tektronix Inc.
- 9 "Signal Averaging and Time Jitter", Appendix to Tektronix SPS Software Manuals.
- 10 D Hannaford "The Application of Picosecond Pulses in Time Domain Metrology". Proceedings of the 1972 Joint Measurement Conference, NBS Gaithersburg Md 1974.



S Ahmad  
British Telecom  
Trunk and Junction Engineering Section  
LLS3.4.2  
Carlton House  
Carlton Ave East  
Wembley, Middlesex  
ENGLAND  
HA9 8QH

Mr S Ahmad gain a BSc (Eng) in Electrical Engineering from London University in 1971. He joined British Telecom (then the British Post Office) in 1970.

Since 1973 he has worked in the External Plant Development Division and been engaged in the development of specialised test equipment and testing methods for coaxial and optical fibre cables.

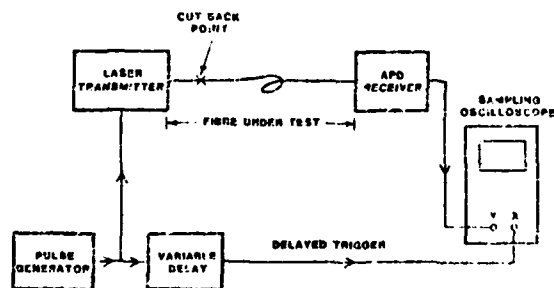


FIG 1

Conventional Measurements for Fibre on Drum



B W Allen  
British Telecom  
Trunk and Junction Engineering Section  
LLS3.4.2  
Carlton House  
Carlton Ave East  
Wembley, Middlesex  
ENGLAND  
HA9 8QH

Mr B W Allen gained a BSc in Electrical Engineering from the University of Salford in 1970, after which he joined British Telecom (then the British Post Office). Since 1977 he has worked in the External Plant Development Division where he has been engaged in the specialised testing of coaxial and optical fibre cables.

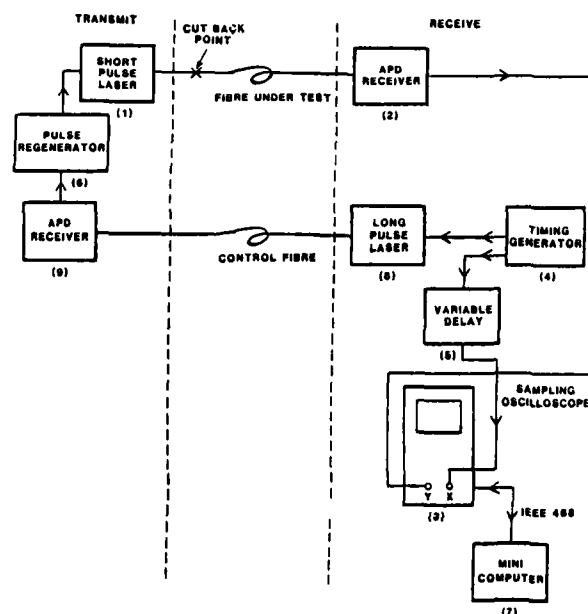


FIG 2

Remote-End Measurement

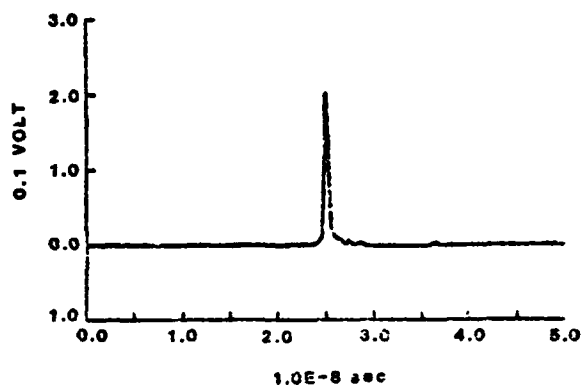


FIG 3  
Short Laser Pulse (Test)

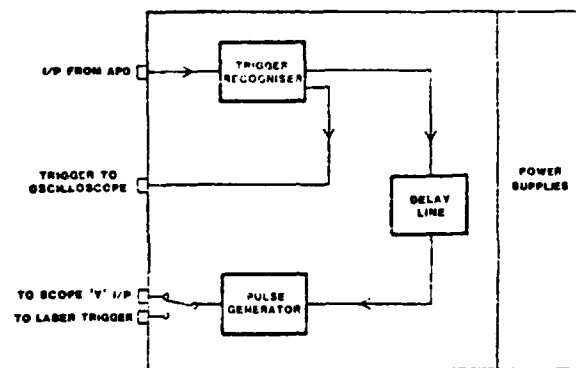


FIG 5  
Pulse Regenerator

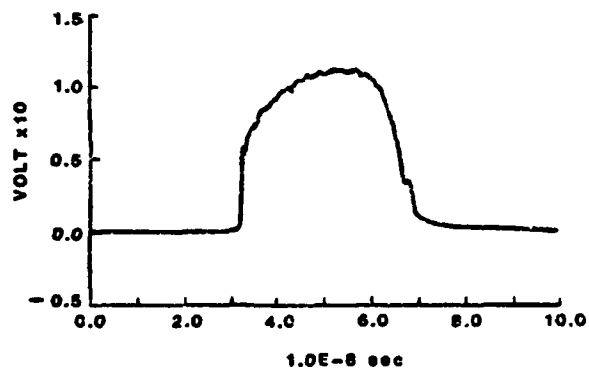


FIG 4  
Long Laser Pulse (Trigger)

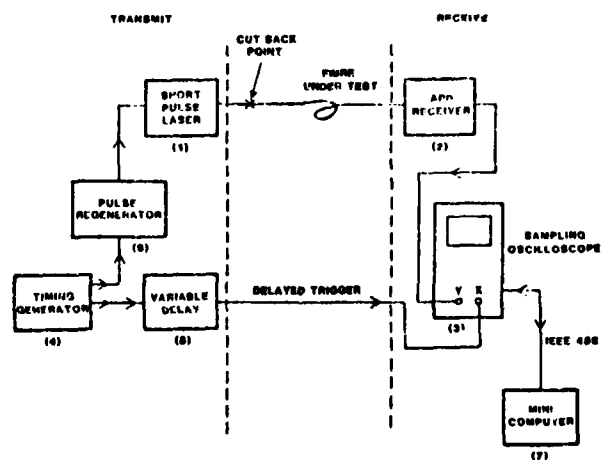


FIG 6  
Near-End Measurement

REMOTE ENDED TRIGGER LENGTH	TEST FIBRE	-3dB BANDWIDTH (MHz)		% ERROR (REMOTE) W.R.T NR END	% UNCERTAINTY DUE TO FREQ. RESOLUTION (10MHz)
		NEAR ENDED	REMOTE ENDED		
4km	A (GREEN) 4km	173.70	172.32	-0.79	$\pm 2.9$
		168.65	168.82	+0.10	$\pm 3.0$
		187.13	184.10	-1.60	$\pm 2.7$
		186.21	184.95	-0.68	$\pm 2.7$
		174.64	172.20	-1.39	$\pm 2.9$
4km	B (RED) 4km	129.67	130.70	+1.00	$\pm 3.9$
		135.20	135.04	-0.12	$\pm 3.7$
		132.29	132.60	-0.23	$\pm 3.8$
		128.24	128.40	+0.12	$\pm 3.9$
		123.11	122.40	-0.58	$\pm 4.1$
8km	A+B (RED + GREEN) 8km	103.19	100.35	-2.62	$\pm 4.8$
		98.06	97.78	-0.29	$\pm 5.1$
		101.75	100.36	-1.37	$\pm 4.9$
		97.08	96.38	-0.72	$\pm 5.2$
		92.75	93.40	+0.70	$\pm 5.4$

FIG 7

-3 dB Bandwidth for Fibre on Drum

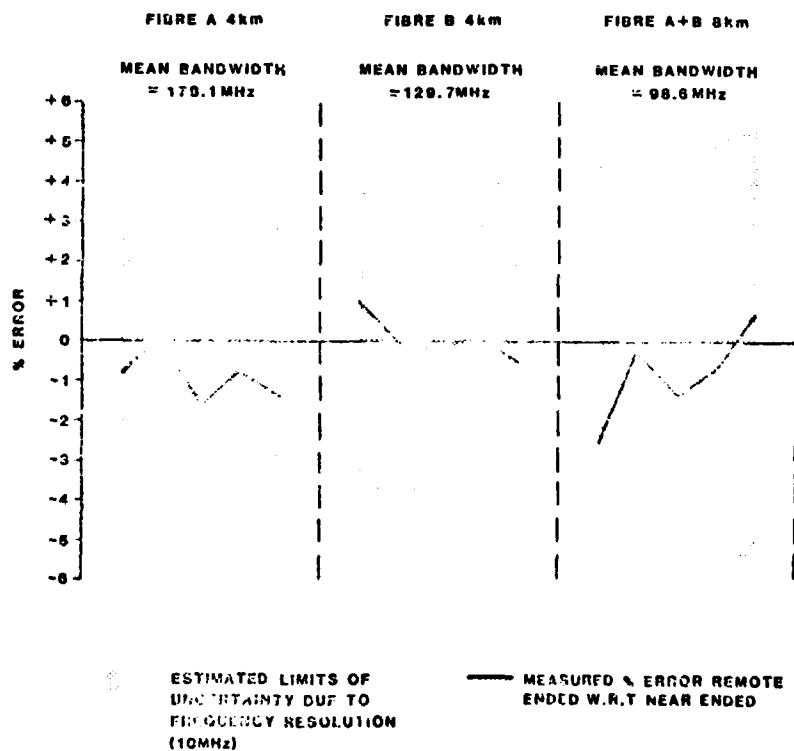
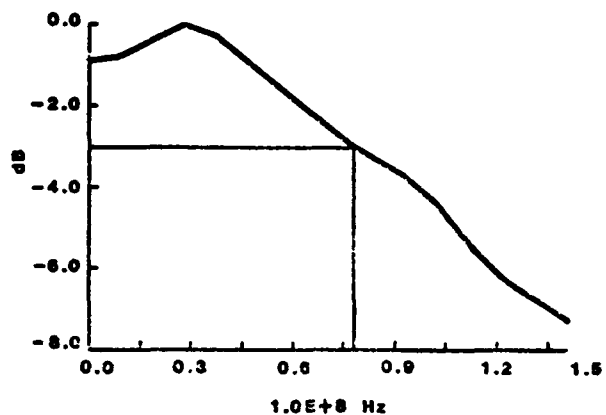


FIG 8

% Error of -3 dB Bandwidth (Remote-End) WRT Near-End for Fibre on Drum



-3dB BANDWIDTH = 82.89MHz  
FIBRE LENGTH = 8800m

FIG 9

Typical Bandwidth Curve

8Mbit/s ROUTE SECTION	FIBRE No.	-3dB BANDWIDTH (MHz)
A 8.8km	5	77.17
	6	88.91
	7	65.93
	8	82.89
B 11.0km	5	39.85
	6	45.16
	7	41.12
	8	42.88

FREQUENCY RESOLUTION 10MHz

FIG 10

-3 dB Bandwidth 8 Mbit/s Route  
(Remote-End Measurement)



## DEVELOPMENT OF SHORT-DISTANCE OPTICAL TRANSMISSION CORD

Masao Yuto, Yyozo Hayashi, Hiroaki Mukunashi, Satoru Iguchi

Sumitomo Electric Industries, Ltd.  
1, Taya-cho, Totsuka-ku, Yokohama 244, JapanAbstract

Two types of optical fiber cords designed for short-distance optical transmission are described. One of them uses plastic fiber as its core material. Its thermal resistance, solvent resistance, and mechanical properties are improved by coating it with a special resin sheathing. The other type is an improved version of the plastic clad silica fiber, in which the protrusion of the core at the ends of the cord has been minimized by selecting the optimal cladding material. Either type is characterized by its large core diameter and high numerical aperture. The ease with which cord ends, including connector attachments can be treated affords them broad applicability as short-distance optical links.

1. Introduction

Silica-glass optical fibers and cables are starting to be widely used for communications and long-distance data links. But such fibers, cables, and related systems are quite expensive because they require excellent transmission properties and high reliability for actual use. Along with the popularization of optical fibers and cables, the need has arisen for short-distance optical transmission cords that are inexpensive and easy to handle.

We have developed two types of optical fiber cords designed for short-distance optical transmission. One is a plastic fiber (All Plastic Fiber) cord usable at temperatures up to 90°C, and the other is a plastic-clad silica fiber (Modified Plastic Clad Fiber) cord with improved connection reliability. Conventional plastic fiber cords which are jacketed with PE, are only usable up to 70°C for long-term use. In contrast, APF cord can be used up to 90°C and has flame retardant properties provided by special coating material and usage of a PVC jacket. M-PCF cord has special cladding material to minimize the amount of fiber protrusion from the first sheath to only one fiftieth that of conventional cords.

Like conventional cords, both of our new cords have the merit of good coupling to LEDs because of their large core diameter and high numerical aperture.

2. Characteristics of New Cords

Two types of cords are intended for use at different distances: APF cords have a 300 dB/km transmission loss using 660nm LEDs and are mainly designed for use as links up to 30m long. M-PCF cords have a 30dB/km transmission loss using 860nm LEDs and are intended for use in links up to 150m long.

The fibers of these cords have high numerical apertures (NA): that of APF and M-PCF are 0.5 and 0.35, respectively. Table 1 shows the cords' structures and characteristics.

3. Initial Properties of New Cords

Initial properties needed for the design of short-distance optical transmission systems are the transmission loss, the numerical aperture and the diameter of the fiber which is inserted into connector plug. For commercial sale, the fluctuations of these properties are also significant. The value of these properties in each process are shown in Table 2.

Transmission losses of the cords are  $287 \pm 30$  dBm/km for (at 3σ value) for the APF and  $22.5 \pm 3.3$  dB/km for the M-PCF. The diameter of the APF coated fiber is  $0.910 \pm 0.51$  (at 3σ value) and that of the M-PCF bulk fiber is  $0.301 \pm 0.024$ . Both of the two cords have adequate initial properties for practical use.

The spectra of Figures 1 and 2 show that the optimum carrier wavelengths are 570 and 650nm for APF cords, and 660 and 800nm for M-PCF cords. However, currently use 660nm LEDs for the APF and 860nm LEDs for the M-PCF because of their reliability and price. For more effective use of the APF cord, the green 570nm LEDs must be commercially supplied.

4. Mechanical Test Results

Short-distance cords must be robust and simple because they are inexpensive and installed in narrow spaces such as vehicles and machine unit controls. Mechanical properties of the cords shown Table 1 for vehicle use were tested (Table 3 and Figure 3 and 4) and it was found that there are no significant problems.

## 5. Thermal and Environmental Test Results

Doped silica fiber for public communications and long-distance data links has been manufactured with great care in order to guarantee that good initial properties will endure. On the other hand, manufacture of short-distance cords requires fewer considerations to achieve the cords' limited aims. For example, the APF consists of plastic material so the thermal resistance has been significant. To check the spread of fire along the cord, the jacket should be flame retardant material. For M-PCF cords, on the other hand, it has been most significant to minimize the amount of core protrusion beyond the first sheath.

For APF cords, the aging properties at high temperature, the loss variations in the heat cycle and during heat shock, and the mechanical properties following the aging test are shown in Figures 5, 6, 7 and Table 4, respectively.

From these results, APF cords with special coating can clearly be used up to a maintained temperature of 90°C. In addition, these cords have good transmission loss in a typical environment, and show little mechanical damage after aging.

With regard to M-PCF cords, in the process of selecting the optimum cladding material, the relationships of cladding material hardness to core protrusions were investigated. The protrusion properties of the new fiber have been confirmed through further testing. Test results are shown in Figures 8 and 9.

The losses monitored in the heat cycle test are shown in Figure 10. The progressive loss variations over the course of the thirty-day test in high temperature conditions are shown in Figure 11.

From these results, it can be seen that M-PCF cords have protrusion values one fiftieth of the PCFs'. Moreover the loss variations in typical conditions are too slight to be considered.

## 6. Applications

Short-distance optical transmission cords have been applied in control and data links in vehicles, ships and factories. APF cords are used primarily in multiplex wiring harnesses in motor vehicles. In these systems, control signals for door windows, vent windows and door lamps are transmitted by fiber optics<sup>[1]</sup>. Photos 1 and 2 show the applications of APF cords to data links and wiring harnesses. M-PCF cords are applied in longer links and systems such as the control of ventilation systems in buildings. Recently the need for lower transmission loss (10dB/km) M-PCF cords for control systems in factories has arisen. In addition, complex cables with metal wires and multi-flat cables will be developed in the near future.

## 7. Reference

- [1] N. Yumoto, et al. "Optical Data Link for Multiplex Wiring", SAE paper 830320

Table 1 Characteristics of New Cords

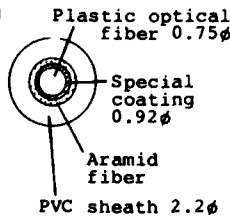
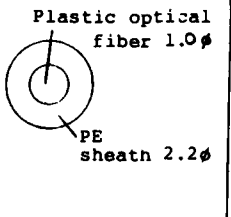
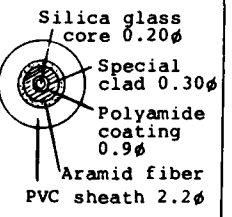
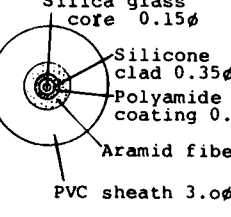
	Plastic cord		PCF cord	
	APF	Conventional	M-PCF	Conventional
Structure				
Characteristics of New Cords	<ul style="list-style-type: none"> <li>• Use at temperature up to 90°C</li> <li>• Good flame retardance</li> <li>• High tension strength</li> </ul>		<ul style="list-style-type: none"> <li>• Good core protrusion property</li> <li>• Easy core polishing</li> </ul>	

Table 2 Initial properties

	Properties		Bulk fiber (core/clad)	Coated fiber	Cord	Measurement
APF	Loss (dB/km)	$\bar{x}$ $\sigma$	309 18	287 16	287 11	Light source: 660nm LED Insert NA: 0.40 Method: Cut back
	Diameter (mm)	$\bar{x}$ $\sigma$	0.754 0.010	0.910 0.017	2.21 0.05	Method: micrometer caliper etc.
M-PCF	Loss (dB/km)	$\bar{x}$ $\sigma$	21.7 1.2	22.7 1.1	22.5 1.1	Light source: 860nm LED Insert NA: 0.40 Method: Cut back
	Diameter (mm)	$\bar{x}$ $\sigma$	0.301 0.008	0.891 0.010	2.16 0.06	Method: Micrometer caliper etc.
	N.A.	$\bar{x}$ $\sigma$	0.339 0.012	— —	0.340 0.010	Method: FFP Length: 2m Value: 90% power

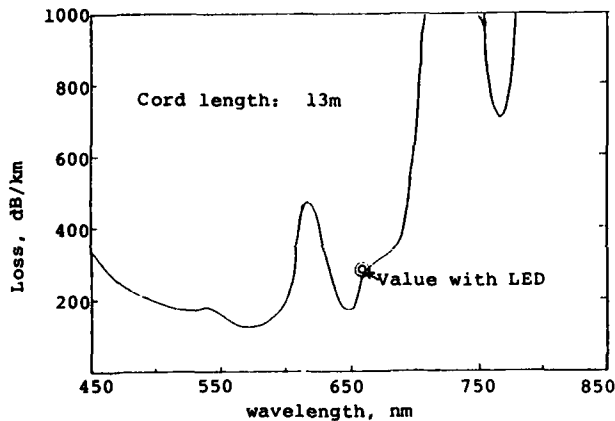


Figure 1 Loss Sepctrum of APF Cord

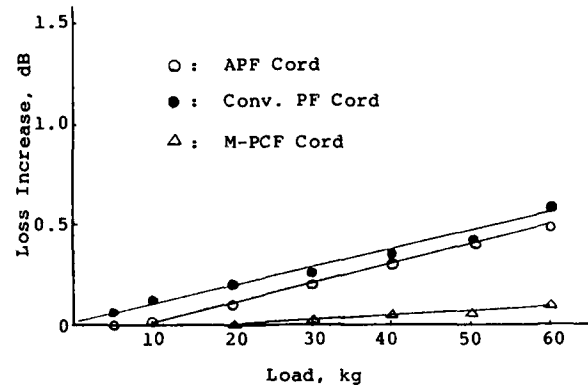


Figure 3 Compression Property

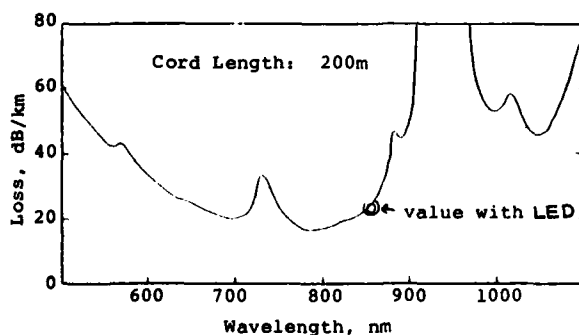


Figure 2 Loss Spectrum of M-PCF cord

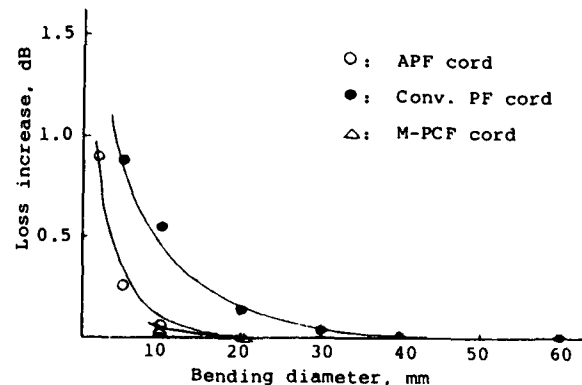

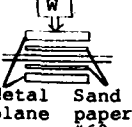

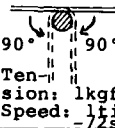




Figure 4 A half bending property

Table 3 Mechanical Tests

Test Cord	Tension	Compression (60kgf)	Bending (a half turn)	Continuous Bending (10 <sup>4</sup> times)	Winding (5 turns)	Twisting (10 turns)
APF cord	0dB (10kgf) Break strength is 25kgf	0.5dB	0.02dB	0.03dB	0.01dB	0dB
M-PCF cord	0dB (10kgf) Break strength is 30kgf	0.1dB	0.01dB	0.06dB	0.01dB	0.01dB
Conven- tional PF cord	Yield strength is 8.5kgf	0.6dB	0.34dB	0.1dB	0.15dB	-
Note	Separation  Length: 300mm Separation Speed: 100mm/min	 Metal Sand plane paper #60 Length: 200mm	Mandrel 20φ 	Mandrel 12φ  90° 90° Ten- sion: 1kgf Speed: 1time -72sec	Mandrel 30φ 	Tension: 10kgf Length: 300mm 

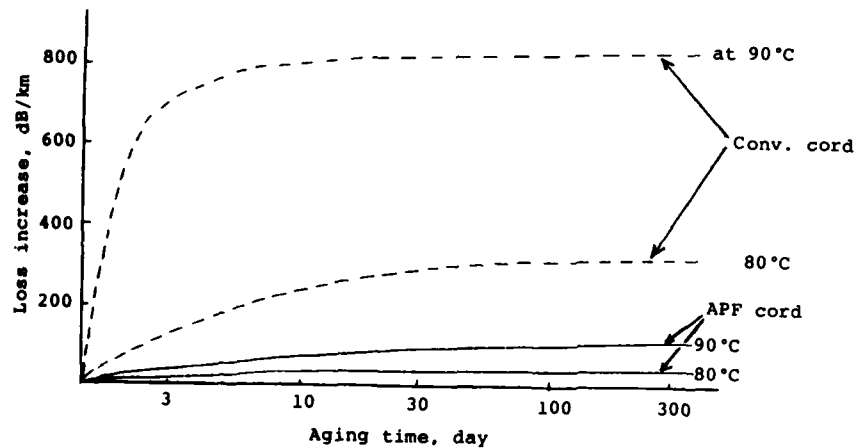


Figure 5 Heat aging properties of APF cord

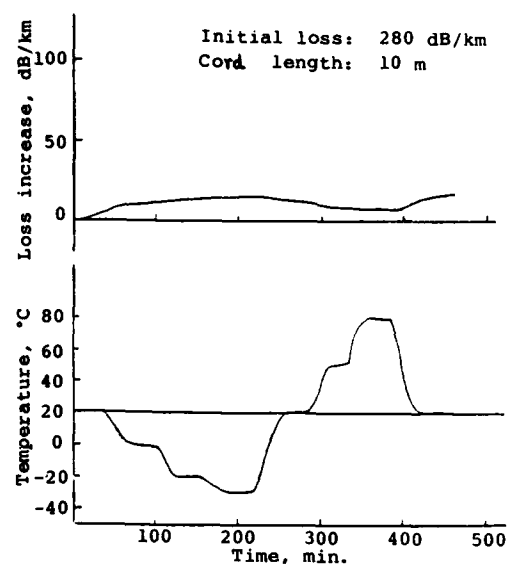


Figure 6 Heat cycle property of APF cord

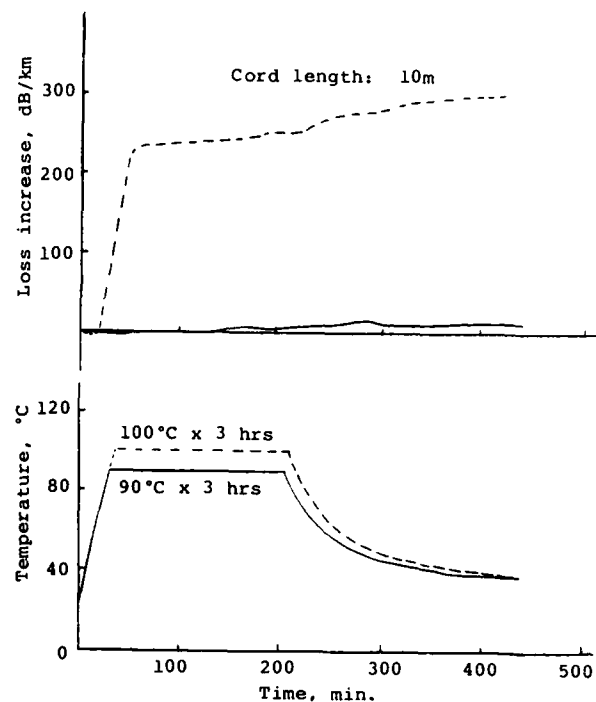


Figure 7 Heat shock properties of APF cord

Table 4 Mechanical Properties after Aging Tests of APF Cord

Item	Evaluation		APF cord	Coated fiber	Bulk fiber
	Properties	Aging Tests			
Continuous Bending	Bending Times at Break	Original	$>10^4$	$>10^4$	4100
		in 70°C water 180 days	$>10^4$	9000	1300
		in 90°C air 320 days	$>10^4$	3900	770
Tension	Strength at Break	Original	29	5.1	4.1
		in 70°C water 180 days	29	5.5	4.2
		in 90°C air 320 days	29	5.8	4.3

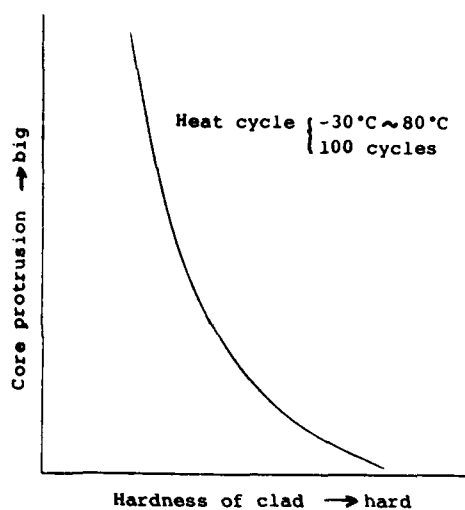


Figure 8 Core protrusion dependence on clad hardness

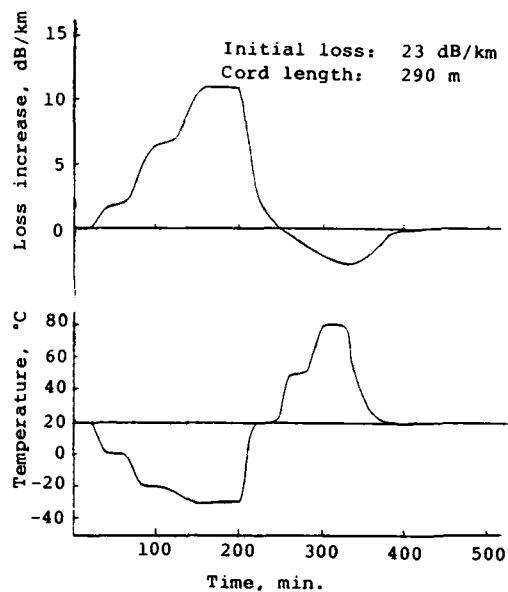


Figure 10 Heat cycle property of M-PCF cord

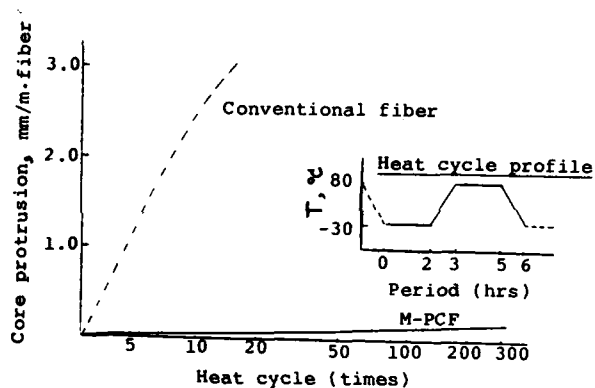


Figure 9 Protrusion properties of M-PCF

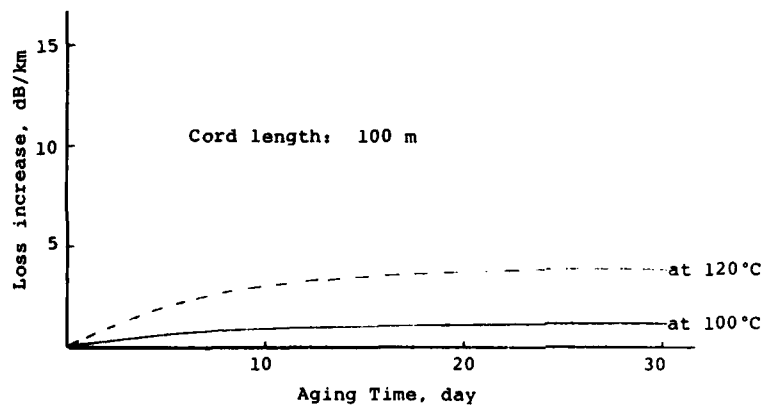


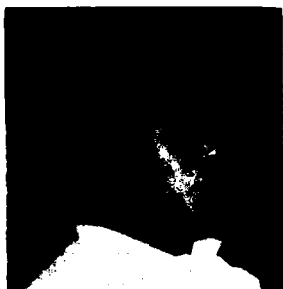
Figure 11 Heat aging property of M-PCF cord



Photo 1 Bidirectional optical data link



Photo 2 Wiring harness for door  
(Combining optical connector cord  
with electrical wiring)



Masao Yuto  
(Speaker)  
Sumitomo Electric  
Industries, Ltd.  
1, Taya-cho, Totsuka-ku,  
Yokohama, Japan

Masao Yuto received his B.S. degree in applied chemical engineering from Kyushu University in 1971. He then joined Sumitomo Electric Industries, Ltd., and engaged in research of plastic materials for optical cables. Mr. Yuto is now a senior engineer of Yokohama R & D Department in R & D Group.



Hiroaki Mukunashi  
Sumitomo Electric  
Industries, Ltd.  
1, Taya-cho, Totsuka-ku,  
Yokohama, Japan

Hiroaki Mukunashi received his B.S. degree in applied chemical engineering from Tohoku University in 1967. He then joined Sumitomo Electric Industries, Ltd., and engaged in research of plastic materials for communication cables. Mr. Mukunashi is now a Chief Research Associate of Yokohama R & D Department in R & D Group, and a member of the Society of Polymer Science of Japan.



Kyozo Hayashi  
Sumitomo Electric  
Industries, Ltd.  
1-3 Shimaya 1-chome  
Konohana-ku,  
Osaka, Japan

Kyozo Hayashi received his B.S. degree in mechanical engineering from Kyushu Institute of Technology in 1971. He then joined Sumitomo Electric Industries, Ltd. Mr. Hayashi is now a senior engineer of Engineering Section, Future Wiring Harness Project Group in R & D Group.



Satoru Iguchi  
Sumitomo Electric  
Industries, Ltd.  
1, Taya-cho, Totsuka-ku,  
Yokohama, Japan

Satoru Iguchi received his B.S. degree from Waseda University. After graduation he joined Sumitomo Electric Industries, Ltd. Mr. Iguchi is now a member of Fiber Optics Systems Engineering Section, Fiber Optics Division, and a member of the Institute of Electrical Communication Engineers of Japan.

# THERMAL PROPERTIES OF LOOSE TUBE SECONDARY COATED OPTICAL FIBRES EXPERIMENTALLY DISCUSSED BY A RELATIVE LIGHT PULSE DELAY TECHNIQUE

Hans Damsgård

Aktieselskabet Nordiske Kabel- og Traadfabriker  
NKT Electronics  
Copenhagen, Denmark

## Abstract

For silicone primary coated optical fibres in loose tubes it is observed that the  $\pm 150^{\circ}\text{C}$  wide temperature interval of no excess loss can be much broader than the temperature interval where the fibre is stress free, and therefore it is most important to be able to control the latter of these intervals as well. The upper limit of this stress free temperature interval is precisely measured by a new interpretation of the temperature versus light propagation time curve, and for the first time it is reported that this upper limit can be controlled over a wide range in agreement with a simple model of the extrusion process. In addition, dynamical relaxation is observed and one result is a shrinkage as low as 0.35% after 160 hours exposure at  $70^{\circ}\text{C}$ . Loose tube fibres with silicone primary coating and polycarbonate secondary coating show excellent and stable optical and mechanical properties in a large temperature window.

experimentally and until now, it has been the practice to identify this interval with the temperature interval where the fibre is stress free.<sup>1,2</sup>

In this work, direct measurements of the upper limit of the stress free temperature interval have been performed by measuring as a function of temperature the change in time delay of short light pulses passing through the loose tube jacketed fibre. By such relative light pulse delay (RLPD) measurements, it has been found that this stress free temperature interval can be much narrower than the temperature interval of no excess loss. Further, it has been observed that in accordance with a simple model of the extrusion process the position of the stress free temperature interval can be accurately controlled by manipulating the extrusion conditions such as back tension force, cooling water temperature, and other extrusion parameters.

## Introduction

To assure long-term optical and mechanical stability of fibre optic cables operating at varying ambient conditions, it is of fundamental importance that the glass fibres are not exposed to external longitudinal stress in order to protect the fibres against static fatigue. Therefore, it is necessary to be able to carefully control the thermal properties of the secondary coated fibres.

One common way to apply the secondary coating to an optical fibre is to extrude a loose tube around the fibre. An optical fibre in a loose tube of a certain radius of curvature will only remain unperturbed in a limited temperature interval due to the difference in thermal expansion coefficient of the glass and plastic materials. These perturbations, occurring at low and high temperatures, might induce excess loss in the optical fibre due to bendings and micro-bendings. The observed excess loss depends strongly upon the hardness of the primary coating material. The temperature interval, where no excess loss is observed, can easily be determined

Finally, it has been shown that this measurement technique is most suitable to study dynamical relaxation phenomena, for example, shrinkage of the extruded plastic tubes at elevated temperatures.

## Measurement Procedure

The measurements were performed using the equipment shown in Fig. 1.<sup>3</sup> Short light pulses ( $\leq 0.3$  ns FWHM) are obtained from an 850 nm laser, and these pulses are divided in two parts in the Y-coupler; one passing through the fibre to be measured placed in temperature controlled environments, the other launched onto the avalanche photodiode through a short reference fibre. The high degree of stability of the 5 MHz external triggering oscillator assures that the relative time difference between the two pulses can be obtained accurately, the measuring time being 5-10 seconds, typically.

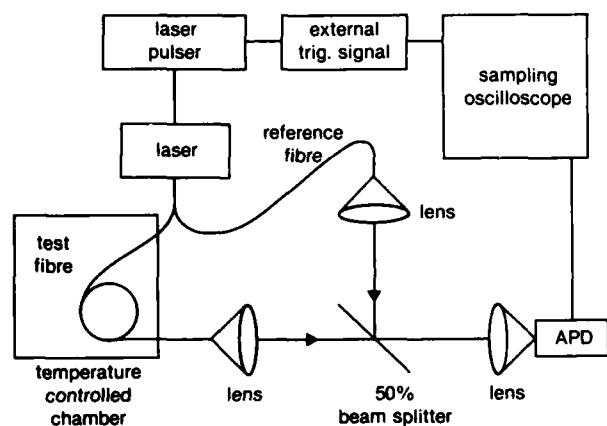


Figure 1. Schematic diagram of relative light pulse delay measurement experiment.

In general, variations in the surrounding physical conditions experienced by the optical fibre imply relative light pulse delay changes, and RLPD-data at different temperatures are related to the stress state of the fibre. However, it is necessary to take into account the dependence of the refractive index on temperature and stress in the evaluation of the data. In all the experiments,  $B_2O_3-P_2O_5-GeO_2$  doped 0.20 NA multimode fibres were used, and in Fig. 2 the elongation versus light pulse delay change curve for that type of primary coated fibre is shown as obtained by our experiments.

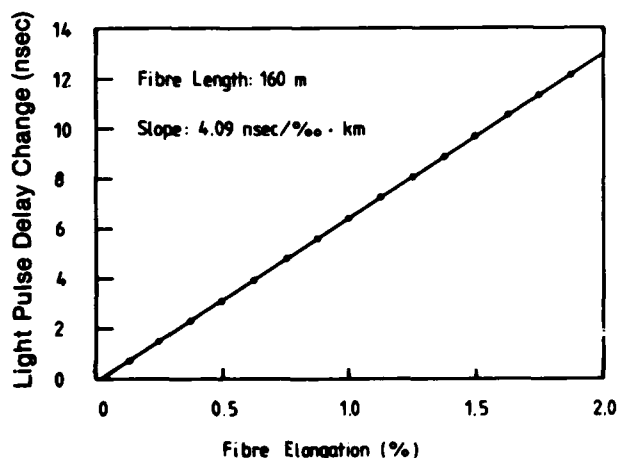


Fig. 2 Transmission time versus fibre elongation curve at 25°C for a  $B_2O_3-P_2O_5-GeO_2$  doped 0.20 NA multimode fibre

The slope is 40.9 nsec/% · km, whereas the pure length effect is

50.0 nsec/% · km. The difference is caused by the decreasing refractive index with increasing stress.<sup>5</sup>

The fast RLPD-data storage makes the method most suitable for observing dynamical processes, for example shrinkage of the (loose tube) jacketed fibres, and such measurements can be performed as accurately as 0.05% on an absolute scale by using the Fig. 2 curve-slope as a conversion factor from delay change to change of fibre length.

A typical RLPD-curve is shown in Fig. 6. At lower temperatures the fibre is in an unstressed mechanical state, i.e., the 38 psec/°C · km of the slope of the curve in that region represents internal physical properties of the doped glass material, only. In contrast, at higher temperatures, the variation of the light pulse propagation time through the fibre is mainly determined by the thermal expansion of the secondary coating material, the mechanical state of the fibre is stressed and a quite different line slope, 180 psec/°C · km, is observed. Also, the direct consequence of the measured shrinkage is seen in Fig. 6, namely a shift of the stress free temperature interval.

#### Theoretical Model of the Extrusion Process

The fibre length relative to the length of the plastic tube may be expressed in terms of the temperature  $T_n$  when of equal length. In a simple model this temperature  $T_n$  is expressed as

$$T_n = T_p - \left( \frac{\Delta l}{l} \right)_F \beta_p^{-1} - \zeta \beta_p^{-1}$$

where  $\beta_p$  is the thermal longitudinal expansion coefficient of the plastic and  $\left( \frac{\Delta l}{l} \right)_F$

is the fibre elongation caused by the applied back tension force and where  $\zeta$  is a geometrical factor taking into account the bending of the secondary coated fibre in the region where the fibre back tension is transferred to the plastic tube.  $T_p$  is the temperature of the plastic tube in said region, and a proper approximation to the formula above is to assume that  $T_p$  equals the temperature of the cooling water source which is located beyond the extruder head.

Disregarding the stress induced at some part of the fibre surface by the coiling of the fibre, the upper limit  $T_u$  of the temperature interval, where the fibre is not exposed to external longitudinal stress and which may be directly measured is given by the equation

$$T_u = T_n + 0.5 \epsilon_F \beta_p^{-1}$$

where  $\epsilon_F$  is the radius of curvature dependent free space for the fibre.<sup>2</sup>

### Experiments and Discussion

#### Comparison between Optical and Mechanical Performance.

The table shows the values of the most important parameters. All of the fibres were 0.20 NA  $P_2O_5 - B_2O_3 - GeO_2$  doped multimode fibres supplied with a 280  $\mu m$  O.D. silicone primary buffer coating. In most of the experiments 88  $\mu m$  O.D. glass fibres were used corresponding to half the cross sectional area of 125  $\mu m$  fibres. The reason being to reduce the degree of mutual interaction between the plastic and the fibre at elevated temperatures. The inner and outer diameter of the polycarbonate plastic tubes were 0.8 and 1.4 mm, respectively.

TABLE OF EXPERIMENTS

Number of Experiment	Back Tension Force (newton)	Cooling Source Temperature (°C)	Fibre Diameter ( $\mu m$ )	Inner Diameter of Plast Tube (mm)	Fibre Length (m)	Measured Upper Limit of Stress-Free Temperature Interval (°C)	Measured Upper Limit Transformed to Coil Curvature: 100 mm
1	1.5	40	125	0.78	2800	30	40
2	1.25	60	88	0.75	620	25	31
3	1.25	20	88	0.78	780	7	14
4	2.0	40	88	0.78	500	-20	-14
5	1.25	40	88	0.77	845	10	16
6	0.5	40	88	0.77	660	39	45

The results of the experimental investigation of the Experiment 1 fibre is illustrated by Fig. 3. At temperatures below 30°C, the fibre is in an unstressed mechanical state as opposed to the temperature region above 30°C. During the

measurements, the actual radius of curvature interval for said fibre was 110 mm to 150 mm implying a weighted average coil curvature  $R = 133$  mm. Hence, by using the thermal coefficient of expansion of the plastic material  $6 \times 10^{-5}/^{\circ}C$ , the lower limit  $T_L$  of the stress free interval, i.e., where the fibre starts to buckle, was calculated to be  $-32^{\circ}C$ . Transformation to  $R = 100$  mm, which is typical in many cable constructions, gives a stress free temperature interval from  $-42^{\circ}C$  to  $41^{\circ}C$ . Now assuming the acceptance of a 1% fibre elongation, which is realistic because this value is less than 1/4 of a typical proof test level, the long term operational temperature region is from  $-42^{\circ}C$  to  $66^{\circ}$ , and this interval becomes significantly extended, whenever the secondary coated fibre is firmly fixed to a strain relief member characterized by a low thermal expansion coefficient.<sup>4</sup>

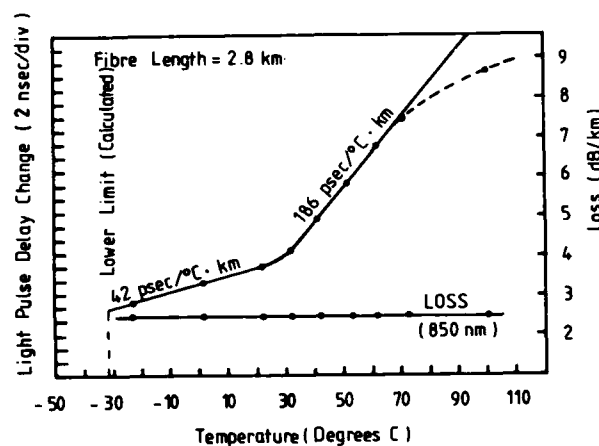


Fig. 3 Stress free and optical temperature intervals for a silicone coated multimode fibre in a loose polycarbonate tube. The full RLPD curve is the delay characteristics predicted by the theoretical model of the extrusion process - Coil curvature range: 110 mm to 150 mm - Note that the fibre might become significantly stressed without inducing additional loss (Exp. 1 - See Table of Experiments)

Also, the optical temperature interval of the same fibre was investigated, and the fibre loss versus temperature curve is shown in Fig. 3 as well. No loss increase was observed from  $-25^{\circ}C$ , which was the lowest measuring temperature, to  $100^{\circ}C$ , from which was concluded that the interval of no excess loss extends far above the temperature interval, where the fibre is stress free. The extremely

satisfactory temperature characteristics with respect to optical attenuation are mainly due to the buffer effect of the primary coating material and to a high degree of thermal stability of the secondary coating.

The two-mode curve, also shown in Fig. 3, is the RLPD-characteristics predicted by the model of the extrusion process which was discussed in the preceding paragraph. The smooth transition from the low to the high slope region around 30°C is due to the actual radius of curvature range 110-150 mm experienced by the fibre and which was also accounted for in the theoretical calculations. The theory compares most satisfactorily to the Experiment 1 data (below 70°C). This item is further discussed in the following sections.

The behavior of the experimentally obtained RLPD-curve above ~70°C is either due to a decreasing plastic stiffness, i.e., the Young modulus starts decreasing with an increase in temperature or due to a fast shrinkage occurring simultaneously with the fibre heating process.

#### Controlling the Fibre Excess Length

In the design of fibre optic cables with respect to temperature characteristics, it should be taken into account that the most suitable stress free temperature interval of the loose tube secondary coated fibre depends on

- type of cable,
- service environments,
- cabling procedure,
- accepted level of fibre elongation,
- and
- specifications in general.

Hence, it is most important to be able to control the fibre excess length in the loose plastic tube. In Fig. 4, it is illustrated that the upper limit  $T_u$  of the temperature interval, where the fibre is not exposed to external longitudinal stress, can be adjusted in almost perfect agreement with the proposed theoretical model of the extrusion process. The back tension force applied to the fibre was changed, and the cooling water temperature was fixed at 40°C in the experiments shown in Fig. 4. The negligible two degrees systematical deviation observed is explained by the approximation introduced in the paragraph dealing with the model of the extrusion process. The fibre remains

some time in ~300°C air before the transfer of the back tension force takes place, and therefore some further cooling or heating occurs in this region: For cooling water temperatures in excess of ~30°C,  $T_p$  will be lower than the water temperature, and the approximation will give too high a value of  $T_u$ . In contrast, cooling water temperatures below the environmental temperature will imply that the theory predicts too low  $T_u$  values. The more pronounced effect of the approximation is seen by Fig. 5.

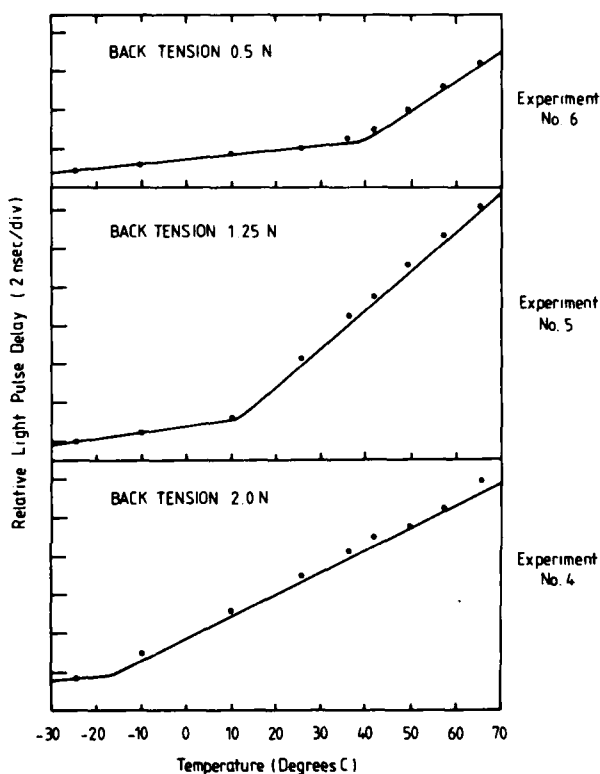


Fig. 4 Controlling the fibre excess length in the loose polycarbonate tube by changing the back tension force for fixed cooling source temperature. The full curves are the delay characteristics predicted by the theoretical model of the extrusion process.

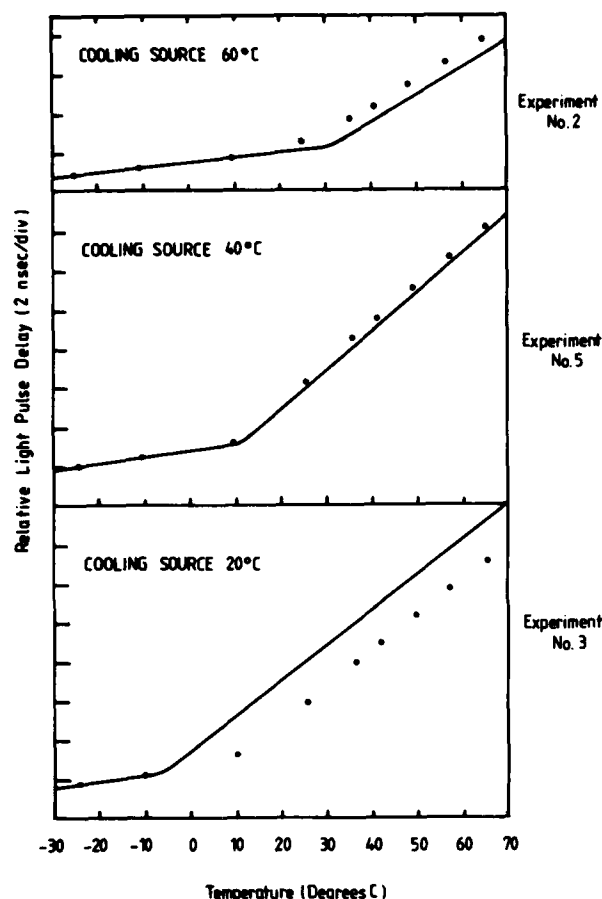


Fig. 5 Controlling the fibre excess length by changing the temperature of the cooling source for fixed back tension force  
The data are given in the Table of Experiments - The full curves are the predictions of the theoretical model which seems to overestimate the effect of the cooling source - See text

### Shrinkage

It has been concluded that it is possible by a uniform well controlled extrusion process to adjust the fibre length relative to the length of the plastic tube in agreement with a theoretical model. Obviously, it is of primary importance to know whether this length ratio does change with time and if so, to find the cause for the change.

Because such dynamical relaxation phenomena are primarily expected to take place at higher temperatures, thermal stability of loose tube polycarbonate

jacketed optical fibres were investigated at elevated temperatures.

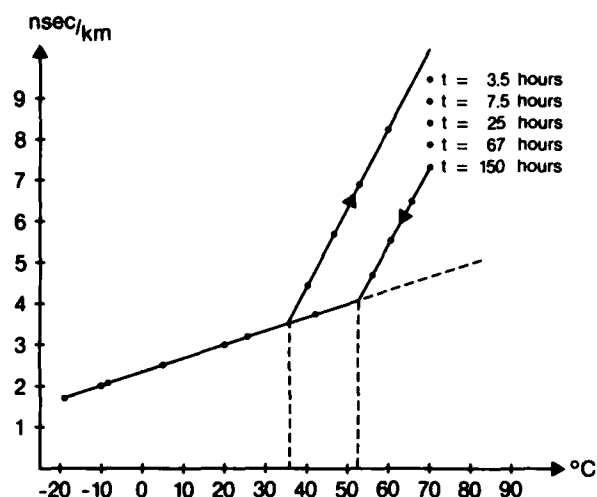


Fig. 6 RLPD measurement before, during, and after shrinkage  
The stress free temperature interval is shifted to the right by the recorded dynamical relaxation

Fig. 6 summarizes the result of a RLPD-measurement before, during, and after shrinkage. The measurements were performed from  $-20^{\circ}\text{C}$  to  $70^{\circ}\text{C}$ , and when  $70^{\circ}\text{C}$  were reached, the fibre was exposed to this temperature for 150 hours. After this procedure, as it is also shown in Fig. 6, the stress free temperature interval was measured again and a  $\sim 17^{\circ}\text{C}$  increase of the upper limit of the interval induced by the 0.73% shrinkage was observed. To investigate the dependence of the shrinkage process on the level of compressive strain experienced by the plastic tube (due to the fibre elongation), a series of 3 experiments was carried out at  $71^{\circ}\text{C}$ , each of these characterized by a specific level of fibre excess length in the plastic tube.

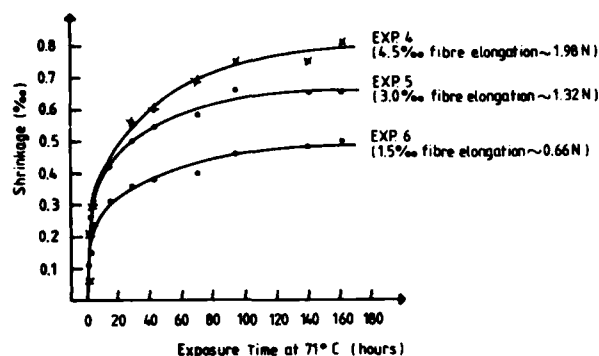


Fig. 7 Dynamical relaxation characteristics for loose tube polycarbonate secondary coated optical fibres at 71°C

The degree of the irreversible dynamical relaxation depends strongly upon the level of compressive strain experienced by the plastic tube

The results are shown in Fig. 7. The lower of the curves refers to a fibre elongation of 1.5% at 71°C, the medium curve to a 3.0% elongation at 71°C, and the upper curve to a 4.5% elongation, also at 71°C. The equivalent forces are 0.66 N, 1.32 N, and 1.98 N, respectively. The cross section area of the tubes are approximately 1 mm<sup>2</sup>. The shrinkage process depends strongly upon the level of compressive strain experienced by the plastic tube induced by the fibre elongation. In Fig. 8, the shrinkage after 160 hours exposure at 71°C is plotted against the actual compressive force acting at the process. The figure indicates a linear relationship and extrapolation to zero compressive strain results in a shrinkage value as low as 0.35% after the 160 hours exposure to 71°C as compared to 0.49% at 0.66 N, 0.66% at 1.32 N, and 0.79% at 1.98 N. Even at very high compressive strain values, the observed shrinkage is as low as 0.8%; hence, the conclusion that polycarbonate exhibits extremely good thermal stability at 70°C.

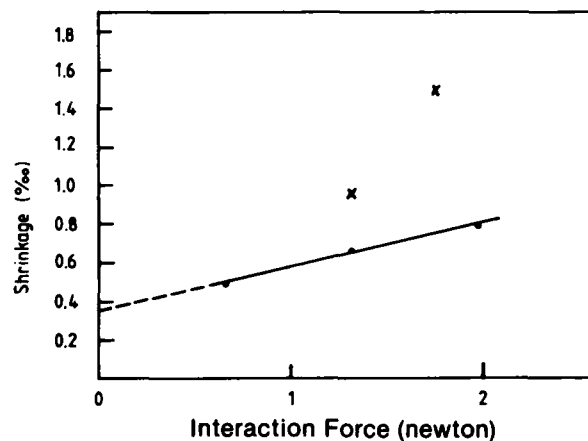


Fig. 8 Shrinkage after 160 hours exposure at 71°C (•) and at 92°C (x) as a function of mutual interaction forces between the glass fibre and the plastic tube material

A similar investigation has been performed at 92°C, and the results are shown in Fig. 9. Here, a faster and larger shrinkage was observed, and also the dependence on the mutual stress interaction force acting between the glass fibre and the plastic tube is more pronounced. However, the shrinkage values obtained at 92°C might be somewhat overestimated because they are based upon a linear RLPD-curve from  $T_u$  to 92°C as it is illustrated by Fig. 3, and it has not been firmly ascertained whether the curved nature of the RLPD-characteristics at temperatures above ~70°C are due to a decreasing Young modulus or to a fast shrinkage occurring simultaneously with the heating process. A remeasurement of the RLPD-curves could give a good deal of information on said problem depending upon whether the thermal expansion coefficient remains unchanged during the relaxation process.

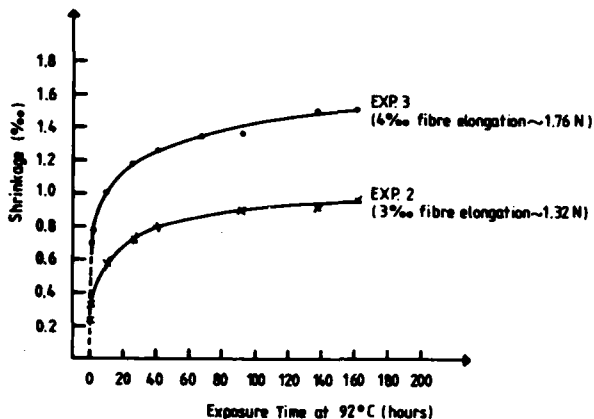


Fig. 9 Shrinkage of loose tube polycarbonate secondary coated fibres at 92°C  
The degree of the irreversible dynamical relaxation depends strongly upon the level of compressive strain experienced by the plastic tube

Anyhow, also at 92°C polycarbonate secondary jacketed optical fibres show excellent thermal stability. Even at a compressive strain as high as 1.34 N, the shrinkage is only 1% for a 160 hours exposure, and for the practical purposes, i.e., much lower mutual interaction forces, the shrinkage is expected to be much less, see Fig. 8.

#### Conclusion

Thermal properties of loose tube polycarbonate secondary coated optical fibres with regard to optical and mechanical performance have been discussed. It has turned out that the fibre length relative to the length of the plastic tube can be accurately measured by obtaining the light propagation time versus temperature characteristics. This is due to a factor 5 slope increase from the region where the fibre is free to move to the region where it becomes stressed by the thermal expansion of the plastic tube.

It was observed that the temperature interval with no excess loss could be much broader than the temperature interval where the fibre is not elongated by the expansion of the plastic secondary coating with the inference that it is much more important to control the stress free temperature interval as opposed to the interval of no excess loss. In fact, it has been observed that the upper limit of the temperature interval, where the fibre is not exposed to longitudinal stress,

can be well controlled over a wide range by adjusting different parameters in almost quantitative agreement with a model of the extrusion process.

Finally, the change of the stress free temperature interval with time has been investigated at 71°C and at 92°C. The observed irreversible dynamical relaxation or the shrinkage of the plastic tubes depend upon the level of compressive strain experienced by the secondary coating material. For compressive strain forces corresponding to less than a 1.5% elongation of a 125µm optical fibre, i.e., a practical relevant situation, the shrinkage would be less than 0.6% for a 160 hours exposure at 70°C and less than 1% for a 160 hours exposure at 90°C.

Hence, loose tube optical fibres with silicone primary coating and polycarbonate secondary coating show excellent optical and mechanical temperature characteristics.

#### References

- (1) Eric G. Hanson, Fiber and Integrated Optics, 3, 113 (1980)
- (2) S. Stueflotten  
Appl. Opt., 21, 4300 (1982)
- (3) A.H. Hartog, A.J. Conduit, D.N. Paine  
Opt. Quant. Electr., 11, 265 (1979)
- (4) R. Kashyap, M.H. Reeve, S. Hornung  
Electr. Lett., 18, 264 (1982)
- (5) L.G. Cohen, J.W. Fleming,  
Bell Syst. Tech. Journ., 58, 945 (1979)



Hans Damsgård  
NKT Electronics  
7 La Cours Vej  
2000 Copenhagen F  
Denmark

Hans Damsgård, né 1956, is a graduate of the University of Aarhus in Physics. Upon graduation, he joined the R&D Department of Nordiske Kabel- og Traadfabriker where he has been working on an industrial Ph.D. project - the thesis dealing with the performance of robust optical fibres.

## BREAKOUT CABLES FOR SHORT HAUL FIBER OPTIC SYSTEMS

F. T. McDuffee

PHALO/Optical Systems Division

ABSTRACT

A breakout cable construction has been designed consisting of individually strengthened and jacketed optical channels which facilitate use of single channel optical connectors. This cable design eliminates the need for a patch panel, breakout box or cable furcation (which are required for standard cable designs) at the cable to electronics interface. The cable design parameters are reviewed along with a detailed cost comparison between use of standard multi-fiber cable and the new breakout cable in short-haul optical links.

BACKGROUND

This product line was designed primarily to address the needs of most short-haul inter-office and inter-building optical systems which require individual connectorization of the optical channels at the cable to electronic interface. Traditionally, the termination of loose tube and tight buffer optical cables has proven difficult to unfamiliar personnel working with outside plant cable primarily due to the fact that fragile components (i.e. the individual optical channels) are exposed when the individual optical channels are broken out for termination. This has resulted in the need to interface optical cables to the electronics with some type of breakout box or patch panel inside the building or at the electronics rack. Typically, cables are spliced to single fiber strengthened cables in the box which are then terminated and routed to the electronics, or the individual fibers are terminated and interfaced to jumper cable assemblies through a patch panel.

Another approach involves furcation of the multi-fiber cable with strengthened furcation tubes. Disadvantages to the intermediate patch panel, breakout box or furcation tubes include the addition of either a fiber to fiber splice or connector to connector splice to the link, the cost of the components and the labor required to implement this approach in the field. With these added costs in mind, it was obvious that elimination of the intermediate cable to electronics interface was highly desirable.

To address these requirements, a series of optical cables consisting of individually strengthened and jacketed channels was designed. Individually terminated, strengthened optical channels

can be broken out close to the electronics and routed to the appropriate device. These cables are typically larger and contain more added material than standard multi-fiber cables. However, the additional cable material costs incurred are much less than the intermediate cable to electronics interface when link lengths less than 500 meters are involved. Often, the breakout cables can be factory terminated, resulting in additional savings and a higher level of quality control of the finished product.

CABLE DESIGN

The breakout cable design is composed of standard sub-units which are simply single fiber strengthened cables. This sub-unit is shown in Figure 1 and consists of a tight buffered optical fiber with aramid strength member and jacket. The sub-unit drawing shows the range of outer diameters used to date and does not indicate the fiber type or sub-unit jacket material since these are dictated by the application and therefore, vary from cable to cable. The sub-units are cabled in a variety of configurations to form a multi-fiber breakout cable. Figure 2 shows the 4 and 6 channel breakout cable configurations.

Central fillers are all dielectric and can be aramid yarn, epoxy S-glass or other suitable all dielectric material jacketed to the appropriate diameters. Fillers are not required for strength since the strength member in the individual sub-units is more than enough to provide reasonable strength for the cable. However, some installers prefer to use a central strength member as a tie-off for pulling cables through ducts. This is not always necessary since the cable can also be pulled by clamping the outer jacket tightly or by tying off to the individual sub-unit strength member material.

Cables have been constructed using both 50 um core, 100 um core and 200 um core optical fiber. The sub-unit jacket materials that have been used to date include flame retardant polyvinylchloride (PVC) and flame retardant thermoplastic rubber (TPR) for non-plenum cables and fluoropolymers for air plenum designs. Since these cables are usually manufactured without a tape to isolate the core from the outer sheath, the choice of outer sheath determines the sub-unit jacket material for non-plenum cable designs. Materials which have been used for outer sheaths are polyurethane, PVC or TPR for non-plenum cables and fluoropolymers for air plenum designs.

For most inter and intra-building installations, the choice of sheath materials usually can be determined with the following items under consideration:

1. Environmental exposure (water, sun, chemicals)
2. Sheath drag resistance
3. Cable flexibility
4. Low smoke requirements (air plenum)
5. Flammability
6. Applicable codes

Item 2 above is the key consideration when choosing TPR over polyurethane or PVC when the cable is pulled through crowded ducts or trays. TPR is harder and pulls over itself and other materials without grabbing or sticking. Therefore, short runs can easily be pulled by hand without the use of lubricants. Polyurethane and PVC provide a more flexible cable than TPR with polyurethane offering the best long term flex resistance.

The best choice of sub-unit jacket material for PVC sheaths is TPR since the PVC will not bond or melt the TPR sub-units during final extrusion. Similarly, PVC sub-units can be used with TPR outer sheaths and TPR sub-units can be used with polyurethane.

Low smoke requirements dictate the use of fluoropolymer jacket materials for both the sub-unit jacket and sheath material. The fluoropolymer cable designs require the use of a glass tape to isolate the cable core from the outer sheath. These air-plenum designs offer the same tensile performance as the equivalent non-plenum designs, however, the flex resistance is much lower due to the nature of the fluoropolymer material. Therefore, the air plenum cables are not suitable for use as a working cable.

Table 1 shows the environmental and mechanical specifications for the 4, 6 and 8 channel breakout cables. As can be seen from the table, these standard designs are very rugged cables due to the high strength member content and jacket material volume. This inherent ruggedness permits use of the breakout cable as a multi-purpose cable.

Breakout cables can be used in aerial, duct, tray or direct burial installations. The cable can be lashed to a messenger wire or possibly used as a self-supporting cable in aerial applications without any design changes, provided proper consideration is given to wind velocity, ice loading and span length. Duct installations may require the incorporation of a water-blocking compound in the cable which can easily be added to the interstitial space between sub-units of the standard cable during the final extrusion process. The individual sub-units require water-blocking only if the cable ends will be exposed to water. Direct burial cable can be made using the standard breakout designs as the cable core with a corrugated metal wrap and polyethylene sheath placed over the core for the necessary environmental protection.

An added advantage of the breakout cable is that hybrid cables (i.e. cables with a combination of optical fibers and electrical conductors) can be made without changing the basic cable design. Electrical power conductors can simply replace a fiber optic sub-unit or be used to replace the

central member or other cable fillers. The sub-unit jacket material in conjunction with the sub-unit orientation in the cable isolates the optical fibers from any macro-bending effects which could be caused by metal conductors in a hybrid design.

#### CABLE TERMINATION PRACTICE

As previously noted, the breakout cables can often be installed with factory terminated connectors. This depends on the specific installation route; however, it must be noted that inter-building installations of factory terminated cables are easily installed. If bends are involved, connectors can still be pulled through the ducts if the cable pulling apparatus is properly installed.

Figure 3 shows a schematic of a terminated breakout cable. Standard practice is to remove the cable outer jacket for the desired length and to slip a piece of 1/2" heat shrink tubing at the jacketed cable edge. This heat shrink tubing is not required for mechanical integrity of the joint but is used for appearance only. The individual strengthened single fiber channels are then cut to the appropriate length and terminated with the appropriate connector.

Since the individual channels of the breakout cable are color coded, it is not necessary to label the individual channels. However, for convenience, individual labels are often used in addition to the color coding. When pulling a factory terminated cable through ducts, the jacketed cable must be gripped and the individual terminated channels must be strain relieved. A central strength member left in place after termination could also be used for pulling the cable into ducts.

#### COST COMPARISON

In order to justify the cable cost increase for a breakout cable versus a non-breakout multi-fiber cable, a detailed cost comparison between the patch panel, breakout box and breakout cable approaches was made and a summary of this analysis is shown in Table 2. The table lists only installation cost items which differ between the various approaches shown. Since precise dollar amounts will vary with industry competitive pricing and time, only relative cost factors can be compared, such as number of man hours to implement a particular cost item, number of splices or connectors, etc. To compare cable costs, a fiber-meter price of seventy cents per fiber meter was assumed for a standard (non-breakout) multi-fiber cable. Based on this standard cost and the fact that the average breakout cable manufacturing costs are 22% more than for an equivalent non-breakout cable (i.e. fiber type and optical performance being equal), a fiber-meter price of eighty-five cents was used in the table. In order to fully understand Table 2, a brief description of each approach will follow.

##### Breakout Box

The breakout box termination approach involves routing the multi-fiber cable into a box

TABLE 1

MECHANICAL/ENVIRONMENTAL SPECIFICATIONSFOR CEOX6 SERIES BREAKOUT CABLES

NUMBER OF SUB-CHANNELS	4	6	8	UNITS
CABLE DIAMETER	9.5	11.2	11.2	mm
CABLE WEIGHT:				
1. TPR	75	90	95	kg/km
2. Polyurethane	83	100	106	
3. PVC	87	105	112	
IMPACT RESISTANCE FOR 100% SURVIVABILITY @ 200 IMPACTS	> 7	> 7	> 7	N-M
CYCLIC FLEX PERFORMANCE				
1. TPR	>1000	>1000	>1000	Cycles
2. Polyurethane				
3. PVC				
CRUSH RESISTANCE	>1600	>1600	>1600	N/cm
CABLE BREAKING STRENGTH (Tensile Load)	6,400	9,600	12,800	N
MAXIMUM INSTALLATION TENSILE LOAD	3,000	4,500	6,000	N
MAXIMUM OPERATING TENSILE LOAD	1,000	1,500	2,000	N
MINIMUM <u>SHORT</u> TERM BEND RADIUS AT:				
1. MAX. INSTALLATION LOAD	200	200	200	mm
2. MAX. OPERATING LOAD	95	112	112	
3. NO LOAD (2.5 X Diameter)	23.8	28	28	
MINIMUM <u>LONG</u> TERM BEND RADIUS AT:				
1. MAX. OPERATING LOAD	200	200	200	mm
2. NO LOAD (10 X Diameter)	95	112	112	
STORAGE TEMPERATURE	-55° to 85°	-55° to +85°	-55° to +85°	°C
TYPICAL ATTENUATION INCREASE AT:				
+65°C	+1.0	+1.0	+1.0	dB/km
-20°C	-1.5	-1.5	-1.5	
-40°C	-2.5	-2.5	-2.5	

TABLE 2  
FIRST COST VERSUS INSTALLED COST  
FOR 6 CHANNEL OPTIC CABLE LINK

	Unit	Breakout Box	Patch Panel	Breakout Cable	
				Field Terminated	Factory Terminated
500 Meters Cable Cost <sup>1</sup>	\$	2,100	2,100	2,550	2,550
1,000 Meters Cable Cost	\$	4,200	4,200	5,100	5,100
1,500 Meters Cable Cost	\$	6,300	6,300	7,650	7,650
2,000 Meters Cable Cost	\$	8,400	8,400	10,200	10,200
Factory Terminated Connectors	Each	12	24	-	12
Field Terminated Connectors	Each	-	12	12	-
Field Splices	Each	12	-	-	-
Patch Cables	\$	84	84	-	-
Field Labor for Termination	Man-Days	2	2	1	-
2 Patch Panels (w/ Bulkheads)	\$	-	600	-	-
2 Breakout Boxes	\$	500	-	-	-
Travel and Living (T & L)	\$	Required	Required	Required	-
Estimated Termination Cost <sup>2</sup> (Excluding T & L)	\$	1,556	2,304	480	420
Estimated Cable & Termination <sup>3</sup> Cost @ 500 Meters	\$	3,716	4,404	3,030	2,970
Estimated Cable & Termination Cost @ 1,000 Meters	\$	5,816	6,504	5,580	5,520
Estimated Cable & Termination Cost @ 1,500 Meters	\$	7,916	8,604	8,130	8,070
Estimated Cable & Termination Cost @ 2,000 Meters	\$	10,016	10,704	10,680	10,620

1. Assume .70/fiber meter for standard cable design, and .85/fiber meter for breakout cable.
2. Assume patch cables are 10 meters long at .70/fiber meter.
3. Includes connector material costs, factory termination costs, field labor @ \$300/man-day.

or housing inside a building. The cable strength member is tied-off in the box and the individual optical fibers are then spliced to single fiber strengthened cables in the box. The single fiber strengthened cables are then routed to the appropriate place inside the building and then terminated with connectors if not factory terminated. Disadvantages of the breakout box include the extra splice at each cable end and the labor required to implement this approach in the field. However, when cable costs dominate (e.g. for long link lengths), this approach can be cost effective. Figure 4a illustrates the breakout box approach.

#### Patch Panel

The patch panel approach is similar to the breakout-box except that the link fiber to single fiber strengthened cable splice is replaced with a bulkhead connector. Implementation of this approach requires field termination of connectors onto the individual fiber channels of the multi-fiber cable. Factory prepared single fiber strengthened cable assemblies can be used for the patch cables. The patch panel offers a higher degree of flexibility than the breakout box method, however, costs are higher due to the increased number of connectors used. Figure 4b illustrates the patch panel approach.

#### Breakout Cable

The breakout cable eliminates the need for the patch panel or breakout box since each optical channel is individually strengthened and jacketed in the form of a single fiber cable. These individual channels can be routed directly to equipment and are often factory terminated for increased cost savings and a higher level of quality control on the finished connector. The field termination and hardware savings justify this approach for link lengths less than 1 km for most installations. Another advantage of this approach is the relative simplicity of termination compared to the installation of a patch panel or breakout box.

### CONCLUSIONS

The cost comparison of Table 2 indicates a significant cost savings can be attained for link lengths less than 500 meters when using breakout cables versus the other two approaches. At longer lengths, the cable costs dominate with the cross over point occurring near 1 km for the breakout-box versus breakout cable comparison. The patch panel approach competes with the breakout cable only after link lengths of greater than 2 km due to the added connector components. Even at the cost cross-over points, the breakout cables (particularly the factory terminated cables) offer the better alternative due to reduced installation requirements. Also, the fact that factory installed connectors can receive a higher level of quality assurance cannot be over-emphasized. A summary of the breakout cable advantages is listed in Table 3.

Although any cost comparison will vary for specific systems, the tradeoffs discussed here should apply to most inter and intra-building systems assuming no unusual system requirements exist. The key tradeoff for considering the use of breakout cables involves a comparison of link cable costs versus cable termination costs. When termination costs dominate, the breakout cable will probably offer the better solution.

TABLE 3. Advantages of Breakout Design

1. Rugged design
2. Multiple use (e.g. aerial, burial, tray, duct)
3. Variety of jacket materials can be used
4. Reduced field labor
5. Fewer parts to order and install
6. Factory termination usually possible
7. Incorporation of electrical conductors possible.

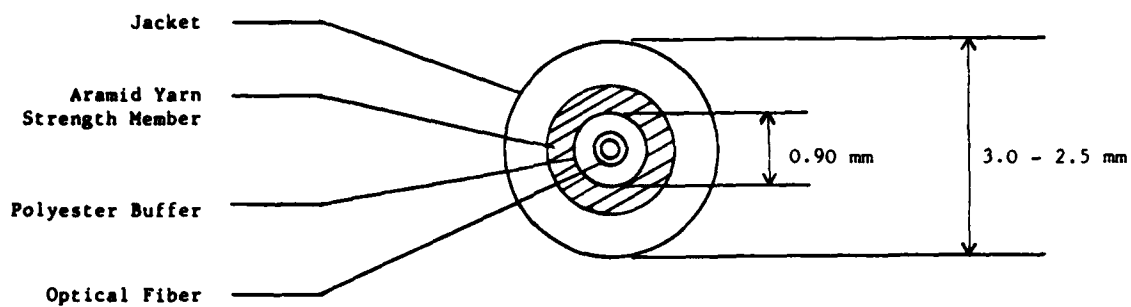


FIGURE 1 Strengthened Single Fiber Sub-Unit

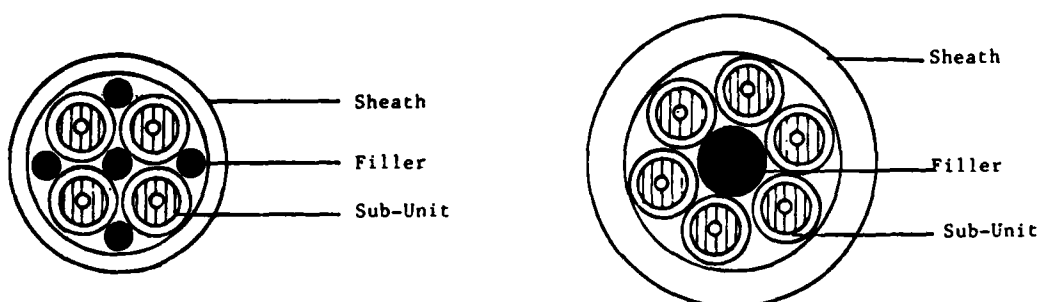


FIGURE 2. 4 and 6 Channel Breakout Cable Designs

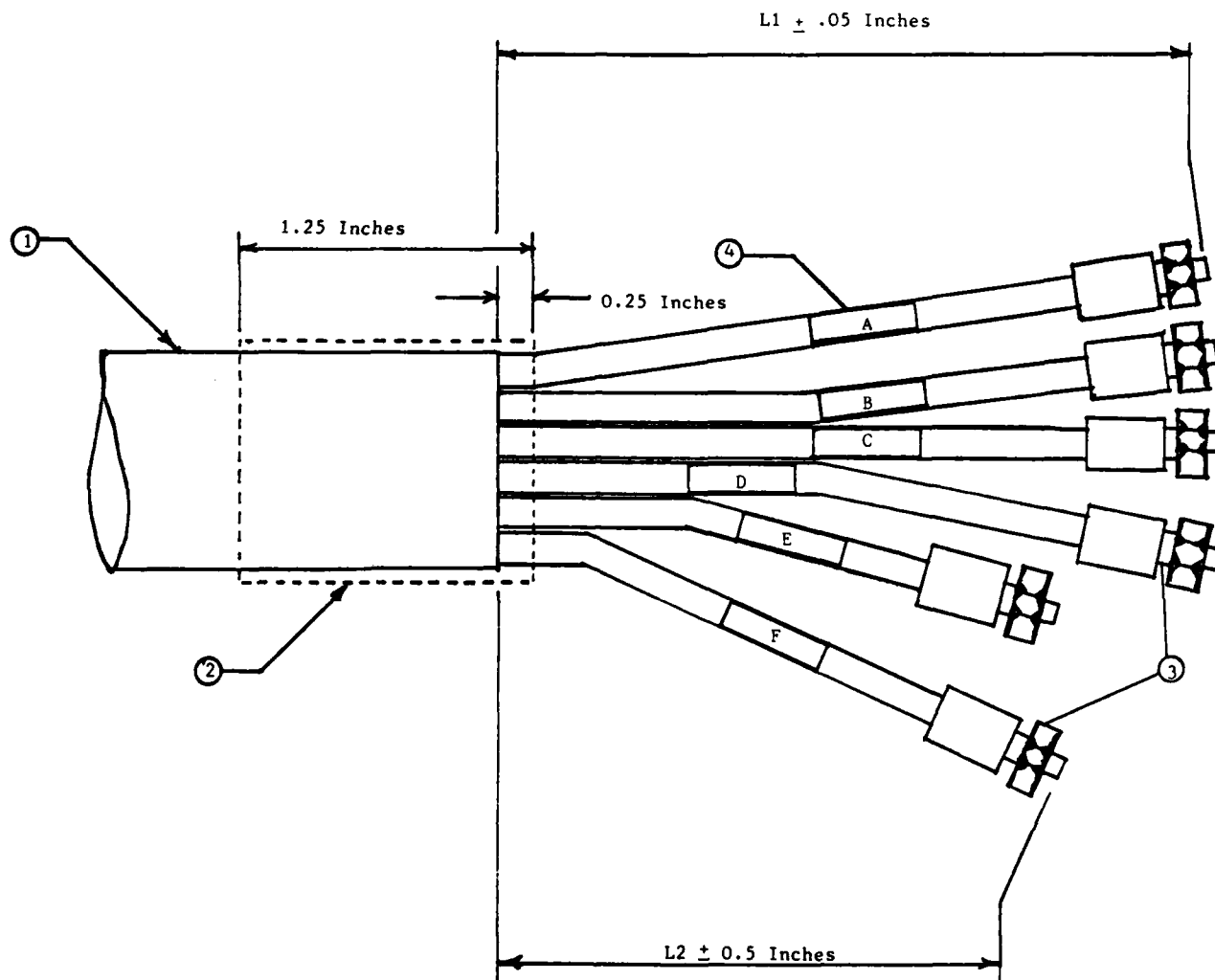


FIGURE 3 Terminated CE-Series Breakout Cable

- 1. CE Series Breakout Cable
- 2. Shrink Tubing

- 3. Terminated Single Fiber Strengthened Channels
- 4. Identification Labels

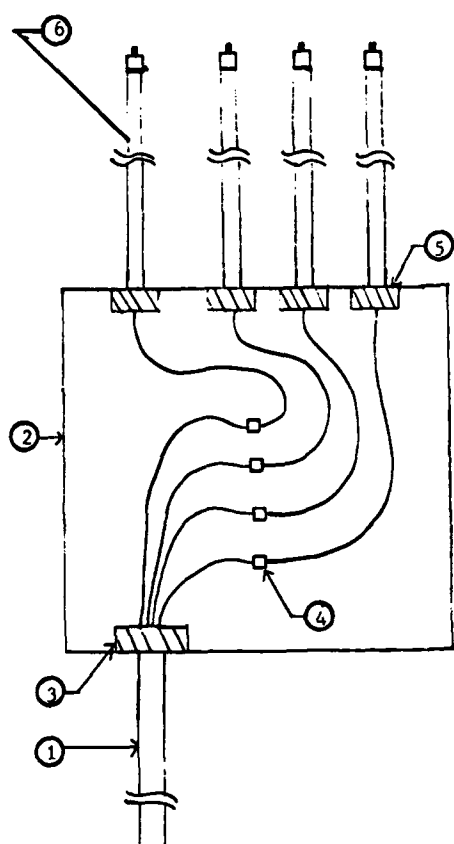


FIGURE 4A Breakout-Box

1. Multi-Fiber Cable
2. Rack or Wall Mounted Box
3. Cable Strength Member Tie-off
4. Fiber-to-Fiber Splice
5. Single Fiber Cable Strength Member Tie-off
6. Terminated Single Fiber Strengthened Cables

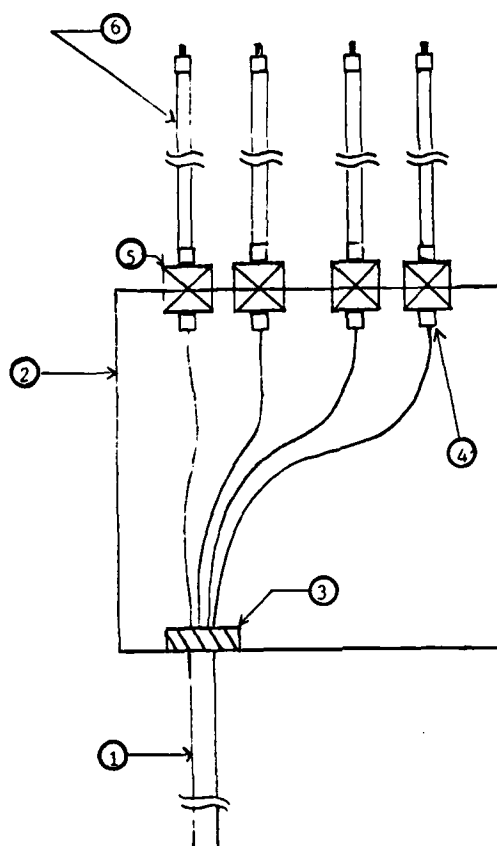
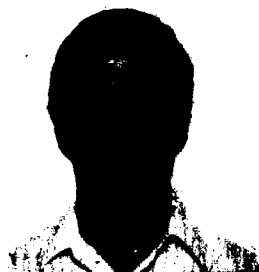


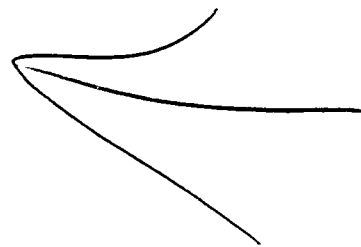
FIGURE 4B PATCH PANEL

1. Multi-Fiber Cable
2. Rack or Wall Mounted Patch Panel
3. Cable Strength Member Tie-off
4. Individually Terminated Fibers
5. Connector Bulkhead Adaptors
6. Single Fiber Strengthened Cable Assemblies



Fred T. McDuffee  
PHALO/Optical Systems Division  
900 Holt Ave  
Manchester, NH

Fred T. McDuffee received a B.S. degree in Physics from Virginia Polytechnic Institute and State University. Previously, he worked in the coupling and measurements group at ITT in Roanoke, VA, developing expertise in fiber splicing and optical couplers. Presently, Mr. McDuffee is Manager of Quality and Components at PHALO/Optical Systems Division, where his concerns include fiber measurements, cable assembly and optical coupler manufacturing.



## Authors Index

Abe, N. ....	155	Ishihara, H. ....	381
Abramson, P. ....	268	Iso, T. ....	70
Adams, D. J. ....	104	Itoh, T. ....	125
Aggarwal, I. D. ....	236, 323	Johansen, E. ....	200
Ahmad, S. ....	414	Kanamori, H. ....	294
Allen, B. W. ....	414	Kato, S. ....	294
Allen, D. B. ....	330	Kawahira, H. ....	54
Amano, Y. ....	30	Keith, R. H. ....	206
Arroyo, C. J. ....	372	Kikuchi, Y. ....	348
Audoux, C. ....	228	Kinard, M. D. ....	243
Bark, P. R. ....	301	Kitayama, Y. ....	54
Benjamin, I. ....	390	Kobayashi, T. ....	348
Blumsack, H. L. ....	236	Kubota, S. ....	54
Blyler, L. L., Jr. ....	144	Kuratani, K. ....	381
Boscher, D. ....	308	Kuwahara, T. ....	294
Bouvard, A. ....	49	Kyoto, M. ....	294
Bursh, T. P. ....	372	Laing, E. D. ....	277
Bury, J. R. I. ....	193	Latoszynski, P. ....	104
Cabey, M. ....	175	Lawrence, D. O. ....	301
Carlson, M. A. ....	111	LeBoutet, A. ....	308
Carter, A. ....	287	LeNoane, G. ....	228
Cassidy, S. A. ....	250	Levy, A. C. ....	88
Cheron, P. ....	228	Licht, R. R. ....	206
Clarke, F. B. ....	390	Linhart, H. ....	94
Cranfield, B. A. ....	193	Link, P. A. ....	37
Dahms, D. G. ....	206	Lombardo, M. ....	17
Damsgård, H. ....	429	Lukas, H. ....	316
Davis, D. D. ....	243	Lutz, D. H. ....	330
de Boer, B. T. ....	1, 104	Mathu, W. L. S. ....	407
Demey, J. P. ....	215	Matsubara, I. ....	54
de Vecchis, M. ....	49, 215	McDuffee, F. T. ....	436
de Vrieze, R. A. ....	83	Meyer, F. K. ....	94
Di Nenno, P. ....	390	Misono, N. ....	348
DiPinto, J. G. ....	330	Missout, B. ....	228, 308
Dobson, P. J. ....	236	Mitsui, T. ....	125
Fentress, V. ....	399	Miwa, M. ....	381
Garmon, J. P. ....	134	Miyamota, Y. ....	30
Geremia, J. ....	354	Mochizuki, K. ....	220
Ghoneim, H. ....	144	Mogi, A. ....	348
Gibson, M. J. ....	287	Monma, M. ....	155
Gieniewski, C. ....	144	Moran, A. L. ....	330
Gomi, T. ....	125	Mori, A. ....	9
Gotthardt, M. R. ....	45	Morris, P. ....	287
Grune, G. L. ....	255	Mottram, K. G. ....	1
Haag, H. G. ....	167	Mukunashi, H. ....	422
Hayasaka, E. ....	155	Murayama, T. ....	348
Hayashi, K. ....	422	Nakajima, T. ....	54
Hayashi, T. ....	70	Nakaseko, M. ....	155
Heintzman, P. ....	76	Nakatani, T. ....	155
Hobgood, R. B. ....	271	Namihira, Y. ....	220
Holte, T. ....	200	Nelson, D. V. ....	399
Hoover, J. R. ....	330	Neumann, R. ....	316
Horima, H. ....	155	Nieuwhof, B. J. ....	83
Hullin, J. P. ....	49, 215	Niirö, Y. ....	220
Hurwicz, D. ....	236	Nonclercq, B. ....	308
Hurwitz, D. ....	323	Odhner, O. R. ....	119
Iguchi, S. ....	422	Ohlhaber, R. L. ....	151
In't Veld, S. ....	323	Ohtake, A. ....	70

Ohtsuka, F. ....	155
Overton, B. J. ....	88
Pacey, G. K. ....	316
Pecsok, R. L. ....	119
Pedersen, J. R. ....	200
Personne, J. ....	215
Pocock, W. ....	354
Poulson, R. ....	49
Prideaux, P. ....	323
Punderson, J. O. ....	330
Quan, X. ....	144
Randa, S. K. ....	111
Reeve, M. H. ....	250
Reifschneider, D. P. ....	111
Roland, D. ....	323
Ruddell, H. J. ....	104
Saen, H. ....	9
Saito, Y. ....	54
Samuelson, G. ....	281
Satani, H. ....	30
Sato, H. ....	294

Sawada, J. ....	381
Sheppard, A. T. ....	183
Shirasawa, T. ....	70
Staath, J. C. ....	215
Sugawara, Y. ....	348
Suzuki, S. ....	294
Sweet, G. C. ....	330
Tachigami, S. ....	70
Tago, N. ....	30
Taylor, D. L. ....	63
Ushitani, S. ....	125
Watanabe, M. ....	294
Webber, R. G. ....	183
Weinraub, W. C. L. ....	243
Woodard, D. P., Jr. ....	24
Yamaguchi, M. ....	125
Yamamoto, H. ....	220
Yoshioka, N. ....	294
Yuto, M. ....	422
Zamzow, P. E. ....	167



**IWCS**

# **International Wire & Cable Symposium**

---

**SPONSORED BY U.S. ARMY COMMUNICATIONS—ELECTRONICS COMMAND  
(CECOM), FORT MONMOUTH, NEW JERSEY  
13, 14 and 15 November 1984  
MGM GRAND HOTEL, RENO, NEVADA**

Please provide in the space below a 100-500 word abstract (20 copies) of proposed technical paper on such subjects as design, application, materials, and manufacturing of Communications and Electronics Wire & Cable of interest to the commercial and military electronics industries. Such offers should be submitted no later than 13 Apr. 1984 to the Commanding General, U.S. Army Communications - Electronics Command, ATTN: DRSEL-COM-3, Fort Monmouth, NJ 07703.

Title: \_\_\_\_\_

Authors: \_\_\_\_\_

Company: \_\_\_\_\_

Address: \_\_\_\_\_

Staple

Fold here

Stamp

Commander  
US Army Communications R & D Command  
ATTN: DRSEL-COM-3  
Fort Monmouth, NJ 07703

Fold here

END

FILMED

2-84

DTIC